Liang Yun · Alan Bliault
Huan Zong Rong

High Speed Catamarans and Multihulls

Technology, Performance, and Applications

Springer

High Speed Catamarans and Multihulls

Liang Yun • Alan Bliault • Huan Zong Rong

High Speed Catamarans and Multihulls

Technology, Performance, and Applications

Springer

Liang Yun
Marine Design and Research Institute of China
Shanghai, China

Huan Zong Rong
Marine Design and Research Institute of China
Shanghai, China

Alan Bliault
Naval Architect
Sola, Norway

ISBN 978-1-4939-7889-2 ISBN 978-1-4939-7891-5 (eBook)
https://doi.org/10.1007/978-1-4939-7891-5

Library of Congress Control Number: 2018939425

Printed on acid-free paper

This Springer imprint is published by the registered company Springer Science+Business Media, LLC part of Springer Nature.
The registered company address is: 233 Spring Street, New York, NY 10013, U.S.A.

Preface

A series of new variations of high-performance marine vessels (HPMVs) have been developed in the last half century, including improvements to planing monohull craft from the 1940s, hydrofoils from the 1950s, air cushion vehicles (ACVs) and surface effect ships from the 1960s, small-waterplane area twin hull (SWATH) craft and wing in ground-effect craft from the 1970s, high-speed catamarans from the 1980s, wave-piercing catamarans (WPCs) from the 1990s, and high-speed trimarans in the first decade of the twenty-first century to the present. The authors have prepared texts discussing ACVs and wing in ground effect craft prior to this volume that focusses on the fast multihull – the catamaran, trimaran and SWATH or semi-SWATH.

The authors have been concerned with HPMVs for a long time. Professors Yun and Rong have more than 40 years' experience at the Marine Design & Research Institute of China, Shanghai (MARIC). Professor Yun has been chairman of the HPMV Design subcommittee of the China Society of Naval Architecture and Marine Engineering (CSNAME) for the last 20 years, as well as vice chairman of the organizing committee of the annual International HPMV Conference, Shanghai, China, since 1996. He has been involved in ACV development in China since the very first prototypes were constructed in Harbin in the late 1950s and has been involved to some extent in the design of many of the other vessel types treated here. Alan Bliault also started working in the ACV industry in its early days as a naval architect with Vosper Thornycroft but became involved in the offshore oil industry in the early 1980s and so has led a double life since that time, in order to maintain his connections with the world of fast marine craft while working for Shell as engineer, manager, and latterly internal auditor.

Designers, scientists, and various organizations, commercial, military, and governmental, have dedicated resources particularly heavily in the last 50 years to find ways in which combinations of hull geometries, hydrofoils, and static or dynamic air cushions can be used to deliver high-speed vessels that can perform very challenging missions. This work continues and is increasingly driven by energy efficiency and environmental impact rather than simply the mission envelope defined by speed/payload/range.

This book takes a broad view of the multihull concept and its design. We go into some depth on the hydrodynamics of such vessels while also aiming to give the reader an appreciation of what it takes to create a multihull as a project, where the underwater configuration is the starting point. A naval architect or marine engineer will be sensitive to the need to strike a balance between the configuration selection based on service requirement and the consequences of that choice of vessel geometric form for the structure, powering, motions, and total cost of ownership (TCO).[1]

Thus, this is a naval architecture book rather than simply a hydrodynamics text. For a more detailed treatment of hydrodynamics for such vessels, readers are referred to texts given in the references and listed in the resources section at the back of the book. University libraries should have access to printed or electronic versions. We will refer to subject matter covered in these other resources as we progress, taking a project delivery approach. Nevertheless, we present an overall approach to selecting and analyzing the form of a multihull vessel based on work at MARIC, where two of the authors have dedicated their careers to high-speed marine technology. This work in turn is linked throughout the text to research in Norway, the UK, Australia, and, more recently, the USA and further developed using the major project execution experience of author Bliault.

We will follow a sequence that can be applied when working on a multihull project. The early part involves looking at options based on available statistical data or some fundamental analysis. Once a starting configuration (or range of examples) is established, the design and analysis cycle can start. To achieve an "optimum" result, you need to have your roadmap set up with the key decision points and core design limitations (including your specification for accept/reject decisions). Without such a roadmap, the design/configuration can easily go off on a tangent and result in one parameter being optimized but a vessel that does not meet an operator's overall requirements. We spend some time discussing these decision points in a project timeline.

A balanced project leads to resilient vessel operation and, with careful maintenance, to a vessel that can be sold for late-life operation, generally in the developing world or a less demanding environment. Many of the larger multihull ferries built in the 1990s remain in service under different ownership. We touch on this issue as well since TCO can be significantly enhanced if the write-off cost at the end of a project is minimized.

Our main focus is the catamaran and trimaran for commercial service at medium and high speeds. Recent decades from the 1980s to the present (2018) have seen a significant market develop globally for passenger vessels, passenger and vehicle ferries (RoPax), and military logistics service as well as some special services for offshore wind farms. Two main inputs apply to these craft: the service envelope

[1]Total cost of ownership (TCO) is often referred to in large capital projects and includes the development cost, design and construction, commissioning and start-up, and operational costs, including decommissioning and disposal. Prior to investment it is important to assess this expenditure stream to determine the present value of the overall investment. A marine vessel project taken end to end will include all these elements.

during its transit and terminal requirements whether quayside docking for ferries or offshore docking, and station keeping for offshore vessels.

This book has evolved a great deal from the early drafts of Profs. Yun and Rong of MARIC. Initial papers were prepared in the early 2000s for the wave-making and wake analysis based on the approach used at MARIC in the 1990s. The work was updated in 2010 by Prof. Yun in preparation for this book with materials for an introduction to concepts including SWATH, wave piercers and hybrids, resistance and stability, seakeeping, and design development. Since that time, Alan Bliault has completed additional chapters regarding propulsion, structural analysis, outfitting, and project execution and updated the earlier material to incorporate the work of researchers and engineers primarily in Australia and the UK so as to reflect, to the extent possible, the global approach to catamaran and multihull design as it stands in the current decade.

We have used a simplistic approach to analysis so as to encourage students to experiment with minimal computational tools. Right now (2018) very sophisticated software is available for line preparation, hydrostatics, and now also much of hydrodynamic modeling. This book aims to provide an understanding of the analytical background of the concepts to be discussed, so that a student or engineer can then use these tools with confidence, rather than treating them as a black box.

In large measure naval architecture is still an art and a hull form that is efficient is generally also pleasing to the eye. There is a complicated combination of properties that must be determined and optimized before one can get to that stage, though. While it is now much easier than it was a couple of decades ago to prepare the key models, without an understanding of the key characteristics of a multihull in comparison to a monohull, it may be difficult to arrive at the desired design, so this understanding is our mission with the book.

Why are multihull vessels important? High-speed marine craft are generally targeted at missions involving low payload mass and higher volume, such as passengers, RoRo freight, or a specific utility or military task. This very requirement was the initial driver behind a vessel type like a high-speed ferry since a monohull has limited volume capacity. In recent decades a number of multihull derivatives have been developed for commercial and military application, including the trimaran and the small waterplane-area twin hull catamaran, or SWATH. We review the challenges associated with the design of these types, while aiming to maintain a focus on the catamaran as fundamental.

In the current decade the Internet has expanded to become a source of extensive reference materials. Throughout the book you will find to links to reference documents that (should be!) available as open-source information. We also provide references to a significant number of texts and papers that may not be immediately accessible to students. If you have difficulty tracing materials, please contact the website at Springer for this book, and we will try to help.

The catamaran has been developed with a number of variations in hull shape – displacement, semiplanning and planing, and small waterplane, combined with semiplaning or planing hydrodynamics. The characteristics of the variations are all

reviewed and their common hydrodynamics discussed as a central thread in the book.

In Chap. 1, we introduce the history, evolution, and development of catamarans, particularly in Norway, Sweden, Australia, the USA, the UK, Japan, and China, and initial concept assessment in Chap. 2. In Chap. 3, the initial calculation of key vessel characteristics and hydrostatics is outlined, allowing a preliminary configuration to be developed based on the concept selected in Chap. 2.

In Chap. 4, theoretical calculation of wave resistance is discussed, both in shallow and deep water. This is developed from the basic equations of equilibrium, velocity potential, wave-making resistance to numerical calculation for wave resistance of catamarans in both shallow and deep water. This chapter is derived from material written as a fundamental course for the theoretical calculation of wave drag and its application to catamarans, small waterplane vessels, and other hull geometrical variations at MARIC. In addition, the book provides computer program code for the calculation of resistance that may be further developed by students.

Chapter 5 describes the drag components of a multihull, their practical calculation for preliminary design (including incorporation of model test experimental results), and the influence of hull parameters on drag. The components introduced are calm water resistance, airflow resistance, appendage drag, and hull-induced wave resistance components derived from Chap. 3. From this chapter readers may understand how to calculate drag and estimate the power requirements of multihull craft at the preliminary design stage.

In Chap. 6, vessel basic motion characteristics are described first, then differential equations for both transverse and longitudinal motion are introduced, including coupled heaving and pitching, as well as their approximate analytical solution. We follow with a general discussion of multihull motions in a seaway and link to standard naval architecture texts and some recent research to direct the student to efficient ways to evaluate the dynamic response characteristics of a selected vessel configuration. This area of design evaluation is especially important for high-speed craft since accelerations can be high if errors are made in configuration selection and the consequences would be severe for human payload, freight, and equipment outfit on the vessel due to vibration.

Chapter 7 describes vessel design development, including evaluation methods to estimate design characteristics at the initial stage of a project, general arrangement evolution, and methods to estimate performance parameters. This chapter provides additional input to update the preliminary analysis presented in Chaps. 3 and 4 to begin concept optimization. This aspect is discussed within the chapter including the direction in which the different concepts will drive the designer.

Chapters 8, 9, and 10 introduce briefly the evolution, application, characteristics, and numerical calculation for wave-making resistance and experimental studies of SWATH vessels, WPCs, planing catamarans, tunnel planing catamarans, and other multihull configurations such as the M craft, the super-slender catamaran, and trimaran.

We continue with Chaps. 11, 12, and 13 on propulsion systems, structural configuration and design, and internal outfit and design. These are intended as an

overview assisting the student or engineer to make choices that can give input into the design spiral that forms the central thread of Chaps. 2, 3, and 7. These choices may create further cycles to be completed, depending on whether they affect the mission specification or the vessel performance envelope.

Finally, Chap. 14, on project delivery, is included so as to get the student thinking about how fast marine craft projects may be planned and executed successfully.

In addition to a section providing a list of Internet links to key technical resources, we supply three appendices that present data on multihull vessels of historical significance, tables that can be used for initial design development, and, finally, specifications and general arrangements of example vessels that may be useful to the student or engineer.

Assembling a textbook of this kind requires a great deal of assistance, and the authors have been fortunate in receiving this from the community of researchers, naval architects, shipyards, and suppliers of key machinery and outfitting worldwide. In what follows, we offer our thanks to the main organizations and individuals who generously provided their assistance. Where images or diagrams require attribution, direct reference is made to the relevant figure in a subsequent listing. Our sincere thanks go to those organizations for their permission to use the material.

Shanghai, China — Liang Yun
Sola, Norway — Alan Bliault
Shanghai, China — Huan Zong Rong

Acknowledgements and Thanks

The authors would like to express their sincere thanks to the leadership of the MARIC, Prof. Xing Wen-Hua, Gao Kang, Prof. Liang Qi Kang (former managing director), and their colleagues at MARIC: Prof. Wu Chen-Ji, Senior Engineer Lv Shi Hai, and the China Society of Naval Architecture and Marine Engineering (CSNAME), as well as the Shanghai Association of Shipbuilding Industry (SASI), Prof. Huang Ping-Tao (President, CSNAME), Prof. Zhou Zhen-Bai (President, SASI), and Prof. Yang Xin-Fa (Secretary General, SASI, Chairman of RINA, Shanghai Branch). Thanks go also to Mr. Jeffrey Hong-bo Hu and Mrs. Q.R. Liu (Senior Engineer, USA) and Mr. Kelvin Xiao Yun (Financial Specialist, Canada) for their help during the writing of this book.

During 2017 we were fortunate to obtain approval from the IMO to include interpretation of key extracts from the IMO High Speed Craft Code applicable to multihulls. Following this DnVGL, Lloyd's Register, and the American Bureau of Shipping agreed to allow us to extract material from their rules to assist in our overview of structural design approaches. These agreements have been very helpful in showing the close connection from initial assessment of hydrodynamic form for a multihull to setting up the design of the structures to construct the vessel.

Thanks also go to Prof. Tony Molland from the University of Southampton, who granted approval to use the material from his and his coworkers' groundbreaking work on catamaran resistance.

Valuable assistance was also provided by Prof. Hoppe on hydrofoil-supported catamarans and Albert Nazarov on the design of high-speed small catamarans.

We would also like to thank Prof. Larry Doctors of the University of New South Wales, Sydney, Tony Armstrong in Perth, and Wayne Murray, CEO of Austal in Thailand for their encouragement to the authors and material supplied to assist in explaining the approach to trimaran design, which is a process requiring the juggling of many more variable parameters than with a catamaran in arriving at an "optimum" design.

Special thanks are also due to Alan Blunden at Fast Ferry International for his support with photos of several vessels and input/guidance on vessel and market statistics.

Approval for the reproduction of images and data from a long list of organizations was received, as listed on the overleaf. It has been quite a journey interacting with all of the people involved and working with the internal processes required. Our thanks go out to all of them for their kind support!

Liang Yun and Huan-Zong Rong would like to express their sincere thanks to their wives, Ms. Li-Hui Qiu and Ms. Ju-Ying Hang, for their support and help during the writing of this book.

Alan Bliault had the support and patience of his wife, Esperance, through this same period, including some challenging extended periods in which Alan focused on the writing and communication with industry officials to the exclusion of much else. She will be relieved once it is in print!

Shanghai, China — Liang Yun
Sola, Norway — Alan Bliault
Shanghai, China — Huan Zong Rong
January 2018

Acknowledgements for Images and Data

Our thanks go to each of the organizations and individuals detailed below for assisting with images and allowing us to use them in the book.

Item	Acknowledgement/Accreditation
Fig. 1.3	Photo © 2017 CupInfo
Fig. 1.4b	Public domain from Smithsonian
Fig. 1.10	Courtesy Alilauro
Figs. 1.6 and 1.11	Courtesy Incat Marketing Pty. Ltd.
Figs. 1.12 and 1.15a, b	Courtesy Austal
Fig. 1.16	Courtesy Afai South
Fig. 5.12	Courtesy Southampton University
Fig. 5.51a	Courtesy Corsica Express
Figs. 6.23 and 6.24	Courtesy Fast Ferry Info with thanks to Alan Blunden
Fig. 6.20	Courtesy Incat Marketing Pty. Ltd.
Fig. 6.30	Courtesy Austal
Figs. 6.31 and 6.32	Courtesy Incat Marketing Pty. Ltd.
Figs. 7.16, 7.17, and 7.18	Courtesy Austal
Figs. 8.2, 8.3, and 8.7	Courtesy Incat Marketing Pty. Ltd.
Figs. 9.11, 9.12, 9.17, 9.18, 9.19, and 9.26	Courtesy Navatek Ltd.
Figs. 9.13a and 9.14	Courtesy Lockheed Martin
Fig. 9.32	Courtesy Pentland Ferries
Fig. 9.33a	Courtesy Damen
Fig. 9.34	Courtesy Abeking and Rasmussen
Fig. 9.35	Courtesy Adhoc Marine Designs, IOW
Fig. 9.36	Courtesy Odfjell Wind Service A.S.
Fig. 9.37	Courtesy Turbine Transfers
Fig. 10.8	Courtesy uimpowerboating.com
Fig. 10.12	Courtesy Kumamoto Ferry Co., Nagasaki, Japan
Fig. 10.13b	Courtesy Incat Crowther

(continued)

(continued)

Item	Acknowledgement/Accreditation
Fig. 10.14b	Courtesy Seacor Marine
Fig. 10.14a	Courtesy Caspian Marine Services / Incat Crowther
Figs. 10.15 and 10.16 to 10.19	Courtesy Austal
Fig. 10.20	Courtesy MCN
Fig. 10.21	Courtesy LOMOcean
Figs. 10.24 and 10.25	Courtesy Mshipco
Figs. 10.26 to 10.28	Courtesy BMT Nigel Gee
Fig. 10.30c	Courtesy Turbojet Hong Kong
Figs. 10.29c, 10.34, and 10.35	Courtesy Hysucat and FASTcc with thanks to Prof. K.G.W. Hoppe
Fig. 10.36	Courtesy Harley Ship Corporation, with thanks to Harold Harley
Figs. 10.37 to 10.40	Courtesy SESEU, with thanks to Ulf Tudem
Fig. 10.41a–c	Courtesy UMOE, Mandal
Fig. 11.7	Courtesy Arneson/Twin Disc
	Courtesy QSPD
	Courtesy Rolla
Fig. 11.7	Courtesy Levidrives
	Courtesy ZF
Figs. 11.9 and 11.25	Courtesy Servogear
Figs. 11.11 and 11.20	Courtesy Wartsila
	Courtesy Hamiltonjet
	Courtesy Rolls Royce KaMeWa
	Courtesy Castoldijet
	Courtesy MJP
Fig. 11.22	Courtesy MTU
Fig. 11.23	Courtesy Scania, material from company website
	Courtesy Cummins, material from their website
	Courtesy MAN, material from their website
	Courtesy GE, material from company website
Fig. 11.24	Courtesy ZF
Fig. 11.24b	Courtesy Reintjes
Fig. 11.26	Courtesy Humphree
Fig. 11.27	Courtesy NAIAD
Fig. 12.3	Courtesy Damen
Fig. 12.4	Courtesy Mackay Rubber
Fig. 12.8	Courtesy Incat Marketing Pty. Ltd.
Fig. 12.10b	Courtesy Rennbootarchiv Schulze, Wikimedia Commons, offshore powerboat racing
Fig. 12.11	Courtesy ABS
Figs. 12.13 to 12.17	Courtesy Incat Marketing Pty. Ltd.
Fig. 13.1	Courtesy Adhoc Marine Designs
Fig. 13.2	Courtesy Incat Marketing Pty. Ltd.

(continued)

(continued)

Item	Acknowledgement/Accreditation
Fig. 13.3	Courtesy South Boats, IOW
Fig. 13.7	Courtesy Incat Marketing Pty. Ltd.
Fig. 13.13a	Courtesy Incat Crowther
Fig. 13.8	Courtesy Survitec
	Courtesy Viking Life
	Courtesy LSAmes
Fig. 13.10a, c	Courtesy Austal
Fig. 13.10b	Courtesy Incat Marketing Pty. Ltd.
Figs. 13.11 and 3.12	Courtesy ISC Ltd.
Fig. 13.14a	Courtesy Curvelle Superyachts
Fig. 13.14b	Courtesy Sabdes, with thanks to Scott Blee
Fig. 13.15	Courtesy One2Three Naval Architects
General	
Material from HSC Code	Thanks to IMO for permission
Material from Rules	Thanks to DnVGL
	Thanks to ABS
	Thanks to Lloyd's Register
Construction Statistics	Thanks to Fast Ferry info
Appendix GA and Specs	Thanks to Incat, Austal, South Boats, Adhoc Designs, Seacor

Contents

About the Authors

Liang Yun Professor Yun has more than 40 years' experience at the Marine Design & Research Institute of China, Shanghai (MARIC). He graduated from the Shipbuilding Engineering Faculty of Da-Lian Polytechnic University in 1953 and completed a postgraduate diploma at the Military Engineering Academy of China in 1955. He has been involved in ACV development in China since the very first prototypes were constructed in Harbin in the late 1950s, the design and prototype construction of WIG craft in the 1990s, and the development of both high-speed catamarans and air cavity vessels from the beginning of the millennium.He was Director of the HPMV division of MARIC from 1983 to 1987 and Deputy Chief Naval Architect of MARIC from 1980 to 1997. He has been a guest professor supporting HPMV postgraduate students at Harbin Engineering University and was Wu Han Water Transportation University in the early 1990s.

Professor Yun has been chairman of the HPMV Design subcommittee of the China Society of Naval Architecture and Marine Engineering (CSNAME) over the last 20 years, as well as vice chairman of the organizing committee of the annual *International HPMV Conference*, Shanghai, China, since 1996.

He continues to play an active role in the promotion and development of HPMV technology in China through his association with the industry and Chinese universities. Prior to the current volume on multihull vessels, Prof. Yun partnered with Alan Bliault on three textbooks covering ACV, WIG, and HPMV technology.

Alan Bliault A naval architect and offshore engineer, Alan is a fellow of the Royal Institution of Naval Architects and graduated from the University of Newcastle upon Tyne. His early career was at Vosper Thornycroft working on the design and operation of hovercraft and air cushion platforms. Subsequently he worked in the offshore industry developing new offshore loading systems. He was responsible for hydrodynamic design for Conoco Hutton Field Tension Leg Platform in the UK and subsequently at Norske Shell for Draugen Platform substructure mechanical outfitting, hydrodynamics, tow-out, and installation in Haltenbanken.

In the mid-1990s he led development of new API and ISO standards for subsea flexible flowlines and risers based in Holland. Through the millennium he led Shell International's development of a floating LNG production system for remote gas fields. Since that time he has held various project management, construction, and research and development roles.

He has worked as a senior auditor in Shell's central internal audit group evaluating risk and management controls on major projects and operating companies worldwide from 2013 to 2016.

He has maintained a keen interest in high-speed marine craft throughout his career, and this led to his partnership with Liang Yun on engineering textbooks, including the present volume on multihull vessels.

Huan-Zong Rong Huan-Zong also has over 40 years' experience at MARIC. In 1967, he graduated from the Department of Mathematics, Fudan University, with a major in mechanics. As an engineer in the Ship Hydrodynamic Laboratory, MARIC, he worked on the calculation of wave resistance and ship form improvement using wave-making theory and wave pattern analysis.In 1982, he received a postgraduate diploma at the China Ship Research and Development Academy, based on his work in marine hydrodynamics, and received an M.Sc. degree from Shanghai Jiao Tong University in 1983.

He became Senior Engineer, Head of CAD, computer division, MARIC, working on uniform B-spline curve fitting with an area constraint, nonuniform B-spline mesh fairing, and hull form generation system

using a nonuniform B-spline technique between 1988 and 1996.

Huan-Zong became professor, principal engineer, and consultant at the Ship Design Technology National Engineering Centre, MARIC, from 1997 to 2012 working on a computer-based hull form generation and hull form design system using a NURBS technique, a ship power estimation system, and a ship damage stability calculation system, all based on Windows.

List of Figures

List of Tables

Chapter 1
Evolution

1.1 Our Subject

This book is about catamarans and multihull craft, their background, the possibilities for their application, and the analytical background in hydrodynamics that allows us to determine their proportions and performance.

Overall, the design of a marine vessel is more of a team event than just applying hydrodynamic analysis, so we provide some thoughts on project planning and execution; then it is up to designers to take up the challenge to build and work with their team to achieve the best possible result.

Our focus is on high-speed motorized craft rather than high-speed sailing catamarans or low-speed utility craft designed simply to use the multihull special attribute of very large deck space. More general treatments of multihulls are described in references [1] and [2]. We refer to these and to several standard texts on naval architecture (e.g., [3–7]) over the course of this book since the principles do not change; it is primarily the impact of a high-speed vessel mission, the interaction between multiple hulls close together, and the extension of some theories to higher speed application that need special attention.

The design and performance of catamarans and multihull craft involves both hydrodynamics and aerodynamics, so the reader will find references in both of these fields. At the back of the book we include a listing of more general reference material including books, journals, and sites on the Internet that can form the start of a search. The Internet changes rapidly, so it may be necessary to perform a more general search if the site listed has changed addresses since the publication of this book or if the site has been succeeded by another one. We also include a listing of key software used by designers at the time of this text's preparation, starting with that used by Austal and Incat. Students can gain access to several of these packages at low cost, which can be useful for project work.

L. Yun et al., *High Speed Catamarans and Multihulls*,
https://doi.org/10.1007/978-1-4939-7891-5_1

Our main focus is the overall configuration and geometry of a high-speed craft using two or more hulls to achieve a particular mission objective and to describe the analysis necessary to design the form of such craft to meet designer goals. Catamarans, along with their derivative configurations, are the main subject. We touch upon power plants, propulsion systems, structures, and outfitting in later chapters, though more for the purpose of giving direction than detailed instructions. Internal outfitting has developed rapidly in the last two decades, borrowing from aerospace for high-speed ferries, and becoming very sophisticated for the private vessels known as superyachts. At present there are few multihull superyachts. Those that have been built use the configuration to maximize the living space with a luxurious outfit.

The book is aimed at students or engineers studying marine technology in college or for themselves, and so we assume knowledge of basic hydrostatics and hydrodynamics. It is useful nevertheless to give some background to key elements, which we do in Chap. 2. It is given as a summary for readers' use, with references to fuller general treatments.

Many high-speed catamarans are displacement or semi-displacement craft owing to their very slender hulls. These craft are designed to slice through waves rather than platform over them as a planing craft would. This design choice brings the challenge of maintaining longitudinal stability in waves at speed and has led to the development of new bow forms as well as the use of stabilizing foils to help control pitch motion in a seaway.

Above a speed equating to a Froude number (Fr_L)[1] of about 0.7 a hull will tend to trim bow upwards because the vessel-induced waves will reach twice the hull length and the vessel will start to experience a significant lifting force component. If the engines are strong enough to accelerate the craft, the dynamic lift force will bring the hull up out of the water it was displacing until it is effectively riding on the surface like a pebble that has been skimmed across water. At $Fr_L > 1.0$, the dynamic force increases sufficiently for a craft to be said to "plane" fully on the water surface given a suitable hull form. In actual fact, there will still be a depression, but it will be small; it constitutes the remains of the hull-induced wave form.

Depending on the underside shape of the hull, a boat may look as if it is skimming or, if the hull has a round or V shape in cross section, it will simply look high in the water. The waves created by a displacement craft and radiating from it will now be a much sharper angled V and appear to emanate from behind the craft itself.

Boats designed specifically to operate in this high-speed region generally have flat or shallow V-shaped hull bottom surfaces to give the best lifting performance. This has two consequences. First, in a seaway the hull may rise out of the water and fall back down again, hitting the surface with a "slam," resulting in high acceleration

[1]The Froude number is usually based on length either directly as waterline Fr_L or indirectly as the cube root of the displacement Fr_V. In this book we will primarily use the waterline length when referring to the Froude number.

forces[2] to the hull. The second consequence is that these motions can be uncomfortable for passengers.

A catamaran can be designed as semiplaning at relatively high actual speed owing to the hull slenderness, causing it to operate at a lower Fr_L compared to an equivalent displacement monohull. This has the potential for improved motion and passenger comfort, an attribute that has been taken advantage of by the largest catamaran builders to build really capable seagoing high-speed ferries. We will discuss this more later on in the design chapter.

Going back to a key attribute of catamarans, it is the large deck area that can be used for low-density/high-volume freight or for spacious passenger accommodations that lend substance to the concept of fast passenger or vehicle ferries and in the military world for delivery of personnel with high-volume supplies and military equipment at significantly higher speed than conventional vessels. By its nature such a craft has relatively low draft, allowing access to a wider range of port facilities and routes than monohull vessels.

The main message here is that multihull configurations can offer mission solutions that are wider in scope than the possibilities offered by a monohull. The first opportunity for such a development was the fast passenger ferry and, more recently, passenger/vehicle ferries. Military missions are now under development, and deployment is occurring particularly in the USA, China, and, recently, Oman, and these vessel types are now also attracting attention in the commercial world for use as superyachts.

Another developing market is for offshore wind farms. Since the early 2000s there has been an increasing number of projects for power generation using fields of offshore wind turbines. These installations require regular inspection and maintenance, so access from shore for personnel, including for fast transit and stable station keeping, presents a challenge while inspection or maintenance work is being carried out by the personnel. The semi-SWATH catamaran and small trimaran form are proving effective for such operations. Looking to the future where renewable energy will become dominant, the demand for such vessels will continue to increase.

We mentioned earlier the semiplaning and planing hull forms for catamarans. Several more multihull configurations exist, including the small-waterplane-area twin hull (SWATH) craft, the trimaran form (generally a slender main hull with outboard stabilizers aft for fast craft), the pentamaran (both bow and stern stabilizer outriggers), and variations based on support by hydrofoil stabilizers.

We will discuss the merits of these and provide some insight on the performance evaluation for different geometries. In our treatment of the theory and analysis of performance for these craft, we will base our analysis on the catamaran form and provide readers with guidelines on the other forms without treating them in equal detail.

[2]Acceleration forces are generally quoted in relationship to the acceleration due to gravity and referred to as "*g*" forces, for example, 0.1 g is 0.981 m/s^2.

1.2 Background

The history of the catamaran goes back to the time when humankind first used a tree trunk for over-water transportation; such a vessel remains common in less-developed parts of the world (Fig. 1.1). While conventional monohull ships started out as dugout logs, the catamaran's origin was as a raft formed by lashing two or more logs together with a space between. Two hulls braced together by means of bracing poles or boards to create a space between them generate the following properties:

- High transverse stability dependent on the space between the two hulls
- Reduced roll angle in waves compared with a single hull
- A sizeable platform for freight or people payload
- Improved seaworthiness in oblique seas

A catamaran so formed nevertheless is a more complex structure than a single-hull vessel, whether propelled by oars or sails. In calm rivers and estuaries, the simpler slender pirogue has persisted for small cargoes, while voyages at sea saw the first application of the catamaran form. Strapping two slender craft together is still simpler than preparing planks of wood and forming them into a more capacious hull, particularly where the available material is tropical hardwood.

The Polynesians are credited with constructing, many centuries ago, the first seaworthy, oceangoing catamarans. They brought this craft type to such a high state of development that they were able to undertake amazing voyages of exploration over vast expanses of the Pacific Ocean, from Tahiti to Hawaii, Easter Island, and, eventually, New Zealand in the period from approximately 1000 AD to the late

Fig. 1.1 Pirogues used for river fishing: short, long, old, and modern (Nkomi River, Gabon (2012))

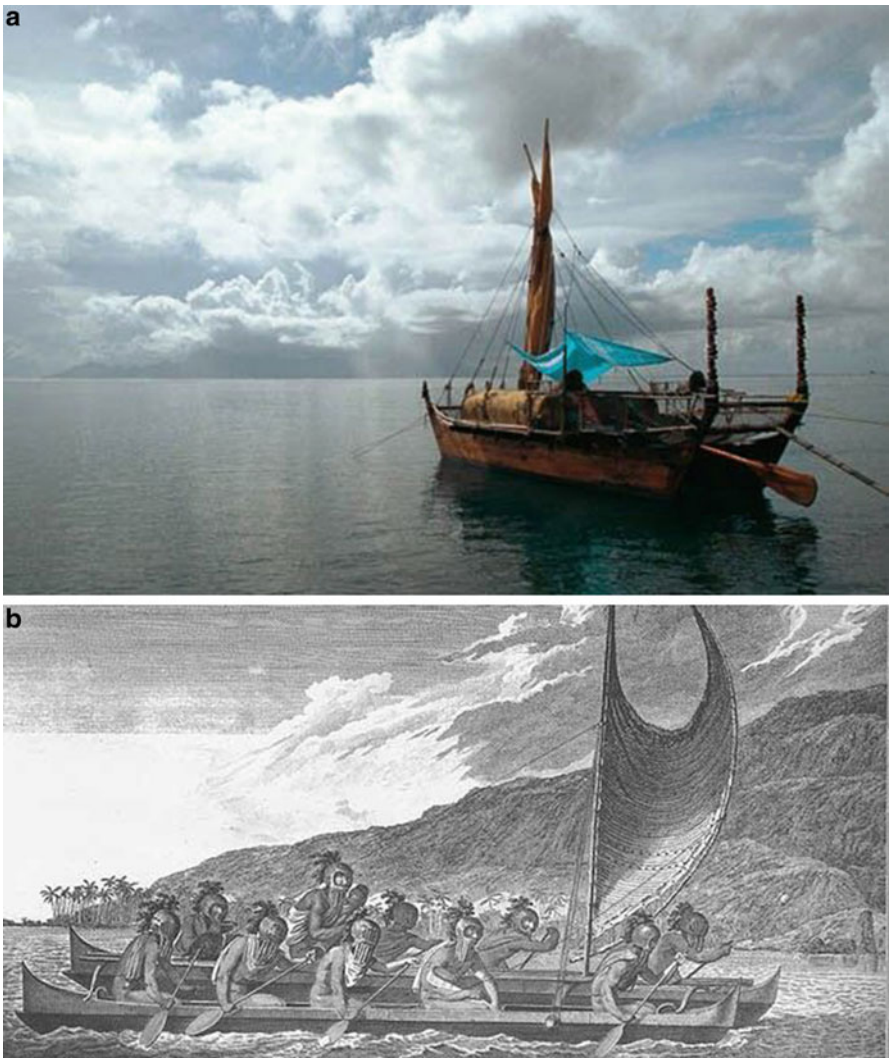

Fig. 1.2 (**a**) Polynesian proa at mooring; (**b**) paddling manpower at speed

eighteenth century (Fig. 1.2) (see resources, general, for Hawaiian voyaging traditions) [8, p. 20, and 9].

For sail-powered craft, sail-carrying ability is a very important function for gaining speed and depends on achieving stability from the hull form and ballast. The monohull form, which will move fast given some forward thrust from the sails, unfortunately has the least stability against the heeling moment of sails when wind is from the beam. The solution for several centuries was to concentrate on achieving the required stability by installing ballast at the bottom of the hull; however, this

Fig. 1.3 Example of fast sailing catamaran on hydrofoils, America's Cup catamarans in 2013

comes at the cost of increasing the displacement, which requires that greater amounts of sail be carried.

Modern sailing yachts have a long extended keel with the ballast weight at the bottom. This reduces the mass required, but the keel fin still induces significant drag loads, in addition to limiting operations to suitably deep water, including docking. The catamaran is able to carry the large amount of sail necessary for high speeds by countering its heeling moment with the inherent stability of two widely separated hulls without the use of significant ballast.

Apart from the catamarans of Polynesia, there was little development of the multihull form elsewhere in the world until the twentieth century. The last century has seen an amazing development of fast sailing catamarans for circuit racing and world circumnavigation challenge events. An example of these from the America's Cup qualification competition is shown below (Fig. 1.3) and the larger craft from the America's Cup competition in 2013 (Fig. 1.4), which has a single design rule based on a catamaran with midship-mounted retractable lifting foil keels (see [10] and resources at end of book for Web sites).

The transition from sailing vessels to mechanical propulsion for commercial and military ships in the nineteenth century, initially to steam engines powered with coal as fuel and later using liquid fuels, meant that the overturning moment of sails at full power was no longer a challenge, so the simple approach of the single hull took the lead for almost the next two centuries.

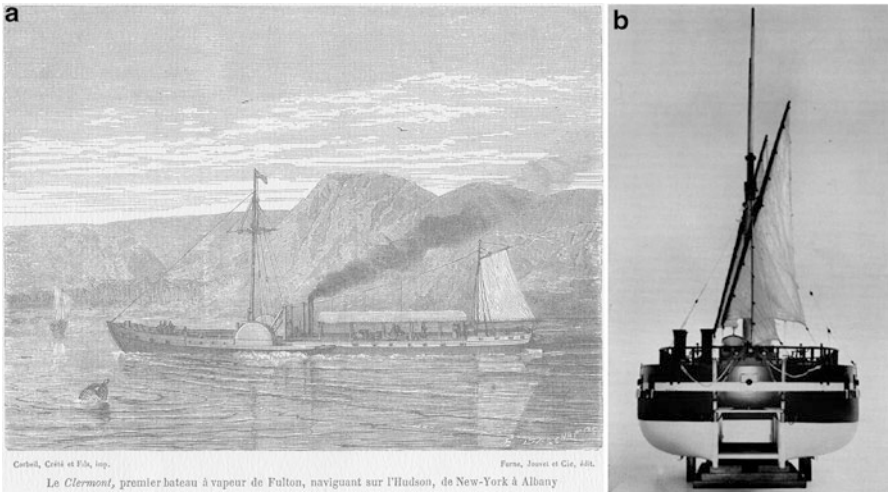

Fig. 1.4 (**a**) Fulton's steamboat Clermont on the Hudson River; (**b**) block catamaran "Fulton the First "

Table 1.1 Fr_L for varying hull lengths

Length, m	10	15	20	25	30	35	40	45	50	75	100
10 Knots	0.53	0.43	0.38	0.34	0.31	0.29	0.27	0.25	0.24	0.19	0.17
15 Knots	0.80	0.65	0.57	0.51	0.46	0.43	0.40	0.38	0.36	0.29	0.25
20 Knots	1.07	0.88	0.76	0.68	0.62	0.57	0.54	0.51	0.48	0.39	0.34
25 Knots	1.34	1.09	0.95	0.85	0.77	0.72	0.67	0.63	0.60	0.49	0.42
30 Knots	1.61	1.31	1.14	1.02	0.93	0.86	0.81	0.76	0.72	0.59	0.51
35 Knots	1.87	1.53	1.33	1.19	1.08	1.00	0.94	0.88	0.84	0.69	0.59
40 Knots	2.14	1.75	1.52	1.36	1.24	1.15	1.07	1.01	0.96	0.78	0.68
45 Knots	2.41	1.97	1.71	1.53	1.39	1.29	1.21	1.14	1.08	0.88	0.76
50 Knots	2.68	2.19	1.90	1.70	1.55	1.43	1.34	1.26	1.2	0.98	0.85

This does not mean that the catamaran concept was not investigated. The first known powered catamaran was a vessel built in England in 1660 by Sir William Petty (Table 1, Appendix 1) [11]. Sir William followed this first craft with several other experimental sail-powered catamarans in the following three decades.

During the steamship era of the nineteenth century it was realized that vessel drag including wave-making resistance increased with speed in square proportion, and this was the reason why ships had great difficulty accelerating to higher speeds. This led Sir William Froude to his towing tank model experiments in Torquay for the British Admiralty and scaling correlation via the nondimensional relation named after him, Fr_L [3, 12].

The best way to reduce the wave-making resistance of a hull is to increase the length/beam ratio (L/b), thereby increasing the slenderness ratio of the ship ($L/\Delta^{1/3}$). A hull with a higher L/B for the same displacement will operate at a lower Froude number at the same speed, incurring lower wave-making drag forces (Table 1.1).

However, this also comes at the cost of decreasing the transverse stability and increasing the hull immersed surface area and friction drag.

This may not be a problem for monohull vessels with low or fixed payloads, such as pleasure craft or small naval craft, but it is a challenge for craft intended for commercial use for freight or passengers. The best solution to the transverse stability problem is to divide the hull along the longitudinal central plane into two demihulls and separate each demihull so as to make a catamaran.

In addition to having two hulls, such vessels can also be symmetric in cross section, rather than asymmetric. This was the route taken by many designers of craft in the later nineteenth century, who also moved to using three hulls, experimenting with longitudinal position and spacing to use wave interference and canceling to minimize induced wave drag at service speed. The aim of these designers was to build craft capable of moving at higher speeds and to build larger craft using the same machinery, since steam machinery was large and its output power limited at that time.

A brief introduction to the history and various types of catamaran can be found online at Wikipedia, in English at www.en.wikipedia.org/wiki/catamaran. The Polynesian craft are discussed and the key types whose hydrodynamic design we cover are introduced.

Expanding somewhat on this material for historical background, a number of steam catamarans were designed and built in the nineteenth century for use on the Mississippi River in the USA (Fig. 1.4), propelled by paddle wheels both outside the hulls and with a wheel between the hulls (see [1] and [13] for a historical perspective).

Most of the experiments during this period seem to have been conducted in the UK and USA and focused on inland shipping in the Great Lakes and on the Mississippi River in the USA and coastal craft in the UK, culminating in two vessels built for service between Dover and Calais in the 1870s. The catamaran lends itself to paddle-wheel propulsion, whether external or between hulls, due to the high transverse stability. Several different layouts were used successfully in the USA in relatively calm river waters. The challenge was somewhat greater in the English Channel owing to the choppy seas, and while mechanically successful, the ferries in service in the 1870s had problems with vibration and motions in the seaway with oblique oncoming waves. Conventional monohull ferry ships took back these routes all the way up to the 1970s, when hovercraft came into service with speedier crossings, and a decade later in the 1980s when wave-piercing catamarans began service on this route took on routes across the Irish Sea. A selection of significant catamarans designed and built during the early evolution is listed in Table 1 in Appendix 1.

In Russia there has been considerable research and development on catamarans for use on inland waterway networks since the early twentieth century. River transport has until recently been the major option for communication between several cities on the Volga and Don River systems owing to a lack of roads and railway connections. A number of different designs were built and used to provide fast transportation between these riverside cities starting in the 1960s. The

development of catamarans paralleled that of high-speed inland hydrofoil craft in the same period [1, 14]. A large number were built in the 1960s and 1970s and provided efficient service for passengers and freight. The catamarans met medium-speed service requirements, while hydrofoils provided rapid transit service. Many such vessels are still in operation today (2017).

It was M.Y. Alferiev who initially proposed catamarans in Russia based on model testing of the longitudinal centerline split configuration (splitting a monohull and moving the two halves apart) with different transverse spacings that he investigated. The coefficient of total resistance was found to be significantly lower than for the original monohull, suggesting a more efficient vessel in catamaran form.

A specific problem with the river system in Russia was that of wash from vessels at higher speeds, and the catamaran was studied to determine whether wave making was less severe with a catamaran. The results were positive, leading to the construction of catamaran cargo vessels in the 1960s. Reference [1] lists five vessels from this era with waterline lengths from 40 to 130 m and speeds from 10 to 15 knots. A further seven vessels are recorded as having been built in the period to 2000. These are all relatively large vessels operating at Fr_L just high enough to gain an advantage from the hulls' wave-making interaction to have lower resistance.

Another issue that affects wave making is water depth. As water depth decreases, so too does the speed at which vessels will create the highest wave pattern before making the transition to "plane" on the surface. Clearly it is best if vessels can avoid this regime by moving either slower or quite a bit faster.

The water depth where most change takes place is where it is shallower than 30% of the craft waterline length. We will discuss this in our chapter on wave drag. For now, suffice it to note that in river and lake environments water depths in a range 5–10 m is not uncommon. The upshot is that craft really need to be designed to operate safely above minimum planing speed, which will normally be in the range Fr_L 0.6–0.75, depending on the exact hull configuration, or to stay below Fr_L 0.4 for vessels that are nonplaning or semiplaning configuration. This latter approach fits well with catamarans that are relatively fine in form (high L/B) and with optimized hull spacing for minimized wave-making drag at service speed. The early catamaran vessels built in Russia operated in this regime.

In 1975, a high-speed passenger catamaran was built to operate in the planing regime; the 47.7 m *Anatoly Uglovsky*. It had a 283-passenger carrying capacity and could travel at up to 45 km/h (30 knots) while powered by just 1200 kW (1800 shp) thanks to the minimized wave-making drag from the slender demihulls and optimized spacing. This vessel was the precursor to a series of passenger catamarans built for river service, though the shallow draft hydrofoils developed by Alexeyev [14] were built in more significant numbers from the 1960s to the 1980s and still operate in both Russia and Europe.

High-speed catamarans for coastal ferry services in the Soviet bloc began with ferries built in Poland in the 1970s and operated in the Black Sea, and later in the decade several Norwegian built Westamaran catamarans were operated on services in the White Sea, in the Black Sea around the Crimea, and in the Far East. Some details are presented in Appendix 1.

In the USA catamaran buildings for offshore operations began with a military vessel. The USS *Pigeon* (ASR-21) (Fig. 1.5). This was the first oceangoing catamaran designed and built for the US Navy. The ship was launched on August 13, 1969, at the Alabama Dry Dock and Shipbuilding Company. It was 251 feet long with an overall beam of 86 feet, and the well between the hulls was 34 feet wide. It was propelled by four diesel engines producing 6000 shp, giving a speed of 15 knots ($Fr_L = 0.29$).

This vessel doesn't really enter the high-speed range, the catamaran form being used to create a large deck platform and high stability. During subsequent decades, several US shipbuilders obtained licenses from fast catamaran designers in Australia and Europe so as to be able to deliver fast ferries for US continental service. The Jones Act prohibits any foreign-built hull from operating commercially within US waters. The licensing arrangements have proven successful for both designers and builders, as a steadily increasing number of fast ferries have been introduced into service in cities such as New York and San Francisco, as well as in the Seattle area.

The reader can probably ascertain from the narrative so far that while in Russia catamaran designs were tailored to the vessel's special needs at home, it was the Scandinavian shipyards (Norwegian and Swedish) that began to have success in exporting their vessels in the 1980s, followed shortly thereafter by Australian designers and yards. Following direct export, the next step was to license their designs to shipbuilders in the Far East and in the USA. This has been one of the strengths of the catamaran business, since exporting the technology to build hydrofoils or hovercraft proved very difficult. For hovercraft there has been some success exporting technology for military craft from the UK to the USA, while for the rest of the world each country involved has tended to develop its own designs. Hydrofoils have tended to be exported as finished products from Russia (protected water craft) and Italy (open seagoing craft).

Fast catamarans are now built in many shipyards around the world. Manufacturing costs limited Scandinavian yards to delivery of specialist vessels for home operations in the first decade of this century, while Australian catamaran designers now have their vessels built in the USA and China as well as at home and export ferries and utility craft on a global scale.

We have taken a quick walk through the development of catamarans, skating gently on the surface so to speak, but what about the motive power to propel catamarans at high speed?

Over the last couple of centuries humans have created mechanical machinery that can deliver the power needed to achieve almost any objective as far as transportation is concerned. Mechanical propulsion began with installations of steam engines and the paddle wheel prior to the screw propeller. Vessel service speeds rose from 8 to 10 knots, through the teens, and into the 20–30 knot range for some commercial vessels in the early part of the twentieth century. In this period it was only experimental, military, and racing craft that achieved speeds much above 20 knots. The introduction of diesel engines began to change that, and for some specialized vessels

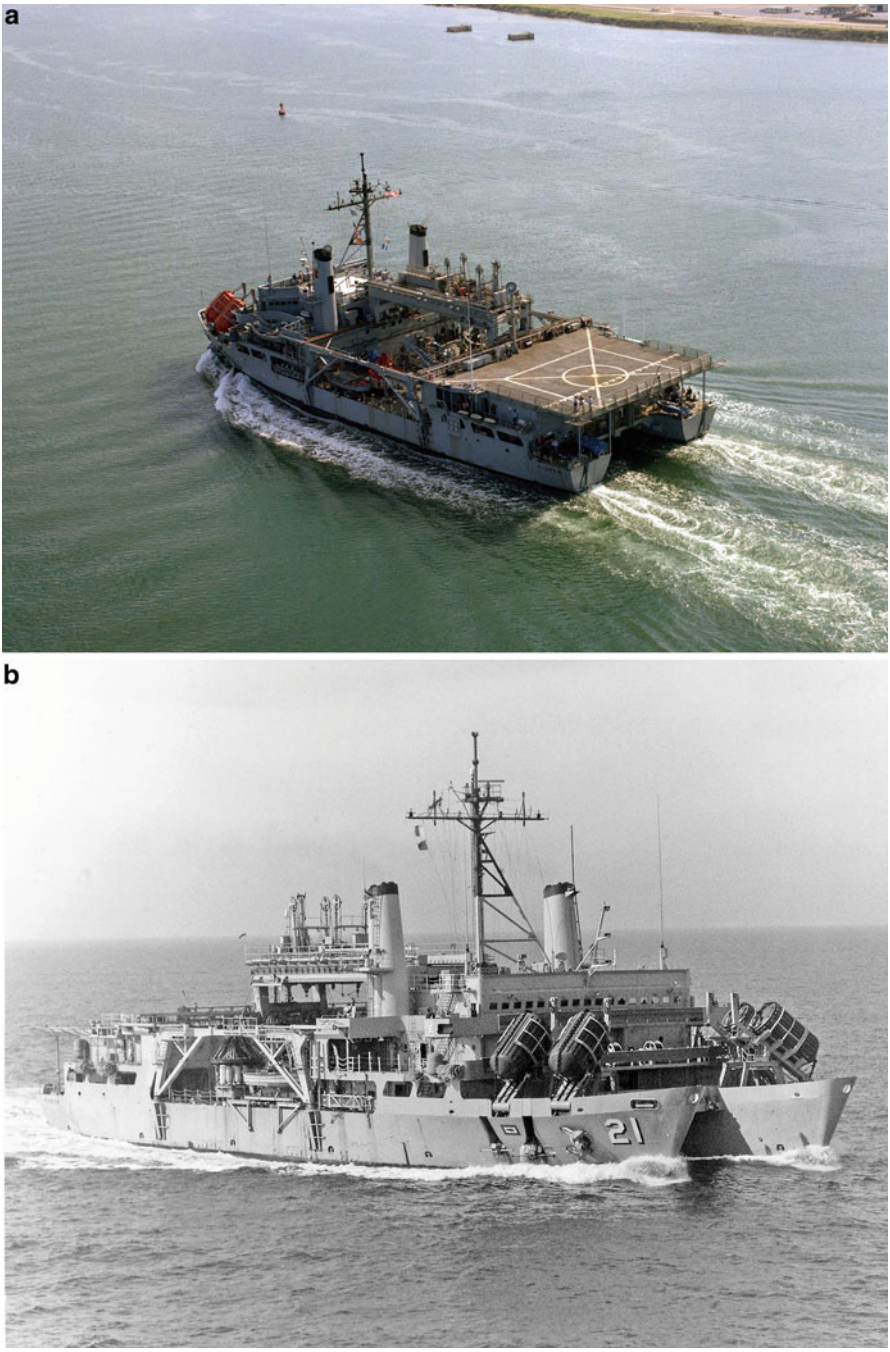

Fig. 1.5 (**a**) Stern view and (**b**) bow view USS *Pigeon* catamaran

gas turbine power began to be installed in the middle of the twentieth century following their development for aircraft propulsion in the 1940s and 1950s.

The development of high-speed commercial vessels, that is, the modern development of the monohull fast craft, can be traced to the Second World War. During that period the materials, engines, and equipment necessary for high-speed craft became available through advances made for aircraft and tanks, such as high-strength aluminum alloy for structures, high-speed diesel engines, and gas turbine power plants for propulsion, together with lightweight reduction gearboxes.

Using these advanced materials and engines, the service speed of monohull planing craft increased to as high as 50 knots during the Second World War, particularly for the torpedo and patrol boats operating at Fr_L 1.25–1.5. However, the impact or slamming load due to pitch and heave in a seaway is so large for monohull planing craft that it was necessary to reduce power in operation so as to reduce vessel speed to be able to maintain reasonable motions that are safe for both the crew and the hull structure. The high-speed potential could only be truly realized in calm conditions. This is not a major issue for military patrol craft, but for a ferry it is a major issue.

The 1950s and 1960s saw the introduction of hydrofoils to passenger ferry service in the Mediterranean and hovercraft on short routes in the UK. The hydrofoils were powered by high-speed diesels, whereas the hovercraft were powered by gas turbine engines modified from aircraft power plants.

Norway had a lot of coastal ferry routes and first noticed the hydrofoils being built in Italy for fast passenger service. The hydrofoils had some success, but they did have some reliability problems in service [15, 16], prompting Norwegian operators and shipbuilders to look for alternatives. The sidewall hovercraft was tried in Oslo fjords but did not attract operator customers on the west coast of Norway.

Commercial catamarans began to develop once high-speed diesel engines became available, with their lower specific weight (Kg/kW) and compact dimensions that could be fitted into a restricted hull space.

Westamarin in Norway started the trend toward catamarans with their designs of asymmetric hull passenger craft in the 1970s [15], following their supply of several hydrofoils built to Swiss Supramar design. The challenge was to achieve an economical service for passengers between the main cities of Norway's west coast, at a speed that could transport people within 3 to 4 h between the main coastal towns. With journeys of that distance, comfort was also a prime requirement.

If we look back for a moment at these competing vessel concepts [14], we can see that beginning in the 1960s and going through the 1990s hydrofoil craft and air cushion vehicles (ACVs), as well as surface effect ships (SESs), developed in parallel in this period with significant operational success. The key was the niche operation. For ACVs to be a success, a part of the route or service needed to be across shallow water where other craft would have a problem. Two locations where this applied were across the Solent between Portsmouth and Ryde in southern England and between Ramsgate in England and Calais in France.

The coastal hydrofoil started its successful development in Italy along the Mediterranean and Adriatic coasts, where deep-water quaysides were not a problem, and the high speed and efficiency meant ticket prices could be competitive with normal

slower ferries. This success spread to other parts of the Mediterranean and to Norway, until passenger demand increased, requiring higher-capacity vessels, hydrofoils being difficult to scale up significantly. The SES or sidewall hovercraft took up this market development challenge aiming at cars as well as passengers and had some success for passenger craft but did not make the breakthrough to passenger and car payloads.

The ACV ferry in the UK reached its zenith in the 1970s with the car and passenger SR.N4 hovercraft that was in service on several routes between England and France. The service speed of the SRN4 (Super 4) was as high as 70 knots – and more in calm conditions during its operation in Dover Strait – and was very successful in delivering a high-speed connection from England to France (quicker than Channel Tunnel journey times), until fuel and maintenance costs overtook it after three decades of service on October 1, 2000. The big challenge for the amphibious ACV are its air propulsion and the resultant noise profile. Ducted air propulsion reduces the noise problem and, together with high-speed diesel engines to minimize fuel costs, has enabled continued economic operations across the Solent for passengers. This was not practical as a development for craft the size of the SR. N4 to carry cars as well as passengers.

The hydrofoil craft built in the same period grew from craft carrying 50 to 100 passengers up to the 450-passenger level. The docking of a hydrofoil and the draft with its hydrofoils under the hull limited the concept to passengers and routes having deep water channels and quaysides for docking.

The SES appeared to have great potential in the early 1970s and was prototyped in the USA for a new high-speed "80-knot Navy." This concept was like a catamaran with an air cushion between the hulls contained by flexible seals at bow and stern [2, 14]. The small-scale test craft SES100B for the planned 3000-ton vessel reached a speed of 90.3 knots during trials. Under encouragement from the success of the test, a development plan for the 3KSES was established in 1974. Unfortunately, the Middle East fuel crisis that year caused a rethink at the US Department of Defense (DOD) and the program was closed down. That cutback affected the career of one of the authors, who was all set up to join one of the teams as part of a group of engineers from the UK when the program was canceled. In some ways it was fortunate because the technology required, though available in theory at that time, was really equivalent to attempting another space mission to the moon while using a tiny part of the budget in relative terms.

Commercial SESs offered a different opportunity, since for passenger service at least they were competitive with the hydrofoil and extended capacity to higher levels. In the 1970s, glass-reinforced plastic hull construction came of age for medium-sized vessels, including a series of monohull mine sweepers and hunters in the UK. Hovermarine, based in Southampton, England, successfully used this technology for its passenger SES for up to 350 passengers and competed with hydrofoils in Hong Kong and several other ferry routes worldwide. For short service routes the 30-knot craft, powered by high-speed diesels, was very economical.

Brødrene Aa in Norway extended this with a series of 30-m, 45-knot vessels aimed at the Norwegian coastal routes, beginning with a craft called the Norcat, also

powered by high-speed diesels [15]. While not becoming the workhorse of this area, the vessel series was successful commercially and has seen service in many parts of the world. The challenge for this large SES initially was the "cobblestone" vibration caused by the dynamics of the cushion in small choppy seas. This was solved by a controlled venting of air from the cushion. The other challenge was interaction of the air cushion and the propulsion system at the stern. In a seaway, the air cushion surface depression could cause air ventilation to the marine propellers, leading to a loss of thrust and cavitation damage to the propellers, increasing maintenance costs. Stainless-steel propellers improved service life compared to bronze propellers, and a change to water jets mounted inside the side hulls represented further improvements for the production vessels following the first-in-class Norcat. Nevertheless, both ventilation fences under the aft part of the hulls' inner wall toward the cushion and careful design of the intake were necessary to avoid ingesting cushion air.

There is a pattern here – technology and concept can push boundaries, as each of these craft types have done. The question, then, is whether operators are ready for the demands of the new technology, whether the challenge is maintenance, passenger or freight handling, or safe operations at higher speeds compared to previously. The solution of new technical problems tended to increase complexity, raising operation or maintenance complexity and costs. Then along comes a further concept that leaves these problems behind and allows the earlier concepts to maintain their presence only in special niches.

Why spend so much time on hovercraft, SES, and hydrofoils? you may ask. Well, these concepts proved the use of aero-derivative gas turbines, and then high-speed diesels in very high-speed craft, also in intensive service. SESs also put to the test a number of the design issues faced by fast catamarans, from structural design to integration of the propulsion system, with lightweight gearboxes and propulsor hull interaction, and devices to stabilize motion, particularly pitch.

The SES is a variation on the planing catamaran that uses a central air cushion to reduce the weight that the hulls must support. The concept uses a geometry for the hull lower surfaces that can operate efficiently in the planing region. If speed is reduced from the 45 knots of Norcat down to 25 to 30 knots, we are back in the semiplaning region that a hull shape adjusted from a displacement vessel can efficiently operate within. The designs of Westamarin in Mandal and Fjellstrand in Omastrand, Norway, were shaped on this basis. Initially Westamarin took the idea of splitting a single monohull longitudinally, and later both shipbuilders adopted the symmetric demihull form. In the 1980s the catamaran came of age and started to steal market share from the other high-speed concepts and to extend the envelope of application.

Since the water plane shape is the main influence on both wave-making resistance and seaworthiness, the distribution of the displacement of a catamaran hull in the vertical direction through the water plane is most important for its performance, operating both in calm water and a seaway. The world does not stand still, so once catamarans had proven practical to design for increasingly larger passenger ferries and that it could combine vehicle and passenger ferries, there began to develop hybrid designs using variations of the water plane and displacement distribution

such as the wave-piercing catamaran (WPC), the semi-SWATH, and the super slender twin hull (SSTH), all aimed at minimal motion in a seaway at high speed.

Modern high-speed catamarans have also adopted the use of stabilizer appendages using dynamic forces to steady motions at high speed. Instead of the trim tabs fitted to hydrofoil craft, catamarans typically have trimmable flaps fitted at the transoms or devices called interrupters that achieve the same objective with lower appendage drag, see [17, 18] and see under resources at the back of this book, under subsection stabilizers. At the bow a number of large catamarans have stabilizer foils suspended beneath the forefoot, and some smaller catamarans have foils across between the bows to dampen pitching.

So far, the classic catamaran with symmetric hulls and the wave-piercing concepts have been extrapolated to the greatest dimensions, which are able to take significant payloads of roll-on/roll-off trucks as well as cars. As size has increased, service speeds have risen to over 40 knots in some cases. Recently a wave-piercing catamaran ferry powered by liquid natural gas (LNG) fuel to its gas turbine engines was built for service in South America (Fig. 1.6).

The rapid development of microprocessors since the 1970s has enabled engine design to optimize fuel burn. Simultaneously improved material quality and manufacturing techniques have allowed increased compression ratios. The combination has delivered higher power, reduced dimensions and weights, and improved fuel efficiency. This applies to both diesel reciprocating engines and gas turbines.

The development of large catamaran ferry designs using alternative fuels will continue as environmental regulations are steadily tightened. Diesel engine

Fig. 1.6 LNG-powered wave-piercing catamaran *Francisco*

manufacturers are now rapidly optimizing gas-powered motors, used in both the marine and trucking markets. The challenge at present is building the distribution infrastructure of LNG for fueling, via bunkering stations for marine vessels. This is under way along the coast of Norway and much of Northern Europe at the time of writing. For the vessels themselves LNG also requires quite different tankage, influencing both compartmentation and design for safety on board.

For all these designs the targets remain:

- Reducing wave-making resistance through the use of high *L*/*B* ratio and slenderness for both demihulls so as to minimize required propulsion engine power output,
- Optimization of the distance between demihulls to minimize wave resistance at the design service speed to counter the larger longitudinal wetted surface of the twin hulls compared to a monohull,
- Minimizing pitching motions and slamming loads through slenderness and demihull forward entry geometry combined with active stabilizers,
- Optimizing vessel maneuverability using hull separation to minimize appendage size for propeller-driven vessels and simplify machinery installation where multiple water jets are sited in each hull by installing steering on one jet only.

1.3 High-Speed Catamaran Development

The core subject of this book are fast catamarans designed for commercial service. The market for this type of craft emerged in the 1970s, as described in the previous section, and designers and shipyards responded in a number of different parts of the world. In what follows, we summarize the developments for ferries in a number of countries and shipyards focusing on the period from the 1970s up to the end of the twentieth century as this was a formative period, beginning in Scandinavia where the modern era of the development of coastal passenger catamarans started. Since around 2000 the industry has become global, with designers and shipyards working together on ferries, utility vessels, military vessels, and, more recently, service vessels for wind farms and oil industry supply vessels. Links to Internet sites with data on some of these vessels are given in the resource section of this book as a starting point for investigation. Some vessels are used as examples in later chapters.

The vessel summary data below give an idea of how configurations have developed as the technology improved in the last part of the twentieth century and provides a reference point for designers. Ferries have continued to be built to greater capacity and speed in the last decade or so, while the trimaran form has matured, and both super slender vessels and SWATH/semi-SWATH configurations have been refined for ferry, military, and utility missions.

We consider a high-speed catamaran to be one with a service speed higher than 25 knots. The nondimensional speed (Fr_L) varies with size, as shown earlier in Table 1.1. The vessels we cover here operate mainly in the region $Fr_L = 0.4–1.0$, with exception of racing craft. The general arrangements of a selection of catamaran and trimaran vessels are shown in Appendix 3 for reference.

1.3.1 Development in Scandinavia

The two main shipyards developing high-speed catamarans in Norway were Westamarin AS and Fjellstrand Aluminium Yachts [14–16, 19], while in Sweden Marinteknik developed its own line of catamaran passenger ferries.

1.3.1.1 Westamarin AS

In 1970, Westamarin AS, located in Mandal close to the southern tip of Norway, developed a high-speed catamaran concept (the W86 series) characterized by the asymmetric transverse section of its demihulls. The W86 accommodated 167 passengers and was powered by two 1100-hp MTU diesel engines, achieving a maximum speed of 28 knots (Fig. 1.7a). Operations of the craft were successful, with the advantages of safety, passenger comfort, low fuel consumption, simple maintenance, and low operating cost, even in comparison to a monohull ferry.

Following successful operation of the Westamaran 86, the company produced a lengthened design based on the W86, the Westamaran 95, with significantly higher power – 3058 kW max rather than the 1956 kW in the W86. The passenger capacity rose from 176 to 205 passengers, and speed increased from 28 up to 31 knots (Fig. 1.7b). The subsequent W100 model had a top speed similar to that of the W86 while taking another 35 passengers and using engines that were similar to that of the W95.

Through the 1970s and the early 1980s, 19 W86 craft and 18 W95 were completed and delivered to various European shipping companies in Norway, Italy, Spain, Denmark, Holland, Sweden, France, and Yugoslavia. Up to 1985 the company also completed a number of other high-speed catamaran designs such as W88, W100, and W120. A total of 45 craft from W86 to W120 were built from 1971 to 1985. All of these craft used the asymmetric demihull, with the flat upright internal side to the hulls. Most of the craft were powered with water propellers, as this was before the water jet was fully developed, and so hull stern quarter lines were shaped differently. The leading particulars of the main Westamarin models are listed in Table 1.2.

Where:

K transport efficiency
S Space between internal sides of two demihulls at midsection in comparison to demihull beam, where *b* represents beam of a demihull at that position

Westamarin ceased building ferries in the late 1980s, while another company in the area, Båtservice, began to build catamaran ferries in glass reinforced plastic (GRP) and carbon-fiber-reinforced plastic. Båtservice has enjoyed steady success since the late 1980s, initially with passenger catamaran ferries and then building the Norwegian Navy SES fast patrol craft and the minehunter vessel fleet. More recently, while continuing with ferries when there is demand, they have moved into the wind farm service vessel market. An example of their catamaran ferries, the 35-m, 33-knot, 250-passenger Solifjell "carbon catamaran" operating out of Tromsø, is shown in the preceding Fig. 1.8. See resources for Båtservice's Web site and full vessel details.

Fig. 1.7 (**a**) Westamaran W86; (**b**) Westamaran W95

Table 1.2 Leading particulars of Westamaran high-speed catamarans

Type of craft	W86	W95	W100	W3700 SC
Length, overall (m)	22.7	29.2	31.7	36.5
Width, overall (m)	9.0	9.25	9.72	9.5
Draught (m)	1.2	1.4	1.7	1.47
Displacement, D (t)	54	74	~84	~120
Passengers	176	205	240	322
Speed, Vc (knots)	26	31	26	32
Vm (knots)	28	32	28	35
Engine output (kw)	2 × 809	2 × 1323	2 × 1323	2 × 2040
Propulsion	Propeller	Propeller	Propeller	Propeller
Demihull configuration	Asymmetric	Asymmetric	Asymmetric	Symmetric
$\mathrm{Fr_L} = v/\sqrt{gL}$	0.966	0.973	0.817	0.952
$\mathrm{Fr_d} = v/\sqrt{g\Delta^{1/3}}$	2.37	2.57	2.199	2.591
$\mathrm{Fr_d}$ (demihull)	2.67	2.88	2.468	2.908
$D/2/(0.1L)^3$(demihull)	2.308	1.486	1.318	1.234
$S = s/2b$	1.0	~1.0	~1.0	~2.0
$K = D$.Vm/102 N (kg.m/s/kW)	4.717	4.517	4.487	5.196
N/D (kW/t)	29.96	35.76	31.5	34.0
$N/(D.v)$ kW/ton.knot	1.07	1.12	1.125	0.97

Fig. 1.8 Båtservice catamaran in Tromsø

1.3.1.2 Fjellstrand Aluminium Yachts AS

Fjellstrand is the foremost shipyard in Norway that developed catamarans in the 1980s and 1990s other than Westamarin AS. The shipyard, located at Omastrand in Hardangerfjord, western Norway, has constructed over 400 vessels from its establishment in 1928 to the present; however, the development and construction of high-speed catamarans started in 1976. The shipyard continues to deliver specialist vessels but stopped production of its catamarans in the late 1990s.

In 1976 the company constructed its first high-speed catamaran named *Traena* for Helgeland Trafikkselskap AS shipping company as a passenger ferry craft. The craft accommodated 119 passengers and was constructed of weldable "marine-grade" aluminum alloy to minimize the hull structure weight. The craft was propelled by two MTU 12 V 493TY70 high-speed diesels driving open-water propellers to achieve a service speed of 26 knots. This craft had asymmetric demihulls with upright internal sides and a high tunnel between the demihulls so as to achieve good seaworthiness. After that first design, the company developed a 31.5 m high-speed catamaran for passenger service (Fig. 1.9a), continuing with asymmetric demihulls, a welded aluminum hull structure, and fixed pitch water propellers. Controllable pitch propellers were installed on later craft of the same type to improve maneuverability.

Since 1985, the company has developed several designs, including a larger 38.8-m catamaran to carry 400 passengers (Fig. 1.9b). The height of tunnel between demihulls was as high as 3 m, which improved seaworthiness compared with earlier craft. In addition, Fjellstrand moved to using symmetric cross-section demihulls. The leading particulars of these craft are listed in Table 1.3.

1.3.1.3 Marinteknik Verkstad AB of Sweden

The development of the high-speed catamaran in Sweden also made rapid progress in the 1980s. The main shipyard engaged in the development was Marinteknik Verksteds AB located in Oregrund.

In the period 1977–1978, Marinteknik designed a water-jet-propelled catamaran vessel named Jetcat. Vessel construction started in November 1979. The craft had a deep V form tapering to an almost zero deadrise aft and with a hard chine at the bow. The hull form had symmetric demihulls with two MTU 12V396TB83 diesel engines and KaMeWa water jet propulsors in each demihull. It was the first application in Sweden where a catamaran used water jet propulsion. The general arrangement for the 33-CPV is shown in Fig. 1.10a and a photo of Alilauro Giove Jet in Fig. 1.10b. It is still in service as of 2018. The designers attracted considerable interest in the new craft during the *International Conference and Exhibition on High Speed Surface Craft* held in Brighton, England, in June 1980 as a result of their innovations.

The midsection demihull profiles showing a Westamaran W86 asymmetric cross section and symmetric cross section of Marinteknik Jetkat respectively can be seen

Fig. 1.9 (**a**) Fjellstrand 31.5-m catamaran; (**b**) 38.8-m catamaran *Victoria Clipper*

in Fig. 1.10c. After the successful introduction of Jetcat, the company developed a series of catamarans in later years, such as JC-F1, PV2400, PV3100, and others. The leading particulars of Marinteknik craft are listed in Table 1.4.

Table 1.3 Leading particulars of Fjellstrand high-speed catamarans

Craft Type	Alamaran 165	31.5 m	38.8 m
Length overall (m)	25.67	31.5	38.8
Width overall (m)	9.28	9.4	9.4
Draught (m)	1.2	2.05	2.40
Speed (knots)	26	26.29	31.5
Passengers	194	292	390
Gross tonnage	197	314	399
Classification	DNV + 1 V2 (Norway)	DNV + 1 V2	DNV + 1 V2
Main engines	2 × MTU12V493TY70	2 × MTU16V396TB63	2 × MTU16V396TB83
Engine speed (rpm)	1400	1650	1650
Power of each (kw)	808.8	1308.8	1510
Propulsion	Water propeller	Water propeller	2 × water jet KaMeWa 63 S62/6
Hull material	Aluminum alloy	Aluminum alloy	Aluminum alloy

The PV2400 was launched in May 1984. This design used symmetric demihulls and a deep V transverse section forward and hard chine (almost rectangular) after section configuration. The craft hull was constructed in welded aluminum alloy that is resistant to saltwater corrosion.

The main engines were later changed from MTU12V396TB83 to MTU16VTB83 with 1540 kW power and 1940 rpm; then the craft was changed with a further conversion to PV3100 with two floors for passengers, cruising speed of 35 knots, and maximum speed of 38.5 knots.

The propulsion for the PV2400 was a pair of KaMeWa type 60/S62/6 water jet pumps with six-blade impellors in stainless steel, a controllable steering scoop, and reverse scoop for both maneuvering and backward motion.

1.3.2 Development in Australia

The key companies working on high-speed catamaran development in Australia are International Catamaran Pty. Ltd. (Incat) and Austal Catamaran Pty. Ltd. (Austal). Incat started on the development of high-speed catamarans in the late 1970s and was the instigator of WPCs. This type of catamaran has a very slender bow form so that the hulls cut through waves rather than ride over them. The development of WPCs will be introduced in Chap. 6. Austal developed its designs independently and uses more traditional forward lines and bow. Both companies have progressed from small passenger ferry craft up to large vehicle and passenger open-sea ferries and military derivatives of these large vessels.

1.3.2.1 Incat

In September 1979, the company completed its first catamaran, the *Jeremiah Ryan*; it was 18 m long, seated 88, and moved at a maximum speed of 26 knots. The craft had a steel hull structure. The company designed and built three more catamarans, called

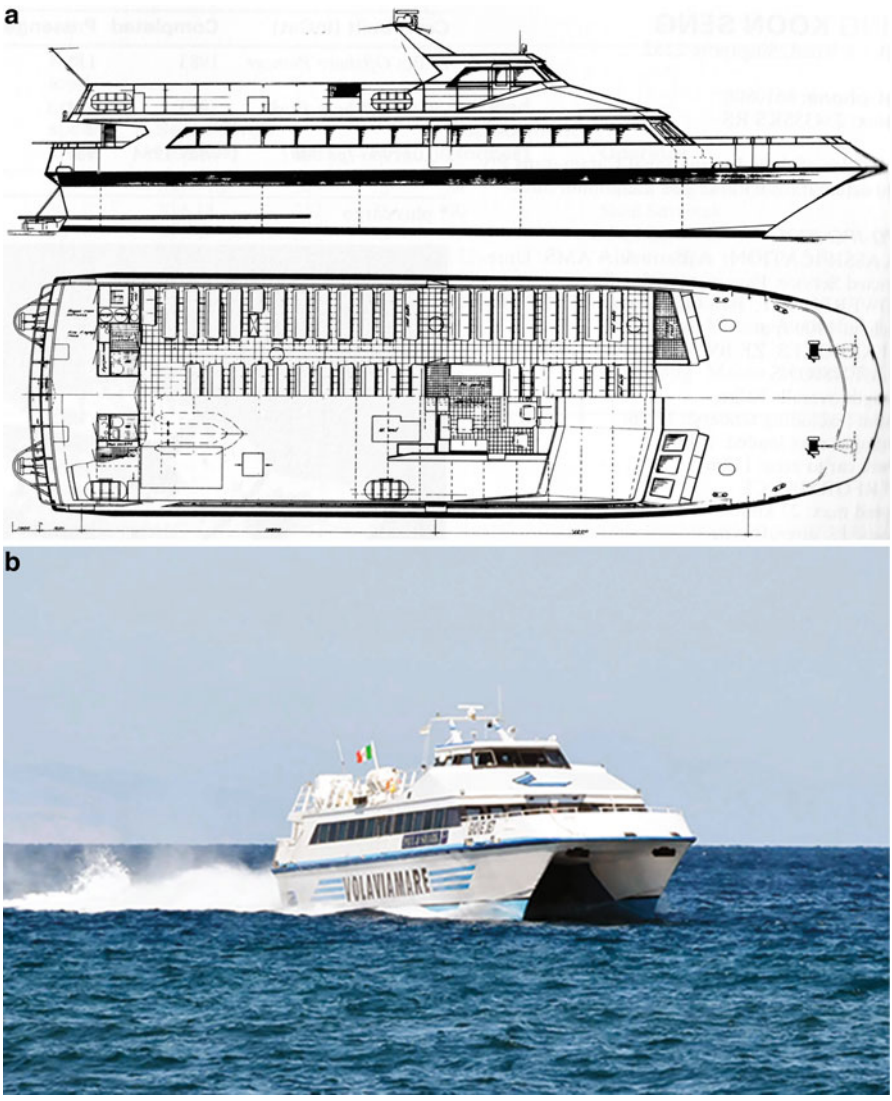

Fig. 1.10 (**a**) Marinteknik Marinjet 33CPV arrangement; (**b**) Giove Jet; (**c**) hull cross-section comparison

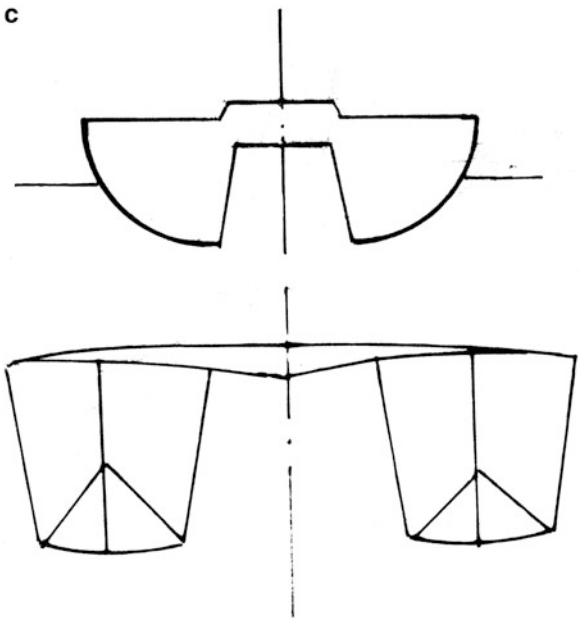

Fig. 1.10 (continued)

Jane Kelly (18 m, 28 knots service speed), *Tiger Lily I* (18 m LOA, speed 22 knots) (Fig. 1.11a), and *Tiger Lily II* (19 m LOA, speed 22 knots). The hulls of all three craft were made of steel, and the super structure was made of aluminum alloy, accommodating 100–150 passengers.

The development of aluminum-hull catamarans in the company started in the early 1980s from a coastal ferry boat named the *Fitzroy* (Fig. 1.11b). The 28-knot craft, with 170 seats, was powered by two 500-hp GM diesel engines and was completed in June 1981. The demihull had symmetric form and deep V lines to fit with rough seas. According to trial reports, the craft could maintain up to 23 knots even in rough seas with waves up to 2 m or more.

The company development of WPCs started with a trial boat called *Little Devil* (Fig. 1.11b). From 1979 to 1985, the company built 20 catamarans for delivery to China, New Zealand, Singapore, and Australia, including designs of 20, 21, 22, 26, and 29 m. Four of the 21-m craft were made in 1982–1983 for Chinese Hong-Macau Shipping Company and were named *Ming Zhu Lake*, *Yin Zhou Lake*, *Liu Hua Lake*, and *Li Jiang Lake*. All of these craft were operated between Hong Kong, Macao, and mainland China. They were constructed in welded marine-grade aluminum alloy, both for hull structure and superstructures, using longitudinal structural frames, a symmetric demihull configuration, water jet propulsion with five-blade impellors 0.8 m in diameter, and Italian engines from Isotta rated 750 hp at 1850 rpm (Fig. 1.9). The leading particulars of these craft are listed in Table 1.5 below.

Table 1.4 Leading particulars of Marinteknik high-speed catamarans

Name	JC-F1	33 CPV	Marinjet 41 CPV SD
Type of craft	Passenger transport	Passenger transport	Passenger transport
Length overall (m)	29.95	33.0	41.5
Width overall (m)	9.4	9.4	11.0
Draught (m)	1.23	1.2	1.2
Hull material	Aluminum alloy	Aluminum alloy	Aluminum alloy
Classification	DNV + 1A2	DNV + 1 V2	DNV + 1A1 R25 light craft EO
Passengers	215	218–276	306
Payload (t)	23	20.5	40
Speed at full payload	30	32	38
Max. speed (knots)	32	35	42
Main engines	2 × MTU12V396TB83	2 × MTU12V396TB83	2 × MTU16V396TB84
Revolution of engine	1900	1940	1940
Power for each (kw)	1180	1180	1945
Fuel consumption (L/h)	581	581	968
Fuel tank volume (L)	7000	7000	10,000
Water tank volume (L)	500	500	1000
Range (NMI)	350	380	275
Propulsion waterjets	2 × water jet	2 × KaMeWa 60/S62/6	2 × MJP650
Auxiliary engine (kw)	24	38	2 × 38
Reduction ratio for main engine	2.025:1	2.02:1	2:1

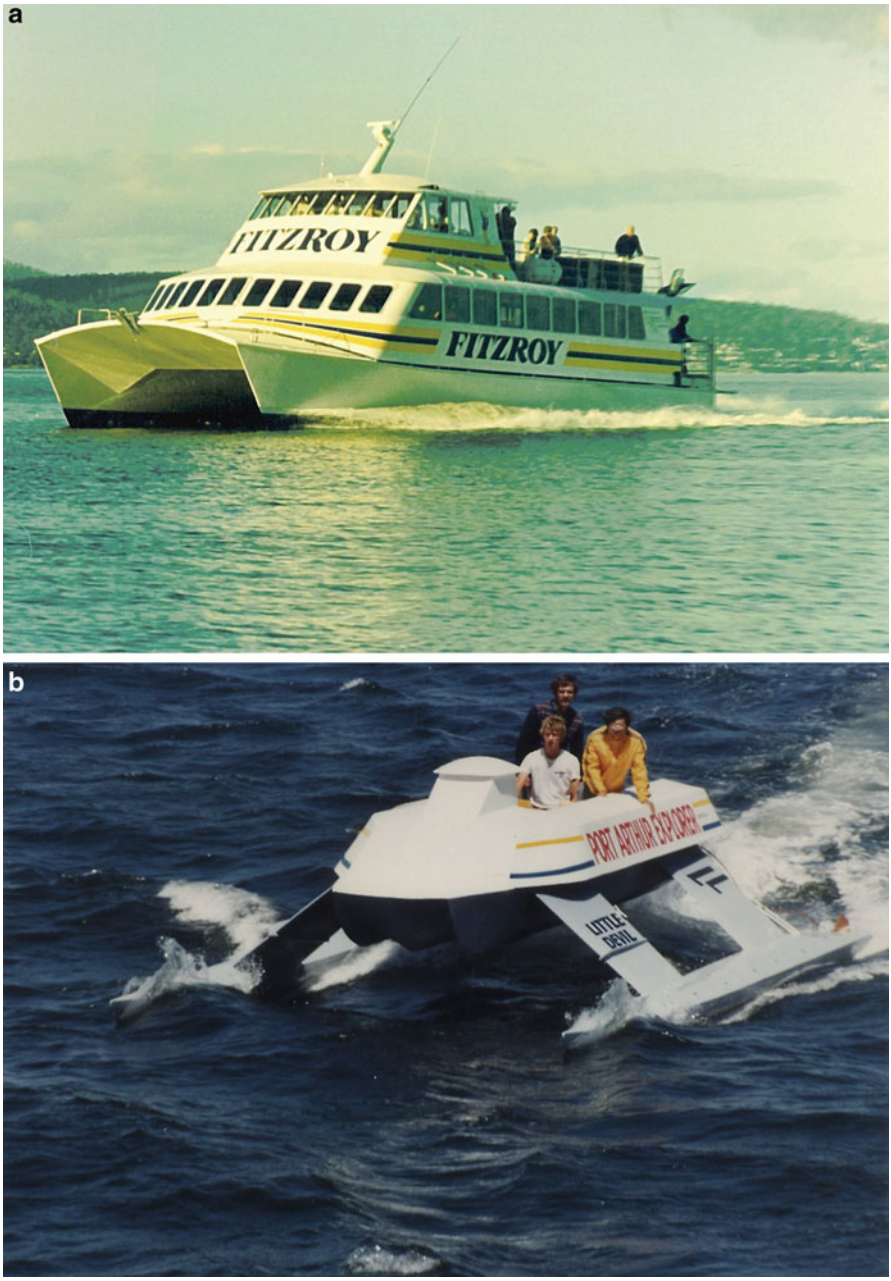

Fig. 1.11 (**a**) 24-m catamaran *Fitzroy*; (**b**) trials wave piercer *Little Devil*

Table 1.5 Leading particulars of high-speed catamarans from International Catamaran Pty Ltd, Australia

Craft type	20 m	21 m	22 m	26 m	29 m
Length overall (m)	20.5	21.9	23	26.14	29.2
Water line length (m)	18.5	19.5	19.5	23.5	25.5
Demihull length (m)	19.9	21.5	21.8	25.6	28.0
Width overall (m)	8.2	8.7	8.7	9.5	11.5
Draft, d (m)	1.5	1.6	1.7	2.2	1.76
Hull depth, T (m)	2.4	2.7	2.71	3.57	2.8
Passengers	100	150	212	400	245
Full displacement (t)	48	48	55	82	93
Dwt (t)	14.25	20.17	22.1	33.2	27.03
Trial speed (knots)	28	29	29	31	29
Service speed (knots)	24	25	25	28	26
Main engine type	GM8V92TI	ID36SS8V	GM12V92TA	GM16V92TA	GM16V92TA
Set	Two	Two	Two	Two	Two
Power (kw)	2 × 367.6	2 × 551.47	2 × 588.2	2 × 985	2 × 882.3
Propulsion type	Water propeller	Water propeller	Water propeller	Water propeller	Water propeller
Demihull shape	Symmetric	Symetric	Symmetric	Symmetric	Symmetric
Seaworthiness	Coastal zone III, wind scale 5, sea state 4	Coastal zone III, wind scale 5, sea state 4	Coastal zone III, wind scale 5, sea state 4	Coastal zone III, wind scale 5, sea state 4	Coastal zone III, wind scale 5, sea state 4

Incat has continued its development from these early craft to work with wave-piercing hull designs in the 1980s based on the success of trials with *Little Devil* and moved to larger sizes with LOAs of 60–120 m capable of transporting significant car and truck payloads as well as passengers. Incat was the pioneer in this hull concept. We develop this further in Chap. 8, where we look at the design of WPCs.

1.3.2.2 Austal

Austal began its development of fast multihull craft from a background of boat- and shipbuilding for the Australian Navy and monohull ferries. Like Incat, its track record progressed through smaller catamarans in the 1980s as the market gained pace. In January 1993, the company won an AUS$21 million contract to build three 40-m catamarans for owners in China. By the early 2000s the company had sold 13 of this vessel type at a total value of AUS$91 million to Yuet Hing Marine Supplies of Hong Kong acting on behalf of Chinese buyers and 35 craft in total to Chinese operators. Example catamarans delivered by Austal in the 1990s are listed in Table 1.6.

Since 2000 Austal has designed and built successively larger catamaran craft and supplied craft to the US Marines and Navy. Its designs include fine-bow-form catamarans that have wave-piercing qualities and have continued with the development of the trimaran form for vessels in a LOA range of 100–120 m. Examples of recent catamarans and a trimaran are shown in Fig. 1.12.

Table 1.6 Austal's early catamaran deliveries

Craft name	*Bali Hai*	*Tong Zhou*	*Flying Dolphin 2000*
Buyer	China	China	Greek
Length, overall (m)	33.6	38.0	47.6
Length, water line (m)	30.7	32.4	43.5
Beam (m)	10.8	11.8	13.6
Draft (m)	1.95	1.3	1.4
Depth (m)	3.5	3.6	3.5
Passengers	301	430	516
Hull materials	Aluminum	Aluminum	Aluminum
Diesel engines	2 × MAN 2842LTE 735 kW at 2300 rpm	2 × MY 16 V396 TB83 1470 kW at 1940 rpm	4 × MTU16V 4000 M70 2320 kW
Propulsion	2 × propellers	2 × MJP J650R water jet	Kamewa 71 SII water jets
Speed (knots)	22	30	42
Classification	DNV	DNV	DNV
Delivered date	March 1990	November 1990	June 1998

Fig. 1.12 (**a**) Austal catamaran *Steigtind*; (**b**) *Shinas* arriving Oman; (**c**) Austal trimaran *Benchijigua*

Fig. 1.13 Mitsui Supermaran CP30 MKIII

1.3.3 Development in Other Countries

1.3.3.1 Japan

Under a licensing agreement concluded in 1973 with Westamarin AS, Mitsui built three super Westamaran CP20s. The craft, which carried up to 182 passengers, had a cruising speed of about 25 knots, comparable to the W86, and operated in waves up to 1.5 m high.

In 1978 Mitsui, employing its own design team, developed the Supermaran CP20HF, seating 195 passengers with a cruising speed of 30 knots. The craft was redesigned for improved seaworthiness and operated in a maximum wave height of 2.5 m. This was followed by two 280-seat Supermaran CP30 MKIIIs that entered service in 1987 (Fig. 1.13). Japan has also focused on the development of the SWATH, a concept that will be introduced in later chapters.

The leading particulars of Mitsui craft can be found in Table 1.7 below.

1.3.3.2 United States of America

The USA has been involved in the development of high-speed catamarans for oceanographic surveys, tourist excursions, fishing services, and, more recently, passenger transportation, for example.

Research and development accelerated in the 1960s and 1970s and grew with the development of SWATH owing to its excellent seaworthiness for military and research missions. A sample of catamarans designed in the USA in the 1970s can be found in Table 1.8.

Since that time, a number of US shipbuilders have teamed up with designers such as Incat and Austal to prepare designs that could be built in the USA. This has resulted in a significant number of passenger ferry catamarans delivered for

Table 1.7 Leading particulars of Mitsui CP series high-speed catamarans, Japan

Craft type	CP20	CP20HF	CP30 MKIII
Length overall (m)	26.46	32.8	40.9
Width overall (m)	8.8	9.2	10.8
Draught (m)	1.18	1.2	1.37
Passengers	182	195	280
Cruising speed (knots)	25	30	28.1
Max. speed (knots)	28.5	30.7	31.1
Main engine power (kW)	2 × 911MTU 12V331TC82	2 × 1867 Fuji Pielstick 16PA4V185-VG	2 × 1867 Fuji Pielstick 16PA4V185-VG
Gross registered tonnage (t)	192	275	283
Propulsion type	Water propeller	Water propeller	Water propeller
Demihull profile	Asymmetric	Asymmetric	Asymmetric

operation in coastal cities such as New York, Seattle, and San Francisco and the development of catamarans and trimarans for the new US Navy Missions, Expeditionary Fast Transport, and Littoral Combat Ship in the first decade of the twenty-first century. The vessel fleets based on these designs will be progressively delivered through the second decade (Fig. 1.15a and b).

1.3.3.3 China

China has been involved with catamaran design for ferry service since the 1970s. The technology available within China in these early years was not competitive with that available outside the country, so it took a considerable amount of time for China's designers and shipbuilders to catch up with those of other countries. China has a large market for passenger water transportation for the following reasons:

- Large population (about 1.3 billion);
- Extended coastline 18,000 km long
- Very large inland waterway system that includes the Yangtze River system through Central China, the Pearl River system in the South, and He Long Jiang River system in Northern China;
- A number of straits between large population centers and important economic zones, such as the Taiwan Strait between mainland China and Taiwan, Bo Hai Strait between San Dong province and Liao Ni province.

In the 1980s and 1990s, high-speed passenger services were developed between Hong Kong and Macau, with departures as frequently as once every 10 min, and from Hong Kong to Kwang-Dong province on the mainland once every 15 min.

Table 1.8 Leading particulars of high-speed catamarans in the USA

Vessel name	*Johnson*	*Shuman* (Fig. 1.14)	*Double Eagle*	*Double Eagle II*	*Rainbow II*	*H & M Speed Twin*
Service	Survey	Survey	Party fishing	Party fishing	Party fishing	Party fishing
Owner	USCE Detroit	USEC Philadelphia	Gilmore	Gilmore	Harold Hayes	H & M
Builder	Marinette	Grafton	Mills	Mills	Breaux	Sermons
Designer	MacLear & Harris	Bond/Grafton	Bond	Bond	Breaux	Bond
Construction	Aluminum	Aluminum	Plywood	Plywood	Aluminum	Aluminum
Demihull form	Semicircular	V	V	V	Concave V	V
Year built	Rebuilt 1970	1970	1967	1969	1970	1970
LOA (m)	15.24	19.8	19.8	19.8	21	19.8
L_{WL} (L) (m)	13.4	18.29	18.29	17.83	18.9	18.29
Width (W) (m)	5.51	7.92	7.92	7.92	7.92	7.92
Demihull beam, b (m)	1.52	2.74	2.74	2.74	3.05	2.74
$(W–2B)/L$	0.184	0.133	0.133	0.137	0.145	0.133
Displacement (t)	21.04	36.3	29.5	28.36	37.5	40.9
SHP	549	1020	640	800	800	800
V, reported knots	16.4	24.2	21.2	23.4	20.8	24
Fr_L	0.73	0.93	0.82	0.91	0.79	0.77
C_b	n/a	0.43	0.363	0.0.408	0.347	0.431
C_m	n/a	0.571	0.49	0.53	0.518	0.557
C_p	n/a	0.573	0.741	0.769	0.67	0.771
Cwp	n/a	0.85	0.835	0.849	0.816	0.845
L/b	8.81	6.67	6.67	6.50	6.2	6.67

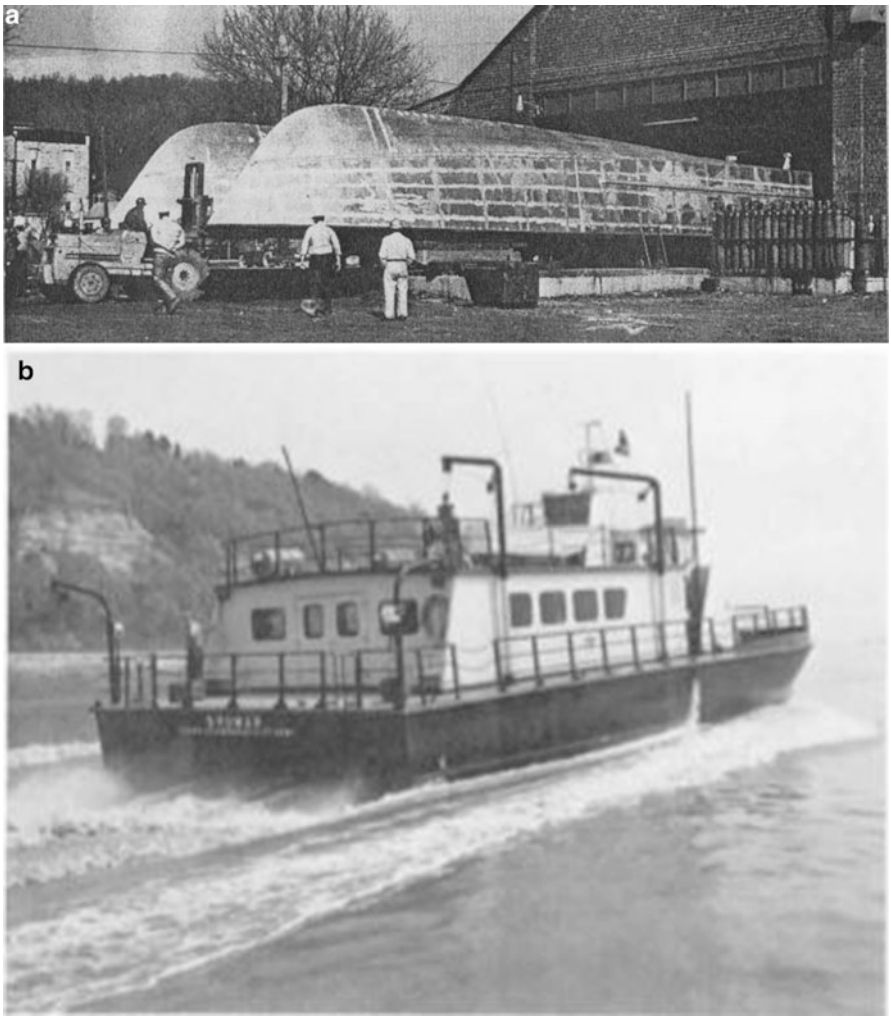

Fig. 1.14 US catamaran ferry *Shuman*: (**a**) hull construction; (**b**) under way

Passenger statistics suggest that approximately 140 million person-trips were made by these ferries every year in the 1990s. Among them, about 7.80 million person-trips were in the Pearl River Delta area between Hong Kong–Macau and mainland China up to Guanghzou. Most such routes are served by high-speed marine craft, including high-speed catamarans. Passenger transport in the Pearl River Delta area is one of the largest and most focused markets of this kind globally, with the inhabitants of the area finding marine transportation more efficient than alternatives using a combination of ferry, rail, and road due to its complex geography.

Fig. 1.15 (**a**) US military catamaran JHSV-1 on trials; (**b**) US military trimaran LCS-2 USS *Independence* at speed

In the 1990s there were about 900 high-speed craft operating worldwide, and about one-third of them were in China, many operating around Hong Kong in the Pearl River Delta. This holds true to this day. The majority of these craft are high-speed catamarans. According to statistics from Ref. [19], the distribution of high-speed craft operating in 1994–1995 in China (not including Hong Kong District) was as follows:

- Total number of high-speed craft of all types operating in China: 155;
- 89 craft were in service in the Pearl River Delta area, including the Mainland China–Hong Kong route, 37 craft on Yangtze and East Sea coastal routes, 16 on the Yellow River, and 13 on the He-Long Jiang River;
- Of the total, 48 craft were constructed in China and 107 craft were from abroad, that is, approximately two-thirds were imported;
- Almost 64% (65 craft) of imported craft were high-speed catamarans, among them, 35 craft were imported from Australia (International Catamaran, Austal), 4 from Sweden (Marinteknik), 4 from Japan (Mitsui CP series), 16 from Norway (Westamarin, Fjellstrand), 4 from Singapore, and 2 from Thailand.

If the catamarans operated by Hong Kong companies are included, perhaps more than 100 high-speed catamarans were operated in China in that period, making it the largest passenger catamaran market in the world. This has created a lot of experience in the operation of high-speed catamarans in these waters, even though most craft were imported rather than from domestic designers and shipyards.

AFAI Southern Shipyard (Panyu) Ltd. in China cooperated with Advanced Marine Design Corporation (AMD) of Australia to construct a fast catamaran passenger-car ferry ship in China in 2000 [14]. The vessel, designated K50, is one of the largest aluminum ferries built in China so far (Fig. 1.16).

The leading particulars of AFAI K50 craft are as follows:

Ship type	K50 high-speed catamaran
Length overall (m)	80.10
Length waterline (m)	72.3
Width overall (m)	19.00
Draft (m)	2.2
Passengers	400–450
Cars	89
Engines	4 Ruston16VRK270
Power (MCR)	5500 kw for each at 1000 rpm
Propulsion	4 KaMeWa 80II water jet propulsion units
Hull material	Welded anticorrosion aluminum alloy type 5083 H116
Range (nautical miles)	220
Speed (knots)	47.8 (full load, 100% MCR of main engines)
	50.10 (light load, 100% MCR of main engines)
Classification	Det Norske Veritas, Norway

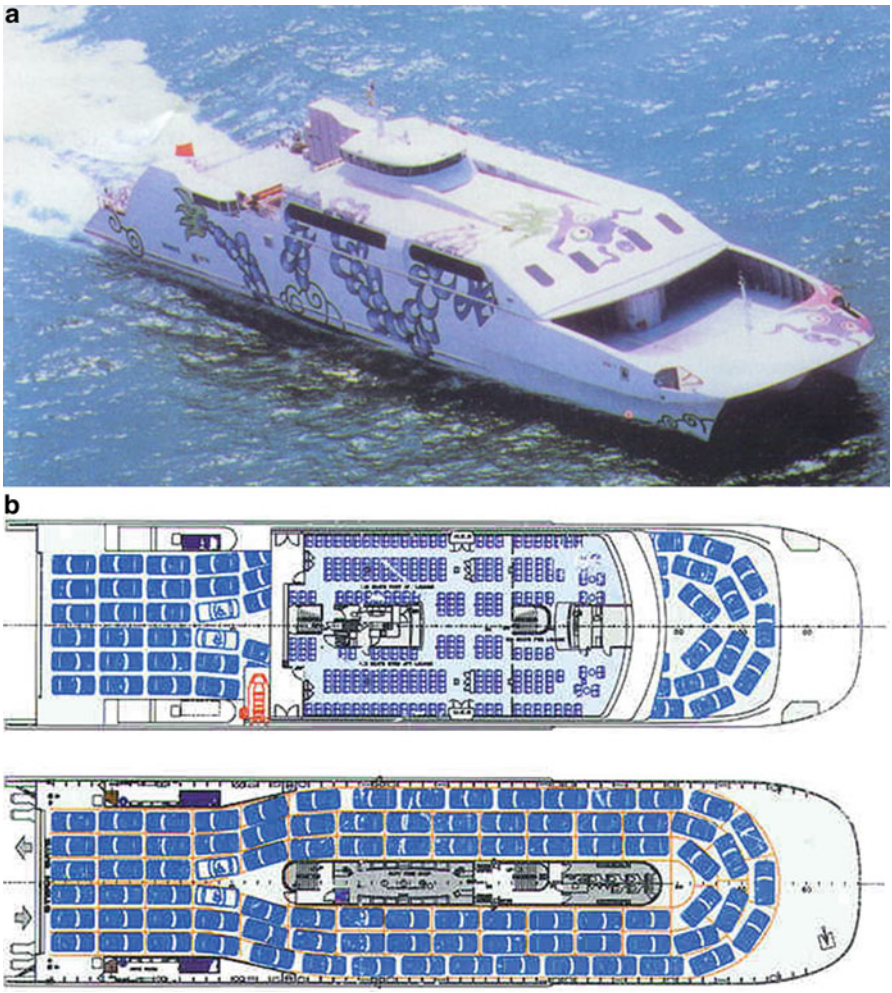

Fig. 1.16 AFAI K50 catamaran: (**a**) photo; (**b**) deck layouts

Flexible mounts between the hull and superstructure were installed to minimize vibration and noise, so that the passenger cabins experience a low ambient noise level of 65 dBA. One hydraulically operated trim regulating tab hinged at the stern end of each hull adjusts the ferry's pitch trimming at sea and gives high motion stability for passengers and crew.

1.4 Recent Developments

In this chapter we have provided some key data for vessels built by the main designers and shipyards as they built the market in the 1980s. Appendix 1 contains a table with details of the even earlier historical development of the market. Data for a sample of larger passenger/vehicle ferries built in the mid-1990s at the peak construction period are shown in Chap. 8, Table 8.4. In Appendix 3 we present a selection of more recent vessel general arrangements and summary technical data covering the range of commercial applications and types.

While Brødrene Aa and Båtservice in Norway have enjoyed continued success with their vessels built in fiber-reinforced plastic for passenger ferries since the 1990s, primarily for the home market, other parts of the world have seen a gradual development of construction capability for vessels up to 120 m in length so far, mainly in aluminum. The largest vessels have continued to be built in Australia by Incat and Austal as they developed their design range in excess of 100 m LOA. There has been a growing group of specialist design houses in Australia, the UK, Holland, and, in the last decade, also in the USA (see resources). They all work with a range of shipbuilders to deliver for operators in the most cost-effective manner. The spread of design experience, through companies associated with those having experience in Europe or Australia, has allowed a significant group of boat builders in the USA to begin building passenger catamaran ferries for operation around New York, San Francisco, and Seattle, for example.

In China also, a number of shipyards have partnered with the same design houses to build catamaran ferries operated around Hong Kong and up to Guangzhou and, more recently, ferries for service between Shanghai and neighboring towns in the Yangtze River estuary. At the time of completing this book (2018), the market for new passenger ferries seems to be very active. At the same time, catamaran ferries built in the 1990s are still in service, transferred from earlier service in Norway and the Channel between England and France to other routes, perhaps with less demanding environments. This is in contrast to other fast ferry craft such as hovercraft or hydrofoils, which seem mostly to be scrapped after their primary deployment.

Figure 1.17 below shows a plot of the aggregate production of catamaran ferries since 1971, including passenger vessels, and both small and large passenger/vehicle ferries. It can be seen that vehicle ferry production took off in 1990 and was significant until 2010; since that time, orders have slowed down. Smaller passenger-only ferry construction has been steady between the 20 and 40 mark and in the last year or so has seen a resurgence as those vessels' popularity for coastal city urban transit has increased.

Two points to note in relation to this plot are that data from locations such as China are still not easy to confirm, so the figure is conservative. Additionally, they do not include utility vessels such as offshore supply vessels, wind farm vessels, or paramilitary or military vessels. Each of these areas is in the process of maturing as market segments for multihull producers.

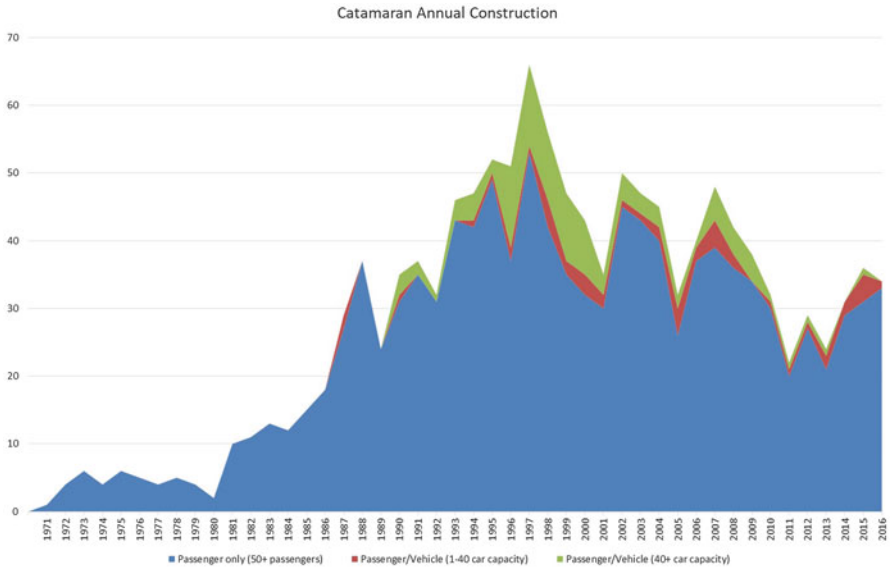

Fig. 1.17 Catamaran ferry annual construction, 1971–2017

The market for wind farm service vessels has matured since the early 2000s and is now substantial, though mostly for small vessels in a range of 20 to 30 m. These vessels face a significant design challenge because offshore transfer needs to be as fast as possible, and then while on site the vessel docking and motions at zero speed need to be as smooth as possible. By their nature, wind farms are in exposed locations, so the seaway is constantly disturbed. Various configurations have been built so far, including more traditional looking catamarans and SWATH and a trimaran SWATH, in an attempt to meet all needs. Add to that the fact such vessels need to transport significant cargo sometimes to be lifted to a turbine by crane for equipment change-outs, and you have a very interesting challenge for a naval architect!

Another development that is gathering pace in the second decade of this century is study of and experimentation with electrical power. One study for San Francisco has shown that it is possible to design a completely electric passenger fast catamaran ferry. Its economy would be controlled by the efficiency and cost of batteries.

This is similar to the technical trajectory for cars and trucks. It may take a while before it is realistic for the larger Ro/Pax fast catamarans, but Incat has already shown that it is possible to design a large catamaran running on LNG (99 m vessel *Francisco* for Buquebus in Argentina/Uruguay) that will comply with the environmental legislation expected to be implemented by the mid-2020s.

1.5 Moving On

In this chapter we have introduced the concept of a catamaran ferry and its development up to and through the recent build-up of a major market in catamaran ferries worldwide. So far we have said little about how the basic configuration is chosen and designs developed, other than to draw attention to the asymmetric or symmetric hull forms, highlight the difference between planing and semi-displacement hull forms, and note that the catamaran has high transverse stability. It may be useful to note that early catamaran ferries from Westamarin and Fjellstrand had a demihull *L*/*b* of 8 to 10, and this progressed to about 13 for the 38.8-m Fjellstrand slender catamaran. It was in Australia that wider spacing was first adopted, and a wave-piercing form was developed and refined as vessel size gradually increased to supply operator demand. The superslender configuration has now been adopted both at the smaller end for river and estuary passenger craft and the larger Ro/Pax ferries, with *L*/*b* in the 17 to 20 region.

If a designer wishes to develop a fast catamaran, there are a number of steps to follow, and we cover these in sequence in the next six chapters. These are general for all catamaran configurations and can be extended to the trimaran concept. Hybrid concepts nevertheless require a little different consideration if they are to be optimized, so we include specific chapters on the WPC, the SWATH, and the other hybrid concepts in separate chapters.

Our treatment of outfitting, hull structures, and other specialist ancillaries is at a summary level, as this text is targeted at the fundamental vessel form and project definition and control such as a managing naval architect would need to apply. We provide guidance on the initial estimation of weights, volumes, and configuration and make reference to texts that should give the reader a starting point to investigate these subjects in more depth. A number of consulting companies specialize in subjects such as internal outfit, so one could approach them to assist rather than building internal competence in a specialized area. The key for a naval architect is to have an understanding of the potential configuration sufficient to maintain a controlled, detailed design process and installation by the appropriate specialist and to ensure compliance with national and IMO safety requirements.

We begin with a discussion on the selection of the initial vessel configuration and follow this with a chapter on vessel static stability and fulfilment of statutory requirements such as IMO [20].

References

1. Dubrovski V, Lyakhovitsky AA (2001) Multi-hull ships. Backbone Publishing Company, Fair Lawn, ISBN 978-0964431126, p 495
2. Faltinsen OM (2005) Hydrodynamics of high-speed marine vehicles. Cambridge University Press, Cambridge, ISBN 978-0-521-84568-7, p 451

3. Principles of naval architecture, revised edition 1967, Society of Naval Architects and Marine Engineers, New York
4. Biran AB (2003) Ship hydrostatics and stability. Butterworth Heinemann, Oxford, UK, ISBN 978-0-7506-4988-9. (BH is an impression of Elsevier, ref Elsevier.com)
5. Munro-Smith R (1965) Naval architecture for merchant navy officers (engineers and navigators). Ernest Benn Ltd, London (before ISBN)
6. Presles D, Paulet D (2005) Architecture Navale, Connaissance et pratique. Editions de la Villette, ISBN 2-915456-14-3. (info at www.paris-lavillette.archi.fr)
7. Doutreleau Y, Laurens JM, Jodet L (2011) Resistance et propulsion du navire (resistance and propulsion of ships – French text). Technosup ENSTA Bretagne, Paris, ISBN 978-2-7298-6490-3
8. Lavery B (2010) Ship, 5000 years of maritime adventure. Dorling Kindersley/The National Maritime Museum 2004, London, ISBN 978-1-4053-5336-6
9. Johnstone P (1980) The sea-craft of prehistory, Chapter 15, the pacific, pages 200 2018, Routledge & Kegan Paul, London, ISBN 0-7100-0500-8
10. America's Cup catamarans – Wiki link – https://en.wikipedia.org/wiki/AC72
11. Sir William Petty catamaran (1662) at http://www.iwhistory.org.uk/RM/catamarandesign/
12. Sir William Froude at http://en.wikipedia.org/wiki/Froude_number
13. American merchant ships and sailors, by Willis J Abbott, illustrated by Ray Brown, Project Gutenberg (http://www.gutenberg.org/)
14. Bliault A, Yun L (2010) High performance marine vessels. Springer, London, ISBN 978-1-4614-0868-0
15. Foss B (1989) Hurtigbåten – Gammeldamens arvtager. Nordvest Forlag, Ålesund, ISBN 82-90330-464
16. Bakka Jr D (2005) Selskabe – Det Stavangerske Dampskibsselskab 50 år, 1855–2005. Omega Trykk as, Stavanger, p 248, ISBN 82-303-0571-4
17. Cave WL, Cusanelli DS (1993) Effect of stern flaps on powering performance of the FFG-7 Class. SNAME Marine Technology 30-1:39–50. ISSN 0025-3316
18. De Luca F, Pensa C (2012) Experimental Investigation on Conventional and Unconventional Interceptors. Int J Small Craft Technol Trans RINA 154:65–72. Part B2, ISSN 0035-8967
19. Jane's high speed marine craft, annual, issues from 1974 through 1993, Jane's Information Group, Coulsdon, ISBN 0-7106-0903-5
20. IMO (2000) International code of safety for high speed craft, publication IA-185E, ISBN 92789 28014 2402. Amendments and resolutions after 2000 are available on IMO website IMO.org

Chapter 2
Initial Assessment

Chapter 1 introduced the reader to the high-speed multihull concept and presented data on some craft that have been built, mostly to provide a historical perspective. For a designer the first step in the design process is to take a look at recent craft that have been built and their form features to compare them with their own ideas.

A designer in a naval architecture firm or at a shipyard may also have data from the yard or firm's earlier vessels to start with. It is always worth taking a look at competitors though! From there it is possible to make a first pass at the desired dimensions and form and start static calculations.

In this chapter we will look at data at our disposal so as to provide examples. We recommend that readers take a look at the websites of the major builders of catamarans and multihulls or perhaps refer to *Jane's High-Speed Marine Transportation* [1] to see the latest information. This may also be the best starting place for university students or independent designers. Check this against some of the plots later in this chapter to assist selection of initial dimensions and characteristics.

If you are looking to develop a craft with more extreme form, whether catamaran, trimaran, or hybrid, it may be best to work from basics and your own knowledge base and just use industry data to cross check. The next few chapters should give you a sufficient basis to go down this route.

2.1 Basic Concepts

Before moving on to the characteristics of multihull craft and their analysis we propose to introduce the basic concepts we will use as we explore these craft. Much of our exploration is an extension of standard naval architecture. The fundamentals are in classic naval architecture texts [2–5]. Normally we would start with our intended payload translated into required cabin or deck area and mass to be transported and relate this to typical statistics for vessels that have been built so far

L. Yun et al., *High Speed Catamarans and Multihulls*,
https://doi.org/10.1007/978-1-4939-7891-5_2

for similar missions, so as to derive expected displacement volume, vessel LOA, and (demi) hull breadth, spacing, and midships depth. To this end, typical data are presented later in this chapter.

2.2 Buoyancy, Stability, and Coefficients of Form

Once we have made an initial selection of overall dimensions for our vessel, the first task will be to develop a line plan for the hulls and determine the static stability. This is now completed in shipyards and naval architecture firms with computer software of varying degrees of sophistication (see Resources, Software).

Our initial quest is a first pass at the displaced volume and center of buoyancy at varying angles of trim and heel (pitch and roll) and the metacenter. Once we combine this information with the estimated center of gravity of the vessel, we can then determine the static stability curves of righting moments.

We will discuss the static parameters in Chap. 3 in more detail, together with the requirements specified by IMO to achieve a safe vessel design. It is clear from even a simple model that a catamaran is relatively stiff in roll, while in pitch the righting moments are low when a slender bow form is used, so other means to provide stabilization at speed may be necessary to provide dynamic stability.

For displacement or semi-displacement vessels this is sufficient to make a start on our design. If we are aiming for a high-speed craft operating in full planing mode, we will need to consider dynamic stability from the beginning. The main issues here will be to maintain steady trim at speed and minimize pitching motion. Deep V hull design with a suitable series of longitudinal spray rails can assist this. Stepped hulls allow further optimization though require care in the configuration of the steps and spray rails to avoid a tendency for the vessel to slide out in a turn due to local transverse flows around the steps.

To enable us to move forward and make an initial assessment of our vessel resistance to derive the necessary powering, it is helpful to calculate some coefficients of form, as used in naval architecture generally. These then enable scaling components of resistance from available generic data to apply to the vessel. The coefficients normally used to plot such data (e.g., resistance against speed) for catamarans are the block coefficient C_b, fineness coefficient C_f, and hull spacing $B/2b$, as follows:

C_b = Displacement vol/($L.\ b.\ d$) related to demihull form, or for full catamaran when comparing with monohulls or other vessels;
C_f = WL area/($L.\ b$) taken from bow to amidships, again usually for demihull form;
C_s = $B/2b$, where B is the centerline spacing between hulls and b is demihull breadth at WL.

Once a form with reasonable static stability is proposed, we begin by assembling the resistance curves and progress with some projected motion data from the plots against the coefficients of form. We may then have to adjust and repeat the cycle

until we home in on our desired characteristics. This should then be sufficient to move forward and make preliminary estimates for structural mass, payload, and outfit mass to verify that these are in the target range before carrying out more detailed analyses of resistance and motion.

It should be noted that when specifying propulsion and powering, a margin is required, first regarding propulsion thrust, and second regarding the power available to generate the thrust. The thrust margin critical speed is the resistance "hump" between slow speed displacement operation and high-speed semi or full planing. A margin of 10% is recommended as a starting point. Reliable powering by diesel or gas engines implies that the engines will run at about 85% of maximum power or thereabouts when the vessel is at service speed in a seaway. Gas turbines are normally operated at a rating close to 100% of the rated power for maximum fuel efficiency at vessel service speed and design sea state.

2.3 Resistance to Motion

The drag or resistance to forward motion comprises two main forces in calm water: from the skin friction on the hull immersed surfaces and from the pressure forces caused by the waves generated by the hull form.

2.3.1 Skin Friction Drag

Water flowing past a vessel hull forms a velocity profile in the boundary layer reducing to zero at the hull surface. Looked at from the point of view of the hull moving forward through the water, it is effectively dragging the boundary layer forward with it at the interface, reducing to zero at the "edge" of the boundary layer. Depending on the Reynolds number, the flow in this layer may be laminar (smooth) or turbulent (multidimensional, variable velocity). Turbulent flow is more energetic, creating higher drag forces. Generally the boundary layer for fast marine vessels is turbulent.

Determining the skin friction drag is simply a matter of determining the Reynolds number at the vessel service speed and associated skin friction coefficient (determined from testing with flat plates) and applying this to the surface area of the hull [2, 6]. If the initially selected hull shape key data have been calculated as in the foregoing buoyancy and stability section, the first element of the resistance curve can be generated.

2.3.2 Wave-Making Drag

As a vessel moves through water, the bodily displacement of the water mass creates a changing pressure field in the water volume around it. While static, it is this pressure field acting on the hull surface that balances the volume displaced and so supports

the vessel. As it moves forward the translation of the pressure field creates a wave pattern at the water surface. This wave pattern requires energy to be generated and corresponds to the "wave-making" or "inertial" drag acting on the forward-moving vessel. Depending on vessel speed, the height and length of the waves generated increase, inducing the vessel to trim bow upward.

Beyond the speed where the principal generated wave is twice the hull length, the trim reduces from its maximum value; nevertheless, the pressure field on the base of the hull is sufficient to support part of the vessel mass. As speed increases further, the proportion of vessel mass that can be supported increases (depending also on the geometric form of the hull) to the point where the majority of the vessel is dynamically supported. This is when a vessel is said to be planing.

We look at the theory for wave-making drag in Chap. 4, including the complicating effects of shallow and constrained waterways that create pressure reflections. Typical curves for catamarans are shown in various figures in Chap. 5 plotted against hull coefficients of form. These can be used to prepare an initial plot for the proposed catamaran design. Planing vessel characteristics are discussed in Chap. 5, as well as in Chap. 7.

2.3.3 Interaction

A key element of catamaran design is the water flow caused by interactions between the hulls, in terms of both frictional resistance and wave interference. As speed increases through the range to service speed, there will be increasing frictional resistance due to the so-called funnel effect of water being accelerated between the hulls and a series of peaks and troughs in additional wave resistance as the generated waves add or cancel the fluid motion in oncoming waves. These effects are greatest for hulls placed close together and rapidly diminish so that beyond a spacing greater than $C_s = 2.5b$ the effect can be ignored for this first phase of assessment. Guidance on this is given in Chaps. 4 and 5.

2.3.4 Added Resistance in Waves

When a vessel is moving forward in a seaway, the orbital motion of water in wind-driven waves impacting on the hull submerged surface will apply additional frictional and inertial forces to the vessel. Since a real seaway is not a sequence of regular waves, the instantaneous effect on the vessel is the sum of the effect of each wave. Waves will also be reflected from the "upstream" hull surfaces applying additional force.

This situation is rather complex, and so naval architects turn to the model test basin, use spectra of waves modeled from statistics taken from the location a vessel is intended to operate, and identify the "added resistance" by deleting the calm water resistance components. Using these data reduced to coefficients linked to the model

geometry and scale enables full-scale vessel total resistance to be assessed, as long as the geometry of the proposed vessel is not too far removed from the model prototype used to generate the resistance factors. We present some example data in Chap. 5.

2.3.5 Appendages

The key appendages for a catamaran are the propellers with their exposed shafting and supports, rudders, stern flaps or interceptors, water-jet intakes, and fixed or moveable stabilizers. It is rather complex to try to estimate additional resistance from these elements in the initial assessment, so it is suggested to simply add a factor to the calm water frictional resistance curve based on the likely additional immersed area of these devices:

$$R_{\mathrm{f}} = C_{\mathrm{f}}.\left(C_{\mathrm{b}}.(L.b.d) + A_{\mathrm{app}}\right).0.5\rho V^2,$$

in which $A_{\mathrm{app}} = \sum(\delta A)$, where δA are the submerged areas of each appendage.

We will discuss appendages in more detail in Chap. 11. A quick reference to this chapter and selection of initial choice of appendages should be sufficient for this first pass at the vessel configuration. It is best to be conservative here to begin with, taking cognizance of the vessel service speed and route or mission.

Typically propeller shafts, supports, and rudders will add 5% to friction drag collectively, while stabilizers may add 3%, bow T foils add 5%, and interrupters or stern flaps may add 3–5% of base friction drag at their maximum deployment. Stabilizers, T foils, and stern appendages are all aimed at improving motion response in a seaway, which in turn will reduce total drag forces and required powering in service; nevertheless, the additional drag will be important for determining performance in calm water.

2.3.6 Propulsion

There are two main choices for propulsion machinery, the gas turbine or the diesel/gas high-speed reciprocating engine. In each case, a reducing gearbox will be required to connect to the propellers or water jets. Water jets rotate at higher speeds than propellers, so the gearbox can be smaller, reducing the installed weight. Reciprocating engine efficiency has advanced considerably in the last two decades, incentivized by environmental regulations introduced by many countries and international organizations. CO_2 emissions are further improved by the use of natural gas as a fuel. At the current top end of the range for high-speed catamarans, the power required demands use of gas turbines due to their very high power density, producing a low installed weight. The challenge is that gas turbines are not as efficient as reciprocating engines, typically 0.4–0.6 L/t per nautical mile compared with 0.3 for a

diesel or gas engine, so in the small and medium range for catamarans reciprocating engines are the baseline choice. We give some statistical data for engine, gearbox, and water jet or propeller installation in Chap. 7, so readers are referred to that chapter for making an initial selection and checking against the preliminary vessel weight and buoyancy estimate made earlier in this chapter using the approach described in the next section of this chapter.

2.3.7 Motion in Waves and Stabilizers

At this stage the main focus is determination of vessel resistance and powering. Once an initial assessment of these has been prepared, and it is confirmed that they are in the right range for the mission objective, one can assess vessel motions through comparisons with existing craft and generic data. The first tasks are to determine the vessel natural periods in roll, pitch, heave, and the damping curve against frequency and check these against the peak period of the sea energy spectrum for the service route or mission. Normally one wishes to keep these two separated so that vessel natural period responses are minimized. In addition, a catamaran will have natural periods in roll and pitch that are close together, so that oblique seas may induce similar levels of these motions at the same time – a corkscrew-like combined motion that can be uncomfortable for passengers. It is recommended to keep the natural periods apart or, if this proves difficult, to introduce damping with stabilizers so as to avoid accentuated natural period response.

2.4 Key Features of High-Speed Catamarans

We need to identify the basic mission for our vessel since this guides us in the selection of dimensions and form, from which we can start the journey of analyzing the static and dynamic characteristics and then optimize them. We start with the vessel configuration, which involves our mission and the influence of the market in deciding on the main dimensions. The starting point is to make some basic decisions on vessel configuration, and for this we need to have a feel for the key features of a multihull.

The key attributes of high-speed catamarans are their efficient performance at high speed, with high usable deck area, high roll stability, seaworthiness, and maneuverability. The flooding resistance, structure weight, cost of construction, maintenance, and repair can all be low with careful design, while the large volume and complex geometry can create challenges if care is not taken to optimize them. The IMO High Speed Craft Code and the rules of classification societies such as DNV and ABS also provide key guidelines [7–9]. We will discuss this topic in more detail in the next chapter.

2.4.1 Resistance/Speed Characteristics

A catamaran comprises two demihulls and a cross structure. This hull form decreases the wave-making resistance at higher Fr_L due to the slenderness of the demihulls; however, this comes at the cost of increased water friction resistance due to increased wetted surface area. Based on statistics from existing craft, the wetted surface of a catamaran will typically be about 40% higher than a monohull craft of equivalent displacement. If we consider the consequences at different speeds, the following observations may be made:

- At a low craft speed of, say, $Fr_L < 0.3$, a catamaran will have no powering advantage over a monohull due to its higher water friction resistance (wave-making resistance is smaller for both craft at low speed).
- At medium speed, say $Fr_L = 0.3$–0.75, wave-making resistance will be the dominant element of total resistance for a catamaran. In this case, the total resistance will decrease compared to an equivalent monohull due to use of high length/beam ratio, L/b, and high slenderness, $L/\Delta^{1/3}$, for each demihull, minimizing total drag and compensating for the higher friction resistance of the two demihulls.
- High-speed craft, say $Fr_L > 0.75$, will have friction resistance equal to wave-making resistance at $Fr_L = 0.75$ and exceeding wave-making resistance at higher Fr_L, so the choice of catamaran hull configuration should be made carefully. A planing geometry with a shallow V bottom and hard chine demihull configuration should be considered so as to use dynamic lift force to reduce friction drag to a minimum.

Consider, for example, a high-speed catamaran, with demihull displacement of 36.5 t, length 27.4 m, and service speed of 32.5 knots, giving $Fr_L = 1.02$, and inverse of demihull slenderness coefficient $C_\Delta = \Delta/(0.1L)^3 = 1.77$. Based on experimental test series results for round bilge high-speed craft, the residual resistance coefficient (coefficient relative to displacement of total resistance minus wave-making resistance) of this catamaran will be $C_R = 1.8 \times 10^{-3}$, which is close to the coefficient for friction resistance. When using a monohull configuration for this craft with a displacement of 73 t, the inverse slenderness and residual resistance coefficients of the craft will be $C_\Delta = 3.54$ and $C_R = 3.0 \times 10^{-3}$ respectively.

The residual resistance coefficient of the catamaran is therefore about 60% of that of the equivalent monohull, and when one considers the increased friction resistance of the craft compared to a monohull due to the increased wetted area from both demihulls, the resistance of both craft will be very similar. Due to the interference resistance caused by the twin hulls, the total resistance of the catamaran will be only slightly larger than the equivalent monohull. To gain an advantage at planing speeds, the catamaran therefore needs a little extra, meaning optimization of the hull spacing to minimize interference, lift from foils, or ram lift from a tunnel form between the hulls. The latter two are concepts applied to racing catamarans with great effect, and we will touch on this later.

In the commercial arena, it has been found that the best zone for the high-speed catamaran is in the speed region $Fr_L = 0.5–0.95$, where hull spacing and form can be optimized for semi-displacement vessels.

Figure 2.1 shows a comparison of total propulsive efficiency (K_η) of some high-speed craft versus Fr_Δ, where 1 = hydrofoil craft, 2 = planing craft, Δ = high-speed-catamaran-specific examples.

Figure 2.2 shows the application zone for high-speed catamarans compared with other high-speed craft, where 1 = planing hull, 2 = displacement monohull, 4 = medium-speed catamaran , 3 = high-speed catamaran, and 5 and 6 show upper and lower boundaries for medium-speed catamarans.

Where $Fr_L >> 1.0$, friction resistance will be very high, and it will be necessary to take additional steps to reduce the hull wetted surface, such as full support by air cushion or hydrofoils. Such craft, for example, the SES and hydrofoil catamaran, require a different design approach (as we discuss in [10], so we refer readers to that text). In this book we will focus on the performance of catamarans, in general with Fr_L in the region 0.5–1.2, that is, medium- and higher-speed catamarans based on the semi-displacement design and wave piercing rather than full planing.

Figure 2.3 [11] shows a comparison of the relative total resistance (R_T/Δ) of three catamaran models with a planing monohull vessel model versus relative speed $v/\sqrt{L}$ (where v = knots, L = feet). It can be seen that the best zone for the catamaran is at a relative speed <3.0, that is, $Fr_L < 1$.

Figure 2.4 below shows typical vessel deck plans for a monohull and a catamaran ferry.

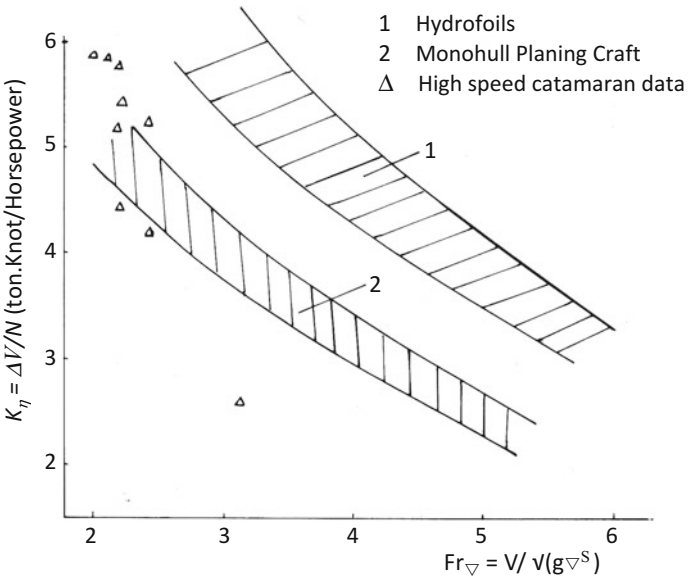

Fig. 2.1 Efficiency K_η versus $F_{r\Delta}$ for hydrofoils, planing craft, and catamarans

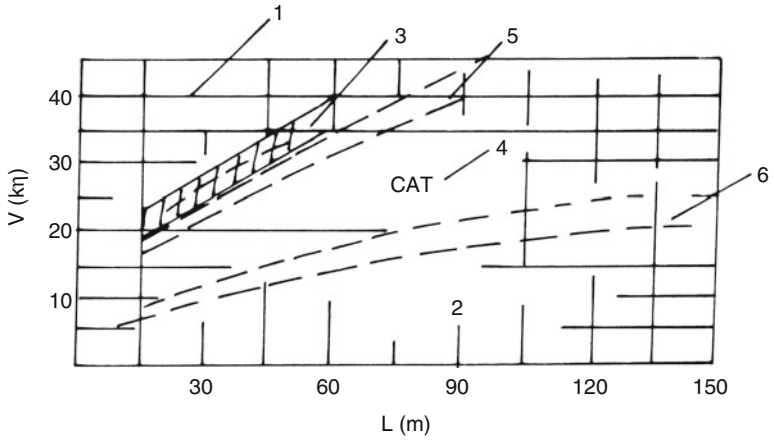

Fig. 2.2 Catamaran operation envelope

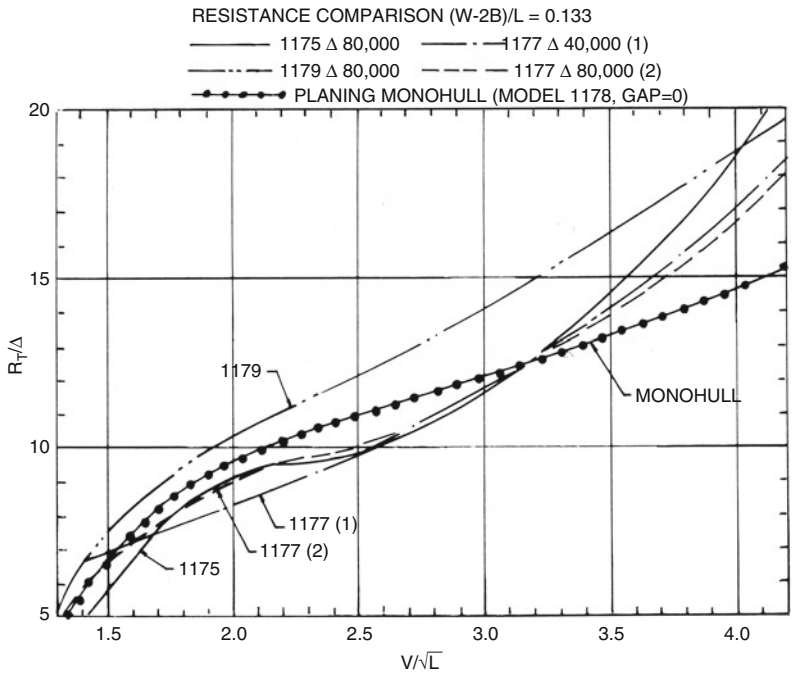

Fig. 2.3 Resistance comparison

2.4.2 Deck Area

The catamaran configuration, by virtue of the bridge structure connecting the demihulls, offers opportunity for greatly increased deck area and payload volume compared to an equivalent monohull craft. This can be seen from the vessel outlines and frontal views in Fig. 2.4a, b.

The catamaran deck area will typically be 40–50% larger than that of a monohull craft. The catamaran offers the opportunity to have multiple passenger decks as well as potential for a vehicle deck at the main deck level, and at each level the potential area will be much more spacious than in a monohull ferry. The result is an attractive vessel for ferry use.

Figure 2.5a shows typical data for catamaran deck area versus length overall (LOA) based on statistical data, and Fig. 2.5b shows the relation between deck area and displacement.

Figure 2.6 shows the overall dimensions versus deck area for both catamaran and monohulls with different length/beam ratios from an analysis in the USA [11].

Figure 2.7 shows statistical data for the comparison of deck area versus displacement and LOA for catamaran and monohull craft from an analysis by MARIC.

The bridge structure of a catamaran offers more volume per ton of displacement than a monohull superstructure. This usable volume, together with high transverse stability, is most useful for particular vessel missions, that is, passenger transport, and vehicle/RoRo cargo.

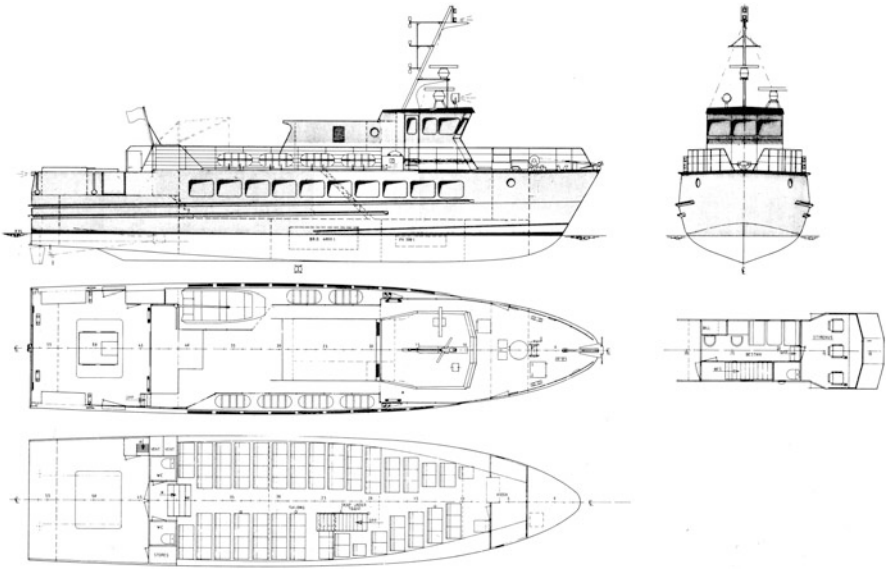

Fig. 2.4 (**a**) GA for Westamaran S80 monohull; (**b**) GA for Westamaran W88

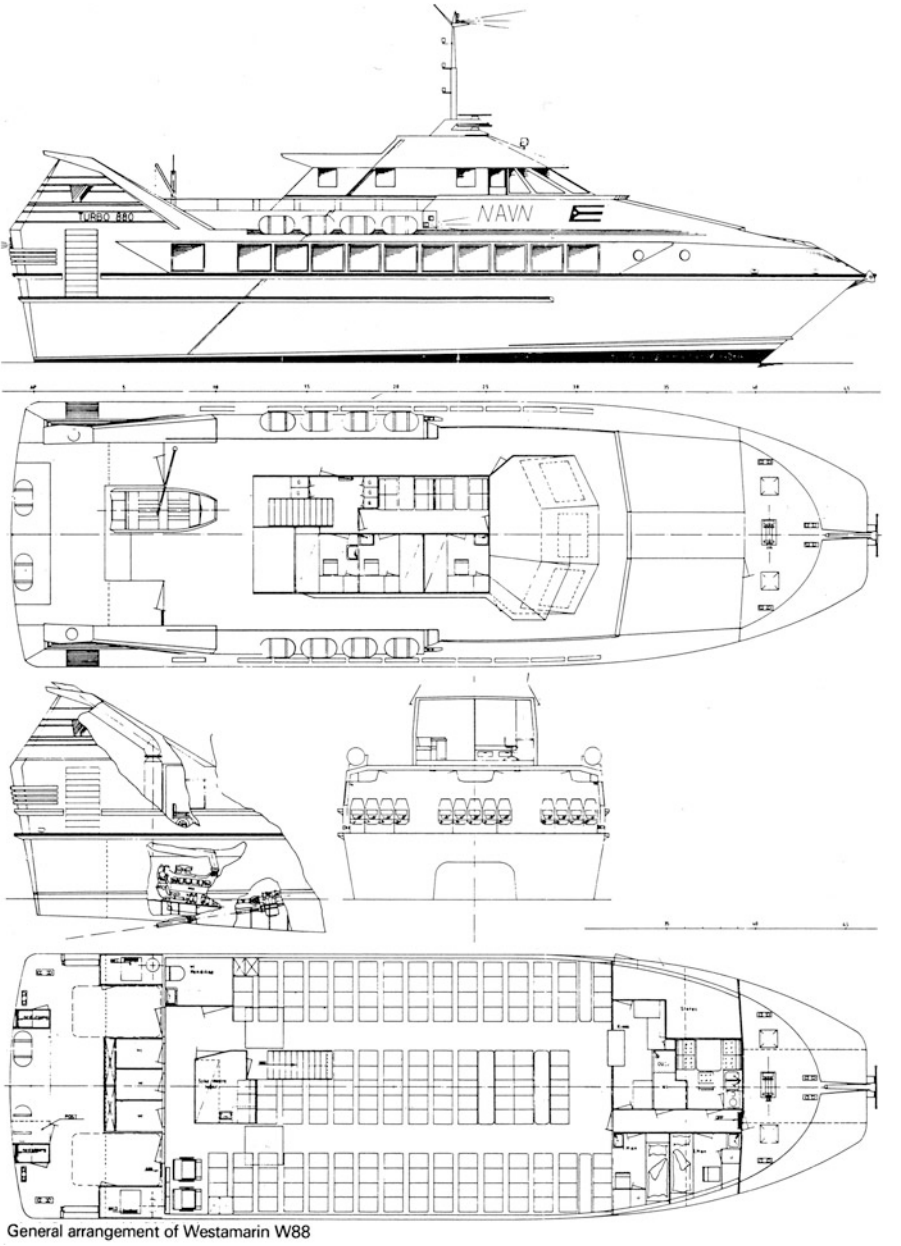

Fig. 2.4 (continued)

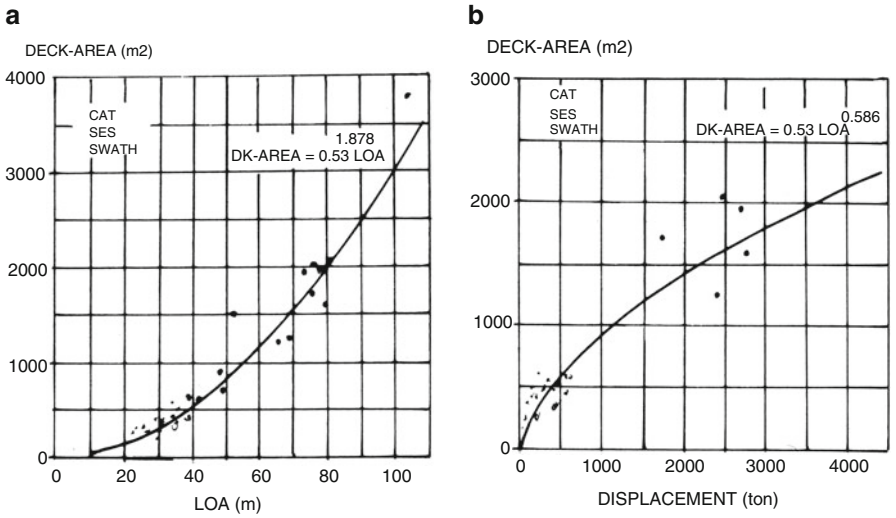

Fig 2.5 Deck area (**a**) versus LOA; (**b**) versus displacement

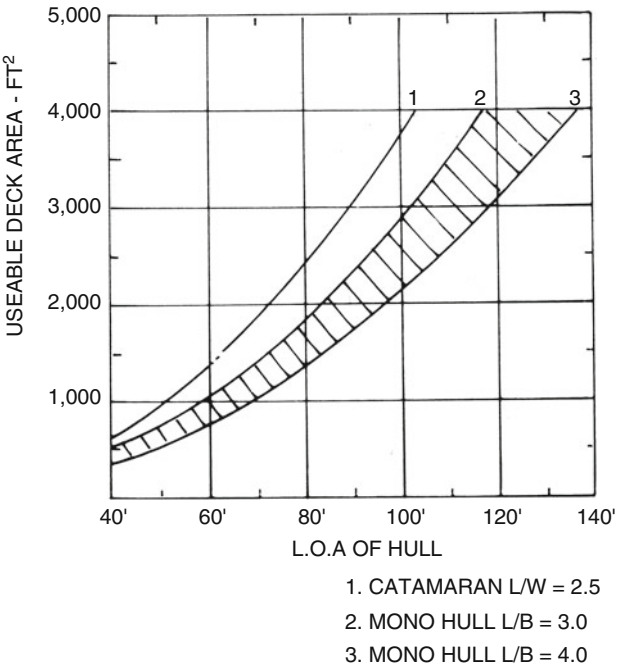

Fig. 2.6 Useable deck area versus length overall (LOA)

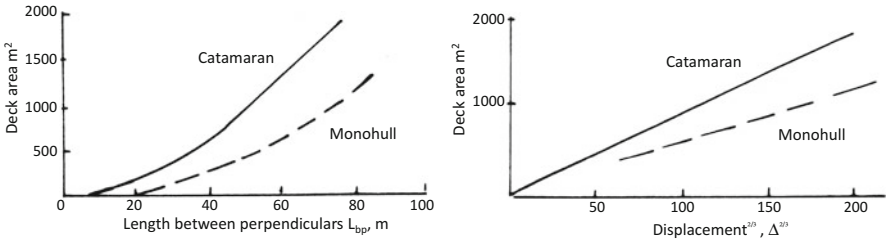

Fig. 2.7 Relation among craft length, displacement, and deck area

2.4.3 Transverse Stability

The catamaran is composed of two separate hulls, giving a large transverse inertia of the waterline area, resulting in high transverse stability, much higher than that of a monohull with equivalent displacement. The metacentric height can be more than 10 times as great as that of a monohull craft.

The transverse stability reserve against overturning moment is also two to four times greater than that of a monohull [12]. This high inherent stability allows a trade-off between stability and other desired capabilities. For example, it is possible to reduce the demihull waterplane area to give a reduction in resistance and wave response in a seaway. The great stability of the catamaran has been an important consideration when selecting this type of ship for some special applications, for instance offshore wind farm maintenance craft. For medium-speed and high-speed catamarans used for ferry missions, the high transverse stability can cause higher accelerations in an oblique seaway and make the vessel uncomfortable for passengers. This means that craft routing needs to be considered when developing the design. In some cases (e.g., the strait between Taiwan and mainland China) conditions are such that a trimaran configuration confer give advantages [13], as the sponsons can be optimized to soften the ride in oblique seas.

2.4.4 Damaged Stability (Compartment Floodable Length)

Catamaran damage conditions are mostly asymmetric, and the damaged heeling angle and roll/pitch angle for a catamaran upper deck must comply with the requirements from the IMO SOLAS rules, so the demihull watertight compartment length must be shorter than in an equivalent monohull.

The subdivision possibilities of a catamaran hull are greater than those of monohull craft because the operational spaces are located primarily in the superstructure rather than within the hull. The arrangement of engine space and water-jet

installation, always located at the rear part of the craft, must be carefully designed to minimize the floodable length in this area, in accordance with the IMO High Speed Craft Code [7].

2.4.5 Seaworthiness

Key seakeeping characteristics of a high-speed catamaran can be outlined as follows:

- Catamaran hulls are slender with a high *L*/*b* ratio, fine waterline entry at the fore body, and low response to waves, so speed loss in a seaway should be less than that of other high-speed craft, such as air cushion vehicle (ACV)/surface effect ship (SES) and monohull planing craft. In addition, the primary wave-making drag peak is also lower than that of these other craft, enhancing its ability to accelerate through the drag peak in rough seas to move toward service speed and planing conditions for high-speed craft.
- Since demihulls are displaced from the vessel longitudinal centerline, roll damping is increased so as to reduce the dynamic rolling angle; however, since the GM is much larger than a monohull, rolling acceleration is high, affecting passenger comfort. In addition, because the *L*/*B* of the whole craft is small, the natural periods for longitudinal and transverse motion are closer to each other, causing a corkscrew-like motion of the vessel in oblique seas, and this can cause serious motion sickness, from slight discomfort through dizziness and nausea to vomiting and complete disability. This can seriously affect the application of catamarans, and designers need to pay careful attention to this when designing vessels. A Chinese catamaran named *Lun Jin*, a 38.8-m craft operating between Hong Kong and mainland China from 1986, experienced seasickness in 70–80% of passengers in a month of winter season operation. This was not acceptable, so the craft was improved by retrofitting roll stabilization equipment, after which it had satisfactory operational performance.
- The motion acceleration caused by sea waves is predominantly vertical acceleration, as roll and pitch amplitudes are small.
- The rolling motion of a catamaran at high speed will be reduced compared to low speed due to increasing damping effect on the craft at higher speeds. The rolling angle and its acceleration will be reduced by a factor of 2–3.5 compared with operation at lower speed.
- There is less "slamming" or "impact acceleration loads" compared with monohull planing craft due to the slender demihulls.
- The longitudinal motion response and speed loss will be smaller for a high-speed catamaran due to its slender demihulls, and seakeeping quality will be high for protection from sea/waves due to its high transverse stability. Nevertheless, from the point of view of ride comfort, the high vertical acceleration and "torsional rolling effect" of a high-speed catamaran in oblique seas can cause discomfort to passengers in high sea states.

So is the seaworthiness of a high-speed catamaran fine or poor? It might be fine in head seas, but in cross seas the torsional or corkscrew motion may cause discomfort, which will actually be worse at low speeds than at high speeds. Additional active stabilization may be needed to minimize this problem.

2.4.6 Maneuverability

Course stability is high for catamarans due to the high L/b of each demihull. This can have its down side for maneuverability. The high transverse spacing between propellers and rudders or water jets mounted at the stern of each hull compensates for this, so that turning and maneuvering are no more difficult than with a typical monohull vessel. The maneuverability of catamarans at lower speeds is also improved using the revolution difference between the propulsion engines in each hull.

The maneuverability will be further improved using water jet propulsion owing to its shallow draft and use of directional and reverse thrust. Larger catamarans that have two water jets in each hull often install just one of the pair with thrust direction controls because this is sufficient both at high speed, where course changes are small, and when berthing since only partial power is required at very low speeds and one of the jet pairs can be shut down. Fine maneuvering during berthing is normally assisted by the installation of small tunnel thrusters at the bows.

2.4.7 Hull Weight

There are weight penalties associated with the large catamaran bridge structures and two additional side walls at the inside face of the demihulls; however, comparisons with monohulls must be carefully made, otherwise the results may be misleading. For weight-limited ships, where the two catamaran hulls must provide the same displacement as a monohull ship, the catamaran incurs a weight penalty. However, if the comparison is by payload volume per ton of displacement, the catamaran and the monohull should have approximately equal hull weights for the same gross payload volume because the monohull would have to be scaled up in displacement to provide a payload volume equivalent to that of the catamaran [14].

2.4.8 Structure Configuration and Equipment

Compared with high-speed craft such as hydrofoils or SESs, the catamaran is a simpler structure and has a less complex power equipment installation, so its construction and maintenance/repair costs are significantly lower than those of

these competitors. This, combined with its ability to scale to similar dimensions to large monohull ferries, has led to its attractiveness for passenger and vehicle ferry service.

In the evolution of SESs, ferry operators and military specialists were very interested in scaling up. An example was the US Navy 3KSES program in the early 1970s. This was a SES with a displacement of 3000 t targeted at a service speed of 80 knots for the US Navy as destroyers and mini aircraft carriers. In Japan the Techno Super Liner (TSL) program worked on competitive 3000 t SES or hydrofoil craft for fast sea transportation at 50 knots in the 1990s [10]. However, both development programs failed to complete due to the very high power that had to be installed and the subsequent extreme operating costs. The 3KSES was effectively stopped by the oil crisis in 1974 when oil producers in the Middle East threatened Western nations with ceasing oil production. This caused the USA to stop military programs such as the 3KSES that were dependent on low-cost, plentiful fuel supplies. Later the TSL in Japan had operational success with its SES but eventually was also stopped by the high fuel costs of the craft, which made it uneconomical to continue the planned coastal utility missions.

In contrast, the catamaran has seen step-by-step improvements in efficiency and scaling up to compete with conventional passenger and RoRo ferries. Computerized structural analysis has assisted in developing configurations that are resistant to fatigue caused by vibration from machinery and the repeated load reversals during travel in a coastal seaway. Meanwhile, construction techniques for welded aluminum structures have significantly improved since the 1970s, including automated parts cutting and preparation and semiautomated welding of subassembly blocks.

The transition to propulsion by water jets rather than external propellers has also led to higher efficiency in propulsion and, thus, minimized power installation for a given mission and vessel size. Many of these improvements have also been applied to monohull fast vessels, and so the choice for an operator has been based on the vessel configuration and fit to his terminal or berthing facilities, together with the vessel earning power.

Shipyards have tended to specialize in a particular vessel type because the investment in developing a design as well as the fabrication equipment for aluminum structures, particularly a large one, is very high. Thus a number of yards in Norway, Sweden, Australia, Holland, and Southeast Asia have become specialist catamaran suppliers, each having their portfolio of designs and often targeting a local or regional market rather than the global market, supported by design houses who have a more global reach.

The consequence for naval architects is that if they are independent designers, they may need to work with one of these yards to allow their design to be built or select a yard that has built craft using the same material. For smaller vessels, many yards worldwide now have experience in building in aluminum alloy or in reinforced plastic, for example, those targeting the superyacht market. The challenge here may be that for a utility craft or ferry, such a yard may not have the lowest costs. A further alternative may be to work with a shipyard that is interested in changing its market to

fast craft. Normally this would be with the intent to improve yard economy. Unless automation is used as a lever, it may be difficult to keep costs low in the initial phases.

This takes us back to hull materials, where in the early days of the smaller catamaran and SES development a number of yards were set up to build in reinforced plastic. Though the larger catamarans are all in aluminum nowadays, some builders supplying the superyacht market and smaller utility vessel market have considerable expertise and capacity for glass-reinforced plastic (GRP)/glass-reinforced epoxy resin (GRE) hull construction, both in Europe and in Asia/China.

Making the choice of structural configuration for a catamaran is a fundamental decision that will affect the design of outfitting in particular, both mechanical and architectural. Depending on the vessel mission and size, it is worth investigating the options open to you as a designer before committing to your main structural material.

Figure 2.8 above shows the structure weight fraction of craft built in various materials – GRP, aluminum, and high-strength marine steel. Note that the structure weight fraction of an aluminum hull can be as much as 45% lighter than that of a high-strength steel hull.

Although the fraction for a GRP hull can be reduced by 20% compared to aluminum, the rigidity of GRP is too low to be the ideal hull material of larger craft. Carbon-fiber reinforcement and the use of epoxy can increase stiffness, but at significant cost.

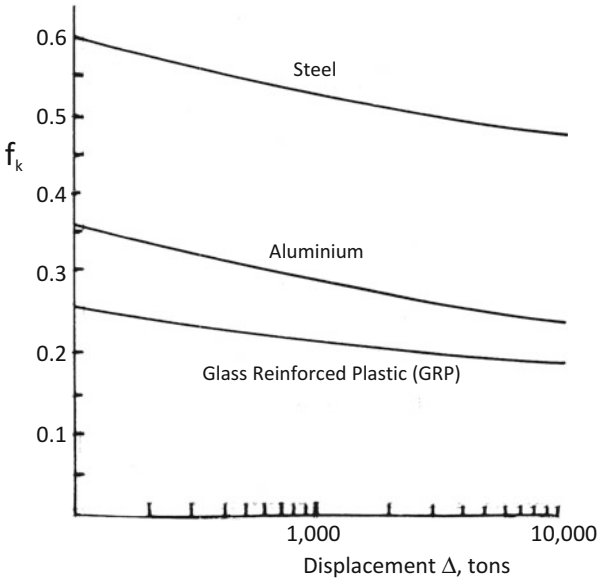

Fig. 2.8 Structure weight fraction

2.4.9 Length-to-Breadth Ratio for Catamarans and Multihull Craft

The *L*/*B* ratio typical for a commercial or military catamaran is typically 4:1 up to 5:1. Wave-piercing craft (WPC) have hulls spread more widely, so the *L*/*B* comes down closer to 3:1 to 4:1. *L*/*b* for typical demihulls is 8 to 10:1 for small utility craft and 13 to 20:1 for SSTH or semi-SWATH vessels. On what basis does one make a first choice for a vessel's overall configuration?

The first steps are to determine the expected payload and, hence, by a factor, the displacement (see the last section in this chapter). If the payload is simply passengers, then 150 kg per person including baggage and a range from 0.3 to 0.6 m^2 deck area may be suitable for the passenger cabin. If vehicles are to be brought on board, an average of 4 × 2 m space and weight allowance of 1800 kg per car may be a useful start. Unless a straight-line drive on and off can be arranged, a lane arrangement must be designed to allow vehicles to circle around, with a radius of typically 5–7 m. A passenger cabin on a RoRo ferry is not normally space limited, so it is simply an estimation of the outfitting payload for the passengers to be carried.

Once the expected payload mass and deck area have been used to estimate vessel displacement, the demihull and catamaran geometry may be drawn up and checked against the target, using *L*/*b* at 8:1 as a starter and centerline spacing of 3*b* (giving overall breadth 4*b*), for example. The superstructure then needs to be checked for deck space and layout for passenger seating and access and for vehicle access, as required. Remaining available space for utility outfit needs to be checked at this stage, depending on the service requirements for HVAC, elevators, stairs, cafeteria, crew quarters, bridge/navigation, and goods storage. If the arrangement seems to have enough space, then at this stage the design can be moved forward to hydrostatic and hydrodynamic assessment.

2.5 Service Applications: Some Thoughts

Based on the characteristics of high-speed catamarans discussed previously, it is apparent that a high-speed catamaran may be suitable for a number of different missions, for example, short-range passenger ferry, car/passenger ferry, patrol boat, rescue boat, oceanographic research vessel, and offshore wind farm service vessel. Some thoughts on these applications are given in what follows to aid selection.

2.5.1 Passenger Ferry Vessels

The motion in a seaway for high-speed catamarans is not conducive to very long route lengths as a passenger ferry. A route length (or route leg between intermediate

terminal points) with a duration of between 0.5 and 2 h is comfortable. Open-sea routes greater than about 60–80 nautical miles are likely to be affected by stormy weather in wintertime, leading to service cancellations for all except craft above 90–100 m LOA. Ferries in the 30–40 m LOA range are useful for routes or route stages of 20–30 nautical miles across open water, or stages up to 60 nautical miles where much of the route is protected.

The issue of motion in open water has been the trigger for designers to look at the trimaran and other configurations, for both commercial and military uses.

Austal has developed a family of trimaran craft at sizes starting at 100 m LOA and aimed at services in more exposed environments such as the Canary Islands, Taiwan Strait, and, more recently, across the English Channel to the Channel Islands.

At smaller sizes, 30–40 m LOA, the focus has been on dynamic stabilization with foils. This was taken to its limit by Fjellstrand in the development of its so-called flying cat, which had foils under the bows and stern to enable it to operate fully foil-borne at service speed. This is the extreme end of the spectrum for the midsize passenger craft.

More widely applied has been the combined use of motion stabilizer foils for roll and pitch and slender areas at the water line and just above it, the so-called thin hull or wave-piercing concept. The leaders in this concept are Incat in Tasmania, with their wave piercers, while different approaches to this challenge have been adopted by Austal and a number of other catamaran designers and builders.

2.5.2 Military, Paramilitary, and Utility Applications

High-speed catamarans hold potential for a number of military and paramilitary applications, based on the following prospective characteristics;

- Very fast “sprint speed” for military defense and attack activities
- Large usable deck supporting variable military roles and equipment layout
- Large cabin area for accommodating crew and extra persons, for example, rescued survivors or illegal immigrants
- Extended loitering capability thanks to the vessels’ static stability, seaworthiness, and broad operational envelope

Figure 2.9 shows the general arrangement of an example catamaran police patrol vessel, and Table 2.1 lists characteristics of a number of existing catamaran patrol vessels [15]. To date the catamaran concept has been used for navy coastal patrol boats, police vessels, offshore economic zone patrol, including fishing protection, coast guard patrol, and, more recently, offshore wind farm personnel transfer and tendering during maintenance. All of these missions benefit from fast transit (or chasing in the case of coastguard or police vessels) and the ability to loiter offshore. The table shows that these craft generally fall within a range 10–30 m in

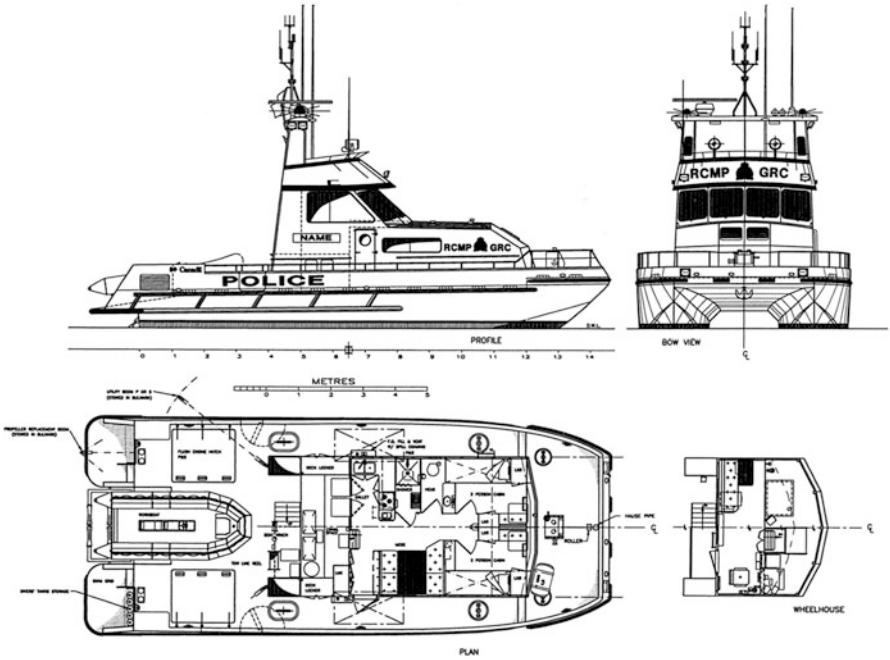

Fig. 2.9 RCMP 17.7-m patrol boat general arrangement

length, the size being dictated by the environmental conditions in the operational area and requirements for motion when loitering, rather than sized from their payload requirements.

Vessels such as wind farm maintenance craft will also have a requirement for self-positioning while nosed up to a windmill access platform, which will require the installation of thrusters and a control system and power supply, either electric or hydraulic, complementary to or independent of the main propulsion. Some designs for this purpose have been proposed utilizing a catamaran form for transit and then having the ability to ballast down to a deeper draft with a smaller waterplane while at the platform, so as to have reduced motion during this phase of operation.

2.6 Benefits of Scaling Up

More car/passenger ferries have been constructed worldwide in recent years because of the advantages from scaling up the sizes of ferries to as much as 120 m in length from passenger-only ferries that ranged in size up to 40 m.

The progression of increasing size has been a steady process since the early 1990s in almost the entire high-performance marine vessel (HPMV) family including catamarans, WPCs, SESs, and hydrofoils, to take advantage of the benefits summarized in what follows, generating strong competition between the concepts. In

Table 2.1 Characteristics of sample catamaran patrol vessels

Vessel name	Builder	Year	Material	LOA (m)	L_{WL} (m)	Beam (m)	Beam at Chine, (m)	Hull separation	Depth
Pursuit	T-craft	1990	GRP	10.00		4.00			
CA3	A. Fai	1990	Aluminum	22.50	21.15	10.00	2.50	7.50	
Nadon	Shore boat	1991	Aluminum	17.75	16.00	6.70	2.15	4.37	1.87
AIN DAR 7 & 8	Båtservice	1991	Aluminum	36.00		11.80			4.20
HKMD police 2	Sea spray	1992	Aluminum	9.90	8.45	4.20	1.30	2.90	
US Army HSPC-1	Trinity	1992	Composite	12.50					
Discovery	Roach B/B	1992	GRP/Kevlar	13.10	11.50	5.49			
Coast guard 2212	T-craft	1992	GRP/foam	22.00		7.00			
Lindsay	Shore boat	1992	Aluminum	17.75	16.00	6.70	2.15	4.37	1.87
Cougar Cat2100	Cougar marine	1992	Aluminum	21.25	19.43	6.47			
SM adamant	FBM	1993	Aluminum	32.00	30.80	7.80			
Damen Alucat 1350	Damen	1993	Aluminum	13.80	11.25	4.51			1.85
Higgett	Shore boat	1993	Aluminum	17.75	16.00	6.70	2.15	4.37	1.87
Response	Sea spray	1993	Aluminum	19.95		8.00			
Recover	Prout Cat'n	1994	GRP	16.50					

(continued)

Table 2.1 (continued)

Vessel name	Draft, m	Power shp	Cruise Speed, knots	Max. Speedknots	Propulsion type	Fuel capac. liters	Water cap liter	Light ship weight tons	Load disp. tons	Notes/ service
Pursuit	0.60	500	20	40	Water jet	800	140		7.00	Foil-assisted
CA3	1.60	1475		28	Propeller	2200	600			Airport rescue
Nadon	0.67	1620	30	35	SPP	4000	450	22.72	27.94	Arneson SPP
AIN DAR 7 & 8	1.85	4370	25	33	CPP	18,235	14,000		210.00	Pollution control
HKMD police 2	0.60	710	30	35	Propeller	1200	400	7.05		Police patrol
US army HSPC-1		800		43	SPP					Army patrol
Discovery			25	30	Water jet					n/a
Coast guard 2212	0.90	2000		37	Water jet	5000	1000			Foil-assisted
Lindsay	0.67	1620	30	33	SPP-fixed	4000	450	23.50	28.75	Custom fixed drive
Cougar Cat2100	1.65	5174	42	53	SPP	13,000			50.5	Customs patrol Spain
SM adamant, now Cardigan Bay	1.10	1360		23	Water jet					Port tender crew boat
Damen Alucat 1350	1.86	1390	21	32	Water jet					Fast rescue
Higgett	0.67	1620	30	33	SPP-fixed	4000	450	23.50	28.75	Custom fixed drive
Response	1.7	1520		25	Propeller	5800				Patrol
Recover	1.00	960			Water jet					Pollution control

Data were taken from Ref. [15] with some additional vessel details found
Limited data available for some vessels
CPP controllable pitch propeller, *SPP* surface-piercing propeller

numbers, the catamaran (including WPC and SWATH) has been the winner, with very large catamarans in a range of 2000–5000 t displacement being completed in recent years and put in continuous service, while upscaling projects for the SES and hydrofoil have not been successful. Part of the success enjoyed with catamarans has been a result of scaling up as a means to improve transport efficiency without changing the complexity of vessels.

2.6.1 Froude Number and Powering

As noted previously in this chapter, the favorable Fr_L for high-speed catamarans operating in semiplaning mode at service speed is about 0.5–1.1, so operational speed at the same Fr_L increases as vessel size increases. However, the increase in speed is smaller than the displacement increase because the latter is inversely proportional to one-sixth the power of the Fr_L increase. In recently produced very large catamarans, displacement has increased by a factor of 10–20, up to 2000–5000 t, but the service speed has only increased from 35 to 45–50 knots, an increase of 30–40%. The power plant requirement, measured in kW/t of displacement, will be reduced with increased vessel sizes and displacement (Fig. 2.10) [16].

2.6.2 Payload Fraction

As displacement increases, the payload fraction can be increased due to a decrease in the vessel's structural fraction (Fig. 2.8). The largest Incat vessels achieve a payload fraction close to 50% of vessel displacement, a very great achievement for the design engineers.

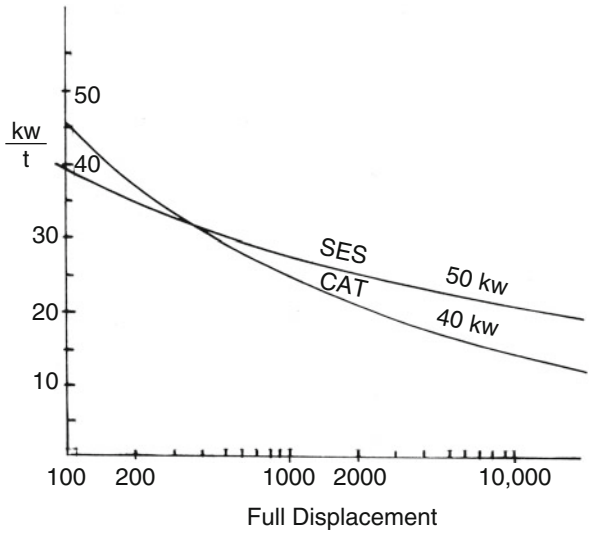

Fig. 2.10 Power versus displacement

2.6.3 Seaworthiness

This is probably the most important reason for increasing vessel size. As size increases, the probability of resonance of the ship with wave frequency in a seaway is reduced owing to an increase in the natural period of vessel motion and increased ship–wave length ratio (L/λ), as well as an increase in encounter frequency in particular, as both size and speed increase while Fr_L remains in a favorable zone.

2.6.4 Specific Power

Figure 2.10 above [16] shows a comparison of specific power (ratio of horsepower of main engines and displacement, kW/t) of a catamaran and SES. Here it can be seen that the reduction in catamaran specific power with increased displacement is sharper than that of the SES. This is due to the catamaran's operating at a more favorable speed with lower Fr_L.

2.6.5 Reduced Speed Loss in Waves

The speed loss of catamarans in a seaway is lower than for SESs, for the following reasons:

- The vertical motion of SESs, that is, both the motion amplitude and accelerations in waves, will be greater than that of catamarans owing to the "cobblestone effect" of cushion air and the leakage of air from the cushion, which generates an increasing draft and a decrease in cushion lift as well as increased resistance;
- The resistance from both fore and rear skirts increases in a seaway due to motion excitation and a large transverse frontal area;
- The probability of air suction into the inlet of propulsion water jets with a flush type of inlet (which mostly applies to high-speed craft due to decreased inlet resistance) will be higher with SESs than catamarans due to the greater vertical motion of SESs. To correct the air ingestion, the power must be reduced to protect the engines from overspeeding, and this results in reduced vessel speed.

Prof. Faltinsen [17] compared the reduction of speed in a seaway for an example catamaran and SES using theoretical calculations. Both craft have the same leading particulars with respect to LOA (40 m), beam (35.3 m for catamaran, 34.8 m for SES), and water jet propulsion, with a flush inlet for both craft.

The shaft power of a catamaran is 2×4150 kW in all sea states, achieving 40 knots maximum speed in calm water, and the propulsion power for SESs is 2×2750 kW in all sea states, achieving 50 knots maximum speed in calm water.

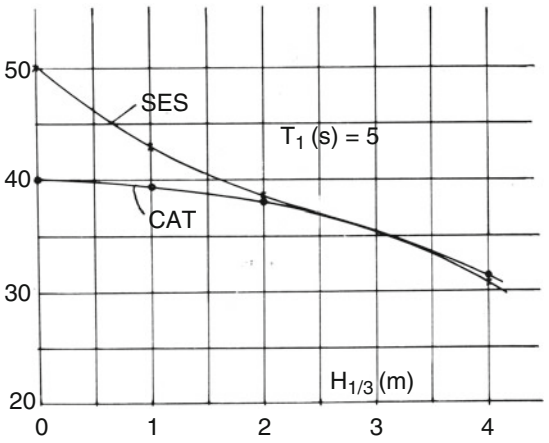

Fig. 2.11 Speed loss in a seaway for catamaran versus SES

The calculation of speed reduction for both craft was carried out in long-crested (unidirectional) waves with the two-parameter JONSWAP spectrum to describe the sea state. Figure 2.11 shows an extract of the calculated results, where the speed represents the speed reduction in the case of air suction into the water jet inlet, $H_{1/3}$ is significant wave height, and T_1 is the mean wave period (s).

From the figure one can see that the speed of the SES in calm water is 10 knots higher than that of the catamaran, while both craft will have the same speed at a wave height of 2 m, and at limiting sea state the speed loss of the SES will be as high as 11.4 knots, while for the catamaran it will be only 2.3 knots.

2.7 Hybrid Configuration Options

Why consider a hybrid? Usually so as to benefit from an additional attribute that satisfies a mission requirement, for example, minimized draft to operate in shallow waters or the use of hydrodynamic lift for a smoother ride at very high speeds. In what follows, we outline the key configurations based on the use of a combination of buoyancy, static air cushion lift, hydrodynamic lift, and aerodynamic lift that all marine craft can bring into play. We go into more detail on this topic in Chap. 10.

In general, all high-speed craft (or HPMVs) can be classified as shown subsequently in Figs. 2.12 and 2.13. Figure 2.12 looks rather complicated and chaotic; however, the figure can be explained in a simple manner as follows [18, 19], so as to help in making a selection of the desired combination of supporting forces. According to the proportion of the four kinds of supportive force used, a series of hybrid craft can be identified. Those using the multihull as part of the configuration are highlighted in italics. Another way of looking at the envelope of types, and therefore possible options, is shown in Fig. 2.13.

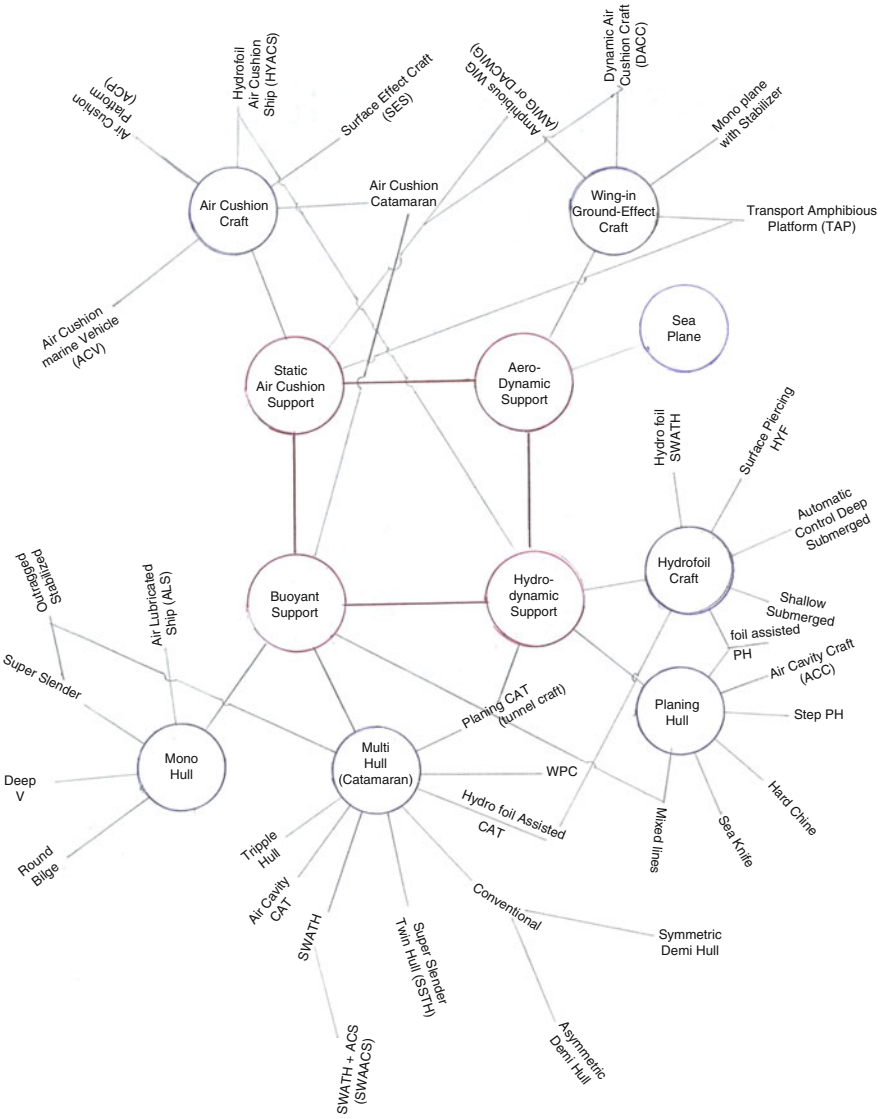

Fig. 2.12 Diagram for the classification of high-performance marine vehicles version 1

1. *Buoyant support*

   (a) Monohull craft

   - Round bilge craft
   - Deep V craft
   - Air lubricated craft with low speed
   - Super slender craft
   - Super thin craft with outrigger stabilizer

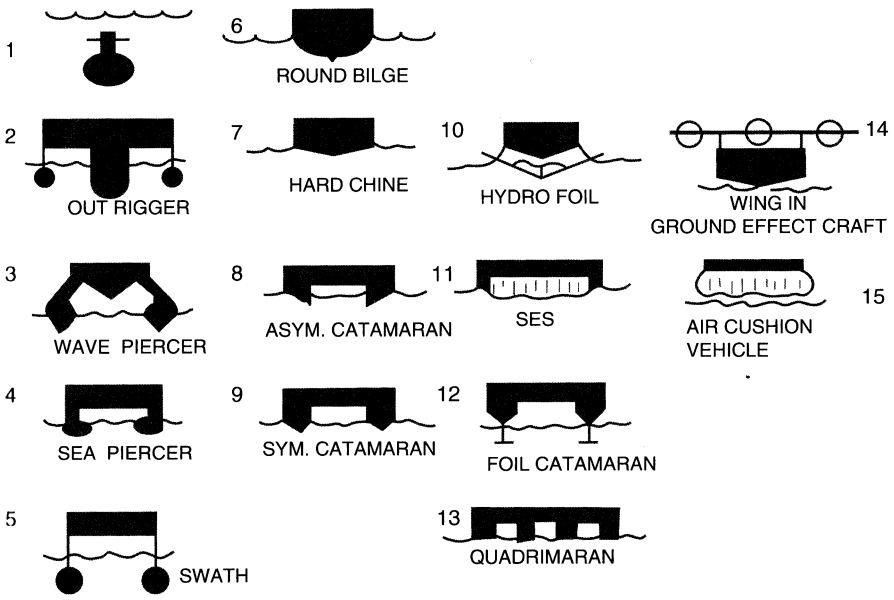

Fig. 2.13 Classification of high-speed craft version 2

(b) Multihull craft

- Conventional catamaran (symmetric demihull, asymmetric demihull)
- SWATH (including SWAACS, i.e., SWATH plus air cushion system)
- Wave Piercer Catamarans, WPC
- Hydrofoil-assisted catamaran (catamaran plus hydrofoil)
- Super slender twin hull, SSTH
- Planing catamaran, that is, tunnel planing craft (merged planing technology in catamaran)
- Air cavity catamaran (merged air lubrication technology into catamaran)
- Trimarans, quadrimarans etc (similar to super thin with outrigger stabilizer, or so-called slice craft)

2. *Hydrodynamic support*

(a) Planing hull

- Hard chine planing hull
- Stepped planing hull
- Hydrofoil-assisted planing hull (merged hydrofoil in planing hull, i.e., planing hull plus fore single hydrofoil)
- Air cavity craft (merged air lubrication into stepped planing hull)
- Sea knife (super critical planing hull for improving seakeeping quality)

- Mixed line planing hull (hard chine for fore and round bilge for rear part of hull for improving seaworthiness), also known as a semiplaning hull

(b) Hydrofoil craft

- Automatic control deep submerged hydrofoil craft (seagoing craft)
- Shallow submerged hydrofoil craft (for inland water operation)
- Surface-piercing hydrofoil with automatic stability augmentation system for improving seaworthiness (seagoing craft)
- Hydrofoil SWATH (hydrofoil plus SWATH)

3. *Static air cushion support*

(a) Air cushion craft

- Air cushion vehicle (ACV)
- Surface effect ship (SES)
- Air cushion platform (ACP), with lower speed for transporting heavy loads in swamps and other areas difficult to access
- Air cushion catamaran (ACC) (merged air cushion in buoyant catamaran)
- Hydrofoil air cushion ship (HYACS) (hydrofoil plus air cushion technology)

4. *Aerodynamic support*

(a) Wing-in-ground effect (WIG) craft

- Airplane configuration, that is, monoplane with stabilizer
- Dynamic air cushion craft
- Amphibious wing-in-ground effect (AWIG) craft or dynamic air cushion wing-in-ground effect (DACWIG) craft (merged air cushion into WIG)

Information on the design of other craft described in the figure can be found in [18, 19] and other references given as resources at the end of this book. We will consider the concept options further in later chapters of this book; meanwhile, we will continue with the basic analysis of catamarans and extensions to wave piercers, SWATH configuration, and the trimaran.

2.8 Synthesis for Initial Dimensions and Characteristics

The data presented earlier provide some insight into the characteristics of catamarans based on data from existing craft and the possibilities for vessel form including various hybrid concepts. A selection of general arrangements and key technical data is given in Appendix 3 to provide a visual reference. That is fine, but what about a new design?

The reader is encouraged to use the flowchart in Fig. 2.14 below as a starting point that links back to the key items discussed in this chapter. The idea is to obtain

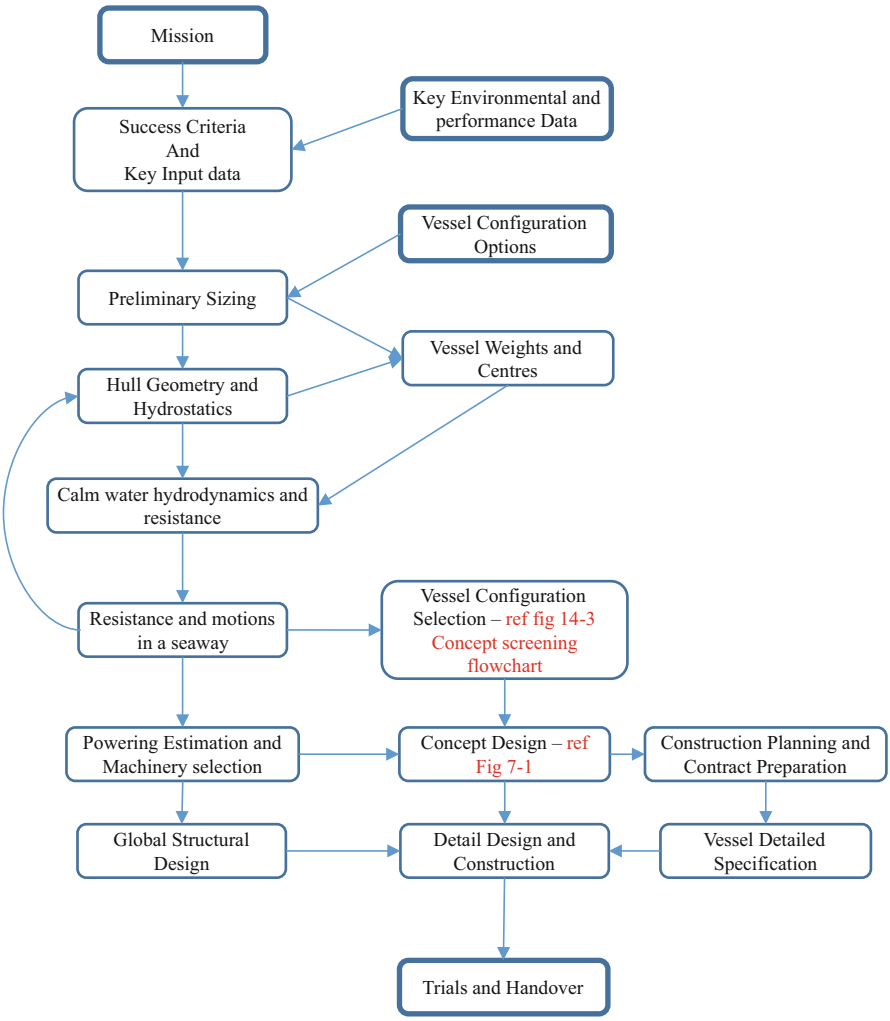

Fig. 2.14 Design flowchart – initial design selection

data for a concept sufficient to allow a first-pass check of static buoyancy and stability before moving on to resistance and performance estimation. We review the statics in Chap. 3 and continue with wave making and calm water resistance in Chaps. 4 and 5. In Chap. 6, we will look at seakeeping before returning to overall vessel design in Chap. 7.

References

1. Jane's high-speed marine transportation editions up to 1999 up to 2012, Stephen J. Phillips, Jane's Publishers, ISBN 0-7106-0903-5, Data referred is from 1999–2000 edition
2. Principles of Naval Architecture, Revised edition (1967), Society of Naval Architects and Marine Engineers, New York
3. Saunders HE Hydrodynamics in ship design. The Society of Naval Architects and Marine Engineers, New York 1965 in 3 Volumes
4. Rawson KJ, Tupper EC (2001) Basic ship theory, 5th edn. Butterworth and Heineman ISBN-13: 978-0750653985
5. Molland AF (ed) (2008) The maritime engineering reference book: a guide to ship design, construction and operation [Hardcover]. Elsevier, p 900 ISBN-13: 978-0750689878
6. Couser PR, Molland AF, Armstrong NA, Utama IKAP (1997) Calm water powering predictions for high speed catamarans, FAST 1997, Sydney, Australia, 21–23 July 1997
7. International code of safety for high speed craft, IMO, publication IA-185E, ISBN 92789 28014 2402, 2000. Amendments and resolutions after 2000 are available on IMO website IMO.org.
8. DnV rules for high speed light craft and naval surface craft (Download from DnVGL internet site)
9. ABS rules for classification of high speed craft (Download from Eagle (ABS publications) internet site)
10. Bliault A, Yun L (2010) High performance marine vessels. Springer ISBN 978-1-4614-0868-0
11. Fry ED, Graul T (1972) Design and application of modern high-speed catamarans. SNAME Marine Technology
12. Catamarans, Chapter 46 in Ship Design and Construction, SNAME, 2 volume edition 2003, ISBN-13: 978–0750689878
13. Armstrong NA, Moretti V (2010) The practical design of a 102m Trimaran Ferry for Taiwan Strait, Proceedings, Shanghai HPMV Conference, April, 2010, Shanghai, China
14. Shao SI (2000) K50 type fast catamaran ferry, proceedings of HPMV'2000 CHINA, April 19–22, Shanghai, China
15. Allan RG (1996) Application and advantages of catamarans for coastal patrol vessels, SNAME Mar Technol 33(2), ISSN 0025-3316
16. Problem concerned with high speed craft with large size, fast ferry international conference, Part 2, April, 1992
17. Faltinsen OM (1991) Speed loss & Operability of catamaran & SES in a Sea Way, FAST'91 Proceedings, Dec. 1991, Norway
18. Bliault A, Yun L (2000) Theory and design of air cushion craft, Pub Arnold/Elsevier, ISBN 0 340 67650 7 and 0 470 23621 3 (Wiley), p 632.
19. Yun L, Bliault A, Doo J (2010) WIG craft and ekranoplan, Ground effect craft technology. Springer ISBN 978-1-4419-0041-8

Chapter 3
Buoyancy and Stability

3.1 Introduction

To develop the design of a multihull vessel, we must start by taking the initial ideas documented from Chap. 2, for example target length and displacement, and by developing the geometry of the hulls determine the hydrostatic characteristics, using some coefficients to guide the geometry.

From a consideration of the coefficients and previous vessel statistics we will have sufficient information to prepare a set of lines. Once we can satisfy Archimedes' law to match buoyancy and mass, an analysis of static stability can be conducted to determine acceptability against criteria from the IMO.

The IMO [1] has devoted considerable effort to preparing guidelines for the design of high-speed craft, including catamarans and multihull vessels, so following a summary of the basic geometric parameters , we will then look at the requirements for stability, including potential damage conditions and consequent compartment flooding, set by the IMO. Other institutions, such as Det Norske Veritas, Lloyds, ABS, and Korean Register [2–7], also have rules that provide guidance on structural design and link back to intact and damaged conditions investigated for stability. We will take a look at these mainly in Chap. 12.

Our first step after selecting our desired overall dimensions and preliminary shape of the hulls based on mission requirements and statistics from vessels that have been built will be to calculate the buoyancy, centers, and coefficients of form using a full set of lines for our own design.

We can then recalculate the static righting moments and plot the stability curves for our craft and recheck these with IMO rules to guide us as to whether we conform to safe design criteria.

Further check against structural criteria given in the classification societies' rules will ensure that we can design an acceptable craft for the geographical area in which the vessel will operate.

L. Yun et al., *High Speed Catamarans and Multihulls*,
https://doi.org/10.1007/978-1-4939-7891-5_3

Thus, the starting point is hull geometry in the form of a set of lines, together with the overall vessel mass and center of gravity (CG). At this time the mass and CG will be initial estimates, most likely still based on statistics as described in Chap. 2. It is normal that a number of cycles will be carried out to recheck once specific structure and outfitting information is available. The final test will be static trials on the actual vessel. We will assume that a preliminary assessment of configuration has indeed been made following the approach in Chap. 2, so that the designer can prepare data at this stage focused on the target mission and optimization within an envelope of desired characteristics.

Our intent with the work based on the hull geometry is as follows:

- Prepare basic hydrostatics—calculation of waterplane and cross-sectional areas, displaced volume, center of buoyancy and mass, coefficients of form, and initial estimates for speed and power in calm water using rules of thumb.
- Adjust hull geometry based on coefficients of form to achieve desired vessel characteristics at specified service speed. Lines may need to be adjusted locally to account for changing characteristics like desired vessel design speed and Fr_L rises and dynamic lift increases as follows:
  - As speed and dynamic lift increase, the bow will pitch up in addition to the effect from hull-form-generated waves. This tendency slows if lines are flattened toward the stern. There is a pitch down moment due to LCG moving forward relative to the center of lift as it moves aft as speed increases toward planning, so the LCG needs to be located further aft for faster vessels, suggesting a static LCB that is also further aft than on slower displacement vessels.
  - Using a finer bow shape gives less lift to steady pitch motion in waves but reduces pitch response, so it is very helpful for a semidisplacement speed regime.
- Determine the effect of increasing the length for the same displacement, that is, a reduction of Fr_L, placing craft back in a semiplaning region and a higher L/b, producing a lower wave-making drag.
- Determine the transverse stability for multihulls—prepare the curves of stability for service condition and minimum and maximum displacement conditions; there are much lower angles before deck immersion than on a monohull. Conduct a first pass assessment of the effect of stiffness (GZ) in roll-on motions.
- Assess compartment flooding and design for safety based on subdivision of IMO rules.

3.2 Buoyancy, Centers, and Coefficients of Form

A number of coefficients of geometric form are used to characterize a hull and allow comparison between designs and scaling from models. Some parameters were introduced in Chap. 2. Here we return to the basics for a moment, since the start to

a design requires determining the basic geometric characteristics and identifying the coefficients derived from the proposed vessel lines and initial design data.

Our starting point is the area of the waterplane and its center. If we repeat the calculation at a series of waterlines down to the keel, we can calculate the total volume and the center of buoyancy. We can also do this using the section areas at each station from bow to stern. Using either method we can determine the block coefficient, prismatic coefficient, and other coefficients of form as follows. Please note that below we relate to a catamaran demi-hull with breadth b, waterline length L and displaced volume V. A catamaran displacement will be 2V.

Waterplane Area
We use the ordinates at the section stations with Simpson's rules to estimate the area.

Waterplane Area Coefficient [Example Value 0.8–0.85]
This is calculated at normal draft and is $C_w = A_w/(L \,.\, b)$.

Transverse Section Area Coefficient [Example Value 0.5–0.6]
Normally calculated for midships section $C_m = A_m/(b \,.\, d)$.

Displaced Volume
We use the cross-section areas at the section stations with Simpson's rules to estimate the volume. This can be done at various drafts from the keel up.

Center of Flotation
This is the center of area of the waterplane, which is useful for determining trim at small angles.

Center of Buoyancy
This is the centroid of the volume displaced by the hull. It has two dimensions, KB, which defines the height from the keel, and LCB, which defines the distance forward or aft of amidships.

Center of Gravity
This is the centroid of the mass of the vessel. It has two dimensions, KB, which defines the height from the keel, and LCG, which defines the distance forward or aft of amidships.

Block Coefficient [Example Value 0.35–0.45]
This is the ratio of the displaced volume to the rectangular block displaced by L, b, and d.

$C_b = V/(L.b.d)$. Note for a catamaran this is determined for each demihull.

Prismatic Coefficient [Example Value 0.6–0.75]
This is the ratio of the displaced volume to a tube the same length as the hull, with the midships cross section, which indicates the fineness of bow entrance and stern taper:

$$C_p = V/(A_m.L)$$

3.3 Static Intact Stability

The first steps are as follows:

- Calculate waterplane area
- Calculate moments of area for waterplane
- Calculate displaced volume using Simpson's rule and the sectional areas at each station. If the bow or stern includes significant curvature, the section spacing can be adjusted so as to maintain accuracy
- Calculate moments of volume about amidships
- Determine centers of buoyancy, KB and LCB
- Calculate the key coefficients, C_b and C_p, at design waterline

The same data for the vessel displacement characteristics, together with the mass and center of gravity for the vessel, are used to assess static stability, calculating the righting moment available from the upward buoyancy force compared with the overturning moment from the vessel mass operating at its vertical centre of gravity (VCG) and any other disturbing forces such as wind or centripetal turning force.

3.4 Transverse Stability

Calculation of catamaran buoyancy is the same as for a conventional monohull craft, taking into account the two separate hulls, as we saw earlier. The calculation of the transverse stability of a catamaran is a little different due to the hull separation.

The initial transverse metacentric height above the vertical CG, $h = \mathrm{GM}$ (m), for a catamaran can be calculated as follows (Fig. 3.1):

$$h = r + z_c - z_g = \frac{2\gamma\left(I_x^d + k_d^2 S_d\right)}{D} + z_c - z_g, \tag{3.1}$$

where

I_x^d Moment of inertia of demihull design waterline area with respect to x-axis of demihull (m^4);
γ Density of water (t/m^3);
k_d, S_d Distance between catamaran longitudinal centerline and demihull centerline (m), and area of demihull design waterline plane (m^2);
z_c, z_g Height of catamaran center of buoyancy and C.G. from baseline (m);
r Initial transverse metacentric radius (normally referred to as BM) (m);
D Displacement of catamaran (t).

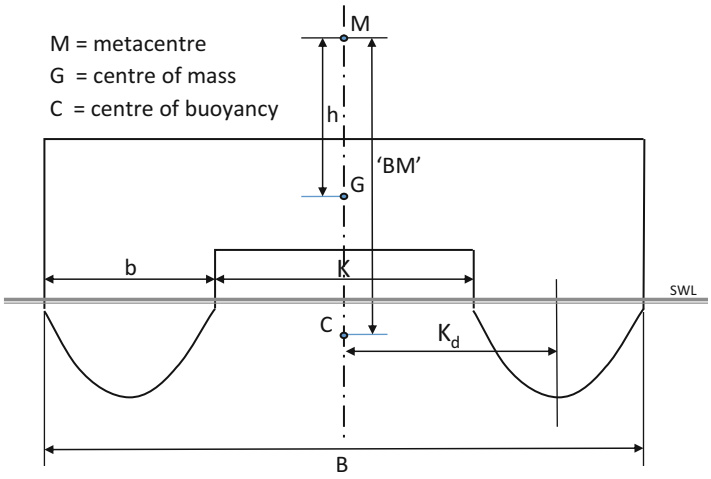

Fig. 3.1 Geometry cross-section diagram

I_x^{d} can be obtained using the lines of the demihulls as follows:

$$I_x^d = \frac{2}{3}\int_{-L/2}^{+L/2} y^3 dx = \frac{2}{3}\Delta L \sum y^3, \tag{3.2}$$

where

y Coordinate value of demihull waterline, from longitudinal central plane;
ΔL Spacing between stations.

If hull lines are lacking at the preliminary design stage, one can use the following formula for an approximate estimation:

$$I_x^{\mathrm{d}} = \frac{D}{2\gamma} \bullet \frac{\alpha^2 b^2}{11.4\delta T}, \tag{3.3}$$

where

α Demihull waterline area coefficient C_{w};
b Demihull beam at midships or central parallel (m);
T Demihull draft at keel (m);
δ Demihull block coefficient C_{b}.

The height of the center of buoyancy z_{c} can also be obtained empirically where there are no hull lines at the initial design stage by referring to the expected waterline area coefficient and the demihull expected block coefficient as follows:

$$z_{\mathrm{c}} = \frac{T}{1 + \delta/\alpha}. \tag{3.4}$$

Thus the transverse metacentric height can be estimated. In comparison with a monohull, the GM will be up to four times as great due to demihull separation.

Since the transverse stability reserve for a catamaran is very large at small angles of heel (say 0–5°), the static transverse restoring moment arm can be assumed linear in relation to the heeling angle at the initial design stage, and the restoring moment can be estimated from

$$M_{\mathrm{sp}} = 0.0174 Dh\theta_{\mathrm{sp}},$$

$$M_{\mathrm{dp}} = 0.0087 Dh\theta_{\mathrm{dp}}, \tag{3.5}$$

where

M_{sp}, M_{dp} Static and dynamic transverse restoring moment, respectively, balancing the heeling moment caused by wind pressure, centrifugal moment during turning, and concentrated passengers at one side of the vessel;
θ_{sp}, θ_{dp} Catamaran static and dynamic heeling angles, respectively (deg).

The heeling moment caused by wind pressure can be expressed by

$$M_{\mathrm{h}} = 0.001 pS_{\mathrm{p}} z_{\mathrm{p}}, \tag{3.6}$$

where

M_{h} Heeling moment (kg-m);
p Wind pressure (kg/m^2), (0.5 ρ V^2);
S_{p} Lateral projected area of catamaran, above sea level (m^2);
z_{p} Equivalent heeling moment arm for wind pressure (m),

where $z_{\mathrm{p}} = T/2 + z_p'$ and

z_{p}' Distance of center of pressure above center of laterally projected area of catamaran above sea surface (m).

To satisfy the requirement for the transverse stability, we have

$$M_{\mathrm{sp}}, M_{\mathrm{dp}} > kM_{\mathrm{h}}/1000, \tag{3.7}$$

where k is a reserve coefficient. Note that here M_{h} is in kg.m from above, while M_{sp} and M_{dp} are in t.m from Eqs. 3.5 and 3.6. In general, the authors have used $k = 3$ against the estimate for wind when making initial estimates before setting out vessel lines; however, the most important thing is to determine the heeling moment so as to predict the rolling angle due to the cases required by the IMO. In most cases, the heel due to wind will be small, but it does need to be determined because it also needs to be taken into account when considering damaged stability, as considered in what follows.

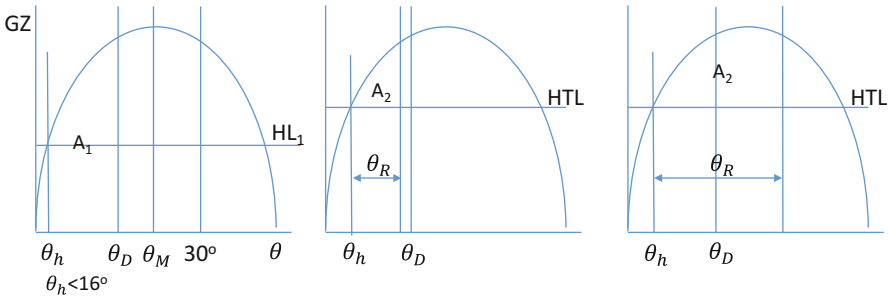

θ_h Roll angle due wind
θ_d Roll angle to down flooding
θ_m Roll angle for Maximum GZ
θ_R Roll angle of vessel due to maximum motion response

A_1 stability moment prior to down flooding when in wind
= total area under GZ curve to least of θ_D θ_M or 30°

A_2 stabilizing moment in wind gusts and passenger crowding or turning
= area bounded by θ_R, HTL and GZ curve ≥ 0.028 m.rad

Fig. 3.2 Intact stability curves

Once the preceding calculations have been made, it is necessary to construct the transverse stability curves for the vessel and verify that the requirements specified by the IMO can be met, as in the following paragraphs.

Note that for a multihull vessel, heeling will be symmetrical at low angles, until the downward-moving deck edge is immersed, unless the cross structure is buoyant and has low clearance from the SWL. The rotation center will then move from the longitudinal centerline toward the upward-moving demihull, unless buoyancy within the cross structure restrains its movement and adds to the stability moment. It is around the point of deck edge immersion or down flooding that the GZ curve will peak (Fig. 3.2). This needs to be kept in mind when the hull and cross structure form above the static waterline are being selected.

The transverse metacentric height (GM_T) will also be important later when analyzing motion in a seaway (Chap. 6), together with a number of the other coefficients calculated for the design proposal.

3.5 Longitudinal Stability

The initial longitudinal metacentric height H (GM_L) can be written

$$H = R + z_c - z_g, \tag{3.8}$$

where R is the initial longitudinal metacentric radius $R = \frac{I_y}{D/\gamma}$, where

$$I_y = 2 \int_{-L/2}^{L/2} yx^2 dx. \tag{3.9}$$

Here x and y are the waterplane line ordinates. If lines are lacking at the initial design stage, R may be estimated as follows for a typical catamaran:

$$R = \frac{\alpha^2}{14\delta} \bullet \frac{L^2}{T}. \tag{3.10}$$

The characteristic of a catamaran is its higher transverse stability than that of a conventional monohull due to demihull separation but a smaller longitudinal stability than that of conventional monohulls due to demihull fineness of form.

The natural period in roll will be closer to the longitudinal natural period, see Eqs. 3.10 and 3.3, due to lower overall length/beam ratio (L/B, where $B = b + 2k_d$) compared to a monohull, and this can cause uncomfortable motion in oblique waves, which will be discussed in later chapters.

3.6 Damaged Stability

Our objective with this calculation is to determine the maximum watertight compartment size suitable for our catamaran, including the influence of the relative position of bulkheads, so as to help us when designing the internal positioning of the main machinery. The starting basis is that the catamaran upper deck watertight compartmentation extends above the damage, limiting flooding to the damaged compartments, with the waterline and free water surface in the damaged compartment(s) at sea level. The requirements for a catamaran are the same as for a conventional monohull and can be expressed as follows:

- The minimum distance from the waterline to the main (upper) deck of a damaged catamaran must be larger than that which satisfies the IMO rules and given classification society;
- The transverse metacentric height of a damaged catamaran in its neutral position must be positive and comply with the requirements for the rules.

The average additional draft ΔT, heeling angle θ, trimming angle ψ, and transverse metacentric height h' for a damaged catamaran can be expressed approximately as follows:

$$\Delta T = P/\gamma S_w,$$

$$tg\theta = \frac{Py_p}{D_0 h_0 + \varepsilon P + \gamma \Delta I_x - \gamma i_x},$$

$$tg\psi = \frac{P\left(x_p - x_f\right)}{D_0 H_0 + \varepsilon P + \gamma \Delta I_y + \gamma i_y},$$

$$h' = \frac{D_0 h_0 + \varepsilon P - \gamma (i_x - \Delta I_x)}{D_0 + P}, \tag{3.11}$$

where

D_0	Displacement;
S_w	Design waterline plane area;
h_0, H_0	Transverse and longitudinal initial metacentric height of intact catamaran;
P	Weight of flooding water (based on flooded compartment volume to SWL);
ε	Distance between center of flooding water to center of added layer of displacement that compensates the flooded compartment;
x_p, y_p	Coordinates of center of gravity of flooding water weight;
ΔI_x, ΔI_y	Additional moments of inertia of water area due to increase of catamaran draft;
i_x, i_y	Moment of inertia of free liquid surface of damaged compartment with respect to transverse and longitudinal axis through C.G of catamaran, where

$$i_x = i_{x0} + k_d^2 s_w \quad \text{and} \quad i_y = i_{y0} + y_p^{'2} s_w; \tag{3.12}$$

i_{x0}, i_{y0}	Moment of inertia of flooded compartment waterline area;
s_w	Area of waterline of flooded compartment;
k_d	Distance between longitudinal centerline of catamaran and demihull;
$y_p^{'}$	Distance between waterline center of area of flooded compartment and catamaran transverse axis.

In general, catamarans have a large stability reserve, floodability is fine, and there is generally no difficulty in satisfying the requirements of the IMO and the classification societies, as long as attention is paid to watertight compartmentation of the demihull structures. This approach is normally consistent with the structural requirements of catamaran demihull design, as it is advantageous to make these "beam" structures of the hulls stiff to ease interaction with the boxlike cross beam and cabin superstructure.

3.7 IMO High-Speed Craft Requirements [1]

The IMO HSC Code generally considers two main conditions for high-speed craft, the displacement mode and the nondisplacement (planing) mode. Additionally, it considers cargo and passenger craft. The HSC code covers all high-speed marine craft. The primary focus of the guidance is stability in the displacement mode considering roll stability with a quasi-static method. Here we review the requirements specific to multihull vessels and give some thoughts of our own for designers.

3.7.1 Intact Buoyancy and Subdivision

The IMO requires sufficient reserve buoyancy in both intact and damaged conditions to be able to meet the stability requirements summarized below by means of watertight compartments that are located below the datum watertight main deck that have structural integrity in both intact service conditions and where damage has been caused to compartments as defined by the rule damage cases. Subdivision of a vessel into watertight compartments needs to be sufficient to fulfill the requirements for continued integrity under the damage conditions discussed in what follows.

Where assessment of heel angles as in the following paragraphs shows that a vessel will heel such that the watertight main deck would be submerged at its outer edge causing entry of water into nonwatertight compartments, it is important that these have adequate drainage as well as structural integrity for this scenario, so as not to unduly influence vessel stability.

Designers of catamarans need to pay special attention regarding the placement of main machinery and propulsion units such as water jets in the aftmost compartments of demihulls since damage to one of these compartments would create a combination of heel and trim that could impact passengers' ability to evacuate the vessel safely. This also highlights the fact that, while the following IMO guidance relates to heel (roll angle), particularly in a damaged state, a catamaran or multihull is likely to face a combined heel and trim state. The requirements for reserve area under the transverse GZ curve are helpful and must be met, but a designer needs to further consider 3D heel and trim situations before deciding that the design is adequate.

As a rule of thumb, the authors of this book recommend that the longitudinal GZ curve also be constructed and the consequences of damaged states be assessed for reserve stability moment in pitch, in addition to the reserve in roll (heeling reserve).

3.7.2 Intact Stability

Four key attributes are required:

- Stability and active stabilization systems must be present and adequate for safety in both displacement and nondisplacement modes and in the transient mode between these two;

- Buoyancy and stability must be adequate for safety when in displacement mode, both intact and when damaged;
- Stability characteristics must be aligned so that the vessel can safely transit from nondisplacement to displacement via the transient mode, in the case of system malfunction;
- The vessel must be able to withstand the effects of passenger crowding to one side and separately maintain a heel angle generally of less than 8° during high-speed turning maneuvers.

The minimum area required under the GZ curve for righting moment against roll angle is as follows:

$$\text{Agz} = 0.055.(30/\theta)\ \text{m.rad},$$

where θ is the smallest downflooding angle for the vessel in roll, or the angle of maximum GZ, or 30°.

The maximum GZ should occur at an angle of at least 10° (see Fig. 3.2 below for a typical GZ plot).

When considering heeling due to wind, passenger crowding, and dynamic roll in turns and rolling in waves, the static inclination should be less than the values described in what follows. Refer to the GZ diagram in Fig. 3.2 for a graphical explanation.

3.7.3 Heeling Due to Wind

$$\text{HL1} = (\text{Pw}.A.Z)/(9800D)\ \ (\text{m})$$
$$\text{HL2} = 1.5\,\text{HL1} \qquad (\text{to allow for gusting})$$

where

Pw 500 Pa;
A Vessel lateral area above lightest service waterline (m^2);
Z moment arm from center of lateral area to a point half of lightest service draft below WL (m);
D Displacement (tonnes).

3.7.4 Heeling Due to Passenger Crowding and High-Speed Turns

A heeling lever should be developed by assuming passengers are grouped on one side of the vessel close to the muster stations for evacuation in an emergency. The IMO specifies that for the purposes of assessing the effects of passenger weight, the following assumptions should be made:

Passenger weight: 75 kg
Passenger CG standing: 1.0 m above deck, sitting: 0.3 m above seat
Passenger distribution: 4/m^2 (or individually located in seats)

3.7.5 Heeling Lever Due to High-Speed Turning

The turning lever should be calculated as follows:

$$\text{Turning lever} = V_0{}^2/(R.g)\ .\ (\text{KG} - 0.5d) \quad (\text{m}),$$

where

V_0 Vessel speed in turn (m/s);
R Turning radius (m);
g Acceleration due to gravity (m/s^2);
KG VCG above vessel keel (m);
d Mean draft (m).

The IMO recommends that, with the exception of rolling in waves and high-speed turns, vessel maximum inclination due to the previously considered effects should be less than 10°.

3.7.6 Rolling in Waves

The IMO requires the effects of vessel roll on stability to be demonstrated mathematically by the designer. The residual area under the GZ curve above HTL (area A2 in Figs. 3.2 and 3.3) and either to the maximum angle of roll or the angle of downflooding, whichever is least, should be equal to or greater than 0.028 m.rad.

In the initial design stage, when vessel motion characteristics are not analyzed, it is recommended to use a roll angle of 15° or (θ_d–θ_h), whichever is less.

The heeling lever to be considered, HTL, is the sum of the heeling lever due to wind and gusting (HL2) and the greater of passenger crowding or high-speed turning.

3.7.7 Buoyancy and Stability in Damaged Condition

Criteria for side damage and bottom damage are specified by the IMO as as listed below.

Damage to the vessel side shell of a demihull, hull, or sponson (vessel periphery):

- Length of damage $0.1L$, $3 + 0.03L$, or 11 m, whichever is least (Category B vessel damage is to be increased by 50% if it occurs forward of amidships), where L is vessel L_{WL};

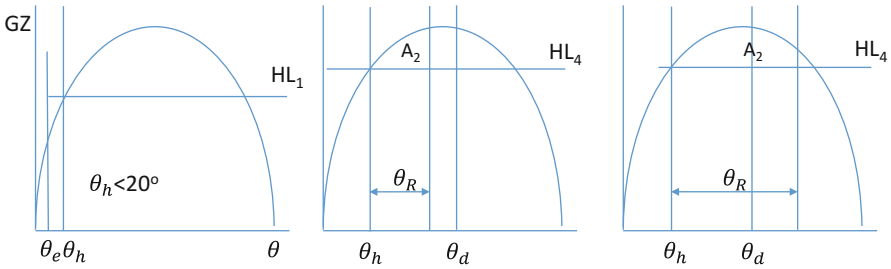

θ_e Equilibrium Roll angle after flooding of damaged compartment
θ_h Roll angle due wind
θ_d Roll angle to down flooding
θ_R Roll angle of vessel due to maximum motion response
A_3 Stabilizing moment in wind and passenger crowding

Fig. 3.3 Damaged stability curves

- Penetration into hull to be the least of $0.2B$, $0.05L$, or 5 m, where B is vessel total beam;
- The vertical extent should be assumed to affect the full depth of the vessel;

Damage to be assumed to bottom of hull or demihull:

- Length as for side damage;
- Transverse damage full breadth of vessel bottom if distance between demihulls is less than 7 m, that is, both hulls are damaged. If spacing is greater than 7 m, then full breadth of a demihull or 7 m, whichever is less;
- Vertical extent to be the lesser of $0.2B$ or 0.5 m.

When calculating the volume of water entering a damaged compartment, the IMO gives the following recommendations for permeability levels:

- Spaces occupied by personnel, void spaces, and spaces for liquid storage: 95%;
- Spaces occupied by vehicles: 90%;
- Machinery compartments: 85%;
- Spaces occupied by cargo or stores: 60%;

Also, recall that water flooding will extend to the equilibrium SWL within damaged compartments.

The criteria for residual stability after damage are as follows:

- The wind heeling angle should be calculated using $P\text{w} = 120$ Pa. The steady wind heeling angle in damaged conditions should not be more than 20°.
- The roll angle in waves should be considered as for intact stability.
- The downflooding angle should be the truncation of the GZ curve (Fig. 3.3).
- In addition to the effect of steady wind, the effect of wind together with passenger crowding should be assessed.

- The residual stability area under the GZ curve should be at least 0.028 m.rad (see GZ diagram for damaged condition as in Fig. 3.3 below).
- It should be noted that as for intact stability, damage to catamarans or multihull vessels will result in significant asymmetrical trim, and so assessment also using the longitudinal GZ curve will be important to verify the pitch attitude of the vessel in a damaged state as well as the angle of heel. If the damage involves aft machinery spaces, the main watertight deck could become submerged close to the stern even though the heeling reserve is shown to be sufficient.
- It may be further noted that the approach of taking bottom damage across both hulls for vessels with demihull spacing less than 7 m may not be conservative. A catamaran may have a greater heel if the specified damage is applied to just one demihull, as with larger vessels, and so this author recommends considering that case even for smaller vessels and making an assessment of longitudinal the trim and GZ reserve.

The following requirements also apply for buoyancy and stability after compartment damage causing flooding:

- For passenger vessels the final waterline should be at least 300 mm below the level of any opening through which further flooding could take place. For cargo vessels the freeboard requirement is 150 mm.
- The angle of inclination in any direction should be less than 10°. While the IMO allows for a temporary maximum of 15°, this needs to be able to be reduced to 10° within 15 min, which may require significant emergency pumping equipment. It is probably better to simply hold to the 10° limit. For cargo craft the limit is 15°.
- Emergency escape stations must be located with suitable freeboard for deployment of survival rafts and other equipment.
- Passenger compartments must not be flooded so as to impede personnel escape.
- Emergency equipment and services must be located so as not to be affected by the orientation and waterline of the damaged vessel.

In light of the foregoing points on damage conditions, let us reflect a little on the circumstances that might inflict damage to help us put together an approach for compartmentation since we have options first concerning the hulls' external geometry and then the spacing of transverse bulkheads.

Side damage will most likely be caused by impact with a quayside or another vessel. There may be sharp penetration or impact over a wide area that deforms the side shell and side frames between bulkheads. Penetration or tearing of the side shell would lead to flooding. Considering the lengths specified earlier and knowing that it might occur anywhere along the hull, the worst case would be for damage to affect two successive compartments, even if the watertight compartments are longer than the damage lengths specified. On this basis the designer needs to ensure that the vessel has stability reserve in case the worst two compartments are punctured.

It may be noted that it is usual to provide a collision damage bulkhead forward of the main accommodations to provide buoyancy and longitudinal safety reserve to

cover the case of head-on collision with another vessel, quayside, or undocumented submerged hazards (rock outcrops or local shallows, perhaps combined with tidal changes or river rapids for inland vessels) (see Chap. 12 concerning structural design). It may therefore be expected that the bottom damage we are concerned with here will be aft of the collision bulkhead.

Bottom damage may occur from grounding. Uneven rocky, coral, or gravel sea or river beds can apply heavy local loadings when combined with vessel speed and cause tearing of the hull plating as well as deformation in the area specified earlier by the IMO. Once again, the damage will affect two compartments, more likely in the area forward of amidships than aft, and in the case of grounding the problem may not be vessel heeling but rather that the flooding damage (to one or both demihulls) prevents the vessel from refloating until a higher tide provides assistance. Once a salvage vessel has pulled the multihull back off the rocks or grounding area, it is then that consideration of the vessel's floating condition while damaged becomes pertinent. The stability reserve with either one or both demihulls damaged needs to be assessed to verify the possibility of safe salvage.

It is also possible that the structure forward of the collision watertight bulkhead will be damaged by a grounding against a rock outcrop so, which would affect one compartment forward and one compartment aft of the collision bulkhead. Designers should look at this to determine whether it is a design control case, if the vessel is to be used in an area where such hazards apply.

Once the compartmentation itself has been selected, verification of structural integrity can be carried out during detail structural design (Chap. 12). The intact structure will be tested against both static and dynamic loadings, while the damaged structure may be tested against static loading plus dynamic loadings with an appropriate safety factor that relates to the static condition after an accident and subsequent recovery to port.

One final item to remember when setting compartmentation: International environmental rules are strict and becoming stricter regarding any pollution of the sea due to spillage. It is important that a designer ensure that in the case of compartment damage, the contents of any internal tankage will remain safe and not be spilled. This also applies to piping carrying fuel, lubricating or hydraulic oil, and so forth. This may be considered a detail at the initial stage of design, but the general approach needs to be followed so as to come up with a resilient design for the owner! We return to this subject in Chap. 13.

3.7.8 Inclining and Stability Verification

Unless a vessel is part of a previously proven and accepted design series and is within 2% in lightweight displacement and 1% deviation of LCG, then inclining tests will be required to verify vessel stability as documented in the stability information book to be maintained by the vessel owners and master during operation. The stability information book prepared for the final design will document

vessel loading condition envelope and associated cross curves of stability. If an inclining test is not practical, an alternative of a detailed lightweight survey and subsequent revision of the stability information book is allowed by the IMO.

3.7.9 Dynamic Stabilization Systems

Many high-speed multihull vessels have dynamic stabilization in the form of foils at the bows, amidships, or stern. Additionally, at the stern, flaps or interrupters may be installed to control the dynamic trim of the vessel at speed. It is important to bear in mind that these systems should not be considered a means to assist in meeting the stability criteria discussed earlier.

Whether a vessel is a displacement, semidisplacement, or planing vessel, it is the buoyancy and, in the case of fully planing craft, the righting forces available from the planing surfaces that provide the righting moment and, thus, the stability reserve, for both the intact and damaged cases. The main issue to deal with concerning dynamic stabilization is that these systems should not apply moments that would further degrade vessel stability, rather than applying damping to the vessel motions. This is particularly important for very high-speed vessels and planing designs.

For intact stability, the interaction of dynamic stabilization systems will be part of the analysis and eventual specification of the system.

For the damaged cases it is recommended that the designer consider the scenario that causes the damage and look at the response of the stabilizer to the timestep-based vessel trajectory. The control system might then be adjusted to respond to motion and accelerations to provide a neutral control force and moment. If this is not possible, the consequences would need to be defined and discussed with the relevant classification society in the first place.

3.7.10 Operation in Conditions Where Icing May Occur

If a vessel is to be operated in a cold region where snow and ice can occur, then accretion should be taken into account for stability calculations. Guidance is provided in annex 5 to reference [1] as summarized in the following table.

Item	Icing allowance to be applied	
1	Exposed weather decks and gangways	30 kg/m^2
2	Projected lateral area of each side of vessel above waterplane	7.5 kg/m^2
3	For rails, booms, small discontinuous objects, and spars (not masts), a factor to be applied for accretion and moment	Factor on lateral area 1.05 Factor on moment due to ice accretion 1.1
4	Care should be taken to assess possible asymmetric accretion on vessel cross structure and consequent reduction of stability	

The IMO code specifies the areas where icing must be considered, for example north of Iceland; above the north coasts of Canada, Russia, and Norway; the Bering and Okhotsk Seas, above 56° latitude in the Baltic Sea; and south of 60° longitude toward the South Pole. A chart is provided for reference. It is noted, though, that within several of these areas, conditions may require anything from 50 to 200% of the aforementioned accretion requirements. A designer (or the operator client) working on a vessel for these areas is likely to be knowledgeable about icing conditions, but it is recommended to take direct advice from the IMO and perhaps the relevant classification society before making a detailed stability evaluation.

The IMO requires such an assessment to cover the expected voyage duration under such conditions, including consumption rates for fuel and consumables.

From the preceding discussion it is clear that snow and ice accretion can be severe, and so a first step for the designer once an assessment of the potential masses have been made would be to look at how these might be reduced by minimizing exposed items as under item 3 in the preceding table and careful design of both horizontal and lateral surfaces.

3.7.11 Considerations for Other Multihull Types

Let us consider configurations beyond the catamaran, such as the trimaran and its cousin, the slender main hull with sponsons. In order that sponsons have minimized drag for vessels operating in the semidisplacement regime, they may have a sharp V form upward from the keel. At very small angles of heel, the stability moment will be small, the main righting moment being provided by the main hull transverse form. As heel increases to, say, 5°, it will be necessary for the sponsons to pick up more buoyancy on the downgoing side and provide support. The design to achieve this should be a curved inner surface from the sponson over to the connection with the main hull, shaped so that the heel angle is restrained to avoid going beyond 10°. Depending on the length of the sponsons, it may also be advantageous to have a spray chine or longitudinal step on the sponson inside surface above the SWL, which will also allow for more buoyancy at heel beyond 5°. The rate of buoyancy increase is important owing to the high CG and slender main hull to avoid having a GZ curve that is low and concave at the initial heel angles. Such a curve would result in the vessel taking a long time to return to vertical in a seaway with transverse wave heading and operating at angles of heel in low side winds. While not a safety issue as such, operation with long periods at heel are disconcerting to passengers, even if for a professional sailor it may be considered normal.

Semiplaning trimarans will have sponsons or outer hulls that operate in the same Fr_L regime, so the rate of generation of buoyancy moment should be high in the initial heel angles up to between 5 and 10°, at the point where the upward-moving sponson hull keel leaves the water or the cross structure connecting to the downward-moving sponson enters the water. It is clearly advantageous for the cross member to be watertight so the GZ curve can continue to rise and a form

satisfying the IMO requirements can be designed. Once the rising sponson has left the water, the geometry is more like an asymmetric catamaran (recall the Polynesian craft!). The center of buoyancy will move as buoyancy is gained by the sponson and then cross structure, so a stepwise calculation with heel is necessary to construct the curve, as opposed to assuming rotation about a fixed center, as might be the case for a displacement or semiplaning trimaran at small roll angles where both sponsons contribute buoyancy.

The foregoing discussion also applies to planing trimarans operating at low speeds. At service speed, the main support will be the dynamic pressure on each planing surface, just as for a planing catamaran. The trimaran will rotate about the center hull at small angles, and righting moments will be generated by the changed orientation of the lift forces.

Depending on the V form of the sponson hulls' cross section, vessel heel may increase to between 5 and 10° before the rising hull keel leaves the water. At planing speeds it is not useful to have a cross structure designed to enter the water as the vessel heels in normal operation due to the sudden drag increase and wave slam forces that might be induced. A planing trimaran therefore needs to meet IMO stability requirements without the cross structure entering the water at speed.

The requirements at low speed and planing speed may not be inconsistent since the vessel will rise from its displacement draft once the transition to planing is achieved.

Finally, if the planing hulls are stepped, the longitudinal distribution of forces will change compared with a simple deep V planing hull. As the vessel heels, generally due to waves or to turning rather than wind, the steps will be open to ventilation on the rising side, while on the down side the step may lose ventilation once it drops below the running waterline at the step. The consequence is increased turbulence in the flow regime at the planing surfaces. In turns, the vessel may slide outward as a result of the centripetal force. Longitudinal spray rails on the V surfaces are necessary to generate resisting force and avoid sliding turns. Spray rails and longitudinal chines are also useful devices to aid vessel stability in a straight line in planing craft.

3.7.12 Stability in Nondisplacement Mode and in Transient Conditions

Several conditions need consideration for vessels that can operate in planing mode either simply through a planing hull configuration or through a combination where a catamaran or multihull has supporting foils mounted at the keel.

At service condition, fully planing, passengers may be expected to be seated, and passenger crowding will apply to displacement mode should an emergency occur. The effect of wind and wind gusts on vessel heel clearly needs to be addressed as well as vessel turning (Fig. 3.4), in this case considering a vessel supported on the

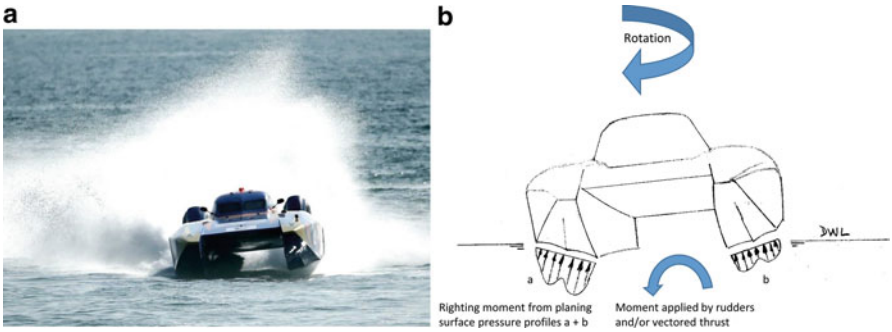

Fig. 3.4 (**a**) Xcat in turn maneuver; (**b**) planing forces in turn maneuver

dynamic lifting forces at the planing surfaces. The GZ curve at service speed therefore needs to be constructed from a determination of dynamic righting forces as the vessel is rolled from vertical. Once the curve has been so constructed, equivalent criteria to those for the displacement case discussed earlier can be applied to test acceptability as in Fig. 3.2.

The racing catamaran shown turning in Fig. 3.4 is banked into the turn. The centrifugal force of the turn at CG is balanced by a centripetal force provided by the turned rudders or propulsion at or below the keel line, and the bow will be turned inward relative to the turning circle achieved so that a velocity vector will exist beam-wise outward, increasing the dynamic pressure on the outer demihull and lowering it on the inner, so that the vessel leans in to the turn. This action is typical of racing craft with a relatively low CG, while large ferry vessels turning at lower speeds and with a high CG will tend to lean out during turns.

Using equivalent criteria for the displacement case and the planing (or planing and foil support) case, it may be considered at the initial design stage that the transient condition for a planing design will also be safe. It should be noted that a planing or hybrid configuration should be analyzed for the static or low-speed displacement condition as well as the service condition while planing or foil support planing and meet the requirement for the displacement case first. The assumption that transient conditions may be assumed to be OK if displacement and service conditions are acceptable in the initial design needs to be tested further in the second round of design. Small changes in hull bottom geometry can have a significant effect on the balance of dynamic forces, and as speed increases, the planing wetted surface will change, affecting the LCB and dynamic metacentric height KM [8]. We discuss this further in Chap. 6 as the response of planing craft to unsteady hydrodynamic flows may be undesirable unsteady motions (porpoising, coupled roll/pitch/yaw, chine running), even though the vessel is quasi-statically stable.

The IMO guidance for nondisplacement mode specifies that calculations or tests should be carried out to show that when subject to any disturbance within the design operational envelope causing roll, pitch, heave, or steady heel, the vessel will return

to original attitude once the disturbance has passed. Additionally, heel angle in calm conditions should not exceed 10° due to passenger movement or beam on winds. When turning, outward heel should not exceed 12° due to wind and centrifugal force (8° due to turning maneuver only).

The analytical approach for planing vessels is subject to research at the time of publication of this book, as discussed in [8]. CFD should help to improve the assessment of dynamic stability, but in the meantime, model testing can assist once a configuration is selected, and vessel trials as required by the IMO for verification of safe performance will need to be completed, as detailed in the HSC Code [1].

3.8 Classification Society Guidelines

ABS, GL Det Norske Veritas, and Lloyd's all refer to the IMO Code of Safety for High Speed Craft for stability criteria. They then provide guidance on structural design to generate a vessel that is resilient to the intact and damaged cases, translated into loading conditions for the vessel structure under study.

Chapter 12 provides an introduction to structural design linked to the classification society guidelines. For the designer, once the overall hull form has been outlined and intact stability confirmed, the damage condition requirements provide a guide to setting up the framing, bulkhead, and watertight compartmentation; then, with an initial configuration available, calculation of hull girder stresses will allow for an optimization cycle to minimize the consequences of damage and compartment flooding, from a static point of view.

Further cycles will be needed to review extreme structure loading cases and ensure compartmentation remains compliant with the rules. The expected design cycles related to vessel stability are shown subsequently in Fig. 3.5.

3.9 Moving on . . .

To get to this point, the designer will have prepared the summary mission requirements and generated data sheets listing key weights and center data for the vessel and outfitting assumed, such as in Appendix 2. Following use of the coefficients of form and quick estimate formulas to select basic attributes, a set of vessel lines will have been prepared, checked against the target form coefficients, and used to test intact and damaged stability.

In many cases, the designer will have two or three hull form options to investigate, either in a geometric series or perhaps more varied, such as comparing a catamaran to a semiswath form or a trimaran form.

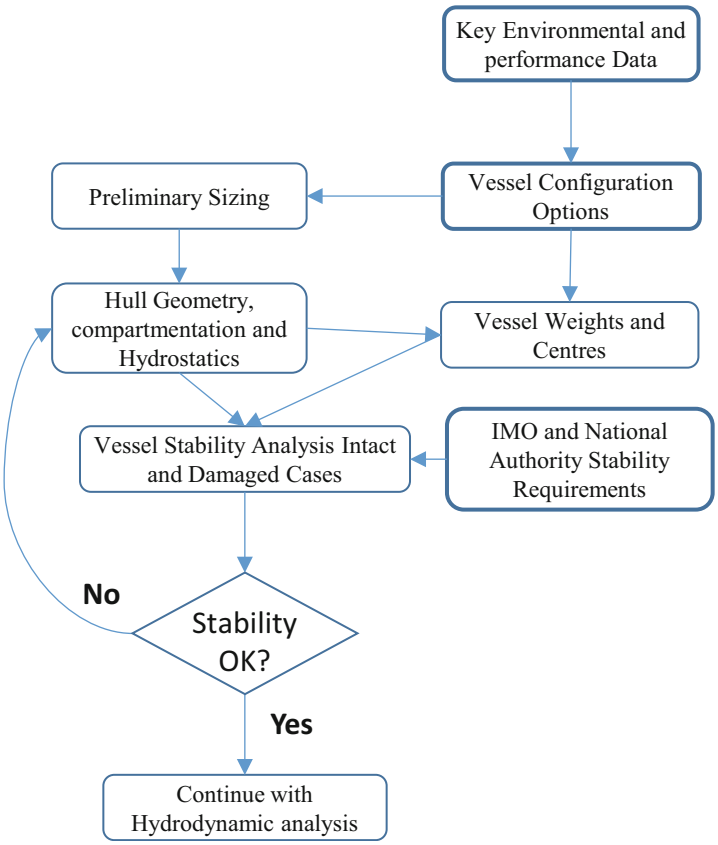

Fig. 3.5 Stability design cycle

While not yet optimized for resistance, motions in a seaway, or structural configuration, the hull lines and vessel overall geometry will now be sufficient to move ahead and look at resistance in calm waters and in a seaway. Once these can be estimated and compared, it will be possible to select a concept for detailed design and start to refine the characteristics of the selected configuration.

If the client has given selection criteria, these need to be kept in mind as the performance estimation and selection process are completed. Even without client specifications it is important for the designer to prepare such criteria, as noted in Chap. 2, so that the selection process can be fact based as the design matures and adjustments can be documented as the project changes, so that changes are not adopted informally, which could cause uncontrolled deviations from the original project.

References

1. International Code of Safety for High Speed Craft, IMO, publication IA-185E, ISBN 92789 28014 2402 (2000). Amendments and resolutions after 2000 are available on IMO web site IMO.org
2. Lloyds Register Rules for SCC (download from Lloyds Register of Shipping site). www.LR.org
3. Lloyds Register Rules for Trimarans (download from Lloyds Register of Shipping site). www.LR.org
4. DnV Rules for High Speed Light Craft and Naval Surface Craft (download from DnVGL site). www.dnvgl.com
5. ABS Rules for Classification of High Speed Craft (download from ABS site Eagle.org
6. Turk Loydu – Rules for High Speed Craft, Chapter 7 (download from Turk Loydu site). www.turkloydu.org/en-us
7. Korea Register of Shipping Rules for High Speed and Light Crafts and also Rules for Recreational Craft at www.krsusa.cloudapp.net/Files/KRRules/KRRules2016/KRRulesE.html
8. D Ruscelli, P Gualeni, M Viviani (2012) An overview of Planing monohulls transverse dynamic stability and possible implications with static intact stability rules, Trans RINA. 153(Part B2), Intnl Jnl Small Craft Tech:B73–86, ISBN1740-0694

Chapter 4
Wave Generation and Resistance

4.1 Introduction

The first component of resistance to address is the creation of a wave form at the surface as the vessel moves forward, displacing the water volume in front of it. The water mass is acted upon by the pressure of the hull surface. The action of gravity on the fluid displaced adds to the energy vector projected by the hull as it moves forward, resulting in the energy dissipating as a pattern of waves radiating outward. If the waves meet another surface, they will be reflected, which will happen in the space between the two hulls of a catamaran and if the vessel is running in a confined waterway.

During the nineteenth century, engineers refined the technique of towing flat surfaces and scale models in water tanks to measure total drag forces, including those due to wave making and frictional resistance. Frictional resistance was then deducted to identify the wave-making drag. This approach was developed first by William Froude [1].

After identifying scaling relationships for the forces, mathematical theories were developed to explain the forces due to generated and incident waves. The theory to allow for the calculation of the wave resistance of single hulls has been available since the late nineteenth century. Many scientists and engineers studied these phenomena, and collectively they developed hydrodynamic theory as we know it today. We use the work of a number of them that link up with analysis for catamarans.

Using the Fourier integral method, in 1899, Michell [2] derived the first integral formula for the wave resistance of a ship running in a nonbounded waterway in steady motion. The formula connects wave resistance directly with the ship hull profile. Michell used the assumptions of a thin ship (beam–length ratio << 1), a linear free-surface condition, and negligible effect of viscosity on fluid flow.

Later, in 1928, Havelock [3] found the Green function satisfied conditions for assuming linear free-surface and wave radiation and developed a mathematical

L. Yun et al., *High Speed Catamarans and Multihulls*,
https://doi.org/10.1007/978-1-4939-7891-5_4

model based on Kelvin sources. In this model the velocity potential could be described in terms of Kelvin sources distributed along the central longitudinal plane of a ship.

Lunde in 1951 [4] also used the Kelvin source method, distributing these on the central longitudinal planes of the two demihulls of a catamaran to derive an integral equation for calculating catamaran wave resistance in a nonbounded waterway in steady motion. Eggers (1955) [5] extended this method to calculate the wave resistance of a catamaran running in steady motion in a narrow waterway. Lin and Day [6] applied both Kelvin sources and dipoles simultaneously distributed on the central longitudinal plane of each demihull of a catamaran to calculate the interference between demihulls (transverse flow) and the effect of the asymmetry of the demihulls themselves.

In cases where the demihulls of a catamaran are very thin (beam–length ratio $<<$ 1), and with very small demihull-width-to-hull-spacing ratio (i.e., hulls substantially apart), distributing Kelvin sources on the central longitudinal planes is still a key method for calculating the wave resistance of a catamaran.

Hsiung [7, 8] developed a numerical calculation method for the Michell integral formula for application to monohull vessels. He used a "tent" function to approximate the hull surface and simplified the Michell integral to a quadratic form, related simply to the offsets of the hull surface. The wave resistance matrix was related only to the Froude number and draft–length ratio. Thus, a hull form could be optimized by a mathematical programming method and the offsets obtained after optimization directly so as to enable various performance calculations using computer-aided design. Hsiung [9] extended this method to a catamaran and used it for optimization of the spacing between demihulls and offsets of demihulls. In this chapter, the application of this method to the wave resistance of a catamaran is the main tool that we present.

Since the mid-1970s, following the advance of computer technology, computational fluid mechanics has developed rapidly, and a number of numerical models for calculating wave resistance have resulted. Among them, the most famous is Dawson's (1977) Rankin Source Method [10]. This was based on the panel method or boundary panel method, and also satisfied the quasi-linear free-surface condition. Dawson distributed Rankine sources ($1/r$) on the hull surface and its image, as well as on the local horizontal region (water surface) around the hull, taking the horizontal plane as a mirror. The source densities or strengths on the panels satisfying the basic equations can be obtained based on these boundary conditions. In addition, the resultant of forces acting on the panels in the direction of flow is equivalent to the wave resistance and can be obtained by integration.

By distributing Rankine sources ($1/\underline{r}$) and dipoles $\frac{\partial}{\partial n}\frac{1}{r}$ simultaneously on the panels, the wave resistance and flow field around a catamaran with asymmetric demihull configurations may be calculated.

Rong [11] developed a numerical method for solving the full nonlinear ship–wave problem based on this approach. Although the panel method has been applied widely in ship hydrodynamics, the instability of its solution and complex pre- and

postprocessing has in the past limited its application to relatively slender hull shapes for stable results. In general, a high-speed catamaran or derivatives such as SWATH and WPC have slender demihulls and beam–length ratios $< < 1$, agreeing with the thin-ship assumption, so calculation results are very satisfactory and may be simplified.

Calculation of catamaran wave resistance based directly on thin-ship theory is therefore sufficient for practical application where the vessel is operating in a displacement or semi-displacement regime where hydrodynamic lift forces are low compared with buoyancy. It should be noted at this point that throughout this chapter, we consider a vessel in displacement mode.

A planing catamaran will also be relatively slender, so an initial estimation of wave generation at speeds below the "hump" prior to planing may be assessed, though for speeds where dynamic support predominates, hydrodynamic forces and equilibrium need to be determined using the semi-empirical methods developed by Savitsky and others, as discussed in Chap. 7.

Since slender hull theory is satisfactory for catamarans, comparison to the panel method will be used to assist in explaining our thin-ship theory approach to catamaran wave resistance in what follows.

4.2 Basic Equations

We use a Cartesian coordinate system fixed in a ship with the origin at amidships, with the *xoy* plane on an undisturbed calm water surface, the *x*-axis along the uniform oncoming flow U_∞ positive to the bow, and the *z*-axis up as positive (Fig. 4.1).

Assuming the fluid is homogeneous, incompressible, inviscid, and ideal and the motion is nonrotational, velocity potential $\phi\ (x,y,z,t)$ exists at any given point, and the velocity field can be deduced from velocity potentials as the vector sum of the potential along each axis:

$$V = \phi_x(x, y, z, t), \phi_y(x, y, z, t), \phi_z(x, y, z, t). \tag{4.1}$$

The velocity potential $\phi\ (x,y,z,t)$ in the flow domain must satisfy the Laplace equation to resolve to a single solution. Only after suitable boundary conditions are specified at the hull surface and water free surface will the solution to the Laplace equation be unique. In the case of a body moving on the water surface, the boundary conditions that must be satisfied to meet this criteria are as follows.

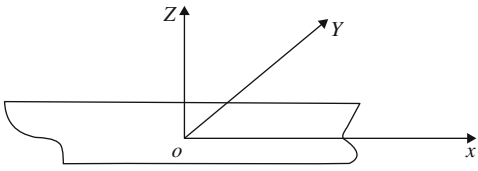

Fig. 4.1 Coordinate system for monohull craft

Kinematic boundary condition on the body surface

Because the body surface S is a solid and fixed wall, it should satisfy

$$\left.\frac{\partial \phi}{\partial n}\right|_S = U_n, \tag{4.2}$$

where n is a unit outward normal vector. The left-hand side of the preceding equation represents the normal velocity of a flow particle point on S, and the right-hand side represents the normal projection of a motion velocity of a certain point on S.

Assume the body surface equation is

$$F(x, y, z, t) = 0. \tag{4.3}$$

The kinematic boundary condition can be deduced from Eq. (4.2) as

$$\frac{DF}{Dt} = F_t + \phi_x F_x + \phi_y F_y + \phi_z F_z = 0 \text{ and } F = 0. \tag{4.4}$$

For constrained waterways the riverbed equation can be represented as

$$z = -H, \tag{4.5}$$

where H is the water depth, which is a fixed boundary that should satisfy the following boundary condition:

$$\phi_z(x, y, -H) = 0. \tag{4.6}$$

Boundary condition at free surface

(1) *Kinematic boundary condition on free surface*

Assuming the equation of the free surface is $F = \zeta(x, y, t) - z = 0$, where ζ is the elevation of the free surface, the boundary condition at the free surface is similar to the kinematic boundary conditions on the body surface. The kinematic boundary condition on the free surface is therefore

$$\frac{DF}{Dt} = \zeta_t + \phi_x \zeta_x + \phi_y \zeta_y - \phi_z = 0 \quad \text{and} \quad F = 0\,. \tag{4.7}$$

Then

$$\zeta_t + \nabla\phi \cdot \nabla\zeta - \phi_z = 0 \quad \text{and} \quad F = 0\,. \tag{4.8}$$

(2) *Dynamic boundary condition on free surface*

Assuming that the free surface is air, according to the Lagrange integral, the dynamic boundary condition on the free surface (equal pressure condition) can be represented as

$$g\zeta + \frac{1}{2}\left(\phi_x^2 + \phi_y^2 + \phi_z^2\right) + \phi_t = 0 \text{ and } \quad F = 0\,. \tag{4.9}$$

Then

$$g\zeta + \frac{1}{2}\nabla\phi \cdot \nabla\phi + \phi_t = 0 \text{ and } \quad F = 0\,. \tag{4.10}$$

Since the free surface is unknown, ς must be eliminated from Eqs. (4.8) and (4.10), and then ϕ on the free surface $z = \varsigma(x, y, t)$ must satisfy the free-surface condition as

$$\phi_{tt} + g\phi_z + \frac{1}{2}\nabla\phi \cdot \nabla(\nabla\phi \cdot \nabla\phi) + 2\nabla\phi \cdot \nabla\phi_t = 0 \text{ and } \quad F = 0\,. \tag{4.11}$$

(3) *Boundary condition at far distance*

To solve the outer domain problem, except for the boundary conditions mentioned earlier, the boundary condition at far distances must be given. Thus, the boundary can be considered closed. This is also called the radiation condition.

In cases where a local disturbance occurs in the far field, then the farther the disturbance is, the less the influence it has on the body. For a body running on the water surface, the radiation condition for there being no wave far upstream (waves have died away) is

$$\nabla\phi = 0, \quad \text{where} \quad \sqrt{x^2 + y^2} \to \infty\,. \tag{4.12}$$

4.3 Panel Method

There are a number of well-proven methods for coming up with solutions to the Laplace equation and boundary conditions summarized earlier. In this section we will introduce the panel method, as applied in ship hydrodynamics (Ogilvie [12]). It is a boundary element method, also called the Green's function method or singularity distribution method. It is a very flexible method for application in situations where complicated boundary conditions exist. The basic characteristic of this method transfers the boundary-value problem of the Laplace equation to solving an integral equation, and the inner/outer flow problem in a three-dimensional domain to finding the singularity distribution on the boundary surfaces. It is substantively a numerical method.

Assuming in the domain that the function τ, $\phi(x, y, z)$ is a harmonic function, ϕ satisfies not only the Laplace equation but also the following boundary conditions:

$$\phi_{xx} + \phi_{yy} + \phi_{zz} = 0 \qquad \text{in domain } \tau, \text{ and} \tag{4.13}$$

$$\left.\frac{\partial \phi}{\partial n}\right|_S = U_n \qquad \text{on boundary } S, \tag{4.14}$$

where n is a unit outward normal vector and U_n is the normal projection of a point velocity on boundary surface S.

According to the third Green's equation, we have

$$\iint_S \left[\phi(P,Q)\frac{\partial}{\partial n}\frac{1}{r(P,Q)} - \frac{1}{r(P,Q)}\frac{\partial \phi(P,Q)}{\partial n}\right] dS = \begin{cases} -4\pi\phi(P) & P \in \tau, \\ -2\pi\phi(P) & P \in S, \\ 0 & P \notin \tau + S, \end{cases} \tag{4.15}$$

where the singularity $Q(\xi, \eta, \zeta) \in S$, $\frac{1}{r(P,Q)}$ represents a space point source, and $\frac{\partial}{\partial n}\frac{1}{r(P,Q)}$ represents a space dipole, which is a harmonic function in the domain $\tau (P \neq Q)$.

The values of $\frac{\partial \phi(P,Q)}{\partial n}$ and $\phi(P,Q)$ on boundary surface S represent the densities of source and dipole, respectively. The preceding equation shows that the potential function at a point can be represented by the singularity distribution on S, being a combination of a space point source and dipole.

When studying the problem concerned with the outward flow from a closed surface, the boundaries can be considered to be $S + S_\infty$, where S_∞ is an assumed outer spherical surface (control surface) and radius $R \to \infty$.

It can be proved that when $\phi \to 0 \ (R \to \infty)$, $R\frac{\partial \phi}{\partial r} \to 0 \ (R \to \infty)$, and thus the integral $\iint\limits_{S_\infty} \left[\phi\frac{\partial}{\partial n}\frac{1}{r} - \frac{1}{r}\frac{\partial \phi}{\partial n}\right] dS \to 0 \ (R \to \infty)$ also tends to 0 as R tends to infinity, where ϕ is a harmonic function in the outward domain of S.

Thus, the third Green's Eq. (4.15) still exists. For the singularity distribution on S, the velocity potential $\phi\ (x,y,z)$ of any point $P(x, y, z)$ on the outward domain of S can be obtained according to this equation.

Actually, $\phi = \frac{1}{r(P,Q)}$ is only a special solution of the Laplace Eq. (4.13). Therefore, the form of ϕ is not unique. If there is a function $G^*(P,Q)$, being a harmonic function everywhere in τ, then clearly the relation

$$G(P,Q) = \frac{1}{r(P,Q)} + G^*(P,Q) \tag{4.16}$$

is still a harmonic function in domain τ and called the Green function. Then the third Green's formula can be rewritten as

$$\iint_S \left[\phi(P,Q)\frac{\partial G(P,Q)}{\partial n} - G(P,Q)\frac{\partial \phi(P,Q)}{\partial n}\right] dS = \begin{cases} -4\pi\phi(P) & P \in \tau, \\ -2\pi\phi(P) & P \in S, \\ 0 & P \notin \tau + S. \end{cases} \tag{4.17}$$

From this equation it can be deduced that

$$\phi(P) = \iint_S \sigma(Q)\ \ G(P,Q)dS, \tag{4.18}$$

where the singularity $Q(\xi,\eta,\zeta) \in S$ and field point $P(x,y,z) \in \tau$ but $\notin S$, where $\in$ and $\notin$ denote equivalent and not equivalent.

If $P(x,y,z) \in S$ and $P = Q, r(P,Q) = \sqrt{(x-\xi)^2 + (y-\eta)^2 + (z-\zeta)^2} = 0$, then integrating the function in Eq. (4.18) gives a singularity.

After some manipulations, we have

$$\left.\frac{\partial\phi(P)}{\partial n}\right|_S = 2\pi\sigma(P) + \iint_{S-P} \sigma(P)\frac{\partial G(P,Q)}{\partial n}dS. \tag{4.19}$$

Inserting boundary condition (4.14) into this equation we obtain

$$U_n|_S = 2\pi\sigma(P) + \iint_{S-P} \sigma(P)\frac{\partial G(P,Q)}{\partial n}dS. \tag{4.20}$$

Then the preceding equation, a Fredholm (bounded linear) integral equation of the second kind, can be used for determining the source densities $\sigma(Q)$. Further description of the Fredholm integral can be found on Wikipedia or in Hazewinkel's *Encyclopedia of Mathematics* (ISBN 978-1-55608-010-4), published by Springer in 2001.

The boundary conditions, with respect to ship hydrodynamics, are rather more complicated than Eq. (4.14). In addition to boundary conditions on a body surface, there are boundary conditions on free surfaces, riverbeds and river banks, and so forth. So the integrated surface S in Eq. (4.20) must include all boundary surfaces.

The discretization of integral Eq. (4.20) can be made by dividing the boundary surface S into the limited panels in Eq. (4.20) and then generating a numerical solution.

Dividing the boundary surface S into N plane panels $S_j, j = 1, \cdots, N$ and letting the surface source density σ_j on S_j remain a constant, then Eq. (4.18) is approximated by

$$\phi(P) = \sum_{j=1}^{N} \sigma_j \iint_{S_j} G(P,Q)dS, \qquad P(x,y,z) \in \tau, \text{and} \notin S. \tag{4.21}$$

In this equation, each of the N panel integrals depends on just the body geometry, not on the source density σ_j. The normal velocity component, from integral Eq. (4.20), is approximated by

$$U_n(P_i) = 2\pi\sigma_i + \sum_{\substack{j=1 \\ j\neq i}}^{N} \sigma_j \iint_{S_j} \frac{\partial G(P_i, Q)}{\partial n} dS, \quad i = 1, \cdots, N, \tag{4.22}$$

where P_i is a particular point on S_i, (usually the center of the panel). If we let $U_n(P_i) = U_{ni}$, the preceding equation can be written as a set of linear equations:

$$\sum_{j=1}^{N} A_{ij}\sigma_j = U_{ni}, \quad i = 1, \cdots, N, \tag{4.23}$$

where

$$A_{ij} = \begin{cases} \iint_{S_j} \dfrac{\partial (P_i, Q)}{\partial n} dS & i \neq j, \\ 2\pi & i = j. \end{cases} \tag{4.24}$$

In solving Eq. (4.23), the source intensity $\sigma_j (j = 1, \cdots, N)$ can be obtained. Inserting these into Eq. (4.21), we obtain the velocity potential at every point $P(x, y, z)$ in domain τ.

4.4 Thin-Ship Theory

4.4.1 Basic Equation for Steady Motion of a Thin Ship [12]

A so-called thin ship represents a ship with a small beam–length ratio B/L. In general, the hulls of catamarans comply with this assumption.

Assuming a ship is moving steadily on the water surface in an unlimited-depth waterway and the velocity of the uniform oncoming flow is U_∞, we obtain the following boundary conditions in steady motion based on the relationships in Sect. 4.4.2.

The velocity potential can be written

$$\phi(x, y, z) = -U_\infty x + \phi(x, y, z), \tag{4.25}$$

where $\phi(x, y, x)$ is a perturbation velocity potential.

Substituting this formula into Eq. (4.7), the kinematic free-surface boundary condition is

$$-U_\infty \zeta_x + \phi_x \zeta_x + \phi_y \zeta_y - \phi_z = 0 \quad z = \zeta(x, y)\,. \tag{4.26}$$

Neglecting the second-order minor terms $\phi_x\zeta_x$ and $\phi_y\zeta_y$, the linearized kinematic free-surface boundary condition is

$$-U_\infty \zeta_x = \phi_z, \quad z = 0\,. \tag{4.27}$$

Substituting Eq. (4.25) into Eq. (4.9), the dynamic free-surface boundary condition is

$$g\zeta - U_\infty \phi_x + \frac{1}{2}\left(\phi_x^2 + \phi_y^2 + \phi_z^2\right) = 0, \quad z = \zeta(x, y)\,. \tag{4.28}$$

Neglecting the second-order minor terms $\frac{1}{2}\left(\phi_x^2 + \phi_y^2 + \phi_z^2\right)$, the linearized dynamic free-surface boundary condition is

$$g\zeta = U_\infty \phi_x, \quad z = 0\,. \tag{4.29}$$

Eliminating the unknown wave elevation ζ in (4.27) and (4.29), the linearized free-surface boundary condition is

$$\phi_{xx} + \frac{g}{U_\infty^2}\phi_z = 0 \quad z = 0 \tag{4.30}$$

Let the equation of a hull surface be

$$y = f(x, z). \tag{4.31}$$

Substituting this equation into Eq. (4.4), the body–surface boundary condition is

$$\phi_y = -U_\infty f_x + \phi_x f_x + \phi_z f_z, \quad y = f(x, z)\,. \tag{4.32}$$

Neglecting the second-order minor terms $\phi_x f_x + \phi_z f_z$, the linearized body–surface boundary condition is

$$\phi_y = -U_\infty f_x(x, z), \quad y = 0. \tag{4.33}$$

Let the riverbed equation be $z = -H$, and then the riverbed boundary condition can be found from Eq. (4.6):

$$\phi_z = 0, \quad z = -H\,. \tag{4.34}$$

The wave boundary condition far upstream, that is, the radiation condition, can be obtained from Eq. (4.12) as

$$\nabla\phi = 0 \quad \sqrt{x^2 + y^2} \to \infty\,. \tag{4.35}$$

In summary, the perturbation velocity potential of a thin ship with steady motion $\phi(x, y, z)$ must satisfy the following equations:

$$\begin{cases} \phi_{xx} + \phi_{yy} + \phi_{zz} = 0, & \text{in domain } \tau, \\ \phi_{xx} + \dfrac{g}{U_\infty^2}\phi_z = 0, & z = 0, \\ \phi_y = -U_\infty f_x, & y = 0, \\ \phi_z = 0, & z = -H, \\ \nabla\phi = 0, & \sqrt{x^2 + y^2} \to \infty. \end{cases} \tag{4.36}$$

According to Eq. (4.29), the equation representing the wave elevation of the free surface can be obtained as

$$\varsigma = \frac{U_\infty}{g}\phi_x, \quad z = 0\,. \tag{4.37}$$

4.4.2 *Velocity Potential and Wave Resistance in Deep Water [4]*

We use the Green's function method as in Sect. 4.4.3 to study the velocity potential and wave resistance of a ship moving steadily on the surface of a waterway of unlimited depth.

As Eq. (4.16) we define the Green's function as follows:

$$G(P, Q) = -\frac{1}{r(P, Q)} + G^*(P, Q).$$

This satisfies all equations in expression (4.36), other than the body–surface boundary conditions. As we are considering unlimited water depth, $H \to \infty$. The function $G(P, Q)$ is called a Kelvin point source. Lunde [4] gave the velocity potential at the field point $P(x, y, z)$ induced by a Kelvin point source at point $G(\xi, \eta, \zeta)$ as

$$G(P, Q) = \frac{-1}{r(P, Q)} + \frac{1}{r_1(P, Q)} + G_1(P, Q) + G_2(P, Q), \tag{4.38}$$

where

$$\begin{gathered} r^2 = (x - \xi)^2 + (y - \eta)^2 + (z - \zeta)^2, \\ r_1^2 = (x - \xi)^2 + (y - \eta)^2 + (z + \zeta)^2, \\ G_1 = \frac{2k_0}{\pi}\int_{-\pi/2}^{\pi/2} \sec^2\theta d\theta \cdot \text{V.P.} \int_0^\infty \frac{e^{k(z+\zeta)}}{k - k_0 \sec^2\theta} \cdot \cos\left[k((x-\xi)\cos\theta + (y-\eta)\sin\theta)\right] dk, \end{gathered} \tag{4.39}$$

$$G_2 = 2k_0 \int_{-\pi/2}^{\pi/2} \sec^2\theta \cdot e^{k_0(z+\zeta)\sec^2\theta} \cdot \sin\left[k_0 \sec^2\theta((x-\xi)\cos\theta + (y-\eta)\sin\theta)\right] d\theta. \tag{4.40}$$

The term V.P. in Eq. 4.39 is the Cauchy principal value integral. The term $k_0 = g/U_\infty^2$ and is a wave number. For gravity waves, k_0 is the wave number in the U_∞ direction, $k_0\sec^2\theta$ is the wave number at the inclined angle θ with U_∞. The wavelength related to k_0 is $\lambda_0 = 2\pi/k_0$, so as velocity increases, the wave number reduces and the wavelength increases.

Ship-generated waves have these characteristics. Initially at low speed the generated waves are shorter in length than the hull, and while energy imparted to the water at the hull surface by the sources increases, this builds the resistance to motion without changing the vessel trim. As speed is increased and the generated waves become longer than the hull length, the hull takes on a steady trim up to a maximum when the wavelength is twice the hull length. This is a peak in the generated wave resistance curve. Beyond this speed as the wavelength increases, the trim flattens out, and while the total resistance continues to increase due to a buildup of frictional resistance as the vessel approaches planing speed, the generated waves appear to die away as their length increases toward infinity.

Equation 4.38 shows that the velocity potential of waves induced by a Kelvin point source is composed of four parts:

- A point source in an unlimited-depth waterway: $-\frac{1}{r}$;
- Point source reflected above the water surface: $\frac{1}{r_1}$;
- Double integral: G_1;
- Single integral: G_2.

According to Eq. (4.37), the wave elevation at the free surface is

$$h(x,y) = \frac{U_\infty}{g}\phi_x(x,y,o).$$

Substituting Eq. (4.38) into this equation, the wave elevation induced by a Kelvin point source can be obtained as follows:

First, noting that $\left(\frac{1}{r}\right)_x = \left(\frac{1}{r_1}\right)_x (z=0)$, it is clear that $\frac{1}{r}$ and $\frac{1}{r_1}$ in Eq. (4.38) should be equivalent and so eliminate each other in finding wave profiles.

Thus,

$$h(x,y) = h_1(x,y) + h_2(x,y), \tag{4.41}$$

$$h_1(x,y) = \frac{-2}{\pi U_\infty} \int_{-\pi/2}^{\pi/2} \sec\theta d\theta \cdot \text{V.P.} \int_0^\infty \frac{k e^{k\zeta}}{k - k_0 \sec^2\theta} \cdot \sin[k((x-\xi)\cos\theta + (y-\eta)\sin\theta)] dk, \tag{4.42}$$

$$h_2(x,y)=\frac{2k_0}{U_\infty}\int_{-\pi/2}^{\pi/2}\sec^3\theta\cdot e^{k_0\sec^2\theta\zeta}\cdot\cos\left[k_0\sec^2\theta((x-\xi)\cos\theta+(y-\eta)\sin\theta)\right]d\theta. \tag{4.43}$$

According to the approximate expression in Eq. (4.42), as $x\to\pm\infty$, we find that $h_1(x,y)\to -h_2(x,y)$ far ahead of the source, which means there is no wave far ahead, while at the same time, $h_1(x,y)\to h_2(x,y)$ far behind the source, so that the wave elevation $h(x,y)=2h_2(x,y)$ far behind, called the spectrum of free waves. Meanwhile, $h_1(x,y)$ is called the spectrum of local waves, which disappears very rapidly beyond a certain distance.

In gravity waves, the dynamic and potential energies are both equal, at 50% respectively of the total. In addition, only the potential energy propagates outward, so only half the entire energy propagates outward following wave patterns. In the case of a ship moving forward, the waves propagate backward in the form of free waves, so half the entire energy propagates backward, and this equals the energy consumed by the wave-making resistance of a ship.

According to Eq. (4.18), to find the velocity potential of a ship in steady motion, the source density of source $\sigma(Q)$ can be distributed on a ship wetted surface, and then the disturbance velocity potential is

$$\phi(x,y,z)=\iint_S\sigma(\xi,\eta,\zeta)G(x,y,z;\xi,\eta,\zeta)dS.$$

Substituting Eq. (4.38) into this equation we obtain

$$\phi(x,y,z)=\iint_S\sigma(\xi,\eta,\zeta)\cdot\left(-\frac{1}{r}+\frac{1}{r_1}+G_1+G_2\right)dS. \tag{4.44}$$

From the force acting on the sources, the wave resistance is

$$R_w=-4\pi\rho\iint_S\sigma(x,y,z)\frac{\partial\varphi}{\partial x}dS, \tag{4.45}$$

where the total velocity potential $\varphi(x,y,z)=-U_\infty x+\phi(x,y,z)$.

The uniform oncoming flow potential $-U_\infty x$, $\frac{1}{r}$, $\frac{1}{r_1}$, and G_1 does not create any wave resistance and it is only G_2 that creates the wave resistance, that is,

$$\begin{aligned}R_w=&-4\pi\rho\iint_S\sigma(x,y,z)dS\iint_S\sigma(\xi,\eta,\zeta)\left\{2k_0^2\int_{-\pi/2}^{\pi/2}\sec^2\theta\, e^{k_0\sec^2\theta(z+\zeta)}\right.\\&\left.\cdot\cos\left[k_0\sec^2\theta((x-\xi)\cos\theta+(y-\eta)\sin\theta)\right]d\theta\right\}dS.\end{aligned} \tag{4.46}$$

Thus,

$$\begin{aligned} R_w &= -8\pi\rho k_0^2 \int_{-\pi/2}^{\pi/2} |A(\theta)|^2 \sec^3\theta d\theta \\ &= -8\pi\rho k_0^2 \int_{-\pi/2}^{\pi/2} \left[P^2(\theta) + Q^2(\theta)\right] \sec^3\theta d\theta, \end{aligned} \tag{4.47}$$

where $A(\theta) = P(\theta) + iQ(\theta)$ is called the wave-amplitude function of the free waves behind a ship:

$$\left.\begin{matrix} P(\theta) \\ Q(\theta) \end{matrix}\right\} = \iint_S \sigma(\xi,\eta,\zeta) e^{K_0 \sec^2\theta\zeta} \left\{\begin{matrix} \cos \\ \sin \end{matrix}\right\} \left[k_0 \sec^2\theta(\xi\cos\theta + \eta\sin\theta)\right] dS. \tag{4.48}$$

According to the principle of linear superposition, the surface S in this equation can be composed of several surfaces, $S_i (i = 1, 2, \cdots, n)$, with different source densities, σ_i. Thus,

$$\begin{cases} P(\theta) = P_1(\theta) + P_2(\theta) + \cdots + P_n(\theta), \\ Q(\theta) = Q_1(\theta) + Q_2(\theta) + \cdots + Q_n(\theta). \end{cases} \tag{4.49}$$

For a thin ship, the sources can be distributed on the central longitudinal plane, $\eta = 0$, writing S' as the projection of the ship surface S on plane $\eta = 0$. Thus, the velocity potential of a thin ship is

$$\phi(P) = -U_\infty x + \iint_{S'} \sigma(Q) G(P, Q) d\xi d\zeta. \tag{4.50}$$

The source density $\sigma(\xi, \zeta)$ can be determined by integral Eq. (4.19). Here the normal direction n is in the y-direction, and according to the body–surface boundary condition (4.33), the left-hand side of the integral equation is

$$\phi_y\big|_{y=0} = \phi_y\big|_{y=0} = -U_\infty f_x(x, z).$$

Since $\eta = 0$ and $y = 0$, the right-hand side of the integral equation is equal to zero, so

$$\sigma(x, 0, z) = -\frac{U_\infty}{2\pi} f_x(x, z). \tag{4.51}$$

Substituting this equation into Eq. (4.48), the wave-amplitude functions of a thin ship can be obtained as

$$\left.\begin{matrix} P(\theta) \\ Q(\theta) \end{matrix}\right\} = -\frac{U_\infty}{2\pi} \iint_{S'} f_\xi(\xi, \zeta) . e^{k_0 \sec^2\theta\zeta} \left\{\begin{matrix} \cos \\ \sin \end{matrix}\right\} [k_0 \sec\theta\xi] d\xi d\zeta. \tag{4.52}$$

Similarly, where the source is distributed on the plane $\eta = \pm b_c/2$, the wave-amplitude functions are

$$\left.\begin{matrix} P(\theta) \\ Q(\theta) \end{matrix}\right\} = -\frac{U_\infty}{2\pi} \iint_{S'} f_\xi(\xi,\zeta).e^{k_0 \sec^2\theta\zeta} \left\{ \begin{matrix} \cos \\ \sin \end{matrix} \right\} \left[k_0 \sec^2\theta \left(\xi\cos\theta \pm \frac{b_c}{2}\sin\theta \right) \right] d\xi d\zeta. \tag{4.53}$$

Taking $\lambda = \sec\theta$, the wave resistance can be represented as the Michell equation with ($\eta = 0$)

$$R_w = -\frac{4\rho g k_0}{\pi} \int_1^\infty \left[I^2(\lambda) + J^2(\lambda) \right] \frac{\lambda^2 d\lambda}{\sqrt{\lambda^2 - 1}}, \tag{4.54}$$

where

$$\left.\begin{matrix} I(\lambda) \\ J(\lambda) \end{matrix}\right\} = \iint_{S'} f_\xi(\xi,\zeta) e^{k_0\lambda^2\zeta} \left\{ \begin{matrix} \cos \\ \sin \end{matrix} \right\} (k_0\lambda\xi) d\xi d\zeta. \tag{4.55}$$

So far, we have been discussing the waves and forces generated by a single hull. We will now move on to use the equivalent approaches to a catamaran.

4.4.3 Catamaran Wave Resistance in Deep Water

We use the *o-xyz* Cartesian coordinate system with the origin located at the center of a catamaran *x,y* plane on an undisturbed calm water surface, with the *x*-axis along the uniform coming flow U_∞ positive to the bow and the *z*-axis up as positive (Fig. 4.2).

The geometric parameters for a symmetric catamaran are as follows: design waterline length L, beam overall B, design draft T, demihull width b, spacing between the demihulls' central planes b_c, and spacing between demihulls b_s (Fig. 4.2).

A catamaran is composed of left and right demihulls. Each demihull is assumed to be symmetric with respect to its central longitudinal plane, and the sources are distributed on the demihulls' central planes $\eta = \pm b_c/2$. Based on the relationships discussed earlier, Eqs. (4.47), (4.49), and (4.53), the formula for the wave resistance of a catamaran can be obtained as

$$R_w = -8\pi\rho k_0^2 \int_{-\pi/2}^{\pi/2} \left\{ \left[P_L(\theta) + P_R(\theta) \right]^2 + \left[Q_L(\theta) + Q_R(\theta) \right]^2 \right\} \sec^3\theta d\theta, \tag{4.56}$$

where for the left and right demihulls respectively

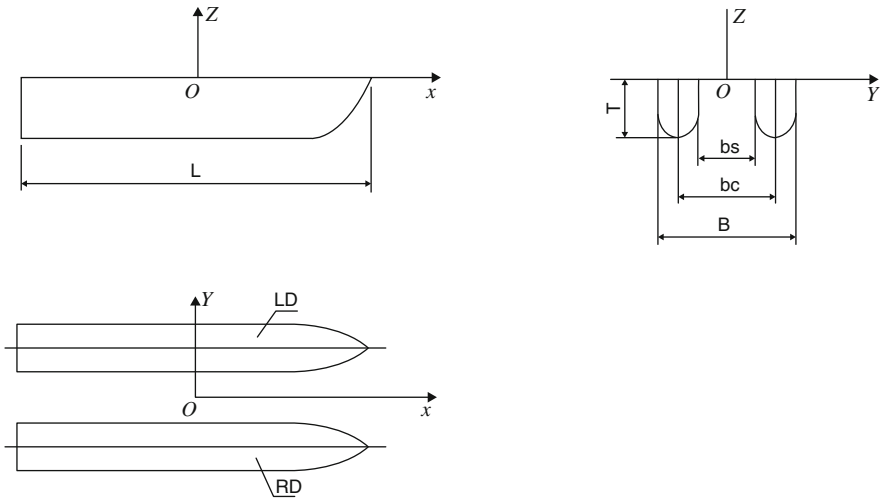

Fig. 4.2 Coordinate system for catamaran

$$\left.\begin{matrix} P_L(\theta) \\ Q_L(\theta) \end{matrix}\right\} = -\frac{U_\infty}{2\pi}\iint_{S'} f_\xi(\xi,\zeta) e^{k_0 \sec^2\theta\zeta} \left\{\begin{matrix} \cos \\ \sin \end{matrix}\right\} \left[k_0 \sec^2\theta\left(\xi\cos\theta + \frac{bc}{2}\sin\theta\right)\right] d\xi d\zeta, \tag{4.57}$$

$$\left.\begin{matrix} P_R(\theta) \\ Q_R(\theta) \end{matrix}\right\} = -\frac{U_\infty}{2\pi}\iint_{S'} f_\xi(\xi,\zeta) e^{k_0 \sec^2\theta\zeta} \left\{\begin{matrix} \cos \\ \sin \end{matrix}\right\} \left[k_0 \sec^2\theta\left(\xi\cos\theta - \frac{bc}{2}\sin\theta\right)\right] d\xi d\zeta. \tag{4.58}$$

In these expressions, $P_L(\theta)$, $Q_L(\theta)$, $P_R(\theta)$, $Q_R(\theta)$ are the wave-amplitude functions for the left and right demihulls respectively. In addition:

$y = f(x,z) \pm \frac{b_c}{2}$ represents the hull surface equation of the left and right demihulls respectively;
b_c is the spacing between the central planes of the demihulls;
S' is the projection of the demihull surface on the x,z plane; in addition, $k_0 = g/U_\infty^2$.

Equation (4.56) can be simplified to the following expression:

$$\begin{aligned} R_w &= -8\pi\rho k_0^2 \int_{-\pi/2}^{\pi/2} \left[P^2(\theta) + Q^2(\theta)\right] \cdot F(\theta) \sec^3\theta d\theta \\ &= -16\pi\rho k_0^2 \int_0^{\pi/2} \left[P^2(\theta) + Q^2(\theta)\right] \cdot F(\theta) \sec^3\theta d\theta, \end{aligned} \tag{4.59}$$

where

$$F(\theta) = 2\left[1 + \cos\left(b_c k_0 \sec^2\theta \sin\theta\right)\right], \tag{4.60}$$

$$\left.\begin{matrix} P(\theta) \\ Q(\theta) \end{matrix}\right\} = -\frac{U_\infty}{2\pi}\iint_{S'} f_\xi(\xi,\zeta) e^{k_0 \sec^2\theta\zeta} \left\{\begin{matrix} \cos \\ \sin \end{matrix}\right\}(k_0 \sec\theta\xi) d\xi d\zeta. \tag{4.61}$$

The preceding formulas are the wave-amplitude functions. The wave resistance of a catamaran, Eq. (4.59), can be rewritten as

$$R_w = 2R_{w0} + R_{wi}, \tag{4.62}$$

where

$$R_{w0} = -16\pi\rho k_0^2 \int_0^{\pi/2} \left[P^2(\theta) + Q^2(\theta)\right] \sec^3\theta d\theta, \tag{4.63}$$

$$R_{wi} = -16\pi\rho k_0^2 \int_0^{\pi/2} \left[P^2(\theta) + Q^2(\theta)\right] \cdot 2\cos\left(b_c k_0 \sec^2\theta \sin\theta\right) \cdot \sec^3\theta d\theta, \tag{4.64}$$

R_{w0} wave resistance of a demihull,

R_{wi} interference resistance of waves generated by demihulls.

Adjusting the spacing between the central planes of demihulls b_c may decrease the interference resistance of waves and even create favorable interference.

In this theory, the sources are just distributed on the demihulls' central planes, but no dipole function has been used to consider the influence of flow around one demihull on the other demihull (e.g., transverse flow) and the influence of the asymmetry of demihulls on the flow. Rong (1984) investigated these influences, and numerical calculation showed that for a modern catamaran with significant spacing of the two demihulls, the influence of the dipole on the flow is very small and can be neglected.

4.4.4 *Velocity Potential and Wave Resistance in Shallow Water*

The disturbance velocity potential of a thin ship running steadily in shallow water $\phi(x, y, z)$ should satisfy Eq. (4.36).

To let the point source $\frac{1}{r}$ located at (ξ, η, ζ) satisfy the boundary condition at the riverbed plane $\phi_z(x, y, -H) = 0$, a reflection of $\frac{1}{r}$ in the riverbed plane must be made, that is, the point source $\frac{1}{r_H}$ located at $(\xi, \eta, -(2H + \zeta))$.

Similar to the velocity potential in deep water, Eq. (4.38), Lunde [4] determined the velocity potential in shallow water at the point $P(x, y, z)$ induced by the source at point $Q(\xi, \eta, \zeta)$ as follows:

$$\phi(P) = \frac{1}{r(P,Q)} + \frac{1}{r_H(P,Q)} + N_1(P,Q) + N_2(P,Q), \tag{4.65}$$

where

$$\begin{aligned}
&r^2 = (x-\xi)^2 + (y-\eta)^2 + (z-\zeta)^2,\\
&r_H^2 = (x-\xi)^2 + (y-\eta)^2 + (z+\zeta+2H)^2,\\
&N_1 = \frac{-4}{\pi}\int_0^{\pi/2} d\theta \ \text{V.P.} \int_0^{\infty} \frac{e^{-kH}(k + k_0\sec^2\theta)\cosh[k(\zeta+H)]\cosh[k(z+H)]}{\cosh(kH)\cdot[k - k_0\sec^2\theta\cdot\tanh(kH)]}\\
&\qquad \cdot \cos[k(x-\xi)\cos\theta]\cdot\cos[k(y-\eta)\sin\theta]dk,
\end{aligned} \tag{4.66}$$

$$\begin{aligned}
N_2 = -4k_0\int_{\theta_0}^{\pi/2} &\frac{\cosh[k_H(\zeta+H)]\cosh[k_H(z+H)]\cdot\sec^2\theta}{\cosh^2(k_HH)\cdot\left[1 - k_0H\sec^2\theta\cdot\ \text{sech}^2(k_HH)\right]}\\
&\cdot \sin[k_H(x-\xi)\cos\theta]\cdot\cos[k_H(y-\eta)\sin\theta]d\theta,
\end{aligned} \tag{4.67}$$

$$k_0 = g/U_\infty^2.$$

k_H satisfies the following equation of k:

$$k - k_0\sec^2\theta\cdot\tanh(kH) = 0. \tag{4.68}$$

Clearly, k is a function of θ, where

$$\theta_H = \begin{cases} \arccos(1/F_H), & F_H \geq 1,\\ 0, & F_H < 1, \end{cases} \tag{4.69}$$

where $F_H = U_\infty/\sqrt{gH}$ is called a Froude number with respect to water depth.

Lunde [4] gave the formula for wave resistance in shallow water as follows:

$$R_w = -16\pi\rho k_0\int_{\theta_H}^{\pi/2}\left[U^2(\theta)+V^2(\theta)\right]\frac{k_H\sec\theta}{\cosh^2(k_HH)\cdot\left[1 - k_0H\sec^2\theta\,\text{sech}^2(k_HH)\right]}d\theta, \tag{4.70}$$

where

$$\begin{aligned}
\left.\begin{matrix}U(\theta)\\ V(\theta)\end{matrix}\right\} &= \iint_S \sigma(\xi,\eta,\zeta)\cosh[k_H(\zeta+H)]\left\{\begin{matrix}\cos\\ \sin\end{matrix}\right\}[k_H(\xi\cos\theta+\eta\sin\theta)]dS\\
&= \iint_{S'}\frac{-U_\infty}{2\pi}f_\xi(\xi,\zeta)\cosh[k_H(\zeta+H)]\left\{\begin{matrix}\cos\\ \sin\end{matrix}\right\}(k_H\cos\theta\xi)d\xi d\zeta.
\end{aligned} \tag{4.71}$$

S' is the projection of hull surface S on plane $\eta = 0$.

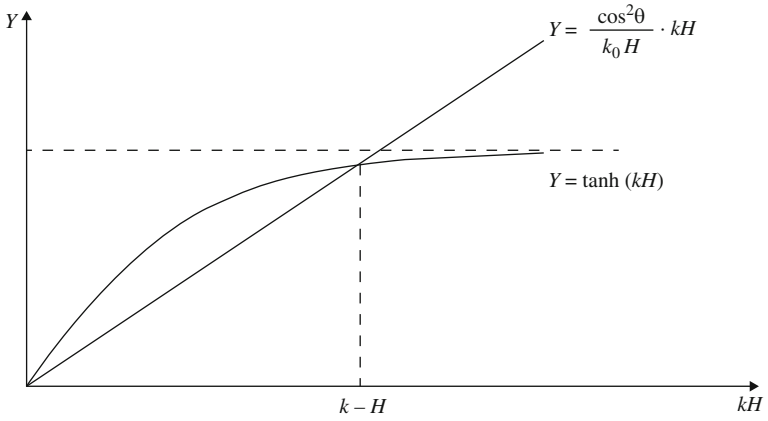

Fig. 4.3 Curve for determining K_H

Investigating the k_H satisfying Eq. (4.68), we can rewrite Eq. (4.68) as

$$\tanh(kH) = \frac{\cos^2\theta}{k_0 H} \cdot kH = F_H^2 \cos^2\theta \cdot kH. \tag{4.72}$$

Taking $kH\ldots$ as an independent variable, we can draw a curve $y = \tanh(kH)$ and a line $y = \frac{\cos^2\theta}{k_0 H} \cdot kH$ as shown in Fig. 4.3. Only when $\frac{\cos^2\theta}{k_0 H} = F_H^2 \cos^2\theta < 1$ does a root k_H in Eq. (4.68) exist. Thus, when $F_H < 1$, k_H always exists, no matter what value θ has. However, when $F_H \geq 1$, only in the case of $\cos^2\theta < \frac{1}{F_H^2}$, that is, $\theta > \arccos\left(\frac{1}{F_H}\right)$, does k_H exist. The integral lower limit in N_2 and R_w with respect to θ is 0 originally. However, after considering the preceding condition, the integral lower limit should be θ_H, and in addition θ_H must satisfy Eq. (4.69).

4.4.5 Catamaran Wave Resistance in Shallow Water

The geometric parameters and coordinate system of a catamaran are given in Fig. 4.2. The wave resistance of a catamaran in shallow water can be obtained as

$$R_w = -16\pi\rho k_0 \int_{\theta_H}^{\pi/2} \left[U^2(\theta) + V^2(\theta)\right] \frac{k_H \sec\theta \cdot F(\theta)}{\cosh^2(k_H H) \cdot \left[1 - k_0 H \sec^2\theta \operatorname{sech}^2(k_H H)\right]} d\theta, \tag{4.73}$$

where

$$F(\theta) = 2[1 + \cos(b_c k_H \sin\theta)]. \tag{4.74}$$

Expression (4.74) represents the factoring of both demihulls and the interference component between the hulls as in Eq. (4.60) for deep water. The wave-amplitude functions $U(\theta)$ and $V(\theta)$ are also the same as in Eq. (4.71).

4.5 Numerical Calculation for Wave Resistance

4.5.1 Introduction

In Sect. 4.4.4, we deduced the formulas for the wave resistance of a catamaran in both deep and shallow water, which included evaluating the integral of a hull surface with respect to the x-direction based on thin-ship theory. The key problem for obtaining the wave resistance is how to represent the hull surface. There are many different numerical methods for calculating the wave resistance of vessels.

Martin [13] assumed that the center of gravity of every transverse area $A(x)$ is located on the same vertical level and simplified the double integral of the wave-amplitude function to a single integral with respect to $dA(x)/dx$. He then used Chebyshev polynomials to fit $A(x)$ and calculated the single integral. We can also use Simpson's formula to calculate the integral.

Hsiung [7] used a set of so-called tent functions to approximate the ship hull surface. The tent function is similar to a first-degree B-spline surface, which has good local support properties. Actually, it is a bilinear surface in every net region (*xz plane*), that is, a ruled surface composed of straight lines. Using this method the double integral of a wave-amplitude function can be simplified to the product of two single integrals. This method simplifies the Michell integral to a standard quadratic form with respect to hull offsets. On the one hand, the wave resistance can be calculated directly by offsets, while on the other hand the hull form can be optimized by a quadratic programming method. Thus, the method has wide application.

4.5.2 Mathematical Expression for Hull Surface

We continue to use the *o-xyz* ship coordinate system in Fig. 4.1. In general, we take a limited number of stations ($i = 1, 2, \ldots, m$) and waterlines ($j = 1, 2, \ldots, n$). The projection of the ship hull surface on the x,z plane and the net divided by stations and waterlines are shown in Fig. 4.4. We define the last point of the underwater part at the stern of a ship as the first station, the first point at the bow as the mth station, the first waterline as the baseline, and the nth waterline as the design waterline.

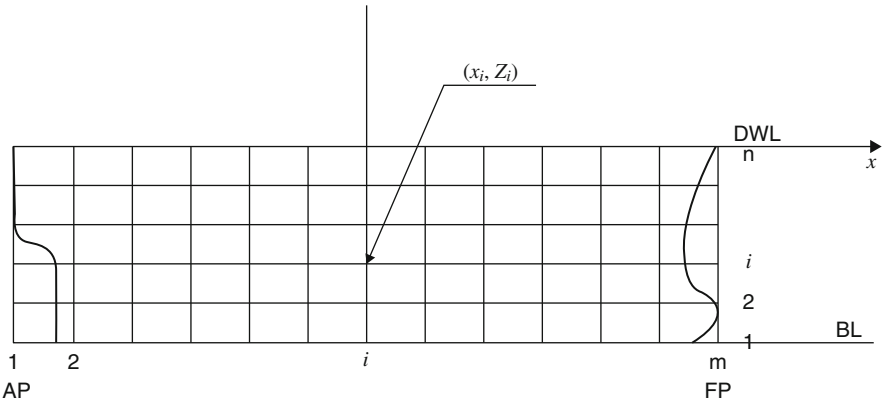

Fig. 4.4 Projection of hull surface curve on *xoz* plane and its net

Considering the curves on the *x,y* plane (the horizontal sections) and a group of given data points (x_i, y_i), $i = 1, 2, \ldots, m$, we use a group of first-degree basic functions $N_{i,\ 1}(x)$, similar to a linear combination of B-spline basic functions, following Farin [14], to construct an interpolation curve:

$$y(x) = \sum_{i=1}^{m} y_i N_{i,1}(x), \qquad x_1 \le x \le x_m, \tag{4.75}$$

where

$$N_{i,1}(x) = \begin{cases} \dfrac{x - x_{i-1}}{x_i - x_{i-1}}, & x_{\text{i-1}} \le x < x_i, \\ \dfrac{x_{i+1} - x}{x_{i+1} - x_i}, & x_{\text{i}} \le x < x_{i+1}, \\ 0, & \text{otherwise}, \end{cases} \tag{4.76}$$

$$i = 2, 3, \cdots, m-1,$$

$$N_{1,1}(x) = \frac{x_2 - x}{x_2 - x_1}, \qquad x_1 \le x < x_2,$$

$$N_{m,1}(x) = \frac{x - x_{m-1}}{x_m - x_{m-1}}, \qquad x_{m-1} \le x \le x_m.$$

An illustration of first-degree basic functions $N_{i,1}(x)$, $i = 1, 2, \ldots, m$, is shown in Fig. 4.5. Every basic function possesses a local support property only, that is, the value of the function beyond a limited region is equal to zero. From Eq. (4.75) it is known that an interpolation curve is the linear combination of basic functions with support from the local property. Thus, the whole interpolation curve is supported by the local properties.

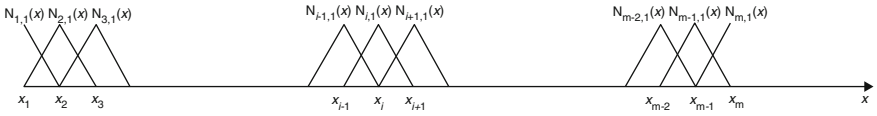

Fig. 4.5 First-degree basic function of $N_{i,\,1}(x)$

Considering surfaces in the *o-xyz* space and a group of given net data points (x_i, y_{ij}, x_j) $i = 1, 2, \ldots, m; j = 1, 2, \ldots, n$, where the net is shown in Fig. 4.4, we can use the Cartesian product of first-degree basic functions to construct an interpolation surface:

$$y(x,z) = \sum_{i=1}^{m} \sum_{j=1}^{n} y_{ij} N_{i,1}(x) N_{j,1}(z), \tag{4.77}$$

where first-degree basic functions $N_{i,1}(x)$ and $N_{j,1}(z)$ can be determined by Eq. (4.76).

Thus, using Eq. (4.76) we can obtain

$$N_{i,1}(x) \cdot N_{j,1}(z) = \begin{cases} \dfrac{x - x_{i-1}}{x_i - x_{i-1}} \cdot \dfrac{z - z_{j-1}}{z_j - z_{j-1}} & x_{i-1} \le x \le x_i, \quad z_{j-1} \le z \le z_j, \\ \dfrac{x - x_{i-1}}{x_i - x_{i-1}} \cdot \dfrac{z_{j+1} - z}{z_{j+1} - z_j} & x_{i-1} \le x \le x_i, \quad z_j \le z \le z_{j+1}. \\ \dfrac{x_{i+1} - x}{x_{i+1} - x_i} \cdot \dfrac{z - z_{j-1}}{z_j - z_{j-1}} & x_i \le x \le x_{i+1}, \quad z_{j-1} \le z \le z_j, \\ \dfrac{x_{i+1} - x}{x_{i+1} - x_i} \cdot \dfrac{z_{j+1} - z}{z_{j+1} - z_j} & x_i \le x \le x_{i+1}, \quad z_j \le z \le z_{j+1}, \end{cases} \tag{4.78}$$

The local properties of an interpolation curve can be extended to develop a surface; thus, the interpolation surface represented by Eq. (4.77) is also supported by the local properties.

The support region for (4.78) is $[x_{i\,-\,1}, x_{i+1}] \times [z_{j\,-\,1}, z_{j+1}]$. In this region, the surface is composed of four bilinear surfaces (a kind of ruled surface). Hsiung in 1984 [8] called it a tent function.

4.5.3 Numerical Calculation for Wave-Making Resistance in Deep Water

We begin by summarizing the expressions for a monohull vessel and then continue with those for a catamaran.

4.5.3.1 Calculation for Wave Resistance of Monohull in Deep Water

We use the Michell Eq. (4.54) to calculate the wave resistance of a ship in deep water. After eliminating the singularity of its integrated function at $\lambda = 1$ by letting $\lambda = u^2 + 1$, Eq. (4.54) becomes

$$R_w = -\frac{8\rho g k_0}{\pi} = \int_0^\infty \left[I^2(u) + J^2(u)\right] \cdot \frac{\left(u^2+1\right)^2}{\sqrt{u^2+2}} du, \tag{4.79}$$

where

$$\left.\begin{matrix} I(u) \\ J(u) \end{matrix}\right\} = \int_{-T}^{0} e^{k_0\left(u^2+1\right)^2\zeta} \int_{-L/2}^{L/2} f_\xi(\xi,\zeta) \left\{\begin{matrix} \cos \\ \sin \end{matrix}\right\} \left[k_0\left(u^2+1\right)\xi\right] d\xi d\zeta. \tag{4.80}$$

Let L, B, and T be, respectively, the length, beam, and draft of a ship. We introduce the following dimensionless variables:

$$x = \xi/L, \quad y = 2\eta/B, \quad z = \zeta/T. \tag{4.81}$$

If we let $\bar{f}(x,z) = 2f(\xi,\zeta)/B$ be the hull function, then the slope function is

$$\bar{f}_x(x,z) = \frac{2L}{B} f_\xi(\xi,\zeta). \tag{4.82}$$

For Froude number $Fr_L = U_\infty/\sqrt{gL}$ we can define the dimensionless wave number as

$$\gamma_0 = k_0 \frac{L}{2} = \frac{gL}{2U_\infty^2} = \frac{1}{2F_n^2}. \tag{4.83}$$

Then a dimensionless wave resistance coefficient for Froude number Fr_L and draft–length ratio T/L can be written

$$\begin{aligned} C_w &= -R_w/\left[8\rho g B^2 T^2/(\pi L)\right] \\ &= \frac{\gamma_0}{2} \int_0^\infty \left[P^2(u) + Q^2(u)\right] \cdot \frac{\left(u^2+1\right)^2}{\sqrt{u^2+2}} du, \end{aligned} \tag{4.84}$$

where

$$\begin{aligned} \left.\begin{matrix} P(u) \\ Q(u) \end{matrix}\right\} &= \int_{-1}^{0} e^{b_d z} \int_{-1/2}^{1/2} \bar{f}_x(x,z) \left\{\begin{matrix} \cos \\ \sin \end{matrix}\right\} (a_d x) dx dz \\ a_d &= 2\gamma_0\left(u^2+1\right) \\ b_d &= 2\gamma_0\left(u^2+1\right)\frac{T}{L}. \end{aligned} \tag{4.85}$$

We take (4.77) to approximate the hull surface $\bar{f}(x,z)$; then

$$\bar{f}(x,z)=\sum_{i=1}^{m}\sum_{j=1}^{n}y_{ij}N_{i,1}(x)N_{j,1}(z). \tag{4.86}$$

Substituting Eq. (4.86) into (4.85) and considering the basic functions local support property, we obtain

$$\left.\begin{matrix}P(u)\\Q(u)\end{matrix}\right\}=\sum_{i=1}^{m}\sum_{j=1}^{n}y_{ij}\cdot\left\{\begin{matrix}C_i\\S_i\end{matrix}\right\}E_j, \tag{4.87}$$

where the values for C_i can be determined from

$$\begin{aligned}
C_i&=\int_{x_{i-1}}^{x_{i+1}}N'_{i,1}(x)\cdot\cos(a_dx)dx\\
&=\int_{x_{i-1}}^{x_i}\frac{1}{x_i-x_{x-1}}\cos(a_dx)dx-\int_{x_i}^{x_{i+1}}\frac{1}{x_{i+1}-x_i}\cos(a_dx)dx\\
&=\frac{1}{a_d}\left\{\frac{1}{x_i-x_{i-1}}[\sin(a_dx_i)-\sin(a_dx_{i-1})]-\frac{1}{x_{i+1}-x_i}[\sin(a_dx_{i+1})-\sin(a_dx_i)]\right\}\\
&i=2,3,\cdots,m-1,\\
C_1&=\int_{x_1}^{x_2}\frac{-1}{x_2-x_1}\cos(a_dx)dx\\
&=-\frac{1}{a_d}\cdot\frac{1}{x_2-x_1}[\sin(a_dx_2)-\sin(a_dx_1)],\\
C_m&=\int_{x_{m-1}}^{x_m}\frac{1}{x_m-x_{m-1}}\cos(a_dx)dx\\
&=\frac{1}{a_d}\cdot\frac{1}{x_m-x_{m-1}}[\sin(a_dx_m)-\sin(a_dx_{m-1})].
\end{aligned} \tag{4.88}$$

Similarly,

$$\begin{aligned}
S_i&=\frac{1}{a_d}\left\{\frac{-1}{x_i-x_{i-1}}[\cos(a_dx_i)-\cos(a_dx_{i-1})]+\frac{1}{x_{i+1}-x_i}[\cos(a_dx_{i+1})-\cos(a_dx_i)]\right\}\\
&i=2,3,\cdots,m-1,\\
S_1&=\frac{1}{a_d}\cdot\frac{1}{x_2-x_1}[\cos(a_dx_2)-\cos(a_dx_1)],\\
S_m&=-\frac{1}{a_d}\cdot\frac{1}{x_m-x_{m-1}}[\cos(a_dx_m)-\cos(a_dx_{m-1})],
\end{aligned} \tag{4.89}$$

and

$$
\begin{aligned}
\mathrm{E_j} &= \int_{z_{j-1}}^{z_{j+1}} N_{j,1}(z)\cdot e^{b_d z}dz \\
&= \int_{z_{j-1}}^{z_j} \frac{z-z_{j-1}}{z_j-z_{j-1}}\cdot e^{b_d z}dz + \int_{z_j}^{z_{j+1}} \frac{z_{j+1}-z}{z_{j+1}-z_j}\cdot e^{b_d z}dz \\
&= \frac{1}{{b_d}^2}\cdot\left\{\frac{-1}{z_j-z_{j-1}}\left[e^{b_d z_j}-e^{b_d z_{j-1}}\right]+\frac{1}{z_{j+1}-z_j}\left[e^{b_d z_{j+1}}-e^{b_d z_j}\right]\right\} \\
j &= 2,3,\cdots,n-1, \\
E_1 &= \int_{z_1}^{z_2}\frac{z_2-z}{z_2-z_1}\cdot e^{b_d z}dz \\
&= \frac{-1}{b_d}\cdot e^{b_d z_1}+\frac{1}{{b_d}^2}\cdot\frac{1}{z_2-z_1}\left[e^{b_d z_2}-e^{b_d z_1}\right], \\
E_n &= \int_{z_{n-1}}^{z_n}\frac{z-z_{n-1}}{z_n-z_{n-1}}\cdot e^{b_d z}dz \\
&= \frac{1}{b_d}\cdot e^{b_d z_n}-\frac{1}{{b_d}^2}\cdot\frac{1}{z_n-z_{n-1}}\left[e^{b_d z_n}-e^{b_d z_{n-1}}\right].
\end{aligned}
\tag{4.90}
$$

Hsiung [7] used a coordinate system complying with the conventional system for a ship line drawing, with the origin at the intersection point at baseline BL and forward perpendicular FP, with the x-axis backward as positive and the z-axis with upward as positive. Using this system, $e^{b_d z_j}$ should be replaced with $e^{b_d(z_j-1)}$ $(j=1,2,\ldots,n)$ in Eq. (4.90).

Furthermore, from Eq. (4.87) we obtain

$$
\begin{aligned}
P^2(u) &= \sum_{i=1}^{m}\sum_{j=1}^{n}\sum_{k=1}^{m}\sum_{\ell=1}^{n} y_{ij}y_{k\ell}C_iC_kE_jE_\ell, \\
Q^2(u) &= \sum_{i=1}^{m}\sum_{j=1}^{n}\sum_{k=1}^{m}\sum_{\ell=1}^{n} y_{ij}y_{kl}S_iS_kE_jE_\ell.
\end{aligned}
\tag{4.91}
$$

Substituting Eq. (4.91) into Eq. (4.84) we obtain

$$
C_w = \sum_{i=1}^{m}\sum_{j=1}^{n}\sum_{k=1}^{m}\sum_{\ell=1}^{n} y_{ij}y_{k\ell}\cdot d_{ijk\ell},
\tag{4.92}
$$

where

$$
d_{ijk\ell}(Fr_L, T/L) = \frac{\gamma_0}{2}\int_0^\infty \left[(C_iC_k+S_iS_k)E_jE_\ell\right]\frac{(u^2+1)^2}{\sqrt{u^2+2}}du.
\tag{4.93}
$$

Note that $d_{ijk\ell}$ depends not on ship offsets but only on the Froude number Fr_L (due to $\gamma_0 = \dfrac{1}{2F_n^2}$) and draft–length ratio, T/L.

If we define one-dimensional variables y_{mm} instead of two-dimensional variables y_{ij}, then

$$\begin{array}{ll} y_{mm} = y_{ij} & mm = i + (j-1) \times m \\ i = 1, 2, \cdots, m; & j = 1, 2, \cdots, n. \end{array}$$

Thus, four-dimensional variables d_{ijkl} can be transferred to two-dimensional variables $d_{mm,\ nn}$:

$$\begin{array}{lll} d_{mm,nn} = d_{ijk\ell} & mm = i + (j-1) \times m & nn = k + (\ell - 1) \times m, \\ i = 1, 2, \cdots, m; & j = 1, 2, \cdots, n, & \\ k = 1, 2, \cdots, m; & \ell = 1, 2, \cdots, n, & \\ \text{max value of } mm \text{ and } nn & \widehat{n} = m \cdot n. & \end{array}$$

In this case, Eq. (4.93) can be written as follows:

$$C_w = \sum_{mm=1}^{mn} \sum_{nn=1}^{mn} d_{mm,nn} y_{mm} y_{nn}. \tag{4.94}$$

Note that

$$d_{mm,nn} = d_{nn,mm},$$

so that Eq. (4.94) is a standard quadratic form and can be written in the following matrix form:

$$C_w = y^T \cdot \widehat{D} \cdot y, \tag{4.95}$$

where

y = column $\widehat{n}$-vector of offsets,
y^T = transpose of y,
$\widehat{D} = \widehat{n} \times \widehat{n}$ is a symmetric matrix and is called the wave resistance matrix for a monohull in deep water.

The integral of Eq. (4.93) can be calculated using Simpson's formula; in general, the step can be taken as $0.1F_n^2$ with 300–500 steps in the calculation.

4.5.3.2 Calculation for Wave Resistance of Catamaran in Deep Water

The geometric parameters and coordinate system for a catamaran are as shown in Fig. 4.2. The demihull function and the net division of the projection of a demihull surface on the *xoz* plane are shown in Fig. 4.4.

Let $\lambda = \sec\theta$ in Eqs. (4.59) and (4.61); then the formula for the wave resistance of a catamaran similar to the Michell integral can be obtained using

$$R_w = -\frac{4\rho g k_0}{\pi}\int_1^{\infty}\left[I^2(\lambda)+J^2(\lambda)\right]\cdot F(\lambda)\frac{\lambda^2}{\sqrt{\lambda^2-1}}d\lambda, \tag{4.96}$$

where

$$F(\lambda) = 2\left[1+\cos\left(b_c k_0 \lambda\sqrt{\lambda^2-1}\right)\right], \tag{4.97}$$

$$\left.\begin{matrix} I(\lambda) \\ J(\lambda) \end{matrix}\right\} = \int_{-T}^{0} e^{k_0\lambda^2\zeta}\int_{-L/2}^{L/2} f_{\xi}(\xi,\zeta)\left\{\begin{matrix}\cos\\ \sin\end{matrix}\right\}(k_0\lambda\xi)d\xi d\zeta. \tag{4.98}$$

Using the dimensionless variables in Eqs. (4.81), (4.82), (4.83) and (4.84), we obtain

$$C_w = \frac{\gamma_0}{2}\int_0^{\infty}\left[P^2(u)+Q^2(u)\right]\cdot F(u)\cdot\frac{(u^2+1)^2}{\sqrt{u^2+2}}du, \tag{4.99}$$

where

$$F(u) = 2\left[1+\cos\left\{\frac{b_c}{L}2\gamma_0(u^2+1)u\sqrt{u^2+2}\right\}\right]. \tag{4.100}$$

The wave-amplitude functions in deep water $P(u)$ and $Q(u)$ can be written as in (4.85).

We use Eq. (4.77) to approximate the hull surface and obtain all of the same formulas as in expressions (4.88), (4.89), (4.90), (4.91), and (4.92). The following equation is applied instead of Eq. (4.93), taking account of the catamaran demihull interference through *F(u)*:

$$d_{ijk\ell}(Fr_L, T/L, b_c/L) = \frac{\gamma_0}{2}\int_0^{\infty}\left[(C_iC_k+S_iS_k)E_jE_{\ell}\right]\cdot F(u)\cdot\frac{(u^2+1)^2}{\sqrt{u^2+2}}du. \tag{4.101}$$

$d_{ijk\ell}$ depends not on ship offsets but only on the Froude number Fr_L, draft–length ratio T/L, and spacing–length ratio b_c/L.

The wave resistance coefficient of a catamaran in deep water C_w is similar to Eq. (4.95) in standard quadratic form. The symmetric matrix of $\widehat{D} = \widehat{n}\times\widehat{n}$ order is called the wave resistance matrix for a catamaran in deep water.

4.5.4 *Numerical Calculation for Wave-Making Resistance in Shallow Water*

We begin by summarizing the expressions for a monohull vessel and then continue with those for a catamaran, similar to our approach to deep water resistance.

4.5.4.1 Calculation for Wave Resistance of Monohull in Shallow Water

Take the dimensionless variables in Eqs. (4.81) and (4.82) and let

$$\bar{k}_H = k_H H. \tag{4.102}$$

Substituting the preceding dimensionless variables into Eqs. (4.70) and (4.71) to calculate the wave resistance of a monohull in shallow water and letting $\sec\theta = u^2 + 1$, we can obtain the following formula for calculating the dimensionless wave resistance coefficient of a monohull in shallow water:

$$\begin{aligned} C_w &= -R_w / \left[8\rho g B^2 T^2/(\pi L)\right] \\ &= \frac{L}{4H}\int_{U_H}^{\infty} \left[U^2(u) + V^2(u)\right] \frac{F_H^2 \bar{k}_H}{\left[F_H^2 \cosh^2 \bar{k}_H - (u^2+1)^2\right]\sqrt{u^2+2}}\, du, \end{aligned} \tag{4.103}$$

where

$$\left.\begin{matrix} U(u) \\ V(u) \end{matrix}\right\} = \int_{-1}^{0} \cosh\left[\bar{k}_H\left(\frac{T}{H}z + 1\right)\right] \int_{-1/2}^{1/2} \bar{f}_x(x,z) \left\{\begin{matrix} \cos \\ \sin \end{matrix}\right\} \left(\frac{\bar{k}_H}{u^2+1} \cdot \frac{L}{H} x\right) dx dz, \tag{4.104}$$

$$a_s = \frac{\bar{k}_H}{u^2+1} \cdot \frac{L}{H},$$
$$b_s = \bar{k}_H \cdot \frac{T}{H}.$$

According to Eq. (4.68), $\bar{k}_H$ should satisfy the following equation:

$$F_H^2 \bar{k}_H - \left(u^2+1\right)^2 \cdot \tanh\left(\bar{k}_H\right) = 0. \tag{4.105}$$

According to Eq. (4.69) we obtain

$$U_H = \begin{cases} \sqrt{F_H - 1}, & F_H \geq 1, \\ 0, & F_H < 1. \end{cases} \tag{4.106}$$

The hull surface $\bar{f}(x,z)$ can still be represented by Eq. (4.86), and so substituting Eq. (4.86) into Eq. (4.104), we have

$$\left.\begin{matrix} U(u) \\ V(u) \end{matrix}\right\} = \sum_{i=1}^{m}\sum_{j=1}^{n} y_{ij} \left\{\begin{matrix} C_i \\ S_i \end{matrix}\right\} E_j, \tag{4.107}$$

where

$$
\begin{aligned}
C_i &= \frac{1}{a_s}\left\{\frac{1}{x_i - x_{i-1}}[\sin(a_s x_i) - \sin(a_s x_{i-1})] - \frac{1}{x_{i+1} - x_i}[\sin(a_s x_{i+1}) - \sin(a_s x_i)]\right\},\\
&\quad i = 2, 3, \cdots, m-1,\\
C_1 &= \frac{-1}{a_s(x_2 - x_1)} \cdot [\sin(a_s x_2) - \sin(a_s x_1)],\\
C_m &= \frac{1}{a_s(x_m - x_{m-1})}[\sin(a_s x_m) - \sin(a_s x_{m-1})],
\end{aligned}
\tag{4.108}
$$

$$
\begin{aligned}
S_i &= \frac{1}{a_s}\left\{\frac{-1}{x_i - x_{i-1}}[\cos(a_s x_i) - \cos(a_s x_{i-1})] + \frac{1}{x_{i+1} - x_i}[\cos(a_s x_{i+1}) - \cos(a_s x_i)]\right\},\\
&\quad i = 2, 3, \cdots, m-1,\\
S_1 &= \frac{1}{a_s(x_2 - x_1)}[\cos(a_s x_2) - \cos(a_s x_1)],\\
S_m &= \frac{-1}{a_s(x_m - x_{m-1})}[\cos(a_s x_m) - \cos(a_s x_{m-1})],
\end{aligned}
\tag{4.109}
$$

$$
\begin{aligned}
E_j &= \int_{z_{j-1}}^{z_{j+1}} N_{j,1}(z) \cdot \cosh\left(b_s z + \bar{k}_H\right) dz\\
&= \int_{z_{j-1}}^{z_j} \frac{z - z_{j-1}}{z_j - z_{j-1}} \cdot \cosh\left(b_s z + \bar{k}_H\right) dz + \int_{z_j}^{z_{j+1}} \frac{z_{j+1} - z}{z_{j+1} - z_j} \cdot \cosh\left(b_s z + \bar{k}_H\right) dz\\
&= \frac{1}{{b_s}^2}\left\{\frac{-1}{z_j - z_{j-1}}\left[\cosh\left(b_s z_j + \bar{k}_H\right) - \cosh\left(b_s z_{j-1} + \bar{k}_H\right)\right]\right.\\
&\quad \left. + \frac{1}{z_{j+1} - z_j}\left[\cosh\left(b_s z_{j+1} + \bar{k}_H\right) - \cosh\left(b_s z_j + \bar{k}_H\right)\right],\right.\\
i &= 2, 3, \cdots, n-1,\\
\mathrm{E}_1 &= \int_{z_1}^{z_2} \frac{z_2 - z}{z_2 - z_1} \cosh\left(b_s z + \bar{k}_H\right) dz\\
&= -\frac{1}{b_s}\sinh\left(b_s z_1 + \bar{k}_H\right) + \frac{1}{{b_s}^2(z_2 - z_1)}\left[\cosh\left(b_s z_2 + \bar{k}_H\right) - \cosh\left(b_s z_1 + \bar{k}_H\right)\right],\\
E_n &= \int_{z_{n-1}}^{z_n} \frac{z - z_{n-1}}{z_n - z_{n-1}} \cosh\left(b_s z + \bar{k}_H\right) dz\\
&= \tfrac{1}{b_s}\sinh\left(b_s z_n + \bar{k}_H\right) + \frac{1}{{b_s}^2(z_n - z_{n-1})}\left[\cosh\left(b_s z_n + \bar{k}_H\right) - \cosh\left(b_s z_{n-1} + \bar{k}_H\right)\right].
\end{aligned}
\tag{4.110}
$$

Similar to the reduction of Eqs. (4.91), (4.92), (4.93), (4.94), and (4.95), we obtain

$$d_{ijk\ell}(F_H, L/H, T/H) = \frac{L}{4H}\int_{U_H}^{\infty}\left[(C_iC_k + S_iS_k)E_jE_\ell\right] \times \frac{F_H^2\bar{k}_H}{\left[F_H^2\cosh^2\bar{k}_H - (u^2+1)^2\right]\sqrt{u^2+2}}du. \tag{4.111}$$

Once again, $d_{ijk\ell}$ depends not on ship offsets but only on the Froude number with respect to water depth F_H, length–depth ratio L/H, and draft–depth ratio T/H.

The wave resistance coefficient of a monohull in shallow water C_w may be determined from expression (4.95) with a standard quadratic form using Eq. (4.111) to represent the disturbance potential. The symmetric matrix of $\widehat{D} = \widehat{n} \times \widehat{n}$ order is called the wave resistance matrix for a monohull in shallow water.

4.5.4.2 Calculation for Wave Resistance of Catamaran in Shallow Water

Similar to the calculation for the wave resistance of a monohull, the dimensionless wave resistance coefficient of a catamaran can be obtained from Eq. (4.73):

$$\begin{aligned} C_w &= -R_w/\left[8\rho g B^2T^2/(\pi L)\right] \\ &= \frac{L}{4H}\int_{U_H}^{\infty}\left[U^2(u) + V^2(u)\right]\cdot\frac{F_H^2\bar{k}_H\cdot F(u)}{\left[F_H^2\cosh^2\bar{k}_H - (u^2+1)^2\right]\sqrt{u^2+2}}du, \end{aligned} \tag{4.112}$$

where

$$F(U) = 2\left[1 + \cos\left(\bar{k}_H\frac{b_c}{H}\cdot\frac{u\sqrt{u^2+2}}{u^2+1}\right)\right]. \tag{4.113}$$

The wave-amplitude functions in shallow water $U(u)$ and $V(u)$ can be written as in Eq. (4.104). $\bar{k}_H$ can be determined from Eq. (4.105), U_H from Eq. (4.106).

Corresponding to Eq. (4.111), in shallow water,

$$d_{ijk\ell}(F_H, L/H, T/H, b_c/H) = \frac{L}{4H}\int_{U_H}^{\infty}\left[(C_iC_k + S_iS_k)E_jE_\ell\right] \times \frac{F_H^2\bar{k}_H\cdot F(u)}{\left[F_H^2\cosh^2\bar{k}_H - (u^2+1)^2\right]\sqrt{u^2+2}}du. \tag{4.114}$$

Again, $d_{ijk\ell}$ depends not on ship offsets but only on F_H, the length–depth ratioL/H, draft–depth ratio T/H, and spacing–depth ratio b_c/H, as previously.

The wave resistance coefficient of a catamaran in shallow water C_w is again similar to Eq. (4.95) in standard quadratic form. The symmetric matrix of $\widehat{D} = \widehat{n} \times \widehat{n}$ order is the wave resistance matrix for a catamaran in shallow water when used with the foregoing relation for disturbance potential.

4.6 Wake Wave Calculation for Monohull and Catamaran

4.6.1 Introduction

In the previous section, we used Hsiung's tent functions to approximate the ship hull surface and obtain the numerical formulas for the wave resistance of a catamaran in both deep and shallow water. Now we also use the tent functions to obtain the numerical formulas for the wake wave height of a monohull and a catamaran with symmetric demihulls in deep water.

4.6.2 Wake Wave Calculation for Monohull and Catamaran in Deep Water

4.6.2.1 Wake Wave Height Induced by a Kelvin Point Source

From Sect. 4.4.2 we know that the wake wave height induced by a Kelvin point source far behind the vessel stern is $h(x, y) = 2h_2(x, y)$.

That is,

$$h(x,y) = \frac{4k_0}{U_\infty} \int_{-\pi/2}^{\pi/2} \sec^3\theta \cdot e^{k_0 \sec^2\theta \zeta} \cdot \cos\left[k_0 \sec^2\theta \left((x-\xi)_{\cos}\theta + (y-\eta)\sin\theta\right)\right] d\theta. \tag{4.115}$$

4.6.2.2 Wake Wave Height Induced by a Monohull

From Eqs. (4.41) and (4.45) we have the following wake wave height induced by a monohull far behind:

$$
\begin{aligned}
h(x,y) = &\frac{4k_0}{U_\infty}\int_{-\pi/2}^{\pi/2}\left\{P(\theta)\cdot\cos\left[k_0\sec^2\theta(x\cos\theta+y\sin\theta)\right]\right.\\
&\left.+Q(\theta)\cdot\sin\left[k_0\sec^2\theta(x\cos\theta+y\sin\theta)\right]\right\}\sec^3\theta d\theta\\
&=\frac{8k_0}{U_\infty}\int_0^{\pi/2}\left\{P(\theta)\cdot\cos\left(k_0\sec\theta\cdot x\right)+Q(\theta)\cdot\sin\left(k_0\sec\theta\cdot x\right)\right\}\\
&\quad\cdot\cos\left(k_0\sec^2\theta\sin\theta\cdot y\right)\cdot\sec^3\theta d\theta,
\end{aligned}
\tag{4.116}
$$

where

$$
\left.\begin{matrix}P(\theta)\\Q(\theta)\end{matrix}\right\} = -\frac{U_\infty}{2\pi}\iint_{S'} f_\xi(\xi,\zeta)e^{k_0\sec^2\theta\zeta}\left\{\begin{matrix}\cos\\\sin\end{matrix}\right\}[k_0\sec\theta\xi]d\xi d\zeta. \tag{4.117}
$$

S' is the projection of the ship surface S on the plane $\eta = 0$. Equation (4.117) is the same as Eq. (4.52).

4.6.2.3 Wake Wave Height Induced by a Catamaran

We again adopt the catamaran coordinate system shown in Fig. 4.2. The sources are distributed on the central plane of each of the demihulls $\eta = \pm b_c/2$. Using relations (4.116) with (4.49) and (4.53), the formula for the wake wave height of a catamaran with symmetric demihulls can be obtained as follows:

$$
\begin{aligned}
h(x,y) = &\frac{8k_0}{U_\infty}\int_0^{\pi/2}\left\{P(\theta)\cdot\cos\left(k_0\sec\theta\cdot x\right)+Q(\theta)\cdot\sin\left(k_0\sec\theta\cdot x\right)\right\}\\
&\cdot\cos\left(k_0\sec^2\theta\sin\theta\cdot y\right)\cdot G(\theta)\cdot\sec^3\theta d\theta,
\end{aligned}
\tag{4.118}
$$

where

$$
G(\theta) = 2\cos\left(\frac{b_c}{2}k_0\sec^2\theta\sin\theta\right). \tag{4.119}
$$

$P(\theta)$, $Q(\theta)$ are as in Eq. (4.117). $G(\theta)$ is called the interference factor of a wake wave for a catamaran and is different from the interference factor $F(\theta)$ of wave resistance. b_c is spacing between the central longitudinal planes of the demihulls. When $b_c = 0$, the wake wave height $h(x,y)$ represented by Eq. (4.118) is double the wake wave height for a monohull. This would actually relate to a monohull with displacement the same as the two catamaran demihulls.

4.6.3 *Numerical Calculation for Wake Wave of Monohull and Catamaran in Deep Water*

We continue to adopt the mathematical expression for hull surface in Sect. 4.5.2 and the dimensionless variables in Sect. 4.5.4. $x = \xi/L$, $y = 2\eta/B$, $z = \zeta/T$, $\lambda = \sec\theta$, and $\lambda = u^2 + 1$.

4.6.3.1 Calculation for Wake Wave of Monohull in Deep Water

From Eq. (4.116) and the preceding formulas, we can obtain the dimensionless wake wave height for a monohull in deep water:

$$\begin{aligned}\bar{h}(x,y) &= -h(x,y)/\left[4BT/\left(\pi LF_n^2\right)\right] \\ &= -\int_0^\infty \left[P(u)\cos\left(a_d x\right) + Q(u)\sin\left(a_d x\right)\right]\cdot\cos\left(c_d y\right)\frac{\left(u^2+1\right)^2}{\sqrt{u^2+2}}du,\end{aligned} \tag{4.120}$$

where

$$\begin{aligned}\left.\begin{matrix}P(u)\\Q(u)\end{matrix}\right\} &= \int_{-1}^{0} e^{b_d z}\int_{-1/2}^{1/2}\bar{f}(x,z)\left\{\begin{matrix}\cos\\\sin\end{matrix}\right\}(a_d x)dxdz, \\ a_d &= 2\gamma_0(u^2+1), \\ b_d &= 2\gamma_0(u^2+1)^2\frac{T}{L}, \\ c_d &= \gamma_0 u(u^2+1)\sqrt{u^2+2}\frac{B}{L}, \\ \gamma_0 &= \frac{1}{2F_n^2}.\end{aligned} \tag{4.121}$$

We also use expression (4.77) to approximate the hull surface $\bar{f}(x,z)$, so that

$$\bar{f}(x,z) = \sum_{i=1}^{m}\sum_{j=1}^{n} y_{ij}N_{i,1}(x)N_{j,1}(z). \tag{4.122}$$

Substituting Eq. (4.122) into Eq. (4.121) and considering the local support property of the basic functions, we obtain

$$\left.\begin{matrix}P(u)\\Q(u)\end{matrix}\right\} = \sum_{i=1}^{m}\sum_{j=1}^{n} y_{ij}\cdot\left\{\begin{matrix}C_i\\S_i\end{matrix}\right\}E_j, \tag{4.123}$$

where C_i, $S_i (i = 1, 2, \cdots, m)$, $E_j (j = 1, 2, \cdots, n)$ are as given in Eqs. (4.88), (4.89), and (4.90).

Similarly, if Hsiung's [7] coordinate system is adopted with the origin at the bow and x positive toward the stern, then $e^{b_d z_j}$ should be replaced with $e^{b_d (z_j - 1)}$ $(j = 1, 2, \cdots, n)$ in Eq. (4.90).

Substituting Eq. (4.123) into Eq. (4.120), we obtain

$$\bar{h}(x, y) = \sum_{i=1}^{m} \sum_{j=1}^{n} y_{ij} d_{ij}, \tag{4.124}$$

where the disturbance potential

$$d_{ij}(Fr_L, T/L, B/L, x, y) = \frac{\gamma_0}{2} \int_0^{\infty} [C_i \cos(a_d x) + S_i \sin(a_d x)] E_j \cos(C_d y) \times \frac{(u^2 + 1)^2}{\sqrt{u^2 + 2}} du \tag{4.125}$$

d_{ij} depends not on ship offsets but only on the Froude number Fr_L (due to $\gamma_0 = \frac{1}{2F_n^2}$), draft–length ratio T/L, beam–length ratio B/L, and a point position (x,y) on the waterplane $(z = 0)$.

As in Sect. 4.5.3, if we define one-dimensional variables y_{mm} instead of two-dimensional variables y_{ij}, then

$$\bar{h}(x, y) = \sum_{mm=1}^{\hat{n}} y_{mm} \; d_{mm}, \tag{4.126}$$

where $\hat{n} = m \cdot n$.

The integral of Eq. (4.125) can be calculated using Simpson's formula. When the variables a_d, b_d, $|x|$ increase (i.e., Fr_L decreases), the oscillation of the integrand becomes serious, so the calculation steps need to be taken as $0.005F_n^2/abs(x)$, with 200 $abs(x)/0.05$ steps in the calculation.

4.6.3.2 Calculation for Wake Wave of Catamaran in Deep Water

Similar to foregoing deduction for a monohull, we have the dimensionless wake wave height for a catamaran with symmetric demihulls in deep water:

$$\begin{aligned} \bar{h}(x, y) &= -h(x, y) / \left[4BT / \left(\pi L F_n^2\right)\right] \\ &= -\int_0^{\infty} [P(u) \cos(a_d x) + Q(u) \sin(a_d x)] \cdot \cos(c_d y) \cdot G(u) \cdot \frac{(u^2 + 1)^2}{\sqrt{u^2 + 2}} du, \end{aligned} \tag{4.127}$$

where

$$G(u) = 2\cos\left(C_d \frac{b_c}{B}\right). \tag{4.128}$$

The wave-amplitude functions in deep water $P(u)$ and $Q(u)$ are as written in Eq. (4.121).

We again take expression (4.77) to approximate the hull surface and obtain the same formula as Eq. (4.124) and the following formula for the disturbance potential:

$$d_{ij}(Fr_L, T/L, B/L, b_c/L, x, y) = \int_0^\infty [C_i \cos(a_d x) + S_i \sin(a_d x)] E_j \cos(C_d y) \cdot G(u) \cdot \frac{(u^2+1)^2}{\sqrt{u^2+2}} du. \tag{4.129}$$

d_{ij} depend not on ship offsets but only on the Froude number Fr_L, draft–length ratioT/L, beam–length ratio B/L, spacing–length ratio b_c/L, and a point position (x,y) on the waterplane $(z = 0)$.

4.7 Programs to Calculate Resistance, EHP, and Wake Wave for Monohull and Catamaran

4.7.1 Introduction

In Sect. 4.5 we introduced the numerical calculation for catamaran wave resistance, and in this section we will introduce the application of this method, that is, how to use this method for the prediction of catamaran wave-making resistance in a preliminary design.

At the preliminary design stage, designers need to be able to vary the geometrical parameters to compare the resistance, propulsive power, and wake generation for near-shore vessel service. With these data it is possible to select favorable principal dimensions, particularly length, beam of demihulls, and separation of demihulls. Once a first review has been made by testing an initial range of parameters for wave-making resistance and wake, the top two or three variants can be selected to use as models for resistance testing in a towing tank.

The theoretical calculation method of wave resistance is a most effective method for the prediction of resistance and initial selection of principal dimensions by running a series of cases with dimensions varied linearly or in proportion so as to plot coefficient variation. At MARIC, we have used such a method for selecting the principal dimensions of high-speed catamarans in preliminary designs and obtained good results. The calculated resistance agreed with test results carried out in the

towing tank at MARIC. Such a theoretical method for the prediction of resistance can also be applied to the resistance calculation of both SWATHs and WPCs and also gives good results compared with model tests. These other concepts will be introduced in subsequent chapters.

The routines calculating wave resistance and wake wave using the numerical method in Sects. 4.5 and 4.6 are embedded in NUBLINE, a hull form generation system developed at MARIC [15, 16]. This makes calculating the wave resistance and wake wave of catamarans very convenient and fast. In the following sections, we present the source code of the kernel program routines in FORTRAN language for reference.

4.7.2 Resistance Calculation

4.7.2.1 Total Resistance

The Michell wave resistance is not generally equal to the real-world "residuary" resistance, as it is based on the "thin-ship" theory with first-order approximation, and, on the other hand, the latter is the remainder of the total resistance minus the skin-frictional and roughness allowance resistance. To compare the wave resistance with the residuary resistance, we subdivide the total resistance of a catamaran including high-speed catamaran, SWATH, and WPC in deep water into

$$R_t = (1 + FFACTOR) \cdot R_w + R_f + R_c, \tag{4.130}$$

where

R_t Total resistance,
R_w Wave resistance,
R_f Frictional resistance according to the ITTC-1957 friction formula,
R_c Roughness allowance resistance,
FFACTOR Form factor.

Thus, the effective horsepower is

$$EHP = R_t \cdot U_\infty. \tag{4.131}$$

We define the dimensionless resistance coefficients by relating the resistance components to $0.5\rho U_\infty^2 S = 0.5\rho g L F_n^2 S$, where S is the wetted area of a catamaran surface, and obtain

$$C_t = (1 + FFACTOR) \cdot \bar{C}_w + C_f + C_c, \tag{4.132}$$

where

C_t Total resistance coefficient,
$\bar{C}_w$ Wave resistance coefficient,

C_f Frictional resistance coefficient,
C_c Roughness allowance coefficient,
C_f Can be calculated from the ITTC-1957 friction formula

$$C_f = 0.075/(LogR_n - 2)^2, \tag{4.133}$$

where $R_n = U_\infty L/\nu$ is the Reynolds number and ν is the kinematic viscous coefficient; C_c is approximately 0.0004–0.0006, which accounts for the roughness allowance for a full-scale ship.

If CAD software such as Maxsurf, Autoship, Fastship, or NUBLINE, for example, is employed to design the lines of a catamaran, the wetted area S can be obtained exactly. The wetted area can also be obtained by the estimation in early stages of design using the method introduced in Chap. 5.

4.7.2.2 Wave Resistance

Equation (4.84) in Sect. 4.5.2 is a dimensionless wave resistance coefficient for the Froude number Fr_L and draft–length ratio T/L. That is,

$$C_w = R_w/\left[8\rho g B^2 T^2/(\pi L)\right].$$

Therefore, $\bar{C}_w$, a dimensionless wave resistance coefficient for $0.5\rho U_\infty^2 S = 0.5\rho g L F_n^2 S$, is as follows:

$$\bar{C}_w = R_w/\left(0.5\rho g L F_n^2 S\right) \quad = C_w\left(\frac{16B^2T^2}{\pi L^2}\right)/\left(F_n^2 S\right). \tag{4.134}$$

4.7.2.3 *FFACTOR* Form Factors

FFACTOR form factors can be determined by model tests. We present the ranges of *FFACTOR* from the examples in Chap. 7, Sect. 7.7.

According to model test results, the total resistance for a real catamaran can be expressed as

$$R_t = 0.5\rho U_\infty^2 S \cdot C_t, \tag{4.135}$$

$$C_t = C_r + C_f + C_c, \tag{4.136}$$

where

C_t Total resistance coefficient,
C_r Residuary resistance coefficient of a test model,
C_f Frictional resistance coefficient according to the ITTC-1957 friction formula,
C_c Roughness allowance coefficient.

Comparing Eq. (4.132) with Eq. (4.136), we obtain

$$FFACTOR = C_r/\bar{C}_w - 1. \tag{4.137}$$

It can be seen that 1 + *FFACTOR* represents the ratio of residual resistance from model tests and the calculated wave resistance. The difference will in general be due to the behavior of water as a real fluid in the influence region around the hull. This will include the internal dynamics of waves generated by the vessel. While the generated waves progress as the transmission of energy via the orbital motion of the fluid, energy is also dissipated by that orbital motion in the nonideal fluid.

4.7.2.4 Catamaran with a Transom Stern

The hull form with a transom stern is employed widely as demihulls on high-speed catamarans and WPCs. When a catamaran moves forward, a "hollow" forms in the water surface directly behind the transom stern. This hollow may be affected by the presence of flaps, wedges, or interrupters to adjust the vessel trim. The length of the hollow is called the "imaginary length." According to the Lagally theorem for unsteady inhomogeneous flow in an inviscid incompressible fluid, the sum of the pressures acting on a body surface is equal to the sum of the pressures acting on an arbitrary flow surface enclosing the body.

When the wave resistance of a catamaran is calculated, we can add one station behind AP in the net of Fig. 4.4, and its length is called the imaginary length. The imaginary length is a function of transom breadth and Fr_L; see Lu et al. [17], who produced an experimental curve of imaginary length for round bilge craft, as shown in Fig. 4.6 in what follows.

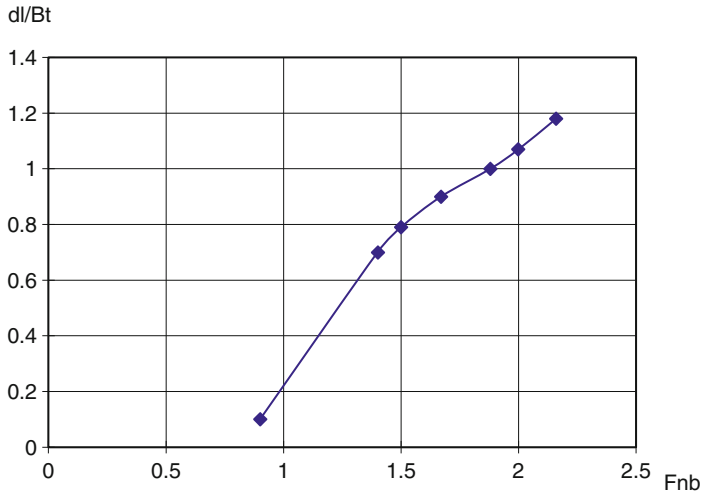

Fig. 4.6 Imaginary length of a round bilge craft at stern

In the figure, F_{nb}, Bt, and dl represent Froude numbers for demihull beam, transom breadth, and imaginary length, respectively. The Froude number for the demihull beam is

$$F_{nb} = Fr_L\sqrt{L/B_d}, \tag{4.138}$$

where waterline length is L, and demihull beam is B_d.

In Chap. 7, Sect. 7.7, the effect of imaginary length on the calculation results of wave resistance will be discussed in detail using examples. Based on the authors' experience, the imaginary length can be taken as 1–1.5 times the transom breadth for most high-speed catamarans when operating in the range of Froude numbers Fr_L from 0.60 to 1.0.

4.7.3 Program Source Code

In this section the source codes of the program kernel routines for calculating wave resistance using the numerical method in Sect. 4.5 are provided in the FORTRAN language for reference. Three subroutines are presented: DMICHELL, CTMICHELL, and DWAKECAL. The first calculates the resistance matrix D; CTMICHELL calculates the resistance components and EHP; and the last, DWAKECAL, calculates the wake wave height profile. Example calculation results can be seen in plots presented in Chap. 7.

The program routines do not have a presentation output; this is up to user. Please note that no guarantees are given related to the use of these routines. Their usefulness or accuracy is the responsibility of the individual using the code.

In what follows, the subroutine purpose, input data required, and output are described. The FORTRAN routine listings are presented following this. The routines should be useable in open-source compilers such as GFortran and linked to output processors according to student or engineer needs.

SUBROUTINE for wave resistance data matrix

DMICHELL (FN, TL, BCL, NOST, NOWL, NTOT, X, Z, D)

Purpose:
This **SUBROUTINE DMICHELL** is for calculating the wave resistance matrix (NTOT, NTOT) of monohull and catamaran with symmetric demihulls using Hsiung's method employing the coordinate system adopted in Sect. 4.5.4.

Input:

FN	Froude number
TL	Draft–length ratio
BCL	Central spacing–length ratio
NOST	Number of stations, ≤ 30.

NOWL	Number of waterlines, ≤ 15.
NOST	NOST $\times$ NOWL, ≤ 450.
X	1D array (NOST), coordinates of stations, FP is 0 and positive toward AP, dimensionless variable.
Z	1D array (NOWL), coordinates of waterlines, baseline is 0 and positive up, dimensionless variable.

Variables:

SM	Coefficients of Simpson's integral.
DELU	Step length of Simpson's integral.
NODU	Step number of Simpson's integral.

Output:

D 2D array (450 $\times$ NTOT), wave resistance matrix

SUBROUTINE for the generation of coefficients, wave resistance, and EHP

CTMICHELL(NOST,NOWL,NTOT,X,Z,Y,L,BD,T,BC,WS,U,CD,FFACTOR, RHO,NU,CF,CW,CT,RF,RW,RT,EHP)

Purpose:

This **SUBROUTINE CTMICHELL** is for calculating frictional, wave, total coefficient and resistance, and EHP of monohull and catamaran with symmetric demihulls using Hsiung's method with coordinate system as in Sect. 4.5.4.

Input:

NOST	Number of stations, ≤ 30.
NOWL	Number of waterlines, ≤ 15.
NOST	NOST $\times$ NOWL, ≤ 450.
X	1D array (NOST), coordinates of stations, FP is 0 and positive toward AP, dimensionless variable.
Z	1D array (NOWL), coordinates of waterlines, base line is 0 and positive up, dimensionless variable.
Y	1D array (NTOT), offsets and start from No.1 to No. NOWL waterline, dimensionless variable.
L	Waterline length, unit is m.
BD	Demihull beam, unit is m.
T	Draft, unit is m.
BC	Central spacing between demihulls, 0 and > 0 is for monohull and catamaran, respectively, unit is m.
WS	Total wetted area, unit is m^2
U	Velocity of ship, unit is knot.
CD	Roughness allowance coefficient

FFACTOR	Form factor
RHO	Density of water, unit is $kg{\cdot}s^2/m^4$
NU	Kinematic viscous coefficient of water, unit is m^2/s.

Output:

CF	Frictional resistance coefficient
CW	Wave resistance coefficient
CT	Total resistance coefficient
RF	Frictional resistance, unit is kN.
RW	Wave resistance, unit is kN.
RT	Total resistance, unit is kN.
EHP	Effective horsepower, unit is kw.

***Called subroutine*:**

SUBROUTINE DMICHELL (FN, TL, BCL, NOST, NOWL, NTOT, X, Z, D)
SUBROUTINE for calculating wake wave height.
DWAKECAL(FN,TL,BDL,BCL,NOST,NOWL,NTOT,X,Z,XX,YY,D)

***Purpose*:**

This **SUBROUTINE DWAKECAL** is for calculating the wake wave height matrix D (NTOT) of a monohull and catamaran with symmetric demihulls.

Input:

FN	Froude number
TL	Draft–length ratio
BDL	Beam–length ratio
BCL	Central spacing–length ratio
NOST	Number of stations, ≤ 30.
NOWL	Number of waterlines, ≤ 15.
NOST	NOST $\times$ NOWL, ≤ 450.
X	1D array (NOST), coordinates of stations, FP is 0 and positive toward AP, dimensionless variable.
Z	1D array (NOWL), coordinates of waterlines, base line is 0 and positive up, dimensionless variable.
XX	X-coordinate of a point on waterplane ($z = 0$), dimensionless variable.
YY	Y-coordinate of a point on waterplane ($z = 0$), dimensionless variable.

***Variables*:**

SM	Coefficients of Simpson's integral.
DELU	Step length of Simpson's integral.
NODU	Step number of Simpson's integral.

Output:

D 1D array (NTOT), wake wave height matrix.

Source Codes:

SUBROUTINE

```
DMICHELL(FN,TL,BCL,NOST,NOWL,NTOT,X,Z,D)
      REAL FN
       INTEGER NOST,NOWL,NTOT
       DIMENSION X(NOST),Z(NOWL)
       DIMENSION D(450,NTOT)
       REAL TL,BCL
       INTEGER M1,M11,N1
       DIMENSION E1(15),E2(15),E(15)
       DIMENSION C1(30),C2(30),C(30),S1(30),S2(30),S(30)
       REAL GAMA,DELU,SM,AIU,U,U2,SQU,FACT
       REAL LMDA,AD,BBD
       REAL XI,DELX,ZI,DELZ,EA,EE,SA,CA
       INTEGER MM,NN,NODU,IU,II,JJ,LL,I1,JA,NA,KK

       M1=NOST-1
       M11=M1-1
       N1=NOWL-1
       DO 201 MM=1,NTOT
        DO 201 NN=1,NTOT
         D(MM,NN)=0.0
    201 CONTINUE
       GAMA=0.5/(FN*FN)
       DELU=0.1*FN*FN
       NODU=301
       DO 250 IU=1,NODU
        IF (IU.EQ.1.OR.IU.EQ.NODU) THEN
        SM=1.0/4.0*DELU
        ELSE IF (((IU/2)*2).EQ.IU) THEN
            SM=4.0/4.0*DELU
           ELSE
            SM=2.0/4.0*DELU
      END IF
        AIU=IU-1
        U=DELU*AIU
        U2=U*U
        LMDA=U2+1.0
        AD=2.0*GAMA*LMDA
        BBD=AD*LMDA*TL
        SQU=SQRT(U2+2.0)
       IF (BCL<=0.0001) THEN
          FACT=SM*0.5*GAMA*LMDA*LMDA/SQU
       ELSE
          FACT=SM*0.5*GAMA*LMDA*LMDA/SQU
      *     *2*(1+COS(BCL*AD*U*SQU))
       ENDIF
        DO 220 II=1,NOST
```

```
      XI=AD*X(II)
      C1(II)=SIN(XI)
      S1(II)=COS(XI)
220   CONTINUE
     DO 221 II=1,M1
      DELX=AD*(X(II+1)-X(II))
      S2(II)=(S1(II+1)-S1(II))/DELX
      C2(II)=(C1(II+1)-C1(II))/DELX
221   CONTINUE
     S(1)=S2(1)
     C(1)=-C2(1)
     DO 222 II=2,M1
      I1=II-1
      S(II)=S2(II)-S2(I1)
      C(II)=-C2(II)+C2(I1)
222   CONTINUE
     DO 230 II=1,NOWL
      ZI=BBD*(1.0-Z(II))
      E1(II)=EXP(-ZI)
230   CONTINUE
     DO 231 II=1,N1
      DELZ=BBD*BBD*(Z(II+1)-Z(II))
      E2(II)=(E1(II+1)-E1(II))/DELZ
231   CONTINUE
     E(1)=E2(1)-E1(1)/BBD
     DO 232 II=2,N1
      I1=II-1
      E(II)=E2(II)-E2(I1)
232   CONTINUE
     E(NOWL)=E1(NOWL)/BBD-E2(N1)

     DO 250 JJ=1,NOWL
      JA=NOST*(JJ-1)
      EA=E(JJ)*FACT
      DO 250 LL=JJ,NOWL
       NA=NOST*(LL-1)
       EE=EA*E(LL)
       DO 250 II=1,NOST
        SA=S(II)
        CA=C(II)
        MM=JA+II
        DO 250 KK=1,NOST
         NN=NA+KK
         D(MM,NN)=D(MM,NN)+EE*(SA*S(KK)+CA*C(KK))
250   CONTINUE
    DO 260 I=2,NTOT
     I1=I-1
     DO 260 J=1,I1
      D(I,J)=D(J,I)
260 CONTINUE
    RETURN
    END
```

SUBROUTINE

```
CTMICHELL(NOST,NOWL,NTOT,X,Z,Y,L,BD,T,BC,WS,U,CD,FFACTOR,RHO,
NU,CF,CW,CT,RF,RW,RT,EHP)
   REAL FN,TL,BCL
     INTEGER NOST,NOWL,NTOT
     DIMENSION X(NOST),Z(NOWL),Y(NTOT)
     DIMENSION D(450,450)
     REAL L,BD,T,BC,WS,U,CD,FFACTOR,RHO,NU
     REAL CHS,RGLS,CWHSIUNG,SE,FN2
     REAL CF,CW,CT,RF,RW,RT,EHP
     INTEGER I,J

     FN=U*0.514444/SQRT(9.81*L)
     TL=T/L
     BCL=BC/L
     CHS=16.0*BD*BD*T*T/(4.1416*L*L*WS)
     RGLS=0.5*RHO*9.81*L*WS*9.81/1000
     RN=U*0.514444*L/NU
     CF=0.075/(ALOG10(RN)-2.0)**2+CD
     CALL DMICHELL(FN,TL,BCL,NOST,NOWL,NTOT,X,Z,D)
     CWHSIUNG=0.0
     DO 25 I=1,NTOT
      SE=0.0
      DO 21 J=1,NTOT
       SE=SE+Y(J)*D(J,I)
21   CONTINUE
      CWHSIUNG=CWHSIUNG+SE*Y(I)
25  CONTINUE
     FN2=FN*FN
     CW=(1+FFACTOR)*CWHSIUNG*CHS/FN2
     CT=CW+CF
     RF=CF*RGLS*FN2
     RW=CW*RGLS*FN2
     RT=RW+RF
     EHP=RT*U*0.514444
     RETURN
     END
```

SUBROUTINE

```
DWAKECAL(FN,TL,BDL,BCL,NOST,NOWL,NTOT,X,Z,XX,YY,D)
      INTEGER NOST,NOWL,NTOT
      DIMENSION X(NOST),Z(NOWL)
      DIMENSION D(NTOT)
      REAL FN,TL,BDL,BCL,XX,YY
      INTEGER M1,M11,N1
      DIMENSION E1(15),E2(15),E(15)
      DIMENSION C1(30),C2(30),C(30),S1(30),S2(30),S(30)
      REAL GAMA,DELU,SM,AIU,U,U2,SQU,FACT
      REAL LMDA,AD,BBD,CD
```

```
      REAL XI,DELX,ZI,DELZ,JA,EA
      INTEGER MM,NODU,IU,II,JJ,I1

      M1=NOST-1
      M11=M1-1
      N1=NOWL-1
      DO 201 MM=1,NTOT
       D(MM)=0.0
  201 CONTINUE

      GAMA=0.5/(FN*FN)
      DELU=0.1*FN*FN/ABS(XX)*0.05
      NODU=201*ABS(XX)/0.05
      DO 250 IU=1,NODU
       IF (IU.EQ.1.OR.IU.EQ.NODU) THEN
       SM=1.0/4.0*DELU
       ELSE IF (((IU/2)*2).EQ.IU) THEN
           SM=4.0/4.0*DELU
          ELSE
           SM=2.0/4.0*DELU
     END IF
       AIU=IU-1
       U=DELU*AIU
       U2=U*U
       LMDA=U2+1.0
       AD=2.0*GAMA*LMDA
       BBD=AD*LMDA*TL
       SQU=SQRT(U2+2.0)
       CD=GAMA*LMDA*U*SQU*BDL
     IF (BCL.LE.0.0001) THEN
        FACT=SM*COS(CD*YY)*LMDA*LMDA/SQU
     ELSE
        FACT=SM*COS(CD*YY)*LMDA*LMDA/SQU
     *     *2*COS(CD*BCL/BDL)
     END IF
       DO 220 II=1,NOST
        XI=AD*X(II)
        C1(II)=SIN(XI)
        S1(II)=COS(XI)
  220  CONTINUE
       DO 221 II=1,M1
        DELX=AD*(X(II+1)-X(II))
        S2(II)=(S1(II+1)-S1(II))/DELX
        C2(II)=(C1(II+1)-C1(II))/DELX
  221  CONTINUE
     S(1)=S2(1)
     C(1)=-C2(1)
       DO 222 II=2,M1
        I1=II-1
        S(II)=S2(II)-S2(I1)
        C(II)=-C2(II)+C2(I1)
  222  CONTINUE
       DO 230 II=1,NOWL
```

```
      ZI=BBD*(1.0-Z(II))
      E1(II)=EXP(-ZI)
230   CONTINUE
     DO 231 II=1,N1
      DELZ=BBD*BBD*(Z(II+1)-Z(II))
      E2(II)=(E1(II+1)-E1(II))/DELZ
231   CONTINUE
     E(1)=E2(1)-E1(1)/BBD
     DO 232 II=2,N1
      I1=II-1
      E(II)=E2(II)-E2(I1)
232   CONTINUE
     E(NOWL)=E1(NOWL)/BBD-E2(N1)
     DO 238 JJ=1,NOWL
      JA=NOST*(JJ-1)
      EA=E(JJ)*FACT
      DO 238 II=1,NOST
       MM=JA+II
       D(MM)=D(MM)+EA*
   *       (C(II)*COS(AD*XX)+S(II)*SIN(AD*XX))
238   CONTINUE
250 CONTINUE
    RETURN
END
```

References

1. Reanalysis of William Froude's studies of planing craft, RINA Transactions Vol 157 Part B1, 2015, pp B33–55, ISSN 1740-0694
2. Michell JH (1898) The wave resistance of a ship. Philos Mag 5(45):106–123
3. Havelock TH (1951) Wave resistance theory and its application to ship problems. Transactions US Society of Naval Architects and Marine Engineers (SNAME)
4. Lunde JK On the linearized theory of wave resistance for displacement ships in steady and accelerated motion. Trans. Society of Naval Architects and Marine Engineers 59:25–76, (1951) , and Bulletins No 1–18 , July 1957
5. Eggers K (1962) Uber die Ernittlung des wellenwitterstandes eine sschiffsmodells durch analyse sein wellensystems. In: Symposium on Ship Theory University of Hamburg, Schiffstechnick, band 9, heft 42
6. Lin WC, Day WG (1974) The still water resistance and powering characteristics of SWATH Ships. In: AIAA/SNAME Advanced Marine Vehicle Conference
7. Hsiung CC (1981) Optimal ship forms for minimum wave resistance. J Ship Res 25(2)
8. Hsiung CC, Dong S (1984) Optimal ship forms for minimum total resistance. J Ship Res 28(3)
9. Hsiung CC, Xu H (1988) Determining optimal forms of a catamaran for minimum resistance by the mathematical programming method. Marz'88, Schiffs -Technik Bd. 35
10. Dawson CW (1977) A practical computer method for solving ship wave problems. In: 2nd Int. Conf. On Numerical Ship Hydrodynamics, Berkeley
11. Rong HZ (1987) A numerical method for solving nonlinear ship-wave problem, 18th ITTC, Kobe Japan
12. Ogilvie TF (1981) Lecture notes on singularity distribution and ship resistance. Dept. of Naval Architecture and Marine Engineering, University of Michigan

13. Martin DW (1961) Polynomial representation of some ship section area curves and the calculation of the associated wave resistance. Q J M.A.M
14. Farin G (1990) Curves and surfaces for computer aided geometric design: a practical guide. Academic Press
15. Rong HZ, Zhang WR et al (1994) NUBLINE system – a hull form generation system using non-uniform B-spline technique. ICCAS 94, Bremen Germany
16. Rong HZ, Qian H et al (in Chinese) (1998) NUBLINE Hull Form Design System Based on Windows. China Shipbuilding, No. 2
17. Investigation on resistance of WPC, XP Lu and etc., (in Chinese), 8th National Seminar on High Performance Ships, 1999

Chapter 5
Calm-Water Resistance

5.1 Introduction to Calm-Water Resistance Data

In Chap. 4 we reviewed the theory behind wave making by a hull as it moves through calm water, and the interactions between the demihulls of a catamaran. The theory is based on an incompressible inviscid fluid and applies to vessels in displacement mode. As mentioned there, the normal way to determine the total resistance for a hull form, and for catamarans, is via scale model testing and to use wave-making theory to enable us to extract that element from total resistance so as to make projections for small geometrical changes added back to the remainder generally referred to as residual drag.

Having set up our target dimensions and form based on Chap. 2 and statics and stability in Chap. 3, we now turn to performance, starting with calm-water resistance, armed with our understanding of the principles of wave generation from Chap. 4. We explain here the principal rationale concerned with the hydrodynamic performance of high-speed catamarans in calm water (resistance in waves is covered in later chapters), and will introduce an approximate prediction of resistance in both deep and shallow water. We will discuss the influence of some parameters such as slenderness, hull separation, demihull lines, stern flap and wedge, and appendages on resistance of catamarans in calm water, to add to the analytical methods.

The main source of up-to-date information for a naval architect or a designer about catamarans and their performance resides in the papers published by marine engineering societies and the conferences they hold, most notably the FAST series of conferences (see resources at back of book) and regular fast-craft conferences run or supported by SNAME, CSNAME, and RINA. These papers can provide useful assistance in design optimization and for following the latest research. Our aim with this textbook is to give a basic outline of catamaran hull design and performance assessment.

First we present a bit of background from a selection of the research that has been done in the last 40 years or so.

L. Yun et al., *High Speed Catamarans and Multihulls*,
https://doi.org/10.1007/978-1-4939-7891-5_5

In 1972, Fry and Graul [1] gave a description of the design and applications of modern high-speed catamarans and compared the performance of catamarans with various demihull configurations (asymmetric and symmetric V-type demihull configuration) with monohull planing craft and showed that there is an optimum speed region for catamarans in the semiplaning region of operation.

Yelmalayev [2] compared the resistance of high-speed catamarans with that of other high-speed craft (e.g., SESs, hydrofoils, monohulls) and pointed out that over a specific range of Froude number, Fr_L, catamaran resistance would be higher than that of a planing monohull due to the fact that catamaran hull forms have lower hydrodynamic lift to decrease the friction area.

Arfiliyev [3] described a theoretical and experimental investigation of resistance of catamarans in deep and shallow calm water. His method is sometimes used for predicting the resistance of catamarans in calm water with a symmetric round bilge demihull configuration, where the lines of new design craft are close to that of the prototype of [3]. However, the data range of test results is narrow for both Fr_L and demihull parameters, so the use of these data is limited.

Song [4, 5] studied a series of model experiments of high-speed catamarans with both asymmetric and symmetric demihull configurations with round bilge and hard chine cross section, carried out in the towing tank of MARIC (Marine Design & Research Institute of China) in the 1980s and 1990s, and analyzed the influence of demihull parameters on the power performance of high-speed catamarans.

Incecik et al. [6] presented a series of model test results of catamarans designed by Vosper International Ltd., carried out systematically in the towing tank of Glasgow University's Hydrodynamic Laboratory, with different demihull parameters, to analyze the resistance, trim, and sinkage of both demihull and catamaran models in calm water and waves.

Wiklund [7] introduced an experimental investigation scheme of a catamaran hull design series'89 in 1993 for studying the hydrodynamic performance of catamarans with hard chine demihulls in the Berlin model basin; however, no publicly available test results have been issued so far.

Insel and Molland [8] and, separately, Molland et al. [9] also introduced a methodology and experimental correlation of a geometric series for determining catamaran resistance based on a significant research program at the University of Southampton in England. Reports available on the university's website are listed in the resources at the back of this book.

Shiro Matsui [10] carried out a model experimental investigation of catamarans with three demihull configurations: a typical round bilge, a mixed form with double chine, and a hard chine demihull form similar to a conventional planing hull. The test results showed the influence of design parameters on residual resistance and the motion of catamarans in both calm water and waves.

Sahoo et al. [11, 12, 13] carried out a series of tests and analytical predictions for hard chine fast catamarans looking at the resistance components and interaction for a geometrical series that linked back to both Molland's work with his team on round bilge hulls and the chined hull series tested earlier in the Berlin model basin.

Working together with N.A. Armstrong and P.R. Couser from Australian Maritime Engineering, A.F. Molland and I.K.A.P. Utama from Southampton University prepared a joint paper [14] to FAST'97 summarizing work on calm-water resistance and powering based on an approach to determining a so-called form factor for catamarans that would apply to the viscous resistance component of drag to account for demihull interaction.

This is a useful point to illustrate diagrammatically the drag components of a catamaran or multihull drag, interpreted from [14] (Fig. 5.1). The intent of a combined scheme of analysis and model testing is to be able to extract the coefficients characterizing the components at model and full scale and the related nondimensional coefficients so that the total calm-water drag for a given vessel design may be calculated.

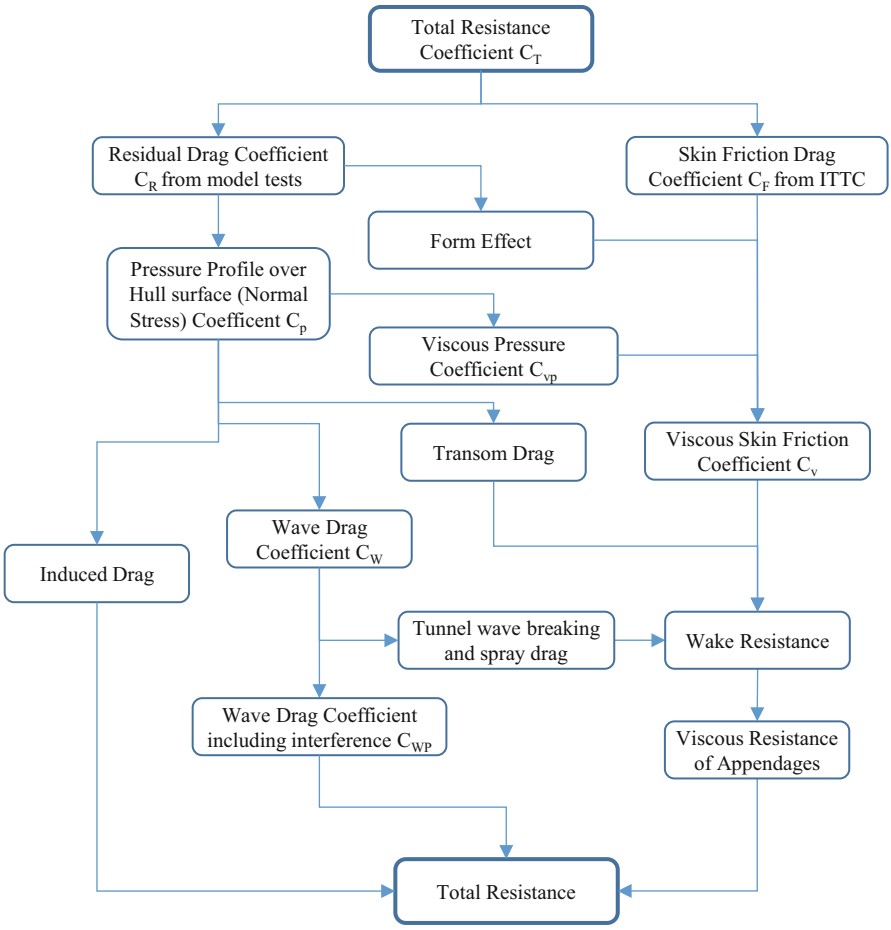

Fig. 5.1 Catamaran resistance components

Since the 1990s, with the increasing ferry operator interest in multihull vessels, there has been a continuation of research into resistance. At the University of Southampton the work by Insel and Molland has been extended, at NTNU in Trondheim work has continued on resistance and motion, and, as we shall see in Chap. 12, research on resistance, motion, and wave loading is ongoing at Australian universities. Significant work has also been carried out in the USA, Germany, Japan, Greece, Italy, China, and Indonesia. Papers have been presented on studies of demihull form, asymmetry, spacing, and stagger for wave resistance, overall resistance through model tests, and motion. In addition to the chapter references, at the back of this book we give a listing of some of these studies as additional references for the student to use as resources and suggest looking into the FAST series of conferences and the material available through RINA and SNAME as a starting point. A wider search on the Internet, using the main search engines or within document libraries such as Scribd, can also be very helpful.

If one takes the body of work in the initial series of references cited earlier and collate together the common thread, a general approach to resistance determination and interpretation can be described and built upon. It is this approach that has been extended in the last 20 years or so as catamaran hull design has become more refined so as to minimize resistance. We will do this in the following sections in this chapter, introducing also work carried out at MARIC.

5.2 Resistance Characteristics and Selection of Demihull Configuration

During the evolution of high-speed catamarans many different demihull configurations have been used for catamaran craft, such as round bilge, hard chine, and planing hull geometry, as well as symmetric and asymmetric demihull configurations. The demihull lines for a vessel are best related to the design operational speed, as follows (and illustrated in Fig. 5.2 on the next page):

(a) Conventional displacement lines for low speed ($Fr_L < 0.5$), asymmetric cross sections for catamaran;
(b) Round bilge symmetric lines for medium speed ($Fr_L > 0.5$);
(c) Round bilge symmetric lines for higher speed with flattened aft and transom;
(d) Round bilge for fore body and flattened lines for rear body and transom stern, that is, mixed lines, as used on high-speed monohulls;
(e) Hard chine V bottom hull used for high-speed monohull craft;
(f) Body plan as used for Westamarin high-speed catamarans, with asymmetric demihull.

Catamaran calm-water resistance can be expressed as twice the resistance for a demihull plus the interference resistance from waves in the demihull spacing. Thus, line design for catamarans should be broken down into two parts, designing demihull lines and then determining the spacing between demihulls for optimum resistance, taking into consideration the structural arrangement for the cross structure.

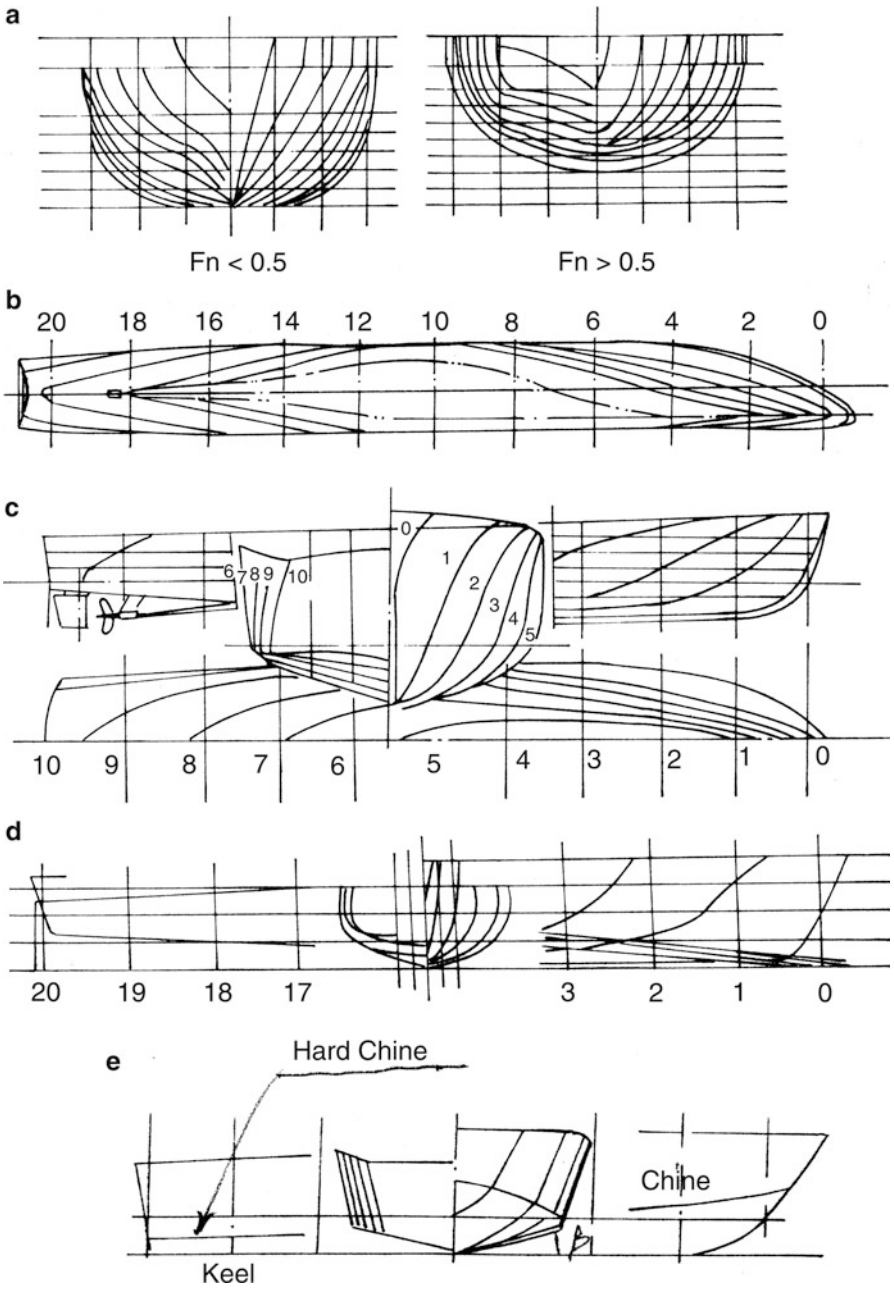

Fig. 5.2 Typical lines for catamaran: (**a**) line plan and body plan for conventional ship Fr_L <0.5; (**b**) round bilge, Fr_L >0.5 with flatter asymmetrical stern lines; (**c**) round bilge for forebody semiplaning aft; (**d**) high-speed round bilge; (**e**) hard chine lines; (**f**) asymmetric demihull for planing catamaran

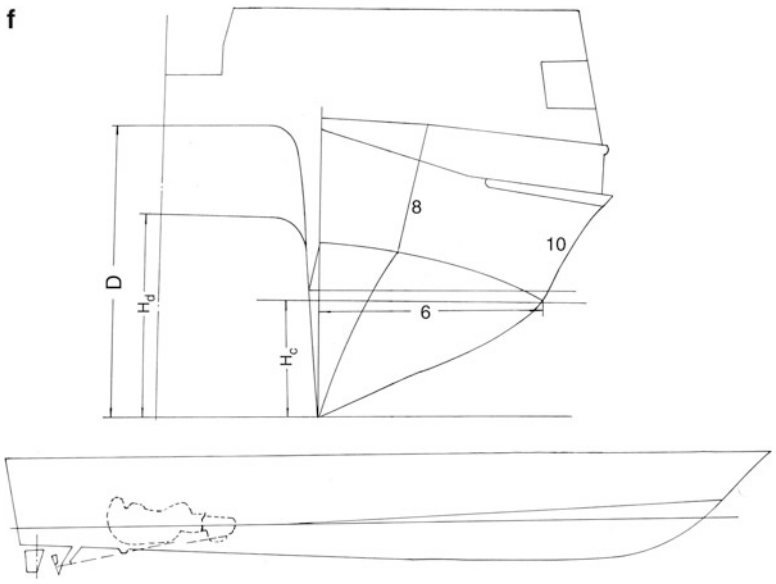

Fig. 5.2 (continued)

Both the demihull lines and the space between demihulls should be designed based on optimization for the intended vessel service speed. The demihull lines not only influence the resistance of demihulls themselves but also the interference resistance.

Selection will focus therefore on how to choose a demihull profile and section, whether round bilge or chined section type, symmetric or asymmetric, and spacing. It may be noted that the vertical wall on the inside of Westamarin catamarans minimized wave making in the tunnel and, thus, wave-making interaction. If this is reversed with a near vertical wall on the demihull outside, then external wash will be minimized. This is currently the form used by many super slender passenger catamarans for river ferries.

5.2.1 Planing Type or Not?

Some catamarans operate at above 35–40 knots and at high relative speed where $Fr_L = 0.8–1.1$ or higher, that is, close to or in the fully planing region for monohull planing craft.

The section shape for many vessels is rounded rather than chined (having a sharp corner between bottom and hull side). This limits the hydrodynamic lifting force generated, hence the term *semiplaning* as applied to them. Wave-piercing catamarans, such as the designs by Incat, use a V bottom to the demihulls while operating in this same semiplaning region. In general, $L/b = 7–12$ for high-speed catamarans and as high as 18 for river catamarans and some wave piercers, and this is another important characteristic for limiting hydrodynamic lift (planing) forces.

Catamarans also have a low displacement-length coefficient Δ/L^3 (represented by ψ), where Δ is in cubic meters, or the inverse, a high demihull slenderness $L/\Delta^{1/3}$ (represented by φ), which is the main characteristic that reduces the wave-making resistance of a demihull operating below $Fr_L = 1$. In general, the slenderness is high, up to 8 or more. Since 2000 or so designers have moved further toward super slender demihull forms with L/b up to 20 for both wave piercers and smaller passenger-only vessels operating in river or estuary traffic.

Owing to the high slenderness, a catamaran will develop a low pitch angle as it accelerates to service speed and generate a hydrodynamic lift force that is a fraction of the vessel total weight rather than supporting the total weight, as with a planing vessel. The vessel equilibrium is affected by the lift, but it is buoyancy that controls the equilibrium.

For a semiplaning vessel, Fig. 5.3a shows the dynamic lift fraction versus Fr_{∇} for a planing hull, and it may be noted that the dynamic lift fraction will be very low for craft with high length/beam ratio ($L/B > 4$) at higher Fr_{∇}. From the figure, one can see that in the case of $Fr_{\nabla} = 1$ and $L/B > 6$–7, the lift fraction of the craft will be lower than 20%.

Therefore, there are two directions to take for fast catamarans: long and slender or, alternatively, if the vessel is to operate significantly above $Fr_L = 1$ ($Fr_{\nabla} = 2$–2.5), then a lower L/b will be necessary. Where dynamic forces fully support a vessel, the planing surface area and center of lift will vary significantly with speed and vessel pitch (angle of attack). At any given speed it is necessary to carry out repeated calculations testing the equilibrium of lift and drag forces and turning moment until a balance is found [15]. This must be repeated over operating speed range where the vessel is planing, meaning above $Fr_L = 1.0$, approximately.

Figure 5.3b shows the resistance/weight ratio and angle of attack versus Fr for five models of a planing hull series. From the figure one can see that there are no peaks on the resistance curve in the case of model slenderness higher than 7.8. In this case the trim angle of the model is also small, so that the model has a very small lift fraction.

In the case of a semiplaning design, with the lift fraction in the range of 20%, it may be sufficient at the initial design stage to determine wave and friction drag together with the vessel trim following a displacement vessel approach and use the trim to assess hydrodynamic lift for this "equilibrium" using the area of the hull bottom out to the bilge using a line out to 30% round the bilge as a means of identifying an effective "dead rise" and bottom area, if the hull sections are not chined. If the vessel is intended for service speeds close to or above $Fr_L = 1.0$, then a dead-rise hull bottom with small bilge radius or bilge chines may be considered useful to gain the maximum lifting effect.

If our target is a true planing catamaran, we would need to take the design in steps, considering both the performance in the planing regime at service speed and also operating in the displacement speed regime. In the latter case, the following discussion applies. For the planing regime, the approach developed by Savitsky and others can be used to determine equilibrium, resistance, and powering. Design

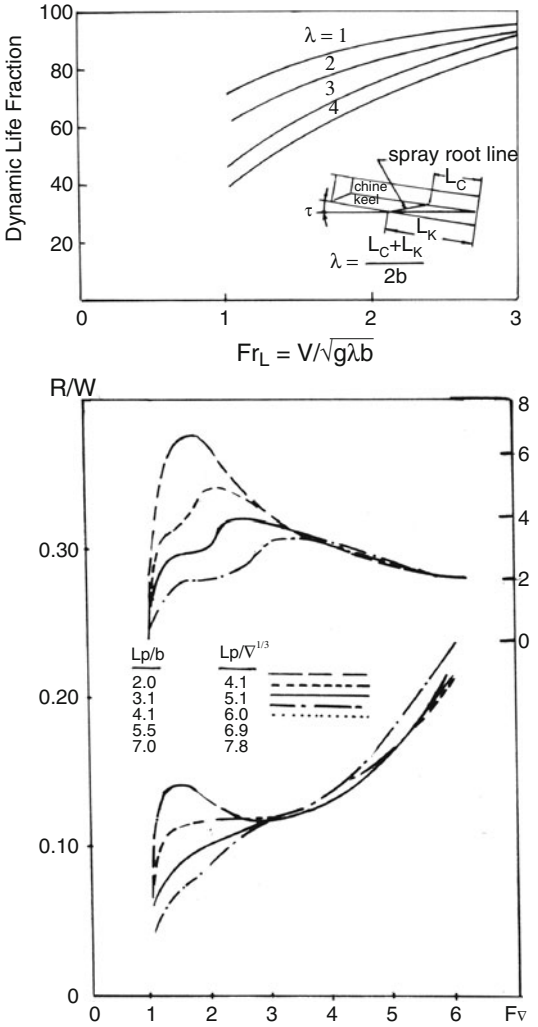

Fig. 5.3 (**a**) Dynamic lift fraction versus speed coefficient Fr_v; (**b**) resistance/weight ratio and angle of attack versus speed coefficient for five models of series

considerations for such craft, generally pleasure, racing, or utility vessels, will be taken up later, at the end of Chap. 7.

Professor David Savitsky [16, 17] derived the hydrostatic and hydrodynamic coefficients to determine the lift and drag of a planing hull based on the following expressions:

$$C_{B_0} = \alpha^{1.1}\left(0.012\lambda^{0.5} + 0.0095\frac{\lambda^2}{\mathrm{Fr}_D^2}\right), \tag{5.1}$$

$$C_{B_\beta} = C_{B_0} - 0.065\beta C_{B_0}^{0.6}, \quad \text{where } \beta \text{ is the dead-rise angle, and} \tag{5.2}$$

$$C_{B_\beta} = \frac{D}{0.5\rho v^2 B^2}. \tag{5.3}$$

Here $\lambda = l/B$ is the wetted length/beam ratio, where l is the average planing length, B the vessel chine beam, α the planing angle, β the dead-rise angle, Fr_{D} the Froude number based on displacement volume D m^3, v vessel speed, and C_{B} the lift coefficient with zero dead-rise angle or positive dead-rise angle β.

The first part of the right-hand side of Eq. (5.1) gives the static lift, and the second part gives the hydrodynamic lift of a planing plate. Equation (5.2) shows the influence of the dead-rise angle on the lift force, where C_{B_β} represents the dynamic load coefficient in the case of dead-rise angle β and C_{B0} when it is equal to zero.

Figure 5.4a, b shows plots of Eqs. (5.1) and (5.2). For catamarans with a demihull length/beam ratio equal to 7, $Fr_L = 1$, and running trim angle at 2°, the dynamic fraction of the demihull lift will be below 10%, even if the dead-rise angle is equal to zero, according to the preceding equation (Fig. 5.4a).

If we consider the influence of demihull dead-rise angle, the dynamic lift fraction should be lower than that. From this point of view, the dynamic lift for high-speed catamarans should be very low, even in the case of higher Fr_L, owing to high demihull slenderness. It is only when a catamaran is specifically designed for Fr_L well above 1.0 that a significant proportion of the mass is supported by planing forces, as is the case for racing catamarans designed for operation at 60 knots and higher. The lines for these craft are like a deep V planing monohull split longitudinally, with the demihull inner walls being vertical.

The lines for the demihulls of commercial high-speed semiplaning catamarans are similar to a displacement fast boat with a slender waterline or other fast displacement vessels, so the lift fraction of these commercially oriented catamarans is small. However, some lift is generated, so one can design the demihull lines to induce a better trim angle, increase lift, and finally reduce the resistance, similarly to fast monohull displacement vessels and high-speed military vessels. See the lines in Fig. 5.1d–f for examples.

The resistance of high-speed catamarans can be considered the resistance of two high-speed slender monohulls plus interference between the demihulls. Initially, if demihull interference is ignored, then total resistance is actually the same as that for two slender monohulls. Figure 5.4c shows $C_{\mathrm{r}} = f(Fr_L, \varphi)$ of a high-speed displacement monohull, where C_{r} is the residual resistance coefficient and φ is slenderness, defined as $\varphi = {}^{L}/_{\nabla^{1/3}}$. Figure 5.4d shows the relationship between the residual resistance of a high-speed catamaran and Fr_L for different slenderness φ, and k/b is the relative hull separation. Note that the same influences exist for both monohull and high-speed catamarans, that is, high slenderness produces lower wave-making resistance.

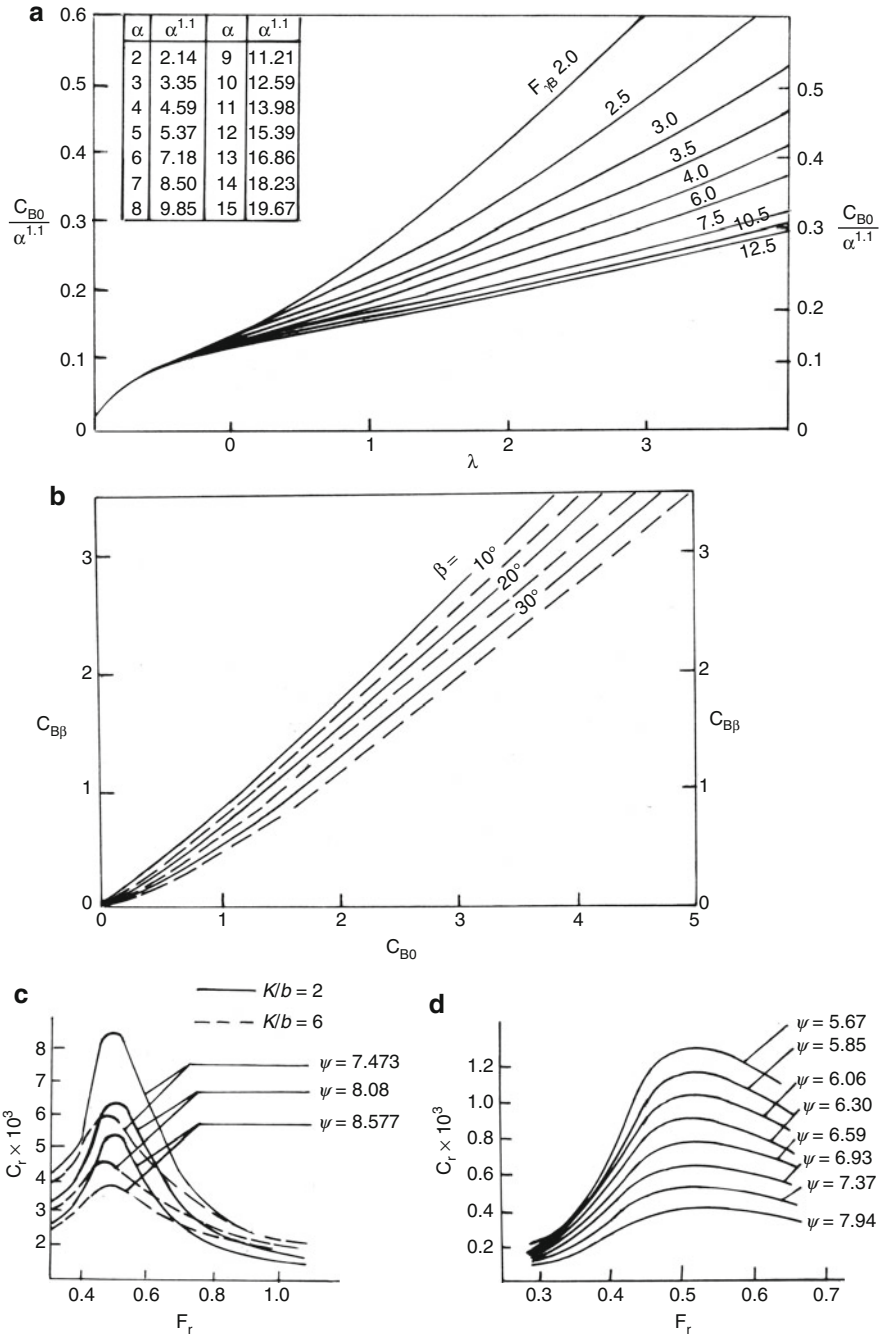

Fig. 5.4 (**a**) $C_{B0}/\alpha^{1.1}$ versus λ for various Fr_v; (**b**) $C_{B\beta}$ versus C_{B0} for various dead-rise angles β; (**c**) residual resistance C_r versus Fr_L for various slenderness ψ; and (**d**) C_r versus Fr_L for various slenderness ψ and relative hull separation K/b

Total resistance can therefore be optimized starting with the form of the demihulls. This can be improved further over the tunnel wave interaction at design speed by the demihull spacing, as we discuss subsequently.

5.2.2 *Interference Effects Between Demihulls*

The difference in flow pattern between the demihulls of high-speed catamarans and around a monohull is that the flow for a catamaran demihull is asymmetric, while for a monohull it is symmetric. On the internal side of a demihull, the flow speed will be increased, which will also lead to a change in the boundary layer thickness and, thus, to increased vortices and viscous interference drag. Flow blockage may occur depending on the exact shape of the demihulls forming the passage and cause the water surface to rise and spray in the tunnel, as well as increase resistance in the case of small hull separation.

The difference in resistance between a catamaran and a monohull is mainly due to the complicated flow interference factors that arise from both viscous and wave-making effects, generating the additional so-called interference drag.

For high-speed catamarans, with each demihull having a high slenderness, the viscous interference effect will be smaller than the wave-making interference effect, and in general, the viscous interference effect can be neglected.

The wave pattern generated by catamarans may be as shown in Fig. 5.5a, b. The wave interference between the demihulls is caused mainly by the diverging wave generated by the two demihulls, interacting in the gap between the two hulls. For this

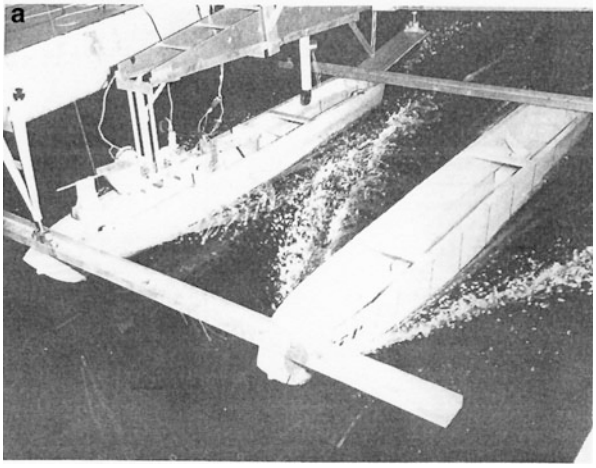

Fig. 5.5 (**a**) Wave pattern for a catamaran model running in towing tank; (**b**) wave pattern for a typical catamaran; (**c**) Kelvin wave profile of catamaran; (**d**) transverse wave interference; (**e**) experimental resistance data for catamaran forms

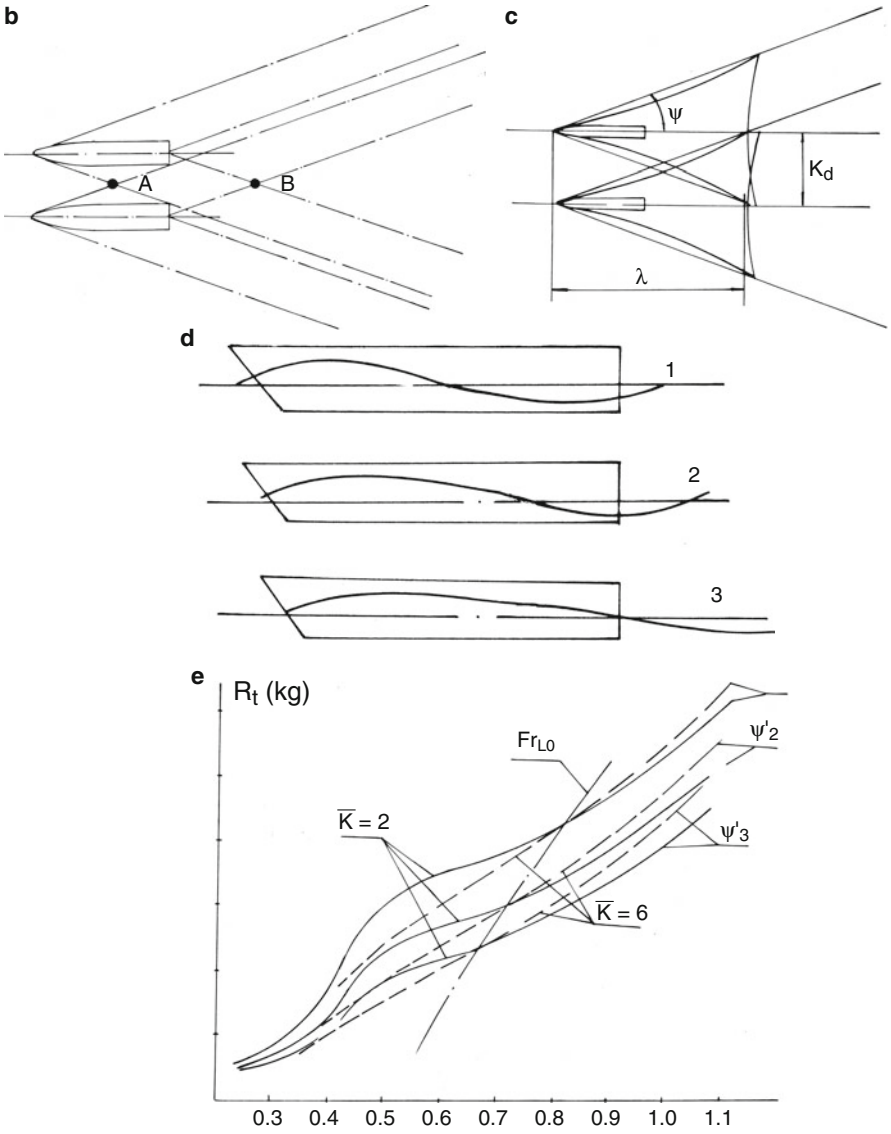

Fig. 5.5 (continued)

reason, the space between the demihulls is an important factor influencing the interference wave, as is the selection of the demihull lines, which generate the diverging wave.

From the figure one can see two divergent wave systems, generated at both the bow and stern of each demihull, that generate interference wave patterns between demihulls at both the forward part and after part of the catamaran, so as to cause an expanding wave pattern from the stern.

From Fig. 5.5b one can see that points A and B are intersection points for both bow and stern divergent waves. It should be noted that at larger hull separation, point A, the intersection point of the bow divergent wave, moves afterwards, so the superposition of such divergent waves with a bow transverse wave is small and leads to a small interference wave and additional wave resistance.

The wave interference problem must be considered based on the Kelvin wave system generated by a moving body on a water surface, as shown in Fig. 5.5c. The intersection of the divergent wave will move toward the stern if the hull separation is enlarged, so the overlap area of transverse waves caused by both demihulls will be decreased. Consequently, this decreases the wave interference between demihulls. For the same reason, in the case of higher demihull slenderness, the angle ϕ is decreased, so wave interference is also reduced.

It is necessary, therefore, to consider the interference caused by not only the divergent wave but also the transverse wave. In the case of a ship moving forward, the ship wave is transmitted afterward, and the bow wave will superpose onto the stern wave, thereby causing wave interference. If the bow transverse wave is transmitted to the stern and in the same phase as the stern wave, meaning the wave peak of the bow wave superposes onto the stern wave peak, then unfavorable interference is generated, and if the bow wave peak superposes onto the trough of the stern wave, then favorable interference is generated.

The phase difference is in terms of the two conditions, that is, the transverse wave length (in terms of ship speed) and the distance between bow and stern wave (in terms of ship length), so the phase difference is related to $\mathrm{Fr_L}$. Figure 5.5d shows the three conditions of transverse wave interference:

1. Unfavorable interference, that is, the bow transverse wave half-length located within ship length. In the case where $Fr_L = 0.5$, the transverse wave peak is transmitted to the stern and superposes on the stern wave peak, causing a most unfavorable interference, as shown in Fig. 5.4d. Therefore, $Fr_L = 0.5$ is called a critical Froude number. With respect to high-speed catamarans, since the transverse bow wave is superposed not only on the stern wave generated by the same demihull but also that by the other demihull, so the interference will be strengthened. Thus, the interference is important not only in terms of $\mathrm{Fr_L}$ but also the hull separation k and demihull slenderness φ since it influences the transmitted transverse wave range, as shown in Fig. 5.5c.
2. For the same reason, where the bow transverse wave half-length exceeds the ship length at high Fr_L, shown as 3 in the figure, this causes favorable interference.
3. Where the bow transverse wave trough is located at the stern and superposed on the stern transverse wave, the interference will be equal to zero, shown as 2 in the figure.

In general, the design Fr_L of high-speed catamarans is higher than 0.5, so it is possible to design a vessel with favorable interference. Clearly, the proposed principal dimensions and range of Fr_L, k, and φ or ψ must all be specified to assess potential favorable interference.

To investigate this, a series of model experimental investigations was carried out at MARIC [18] to derive favorable Fr_L related to demihull slenderness and hull separation, K_d/b (see Fig. 3.1 for definitions). The test models were of round bilge form, and the draft was changed to form different slenderness and b/T cases for investigation, see Table 5.1 below. Since, in general, b/T has a lesser influence on resistance, the influence of slenderness on resistance and more favorable Fr_L could be studied separately.

Five hull separations, $K_d/b = 6, 3.2, 2.6, 2.0, 1.6$, were used for tests.

In what follows, Fig. 5.5e shows the resistance curves of models for $K_d/b = 6$ (max.) and 2.0 (rather small), and the inflection point Fr_{L0}, that is, the inflection Fr_L between the different geometries, can be found in the figure, ranging from Fr_L 0.66 to 0.83.

According to the test results, the regression formula for inflection Fr_{L0} for wave interference can be obtained as

$$Fr_{Lo} = 0.55 + 0.042\left[\frac{0.166}{\left(\frac{k_d}{b} - C_p\right)^{7/4}} + 1\right]\left(\frac{\nabla}{(0.1L)^3}\right)^2.$$

Using this formula, a designer may select the proper geometric parameters and inflection Fr_{L0} and try to determine the desired Fr_L above the inflection Fr_{L0}.

Table 5.2 below shows the inflection Fr_L calculated using this formula and the design Fr_L of various practical high-speed catamarans for the reader's reference. From the table it can be seen that the Fr_L designs are greater than Fr_{L0} for all high-speed catamarans, and this is reasonable.

Table 5.1 Main geometrical parameters of test models at MARIC

	L/b	B/T	C_p	ψ
Design waterline	10.53	2.375	0.629	1.896
Overloaded	10.53	2.036	0.657	2.396
Light load	10.53	2.664	0.606	1.585
Series 64 in USA	8.45–18.26	2–4	0.63	0.529–1.93

Table 5.2 Fr_{ld} (design Fr_L) and Fr_{L0} (inflection Fr_L) for some high-speed catamarans [18]

Craft name	MXA 1700	AZ100	Shuman	Double Eagle	Double Eagle II	High-Speed Twin	Yong Xin	IET catamarans
ψ	3.47	2.83	2.912	2.35	2.421	2.035	1.25	1.77
Fr_{l0}	1.114	0.928	0.936	0.805	0.820	0.743	0.632	0.704
Fr_{ld}	1.272	1.068	0.930	0.820	0.912	0.775	0.918	0.941

5.2.3 *Symmetric or Asymmetric Demihull*

Since the wave resistance of catamarans is mainly caused by demihulls, demihulls with low slenderness and large entrance waterline angles at the bow will generate large divergent waves. An asymmetric demihull with vertical upright plane on one side will generate lower divergent waves owing to the small water entrance angle at this side.

Figure 5.6 shows two types of asymmetric demihull. L is the demihull length, b the beam, and k the space between the demihulls. The left part of the figure shows that the flat hull wall is designed on the demihull external side with a very fine waterline entrance angle, so the external wave height should be small, which is very suitable for inland catamarans, as it will generate lower external transverse waves, lessening the wave impact on a river bank or lake shore.

The alternative is shown in the right part of the figure where the flat part is at the demihull's internal side. In this case the divergent wave between the demihulls will be small and so generate a small divergent wave between the demihulls and less wave interference. This form is often used for very fast vessels, including planing catamarans.

From this point of view, the asymmetric demihull may be suitable for catamarans in particular applications:

- High speed and operated in inland waterways (flat external surface);
- Small space between demihulls, minimizing interference drag (flat internal surface).

The second case is exactly where Westamarin started with its designs for passenger ferries in the 1970s. The challenge with an asymmetric demihull is that it will cause greater wave resistance due to a higher (external) waterline entrance angle at the bow (double the angle for a symmetric demihull), generating a larger divergent wave at the external side, and this will negate the decrease in interference wave drag

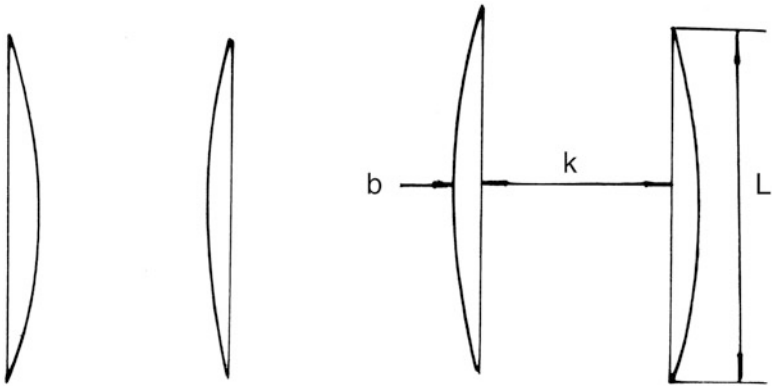

Fig. 5.6 Two types of asymmetric demihull

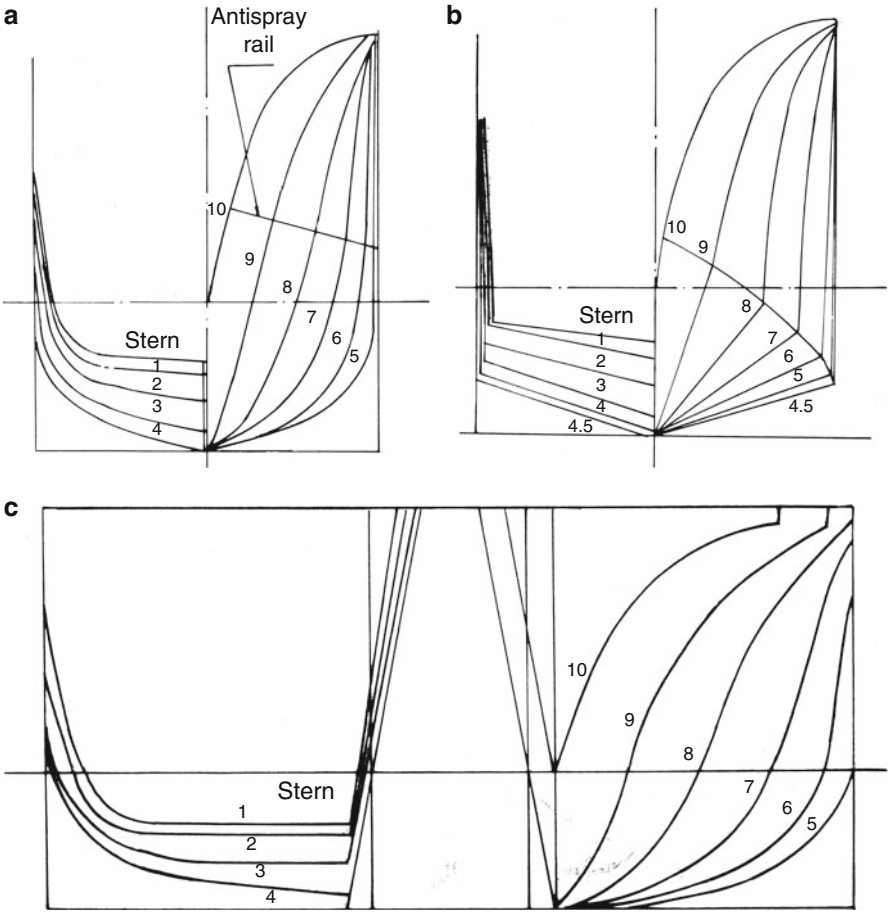

Fig. 5.7 (**a**) Lines for round bilge; (**b**) hard chine; (**c**) asymmetric demihull

if there is more space between the demihulls. It only works positively for narrow hull spacing where interference is itself significant. Perhaps this is one of the reasons why designers mainly use the symmetric demihull on modern high-speed catamaran ferries.

Figure 5.7a shows a catamaran with a symmetric demihull and round bilge configuration, and Fig. 5.7b shows it with a symmetric demihull in a hard chine configuration. Figure 5.7c shows a asymmetric demihull of a catamaran model manufactured at MARIC.

Resistance tests were carried out in the towing tank at MARIC on the vessels with lines in Fig. 5.6c [4], and the results of the tests in calm water are shown in Fig. 5.8a below. The data were reduced to R/Δ against vessel speed in knots or as Fr_L.

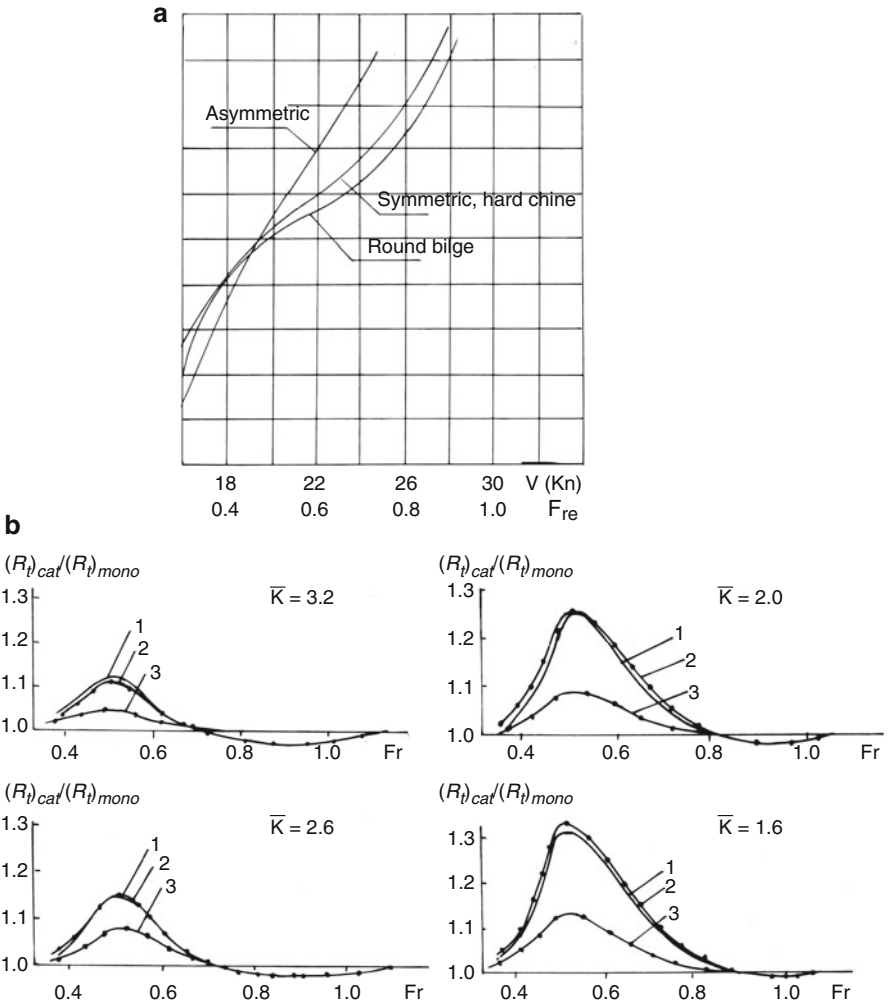

Fig. 5.8 (**a**) Calm-water resistance R/Δ versus speed v; (**b**) interference drag coefficient versus demihull cross section

The tests produced the following results:

- The resistance is lowest for asymmetric demihull below $Fr_L = 0.45$ due to small interference wave drag;
- Above $Fr_L = 0.45$, the resistance of a symmetric demihull catamaran will be lower than an asymmetric one owing to the aforementioned reasons;
- Below $Fr_L = 0.8$ the resistance of a symmetric demihull with a round bilge will be lower than in hard chine form; however, at higher Fr_L the difference will be small

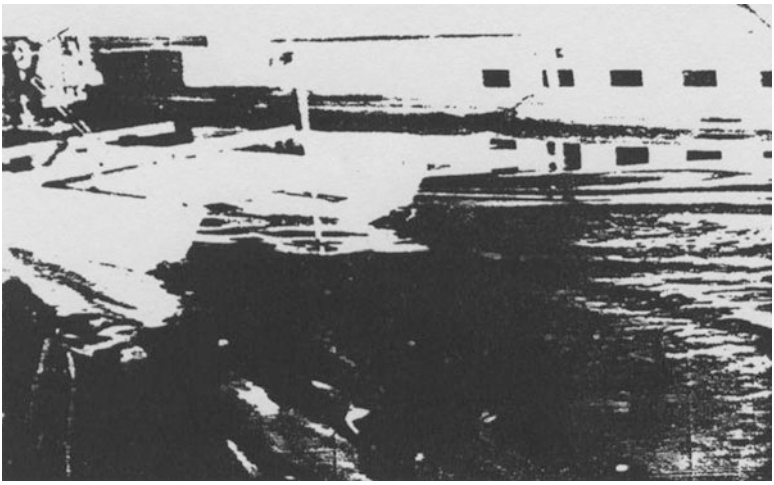

Fig. 5.9 Running attitude of catamaran in towing tank. Model is running at 15.1 knots and has *K*/*b* of 3.2

and may be even higher for a round bilge than a hard chine owing to some dynamic lift contributed by the latter.

Figure 5.8b below shows the influence of demihull transverse section on the interference drag coefficient of catamarans at different hull separations and Fr_L. Note that the interference drag coefficient for asymmetric demihulls is lower than that on symmetric demihull catamarans, whether there is favorable or unfavorable interference. This is due to the lower wave resistance generated by the internal side of demihulls because of the sharp internal side of the bow and small entrance angle.

Meanwhile, the influence of a demihull transverse section (hard chine or round bilge) mainly influences the resistance of demihulls, less so the wave interference, that is, the interference drag coefficients for both hard chine and round bilge configurations of demihulls are similar.

Figure 5.9 shows the running trim of a catamaran towing tank model in calm water at MARIC.

Figure 5.10 shows the drag/weight ratio ε and trim angle φ of a catamaran model with asymmetric demihull with flat internal side and different spacing between demihulls [4]. It is shown that the resistance/weight ratio of all the models will be very close due to the flat internal sides of the demihulls, while the resistance is higher than that of a monohull where Fr_L is higher than 0.5.

To sum up, the most important factors for catamarans are slenderness and space between demihulls as well as demihull configuration. The influence of the first two factors will be discussed further later in this chapter.

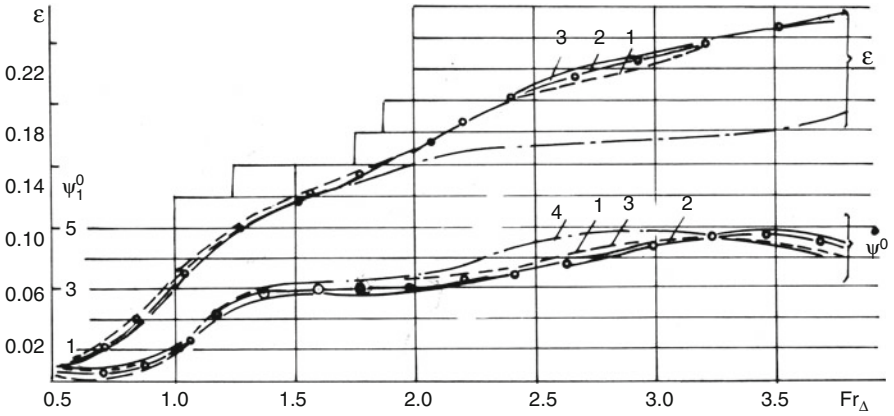

Fig. 5.10 Drag/weight ratio ε and trim angle ψ of a catamaran model with asymmetric demihulls with different spacing $\bar{C}$ between demihulls

5.3 Approximate Calculation for Resistance in Deep Water

In Chap. 4 we introduced a theoretical calculation for the wave-making resistance of catamarans in calm water, which should be very useful in the selection of the principal dimensions. However, for a feasibility study and initial project design, designers must estimate the preliminary design performance for vessel powering and offer a design for the client based on this total resistance and powering estimate.

In this section, we will introduce a method for estimating catamaran resistance, particularly for the estimation of wave-making resistance based on model test data. For more precise estimation of this drag, one can correlate using towing tests on a near final configuration in later design stages.

The resistance of catamarans can be expressed as

$$R_t = 2R_w + R_i + 2R_f + R_{cs} + R_{ap} + R_a, \tag{5.4}$$

Where

R_t Total resistance of catamarans;
R_i Interference resistance caused by wave interference of both demihulls;
R_w Wave resistance caused by one demihull;
R_{cs} Resistance caused by cross structure;
R_f Water friction resistance caused by each demihull;
R_{ap} Appendage drag;
R_a Air drag.

Since in general the cross structure is above the water surface, this resistance can be assumed to be zero at an early design stage, so Eq. (5.4), can be rewritten as

$$R_t = 2R_w + R_i + 2R_f + R_{ap} + R_a. \tag{5.5}$$

5.3.1 *Wave-Making Resistance* R_w

Theoretical Method

Using Chap. 4, one can calculate the wave resistance, including the wave interference drag, using an analytically based computer program. However, it does not include the viscous interference drag in this method, but one can predict such interference drag with the aid of model test results from research conducted at the University of Southampton, UK, which is introduced in what follows, and total drag predictions should be accurate for fine-form round bilge vessels. Alternative test series data for chine form hulls are given in references [11, 12]. Figure 5.11 shows the wave-making resistance calculated by theory for different demihull spacings by Arfiliyev [3].

Model Test Series Completed at University of Southampton

Insel, Molland, and associates at the University of Southampton in the UK [8] used four (National Physical Laboratory, NPL) high-speed monohull models as the (symmetrical) demihulls of catamaran models with different separations, S, shown in Fig. 5.12a, b, to study catamaran resistance with regulated variations in form. Details of the four models are shown in Table 5.3.

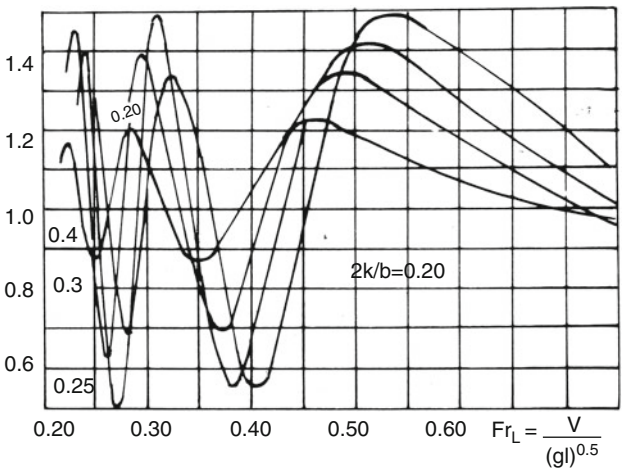

Fig. 5.11 Wave-making resistance ratio of a catamaran at various hull separations ($2K/b$), according to theoretical calculation

Model C2 used the Wigley form, which has symmetrical parabolic lines forward and aft and has a rectangular profile. Models C3, 4, and 5 have an increasing length-to-displacement ratio and diminishing wetted surface areas. They show a round bilge profile and lines, with transom stern form based on the National Physical Laboratory round bilge monohull series tested by David Bailey's team in the 1970s. This approach enabled correlation with the earlier test programs. Catamaran demihull spacings S/L of 0.2, 0.3, 0.4, and 0.5 were tested.

In the table L, B, and T are the length, beam, and draft of demihull, and $L\nabla^{\frac{1}{3}}$ is the length-to-displacement ratio. The body plans of the model demihull series are shown in Fig. 5.12a.

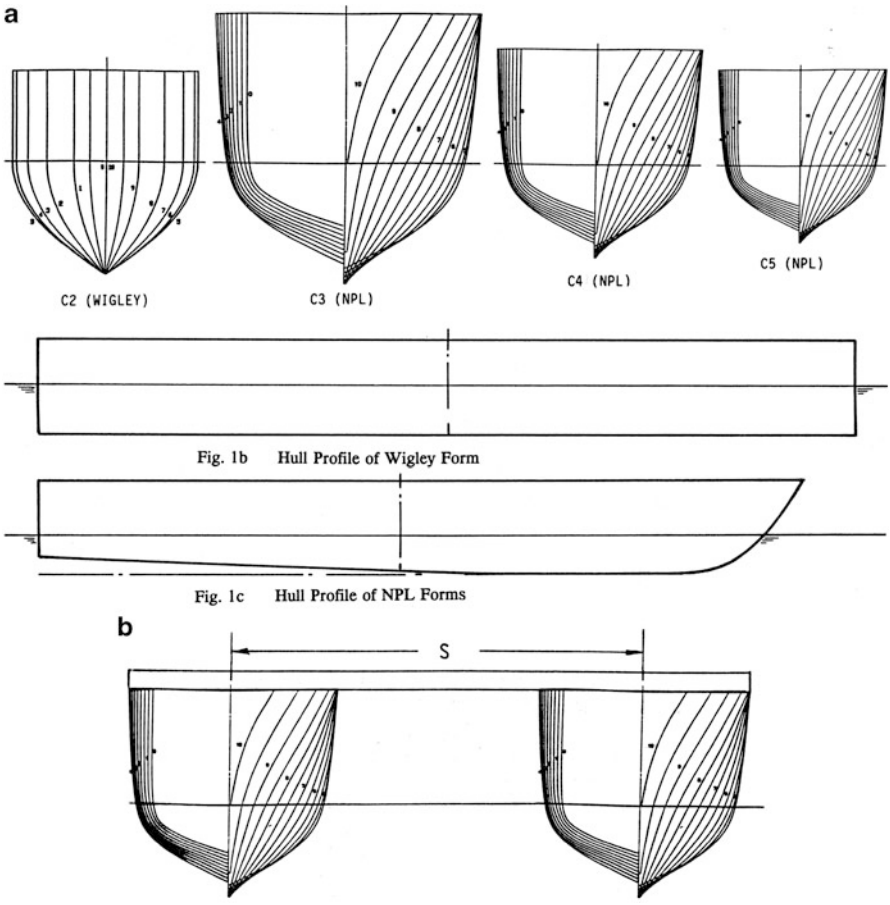

Fig. 5.12 Molland: (**a**) initial series body plans and profile; (**b**) demihull spacing diagram; (**c**) second series body plans

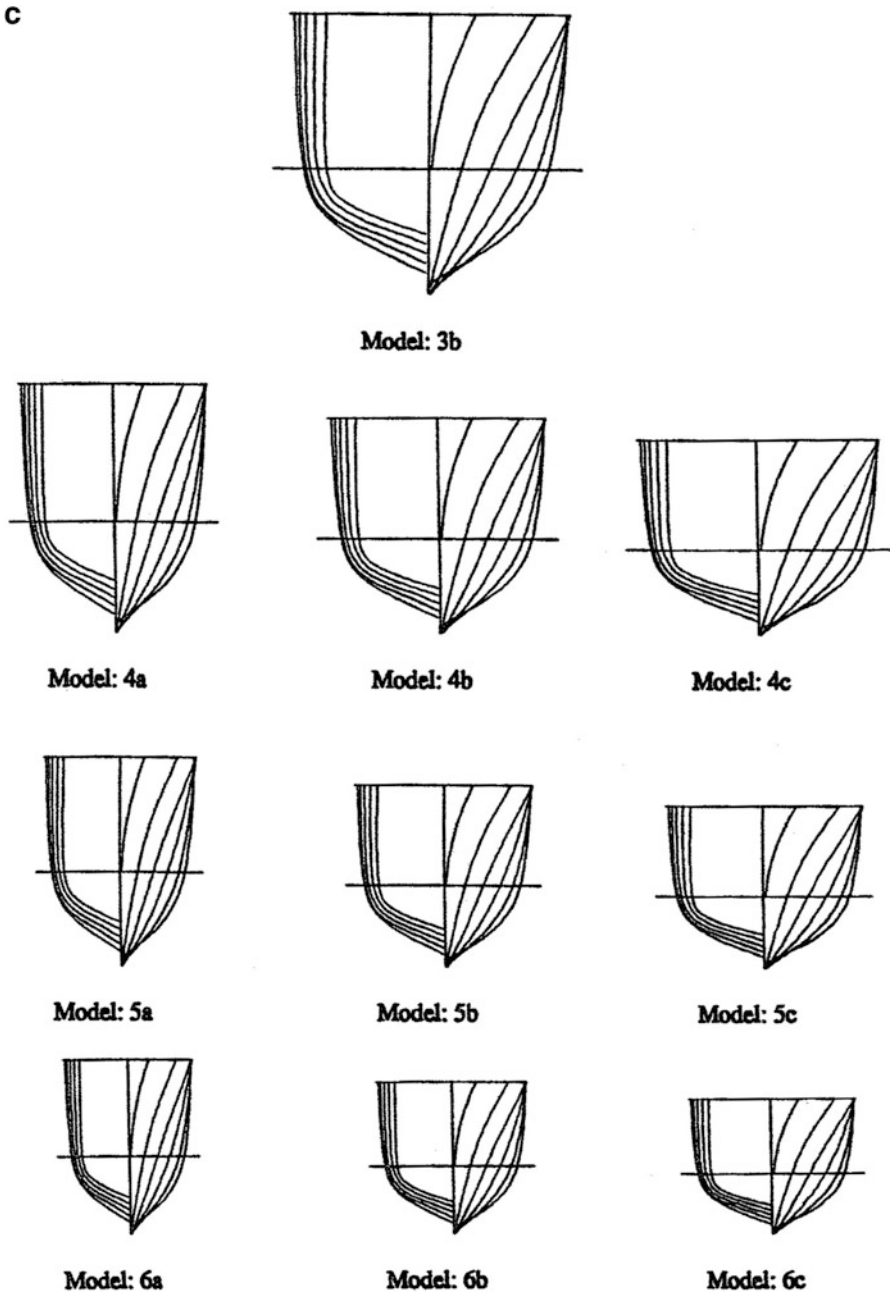

Fig. 5.12 (continued)

Table 5.3 Details of models with catamaran demihull form

Model	C2	C3	C4	C5
L, m	1.8	1.6	1.6	1.6
L/B	10.0	7.0	9.0	11.0
B/T	1.6	2.0	2.0	2.0
$L\nabla^{\frac{1}{3}}$ slenderness	7.116	6.273	7.417	8.479
C_B, block coefficient	0.444	0.397	0.397	0.397
C_p, prismatic coefficient	0.667	0.693	0.693	0.693
C_M, midsection coefficient	0.667	0.565	0.565	0.565
A (m^2), wetted surface area	0.482	0.434	0.338	0.276
LCB (%L) longitudinal center of buoyancy from amidships	0	−6.4	−6.4	−6.4
Material	GRP	FOAM	FOAM	FOAM
Hull	Parabolic	Round bilge	Round bilge	Round bilge

The total drag coefficient was obtained in towing tank tests, and the wave resistance was obtained by the multiple longitudinal cuts of the wave pattern in the towing tank during the tests, while the viscous drag was obtained by making a wake traverse analysis of the running model tests from measurement of the wake wave pattern during testing.

The total drag coefficient was expressed by Insel and Molland as

$$C_{tCAT} = (1 + \phi k)\,\sigma C_F + \tau C_w, \tag{5.6}$$

where:

C_{tCAT} Total resistance coefficient of CAT;
C_F Coefficient of friction resistance, obtained from ITTC 1957 correlation line;
C_w Wave resistance coefficient of individual demihull;
$+k$ Form factor of individual demihull;
ϕ Factor taking account of pressure field change around demihull;
σ Factor taking account of velocity augmentation between two demihulls, calculated from an integration of local frictional resistance over wetted surface;
τ Wave resistance interference factor.

For practical purposes, ϕ and σ are combined into a viscous resistance interference factor β, where $(1 + \phi k)\sigma = (1 + \beta k)$, so that

$$C_{tCAT} = (1 + \beta k)C_F + \tau C_w. \tag{5.7}$$

Note that for the demihull in isolation, $\beta = 1$, $\tau = 1$.

Insel and Molland found from their tests that the form factor k was of order 0.1, though this varied with the spacing between hulls. They also found in their tests that for smaller demihull spacing, the wave form between the hulls broke, particularly in

the "hump speed" range of Fr_L 0.42, where wave length was close to vessel length and, so, additive. It may be noted that for transom form vessels this is the speed at which flow clears the transom and forms a "rooster tail" behind the vessel, which flattens out as speed increases toward planing.

We can use the material in Chap. 4 to assess the value τC_w against Fr_L and deduct this from the total resistance predicted from model tests to determine "residual" resistance and so predict βk and C_F. The total resistance can then be predicted for the full-scale vessel. The viscous factor and form factor are almost constants and vary little with Fr_L as the viscous forces are proportional to vessel velocity^2.

Based on the previously given test results, Molland et al. [9] carried out an analysis on a series of catamaran hull forms and generated a series of plots for the prediction of catamaran resistance for use in design. Figure 5.12c on the next page shows the ten body plans used for the model demihulls. The notation and main parameters of models, as well as the details of the models, are shown in Tables 5.4 and 5.5.

The data and body plans reviewed here are taken from Southampton University Ship Science Reports 71 and 72 listed in the resources at the back of this book, with permission from and thanks to Tony Molland and Southampton University. References [8, 9] summarize this work.

From their test results, LCB has less influence on the resistance of a catamaran, so they took the LCB as constant for all models, −6.4% L (behind the midsection of the models).

Table 5.4 Notation and main parameters of models

$L\nabla^{\frac{1}{3}}$	$B/T = 1.5$	$B/T = 2.0$	$B/T = 2.5$	C_p
6.3		3b		0.693
7.4	4a	4b	4c	0.693
8.5	5a	5b	5c	0.693
9.5	6a	6b	6c	0.693

Table 5.5 Details of models

Model	L, m	L/B	B/T	$L\nabla^{\frac{1}{3}}$	C_B	C_p	C_m	A, m^2	LCB (%L)
3b	1.6	7.0	2.0	6.27	0.397	0.693	0.565	0.434	−6.4
4a	1.6	10.4	1.5	7.40	0.397	0.693	0.565	0.348	−6.4
4b	1.6	9.0	2.0	7.41	0.397	0.693	0.565	0.338	−6.4
4c	1.6	8.0	2.5	7.39	0.397	0.693	0.565	0.340	−6.4
5a	1.6	12.8	1.5	8.51	0.397	0.603	0.565	0.282	−6.4
5b	1.6	11.0	2.0	8.50	0.397	0.693	0.565	0.276	−6.4
5c	1.6	9.9	2.5	8.49	0.397	0.693	0.565	0.277	−6.4
6a	1.6	15.1	1.5	9.50	0.397	0.693	0.565	0.240	−6.4
6b	1.6	13.1	2.0	9.50	0.397	0.693	0.565	0.233	−6.4
6c	1.6	11.7	2.5	9.50	0.397	0.693	0.565	0.234	−6.4

Nomenclature

A Static wetted surface area, m^2;
B Demihull maximum beam, m;
L Demihull length, m;
T Demihull draft, m;
S Separation between CAT demihull centerlines, m;
Δ Volume of displacement of demihull, m^3;
C_b Block coefficient;
C_p Prismatic coefficient;
$L\nabla^{\frac{1}{3}}$ Length displacement ratio;
R_t Total resistance;
C_t Coefficient of total resistance, $= R_T/\frac{1}{2}\rho A v^2$;
C_{wp} Wave resistance coefficient, $= R_{wp}/\frac{1}{2}\rho A v^2$;
S/L Separation-to-length ratio.

From the test results, the form factors from C_{wp} measurements can be obtained in Table 5.6.

The residual resistance coefficients of the models obtained are listed in Tables 5.7a, 5.7b, 5.7c, 5.7d, 5.7e, 5.7f, 5.7g, 5.7h, 5.7i, and 5.7j on the following pages. $C_R = C_T - C_{FITTC}$, where C_{FITTC} is the friction drag coefficient determined

Table 5.6 Form factors from model C_{wp} measurements

$L\nabla^{\frac{1}{3}}$	B/T	Model	Monohull $1 + k$	$S/L = 0.2$ $1 + \beta k$ β	$S/L = 0.3$ $1 + \beta k$ β	$S/L = 0.4$ $1 + \beta k$ β	$S/L = 0.5$ $1 + \beta k$ β
6.3	2.0	3b	1.45	1.60 1.33	1.65 1.44	1.55 1.22	1.60 1.33
7.4	1.5	4a	1.30	1.43 1.43	1.43 1.43	1.46 1.53	1.44 1.47
7.4	2.0	4b	1.30	1.47 1.57	1.43 1.43	1.45 1.50	1.45 1.47
7.4	2.5	4c	1.30	1.41 1.37	1.39 1.30	1.48 1.60	1.44 1.47
8.5	1.5	5a	1.28	1.44 1.57	1.43 1.54	1.44 1.57	1.47 1.68
8.5	2.0	5b	1.26	1.41 1.58	1.45 1.73	1.40 1.54	1.38 1.46
8.5	2.5	5c	1.26	1.41 1.58	1.43 1.65	1.42 1.62	1.44 1.69
9.5	1.5	6a	1.22	1.48 2.18	1.44 2.00	1.46 2.09	1.48 2.18
9.5	2.0	6b	1.22	1.42 1.91	1.40 1.82	1.47 2.14	1.44 2.00
9.5	2.5	6c	1.23	1.40 1.74	1.40 1.74	1.45 1.96	1.44 1.91

Table 5.7a Model 3b residual resistance coefficient (C_T–C_{FITTC})

Fr_L	Monohull C_R	$S/L = 0.2$ C_R	$S/L = 0.3$ C_R	$S/L = 0.4$ C_R	$S/L = 0.5$ C_R
0.20	2.971	3.192	3.214	2.642	2.555
0.25	3.510	4.540	3.726	4.019	3.299
0.30	3.808	5.303	4.750	4.464	3.938
0.35	4.800	6.771	5.943	5.472	4.803
0.40	5.621	8.972	7.648	7.085	6.589
0.45	8.036	12.393	12.569	10.934	9.064
0.50	0.038	14.874	14.237	12.027	10.112
0.55	8.543	15.417	12.275	10.538	9.394
0.60	7.626	12.818	10.089	8.962	8.361
0.65	6.736	8.371	8.123	7.592	7.488
0.70	5.954	5.954	6.852	6.642	6.726
0.75	5.383	5.383	5.934	5.921	6.078
0.80	4.911	4.911	5.289	5.373	5.537
0.85	4.484	4.484	4.814	4.949	5.046
0.90	4.102	4.102	4.452	4.543	4.624
0.95	3.785	3.785	4.172	4.236	4.335
1.0	3.579	3.579	3.936	3.996	4.099

Coefficients $\times 10^3$

Table 5.7b Model 4a residual resistance coefficients ($C_T - C_{FITTC}$)

Fn	Monohull C_r	$S/L = 0.2$ C_r	$S/L = 0.3$ C_r	$S/L = 0.4$ C_r	$S/L = 0.5$ C_r
0.2	1.909	2.327	2.564	2.495	2.719
0.25	2.465	3.148	3.315	2.937	3.484
0.30	3.273	3.954	4.283	4.396	3.875
0.35	3.585	5.073	4.576	4.064	4.173
0.40	4.100	4.874	5.871	5.900	5.109
0.45	5.305	8.111	7.953	7.220	6.299
0.50	5.526	8.365	7.150	6.650	6.140
0.55	5.086	7.138	5.990	5.692	5.615
0.60	4.431	5.878	5.090	4.880	4.981
0.65	3.924	4.815	4.392	4.269	4.387
0.70	3.477	4.047	3.949	3.834	3.911
0.75	3.128	3.556	3.594	3.512	3.570
0.80	2.904	3.224	3.187	3.252	3.296
0.85	2.706	2.923	2.966	3.054	3.070
0.90	2.544	2.729	2.839	2.881	2.873
0.95	2.398	2.550	2.657	2.767	2.707
1.00	2.272	2.433	2.437	2.687	2.558

Table 5.7c Model 4b residual resistance coefficients ($C_T - C_{FITTC}$)

Fr_L	Monohull C_r	$S/L = 0.2$ C_r	$S/L = 0.3$ C_r	$S/L = 0.4$ C_r	$S/L = 0.5$ C_r
0.2	2.613	2.929	2.841	2.721	2.820
0.25	2.629	3.868	3.374	3.365	3.396
0.30	3.532	4.311	4.113	4.150	3.902
0.35	3.763	5.483	4.816	4.557	4.329
0.40	4.520	5.897	5.934	5.940	5.716
0.45	5.402	7.748	7.777	7.078	6.741
0.50	5.389	8.420	7.669	6.922	6.581
0.55	4.865	8.099	6.639	6.145	5.921
0.60	4.276	7.159	5.471	5.315	5.209
0.65	3.787	6.008	4.620	4.605	4.593
0.70	3.394	4.769	4.061	4.098	4.125
0.75	3.098	4.041	3.641	3.718	3.786
0.80	2.848	3.605	3.326	3.440	3.520
0.85	2.647	2.647	3.153	3.247	3.319
0.90	2.476	2.476	2.917	3.078	3.131
0.95	2.361	2.361	2.834	2.968	2.998
1.00	2.347	2.347	2.347	2.882	2.870

Table 5.7d Model 4c residual resistance coefficients ($C_T - C_{FITTC}$)

Fn	Monohull C_r	$S/L = 0.2$ C_r	$S/L = 0.3$ C_r	$S/L = 0.4$ C_r	$S/L = 0.5$ C_r
0.2	2.169	2.983	2.830	2.801	2.690
0.25	2.506	3.718	3.459	3.412	3.336
0.30	2.987	4.401	4.110	4.067	3.960
0.35	3.349	5.336	4.777	4.321	4.275
0.40	4.371	5.905	5.850	5.919	5.722
0.45	5.525	8.567	8.454	7.605	7.061
0.50	5.512	9.474	7.892	7.013	6.633
0.55	5.021	8.316	6.625	6.087	5.907
0.60	4.473	6.845	5.522	5.249	5.204
0.65	3.995	5.584	4.720	4.617	4.637
0.70	3.632	4.718	4.167	4.165	4.203
0.75	3.360	4.216	3.785	3.845	3.871
0.80	3.119	3.784	3.503	3.587	3.608
0.85	2.922	3.459	3.276	3.364	3.387
0.90	2.743	3.276	3.089	3.165	3.190
0.95	2.603	3.076	2.934	3.003	3.017
1.00	2.481	2.904	2.821	2.875	2.875

Table 5.7e Model 5a residual resistance coefficients ($C_T - C_{FITTC}$)

Fr_L	Monohull C_r	$S/L = 0.2$ C_r	$S/L = 0.3$ C_r	$S/L = 0.4$ C_r	$S/L = 0.5$ C_r
0.2	1.865	2.565	2.565	2.381	2.392
0.25	2.485	3.074	2.991	3.031	3.123
0.30	3.009	3.959	3.589	3.686	3.473
0.35	3.260	4.018	3.756	3.589	3.716
0.40	3.677	4.472	4.604	4.616	4.403
0.45	4.103	6.968	5.563	5.009	4.929
0.50	3.884	5.805	4.950	4.581	4.501
0.55	3.442	4.914	4.221	4.015	3.966
0.60	3.063	4.065	3.596	3.516	3.499
0.65	2.736	3.429	3.318	3.126	3.140
0.70	2.461	3.004	2.827	2.845	2.882
0.75	2.278	2.705	2.615	2.658	2.699
0.80	2.138	2.494	2.465	2.519	2.559
0.85	2.038	2.342	2.351	2.406	2.453
0.90	1.931	2.231	2.260	2.308	2.354
0/95	1.871	2.153	2.183	2.238	2.272
1.00	1.818	2.100	2.124	2.179	2.201

Table 5.7f Model 5b residual resistance coefficient ($C_T - C_{FITTC}$)

Fr	Monohull C_r	$S/L = 0.2$ C_r	$S/L = 0.3$ C_r	$S/L = 0.4$ C_r	$S/L = 0.5$ C_r
0.20	1.406	2.288	2.849	2.538	3.006
0.25	2.362	2.843	3.200	3.260	3.093
0.30	2.632	3.643	3.539	3.693	3.330
0.35	2.890	4.194	3.952	3.711	3.437
0.40	3.514	4.520	4.687	4.622	4.303
0.45	3.691	5.506	5.218	4.960	4.648
0.50	3.518	5.581	4.903	4.632	4.324
0.55	3.125	4.927	4.323	4.057	3.804
0.60	2.851	4.177	3.783	3.504	3.286
0.65	2.599	3.555	3.302	3.090	2.872
0.70	2.285	3.051	2.989	2.759	2.576
0.75	2.155	2.744	2.752	2.515	2.396
0.80	2.010	2.529	2.584	2.327	2.310
0.85	1.938	2.383	2.462	2.163	2.322
0.90	1.830	2.298	2.375	2.111	2.382
0.95	1.852	2.221	2.324	2.128	1.852
1.00	1.803	2.186	2.279	2.145	1.803

Table 5.7g Model 5c residual resistance coefficients ($C_T - C_{FITTC}$)

Fr_L	Monohull C_r	$S/L = 0.2$ C_r	$S/L = 0.3$ C_r	$S/L = 0.4$ C_r	$S/L = 0.5$ C_r
0.20	2.517	2.731	2.801	2.718	2.983
0.25	2.756	3.256	3.199	3.203	3.290
0.30	3.010	3.445	3.599	3.386	3.371
0.35	3.273	3.937	3.779	3.623	3.625
0.40	3.687	4.635	4.813	4.731	4.519
0.45	3.891	5.908	5.543	4.969	4.644
0.50	3.621	5.864	5.016	4.513	4.340
0.55	3.232	5.095	4.274	3.945	3.855
0.60	3.048	4.231	3.703	3.495	3.512
0.65	2.685	3.576	3.267	3.183	3.187
0.70	2.417	3.074	2.930	2.920	2.936
0.75	2.205	2.771	2.741	2.717	2.779
0.80	2.076	2.558	2.632	2.564	2.594
0.85	1.903	2.434	2.607	2.476	2.514
0.90	1.863	2.346	2.599	2.404	2.454
0.95	1.915	2.259	2.550	2.341	2.358
1.00	1.785	2.213	2.481	2.256	2.281

Table 5.7h Model 6a residual resistance coefficient ($C_T - C_{FITTC}$)

Fr_L	Monohull C_r	$S/L = 0.2$ C_r	$S/L = 0.3$ C_r	$S/L = 0.4$ C_r	$S/L = 0.5$ C_r
0.20	1.916	2.727	2.660	2.807	2.484
0.25	2.257	3.379	3.244	3.595	3.515
0.30	2.443	3.792	3.548	3.761	3.665
0.35	2.527	3.665	3.381	3.754	3.566
0.40	2.723	4.377	4.403	4.257	4.009
0.45	2.796	4.703	4.593	4.339	3.998
0.50	2.658	4.592	3.974	3.855	3.635
0.55	2.434	3.799	3.382	3.338	3.243
0.60	2.246	3.193	2.994	2.955	2.916
0.65	2.111	2.812	2.703	2.689	2.651
0.70	1.917	2.534	2.496	2.505	2.475
0.75	1.781	2.367	2.348	2.379	2.336
0.80	1.633	2.253	2.261	2.304	2.243
0.85	1.544	2.176	2.194	2.230	2.171
0.90	1.478	2.110	2.155	2.146	2.093
0.95	1.528	2.062	2.110	2.047	2.021
1.00	1.521	2.027	2.064	1.976	1.962

Table 5.7i Model 6b residual resistance coefficient ($C_T - C_{FITTC}$)

Fr	Monohull C_r	$S/L = 0.2$ C_r	$S/L = 0.3$ C_r	$S/L = 0.4$ C_r	$S/L = 0.5$ C_r
0.20	1.755	2.864	2.297	2.933	2.353
0.25	2.136	3.217	3.235	3.203	2.335
0.30	2.255	3.769	3.162	3.251	2.833
0.35	2.150	3.667	3.299	3.502	3.158
0.40	2.639	4.007	3.721	3.913	3.470
0.45	2.696	4.534	4.092	3.950	3.570
0.50	2.510	4.379	3.771	3.592	3.393
0.55	2.338	3.734	3.202	3.196	3.085
0.60	2.084	3.144	2.762	2.866	2.662
0.65	1.900	2.738	2.507	2.635	2.565
0.70	1.747	2.477	2.355	2.468	2.378
0.75	1.656	2.311	2.249	2.339	2.268
0.80	1.575	2.184	2.158	2.241	2.214
0.85	1.527	2.093	2.068	2.172	2.112
0.90	1.523	2.052	2.056	2.129	2.064
0.95	1.482	2.020	2.046	2.089	2.048
1.00	1.426	2.001	2.001	2.063	2.036

Table 5.7j Model 6c residual resistance coefficients ($C_T - C_{FITTC}$)

Fr	Monohull C_r	$S/L = 0.2$ C_r	$S/L = 0.3$ C_r	$S/L = 0.4$ C_r	$S/L = 0.5$ C_r
0.20	1.882	2.979	1.909	2.608	2.515
0.25	2.395	3.169	3.328	3.056	2.911
0.30	2.581	3.539	3.401	3.252	3.191
0.35	2.666	3.531	3.309	3.385	3.366
0.40	2.785	3.684	3.774	3.813	3.629
0.45	2.816	4.229	3.932	3.813	3.676
0.50	2.626	4.154	3.719	3.527	3.446
0.55	2.394	3.573	3.256	3.187	3.145
0.60	2.177	3.080	2.855	2.866	2.851
0.65	2.006	2.809	2.595	2.609	2.608
0.70	1.866	2.504	2.437	2.432	2.487
0.75	1.754	2.305	2.331	2.345	2.358
0.80	1.682	2.165	2.199	2.232	2.297
0.85	1.633	2.138	2.167	2.210	2.249
0.90	1.568	2.108	2.120	2.174	2.227
0.95	1.628	2.078	2.121	2.149	2.227
1.00	1.672	2.067	2.134	2.157	2.193

using the ITTC 1957 correlation for the hull fluid friction based on submerged surface area.

It should be noted that this work is based on a clean hull without appendages, so the drag of appendages will have to be added (see description later in the chapter) once the "bare hull" drag assessment has been verified and before projections for vessel powering are carried out.

It may also be noted that from the testing and analysis in [8] when determining the frictional resistance, the form factors for these four model forms as isolated demihulls and interference factor β as catamaran are as follows:

Model	C2	C3	C4	C5
k	0.1	0.45	0.3	0.17
$(1 + k)$	1.1	1.45	1.3	1.17
β (approx.)	2.0	1.3	1.5	2.3
$(1 + \beta k)$	1.20	1.59	1.45	1.39

It can be seen that as the slenderness increases (Table 5.3) from C3 to C5 the "monohull" form factor reduces because the form more closely resembles the flat plate area that is implicit in the ITTC calculation. In contrast, the catamaran interference factor increases, but not enough to counter the improvement based on demihull slenderness. The same trends are seen in the results in Table 5.5 from the subsequent hull form series analyzed.

From these tables one can estimate the residual resistance and powering of a design at the initial design stage. Using those data with calculated friction resistance, for example (as in Eqs. 5.6 and 5.7) and the assessment of wave drag using the methods of Chap. 4, total resistance can be assessed.

To account for the viscous and form effect of a catamaran, designers also have to use a scaling coefficient to predict the resistance from model test results in a towing tank to full scale as follows:

$$C_{\text{Tship}} = C_{\text{Fship}} + C_{\text{Rmodel}} - \beta k\left(C_{\text{Fmodel}} - C_{\text{Fship}}\right). \tag{5.8}$$

The scaling coefficient is due to the difference in Reynold's number (Re) between the model and the ship. The friction coefficient can be obtained from the 1957 ITTC data, as in the next section. When using the theoretical calculation of wave drag from Chap. 4, the viscous and form effect must be added owing to the nonnegligible value (Chap. 7, Sect. 7.7).

5.3.2 *Predicting Catamaran Resistance in Calm Water Using Monohull Data*

There are a lot of test data on the resistance coefficient of monohulls, so the resistance coefficients can be obtained from such data where suitable hull geometries have been tested. One must then add the form factor, viscous effect, and wave

interference effect, β, k, and τ, from the previous tables to Eq. (5.9), where C_w used is the monohull wave resistance coefficient:

$$C_{tCAT} = (1 + \beta k)\, C_F + \tau C_w. \tag{5.9}$$

5.3.2.1 Arfiliyev's Method

A method for estimating catamaran residual resistance was developed by Arfiliyev of the former USSR [3]. The method is based on experimental results from a series of catamaran models that form a geometric series with symmetric demihull lines and typical principal dimensions and lines for high-speed catamarans, as are shown in Fig. 5.13a, b below. For these models the notation used is hull separation k, demihull beam b, draft T, and length L.

Figure 5.11, presented earlier before the tables, shows the wave-making resistance ratio $\overline{R_w}$ of a catamaran at various relative hull separations k/L, based on theoretical calculations completed by Arfiliyev, where $\bar{R}_w = (2R_w + R_i)/2R_w$. From the figure one can see that the wave making is very complicated when $Fr_L < 0.5$ owing to strong wave interference by both demihulls; however, it is more regular and simple after $Fr_L > 0.5$.

From the figure one also can see that interference drag might be either positive, indicating unfavorable interference, or negative, indicating favorable interference. The calculation of catamaran resistance should be analyzed carefully and separated into the two regions, that is, before and after $Fr_L = 0.5$, and we refer to this Froude number as the critical Froude number.

Fortunately, the operational relative speed of most high-speed catamarans is above $Fr_L = 0.5$, often in the region 0.7–1.1, and with high slenderness, giving no clear resistance hump. We normally are used to estimating the resistance above the critical Fr_L and interpolate downwards in speed.

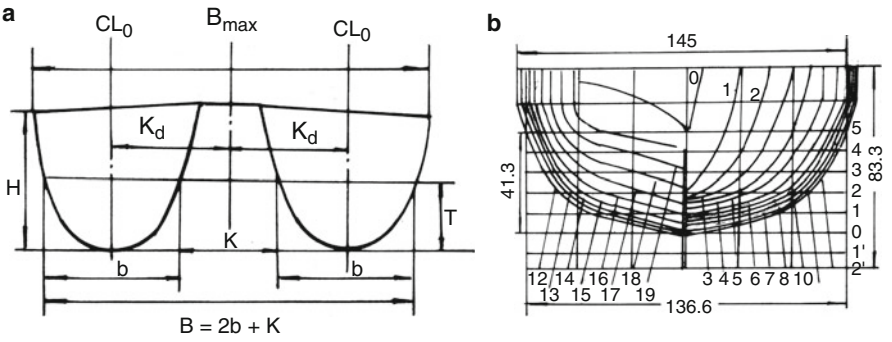

Fig. 5.13 Arfiliyev: (**a**) catamaran cross-section definitions; (**b**) typical demihull lines for tests above Fr_L 0.5, where L/b = 15, b/T = 3.275, and δ = 0.47 for this model

The residual resistance R_r after extraction of the viscous friction drag according to ITTC 1957 as in section (2) below contains wave-making resistance plus form drag and can be expressed as

$$R_r = \tfrac{1}{2}\rho_w v^2 S_w C_r, \tag{5.10}$$

where

S_w Wetted area of demihulls, m^2;
ρ_w Water density, $N \bullet s^2/m^4$;
v Vessel speed, m/s;
C_r Residual drag coefficient;
R_r Residual resistance (N), which can be expressed as

$$R_r = f\left(Fr_L, \bar{k}, L/b, b/T, \delta\right), \tag{5.11}$$

where

$\bar{k} = k/b$;

δ Block coefficient of demihull;
L/b Length/beam ratio of demihull;
b/T beam/draft ratio of demihull.

In relation to the demihull lines shown in Fig. 5.13b (Arfiliyev) earlier, three groups of models were manufactured and tested in the towing tank at MARIC with constant <L/b>, <b/T>, <δ> in each group. There is only one variant in each group, and three groups of curves were obtained using the model test results as follows:

$$\begin{aligned} C_w^{L/b} &= f_{L/b}(L/b) \quad \text{where } Fr_L, b/T, \delta, \bar{k} \text{ are constant;} \\ C_w^{b/T} &= f_{b/T}(b/T) \quad \text{where } Fr_L, L/b, \delta, \bar{k} \text{ are constant;} \\ C_w^{\delta} &= f_{\delta}(\delta) \quad \text{while } Fr_L, L/b, b/T, \bar{k} \text{ are constant.} \end{aligned} \tag{5.12}$$

After recalculation of the test results, the residual resistance coefficient can be expressed as

$$C_r = C_r^{L/b} \chi_{b/T} \chi_{\delta}. \tag{5.13}$$

The element $C_r^{L/b}$ is the residual resistance coefficient, according to the first test groups expressed in Eq. (5.12), and the influence factors are as follows:

$\chi_{b/T}$ Influence factor of b/T on residual drag coefficient, according to b/T group test results;
χ_{δ} Influence factor of δ on residual drag coefficient, according to δ group.

The test results were found as follows:

Figure 5.14a shows the curves for the calculation of the residual drag coefficient C_r of catamarans versus L/b, and Fr_L at constant hull separation $k/b = 1.0$ in deep water and Fr_L over critical number 0.5.

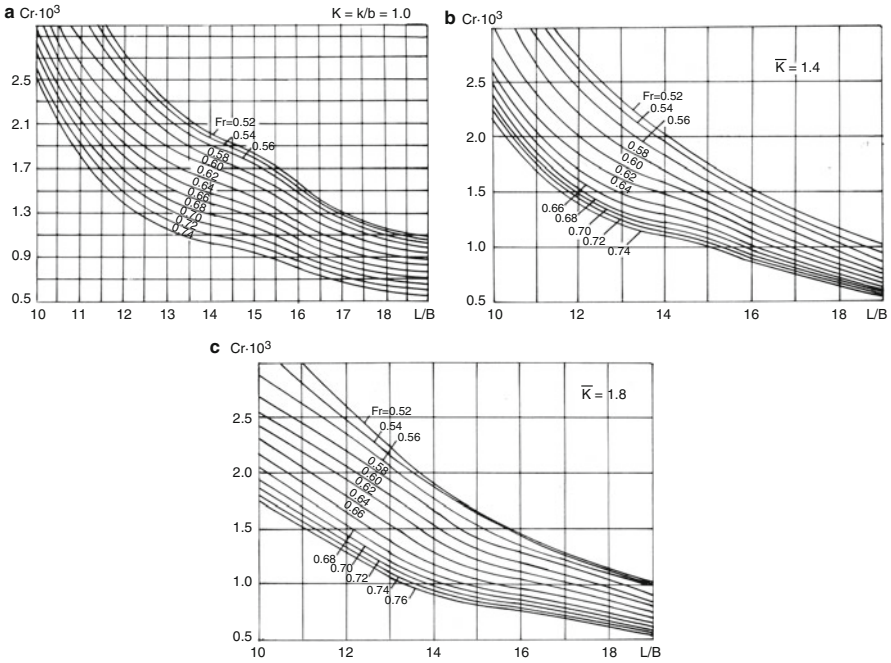

Fig. 5.14 Residual resistance coefficient ($C_r.10^{3)}$ of catamaran versus *L*/*b*: (**a**) *K*/*b* = 1.0; (**b**) *K*/*b* = 1.4; (**c**) *K*/*b* = 1.8

Figure 5.14b, c shows the residual drag coefficient in the same condition mentioned earlier, however, with $k/b = 1.4$ and 1.8, respectively.

Figure 5.15a shows an influence curve group (correction coefficient) of the demihull block coefficient on the residual drag of catamarans versus δ, Fr_L at constant $k/b = 1.0$ in deep water and Fr_L over critical number 0.5.

Figure 5.15b, c shows the correction coefficient in the same condition, however, with different hull separation, $k/b = 1.4$ and 1.8, respectively.

Figure 5.16a shows the influence curve group of b/T on the residual drag of catamarans versus Fr_L at constant $k/b = 1.0$ in deep water and Fr_L over critical number 0.5.

Figure 5.16b, c shows the correction coefficient in the same condition mentioned earlier, however, with different hull separation, $k/b = 1.4$ and 1.8 respectively.

Using these curves, it is not difficult to estimate the residual drag of catamarans in deep water above the critical Fr_L with precision where the target craft lines are close to those in Fig. 5.13b (Arfiliyev body plan).

Based on these data, designers can use interpolation to estimate the influence of hull separation in a range of *k*/*b* from 1.0 to 1.8. Unfortunately, the test range for Fr_L is limited to 0.52–0.75, so that in the case of Fr_L above 0.75 and *k*/*b* exceeding 1.8, designers are obliged to use extrapolation for the estimation of hull interference effects.

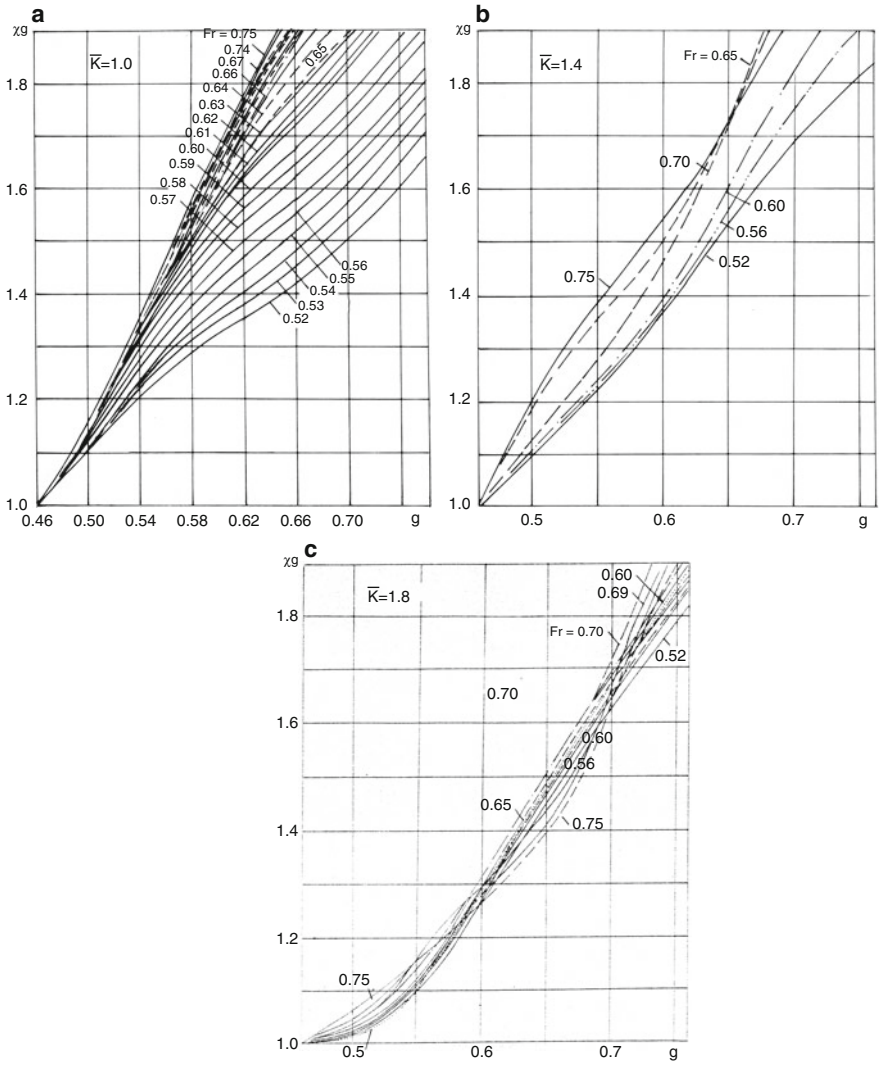

Fig. 5.15 Influence coefficient χ_δ on residual resistance of catamaran versus L/b: (**a**) K/b = 1.0; (**b**) K/b = 1.4; (**c**) K/b = 1.8

5.3.3 Friction Drag

The basic friction drag of each demihull can be calculated using ITTC 1957 as follows:

$$R_\mathrm{f} = 1/2\rho_\mathrm{w} v^2 S_\mathrm{w}(C_\mathrm{f} + \Delta C_\mathrm{f}), \tag{5.14}$$

where

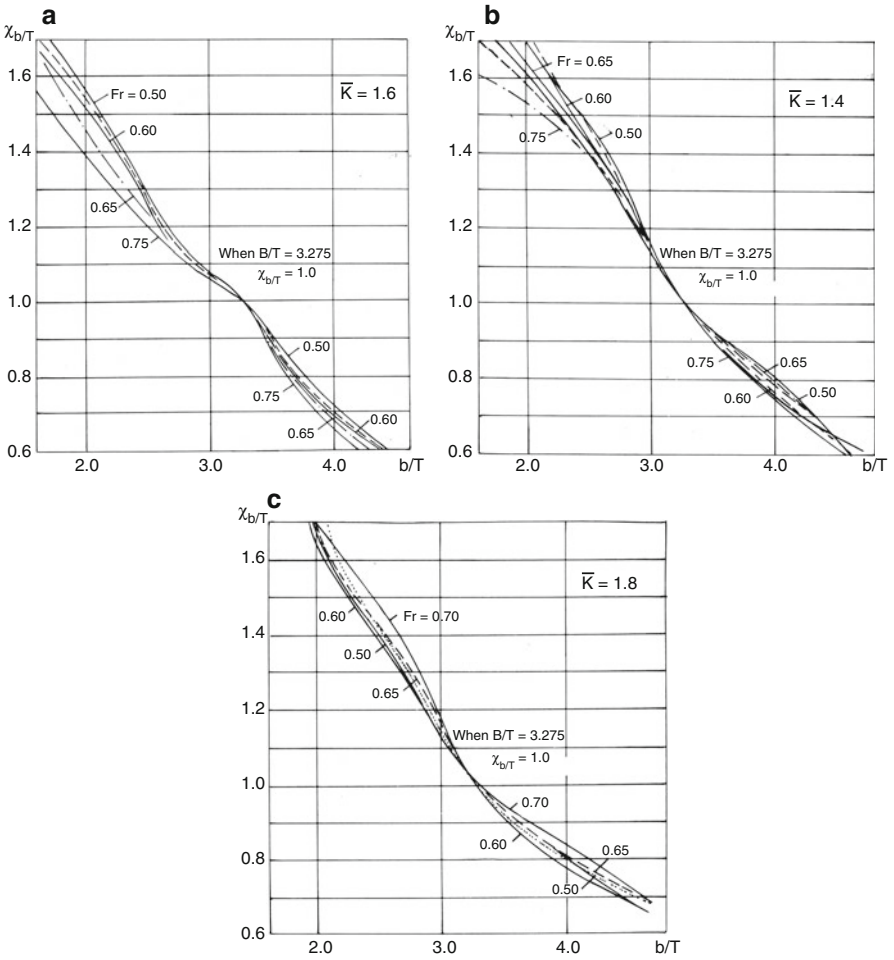

Fig. 5.16 Influence curve of $\chi_{b/T}$ on residual resistance of catamaran: (**a**) K/b = 1.0; (**b**) K/b = 1.4; (**c**) K/b = 1.8

C_f is the friction coefficient for a smooth plate and can be expressed as

$$C_f = \frac{0.455}{(\log R_e)^{2.58}}, \tag{5.15}$$

$$R_e = \frac{vL}{\gamma} \tag{5.16}$$

R_e Reynold's number;
L calculated demihull length, m

γ Dynamic viscous coefficient of water, m^2/s, $\gamma = 1.14 \times 10^{-6}$, when water temperature $t = 15\ ^\circ C$;

ΔC_f Additional friction coefficient for surface roughness of demihull, can be taken as 0.4×10^{-3} for estimation purposes; for more detailed information see reference [19];

S_w Wetted surface area of each demihull, can be determined in approximation as in the following expressions (refer to Eqs. 5.10 and 5.11 for explanation of symbols):

$$S_w = V^{2/3}\left(5.1 + 0.074\frac{L}{T} - 0.4\delta\right) \quad \text{or} \quad S_w = L(1.36T + 1.13b\delta), \tag{5.17}$$

where V is the volumetric displacement of each demihull.

It should be noted that this is the starting point for any analysis as described in earlier sections, where the impact of the demihull form and spacing is taken in to account.

5.3.4 *Underwater Appendage Drag and Air Profile Drag [19]*

5.3.4.1 Drag Due to Rudders and Other Appendages

Drag due to rudders and other foil-shaped appendages, such as propeller and shaft brackets, can be written

$$R_r = C_{fr}(1 + \delta v/v)^2(1 + r)S_r q_w, \tag{5.18}$$

where R_r is the drag due to the rudder and foil-shaped propeller and shaft bracket (N) and C_{fr} is the friction coefficient, which is a function of R_e and the roughness coefficient of the rudder surface. In this case, $R_e = vc/\gamma$, where c is the chord length of rudders or other foil-like appendages (m); $\delta v/v$ is the factor considering the influence of propeller wake, where $\delta v/v = 0.1$ in general or $\delta v/v = 0$ if there is no effect of propeller wake on this drag; v is craft speed (m/s); r is an empirical factor considering the effect of shape; $r = 5\ t/c$, where t is the foil thickness; S_r is the area of the wetted surface of the rudders or foil-like appendages (m^2); and $q_w = 0.5\ \rho_w\ v^2$ is the hydrodynamic head due to craft speed.

This equation is suitable for rudders or other foil-shaped appendages totally immersed in water.

5.3.4.2 Drag of Shafts (or Quill Shafts) and Propeller Boss

The drag can be written

$$R_{\mathrm{sh}} = C_{\mathrm{sh}}(d_1 l_1 + d_2 l_2) q_{\mathrm{w}}, \tag{5.19}$$

where R_{sh} is the drag of the shaft (or quill shaft) and boss (N); d_1, d_2 are the diameters of the shaft (quill shaft) and boss, respectively (m); and l_1, l_2 are the wetted length of the shaft and boss, respectively (m). For a fully immersed shaft (quill shaft) and boss and $5.5 \times 10^5 > R_e > 10^3$, the coefficient C_{sh} may be defined as

$$C_{\mathrm{sh}} = 1.1 \sin^3 \beta_{\mathrm{sh}} + \pi C_{\mathrm{fsh}}, \tag{5.20}$$

Where β_{sh} is the angle between the shaft (quill shaft), boss and entry flow (for stern buttocks), C_{fsh} is the friction coefficient, which is a function of Re, where

$$R_e = v(l_1 + l_2)/\gamma, \tag{5.21}$$

and also includes the roughness factor, for example, if $\beta_{\mathrm{sh}} = 10^0 - 12^0$, with the shafts are fully immersed, then we take $C_{\mathrm{fsh}} = 0.02$.

5.3.4.3 Drag of Strut Palms

Similar to Eq. (5.18), the drag of a strut palm can be written

$$R_{\mathrm{pa}} = 0.75 C_{\mathrm{pa}} \left(h_{\mathrm{p}}/\delta\right)^{0.33} y h_{\mathrm{p}} (\rho_{\mathrm{w}}/2) v^2, \tag{5.22}$$

where R_{pa} is the strut palm drag (N), y is the strut palm width (m), and δ is the thickness of the boundary layer at the strut palm:

$$\delta = 0.01 x_p \ (\mathrm{m}),$$

where x_{p} is the distance between the waterline stagnation point and strut palms (m), h_{p}.

5.3.5 Aerodynamic Profile Drag

Aerodynamic profile drag can be written

$$R_{\mathrm{a}} = 0.5 C_{\mathrm{a}} \rho_{\mathrm{a}} S_{\mathrm{a}} v^2, \tag{5.23}$$

where

C_{a} is the aerodynamic profile drag coefficient; in general, we take 0.4–0.65 for high-speed catamarans;

S_{a} Frontal cross-section area of hull above water surface, m^2;

V Craft speed, m/s;
ρ_a Air mass density, Ns^2/m^4.

After calculating the total craft drag, the necessary engine power can be estimated as follows:

$$N = \frac{Rv}{102\eta_p\eta_m\eta_h}, \tag{5.24}$$

where

R Total resistance of craft, kgf;
v Craft speed, m/s;
N Output of engines, kW;
η_p Propeller efficiency;
η_m Transmission efficiency;

$\eta_h = \frac{1-t}{1-\omega}$ Hull efficiency for propulsion, t thrust reduction coefficient, ω wake coefficient.

5.4 Approximate Estimation of Resistance in Shallow Water

The only difference for resistance between a craft operating in deep and shallow water is wave-making drag. The theoretical calculation for wave-making drag in shallow water can be found in Chap. 4. It is well known that there is a more marked resistance peak of craft operating in shallow water, which influences the selection of service speed, and designers must pay more attention to acquiring greater power reserves on the main engines to ensure acceleration through the hump speed in shallow water.

Since the hump speed will be significantly lower than the catamaran's cruising speed, it is extremely important to estimate the hump speed and peak resistance in the initial phase of design and to select main engines with a power reserve so as to overcome the hump resistance and accelerate through the hump speed effectively and speedily.

Figure 5.17 [3] shows the test results of the residual coefficient C_r versus Fr_L of catamaran models in shallow water. The model lines can be found in Fig. 5.13. H_φ is the depth of a riverbed, and F_{rH} is the critical Froude number with respect to water depth, that is, at that relative speed the residual drag coefficient is highest, meaning the resistance peak:

$$\begin{aligned} F_{rH} &= v/\sqrt{gH_\varphi}, \\ Fr_L &= F_{rH}\sqrt{H_\varphi/T}\sqrt{T/L}. \end{aligned} \tag{5.21}$$

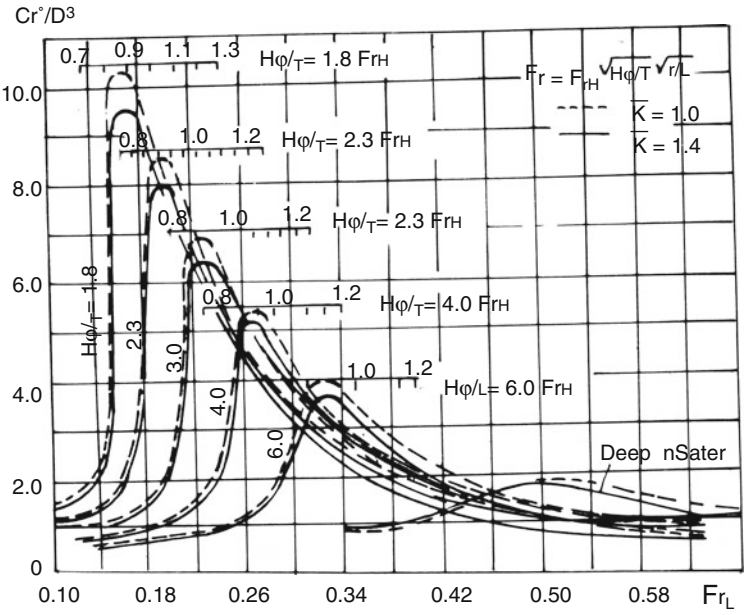

Fig. 5.17 Test results of residual drag versus Fr_{L} of catamaran models in shallow water

From the figure it is noted that the Fr_{H} varies with relative water depth H/T on which the catamaran operates, and the shallower the water depth, the higher the resistance and the lower the Fr_{H}. However, it seems the hull separation has less influence on the residual drag, that is, the residual drag coefficients of the models at $k/b = 1.0$ and 1.4 are very close in value. Perhaps this is because the wave drag of catamarans in shallow water and at critical speed is so high that it masks the influence of hull separation of the craft. This property can be validated for a design using the theoretical analysis in Chap. 4.

The approximate estimation of wave resistance in shallow water can be determined as follows. The most important thing is to define the critical speed and drag peak at this speed to determine the power output of the main engines. Reference [2] also used the test results of three groups of catamaran models and defined the residual drag coefficients of catamarans operating in shallow water.

Figure 5.18 shows the critical speed versus block coefficient of a demihull and relative water depth, that is,

$$F_{rH} = f\left(H_{\varphi}/T, \delta\right). \tag{5.22}$$

Then the critical speed can be defined by the following equation:

$$F_{rH} = F_{rH}^{\delta} \chi_{L/b} \chi_{b/T}. \tag{5.23}$$

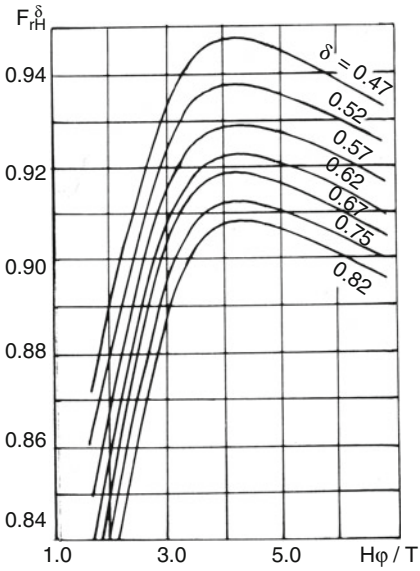

Fig. 5.18 Critical Fr_h versus δ and H_φ/T

Here F_{rH}^{δ} can be found from Fig. 5.18 at the specific δ of the craft with $L/b = 15$, $b/T = 3.275$; then the influence factors of L/b and b/T on the critical speed can be found from Figs. 5.19 and 5.20 for application to the target design.

Figure 5.19 shows the influence factor of L/b on the critical speed of catamarans at different water depths.

Figure 5.20 shows the influence factors of b/T on the critical speed of catamarans at different water depths. It should be noted that the estimation does not consider the influence of hull separation k/b due to the aforementioned reasons.

Then the critical speed can be written

$$v_{\mathrm{cr}} = F_{rH}\sqrt{gH_{\phi}}. \tag{5.24}$$

Using the same method, the residual drag coefficient can be expressed as

$$C_{\mathrm{r}} = \bar{C}_{\mathrm{r}}^{\delta}\chi_{L/b}\chi_{b/T}, \tag{5.25}$$

where $\bar{C}_{\mathrm{r}}^{\delta}$ is the ratio of residual drag coefficient of catamarans at critical speed and in shallow water whose maximum values in deep water, $\chi_{L/b}\chi_{b/T}$, are the influence factors with respect to L/b and b/T, respectively.

Figure 5.21 shows the residual drag coefficient of catamarans at critical speed F_{rH} in shallow water at various δ and H_φ/T, however, keeping $L/b = 15$ and $b/T = 3.275$.

Figure 5.22 shows the influence factor $\chi_{L/b}$ of L/b on residual drag coefficient of catamarans at critical speed in shallow water. Figure 5.23 below shows the influence factor $\chi_{b/T}$ of b/T on the residual drag coefficient at critical speed in shallow water,

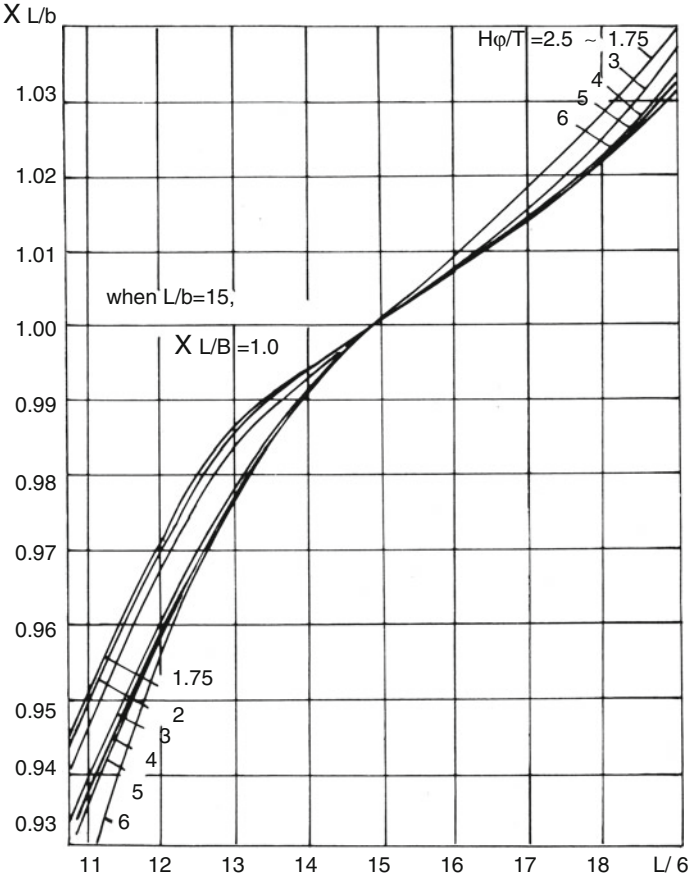

Fig. 5.19 Influence factor of demihull length/beam ratio ($\chi_{L/b}$) on critical Froude number Fr_{h0} of catamaran in shallow water. When L/b = 15 it is 1.0

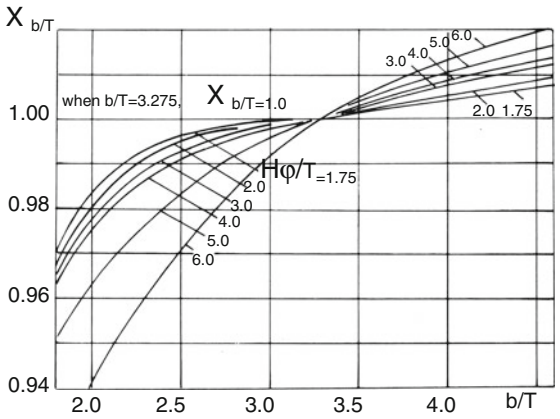

Fig. 5.20 Influence factor of b/t, $\chi_{b/T}$ on Fr_h at different H_φ/T

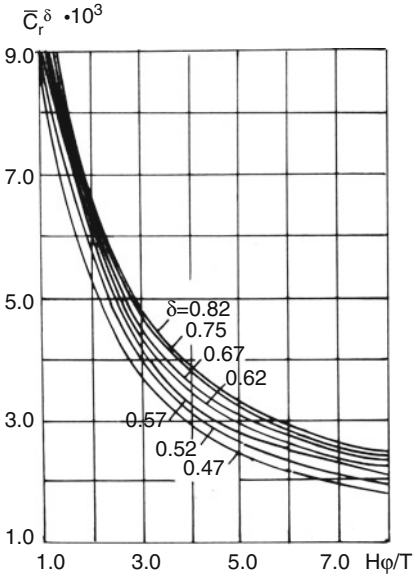

Fig. 5.21 Residual resistance coefficient of catamaran versus critical Fr_h in shallow water, $C_r^{\delta} = f(\delta, H_{\varphi}/T)$

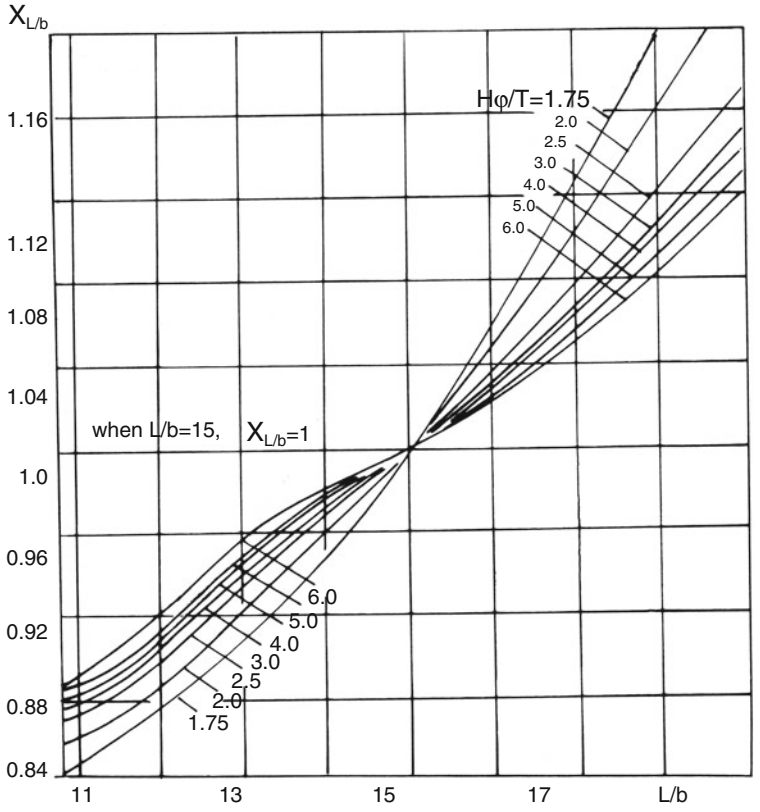

Fig. 5.22 Influence factor $\chi_{L/b}$ on residual drag coefficient C_r^{δ} of catamaran at critical Fr_h in shallow water

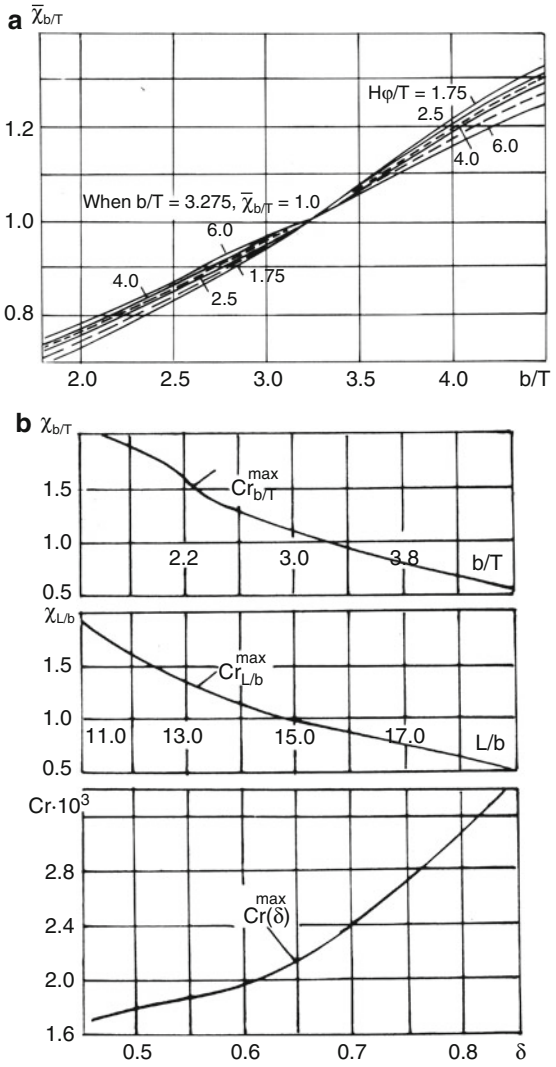

Fig. 5.23 (**a**) Influence factor $\overline{\chi}_{b/T}$ on residual drag coefficient C_r^{δ} of catamaran at critical Fr_h in shallow water; (**b**) in deep water

while Fig. 5.23a shows the influence factor for a catamaran at critical speed in deep water.

Then the relative residual drag coefficient C_r of catamarans at critical speed F_{rH} can be written

$$C_r = \bar{C}_r^{\delta} \chi_{L/b} \chi_{b/T}. \tag{5.26}$$

The residual drag of catamarans at critical speed can be expressed as

$$R_r = \frac{1}{2}\rho_w S_w C_r C_r^{max} v_c^2, \tag{5.26a}$$

where:

S_w Area of wetted surface;
v_c Critical speed;
C_r^{max} Maximum coefficient of residual drag of craft in deep water, can be expressed as

$$C_r^{max} = C_{r(\delta)}^{max} \cdot \chi_{L/b}^{max} \cdot \chi_{b/T}^{max}. \tag{5.26b}$$

The aforementioned coefficients are the maximum values for catamarans at calculated L/b, b/T, and δ, which can be found in Fig. 5.24.

Thus the hump resistance of catamarans at critical speed in shallow water can be defined, and designers can judge whether the craft is able to get through the hump resistance with the installed power specified and compared to the requirements at the cruising speed of the vessel.

The resistance of catamarans operating above hump speed in shallow water can be defined as follows, where in general the resistance might be lower than that in deep water:

$$C_r = C_r^0 \chi_{L/b} \chi_{b/T} \chi_\delta, \tag{5.27}$$

where

C_r Residual drag coefficient of catamarans operating in shallow water;
C_r^0 Basic residual drag coefficient of catamarans operating in shallow water over hump speed, at different water depths and hull separations (Fig. 5.24);

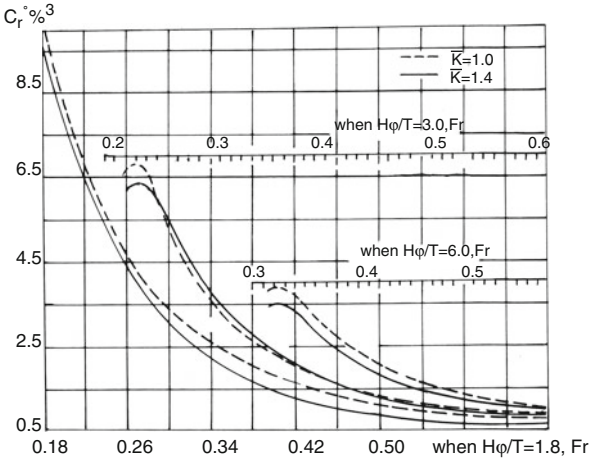

Fig. 5.24 Residual drag coefficient of catamaran operating above critical speed in shallow water at three-hull H_φ/T and two-hull separation ratio k/b

$\chi_{L/b}$ Influence factor of L/b on residual drag coefficient of catamarans in shallow water at different water depths $H_{\phi/T} = 1.8, 3.0, 6.0$ over hump speed (Fig. 5.25a–c);

$\chi_{b/T}$ Influence factor of b/T on residual drag coefficient of catamarans in shallow water, over hump speed, at different water depths, H_{ϕ}/T=1.8, 3.0, 6.0 (Fig. 5.26a–c);

χ_{δ} Influence factor of δ on residual drag coefficient of catamarans operating over critical speed in shallow water, at different water depths, H_{ϕ}/T=1.8, 3.0, 6.0 (Fig. 5.27a–c).

The residual drag coefficient can be obtained from Figs. 5.24, 5.25, 5.26, and 5.27 and Eq. 5.27 by means of interpolation and extrapolation for the target design.

In the case where $Fr_L = 0.5$–0.65 for catamarans in shallow water over the critical speed, Arfiliyev and Madorsky [3] also recommend an experimental method for the estimation of drag as

$$C_{\mathrm{r}}^{'} = C_{\mathrm{r}}^{L/b} \chi_{b/T}^{'} \chi_{\delta}^{'}, \tag{5.28}$$

where $C_{\mathrm{r}}^{'}$ is a residual drag coefficient for catamarans in shallow water at $Fr_L = 0.5$–0.6, and $C_{\mathrm{r}}^{L/b}$ is a residual drag coefficient for catamarans in shallow water at $Fr_L = 0.5$–0.6, at different L/b and $H_{\phi/T}$ (Fig. 5.28).

Parameters $\chi_{b/T}^{'}\chi_{\delta}^{'}$ and influence factors of b/T and δ on the residual drag coefficient of catamarans in shallow water at $Fr_L = 0.5$–0.6 respectively are shown in Fig. 5.29a, b.

In the situation where the demihull lines of a target design are not close to those of the experimental models in Figs. 5.12 or 5.13 or other test data that the designer can have access to, the estimation of drag mentioned previously should be corrected, as

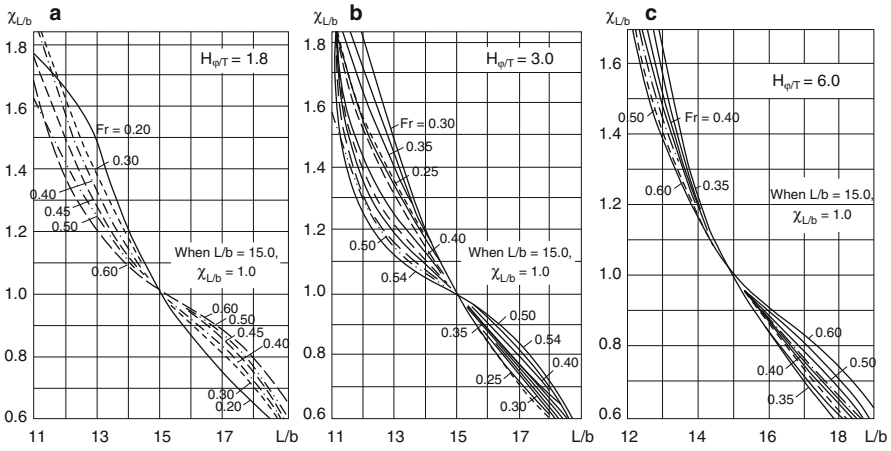

Fig. 5.25 Influence coefficient $\chi_{L/b}$ on residual drag coefficient of catamaran operating over critical speed in shallow water: (**a**) H_{φ}/T = 1.8; (**b**) H_{φ}/T = 3.0; (**c**) H_{φ}/T = 6.0

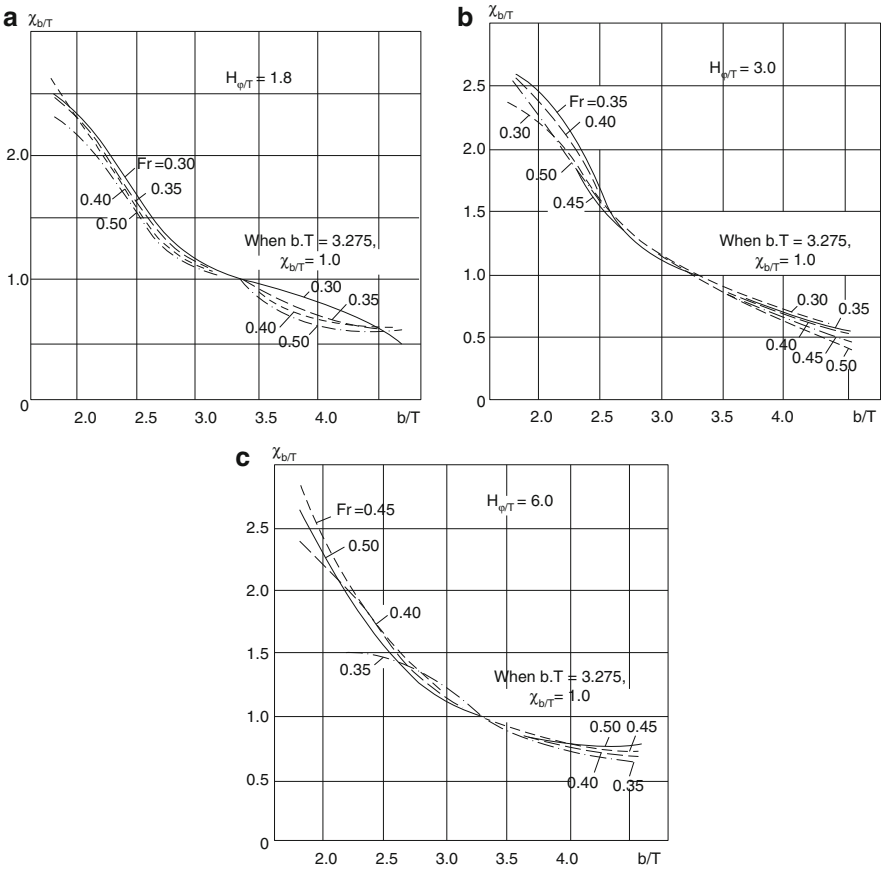

Fig. 5.26 Influence factor $\chi_{L/b}$ on residual drag coefficient of catamaran operating over critical speed in shallow water: (**a**) H_φ/T = 1.8; (**b**) H_φ/T = 3.0; (**c**) H_φ/T = 6.0

the range of demihull parameters, particularly the Fr_L range of the models available, is rather narrow, so drag needs to be estimated by extrapolation, and this will reduce the potential accuracy of the prediction.

For a more precise prediction of drag in shallow water, it is recommended to use model experiments in towing tanks where possible, while realizing that this can only be justified once a design target is identified through initial estimates and has promise for construction. Most model test tanks are not set up for shallow-water testing, so the extrapolation from "deep-water" tests to the intended shallow water operation remains an exercise of analysis and interpolation in most cases. Southampton University has carried out additional testing in shallow water on its catamaran series, and the reader is encouraged to refer to these reports, as listed in the resources at the end of the book, as a starting point.

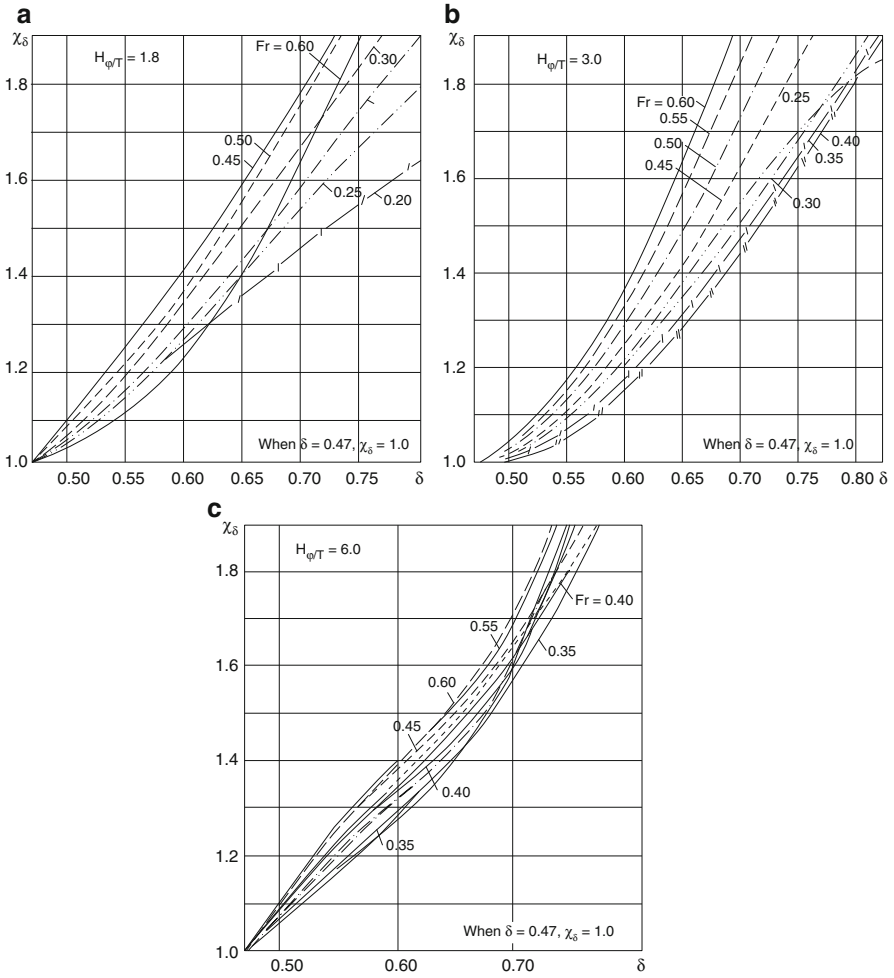

Fig. 5.27 Influence factor χ_δ on residual drag coefficient of catamaran operating over the critical speed in shallow water: (**a**) H_φ/T = 1.8; (**b**) H_φ/T = 3.0; (**c**) H_φ/T = 6.0

5.5 Influence of Hull Parameters on Resistance in Calm Water

5.5.1 Influence of Displacement/Length Coefficient $\Delta/(0.1\mathrm{L})^3$

As for a conventional displacement monohull, the displacement/length coefficient is the most important factor influencing the wave-making resistance of catamarans. We introduce model experimental investigations from some technical institutions, including MARIC, as follows.

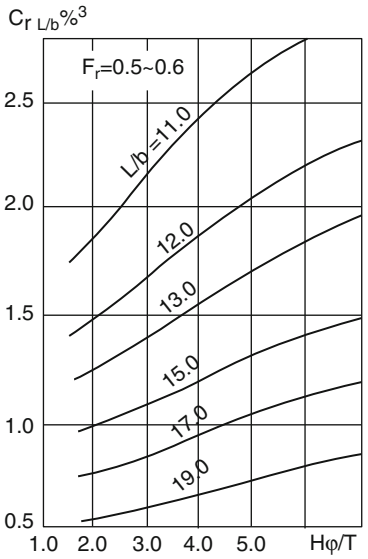

Fig. 5.28 Residual drag coefficient of a catamaran in shallow water at Fr_L = 0.5–0.6, at different L/b and H_φ/T

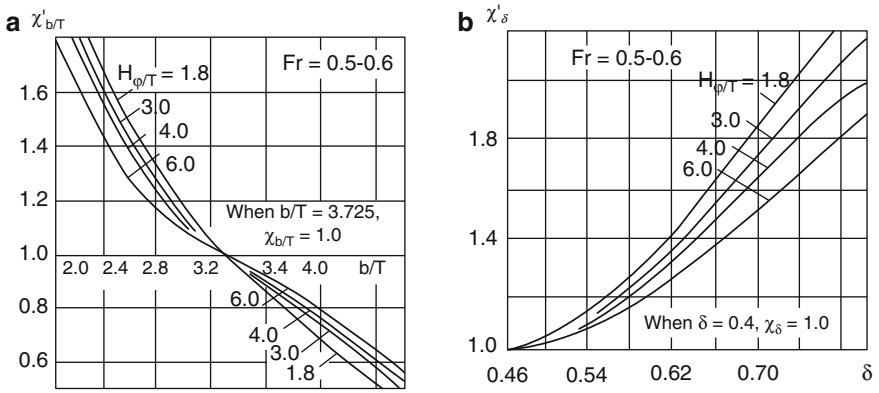

Fig. 5.29 Influence factors: (**a**) influence factor $\chi'_{b/T}$ on residual drag coefficient of catamaran in shallow water at Fr_L = 0.5–0.6 at different b/T and H_φ/T; (**b**) influence factor χ'_δ

1. *MARIC* [4, 5]

Tests were carried out using demihull model lines as shown in Fig. 5.6a, that is, three types of craft lines all with a round bilge, for the investigation. Basic leading particulars for the full-scale vessel are as follows:

Design waterline, L	30.0 m
Demihull beam, b	2.85 m
Basic draft, T	1.2 m
L/b	10.53
b/T	2.375

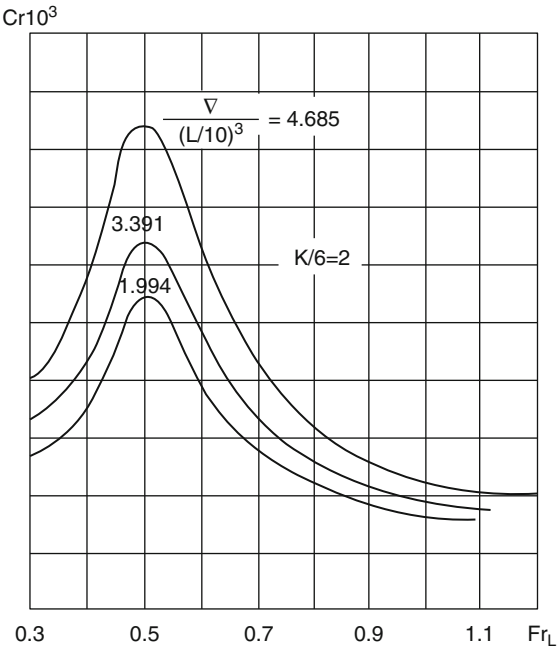

Fig. 5.30 Influence of $\nabla/(0.1L)^3$ on residual drag coefficient of catamaran at different Fr_L

The model draft can be changed to adjust to different displacements and displacement/length coefficients.

Figure 5.30 shows the influence of the displacement/length coefficient on the residual drag coefficient of catamarans at hull separation $k/b = 2$. From the figure one can see that as the displacement/length increases (i.e., reducing slenderness), wave-making resistance increases, particularly at the critical $Fr_L = 0.5$ due to large interference drag. The interference drag is also verified by the tests as influenced by hull separation, which will be described in Sect. 5.5.2.

Since high-speed catamarans often have $L/b = 8$–10 and k/b around the 2, the test results can be useful for estimation of residual drag of high-speed catamarans as follows:

$$C_r = f\left(Fr_L, \Delta/(L/10)^3\right), \tag{5.29}$$

where C_r can be found in Fig. 5.31a, b.

2. *Glasgow Hydrodynamic Laboratory*

A test program with ten experimental model arrangements was carried out in the towing tank at Glasgow Hydrodynamic Laboratory [6] to measure their resistance,

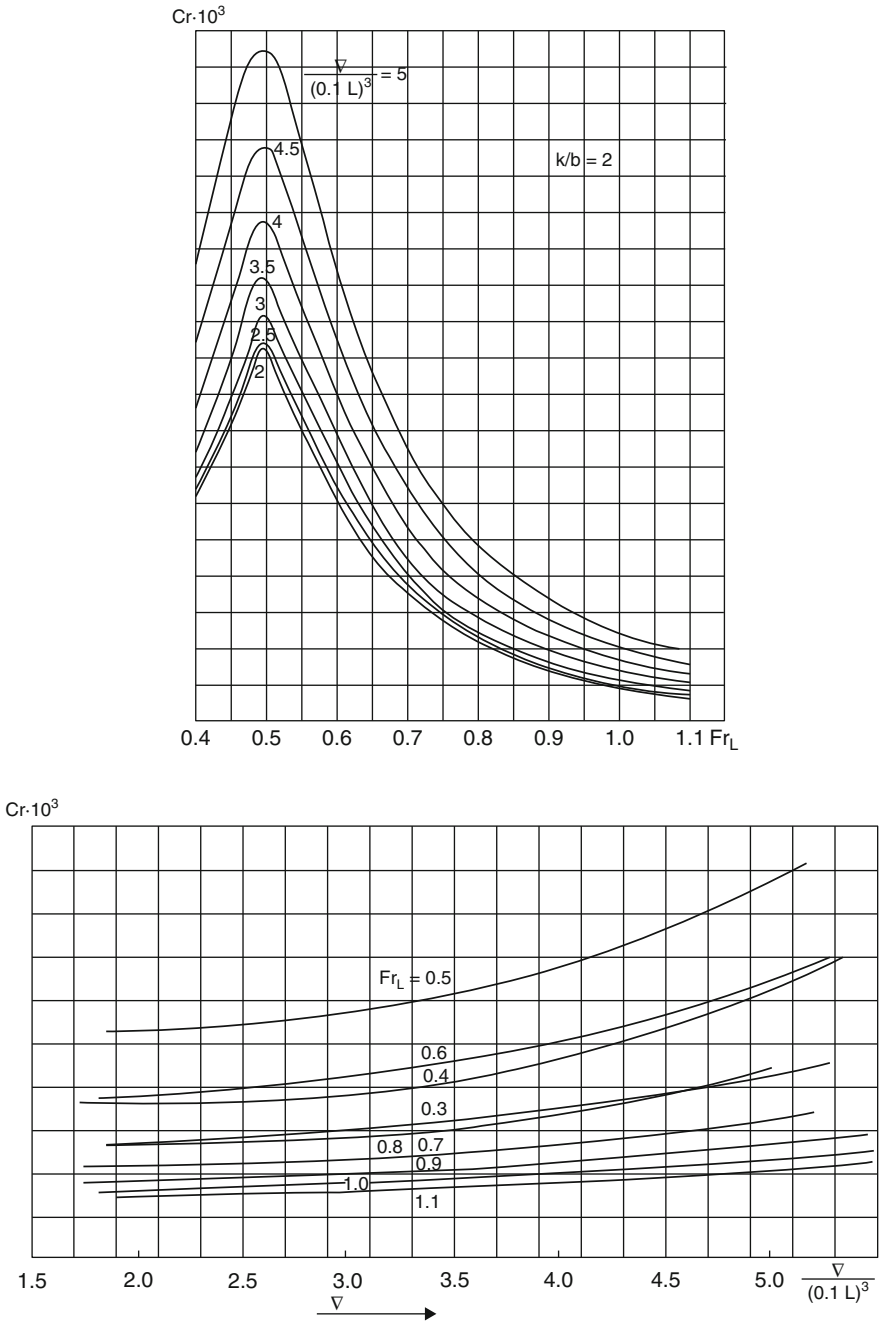

Fig. 5.31 (**a**, **b**) Curves for predicting residual drag coefficient of a catamaran at different $\nabla/(0.1L)^3$ and Fr_L at hull separation ratio $K/b = 2$

Table 5.8 Glasgow Hydrodynamic Laboratory catamaran model parameters

Condition	Model	Draft (cm)	LCG % from transom	Centerline separation (cm)	Disp. (kg)	$\Delta/(L/10)^3$ of Demihull	k/b	b/T
1	Demihull	3.5	40		6.066	0.76		4.18
2	Demihull	4.5	40		8.499	1.062		3.25
3	Demihull	4.5	36		8.499	1.062		3.25
4	Demihull	4.5	44		8.499	1.062		3.25
5	Demihull	5.5	40		11.018	1.377		2.66
6	Demihull	6.5	40		13.309	1.516		2.25
7	Catamaran	3.5	40	30	12.132		1.05	
8	Catamaran	4.5	40	37.5	22.85		1.56	
9	Catamaran	5.5	40	42.5	28.85		1.97	
10	Catamaran	6.5	40	45	30.35		2.07	

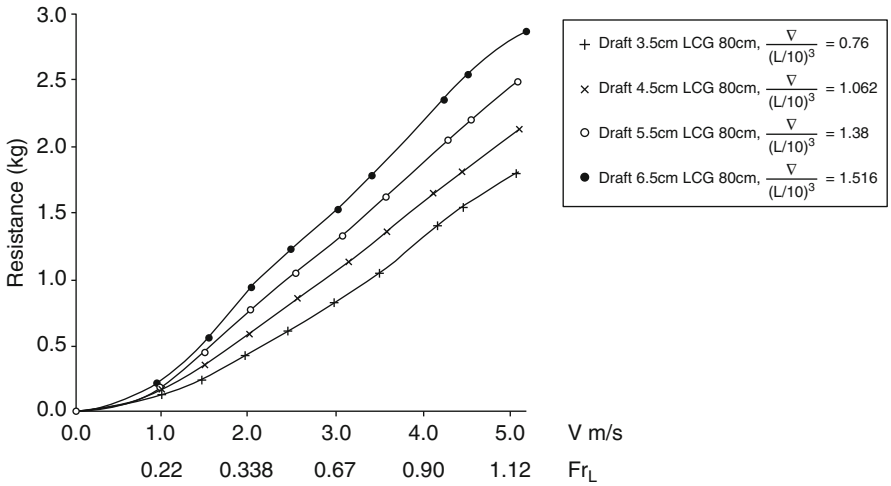

Fig. 5.32 Resistance measurements of Glasgow University 2-m demihull mode

trim, sinkage, and so forth, in both calm water and waves, with a sequence of parameter variations.

The model length $L = 2$ m, demihull beam $b = 14.65$ cm, $L/b = 13.65$, and the characteristics at each parametric condition are as listed in Table 5.8 below. Individual demihulls were tested in tests 1–6 and full catamarans in tests 7–10.

Figure 5.32 below shows the resistance measurements of the demihulls of catamaran models in cases 1–6. Figure 5.33 shows the resistance measurements of the catamarans in tests 7–10. Note that the resistance trend versus Fr_L for both demihull and catamarans is almost the same. The most important factor influencing

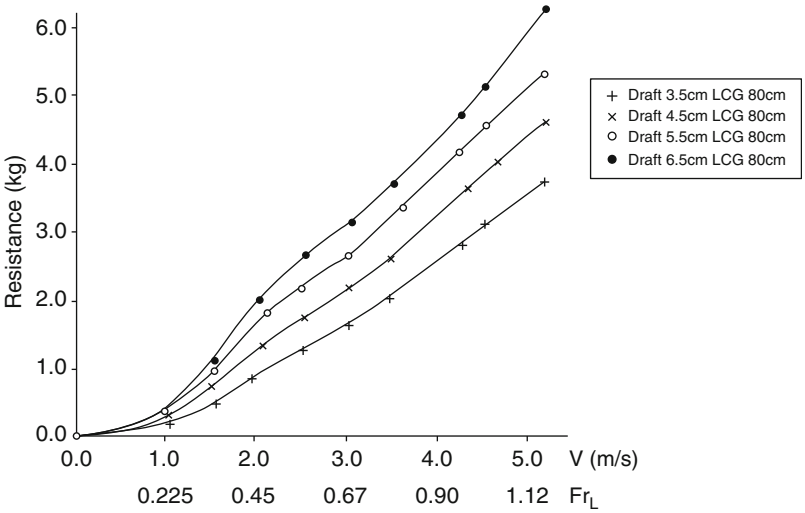

Fig. 5.33 Resistance measurements of Glasgow University 2-m catamaran model

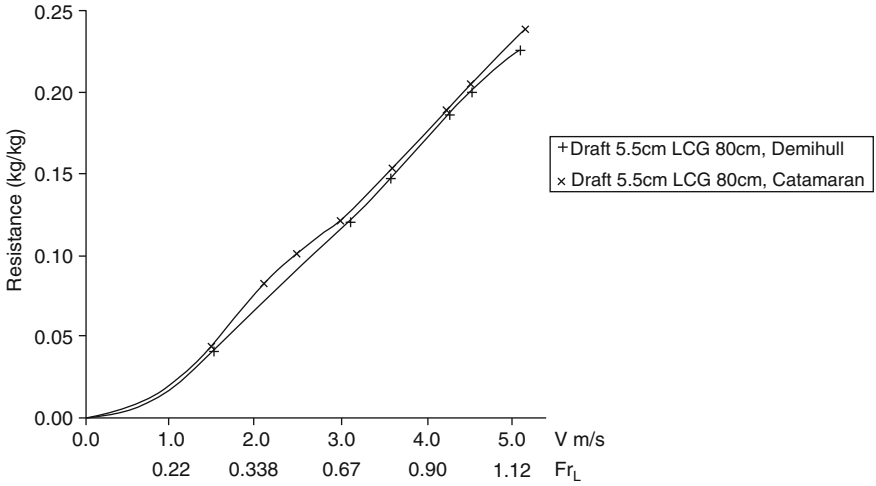

Fig. 5.34 Resistance measurements of Glasgow University 2-m catamaran versus demihull

the wave-making resistance is displacement-to-length coefficient, similar to the test results at MARIC.

The figure also shows that there is a small peak resistance at $Fr_L = 0.5$; however, the peak is small due to the small displacement-to-length coefficient of the models.

Figure 5.34 shows a comparison of the specific resistance (drag/displacement, kg/kg) of both demihull and catamarans, and the two curves are very close. This

suggests the interference drag of these particular catamarans is small due to the high demihull slenderness, and it demonstrates that slenderness is the critical factor influencing catamaran resistance.

3. *Shiro Matsui of Japan* [10]

Shiro Matsui carried out towing tank model experiments, with three different demihull lines, shown in Fig. 5.35, where:

(a) Shows the model with typical round bilge, M.S. 9064-R;
(b) Shows a mixed form with double chine M.S.9345-M. Leading particulars of this model are the same as for M.S. 9064-R, and the double chines are in the region of 20% model length forward of the stern transom;
(c) Shows a hard chine form M.S.9315-C similar to conventional planing hull

Figure 5.36 shows the effect of slenderness (also displacement/length coefficient) on residual drag coefficient C_r and demonstrates the same tendency mentioned earlier, that the more slender the demihull, the lower the residual drag.

This result should be correct no matter what form and what other parameters of demihull there are. However, in the case of craft with wide demihulls that generate significant hydrodynamic lift, meaning planing catamarans, the running attitude will be rather different, and the craft will have different design characteristics, which we will follow up on a little later. We move first to consider the hull separation coefficient *k*/*b*.

5.5.2 *Influence of Hull Separation Coefficient* k/b

Hull separation is another important factor affecting interference drag, in addition to the demihull slenderness, particularly at critical $Fr_L = 0.5$.

Figure 5.37 [4, 5] shows model test results in MARIC for different *k*/*b* and two slenderness conditions and shows that a higher hull separation gives a lower residual drag coefficient, particularly at critical Fr_L. In addition, it will be lower for demihulls with a higher slenderness (small displacement/length ratio). The figure also shows that the interference drag will decrease rapidly with increased Fr_L, which agrees with the test results at the Glasgow Hydrodynamic Laboratory shown in Fig. 5.34.

Figure 5.38 below shows the relative residual drag coefficient $\Delta C_r = \frac{C_{rCAT} - C_{rD}}{C_{rD}}$ (%) versus Fr_L at different displacement length coefficients and constant hull separations *k*/*b*, where C_{rCAT} and C_{rD} are the residual drag coefficient of a catamaran and demihull, respectively. It seems there are occasionally negative ΔC_r at higher Fr_L, which suggests the interference drag is a negative value, perhaps due to the favorable interaction between the bow divergent waves with stern wave systems.

Figure 5.39 shows the influence of spacing $k/b = 2$, 2.6, and 3.2 at different Fr_L, and it is noted that at critical speed $Fr_L = 0.5$–0.6 significant drag reduction can be achieved by increasing hull separation; however, as speed is increased, the residual

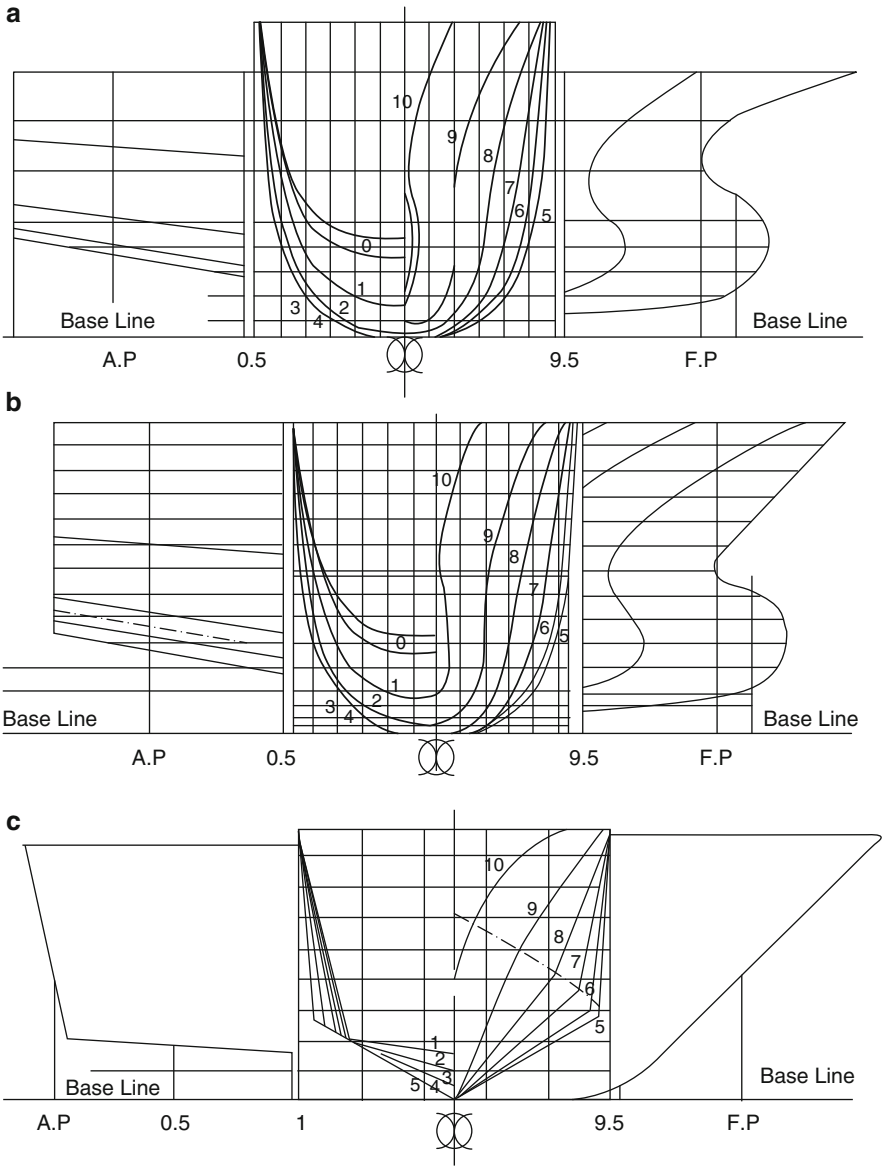

Fig. 5.35 Lines plans of models (**a**–**c**)

drag coefficient will be similar for the three hull separations tested, with a difference down to 5% of total resistance. This suggests the best k/b of high-speed catamarans with higher relative speed might be equal to or slightly less than 2.

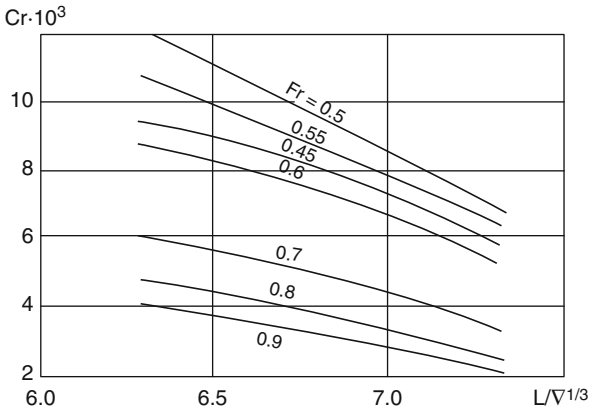

Fig. 5.36 Effect of slenderness on residual drag coefficient

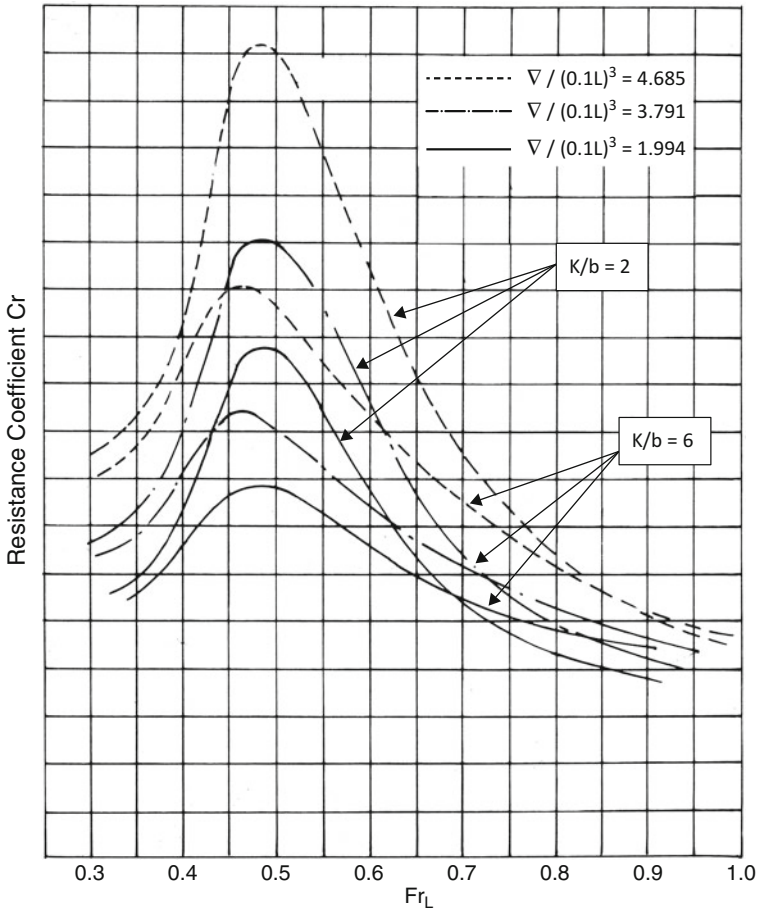

Fig. 5.37 Effect of spacing on residual drag coefficient C_r versus K/b, Fr, $\nabla/(0.1L)^3$

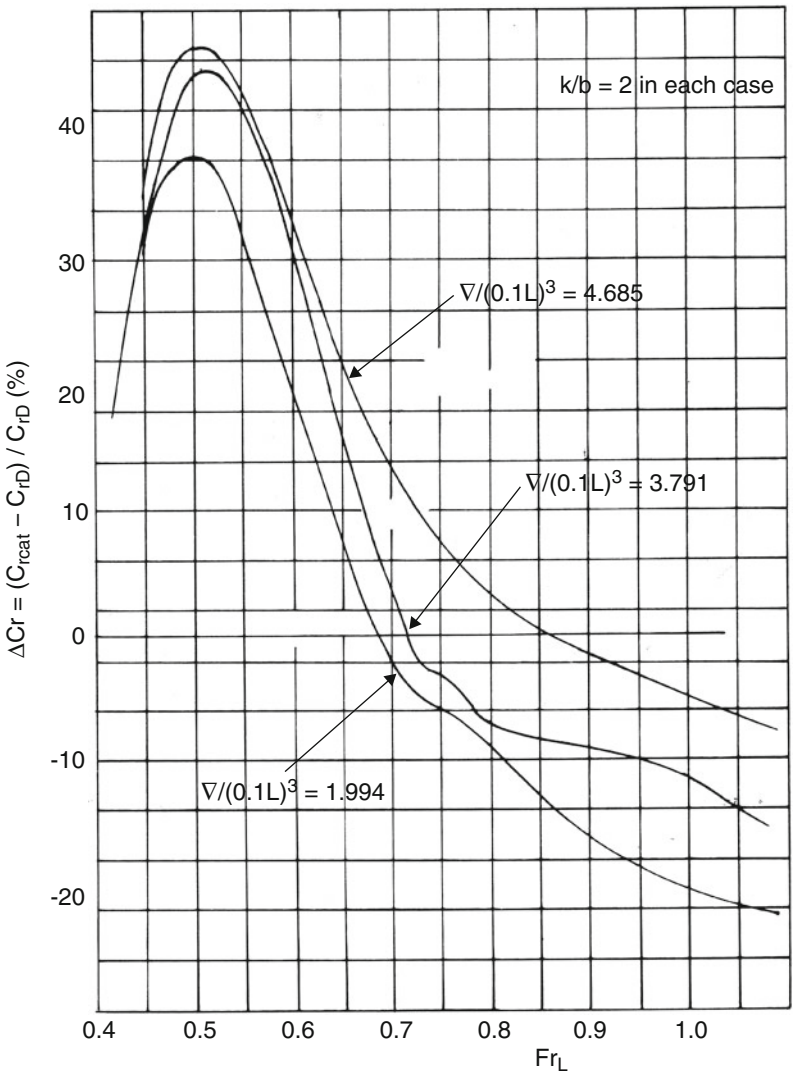

Fig. 5.38 Effect of fullness on ΔC_r versus Fr_L at constant $K/b = 2.0$

Figure 5.40 [4] below shows the effective horse power (EHP) of catamarans at constant $k/b = 2$ and double demihulls at different Fr_L; it is noted that the EHP for both conditions are close after $Fr_L = 0.75$; however, there is a small EHP peak on the catamaran curve at critical speed, so designers must pay more attention to such cases. However, in most cases for high-speed catamarans with higher Fr_L and logically larger engine output to achieve cruising speed, designers may not need to worry about this small drag peak. If there is a powering issue, one might enlarge the hull separation or demihull slenderness to reduce the drag peak.

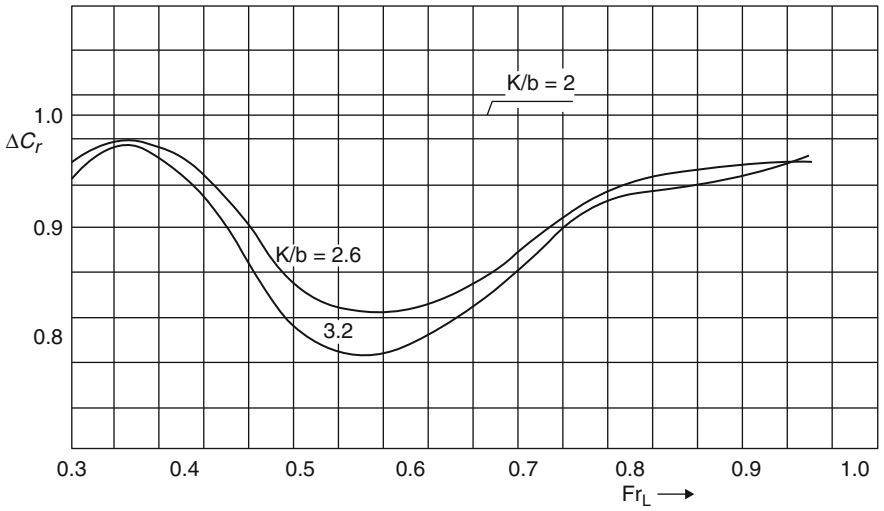

Fig. 5.39 Effect of spacing on ΔC_r versus K/b, Fr_L

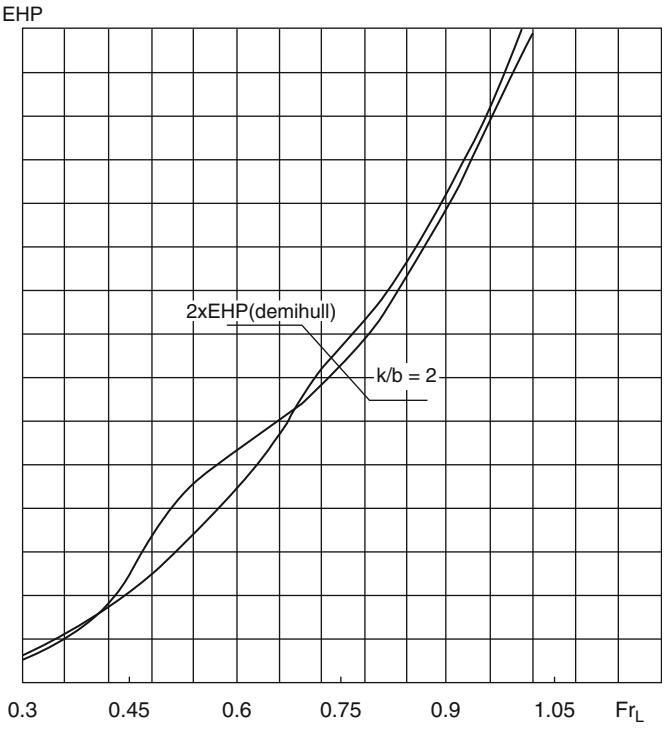

Fig. 5.40 EHP of catamaran model and double demihulls versus Fr_L at constant K/b = 2.0

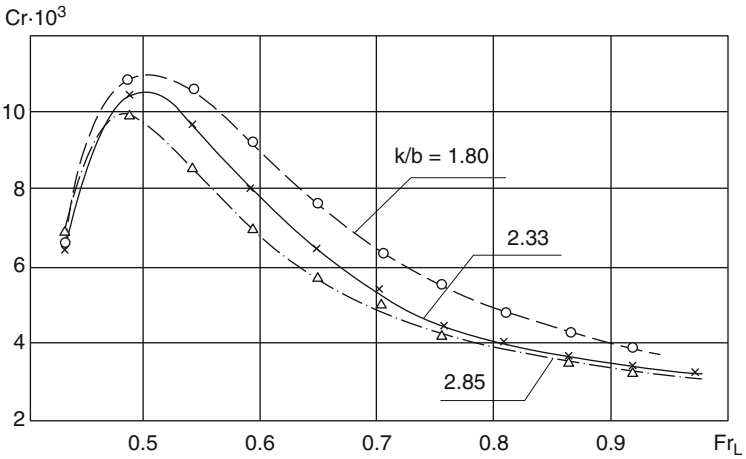

Fig. 5.41 Residual drag coefficient versus K/b, and Fr_L

Fig. 5.42 ΔC_r versus K/b and Fr_L

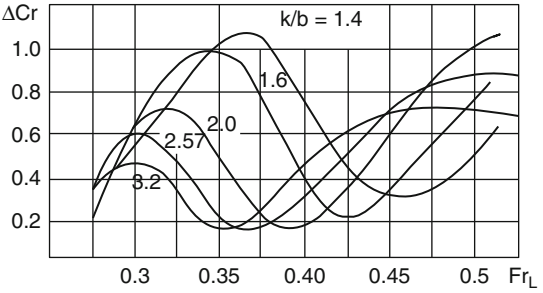

Figure 5.41 shows test results for catamarans in Japan, with the same trend mentioned earlier, regardless of the different hull form.

Figure 5.42 shows the $\Delta C_r = \frac{C_{rCAT}}{C_{rD}} - 1$ versus medium-range Fr_L (below critical) at different k/b. Note that there is an envelope curve for lower ΔC with respect to the drag trough at increasing Fr_L as k/b decreases. It is possible, therefore, to find an "optimum" k/b for different Fr_L for vessels designed to operate at medium speed.

5.5.3 *Influence of Hull Form*

As shown in Fig. 5.34, there were three types of model lines in the tests used by Matsui: round bilge, mixed round bilge and chine form, and hard chine type, including lines with double chine and single hard chine. Figure 5.43a below shows the effect of hull form on C_r from these tests. It is shown that:

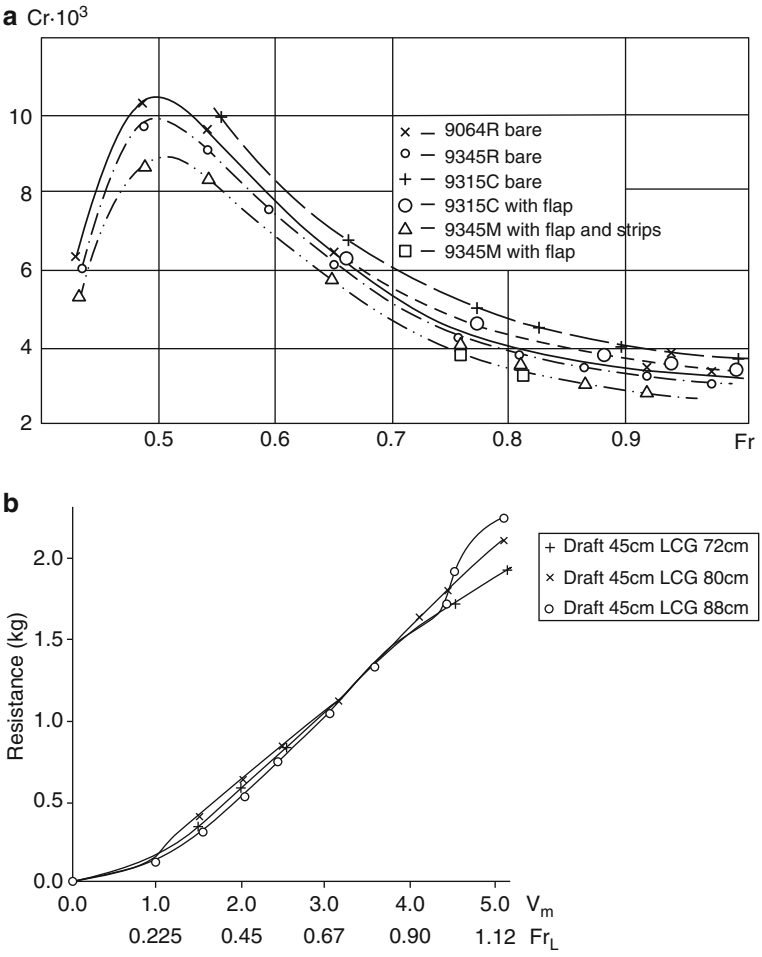

Fig. 5.43 (**a**) Effect of hull form on C_r; (**b**) effect of LCG on C_r

- At $Fr_L = 0.809$, the residual drag of mixed lines (M.S.9345-M) is 7.5% lower than that of a round bilge (M.S.9064-R);
- The residual drag of hard chine lines (M.S.9315-C) with slenderness$L/\Delta^{1/3} = 6.662$ is highest compared with that of the two forms mentioned earlier at operational speed $Fr_L = 1.0$, which indicates that the catamaran is still in displacement mode due to high L/b and slenderness, as explained in Sect. 5.5.1.

To summarize, the selection of demihull lines is similar to the approach in monohull design, based on a consideration of Fr_L, L/b, and slenderness; however, the difference in residual drag between the three hull forms is not large because all of these models are in displacement mode, and only a small part of lift is generated by hydrodynamic forces.

5.5.4 *Influence of Longitudinal Center of Gravity on Catamaran Resistance*

Reference [6] documents towing tank model tests carried out with different longitudinal centers of gravity (LCGs) with test results as shown in Fig. 5.43b. It can be seen that up to a model speed of 3.5 m/s ($Fr_L = 0.79$), the total resistance *decreases* as the LCG moves forward, whereas the total resistance *increases* as the LCG moves forward when the model speed exceeds 3.5 m/s. The results are apparently similar to those for displacement craft; however, the difference in total drag between three LCG positions is rather small, so LCG position is not as sensitive as that in other hydrodynamically supported vessels such as ACVs, SESs, and hydrofoils.

5.6 Other Measures for Reducing High-Speed Catamaran Resistance

5.6.1 *Stern Flap and Wedge*

The stern flap is a short plate hinge mounted at the bottom edge of the transom and extending partly or wholly across the transom beam so as to adjust vessel trim and improve the residual drag at high Fr_L. Trim flaps or tabs can be quite small due to the longitudinal moment produced by its lift. They often reduce the rooster tail wave at the stern and improve the virtual waterline. Such devices work best on semiplaning or planing vessels with a transom stern.

Figure 5.44a shows the test results of [10] by Matsui, demonstrating that the trim angle of the catamaran at $Fr_L = 0.67$ (3 m/s at model scale) is reduced from 2.6° (without flap) to 1.0° at flap angle −7° (flap down).

Figure 5.44a, b shows the total resistance and residual resistance coefficient of catamarans with and without flap versus Fr_L, and it can be seen that resistance is reduced by 5% at flap angle +2°, and 5.3 % at flap angles –4°, and 6.7 % at flap angle –7° respectively. A negative angle means the flap rotates down to create a positive angle of attack to an oncoming stream, and a positive angle means the flap rotates upwards. Since the flow from the transom when unconstrained rises up toward still water (actually toward a so-called rooster tail geometry), even +2° still has a significant angle of attack to the flow, generating a pitch trimming moment for the vessel.

Reducing the bow-up trimming angle will decrease the residual drag, but it will also increase the wetted surface area of the craft and frictional drag so there is an optimal flap angle for catamarans at different Fr_L.

An alternative to the stern trim tabs is to use a fixed wedge at the stern, which obviates the need to install any mechanical system. Figure 5.45 below shows the test results of demihull models [6] with and without a wedge (similar to the stern flap) at the low edge of the stern, and it is noted that the demihull resistance (just like a monohull) may be decreased by up to 5% in almost the entire range of Fr_L.

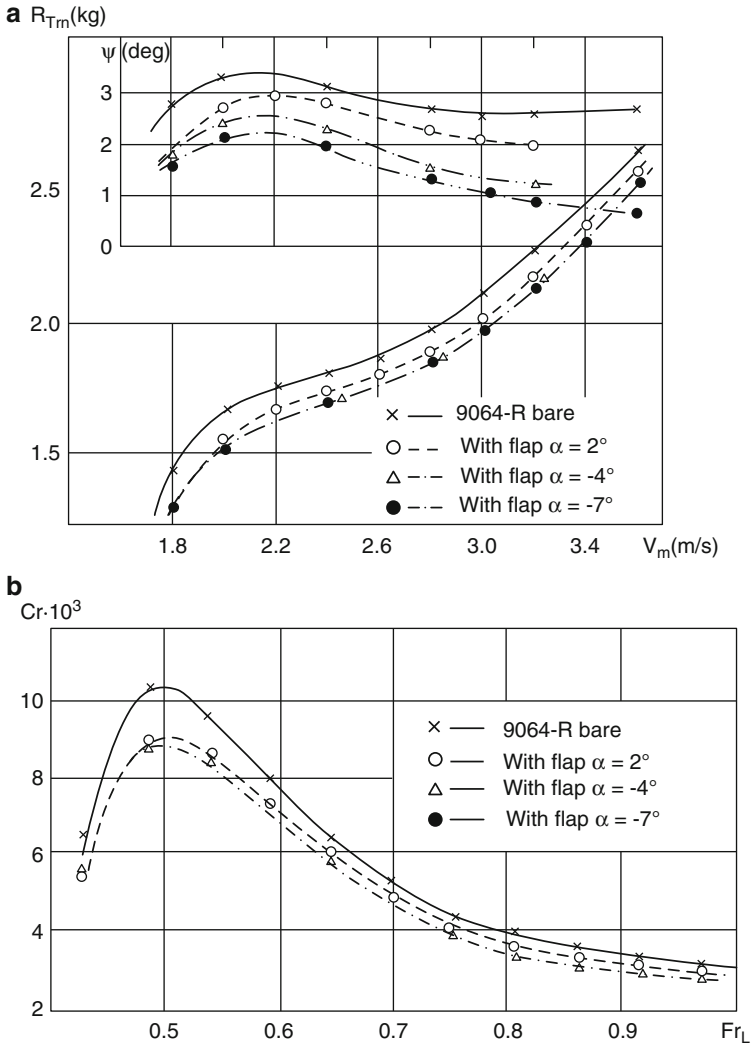

Fig. 5.44 Cr versus Fr_L of catamaran model (**a**) with and (**b**) without flap

5.6.2 Wave Suppression Hydrofoil

To improve the bow wave system between demihulls, tests of antiwave hydrofoils fitted on the inner sides of demihulls were carried out on the round bilge model of [10], with both a whole-span hydrofoil (span of hydrofoil equal to spacing of demihull) and half-span hydrofoil (span of hydrofoil equal to 0.4 hull separation k), as well as an aspect ratio of the hydrofoil equal to 2.36.

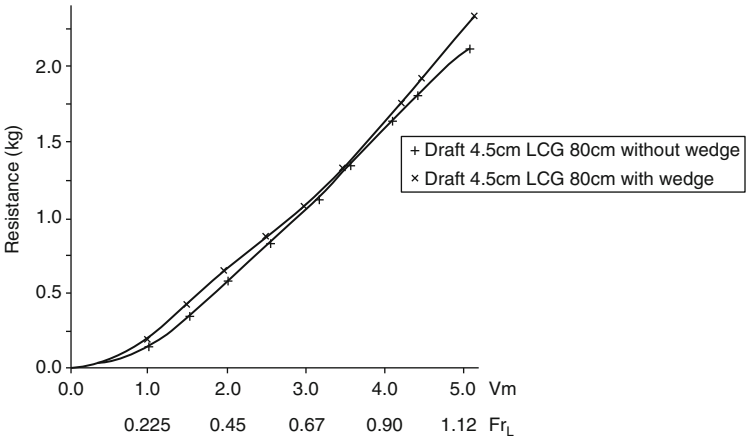

Fig. 5.45 Resistance of catamaran model with and without wedge versus Fr_L

The hydrofoils were mounted on models with stern flaps so as to balance the longitudinal moment and obtain a satisfactory trim angle.

The test results showed that the effect of the hydrofoils was small, occasionally with some improvement, but not a total success, perhaps because it is very difficult to fix the optimal installation angle of a hydrofoil to cope with different running attitudes at varying speeds.

The same test was carried out by the authors [20] on SESs (SES plus bow-fixed hydrofoils on the inner sidewalls of SESs), and obtained similar results.

The upshot is that for bow-mounted foils, it is necessary to have an active system to adjust the foil attitude dynamically during craft operation. For very large catamarans these types of control have been installed with the aim being rather to achieve motion suppression than a reduction in resistance.

5.6.3 Effect of Bow Spray Strips

Some bow spray strips have been mounted on catamaran models [10], and test results indicate that resistance may be reduced, but only slightly. However, it will reduce the spray, thereby improving the navigator's vision.

Spray strips will also improve seakeeping quality, which will be introduced in the next chapter.

5.6.4 *Interceptors*

The working principle of interceptors and their configurations [21, 22] are as shown in Fig. 5.46; the interceptors are the plates mounted at the transom stern, which can be controlled to protrude under the stern bottom, for resisting flow, so as to increase the bottom pressure and lift as well as reduce the wetted surface and resistance. The protrusion depth can be adjusted at various running conditions and waves to obtain optimum results.

Since the protrusion depth is very small, in general, in the boundary layer of the flow, ($h/L = 0.075$–0.12%, where L is vessel length and h protrusion depth), the additional resistance is small, but significant lift is achieved and the wetted surface and trimming angle are reduced, so the hydrodynamic properties with interceptors will improve.

Figure 5.47 shows the schematization of the 2D hydrodynamics of interceptors [22], and Fig. 5.48 shows the configuration of the interceptors mounted on the 40-m-long high-speed hydrofoil-assisted catamaran Superfoil 40 [23] at a speed of 55 km. From the figure one can see that the interceptor protrusion depth can be controlled vertically by means of hydraulic actuators or electric motors to adjust the trim before and after critical Fr_L, in waves, and so forth. The side skeg at the stern is used to guide the flow lines at the stern to improve the hydrodynamic properties.

Figure 5.47 shows the flow vectors and pressure profile under the bottom due to the interceptor, and it shows that the pressure increases significantly at the bottom before the transom owing to the interceptor.

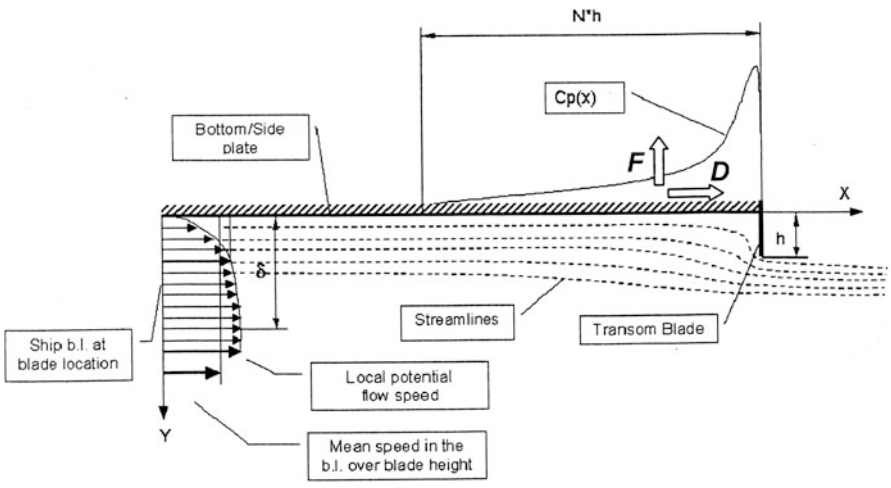

Fig. 5.46 Interceptor working principle schematic

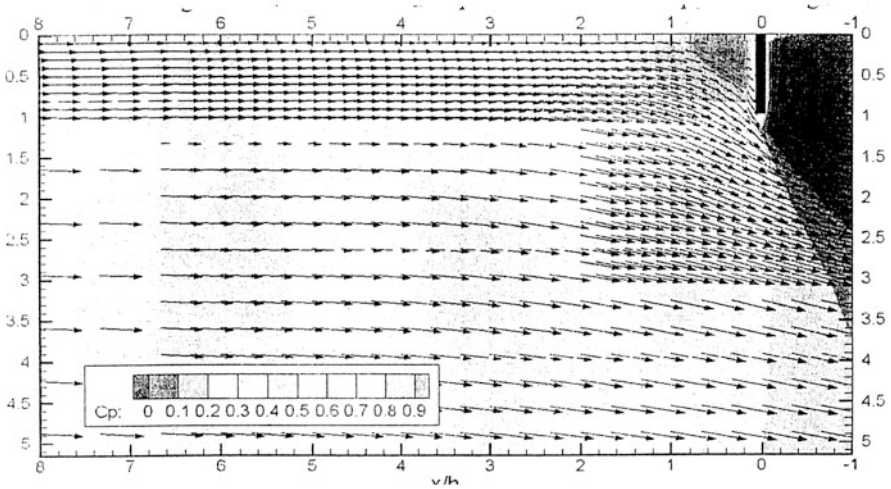

Fig. 5.47 Flow and pressure vectors due to interrupter mounted at stern

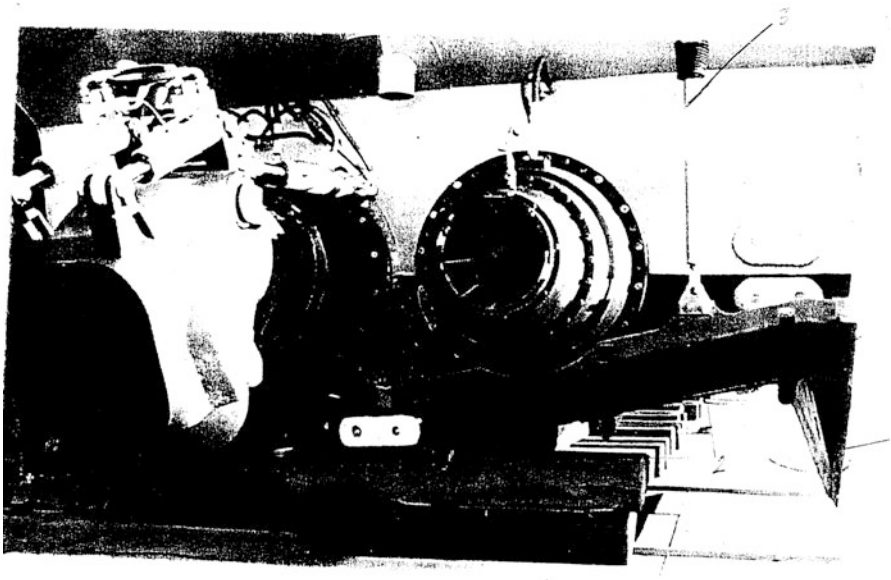

Fig. 5.48 Stern of superfoil vessel with interrupters

5.6.4.1 Test Results of of A. Mancini's Investigation

Mancini carried out an experimental investigation in 2005 [22]. Tests were conducted on three different models at INSEAN, and their leading particulars are outlined in Table 5.9 below:

Table 5.9 Model hull forms tested by Mancini

Model	A	B	C
Features	Planing monohull with lower length/beam ratio	Planing monohull with higher length/beam ratio	CAT
L_{PR}/B_{px}	2.88	4.72	12.09
$A_p/\nabla^{\frac{2}{3}}$	6.15	3.54	–
β^0	16	14.8	14.5
β_T^0	12.7	7.9	14.5
$L_{WL}/\nabla^{\frac{1}{3}}$	4.28	5.65	5.87

Where

L_{pr}	Projected length of hard chine, m;
B_{px}	Maximum width at hard chine, m;
A_p	Wetted surface area at bottom, m^2;
∇	Displaced volume, m^3;
β, β_T	Dead-rise angle at midsection and stern, respectively;
$L_{WLl}/\nabla^{\frac{1}{3}}$	Length/displacement ratio.

Since we are discussing the effect of interceptors on catamarans, only the test results of models B and C need be considered.

Figure 5.49 shows the test results of model B, which is the monohull model with higher planing length/beam ratio and smaller planing surface area. From the figure one can see that the decrease in resistance is approximately 9.5% at volume Froude number, $F_{r\nabla} = v/\left(g\nabla^{\frac{1}{3}}\right)^{\frac{1}{2}} = 1.7$; however, in the case of volume Fr_D at 2.0–2.7, the decrease in resistance is 17% with a decrease in the trimming angle as the speed increases rather than an increasing trim.

Figure 5.50 shows the test results for catamaran model C with an interceptor, at $h/L_{PR} = 1.14 \times 10^{-3}$(where h is the protrusion depth of the interceptor and L_{PR} is the length between perpendiculars) and different Fr_D; when Fr_D is between 1.6 and 2.20, the decrement of resistance is small, but at Fr 2.4, the decrease in resistance is as high as 10%. It may be noticed that for the catamaran the trim effect of the intruder/interceptor is far less marked compared to no interceptor.

Meanwhile, the trim angle (bow up) reduces at high speed on the catamaran with interceptors. This is most favorable for reducing catamaran resistance since, on a conventional catamaran, the trim angle will increase at high speed owing to the slender demihull form, and this will increase the resistance.

Tests were carried out for both interceptor and flap on planing model A, where h/L_{PR} is the relative protrusion depth, and θ is the initial trim angle of the models for speeds at displacement Fr_D of 2.15, 2.8, and 3.45. These showed that while the flaps

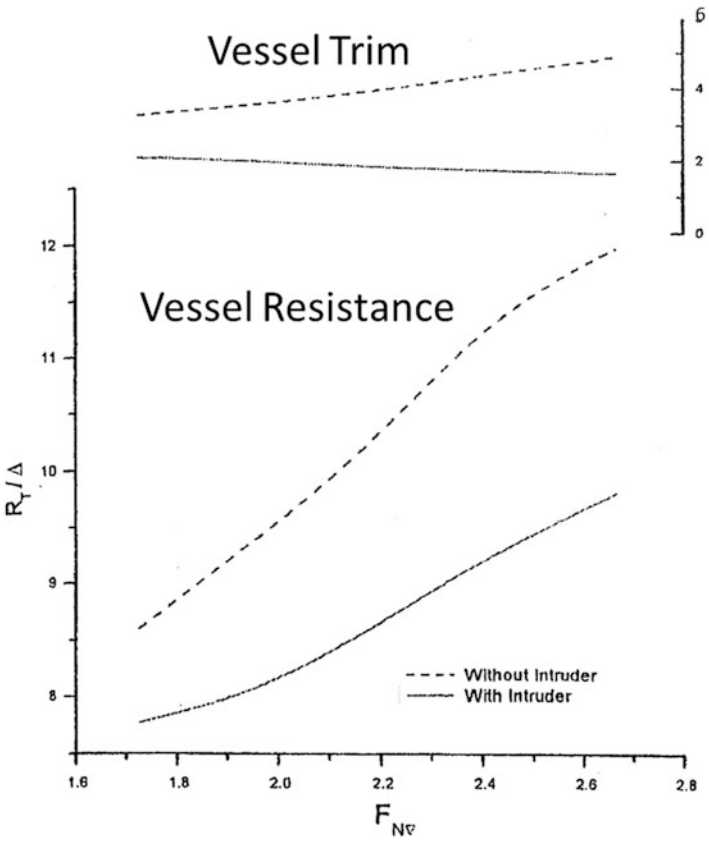

Fig. 5.49 Test results model B

and intruders could be adjusted to achieve the required trim, the interceptors could be adjusted to achieve greater resistance reduction. The optimum relative protrusion of an interceptor changes with Fr_D and θ, so interceptors do have to be adjusted either automatically or manually. In comparison with a flap, the setting of an interceptor is nevertheless rather more forgiving.

The higher the craft speed, the more effective are the interceptors. On the hydrofoil-assisted catamaran Superfoil (see also Chap. 10), the effectiveness is high thanks to the very high volume Fr_D (3.89); in addition, with the aid of a bow hydrofoil, the whole fore part of the bottom is clear of the water surface, so the wetted length at the rear bottom is very small, giving a small wetted-length-to-beam ratio of the demihull compared with that on a conventional high-speed catamaran. So the hydrodynamic properties of this craft are improved with interceptors.

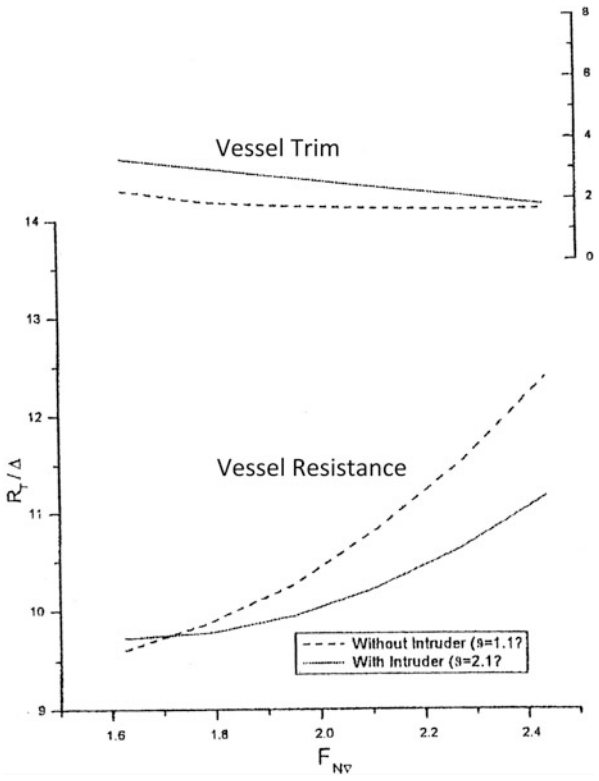

Fig. 5.50 Test results model C

5.6.5 Steering Interceptor for Improving Maneuverability

Using the hydrodynamic principle for interceptors, interceptors can also be mounted on the outer side of demihulls of high-speed vessels to provide lateral forces to improve maneuverability.

Figure 5.51 shows the high-speed monohull craft *Corsica Express III* and its Humphree steering configuration. Figure 5.52 shows the steering interceptor configuration for a semi-SWATH, type STENA HSS 1500 demihull. Figure 5.52b, c shows details of an interceptor and associated actuator fitted on the transom of the Stena HSS1500 for steering control.

The advantages of the steering interceptor (SI) can be outlined as follows:

- Reduced resistance and fuel savings: obviates the need to install steerable waterjet to provide steering force and moment to reduce hull resistance and save fuel;
- Reduced and simplified maintenance thanks to less complex waterjet installation;
- As a reserve control surface SI can be combined with a steerable waterjet, so that SI can be used at high speed and waterjet controls at low speed;

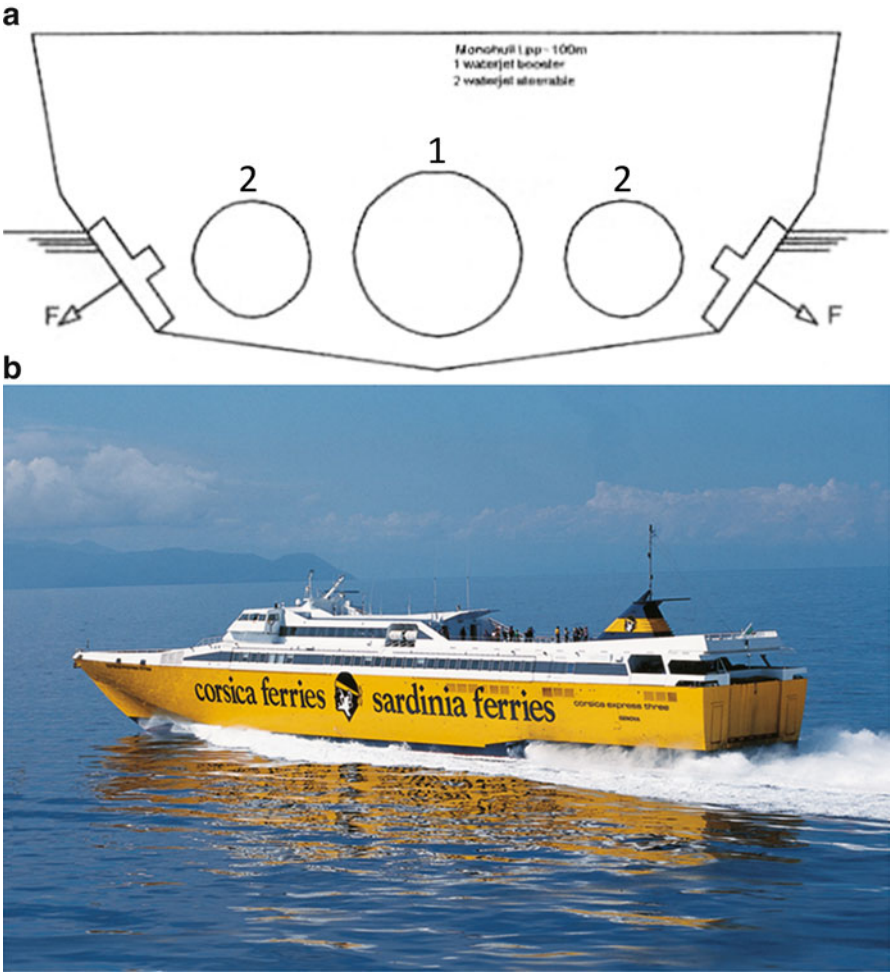

Fig. 5.51 (**a**) *Corsica Express III* with intruder steering configuration: (**b**) photo of *Corsica Express III*

- Improved seakeeping quality by fixing waterjets (not using them for steering) but using a steering interceptor for course keeping. This enhances speed by 1 knot at high speed in a significant wave height of 2.0 m and 2.0 knots in 3.25 m waves for HSS1500 (Fig. 5.53).

  Figure 5.53 shows the speed gain with interceptor steering.

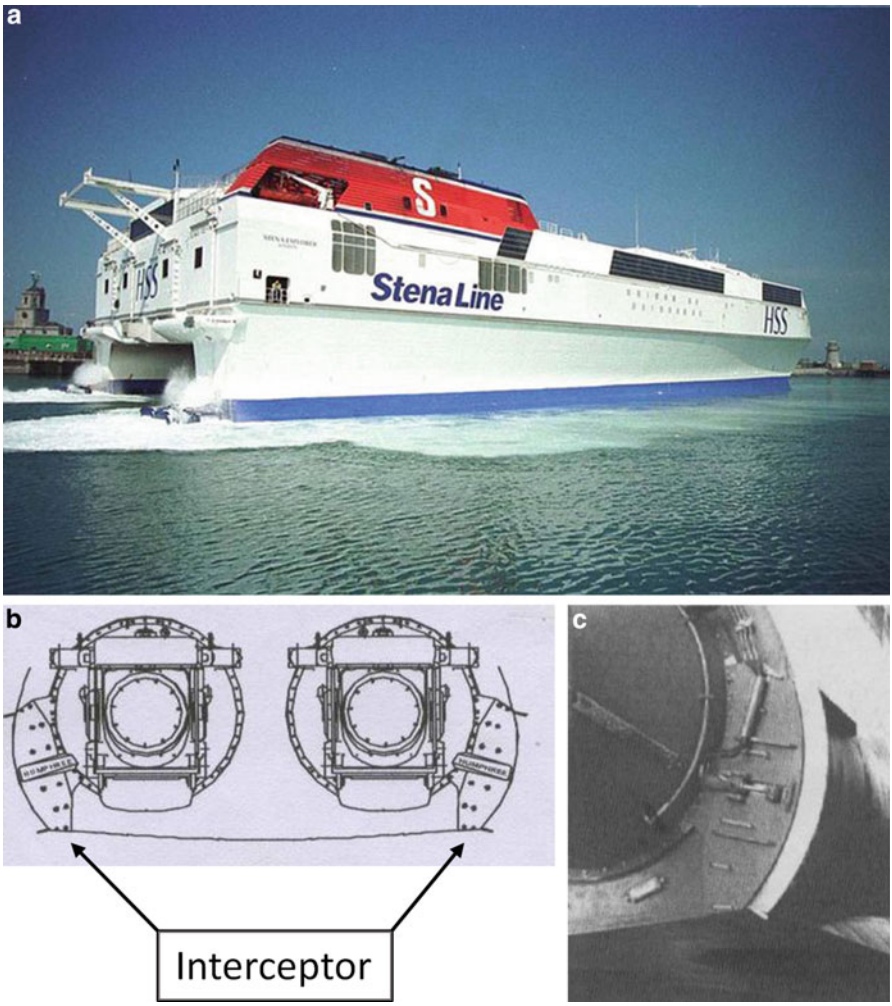

Fig. 5.52 (**a**) Stena Explorer stern; (**b**) steering interceptor diagram for Stena HSS-1500; (**c**) detail of interceptor and actuators

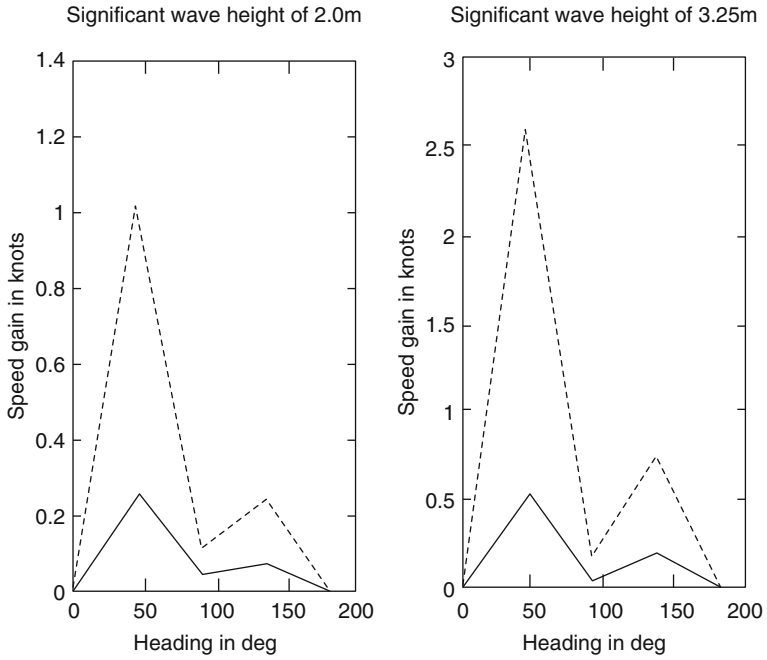

Fig. 5.53 Speed gain with interceptors

References

1. Fry ED, Graul T (1972) Design and application of modern high-speed catamarans. SNAME Marine Technology
2. Yelmalayev: hydrodynamic characteristics of high speed catamaran, shipbuilding, Saint Petersburg, USSR, No 8, 1976 (in Russian)
3. Arfiliyev MY, Madorsky GS (1976) Inland transport catamaran, Transport Press, USSR, (in Russian, or Chinese translation)
4. Song GH (1996) Drag performance of high speed catamaran (1)(2), Ship & Boat, Marine Design & Research Institute of China (MARIC), Shanghai, China (in Chinese)
5. Song GH (1987) Catamaran class B, research & design of ships, Chinese naval ships academy, vol 11 Beijing, China (in Chinese)
6. A Incecik, Morrison BF, Rodgers AJ (1991) Experimental investigation of resistance & seakeeping characteristics of a catamaran design, FAST'91 Proceedings, Trondheim, Norway
7. Wikland KM (1993) The feature for high speed craft, FAST'93 proceedings, Dec 1993, Yokohama, Japan,
8. Insel M, Molland AF (1992) An investigation into the resistance components of high speed displacement catamarans. Transactions of Royal Institution of Naval Architects. pp 1–20. ISSN 0035-8967
9. Molland AF, Wellicome JF, Couser PR (1996) Resistance experiments on a systematic series of high speed displacement catamaran forms-variation of length-displacement ratio and breadth-draught ratio, Transactions of Royal Institution of Naval Architects. pp 555–571, ISSN 0035-8967

10. The experimental investigation on resistance & seakeeping quality of high speed catamaran, Shiro Matsui, Fast'93, 1993, Yokohama, Japan
11. Pham XP, Kantimahanthi K, Sahoo PK. Wave resistance prediction of hard-chine catamarans through regression analysis, 2nd international European Conference on High Performance Marine Vehicles (HIPER 2001), Hamburg, Germany, pp 382–394
12. Sahoo PK, Salas M, Schwetz A (2007) Practical evaluation of resistance of high-speed catamaran hull forms—Part I, Ships and offshore structures published by Taylor and Francis 2:4, pp 307–324. Also available by download from University of Tasmania at www.eprints.utas.edu.au/3601
13. Sahoo PK, Mason S, Tuite A (2008) Practical evaluation of resistance of high-speed catamaran hull forms—Part II, Ships and offshore structures published by Taylor and Francis 3:3, pp 239–245. Also available by download from University of Tasmania at www.eprints.utas.edu.au/7731
14. Couser PR, Molland AF, Armstrong NA, Utama IKAP (1997) Calm water powering predictions for high speed catamarans, FAST 1997, Sydney, Australia, 21–23 July 1997
15. Savitsky D. Overview of Planing hull development, HPMV'92 proceedings, June 1992, USA
16. Savitsky D (1964) Hydrodynamic design of planing hulls, marine technology, vol 1. Society of Naval Architects and Marine Engineers, New York
17. Savitsky D, Ward Brown P Procedures for hydrodynamic evaluation of planing hulls in smooth and rough water, marine technology, vol 13. Society of Naval Architects and Marine Engineers, New York
18. Wang YC (1992) Resistance features of high speed catamaran, Proceeding of domestic conference on ship resistance and performance, (in Chinese)
19. Hoerner SF (1965) Fluid dynamic drag. Published by the author, Hoerner fluid dynamics, Brick Town, New Jersey. ISBN-13: 978-999883163.
20. Stephen Brizzolara: "Hydrodynamic analysis of interceptor with CFD methods", Proceedings, FAST 2003
21. Bliault A, Yun L (2000) Theory and design of air cushion craft, Pub Arnold/Elsevier, ISBN 0 340 67650 7 and 0 470 23621 3 (Wiley), p 632
22. Christer Wilmark et al.:(2001) Interceptor steering boats performance of high speed vessels. The Scandinavian Shipping Gazette
23. Mancini A (2006) A moriconi, intruder: a device to improve hull performance, Proceedings, HPMV CHINA, Shanghai, China
24. Stanislav P, Yun L (2005) "A brief introduction to a high speed passenger craft—hydrofoil assisted catamaran, Superfoil 40", Proceedings HPMV CHINA, Shanghai, China

Chapter 6
Seakeeping

6.1 Introduction

So far we have discussed the wave making of a vessel in calm water and the analysis of drag generated by the vessel-induced waves in Chap. 4, followed in Chap. 5 by an estimation of the other key components of drag that make up total resistance.

The next step is to look at the motions of a vessel in a seaway and the influence of the hull form on the motion response as well as dynamic stability. Once key relationships have been established, it should be possible to adjust the vessel geometry or install appendages that can dampen motions so as to enable safe and comfortable passage for passenger and freight cargo.

When traveling in a seaway, a vessel will experience pitching, roll, and heaving forces and moments as wind-induced waves pass by the vessel. Catamarans or multihulls have a more complex response to wind waves than monohulls due to the separation of the hulls creating different responses at the same point in time. Depending on their orientation to the oncoming seaway, multihull vessels will experience significant torsional moments.

We start our investigation of multihull seakeeping with basic motion characteristics and then summarize the theory for coupled motions.

The main purpose of these analyses is twofold:

- Identify the motions and accelerations on the vessel hull to enable structural analysis. The vessel operational limits may then be determined by this response, and additionally the service life due to fatigue will be defined by this.
- Identify the motions and accelerations applied to a cargo of people or freight. In this case the operational limits may be set lower than the structural limitations due to the motion boundaries that define the onset of motion sickness for people or requirements to limit vibration motion to sensitive freight.

L. Yun et al., *High Speed Catamarans and Multihulls*,
https://doi.org/10.1007/978-1-4939-7891-5_6

In the first part of this chapter we focus on the catamaran. Then we consider the case of hull forms that have finer lines at or above the waterline, that is, the wave-piercing form and the small-waterplane-area twin-hull (SWATH) form.

6.2 Multihull Motion Characteristics in Waves

The motion of a catamaran is rather different from that of a conventional ship due to the demihull separation and slender hull form. Owing to the high transverse stability, roll motions are very small compared with a monohull. The natural periods of roll and pitch are much closer, and the movements can be jerkier due to the high roll damping. In oblique seas the motions follow a corkscrew trajectory and can make personnel movement difficult and engender sickness in higher sea states. Designers have worked on this issue for many years, and it is part of the reasoning behind the wave-piercer concept and the small-waterplane designs.

The responses in the motion of a catamaran differ from those of conventional ships as follows.

6.2.1 Roll Motion: Influence of Short Roll Period and Strong Roll Damping

The natural roll period can expressed as

$$T_\theta = \frac{1}{2\pi}\sqrt{\frac{I_x + \lambda_x}{Dh}}, \tag{6.1}$$

where

D Displacement,
h Metacentric height above CG,
I_x Moment of inertia in roll,
λ_x Added mass moment of inertia in roll.

Figure 6.1 shows a cross section of a catamaran with the nomenclature that will be used in this chapter.

The initial transverse metacentric height of a catamaran is higher than that of monohull (up to two to four times), and the mass moment of inertia of a catamaran may be smaller than that of a monohull (up to 15–20% lower) due to the mass distribution's being more centralized than the buoyancy, so the catamaran roll period is shorter.

Roll damping is rather high due to demihull separation, so the first feature of catamaran roll motion is a very fast roll together with fast attenuation due to the higher roll damping, particularly on a catamaran with hard chine demihulls. This is

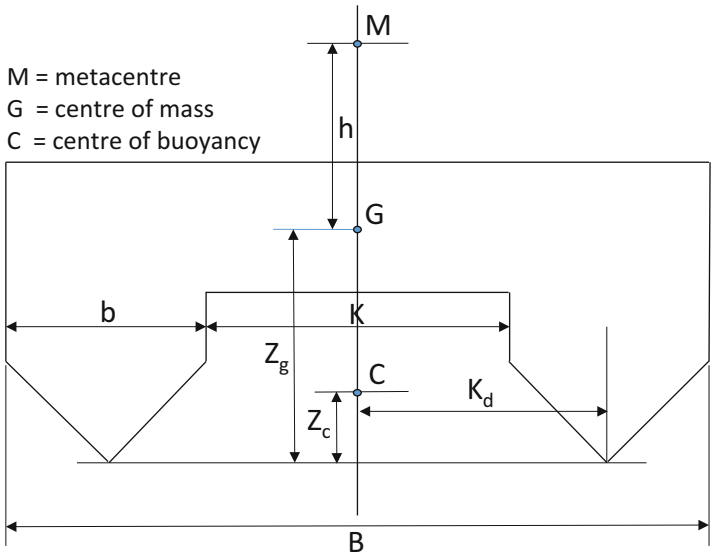

Fig. 6.1 Catamaran dimensions

Table 6.1 Nondimensional damping coefficient of roll motion

Model number	9064-R round bilge		9345-M mixed	9315-C hard chine
Condition	Bare hull	With stern flap, spray strips	Bare hull	Bare hull
Damping coefficient ν	0.0387	0.0649	0.0502	0.1164

one reason why designers use such lines for catamarans to improve their seakeeping even without reaching planing speeds.

Table 6.1 below shows the nondimensional damping coefficient ν for three of the models found in reference [1] of Chap. 5, where 9064-R is a model with a round bilge form, 9345 is a model with mixed body plan, and 9315-C is a hard chine model.

From the table one can see that the roll damping coefficient of a catamaran with hard chine is almost three times larger than that of round bilge hulls, and the damping coefficient of a catamaran with stern flap and spray strips is significantly enhanced compared to the bare hull model.

The pitching motion of a catamaran is rather different from the roll motion, with lower motion damping, resulting in larger pitching angles, due to the small L/B ratio (length to overall breadth) for a catamaran.

Figure 6.2 shows a comparison of roll and pitching angles of a conventional catamaran and monohull in waves for different headings.

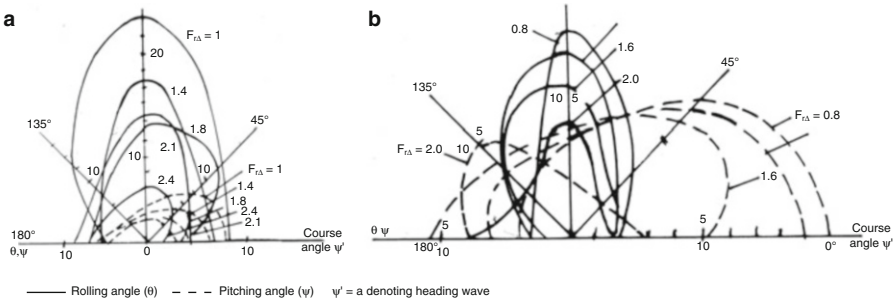

Fig. 6.2 Comparison of rolling and pitching angles of catamaran models with monohulls

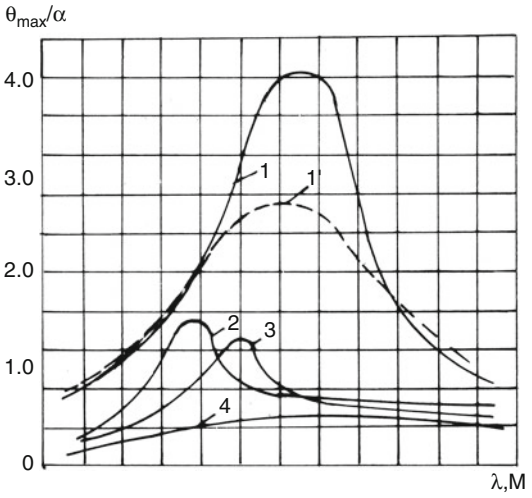

Fig. 6.3 Comparison of relative roll angle of monohull with catamaran and SWATH

Figure 6.2a shows the motion of the conventional monohull model, $k/b = 0$, in waves with wave height and waterline/length ratio $h_{w3\%}/L_{WL}$ equal to 0.06, where $h_{w3\%}$ represents waves at 3% occurrence. The figure shows the craft motion at different course angles $\psi'(\psi' = 0$ represents waves coming from the bow at 0° heading).

Figure 6.2b shows the motion (roll and pitching angle θ, ψ) of the catamaran model, with hull separation $k/b = 2$, $h_{w3\%}/L_{WL} = 0.07$, at different course angles. The catamaran roll angle is reduced by between 73% and 81.4% of conventional monohull ship motion; however, the pitching angle of the catamaran is significantly larger than that of the monohull.

Figure 6.3 [2] shows a comparison of the relative maximum roll angle $\theta_{\max}/\alpha$ (where α represents the wave steepness) for different hull forms, based on testing carried out in Japan. In the figure the numbered curves are as follows: 1: monohull, 1′: monohull with roll damping devices, 2: catamaran, 3: SWATH with single strut, 4:

SWATH with double struts at one side. It can be seen that the maximum roll angle for a catamaran is much lower than that of a conventional monohull.

The damping force (and moment) for a catamaran is four to seven times higher than that of a monohull. The damping increases with vessel speed, so the roll angle and roll angle acceleration of a catamaran at high speed will be less than at lower speed by 3–3.5 and 2–2.5 times, respectively, owing to the high damping coefficient [3]. Also, since the natural roll motion at its natural frequency will be damped and decay quickly, in a seaway the superposition of natural roll motion on the forced roll motion caused by encountered waves will be less than that on a monohull, so the seaworthiness (dynamic response) of a catamaran may be said to be improved compared to a monohull ship.

6.2.2 Torsional Motions

Since the natural periods of both roll and pitching are close to each other, due to the higher transverse and lower longitudinal waterplane moment of inertia (see Chap. 3 for a review), a so-called corkscrew motion of a catamaran, that is, motion on the catamaran diagonal axis may be generated in oblique seas and make for a very uncomfortable feeling for crew and passengers. The torsion across the diagonal is also a serious issue for the design of the hull connecting structure and for larger vessels can be the dimensioning load case. An illustration was shown earlier in Fig. 6.2b. This is a very important factor affecting the seaworthiness and operation of catamarans.

6.2.3 Wave Interference Between Demihulls

The wave system caused by catamaran roll motion is different from that of a monohull due to the waves generated between the demihulls. These radiate toward the opposing demihull and interact with each other as they do, imposing more loads on the hulls. This causes the added mass coefficient and damping coefficient to be rather different from a monohull, so direct knowledge of the interaction is necessary for a study of catamaran motions, rather than interpolation from monohull data.

The previously mentioned Fig. 6.4 shows a wave system caused by the roll and heaving motion of monohull. Panel a shows the waves caused by the roll and heaving motion of a monohull on calm water, panel b shows the encounter waves athwart the craft side, and panel c shows craft motion in beam seas,

where

1. Wave caused by craft motion
2. Encounter wave athwart the craft side
3. Beam wave through craft
4. Reflective wave from craft

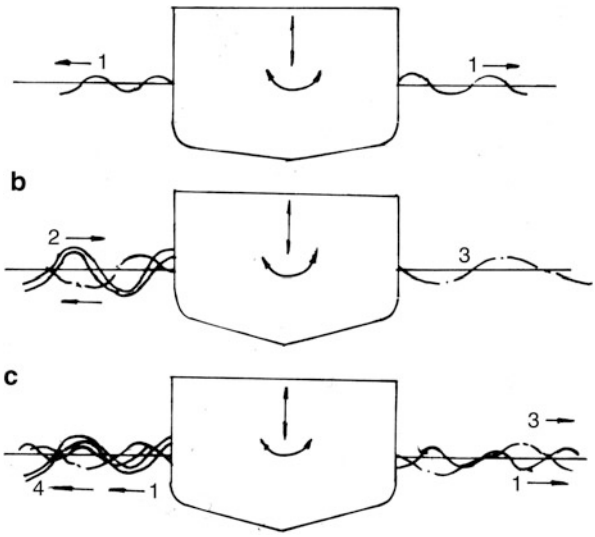

Fig. 6.4 Wave system caused by rolling and heaving of a monohull craft: (**a**) on calm water; (**b**) wave athwart the craft side; (**c**) craft motion in beam seas

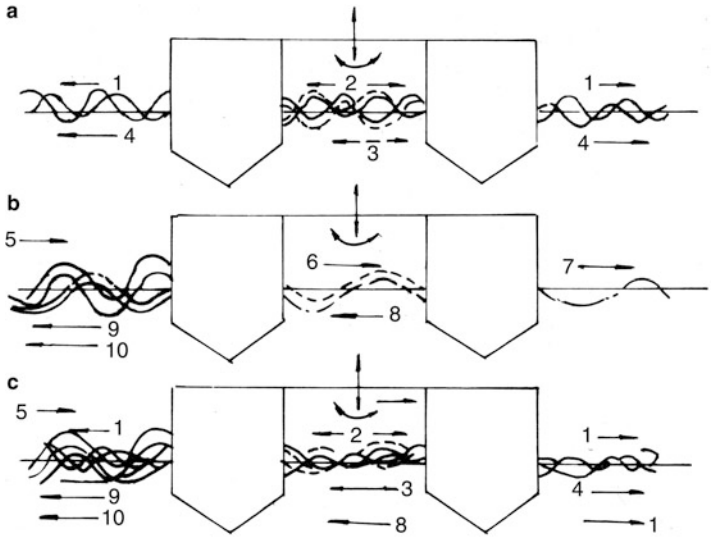

Fig. 6.5 Wave system caused by rolling and heaving motion of catamaran: (**a**) on calm water; (**b**) wave athwart the craft side; (**c**) craft motion in beam seas

Figure 6.5 shows a wave system caused by the roll and heaving motion of a catamaran and the encounter waves and generated waves mentioned earlier; in this case the internal wave generation between the hulls creates a more complex situation:

1. Wave caused by craft motion, outside demihulls
2. Wave caused by craft motion, between demihulls

3. Reflective wave of 2, between demihulls
4. Reflective wave of 1, outside demihulls
5. Wave athwart craft side
6. Wave athwart and across craft side and between demihulls
7. Wave across demihull
8. Reflective wave of 6
9. Reflective wave of 5
10. Reflective wave of 8 across demihull

It can be seen that the induced wave system of a catamaran is rather different from that of a monohull, and the resulting wave amplitude is related to the phase lag of incident and reflective waves. The phase lag is related to the hull separation rather than the roll damping coefficient.

The heave damping and catamaran water added mass are larger because of the two hulls and their separation, and the roll motion of a catamaran can therefore be considered in a similar way to a pair of demihulls in heaving motion. Nevertheless, owing to the internal wave generation and interaction when rolling, the damping and added mass coefficients of catamarans are rather different from the sum of a pair of hulls. This is why the test and theoretical data of both the water added mass and damping coefficient of a monohull cannot be applied directly to that of catamaran.

Another important characteristic of the motion of a catamaran in waves is the asymmetry of the perturbation forces and moments acting on each of the demihulls. The wave perturbation force acting on the first demihull is larger than the force on the second demihull due to the loss of energy when interacting with the first demihull.

Depending on the wave incident direction, incoming waves may impact on the first demihull and not on the second (for 90° beam seas) or partially on the bow area or stern area of the second hull (oblique head or stern seas), and the reflected waves will also radiate at the mirror angle to impact with the demihull. The wave system both inside and outside the catamaran demihulls is complex, to say the least, so the theoretical calculation of the motion of a catamaran represents a huge challenge. More recently, computer analysis using finite-element methods has advanced our understanding, but at present we remain heavily dependent on model testing and evaluation from full-scale trials.

Where does this get us just now? Well, we will continue here with our analytical approach to understanding the challenge. For the purposes of vessel design, it may be proposed that the internal waves within a catamaran demihull enclosure will have the following effects:

- The phase lag effect for generated internal waves may increase the effective damping for vessel roll motions, so the overall effect on motion amplitude is slight, though the oscillating forces applied to the hull surfaces on the inside of each demihull may increase somewhat, affecting the fatigue life of the hull structures.
- At oblique vessel headings, the reflected waves from the “far” demihull that do not impact on the near hull but are dispersed as they radiate represent a loss of

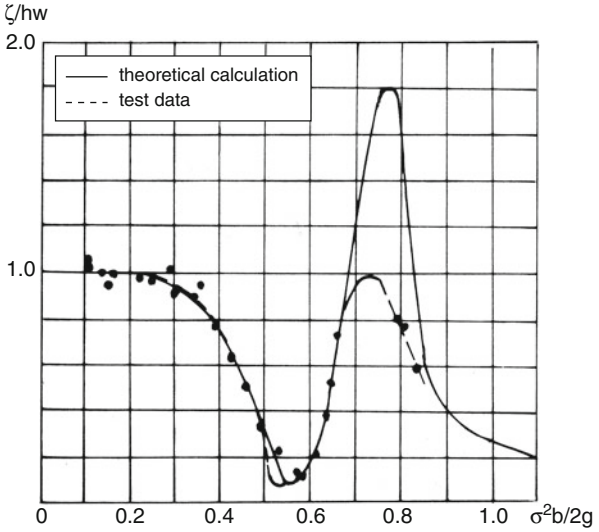

Fig. 6.6 Relative amplitude of heaving motion of catamaran model tested in Japan

energy that will contribute to the combined roll/pitch motion. Thus, analytical prediction of this combined motion may not be conservative.

- The speed of the vessel through the seaway will induce an angle of reflection on internally generated waves, which will further complicate the aforementioned two items, generally reducing the first effect and increasing the second effect. See the subsequent discussion in Sect. 6.4 for further thoughts on this topic.

Figure 6.6 shows the relative amplitude of the heaving motion of the catamaran models tested in Japan, showing both the analytical response prediction and model test results. In the diagram the parameters are heaving amplitude, ς, wave height, h_w, natural frequency of roll motion, σ, and demihull beam, b. It can be seen that the relative amplitude of heaving will be minimized when $\sigma^2 b/2g = 0.6$ owing to favorable wave interference between demihulls.

This suggests that hull separation should be fixed not only in terms of drag optimization and in consideration of the general arrangement but also in terms of favorable wave interference between the demihulls to minimize wave impact forces and induced motions.

The catamaran roll natural frequency can be expressed approximately as

$$\sigma = \sqrt{\frac{h}{kk_d}}, \tag{6.2}$$

where

h Initial transverse metacentric height;

k Coefficient in terms of catamaran transverse mass distribution considering also the water added mass; in general, $k = 1.3$–1.5 in the case of motion away from resonance;

k_d Distance between catamaran and demihull longitudinal center planes.

6.2.4 *Effect of Craft Speed and Control Surfaces for Improving Seakeeping Quality*

Figure 6.7 [4] shows a comparison of the energy spectrum and roll response with and without control surfaces. Figure 6.7a shows the comparison of a roll energy spectrum, and one can see that the energy spectrum for the high-speed catamaran with control surfaces would be reduced compared with that without such motion controls, particularly close to resonance frequency. Figure 6.7b shows the roll frequency response curves of three types of catamaran (the leading particulars and hull sections can be found in Chap. 5). One can see that the roll response of a catamaran with hard chine is smallest, even without trim tabs (flap) and spray strips.

Installing automated stabilizing control surfaces or even some type of fixed surface can nevertheless improve the seakeeping quality of a high-speed catamaran without going to a full planing configuration. Antiroll fins installed at the internal sidewall can reduce the roll motion and so improve passenger comfort.

Figure 6.8a [4] shows the pitch response curves of a round bilge catamaran model at different ratios of ship to incident wave length in regular head waves for different Fr_L, where λ represents wave length and α wave steepness. It is found that faster speeds generate less pitching due to the increased damping coefficient of pitching motion. The results are similar to those shown in Fig. 6.2 for different wave headings as well as Fr_L values.

Figure 6.8b shows the heave response curves of the same model in the same operating condition, and with similar results, that is, higher speed gives less heave amplitude response.

Figure 6.9 shows the acceleration frequency response curve for a catamaran with round bilge body sections. The maximum acceleration amplitude of a catamaran increases with speed owing to an increase in encounter frequency, similar to conventional ships.

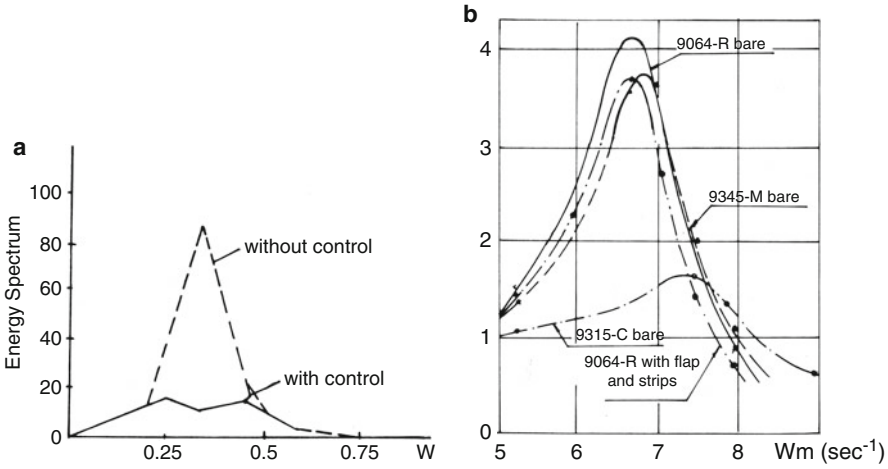

Fig. 6.7 (**a**) Comparison of roll energy spectrum; (**b**) rolling frequency response curves

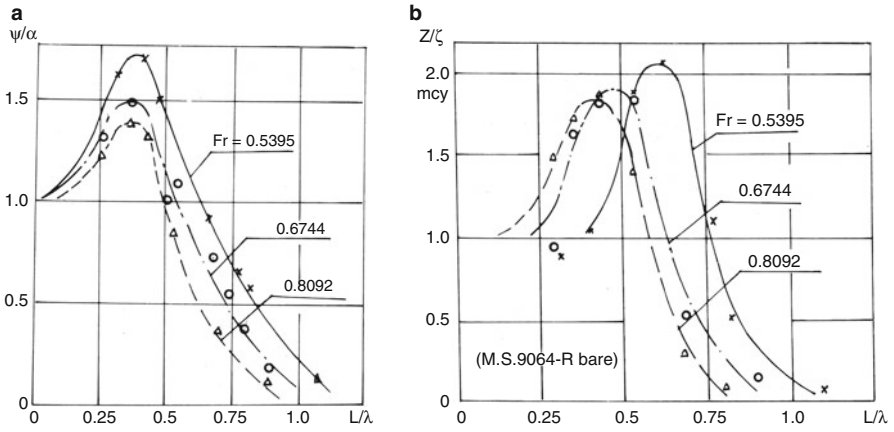

Fig. 6.8 (**a**) Pitching frequency response curve; (**b**) heaving frequency response curves

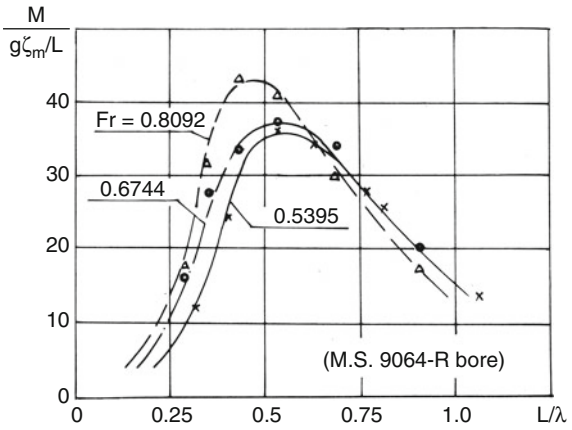

Fig. 6.9 Acceleration frequency response curves

Figure 6.10 shows the frequency response curves for incremental resistance of a catamaran in head waves. It can be seen that added resistance increases with speed, and it seems that some devices for improving craft motion, such as flaps and spray strips, do not decrease the catamaran added resistance.

6.3 Differential Equation of Rolling Motion for Catamarans

6.3.1 Introduction

The rapid roll motion of a catamaran and coupled longitudinal and transverse torsional motion in oblique seas can cause high vertical acceleration, making crew

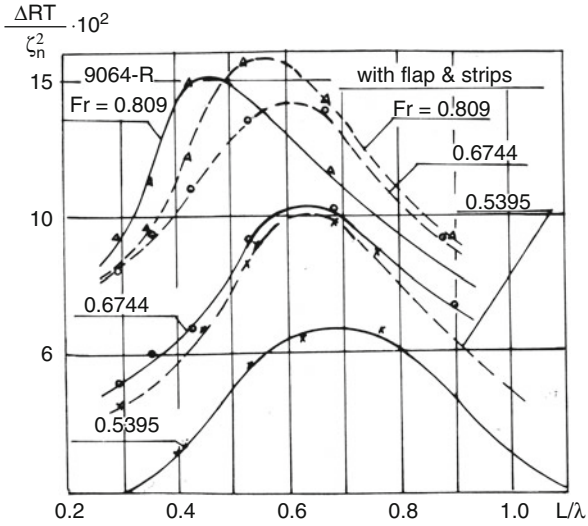

Fig. 6.10 Increment in resistance frequency response curves in head waves

and passengers uncomfortable and even cause dangerous conditions for the vessel structure in rough seas. This is due to the fact that catamarans have a high transverse metacentric height and stiff static transverse stability. It is therefore important to carry out a dynamic analysis of a catamaran operating in waves so as to minimize motions to the extent possible.

The analysis of a catamaran operating in waves is, however, rather complicated owing to wave interference between the demihulls, the influence of demihulls on wave disturbance forces, and moments acting on the catamaran, as well as the roll damping and water added mass coefficient of a catamaran, which are rather different from those of conventional monohull ships.

To simplify the issue and obtain an approximate solution for the dynamic analysis of a catamaran operating in waves, the aforementioned issues can be resolved using the following procedure:

- Use general formulas and equations to establish the transverse differential equation of roll motion;
- Neglect the effect of demihulls on wave profiles crossing two demihulls in beam seas, that is, comply with Froude–Krylov assumptions, irrespective of the significant influence of demihulls on the wave profile aft of the demihulls, as discussed earlier;
- Neglect craft speed, and assume that the craft is in static condition;
- Use model test data and theoretical estimations for water added mass and damping coefficients of conventional monohull craft applied to catamarans with a similar demihull form, however using an approximate correction with the aid of empirical methods;
- Neglect the coupling of both roll and heaving motion of catamarans in waves.

In short, the aim of such a dynamic analysis is to carry out calculations for the motion parameters, for instance, maximum roll angle, acceleration, and roll natural period, of a catamaran in waves for the preliminary overall design of a catamaran; the aim is not to conduct an exhaustive investigation of the theoretical analysis of catamaran motions in waves.

6.3.2 *Simplified Differential Equation of Catamaran Roll Motion in Waves and Its Solutions [3]*

The roll motion of a *conventional monohull* in regular waves can be expressed as a linear differential equation of second order as follows:

$$(I_x + \Delta I_x)\ddot{\theta} + 2N_\theta\dot{\theta} + Dh\theta = \alpha_m\left[\left(Dh - \Delta I_x\omega^2\right)\sin\omega t + 2N_\theta\omega\cos\omega t\right], \quad (6.3)$$

Where:

I_x	Moment of inertia of mass through CG with respect to x-axis of ship;
ΔI_x	Moment of inertia of added mass of ship;
$\theta, \dot{\theta}, \ddot{\theta}$	Roll angle, angular velocity, and acceleration respectively of ship;
$2N_\theta$	Proportional constant of damping moment with angular velocity;
D, h	Displacement and initial transverse metacentric height;
$\alpha_m = \chi_\theta kr$	Effective wave steepness, where χ_θ is the attenuation coefficient for the roll angle;
$k = 2\pi/\lambda$	Wave number;
r	Half wave height;
λ	Wave length;
$\omega = 2\pi/\tau$	Circular frequency of waves, where τ is the wave period.

The first term on the left-hand side of Eq. (6.3) represents the moment of inertia of the ship and its added mass, the second term represents the damping moment, and third term is the restoring moment. The various terms on the right-hand side represent the disturbance moment, that is, restoring, damping, and added mass moment, caused by waves.

The differential equation of a *catamaran* in regular beam waves can also be expressed as

$$\begin{aligned}&(I_x + \Delta I_x)\ddot{\theta} + 2N_\theta\dot{\theta} + Dh\theta \\ &\quad = \chi_\theta kr[(Dh - \Delta I_x\omega^2)\sin(kk_d - \omega t) + 2N_\theta\omega\cos(kk_d - \omega t)].\end{aligned} \quad (6.4)$$

The first term on the left-hand side of Eq. (6.4) represents the moment of inertia of the craft itself and added mass of water, the second term is the damping moment, and the third term is the restoring moment of the catamaran. The terms on the right-hand side are the perturbation moments acting on the catamaran by the waves,where:

I_x Moment of inertia of mass of catamaran;
ΔI_x Moment of inertia of added mass of water;
$\theta, \dot{\theta}, \ddot{\theta}$, Roll angle, angular velocity of roll, angular acceleration velocity of roll of catamaran, respectively;
χ_θ Attenuation coefficient of roll angle;
k Wave number, $k = 2\pi/\lambda_\omega$;
k_d Distance between longitudinal centerlines of catamaran and demihull;
ω Circular frequency of wave, $\omega = 2\pi/\tau$, where τ is the wave period;
r Wave amplitude;
h Transverse metacentric height of catamaran.

To solve the foregoing differential equation, both the catamaran added mass of water and damping moment have to be derived for the demihulls, and we must also consider the interference effect of the wave system between demihulls on the response coefficient of the catamaran.

After reorganization Eq. (6.4) can be written

$$\ddot{\theta} + \frac{2N_\theta}{I_x + \lambda_{44}}\dot{\theta} + \frac{Dh}{I_x + \lambda_{44}}\theta = \chi kr \frac{\sin kk_d}{kk_d}\left[\begin{array}{l} \dfrac{Dh}{I_x + \lambda_{44}}\left(fkk_d - q_\lambda \dfrac{\lambda_\varsigma k_d^2 \omega^2}{Dh}\right)(\cos\omega t - d\sin\omega t) + \\ 2q_\nu \dfrac{\nu_\varsigma k_d^2}{I_x + \lambda_{44}}\omega(d\cos\omega t + \sin\omega t) \end{array}\right], \tag{6.5}$$

where

λ_{44} Moment of inertia of water added mass of catamaran, which can be expressed as

$$\lambda_{44} = 2\left(\lambda_\theta + \lambda_\varsigma k_d^2\right),$$

where $N_\theta = \gamma_\theta + \gamma_\varsigma k_d^2$, the damping moment coefficient,

and it is assumed that

$$f = \frac{\chi_\theta}{\chi_\varsigma}, \quad q_\lambda = 1 + \frac{\lambda_\theta}{\lambda_\varsigma k_d^2}, \quad d = \frac{\cos kk_d}{\sin kk_d}, \quad q_\nu = 1 + \frac{\nu_\theta}{\nu_\varsigma k_d^2}, \tag{6.6}$$

where

λ_θ Inertia moment of added mass of demihull about x-axis of demihull;
ν_θ Roll damping coefficient of demihull;
ν_ς Heaving damping coefficient of demihull;
$\lambda_\vartheta, \lambda_\varsigma$ ZWater added mass of demihull about demihull x-axis and water added mass of demihull along z-axis; in general we take $q_\lambda = 1$.

Some notations are also used for Eq. (6.5) as follows:

ν_c Roll attenuation coefficient, $\nu_c = \frac{N_\theta}{I_x+\lambda_{44}}$;

ω_r Natural roll frequency, $\omega_r = \sqrt{\frac{Dh}{I_x+\lambda_{44}}}$;

ν' Relative roll attenuation coefficient, $\nu' = \dfrac{\nu k_d^2}{(I_x+\lambda_{44})\omega_r}$;

ω_h Natural heaving frequency, $\omega_h = \sqrt{\frac{2\gamma S_c}{D/g+2\lambda_\varsigma}}$;

S_c Area of waterplane;

ε Water added mass coefficient, $\varepsilon = \frac{2\lambda_\varsigma}{D/g+2\lambda_\varsigma}$;

p_c Relative increment of initial transverse metacentric height, $p_c = \dfrac{k_d^2 S_c}{V \cdot h}$;

V Volumetric displacement of catamaran.

Then (6.5) can be rewritten as

$$\ddot{\theta} + 2\nu_c\dot{\theta} + \omega_r^2\theta = \chi_\varsigma kr\omega_r^2 \frac{\sin kk_d}{kk_d} \times \sqrt{(1+d^2)\left[\left(fkk_d - q_\lambda p_c \varepsilon \frac{\omega^2}{\omega_h^2}\right) + 4q_\nu \nu'^2 \left(\frac{\omega}{\omega_r}\right)^2\right]} \times \sin(\omega t + \vartheta), \tag{6.7}$$

where

ω Wave frequency,

ϑ Phase angle.

Then the roll angle can be solved as

$$\theta = \chi_\varsigma kr \frac{\sin kk_d}{kk_d} \sqrt{\frac{\left[\left(fkk_d - q_\lambda p\varepsilon\frac{\omega^2}{\omega_h^2}\right) + 4q_\nu^2\nu'^2\left(\frac{\omega}{\omega_r}\right)^2\right](1+d^2)}{\left[1-\left(\frac{\omega}{\omega_r}\right)^2\right]^2 + 4\frac{\nu_c^2}{\omega_r^2}\left(\frac{\omega}{\omega_r}\right)^2}} \times \sin(\omega t + \beta), \tag{6.8}$$

where β is the total phase angle of the forced oscillation.

After calculation, and making the assumptions that $q_\nu = 1.15$ and $q_\lambda = 1$ for a conventional catamaran, the maximum roll angle θ_m and total phase angle β can be written

$$\theta_m = \chi kr \frac{\sin kk_d}{kk_d} \sqrt{\frac{\left[\left(fkk_d - p_c\varepsilon\frac{\omega^2}{\omega_h^2}\right)^2 + 5.3\nu'^2\left(\frac{\omega}{\omega_r}\right)^2\right](1+d^2)}{\left[1-\left(\frac{\omega}{\omega_r}\right)^2\right]^2 + 4\frac{\nu_c^2}{\omega_r^2}\left(\frac{\omega}{\omega_r}\right)^2}}, \tag{6.9}$$

$$\sin\beta = \frac{\left(\omega_r^2-\omega^2\right)\left[\left(fkk_d - p\varepsilon\frac{\omega^2}{\omega_r^2}\right) + 2.3\nu'^2\frac{\omega}{\omega_r}d\right] - 2\nu_c\omega\left[2.3\nu'\frac{\omega}{\omega_r} - \left(fkk_d - p\varepsilon\frac{\omega^2}{\omega_h^2}\right)d\right]}{\sqrt{\left(1+d^2\right)\left[\left(\omega_r^2-\omega^2\right)^2 + 4\nu_c^2\omega^2\right]\left[\left(fkk_d - p\varepsilon\frac{\omega^2}{\omega_h^2}\right) + 5.3\nu'^2\left(\frac{\omega}{\omega_r}\right)^2\right]}}.$$

Then the roll angle at every frequency can be obtained using the preceding equations. The key issue is how to obtain the various coefficients and parameters in the equations.

In the calculation of maximum roll angle, the wave frequency can be assumed to be the same as the roll natural frequency of the catamaran: $\omega = \omega_r = \sqrt{\frac{Dh}{I_x+\lambda_{44}}}$.

The wave length can be written

$$\lambda_w = 1.56T_w^2, \text{where } T_w = \frac{2\pi}{\omega}.$$

The wave height can be written

$$h_w = 0.17\,\lambda_w^{\frac{3}{4}}.$$

Then the wave amplitude can be written

$$r = 0.5\,h_w.$$

When calculating the catamaran roll motion in irregular waves, the wave lengths for analysis can be taken using the requirements of ship classification rules, and the wave frequency can be expressed as

$$\omega = \frac{2\pi}{0.8\sqrt{\lambda_w}}.$$

The catamaran maximum relative linear acceleration, $\bar{A}_m$, which is a very important factor affecting passenger comfort, can be written as follows:

$$\bar{A}_m = A_m/g = \frac{1}{T_c^2}\cdot\frac{2\pi^2}{g}\cdot B_p\cdot\theta_m, \tag{6.10}$$

where

θ_m Maximum roll angle, obtained from Eq. (6.9);
B_p Width of upper deck, where passenger accommodations are located;
T_c Calculated roll period in waves, which can be written

$$T_c = \beta_c \frac{2\pi}{\omega_r}, \tag{6.11}$$

where

β_c Correction coefficient, always larger than 1. This is because the forced roll period is always larger than the wave period, to some extent based on full-scale observations, which can be expressed as

$$\beta_c = 1 + 0.15 \frac{b}{T} \bar{k}^{3/2}, \tag{6.12}$$

where

$\bar{k} = k/b$;
b/T Beam/draft ratio of demihull.

6.3.3 Determination of Catamaran Water Added Mass [5]

To calculate the maximum roll angle, maximum vertical acceleration, and roll characteristics of a catamaran in waves, we have to determine the water added mass and other coefficients for a catamaran. We introduce some empirical formulas here as a starting point with the intent that more precise evaluation can be completed once the final demihull lines have been chosen and physical testing can be used to verify these initial estimates and comparison with similar vessel data.

The water added mass of a demihull in the vertical direction λ_{33}^d can be written

$$\lambda_{33}^d = 0.85 \frac{\pi}{4} \cdot \frac{\gamma}{g} L b^2 \frac{\alpha^2}{1+\alpha}, \tag{6.13}$$

where

L, b Length and beam of demihull;
α Coefficient of waterplane.

Note that in the equations in this section the subscripts carry the following meanings:

11 = water added mass of body on x-axis, 22 on y-axis, 33 on z-axis;
44 = moment of inertia of added mass on x-axis, 55 on y-axis, 66 on z-axis.

To predict the interference effect of twin demihulls on wave making and, consequently, on the catamaran water added mass, the additional added mass between the hulls is assumed to be contained by an ellipse horizontally with maximum breadth at amidships and a parabola in the vertical plane, which can be written as follows:

$$\Delta\lambda_{33} = 0.21\rho\pi TL\frac{b^3}{k_d^2}\cdot\frac{\alpha^3}{(1+\alpha)(1+2\alpha)}, \tag{6.14}$$

where

L, b, T Length, beam, and draft of demihull;
α Waterplane coefficient of demihull;
ρ Water density.

Then the total added mass of water of the catamaran can be written

$$\lambda_{33} = 2\left(\lambda_{33}^d + \Delta\lambda_{33}\right) \tag{6.15}$$

or as follows:

Considering the wave interference between the demihulls, the heaving added mass of a demihull can be written

$$\lambda_\varsigma = 1.6\lambda_{33}^d. \tag{6.16}$$

Then the moment of inertia of the total catamaran caused by the added mass of the demihulls, considering the demihulls x-axes are rotated to some angle during craft roll, can be written briefly as

$$\lambda_{44} = 2.5\lambda_\varsigma k_d^2, \tag{6.17}$$

where k_d is the demihull spacing from its centerline to the catamaran's longitudinal centerline.

6.3.4 Mass Moment of Inertia of Catamaran Mass

The moment of inertia of each demihull mass around the x-axis of the demihull can be written

$$I_{xd} = \frac{D}{2g}\left(\frac{b^2\alpha^2}{11.4\delta} + \frac{H^2}{12}\right), \tag{6.18}$$

where

H Depth of demihull;
D Displacement of demihull;

δ Block coefficient;
b Demihull breadth;
α Waterplane area coefficient.

The moment of inertia of the catamaran mass (sum of demihulls and spacing) can be written

$$I_x = \frac{D}{12g}\left(B^2 + 4z_g^2\right), \tag{6.19}$$

where

B Catamaran breadth;
z_g Center of gravity height above baseline.

6.3.5 *Damping Coefficient*

The damping moment is proportional to the angular velocity of roll, from Eq. (6.6), and can be expressed as

$$N_\theta = \nu_\theta + \nu_\varsigma k_d^2 \qquad (\text{kg} - \text{m} - \text{s}), \tag{6.20}$$

where

ν_θ Damping coefficient for angular oscillation of demihull, and can expressed as

$$\nu_\theta = 0.1\sqrt{\frac{D}{2}h\left(I_x^d + \lambda_{44}^d\right)} \qquad (\text{kg} - \text{m} - \text{s}), \tag{6.21}$$

where

I_x^d Moment of inertia of demihull displacement about demihull x-axis:

$$I_x^d = \frac{D}{2g}\left(\frac{b^2\alpha^2}{11.4\delta} + \frac{H^2}{12}\right) \tag{6.22}$$

h Depth of demihull at amidships, m;

λ_{44}^d Moment of inertia caused by water added mass of demihulls, which can be expressed as

$$\lambda_{44}^d = 2\lambda_{33}^d k'^2 \qquad (\text{kg} - \text{m} - \text{s2}), \tag{6.23}$$

where

k' Radius of moment of inertia of added mass about x-axis of demihull; in general, it can be taken as $b/4$, where b is the beam of the demihull;

λ_{33}^{d} Can be obtained from Eq. (6.14).

Note the foregoing comparison with Eq. (6.23) for demihull added mass moment of inertia to Eq. (6.17) for the vessel added mass moment of inertia.

The damping coefficient on the vertical oscillation for each demihull can be determined by the Haskind equation:

$$\nu_{\varsigma} = \frac{1}{2}\rho\frac{\omega^3}{g}S_d^2 x^2\left(\frac{T}{\lambda_w}\right)\chi\left(\frac{L}{\lambda_w}\right) \qquad (\text{kg} - \text{s/m}), \tag{6.24}$$

where

$\rho = \gamma/g$ Density of water, kg · s^2/m^4;

ω Circular frequency of wave, 1/s;

g Gravity acceleration, m/s^2;

$\chi^2\left(\frac{T}{\lambda_w}\right)$ Coefficient, found in Fig. 6.11 on next page, that is a function of $\chi = \delta/\alpha$, and T/λ_w;

λ_w Wave length, m;

$\chi\left(\frac{L}{\lambda_w}\right)$ Coefficient that can be found in Fig. 6.12, function of ship wave length ratio and waterplane coefficient.

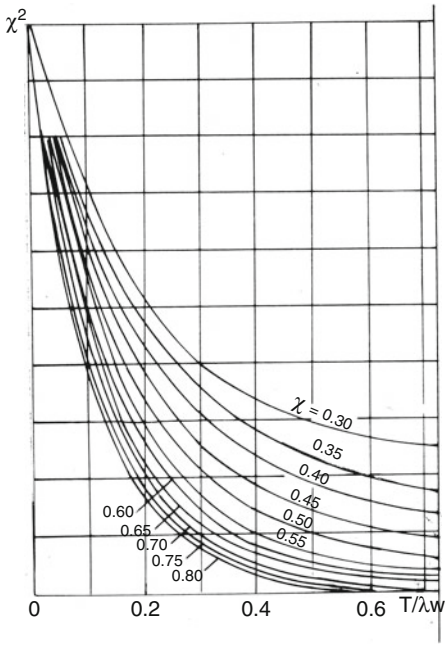

Fig. 6.11 $\chi^2 = f(\chi, T/\lambda_w)$

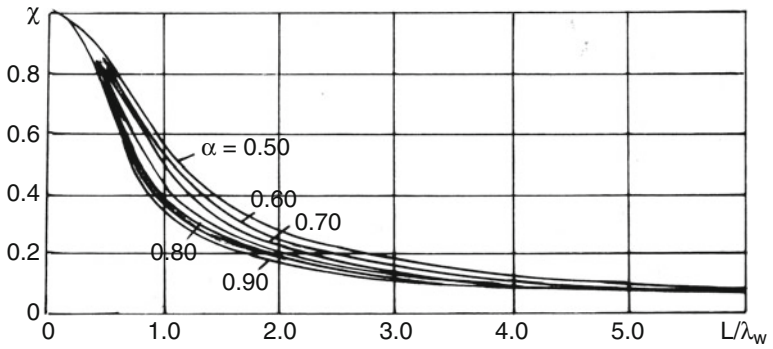

Fig. 6.12 $\chi(L/\lambda_w) = f(\alpha, L/\lambda_w)$

6.3.6 *Influence Coefficients of Catamaran Cross-Section Shape on Heave and Roll Motions*

- *Influence coefficient of catamaran cross-section shape on heaving* χ_ς

Similar to the heaving of a conventional ship in waves, the influence coefficient of cross-section form (beam and draft) on vessel roll motion must be considered, and for catamarans the additional influence coefficient caused by the wave interference between demihulls should be considered as well, so the final consideration of such an influence should be written as follows:

$$\chi_\varsigma = \chi_{\varsigma b}\chi_c\chi^0_{\varsigma T}, \tag{6.25}$$

where

χ_ς Influence coefficient of both draft and beam of demihull;
$\chi_{\varsigma b}$ Influence coefficient of beam of demihull; can be written

$$\chi_{\varsigma b} = 1 - 1.73\alpha\left[\frac{b\left(1+\frac{n}{n-k}\right)}{\lambda_w}\right]^2, \tag{6.26}$$

where

$\bar{k} = k/b$;
$n = 1 + 2.5\bar{k}^m$;
$m = 2.5$ for catamaran at speed lower than $\mathrm{Fr_L} = 0.2$–0.4;
$m = 1.5$ for catamaran at speed higher than critical speed and $\mathrm{Fr_L} = 0.6$–0.75;
χ_c Influence factor of interference of demihulls, a function of hull separation, can be written

$$\chi_c = 1 + \frac{0.5}{0.5 + 0.75\sqrt{k}}; \tag{6.27}$$

$\chi^0_{\varsigma T}$ Influence coefficient of draft of demihull, but not considering interference of demihull;

$$\chi^0_{\varsigma T} = 1 + \chi kT + \frac{\chi}{2(2-\chi)}(kT)^2 - \frac{\chi}{6(3-2\chi)}(kT)^3, \tag{6.28}$$

where

$\chi = \delta/\alpha$;
δ Block coefficient of demihull, and α is waterplane area coefficient.

To simplify the calculation, some graphs for the calculation of the coefficients were prepared and are presented below, where

$\chi^0_{\varsigma T}$ can be obtained in Fig. 6.13,

χ_c can be obtained in Fig. 6.14,

$\chi_{\varsigma b}$ can be obtained in Fig. 6.15 for a catamaran at a speed higher than the critical speed, $\mathrm{Fr_L} = 0.6$–0.75.

- *Influence coefficient of catamaran cross-section shape on roll* χ_θ

Similar to the calculation of the influence coefficient for heaving motion, the influence coefficient of the catamaran beam and draft on roll, χ_θ, can be written

$$\chi_\theta = \chi_{\theta B}\chi_{\theta T}, \tag{6.29}$$

$$\chi_{\theta T} = \chi_c\chi^0_{\theta T}, \tag{6.30}$$

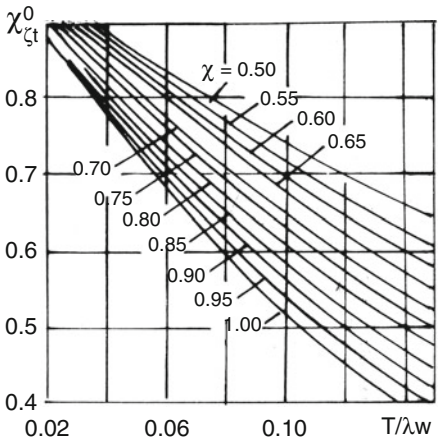

Fig. 6.13 $\chi^0_{\varsigma T} = f(T/\lambda_w, \chi)$

Fig. 6.14 $\chi_c = f(\bar{k})$

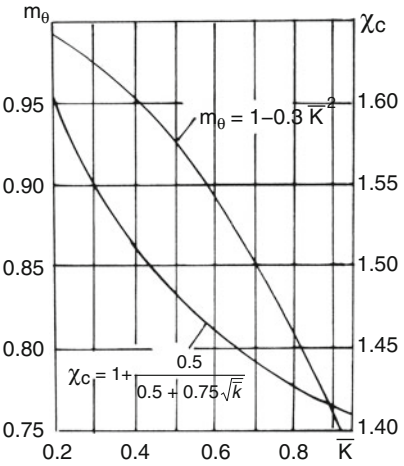

Fig. 6.15 $\chi_{\varsigma b} = f(\bar{k}, \alpha b^2/\lambda_w^2)$

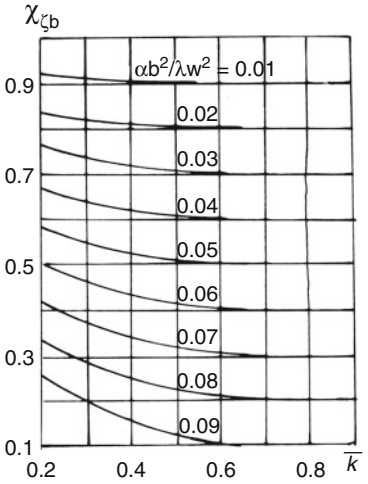

$$\chi^0_{\theta T} = 1 - \frac{6\chi^3}{(1+\chi)(1+2\chi)}kT + \frac{1.5\chi^3}{(2-\chi)(2+\chi)}(kT)^2 - \frac{\chi^3}{3(3-2\chi)(3-\chi)}(kT)^3, \tag{6.31}$$

where

Fig. 6.16 $\chi^0_{\theta T} = f(\chi, T/\lambda_w)$

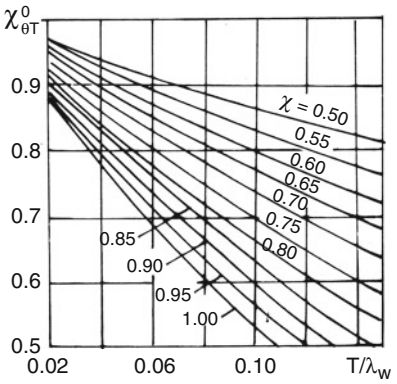

$\chi = \delta/\alpha$;
$k = 2\pi/\lambda_w$
$\chi^0_{\theta T}$ can be obtained in Fig. 6.16, and χ_c can be obtained in Fig. 6.14;

$$\chi_{\theta B} = m_\theta \left[1 - \sqrt{\alpha}\left(\frac{B}{\lambda_w}\right)^2\right], \tag{6.32}$$

where

B Beam of catamaran, m;

$$m_\theta = 1 - 0.3\bar{k}^2; \tag{6.33}$$

$\chi^0_{\theta T}, m_\theta$ can be obtained in Figs. 6.16 and 6.14, upper curve in diagram, respectively.

6.4 Differential Equation for Coupled Pitching and Heaving Motion

6.4.1 Introduction

The forces acting on a high-speed catamaran in waves, and thus the differential equation of motion and its solution, are similar to that for conventional displacement ships. However, there are some special features concerning the longitudinal motion of a catamaran in waves as follows:

- The interference effect both on water added mass and damping coefficient have to be considered during the calculation of longitudinal motion of a catamaran in waves;
- Since the body plane lines of high-speed catamarans generally have a semiplaning form with spray rails or hard chine configuration, both water added mass and damping coefficients are different from those of conventional displacement monohull vessels with round bilge form, and one cannot use such coefficients from conventional monohulls for a high-speed catamaran.

In this section we will introduce the differential equation of longitudinal motion of a catamaran in waves and its approximate solution considering wave interference between the demihulls of the catamaran and taking form into account.

The features of modern high-speed catamarans are high speed ($Fr_L = 0.7–1.0$), high slenderness or length displacement ratio of the demihull (>8.00), small entrance angle of the bow waterlines, and large demihull separation ($k/b = 2.5–5.0$). In general, therefore, the interaction of the divergent waves made by the demihull would be behind the stern of such craft, and a transom would be clear of water.

Reference [6] shows figures comparing the measured and calculated data of the largest of the models by Wellicome et al., and it was concluded that it could not be demonstrated that the computed or measured data showed a strong variation of maximum response amplitude operators of both pitching and heaving motion of a catamaran in head seas with varied hull spacing, including a comparison with a monohull equivalent to the complete catamaran or to the infinite spacing case.

Then Michael R. Davis [7] concluded that hydrodynamic interaction between the hulls was very small and that head sea response of a twin hull vessel was very similar to that of a monohull of the same geometry. For these reasons, the interference of the demihulls may be neglected, and one can use the differential equations of coupled pitching and heaving motion of a monohull craft that are equivalent to the catamaran demihull. This was validated by both theoretical calculations and experimental investigations in reference [8]

6.4.2 *Differential Equation of Motion for Catamaran Coupled Pitching and Heaving*

The differential equation of motion can be described as follows [9–11]:

$$(m + a_{33})\ddot{z} + b_{33}\dot{z} + c_{33}z + a_{35}\ddot{\psi} + b_{35}\dot{\psi} + C_{35}\psi = F_{ZC}\cos\varpi_e t + F_{zs}\sin\varpi_e t, \tag{6.34}$$

$$\left(I_{yy} + a_{55}\right)\ddot{\psi} + b_{55}\dot{\psi} + c_{55}\psi + a_{53}\ddot{z} + b_{53}\dot{z} + c_{53}z = M_{\psi c}\cos\omega_e t + M_{\psi S}\sin\omega_e t,$$

where

M Half of craft mass (henceforth also represents the demihull);
A_{33} Heaving added mass;
B_{33} Heaving damping coefficient;
C_{33} Heaving restoring force coefficient;
$\ddot{z}, \dot{z}, z$ Heaving acceleration, velocity, and displacement;
$\ddot{\psi}, \dot{\psi}, \psi$ Pitching acceleration, velocity, and displacement;
A_{35} Heaving added mass due to pitching;
B_{35} Heaving damping coefficient due to pitching;
C_{35} Heaving restoring force due to pitching;
ω_e Encounter frequency;
T Time;
F_{zc}, F_{zs} Sin and cos parts of wave heaving perturbation force;
I_{yy} Moment inertia of half craft about y-axis via the CG;
A_{55}, b_{55}, c_{55} Pitching added mass, damping moment, and restoring moment coefficients;
A_{53}, b_{53}, c_{53} Static moment coefficients of added mass, damping, and restoring forces;
$M_{\psi c}$, $M_{\psi s}$ Cos and sin parts of wave pitching perturbation moments.

Meanwhile Eq. (6.34) for forces and moments can also be written in simple form:

$$\begin{aligned} m\ddot{z} &= F, \\ I_{yy}\ddot{\psi} &= M, \end{aligned} \tag{6.35}$$

where

F Vertical force acting on craft, including inertia, damping, and restoring forces;
M Moments acting on craft about GY-axis;

Then, considering the fluid motion about the craft in two dimensions during craft motion, the force and moments can be determined using the strip method to integrate along the vessel length, L, as

$$\begin{aligned} F &= \int_L F(x)dx, \\ M &= -\int_L F(x)xdx, \end{aligned} \tag{6.36}$$

where x is the coordinate location along the craft length L, using the right-hand rule for GXYZ coordinates, and positive M is for bow down pitching.

Then the force at the demihull transverse section at x can be assembled from the sum of static fluid, damping, and inertia forces, due to heaving, pitching, and vessel forward speed, as well as wave perturbation, so that we have

$$\begin{aligned} F(x) &= -2\rho g y_w\left(z - x\psi - \varsigma_x^{\cdot}\right) - N_Z(x)\left(\dot{z} - x\dot{\psi} + U\psi - \varsigma_x^{\cdot}\right) \\ &\quad - \frac{d}{dt}\left[m_z(x)\left(\dot{z} - x\dot{\psi} + U\psi - \varsigma_x^{\cdot}\right)\right] = -2\rho g y_w\left(z - x\psi - \varsigma_x^{\cdot}\right) \\ &\quad - N_z(x)\left(\dot{z} - x\dot{\psi} + U\psi - \varsigma_x^{\cdot}\right) - m_z(x)\left(\ddot{z} - x\ddot{\psi} + 2U\dot{\psi} - \varsigma_x^{\cdot}\right) \\ &\quad + U\frac{dm_z(x)}{dx}\left(\dot{z} - x\dot{\psi} + U\psi - \varsigma_x^{\cdot}\right), \end{aligned} \tag{6.37}$$

where

U	Ship speed; note that from the equation, one can see that the damping coefficient increases rapidly with an increase in ship speed, so as to decrease both heaving and pitching displacement;
Y_w	Half-width of waterline;
$N_z(x)$	Heave damping coefficient at x transverse section;
$M_z(x)$	Added mass at x transverse section;
$\varsigma_x^{\cdot}$	Effective wave ordinate at x section, considered "Smith" effectiveness.

After inserting Eqs. (6.36) and (6.37) into Eq. (6.35) and sorting out, then comparing this with Eq. (6.34), we obtain the various coefficients in the differential equation, as follows:

$$a_{33} = \int_L m_z(x)dx; \qquad a_{53} = -\int_L m_z(x)xdx;$$

$$b_{33} = \int_L \left[N_z(x) - U\frac{dm_z(x)}{dx}\right]dx; \qquad b_{53} = -\int_L \left[N_z(x)x - Ux\frac{dm_z(x)}{dx}\right]dx;$$

$$c_{33} = 2\rho g\int_L y_w dx; \qquad c_{53} = -2\rho g\int_L y_w xdx;$$

$$a_{35} = -\int_L m_z(x)xdx - \frac{U}{\omega_e^2}\int_L \left[N_z(x) - U\frac{dm_z(x)}{dx}\right]dx;$$

$$b_{35} = -\int_L \left[N_z(x)x - 2m_z(x)U - Ux\frac{dm_z(x)}{dx}\right]dx;$$

$$c_{35} = -2\rho g\int_L y_w xdx;$$

$$a_{55} = \int_L m_z(x)x^2dx - \frac{U}{\omega_e^2}\int_L \left[N_z(x)x - Ux\frac{dm_z(x)}{dx}\right]dx;$$

$$b_{55} = \int_L \left[N_z(x)x^2 - 2Um_z(x)x - Ux^2\frac{dm_z(x)}{dx}\right]dx;$$

$$c_{55} = 2\rho g\int_L y_w x^2 dx.$$

The cos and sin parts of the wave perturbation forces and moments can be expressed as in Eq. (6.38) below:

$$\left(\frac{F_{za}}{\zeta_a}\right)^{\cos}_{\sin}\varepsilon_{F_\zeta} = 2\rho g\int_L y_w e^{-kT\cdot\,{}^{\cos}_{\sin}}kxdx \mp \int_L \left[N_z(x) - U\frac{dm_z(x)}{dx}\right]e^{-kT\cdot\,{}^{\sin}_{\cos}}kxdx$$
$$-\omega^2\int_L m_z(x)e^{-kT\cdot\,{}^{\cos}_{\sin}}kxdx;$$

$$\left(\frac{M_{\psi a}}{\zeta_a}\right)^{\cos}_{\sin}\varepsilon_{M\zeta} = -2\rho g\int_L y_w x e^{-kT\cdot\,{}^{\cos}_{\sin}}kxdx \pm \omega\int_L \left[N_z(x) - U\frac{dm_z(x)}{dx}\right]xe^{-kT\cdot\,{}^{\sin}_{\cos}}kxdx$$
$$+\omega^2\int_L m_z(x)xe^{-kT\cdot kT\,{}^{\cos}_{\sin}}kxdx, \tag{6.38}$$

where

F_{za} Amplitude of perturbation force due to waves;
$\varepsilon_{F\zeta}$ Phase angle of perturbation force with waves;
$M_{\psi a}$ Amplitude of perturbation moment due to waves;
$\varepsilon_{M\zeta}$ Phase angle between perturbation moment and waves.

$$F_{za} = \sqrt{F_{zc}^2 + F_{zs}^2},$$

Then (6.39)

$$M_{\psi a} = \sqrt{M_{\psi c}^2 + M_{\psi s}^2}.$$

Then the special solution of Eq. (6.34) for heave and pitch is

$$z = z_c \cos \omega_e t - z_s \sin \omega_e t = z_a \cos(\omega_e t + \varepsilon_{z\zeta}),$$
$$\psi = \psi_c \cos \omega_e t - \psi_s \sin \omega_e t = \psi_a \cos(\omega_e t + \varepsilon_{\psi\zeta}), \tag{6.40}$$

where

ω_e Encounter frequency;
z_a, ψ_a, $\varepsilon_{\psi\zeta}$, $\varepsilon_{z\zeta}$ Heaving and pitching amplitude, and the phase angle between the heaving and pitching and the waves, respectively.

Then

$$z_a = \sqrt{z_c^2 + z_s^2},$$
$$\psi_a = \sqrt{\psi_c^2 + \psi_s^2}. \tag{6.41}$$

6.4.3 Determination of Added Mass and Damping Coefficients and Natural Periods

The key to solving the coupled pitching and heaving differential equation is to determine both the added mass and damping coefficients. Here we introduce a simple method to define such coefficients that does not need any offset of craft lines and can be used at the initial concept design of catamarans.

6.4.4 Contrikov's Method for Added Mass and Damping

Contrikov made regression analysis of graphs describing the coefficients of both added mass and damping of the cross section of a monohull ship in heaving motion carried out by Fukuzo Tasai of the Research Institute for Applied Mechanics, Kyushu University, in the mid-1960s. The coefficients obtained can be expressed as A_3 and C_0 in what follows, Eq. (6.42). It may be noted that for a catamaran in heave and roll, rolling motion effectively "heaves" the demihulls at small roll angles, so this provides useful data for catamaran coupled motions:

$$\bar{A}_3 = \sum_{i=0}^{4} \sum_{k=0}^{2} \sum_{l=0}^{2} a_{ikl} \xi_d^i \left(\frac{d}{B}\right)^k \sigma^l, \tag{6.42}$$

$$C_0 = (d/2)^2 C = \sum_{i=0}^{4} \sum_{k=0}^{2} \sum_{l=0}^{2} b_{ikl} \xi_d^i \left(\frac{d}{B}\right)^k \sigma^l,$$

where

Table 6.2 Regression coefficients of a_{ijl}, b_{ijl}

i, k, l	a_{ikl}	b_{ikl}	i, k, l	a_{ikl}	b_{ikl}
0,0,0	2.2102	6.5418	3,1,1	−78.8555	−74.6699
1,0,0	−11.0964	−28.2111	4,1,1	16.8600	14.8633
2,0,0	27.3812	42.3544	0,2,1	−3.4149	−6.3947
3,0,0	−19.3812	−23.9681	1,2,1	24.0855	40.4441
4,0,0	4.4314	4.8685	2,2,1	−46.5159	−51.9258
0,1,0	−6.0134	−6.1183	3,2,1	30.3940	27.2324
1,1,0	36.2004	38.7077	4,2,1	−6.4753	−5.2692
2,1,0	−80.3705	−50,7135	0,0,2	0.4612	9.7853
3,1,0	56.9283	26.7735	1,0,2	−4.0683	−52.7271
4,1,0	−129,728	−5.1945	2,0,2	1.4359	81.6971
0,2,0	2.3129	2.4644	3,0,2	1.6235	−49.2273
1,2,0	−14.4029	−14.6185	4,0,2	−0.8189	10.2915
2,2,0	30.9950	18.5078	0,1,2	−2.1326	−8.0976
3,2,0	−21.7970	−9.2339	1,1,2	16.0122	66.5850
4,2,0	4.9468	1.6751	2,1,2	−23.3070	−87.4029
0,0,1	−2.8107	−15.1006	3,1,2	10.5205	48.0897
1,0,1	20.6434	77.4020	4,1,2	−1.2310	−9.8324
2,0,1	−37.3756	−116.7440	0,2,2	0.8927	3.8935
3,0,1	23.1179	69.1435	1,2,2	6.3716	−26.1503
4,0,1	−4.8009	−14.2832	2,2,2	9.2028	33.3911
0,1,1	8.5736	15.2720	3,2,2	−4.0630	−17.6554
1,1,1	−61.3614	−106.6744	4,2,2	0.4603	3.4641
2,1,1	120.2025	138.9335			

$$\xi_d = \frac{\omega^2}{g} d, \quad \sigma = S/Bd,$$

S, B, and d are the area, width, and draft of the calculated section, while a_{ikl} and b_{ikl} can be obtained from Table 6.2 below.

Then the damping and added mass coefficient of transverse section x can be stated as

$$\begin{aligned} N_z(x) &= \frac{\rho g^2 \bar{A}_3^2}{\omega^3}, \\ m_z(x) &= \frac{1}{8}\rho\pi B^2 C, \end{aligned} \tag{6.42a}$$

where C is derived from C_0 in Eq. (6.42) above.

6.4.5 Determination of Natural Periods of Motion

The natural period of heaving and pitching motion of a catamaran T_h, T_p can be written

$$T_h = 2\pi\sqrt{\frac{D+\Delta D}{g\gamma S_c}}, \tag{6.43a}$$

$$T_p = 2\pi\sqrt{\frac{I_y+\Delta I_y}{D(R+z_c-z_G)}}. \tag{6.43b}$$

Some parameters in these equations can be determined by empirical formulas for preliminary estimation before full motion analysis, as follows:

$$I_y = 0.07\frac{\alpha}{g}DL^2, \tag{6.44}$$

$$\Delta I_y = 0.055\frac{\gamma}{g}b^2L^3\frac{\alpha^2}{(3-2\alpha)(3-\alpha)}, \tag{6.45}$$

$$\Delta D = 0.85\gamma\frac{\pi}{4}Lb^2\frac{\alpha^2}{1+\alpha}, \tag{6.46}$$

$$R = \frac{\alpha^2}{14\delta}\cdot\frac{L^2}{T}, \tag{6.47}$$

$$i_y = RV_d, \tag{6.48}$$

where

T Catamaran draft;
V_d Volumetric displacement of a demihull;
i_y Moment of inertia of catamaran waterplane about y-axis.

Using the preceding equations, both the heaving and pitching natural period can be calculated with approximate values.

6.5 Differential Equation of Longitudinal Motion in Waves

6.5.1 Simplified Differential Equation of Motion

Similar to conventional ships, the simplified differential equation of *uncoupled* pitching and heaving motion of a catamaran can be written

$$\left(\frac{D+\Delta D}{g}\right)\ddot{\xi}+kS_d\dot{\xi}+\gamma S_d\varsigma=a_0\cos\omega t+b_0\sin\omega t,$$
$$\left(I_y+\Delta I_y\right)\ddot{\psi}+ki_y\dot{\psi}+D\left(R+z_c-z_g\right)\psi=a_1 con\omega t+b_1\sin\omega t. \tag{6.49}$$

This may be compared with the full equation of motion presented above in Eq. (6.34), where

D	Displacement of each demihull of catamaran;
ΔD	Added displacement due to water added mass of demihull;
k	Damping coefficient;
S_d	Waterplane area of a demihull;
Ψ	Pitching angle;
ζ	Heaving amplitude;
I_y	Moment of inertia of mass of catamaran about y-axis;
ΔI_y	Moment of inertia of added mass of catamaran;
i_y	Moment of inertia of waterplane about y-axis;
R	Longitudinal metacentric radius;
z_c	Height of center of buoyancy of catamaran;
z_G	Height of center of gravity of catamaran;
a_0, b_0, a_1, b_1	Coefficients of interference force of waves.

6.5.2 Full Differential Equations of Longitudinal Motion of Catamaran in Waves

To calculate the maximum amplitude of both heaving and pitching motion and maximum vertical acceleration of a catamaran in waves, the added mass and damping coefficient as well the interaction factor between demihulls must be considered in the calculation of catamaran motion in waves.

The *coupled* heaving and pitching differential equation of a catamaran in waves can be written as follows:

$$\begin{aligned}
&\left(\frac{D}{g}+\Delta M\right)\ddot{\varsigma}+\nu_{\varsigma}\dot{\varsigma}+2\gamma S_d\varsigma+\Delta M x_1\ddot{\psi}+\left(\nu_{\varsigma\psi}-v_0\Delta M\right)\dot{\psi}\\
&\quad+(2\gamma S_d l-v_0\nu_{\varsigma})\psi=r\left(\gamma a_0-\omega^2 a_0''-\omega b_0'\right)\cos\omega_e t\\
&\quad-r\left(\gamma b_0-\omega^2 b_0''+\omega a_0'\right)\sin\omega_e t\\
&\left(I_y+\Delta I_y\right)\ddot{\psi}+\left(\nu_{\psi}+\frac{v_0^2}{\omega^2}\nu_{\varsigma}\right)\dot{\psi}+\left(DH-v_0^2\Delta M\right)\psi+\Delta M x_1\ddot{\varsigma}+\left(\nu_{\varsigma\psi}+v_0\Delta M\right)\dot{\varsigma}\\
&\quad+(2\gamma S_d l+v_0\nu_{\varsigma})\varsigma=r\left(\gamma a_1-\omega^2 a_1''-\omega b_1'\right)\cos\omega_e t\\
&\quad-r\left(\gamma b_1-\omega^2 b_1''+\omega^2 a_1'\right)\sin\omega_e t,
\end{aligned}\tag{6.50}$$

where

ν_{ς}, ν_{ψ}, $\nu_{\varsigma\psi}$	Damping coefficients;
ΔM, ΔI_y	Water added mass and moment of inertia of added mass about y-axis of catamaran;
$\Delta M x_1$	Static moment of water added mass about y-axis through CG of catamaran;
a_0, b_0, a_1, b_1	Coefficients of main part of perturbation force of waves;
a_0', b_0', a_1', b_1'	Coefficients of perturbation force due to damping force;
a_0'', b_0'', a_1'', b_1''	Coefficients of perturbation force due to added mass;
$S_d l$	Static moment of waterline plane about CG of catamaran;
$\omega=2\pi/\tau$	Wave frequency;
$\tau=\lambda_w/c$	Wave period;
c	Wave speed;
$\omega_e=$	$\omega(1+v_0/c)$ Apparent frequency of heading wave encounter;
v_0	Ship speed;
r	Half of wave height.

Using the strip theory method, the foregoing added mass, damping, and perturbation force coefficients can be written as follows:

$$\begin{aligned}
&\nu_{\varsigma}=2\int\nu_0(x)dx; && a_0=4\int y_1\cos kx dx; && a_1=4\int xy_1\cos kx dx;\\
&\nu_{\varsigma\psi}=2\int x\nu_0(x)dx; && a_0'=2\int\nu_0(x)\cos kx dx; && a_1'=2\int x\nu_0(x)\cos kx dx;\\
&\nu_{\psi}=2\int x\nu_0(x)dx; && a_0''=2\int\mu_0(x)\cos kx dx; && a_1''=2\int x\mu_0(x)\cos kx dx;\\
&\Delta M=2\int\mu_0(x)dx; && b_0=4\int y_1\sin kx dx; && b_1=4\int xy_1\sin kx dx;\\
&\Delta M x_1=2\int x\mu_0(x)dx; && b_0'=2\int\nu_0(x)\sin kx dx; && b_1'=2\int x\nu_0(x)\sin kx dx;\\
&\Delta I_x=2\int x^2\mu_0(x)dx; && b_0''=2\int\mu_0(x)\sin kx dx; && b_1''=2\int x\mu_0(x)\sin kx dx;
\end{aligned}\tag{6.51}$$

where

$\nu_0(x)$, $\mu_0(x)$ Damping coefficient and water added mass coefficient of a demihull for each frame station that can be obtained in this and the following sections;
y Abscissa of waterline:

$$k = 2\pi/\lambda_w, \text{ the wave number.}$$

The plots for the damping coefficients are shown in Fig 6.17a–d, and the plots for the coefficient of water added mass for each station of the demihull can be obtained from Fig. 6.18, that is,

$$\mu_0(x) = f\left(\frac{\pi b}{\lambda_w}\right), b/2T, \beta).$$

The preceding damping and added mass coefficients do not consider the effect of wave interference between demihulls, that is, the effect of hull separation on the damping and added mass coefficients.

The influence factors for demihull interference can be written

$$\begin{aligned} \overline{\nu}\left(\bar{k}\right) &= \frac{\nu(x)}{2\nu_0(x)}, \\ \overline{\mu}\left(\bar{k}\right) &= \frac{\mu(x)}{2\mu_0(x)}, \end{aligned} \tag{6.52}$$

where

$\nu_0(x)$, $\mu_0(x)$ Damping and added mass coefficients for each demihull station, without consideration of interference effect;

$\nu(x)$, $\mu(x)$ Damping and added mass coefficients for each catamaran station, considering interference effect of catamaran hull separation;

$\overline{\nu}(K/b), \overline{\mu}(K/b)$ Interference factors, which can be obtained from Fig. 6.19 [3], in which the solid line represents the influence factor for two flat plates and the dashed line that for an elliptical cylinder. However, the factors are almost the same in the case of K/b greater than 1.0, which is the majority of modern high-speed catamarans.

In the case of higher spacing, and thus with a smaller interference factor, catamaran pitching and heaving amplitude in waves can be obtained in a similar way to the solution of the differential equation for conventional ships, thus applying the influence factors to the added mass and damping to solve the differential equation of motion for a unit wave amplitude to determine the response amplitude operators.

Then, to determine the response in a seaway, spectral methods are used to generate the mean, significant, and maximum values in a particular seaway energy spectrum. For this readers are referred to the classic naval architecture texts.

It should be recalled that this type of analysis will provide useful results for typical operational sea states when responses are expected to be linear or nearly linear. Response in extreme sea states where wave impact may occur on catamaran

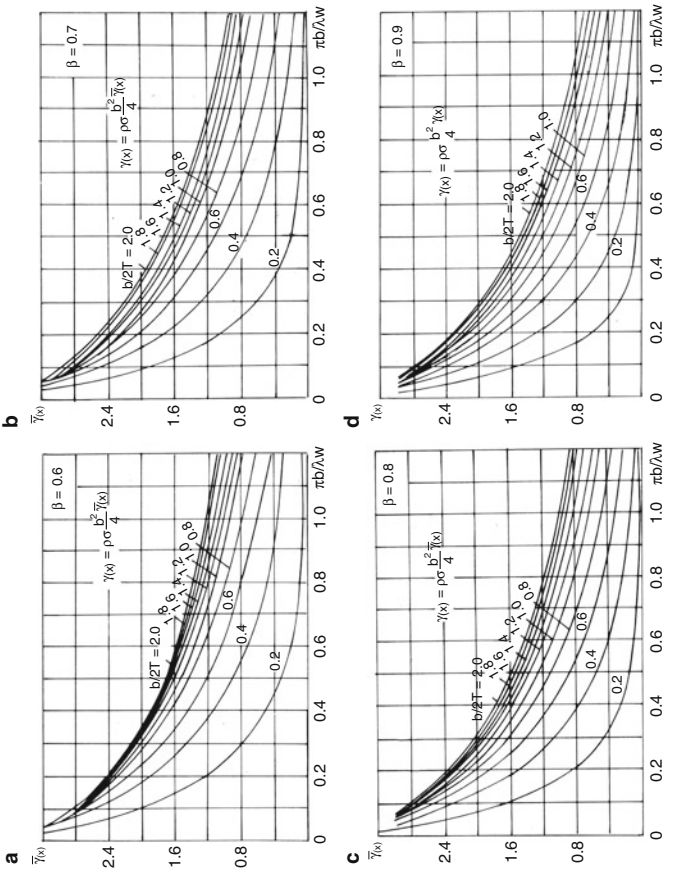

Fig. 6.17 $\gamma_0(x) = f(\pi b/\lambda_w, b/2T, \beta)$ plots (**a–d**)

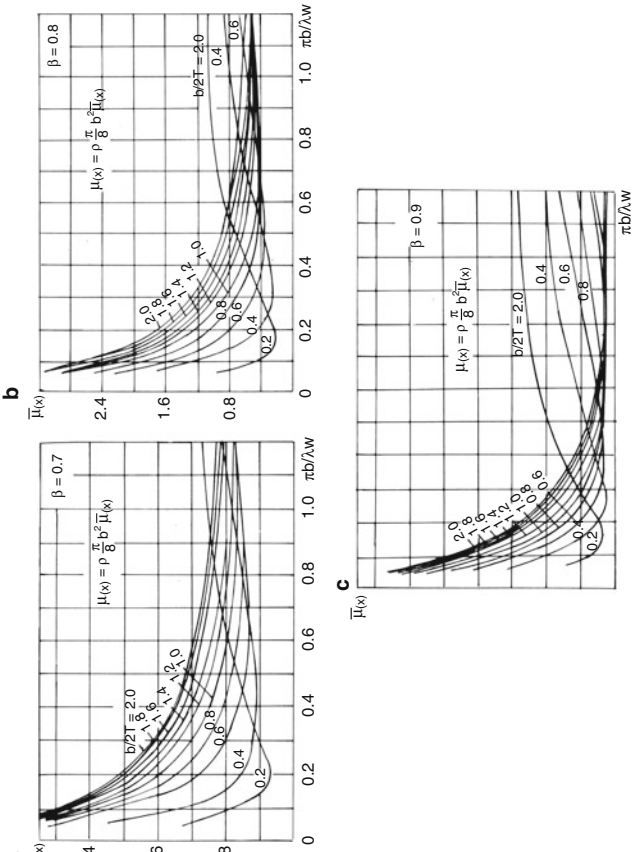

Fig. 6.18 $\mu(x) = f(\pi b/\lambda_w, b/2T, \beta)$ plots (**a**–**c**)

Fig. 6.19 $\overline{\mu}(\overline{k}) = f(\overline{k})$

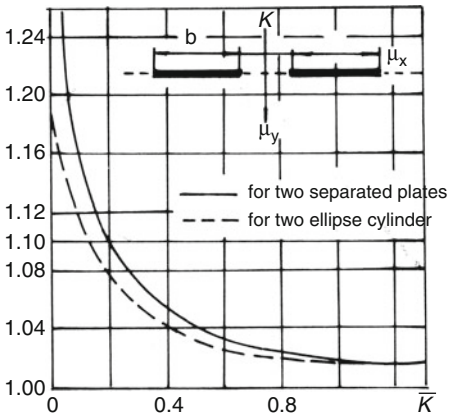

cross structure will require a time domain analysis. This is further discussed in Chap. 12, where we cover vessel motions in more detail and the input to structural analysis.

6.6 Measures for Improving Catamaran Seakeeping Qualities

6.6.1 Improving Seakeeping Qualities of Modern Catamarans

We refer to modern high-speed catamaran designs as those aiming at service speed above 35 knots, wider deck area and cabin volume for accommodating low-density goods (e.g., people, cars, and trucks), large displacement, and fine seakeeping quality, with a low seasickness rate and maintaining high speed in waves, for example:

- Large passenger-car ferry ships, operating in coastal environment and rough seas;
- Naval sealift ships.

Such vessels would have high motions and accelerations when using conventional catamaran lines and form when at high speed in rough seas. The design challenges related to the seakeeping quality of high-speed catamarans can be outlined as follows:

- Similar to the conventional catamaran, the coupled longitudinal and transverse motion of a high-speed catamaran operating on bow quartering course in waves, particularly at lower speed, might occur on the high-speed catamaran making a so-called corkscrew or drunken motion for passengers and crew, creating a higher

seasickness rate. This is due to lower length beam ratio of such craft (L/B = 2.5–3.5), thus causing the natural period for both pitching and roll oscillation to be close together;

- Wave encounter frequency is higher due to the high speed, $\omega_e = \frac{2\pi(c - v\cos\chi)}{\lambda}$, where ω_e is the encounter frequency, c the wave speed, v the craft speed, λ, χ the wave length and wave direction, respectively.

In case of head seas, $\omega_e = \frac{2\pi(c+v)}{\lambda}$, since χ is 180°, so at resonance for the same encounter wave frequency with pitching and heaving natural frequency, a large motion amplitude will be caused. The peak response amplitude operator (RAO) of both pitch and heave, $\psi/k\zeta_a$ and z/ζ_a, is as high as 2 to 2.5

- Due to the high ω_e and RAO, the heaving and pitching acceleration of a high-speed catamaran in head or bow quarter seas is also high, causing a high superposed vertical acceleration by both pitching and heaving, as well as roll, at the encounter frequency. In general, this will be at 0.4 to 2.5 rad/s, 0.06 to 4 Hz, exactly where seasickness is most likely for people in general.
- The speed loss in waves will be significant due to the high vertical acceleration and slamming, which might cause discomfort for passengers and damage to both hull structure and equipment, causing the captain to reduce power and speed in service.
- In contrast with the conventional catamaran, the RAO of vertical acceleration will be higher in head waves than bow quarter seas, as in this latter case the encounter frequency is reduced.

One clear method to improve catamaran roll and heave response is to reduce the area of the hull waterplane at and above the still waterline to the minimum practical level for static stability and having most of the displaced volume below the operational waterplane and strutlike support above this to the payload structure.

This is the concept of the SWATH vessel. However, resistance will be increased due to the increased wetted surface and is not really suitable for high-speed vessels.

An alternative is the wave-piercing catamaran (WPC) for improving seakeeping quality, particularly decreasing the speed loss in waves. This concept uses a reduced waterplane form in the bow section of the catamaran and a more traditional stern half of the hull. However, as in the SWATH, the reduced waterplane means that pitch stability is reduced, and appropriate dynamic stability requires control systems with fin or foils and thus increases the complexity of system installation, maintenance, and operating costs.

Davis and Holloway of the University of Tasmania, Australia [12], tested and recorded the vertical acceleration on a WPC in service at the different wave directions. Figure 6.20 shows the Incat 86-m vessel used in the sea trials to record motion data, and Fig. 6.21 shows the acceleration (rms) relative to wave height (rms), $\left(\ddot{z}_R = \ddot{z}_{rms} \bullet \frac{L_{WL}}{h_{w1/3}} \bullet g\right)$, observed at the center of gravity (dimensionless units, rms acceleration, length/g.rms wave height).

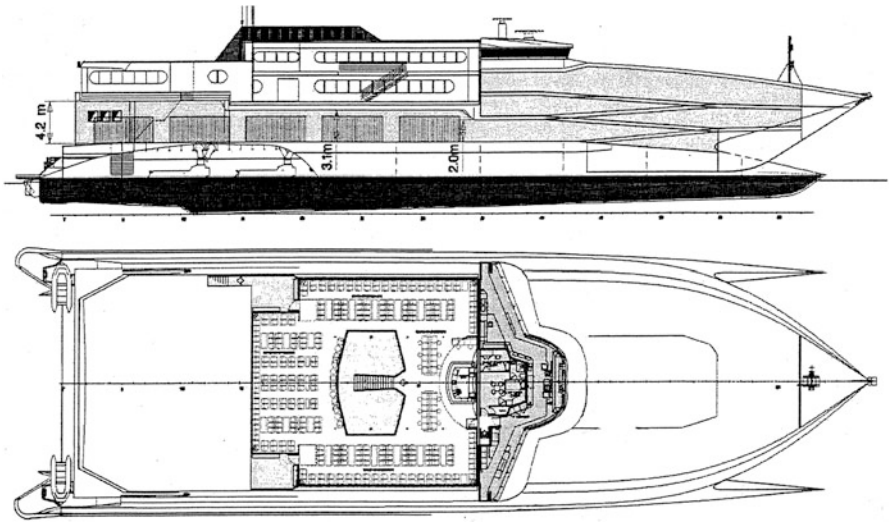

Fig. 6.20 Incat 86-m vessel general arrangement

Fig. 6.21 Measured acceleration data

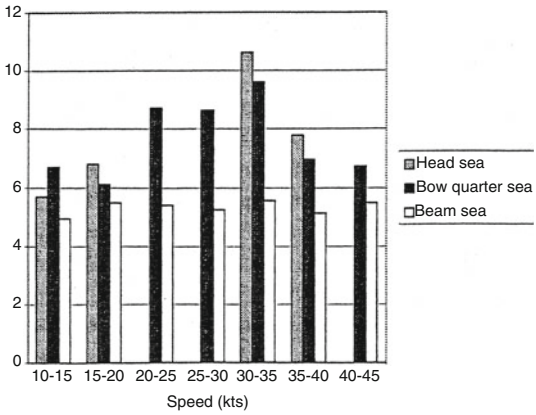

The results from these trials showed that stern tabs and a bow stabilizer foil had a measurable effect on motion response. The tabs improved vessel trim, while the bow foil added damping to the motion response. Figure 6.21 below shows that while head seas produce the greatest heaving at 30 to 35 knots, the bow quartering seas caused almost as high a response and over the whole speed range.

6.6.2 *Measures for Improving the Seakeeping Quality, the Semi-SWATH*

The semi-SWATH is a ship form between the conventional catamaran and SWATH, where the design waterline is constricted and so the displaced volume is partly moved below the design waterplane deeply so as to form a lean design waterplane and lines as well as sharp bow for reducing the wave forcing, but without increasing the draft.

On these craft the frame section is flared above the design waterline for safe operation in waves and obviates the need to use any active control system. Consequently, the body plan of the semi-SWATH looks a little like a typical old Greek amphora [8] or a vase [13].

Semi-SWATHs have been developed with different variations in hull geometry as follows:

- Waterplane *partly constricted* type (WPCP): as shown in Fig. 6.22a, b [14]. Nigel Gee and Edward Dudson of BMT Nigel Gee Associates Ltd., UK, developed this type of semi-SWATH, with the waterplane partly constricted – mainly forward of amidships and at the bow, with a small bulbous bow and an almost conventional type of catamaran aft of amidships. Figure 6.23a shows the bow and fore part of craft "X," designed by BMT Nigel Gee Associates Ltd. for the US Navy, and Fig. 6.22b shows the schematic body plan for this craft.
- Design waterplane *wholly constricted* type (WPCW), as shown in Figs. 6.23a, b and 6.24: Stig Bystedt, technical director of Stena Rederi, together with the shipyard Finnyards, created this type of semi-SWATH type designated HSS 1500 [15], with the waterplane constricted over the full hull length, with a small and sharp bulbous bow. Figure 6.23a shows the structure of one hull and Fig. 6.23b the bulbous bow of the Stena HSS being constructed at Finnyards. Figure 6.24a shows the HSS1500 in service, Fig. 6.24b the vessel general arrangement.

Danyard A/S, Denmark, also designed and built two semi-SWATH type vessels for the Mols line ferry service, as shown in Fig. 6.25a, b [16, 17].

The Seajet 250 also had a semi-SWATH hull arrangement, with the stern hull form constrained as far as possible to meet the requirements of the waterjet and gas turbine engine arrangement.

6.6.3 *MARIC Semi-SWATH and Its Improvements in Seakeeping [18, 19]*

To develop a proposal for a high-speed catamaran passenger-car ferry to operate across the Taiwan Strait, MARIC carried out both theoretical and experimental investigations of semi-SWATHs to compare with other vessel form types and bow

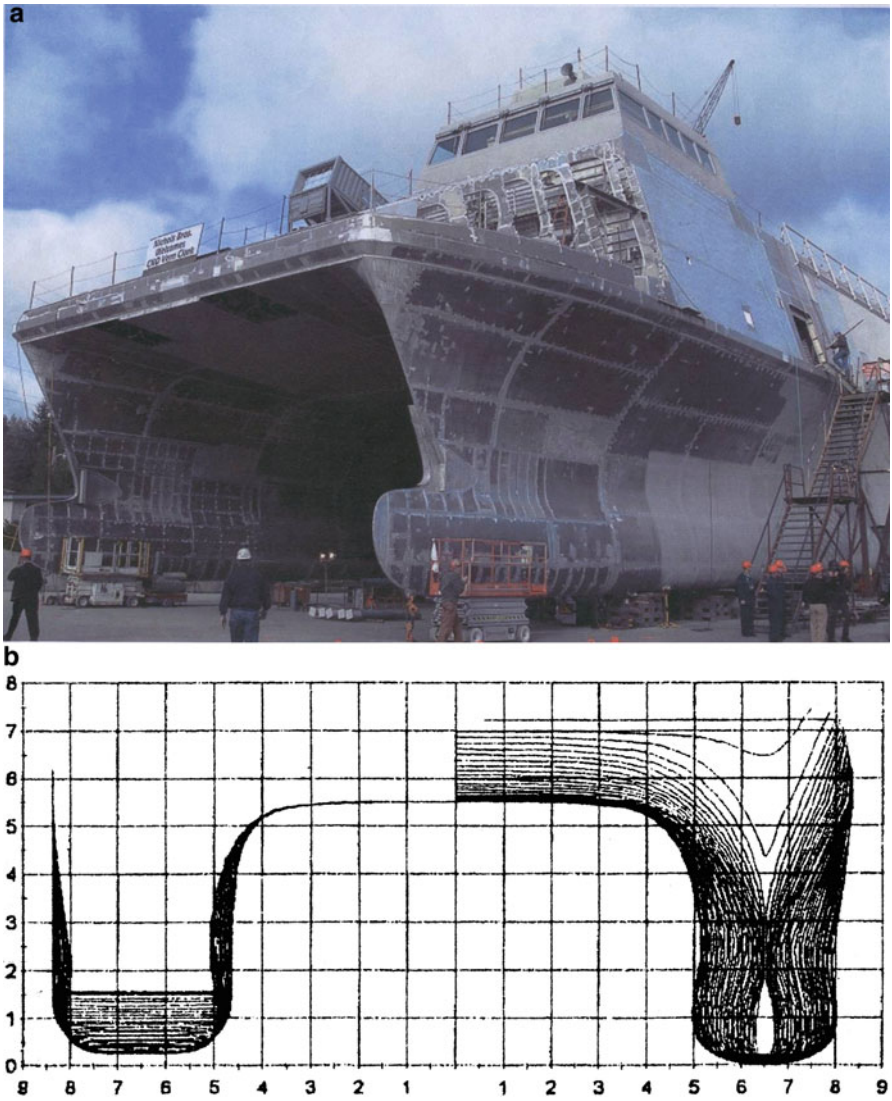

Fig. 6.22 (**a**) Seafighter bow area; (**b**) body plan

types including the conventional type of catamaran that had been designed at MARIC a number of years previously.

The form features of the semi-SWATH incorporated into the design were constriction of the waterline on each demihull to give smaller pitching and heaving restoring forces (moments) and perturbation forces (moments) compared with traditional catamaran lines. A comparison was carried out with a conventional high-speed catamaran with the same dimensions, displacement, relative speed (Froude

Number Fr_L), and slenderness and separation of demihull, length beam ratio of demihull, and so forth.

The ratio of the nondimensional waterplane constriction ratio $A_w/\Delta^{2/3}$ (where A_w is the waterplane area, $\Delta^{2/3}$ the volumetric displacement coefficient) for conventional, wave-piercing, and reduced-waterplane catamarans were 1, 0.8, and 0.5 approximately, and the ratio of the vertical prismatic coefficient (the distribution of displacement under the designed waterline) C_{vp} was 1: 1.12: 1.35 approximately.

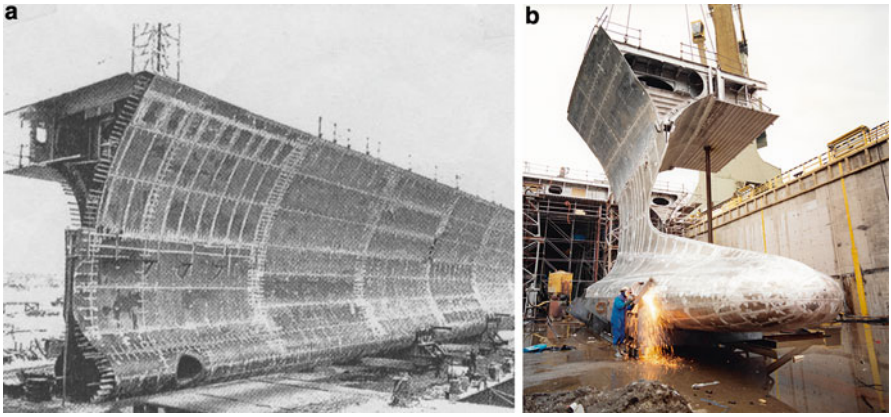

Fig. 6.23 (**a**) HSS1500 structure; (**b**) bow section in basin

Fig. 6.24 (**a**) Stena HSS1500; (**b**) general arrangement

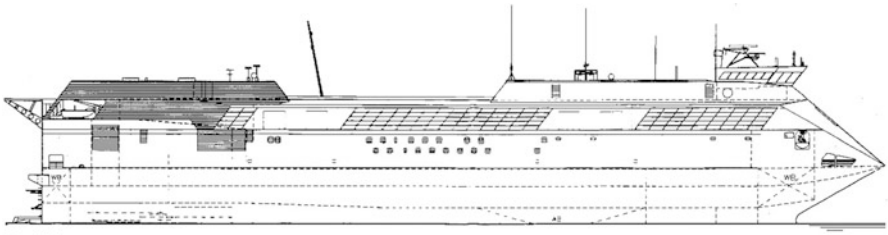

Profile

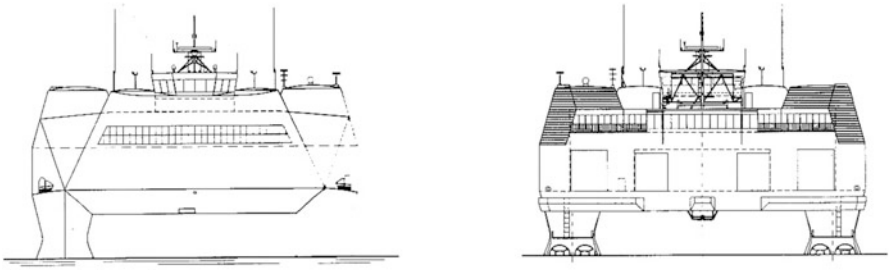

Bow and stern views

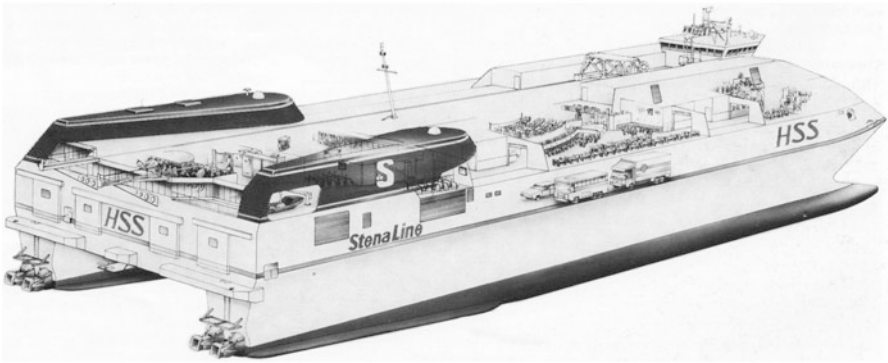

Cutaway view showing canted bilge keels protecting waterjet inlet flow

Fig. 6.24 (continued)

That meant most displacement was moved to below the waterplane, giving the following results:

(a) The heaving restoring force coefficients C_{33} (Eq. 6.34) for the three types of high-speed catamaran decreased at a ratio of 1: 0.85: 0.65 approximately, and pitching restoring moment C_{55} at a ratio of 1: 0.75: 0.65, thereby reducing the longitudinal metacentric arm at a ratio of 1: 0.7: 0.4 approximately and increasing the natural pitching period;
(b) The wave perturbation force and moment coefficients dropped significantly.

Different shapes of "bulbous bow" are shown in Figs. 6.22, 6.23, and 6.25 that are used together with a reduced waterplane on high-speed vessels. Their use on high-

speed catamarans needs a little explanation since the slender hull form is already a low-wave-generating form. The effect of a bulbous bow for improving the interference of both transverse and divergent waves for reducing wave-making resistance is weak in the case of a high-speed catamaran with high Froude number ($Fr_L = 0.75$ to 1.0) and high slenderness ($L_{WL}/\Delta^{1/3} > 8.0$), as well as large separation between the demihulls ($K_d/b > 3.0$). The small reduction of wave making cannot compensate for the increase in the wetted area of a bulbous bow, with associated friction resistance,

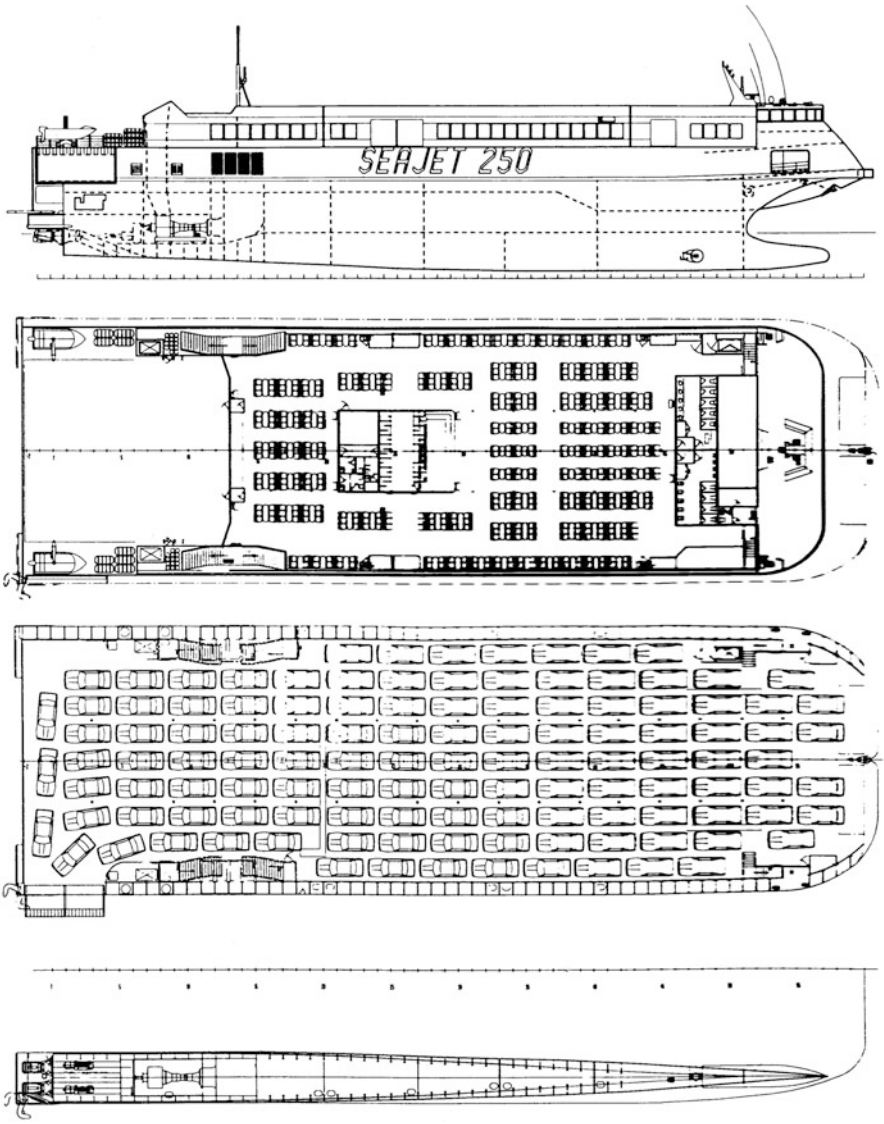

Fig. 6.25 (**a**) Danyard Seajet 250 general arrangement; (**b**) Danyard Seajet

Fig. 6.25 (continued)

since part of the friction drag will be over 50% of the total resistance when a restricted waterplane form is used.

With careful design, the effect can be neutral as far as resistance is concerned, as illustrated by Fig. 6.28, taken from the comparative tests carried out at MARIC.

However, due to the fact that most of the moving vessel-displaced volume is below the waterplane, a small and sharp bulbous bow can be shaped. The result of this geometry is lower pitch forcing as the vessel (hence the name "wave piercer" coined by Incat) operates in a seaway, and the overall waterplane restriction reduces the heave forcing, particularly for the more extreme restricted-waterplane areas of the Seajet 250, the Seafighter, and the HSS vessels.

So the objective of the "sharp" bulbous bow on semi-SWATHs or wave piercers is rather different from that of the conventional bulbous bow.

- Bow profile: The frame offsets above the waterline should be flared, particularly at the bow, to provide adequate transverse and longitudinal dynamic stability in waves, particularly against the "nose in" ("plough in") in following and stern quartering seas;
- Stern profile: Similar to the conventional catamaran, the main engines and waterjet pumps will be arranged in the after part of the vessel and at the stern. Transom and stern size will be dimensioned by the requirements for this outfit, particularly in the case of using two sets of propulsion system in one demihull. The designer has to look carefully at the geometry for the main machinery outfit, as it may be necessary to use a full or partly tandem positioning rather than

parallel so as to allow the waterline breadth to be kept consistent with the forward vessel lines.

- Location of LCB and LCF: Similar to the conventional catamaran, the semi-SWATH has a fine bow and fore part and wider stern, so the LCB will be located aft of the midship section (normally about 3–4%). The fine forward part will be compensated by the bulbous bow, so as to keep the LCB unchanged. However, due to the widened waterline at the stern for arranging engines and waterjet pumps, and lean waterline at the bow, the LCF may be moved afterward, making LCF < LCB (measured from transom). The further aft these centers are located, the greater the tendency for a vessel to pitch nose down in a seaway. The bulbous bow volume helps to mitigate this; nevertheless, the difference between the location of both the LCB and LCF should not be too large and should be not too far aft of the waterplane center of the area so as to avoid "nose in" in following seas and wave slamming at the bow in head seas.

To carry out both theoretical and experimental investigation of semi-SWATHs for a passenger-car ferry to operate in the Taiwan Strait and perform a comparison with conventional catamarans, MARIC worked on the investigation for a standard series of semi-SWATHs, with different bulbous bow geometries (e.g., ellipse, nabla, delta, and reverse delta) as well as a series of conventional catamarans with the same dimensions and nondimensional characteristics, that is, the same L/b, demihull slenderness, Fr_L, hull separation, b/T, and block coefficient, to allow for comparison.

The leading particulars of the vessels at full scale are as follows [18]:

Length overall:	66.1 m
Width overall:	16.6 m
Length of waterline:	58.4 m
Molded depth:	5.7 m
Passengers:	645
Cars:	46
Service Speed:	38 knots
Main engines:	4 × MTU20V4000M93L (4300 kW each)
Waterjet:	4 × KeMeWa 90SII

The general arrangement of the craft is shown in Fig. 6.26, and towing tank tests, carried out at a model scale ratio of 1:20 [19], are shown in Fig. 6.27.

Tables 6.3, 6.4a, and 6.4b below show the model data and test results in tabular form.

The type of semi-SWATH modeled was taken as a constrained waterplane catamaran with sharp bulbous bow form, with the bulb geometry varied for some tests. Results are shown in the figures below after the explanations. The test results that include improvement of seakeeping quality in head seas at a maximum speed of 40 knots can be outlined as follows.

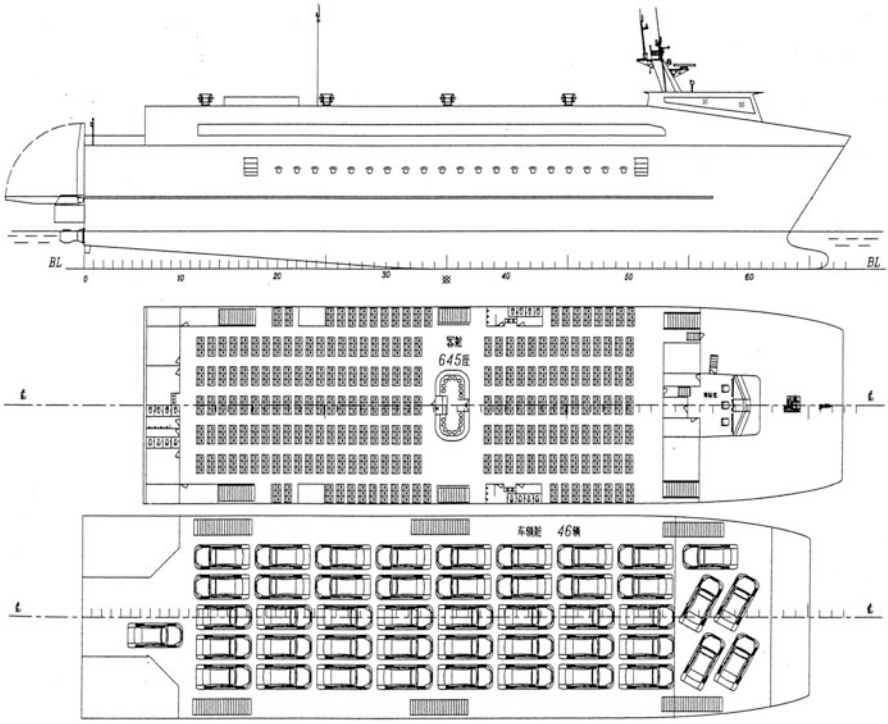

Fig. 6.26 MARIC semi-SWATH catamaran ferry

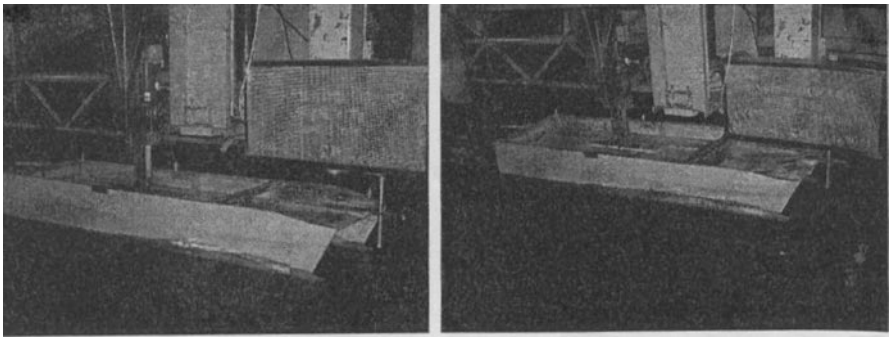

Fig. 6.27 Model tests for resistance and seakeeping

6.6.3.1 Resistance Characteristics

Resistance in calm water is almost the same as that of the conventional catamaran, as shown in Fig. 6.28a. Various type of bulbous bow with different types (ellipse, nabla, delta, and reverse delta) and coefficients have been tested by other researchers

Table 6.3 Leading particulars of both conventional catamaran and semi-SWATH models

Item	Unit	Catamaran	Semi-SWATH
L_{pp}	m	2.71	2.71
B_{max}	m	0.836	0.837
T	m	0.12	0.142
Displacement	m^3	0.067	0.067
S_w, wetted surface area	m^2	1.658	1.906
Hull separation	m	0.65	0.65
Lcg	m	−0.175	−0.184

Table 6.4a Test results of seakeeping quality for conventional catamaran in irregular waves, significant response (mean of highest 1/3)

H1/3	T, s	Rw	Zeta1/3	Z1/3, m	Af1/3, g	Am1/3, g	Aa1/3, g
1.0	5.8	0.8	0.54	0.37	0.23	0.14	0.18
1.5	6.1	2.04	0.90	0.65	0.38	0.24	0.28
2.0	6.4	3.96	1.31	0.98	0.54	0.34	0.39
2.5	6.7	6.56	1.74	1.34	0.70	0.45	0.50
3.2	7.0	11.05	2.32	1.9	0.92	0.61	0.65
4.0	7.6	17.07	2.99	2.43	1.17	0.76	0.78

Table 6.4b Test results of seakeeping quality for semi-SWATH in irregular waves, standard deviation values, significant response (mean of highest 1/3)

H1/3	T, s	Rw	Zeta1/3	Z1/3, m	Af1/3, g	Am1/3, g	Aa1/3, g
1.0	5.8	0.73	0.47	0.18	0.005	0.04	0.08
1.5	6.1	1.73	0.80	0.32	0.08	0.07	0.13
2.0	6.4	3.15	1.16	0.49	0.11	0.10	0.17
2.5	6.7	4.93	1.55	0.67	0.14	0.12	0.22
3.2	7.0	7.95	2.15	0.91	0.18	0.16	0.28
4.0	7.6	11.5	2.76	1.21	0.22	0.19	0.34

[20–22], with volume coefficient $C_{VPR} = V_{PR}/V_{wL}$, where (V_{PR} represents the volume of the bulbous bow protruding from the vessel stem, V_{wL} is displacement); transverse section coefficient $C_{ABT} = A_{BT}/A_{MS}$, where A_{BT} is the transverse projected area of the protruded bulbous bow, A_{MS} is the transverse midsection of the ship; lateral coefficient $C_{ABL} = A_{BL}/A_{ms}$, where A_{BL} is the longitudinal projected area of the bulbous bow; length coefficient $C_{LPR} = L_{PR}/L_{pp}$, where L_{PR} is the protruded length of the bulbous bow, L_{pp} is the length between perpendiculars; width coefficient $C_{BB} = B_B/B_{MS}$, where B_B is the width of the bulb, B_{MS} the width of the midsection; and depth coefficient $C_{LB} = z_B/T_{FP}$, where Z_B is the distance between the baseline of the ship and the highest point of the bulb, and T_{FP} is the draft at the bow perpendicular.

Unfortunately, the reduction of wave-making resistance for various types of bulb cannot compensate for the increase in friction due to the increase in the wetted area

of the bulb and the total resistance increment of a semi-SWATH in calm water, except when using a transom interceptor for decreasing the vessel trim angle at high speed. This will make the total resistance of the semi-SWATH close to that of the conventional catamaran.

The resistance increment in a seaway is small for the semi-SWATH, as shown in Fig. 6.28b, h, showing R with respect to wavelength. There is about a 30% decrease in sea state 4 compared with the conventional catamaran due to lower longitudinal motion velocity and sharp bow. Thus, this is a significant gain.

6.6.3.2 Pitching Response

Pitching amplitude was approximately the same as in the conventional catamaran, as shown in Fig. 6.28c, I, and due to the large wave perturbation moment (Ma) and small pitching damping coefficient, with these being similar between the semi-SWATH and conventional catamaran, due to fine forward part and wider stern for arranging the power plant on both vessel designs.

6.6.3.3 Heaving Response

Heaving amplitude decreased significantly in comparison with the conventional high-speed catamaran, as shown in Fig. 6.28d, in which heaving amplitude is Za, wave amplitude ζ_a, wave length λ, and waterline length L, and it can be shown that the peak heave amplitude dropped by 50% in regular waves and approximately 50% in irregular waves with significant wave height 2.5 m (sea state 4, with Jonswap wave energy spectrum; all values in irregular waves are significant values). This could be due to the following factors:

(a) Wave perturbation coefficient decreased significantly, about 35% reduced for F_{za} in calculations (Eq. 6.50) due to the constriction of the waterplane over the whole length, particularly at the midpart of the vessel;
(b) The natural heaving period increased, and consequently, the difference between the vessel response natural frequency and wave encounter frequency increased so as to decrease the heave amplitude;
(c) The heaving damping coefficient increased at the high operating speed of 40 knots.

6.6.3.4 Vertical Acceleration

The forward vertical acceleration decreased significantly as shown in Fig. 6.28e, k, where Acf is forward vertical acceleration. This drops by about 70% compared with a conventional catamaran at peak value in regular waves and 80% in irregular seas at a significant wave height of 2,5 m (SS4).

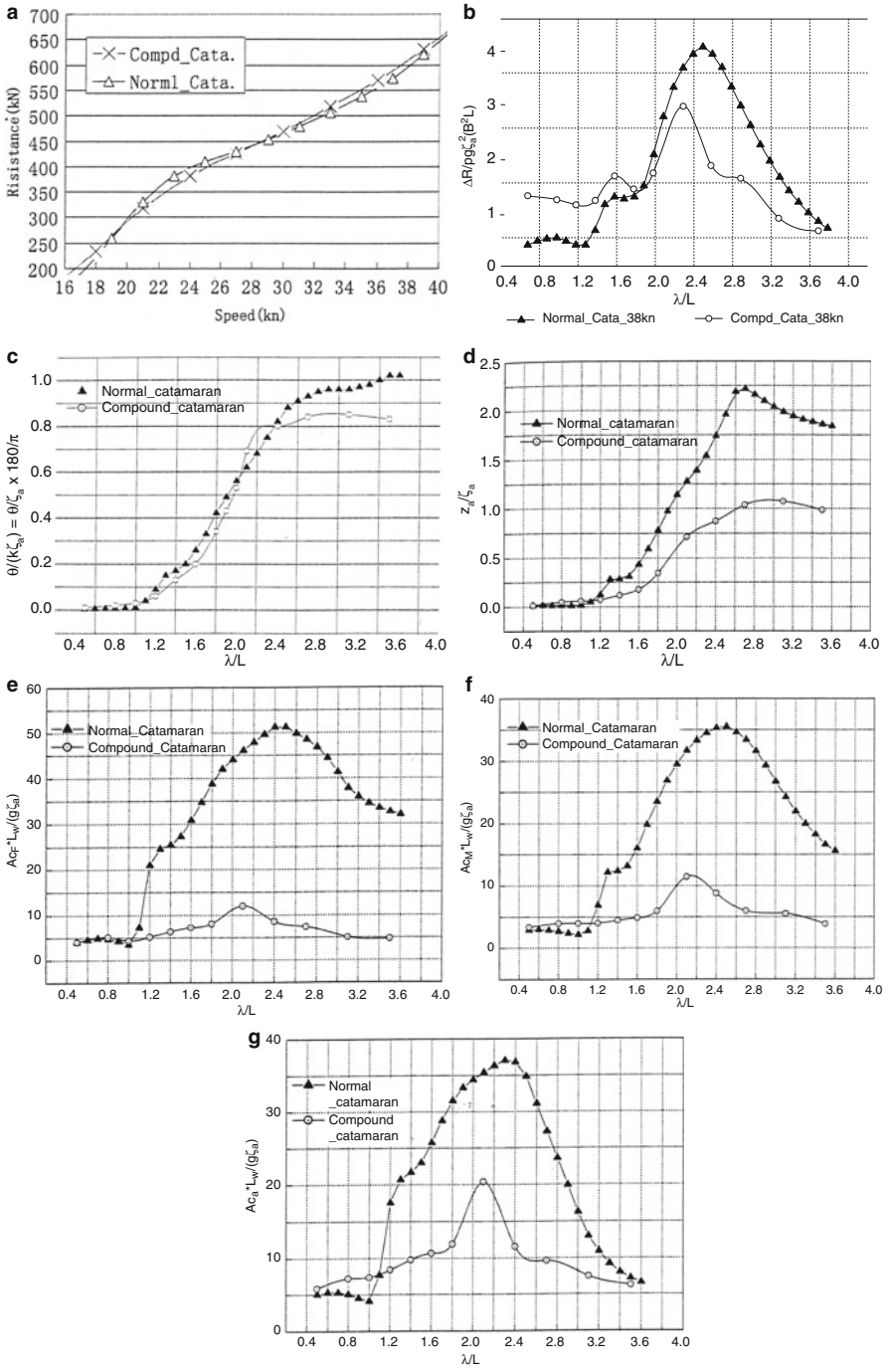

Fig. 6.28 (**a**–**u**) Test results

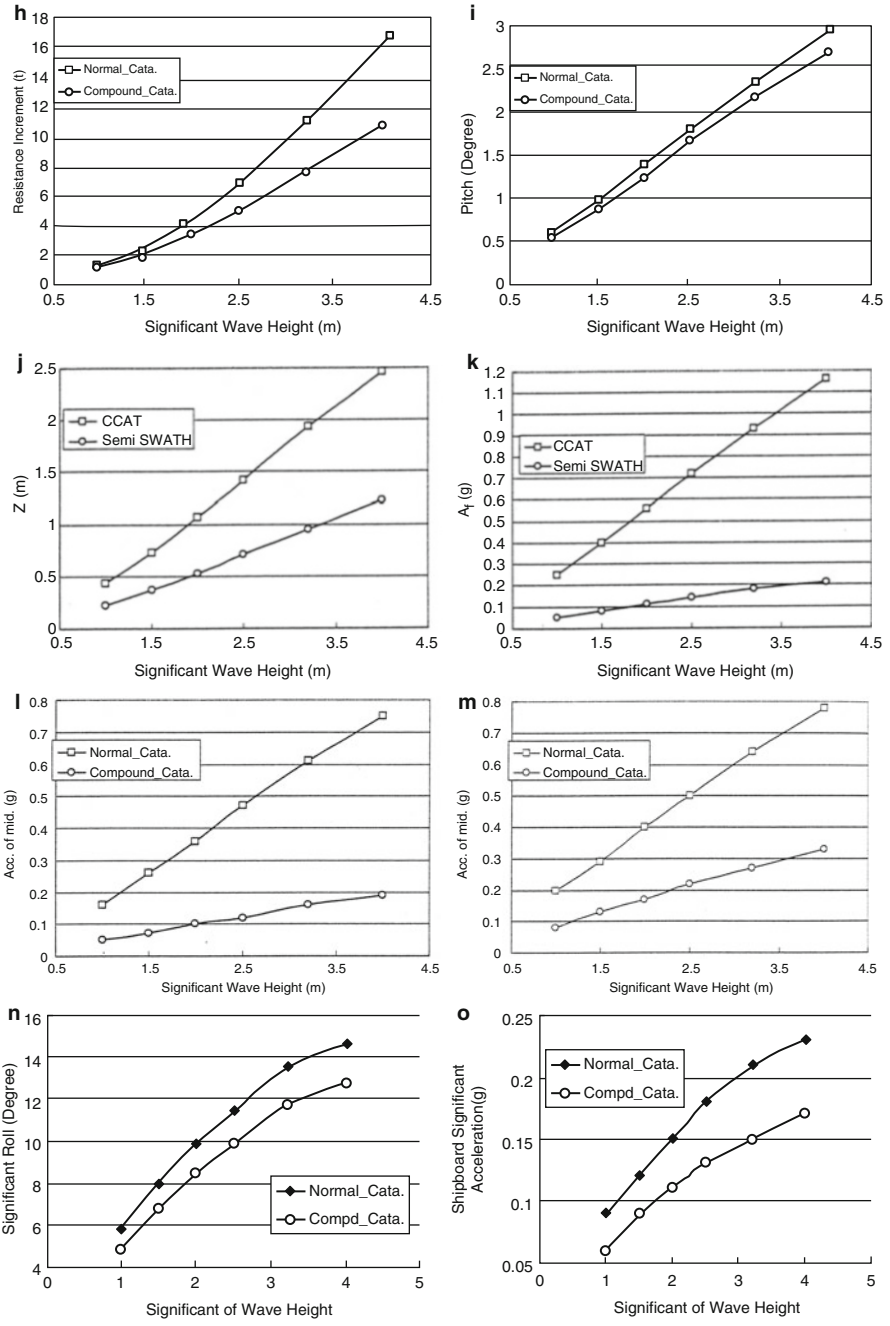

Fig. 6.28 (continued)

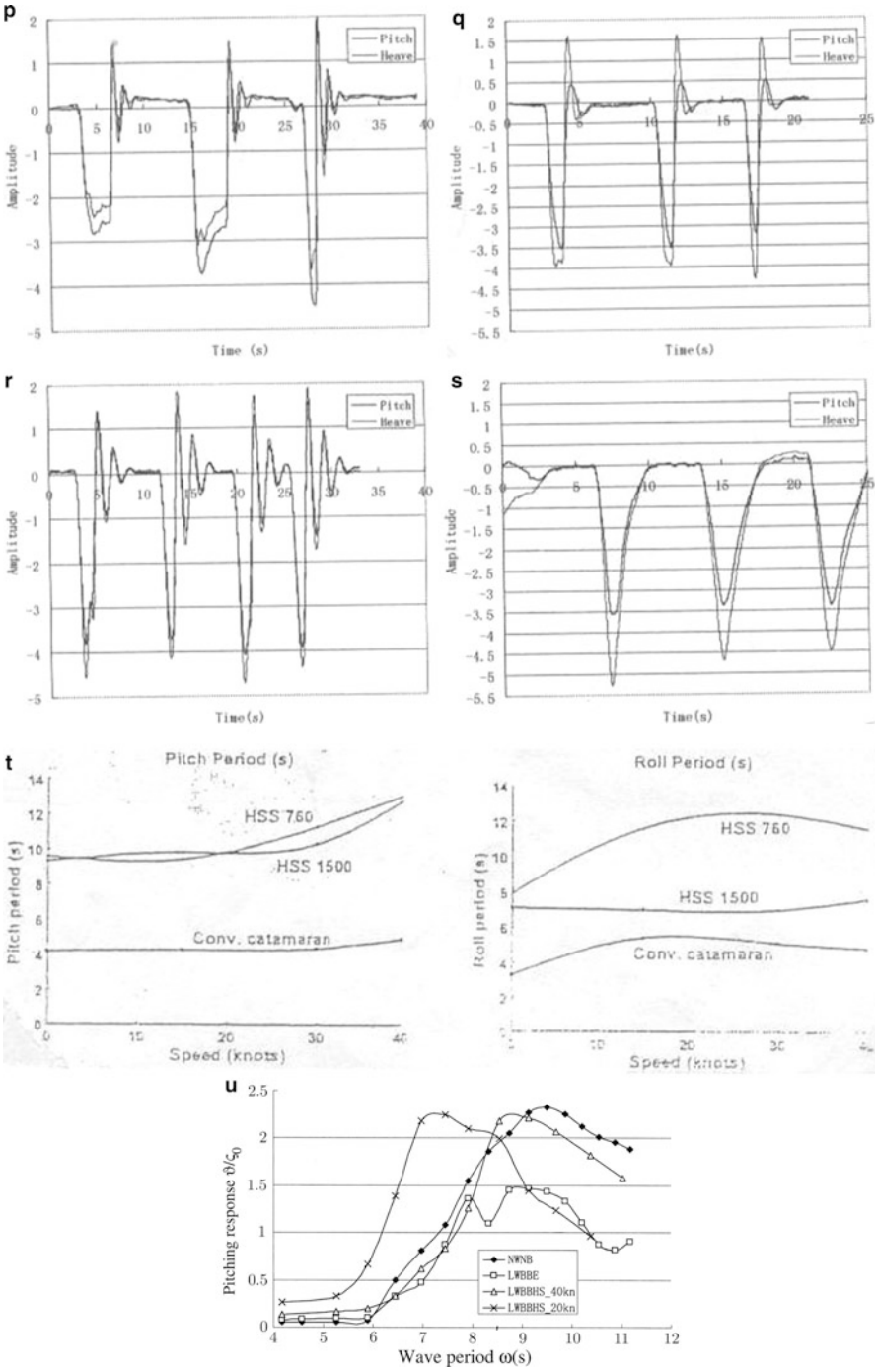

Fig. 6.28 (continued)

This could be due to the following factors:

(a) Decrease in both pitching and heaving natural frequency, so that the vessel peak response is further into the area of the wave energy spectrum tail where energy is low, so responses are reduced;
(b) Heave amplitude decreased.

Vertical acceleration in the midships area also decreased about 70–80%, as shown in Fig. 6.28f, l, respectively, for response to varying regular wave length and response to irregular sea states, for the same reasons. Vertical acceleration at the stern decreased about 50%, however, not as much as in the forward and midpart of the craft. This could be due to the vessel lines being larger in this area with the center of buoyancy aft of midships for the semi-SWATH vessel, the lines in the aft portion being closer to those of a conventional catamaran.

When a semi-SWATH vessel is running at high speed and in head seas, the pitching and heaving damping increase, so as to significantly increase the longitudinal natural period. Figure 6.28p, q, shows the longitudinal motion, that is, the pitching and heaving amplitude at the bow of a conventional catamaran at a model speed of 2.1 m/s and 4.2 m/s, respectively (equivalent to 19 knots and 38 knots for real craft), and Fig. 6.28r, s shows the same condition, however, for the semi-SWATH.

From the figures one can see that for the conventional catamaran, the pitching natural period of the model increases from 1.1 to 1.9 s, as the model speed increases from 2.1 to 4.2 m/s. However, on a semi-SWATH, the pitching natural period increases from 1.7 s to a greater value of about 7 s and cannot be predicted precisely due to the very heavy damping.

At the same time, from Fig. 6.28t [15], one can also see that on the semi-SWATH type HSS1500, the pitching natural period increases at high speed (40 knots) to as high as 13 s, compared with 5 s for the conventional catamaran at the same speed. This could be due to the S shape of the body plan on the semi-SWATH, particularly at the bow. From this viewpoint, a craft with fully semi-SWATH will have better seakeeping quality compared with a partly semi-SWATH configuration, which has been verified in tests [18, 19].

In the case of operation in irregular waves, since the semi-SWATH natural pitching frequency at high speed is reduced further at speed compared with the wave encounter frequency, the craft is running in supercritical motion mode, that is, "platforming" operation, so as to reduce vertical acceleration, which can be shown both in the figures and actual results in the towing tank. During the experiments, the semi-SWATH model moved slowly in the vertical direction when at high speed in head seas owing to the high damping coefficient and longer natural period.

6.6.3.5 Changes in Motion Damping and Response at High Speed

In irregular seas, a 54-m-long semi-SWATH running at high speed (38–40 kn) in head seas would encounter wave lengths of L to 2 L, that is, 54–108 m at an

encounter period of 1.8 to 3.2 s; however, both the pitching and heaving natural period for the vessel will be 16–20 s. The vessel motion response at 1.8–3.2 s will therefore be very low, even if this is the peak of the wave energy spectrum as in sea states 2 to 4, as would be experienced by typical ferry vessels. Figure 6.28u shows the pitching response ϑ/ς_0, that is, pitching amplitude (degrees) per wave height (m) versus wave period ω of the model mentioned earlier, where Δ, $\times$ represent the model speed at 20 and 38 knots, respectively. One can see that the pitching amplitude peak is at a wave period of 8.5 s, speed 38 knots, while the encounter wave period is 3.4 s of a real ship, much less than the pitching period 29 s. Because the peak is not close to the resonance period but induced by a large wave length ($\lambda/L = 2.1$) and another peak induced by the resonance of the period will be at a wave length ratio as high as 5, the irregular wave excitation is where the wave power spectrum is very low.

It is clear from this work that the use of a restricted waterplane can generate significant improvements for vessel motions in a seaway as long as the size of the vessel allows the Froude number to be in the displacement or semiplaning region at high speed. We will go further into this in Chap. 9 and Chap. 8 to a certain extent considering the balance between vessel motions and resistance.

6.6.3.6 Oblique and Beam Sea Motion Response Characteristics and Improvement Measures

The theoretical calculation for catamaran motion response in waves was described in a previous section of this chapter. However, since the demihull separation for a high-speed catamaran is usually large, normally the added mass and damping moments around the demihull centerline used in Eq. (6.6) can be neglected, that is, $\lambda_\theta = 0$, $\nu_\theta = 0$, $q_\lambda = 1$, $q_\nu = 1$. Thus, the roll motion calculation, just like the longitudinal motion discussed earlier, can be carried out using the strip method, and the interference effect of demihulls in the calculation of roll motion can also be neglected owing to the large separation.

Thus, with respect to the technical issue of demihull separation affecting the roll (and heave) motion, the issues here are not interference of demihulls, but the wave perturbation moment (force) on the roll and heave, just as for longitudinal motion. For instance, if the wave length is equal to the separation of demihulls in beam seas, the perturbation moment of waves will be equal to zero, so the roll amplitude will also be equal to zero, while the heaving motion will be at its maximum. In contrast, if the wave length approaches infinity, the roll amplitude will be equal to the wave steepness, just as for longitudinal motion.

Alberto Francescutto [23] carried out experimental investigations of roll motions of catamaran models with three different separations: S_1/L_{WL}, S_2/L_{WL}, S_4/L_{WL}, equal to 0.195, 0.28, 0.504, respectively, as shown in Fig. 6.29d, and obtained test results as shown in Fig. 6.29a–c.

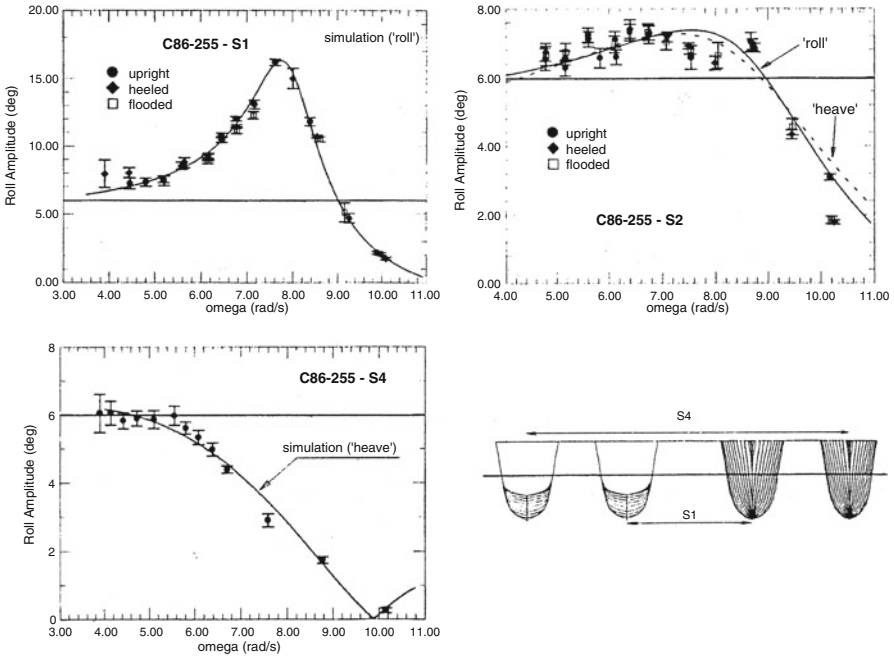

Fig. 6.29 Roll motion amplitude C86-255 versus wave frequency at separation: (**a**) S1; (**b**) S2; (**c**) S4; (**d**) hull spacing

From the figures some observations may be made:

- In the case of small separation shown in Fig. 6.29a, the experimental roll motion amplitude versus frequency for the catamaran model C86-255 in all tested conditions with hull separation S_1 is close to the theoretical projection (solid curve). The horizontal solid line represents the low frequency limit. The test results show a resonant response at around 7.5 rads/s. The response does not die away to the zero low frequency end, indicating that interaction effects between the hulls may be influencing the response.
- In the case of the largest separation, $S_4/L_{WL} = 0.504$, as shown in Fig. 6.29c, the peak roll amplitude response has disappeared, and the maximum roll amplitude is approximately equal to the low frequency limit (wave slope). In the case of wave frequency equal to 9.9 rad/s, where the wave length is just equal to the hull separation, the roll amplitude is equal to zero, that is, both demihulls are supported on the wave peaks or troughs, and in such cases, the heave amplitude will be at its maximum.
- Figure 6.29b shows the middle condition of panels a and c, mentioned earlier.

An increase in hull separation causes a decrease in roll motion, so one can say that the decision on hull separation will be made on the basis of the transverse motion,

not the longitudinal motion, of a catamaran at high speed, Fr_L, slender demihulls, and also in terms of predominant wave direction and energy spectrum at which the high-speed catamaran is operated. A larger separation certainly appears from these results to have advantages where open sea operation is concerned, and perhaps this is why it is adopted on modern high-speed passenger-car ferry catamarans.

Three different loading conditions of the models for the tests were also carried out for each hull spacing S_1, S_2, and S_4, that is, an intact ship in an upright equilibrium condition, an intact ship in a heeled state due to asymmetric loading, and a "damaged" ship in a heeled state due to asymmetric flooding. The test results show the same tendency of roll motions in waves, as shown in Fig. 6.29a–c.

Roll motion tests of a semi-SWATH and a comparison with the conventional catamaran at zero speed and in beam seas were also carried out at MARIC, as shown in Fig. 6.28n, o. From the figures one can see that the roll amplitude decreases by about 10–15% compared with the conventional catamaran in irregular waves, and vertical acceleration reduced by about 25–30% owing to the increase in the roll natural period of the semi-SWATH, even though the roll damping coefficient may be decreased owing to the hull lines.

Table 6.5 shows the maximum roll amplitude (degrees) of the MARIC semi-SWATH catamaran calculated in irregular seas with a certain wave average period, different wave directions, at speeds of 38 and 20 knots, with a significant wave height of 2 m [19].

This compares with equivalent maxima of approximately 6.25° for 96-m catamaran and 4° for a 102-m trimaran calculated by Armstrong and Morretti in reference [24]. It is apparent that the roll angle of a catamaran is larger than that of a trimaran. The catamaran roll angle might be reduced by expanding the hull separation, as shown previously; however, it will come at the cost of increasing the structural weight.

Figure 6.30 [25] shows the results of an operability analysis carried out by Austal of three equivalent monohull, catamaran, and trimaran vessels, designed for 1000 t, in the Western Pacific area, for a selected number of motion criteria. The superior operability of the stabilized trimaran is clearly illustrated. From the figure one can see that the lower operability of the catamaran versus trimaran is mainly due to the motion response in beam and quartering seas.

Table 6.5 Maximum roll angle (degrees)

Wave direction	$V = 20$ knots	$V = 38$ knots
Head quartering	3.24	2.8
Beam seas	6.7	6
Follow quartering	4.1	3.6

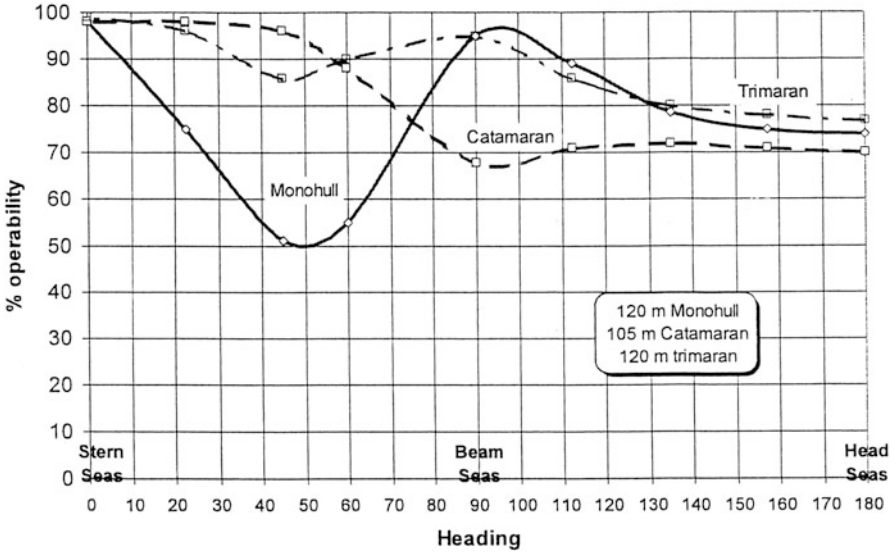

Fig. 6.30 Operability versus heading

6.7 Motion Characteristics of Catamaran Forms in Oblique Seas

Study of catamaran motion operating in oblique seas is very important since in some cases the vessel motion and vertical acceleration in bow quartering seas might be higher than when operating in head seas. This is due to the coupled longitudinal and transverse motions, and the similar pitching and roll natural periods, causing higher vertical and lateral accelerations and seasickness.

Davis and Holloway (University of Tasmania, Australia) carried out both theoretical investigations and empirical tests [26] on a model of an 80-m-LOA catamaran using hulls similar to the full-scale Incat 86-m WPC vessel, as shown in Fig. 6.20, to obtain the influence of wave height and two demihull separations on the vertical accelerations of the model and projected passenger motion sickness incidence (MSI).

Projections were made for acceleration at the bow, amidships, and stern locations in sea states up to 5 m significant wave height in head, oblique, and beam seas, and an estimate of MSI was calculated from the accelerations. It was found that the MSI was reduced when demihull separation increased from 20 to 40%, as shown in Table 6.6 indicating results in 1- and 3-m seas, particularly in oblique 120° waves, and wave height 1 m, when it is about three to five times lower due to the decrease of roll amplitude.

Table 6.6 MSI in percentage with different demihull separations

Significant wave height, m	1 m	3 m	1 m	3 m	1 m	3 m	1 m	3 m
Wave course, °	180	180	150	150	120	120	90	90
MSI (%), at bow,								
40% separation/	10	75	9	60	6	36	0.7	5.5
20% separation	12	78	15	75	22	60	2.2	11
MSI, at LCG								
40% separation/	9	60	8	43	3	3	0.3	4
20% separation	12	70	12	60	16	45	1.5	8

In the case of small and oblique seas (120°), the MSI will be as high as in head seas, particularly at 20% separation, owing to the increase in roll amplitude; furthermore, it is amplified by an increase in pitching angle related to an increase in the effective wave length, at which the wave peak energy is located. Thus, at a small wave height, the captain would find it best to change the navigation course from oblique (bow quartering seas) to head seas, but not in large waves, as shown in Fig. 6.31.

In general:

MSI increases with wave height;
MSI is highest at the bow;
MSI is lower in beam seas, particularly in the case of large separation (40% separation),

At the same time, Davis and Holloway [12] also carried out motion analysis using calculations for an 86-m WPC RoPax vessel at 38 knots, as shown in Figs. 6.32 and 6.33.

Figure 6.32 shows the predicted variation of dimensionless acceleration relative to wave height $\left(\ddot{z}_R = \ddot{z}_{rms} \bullet \frac{L_{WL}}{h_{w1/3}} \bullet g\right)$ with location, speed, and sea direction. The bars are left to right in each group in the order as listed in the legend. The figure shows the relative acceleration at many locations on the vessel. Figure 6.33 shows the predicted variation of motion sickness (MSI) also with location, speed, and sea direction, in terms of vertical acceleration and frequency of accelerations, but not including the effect of lateral acceleration.

From the figures, some features of the vessel seakeeping quality in oblique seas (bow quartering seas) may be observed:

- MSI increases with ship speed;
- At high speed, the maximum MSI still occurs in head seas, not in bow quartering seas. At low speed the maximum MSI may be off centerline in beam seas, as shown in Fig. 6.33;
- In general, the MSI of a high-speed catamaran is not large in beam seas compared with head seas;
- In bow quartering seas, the difference in MSI at different transverse directions of ships, that is, port, centerline, and starboard, are not obvious; however, this

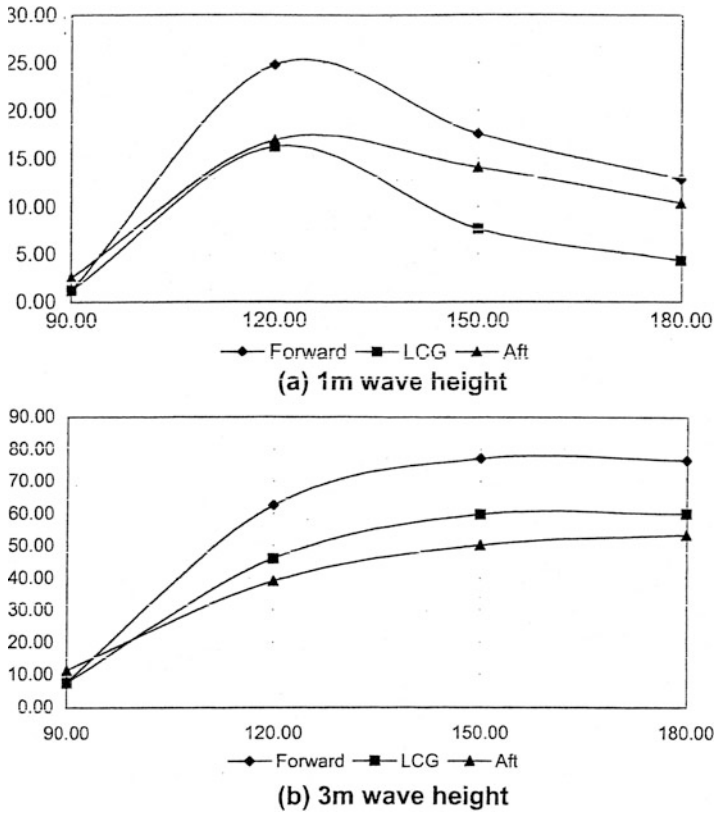

Fig. 6.31 (**a, b**) Variation of MSI with wave direction for two wave heights 80-m hull

demonstrates that the "corkscrew" effect on the high-speed catamaran (with high speed, high slenderness, and large separation of demihulls), though not remarkable, is still not clarified through this work.

6.7.1 Seakeeping Behavior of MARIC Semi-SWATH in Oblique Seas

Seakeeping model investigation of semi-SWATH motions in waves with different directions was also carried out at MARIC [18, 19]. Tables 6.7a and 6.7b below show a comparison of vertical acceleration at different locations on the vessel and in different wave directions. The measurement point of vertical acceleration at the bow center was taken as 1, and the table lists the ratio of vertical acceleration at various measured points with that at the bow center.

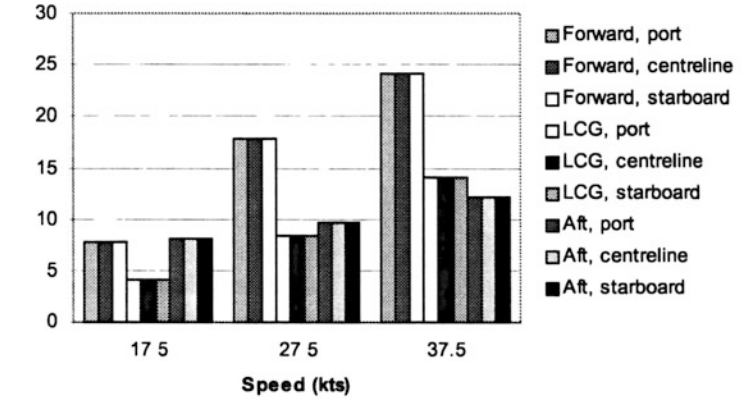

(a) Head seas

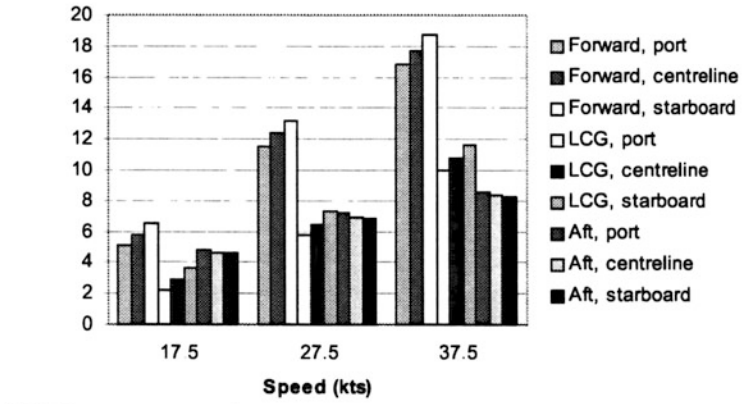

(b) Bow quartering seas

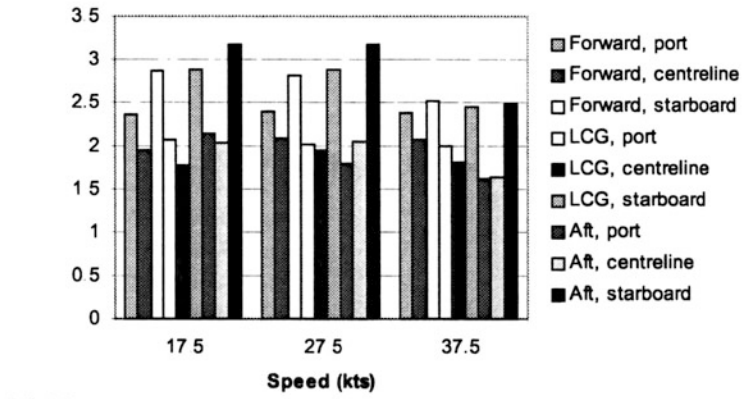

(c) Beam seas

Fig. 6.32 Dimensionless acceleration with direction of sea heading

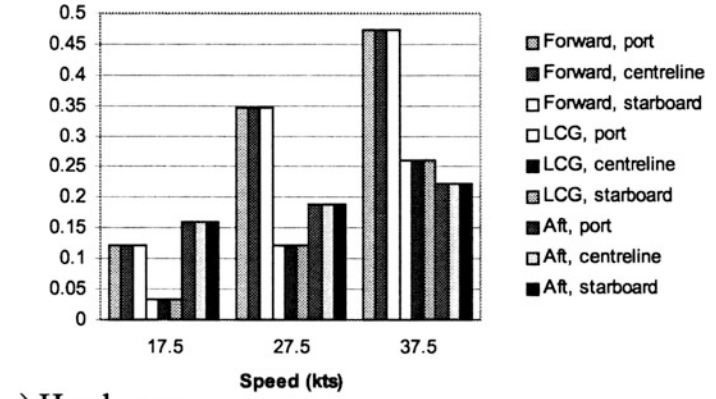

a) Head seas

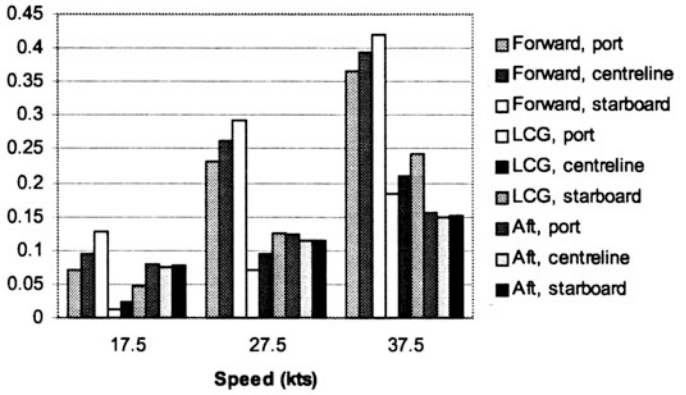

b) Bow quartering seas

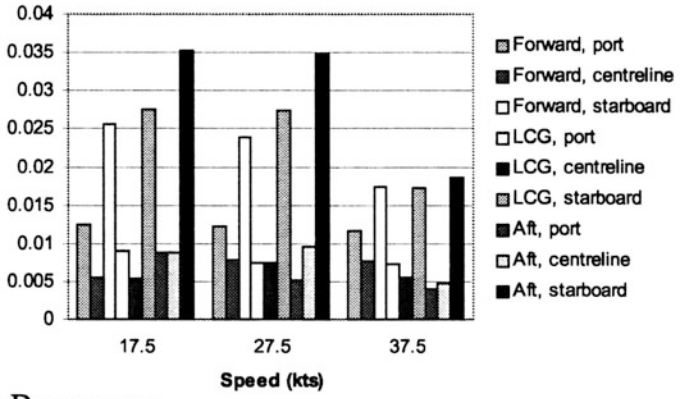

c) Beam seas

Fig. 6.33 Predicted MSI with seas direction

Table 6.7a Craft speed 38 knots, significant wave height 2 m, and vertical acceleration ratio

	A1	A2	A3	A4	A5	A6
Head seas	1	1	1.3	–	–	–
Bow quartering	0.83	0.75	1.14	0.89	0.73	0.98
Beam seas	–	–	0.39	–	0.59	–
Stern quartering	0.107	0.18	0.214	0.16	0.22	0.23
Following seas	0.58	0.143	0.57	–	–	–

where $a_{1,2,3,4,5,6,}$ represent measure points located at bow center A1, midcenter A2, stern center A3, bow port side A4, mid port side A5 and stern port side A6 respectively.

Table 6.7b Craft speed 20 knots, significant wave height 2 m, vertical acceleration ratio

	A1	A2	A3	A4	A5	A6
Head seas	1	0.93	2	–	–	–
Bow quartering	0.72	0.84	1.33	0.69	0.93	1.47
Beam seas	–	0.55	–	–	0.73	–
Stern quartering	0.187	0.25	0.33	0.33	0.32	0.45
Following	0.26	0.13	0.28	–	–	–

From the table, some points can be observed as follows:

In the case of both speeds, at 38 and 20 knots, the vertical acceleration of the model in head seas is still highest compared with other wave directions.

In the case of 38 knots:

- The acceleration at the stern is greater than at the bow, which is characteristic of this model, which can be improved by means of adjusting the LCG and LCB;
- Acceleration in following seas is better;
- Vertical acceleration in beam seas does not seem bad, probably owing to the larger hull separation of this model; however, the roll angle is larger, which may influence the operability.

In the case of 20 knots:

- The vertical acceleration at the stern port in bow quartering seas is higher owing to the superposition of both longitudinal and transverse motions; in addition, in this case, the encounter wave period (7.6 s) is close to both the natural pitching period (7.46 s) and the roll period (5.68 s) to encourage resonance and corkscrew motion.

With respect to the corkscrew problem, this will improve on a semi-SWATH at high speed (40 knots) due to the following factors:

- The difference between pitching and roll response will be increased at high speed because of the increase in the pitch damping, so as to alleviate the corkscrew motion;

- The roll amplitude of the semi-SWATH is reduced due to a large hull separation, with the consequence that roll acceleration will also be reduced;
- The pitching acceleration of the semi-SWATH also decreases at high speed owing to the supercritical operation, as mentioned earlier in the chapter.

According to the vertical acceleration test results mentioned, it seems that the corkscrew phenomenon, which influences motion sickness, only happened on the semi-SWATH at lower speed (20 knots) but not at high speed (38 knots) owing to the lower vertical acceleration of the craft in oblique seas compared with head seas. This is predicted by ISO 2631, so the vertical acceleration was taken as the main criterion for predicting motion sickness, but the other motion parameters, particularly lateral acceleration, roll angle, and velocity, were not considered.

According to [27], the authors of this paper used a new approach to predicting motion sickness in ships using all six degrees of freedom. In addition, full-scale trials were carried out on board two different high-speed vessels, a monohull and a catamaran, in order to measure motions and their effects on passengers and possible motion sickness. The accumulated results were compared with existing methods and criteria for the prediction of MSI as well as with the newly developed and validated six-degree-of-freedom time domain model that was based on sensory conflict theory incorporating information about the human motion sensory system.

From the investigation, they obtained the following findings:

- Using ISO criteria for predicting the MSI for a high-speed catamaran underpredicts real craft conditions. The full-scale tested MSI value is 70–80% higher than the value predicted by ISO.
- The test results for a conventional monohull is close to the ISO predicted value.

Using the model with six degrees freedom as in [27] is therefore more precise than using only one parameter (vertical acceleration) as defined by ISO for predicting MSI, particularly for high-speed catamarans. This is likely because of the more complex motion of a catamaran with combined pitch and roll at similar frequencies and the combination of directions helping to aggravate human sensory perception.

The MSI on a semi-SWATH will be improved compared to a normal catamaran since the accelerations in both directions will be lower for a given sea state. There will still be influence from lateral accelerations at similar frequencies on a SWATH, so the tendency will still be along the same lines as the catamaran. Further investigations, both on models and real vessels, on the prediction of MSI considering more motion parameters, including the influence of roll angle, velocity, and lateral acceleration, will be helpful to optimize semi-SWATH design.

It may be noted that the motions on the Stena HSS semi-SWATH on voyages between Hook of Holland and Harwich across the southern North Sea did not seem to exhibit significant corkscrew motion, at least in the experience of author Bliault, who had cause to use the service regularly in the mid-1990s. Personal experience with this vessel was relatively comfortable, with more attention paid to the various restaurant facilities and the cinema on board.

6.8 Motion Characteristics in Following Seas

As far as SWATHs are concerned, there are two disadvantages faced by the designer: possible plough-in (bow pitch down) in following seas, and the requirement for precise calculation of load distribution in the longitudinal direction. To avoid plough-in at high sea states and following seas, active control systems for controlling the fins located at both the bow and stern of a SWATH need to be installed on the craft.

Similarly, on a semi-SWATH, the S shape of the body plan with constrained waterline area at the bow will lead to lower static longitudinal stiffness. Therefore, some measures are suggested for consideration in the design as follows:

- Use a flared body plan at the bow above the waterline to reduce the tendency toward plough-in in following seas, and verify this in model tests;
- Antispray rails may be mounted in the bow area nearby and slightly over the design waterline for spray deflection and to protect the hull against plough-in in following seas. This has been tested at MARIC, and satisfactory results were obtained.

  Such spray rails were also mounted at the sidewall of an SES, with three rows vertically, both at the inner and outer sides of the sidewall at the bow, combined with a responsive bow skirt, and gave an excellent seakeeping quality without plough-in for the full-scale craft in operation for a number of years [28].
- Installing a ride control system [29] may be the best way to improve seakeeping quality; however, this results in high costs and a more complex structure owing to the induced local loadings that must be distributed to the hull shell and internal primary structure.

References

1. Matsui S (1993) The experimental investigation on resistance & seakeeping quality of high speed catamaran. In: Fast'93, Yokohama, Japan
2. Batuyev AD. Characteristics of rolling motion on catamaran, Shipbuilding, No. 8, 19
3. Zhao LE et al (2000) High performance marine vehicle-its hydrodynamic principle and design. Harbin Engineering University Press, China (in Chinese)
4. Zhang M et al (2001) High performance marine vehicles in 21st century. China Defense Industrial Press, Beijing, China, July 2001, (in Chinese)
5. Gu MX (1964) Rolling motion of ship, Press of Harbin Military Engineering Academy of China (in Chinese)
6. Wellicome JF et al (1995) Experimental measurements of the seakeeping characteristics of fast displacement catamarans in long crested head seas, Ship Science Report 89, University of Southampton, UK, Dec 1995
7. Michael R, Davis et al (2003) Motion & discomfort on high speed catamaran in oblique seas. Int Ship Prog 50(4):333–370
8. Holloway DS, Davis MR (2003) Experimental seakeeping of Semi-SWATH at High Froude Number. In: Proceedings of RINA

9. Gerritsma J, Beukelman W (1967) Analysis of the modified strip theory for the calculation of ship motion and wave bending moments. Int Shipbuild Prog 14(156)
10. Tao YS et al (2000) A discussion on Seakeeping prediction method in ship optimization design. J Ship Mech 4(2). China (in Chinese)
11. Tao YS et al (1996) Seakeeping Quality of Ships. Shanghai Jao-Tong University Press, China (in Chinese)
12. Davis MR, Holloway DS (2003) Wave response of an 86m high speed catamaran with active T-foil & stern tabs. In: Proceeding of Royal Institute of Naval Architects
13. Liu SH, Yun L et al Research reports on Semi-SWATH crafts, MARIC, 2006–2009, Shanghai, China (in Chinese)
14. Gee N (2005) The X-craft – A potential solution to littoral warfare requirements. In: Proceedings, HPMV Conference, Shanghai, China
15. Stena Reports on 18 Months of HSS 1500 Service and Concept Design, Fast Ferry International, Nov 1997
16. Car Ferry Design Unveiled at Exhibition, Fast Ferry International April 1994
17. Schack C (1995) Research on Semi-SWATH hull form. In: FAST 1995, Third International Conference on Fast Sea Transportation, Travemunde, Germany, Vol 1, pp 527–538
18. Liu SH, Yun L, et al (2010) A high speed ferry catamaran with semi-SWATH configuration-an additional science report. In: Proceedings of HPMV International Conference, Shanghai, China, April 9, 2010
19. Test Report of Semi-SWATH models in Towing Tank, Shanghai, Ship & Shipping Research Institute, Ministry of Communication of China, 2008
20. Keuning A (2001) The effect of bow shape on the seakeeping performance of a fast monohull, FAST
21. Kracht A (1978) Design of bulbous bows. Transactions of Society of Naval Architects and Marine Engineers, New York
22. Royce R (2005) Bulbous bow resistance reduction of semi-planing vessel, FAST
23. Francescutto A et al (2001) Dynamic stability and roll motion modelling of multihulls, FAST 2001, Southampton, UK
24. Armstrong NA, Moretti V (2010) The practical design of a 102m trimaran ferry for Taiwan strait. In: Proceedings, Shanghai HPMV Conference, April, 2010, Shanghai, China
25. Armstrong NA (2003) A new generation of large fast ferry from concept to contract. In: Proceedings, FAST
26. Davis MR, Holloway DS (2003) Effect of sea ride controls , hull form and spacing on motion and sickness incidence for high speed catamarans. In: Proceedings of Seventh International Conference on Fast Sea Transportation (FAST 2003), Ischia, Italy, Section E, pp 1–10
27. Vesveniotis CS (2003) Prediction of motion sickness in high speed craft, University of Glasgow, Strathclyde, UK, Proceedings, HPMV, Shanghai, China
28. Yun L et al (2007) The Evolution of SES-from thin sidewall to air cushion catamaran, Science report, MARIC, China
29. Shigohiro R Evaluation method of ride control system for fast craft from the viewpoint of passenger comfort. In: Proceedings of the 7th International Conference on Fast Sea Transportation, FAST'03, Ischia, Italy, Paper: P2003-7, ISBN: 99-901174-0-0

Chapter 7
Principal Dimensions and Design

7.1 Introduction

Our aim in this chapter is to take you into the second round of the design spiral. Previous chapters introduced some basics, so that you should have been able to set out your vessel mission and, based on that, select initial dimensions or a range of potential dimensions and characteristics from which to home in on a design to detail out and refine.

So far we have looked at static stability based on an initial line plan and sample regulations to check against. We followed this with wave-making theory and an analysis of resistance components that we can use to verify our initial vessel configuration and lines. Finally, we looked at equations of motion and seakeeping estimation derived from these.

While the initial configuration might be based on an existing vessel or vessel series, we have not gone through a rigorous check based on an estimation of the weights and centers for all the major elements making up a vessel. The initial data sheet may have included some data but will necessarily have been at a summary level. Now we need to move down a level of granularity toward detailed weight and center estimates for all the major items and recheck that the vessel displacement matches. If this is a close match, we can move forward to detail the design of the hull and superstructure, verifying as we go along that the design remains within the programmed allowances and margins. An outline of our design process is shown on the next page, Fig. 7.1, expanded from the overall roadmap in Fig. 2.14.

At this stage it is useful to remember that it is also important to cross check with your potential client or clients to find out what their priorities are. You will then be able to direct your refinements to meet those priorities.

In the first part of this chapter we review a number of operational design parameters for catamaran and multihull vessels such as seaworthiness, safety, and environment that interact with constraints on vessel dimensions. We will then continue with regression analysis from a relevant sample of existing catamaran

L. Yun et al., *High Speed Catamarans and Multihulls*,
https://doi.org/10.1007/978-1-4939-7891-5_7

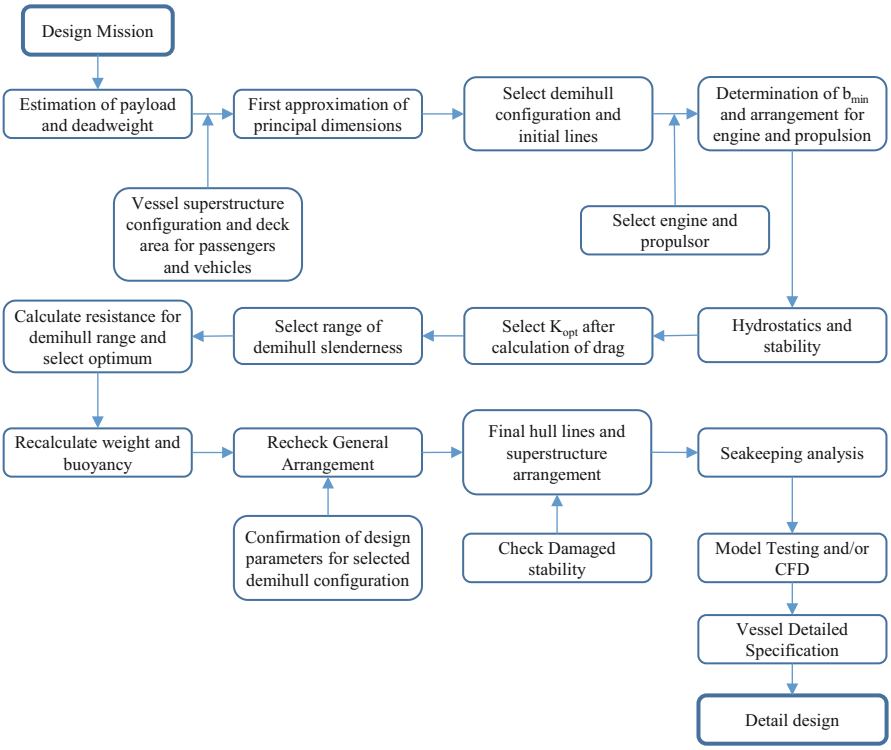

Fig. 7.1 Concept design flowchart

ferries and some data from larger fast monohull ferries. We will discuss what these data suggest to us when preparing the design for a new vessel and the directions our design may take depending on the mission that we have for our design.

This input can then be used together with analysis following the approach in Chaps. 3, 4, 5, and 6 to develop the vessel design and start the optimization spiral before going into detailed design aspects such as structural design, mechanical and systems design, internal outfitting, and finally design for construction linked to the capabilities and techniques available at the boat or shipyard selected for the build. Design for construction is normally a cooperation between the naval architect and the shipyard aimed at optimizing delivery against quality and target cost.

At some stage it may be necessary to carry out model testing of the new vessel design to verify the assumptions made, at least for larger vessels. If the vessel is small, then the prototype can be used as a full-scale testbed, and modeling of the design in CFD programs utilized instead as a means to optimize the hull form as far as possible before building the prototype.

7.2 Design Characteristics and Limitations

To recap from Chap. 2, the methodology for the design for high-speed catamarans is similar to that for other high-performance marine vehicles that the authors have described in [1] and [2]. The design process is summarized at a high level in Fig. 2.14 and at the next level down in Fig. 7.1. The starting point is the design brief or mission requirement for the client operator. Key elements are the service speed, service route and range or environmental envelope, payload mass, volume and distribution, and seaworthiness requirements, including the requirements for the transverse stability and damaged flooding resistance demanded by classification societies and the IMO. This last aspect was covered in Chap. 3.

Some vessels have additional requirements, such as draft limitations, external wave making and wash, noise, and vibration. We discuss the impact of each of these in what follows.

After defining the key attributes to satisfy the mission in an initial data sheet (Appendix 2), it is useful to consider other issues that will affect the vessel dimensions, mass, center of gravity, and so forth.

The outfitting will have a significant influence on the configuration, for example, if LNG is used as fuel for the main engines or if the installation of powered ramps and door closures for vehicles and for passengers is necessary, as well as the configuration of the superstructure as such. Military vessels also have requirements for "battle hardening" core areas of the hull and superstructure as well as offensive and defensive weapons outfitting.

A little further along the design spiral, auxiliary electrical power generation and distribution, HVAC, noise and vibration dampening, and instrumentation and control systems all have to be considered, as we introduce in Chap. 13.

The key at this stage of a project is to identify all the possible "knowns" and include these in volume, weight, and CG calculations either as specific data or as a specified part of the design allowances or margins. That way, later on in the process, "surprises" will be avoided. Such surprises are usually negative for the project outcome, since they usually come with project cost increases, reduced vessel capability, and delayed delivery. As a starting point, a check list is presented below for items to consider and use to add detail to the second vessel data sheet (Appendix 2). This is not meant as a complete list but rather as a means to trigger the designer's thought process. The challenge that a designer faces in the initial stages of a project is that, often, to keep things simple, it is easier to have global growth allowance and estimation margins. While these are needed, it is best to minimize them by being as specific as possible about the components required. State the requirement, make a rough estimate of the weight and location, and identify an uncertainty band. This rigor can help in discussions with the client to manage expectations, while reducing estimation and growth margins down to the 10% to 20% level, which can be handled in a typical project management environment.

It is often the case that at the start of a project, many of these issues may not be clear, and so taking a simplistic approach, as discussed in Chap. 2, is the best means

of making a start. After the first round of initial specification and performance estimation, now is the time to go deeper and try to identify as complete a list as possible and be clear with the client that further additions may not be practical. The end result of this exercise may be a need to revisit the initial vessel lines so as to adjust to accommodate the main engines and power train, for example. A revisit of Chap. 2 will usefully wait until you have checked out the various relationships in this chapter so as to adjust to all the influences in a coordinated way.

At this stage much of the detail referred to here is covered by comparison with statistics from existing vessels. Since this is an approach based on generalized statistics, it is important that a designer note any special items required for their vessel as in Table 7.1 and consider the weight or space requirements as an additional factor when comparing against existing vessels, unless review of the existing vessels used for comparison shows they have the outfit as a standard. For example, if the vessel requires special hydraulically operated vehicle ramps and doors to access quay facilities available along the service route, then the mass should be added in as fixed payload or the effective cargo payload reduced to compensate.

Table 7.1 Memory jogger for special outfit requirements

Item	Description	Special requirement
1	Active roll stabilizer	Stabilizer fin installation and hydraulic power
2	Bow hydrofoil stabilizer	Support structure, hydrofoil, power system
3	Stern trim flap or interrupter	Flap or interrupter, support structure, power system, control system
4	Special storage space and payload	Space for bicycles, skis, children's prams or other outsize passenger luggage, or small freight packages
5	Docking interface	Measure quayside, vehicle ramps, and so forth for fit dimensions with vessel stern specification
6	Open deck at bow	Deck arrangement for docking crew, and passenger access including hydraulic ramp
7	Open deck at stern, each side	Deck arrangement for docking crew with mooring equipment and personnel ramps Access to area for passengers for fresh air?
8	Vehicle hydraulic ramp	Ramp, support structure, power, local controls, instrumentation to bridge
9	Personnel hydraulic ramp	Ramp, support structure, power, local controls, instrumentation to bridge
10	Lift	Personnel or freight lifts to cabin levels from vehicle decks
11	Anticollision outfit	Radar
12	Outfit for night operation	Radar, sonar, low-light vision system
13		
14		
15		*Add other key information to check*
16		*And ensure data sheets are complete*
etc		

It is not possible to define everything at an early stage, so some design development allowances and margins to cover estimation accuracy are also needed. Once a prototype has been built, these items can all be revisited with a view to optimizing them for a production series or standardized stock design. The allowances and margins need to be recorded in the vessel design data sheet for reference and adjustment as the design progresses so the data sheet should be managed as a "live" document.

We will begin with a summary of factors that influence catamaran performance and then present the regression data from existing vessels as a guide to check the initial estimates of dimensions and form. These will build on the initial geometry and static design parameters discussed in Chaps. 3 and 4, as indicated earlier in Fig. 7.1 showing the design process we follow. We will track the steps of this process through the rest of the chapter.

7.2.1 Seakeeping and Motion Tolerance

The motions that are tolerable to passengers can be characterized by the RMS values of vertical acceleration, rolling and pitching angle, and the tolerable exposure period of passengers to the motion. The most widely used standard for acceptable motions limits is ISO Standard 2631.

Figure 7.2 shows the severe discomfort boundaries for passengers on board. The limitations specified in ISO 2631 are a function of vertical acceleration, motion frequency, and the tolerable exposure period.

Figure 7.3 shows the effect of motion and acceleration on decreased working efficiency due to personnel fatigue and discomfort or motion sickness for passengers. The left side of the figure shows the limitation to avoid motion sickness for passengers and crews, and the right shows fatigue-decreased work efficiency. The limitation of vertical acceleration is also a function of frequency and tolerable time duration.

The limiting sea conditions for passenger comfort for a 28-m high-speed catamaran named *Prinsessen*, operated at a speed of 25 knots for a half hour along the coast of Norway, are shown as an example in Table 7.2. The vessel motion limits are based on the criteria of ISO 2631 as illustrated in Figs. 7.2 and 7.3 and detailed in Table 7.3.

When the design of a new catamaran is carried out, seakeeping analysis is necessary to predict the rolling and pitching angle of vessels in various wave directions and speeds, vertical accelerations, including possibly accelerations due to bow immersion in the waves and slamming, and so forth. Using seakeeping analysis and a comparison with the limits from ISO 2631 [3], the operational limits for comfort and safety can be set, similar to the example in Table 7.2 and criteria in Table 7.3.

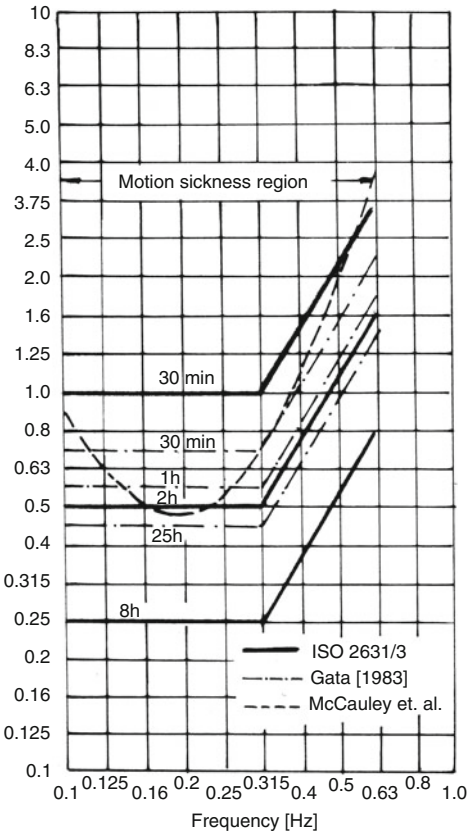

Fig. 7.2 Severe discomfort boundaries

Key to numbers in diagram

1. Body Resonance, 4 to 8 cycles/sec
2. Negligible response at this acceleration
3. Light response
4. Medium response
5. Serious response
6. Frequencies experienced when working and running
7. ISO Criteria for exposure over 8 hours, high frequency
8. ISO Criteria for exposure over 1 hour, high frequency
9. ISO Criteria for exposure over 1 minute, high frequency
10. ISO Criteria for exposure over 8 hours, low frequency
11. ISO Criteria for exposure over 2 hours, low frequency
12. ISO Criteria for exposure over 20 minutes, low frequency
13. Low frequencies creating discomfort
14. High frequencies creating fatigue and reduced focus

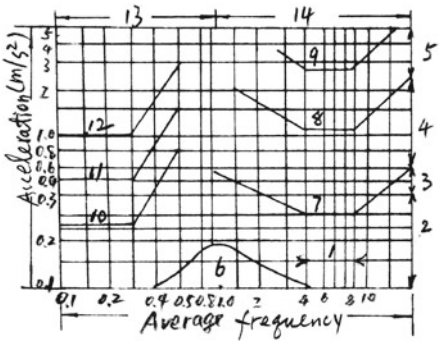

Fig. 7.3 Effect of motion on physiological response: comfort and fatigue

Table 7.2 Limitation of comfort for passengers on HSCAT *Prinsessen* of Norway

Wave direction	Significant wave height, m	Vessel motion	Suggested max. speed
0° (head waves)	1.2	Vertical acceleration	Service speed (25 knots)
45°	1.1	Vertical acceleration	Service speed
90°	1.2	Rolling motion	Service speed
135°	2.0	Rolling motion	Service speed
180°	2.3	Pitching motion	Service speed

Table 7.3 Comfort and safety limitation for high-speed vessels

Limitation	Motion	Value	Comment
Passenger comfort	Vertical acceleration at CG	0.15 g (RMS)	1 h operation at 1 Hz
	Pitching	1.5° (RMS)	
	Rolling	2.0° (RMS)	
Passenger safety	Vertical acceleration at CG	0.27 g (RMS)	0.5 h operation
	Lateral acceleration	0.1 g (RMS)	0.5 h operation
	Pitching	2.0° (RMS)	0.5 operation
	Rolling	4.0° (RMS)	0.5 operation
	Lateral acceleration	0.15 g (single amplitude)	Max. value for person standing
	Lateral acceleration	0.25 g (single amplitude)	Max. value for person standing but holding rail
	Lateral acceleration	0.45 g (single amplitude)	Max. value for person sitting
For structural design and safety of vessels	Vertical acceleration (at CG)	1.0 g (max. value) 0.33 g (RMS)	Normal design limitation
	Pitching and slamming	Bow down, immersed in water	In terms of, e.g., ship design, speed, and wave direction

To avoid, or at least minimize, the torsional oscillating motion on a catamaran in oblique seas, both pitching and rolling natural period have to be predicted, and to avoid torsional motion, a large difference between them is recommended.

Table 7.4 shows the acceptable acceleration levels from ISO, and the roll and pitch angles based on NATO requirements for military vessels and STANAG 4154 [4] for normal operation. The recommended design extreme motion limits for crew and helicopters on military vessels are shown in the following Table 7.5. These data will affect the approach to operational envelope for a military vessel and requirements for speed reduction in severe weather during a deployment.

Table 7.4 Recommended limits for RMS accelerations based on IMO HSC, ISO, and NATO standards

Item	Location	Referred standard	Standard type/units and Limiting value,	RMS
1	CG	ISO passenger health	Vertical acceleration/g	0.20
2	Deck	HSC code normal operation	Lateral acceleration/g	0.07
3	CG	STANAG personal limit	Roll angle/(°)	4.00
4	CG	STANAG personal limit	Pitch angle/(°)	1.50
5	CG	ISO passenger safety	Vertical acceleration/g	0.25
6	Deck	HSC code worst condition	Lateral acceleration/g	0.115
7	CG	STANAG personal limit	Roll angle/(°)	4.00
8	CG	STANAG passenger safety	Pitch angle/(°)	2.00
9	CG	ISO comfort (1/2 h)	Vertical acceleration/g	0.10
10	Deck	ISO comfort	Lateral acceleration/g,	0.025

Table 7.5 Motion limitation for surface naval ships [1, p. 369]

Subsystem	Motion	Limitation (significant single amplitude)	Location
Crew	Roll	8°	LCG
	Pitch	3°	LCG
	Vertical acceleration	0.4 g	Bridge/wheelhouse
	Roll	3°	Bridge/wheelhouse
Helicopter	Roll	5°	LCG
Helicopter	Pitch	3°	LCG

Having presented the preceding data setting-out criteria, the question for a designer is how to respond. Initially, once the vessel lines and initial estimates of seakeeping response have been made, by reference to the approach in Chap. 6, a number of alternatives are available.

If the vessel response is favorable, or close to favorable, for the mission criteria, it may be possible to adjust the lines or demihull spacing to improve towards the target. If the acceptable motions require reduced service speed, which would impair mission success, three further options may be considered:

- Install dynamic control surfaces such as bow-mounted stabilizing foils
- Consider adjusting hull geometry toward semi-small-waterplane-area thin-hull (SWATH) and wave-piercing forms
- Consider more radical hull geometries such as the trimaran form

We discuss the wave-piercing and SWATH forms in the next chapters and control surfaces under appendages in Chap. 11.

7.2.2 *Design for Safety*

Safe operation is a most important criterion for high-speed catamarans as the consequences of an incident at high speed can be very serious both to the vessel itself and to other vessels. In locations such as Hong Kong, traffic is heavy both during the day and at night, when conditions for navigation are more difficult.

According to a statistical analysis of marine accidents in Norway, almost 85% of casualties in incidents are related to vessel collision and groundings due to off-course navigation. A significant proportion of fast ferry accidents in other parts of the world have been due to collisions in fog or low visibility conditions while operating in busy traffic locations such as the Hong Kong area or collisions with quayside structures due to problems with docking control.

The designer of high-performance marine vessels therefore needs to ensure the design has appropriate measures against damage due to grounding and collision. Clear requirements are specified in the rules and regulations of classification societies as well as the IMO [5]. Structural and subdivision requirements first come to mind and have a main impact on demihulls and cross structures. Important related requirements that affect the vessel layout, particularly passenger and vehicle spaces, are those associated with fire protection and passenger and crew evacuation.

The human factor is an extremely important one influencing vessel safety. This aspect relates to bridge design, including field of vision, ergonomics, instrumentation including navigation aids, and communications outfitting. Additionally, the facilities to ensure passenger safety are critical.

Key technical factors for ensuring safety are as follows:

- Appropriate navigation equipment (e.g., radar, radio, navigation devices, night vision instruments);
- Seats conforming to safety regulations including seat belt restraints as appropriate;
- Internal outfitting including service spaces for passenger cabins that cater to typical usage rates during a voyage and provide comfortable lighting and atmosphere;
- Balanced general arrangement, including personnel evacuation routes and emergency equipment;
- Fire protection equipment;
- Adequate escape and rescue equipment;
- Ergonomics and efficiency for the wheelhouse and its equipment;
- Clearly defined operational guidelines and environmental limits for vessel operation and navigation covering the certified service envelope.

We discuss much of this list in Chap. 13.

Most technical measures and requirements are stipulated in the rules and regulation of classification societies and the IMO. The application of some of the aforementioned criteria is an issue of ongoing discussion among ship designers, owners, and shipping classification societies, including seat design and the application of seat

belts in the passenger cabin. If designers consider their project in terms of total value (total cost of ownership or TCO), it is generally wise to take a conservative approach, especially to safety-related issues, and simply look carefully at the cost of inclusion. This is because regulation continues to develop as experience is gathered.

Taking seats as an example, if seat belts are included, then the supporting structural design will have to account for the acceleration of the passengers on the seats via the seat belt attachments. Over any 20-year period typical for the replacement lifetime of a ferry or military vessel, safety regulations globally tighten, whereas if a vessel structure is not designed for seat belt loads, it is unlikely to be able to be upgraded even if the seats could be. In the meantime, the reduced operational stresses in the structure by taking a conservative approach will likely improve the fatigue resistance of the vessel structure, so that conditions at time of selling on can be demonstrated as more reliable.

Some operational standards for safety as shown in Table 7.6 should also be implemented for the projected vessel and checked in the design stage.

7.2.3 Restrictions on Overall and Demihull Beam

The demihull beam, particularly at the demihull stern half behind amidships, will be limited mainly by the main engine dimensions and propulsion configuration. From the point of view of drag, the demihull beam, particularly at the waterline, should be kept as fine as possible to minimize residual drag for catamarans in displacement mode. For vessels designed for higher speed in the semiplaning or planing region, it may be advantageous to have a wider stern waterline leading to a wider transom stern. This will also give more flexibility for the propulsion system installation.

The catamaran overall beam comprises two demihull beams and the separation between them. Hull separation will be affected by wave-making drag and design for the cross-structure transverse strength. Larger hull separation will reduce the wave interference drag but increase structure weight. In addition, for high-speed open-water catamarans, the influence of hull separation will be less, as described in Chap. 5, so the hull structural design and weight may be the controlling factors. The overall beam will also be influenced by port docking requirements, navigation route whether riverine or coastal, and the superstructure volume requirements for passengers and vehicles or freight.

The best approach to selecting demihull dimensions and overall vessel beam is to start with the mission requirements that define payload mass, deck area, and volume and then use the ratios for form presented in Chap. 2. The first turn of the design spiral can then be started by preparing a range of dimensions that appear to fit and test the static buoyancy and stability as in Chap. 3. Once this works, the basics of wave making and estimation of total resistance can be made as in Chaps. 4 and 5. We present an example of such a parametric analysis that was carried out by Prof. Rong of MARIC later in this chapter for guidance. At this stage, dynamics as in Chap. 6

Table 7.6 Safety standard

Safety standard		Criteria			Remarks
Influence level	Definition	g (nondim.)	Rate of change in g $(m/s^2)/s$	Kind of load	Guidance on consequence or mitigation
1	**No consequence**				
		0.08	0.2	Max. horizontal force	Can be balanced by seniors holding rails
2	**Low consequence**				
Low	Medium uncomfortable	0.15	0.2	Max. horizontal force	Can be balanced by ordinary person holding rail
High	Medium uncomfortable	0.15	0.8	Max. horizontal force	Person sitting has to hold rail as well
3	**Important consequence**				
Low	Safety decreased	0.25	2.00	Max. horizontal force	Person has to hold with max. force to avoid falling
High	Significant safety decrease	0.45	10.00	Max. horizontal force	Person will fall from seat in case of seat belt not fastened
4	**Dangerous consequence**				
	Influence on structure strength criteria	Design load case		Max. vertical load	Boundary condition for damage to structure
5	**Extreme consequence**				**Personal injury, freight damage**
Low	Touch ground	Grounding load IMO		Max. forward force	Protection for passengers can reduce injuries
High	Collision	Collision load IMO		Max. forward force	Person injured, vessels in emergency

can be reviewed by inspection before testing the configuration further using the regression data presented in this chapter.

Having developed the vessel this far, the next step is to recheck the dimensions using the regression data later in this chapter and to create a layout for the main propulsion after reviewing options and making a first selection (Chap. 11) to see whether this fits. If not, adjust the lines and recycle the design spiral based on the revised data. Once the vessel configuration has been verified or adjusted, a recycle through resistance can be made and seakeeping assessed through model testing.

7.2.4 Limitations on Draft

The limitation on draft depends upon the depth of river and other waterway that will be navigated. Unless a SWATH or semi-SWATH form is being selected, the main issue will be the lines at the aft part of the vessel to accommodate the propulsion equipment, particularly waterjet intakes. These encourage use of straight keel lines toward the stern that fit well with a rectangular transom stern and small bilge radius. This installation also gives the minimum vessel draft and so is the most suitable option for craft operating in shallow waters such as rivers and lakes.

Free propellers are suited to most geometries, though curved keel and deep-V keel geometries are most common as they provide more clearance from the hull for a propeller and so less turbulence and a tendency to cavitation at high service speeds.

Resolving the selection of stern lines and propulsion system is directly connected to work under item 3 earlier.

7.2.5 Wave-Making Issues in Restricted Waterways Such as Rivers

When operating a catamaran in inland waters such as lakes, rivers, and other narrow waterways, the wave height, especially maximum wave height, caused by the catamaran itself is an important factor influencing the safety of nearby boats and waterway embankments due to the impact load acting on the infrastructure and motions affecting other vessels or anchored boats.

Experimental investigation and analysis of wave generation by a high-speed catamaran on inland rivers was carried out at MARIC [6]. The researchers aimed to make some advances in reducing the wave making caused by vessels running at high speed in narrow waterways as follows:

- Demihull designed with an asymmetric form, that is, its external side is a vertical plane;
- Installation of forward spray strips;
- Installation of forward and aft wave elimination fins;
- Experimenting with various hull separations *k/b* between 2 and 8.

The experimental results are presented here for reference. The principal dimensions of the catamaran are listed as follows:

Item		Full-scale dimension
L_{WL} (m)	Waterline length	38
b (m)	Demihull breadth	2.25
L/b		16.897
T (m)	Draft at waterline	1.2
b/T		1.875

(continued)

Item		Full-scale dimension
C_b		0.508
C_p		0.646
Model scale		1:15

A wave probe was installed on the towing tank wall, and since the breadth of the tank is 5 m, the location of the wave probe from the longitudinal center plan of the catamaran is 2.5 m. Because of the reflection of ship waves at the wall, the measured wave height at the tank wall is equal to double the wave height at this point when there is no wall. This simulated a wave reaching the river bank or nearby boat at a distance of about 37.5 m.

The body plan and profile of the demihull are shown in Fig. 7.4, and these very closely resemble a half hull cut from a conventional ship at the longitudinal central vertical plane, except that this vertical plane is located on the external side of the demihull.

The wave pattern measurement system is shown in Fig. 7.5, and the wave height trace measurements used are shown in Fig. 7.6.

The maximum wave height and average wave height of the test results are shown in Table 7.7.

The maximum and average wave heights are shown in Fig. 7.7; they decrease with increasing k/b and $\mathrm{Fr_L}$.

Figure 7.8 also shows that when $k/b = 3.2$, the maximum wave height will decrease rapidly with increasing Fn. Figure 7.9 shows the relation of residual drag with k/b and $\mathrm{Fr_L}$. We find the same result in Chap. 4, that is, the residual drag coefficient will be almost the same at different k/b where it is larger than 3.0–4.0.

This model experimental investigation also showed that spray strips and wave-eliminating fins cause a 15% decrease in wave-making height at $\mathrm{Fr_L} = 0.6927$.

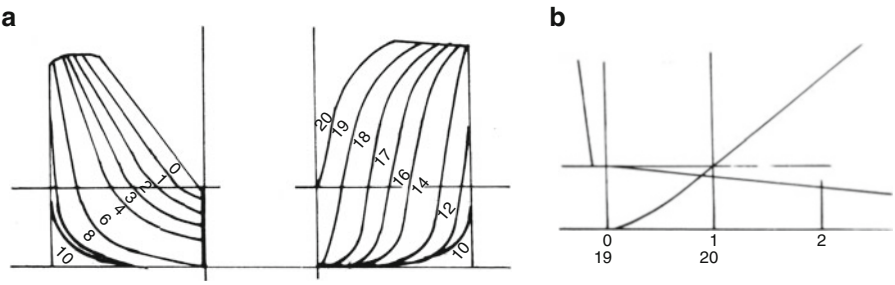

Fig. 7.4 (**a**) Body plan of model; (**b**) bow and stern plan of model

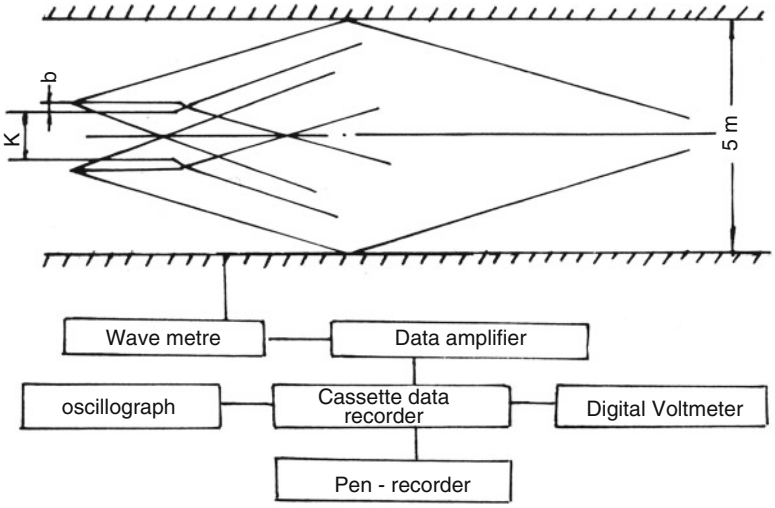

Fig. 7.5 Wave pattern measurement system

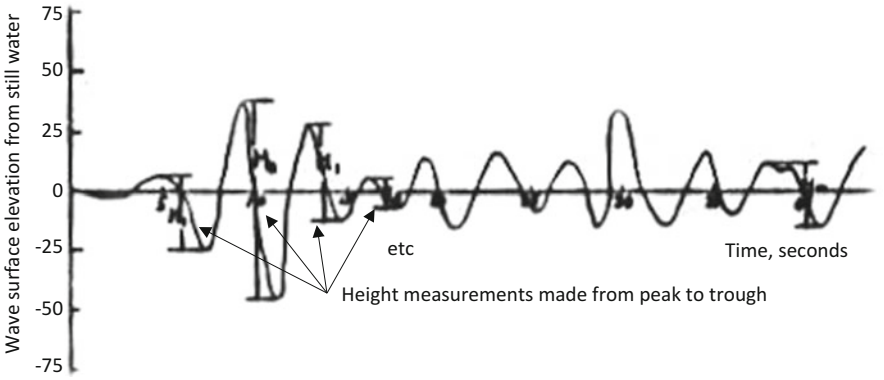

Fig. 7.6 Wave height analysis at ship model

Table 7.7 Test results of catamaran, maximum wave height, and average wave height [6]

Fr_L		0.4795		0.586		0.6927	
Item	K/b	H_m	$\bar{H}$	H_m	$\bar{H}$	H_m	$\bar{H}$
1	2.0	105.8	56.44	120.0	57.34	94.8	55.18
2	2.6	109.3	53.51	111.0	51.69	77.6	50.68
3	3.2	112.6	51.50	101.0	51.23	78.5	48.75
4	5.0	87.1	46.96	87.0	48.44	76.1	50.69
5	6.0	80.9	43.91	80.3	47.63		
6	8.0	86.5	43.91	78.0	50.04	84.9	55.28

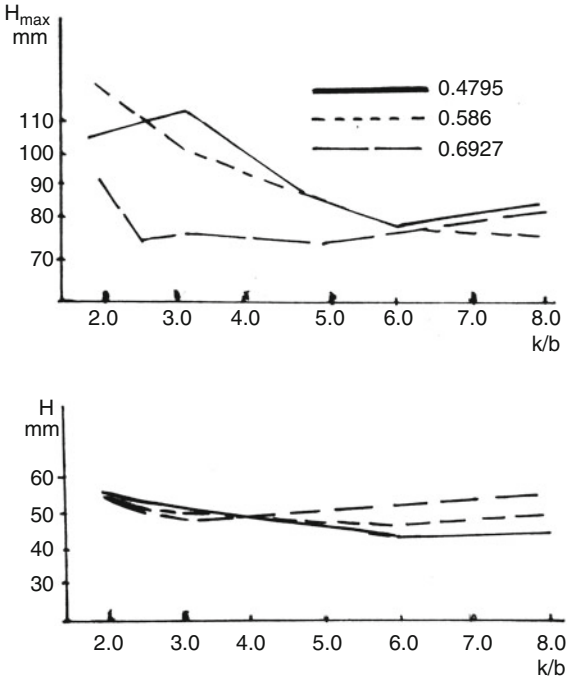

Fig. 7.7 $H_{max}, \bar{H}$, versus k/b

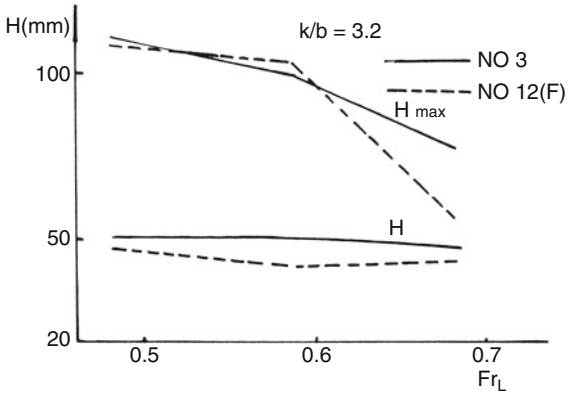

Fig. 7.8 $H_{max}, \bar{H}$, versus Fr_L

7.2.6 Limiting Vibration and Noise

Nowadays there are no regulatory requirements for vibration and internal noise for high-speed marine vessels; however, operators always seek the lowest level of vibration and levels of internal noise possible so as to maximize passenger comfort.

Greater passenger comfort leads to higher utilization and, therefore, economy for the operator, so lower vibration and noise levels in passenger cabins are important

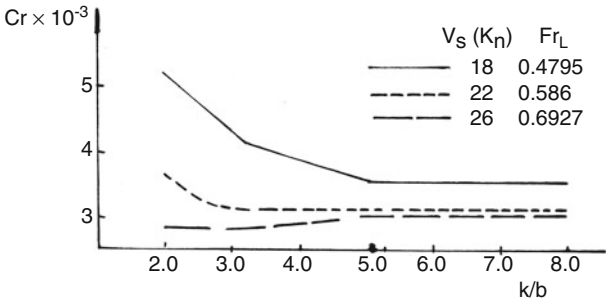

Fig. 7.9 C_r versus k/b, Fr_L

factors for competition in the ferry and fast ferry market, and designers have to pay serious attention to these issues to deliver the best quality performance.

The following factors will influence noise and vibration levels in passenger cabins:

- General arrangement: The internal noise and vibration levels can be reduced if the vibration and noise sources, such as main engines and water propellers, can be separated from the passenger cabins either by isolation or by distance.
- Noise sources in cabin: Where some noise sources, for example hydraulic pipelines and HVAC machinery and ducting, might be routed through or next to passenger cabins, they have to be isolated using noise insulation and separated where possible from passenger cabins and saloons. Particular care is needed to ensure that noise from HVAC and heating systems is not transmitted through ducting by fitting suitable noise baffles. This also applies to machinery noise that could travel through such ducting from the machinery spaces to passenger spaces.
- Isolation of cabins:
  - Efficient noise-damping and noise-absorbent material have to be used as isolation material in passenger cabins.
  - Noise-isolation and vibration-isolation measures should be adopted in the cabin area close to water propellers.
  - Vibration-absorption devices can be installed between the demihulls' primary cross structure and upper-level superstructure on larger vessels to improve vibration and noise levels in passenger cabins.
- Machinery bays with remote control and passenger cabins with noise insulation are suggested to improve both vibration and noise levels.
- Vibration damping for engines: Mounting of main and auxiliary engines on vibration dampers or on subframes that are resiliently mounted to the hull should be considered.

Some rules for cabin noise levels on conventional ships from various countries are listed in Table 7.8 for reference on criteria. To achieve these levels, noise insulation will need to be installed on the walls enclosing the main and auxiliary

Table 7.8 Rules for cabin noise level on conventional ships of various countries, dBA [1, p. 372]

Country	UK	Japan	USA	Germany	Expectation
Date made effective (day. month.year)		01.07.75	01.03.68	01.06.68	2018
Suitable range	Shipping	Ships <3000 t	Merchant ships	Ships with German crews	Fast ferries
Machinery control area continuous	75	75			75
Machinery area noncontinuous	110			110	100
Machinery area continuous	90	85	90	90	90
Accommodations	60	60–65	56	65	55
Navigation cabin	65		65	60	60
Bridge	68			65	60
Radio room	60			60	60
Kitchen	70				70
Dining room	75			65	65–70
Unsheltered deck	75				75
Corridors	80		61		60

machinery. Installation of HVAC ducting will require special care so as to avoid noise channeling to cabin vents. Cabin flooring will need sound-deadening covering, and cabin ceilings should generally be outfitted with paneling that absorbs sound. At the detailed design stage, estimates will be made for each of these items on an area basis so as to identify mass and procurement/installation cost.

7.3 Use of Statistical Data to Evaluate Principal Dimensions

7.3.1 Collating Reference Data of High-Speed Catamarans

The aim of collating reference data for high-speed catamarans is to obtain guidance on the leading particulars of a range of vessels for designers to select data to compare with the target new design. We do this to create useful regression equations to identify typical principal dimensions based upon the material. In this section we show analyses of two different sets of data for leading particulars of high-speed ferries:

- Data for fast ferries up to 150 m L_{WL} (Sect. 7.3.2.1 below)
- Data for fast catamaran ferries up to 50 m L_{WL} (Sect. 7.3.2.2 below)

The first set is extracted partly from Fast Ferry International (FFI) data specifically for catamarans and partly from a wider data set of fast ferries including monohulls in

the 50- to 150-m-L_{WL} range. The second set includes example data for 105 high-speed catamarans from Australia, Norway, Japan, USA, and Sweden extracted from FFI, together with information available from ferry builders' websites.

The purpose of this is to give an example for assembling tables of characteristics from similar size vessels, or over a range, to generate meaningful parameters for comparison with the selection made by the designer following the approach presented starting in Chap. 2.

It is important to challenge these data for your new design; most likely you will need to collect additional data and extend or replot the curves for yourself since vessel design is continuously evolving, and this will allow you to make selections closer to an "optimum" for the new design and reduce design cycling.

Key sources of data are the websites of the principal designers and shipyards and databases such as those maintained by Fast Ferry Information (successor to Fast Ferry International) on a database. Links to sources are given in the resources listing at the back of this book.

7.3.2 Sample Regression Formulas for Estimation of Principal Characteristics

7.3.2.1 Statistical Relation between Various High-Speed Catamarans' Principal Data

Vessel data are available from a number of sources, including the shipyards themselves. We have extracted sample data for vessels in a range up to 150 m L_{WL} for fast monohull and catamaran ferries to plot trends of the parameter relationships. This material is discussed in this section. In the following Sect. 7.3.2.2, we present sample plots for a smaller sample of catamarans in a L_{WL} range up to 30 m. Based on these data, regression relations between various principal dimensions of high-speed catamarans can be estimated as summarized below. This gives an idea of what has been used to date by designers.

The data sets plotted are generalized, rather than being a selection based on a target size, payload, route, or turnaround, for example. It is recommended that designers search for data on a representative sample of vessels and plot equivalent relationships to compare with their preliminary principal dimensions and data. In some areas, the relationships will be similar to our data below, which should be encouraging! Nevertheless, do not be tempted to avoid doing your own research. A bit of diligence here will avoid recycles. Remember that the further we go along the path of project design, the more difficult it gets to change, and the more expensive it becomes in time and money.

Fast Ferry International regularly published articles [7] and informative tables on an annual basis up to 2012 and, as Fast Ferry Information, continues to maintain an electronic database (see resources) covering catamaran fast ferries. The database is specific to fast ferries and goes back as far as 1956, so historical trends for

parameters can also be evaluated. We have taken a small sample of these data for vessels in a range of 20 to 30 m L_{WL} to plot a number of parameter relationships under Sect. 7.2 in what follows. It should be reiterated that the regression plots represent vessels from the past, so while they are useful as an initial guide, and as a view of the statistical relationships that can be useful, designers need to check for themselves statistics for vessels with characteristics close to their chosen designs; this will require direct access to the data mentioned earlier, whether from the FFI database or from designer and builder publicly available data.

Note that similar data are available from Jane's High-Speed Marine Transportation [8, 9], though in this case the focus is on recent designs and vessels constructed for each annual publication; some data from this source have also been used in the regression analysis.

(a) *Length overall and length of waterlines* L_{OA}~L_{WL}

Figure 7.10a, b shows the relation between length overall and length of design waterline, and the statistical relation between them can be expressed as follows (all data in meters):

When

$$\begin{array}{ll} L_{OA} < 150\text{ m}, & \text{then} \quad L_{WL} = 0.8785 L_{OA}, \\ L_{OA} < 50\text{ m}, & \text{then} \quad L_{WL} = 0.8878 L_{OA}. \end{array} \tag{7.1}$$

From the figures, it can be seen that the data in the plot are rather focused.

(b) *Relation between demihull draft and width* (b–T)

Figure 7.10c, d shows the relation between b and T and can be regressed as follows:

When

$$\begin{array}{ll} b < 9\text{ m}, & \text{then} \quad T = 0.552b, \\ b < 5\text{ m}, & \qquad\quad T = 0.17\text{b} + 0.99. \end{array} \tag{7.2}$$

It can be seen that the points are not so scattered, particularly in case of $b < 9$ m

(c) *Relation between length of waterline and maximum beam* L_{WL}~B

Figure 7.10e shows when

$$L_{WL} < 50\text{ m}, \quad \text{then} \quad B = 1.3394 L_{WL}^{0.5922}.$$

Figure 7.10f shows when

$$L_{WL} < 150\text{ m}, \quad \text{then} \quad B = 0.5845 L_{WL}^{0.85}. \tag{7.3a}$$

(d) *Relation between hull depth D and length of waterline* L_{WL}

As Fig. 7.10g shows,

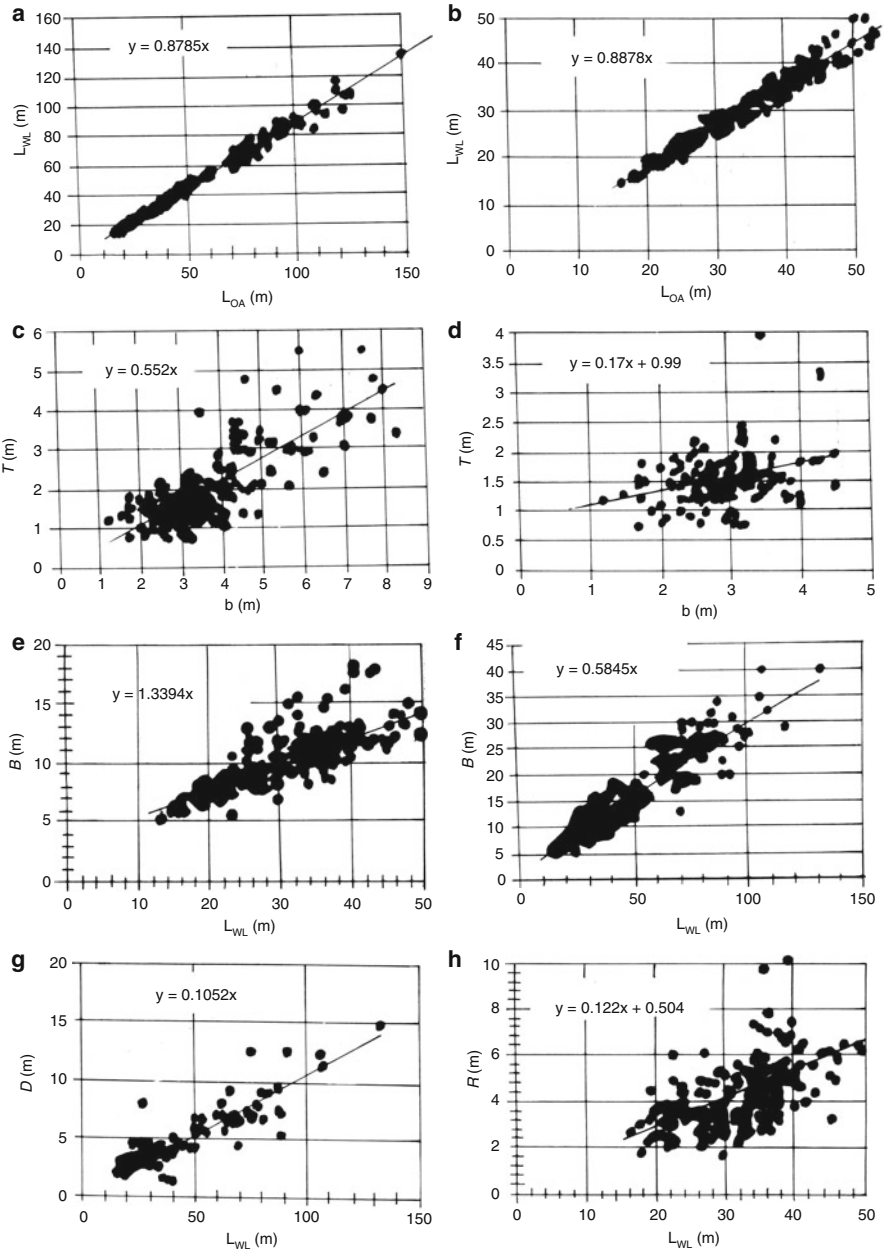

Fig. 7.10 Statistical plots (**a–i**) for parameter estimation

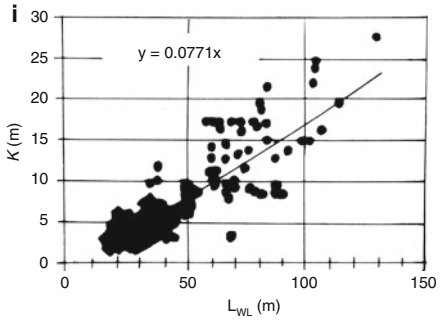

Fig. 7.10 (continued)

$$D = 0.1052\, L_{\mathrm{WL}}. \tag{7.3b}$$

(e) *Demihull separation k* versus L_{WL}

From Fig. 7.10h, when

$$L_{\mathrm{WL}} < 50 \text{ m}, \quad k = 0.122 L_{\mathrm{WL}} + 0.504.$$

From Fig. 7.10i, when

$$L_{\mathrm{WL}} < 150 \text{ m}, \quad k = 0.0711 L_{\mathrm{WL}}^{1.1656}. \tag{7.3c}$$

From this figure it can be seen that the points are very scattered, indicating a range of choices have been made by designers for similar vessel lengths. We have discussed the influence of demihull separation on wave making, resistance, and motion, so that this parameter is complex to optimize. The relation here (very much an average value) may be useful to compare with the choice you made as designer based on using the procedures in earlier chapters. Does your mission requirement place you out on the edge of this plot, or in the middle? If your mission is special, then being on the edge may be justified. If there is nothing special about the mission, you should (at least at this stage) be closer to the average, that is, following the foregoing relation.

(f) *Deck area* $L \times B$ *(*m^2*)* versus *number of passengers and cars*

Figure 7.11a shows the relation between deck area and number of passengers:

$$P_{ax} = 0.8312(LB). \tag{7.4a}$$

The data are also very scattered due to different arrangements of passenger cabins (e.g., length, layer, class) and operational area (e.g., seakeeping requirements).

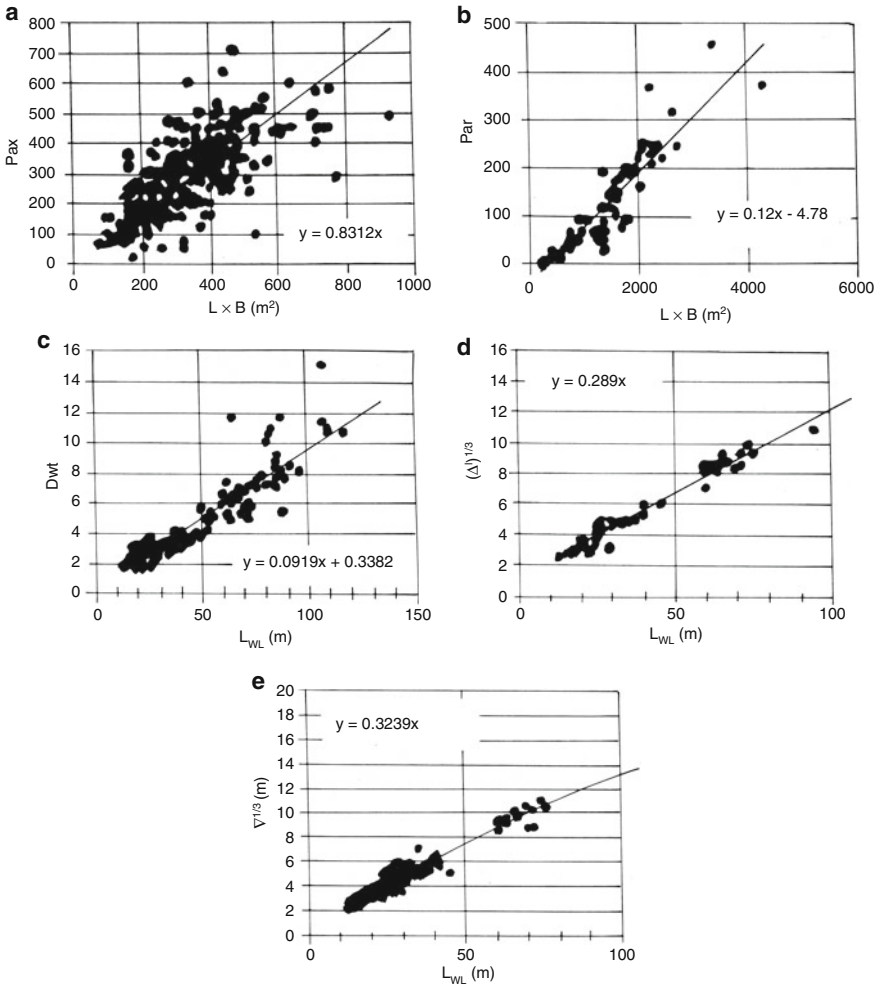

Fig. 7.11 (**a**) S = $L_{wL} \times B_{max}$ versus passengers; (**b**–**e**) further statistical plots

Figure 7.11b shows that the relation between deck area and car number is less scattered:

$$N_c = 0.12(LB) - 42.78. \tag{7.4b}$$

(g) *Relation between* L_{WL} *and deadweight* $(DWT)^{1/3}$, *light weight displacement* $(\Delta^l)^{1/3}$, *and loaded volumetric displacement* $(\nabla)^{1/3}$

From Fig. 7.11c:

$$(\mathrm{DWT})^{1/3} = 0.919 L_{\mathrm{WL}} + 0.3382.$$

From Fig 7.11d:

$$\left(\Delta^{l}\right)^{1/3} = 0.289 L_{\mathrm{WL}}{}^{(0.809)}.$$

From Fig 7.11e

$$\nabla^{1/3} = 0.3239 L_{\mathrm{WL}}{}^{(0.8032)}. \tag{7.5}$$

7.3.2.2 Relationships from High-Speed Catamaran Data Sample with $L_{\mathrm{WL}} < 50$ m

(a) *Freeboard* $(D - T)$ versus L_{WL}

From Fig. 7.12a one can see that the points are focused around the regression line that can be expressed as follows:

$$(D - T) \cong 5\% L_{\mathrm{WL}}. \tag{7.6}$$

(b) *Deck area (LB) maximum* versus *number of passengers*

From Fig. 7.12b one can see that the data points here are rather scattered. The relation between deck area LB and number of passengers can nevertheless be identified at the upper and lower limits, according to the arrangement of passenger cabins. The upper limit relates to high-speed catamarans with more deck levels with passenger saloons, while the lower limit line relates to a single passenger saloon.

Points ⊗ show vessels with waterjet propulsion, with such vessels tending to have longer upper decks. This attribute is separate from the aforementioned relation in the figure, but it may be a useful guide. It is useful to compare these plotted data with the relation for ferries up to 150 m long presented earlier.

(c) L_{WL} versus $(\mathrm{DWT})^{1/3}$

In general, at the initial design stage, the DWT can be determined by factoring from the technical specifications from the client (from vessel passenger capacity, cargo mass, and route length); the waterline length can then be plotted for existing vessels to see the relation. Using the vessel data set as plotted in Fig. 7.12c, the regression formula can be expressed as

$$\mathrm{DWT} = \left(3.7 + 0.05^{*}\left(L_{\mathrm{WL}} - 18\right)\right)^{3} \quad (\mathrm{tons}). \tag{7.7}$$

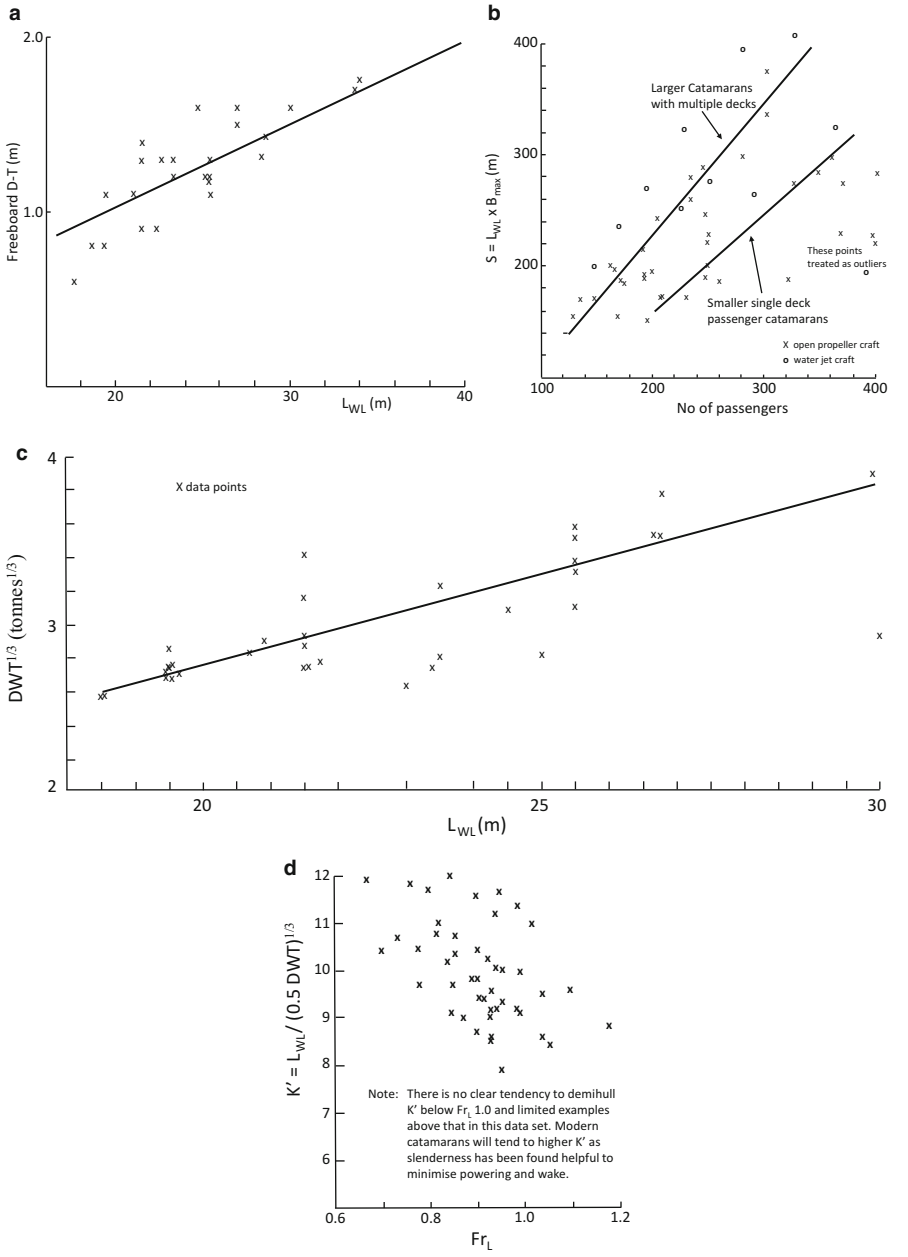

Fig. 7.12 Displacement versus SHP required for various speed/length ratio, and further statistical plots (**a**–**d**)

This relation applies to the sample range between 18 and 30 m length plotted in the diagram.

The relation between deadweight and displacement, D, of vessels can be expressed as

$$D = k_1 \mathrm{DWT}, \tag{7.8}$$

where k_1 is an empirical factor that can be taken by the designer from an available prototype. Otherwise, use 0.25–0.4 for passenger vessels (higher when hull is nonmetallic) and 0.3 to 0.5 for larger passenger and vehicle ferries. Design in an aluminum structure is becoming more sophisticated, and at the same time shipyard fabrication is becoming more automated, enabling lighter structures. Design of nonmetallic hulls using carbon or aramid fibres and resin for minimized mass is a specialist capability and so support may be needed by designer or shipbuilder.

There is considerable variation stemming from the mission (e.g., pax versus cargo, versus service speed) for DWT, so it is recommended to check first against this relation and compare it with a weight breakdown for fixed and moveable payload/deadweight.

If the DWT is significantly different from Eq. (7.8) when starting with $\mathrm{L_{WL}}$, it will be necessary to work in reverse to check vessel dimensions by estimating displacement D (between two and four times DWT depending on increasing size) and then adjusting the hull lines.

Accounting for the necessary passenger/cargo deck area and layout may help to guide first priorities on whether to extend $\mathrm{L_{WL}}$, scale accommodation deck breadth and width in proportion, or scale the demihull $\mathrm{L_{WL}}$, b, and t without changing the accommodation deck overall plan dimensions.

(d) *Demihull slenderness* $\frac{L_{\mathrm{WL}}}{(\mathrm{DWT}/2)^{1/3}}$ versus Fr_L

Figure 7.11d shows a plot of high-speed catamaran slenderness data (based upon DWT) versus Fr_L, that is, $k' = \frac{L_{\mathrm{WL}}}{(\mathrm{DWT}/2)^{\frac{1}{3}}}$ versus Fr_L. It should be noted that even though the data points are also very scattered, the tendency of the curve is clear: the demihull slenderness is highest in the case of $Fr_L = 0.8$ to 0.85 then drops down with an increase in Fr_L, which may be due to the fact that most high-speed catamaran operations are concentrated in the region $Fr_L = 0.85$–1.0, in which the residual drag is largely friction drag, so that increased demihull length will cause only a small decrease of residual resistance while increasing friction resistance due to an increase in wetted surface. The interference drag will decrease as Fr_L increases no matter how high the slenderness.

The arrangement of propulsion equipment also affects demihull dimensions, for example, using waterjet propulsion located in the rear part of the demihulls rather than water propellers located under them may lead to longer waterline length and, so, slenderness.

The determination of demihull length has to be considered carefully according to the specific situation, which will be discussed in subsequent sections.

If displacement is used instead of DWT, then the slenderness of high-speed catamarans can be shown to be concentrated at $L_{WL}/b = 6.5–8.5$. It is probably easier to use relations 7–8 and 7–9 to establish realistic L_{WL} and look at demihull slenderness from that point of view, as discussed in (c) above in the first instance.

As in Chap. 5, for medium-speed vessels ($Fr_L = 0.5–0.75$), residual drag is larger than friction drag, so it is advantageous to use a higher length/beam ratio or slenderness, up to between 9 and 15 for the demihulls.

In the case of higher speed, $Fr_L > 0.75–0.85$, the residual drag will contain a much higher proportion of friction drag (typically 75–85%), and so slenderness should be determined based on design-specific calculations or test results. Start with a demihull slenderness of 6–8 and adjust once calculations are available.

7.4 Further Considerations for Principal Dimensions and Form

7.4.1 Hull Separation k/b

In the case of medium-speed vessels ($Fr_L = 0.3–0.55$), *k/b* plotted in Fig. 5.41 indicates that there are favorable hull separations for minimum residual drag coefficient. However, at high speed ($Fr_L > 0.75$), the wave interference drag is only a small part of residual drag, and in general *k/b* may be taken at about 2 so as to balance optimization of drag with growth in hull structure scantlings and mass necessary to provide structural strength and stiffness.

Based on experimental investigations at MARIC, hull separation will only weakly influence the residual resistance coefficient of high-speed catamarans with hard chine demihull lines as shown in Figs. 7.13 and 7.14. It is shown in the figures that in the case of $Fr_L = 0.775$, *k/b* has almost no effect on residual drag.

As described in Chap. 5, in the case of $Fr_L > 0.75$, when demihull slenderness $\psi > 8$, the wave interference between demihulls is low and may be neglected. As in Fig. 5.36, when $Fr_L > 0.8$ and $k/b > 2.5$, the influence of *k/b* on C_r, the coefficient of residual resistance, is small for any slenderness ratio. This condition can be verified from Fig. 5.25, so that when $Fr_L > 0.75$, the ΔC_r (the difference in residual resistance at such *k/b* with that at *k/b* of 2) is almost the same as when $k/b = 2.6$ or when $k/b = 3.2$.

In addition, from Chap. 6 one can see that the hull separation does not greatly affect the seakeeping quality of modern catamarans with $k/b > 3$ in head seas, and the calculation of the seakeeping quality of the vessel can be carried out treating it as two monohull vessels connected together.

In contrast, the hull separation greatly affects the transverse motion of the catamaran in beam seas. A bigger hull separation produces smaller transverse motion and rolling angle so as to reduce vertical acceleration. This happens due to an increased roll damping moment as the hull separation is increased.

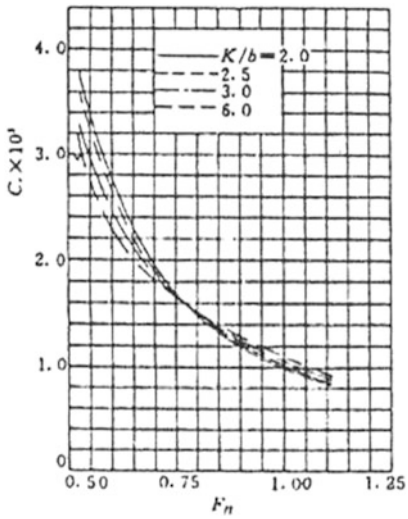

Fig. 7.13 Residual drag coefficient of hard chine catamaran versus Fr_L

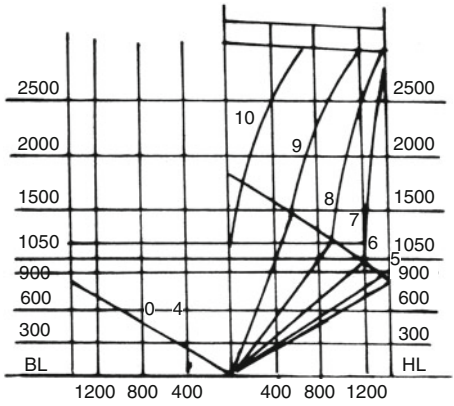

Fig. 7.14 Body plan of hard chine catamaran demihull

High vertical acceleration will occur on catamarans in bow quartering seas owing to the superposition of both longitudinal and transverse motion, and in addition there is motion phasing (corkscrew motion) that can accentuate the vertical extreme, so designers have to consider the following when deciding on hull separation:

- Theoretical calculations and model testing for the seakeeping quality, including motion sickness incidence (MSI), have to be carried out using the specific conditions of sea state and wave spectrum on the intended operational route or for the environmental envelope of operation, to select the best hull separation;
- The transverse strength and stiffness of the hull structure has to be checked since a bigger hull separation leads to reduced transverse stiffness and strength with the

same hull structure, so structural scantlings have to be increased to maintain stiffness and structural integrity to compensate;
- The general arrangement should be laid out rationally for both cars and passengers on decks; accelerations are lowest at the vessel center, so induced loads are also lowest. In the fore and aft directions, accelerations increase toward the bow, and athwartships accelerations are highest out over the demihulls.

7.4.2 *Demihull Beam/Draft Ratio,* b/T

To minimize residual drag, a decrease in *b/T*, that is, a deeper and thinner demihull shape, will be favored; however, from the point of view of increasing lift toward the stern so as to decrease trim angle and drag, an increase of *b/T*, particularly at the stern area, will be favored.

As discussed in Chap. 5, the demihull beam/draft ratio does not play a significant enough role in resistance to become a control for vessel dimensions. In general, for high-performance marine vessels, particularly for high-speed passenger-car ferries and high-speed naval sealift vessels, the controlling factor is the dimensions to install required propulsion engines and power trains due to high speed and to provide the necessary displacement. The demihull beam at the stern usually depends upon the size of waterjets and transmission as well as their arrangement. The demihull beam at amidships is usually close to that at the stern.

The draft selected also depends upon the depth of the river and seabed over the route where the vessel is to operate, as well as the arrangement of propulsion and main engines, so the vessel mission will usually determine the T, and b is a resultant of other factors.

The demihull block coefficient C_b is usually close to 0.5 for a catamaran. Now, displacement $D_{\mathrm{fw}} = 2L_{\mathrm{WL}} \,.\, b \,.\, T \,.\, C_b$. ($\mathrm{m}^3$ or tons in freshwater, $D_{\mathrm{sw}} = D{*}1.025$ in saltwater). If b and T are determined by the cross section needed for the main machinery, it will tend to be parallel from midships to transom stern, and so it is clear that to increase $\mathrm{L_{WL}}$ we will need to design a finer form forward of amidships so as to reduce C_b a bit. For slower vessels where T is not restricted, we could deepen the demihull draft somewhat, but only if we can find ways to squeeze the cross-section breadth at the waterline. It can be seen, therefore, that demihulls closely fitting the main machinery are a general result.

7.4.3 *Demihull Depth*

Demihull depth, and more precisely the demihull freeboard ($H_{\mathrm{f}} = D - T$, where D is depth and T is draft of demihull), will be determined by seaworthiness requirements. According to statistical data from the data set analyzed, the $D - T$ (freeboard at amidships) of a high-speed catamaran operating at sea will be equal to approximately 5% $\mathrm{L_{WL}}$. This should be regarded as a starting point since, while this freeboard value

may be suitable as the height for the main deck, it may be necessary for the cross-structure base of the structure to be higher than this level depending on the operational environment and vessel motions. To design a simple structure through the demihulls, it may be best to use a higher freeboard at amidships. Second, when considering freeboard, it is important to review the demihull compartmentation and compliance with the requirements of the IMO or relevant classification society.

7.4.4 Demihull Line Plan

In Chap. 2 we introduced the main inputs to sizing a catamaran and its demihulls from a static point of view. The breadth, draft, freeboard, C_b, and various other characteristics link to the vessel mission and operational environment. In Chaps. 3, 4, 5, and 6 we showed how wave making, overall resistance, and motions in a seaway also influence the main parameters.

These alone will not generate hull lines automatically as the designer has other choices that interact with the vessel powering and control systems that are selected. We introduce some thoughts here and will continue in the next chapters to discuss the concept refinements that have developed over the last two decades in connection with multihull vessels. Some additional thoughts for smaller catamarans are presented at the end of this chapter.

For high-speed catamarans with $Fr_L > 0.75$, the interference drag will be small in the case of normal hull separation, typically $k = 2b$, so the demihull lines as such become important to optimize drag. In general, medium-speed vessels with Fr_L close to 0.75 or lower, the round bilge or mixed lines (round bilge for fore part, and close to hard chine for rear part) may be selected as the initial line plan. However, for higher speed vessels, say $Fr_L = 0.85$ and up to 1.0 or even more, particularly for seagoing operation, the hard chine configuration with various hull cross sections (symmetric, asymmetric with internal or external side vertical, shallow V, deep V, and fine forward double curved form with minimum bilge radius to flattened lower surface and sides aft), as noted in Chap. 5, might be selected.

The profiles of bow and stern waterlines are very important owing to their effect on running attitude and vessel resistance. The waterline shape at the bow of a high-speed catamaran with high slenderness ($\frac{L_{WL}}{\nabla^{1/3}} = 8 - 8.5$) may be almost linear with about 7° of half entrance angle so as to decrease the wave-making drag.

The immersed transom area A_0 (at rest) will affect the lift at the stern and, thus, vessel trimming angle, so it influences drag. For high-speed vessels, the stern will be located at the wave trough in the worst case, so an increase in transom static immersed area will increase the lift at the vessel's stern and decrease the trimming angle so as to decrease the drag.

In addition, waterjet propulsion and propellers are installed in the stern half of the demihull, so the lines of the stern and transom have to be considered to fit the arrangements of waterjet inlet and minimize the duct length so as to reduce the water weight in the waterjet propulsion duct. Alternatively, the demihull lines below the

stern area have to accommodate the arrangement of water propellers and transmission if these are selected.

In recent years, many large catamarans have been designed as high-speed passenger-car ferries and for naval high-speed sealift. Seaworthiness is extremely important for these ships, so the demihull lines should be designed in terms of both powering performance and seaworthiness, particularly the latter. The motion response and seaworthiness challenge have caused major catamaran shipyards to refine catamaran hulls with fine lines forward and, where possible, also with restricted waterline dimensions and above water flare. We will discuss these aspects further in the next chapter; in the meantime, a few remarks are offered regarding approaches to restricted waterline geometry or semi-SWATH form.

- *Selecting semi-SWATH section for whole length*: Such a design can be adopted on vessels without an automatic ride control system to reduce the construction and maintenance cost but still with satisfactory seaworthiness for medium-speed vessels. In such cases, the S profile body plan will be extended for the entire demihull length, with a small bulbous bow and great hull separation as well as demihull slenderness for good seakeeping (small motion values and MSI) both in head and bow quarter seas.
- *Selecting semi-SWATH profile over forward part of vessel* and using an automatic ride control system, that is, hydrofoil at bow under or parallel with the hull bottom as well as interceptors at transoms. The fine forward form and small-waterplane area reduces the response to waves, while the automatic control systems provide damping to reduce bow down tendency and wave slamming. The feature of this semi-SWATH is the forward lines with an S-type body plan, as described in Chap. 5, and also with a small bulbous bow. The bulbous bow may be designed not to improve the resistance of vessels in calm water, since at such a high Froude number a bulbous bow does not play a significant role in reducing resistance. However, a small bulbous bow is necessary for semi-SWATH vessels with an S body plan at the bow for reducing the entrance angle of the waterline at the bow for a reduction in resistance in a seaway (Chap. 6).

7.4.5 Other Measures

The use of a stern flap or wedge, particularly with automatic control systems, are definitely helpful for improving the drag and seakeeping quality, as explained in Chaps. 5 and 6.

Wave depression or spray rails at the bow are also useful for reducing the bow wave and spray of catamarans at higher speed ($Fr_L > 0.6$), both in calm water and waves.

Experimental investigations at the Berlin Model Basin on 17 different spray rail configurations demonstrated that well-shaped spray rails, if combined with a transom wedge, are the most effective devices to reduce the hull resistance of a given

semidisplacement round bilge hull [10]. According to the reference paper, by means of this rail system, which is used in combination with a transom wedge, an overall gain in effective power of 5–6% for one rail and 8–10% for both rails could be achieved in a speed range of $Fr_L = 0.5–0.9$.

In addition, the rail system improves the seakeeping qualities of the semidisplacement round bilge hull due to a reduced deck wetness and an increased visibility from the bridge. Similar results are also obtained on high-speed catamarans. The spray rail system geometric features can be seen in Fig. 7.15a–c.

7.5 Considerations for Vessel General Arrangement

Some considerations for general arrangement in preliminary design are as follows.

7.5.1 Catamaran Vessel Profile

It is normal on high-speed vessels to arrange the above waterline profile so that the center of area is aft of amidships, as shown in Figs. 7.16, 7.17, and 7.18. This assists in giving stability related to wind forces at high speeds and in higher sea states where the wind velocity will also be high. Passenger craft require significant window area for passenger comfort. The structural design of window apertures and the quality of toughened glass available has advanced greatly in the last two decades, so that it is now possible to have large windows with excellent visibility for passengers, including use of UV shielding and colored glass to provide an impression of a continuous line to the vessel, as shown in the figures. Smaller vessels, as shown in Fig. 7.16, tend to be more governed by practical aspects and have a squarer profile; nevertheless, the front of both passenger cabins and the navigation bridge is generally inclined so as to minimize air drag at speed. Larger vessels exhibit rake of above 45° in some cases (Fig. 7.18).

7.5.2 Passenger Cabin

Passenger cabins have to be arranged in the superstructure at the upper deck in order to give good vision, space for access as well as seating, and comfortable arrangement including kiosk and table areas for meals on larger vessels. The largest ferries might also have a movie theater or games area (see Appendix 3 for examples). Aviation-type seats should be arranged with no more than four seats in a row with two entrances in the central area, and three seats with one entrance at the side (Fig. 7.17). This will facilitate evacuation in an emergency.

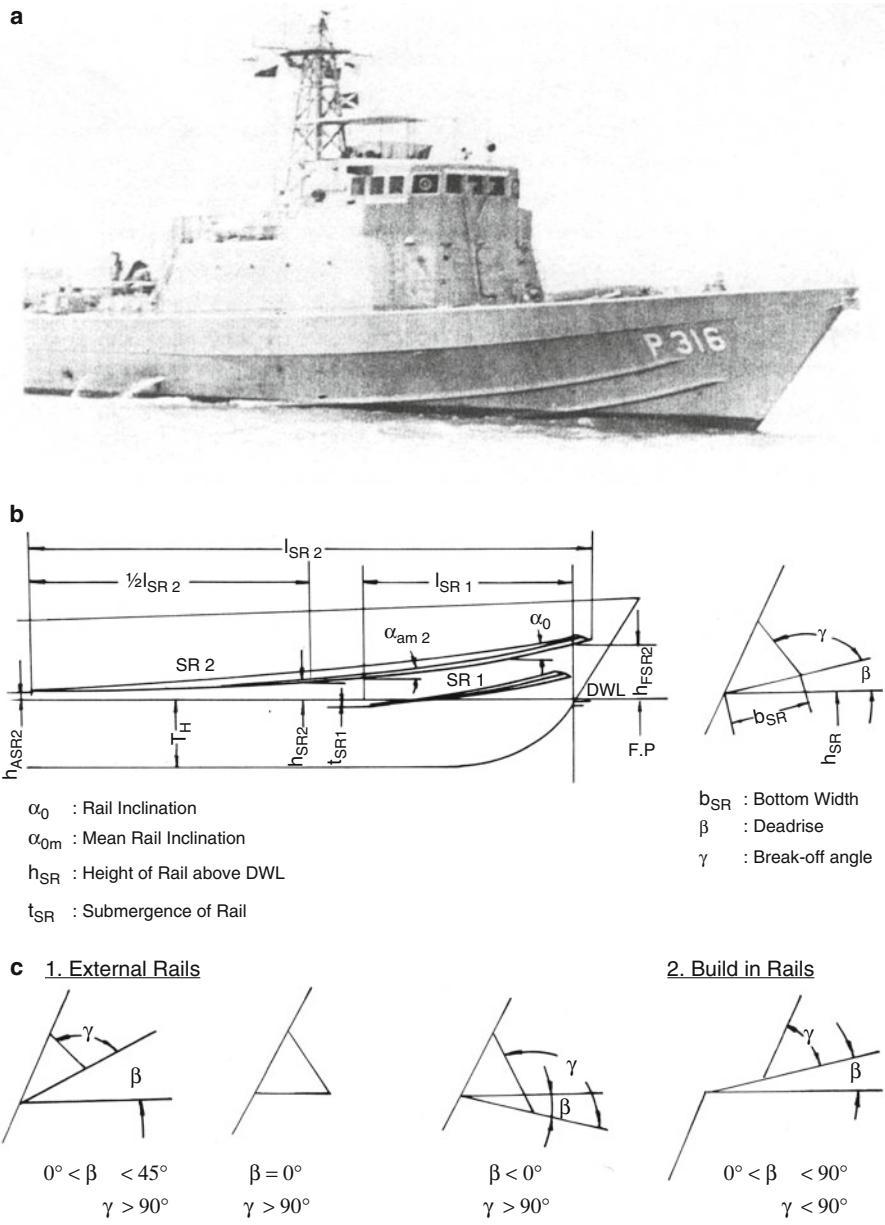

Fig. 7.15 (**a**) PS316; (**b**) PS316 spray rail diagram; (**c**) spray rail geometry

Fig. 7.16 Zhao Quing 42-m passenger catamaran ferry by Austal

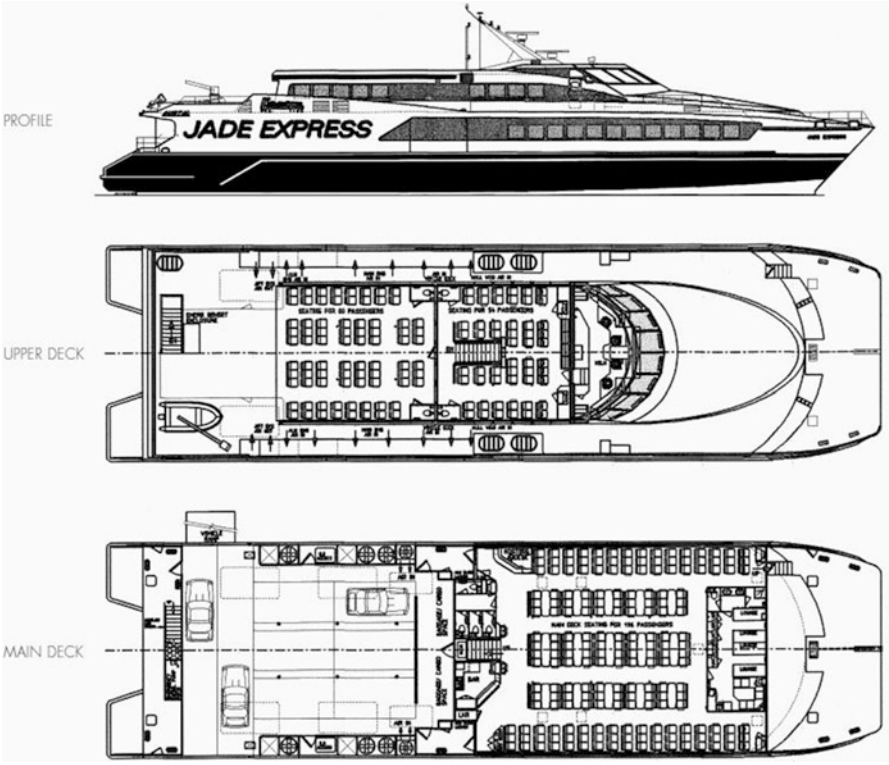

Fig. 7.17 General arrangement of Austal Auto Express 48 passenger and vehicle ferry Jade Express

Fig. 7.18 Photo of Jade Express

The evacuation corridors for passengers have to be arranged in case of emergency. In general, at least four doors for exit/entrance of passengers have to be arranged in a passenger cabin at the main deck level (Fig. 7.17) [5] and with boarding gates for entrance/exit and possibly also forward doors for emergency exit depending on the number of passengers.

7.5.3 DemiHulls

In general, the main engines and waterjet propulsion system are arranged at the rear half of a demihull, with auxiliary machinery bays and some auxiliary holds also arranged in the demihulls for machinery removal. No passenger facilities can practically be put into the demihull space for safety reasons.

The demihull beam main cross section is therefore controlled by the width and height plus access around a high-speed diesel in most cases. Only the largest high-speed catamarans have gas turbines installed.

7.6 Update of Principal Dimensions

The procedure can follow a flowchart as in Fig. 7.1 We continue here to revisit the main parameters started in Chap. 3 as follows.

7.6.1 Preliminary Design

7.6.1.1 Design Mission

In Chap. 3 and earlier in this chapter we referred to design data sheets for the target vessel. Templates are contained in Appendix 2. These data sheets provide the starting point for comparing with the parameters plotted from regression analysis in the previous section, as well as plots presented in Chaps. 5 and 6.

Before launching into a full evaluation of the main parameters as detailed in what follows, it is worthwhile to review these data sheets and, if necessary, make adjustments. In the process to this point, you have probably found new data on components of payload or weight applicable to your new vessel or adjusted parameters as a result of a discussion with the client. Aspects worth homing in on are maximum payload and light payload, with associated ballast water that may be needed for static trim, route length, and associated fuel tankage, including reserves for main engines, as well as the auxiliary power required.

By now you may have selected the catamaran configuration. If you are looking at a SWATH or a wave-piercing configuration, it is best to review the next two chapters first before going too far into the design stage. Meanwhile, we will continue with a recheck process for the principal particulars. Once this stage has been completed, you will probably be ready to prepare a model test or carry out CFD on your configuration. We will discuss the subsequent stages in Chap. 14, following a review of WPCs, SWATHs, and other multihulls, and talking through aspects such as propulsion and machinery, structures, and outfitting that need to be decided on before detail design is completed in an efficient fashion.

7.6.1.2 Calculation of Payload and Deadweight

We take a passenger high-speed catamaran as an example; payload will be

$$W_{pas} = nw_p, \tag{7.9}$$

where

W_p Weight of each passenger; in general we take 100 to 120 kg for each;
n Passenger number.

Then the DWT can be calculated as $\text{DWT} = k_{\text{DWT}} W_{pas}$, where k_{DWT} can be taken from a suitable prototype. In general, we use 1.2–1.35 for an ordinary passenger catamaran to cover baggage.

If the vessel is for vehicles as well as passengers, the number of vehicles required needs to be specified; then the DWT for this cargo will be

$$W_{pv} = n \cdot 2300 \text{ kg}$$

where

W_{pv} is the passenger vehicle component of the total vessel deadweight (DWT)

Here we are assuming a typical car (assume passengers assessed separately) mass is around 2 t. Today a typical crossover SUV will weigh close to 2 t, as will a pickup or midrange car. A small car may weigh rather less, down to perhaps 1250 kg empty, while an electric car such as a BMW i3, VW Golf, or Renault Zoe will be in the 1500 kg range. The average of the preceding numbers allows for baggage and fuel in the vehicle. If trucks are to be carried, then a closer assessment of the number and sizing is required since a typical tanker truck or container truck may well have a total axle weight of up to 50 t while taking a floor space of three to four cars.

Having generated the core payload of passengers, or passengers and vehicles, we now need to look at all the other inputs to payload and deadweight.

7.6.1.3 Weight Calculation

The following series of typical characteristic data can be used prior to a detailed calculation (second or third round of design spiral).

Hull weight:

$$W_h = k_h L_{\mathrm{WL}} B. \tag{7.10}$$

Power plant:

$$W_p = k_p n N, \tag{7.11}$$

where

n Engine number,
N Engine power.

Fuel weight:

$$W_F = q_e \frac{R}{v_c} n N_c K_L, \tag{7.12}$$

where

q_e Specific fuel consumption, kg/kw-h;
R Range, nautical miles;
v_c Cruising speed, knots;
N_c Power for each engine at cruising speed, kW;
K_L Coefficient for lubrication oil, and others.

Weight for electrical system:

$$W_E = K_E D^{2/3}. \tag{7.13}$$

Provision weight:

$$W_{\text{Pro}} = K_{\text{Pro}} D \tag{7.14}$$

Reserve displacement:

$$W_{\text{Res}} = K_{\text{Res}} D. \tag{7.15}$$

Then total weight W can be written

$$W = W_H + W_P + W_F + W_E + W_{\text{Pro}} + W_{\text{Res}} + W_{\text{Pas}} + W_{\text{pv}}. \tag{7.16}$$

All of the previously mentioned coefficients can be based on the prototype used for comparison, or typical values for the coefficients based on review by the designer of existing vessel data can be chosen. If W is not equal to D, then the principal dimensions have to be changed, and the regression has to be carried out until total weight is close to assumed displacement (Sect. 7.6.1.5).

7.6.1.4 First Check of Principal Dimensions

The principal dimensions L_{WL}, Bm, D, T can be obtained from regression Eqs. (7.1), (7.2), (7.3), and (7.4) as a first approximations.

These data can then be compared with the dimensions and other data developed by the designer from the first-pass work following Chaps. 2, 3, 4, 5, and 6 to assess whether the design appears to be close to the average or is far from it. If it is far from average, it is worthwhile to look at the input data to see whether there are assumptions than can be adjusted to bring the parameters closer to the "average" as this will provide flexibility for optimization in the next stage of design.

7.6.1.5 Calculation of Principal Parameters

The principal parameters, Fr_{L}, $F_{r\nabla}$, $\frac{L_{\text{WL}}}{D^{1/3}}$, $\frac{D}{(0.1L_{\text{WL}})^3}$, $L_{\text{WL}}/(\text{DWT})^{1/3}$, can be calculated according to above data, and checking the slenderness in Fig. 7.12b

7.6.1.6 Selecting Lines and Demihull Configuration

Based on the mission, Froude number, and slenderness, designers can judge and select the type of demihull profile and configuration, that is, symmetric, asymmetric,

round bilge, hard chine, mixed, deep V, and others. Then a line plan can be developed. There will be some cycling around between items 2, 3, and 4 of this procedure until a balance is struck. At this point the static stability of the vessel has to be rechecked, which will include an assessment of pitch, roll, and heave natural periods. If pitch and roll natural periods are too close together, steps need to be taken to separate them or provide damping for one or both motions.

7.6.1.7 Checking Passenger Cabin Area

With a basic arrangement of passenger cabins, that is, how many deck levels there are for passenger cabins in the design, luxury or ordinary, and so forth, the passenger cabin area can be checked according to Figs. 7.11a, b and 7.12.

7.6.1.8 Selecting Main Engines

Residual drag, total drag, and main engine power in a first approximation can be calculated according to Fig. 5.34 and other relationships in Chap. 5. The main engine type and number can be selected according to the required power. Typically, for a catamaran this will be one or two in each demihull. Further data to assist power plant selection are discussed in Chap. 11.

7.6.1.9 Determination of b_{min} and Estimation of Arrangement of Machinery Bay

Once the main engines have been selected, the minimum demihull beam can be determined depending on the arrangement of the main engines and propulsion system (e.g., water propeller, waterjet propulsion, surface piercing propeller, fixed- or adjustable-pitch propellers) in the machinery bays.

7.6.1.10 Selecting Optimum Hull Separation

One can select three or more hull separations, $\bar{k}_1, \bar{k}_2, \bar{k}_3$ (around $k/b = 2.0$), to calculate the vessel drag; then the optimum k/b can be judged according to the calculations. The calculation can be done according the method explained in Chap. 5 (e.g., Figs. 5.36, 5.39, and 5.41).

7.6.1.11 Selecting Optimum Relative Principal Dimensions, Such as Slenderness, *L/b*, *b/T*

1. *Selecting optimum displacement/length ratio, or slenderness*

Taking the constant block coefficient δ using the prototype lines and T selected based on the draft requirement from the client or determined from route and terminal data, if displacement is held constant, then one can take slenderness K_2 between 3 and 5; then

$k_{21} = \frac{L_{\mathrm{WL1}}}{(D)^{1/3}}, k_{22}, k_{23}$. Then $L_{\mathrm{WL1}} = k_{21}(D)^{1/3}$, so L_{WL2}, L_{WL3}can be obtained,

$$b_1 = \frac{D/2}{L_{\mathrm{WL}} T \delta}, \text{and } b_2, b_3 \text{ can be obtained from same relation to varied } L_{\mathrm{WL}}, \tag{7.17}$$

where T represents the draft from the baseline.

2. *Selecting several L/b, b/T and keeping D, T, and δ constant, then*

$$b = \frac{D/2}{L_{\mathrm{WL}} T \delta} = \frac{D/2}{\frac{L_{\mathrm{WL}}}{b}} \cdot \frac{b}{T} \cdot \delta T^2. \tag{7.18}$$

7.6.1.12 Calculation of Resistance for Different Variants and Selecting Optimum Principal Dimensions

This calculation can be completed using the method introduced in Chaps. 4 and 5, and the optimum principal dimensions can initially be based on the calculation results. As a guide, we present in what follows a parametric analysis carried out by Prof. Rong of MARIC for wave resistance and wave wake generation, compared with actual model tests. These data provide one resource to allow interpretation against the dimensions and form of the designer's target new vessel. Alternative data sets were referred to in Chap. 5, which can also be used for comparison and the selection of vessel characteristics.

7.7 Wave Resistance Calculation Compared to Model Tests

7.7.1 Introduction

Wang (1994) [11] conducted extensive experimental investigations on resistances of three high-speed catamaran models, whose demihull forms were a typical round bilge form, a hard chine hull form, and an asymmetric round bilge form, in the

towing tank at MARIC. Rong [12] performed numerical tests on the round bilge form of one of Wang's models using subroutine CTMICHELL in Sect. 4.7.3. Comparing the calculations with test results, he obtained satisfactory results that may be described as follows.

7.7.2 Test Model

This model is a typical round bilge form with a transom stern. The body plan is shown in Fig. 7.19. The scale of the model to the real high-speed catamaran is 1:15 and the full-scale principal dimensions of the real high-speed catamaran are given in Table 7.9 below.

7.7.3 Wave Resistance and Effect of Imaginary Length

Rong [12] calculated the wave resistance coefficient $\bar{C}_w$ of the tested model for $b_c/B_d = 2.0$ at $Fr_L = 0.3$–0.96 using the numerical calculation method in Sect. 4.7.2.

The numbers of stations and waterlines were taken to be 21 and 7, respectively. Because high-speed catamarans have transom sterns, one station is added behind AP, whose length is called the imaginary length, and so the total station number is 22.

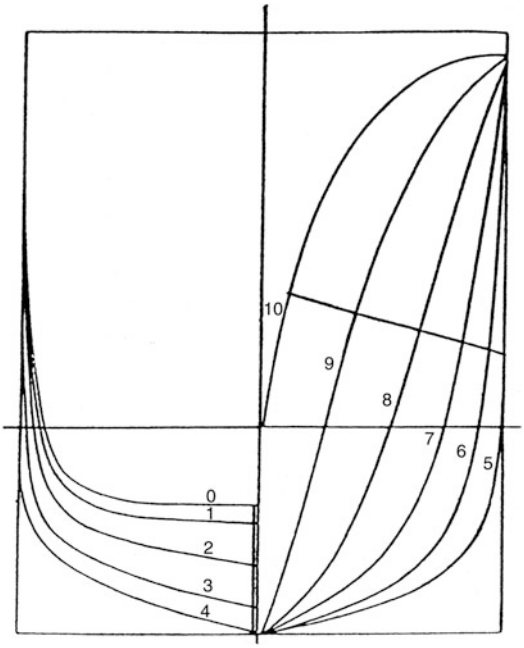

Fig. 7.19 Body plan of a high-speed catamaran

Table 7.9 Particulars of full-scale high-speed catamaran

Item	Ship Data
Waterline length, m	30.0
Demihull beam, m	2.85
Draft, m	1.20
Total wetted area, m^2	202
Displacement volume, tons	102
Demihull block coefficient	0.500
Demihull prismatic coefficient	0.629
Demihull waterline coefficient	0.785
Length/beam ratio	10.53
Draft-length ratio	0.040

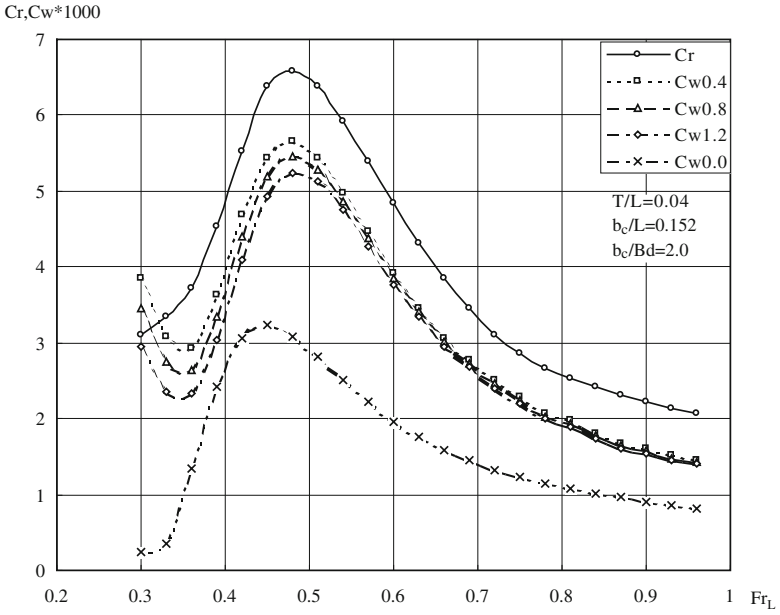

Fig. 7.20 Effect of imaginary length on C_w ($b_c/B_d = 2.0$)

Figure 7.20 shows the results of the test and calculation. In this figure, C_w means $\bar{C}_w$ in formula (4.7-2). The figure gives curves C_r and C_w at $Fr_L = 0.3$–0.96, and C_w 0.4, C_w 0.8, C_w 1.2, and C_w 0.0 represent the wave resistance coefficients for the imaginary lengths, which are 0.4, 0.8, 1.2, and 0.0 times of the transom breadth, respectively. Obviously, the curve of C_w 0.0, not considering any imaginary length, is very different from C_r and the imaginary length must be added to predict wave resistance. The other curves C_w have the same shape and move up as the imaginary lengths decrease. They have obvious differences at $Fr_L < 0.55$ and they approach the same value when $Fr_L > 0.55$.

The imaginary length can be selected based on the imaginary length curve in Fig. 4.6, Sect. 4.7.2. We can take it as 1.2 times the transom breadth at $Fr_L > 0.55$, which is more convenient for practical use.

7.7.4 Comparison of Calculation with Test Results

Calculations were carried out with five spacing/beam ratios: $b_c/B_d = 1.6, 2.0, 2.6, 3.2,$ and 6.0, where b_c is the demihull to centerplane spacing, at the same displacement, and $Fr_L = 0.30$–0.96. The imaginary length/transom breadth ratio was taken as 1.2.

Figure 7.21a–e shows the results of tests and calculations for residuary and wave resistance coefficients. In these figures, C_w means $\bar{C}_w$ in Eq. (8.7-2) and $C_{wr} = 1.25C_w$ (i.e., form factor $FFACTOR = 0.25$). It was found that C_r and $\bar{C}_w$ have the same shape and same tendency at $Fr_L = 0.36$–0.96. There are obvious wave troughs at $Fr_L = 0.35$ in the curves C_w, and these do not occur in the curve forC_r. This may be due to the creation of strong viscous effects in the low- and medium-speed ranges for general ships, even though the length/beam ratio is approximately 10.0. Fortunately, most high-speed catamarans operate in the high-speed range, $Fr_L \geq 0.60$. When the spacing/beam ratio b_c/B_d is 2.0, 2.6, and 3.2, the curves C_{wr} agree with C_r, while at $Fr_L = 0.42$–0.80, C_{wr} is less than C_r at $Fr_L \leq 0.42$ and $Fr_L \geq 0.80$. In general, the spacing/beam ratio b_c/B_d is usually at 2.0–3.2, so we can take $FFACTOR = 0.25$ as a constant and get a good result, which is more convenient for practical use.

Figure 7.22 shows the results of C_r and C_w for $b_c/B_d = 6.0$, a high-speed catamaran, and *Cmono* for a monohull, the demihull of the high-speed catamaran. C_w agrees with *Cmono* very well when $Fr_L \geq 0.57$, and C_w is slightly greater than *Cmono* when $0.35 \leq Fr_L \leq 0.57$. So the interference between demihulls can be neglected at $Fr_L \geq 0.57$ when $b_c/B_d \geq 6.0$.

Comparisons of experimental and calculated total resistance and powering results for $b_c/B_d = 2.0$ are shown in graphical form in Figs. 7.23 and 7.24. The total resistance curves shown in Fig. 7.23 demonstrate good agreement between calculated, Rtc, and experimental results, Rte; however, there are some discrepancies that are mainly due to the differences in the wave resistance coefficients, as shown in Fig. 7.21b. Moreover, the calculated total resistance, Rtce, including $FFACTOR = 0.25$, agrees with Rte fully at $Fr_L \leq 0.80$. We arrive at the same conclusion for the EHP curves shown in Fig. 7.24. EHPe, EHPc, and EHPce represent experimental, calculated, and calculated, including $FFACTOR = 0.25$, effective horsepower, respectively.

7.7.5 Effect of Spacing/Beam Ratio

Residuary resistance coefficient curves C_r at different spacing/beam ratios, $b_c/B_d = 1.6, 2.0, 2.6, 3.2,$ and 6.0, are shown in Fig. 7.25. Cr1.6 represents C_r for $b_c/$

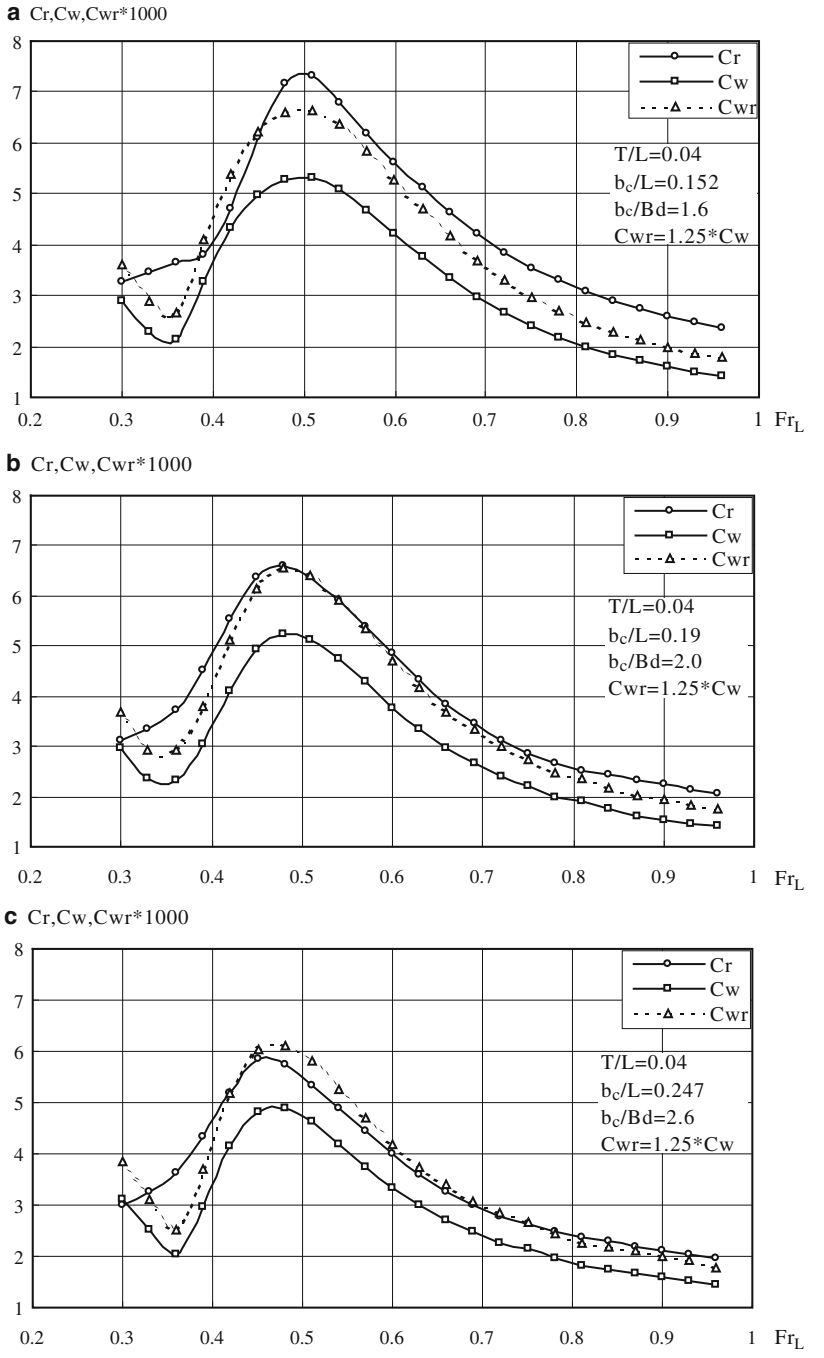

Fig. 7.21 Comparison of C_r with C_w, with b_c/B_d having the following values: (**a**) 1.6; (**b**) 2.0; (**c**) 2.6; (**d**) 3.2; and (**e**) 6.0

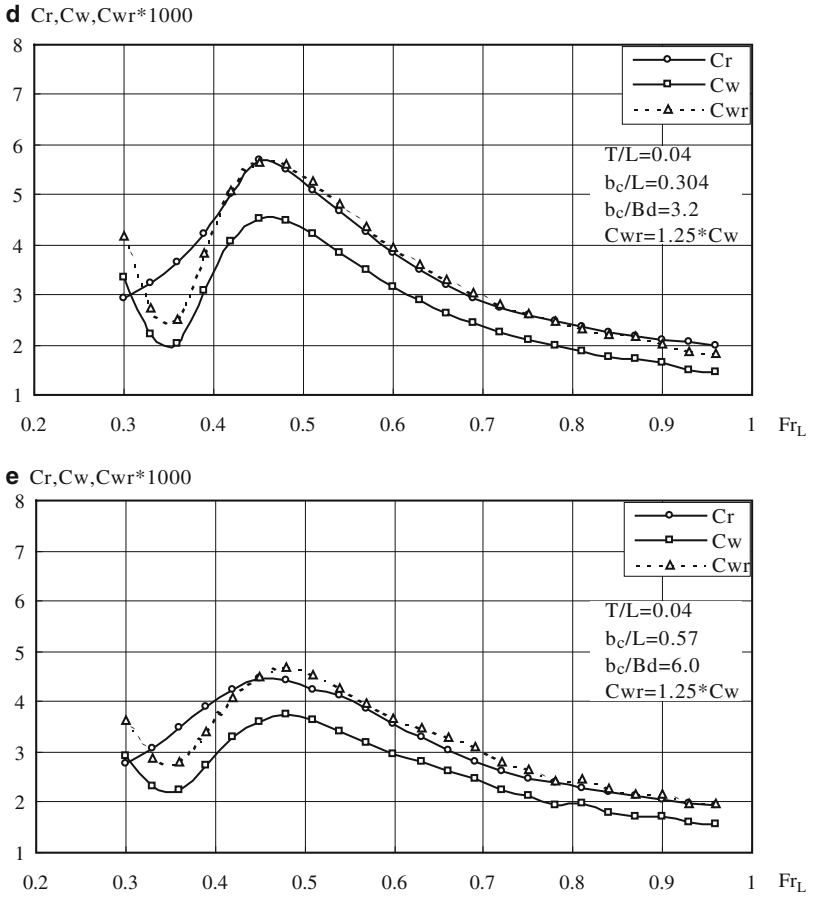

Fig. 7.21 (continued)

$B_d = 1.6$, and so on. It can be seen that residuary resistance increases at $Fr_L \geq 0.48$ when the spacing between demihulls is reduced. In particular, in the "hump" region ($Fr_L = 0.48$–0.60), the resistances are largely dependent on the spacing/beam ratio, b_c/B_d. If the spacing/beam ratio is too small, the increment in resistance will be significant. Note that if a moderate spacing/beam ratio, $b_c/B_d = 2.0$–3.0, is chosen, the resistance at $Fr_L \geq 0.70$ will only slightly increase in comparison with $b_c/B_d = 3.2$. Therefore, it is not necessary to select too large a spacing/beam ratio in practical design to decrease resistance.

Wave resistance coefficient curves C_w including $FFACTOR = 0.25$ at different spacing/beam ratios, $b_c/B_d = 1.6$, 2.0, 2.6, 3.2, and 6.0, are shown in Fig. 7.26. C_w 1.6 represents C_w for $b_c/B_d = 1.6$ and so on. We draw the same conclusion as earlier. Thus, we can predict the effect of the spacing/beam ratio well using Hsiung's method from Sect. 4.5.3 and the program in Sect. 4.7.3. for displacement and semiplaning catamarans.

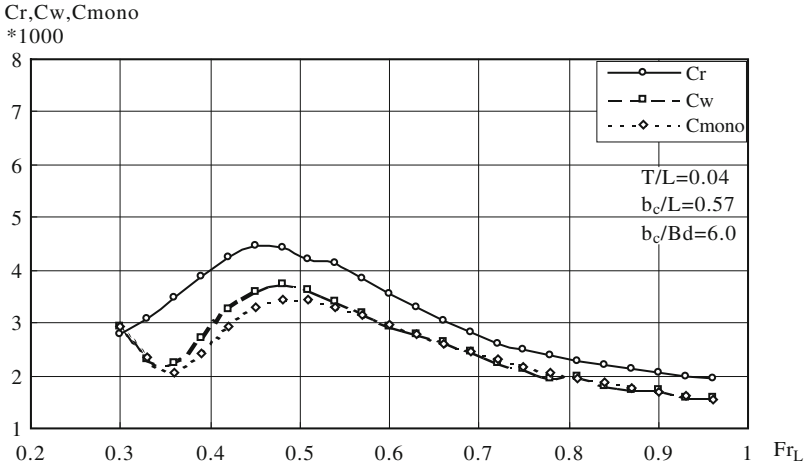

Fig. 7.22 Comparison of monohull with twin hull C_w (b_c/B_d = 6.0)

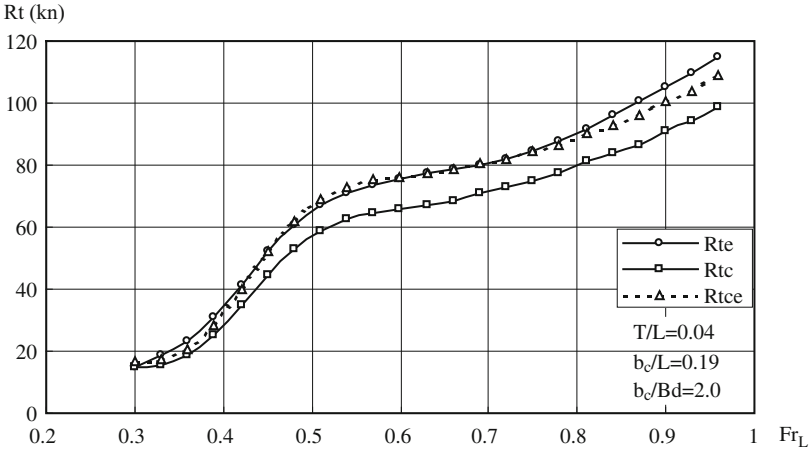

Fig. 7.23 Comparison of Rte with Rtc (b_c/B_d = 2.0)

7.7.6 Effect of Length/Displacement Ratio

Tests were carried out on the model with three test loading conditions, and the principal dimensions and the loading conditions corresponding to a real high-speed catamaran are given in Table 7.10.

Residuary and wave (including *FFACTOR* = 0.25) resistance coefficient curves at Fr_L = 0.45, 0.48, 0.63, 0.69, 0.81, and 0.96 and under different loading

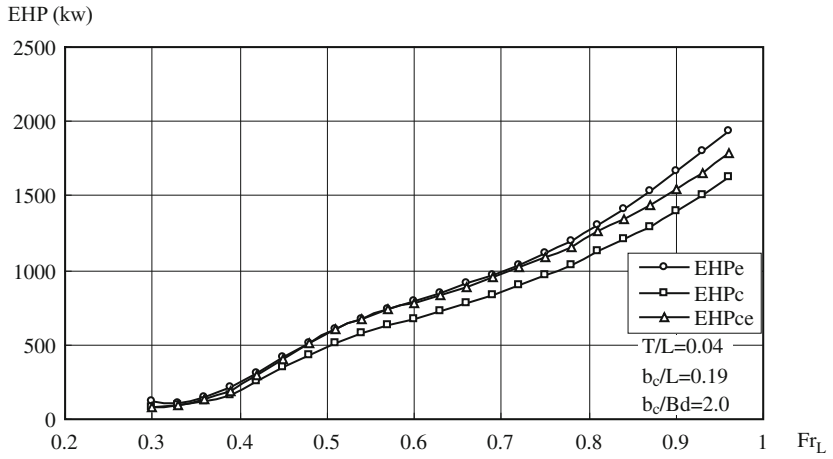

Fig. 7.24 Comparison of EHPe with EHPc (b_c/B_d = 2.0)

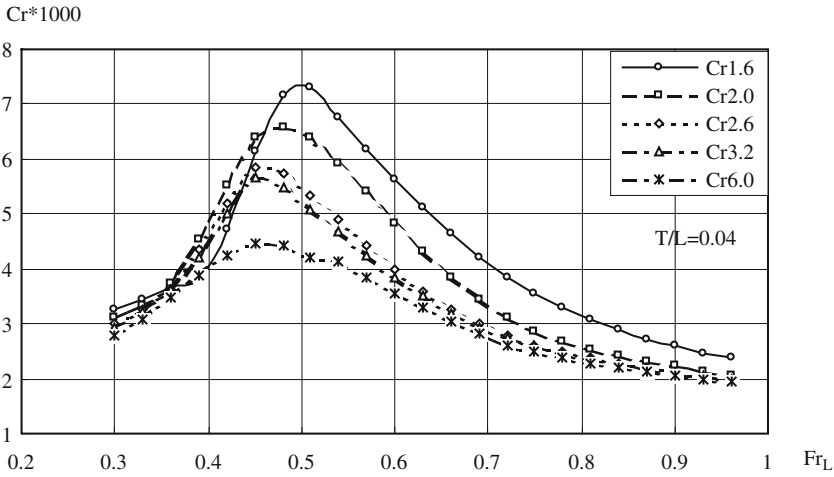

Fig. 7.25 Effect of spacing/beam ratio on C_r

conditions, length/displacement ratios, $L/\nabla^{1/3} = 6.742$, 6.421, and 5.977, and for $b_c/B_d = 2.0$ are shown in Fig. 7.27.

CrFn0.45 and CwFn0.45 represent C_r and C_w at $\mathrm{Fr_L} = 0.45$, respectively and so on. It can be found that the resistance decreases fast as the value of $L/\nabla^{1/3}$ increases at $\mathrm{Fr_L} = 0.45$–0.69, but the change in resistance is smaller as $L/\nabla^{1/3}$ increases at $\mathrm{Fr_L} \geq 0.81$.

Moreover, corresponding residuary and wave resistance coefficient curves are very close for all $\mathrm{Fr_L}$. Thus, we can predict the effect of the length/displacement ratio well using Hsiung's method from Sect. 4.5.3 and the program in Sect. 4.7.3.

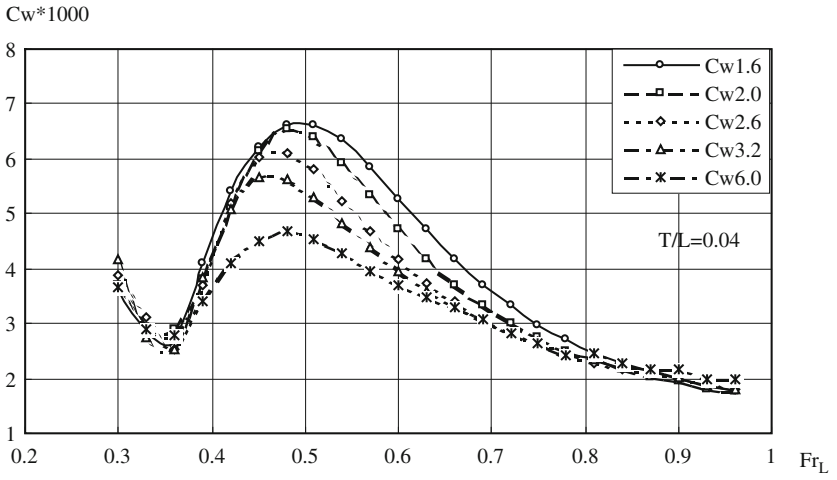

Fig. 7.26 Effect of spacing/beam ratio on C_w (*FFACTOR* = 0.25)

Table 7.10 Particulars and loading conditions of full-scale high-speed catamaran

Item	Light	Design	Full
Waterline length, m	29.7	30.0	30.2
Demihull beam, m	2.85	2.85	2.85
Draft, m	1.07	1.20	1.40
Total wetted area, m^2	185	202	226
Displacement volume, t	85.5	102	129
Length/displacement ratio	6.742	6.421	5.977

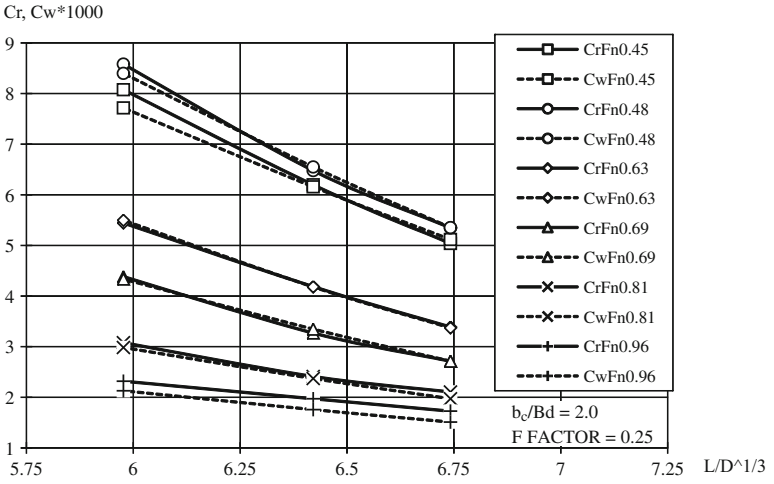

Fig. 7.27 Effect of $L/\nabla^{1/3}$ on C_r and C_w (b_c/B_d = 2.0)

7.8 Evaluation of Wave Wake

7.8.1 Introduction

Rong [13] carried out numerical tests on the high-speed catamaran model in Sect. 7.7 using the subroutine DWAKECAL in Sect. 4.7.3 to calculate wake wave heights. He undertook serious investigations on the effect of Fr_L, spacing/beam ratio, position Y, and length/displacement ratio on wake wave height and the effect of Fr_L on maximum wake wave height.

Because the model was not instrumented/tested for wake wave height, we cannot compare calculation results with the test. Fortunately, calculation results coincide with the test results of some papers, such as that of Doctors [14]. Thus, the following calculation results are useful for predicting wake wave height.

7.8.2 Effect of Fr_L on Wake Wave Height

Rong [13] calculated the wake wave height curves of the tested model for a spacing/beam ratio of $b_c/B_d = 3.2$ and the transverse position $Y = 37.5$ m from the model centerline at $Fr_L = 0.35$, 0.39, 0.43, 0.48, 0.55, 0.60, 0.65, 0.70, 0.75, and 0.80 using the subroutine DWAKECAL in Sect. 3.7.3.

The numbers of stations and waterlines were also taken as 21 and 7, respectively. Because the high-speed catamaran being modelled has a transom stern, one station is added behind AP, whose length is called the imaginary length, and so the total number of stations is 22.

Figure 7.28a–j shows the results of the calculations; the oscillation frequency of the wake wave decreases as Fr_L increases.

7.8.3 Effect of Froude Number on Maximum Wake Wave Height

Figure 7.29 shows the effect of Fr_L on maximum wake wave height for a spacing/beam ratio of $b_c/B_d = 3.2$ and transverse position $Y = 37.5$ m from the model centerline at $Fr_L = 0.35$–0.80.

The "maximum wave height" is defined as being the maximum consecutive peak to trough (or trough to peak) rather than the difference between the highest peak and the lowest trough.

The maximum wave height increases rapidly as Fr_L goes from 0.35 to 0.55 but it varies rapidly in the speed range Fr_L from 0.55 to 0.8 with the lowest trough at $Fr_L = 0.7$ and the highest peak at $Fr_L = 0.8$.

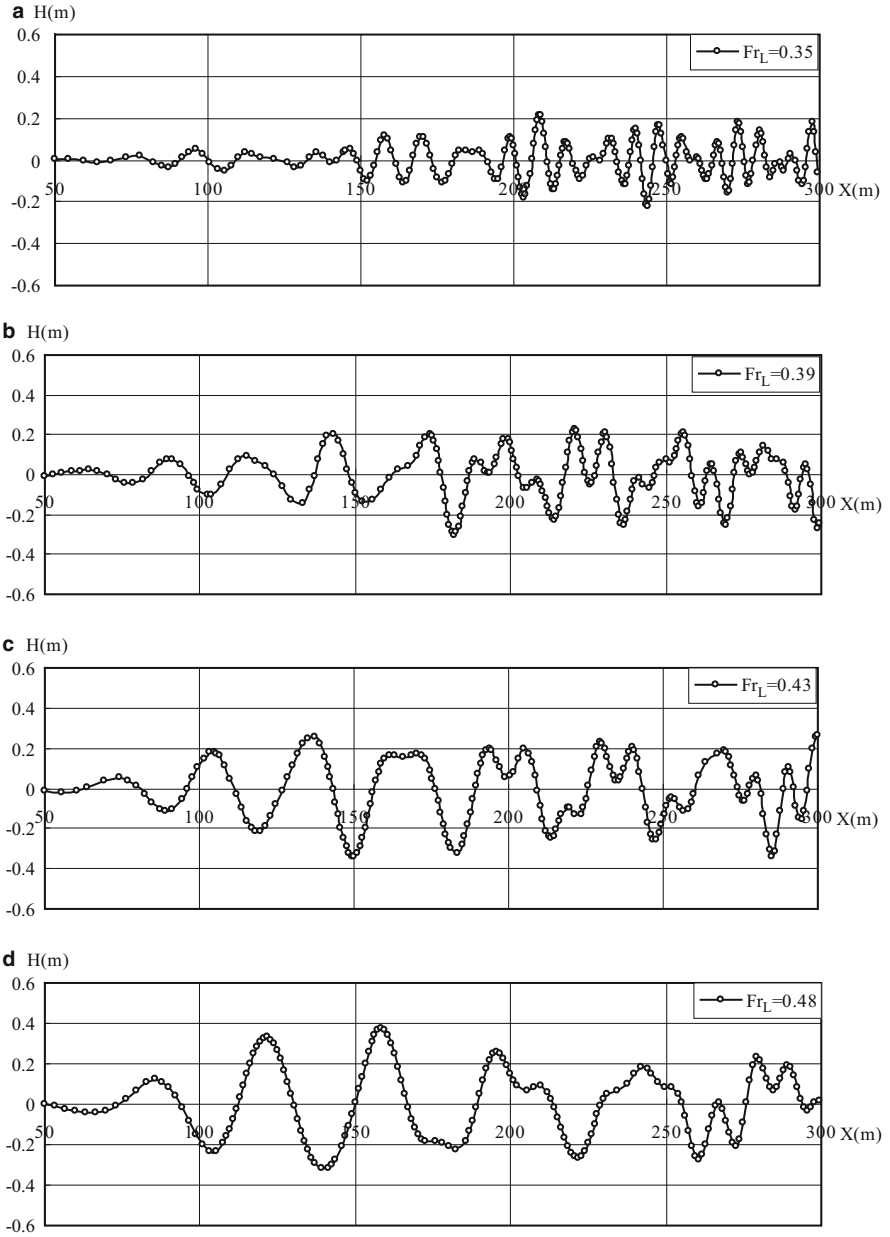

Fig. 7.28 Effect of Fr_L on wake wave height with the following values of b_c/B_d, Y, and Fn:(**a**) $b_c/B_d = 3.2$, $Y = 37.5$ m, $Fr_L = 0.35$; (**b**) $b_c/B_d = 3.2$, $Y = 37.5$ m, $Fr_L = 0.39$; (**c**) $b_c/B_d = 3.2$, $Y = 37.5$ m, $Fr_L = 0.43$; (**d**) $b_c/B_d = 3.2$, $Y = 37.5$ m, $Fr_L = 0.48$; (**e**) $b_c/B_d = 3.2$, $Y = 37.5$ m, $Fr_L = 0.55$; (**f**) $b_c/B_d = 3.2$, $Y = 37.5$ m, $Fr_L = 0.60$; (**g**) $b_c/B_d = 3.2$, $Y = 37.5$ m, $Fr_L = 0.65$; (**h**) $b_c/B_d = 3.2$, $Y = 37.5$ m, $Fr_L = 0.70$; (**i**) $b_c/B_d = 3.2$, $Y = 37.5$ m, $Fr_L = 0.75$; (**j**)$b_c/B_d = 3.2$, $Y = 37.5$ m, $Fr_L = 0.80$

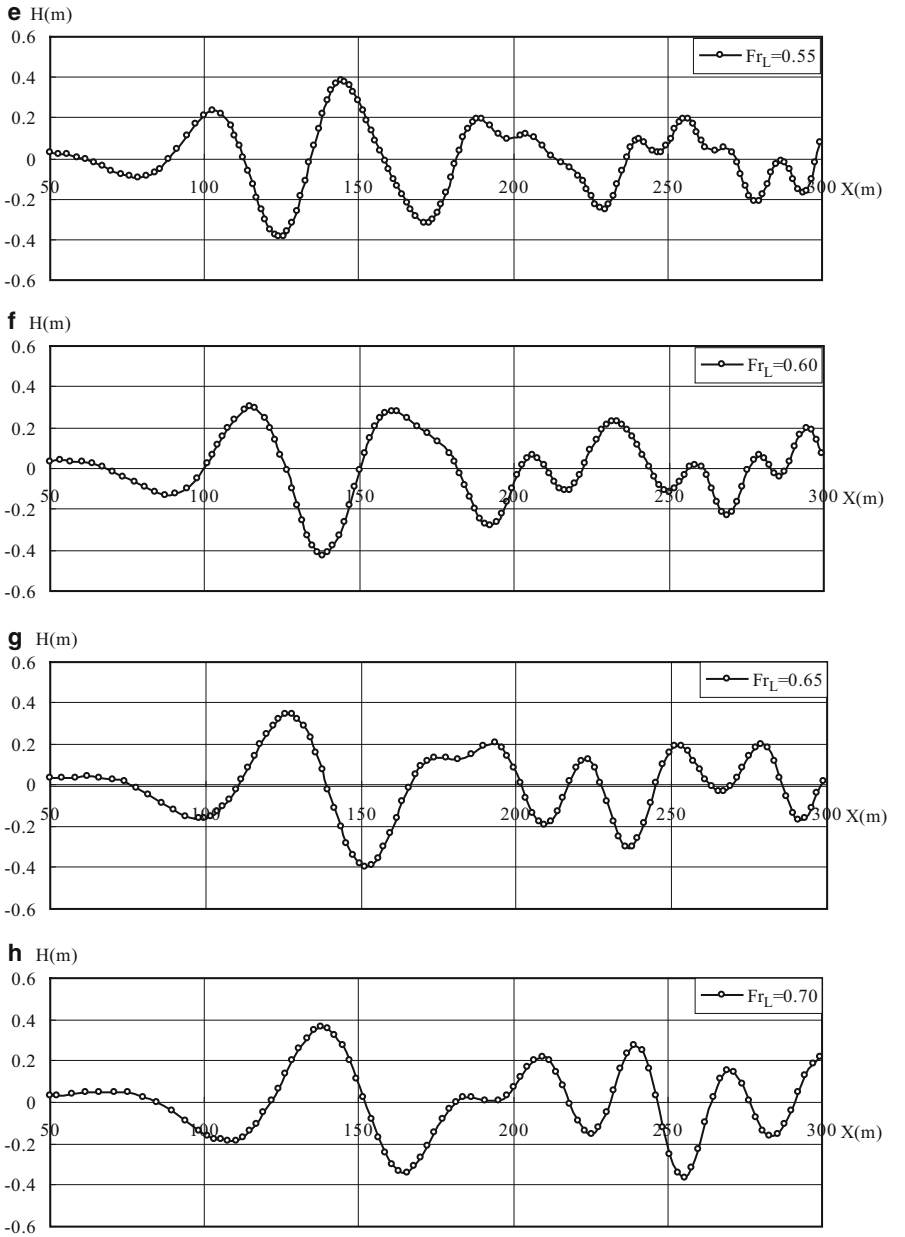

Fig. 7.28 (continued)

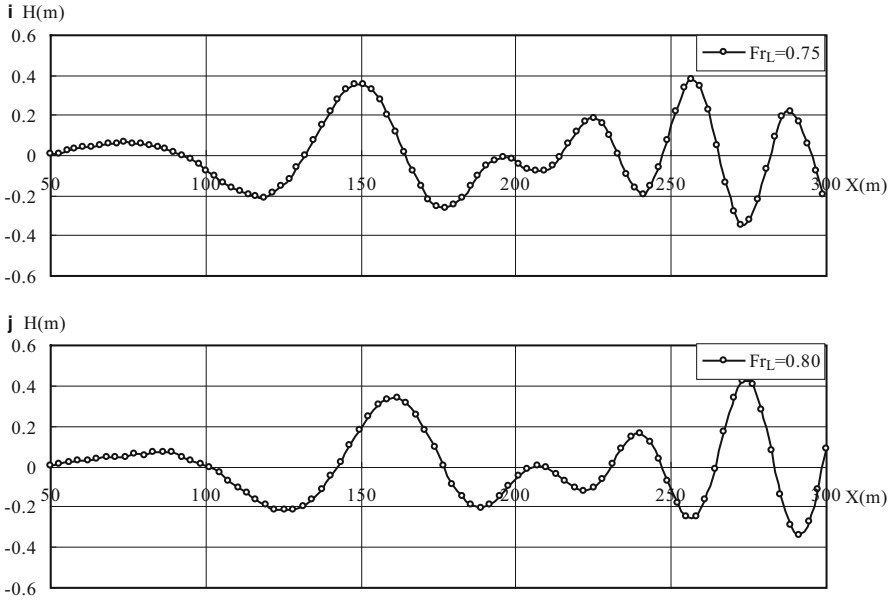

Fig. 7.28 (continued)

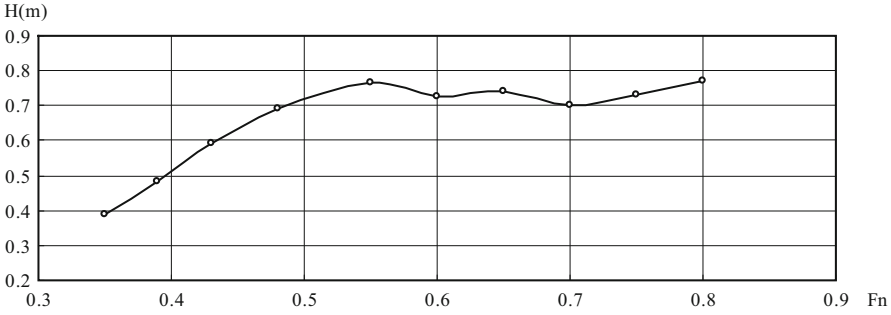

Fig. 7.29 Effect of Fr_L on maximum wake wave height (b_c/B_d = 3.2, Y = 37.5 m)

7.8.4 Effect of Spacing/Beam Ratio on Wake Wave Height

Figure 7.30a, b shows the effect of the spacing/beam ratio b_c/B_d on the wake wave height for the transverse positions $Y = 37.5$ m and 20.0 m from the model centerline at $Fr_L = 0.70$. The maximum wake wave height decreases as the spacing/beam ratio increases for different positions. Thus, we can select the larger spacing/beam ratio in practical design to decrease the maximum wake wave height.

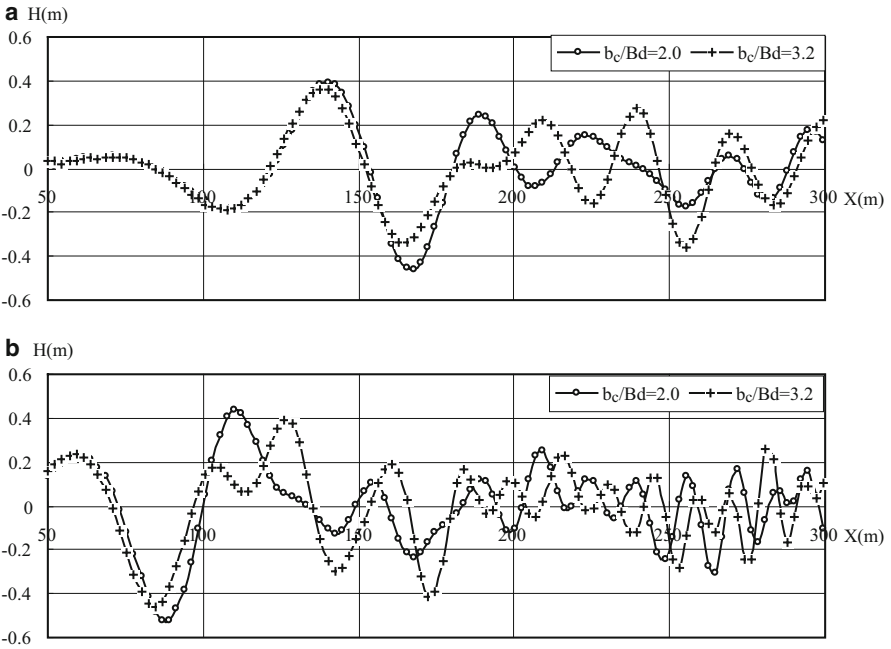

Fig. 7.30 Effect of spacing/beam ratio on wake wave height with following values of Fr_L and Y: (**a**) $Fr_L = 0.70$, $Y = 37.5$ m; (**b**) $Fr_L = 0.70$, $Y = 20.0$ m

7.8.5 *Effect of Position* Y *on Wake Wave Height*

Figure 7.31a, b shows the effect of the transverse position from the model centerline Y on the wake wave height for a spacing/beam ratio of $b_c/B_d = 2.0$ and 3.2 at $Fr_L = 0.70$. The maximum wake wave height decreases as position Y increases for different spacing/beam ratios. This coincides with the wake wave seen in MARIC tests.

7.8.6 *Effect of Length/Displacement Ratio on Wake*

Figure 7.32a–c shows the effect of the length/displacement ratio on the wake wave height for $b_c/B_d = 3.2$ and $Y = 37.5$ m at $Fr_L = 0.39$, 0.48, 0.70. S, M, and L represent length/displacement ratio $L/\nabla^{1/3} = 5.977$, 6.421, and 6.742.

The maximum wake wave height decreases as the length/displacement ratio decreases for different Fr_L. Therefore, we can select the lower length/displacement ratio in practical design to decrease the maximum wake wave height.

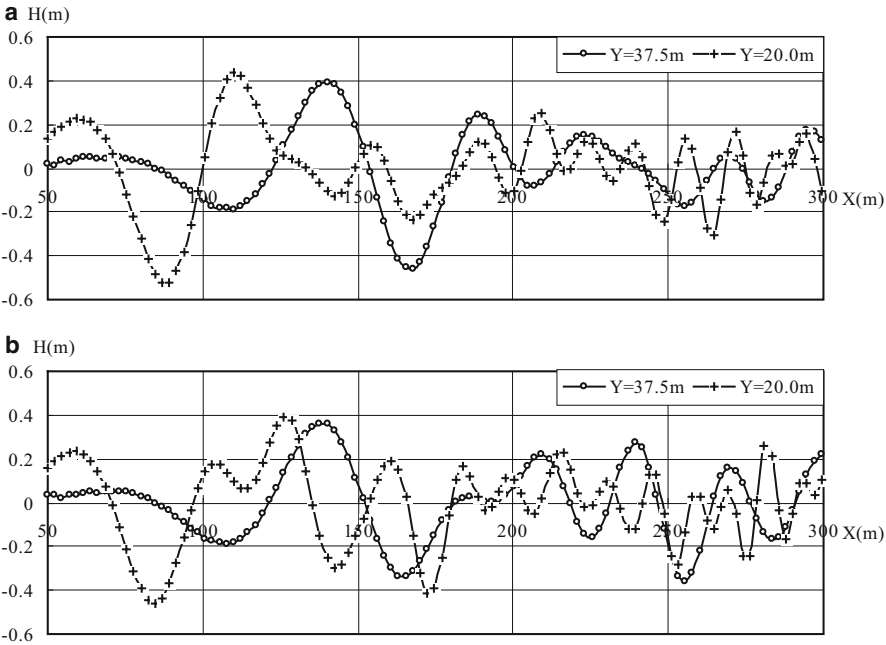

Fig. 7.31 Effect of position Y on wake wave height with the following values of $Fr_L = 0.7$ and b_c/B_d: $Fr_L = 0.7$, $b_c/B_d = 2.0$; (**b**) $Fr_L = 0.7$, $b_c/B_d = 3.2$

7.9 Small Catamarans – All Speed Ranges

Albert Nazarov of Albatross Marine Design [15] presented a paper to the *Second Chesapeake Power Boat Symposium* in March 2010 discussing the design of small power catamarans in the length range of 6 to 24 m that gives useful guidance for catamaran design, particularly planing vessels and smaller craft. The key points of the paper are summarized in what follows. Readers are encouraged to refer to the paper where sample line plans for displacement, semiplanning, and planing craft and specifications of the 16 vessels referred to can also be found. Another paper [16] builds on this one, giving further details on the proposed design methodology.

The focus of the paper is a practical approach to designing catamarans for pleasure or utility use derived from designing, building, and testing 16 different vessels. Like our description of the different basic hull shapes for displacement, semiplaning, and planing vessels, Nazarov also describes these shapes, noting that a catamaran is effectively designed around the tunnel between the hulls, with the tunnel shape and dimensions having a primary influence on the resulting boat performance. He notes that planing catamarans will have wider hulls and a smaller width of the central tunnel so as to avoid having the boat be too stiff in roll and giving an uncomfortable ride. Once the vessel is planning, the interaction between

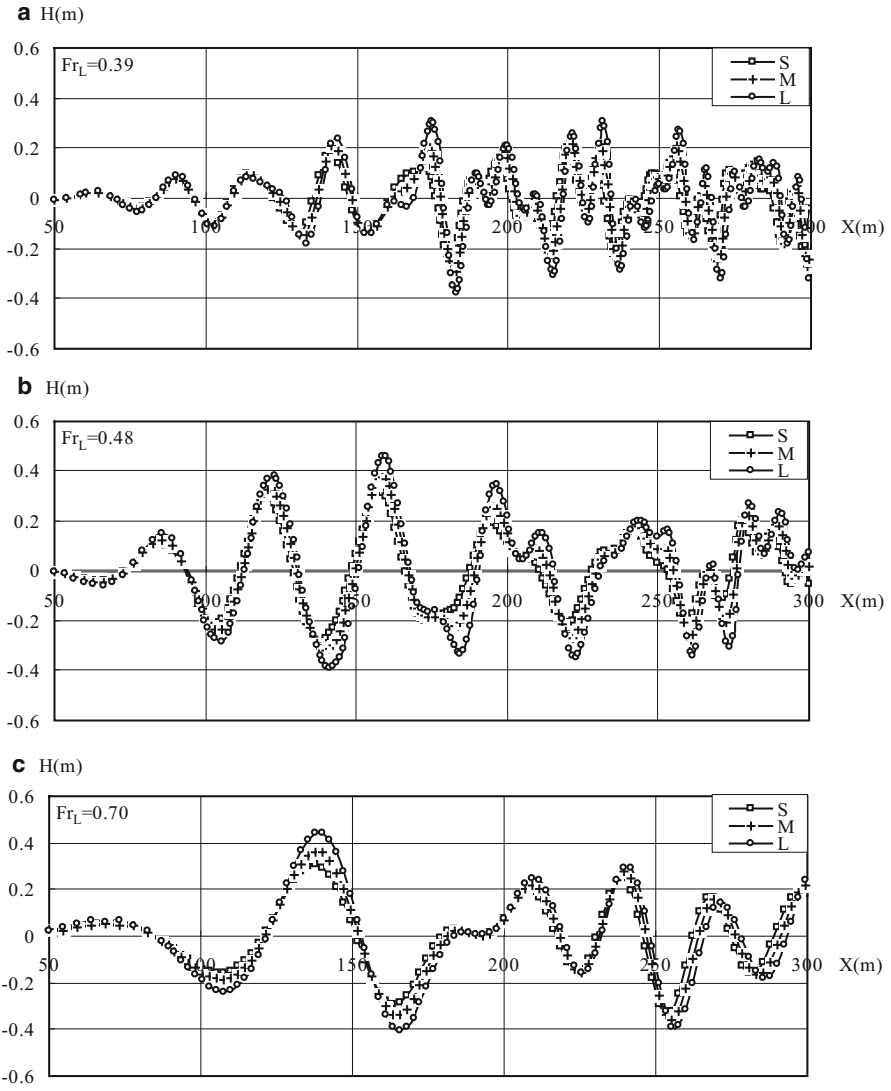

Fig. 7.32 Effect of length/displacement ratio on wake at different values of b_c/B_d, Y, and $\mathrm{Fr_L}$: (**a**) b_c/B_d = 3.2, Y = 37.5, $\mathrm{Fr_L}$ = 0.39; (**b**) b_c/B_d = 3.2, Y = 37.5, $\mathrm{Fr_L}$ = 0.48; b_c/B_d = 3.2, Y = 37.5, $\mathrm{Fr_L}$ = 0.70

the hulls for wave making is less, particularly if the inner walls are vertical or near vertical, so there is more flexibility to design in this respect than slower semiplaning or displacement boats.

7.9.1 Hull Shape

Nazarov defines two factors affecting the isolated demihull shape: the length/displacement ratio (LDR $= L_{WL}/V^{0.33}$, where V is the displaced volume, m^3) for displacement catamarans and the static load factor, C_Δ, where $C_\Delta = V/(2\ B_{cd})^3$ and B_{cd} is the beam at the chine of the demihull (m) for planing boats operating above $Fr_L = 1.0$ or $Fn_\Delta = 2.5$.

By taking twice the demihull width, the approach is similar to considering the planing surface of a monohull planing craft, ignoring the central tunnel. Here the displaced volume is that for the craft at rest. Clearly the wider the aggregate demihull width, the greater will be the planing surface, reducing the surface pressure needed to support the boat in planing mode. Nazarov recommends that designers use $C\nabla$ 0.5 to 0.7 for successful planing, noting also that many fast monohull vessels have $C\nabla$ in a range of 0.2 to 0.5.

It may be observed that the lift generated by the two asymmetric demihulls of a planing catamaran will be somewhat less than that of a monohull due to the vertical wall at the keels and the decline in pressure toward that point. The reduction may be in the region of 10%, so for catamarans this should be taken into account for planing area assessment when calculating both dynamic trim and drag.

Nazarov's example catamaran designs have LDR in a range of 5 to 7.6 with no clear distinction between vessels for different speeds; small craft appear to be more toward 5 while some designs are at 7 and 7.6. A higher LDR gives a finer hull form, and so lower wave-making drag, which is important for slower boats. The LDR can also relate to a lighter loading for a planing catamaran, which is helpful for acceleration up to planing.

Dynamic lift will also be dependent on the lower hull dead rise and whether there is warp toward the stern. Nazarov used dead-rise angles mostly in a range of 20 to 30°, which is also typical of a fast monohull, with slower vessels having a warp down to about half that angle at the stern, while faster vessels tend to have almost parallel cross section aft of amidships with two or more longitudinal spray rails and a downward-facing chine rail. One of Nazarov's high-speed planing examples also has two steps in the after part of the hull [15].

The present authors suggest a designer start with C_Δ around 0.5 and, once the structural weight for the boat has been estimated, make another cycle to see if this can be maintained or allow it to be higher and increase installed power to compensate, so as to maintain the desired design speed. Designing for much lower than 0.5 may demand special construction, in carbon fiber for example, so as to save weight, but this will come at significant cost, which may not be justified, unless the vessel is for competition.

Concerning demihull slenderness, efficient displacement and semidisplacement catamarans have a L_{WL}/B_{cd} of 10 to 12, while for faster planing boats this may reduce down to as far as 8. For small craft like this there is a useful lower limit to demihull width to allow access and machinery installation for personnel. Nazarov notes that demihulls are generally wider than 1 m.

Slower displacement or semidisplacement boats will normally be designed with a rising keel line toward the stern so as to minimize resistance, while faster semiplaning and planing craft will have a transom stern that may be the same draft as at amidships. Nazarov recommends that semiplaning vessels operating in a range of Fr_L 0.5 to 1.0 have linearly increasing transom areas compared to amidships from 0 to 0.05 up to 1.0 as the design transitions to full planing.

Regarding the dead-rise angle at the stern, apart from hydrodynamic performance, there is also an issue of integration with the propulsion system. A 10- to 15-m boat may have outboard motors attached to the stern of each demihull, or perhaps inboard motors and a z-drive unit at the transom, in a power range up to 250 shp. This is okay with a single unit on each hull, while for larger boats the power rating may mean larger engines mounted further forward driving a traditional propeller configuration below the keels or perhaps linked to a waterjet propulsion unit, or for a design aimed at above 50 knots perhaps a surface drive unit. In either of the latter cases, careful review of the hull shape aft of amidships is needed, since for a waterjet in particular it would be advantageous to have a flat area around the inlet, or at least a lower dead-rise angle. This is a rather specialist area, and so it is recommended to seek advice from a waterjet supplier if this power option is considered.

Above $Fr_L = 1$ or $Fr_v = 2.5$, a boat is expected to fully plane, so a hard chine form with asymmetrical demihulls may be the baseline, and below $Fr_L = 0.4$ or $Fr_v = 1.0$ the boat will be in displacement mode and so a round bilge form would be adopted. In between we have the speed range where dynamic lift is increasingly effective, and so use of a chined demihull section will be helpful. Combining this with the need to increase the transom area as speeds approach full planing one can see a natural tendency to adjust the demihull cross section from amidships or slightly forward and back to the stern, changing to a symmetrical shallow chined form and extending this forward to the bow for higher-speed boats. Figure 7.33 gives a diagrammatic view of these forms against Fr_l.

As vessel design speed is increased and dynamic lift becomes significant, the form discussed previously will tend to drive the center of buoyancy toward the stern. A displacement vessel will have a CB perhaps up to 5% aft of amidships. Semiplaning vessels will have finer forward lines, so the CB (of a boat at rest) will move sternward to perhaps 10% at Fr_l of 1.0 and as high as 15% for high-speed vessels without stepped hulls or remain around 10% for stepped-hull design. The fineness of the forward form is most important for vessels operating in a Fr_L range up to 0.6. For these vessels a demihull prismatic coefficient C_P below 0.6 is recommended by Nazarov. This is the speed range where wave making and demihull wave making interference are greatest, as discussed in Chaps. 2 and 4, and is the range where for larger vessels the super slender form has been introduced with great success.

As design speed is increased through the semiplaning range of Fr_L, the C_P for these small vessels will increase as the form is changed toward a chined shape so that above $Fr_L = 1.0$ the C_P may be in the range 0.7 to 0.8 for the at-rest demihull. Note also that for a planing vessel, while the form of the planing surface will be triangular,

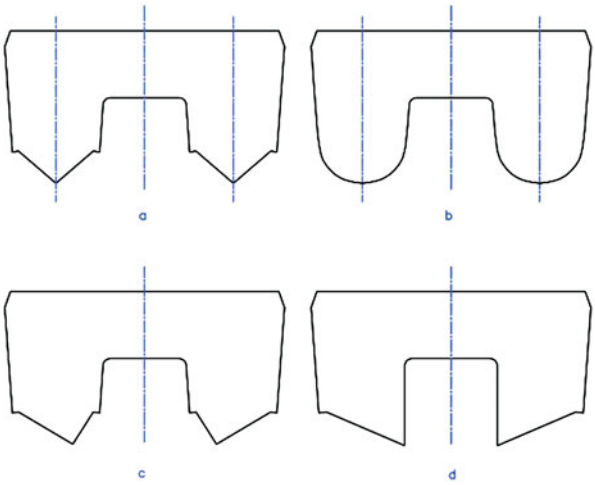

Fig. 7.33 Body plans for fast catamarans

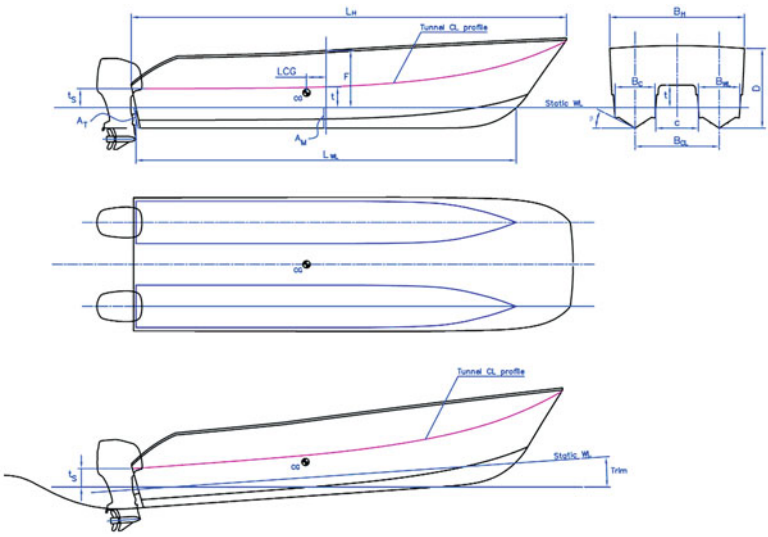

Fig. 7.34 Planing catamaran

it is important that there be sufficient buoyancy in the bow area to lift the hulls as waves are negotiated (contrary to the approach for wave-piercing catamarans discussed in Chap. 9), and this leads to the characteristic form of a fast powerboat with a sharp flared bow as in Fig. 7.34.

Figure 7.35 below shows the recommended envelope of LCB and C_P against an *x*-axis of Fr_L and Fr_v by Nazarov.

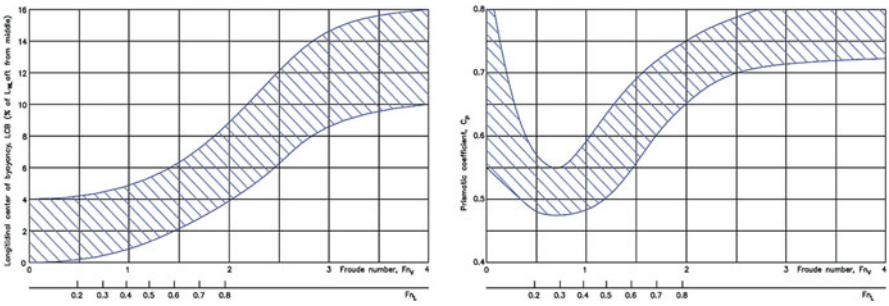

Fig. 7.35 Design envelopes for (**a**) LCB and (**b**) CP with Fr_L

7.9.2 Tunnels

The tunnel between demihulls of a fast catamaran needs to be considered from three aspects, as further considered below:

- Hull spacing (c) and so tunnel width compared to demihull beam, and length
- Tunnel roof height (t) from SWL
- Tunnel shape from bow to stern

7.9.2.1 Spacing

In Chap. 4, we went through in some detail the optimization of demihull spacing from the wave-making resistance point of view. Nazarov's comment is that slower small catamarans tend to have wider spacing for optimized resistance compared with planing craft.

Relating hull spacing to demihull beam as we did earlier in the book, Nazarov's lower speed designs have B_{cl}/c in a range of 2 to 3, while the higher-speed planing designs have values of 1 or less. Nazarov recommends the lower spacing to give lower roll stiffness for those craft that have wider demihull beams, as mentioned earlier.

The lower spacing is also consistent with having an asymmetric hull section and so lower wave-making interaction as a boat is accelerated. Nazarov recommends a spacing of between 0.1 and 0.2 of vessel L_{WL} for planing craft, which would mean the L_{WL}/B_{WL} for such planing vessels would stay similar for larger craft.

In actual fact, as such vessels are scaled up, the tendency is to scale up the length more than the vessel breadth, even for planing craft, and use stepped-hull forms to optimize planing support. This is evident in Class 1 offshore racing catamarans (Fig. 10.8). The tunnel width is nevertheless relatively smaller than on semiplaning catamarans, as also shown in the section on MARIC planing catamaran studies in Chap. 10.

7.9.2.2 Height

Tunnel height has to be set so as to avoid (so far as possible) impact with the sea surface. At the bow this means any cross structure needs to be at a freeboard to avoid slamming due to the design sea state. Nazarov quotes from his experience and model testing that for the small catamarans slamming generally begins when the significant sea state $h_{1/3} = 2$ t, where t is the cross-structure deck clearance from SWL at amidships, at rest.

This is likely also to depend on the exact form of the bow area and how much additional clearance can be designed for at the front of the cross structure. Clearly it is advantageous to ramp the tunnel up toward the bow so the surface facing oncoming waves are canted, up to the deck edge level if the tunnel extends all the way to the bow. Typically the demihull freeboard may be more than twice the tunnel height. Where wide demihull spacing is used, it will be useful to include a wave-breaking wedge form in the bow part of the tunnel, extending halfway back to amidships, as this is the area most affected by slamming in high waves. Such a structure can also add strength to the cross structure above the tunnel in this highly loaded area.

If we turn our thoughts back to Chap. 3 and vessel stability for a moment, then in order to design the overall form of our catamaran, we first select the form of our demihulls and spacing, and then we need to consider both the likely operational sea state to make a preliminary location and wet deck shape for the cross structure and check out the demihulls' freeboard intact and damaged so as to have a stable vessel. The demihull freeboard will then guide the shape of the cross structure as it crosses the beam of the demihull integrating with the hull shell, frames, and bulkheads.

7.9.2.3 Shape

The tunnel for a planing catamaran will have increased clearance from the SWL when the boat is at speed but first needs to negotiate acceleration through hump speed. Since this is in a seaway, the tunnel roof shape and height should follow the foregoing recommendations based on the expected design limiting sea state. Since a planing vessel will experience impact loads much higher than a slower vessel (proportional to velocity^2) the additional height on the plane will assist at limiting slamming loads. Nazarov takes a less cautious view, suggesting a tunnel height at amidships of 2% to 3% of boat L_{WL}.

The tunnel roof may be designed parallel aft of amidships or, on slower boats, to have a rise or step upward in the stern area, while high-speed craft may have a roof tapered further to the SWL to generate higher pressure in this region from the air and spray flow. Both Nazarov and the present authors recommend, nevertheless, keeping the tunnel roof line above the SWL.

Note also that for boats operating in the Fr_L 0.4 to 0.7 region, the demihull inner side shape forming the sides of the tunnel will have important input to the wave-

making interaction, as discussed in Chap. 4 and earlier in this chapter; so in addition to demihull spacing, an asymmetric cross section can be used to either optimize resistance or minimize the external wake for confined waterways.

7.9.3 Above-SWL Configuration Air Drag

A pleasure or utility catamaran will have a superstructure designed around the functional needs of its mission and the personnel. A sport fishing vessel may have a flying bridge as well as cabins laid out on the floor space provided by the cross-structure area, with only storage spaces and machinery in the demihulls.

Nazarov notes that small catamarans will have a higher aerodynamic resistance than a monohull vessel owing to the higher presented area of the superstructure and cross structure between the hulls. The superstructure of small utility boats is likely to be bluff and practical rather than streamlined, so the air drag coefficient C_D may be as high as 0.6 to 0.8. Fast planing vessels need to carefully consider streamlining and minimization of drag-inducing external small appurtenances so as to reduce C_D, to below 0.5 if possible. The present authors recommend referring to Hoerner [17] to prepare air resistance calculations.

It may be noted that, specially for small craft but also larger vessels, where utility reasons lead to a profile with more windage forward, this will reduce vessel directional stability in high wind conditions. As discussed earlier in this chapter in Sect. 7.5.1, multihull ferries generally have aerodynamic center of pressure well behind amidships to minimize this issue. Where this is overridden by utility factors, it will be necessary to provide additional directional stabilization from rudders or fins at the stern.

A first-pass approach to checking directional stability and sizing such appendages will be to determine the turning moment from the expected extreme wind assumed from the beam for the above-water profile, then determine the center of hydrodynamic pressure from the submerged hull profile and determine the hydrodynamic corrective turning moment as the vessel is turned against its direction of motion by, say, 15°, 30°, or 45° at its operational speed (and to check at maximum speed perhaps). If the stabilizing hydrodynamic moment exceeds the wind turning moment, the vessel is probably directionally stable, but if it requires 10° or more from the initial direction of motion, then additional hydrodynamic stabilizing forces will be needed.

The traditional propulsion arrangement with canted drive shaft, propeller, and rudder provides such stabilizing moments, and the main task is to size the rudder both for directional stability and to provide sufficient turning moments for craft maneuvering. Where a waterjet, stern drive, or surface drive is used for propulsion, they will rely on the after-hull underwater form to be directionally stable, so it is important for the designer to check this out early on in design, adding fins or strakes as required.

Fig. 7.36 Albatross Marine AT1500 catamaran

Fig. 7.37 Albatross Marine AS14 fast ambulance

The target is to achieve a balance of the hull profile and above-water profile that will protect against a "broach" to a broadside condition to waves in the design envelope of winds and waves.

Figures 7.36 and 7.37 show examples of catamaran vessels designed by Albatross Marine Design based on these principles.

7.10 Moving on from the Hydrodynamic Form

In this chapter, we have used relations based on statistics or model test correlations to define or check the overall dimensions for a catamaran. These data then need to be used to check against the initial hull form developed in Chaps. 2 and 3, reevaluate calm-water resistance, and take a look at seakeeping as in Chap. 6. Once the desired main dimensions and form balance with the functional design requirements and meet the criteria for desired speed and motion based on the estimations, it is possible to

move forward to work on propulsion, structural design and analysis, and internal outfitting. We discuss these subjects in Chaps. 11, 12, and 13. Before that, we will look at multihull design variations so as to highlight where they may offer opportunities and may need a different approach to defining their form.

We start with wave-piercing catamarans, continue with SWATH vessels and then consider a number of hybrid configurations, and go into a little more detail on the study of planing catamarans at MARIC.

References

1. Bliault A, Yun L (2000) Theory and design of air cushion craft, Pub Arnold/Elsevier, ISBN 0 340 67650 7 and 0 470 23621 3 (Wiley), p 632
2. Yun L, Bliault A, Doo J (2010) WIG craft and ekranoplan, ground effect craft technology. Springer, ISBN 978-1-4419-0041-8
3. ISO 2631 mechanical shock and vibration – evaluation of human exposure to whole-body vibration (at https://www.iso.org/obp/ui/#iso:std:7612:en)
4. STANAG 4154-2000 common procedures for seakeeping in the ship design process, available via. https://infostore.saiglobal.com/store/Details.aspx?productID=456533
5. IMO (2000) International code of safety for high speed craft, publication IA-185E, ISBN 92789 28014 2402. Amendments and resolutions after 2000 are available on IMO web site IMO.org
6. Song GH et al (1988) The research of wave-element for a high speed catamaran in inland river. In: Proceedings of International HPMV Conference, Shanghai, China, 2–6 Nov 1988
7. Armstrong T (2000) Statistical analysis of the characteristics of catamarans. Fast Ferry International, Great Britain
8. Jane's high speed marine craft, annual, issues from 1974 through 1993, Jane's Information Group, Coulsdon, ISBN 0-7106-0903-5
9. Jane's high-speed marine transportation editions up to 1999 up to 2012, Stephen J. Phillips, Jane's publishers, ISBN 0-7106-0903-5, Data referred is from 1999–2000 edition
10. Burkhard M-G (1991) The effect of an advance spray rail system on resistance and development of spray of semi-displacement round bilge hulls. In: Proceedings, FAST'91, Trondheim, Norway
11. Wang C-Y (1994) Resistance characteristic of high-speed catamaran and its application. (in Chinese). Shipbuilding of China, No.3
12. Huan-Zong R (2002) Application of linearized theory of wave resistance to high speed catamaran, SWATH and WPC. (in Chinese). Research report, MARIC
13. Huan-Zong R (2002) Calculations of wake wave for a catamaran by using linearized theory. (in Chinese). Research report, MARIC
14. Doctors LJ (1991) Waves and wave resistance of a high-speed river catamaran. FAST'91, China
15. Nazarov A Power catamarans: design for performance. Second Chesapeake Powerboat Symposium, Annapolis, Maryland, March 2010
16. Nazarov A Catamarans: design approaches and case studies. Trans RINA, Vol 156, Part B2, Intl Jnl Small Craft Technology, Jan–Jun 2014
17. Couser PR, Molland AF, Armstrong NA, Utama IKAP (1997) Calm water powering predictions for high speed catamarans, FAST 1997, Sydney, Australia, 21–23 July 1997

Chapter 8
Wave-Piercing Vessels

8.1 Introduction

In the next three chapters, we will introduce a number of hybrid vessel types linked with the catamaran configuration that aim to improve seakeeping and seagoing performance. We start with the wave-piercing catamaran (WPC) and then continue with the small-waterplane-area twin hull (SWATH) in Chap. 9 and other multihulls in Chap. 10. We will briefly touch on the WPC plus air cushion support in this chapter, SWATH plus air cushion support in the next chapter, and concepts such as the tunnel planing craft (TPC) and super-slender twin hull (SSTH) in Chap. 10 to give a flavor of the challenges presented by hybrid designs and the performance tradeoffs that they introduce. There are similarly a number of options for vessels with a central hull and outrigger support, such as the high-speed trimaran and the pentamaran. These can also employ additional concept adjustments such as hydrofoils to enhance performance. We will give a flavor of these also in Chap. 10.

The aforementioned vessel types have different hull lines and configurations, hydrodynamic mechanisms, and performance characteristics, as well as structural features, making a simple comparison of their features across the board a little complex. For this reason, in this and next two chapters, we will focus on the catamaran's close relatives, such as the WPC, SWATH, TPC, SSTH, and their hybrids.

All high-speed craft (or high-performance marine vehicles) are supported by some combination of hydrostatic support (buoyancy), static air cushion lift, hydrodynamic support, and aerodynamic support. We introduced craft supported by static air cushion in [1] and those supported by aerodynamics in [2]. Here we focus on the catamaran supported mainly by buoyancy with a proportion by hydrodynamic lift and primarily using hydrodynamic forces to stabilize its motion while at speed. We will discuss fins or hydrofoils that function as a control mechanism to adjust the running trim and provide damping force and moment for improving the seakeeping in our Chap. 11.

L. Yun et al., *High Speed Catamarans and Multihulls*,
https://doi.org/10.1007/978-1-4939-7891-5_8

8.2 Features of Wave-Piercing Vessels

The concept for a wave-piercing craft is a hybrid combining elements of a catamaran, semi-SWATH, and semiplaning monohull high-speed vessel. The advantages and disadvantages of the three types individually are summarized briefly in the following table. The idea for the WPC is to merge the advantages of the three concepts while avoiding the disadvantages so as to create a generally improved performance compared with a simple catamaran form.

The design target for a wave-piercing vessel is to combine the low motion and accelerations of a SWATH or semi-SWATH when operating in waves while minimizing drag using a semiplaning hull form. To achieve this, a WPC has a larger waterplane area than a SWATH, but with considerable tumble home above the waterline. Effectively, the so-called SWATH characteristic is applied to the hull above the waterline so that in waves the tendency is to slice through rather than to "ride" the waves. Since catamaran demihulls do not have sufficient buoyancy to lift the bow out of waves, in higher sea states waves may impact with the catamaran's connecting structure, and in the bow area this is formed like a central hull and bow with its keel above the calm-water waterline. A typical cross section of a modern WPC is shown in Fig. 8.1, while further indications of the geometry are seen in Figs. 8.2 and 8.3a–c. The prototype WPC craft had a raised central hull/cabin supported on struts from the demihulls (Figs. 8.3 and 1.11b).

The modern WPC is characterized by demihull slenderness under the design waterline, similar to a normal catamaran, and with reduced beamwise dimensions above the demihull design waterline, not quite as thin as a SWATH but sufficient for improving seakeeping quality. This geometry avoids the difficulties associated with the arrangement of the main engines in the demihull that occur for a SWATH (Chap. 9) and allows the vessel to be designed for semiplaning operation at service speed.

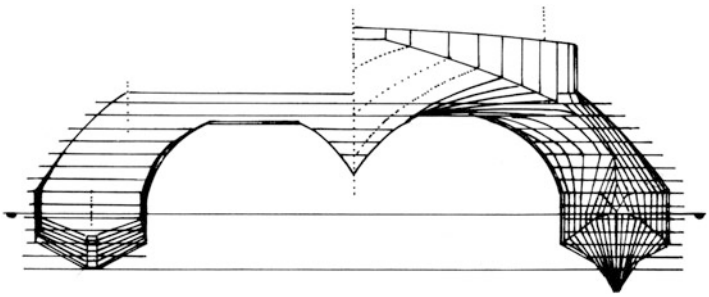

Fig 8.1 WPC configuration features

Fig. 8.2 Wave-piercing bow in action – US Navy HSV-2 – Incat Hull 050

Advantages	Disadvantages
Semiplaning monohull vessel	
• Fine seaworthiness	• Low transverse stability for high slenderness
• Good high-speed performance	• High motions and accelerations in a seaway
	• Low-volume and deck area for payload
High-speed catamaran	
• Simple structure	• Challenging structural design for large craft
• Low-cost construction	• Poor seaworthiness in beam seas
• Large usable deckhouse area	
• Medium speed	
SWATH	
• Extreme seaworthiness	• Large wetted area, friction drag at high speed
• Large deck area	• Poor longitudinal stability
	• Deep draft
	• Sensitive to weight distribution and changes
	• Complicated power transmission

Key features of WPCs are summarized in what follows.

1. *Hull slenderness*. A typical demihull slenderness ratio is $L/\nabla^{1/3} = 9 - 11$, with L/b in a range of 10–19 and $b/T = 1.2–2.3$ (see Tables 8.4a and 8.4b for examples of vessel characteristics). This is rather slender and with deeper draft compared with conventional catamarans, so the waterline entrance angle at the bow is smaller than that on a high-speed catamaran. Figure 8.4 shows a typical relation between the unit power $P/v_s\nabla$ and volumetric Froude number

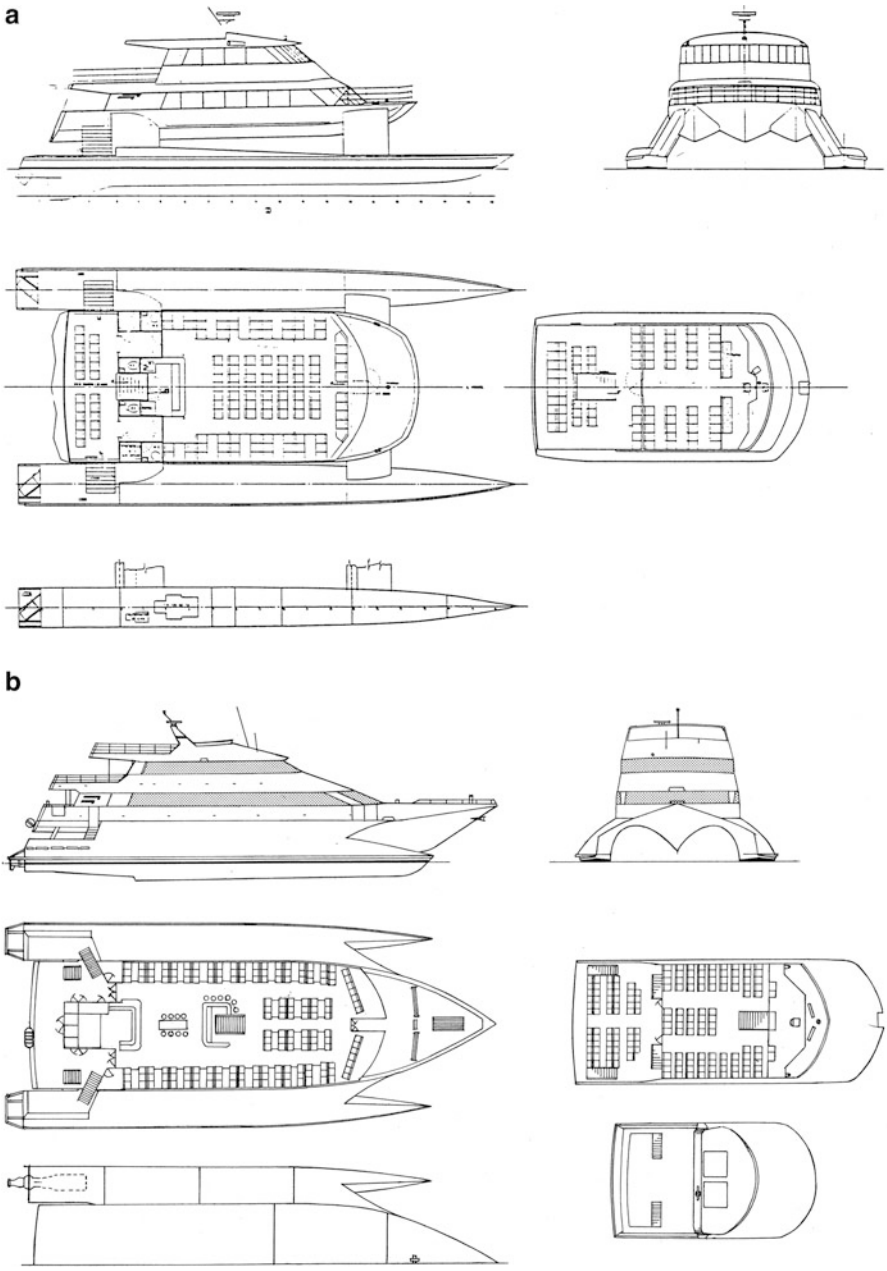

Fig. 8.3 (**a**) Profile of 23-m Incat WPC *Spirit of Victoria*; (**b**) general arrangement of Incat 39-m WPC; (**c**) Incat 74-m WPC Seaspeed Jet

Fig. 8.3 (continued)

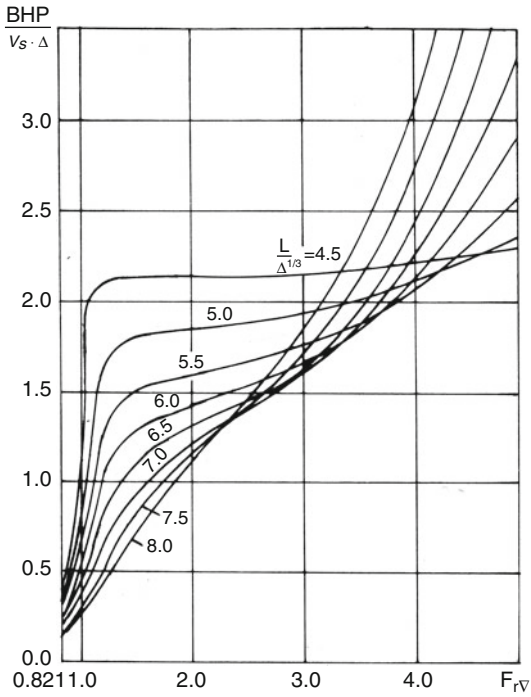

Fig 8.4 Power per tonne knot relationship with Fr_L

$F_{r\nabla} = v_s/\sqrt{g\nabla^{1/3}}$, where v_s is the ship speed, P the engine power, and ∇ volumetric displacement. It can be seen that increased slenderness will cause a reduction in the required total power, where $F_{r\nabla} < 3.0$ due to a decrease in wave-making resistance, similar in principle to a high-speed catamaran with high slenderness. However, for $F_{r\nabla}$ larger than 3.0, the total power will be higher at high slenderness owing to the increased friction resistance. So the ideal for WPCs is $F_{r\nabla} = 0.75–1.1$.

2. *Low demihull freeboard and thinner struts*. A WPC demihull freeboard is low, particularly at the bow. The reserve buoyancy at the bow is reduced, which decreases wave perturbation and heaving and pitching motions in waves. The demihull configuration above the design waterline is rather different from that on ordinary high-speed catamarans in the area interfacing with the bridging structure, with thinner configuration, while being curved and transitioning smoothly into the connecting structure on the inside underneath (Fig. 8.1).

   Variations to the geometry shown in Fig. 8.1 have been used because the vessel type has matured and vessels with this configuration have increased in size. Early and smaller vessels had struts connecting the superstructure and were also thinner, similar to a SWATH, so as to reduce the interference of waves and improve longitudinal motions reduce added resistance and speed loss in waves. Typically, two struts were arranged on each side of a WPC (Fig. 8.3); however, this gradually changed to single-strut type to reduce drag and simplify the construction, employing a demihull extended above the design waterline as a single structure to merge with the bridging superstructure (Fig. 8.3b). This last feature also made the main engine and transmission installation easier within the demihull space.
3. *Bow and stern shape*. The vessel transverse section in the bow area is usually formed as a deep V lower surface configuration (Fig. 8.1). The keel can be curved down under the base plane in the forefoot so as to increase the transverse section area and steepness of the deep V. This will increase the pitch damping force and help prevent the bow from emerging from the water surface in waves. At the same time, since the horizontal half angle of entrance can be reduced ($\alpha/2 \leq 6–10°$), the calm-water wave resistance and the resistance increment in a seaway can also be reduced.

   The stern shape of a WPC will be similar to that on an ordinary high-speed catamaran. Since WPC service speed is higher and waterjet propulsion is normally employed on such vessels, the stern is of a transom type with a small deadrise angle, and the connecting structure rising from the demihulls should be shorter than the demihull at the both bow and stern (Fig. 8.3), so as not only to reduce heaving and pitching moments but also to leave enough area on the demihull deck at the stern for installing and removing main engines.
4. *Clearance between sea surface and superstructure*. The demihull shape of a WPC allows the vessel to cut through waves rather than contouring them, resulting in wave peaks reaching a higher elevation relative to the front of a catamaran connecting bridge structure. In addition, when a WPC pitches down in

longer waves, as the pitch restoring moment is lower there is greater potential for water impact with the bridge front.

To mitigate this, WPCs have to be designed with a central bowlike geometry. This will reduce the potential impact load from waves and provide righting moments. The body plan of the central hull is of a V shape with a large flare configuration (Figs. 8.1, 8.2, and 8.3). This also gives the vessel reserve buoyancy against "plough-in" or "pitch-in" in following waves.

The exact geometry of the central bow structure, including the keel height above the static waterline, flaring, and volume, has been refined by the concept's inventors AMD and Incat over the years, supported by model testing and experience with vessels in service.

5. *Demihull separation*. The vessel beam and demihull ratio, *B*/*b*, of WPCs is as high as 5.5–6 instead of 3–4 for other high-speed catamarans, so the interference effect for hull separation should be slight or potentially favorable. The transverse stability will be similar to that of a simple catamaran, even though the superstructure is higher with corresponding higher CG as the wider spacing will compensate and maintain GM. The demihull form will provide higher damping than a simple catamaran, so that the roll angle may be minimized in waves.
6. *Connecting structure and central hull*. The shape of the connecting structure and central hull will provide reserve displacement for a WPC and, consequently, influence the control of the running trim and seakeeping quality. In general, the transverse section of connecting structure is of an arch type (Figs. 8.1 and 8.3), which is favorable for reducing the wave-impacting load and maximize transverse strength as well as resistance to fatigue damage of the hull structure. In early vessels of this type, the central hull transverse section included a deep V and extension downward to improve the wave-impacting load on the central hull and provide buoyancy during pitch down to prevent plough in rough seas. Experience has shown that it is sufficient to implement wave-pressure-reducing geometry further away from the nominal waterline because the support is only required in extreme conditions.

Figure 8.3a–c shows respectively the profiles of 23-, 39-, and 74-m WPC types illustrating the attributes described earlier.

Typical performance features of WPCs may be listed as follows:

1. *Service speed*: The vessel will be operated at rather higher speed, say, $Fr_L = 0.75–1.1$, and $Fr_D = 2.4–3.0$ and higher.
2. *Damage stability*: The WPC demihull and above-water form lend themselves to compartmentation, providing high resistance to flooding damage. Typically a WPC vessel can have compartmentation that satisfies two flooded holds. In addition, the central hull is watertight, so it provides additional buoyancy in a damaged condition, so it is rather different from the conventional catamaran in the calculation for stability and floodability. The central "hull" will not submerge until significant roll or pitch trim, so the designer has to ensure through the use of the two compartments damage stability criteria for the demi-hulls that the righting

Table 8.1 Analytical results of heeling and trimming angle of 28-m WPC in damaged condition

Damage condition	Location of flooding	Heel angle (°)	Trim angle (°)
Asymmetric	Hold no 1(stern peak)	1.43	1.59 (stern down)
Asymmetric	2	4.02	3.61 (stern down)
Asymmetric	3	4.01	1.73 (stern down)
Asymmetric	4	1.86	0.81 (bow down)
Asymmetric	5	2.95	2.95 (bow down)
Asymmetric	6 (bow peak)	0.89	1.21 (bow down)
Symmetric	1 (stern peak)	0	5.15 (stern down)
Symmetric	6 (bow peak)	0	3.56 (bow down)

moment has a steady slope providing resistance to sudden roll subsidence when the demihulls submerge.

Table 8.1 shows a calculation of both heeling and trimming angles of a 28-m WPC in a damaged condition with asymmetric flooding of one hold in a demihull. From the calculation it may be noted that the flooding resistance is satisfactory, with the largest heel angle being around 4° and pitch angle just over 5°.

3. *Seaworthiness*: Since a WPC has a reduced waterplane area above the static waterline, it will have longer natural periods for heave, pitch, and roll, much like a SWATH but with higher damping in heave and roll. This gives it nice seakeeping properties, including lower speed loss, lower motion amplitude in waves and so also lower vertical acceleration.

   Figure 8.5 shows the influence of hull separation on both heaving and lateral acceleration. It was found that as demihull separation is increased, the response is lower heaving and lateral acceleration.

   Trials of 30-m vessel prototype *2001* and model experiments of a 71-m wave piercer of International Catamarans Ltd. of Australia, in a towing tank, gave test results as shown in Fig. 8.6. It was found that the vertical acceleration (RMS value) is less than 0.08 g in 2 m significant wave height and 0.2 g at 4 m significant wave height.

   A 74-m WPC, the *Hoverspeed Great Britain*, on delivery from International Catamarans in Australia to the UK for Sea Containers Ltd., took just 79.9 h to complete the leg from New York in the USA to the southwest of England. This was a 5400-nautical-mile voyage and broke the historic transatlantic speed record (the Blue Riband) with an average speed across the Atlantic Ocean of 36.6 knots during the major ocean passage. The rate of seasickness was also low thanks to its "platforming" ride, which was up to ten times less compared with conventional catamarans (from 20% down to 2% sickness rate).

4. *Power transmission*: It is practical to locate the main engines and transmission in the demihulls so as to reduce transmission shaft lengths compared with those of a SWATH and simplify the mechanical transmission, enhancing efficiency. In early designs which had struts supporting the main deck the main engine air inlet ducts, exhaust pipe, electric cables, and access for crews was made via the

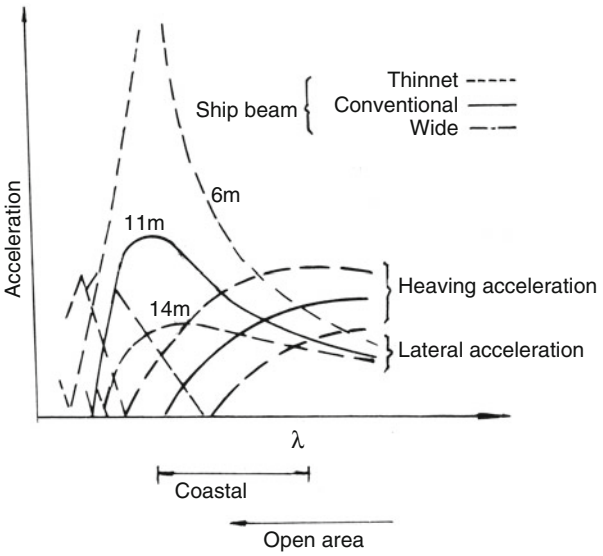

Fig 8.5 Influence of hull separation on vertical accelerations

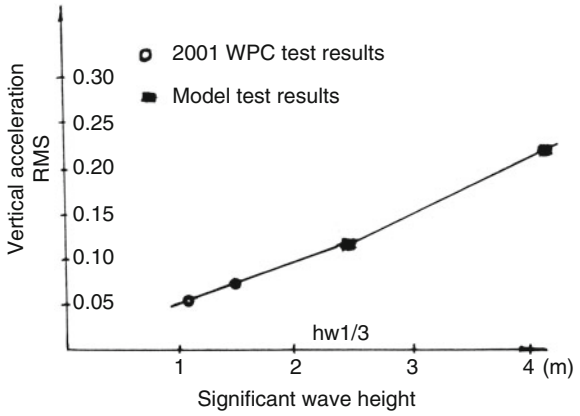

Fig. 8.6 Motions response data for 30-m WPC full scale and 71-m WPC from model tests

Table 8.2 Test data of maneuverability on 37-m WPC

Turning performance	*Turn left*	*Turn right*
Engine load	4/4	4/4
Jet angle for waterjet propulsion (°)	30	30
Turning time: Starting →5°	2 s	2 s
Starting→90°	22 s	23 s
Starting→180°	42 s	42 s
Go-ahead distance, m	190	200
Max. turning diameter, m	240	240
Stopping performance		
Power load	4/4 → max. reverse power rate	
Stopping situation	20 s	
Stopping distance, m	130 m	
Operating conditions		
Draft at bow and stern, m	1.31 & 1.46	
Trim, stern down, m	0.15	
Displacement, t	125	
Max. speed at max. power output, 4/4, knots	31.65	

struts and this constrained their dimensions. Once the concept matured, the demihull configuration above water was adjusted so that these services and access became simple to arrange in the aft area of the deck support structure.

5. *Maneuverability*: A WPC has high maneuverability owing to very large demihull separation and so also separation of the propeller(s) and associated rudder(s), or waterjet(s). This gives each propulsor a high turning moment about the vessel vertical centre of rotation. Table 8.2 shows the maneuverability of a 37-m WPC.

8.3 WPC Development

The design concept of WPCs was invented by Philip Hercus, Chairman and Technical Director of International Catamarans Ltd. of Australia. The first 8.7-m prototype, named *Little Devil*, was built and tested in 1983 and enjoyed great success (Fig. 1.11b).

The seaworthiness of the prototype WPC was a great success as the vessel operation in wave-piercing mode in a seaway showed low speed degradation and low motion amplitude as well as acceleration. In addition, the calm-water performance was good. The seakeeping quality was close to that of a SWATH; however, some of the disadvantages of a SWATH were avoided, so the prospects for commercial vessel development looked promising.

In a short period of time, from 1983 to 1989, a series of high-speed passenger vessels, with lengths of 28, 37, 49, 74, and 104 m, were designed and completed for service as passenger and RoPax ferries operating on coastal and up to oceangoing

routes. These vessels have made a real impact on the fast ferry market and led to historical changes in the development of water transportation around the world.

Table 8.3 below shows the quick development of the WPC in the short period of time between 1987 and 1989 compared with the overall market.

In 1989, a 37-m WPC, weighing 125 t and named *Quicksilver*, completed an operational demonstration around the coast of Australia and operated smoothly at an average speed of 24 knots in winds averaging 25–30 knots and in 3- to 5-m wave height, making a deep impression on passengers and operators (Fig. 8.7).

In June to July of the same year, another 39-m WPC, named *Prince of Venice*, was delivered from Australia via the Indian Ocean and Mediterranean Sea to Yugoslavia, during which the vessel encountered seas with wave heights up to 3.7–6.0 m and was still able to run smoothly at 16.2 knots average speed through rough seas.

A number of WPCs followed the *Prince of Venice*, and in 1990 the first 74-m passenger-car WPC ferry, *Hoverspeed Great Britain*, was delivered for service across the Channel between England and France.

Two subsequent Incat vessels, both 91-m wave-piercing designs, broke the record crossing the Atlantic Ocean: the *Catalonia*, 3 days 4 h 32 min at an average speed of

Table 8.3 Delivered and ordered WPCs, 1987–1989

	Delivered craft			Ordered craft			Total craft		
Year	1987	1988	1989	1987	1988	1989	1987	1988	1989
WPCs	1	3	5	9	7	7	10	10	12
All high-speed craft	50	70	56	75	75	82	125	145	138
WPC %	2	4	10	12	10	9	8	7	9

Data courtesy Fast Ferry Information and Incat

Fig. 8.7 Incat WPC *Quicksilver*

38.877 knots, and the *Cat-Link V*, in 3 days 2 h 20 min at an average speed of 41.284 knots. Many Incat vessels have had multiple owners and operators. The *Cat-Link V* was renamed the *Fjord Cat* when it entered service between Denmark and Norway some years after its Blue Riband run.

Continuing development and demand saw nine 74-m, three 78-m, three 81-m, four 86-m, and four 91-m WPCs built up to 1999. Incat Australia has built a series of 96-m combination RoPax catamarans, designed to accommodate up to 600 passengers and 105 cars as well as having 415 truck lane meters for Ro-Ro freight in the 2000s; since 2010 the company has further increased the size of its largest designs to above 120 m in length.

The group of the designers who worked together at International Catamaran Designs in Sydney and International Catamarans Tasmania in the initial stages of wave-piercer development separated and formed their own company, called Advanced Multihull Designs, in the 1990s in Sydney and continued with their own approach to the wave-piercer configuration, licensing their designs for construction by partnering shipyards. In 1994 fast ferry demand led to the development of the K class design by AMD, a ferry suited to very high-speed operation on relatively sheltered routes. Two K class vessels with 50-knot service speed were completed under license by Afai Shipyard in China (Chap. 1). Later, in 1997, AMD designed the world's fastest catamaran ferry, the 77-m gas-turbine-powered *Luciano Federico L* that operates in Argentina.

We present in Tables 8.4a and 8.4b statistics from a selection of Incat and AMD vessels built over the last 20 years, ranging in length from 31 m to 120 m LOA.

$^{*}L/\nabla^{1/3} \cong L/(3\mathrm{Dw})^{1/3} = \left(L/\mathrm{Dw}^{1/3}\right) \times 0.69.$

Slenderness for demihull: $L/(\nabla/2)^{1/3} = \left(L/\nabla^{1/3}\right) \times 1.26 \cong \left(L/\mathrm{Dw}^{1/3}\right) \times 0.9.$

Therefore, the slenderness with respect to the deadweight in the table implies approximately equal to 1.10 slenderness for demihull.

Transport efficiency: $K_{\mathrm{p}}\left(\frac{\mathrm{Pass} \times \mathrm{km/h}}{\mathrm{kw}}\right)$.

In Australia WPC design has continued to be developed at Incat, based in Hobart, Tasmania, as well as designers Advanced Multihull Designs (AMD) and One2Three. The latter two organizations have used separate shipyards in different parts of the world to construct their vessel designs, while Incat builds larger vessels itself in Hobart and has a large network of builders around the world for smaller ferries. The technology for wave piercing and optimization of high *L*/*b* catamarans has been developed and refined independently by these organizations based on the experience they have gained with successive vessel builds.

Table 8.4a Leading particulars of a selection of Incat and AMD WPCs

Type	25 m	37 m	39 m	49 m	52 m	77 m
Name	*Fei Ying*	*Quicksilver V*	*Prince of Venice*	*Condor*	*Haras 1 and 2*	*Luciano Federico L*
Design	AMD 150	International catamarans	International catamarans	International catamarans	AMD 520P	AMD 1530
Year completed	1998	1989	1989	1990	2008/9	1997
Operation country	China	UK	Europe	UK	Oman	Argentina
Constructor	Hang Tong	NQEA	NQEA	NQEA	Rodriquez	Izar Bazan
LOA, m	25.0	38.6	39.6	48.7	52.1	77.32
L_{bp}, m	22.8	31.4	31	40.5	47.6	72.3
BOA, m	9.57	15.6	15.6	18.2	18.2	19.5
b, m	2.6	2.6	2.8	3.3	4.3	4.7
T, m	1.8	1.3	1.60	1.90	2.0	2.15
Relative hull separation k_d/b	2.68	5.0	4.2	4.52	3.25	3.15
Deadweight Dw, t	21	~40	~40	63	32.8	142
Power, kW	Diesel 2 × 1674	GM16V 92TA 2 × 1230	DDC16 V149TA 2 × 1435	MWM TBD 604 V16 4 × 1682	Diesel 4 × 11740	ABB GT35 2 × 15800
Propulsion	2 × prop	2 × WJ KaMeWa 63/S62	2 × WJ KMW 63 S62	4 WJ (J650R)	4 × WJ KMW S61 SII	2 × WJ KMW 112 SII
V_{max}, knots	31	31.2	31	37.5	42	60
V_s, knots	28	27.0	27	35.0	40	57
Passenger	180	340	303	450	200 + 24	446
Car (trucks + cars)	0	0	0	0	0	52
Fr_L (based on V_m)	1.07	0.914	0.914	0.967	1.0	1.16
Transport efficiency, K_p, based on V_m	4.67	5.01	7.0	5.02	1.58	4.79
$L/Dw^{1/3}$	8.27	9.09	9.08	10.17	11.57	13.88
b/T	1.44	2.0	1.75	1.74	2.15	2.19
B/b	3.68	6	5.57	5.51	3.6	4.15
L_{bp}/b	8.77	12.08	11.07	12.27	11.07	15.38

Table 8.4b Leading particulars of a selection of Incat Tasmania WPCs

Type	31 m	74 m	81 m	86 m	96 m	112 m	130 m
Name	*Incat Tassie Devil*	*Sea Speed Jet*	*Jaume II*	*Champion Jet 2*	*Manannan*	*Incat Natchan World*	*130 m Ecoship*
Design	Incat 017	Incat 023	Incat 038	Incat 042	Incat 050	Incat 065	Incat
Year completed	1986	1990	1996	1997	1998	2013	Design
Operation country	Australia	Greece	Spain	Greece	UK	Japan	Australia
Constructor	Incat	Incat	Incat	Incat	Incat	Incat	Incat
LOA, m	30.5	74.3	81.1	86.3	96.0	112.6	130
L_{bp}, m	25.0	60.0	66.3	78.4	86.0	105.6	123.6
BOA, m	13.0	26.2	26.0	26.0	26.0	30.5	31.2
b, m	2.2	4.3	4.3	4.3	4.5	4.7	4.7
T, m (ex bow T foil)	2.15	2.5	3.0	3.5	3.7	3.93	4.0
Relative hull separation k_d/b	4.91	5.09	5.09	5.09	4.78	4.17	4.47
Deadweight, t	~20	198	320	380	800	880	1300
Power, kW	Diesel 2 × 830	Diesel 4 × 3560	Diesel 4 × 5500	Diesel 2 × 14160	Diesel 4 × 7200	Diesel 4 × 9000	GT 2 × 23,000
Propulsion	2 × prop	4 × WJ	4 × WJ	2 × WJ	4 × WJ	4 × WJ	2 × WJ
V_m, knots	31	42	44.0	48	51.0	45.0	55.0
V_s, m	28	35	38.0	42	35.0	35–38	60.0
Passengers	196	600	700	800	600	800	1376
Cars/trucks	0	84	173	200	245	300/120	460
Fr_L (based on V_m)	1.02	0.89	0.89	0.89	0.90	0.64	0.61
Transport efficiency K_p (based on V_m)	6.92	11.91	12.12	11.98	13.41	11.22	12.3
$L/Dw^{1/3}$	9.37	10.31	9.71	10.85	9.28	11.04	11.35
b/T	1.02	1.72	1.43	1.23	1.29	1.20	1.18
B/b	5.91	6.09	6.05	6.05	5.78	6.49	6.64
L_{bp}/b	11.36	13.95	15.42	18.23	19.11	22.47	26.3
Ride control system		Tabs	Tabs	Tabs + T foil	Tabs + T foil	Tabs + T foil	Tabs + T foil

8.4 Comparison with Other High-Speed Craft

The WPC has been well proven as a concept in the three decades since the first trials in the early 1980s, as a large number of vessels have been constructed and put into operation by Incat, Incat Crowther, and shipyards licensed by AMD. The steady development in numbers of craft built and their size, up to 120 m LOA, has meant that a lot of model tests have been carried out by both Incat and AMD of Australia. Key elements of the concept were patented at an early stage, and so, due to confidentiality of intellectual property rights for Incat and AMD, technical information is not complete in the public domain. At an early stage in the concept development, technical information was difficult to clarify, and so Marine Design & Research Institute of China (MARIC) carried out its own independent investigation during the early 1990s. We present some of that material here for the reader's reference.

To investigate such technology, experimental investigation was conducted at both MARIC and Harbin Engineering University of China for a number of years in 1992 and 1993, respectively. In addition, some comparison of speed performance and seakeeping quality between the WPC and high-speed catamaran as well as comparison with high-speed monohull vessels with round bilge and deep V shape was conducted at these facilities. We summarize that work in the following paragraphs.

Experimental Investigations in MARIC

At MARIC a preliminary experimental investigation was carried out in the early 1990's, beginning in 1992 to study the hydrodynamic performance of WPCs and to compare the performance with various other high-performance marine vehicles that MARIC has worked on.

The experimental investigation was carried out in a towing tank at MARIC, and the research object was a 450-passenger WPC for operation at a service speed of 35 knots. The reference vessel WPC was a well-proven 49-m WPC developed by International Catamarans Ltd. However, since no detailed technical specification or performance data for the Incat WPC were available publicly at that time, the test results of the MARIC research should not be considered to accurately represent the Incat vessel performance but rather as "typical" for a WPC and useful primarily as realistic data to compare the WPC with other high-speed vessels.

The leading particulars of both the WPC at MARIC and the reference WPC are listed in Table 8.5. There are some differences due to the target of the MARIC investigation, so relative to the Incat vessel, the demihull slenderness of MARIC's WPC was increased with the intent of further improving the seakeeping quality, and the demihull separation was decreased to improve the transverse strength of the WPC.

The performance comparison for the various vessels tested can be summarized as follows.

Table 8.5 Principal dimensions of wave piercing catamaran for Incat and MARIC

Craft for model test investigation	Dimensions	MARIC's research model	49-m WPC for reference
Loa	m	50.2	48.7
Boa	m	14.2	18.2
b	m	3.0	3.3
T	m	1.8	1.9
L_{WL}	m	47.5	42.5
Height of tunnel, *H*	m	4.4	Not available
Displacement	t	265	250
Depth, *D*	m	6.4	Not available
Maximum speed, V_m	knots	35	35
Power	kW	2 × 3300	4 × 1682
Demihull slenderness		9.317	8.5
B/*b*		4.73	5.52

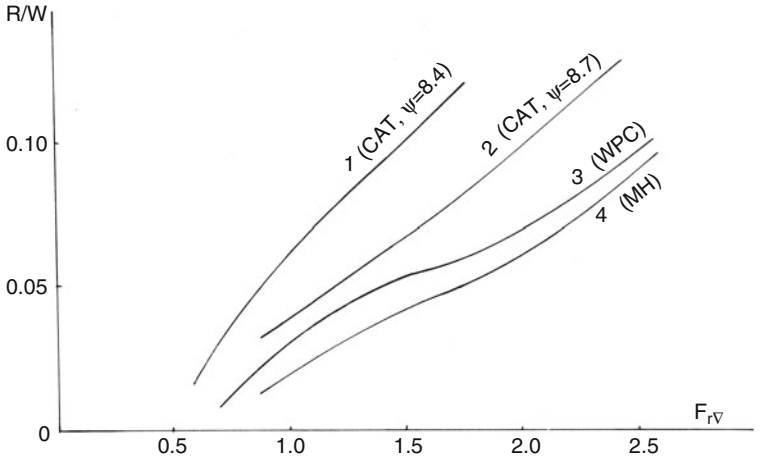

Fig. 8.8 Resistance comparisons in calm water

Resistance in calm water

Figure 8.8 shows a comparison of the resistance of the different vessels tested in calm water, where the curves are labeled as follows:

1. Test data of catamaran from [3] with demihull slenderness $L/\nabla^{1/3} = 8.4$, where ∇ is demihull volume displacement;
2. Catamaran with demihull slenderness 8.7;
3. Test data of WPC with demihull slenderness 9.3;
4. Monohull displacement vessel with slenderness 10.0.

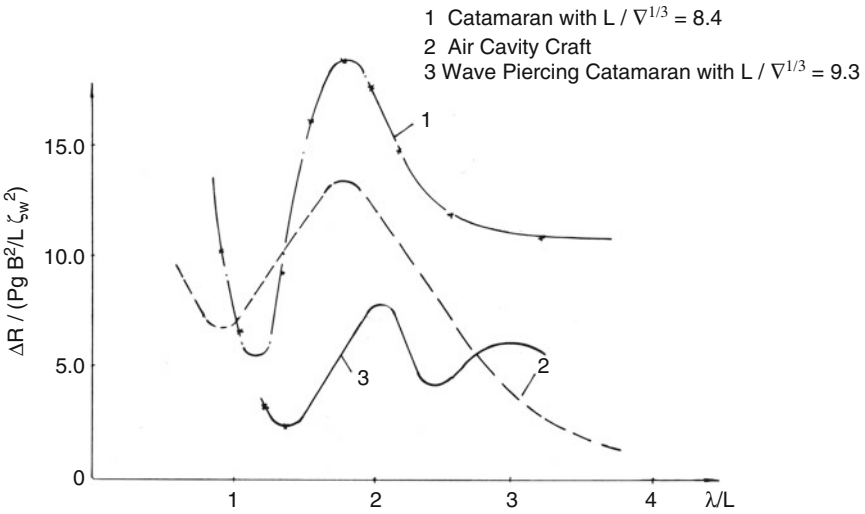

Fig 8.9 Additional resistance in waves versus wave length/craft length ratio

From the figure one can see that the resistance of a WPC in calm water is lower than that of a catamaran, possibly owing to high demihull slenderness and lower b/T, which would reduce the wave-making resistance and friction resistance as well, and close to that of a super slender monohull vessel (however, at the cost of poor transverse stability).

Additional resistance in waves

Figure 8.9 shows the additional (wave) resistance of various vessel designs in waves versus wave/vessel length ratio, where:

ς_w Wave amplitude;
λ Wave length;
∇R Additional resistance of vessel in waves.

The curves in the figure are labeled as follows.

1. Catamaran with slenderness coefficient 8.4 [3];
2. Air cushion catamaran (ACC) with thickened side-walls [4];
3. Tested WPC.

The WPC additional resistance is smallest owing to wave-piercing effects.

Heave response in waves

Figure 8.10 shows the heave motion response of the vessels in waves, where z represents the motion amplitude of heave in waves.

1. Catamaran [3];

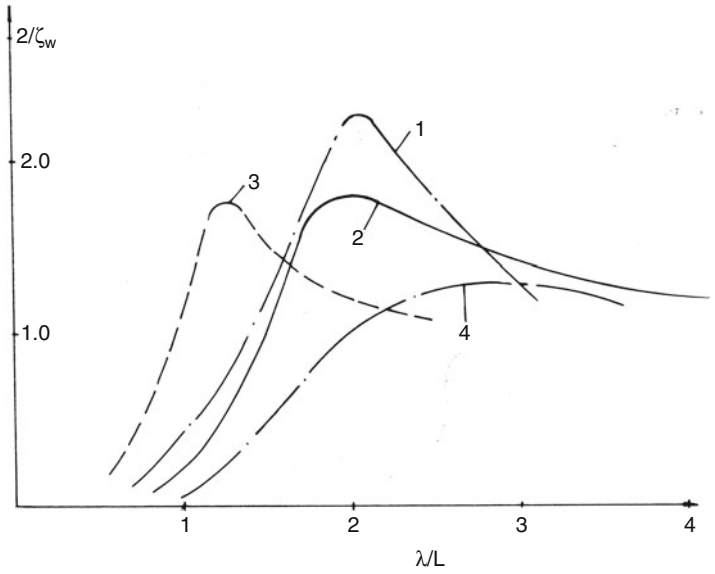

Fig. 8.10 Heave motion response comparisons

2. WPC;
3. SSTH [5];
4. ACC [4].

This plot shows that the WPC heave response is much lower than that of a normal catamaran or SSTH at lower ratio of wave length to vessel length; however, it is higher than that of an ACC, perhaps owing to the high damping coefficient of the ACC air cushion.

The heave motion of an ACC will be highly damped as the air cushion will be leaked or compressed during heave motions, which will serve to rapidly decrease and increase the air cushion pressure. The ACC therefore has a very high heave damping and stability coefficient. Since the ACC has very low water drag, this damping is not "costly" to performance, while for a catamaran with immersed demihulls, it is less costly to have a rather slender immersed hull.

The benefit is illustrated by the difference in heave response of the WPC or SSTH with the standard catamaran hull form.

Pitch response in waves

Figure 8.11 shows the pitch response of a wave-piercing craft in waves compared with other types, where ψ represents the pitch response of the vessel and $\chi = 2\pi/\lambda$, so $\psi/\chi\varsigma_w$ represents the nondimensional pitch amplitude of the vessel in waves. The curves are as follows:

1. ACC [4];
2. WPC;
3. Catamaran [3].

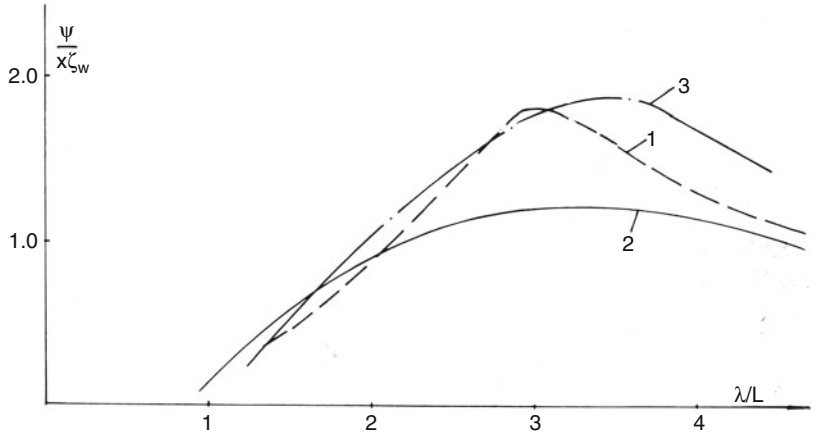

Fig. 8.11 Pitch response in waves comparison

WPC pitch response is greatly improved compared to the other vessel types at all wave frequencies, perhaps partly owing to lower wave disturbance and longer natural period of longitudinal motion. The natural frequency of motions of the WPC from MARIC experimental data is as follows:

1. Heave natural frequency $\omega_h = 0.37$, 1/s;
2. Pitch natural frequency $\omega_p = 0.32$, 1/s;
3. Roll natural frequency $\omega_r = 0.39$, 1/s.

It should be noted that the natural frequencies of all three motions (roll, heave, and pitch) are close to each other, which will cause significant coupled motions for roll, heave, and pitch, and would then create total motions that are not very comfortable for passengers. It was concluded from the tests that more attention has to be paid to the relations of the different motions as described in Chaps. 5 and 6. This issue is perhaps not specific to characteristics of WPCs; rather, it is a general issue for catamaran configurations and in this case may be due to nonoptimal design of this model as tested at MARIC. Therefore, it was concluded that further research on such issues was needed so as to be able to optimize pitch response and minimize coupled motions that may cause passenger seasickness.

At the early stage of large WPC development, when the first 74-m WPC was put into operation across the English Channel, it was found that the seasickness rate of passengers on board was high. This was probably due to the coupled resonance motions (rolling pitching and heaving motion) that occurred on the vessel operating on the English Channel route, with the close natural frequency for all three motions of the vessel, as mentioned earlier. The problem was eventually resolved for the vessel by installing antirolling/pitching fins with an automatic control system.

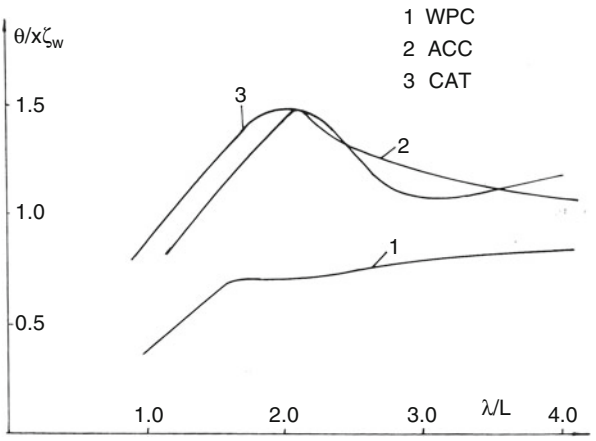

Fig. 8.12 Roll response of craft models in beam seas at zero speed

Roll response in waves

Figure 8.12 shows the nondimensional roll response of the vessel models in beam seas at zero forward speed. The WPC has much lower response than both the ACC and catamaran, perhaps owing to less wave disturbance of the thinner and inward inclined structure between the demihulls and the WPC central hull and its lower roll natural frequency. The curves are as below:

1. WPC;
2. ACC [4];
3. Catamaran [3].

The reduction in roll amplitude of the WPCs is demonstrated at almost all wave/vessel length ratios.

Vertical Acceleration Response of Vessel Models at Bow

Figure 8.13a shows the vertical acceleration response of each of the vessel models at their bow. The acceleration at the WPC bow is far lower than that on the ACC and catamaran, particularly at long wave lengths, that is, $\lambda/L > 2$. This may be due to the wave-piercing effect, platforming through the waves, particularly for waves longer than twice the hull length, where the reduction appears to be of order 30%.

Seasickness Rate

Figure 8.13b shows the vertical acceleration RMS value at vessel midposition and the prediction of seasickness rate for passengers on the WPC vessel. The figure's curve 1 shows accelerations for the MARIC WPC running at 30.4 knots, in significant wave height of 1.63 m. The greatest vertical acceleration of the vessel is located at 0.3–0.4 Hz wave encounter frequency, corresponding to $\lambda/L = 1.5$. A vertical acceleration of 0.156 g was measured, and in this case passengers can only tolerate this motion for no more than half an hour.

However, if the length of the WPC is increased to 74 m, as in curve 2 in the figure, then $A_{rms} = 0.067$ g, and tolerance duration is extended to 8 h.

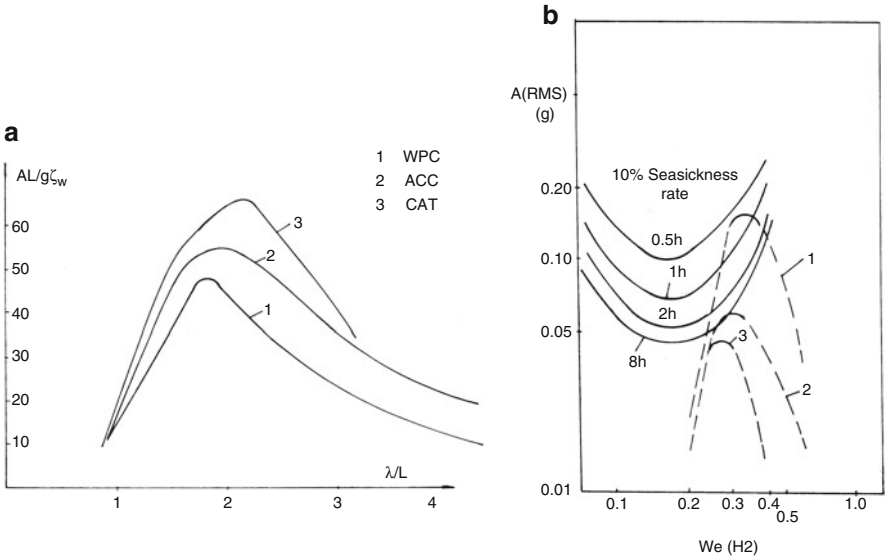

Fig. 8.13 (**a**) Vertical accelerations at bow; (**b**) seasickness rate versus acceleration

Figure 8.13b also shows the estimated vertical acceleration for a 74-m WPC with an automatic control system on stern trim tabs (curve 3), and the seasickness rate is further reduced.

Experimental Investigations at HEU

A comparison of experimental results for three high-speed craft, including a WPC, high-speed monohull vessel with round bilge, and a deep V monohull, was carried out at the High-Performance Marine Vehicle Research Center, Harbin Engineering University, Harbin, China, in 1992. The test results and their analysis are introduced briefly as follows.

Powering Performance

The model experiments for the three models (a WPC, high-speed monohull with round bilge, and monohull with deep V configuration) were carried out in the towing tank of the HEU. The test results were scaled to the same displacement of 600 t as shown in Fig. 8.14 and Table 8.6. Figure 8.14 shows a comparison of the projected effective power of each of the three vessel models required plotted against the speed in knots.

The figure shows that the effective power of a WPC is higher than that of the other vessels at lower speed; however, at higher speeds above 25 knots the required power for the deep V monohull is higher, and by 30 knots the round bilge catamaran's required power is also higher. These results agree with MARIC's own experimental results.

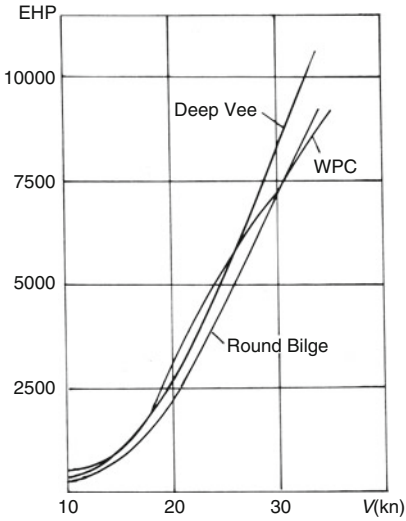

Fig. 8.14 Comparison of effective power of models at HEU

Table 8.6 Seakeeping comparison for three types of high-speed vessel

	Pitching, °	Heaving, m	Vertical acceleration at bow, g	Vertical acceleration at stern, g	Added resistance, kN
(a) At wave height $H_w = 2.0$ m ship speed $V_s = 18$ knots					
WPC	2.48	0.85	0.60	0.24	0.95
Deep V MH	2.17	0.43	0.41	0.24	2.48
MH with round bilge	2.75	0.65	0.62	0.30	2.63
(b) $H_w = 2.0$ m, $V_s = 30$ knots					
WPC	1.44	0.73	0.45	0.30	1.51
Deep V MH	2.10	0.57	0.58	0.37	3.06
MH with round bilge	2.56	0.83	0.74	0.42	2.92
(c) $H_w = 3.5$ m, $V_s = 18$ knots					
WPC	5.25	1.84	0.83	0.37	3.31
Deep V MH	4.33	1.14	0.64	0.39	5.44
MH with round bilge	5.13	1.46	0.83	0.45	5.77
(d) $H_w = 3.5$ m, $V_s = 30$ knots					
WPC	3.87	2.06	0.82	0.57	7.30
Deep V MH	4.54	1.47	1.03	0.65	9.08
MH with round bilge	5.33	1.92	1.33	0.74	9.23

Seakeeping
The test results of heaving and pitching amplitude, vertical acceleration at bow/stern, and added resistance for three models at the 2.0- and 3.5-m height regular bow waves, at vessel speeds of 18 and 30 knots, are listed in Table 8.6. The motions of the WPC at low speed (18 knots) in rough seas is close to that of the other vessels; nevertheless, the resistance at this speed is less than that of the two other catamarans. In addition, at high speed, the WPC's seakeeping quality is much better than that of the other high-speed vessels, with both the motions and the added resistance being lower.

The test results suggest that the advantages are really with the WPC, much like the results of the experimental investigation at MARIC summarized earlier.

8.5 Investigation of Wave-Piercing ACC

Background
From the MARIC experimental results with the WPC, the natural periods of roll, heave, and pitch motion for this design are close to each other, causing sensitivity to corkscrew motions in oblique seas. In addition, the heave amplitude of the WPC, particularly in the medium-frequency wave encounter region, is rather large owing to a lower heave damping coefficient. Such motions induce high loadings, so that the transverse structure strength would also have to be increased owing to the large demihull separation.

An experimental investigation using one approach to improving such motions was carried out at MARIC [6]. The design idea was to use the basic advantages of the WPC and merge this with air cushion technology so as to form a novel type of craft, called a wave-piercing air cushion craft (WPAC), as follows:

- Keep the original configuration of the WPC unchanged, but use a pair of bow/stern skirts with high responsive characteristics as shown in Fig. 8.15a, b. The key function of the so-called responsive skirts is that the skirts are able to deform and yield to the waves passing through the skirts while operating in a seaway, thereby reducing the additional wave drag and longitudinal motions.
- Add a lift system for the craft applying air cushion pressure to the bow and stern skirts and support part of the vessel weight so as to reduce the load acting on the demihulls and thus improve the effective transverse strength of craft.
- Since the air cushion has a high damping characteristic, the heave motion of a WPC might be improved with the aid of an air cushion system, and the roll and pitch motions would be damped by action of the skirt system together with the main cushion damping.

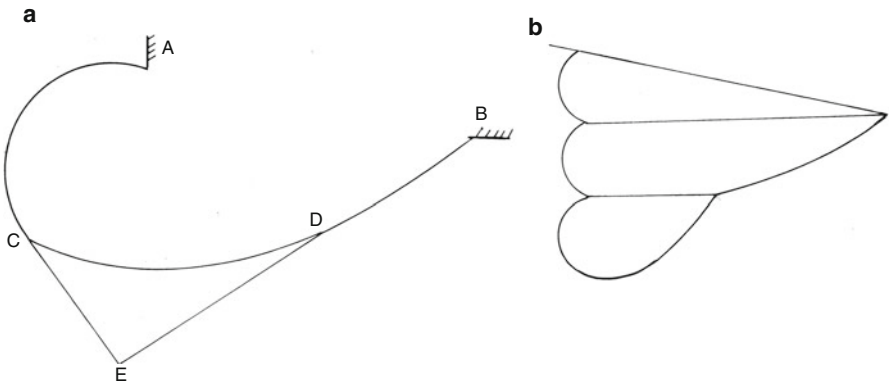

Fig. 8.15 WPAC skirt configuration: (**a**) bow skirt; (**b**) stern skirt

Table 8.7 Principal dimensions of WPC and WPAC

		WPC	WPAC
Loa, L	m	50.2	50.0
Boa, B	m	14.2	12.0
Depth, D	m	6.6	6.0
L_{WL}	m	47.4	47.2
Demihull beam, b	m	3.0	2.6
Height of tunnel, H	m	4.4	4.0
Draft, T	m	1.8	0.9
Overall weight, W	t	265.0	265.0
Payload	t	−60.0	−60.0
Speed, max., V_m	Knots (Fr_L)	35.0 (0.83)	42.0 (1.0)
Engines		2 × MTU16V538TB92	2 × MTU16V538TB92 for prop 2 × MTU8V396TB84 for lift
Total power	kW	3300.0	4210.0
Seakeeping quality		Sea state 5, normal operation	Sea state 5 normal operation

Experimental Results and Analysis

The experiments were carried out in a towing tank at MARIC [6]. The leading particulars and target performance of both the WPC and WPAC, with scale ratio $\lambda = 20$, are as follows (Table 8.7).

The test results and comparison for both craft models follow.

Resistance in Calm Water

Figure 8.16 shows the resistance of both craft in calm water, where the curves are labeled as follows:

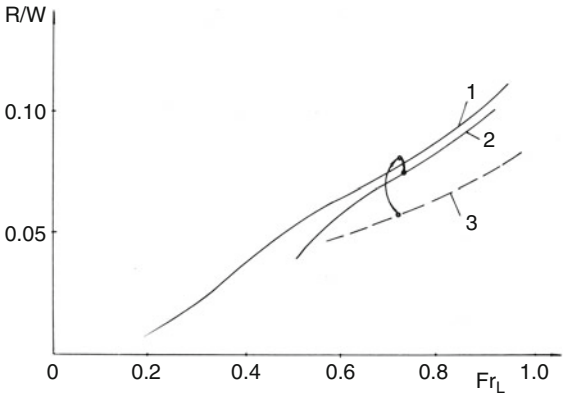

Fig. 8.16 Resistance of WPC and WPAC in calm water

1. WPC with demihull slenderness 9.3;
2. WPAC with air cushion support ratio $k = \nabla_c/\nabla = 0.48$, where ∇_c represents the air cushion lift proportion of the total craft weight;
3. WPAC with $k = 0.73$.

The points in the figure represent the corresponding relative resistance of the WPAC, that is, including the equivalent resistance consumed on lift power. This can be written

$$R_c = R_t + R_L = R_t + \frac{Q\nabla_c k_c}{vS_c\eta_F\eta_M}, \tag{8.1}$$

where

R_c Corresponding resistance, kg;
R_t Total resistance of craft measured in towing tank, kg;
R_L Equivalent resistance consumed on lift power, kg;
Q Air cushion flow rate, m^3/s;
$k_c = P_c/H$;
S_c Air cushion area, m^2;
V Model speed, m/s;
η_F, η_M Efficiency of fan and mechanical transmission of lift system, respectively.

From the figure one can see that the resistance of the WPAC with $k = 0.73$ (3) is lower than the WPC, particularly at high Fr_L; however, when considering the corresponding resistance, the resistance of the WPAC is almost equal to that of the WPC at 0.8 Fr_L. The advantage of the WPAC will be realized only at high speed, say $Fr_L > 1$.

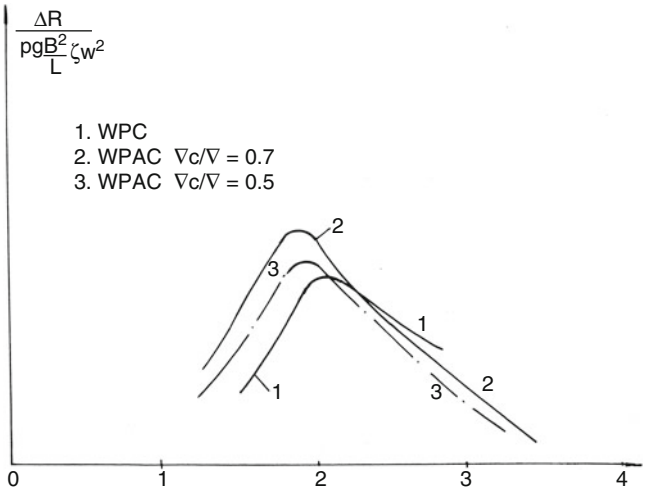

Fig. 8.17 Additional resistance coefficient of WPC and WPAC in waves

Resistance in Waves

Figure 8.17 shows the additional resistance of the craft in waves, and it is found that the resistance of both the WPC and WPAC are almost the same in longer waves, while in shorter waves the added resistance of the WPC is lower, owing to the wave-piercing effect for the WPC, while the cushion dynamics actually induce higher additional resistance. This really demonstrates the advantage of the WPC from the point of view of resistance in waves.

Heave Response

Figure 8.18 shows the heave response of the craft, where the heave amplitude of the WPAC with high responsive bow/stern skirts is far lower than the WPC (up to more than 50%) due to the high damping coefficient. The down side of the lower heave response is that the bow and stern skirts have to respond to the waves in phase to minimize additional drag, while to minimize motion, out-of-phase response is favored.

From the point of view of improving heave response of craft in waves, perhaps the WPC + AC is reasonable, while the required damping needs to be optimized so as to minimize the added resistance, as noted previously.

Pitch Response

Figure 8.19 shows the pitch response of the craft in waves. The WPAC relative pitch amplitude at $k = 0.5$ is much lower than that of the WPC (about one-third lower), probably also due to the high damping effect of the WPAC from the cushion.

Perhaps there is an optimal k for the WPAC, and too high an air cushion effect would decrease the advantage of the wave-piercing effect, so the optimized k might be at a lower level. The work did not pursue this much further since, as discussed in

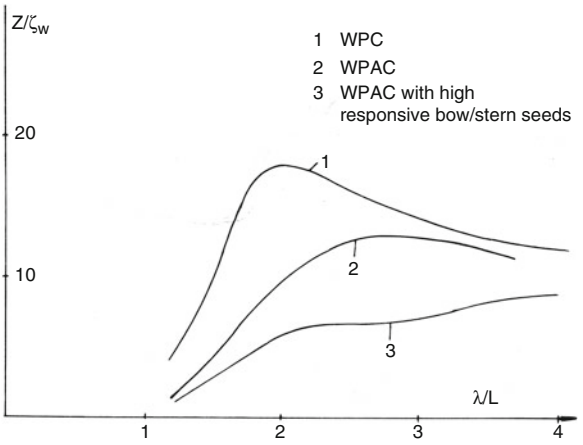

Fig. 8.18 Heave response of WPC and WPAC in waves

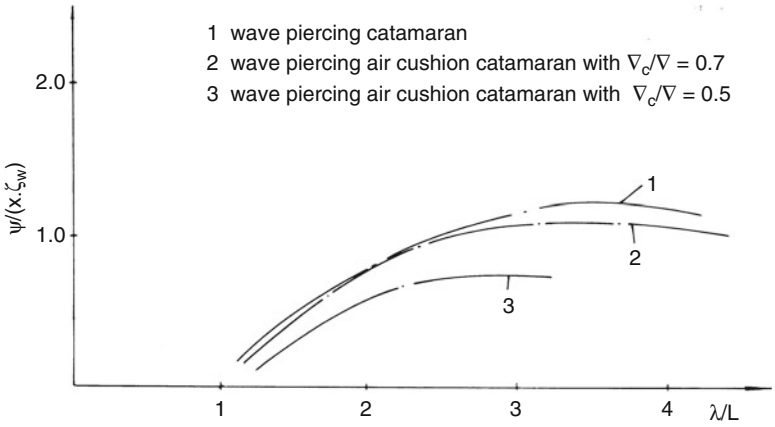

Fig. 8.19 Pitch response of WPC and WPAC in waves

what follows, the air cushion has other consequences that mean it is not an overall better concept than the basic WPC.

Vertical Acceleration Response

Figure 8.20 shows the vertical acceleration response of the craft in waves. Note that the vertical acceleration of the WPAC with $k = 0.5$ is lower than that of the WPC, particularly for peak vertical acceleration (almost 25% lower), and improves the impact load of craft owing to the high damping effect of the air cushion.

Conclusions

Merging an air cushion with wave-piercing technology to generate an air cushion effect will enhance the damping coefficient and reduce both heave and pitch motion and improve the impact load acting on the central hull and seaworthiness. However,

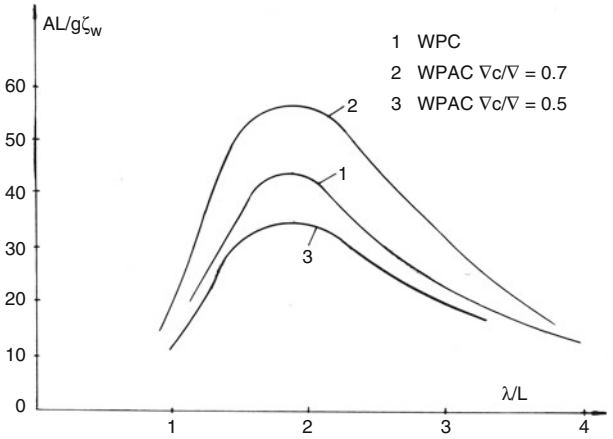

Fig 8.20 Vertical acceleration response of WPC and WPAC at bow in waves

the WPAC resistance in both calm water and waves is not improved over the WPC, except for much higher calm-water speed and Fr_L.

The WPAC will require a separate power system for the cushion system as well as a cushion venting system. This is in addition to the skirt system, which increases maintenance consequences. Considering this, the WPAC is not immediately attractive as an alternative concept to WPC for improving motion response at least for service speed where $Fr_L < 1.0$.

The use of forward-mounted pitch control hydrofoils and stern-mounted flaps or interrupters was introduced in the mid-1990s to provide improvements in motion response on a WPC, achieving similar results to that available from a WPAC while being significantly less complex and costly to achieve the same result.

Similar to the high-speed catamaran, the modern WPC is characterized by a simple configuration and without complicated equipment outfit. It has fine seaworthiness and powering performance and this combination has been the reason for the steady buildup of the WPC ferry fleet in recent years. Its relative simplicity has enabled scaling up, so far to 120-m vessels, with the prospect for even larger craft as structural design optimization progresses with modern finite-element analysis software.

It is also easier to successfully deploy the technology to other countries. One example is a license that was purchased to use the WPC patent from AMD of Australia, and a large WPC with 99.78 m LOA, 19.98 m beam, 7.30 m depth, 570 t payload, and the capacity to accommodate 460 passengers and 94 cars or 24 trucks was built in Japan.

The ship is equipped with four caterpillar diesel propulsion engines; two of the four are of the type 316 (5420 kW for each), and the other two are diesels of the type 3612 (4060 kW for each), so the total power is 18,960 kW. The propulsion of this vessel comprises four sets of KPJ-169A waterjet propulsion to enable operational

speeds of up to 35.5 knots (max.) and 30 knots (service). The vessel is also equipped with an automatic control foil at the bow and automatic control tabs at the stern to improve rolling, pitching, and heaving motions of the vessel in waves.

8.6 Comparison of Calculation and Model Tests for WPC

We present here a comparison between the test model and full-scale results taken from Lu (1999) [7] and Zhao (1995) [8] and analytical predictions by Prof. Rong in 2002 [9]. The model scale ratio to the real WPC is 1:33.3. The full-scale principal dimensions of the real WPC are given in Table 8.8. The model is a typical example of a WPC with a deep V-type hull cross section forward, a hard chine midsection, and transom stern. The body plan is that shown in Fig. 8.1.

Rong (2002) [9] calculated the wave resistance coefficient $\bar{C}_w$ of the tested model at $Fr_L = 0.3–1.0$ using the numerical calculation method presented in Sect. 4.5.3 and the program in Chap. 4.

The numbers of stations and waterlines were taken to be 21 and 9, respectively. Waterlines were inserted at intersection points between knuckle curve and station lines.

Because the WPC has a transom stern, one station is added behind Aft Perpendicular, as the imaginary length, and so the total number of stations is 22. The imaginary length is taken as 1.2 times the transom breadth.

Figure 8.21 shows the results of the test and calculation. In this figure, C_w is the same as $\bar{C}_w$ in Eq. (4.132) and $C_{wr} = 1.25C_w$ (i.e., form factor FFACTOR = 0.25) at $Fr_L = 0.3–1.0$.

Table 8.8 Particulars of full-scale WPC

Item	Ship
Waterline length, m	52.0
Demihull beam, m	4.40
Draft, m	2.00
Total wetted area, m^2	651
Displacement volume, t	554
Demihull/center plane spacing, m	16.0
Demihull block coefficient	0.590
Demihull prismatic coefficient	0.776
Demihull midship coefficient	0.76
Length/displacement ratio	8.05
Length/beam ratio	11.82
Draft/length ratio	0.0385
Spacing/beam ratio	3.6364
Spacing/length ratio	0.3077
Design Froude number	0.70

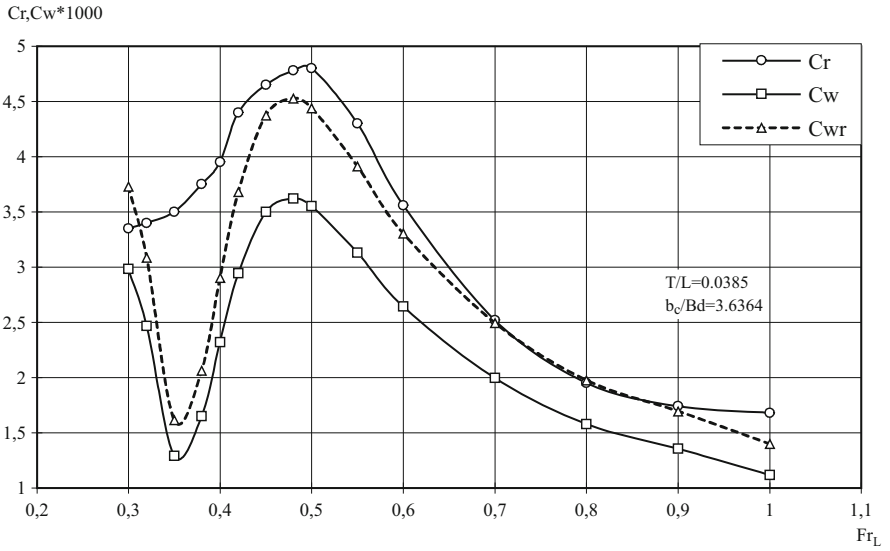

Fig. 8.21 Comparison of C_r with C_w for WPC

It was found that C_r from model testing and $\bar{C}_w$ from the analysis have the same shapes and same tendency at $Fr_L = 0.36$–1.0. But there is an obvious wave trough at $Fr_L = 0.35$ in the curve for C_w but none in the C_r curve.

This may be due to the creation of strong viscous effects in the low- and medium-speed ranges for displacement vessels due to interaction. The C_{wr} curve agrees with C_r well at $Fr_L = 0.65$–0.90, but C_r is greater than C_{wr} gradually at $Fr_L \geq 0.90$, and this may be due to an increment of spray resistance.

Thus, the analytical prediction of residual resistance for a WPC form may be used (with some care) for speeds above approximately $Fr_L = 0.45$, which is useful for initial estimation purposes. Below $Fr_L = 0.45$ careful estimation of the viscous drag on the hulls is required because it is not simply estimated by the traditional means based on Reynolds number and friction coefficient applied to hull surfaces due to interactions with generated waves and wave interactions.

References

1. Bliault A, Yun L (2000) Theory and design of air cushion craft. Arnold/Elsevier, UK, ISBN 0 340 67650 7 and 0 470 23621 3 (Wiley), 632 pp
2. Yun L, Bliault A, Doo J (2010) WIG craft and ekranoplan, ground effect craft technology. Springer, New York, ISBN 978-1-4419-0041-8
3. Song GH (1987) Catamaran class B, research & design of ships, vol 11. Chinese Naval Ships Academy, Beijing, China (in Chinese)

4. Faltinsen OM (1991) Speed loss & operability of catamaran & SES in a sea way. In: FAST'91 proceedings
5. Sato R, Miyata H (1991) Hydrodynamic design of fast ferries by the concept of super slender twin hull. In: Proceedings of FAST 91, Trondheim
6. Mao T, Ming T (1996) Novel hybrid craft – experimental investigation on wave piercing air cushion catamaran craft (WPAC). In: Information & trend. High Performance Marine Vehicle Design Subcommittee of CSNAME, Shanghai (in Chinese)
7. Lu X-P et al (1999) Investigation on resistance of WPC (in Chinese). In: 8th national seminar on high performance ships
8. Zhao L-E et al (1995) Investigation on performances and hull form design of wave piercing catamaran (in Chinese). In: Symposium on seminar of ship resistance and performance
9. Rong H-Z (2002) Application of linearized theory of wave resistance to HACAT, SWATH and wave piercing catamaran (in Chinese). Research report, MARIC

Chapter 9
Small-Waterplane-Area Twin-Hull Vessels

9.1 SWATH Evolution

The idea of using cylindrical hulls placed well below the free surface with one or more thin struts through the waterplane is based on an attempt to reduce wave-making resistance by bringing the bulk of the displaced volume below the surface and connect to the payload-carrying structure above the surface with as small surface-piercing struts as possible. This technique took advantage of the fact that a submarine makes no surface waves and has wave resistance while making motion under the water surface.

Siedl [1] provided a summary of early works and references. In 1880, C. G. Lundborg devised a single-hulled ship based on the principle, though the vessel may have had stability issues as a single hull, perhaps acting more like a submarine close to the surface. To counter the stability problem, other inventors considered twin-hull and multiple-hull vessels. For example, in 1905, A. Nelson in the USA patented a twin-hulled vessel whereby the buoyancy was provided by a pair of cylindrical submerged hulls and the above-water portion of the vessel was supported by struts.

Stenger designed the first medium-waterplane-area vessel in 1966. In 1968 this approximately 40-m vessel, the *Duplus*, called a small-waterplane-area twin hull (SWATH), was launched [2] or [3, Sect. 1.5.3]. The SWATH can also be referred to as a semi-submerged craft (SSC) as it has similarities to semi-submersible drilling rigs with submerged pontoons and column supports to the main working deck.

More recently, patents for designs by Leopold (1967, 1969), Lang, and Seidl have been granted. The latter exhibits a lower hull of "substantially varying" cross section, whereas all previously mentioned designs have two lower hulls that are torpedo-shaped or elongated bodies of essentially constant section. All these designs possess a single- or twin-strut design.

In 1973, the first vessel of this kind aimed at higher operational speed was constructed in the USA [4]. The SWATH, named the SSC *Kaimalino*, demonstrated that such craft had entered into a period of practical application (Fig. 9.1a). The craft

L. Yun et al., *High Speed Catamarans and Multihulls*,
https://doi.org/10.1007/978-1-4939-7891-5_9

Fig. 9.1 SWATH "Kaimalino"

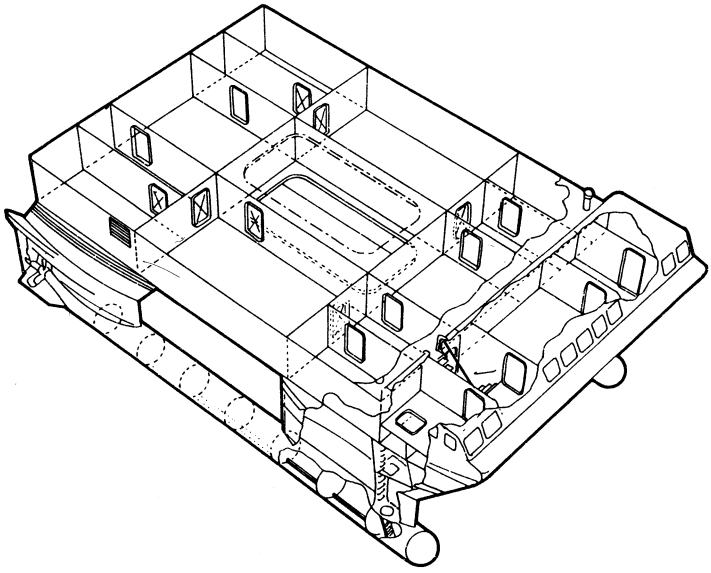

Fig. 9.2 *Kaimalino* compartmentation layout

is of semi-submerged form, with much of the displacement submerged under the water surface, and a large boxlike superstructure with utility and passenger cabins high above the water surface supported by extremely thin struts to form a carrier vessel (Figs. 9.1b and 9.2). The trial vessel was built with just a flat main deck as in the photo in Fig. 9.1a.

The lower hulls are of a circular or elliptical transverse section with the length/diameter ratio variable between 15 and 19 and providing 65–90% total buoyancy, outfitted with fuel and water tanks, ballast tanks, power transmission and even main engines, as well as fins and their control system for improving stability. The struts have slender streamline-shaped horizontal sections providing about 15–20% buoyancy and with a 5/15 length/thickness ratio.

A series of builder trials were carried out on the SSC *Kaimalino* before delivery; however, more tests were then completed in operation at sea around Hawaii, such as stress measurements on the hull structure, speed and maneuverability tests, vibration, and seakeeping tests. Since then, more than 100 helicopter landing and take-off tests were also carried out in rough seas [sea state (SS) 4]. Hawaii has an exposed ocean route between its islands with significant swells, hence the need to improve seagoing performance, a very useful test area for SWATH vessels. The performance of the SSC *Kaimalino* has stood the test of time, and it remains a reliable and passenger-friendly ferry.

Such systematic tests verified its seakeeping performance and confirmed her capability as well as positive prospects for such craft in the future.

SWATHs have the following main advantages and features:

- *Decreased wave-making resistance*: The wave-making resistance is very small; however, the friction resistance is great due to the large wetted surface area (60% larger than conventional monohulls) because of the large underwater hull volume and deep draft. Therefore, the total resistance is larger than that of monohull craft at low speed; nevertheless, the total drag will be reduced at medium speed.
- *Decreased motion in waves*: Since the wave disturbance to the craft is weak due to only the sharp strut contact with the water surface, the seakeeping quality is improved greatly compared with conventional craft. The US Coast Guard carried out a comparison seakeeping test of the SSC *Kaimalino* (220 t displacement) with a patrol ship weighing 3100 t in SS 3 and found that the motions for both craft are almost identical, and even a little lower for the SWATH (Fig. 9.3a). The seakeeping quality of this SWATH was also compared with a ferry boat named *Hawaii* with 100 t of displacement, at 18 knots in SS 4, and encouraging test results, shown in Table 9.1 and Fig. 9.3b, were obtained, with much lower motions.
- *"Stable platform"*: From the seakeeping tests of the SSC *Kaimalino* in SS 4 at 18 knots one can find that the pitching, rolling, and heaving displacements are $\pm 0.5°$, $\pm 0.7°$, and ± 0.3 m, respectively, so a helicopter weighing 6.8 t had no difficulty landing on the deck of the craft. The pilots even considered that the landing on this SWATH was as easy as on a helicopter carrier weighing 4200 t. In addition, the SWATH has a wide and spacious upper deck area for accommodating cabins, for passengers, working, or military applications.
- *Fine maneuverability and course-keeping ability*. The profile of a SWATH with longer underwater twin hulls shows a fine course-keeping quality. In addition, the wide space between the propellers in each hull provides a large turning moment even at low speed. Figure 9.4a shows the ratio of turning diameter to ship length

of three SWATHs, the SSC *Kaimalino* and the Japanese ships the *Seagull* and the *Ohtori*, versus speed. It is found that the turning diameter ratio to vessel length of a SWATH is close to that of a conventional monohull craft. Nevertheless, since the length of a SWATH is usually smaller than that of a monohull vessel, the absolute turning diameter is favorable. The craft maneuverability at zero speed is encouraging, even with the ability to turn on the spot. In addition, the positioning ability of a SWATH is fine, for example, the SSC *Kaimalino* was able to hold static position in rough seas for 21 h, which is very suitable for military and ocean engineering applications.

- *Lower speed loss in rough seas*. Figure 9.4b below shows the comparison of speed loss of various existing high-performance marine vessels in waves. It was found that the speed loss of SWATH in rough seas is lowest;
- *Larger deck area and spacious cabins in superstructure*: Similar to a catamaran, the deck area and working cabin or passenger cabin area in the superstructure are larger compared with conventional monohull ships, owing to the large hull separation. A comparison of a harbor surveillance ship with a SWATH configuration or conventional ship with the same displacement is given in the listing below [5]:

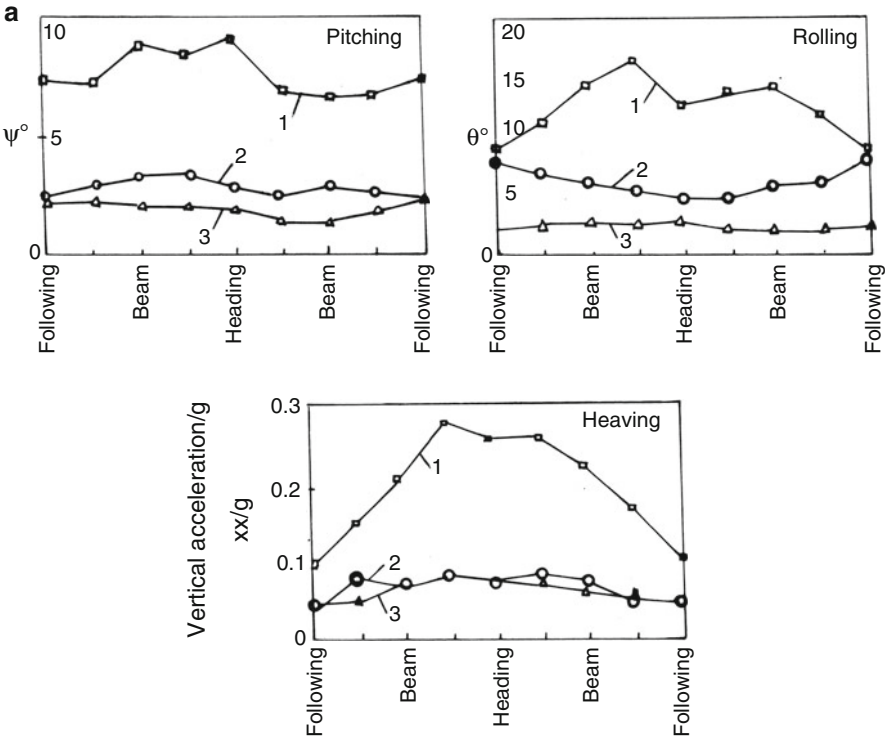

Fig. 9.3 (**a**) *Kaimalino* motion data; (**b**) comparison motions with ferry *Hawaii*

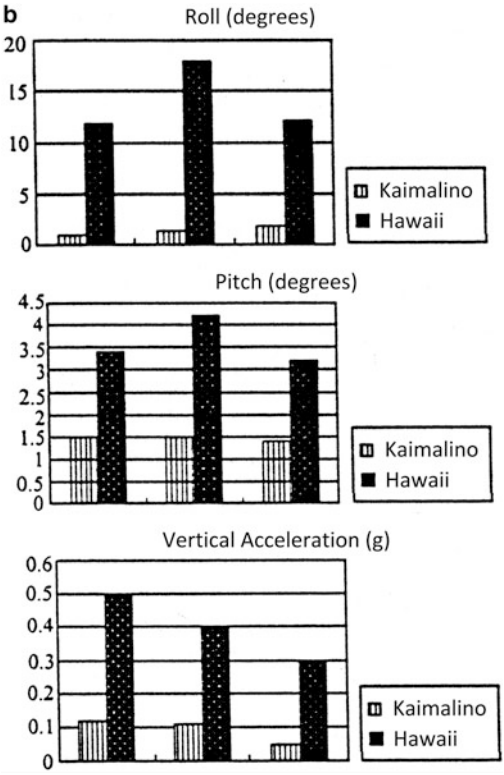

Fig. 9.3 (continued)

Key	Dimension	SWATH version	Conventional ship
LOA	m	28.7	32.2
BOA	m	9.4	5.4
T	m	2.14	1.35
Displacement	t	95.0	95.0
Area of meeting room	m^2	30.4	19.8
Total area of superstructure	m^2	129.4	62.9
Total area of upper deck	m^2	213.9	149.7
Wetted area	m^2	270.0	152.0
Waterplane area	m^2	22.0	120.0

Figure 9.4c shows the relation between the deck area and displacement of both SWATH and conventional monohull craft [6].

- *Fine propeller performance*: Since the SWATH draft is deeper than that of a monohull, in addition, with a wide hull separation, the propeller diameter can be larger than that on conventional ships, so the efficiency and cavitation margin of SWATH propellers will be improved. In addition, underwater hulls are usually of

Table 9.1 Comparison of seakeeping test results for *Kaimalino* and *Hawaii*

Motion	Heading	*Kaimalino*	*Hawaii*
Rolling motion (°)	Head waves	1.6	11.9
	Beam waves	1.5	18.0
	Following waves	1.9	12.2
Pitching angle (°)	Head waves	1.5	9.4
	Beam waves	1.6	4.2
	Following waves	1.4	3.2
Heaving acceleration (g)	Head waves	0.12	0.5
	Beam waves	0.11	0.4
	Following waves	0.05	0.3

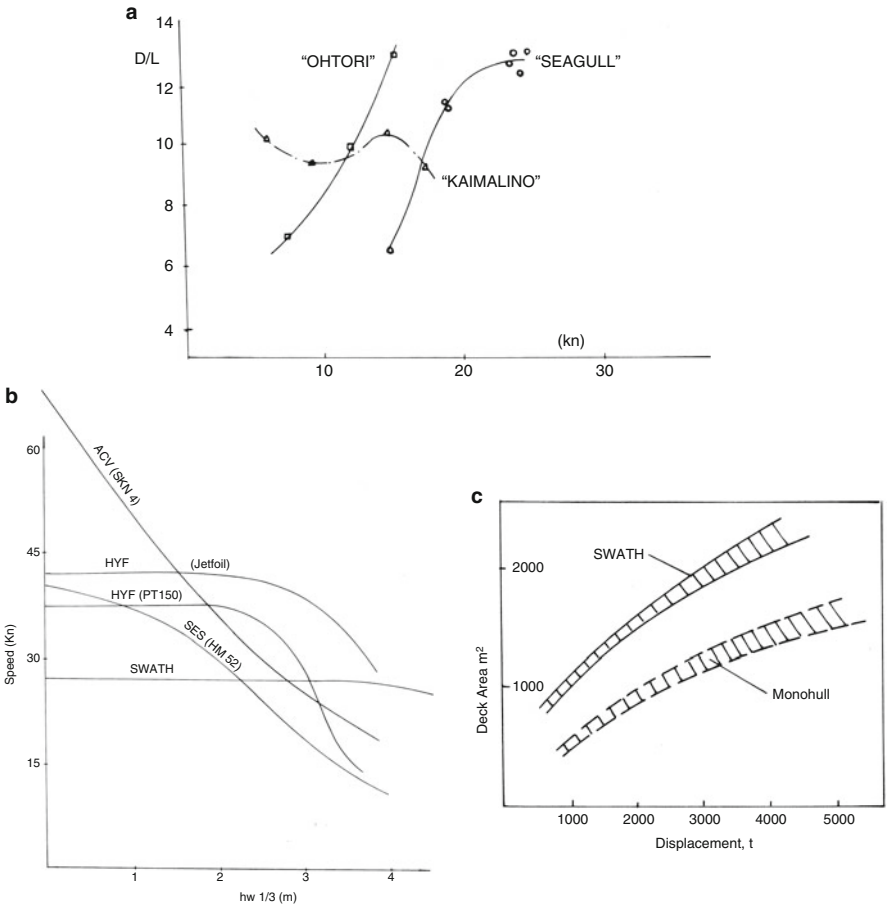

Fig. 9.4 (**a**–**c**) SWATH characteristics

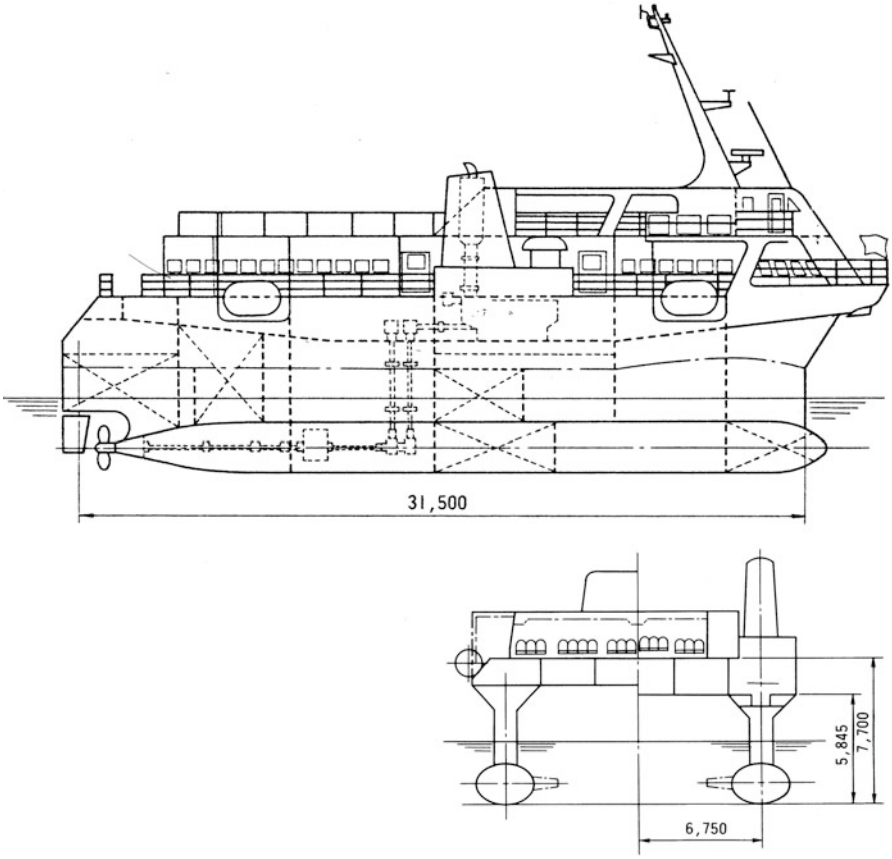

Fig. 9.5 Profile of SWATH *Seagull*

regular slender cylindrical body shape, so the wake around the propeller disc is more uniform, which improves hull efficiency.

The result is that the total propulsion efficiency of a SWATH may be increased by 10–40% compared to conventional monohull craft. For these reasons, many marine engineers became interested in the development of such craft following the appearance of the SSC *Kaimalino*, especially in Japan. Research and development in Japan was initiated by Mitsui in the early 1970s [7]. The first Japanese experimental 11-m SWATH vessel, the *Marine Ace*, was constructed in 1977 under the sponsorship of the Japan Marine Machinery Development Association.

The first commercial passenger ferry, the *Seagull*, was constructed in 1979, and extensive sea trials were carried out and extensive test data on it were gathered. The *Seagull* entered into service between Tokyo/Atami and Oshima Island in the Pacific Ocean in September 1981. Figure 9.5 shows the profile of the *Seagull*. Comparison seakeeping tests for the *Seagull* with another high-speed monohull craft of almost

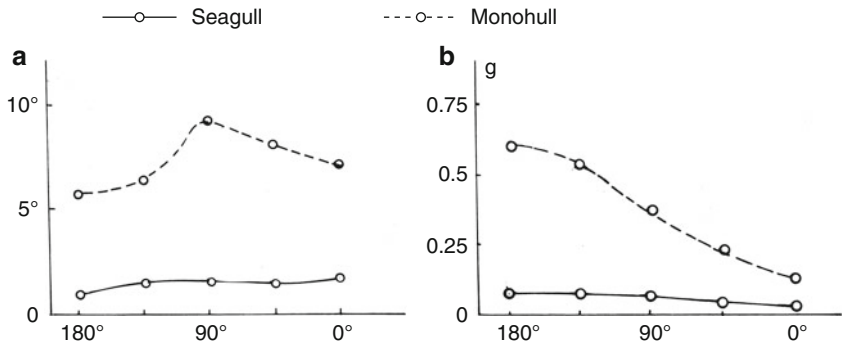

Fig. 9.6 Motion comparison of *Seagull* with monohull craft in waves

same length (35 m) were carried out at a speed of 24 knots in SS 3–4. The comparison tests were observed onboard a ship and by helicopter simultaneously.

Figure 9.6 shows a motion comparison of the *Seagull* with monohull craft at a speed of 24 knots in SS 3–4. It was found that the significant value (highest third) roll angles of SWATH at various wave directions (Fig. 9.6a) are only about 1.5°, compared with 9° on monohull craft. The vertical accelerations of a SWATH at various wave directions are below 0.1 g, compared with 0.6 g for monohull craft under the same conditions (Fig. 9.6b). The speed loss for the SWATH is below 2%, which is much lower than that on the monohull.

Using the operational experience with the *Seagull*, Mitsui developed a new passenger SWATH design called the *Seagull* 2 (Fig. 9.7), and this took over service from the *Seagull* in December 1989, that is, after 10 years of operation of her prototype the *Seagull*, which had enjoyed a good reputation for her comfortable ride and regular service among passengers during her service. The *Seagull 2* can run at 30.6 knots at maximum continuous rating and 27.5 knots at service with 410 passengers.

The trials and in-service performance were encouraging. Figure 9.8 shows the speed loss in a seaway of both the *Seagull* and *Seagull 2*. The performance in waves of *Seagull 2* was much better than that of her prototype, and the service speed during the year overall could be maintained as scheduled using the design power margin of the engines to compensate for the speed drop.

Figure 9.9a shows the vertical acceleration of *Seagull 2* in various SSs. The vertical acceleration level is quite low, whether at the bow, midship, or stern part of the craft. In general, it is lower than 0.1 g in rough seas with waves up to 2.5 m. The lower vertical accelerations guarantee lower passenger seasickness on the craft in a seaway. Figure 9.9b shows the relation of seasickness of passengers on the *Seagull 2* with SS, demonstrating that the seasickness level is very low at less than 0.6% for the average seasickness ratio.

Fig. 9.7 SWATH *Seagull 2*" in operation

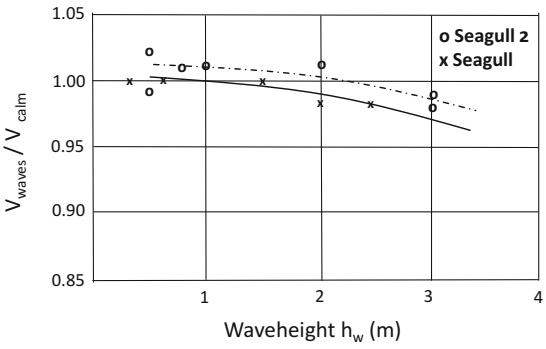

Fig. 9.8 Speed loss of *Seagull* in waves

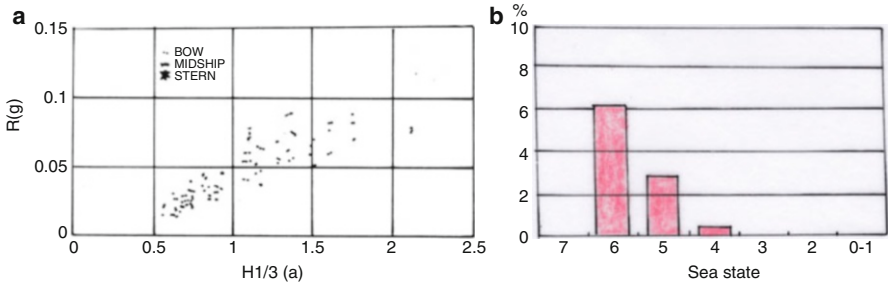

Fig. 9.9 (**a**) Vertical acceleration of *Seagull 2* in waves; (**b**) relation of seasickness of passengers on *Seagull* with sea state

The general arrangement (GA) and hull form of *Seagull 2* (as shown in Fig. 9.10) were selected considering the following criteria:

- Comfortable ride and service speed of more than 27.5 knots to replace *Seagull*;
- High operability as a logistical life line for isolated islands in rough open seas;
- Performance and facilities that make passengers want to take repeat voyages on this famous sightseeing route.

Key data for a sample of SWATH vessels completed up to the early 2000's is shown in Table 9.2. Most of the examples are slow-speed craft operating well below

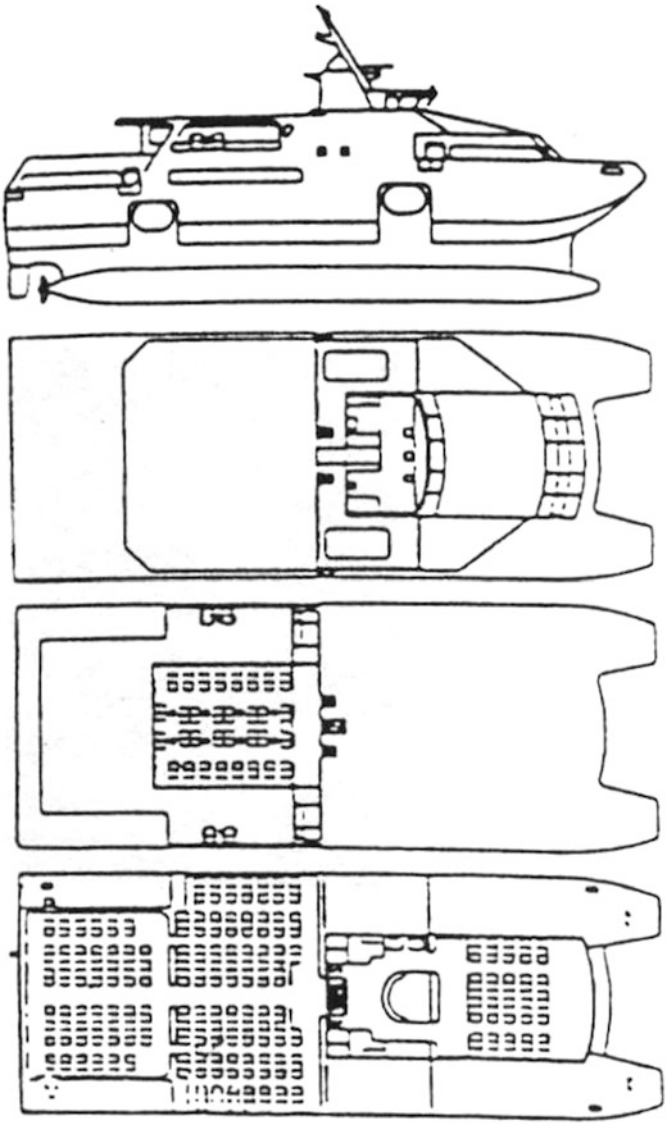

Fig. 9.10 General arrangement of *Seagull 2*

the 25 knots considered to be characteristic of fast craft. It was with the emergence of the less extreme hull form between the multistrutted craft and the wave piercer form discussed in Chap. 8 that the SWATH form could develop. These more recent craft have a super-slender waterplane and continuous hull form rather than the dual-strut form adopted on the *Seagull 2* or *Navatek 400*.

9.2 SWATH Characteristics and Limitations

The SWATH has a lot of positive points concerning motion reduction and, hence, its ability to operate in rough environments. Nevertheless, it comes with a number of challenges in connection with by the hull form, as follows:

- *Deep draft*: This limits its application in bounded waterways, such as harbors and piers, and limits its development for scaling to larger size ships.
- *Sensitive to weight distribution*: Since the buoyancy change for increased draft is very small due to the small waterplane area of the craft, it is extremely sensitive to weight distribution. This strongly influences the design and construction of SWATHs, meaning more attention has to be paid to weight control during design and construction, and influences the distribution of weight, meaning the changeable weight/payload elements have to be controlled more strictly. For instance, a ship with a displacement of 100 t, where the load error is 10 t, the effect of draft on monohulls, catamarans, and SWATHs is 0.01 m, 0.05 m, and 0.5 m, respectively [8], so weight control is one of the key points for SWATH design.
- *Poor damaged stability*: The damaged stability is poor compared with conventional ships for the reasons discussed earlier, particularly in the case of asymmetric flooding. For this reason, controllable ballast tanks and an active transfer system have to be arranged in ships' hulls to control trim, with a consequence of higher ship light weight.
- *Less usable space*: Since the struts and lower hulls are too narrow to be usable cabin and utility space, the usable space is lower compared with conventional multihull vessels.
- *Lower transportation efficiency*: Due to the large wetted surface and more complicated cross structure, lower hull, and struts as well as system for trim control, power transmission, and ballast system, the lightweight proportion of a SWATH may be larger than that of conventional ships by up to 10–40%. For this reason the transportation efficiency will be lower than that of a high-speed catamaran, as shown in Table 9.3; even the hydrodynamic efficiency for SWATHs are not lower at Fr_L equal to 0.7–0.8, owing to lower wave resistance, as can be found in the same table. To sum up, the economy of a SWATH is rather lower than that of a conventional catamaran.

Table 9.2 SWATH vessel leading particulars

Ship name	*Kaimalino*	*Marine ACE-1*	*Marine ACE-1a*	*Seagull*	*Kotozaki*	*Ohtori*
Country	USA	Japan	Japan	Japan	Japan	Japan
Completed	1973	1977	1978	1979	1980	1981
Application	Working ship	Test	Test	Passenger ferry	Marine survey	Marine survey
Grt, t	..	29.91	31.56	672.08	..	..
Displ., t	193	18.4	22.2	338	236	239
LOA, m	26.8	12.3	12.35	35.9	27.0	27
BOA, m	13.7	6.5	6.5	17.1	12.5	12.5
Draft, m	4.66	1.55	1.55	3.15	3.2	3.4
Speed, knots	25	17.3	15.4	27.1	20.5	20.6
Main engine	2×Gas Turbine	2×Petrol Engine	2×Petrol Engine	2×Diesel	2×Diesel	2×Diesel
Total power, (N) kw	3132	298	298	6040	2834	2834
Machinery Location	Cross Structure	Cross Structure	Cross Structure	Cross Structure	Cross Structure	Cross Structure
Transmission type	Chain Drive	Bevel Gears	Bevel Gears	Bevel Gears	Bevel Gear	Bevel Gears
Propeller	3 blades adjustable-pitch propeller	3 blades fixed-pitch propeller	3 blades fixed-pitch propeller	3 blades fixed-pitch propeller	Adjustable-pitch propeller	Adjustable-pitch propeller
Stability fins	Automatic	Automatic	Automatic	Automatic	Manual	Manual
Strut type	Twin strut	Twin strut	Twin strut	Single strut	Single strut	Single strut
Deck material	Al	Al	Al	Al	Al	Steel
Strut material	Steel	Al	Al	Al	Steel	Steel
Lower Hull	Steel	Al	Al	Al	Steel	Steel
Fr_L	0.79	0.66	0.72	0.74	0.64	0.647
$C = \frac{D^{2/3}v^3}{N}$	222.3	161.9	129.4	213.3	154.9	158.5

(continued)

- *Complicated power transmission*: The main engines are typically located on the upper cross structure, which is the most traditional arrangement on SWATHs, as shown in Table 9.2. The propellers are located at the stern of the submerged hull so that a complicated Z-type drive with bevel gears, or inclined shaft drive with universal joints, or belt drive, or electric drive must be installed. All such arrangements make the design more technically complicated and higher risk and generate more weight and costs.

If the main engines are located in the lower hull with direct power transmission, this can reduce some of the transmission problems mentioned earlier; however, the design, installation engines during construction, and repair as well as maintenance

Table 9.2 (continued)

Name	*Betsy (ex Suave Lino)*	*Charwin*	*Kaiyo*	*Halcyon SD-60*	*Marine Wave*	*Sun Marina*
Country	USA	USA	Japan	USA	Japan	Japan
Completion Year	1981	1984	1984	1985	1985	1987
Application	Offshore tender	Fishing vessel	Submarine support ship	Test demonstration	Luxury boat	Luxury boat
GRT t	..	..	..	57	..	..
Displ., t	40	193	2849	52	19	19
(Pax) + Crew	(n/a)	(n/a)	(40) +29	(20) +3	(17 total)	(33 total)
(cars)	(−)	(−)	(−)	(−)	(−)	(−)
LOA	19.2	25.3	61.55	18.3	15.1	15.05
BOA	9.1	12.2	28.00	9.1	6.2	6.4
T	2.13	2.74	6.3	2.13	1.6	1.6
Speed, knots	18	10	14.1	20	18	20.5
Main engine	2×Diesel	2×Diesel	4×Diesel	2×Diesel	2×Diesel	2×Diesel
Power, kW	632	485	7400	761	373	447
Machinery location	Cross structure	Cross structure	Cross structure	Cross structure	Cross structure	Cross structure
Transmission	Bevel Gear	Belt	Electric	Belt drive	Inclined shaft	Inclined shaft
Propeller FP – fixed AP – adjustable	2 FP prop	2 FP prop	2 AP prop 4 blade	2 CP prop	2 FP prop	2 FP prop
Fin	Active	No data	Active	Active	Active	active
Strut	Single	Single	Single		single	single
Deck material	Al	Steel	Steel	Al	GRP	GRP
Strut	Al	Steel	Steel	Al	GRP	GRP
Hull	Al	Steel	Steel	Al	GRP	GRP
Fr_L	0.674	0.35	0.29	0.768	0.768	0.867
C	144.2	91.89	101.4	195.6	148.8	183.4

(continued)

during operation will be more complicated than under the traditional approach unless the size of the lower hull is increased with drag penalty. An alternative available since the early 2000s is to install a diesel electric drive with the main engines above and electric motors direct coupled to the propeller. Another alternative would be a high-pressure hydraulic drive. Both such systems are rather more expensive to install than a mechanical transmission.

- *Complex ride control system*: Such a system is needed to maintain dynamic longitudinal stability and maximize seaworthiness.

Table 9.2 (continued)

Name	*Chubasco*	*Frederick G Creed*	*T-AGOS 19 USS Victorious*	*Bay Queen*	*Seagull 2*	*FDC 400 Patria*	*Aegean Queen*
Country	USA	USA	USA	Japan	Japan	UK	Greece
Completion Year	1987	1989	1989	1989	1989	1989	Design 1991
Application	Luxury boat	Fisheries patrol	Subsea survey	Multipurpose	Passenger ferry	Passenger ferry	RoPax Ferry
GRT, t	..	..	..	..	..	..	2544
Displt	76	80.26	3450	40	350	180	1060
(pax) + crew	(11) +3	(125)	(5) +19	(−) +40	(410) +7	(400) +10	(752)
(cars)	(−)	(−)	(−)	(−)	(−)	(−)	(80)
LOA	21.95	20.4	71.3	18	39.3	36.5	51.5
BOA	9.45	9.75	28.6	6.8	15.0	13.10	31.7
T	3.05	2.6	7.56	1.6	3.25	2.74	5.0
Speed, knots	20.0	25	10.4	20	30	30	30
Main engine	2×Diesel	2×Diesel	4×Diesel	2×Diesel	4×Diesel	2×Diesel	4×Diesel
Power, kW	1119	1610	3341	1266	7882	4022	14,914
Machinery location	Lower Hull	Lower Hull	Cross Structure	Cross structure	Cross Structure	Cross Structure	2 in line in each lower hull
Transmission	Straight gearbox	Straight gearbox	Electric	Belt drive	Bevel gears	Inclined shaft	Gearbox
Propeller FP: fixed CP: variable	2 FP prop 4 blade	2×FP prop	2 FP prop 5 blade	2 FP prop 3 blade	2 prop	2 FP prop 3 blade	2 CP prop 5 blade
Fin	Gyro active	active	active	active	active	active	active
Strut	single	single	twin	single	single	single	single
Deck material	Al	Al	Steel	Al	Al	Al	Al
Strut	Al	Al	Steel	Al	Al	Al	Al
Hull	Al	Al	Steel	Al	Al	Al	Al
Fr_L	0.701	0,909	0.202	0.774	0.786	0.816	0.69
C	171.3	241	102	98.73	226.9	285	250

(continued)

The issue to tackle before adopting a SWATH configuration is the balance of demands for the vessel mission. The *Seagull 2* mission was aimed at continuous service in relatively rough seas as a ferry. Not many fast ferry routes have to face this kind of challenge. One mission that does have such a challenge is the offshore wind turbine service and maintenance market. Such wind farms are typically in an exposed location where winds are reliable, resulting in SSs that are also rough rather than calm most of the time. We will look at how some of these vessels have adapted the SWATH approach later in the chapter. In the meantime, what follows is a general overview of applications for SWATHs as they have developed, which gives a flavor.

Table 9.2 (continued)

Name	*Navatek 1*	*2000 Class*	*Hibiki*	*T-AGOS 23 USS Impeccable*	*Radisson Diamond**	*Customs 201*
Country	USA	USA	Japan	USA	USA	China
Completed Year	1989	1989	1990	1992	1992	2001
Application	Passenger	Subsea survey	Military survey	Military survey	Passenger	Customs craft
GRT, t	..	..	..	..	20,295	..
Displ. D, t	365	80	3700	5368	12,000	228
(pax) + crew	(450)	(.)	(5) + 19	(25) + 25	(354) +150	(n/a)
LOA, m	40.24	20.43	67.0	85.78	131.2	35.0
BOA, m	16.16	9.75	28.6	29.16	30.96	13.3
T, m	3.7	2.59	7.56	7.9	7.6	2.8
Speed, knots	17.5	25	11.0	12.0	14.15	17.5
Main engine	2×Diesel	2×Diesel	4×Diesel	4×Diesel	4×Diesel	2×Diesel
Power, kW	1912	1610	2386	3710	11,345	2240
Machinery location	Lower hull	Lower hull	Cross structure	Cross structure	Lower hull	Cross structure
Transmission	Directly	Directly	Electric	Electric	Directly	Inclined shaft
Propeller FP: fixed AP: adjustable	2× AP Prop	2× FP Prop	2× FP prop 4 blade	2× FP prop 5 blade	2× ducted Prop	2× FP prop
Fins	Active	Active	Active	Active	Active	Fixed
Strut	Twin strut	Single	Single	Single	Single	Twin
Material	Al	Al	Steel	Steel	Al	Steel
Fr_L	0.45	0.91	0.22	0.31	0.203	0.486
C	191.0	240.6	177.3	102	174.2	119.5

**Radisson Diamond* now *China Star*

9.3 SWATH Applications

9.3.1 Civil Applications

The SWATH was developed for special civil applications requiring large passenger or personnel operational space and relatively low payload variation, where extreme stability and ride comfort are required in year-round high SS environments with high operational reliability. Some SWATHs for civil application have been constructed as follows:

Table 9.3 Comparison of hydrodynamic and transportation efficiency between SWATH and high-speed catamarans

Ship name	*Seagull* 2	*FDC 400*	*AMD 200*	*Cata-marin*	*W95*	*W100*	*Mackinac express*
Type of ship	SWATH	Semi-SWATH	HSCAT	HSCAT	HSCAT	HSCAT	HSCAT
Speed (v), knots	30	30	25	28	31	26	27
Displacement, t (D)	200	180			74	84	
LOA	39.3	36.5	28	26.15	29.2	33.3	25.16
Power (N), kW	7882	4022	1680	1970	2646	2646	1678
Passenger, P	410	400	235	400	205	240	330
Fr_L	0.78	0.816	0.775	0.945	0.99	0.8	0.955
N/P, kW/passenger	19.2	10.05	7.15	4.92	12.9	11.0	5.07
Hydrodynamic Efficiency, K_η	6.9	6.76			4.37	4.16	
Transportation Efficiency, K_p	2.89	1.53	6.48	10.5	4.45	4.37	9.8

In the foregoing table:
$K_\eta = vD/102N$, with units (km/s)·kg/kw and $K_p = Pv/N$, with units Pass·(km/h)/kw

- Passenger ferry ship *Seagull* series (Figs. 9.5 and 9.7) operating on the route between Tokyo/Atami and Oshima Island in the Pacific Ocean in offshore Japan, and *DFC-400* (Figs. 9.29 and 9.30) in the North Sea, or Chinese navigation route in Bo Hai Bay and Taiwan Strait, where large passenger flows are possible due to routes cutting distance compared with ground transportation while the routes are exposed, resulting in a high SS [9, 10];
- Ship for excursion and cruising utility, the *Navatek 1* (Fig. 9.11a, b), where spacious, stable, quiet, comfortable cabins (even casino available) arranged on a superstructure can be operated in the ocean;
- Marine survey ships *Ohtori* and *Kotozaki* (Fig. 9.12) of Japan, which require extreme seaworthiness to operate in the ocean year round;
- Fishing boats and excursion boats as well as luxury boats operating in exposed seas with rather small displacement, for example, the *Chubasco* and *Suavolino*;
- Utility ships and other paramilitary missions for application in rough sea, such as the *Customs 201*;
- Since the early 2000s both catamaran and trimaran variations of the SWATH geometry have been designed and built for wind farm maintenance operations where the ability to hold station and have minimum motion for personnel transfer to a wind turbine structure together with rapid transit from base to turbine farm offshore is a key attribute.

9.3.2 Military Applications

SWATH operational characteristics are attractive for some military applications, and government and military administrations are able to consider vessels with lower economic efficiency due to the lower annual usage rate or special mission requirements. The following elements may suggest a SWATH will be the right choice:

- Fine seaworthiness as well as spacious deck area and deckhouse provide a stable flying deck and support for palletized or modular military hardware outfit. In 1976, some landing and launching tests for helicopters (more than 80) were carried out on the relatively small SSC *Kaimalino* at 220 t (Fig. 9.1), and the test results demonstrated that such operations could be carried out year round;
- High operability for SWATHs year round due to extreme seaworthiness. According to statistical investigations of the US Navy in 1983, conventional monohull ships weighing 2760–1150 t could be operated at full speed only in the case of SS below 5. In addition, the probability of navigation without limitations for a conventional frigate with 122 m in length in winter in the North Atlantic Ocean is only 30% and only 55% for destroyers or cruisers with 167.6 m long. In

Fig. 9.11 SWATH *Navatek 1*: (**a**) the vessel; (**b**) profile and general arrangement

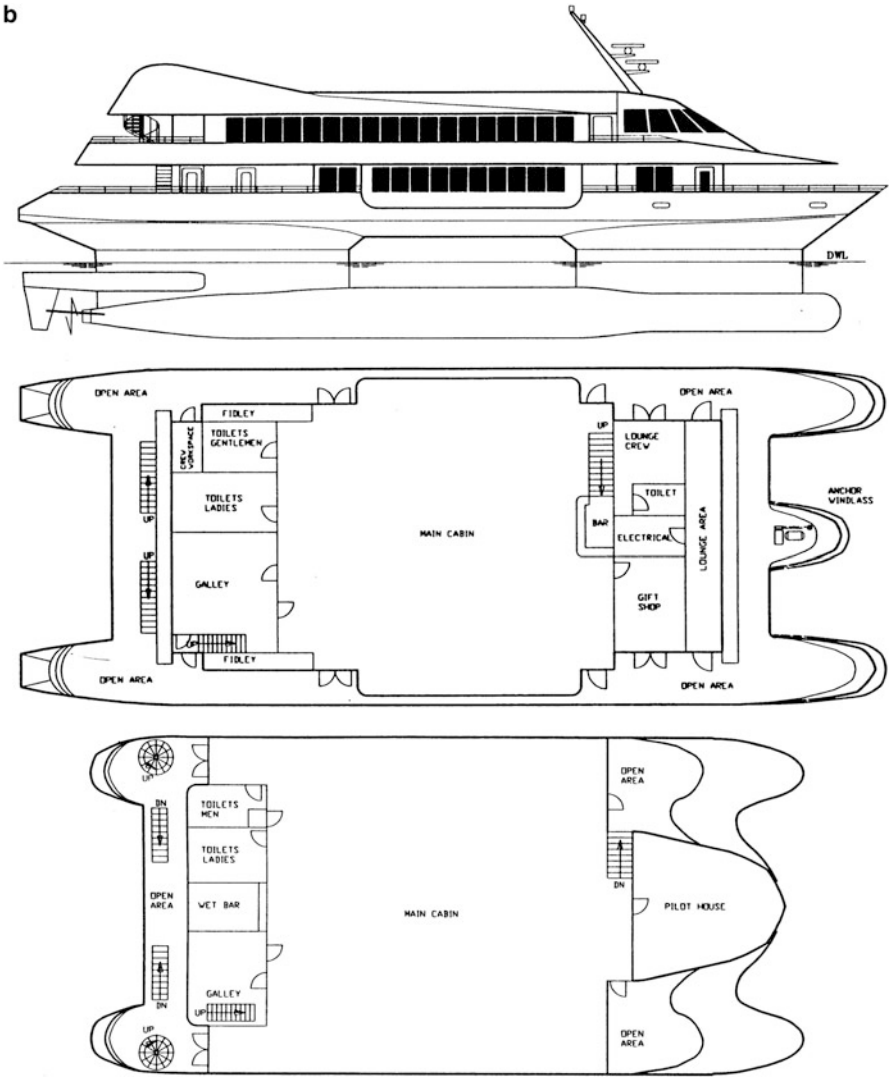

Fig. 9.11 (continued)

the North Atlantic Ocean, the navigation rate without limitations for year round operation are 45% for conventional frigates and 70% for conventional destroyers; however, in the case of SWATHs, which might be navigated year round, regardless of the SS. Unless dash speed is important, a SWATH may improve overall usability;

- Fine maneuverability and stable motion performance of SWATHs in rough seas allow a stable base for guided missiles and artillery. According to shot tests carried out by a Rockwell research team in 1981, the percentage of hits of

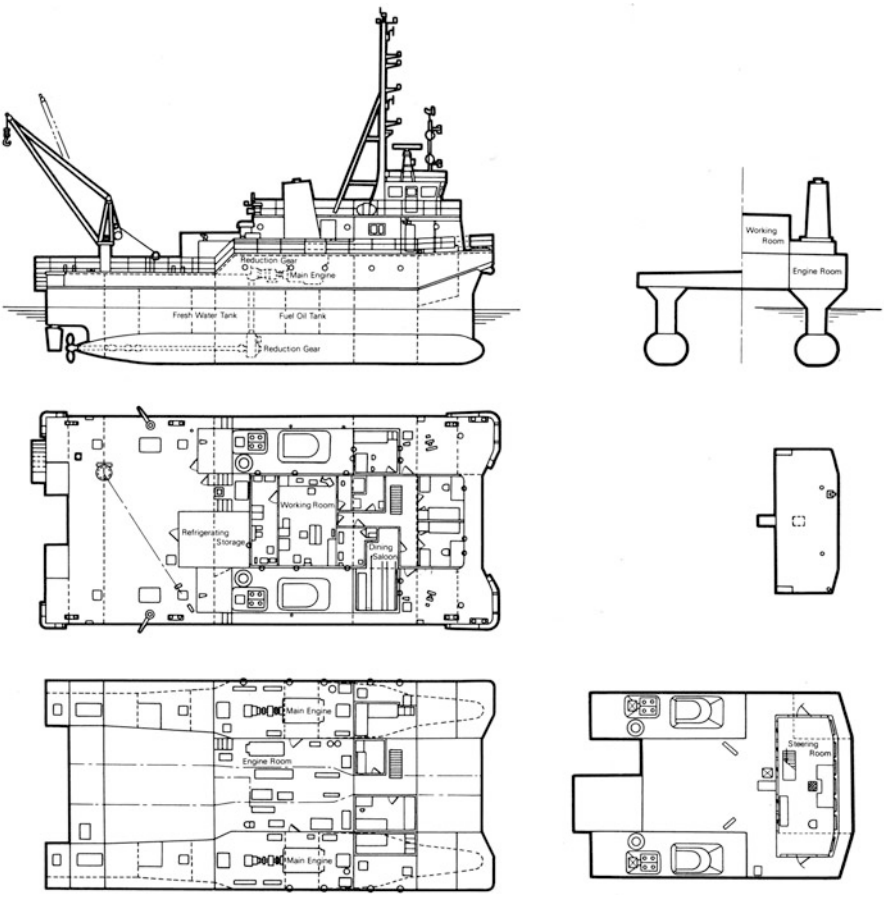

Fig. 9.12 Profile and general arrangement of SWATH *Kotozaki*

weapons on a SWATH could be enhanced by up to 10–40% compared to conventional warships;

- Deep draft might be a defect for commercial vessels, but it could be an advantage for warships because it would allow for mounting a propeller with a larger diameter and lower revolution so as to reduce the load on propellers and the occurrence of cavitation. In addition, a deeply immersed lower hull makes it easier to install acoustic equipment, and this would lead to reduced noise levels caused by ship machinery, so that the SWATH lends itself to submarine detection and other underwater operations when used as the mother ship;
- High damage tolerance due to twin hulls and deep draft, as long as the compartmentation of struts is taken care of and the ballast system is sized correctly;
- Making a stealth superstructure thanks to its architectural peculiarity, like the US SWATH type *Sea Shadow*, which is also extremely important for modern warships. Figures 9.13 and 9.14 show the frontal view and configuration of this ship

[11], and the inclined A shape superstructure shows the stealth peculiarity of the ship, on which the US Navy spent approximately $196 million for research in the 10 years prior to 1993.

Research on the stealth (reduced radar and physical visibility) concept for warships has been ongoing for years under the leadership of the US Navy, which has used the approach for both stealth aircraft, such as the Lockheed F-117A, and with a SWATH ship prototype. The peculiarity of the hull profile of the *Sea Shadow* to the ship community is similar to the peculiarity of the stealth aircraft F-117A for the aircraft community.

The *Sea Shadow* is 49.99 m in length overall and 20.73 m wide and has a displacement of 560 t, a disposable weight of 51 t, a draft of 4.42 m, and a maximum low hull diameter of 3.048 m; clearance between above body and water surface is 2.438 m. Propulsion is by a diesel-electric motor system, with the diesel located at the main deck and electric motors located in the underwater hulls, giving a service speed of 13 knots. The craft can be operated normally in SS , and operated safely in SS 5.

The vessel cross section (Figs. 9.13a and 9.14) is like the letter A and rather different from that of a conventional SWATH. Figure 9.13b shows seakeeping test results of the *Sea Shadow* model, indicating that the type of struts with an inclination angle of 45° is most suitable for the craft operated in rough seas with a satisfactory motion response. The rationale is that the damping and added mass coefficient of this type of model will increase so as to decrease motion. Actually, the motion of *Sea Shadow* within its operating envelope was said to be comparable to that of the conventional SWATH with 4000–5000 t displacement.

A series of design measures connected to stealth were made on the craft: stealth hull profile, configuration, and material. The hull profile was composed of a series of

Fig. 9.13 (**a**) Frontal view of *Sea Shadow*; (**b**) influence on strut inclination angle on heaving motion

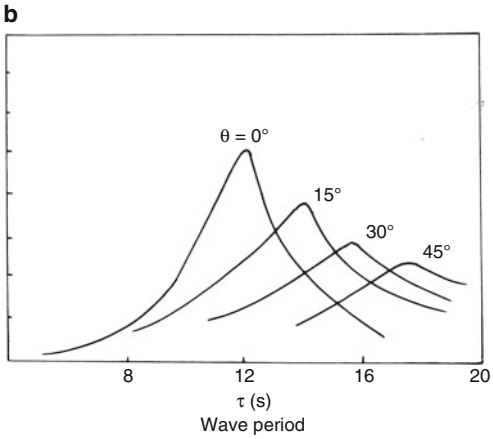

Fig. 9.13 (continued)

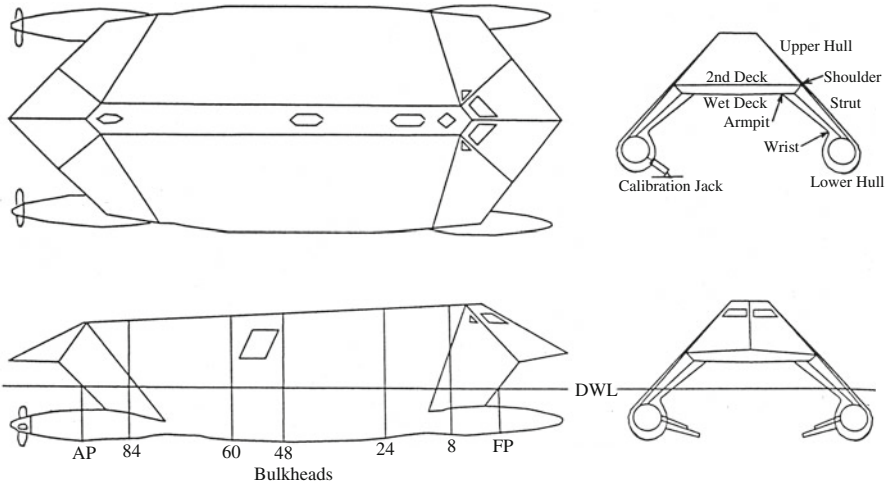

Fig. 9.14 *Sea Shadow* configuration

smooth panels, like on F-117A aircraft, with an inclination angle larger than 39°, in order to deflect reflected radar wave from enemy radar upward or downward. The hull structure is also covered in materials for absorbing enemy radar waves.

For these reasons it is apparent that a suitably designed SWATH might be used for military applications, once it is scaled up from the trial dimensions of *Sea Shadow*, as follows:

- So-called carrier ships, such as aircraft carriers or helicopter carriers, due to their large superstructure volume, deck area, and seaworthiness;

- Antisubmarine warships;
- Submarine salvage and support ships;
- Patrol ships and boats that can access a location quickly while also cruise at lower speed offshore on patrol to protect a nation's exclusive economic zone.

9.4 SWATH Performance

9.4.1 Calm-Water Resistance

The parameters that influence the resistance and other performance aspects of SWATH ships are more numerous than for conventional monohull ships or even the conventional catamaran. For instance, the parameters concerned with the transverse dimensions of a conventional ship are only the beam; however, with SWATHs, there are four: thickness of struts, centerline spacing between the two hulls, beam of submerged hull, and platform height. The length parameter for a conventional ship is one (L_{WL}), but on SWATHs there are three (L_h, L_{bs}, L_{ss}) (Fig. 9.15) and for height also three parameters versus one.

For these reasons, it is difficult to determine the dimensional parameters of a SWATH in preliminary design by model tests in a towing tank directly because there are too many models and test variations required. Fortunately, the slenderness of both struts and the lower hull are so large that it is possible to predict the main part of the total resistance of a SWATH, wave-making drag, with the aid of theoretical calculations, as was introduced in Chap. 3, and we continue this thread in the next sections of this chapter.

A comparison of the combination of design parameters of a SWATH with those of a conventional monohull ship and catamaran are listed in Table 9.4.

Based on the theoretical calculation for resistance (and in some cases for longitudinal dynamic stability as well), the selectable variants may be decreased significantly, and necessary model tests might then be carried out for final selection.

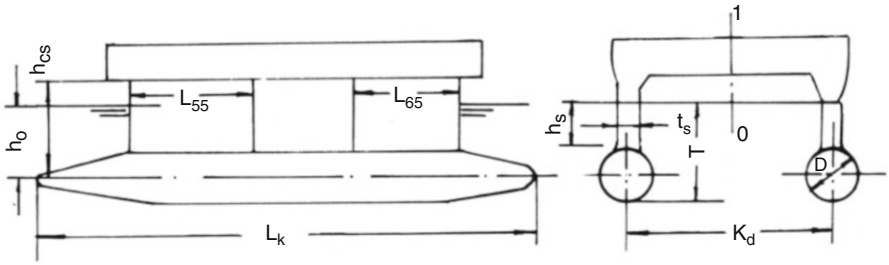

Fig. 9.15 Principal dimensions of SWATH

Table 9.4 Comparison of parameter combinations of SWATH, monohull, and catamaran

	Length	Width	Height	Draft	Displacement	Number of variables	Combinations of design parameters*
Conventional monohull ships	1	1	1	1	1	5	$3^5 = 243$
Catamaran	1	2	2	1	1	7	$3^7 = 2187$
SWATH	3	4	3	1	1	12	$3^{12} = 531{,}441$

*If three variants are used for each parameter.

The total resistance of a SWATH can be expressed in the same way as a catamaran as follows with respect to velocity, v:

$$R_t = \frac{1}{2}\rho_w v^2 \left(C_r + C_f + \Delta C_f\right) S_w = \frac{1}{2}\rho_w v^2 S_w C_t. \tag{9.1}$$

Then the engine power can be expressed as

$$N = \frac{R_t v}{102\eta_p \eta_m} = \frac{D^{2/3} v^3}{C}. \tag{9.2}$$

In this equation the wetted area S_w can be expressed as $D^{2/3}$, and C is the admiralty coefficient, similar to the power expression for conventional ships. Table 9.2 earlier in the chapter included data for the factor C for various SWATH ships.

Figure 9.15 shows the principal dimensions of a model that was tested by the Unites States Naval Research Laboratory, Washington DC. The configuration of this SWATH is with vertical rather than canted wave-piercing struts.

Figure 9.16a shows a comparison of a theoretical calculation of a SWATH-IV model with test results. The practical calculation method for the wave resistance of a SWATH will be introduced in the next section.

From the calculations, as in reference [8], it is noted that approximately 40–60% of the total resistance is wave-making resistance, so the geometric parameters of lower hulls and struts are very important to determine to decrease the total resistance. Figure 9.16b shows the influence of the length and diameter ratio of the lower hull L_h/D on wave-making resistance [8]. It is apparent that the higher this ratio, the lower the wave-making resistance coefficient; however, it will also cause an increase in the wetted area and the friction resistance for a given vessel displacement.

The main geometrical parameter for strut influence on wave-making resistance is the strut thickness, which influences the angle of entry at the leading edge and the fineness of the trailing edge

From the analysis it is noted that there are six wave-making resistance components caused by a SWATH with a single strut, shown in Fig. 9.16c, where:

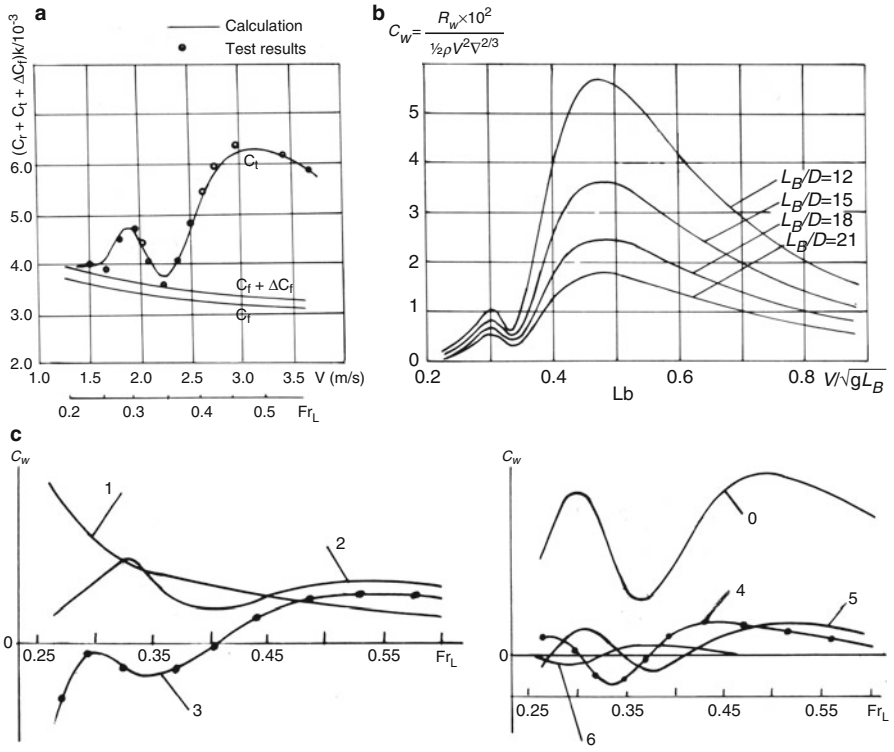

Fig. 9.16 (**a**) Calculation and test data for SWATH-IV model of NSRDC; (**b**) influence of Le on wave-making resistance; (**c**) wave resistance for single-strut SWATH

0. Total wave-making resistance
1. Strut wave making,
2. Wave making caused by submerged hull (demihulls),
3. Interference wave making caused by strut and submerged hull,
4. Intersection interference wave making caused by submerged hulls and struts,
5. Interference wave making caused by both submerged hulls,
6. Interference wave making caused by struts.

Since the wetted area of a SWATH is much higher than a displacement monohull, the friction resistance is also increased significantly, and this limits the speed of SWATHs, which are seldom designed for speeds in excess of 28 knots. The concept of the SWATH, with fully submerged lower hulls, does not allow for the use of surface planing and dynamic lift, as with a catamaran or trimaran, so the limits of displacement operation define its useful speed envelope.

In general, the ratio of wetted area between conventional monohulls, catamarans, and SWATHs may be as follows:

$$C_s \text{ ratio} = 1.0 : 1.4 : 2.3.$$

where $C_s = S/\sqrt{\nabla L}$, S, ∇, L represent wetted area, volume displacement, and length of SWATH, respectively.

The wetted area, being 60% higher than that of a typical catamaran and having a small waterplane, means that frictional resistance dominates for the SWATH. It was found to be more advantageous to have a single-strut form for most missions for SWATHs after the initial vessels were built because, though wave resistance is increased, this form can be much more stable in heave and pitch and so tolerant of payload mass and CG variation. So what will guide the through-water configuration in the start of a design?

9.4.1.1 Choice of Through-Waterplane Configuration

The issues discussed here are mainly concerned with the type of strut to be selected for a SWATH vessel, that is, a single strut or twin struts. The single strut is an extension of the small-waterplane-area catamaran, while the twin struts are as in the SWATH-IV. The following points may be noted:

- *Resistance*: Twin struts should be worse than single-strut vessels based on model test results found in [1, 10, 12, 13], particularly in the case of high speed, where the strut spray drag will be dominant in resistance. In the case of twin struts, the separation between the fore and aft struts has to be enlarged in order to avoid the effect of spray caused by struts at higher speed.
- *Seakeeping*: The SWATH is characterized by its small waterplane area, which reduces the wave disturbance force as well as moment and natural heave and roll frequency (Chaps. 2 and 4). In the case of single struts, the natural heave period will be shorter than that of twin struts. In addition, since the motions of a SWATH are much better in vertical mode, the horizontal motions and accelerations are sensed more easily by passengers and therefore need to be minimized. A twin-strut configuration will tend to have less transverse acceleration in beam seas.
- *Stability:* A SWATH is also characterized by low static transverse and longitudinal initial stability due to the small waterplane area; in addition, the static initial transverse stability can be improved and checked by proper hull separation; however, the longitudinal stability will be more sensitive if the LCG changes as a result of movement of passengers or other dynamic payload.
- *Operational issues*: For the aforementioned reasons, the single-strut configuration will be more suitable for passenger ferry application due to its better longitudinal stability than a twin strut. However, in the case of a SWATH with significant operation at low and zero speed, for example, whale watching, nature excursions, wind farm maintenance, or other applications requiring fast access to a site and then station keeping, the twin-strut configuration can prove more advantageous.

- *Mechanical system installation*: There are two options for a SWATH: install all machinery in the upper structure and arrange mechanical transmission to shafts and propellers at the stern of the submerged hulls, or make the hull large enough to accommodate the machinery and design the strut structure to provide access, ventilation, motor intake, and exhaust. For a small vessel the first option may be simpler, while for larger vessels the complication of extensive transmission systems may demand machinery installed in the lower hulls. This is not so difficult where the SWATH is a single-strut design.
- *Transverse wave loads*: A single-strut SWATH design will attract higher transverse wave loads than a two-strut-per-hull configuration, so the upper structure connecting to the struts will be more substantial to accommodate the load.

9.4.1.2 Stability

Because the waterplane area is small in order to reduce the effect of an undulating sea surface, the displaced volume is deeply submerged below the water surface. The vertical center of gravity is high due to the wet deck and superstructure requirement of having a certain clearance above sea level. Taking these two together, the initial transverse stability is lower than that of a conventional ship. An increase in the waterplane area will cause a reduction in the heave natural period so as to reduce seakeeping quality.

Increasing the hull separation has less of an effect than on a conventional catamaran due to small waterplane area. However, fortunately, at larger inclinations the sponson (watertight lower part of the superstructure) gives a greater reserve buoyancy to enhance the transverse stability of a ship with a large heeling angle. Figure 9.17 shows the intersection of inclined waterplanes of the US SWATH *Navatek 1*, and Fig. 9.18 shows the righting arm and heeling arm caused by passenger crowding on the ship with 12.5-m draft; in the figure, "1" represents the righting arm and "2" the heeling arm.

From the figures one can see that the righting arm will increase with a small inclination angle and at a greater rate with inclination angles larger than 8°, despite the small initial static transverse metacentric height. This is due to a broadening of the struts just above the design draft to provide increased buoyancy and the large sponson at the upper deck.

As the deck house is not considered to be watertight, the angle of reversal of the transverse stability curve is mostly at the height of the deck house entrance coaming, and the point of downflooding over the deck house door entrance coaming is the point of reduction of stability, as can be seen in Fig. 9.17.

Figure 9.19 shows the calculated intact and damaged righting arm curve of *Navatek 1*, where "1" represents the intact righting arm, "2" shows the righting arm of the ship in case of flooding of the aft machinery bay, and "3" denotes flooding of the engine room, both of which are located in the ship submerged hulls.

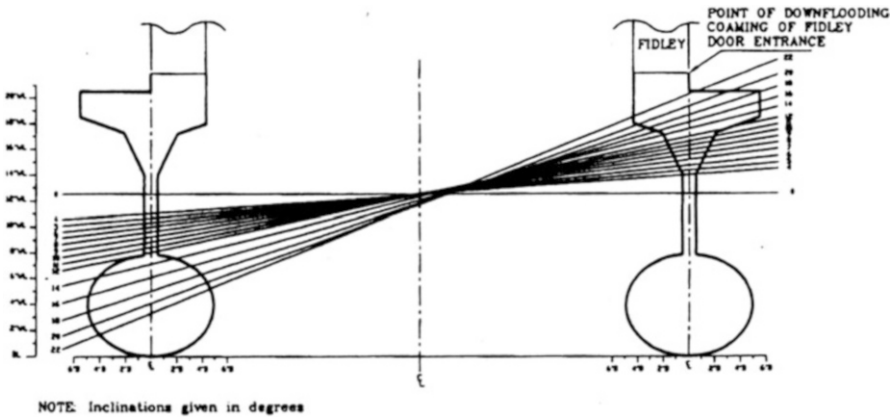

Fig. 9.17 Intersection of inclined waterplanes of *Navatek 1*

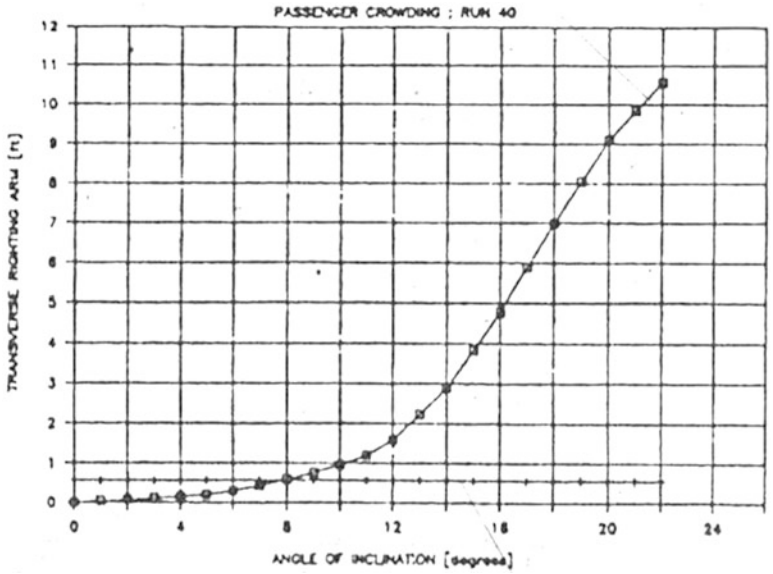

Fig. 9.18 Righting arm curve for 12.5-feet draft of *Navatek 1*

From the figure one can see the righting arm is positive in damaged condition, and both flooding conditions are still satisfied, even without considering counterballasting measures.

The calculation method for static transverse stability is the same as for a conventional catamaran, and the criteria as well as the standard for the transverse stability of a SWATH are also the same as for conventional catamarans (Chap. 2).

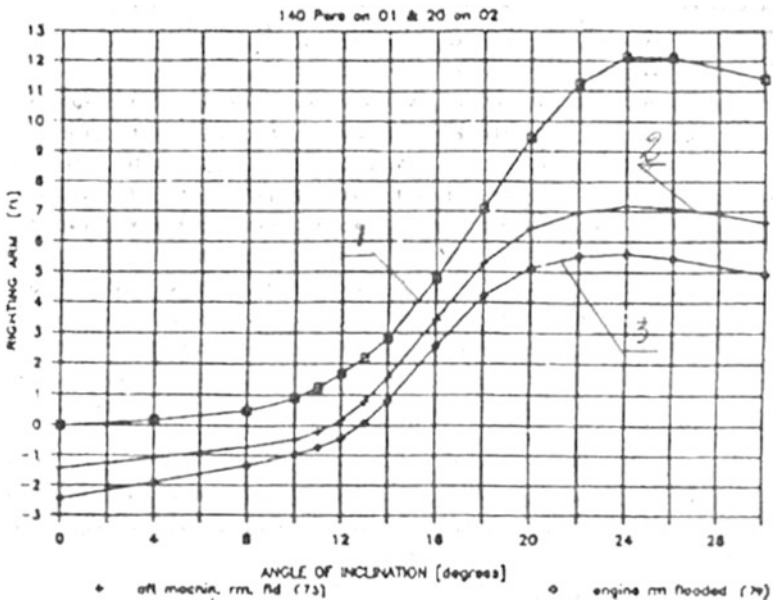

Fig. 9.19 Intact and damaged righting arm curve *Navatek 1*

9.4.2 Static Longitudinal Stability

The definition of SWATH longitudinal stability is "the ability of a SWATH to return to its initial upright state by restoring moments that cancel the external disturbance moment that caused the trimming of the ship.".

The calculation method for the longitudinal stability of a SWATH is the same as for a conventional catamaran (Chap. 2), and it has been found that the static longitudinal stability of a SWATH is lower than that of a conventional catamaran owing to its small waterplane area or areas on the struts. Therefore, it is important to calculate and assess the longitudinal stability, including some geometric variation, and to design carefully the lines of struts and hull above water to satisfy stability requirements.

9.4.3 Dynamic Longitudinal Stability

It is most important to consider dynamic longitudinal stability because normally a SWATH is unstable if no measure has been taken, such as adding fins at the stern of the demihulls, rather like a submarine. This is particularly the case for a two-strut SWATH, while a single-strut SWATH does have directional stability. Dynamic pitch stability is a challenge for both configurations and may demand controllable fins at the demihull bows also to dampen long period motions from ocean swell.

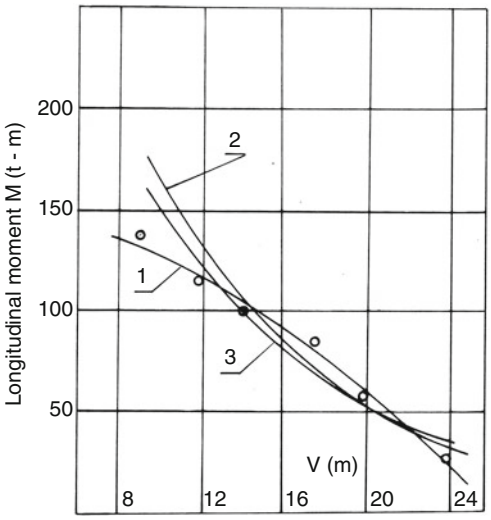

Fig. 9.20 Fluid dynamic trimming moment (bow down) and stabilizing moment of fins of SWATH model M8502

Since the submerged hull shape of a SWATH is cylindrical, an unstable trimming moment (bow down) with respect to the square of speed, and so-called Munk moment will act on a SWATH. Therefore, it is necessary to install a pair of fins at the stern to provide a stabilizing moment, just as that on both submarines and torpedoes.

Figure 9.20 shows the bow down fluid dynamic moment (line 1) of a SWATH model [10] at various speeds with 2° of bow down trimming angle; this must be balanced by restoring moments caused by fins, either variant 3 (line 2) or variant 7 (line 3).

In addition, a SWATH is dynamically unstable in longitudinal motion at speed if there are no fins to control pitch and yaw owing to the low damping moment from its special underwater hull lines and the interaction of the ship's struts. Therefore, it is necessary to install both horizontal and vertical fins to enhance the longitudinal damping moments.

Stable longitudinal motion can be obtained for a SWATH with proper fins mounted, even without automatic control systems.

The design idea for a stable SWATH is therefore as follows. If the longitudinal motion of a SWATH equipped with stabilizing fins is stable, then the characteristic root of the motion equation should be negative or at least have a negative real part. This characteristic is related to the stabilizing fins; if the stabilizing fin design provides forces that satisfy the aforementioned requirements of characteristic roots, then the design should be successful. If not then it will be necessary to make the fins larger, and recalibrate the root of the motion equation. A detailed explanation and associated computer program are available in [14].

9.4.3.1 Seakeeping

Seakeeping quality is a very important feature for SWATHs, so we will discuss it in more detail in what follows.

9.4.4 Theoretical Calculation

Because SWATH ships are extremely slender at the waterline, computer programs based on strip theory can provide sufficiently accurate results for design purpose, particularly for those with single struts, as outlined in Chaps. 4, 5, and 6 introducing the theoretical calculation of the resistance and seakeeping quality of catamarans.

9.4.5 Motion Natural Frequency

At first, one has to determine the area of the waterplane. The waterplane area is a double-edged sword, influencing the seakeeping quality and stability, particularly longitudinal stability, affecting ship safety. A tradeoff design approach needs to be used, and decisions will be made following detailed calculations for both stability (including static and dynamic transverse and longitudinal stability) and seaworthiness.

To avoid the resonance of ship natural frequency motion with wave encounter frequency, the natural periods of a SWATH have to be significantly larger than the encounter wave period. This is not difficult for SWATH to achieve, as demonstrated in existing ships, illustrated by Table 9.5.

It can be seen that the natural periods of a SWATH are far larger than those of sea waves, in which ships operate in accordance with their size. Therefore the ratio of the

Table 9.5 Natural periods of some SWATHs

Name	*Kaimalino*	*Marine Ace*	*Seagull*	*Kotozaki*	*Customs 201*	*FDC 400*	*Aegean Queen*
Country	USA	Japan	Japan	Japan	China	UK	Greece
Lbp, m	27	11.0	31.5	25.0	31.0	36.4	50
BOA, m	14	6.5	17.1	12.5	13.3	13.0	31.7
Type of strut	Twin	Single	Single	Single	Twin	Single	Single
Displacement, t	217	18.4	343	236	228	180	1050
Natural period heave, s	12	5.5	6.2	5.8	n/a	5.5	8.5
Pitch	9.5	4.8	9.5	8.9	8.1	5.5	14.7
Roll	13	11.2	10.9	10.7	10.3	8.0	8.8
Speed, knots	25	17.3	27.1	20.5	17.5		30

encounter frequency of a SWATH compared with its response natural frequency, particularly in head seas and at high speed, i.e. the tuning factor $\Lambda = \omega_e/\omega_n \gg 1$, where ω_e represents the frequency of wave encounter and ω_n the natural period of motion.

In this case, the ship will be operated in supercritical mode and under so-called platforming. The motion amplitude will be decreased, and vertical acceleration will be decreased significantly in inverse square proportion to period with acceleration, as shown in Eq. (5.21), that is, $\bar{A}_m = \dfrac{A_m}{g} = \dfrac{1}{T^2} \cdot \dfrac{2\pi^2}{g} B_p \cdot \theta_m$, which is a critical factor that influences passenger seasickness. It should be noted, nevertheless, that unless significant damping is available from appendages such as horizontal and vertical fins, the effect of low period water particle oscillations from swells will generate low-frequency heave and pitch motions, which may also manifest as low-frequency corkscrew motion in oblique seas. Careful attention to damping is therefore required by the designer.

9.4.6 *Some Calculation and Experimental Results for SWATH*

Figure 9.21 shows the calculation results for a SWATH passenger-car ferry weighing 1050 t with a length of 51.15 m and speed of 30 knots, designed and tested by National Technical University of Athens, planned to operate in the Aegean Sea [15].

Figure 9.21a, b shows the heave and pitch motion coefficients versus the relative encounter frequency, respectively. Note that the motion coefficients at all ranges of frequency are small in the case of ships with fins due to the large damping coefficient contributed by the fin of a ship at high speed.

However, at zero speed the situation is quite different. Figure 9.21c, d shows the heave and pitch motion coefficients versus relative encounter wave, respectively. From the figures it is seen that there is a peak response of motion around 1.0–2.0 of the relative encounter frequency, $\omega_e \sqrt{\frac{L}{g}}$. Therefore, the critical frequency will be at 0.442–0.884 and the period at 14.2–7.1 s. This is far larger than the period of most waves in the Aegean Sea.

Figure 9.22a shows the response amplitude operators (RAOs) of the SWATH *Navatek 1* [1] in bow quartering seas and for various speeds. The roll motion has a resonance for the loading condition shown in the vicinity of 16 s; however, because damping increases in proportion to the square of the motion, the response is much less for larger roll angles. In addition, it is seldom that long waves at a 16-s wave period are encountered in seas appropriate for operation of this size ship.

Figure 9.22b shows the vertical acceleration at the bow of the *Navatek 1* due to a combination of heave and pitch. Note that there is a response peak at zero speed. Figure 9.22c depicts the horizontal acceleration RAO at the bow, containing the

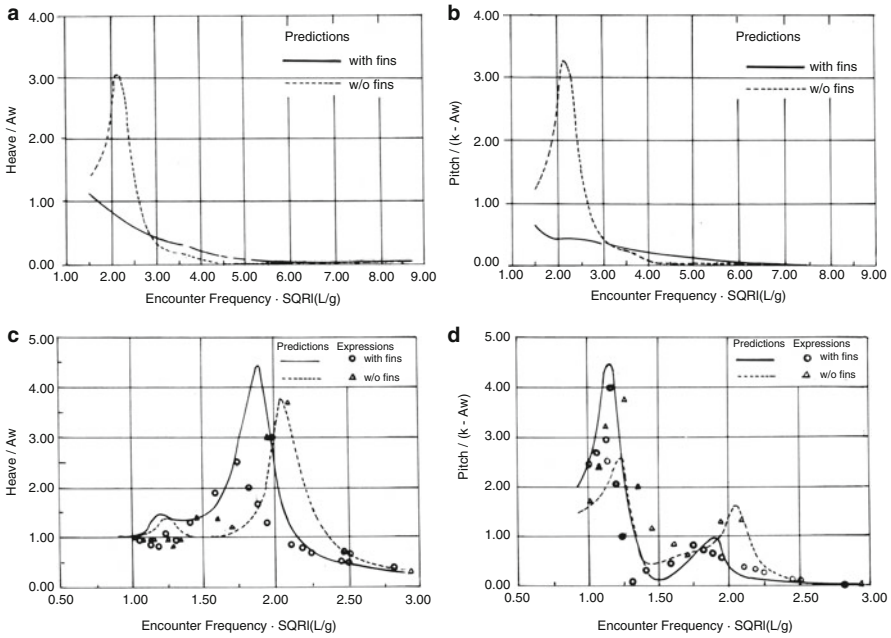

Fig. 9.21 (**a**) Heave motion coefficient for SWATH-NTUA 1; (**b**) pitch motion coefficient for SWATH-NTUA 1; (**c**) heave motion coefficient, zero speed; (**d**) pitch coefficient, zero speed

contribution from sway, roll, and yaw. These accelerations are even lower than the vertical ones, but they are also important for the ship because the comfort of walking around is greatly enhanced when the horizontal acceleration is kept lower.

Figure 9.23a shows a comparison of the energy spectrum of the heave and pitch motion on the SWATH *Seagull* 2 [7] with automatic ride control off and on, respectively. Note that the motion spectrum of the ship is reduced significantly with the automatic system on. This is why an automatic system would be mounted on modern SWATHs, despite its high cost.

9.4.7 Seasickness Frequency Onboard SWATH Vessels

The frequency of seasickness of passengers on SWATHs is a very important criterion for judging ships' performance and is believed to be more sensitive than all RAO and cumulative probabilities of exceedance of acceleration levels because it includes human factors such as response to engine vibration, noise, passenger cabin layout, and others. Table 9.6 summarizes the seasickness rates of various SWATHs based on tests carried out.

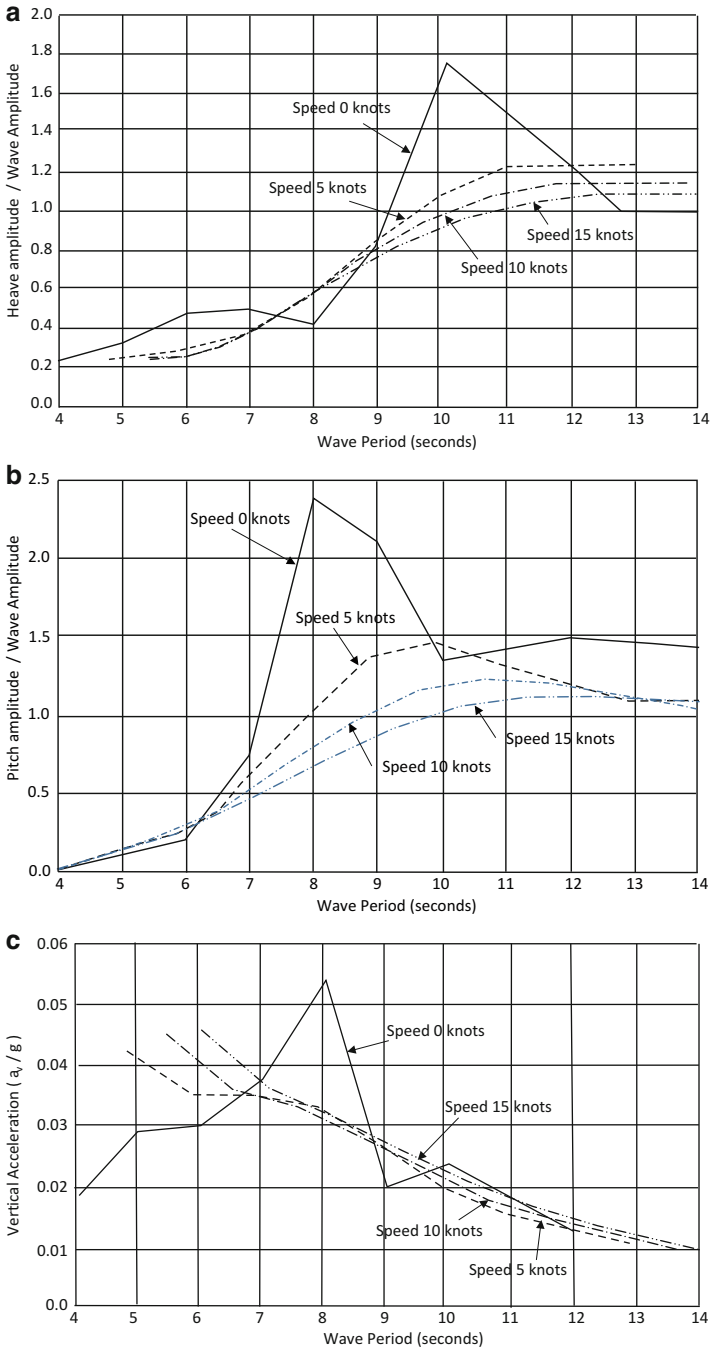

Fig. 9.22 (**a**) Roll RAOs; (**b**) vertical acceleration; (**c**) horizontal acceleration

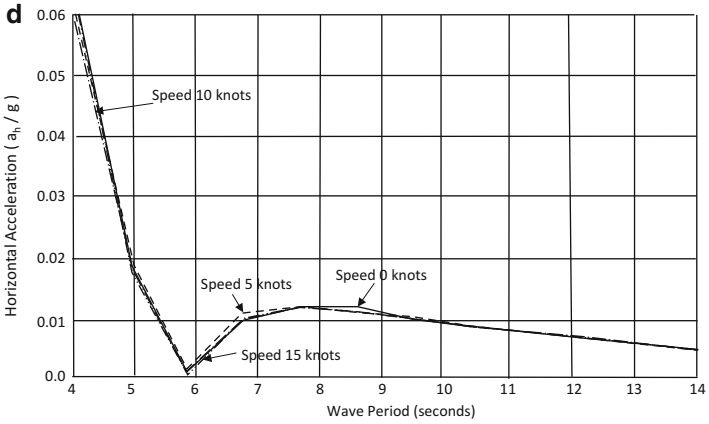

Fig. 9.22 (continued)

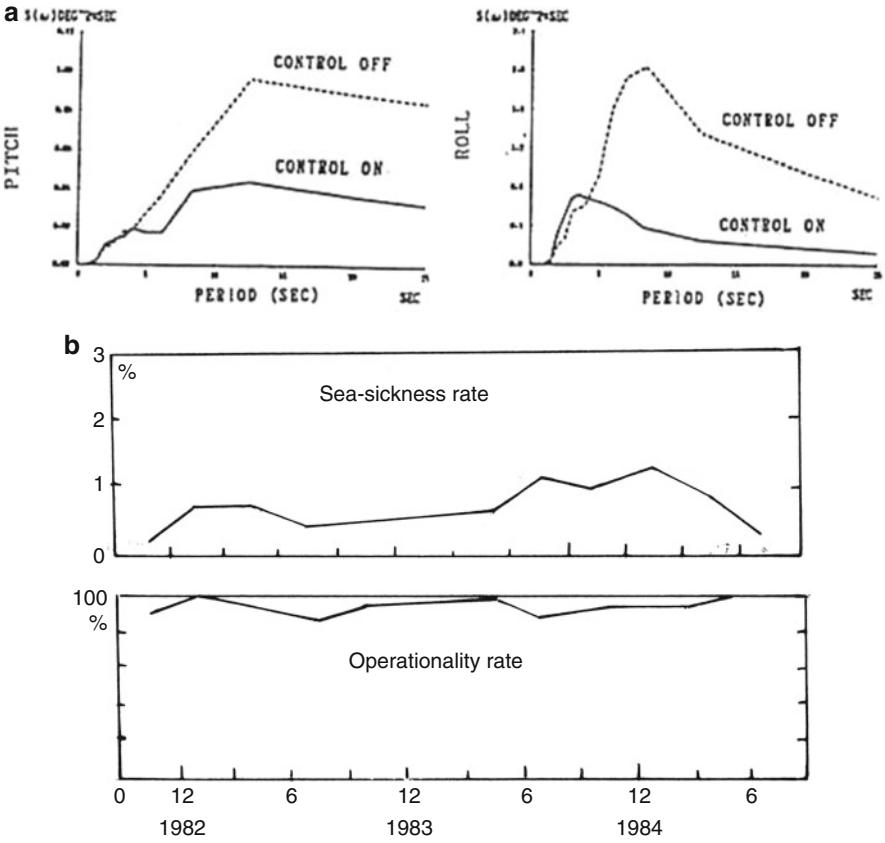

Fig. 9.23 (**a**) Comparison of energy spectrum of ship motions; (**b**) sea sickness and operability

Table 9.6 Seasickness rate of example SWATHs

Ship name	*Seagull* 2			*Navatek 1*	*Customs 201*
Country	Japan			USA	China
LOA, m	39.3			40.25	35
Displacement, t	360			365	228
Sea state	4	5	6	4–5	4
Seasickness rate, %	0.4	2.4	6	0.5 to 1	0.6

Figure 9.23b shows the seasickness and operability data for the passenger SWATH *Seagull* monitored during the 3-year period 1982–1984. Note that the seasickness rate throughout the year is low, and the operational reliability rate was over 90% year round.

9.4.8 *Influence of Fins on Seakeeping Quality [8]*

As mentioned earlier, since there is an unstable Munk moment acting on a SWATH at speed, in general, a pair of fins has to be mounted on the internal side of both lower hulls, either passive or with active control systems for improving longitudinal stability and seakeeping quality by increased damping and added mass coefficient.

Figure 9.24a shows the influence of fin location on the longitudinal motion of SWATHs, where:

1. Fins located at 35% L after midship section,
2. At midships,
3. At 26.5% L before midships,
4. Without fin.

The figure demonstrates that the influence of the location of fins on longitudinal motion is small.

Figure 9.24b shows the influence of fin size on the longitudinal motion of SWATHs, where aspect ratio (AR = 1.2) and location of fins (at 25.66 m after midships) are constant, but the fins' projected area changes as follows:

Curve	1	2	3	4	5	6
Area of fins, m^2	1.2 × 24	1.0 × 24	0.8 × 24	0.6 × 24	0.4 × 24	0

It can be seen in Fig. 9.24b that the influence of fin area on longitudinal motion is significant.

Figure 9.24c shows the influence of the joint action of both bow/stern fins on the longitudinal motion of a SWATH, where

1. Without fin,
2. With both bow and stern fins,

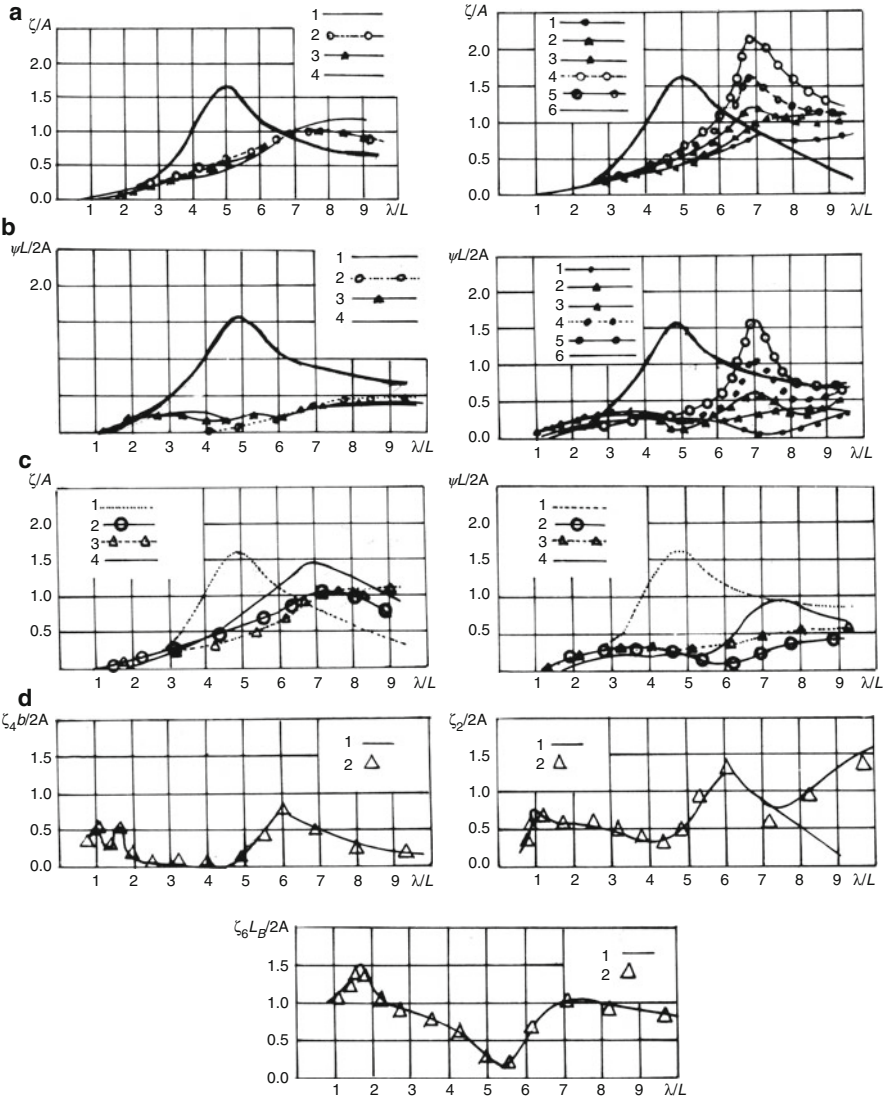

Fig. 9.24 Influence of fins and location on longitudinal and transverse motion, (**a**–**d**)

3. With stern fin only,
4. With bow fin only.

It is seen that the influence of fins mounted at both the bow and stern is greatest; meanwhile, since the stern fin size has to be greater than that of bow fins due to the requirements of longitudinal stability, the function for improving seakeeping quality for stern fins is greater than that for bow fins.

Figure 9.24d shows the influence of fins on the transverse motion of SWATHs, where

1. Without fins,
2. With fins.

The influence of fins on the transverse motion of SWATHs is very slight.

9.4.8.1 Arrangement of Propulsion System

The traditional propulsion system arrangement is that the main engines are located in the cross structure and propellers located under the water, the power being transmitted via shafts and bevel gears (as Z drive), pairs of universal joints (inclination shafts), belt drive, and so forth (Table 9.2). The most common power transmission used is the Z drive type.

The power transmission train for an engine housed in the topside structure is significant, as is the initial cost and maintenance cost. The noise and vibration levels for the components of the power transmission can also be a challenge. Alternative power transmission types, meaning direct transmission, that is, main engines located in lower hulls, has been used in some SWATH projects. The following measures may be taken:

- Using high-speed diesels with narrower transverse dimensions;
- Designing the submerged hull and struts with a varying transverse section along the longitudinal direction and widening transverse size of struts to facilitate the installation, maintenance, and repair of the main engines (Figs. 9.25, 9.26, and 9.27);
- Using two engines driving one shaft and propeller so as to decrease the transverse size of the engine room (Fig. 9.25);
- Using an electric generator–motor driving system.

Figure 9.25a–c shows the arrangement of engines and changing section along the longitudinal direction as twin engines connected to one shaft system for direct power transmission of design project of SWATH named “Aegean Sea”.

Figure 9.26 shows the direct power transmission of the SWATH *Navatek 1*.

Reference [9] compares the positives and negatives of two SWATH projects in China with different power transmission and concluded that, based on the construction experience in China at that time, the direct power transmission design project would be better than a Z drive, as shown in following table.

From Table 9.7 it can be seen that the variant with direct power transmission is characterized by lower construction and maintenance costs, fine stability, and low operational risk, so it is more reliable, even at the cost of 1.5 knots in speed capacity.

Figure 9.27a, b shows the vessel GA for the two projects, and Fig. 9.27c shows the considerations for construction and repair with respect to the main engines of Darlian 2. It is shown that space for maintenance is available, and the main engines can be removed.

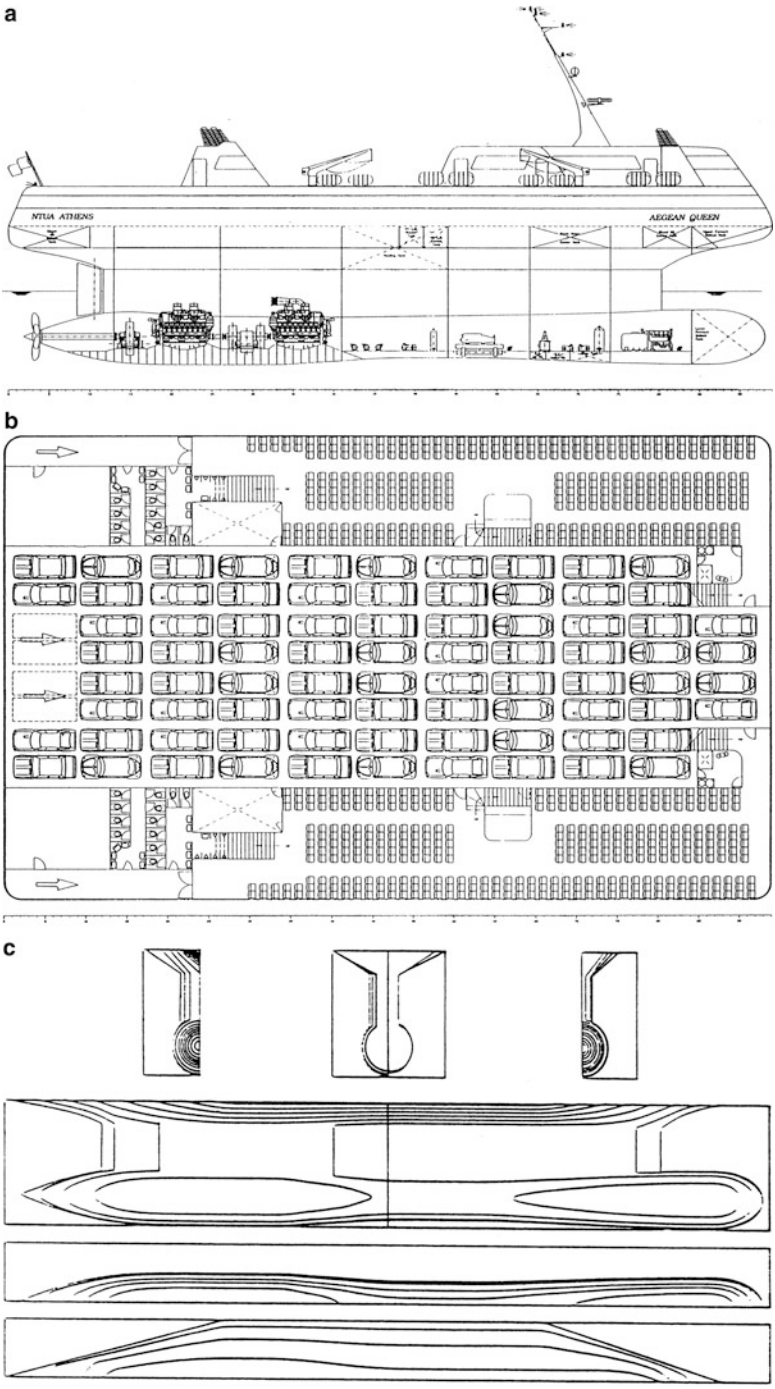

Fig. 9.25 (**a**) Profile of passenger/car ferry *Aegean Queen*; (**b**) car and passenger deck arrangement; (**c**) lines of *Aegean Queen*

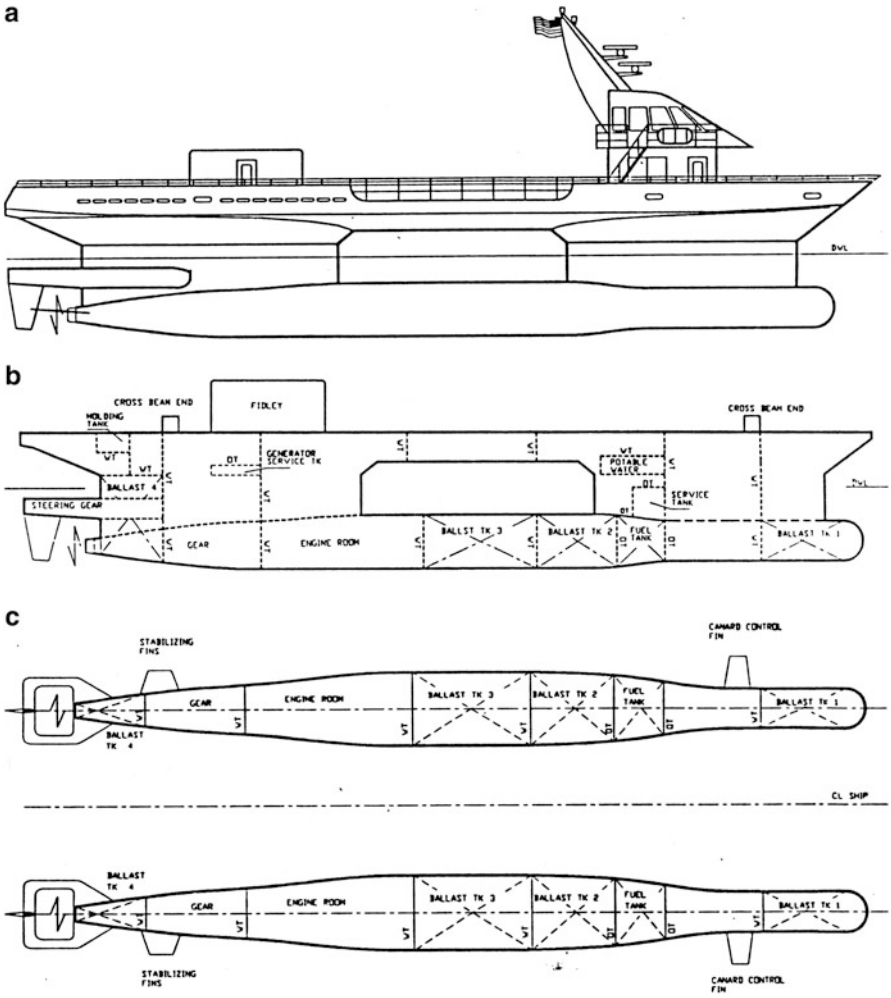

Fig. 9.26 (**a**) Profile; (**b**) compartmentation; and (**c**) lower hull of *Navatek 1*

To sum up, the following are the key challenges for SWATH designers:

- Optimization of ship form according to main performance of SWATH mentioned earlier;
- Options of fin area and location as well as their automatic systems, according to requirements for stability;
- Design of propulsion system (mainly dealing with the arrangement of propulsion system);
- Hull structures.

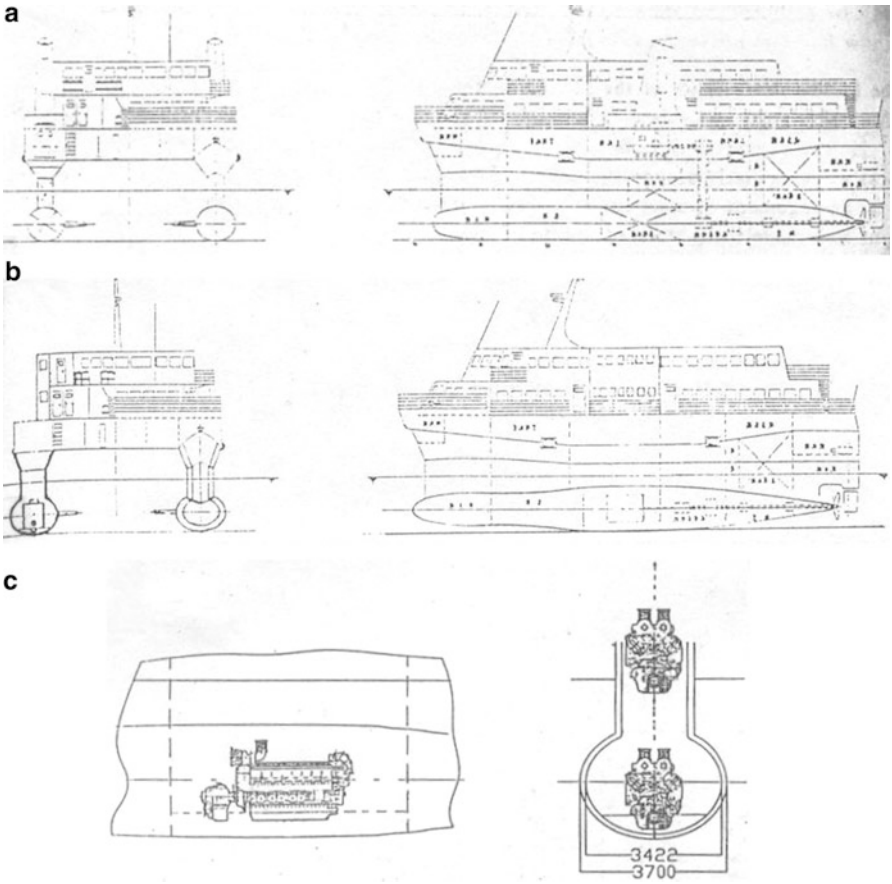

Fig. 9.27 (**a**) General arrangement of Darlian 1; (**b**) Darlian 2; (**c**) main engine room arrangement

9.4.8.2 Transverse Wave Load on Hull Structure

Considering the SWATH configuration, note that the structural stiffness of the lower and upper hulls is high due to the vessel's cylindrical body and trunk for both hulls. However, since the thickness of struts is rather small, the joints between both the upper and lower hulls and the struts are weak. Because the longitudinal moment of inertia of the lower hull structure is large, the Munk moment and wave load acting on the lower structure do not cause serious stress on the structures.

In the case of the SWATH's lateral motion, the Munk moment and wave load will act on the lower hulls and struts, leading to severe stress on the joints between the upper hull and struts. Therefore, the calculation of the transverse wave load and the dimensioning of a strengthening structure and has to be addressed in vessel design.

Table 9.7 Comparison of various performances and factors of SWATH between two design projects on arrangement of main engines

Design project	Darlian 1 (Fig. 9.26a)	Darlian 2 (Fig. 9.26b)
Power transmission	Z drive with two pairs of bevel gears	Direct
Displacement, t	383	383
Number of passengers	512	566
Lower hull length, m	31.6	32
Lower hull diameter, m	2.8 (horizontal)	3.71 (horizontal)
	2.2 (vertical)	2.91 (vertical)
Strut breadth, m	1,2	1.96
Speed, knots	18.8	17.3 (8% lower)
EPS, kW	2260	2841 (20.5 higher)
Total mechanical transmission efficiency	0.904	0.96
GMT (transverse), m	3.519	5.753
GML (longitudinal), m	7.589	8.58
TPC (ton/cm immersion)	0.657	0.829 (20.7% up)
Moment/cm trim	0.878	0.99 (11.3% up)
Moment/degree heel	23.5	38.4 (38.8% up)
Cost factor	1	0.91
Annual net income factor	1	1.16
Risk in operation	Medium	Lower
Operations/maintenance complexity	High	Easy

9.5 Wave Resistance from Calculation and Model Testing

A SWATH model was tested on a scale of 1:20 by MARIC. The full-scale principal dimensions of the real SWATH are given in Table 9.8, and the model is a typical example of a SWATH arrangement of hulls with submerged bodies and single struts. Each demihull is a combination of a body and a strut. The body has circular cross sections at the parallel middle part and with parabolic change at the stern. But at the bow, the cross section consists of a rectangle and two semicircles on its sides, called a waist drum form, and its area has parabolic change. The struts are cylinders that have parallel horizontal sections and a parabolic bow and stern. Thus, bodies of different diameter and prismatic coefficient and struts of different thickness could easily be combined for model testing.

Rong (2002) [16] calculated the wave resistance coefficient $\bar{C}_w$ of the tested model for $Fr_L = 0.152–0.607$ using the numerical calculation method presented in Chap. 4 and the program in Sect. 4.5. The combination of the body and strut of the SWATH is treated as a thin ship. Here strut length is considered the waterline length, approximately. The numbers of stations and waterlines were taken to be 24 and 12 (from 1 to 11 for the body and 11 to 12 for the strut), respectively.

Table 9.8 Leading particulars of full-scale SWATH

Item	Ship
Body length, m	58.000
Body maximum beam, m	7.200
Strut length/waterline length, m	53.000
Strut maximum beam, m	2.900
Draft, m	6.500
Total wetted area, m^2	1930.000
Demihull to centerplane spacing, m	20.600
Body length/beam ratio	8.060
Strut length/beam ratio	18.200
Draft/length ratio	0.123
Body spacing/beam ratio	2.860
Strut spacing/beam ratio	7.100

Unlike high-speed catamarans (HSCATs), most SWATHs operate in the medium-speed range, $Fr_L = 0.25$–0.38. In Sect. 8.7 it is shown that the Michell wave resistance could not produce satisfactory results in the low- and medium-speed ranges for general ships, even though the length/beam ratio was approximately 10.0. But in this case the struts of the SWATH created the main wave-making resistance. Moreover, their thickness was very thin and the length/beam ratio was very large, 18.20 in this example, which is much greater than 10.0 and very closely approximates the hypothesis of a "thin ship." Thus, we could have expected satisfactory results.

Figure 9.28 shows the results of the test and calculation. In this figure C_w means $\bar{C}_w$ in Eq. (8.7.2). The test only gives C_r at $Fr_L = 0.152$–0.369. The calculation curves predict the wave peaks and troughs of the curve at $Fr_L = 0.20$–0.38 correctly, which appear only a little early. However, the troughs of the test curve are too high, and this may be due to the creation of viscous effects. Thus, SWATH designers should stay away from $Fr_L = 0.30$ and approach $Fr_L = 0.27$ or 0.35 if possible.

9.6 Fast Displacement Catamarans

If the waterplane area is widened from the extreme configuration used for a pure SWATH, one arrives at a configuration that is less sensitive to payload variations while at the same time having minimized motions in a seaway. The configuration might be likened to a wave-piercing catamaran where the design waterline is above the lower hulls. This configuration has been called a fast displacement catamaran, as it operates exclusively in displacement mode rather than taking advantage of dynamic lift to some extent, as a wave-piercing craft will do.

The first fast displacement catamaran (FDC 400) was built by FBM Marine of the UK in 1989 [17]. The design objectives were to extend the capability of the catamaran concept to longer and more exposed sea routes, to reduce degradation

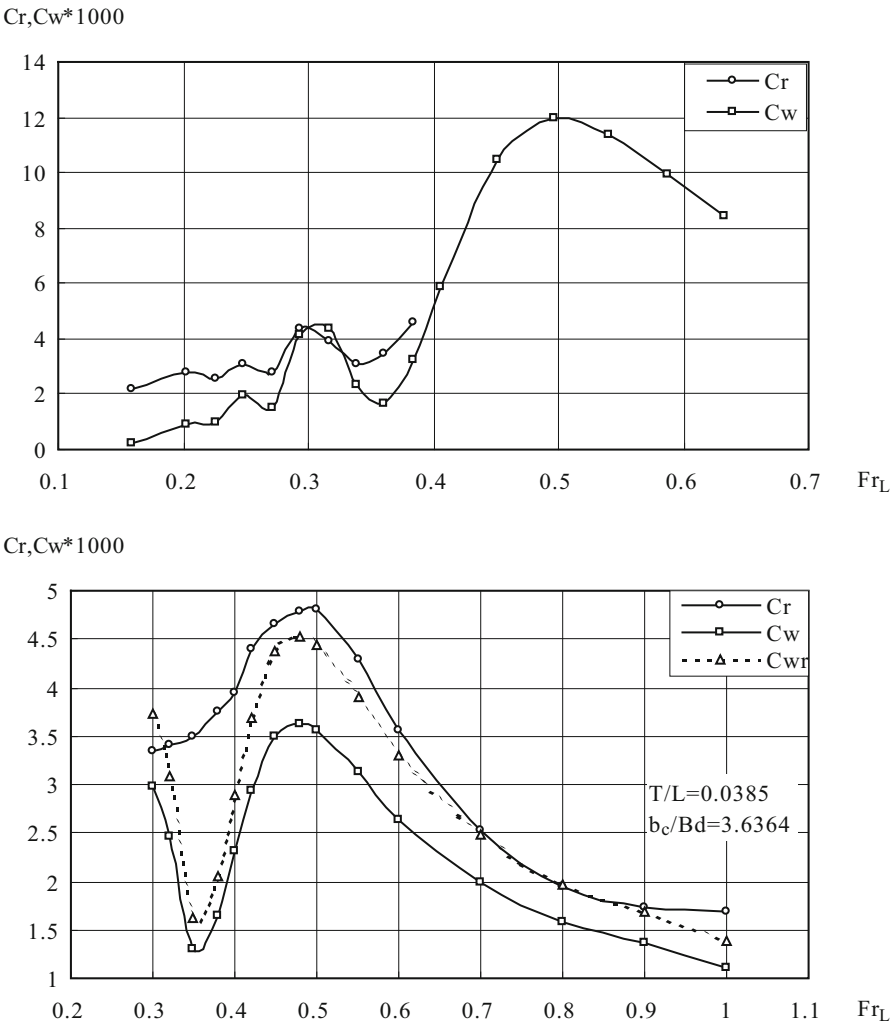

Fig. 9.28 Comparison of C_r with C_w for the SWATH

in waves and to significantly lower accelerations that could lead to passenger sickness and crew fatigue in open sea conditions. In short, the design objective was to improve seaworthiness with the aid of a so-called medium-waterplane-area concept, that is, the area of the waterplane represents a compromise between the conventional type of catamaran and that of a SWATH.

There are twin underwater hulls of a cylindrical type, a single strut (or, rather, a waterline area that is reduced as much as possible), and a catamaran-type superstructure (not a "carrier" type like early SWATH vessels) on the ship, as shown in Figs. 9.29 and 9.30. The principal dimensions are shown in Table 9.2.

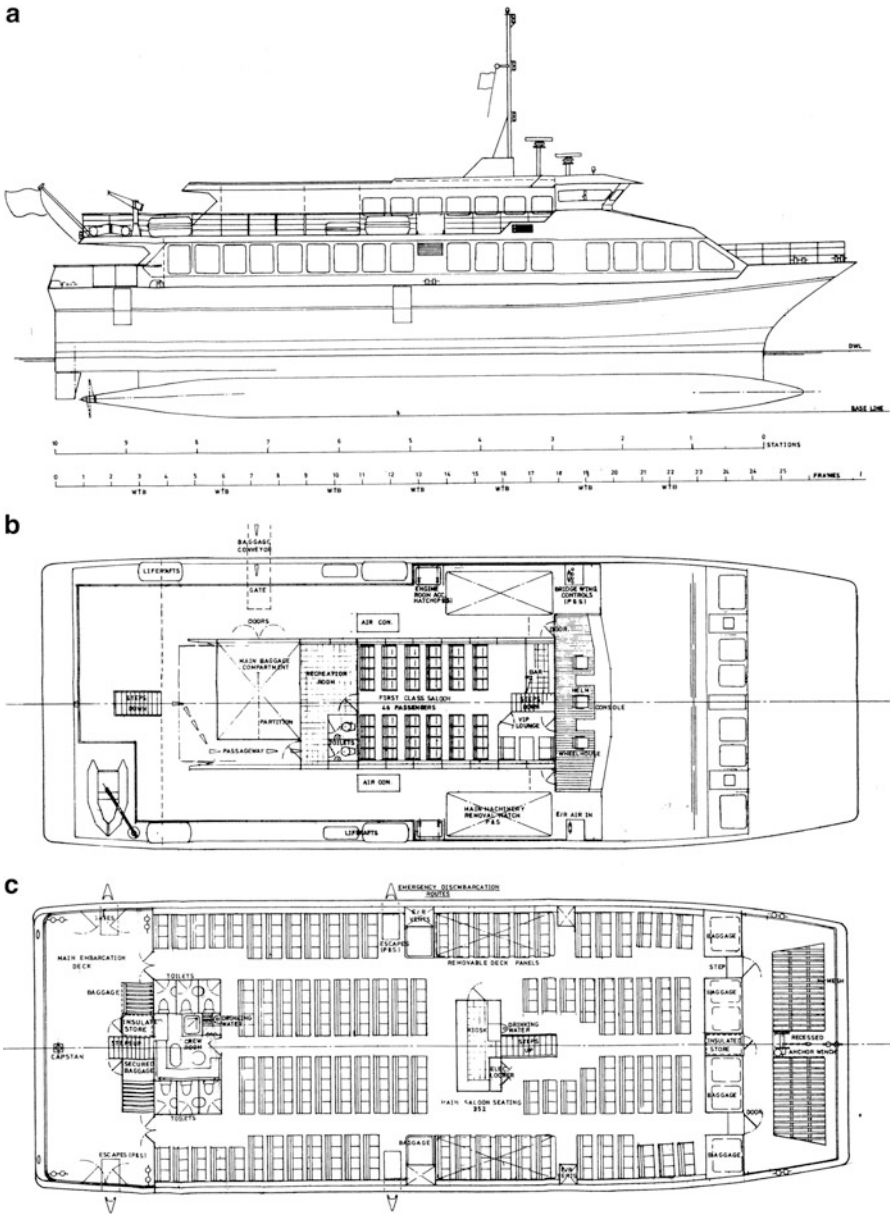

Fig. 9.29 (**a**) Profile of FDC 400; (**b**) deck plans of FDC 400

Fig. 9.30 FBM FDC400 *Patria* at speed

The design features of the FDC are as follows:

- Compared with the catamaran, the ship has a decreased waterplane to improve seakeeping quality and slices through waves so as to reduce speed loss in waves.
- Compared with the SWATH, the ship has improved inherent longitudinal stability due to increased buoyancy of the waterplane area. Without the use of bow fins or control system, and only with aft fins to vary vessel trim, operation need only be manually controlled from the wheelhouse [14]. For these reasons, the cost and operation of a FDC is lower than those of a SWATH.

- As shown in Table 9.5, the natural motion periods of the FDC 400 are also between those of the SWATH and conventional catamaran.
- Comparison of vertical acceleration and speed degradation in waves with other high-speed craft, such as planing monohull vessels, HSCATs, and surface effect ships (Fig. 9.31), has shown that the seakeeping quality of the FDC exceeds that of those alternatives.
- The stern form of the FDC is similar to that of a SWATH, so the craft has no underwater appendages and can have larger propeller diameters so as to enhance propulsion efficiency compared with conventional propeller-driven catamarans. This may not be a significant advantage if one considers a catamaran with waterjet propulsion, but overall the efficiency may be comparable, which is an achievement in itself.

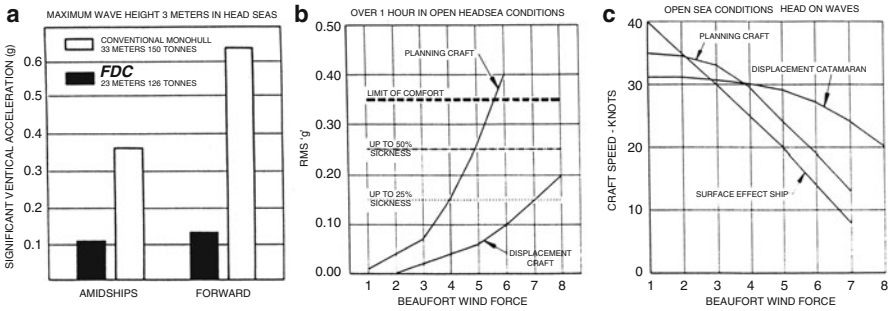

Fig. 9.31 (**a**) Comparison of vertical acceleration of FDC 400 with monohull craft with similar size; (**b**) comparison of vertical acceleration in RMS g; (**c**) speed degradation in regular waves

In 2007 Pentland Ferries in Scotland contracted with FBM to design and build a catamaran ferry for a route across the Pentland Firth to Orkney. FBM, together with Sea Transport Solutions in Australia, designed a 70-m catamaran of the FDC type that began service after delivery voyage from FBM's shipyard in Cebu, Philippines, in June 2009. This vessel has a relatively small diameter cylindrical lower hull shape and highly flared hulls above water, as shown in Fig. 9.32b. This enables the main machinery to be installed within the demihulls. The hulls and main connecting structure are steel, and the superstructure is in aluminum. Key statistics for the vessel are LOA 70 m, BOA 20 m, draft 2.2 m, 350 passengers, and 58 cars or 32 cars and 9 trucks. The ferry operates at a service speed of 15 knots, and its maximum speed is 19.7 knots.

In April 2017, Pentland Ferries ordered a new ferry to replace the *Pentalina*, designed by BMTNGL, somewhat larger, at 84.5 m LOA and had a capacity for 98 cars and 430 passengers, with less pronounced semi-SWATH characteristics, closer to a slower-speed wave-piercing form with a fine forward half of the hull and parallel after body, having rather less hull flare above water. This vessel also has a steel hull and aluminum superstructure. It is constructed in Vietnam at the Vung Tau shipyard and will begin service in 2019 with a slightly higher service speed of 16 knots.

BMT prepared a 37-m full-SWATH design for 181 passengers together with Damen in Holland in 2004 for passenger service in Zeeland between Vlissingen and Breskens at a service speed of 14.5 knots. Two vessels have been constructed, the *Prins Willem Alexander* and the *Prinses Maxima*. The vessel and GA are shown in Fig. 9.32a, b.

While the MV *Pentalina* and the full-SWATH Zeeland ferries are below a speed that one might consider fast, where 25 knots is generally considered the dividing line, it may be argued that in fact these should be considered fast since they are designed to cope with rather exposed SSs and so, using the semi-SWATH or full-SWATH approach, are able to maintain service speed in heavy weather with minimized motion and acceleration. The Patria demonstrated that it is practical to

Fig. 9.32 FBM *Pentalina* RoRo ferry: (**a**) the vessel; (**b**) inset steel hull construction showing above water cross section

design a semi-SWATH for 30-knot service. In the case of the Pentland and Zeeland services the economical equation for the operators and passengers has led to lower-speed ferries. The multihull form then supplied the desired payload and service areas.

A similar approach of balancing service speed and motion performance has been developed through market feedback for small patrol vessels and offshore crew transfer for wind farm maintenance.

9.7 Patrol Vessels and Wind Farm Service Craft

Since 2000, the SWATH form has been used by a number of designers and shipyards for utility vessels requiring a rapid deployment to a location or a patrol area followed by the ability to loiter or hold position with minimized vessel motion for crew comfort or personnel transfer. Typical of this type are wind farm service vessels and offshore survey vessels. The key data for a selection of these are summarized in Table 9.9, and examples are shown in Figs. 9.33, 9.34, 9.35, 9.36, and 9.37.

Abeking & Rasmussen has designed and built a significant number of SWATH vessels for paramilitary duties in the Baltic and pilot vessels for ports in Germany, Holland, and Belgium. The company's initial vessel was the *Natalia Bekker* for offshore transfer service, and it can be seen from Table 9.9 that this vessel had diesel electric propulsion with fixed-pitch propellers. On later vessels it moved to diesel propulsion and Servogear CP propellers for control. These vessels do not have active fins or other motion damping.

Danish Yachts has also constructed a series of offshore crew transfer SWATH vessels for service speed in the 18–20 knot range for Odfjell Wind Service. Danish Yachts builds vessels in carbon fiber reinforced polymer that allows the geometry of the lower hulls to be more complex. The lower hulls have a cross section with an upper surface that is almost flat so that the response to waves can provide more motion cancellation. Odfjell is increasing its fleet with a further four 32-m SWATH vessels with higher service speed and is moving to aluminum construction in 2018. Both Danish Yachts and A&R use a twin-strut SWATH geometry.

Adhoc Designs and BMTNGL, on the other hand, have chosen a single-strut design for their vessels, which are aimed at a higher maximum speed (close to 28 knots) and service speed around 24 knots. Both of these vessels have active motion damping installed. In the case of Adhoc's Typhoon (two vessels are operated by MCS in Scotland), the vessel is fitted with four fins following normal practice for SWATHs. BMTNGL has installed forward T foils under the forefoot of each demihull and interrupters at the stern, having in mind high-speed service at lower draft, while the bow motion damping at the deeper draft is effective with the T foils at slow and zero speeds. Bow T foils or the equivalent can assist in damping for personnel transfer, and for larger vessels a hydraulic gangway system can be helpful (see Chap. 13 for more details).

Because wind farms are constructed at more remote and exposed locations, the design challenges will continue to increase. On the one hand, economical fast transfer is important to get personnel to the workplace efficiently. Once on site, though, the same vessel must be able to interface with the offshore structure at zero speed and, if possible, with almost zero bow heave motion.

This drives the design toward a hull shape rather than circular lower hulls so the vessel can be de-ballasted to ride higher and faster as weather permits for the transit, ballasting down once approaching a site to operate like a semi-submersible drill rig while on location.

Table 9.9 Sample SWATH patrol vessels and wind farm service craft

Patrol and service vessels	A&R	A&R	A&R	Danish Yachts	Adhoc	BMT Nigel Gee
Design/class				SWATH	Typhoon	XSS
Name	Natalia Bekker	Skrunda	Jakob Prei	SWATH 6 Lina	SWATH 2	Cymyran Bay
Operator	AG Ems Maritime Offshore	Latvian Navy	Estonian Waterway Authority	Odfjell FOB	MCS	Turbine Transfers
Service	Port service	Patrol, Latvia	Survey, Estonia	Wind Service	Wind Service	Wind Service
Year	2010	2011	2012	2011	2016	2013
Type, single or two strut	2	2	2	2	1	1
Passengers	12	–	12 max	12	12	12
Crew	3	8–10	3	3	3	5
Speed, max. knots (cruise)	18	21	20 (12) survey	20 (18)	24 (22)	29 (25)
Displacement, t	c125	c125	c125	c120	95	n/a
LOA, m (L_{WL})	26.4	25.7	26.4	24.7 (23.7)	26.7 (23.5)	28.1
Vessel beam, m	13	13.5	13	10.6	9.8	8.5
Vessel draft, m (cat mode)	2.7	2.7	2.7	2.5 (1.8)	2.06	1.85
Lower hull length, m	24	24	24	24	24	28
Lower hull breadth, m	2.5	2.5	2.5	2.6	1.5	2.2
Strut breadth, m	1.5	1.5	1.5	1.25	0.8	1.4
EPS, kW	2×900 MTU 12 V2000	2×809 MAN D2842	2×809 MAN D4892	2×900	2×1029 MAN	2×1076 MTU

(continued)

Table 9.9 (continued)

Patrol and service vessels	A&R	A&R	A&R	Danish Yachts	Adhoc	BMT Nigel Gee
Engine location	Upper hull	Lower hull	Lower hull	Lower hull	Upper hull forward	Upper hull
Power transmission	2× 710 kW electric motor	Shaft drive	Shaft drive	Shaft drive and gearbox	Canted drive to ZF3050A gearbox	Canted drive to ZF3050A gearbox
Propulsion FPP fixed-pitch propeller CPP variable-pitch prop	FPP	Servogear CPP	Servogear CPP	Servogear CPP	Propellers	MJP550 waterjets
Hull material	Al	Al	Al	CFRP	Al	Al
Control surfaces	–	–	–	–	4 fins	T foils NAIAD
Notes	Lower hull variable diameter	5 sister vessels Waves up to 3.5 m	Lower hull variable diameter	6 off 24 m vessels at FOB 4 off 32 m in build	MCS SWATH 1 and 2 bow thrusters	Turbine Transfers Rhosneigr Bay also

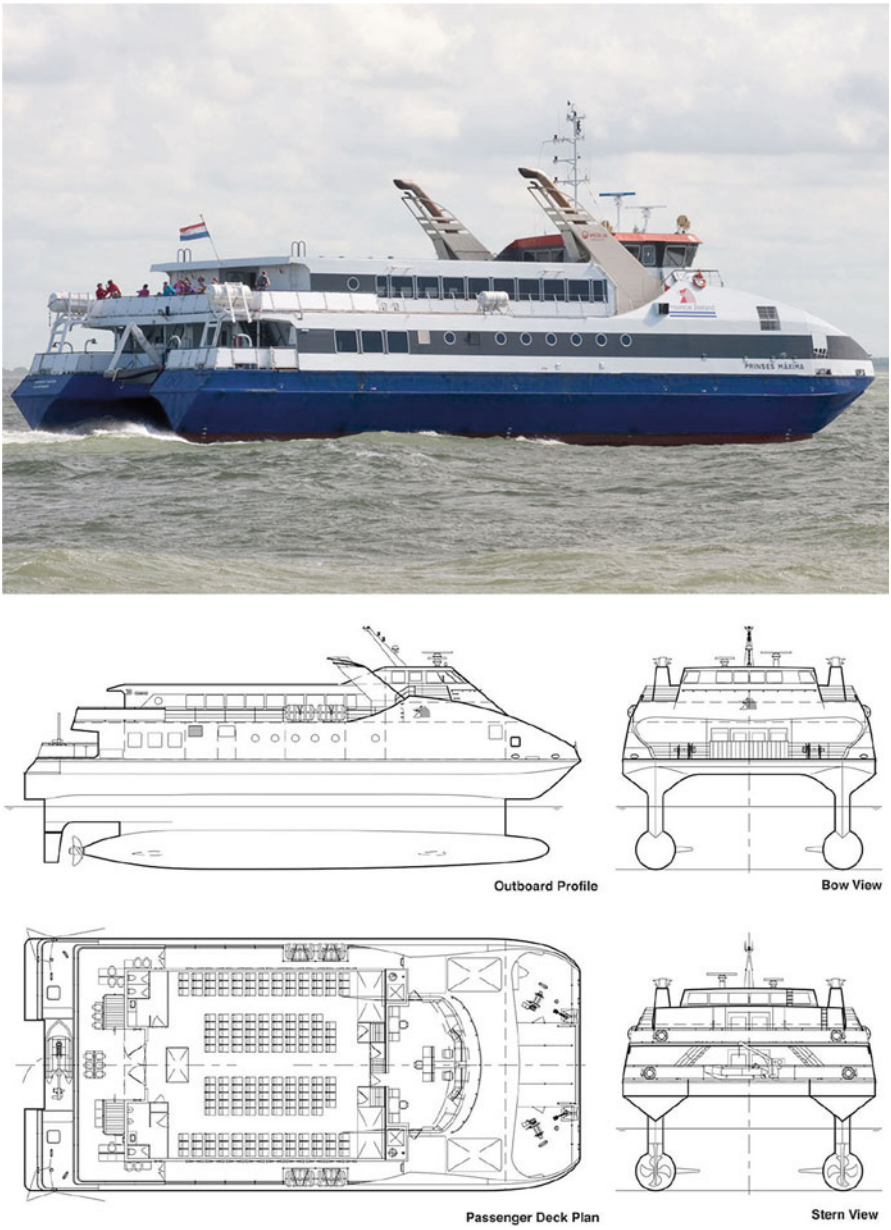

Fig. 9.33 BMTNGL and Damen Zeeland SWATH ferry *Prinses Maxima*: (**a**) the vessel; (**b**) general arrangement

Fig. 9.34 Abeking & Rasmussen SWATH oceanographic survey vessel Jakob Prei

Fig. 9.35 Adhoc Marine Typhoon Class wind farm service vessel SWATH-1 operated by MCS

It may be noted that where vessels are used to support the construction phase of a wind farm, they may be required to remain offshore for long periods to provide tender services for crew transfer between the multiple turbine locations rather than simply providing a ferry service from shore. This duty has a further consequence for

Fig. 9.36 Danish Yachts 27-m wind farm service SWATH vessel Lina operated by Odfjell

Fig. 9.37 BMTNGL wind farm service vessel *Cymyran Bay* operated by Turbine Transfers

vessel specification, including accommodation, equipment and consumables storage, and the nature of the dynamic positioning system installed, in addition to the preference for twin struts at each demihull to reduce the directionality of response while on station.

The Odfjell 24-m vessels have an offshore endurance of up to 7 days, and while they have a transit speed of 20 knots, the larger 32-m vessels can transit at between 30 and 34 knots and have an endurance of up to 14 days, which is a typical offshore work shift in Europe.

The air cushion catamaran has also entered this market, with vessels designed and built by UMOE Mandal; see Chap. 10 for more on this topic.

References

1. Seidl LH et al (1993) Design and operational experience of the SWATH ship Navatek 1. SNAME Marine Technology vol 30
2. Bliault A, Yun L (2010) High performance marine vessels. Springer, New York. ISBN 978-1-4614-0868-0
3. Dubrovski V, Lyakhovitsky AA (2001) Multi-hull ships. Backbone Publishing Company, USA ISBN 978-0964431126, 495 p
4. SWATH ships, Kennell C Technical and research bulletin 7–5 prepared for panel SD-5 (Advanced surface ships and craft). SNAME, USA p 1992
5. Introduction to a coastal SWATH, proceedings of 4th International Boat Show and Conference on HPMV, April, 1999, Shanghai, China
6. Ming Z et al (2001) High performance marine vehicles in 21st century. Defense Industrial Press of China, Beijing (in Chinese)
7. Komoto M et al (1992) High speed passenger craft developed and constructed by Mitsui, Proceedings of 2nd international conference on high performance marine vehicles (HPMV'92CHINA), Shen Zhen, China
8. Lian-En Z et al (2001) Hydrodynamic principle and design of high performance marine vehicles. Press of Harbin Engineering University, China (in Chinese)
9. Bo LH, Yuan DL (1992) A crucial technique in SWATH design—arrangement research of the propulsion system, Proceedings of HPMV'92 CHINA
10. Wong TL et al (1988) Problems concerned with the performance design of SWATH, ship engineering, June, 1988, (in Chinese)
11. Reed A et al (1997) Seakeeping and structural performance of the A-Frame SWATH vessel sea shadow. SNAME Trans 105
12. Cao YQ (1984) Development of SWATH in home and abroad, 2nd domestic conference on HPMV, June, 1984, China, (in Chinese)
13. Salvesen N et al (1985) Hydro-numeric design of SWATH ships. Trans SNAME 93
14. Huang DL, Li XQ (1987) The motion and its control of SWATH ships in longitudinal plane. J Dalian Inst Technol 4 (in Chinese)
15. Papanikolaou A et al (1991) Preliminary design of a high-Speed SWATH passenger/car ferry. Mar Technol 28(3):129–141
16. Rong H-Z (2002) Application of linearized theory of wave resistance to HACAT, SWATH and WPC (in Chinese), Research report, MARIC
17. First FBM Marine FDC 400 on Trials (1989) Fast Ferry International, Dec, 1989

Chapter 10
Other High-Speed Multihull Craft

10.1 Introduction

In previous chapters we introduced catamarans of a displacement or semiplaning type with some information on resistance for the planing hull form as used mainly by wave piercers. We explained that, owing to the catamaran demihull's slender length/beam ratio aimed at reducing wave-making drag, such craft would not operate in the planing region as the Froude number Fr_L remains below around 0.75, even for high service speed (Table 1.1), so the hydrodynamic lift proportion would not be more than 20% of displacement, even if a hard chine demihull form is used. In this chapter we will discuss other design alternatives for high-speed vessels, including those targeted at speeds above $Fr_L = 1.0$.

The approach of using slenderness to reduce wave making is helpful for larger craft to minimize powering, but it does have its down side regarding seakeeping for catamarans, as we saw in earlier chapters. The small-waterplane-area twin-hull (SWATH) vessel with multiple struts can reduce oblique sea motions for slower-speed craft in the range Fr_L 0.2–0.5, but another configuration, such as the semi-SWATH, wave piercer, or the trimaran or possibly its cousin the stabilized slender monohull, is needed for more flexible high-speed performance delivery (Fr_L 0.5 up to about 1.0) in exposed environments.

Wave-piercing craft, discussed in Chap. 8, generally operate in the semiplaning regime of Fr_L 0.5–0.9 and have V-shaped lower hulls, giving hydrodynamic lift (e.g., Fig. 8.1). Their bow shape is formed so as to give a platforming ride through waves while utilizing hydrodynamic support as much as possible at their operating Fr_L regime. Having a classic catamaran form does nevertheless have consequences for performance in exposed environments. The wave piercer works well at very large size, but what about smaller vessels for high speed and Fr_L? Can semiplaning or planing vessels or other hybrids using aerodynamic or hydrodynamic support and stabilization achieve high-quality seakeeping performance for speeds in the range Fr_L 1–3?

L. Yun et al., *High Speed Catamarans and Multihulls*,
https://doi.org/10.1007/978-1-4939-7891-5_10

We discuss a number of configurations after looking at two extremes for the basic catamaran form targeting higher service speeds – geometries suitable for very fast planing catamarans and extremely fine hull form catamarans working at lower Fr_L that seek to minimize wave drag and wake.

We will continue with the alternative geometries such as the trimaran and pentamaran and then go back to look again at alternative hydrodynamic and aerostatic supports that have been tried out to minimize powering for smaller planing catamarans at higher speeds, including the following types of forms:

- Triple planing hull (TPH);
- Hydrofoil-assisted planing catamaran (HPC);
- Air-cavity catamaran (ACCAT)

We will close this chapter with a discussion on how to navigate between these options to assess whether they can improve upon a basic catamaran configuration where that needs to remain the basis. Included in this is further consideration of the SWATH and wave-piercing forms introduced in some detail in the last two chapters.

Starting with the catamaran variants we consider demihulls with two different extremes of geometry:

- Demihulls with higher b/L and a low static load coefficient $C_\Delta = \Delta/b^3$, where Δ is the weight supported by each demihull. As the static load coefficient is small and the form is less slender, the craft may be supported by hydrodynamic lift if the lower demihull is formed with planing surfaces. This form is generally called the planing catamaran (PCAT) or TPH;
- Demihulls with extremely slender form, that is, high $L/\Delta^{1/3}$, so as to decrease as much as possible the wave-making resistance and disturbance force from the demihulls, both in calm water and in waves. This form is generally referred to as a super slender twin-hull (SSTH) craft.

10.2 Planing Catamaran and Tunnel Planing Catamaran

Starting with the background, the key characteristics of planing monohull craft are as follows:

- Low static load coefficient, $C_\Delta = \Delta/B^3$, where B is the vessel beam in this instance:
- Low resistance/vessel weight ratio at high Fr_L, as a result of being supported by increasing hydrodynamic lift on the hull lower surfaces as speed increases, decreasing the hull wetted area and friction resistance;
- Greater compactness than a very slender displacement vessel since the L/B ratio does not need to be high;
- High maneuverability assisted by its low L/B.

However, the design challenges for these vessels are as follows:

- High impact loads acting on planing surface during operation in waves;
- High vertical acceleration from heave and pitch motions and high wave encounter frequency.

A planing monohull at speed in a seaway will ride through the upper parts of waves. In the extreme, a racing craft can jump from crest to crest with the hull out of the water as it passes over the trough. While most craft do not ride so high, the effect of each passing wave crest is to apply a repeated rapid pressure profile to the hull underside. Depending on the wave length and steepness, the pressure profile may be sharp enough to cause shock loads on the hull surface (referred to as slamming). The overall pressure profile lifting and releasing the hull from the wave crest causes overall acceleration, while shock loads, when they occur, can increase the downward deceleration of the vessel and in addition apply stresses to the structure that can rapidly fatigue structural connections and joints.

Racing and personal cruising vessels reduce this somewhat by using a deep V geometry for the lower surfaces. Longitudinal spray rails or spray chines on the V surface and bilge corner (corner chine) turn the water flow away from the V surface as the hull moves downward becoming immersed in the sea surface. This creates aeration of the water flow, hence the name *spray rails*, and helps to dampen the pressure on hull surfaces and reduce friction drag. Global vessel accelerations at high speed are nevertheless high enough to be uncomfortable for passengers and outside the limits discussed in Chap. 7. Sprung and damped seating and, for racing craft or higher-speed recreation craft, multianchor seat belts (racing type with push release at the stomach) are needed for the helmsman, navigator, and engineers so as to absorb shocks and restrain body movement (see *Resources, outfit* for examples of suppliers). Associations that govern offshore racing such as the Royal Yacht Association in the UK include regulations for personnel safety equipment that would need to be consulted.

It is the seakeeping quality of a planing monohull in a seaway that makes it less suitable for service as a high-speed passenger ferry than a catamaran. This has encouraged the development of a range of other high-speed marine craft to try to overcome the motion and acceleration challenges while taking advantage of the lower relative resistance and high maneuverability of the planing monohull.

The PCAT represents just such an attempt. It uses the catamaran form to improve the seaworthiness of the basic planing monohull so that it may be applied to fast ferry service. The hydrodynamic configuration of a simple PCAT is similar to that of a catamaran, with asymmetrical section demihulls, each of which is a slender planing monohull (Fig. 10.1a).

The tunnel planing catamaran (TPC) is slightly different in that it has asymmetric demihulls formed by a reducing height tunnel along the longitudinal central plane from bow to stern so as to provide some additional aerodynamic and hydrodynamic lift (Fig. 10.1b). The top of the tunnel may be of a V configuration with a dead-rise angle of 10–15°, as in the figure, to reduce wave slamming and form a stable ram air lubrication layer at high speed.

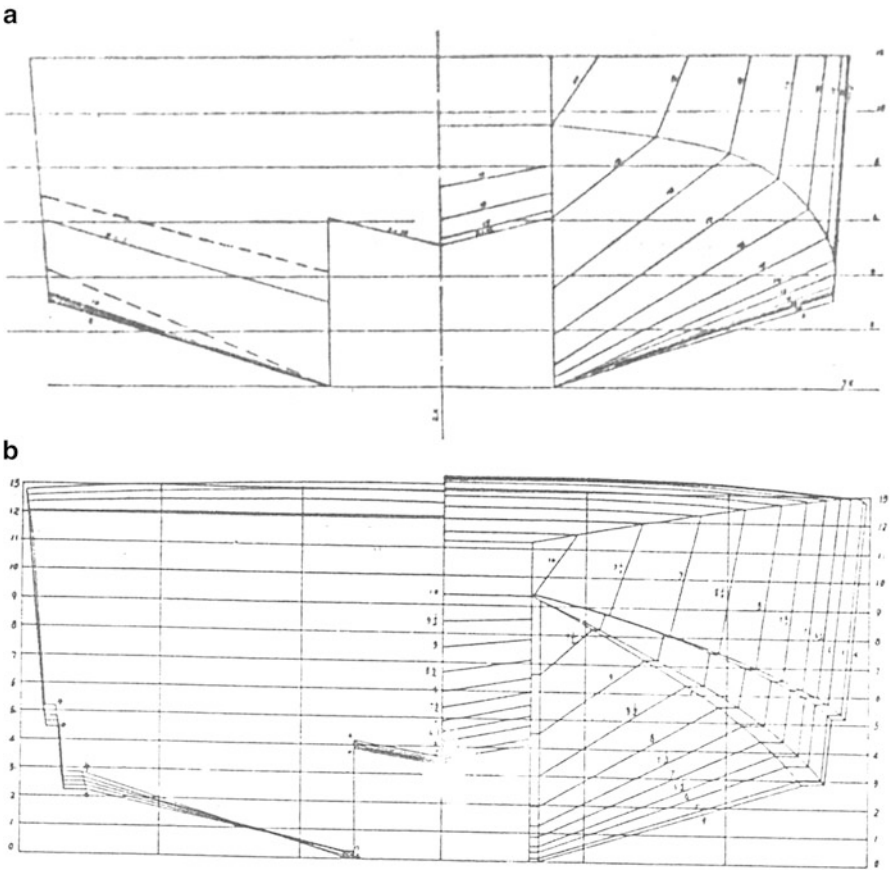

Fig. 10.1 (**a**) Planing catamaran model C body plan; (**b**) TPC model D body plan

This approach has been used successfully for cruising and racing boats. The TPC form is used for both high-speed offshore racing powerboats (Fig. 10.2) and for circuit racing hydroplanes. These ultra-high-speed craft also use a transverse stepped planing surface to further reduce drag at high speed and dampen the porpoising motion characteristic of many planing craft at high speed in waves.

The PCAT with symmetrical hulls will need to have wide spacing between the demihulls to minimize the wave interaction between them as the vessel is accelerated through the drag hump up to planing. This is the option adopted for the wave-piercing craft discussed in Chap. 8, so we refer readers back to that chapter if the design target vessel is to be large scale with Fr_L below 1.0. Smaller PCAT vessels would retain the lower L/B as discussed in Chap. 7. To improve acceleration performance, some catamarans with this configuration have been designed with hydrofoil support. We discuss that configuration later in this chapter.

Fig. 10.2 Offshore racing catamaran

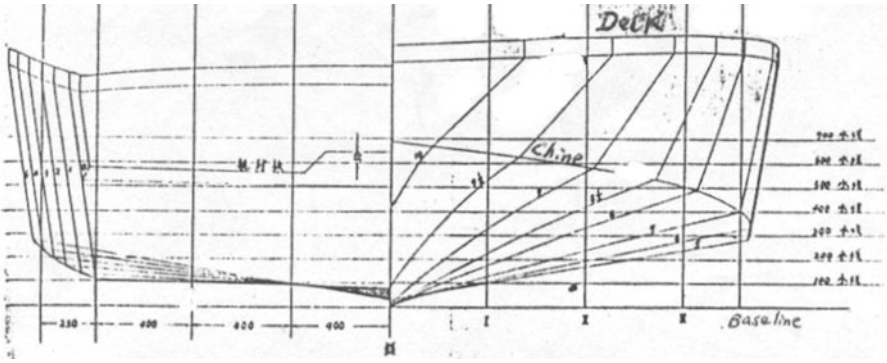

Fig. 10.3 Body plan of conventional planing monohull model B

The TPC, particularly for small-displacement, high-speed craft ($F_{r\nabla} > 4.0$), has good takeoff capability to planing, stable, high-speed running, low dynamic trim angle, good seakeeping quality, high transverse stability, and good maneuverability.

Typical characteristics of TPC can be summarized as follows:

- The planing surfaces from a monohull form are split into two slender demihulls designed to ride at low operating trim angle (see body plans in Figs. 10.1b and 10.3). The tunnel is designed as a reducing volume from bow to stern so as to create an overpressure of the air in the tunnel aiming to dampen motions in waves

and, consequently, the impact load on the hulls and to improve the seakeeping quality. The speed loss of such craft in waves may also improve compared with conventional planing monohulls.

- The tunnel shape is contracted from bow to stern with the elevation at the stern at or below the static waterline to create a so-called ram air effect as the vessel accelerates on to the plane. As the craft accelerates, the tunnel volume increases, and so the effective lift remains steady and both pressure and air lubrication help to minimize the resistance of the demihull inside walls.
- During TPC takeoff, the aerodynamic lift is affected by the tunnel transverse section area change and can be designed to provide more support toward the stern so the change of trim angle with speed is smaller, giving reduced drag hump during takeoff. On conventional planing monohull craft, the adjustment of hydrodynamic lift center and, therefore, trim requires trim tabs at the stern.
- The transverse static and dynamic stability are higher than a monohull. Generally, a planing catamaran will have a fuller form for the demihulls than a displacement catamaran but closer spacing, so transverse stability will be similar.
- The slender planing surfaces of a TPC will have less of a tendency to cause porpoising motions, as occurs on conventional planing monohull vessels; in addition, the widened hull increases the distance between two water propellers, improving the maneuverability.
- It has a large deck area for the arrangement of passenger and utility spaces, similar to a displacement catamaran, while the space in the wider demihulls gives greater freedom for machinery arrangement and keeping the mass center of gravity (CG) low.

Cougar Marine of the UK (Now Cougar Powerboats Ltd.) has designed and built TPC vessels in the 5- to 50-t displacement range during the 1980s and 1990s. Leading particulars of the craft are listed in Table 10.1. A 40-t Cougar TPC named *Challenger* [1, 2] broke the speed record for crossing the Atlantic Ocean following a route of 2819 nautical miles at a speed close to 50 knots in 1985, demonstrating it was possible for a relatively small high-speed catamaran vessel to take on very rough

Table 10.1 Leading particulars of TPC models

Type	CAT900	CAT1400	Cougar20	CAT2000	CAT2100
Length, oa, m	9.7	14.30	17.68	19.88	21.60
Length at chine, m	9.20	14.00	17.68	19.80	21.0
Beam, m	2.89	5.00	6.71	6.24	5.50
Draught, m	0.78	1.20	1.37	1.38	1.5
Power, kW	312	735	1863	2881	4413
Speed, knots	42	38	47.75	50	51
Displacement, t	4.80	12.40	20	36	53.23
Hull depth, m	1.27	1.94	2.42	2.84	2.60
$F_{r\nabla} = v/\sqrt{g\nabla^{1/3}}$ Fr_L	5.31 2.0	4.10 1.8	4.76 2.0	4.50 1.9	4.32 1.86

seas and maintain high speed. The motions cannot be recommended as suitable for paying passengers, though! Later a larger Incat wave piercer for ferry service in the UK followed a similar route across the Atlantic on its delivery voyage from Tasmania, demonstrating its resilience at high speed as well and improving on the records set by the much larger high-speed passenger liners for the Blue Riband trophy.

From the table one can see that $Fr_V > 4.0$ for all of the craft in the table, and Fr_L is also in the region close to 2 so well in to the planing region at speeds where aerodynamic forces are significant and cavitation/ventilation is an issue for propellers or waterjets. Semi-submerged propellers were used on such craft, operating in full ventilation mode and connected to steerable *z*-drives or direct stern drives, removing the need for a rudder. Because there were no other underwater appendages, the propulsion efficiency was improved, as was maneuverability.

Since this early series of fast planing catamarans was built, offshore powerboat racing has encouraged builders in the USA and other countries to build such craft, and the racing experience has enabled top speeds of up to 200 km/h (140 mph) to be achieved in offshore conditions during the period since 2000.

The success of the fast catamarans built by Cougar encouraged MARIC and Harbin Engineering University to carry out investigations of the hydrodynamic performance of TPC vessels. We outline this work in the following paragraphs.

Experimental Investigation of TPC at Harbin Engineering University, China
An experimental investigation of TPC performance was carried out at Harbin University using a high-speed towing tank (Length × Beam × Depth = 510 × 6.5 × 6.8 m) [3]. Two TPC models were tested. The model type C, shown in Fig. 10.1a, has a deep and wide tunnel, designed for operation in coastal areas, and model type D, shown in Fig. 10.1b, has a narrow and shallow tunnel, designed for operation in rivers. These were compared with a monohull form model B, as shown in Fig. 10.3.

The models were made with both wood and glass-reinforced plastic (GRP) coated by lacquer with a smooth surface and painting with waterline and frame symbols for taking pictures and making video recording. To record the running attitudes, wetted length, and spray in the tunnel of models in various conditions, the top plates of the model tunnel were made using transparent plastic. The leading particulars of the models are listed in Table 10.2.

The lines and body plan of TPC model types C and D can be found in Fig. 10.1a, b, respectively. From the figures one can see that the tunnel is continuous and contracting from bow to stern on both designs, but on model C the tunnel is higher. Type D is designed for inland river operation and has two longitudinal bilge spray chines for generated wave suppression and reduction of resistance at high speed.

Test Results

(A) Figure 10.4 shows the relative resistance versus Fr_V, where V is the displacement volume, curve C shows the TPC with a wide tunnel, and B indicates the conventional planing craft shown in Fig. 10.3. From the figure it can be seen that

Table 10.2 Test conditions of both TPC and HPC models

Description	Parameter	Value
Max. beam at hard chine	B_{cx}, m	0.884
Beam at transom hard chine	B_{ct}, m	0.878
Beam ratio	B_{ct}/B_{cx}	0.99
Relative tunnel beam for model C	$(b/B_{cx})_C$	0.27–0.32
Relative tunnel beam for model D	$(b/B_{cx})_D$	0.22–0.24
Relative tunnel height for model C	$(h/B_{cx})_C$	0.206
Relative tunnel height for model D	$(h/B_{cx})_D$	0.133
Projected length at hard chine	L_c, m	2.61
Length/beam ratio	L_c/B_{cx}	2.95
Projected area under hard chine	A, m^2	2.135
Ratio for projected area	$A/L_c \cdot B_{cx}$	0.925
Dead-rise angle at amidship	β, deg (°)	17
Dead-rise angle at transom	β_t, deg (°)	15

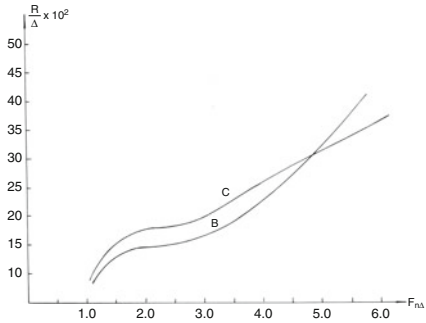

Fig. 10.4 Relative resistance of models C, B versus Fr_L

at low speed, the resistance of C (TPC) is higher than the monohull model B. This is due to the tunnel's making the planing surface discontinuous in transverse section so as to reduce the planing effect and increase resistance.

At high speed, the TPC resistance is lower than that of the conventional planing craft (B) owing to the ram air cushion in the tunnel, generating an air cushion to provide lift acting at the top of the tunnel. In addition, since the tunnel is contracting from bow to stern, the friction at the stern will be decreased owing to air lubrication effects from the generated and contained spray.

Additionally, the air cushion generates a lift acting on the tunnel, and the center of aerodynamic lift moves aftward owing to the contraction toward the stern. Thus, the vessel trim angle will decrease at high speed, reducing the wave-making resistance.

This physical phenomenon was observed during model testing in the towing tank, with the water flow with merged air and water spray blown out under the tunnel at the stern part of the model.

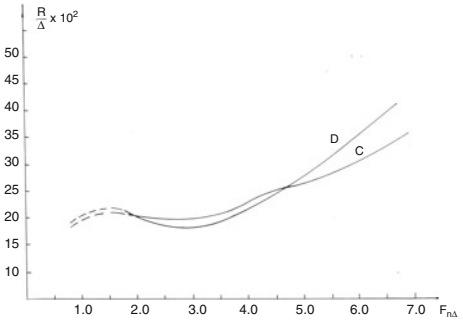

Fig. 10.5 Relative resistance of models C, D versus Fr_L

(B) Figure 10.5 shows the resistance comparison of the TPC with different tunnel widths. It was found that the resistance of C (wide tunnel) is lower than that of D (narrow tunnel) owing to the ram air cushion effect mentioned previously. Also, the peak wave-making drag of C (drag hump) is slightly lower than that of D, perhaps because model C has a higher relative tunnel roof, causing less interference drag at lower speeds when the ram air effect is low.

(C) The influence of the static load coefficient $C_\Delta = \Delta/B^3$ is shown in Fig. 10.6, where Δ represents the volume displacement of the craft and B the overall breadth. From the figure one can see that large $C_\Delta$causes high peak drag and demonstrates the sensitivity to hump drag. According to the test results of model D with C_Δ= 0.22–0.37, the hump drag is located at $F_{r\Delta}$= 1.75, and craft will take off above 2.0 to fully plane at $F_{r\Delta} = 3$ and higher. After taking off, the relative drag will drop down, and higher C_Δ gives lower relative drag, indicating that wide craft and planing surfaces are more efficient. The static load coefficient therefore needs to be considered both for efficient takeoff, as it affects the design for lower Fr, and also for planing speeds after takeoff when looking at the target service speed. Start by looking at the hump drag and profile so as to achieve efficient acceleration and then adjust if necessary for service or maximum speed.

(D) Figure 10.7 shows the influence of the longitudinal center of gravity (LCG) on relative resistance, where $x_g/L_c = 0.36$, 0.34, and 0.32, respectively, where x_g is measured from the transom. It is found that hump drag is very sensitive to LCG position, and moving the CG aftward will cause less hump drag, possibly due to higher trim angle during takeoff, however, after takeoff it will cause larger drag due to larger wave-making resistance. This effect may be reduced dynamically if trim tabs or interrupters are installed at the transom so as to move the center of hydrodynamic lift towards the stern. The lines of the TPC tend to place the center of buoyancy more to the stern of amidships than on other catamarans; nevertheless, it is important that the vessel LCG be set in the region $x_g/L_c = 0.4$ to 0.35 with static trim as flat as possible, so as to give flexibility to the hydrodynamic devices so they can operate effectively.

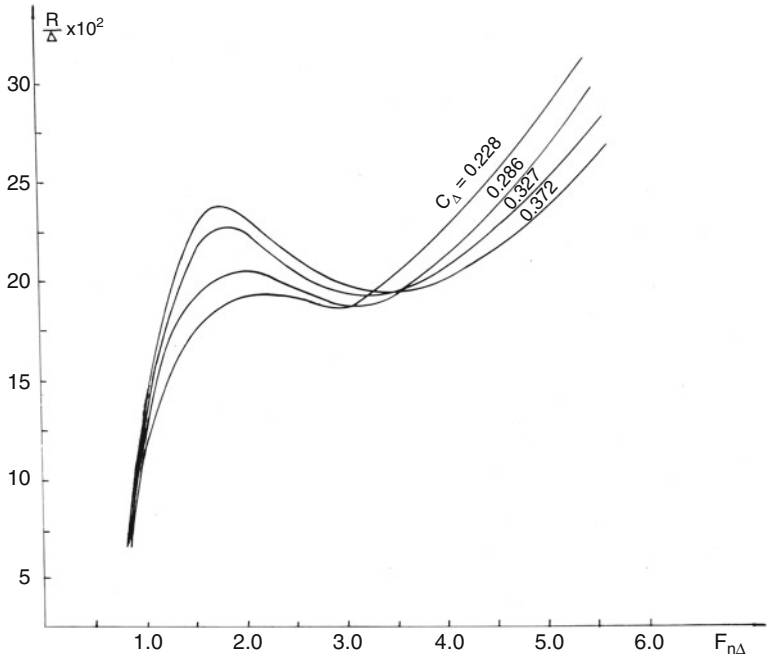

Fig. 10.6 Influence of static load coefficient on resistance of TPC

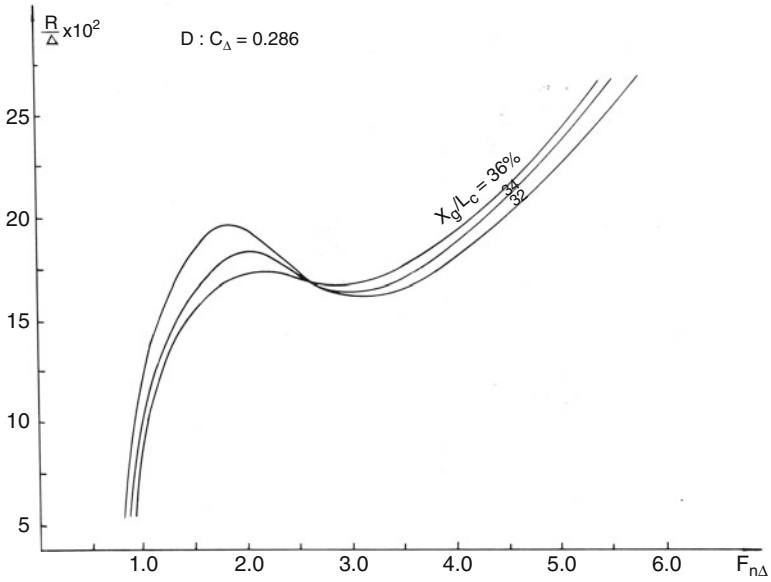

Fig. 10.7 Influence of LCG on resistance

Fig. 10.8 Offshore racing catamaran wave hopping

It should be noted that these results are from models in a towing tank using Froude scaling and calm water, so that aerodynamic flows and forces would not be to scale (they will be much reduced). The effect of the tunnel geometry on the hydrodynamic flows was therefore the key element in the model results. Two important conclusions from this work are that the tunnel geometry is important for obtaining minimized resistance at high speed and that it affects both the drag peak and the balance of the dynamic trim.

What we learn from this work is that it is possible to design a planing catamaran for high-speed operation and optimize it for a resistance profile by adjusting the tunnel geometry. This would be our first step in developing such a craft. A second step would be to refine the demihull lines including the *V* angle and spray strakes to provide the best possible motion damping in waves. Finally, the addition of one or more transverse steps may provide additional resistance minimization and motion stabilization at high speed (e.g., Fig. 10.8). Designer Lorne Campbell has useful information and lectures on planing craft and steps at his Internet site, see resources for link.

Racing boat designers have optimized designs through the evolution of full-scale prototypes. Fast ferry catamaran designers use model test series to optimize their vessel hull geometry. For the TPC, model testing can lead to an initial stage of selection, while larger-scale prototype testing in a seaway would be needed for the seakeeping optimization due to the challenge of Bernouli scaling for the aerodynamics. We then still have the question of whether global motions will be low enough to allow paying passengers or freight.

Presently passenger and vehicle ferry operations provide services that "fit" with client demand with service speeds in the range 25 to 40 knots. Experience through the 1990s and 2000s showed that large craft aimed at higher speeds, even in a range of 40 to 50 knots, have installed power and weather limits that make operation less economically viable.

Perhaps military personnel and weapons payload but not commercial payload are an interesting alternative for this concept. The challenge to reduce vertical accelerations led to development of the surface effect ship (SES), which is a variation on the planing catamaran, and to the 'M' craft in the USA. The SES has been developed successfully for offshore patrol and strike craft in Norway. The problem is that such craft have limitations in higher sea states (SSs) and required powering, so application has remained a niche so far.

One alternative, also discussed in what follows, is to support much of the vessel displacement on foils between the planing hulls rather than use ram air in a conical volume tunnel. This technique has been successful so far at small sizes; see later on in this chapter for sport and utility vessels.

We will discuss the bigger picture on this in Chap. 14, but in the meantime let us leave TPCs with the thought that technically such vessels can be designed and optimized and, in the form of racing craft, can operate at speeds in excess of 100 knots in an open seaway. Going back to our ferry challenge, can we simply further extend the L/b and have a vessel that can operate at higher speed while Fr_{L} is kept below planing?

10.3 Super Slender Twin-Hull Vessels

Displacement and semiplaning passenger ferry catamarans have been built for service speeds up to 40 knots with Fr_L below 0.75, though more commonly these craft have service speeds in a range of 25 to 35 knots due to the obstacle of wave-making resistance at high Fr_L. Of course, the large wave-piercing catamaran (WPC) is an exception to this, as are the very large passenger/vehicle semiplaning catamarans, which operate in a Fr_L range of 0.4 to 0.6 owing to their size.

Another solution to achieving a higher service speed, and particularly for low wake operation for the smaller passenger craft, is the SSTH form, [4, 5], that is, to further extend the length of the twin hulls to increase the demihull slenderness and so to decrease Fr_L, thereby decreasing the wave-making drag and wake generation for operation in restricted waterways.

This may be thought of as being similar to the lengthening process applied to a number of large ocean liners in the latter part of the twentieth century. For example, the length of the high-speed conventional passenger liner *United States* was extended, giving a length/beam ratio that increased to 10 and Fr_L that reduced to 0.38.

The Thames River 23-m waterbus is a catamaran with a SSTH with a length-to-demihull-length/beam ratio of 18, for 62 passengers, operating at 25 knots, and

Fig. 10.9 Thames Clippers waterbus, 23 m

powered by two diesel engines each of 500 kW power output; it is operated as a commuter vessel in London by Thames Clippers (Fig. 10.9).

The main feature of the SSTH is a demihull with extreme slenderness, even more slender than the WPC, with slenderness $\psi = L/\nabla^{1/3} > 10.0$, $L/b > 15$. Since the twin hull is so slender, the wave-making drag is not difficult to calculate using theoretical methods, so total resistance for the ship can be predicted, and optimum leading particulars can be determined accurately from theoretical analysis.

Change of payload may give only a small influence to the ship speed and running trim compared with high-speed ships with dynamic support or the payload-sensitive SWATH. In addition, the configuration is rather simple, and there is no special equipment that would create difficulties in scaling the concept to a larger size. The very long twin hull is probably is not an ideal solution owing to an increase in the friction drag and increased hull longitudinal strength challenges, leading to potentially higher vessel lightweight proportion and lower payload fraction. The configuration nevertheless lends itself to all-passenger ferries for restricted waterways where vessel wash is a key factor and the payload fraction from passengers is low.

China has many inland waterways, and higher speed river buses are of interest, so MARIC has carried out a review of this form based on published research. References [4] and [5] introduced research in this field in Japan by a team from Ishikawajima-Harima Heavy Industries Co., Ltd (IHI) and Tokyo University in Japan.

To minimize the total resistance, in addition to increasing the demihull slenderness, other measures should be taken to minimize wave-making drag. Reference [4] shows that the application of "lightly" asymmetric demihulls (i.e., 40–45% of displacement for inner half of demihull and 55–60% for outer half of demihull) is

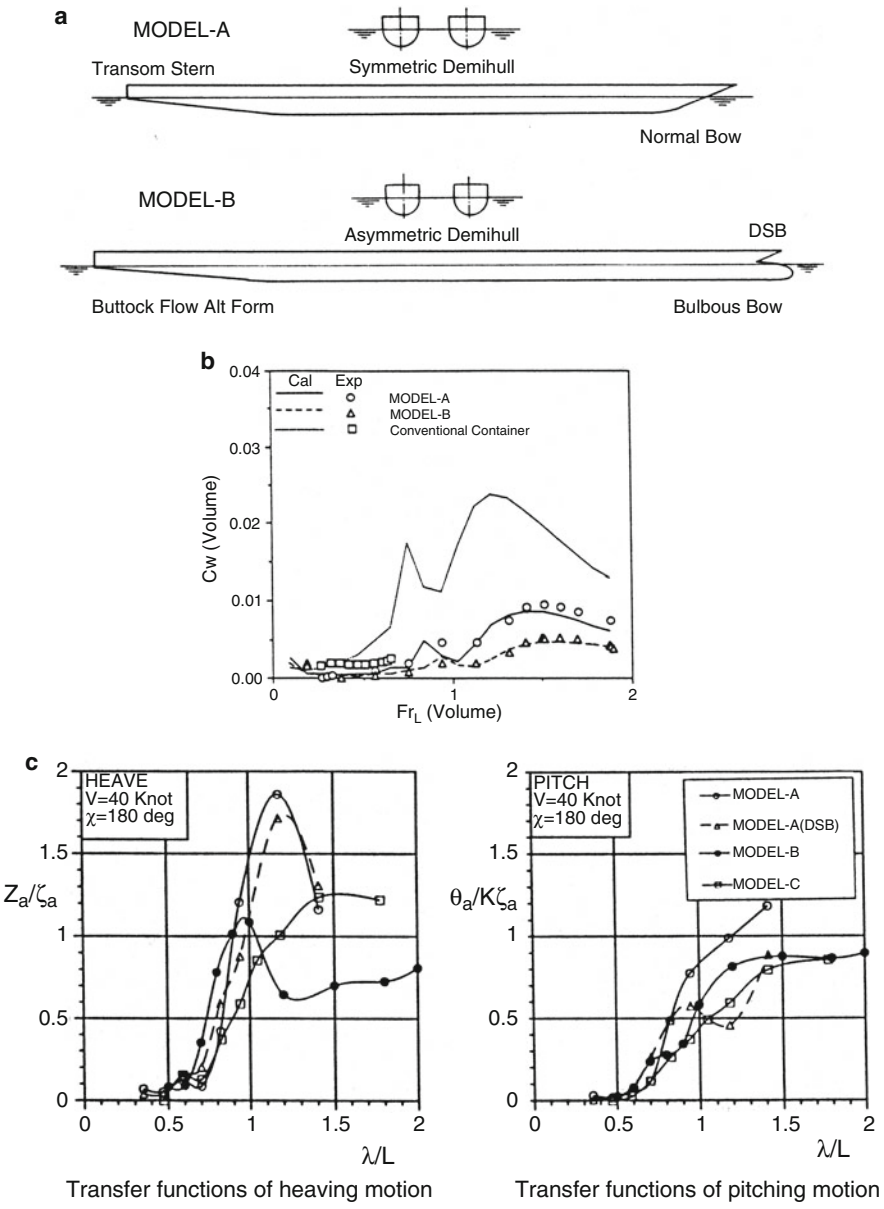

Fig. 10.10 (**a**) SSTH analytical studies model A and B; (**b**) wave resistance, (**c**) heave; and (**d**) pitch response

favorable for decreasing wave-making resistance. The use of a bulbous bow can also reduce the wave-making drag further for such SSTHs.

Figure 10.10a shows two typical types of SSTH studied by IHI and Tokyo University, where model A shows a symmetric demihull without bow bulb and

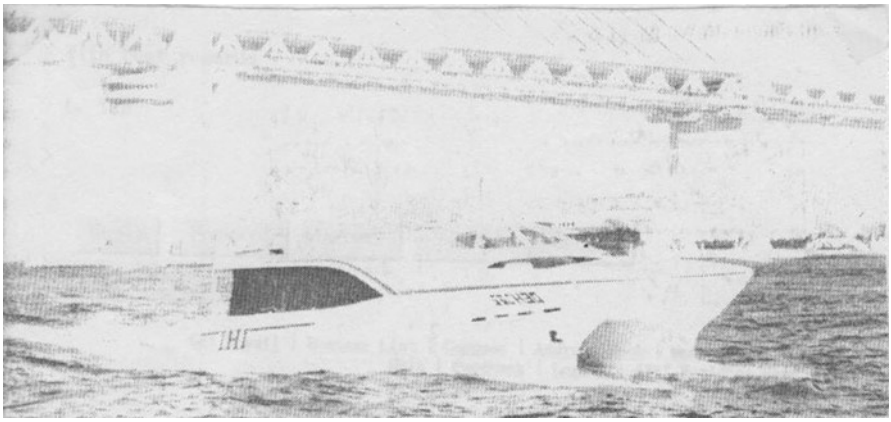

Fig. 10.11 IHI test prototype

with typical trapezoid stern, and model B has more slender and lightly asymmetric demihulls, with bow bulb and longitudinal flow stern lines. Figure 10.10b shows the theoretical calculation and experimental results for the SSTH models.

At the same time, the seakeeping quality can also be improved using a slender demihull. Figure 10.10c shows the transfer function for SSTH longitudinal motion; note that model B, with a high demihull slenderness, has a lower longitudinal response than model A in waves, particularly for heaving motion.

In this figure, the experimental results of a further model C with a pitching-motion-damping hydrofoil are also presented, and it can be seen that the contribution to reducing longitudinal motion is very large.

It is clear that the SSTH has potential for improving power performance and seakeeping quality to a certain extent; however, this comes at the cost of an increase in the hull structural weight. This may be a serious disadvantage of such craft. The question that arises is just how far one should go in increasing L/b.

To obtain confidence in applying the SSTH concept to large ships, over 50 m long, IHI constructed a 30-m-long experimental vessel and conducted various open-sea tests, including tests of speed performance, maneuvering, seakeeping ability, and monitoring strain gauges that measure stresses in the hull structure during ship trials.

The first SSTH, named *Toraidento* (Fig. 10.11) was completed and put into operation in Japan in 1991. The leading particulars are listed in Table 10.3. The trials demonstrated that the craft had a fine seakeeping quality. Based upon the successful test of the 30-m ship, IHI designed a 70-m passenger car SSTH ferry, *Ocean Arrow* (Fig. 10.12), with leading particulars as in Table 10.3. The *Sea Arrow* entered service in 1998. Reference [6] describes a program of data monitoring following its introduction to service.

The success of the *Sea Arrow* has shown that the SSTH concept offers a useful alternative to the wave-piercer concept for higher-speed large vessels, keeping Fr_L below 0.75 even at 40 knots and providing passenger comfort for at least shorter

Table 10.3 Leading particulars of 30- and 70-m SSTHs

Ship type	30 m (Fig. 10.11)	70 m (Fig. 10.12)
Length overall, m	30.4	72.1
L/*b*	21.0	22.0
Breadth, m	5.6	12.9
Depth, m	2.0	5.6
Draft, m	0.88	2.1
Gross tonnage, t	40.0	1687
Passenger capacity	66	430 persons and 51 cars
Max. speed, knots	28.2	31.3
Froude number, Fr_L	0.9	0.78
Main engines	2 × MTU8V183TE92, diesel	2 × MTU16V595TE70L, diesel
Power, kW	2 × 441	2 × 3925
Revolutions, rpm	2300	
Propulsion system	Propeller	Fixed-pitch propeller
Endurance, NMI	200	950
$k_p = pv/N\left(\frac{p \cdot km/h}{kw}\right)$	3.91	
Hull material	Aluminum alloy	Aluminum alloy
Crew	3	10
Navigation region	Calm water	Seagoing
Builder	IHI AMTEC	IHI
Completed date	October 1991	1997

journeys such as the Tokyo Bay service provided by *Ocean Arrow*, which takes around 30 min.

In the last few years designers such as One2three, Incat Crowther, and Damen have employed the SSTH form for low-wash river ferries, with *L*/*b* in a range between 15 and 20. Two examples are shown in Fig. 10.13a, b, the 33-m Thames Clipper commuter ferries that operate along the Thames River in London (*L*/*b* = approx. 18) by One2three/Incat and the 40-m ferry for Hong Kong Pearl River Estuary services by Incat Crowther. A larger, 70-m offshore crew transfer and supply vessel has also been designed by Incat Crowther for operation in the Caspian Sea, also with *L*/*b* = 18, and is shown in Fig. 10.14. Two vessels were constructed by Austal and placed in operation by Caspian Marine Services out of Baku, Azerbaijan. While the river ferries are designed for 25- to 30-knot operation, the crew boat operates at between 30 and 35 knots.

Austal also delivered two 57.6-m high-speed crew transfer vessels to Swire Pacific Offshore (SPO) in early 2017, also designed by Incat Crowther with high *L*/*b* and constructed by Austal's shipyard in the Philippines. The 40-knot *Offshore Express 57* large crew transfer vessel is capable of transporting 90 personnel (plus cargo) to offshore platforms safely in up to SS 6 conditions with wave heights between 4 and 6 m. Vessels of this size and capability are becoming an efficient alternative to offshore personnel transfer by helicopter, where platform access from

sea level is a practical option. To assist this, an Ampelmann (see resources) motion-compensated "walk-to-work" (W2W) gangway that allows for the safe transfer of personnel to offshore platforms is installed. Aided by a Class 2 dynamic positioning (DP) control system, the vessel has built-in redundancy to successfully complete transfers in the event of an engine or bow thruster failing. This development follows a similar approach to that being developed for wind farm crew transfer vessels (Chap. 13).

Similar offshore crew and supply vessels in the 2×57 m and 2×70 m classes designed by Incat Crowther have been built by Gulf Craft for Seacor Marine in 2008 and 2013. The latter 70-m vessels are operated by Leopard and Lynx at up to 42 knots and have Class 3 DP similar to deep water subsea service vessels (see resources for reference links). A specification summary is shown in Appendix 3.

Fig. 10.12 *Ocean Arrow* SSTH ferry: (**a**) cutaway; (**b**) at speed; (**c**) general arrangement

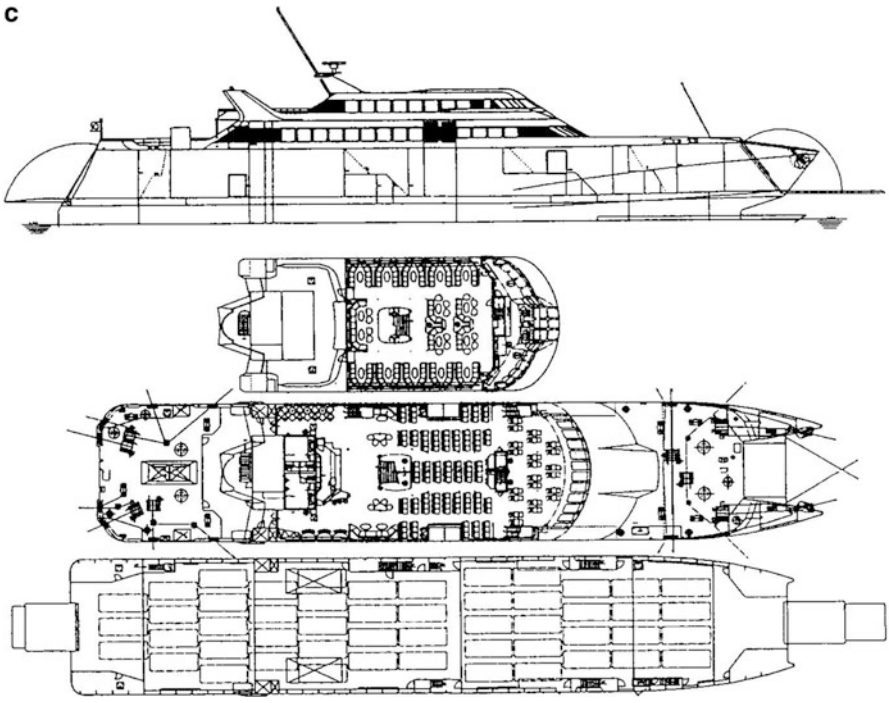

Fig. 10.12 (continued)

10.4 Fast Trimarans

The trimaran form as such is not a new one as the Polynesians used these craft a millennium ago. More recently, in the middle part of the twentieth century, the form was used for world water speed records [7].

The most recent development in high-speed vessels has been led by Austal shipbuilders of Henderson, Western Australia, for ferries in the 90- to 120-m-length overall (LOA) range and for the military derivative which they build in the USA for the US Navy. Austal has also developed a smaller 27-m vessel aimed at offshore wind farm maintenance. Other Australian designers, such as One2three, have also designed trimarans in the smaller 50-m-LOA range for ferry and luxury yacht applications.

Rather than having three similarly dimensioned hulls in parallel, the Austal craft have a configuration with a slender central hull that provides the majority of the displacement and two side hulls (sponsons or amahs) in the after half of the vessels' overall length that act as stabilizers rather than providing primary payload support. This configuration allows a much larger passenger/payload space in the after half of the vessel superstructure than a monohull.

Fig. 10.13 (**a**) Thames River 33-m SSTH ferry; (**b**) Incat Crowther 40-m ferry for Hong Kong

Austal employs asymmetrical V-shaped cross section to the two outrigger stabilizers to provide controlled stability in roll that is not as stiff as a catamaran, and so motions and roll accelerations are lower than a typical high-speed catamaran. The stabilizers, being somewhat shorter than the main hull, will operate at a higher Fr_L so the slender V form minimizes drag.

Fig. 10.14 SSTH high-speed supply vessels: (**a**) Caspian Marine Services 70-m vessel; (**b**) Seacor Marine 57-m vessel

A photo is shown in Fig. 10.15, while the GA is shown in Appendix 3 for reference.

An alternative approach has been taken by other designers using a wider spacing to the outrigger sponsons and wider beam and symmetrical cross section leading to a much stiffer roll response. We will come back to this form after reviewing Austal's development.

Fig. 10.15 Austal 102-m trimaran

The Commercial Opportunity

The key opportunity with this form is for improved open ocean motions and therefore application for ferry service over routes served by slower traditional monohull displacement ferries with service speeds of 12 to 20 knots. Example routes that may be suitable are the longer cross-channel route between England and France (Poole to UK Channel Islands or St. Malo), routes in the Canary Islands, and routes across the Taiwan Strait to mainland China. So far there is a vessel in service on the first two routes, while at present the Taiwan Strait remains a study, which we will look at later on (with many thanks to Austal for the technical data) [8].

Setting Configuration

Preliminary requirements for such a vessel, like a catamaran ferry, are initially the space required for vehicles, in-lane meters for trucks, and a minimum number of cars. Once these are selected, the passenger space, which is normally in accommodation over the vehicle deck, should at least accommodate the capacity of the cars carried, as a rule of thumb. So if car capacity is to be 250, then passenger arrangements should be in a range of 1000 or more. The floor area and arrangement required for roll-on and roll-off of the cars and trucks will suggest the beam dimensions and the length of the car deck. This will provide the starting point for overall vessel dimensions. If the sponsons are disregarded as a starting point, the displacement and dimensions of the main hull can be set, bearing in mind the additional mass of the extended hull over the sponsons, providing the payload accommodation, and the sponsons themselves. Some guidelines concerning vessel mass can be taken from the information in Chap. 2.

The stabilizing sponson trimaran design approach can differ from that of the catamaran since the outrigger sponsons or "amahs," as Austal calls them, can be dimensioned, located, and formed to provide transverse stability without needing to accommodate machinery, all of which can be housed in the main hull. If the sponsons are positioned toward the stern, the passing of waves through the space between the sponson and the main hull under the wet deck will not have the same potential wave impact issue as on a catamaran bridging structure.

A number of studies have been carried out over the last decade or so regarding positioning and spacing of sponsons [9, 10]. The first reference details work in the UK prior to the development of the Royal Navy trial trimaran HMS *Triton*. The second paper details analysis and model tests to investigate trimaran sponson positioning and interference effects by Austal as part of its trimaran development program. This latter work in particular indicated a very complex relationship between sponson position and size and total resistance for different sizes of vessel.

The first requirement is to provide roll stability. If spacing is increased, then sponson volume can be decreased as far as stability is concerned. For vessels operating at Fr_L in a range of 0.3–0.6 with sponsons operating at 0.6–1.0 perhaps depending on their length, the spacing can have a beneficial interaction and so optimization can be worthwhile. In this case, sponson positioning more forward to amidships has been found to be helpful from the point of view of minimized wave resistance but has a negative effect on maneuverability. For vessels such as Austal craft operating at around 0.8 for the main hull but closer to 1.1 for the sponsons, this means that the sponsons will be close to the planing speed range, so the wave making will have a different interaction with the main hull depending on the precise shape of the sponson. The Austal approach to sponson shape for large craft has been to use low draft with asymmetry toward the main hull, thereby minimizing wave making external to the craft.

Note also that where the main hull is below planing speed, if the sponsons "plane," they will not lift the vessel like a planing craft, so the planing forces will simply add roll stiffness and stresses in the connecting structure at service speed.

Stability

The static stability of a trimaran will comprise the normal righting moment of the central hull rolling about its center of buoyancy, plus the righting moment from the rotation of sponsons (one down into and one up out of the waterplane):

$$\begin{aligned} \mathrm{BM} &= I/V + 2\left(A \cdot h^2\right), \\ \mathrm{GM} &= \mathrm{BM} + \mathrm{KG}, \end{aligned} \tag{10.1}$$

where A is the sponson waterplane area and h the lever arm about the main hull centerline.

Once the static metacenter is defined, the roll natural period can be estimated, as in Chap. 3. The smaller the sponson volume, the less influence on metacentric height. A monohull with fine form, as is used for the trimaran, might on its own have a GM in a range of 2–3 m. Austal found for it 102-m design that sponsons

dimensioned to raise the GM to between 6 and 8 m was sufficient to reduce vessel roll motions to below 2° for almost all vessel sea headings. This softer roll motion contrasts with that experienced by large catamarans that generally have GM in a range above 10 m. It also helps to avoid the close coupling of the roll and pitch motion characteristic of catamarans.

There is a trade-off for passenger comfort between accelerations and roll angle envelope. For military vessels this also applies to the operability of helicopter landing decks. The sponson static displacement volume and volume increase above the waterline can be adjusted over a wide range. If the sponson waterplane area is very low and vertically slim, the vessel may have low roll acceleration but experience much higher roll angles in service, and righting time may increase. One way to balance this at service speed is through the use of dynamic stabilization, while at low speeds and when traveling in oblique seas there still needs to be enough buoyancy in the sponsons to control rolling satisfactorily in the limiting operational SS.

Resistance and Propulsion

The large trimaran such as that studied by Austal for the Taiwan Strait (the 102-m vessel eventually built and put in service in the UK) could be initially dimensioned using the theory presented in Chap. 4 since the main hull and sponsons are all fine forms with high *L*/*b*. Austal has available the CFD program SHIPFLOW, which was used to model the vessel and test geometry adjustments prior to subjecting the design to model testing. The model tests aligned with the SHIPFLOW results.

Figure 10.16 shows a comparison of model tests and full-scale trial data for the total resistance coefficient in calm water, demonstrating close agreement between the different results.

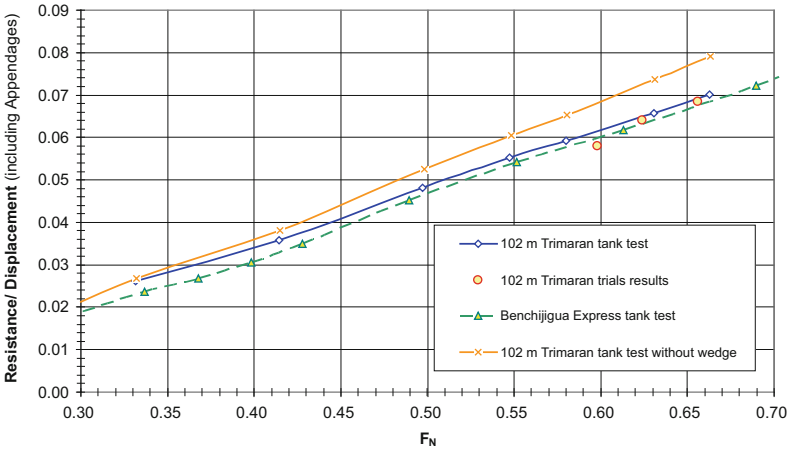

Fig. 10.16 102-m trimaran resistance trial comparison

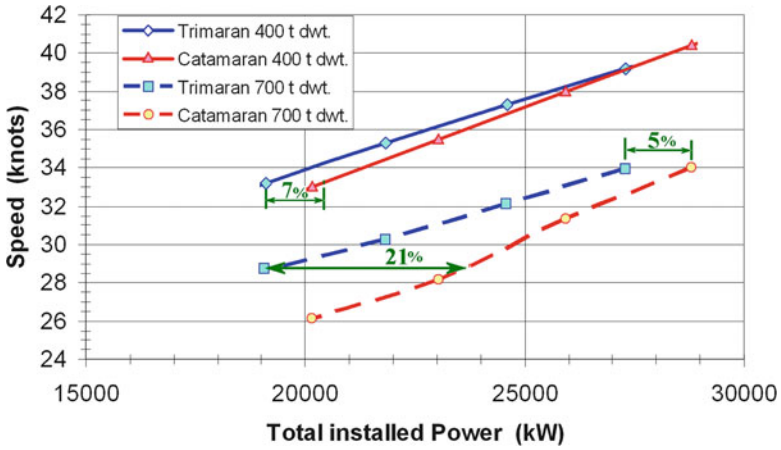

Fig. 10.17 Powering comparison with catamaran

Austal also compared resistance at two displacements (400 and 700 t) for the 102-m trimaran compared with an 88-m catamaran. This was translated into speed achieved by a power rating applied through similar waterjet installations. The results are shown in Fig. 10.17. The findings were that at full power and loaded displacement, the trimaran had a 5% advantage that increased to 20% or so at power reduced to 30 knots. At a light weight, the differences were much smaller.

The fact that the advantage occurs as displacement is increased suggests that the friction resistance on the catamaran hulls is the culprit here, since the catamaran hulls will be of finer form and should generate lower wave-making drag.

Motions and Interaction with Vessel Geometry

Austal calculated the RAOs for roll, pitch, and heave motions and for vertical acceleration for both the 102-m trimaran and an example 98-m catamaran. The results are shown in Fig. 10.18a–d. The one characteristic that is similar is the heave response. The responses in roll and pitch are much improved over the trimaran, and this feeds through to the acceleration response, which is significantly reduced for head and quartering seas in the critical response range of wavelength to ship length of 0.7 to 1.7.

The RAOs give an impression of motion response, while what a passenger feels is derived from the vessel response to an actual seaway, that is, an average response to the seaway wave spectrum. Austal calculated the RMS responses to Pierson Moscovitz spectra with a 2.5-m significant wave height for vessel speed of 37 knots at a range of zero crossing periods (zero crossing period decreases as vessel speed increases). The results for vertical acceleration and for roll angle in beam seas are shown below in Fig. 10.18a, b. Trends similar to those for the RAO's are seen with the trimaran response, which is significantly lower than that of the catamaran.

The trimaran and catamaran key data used for the analysis are as follows (Table 10.4).

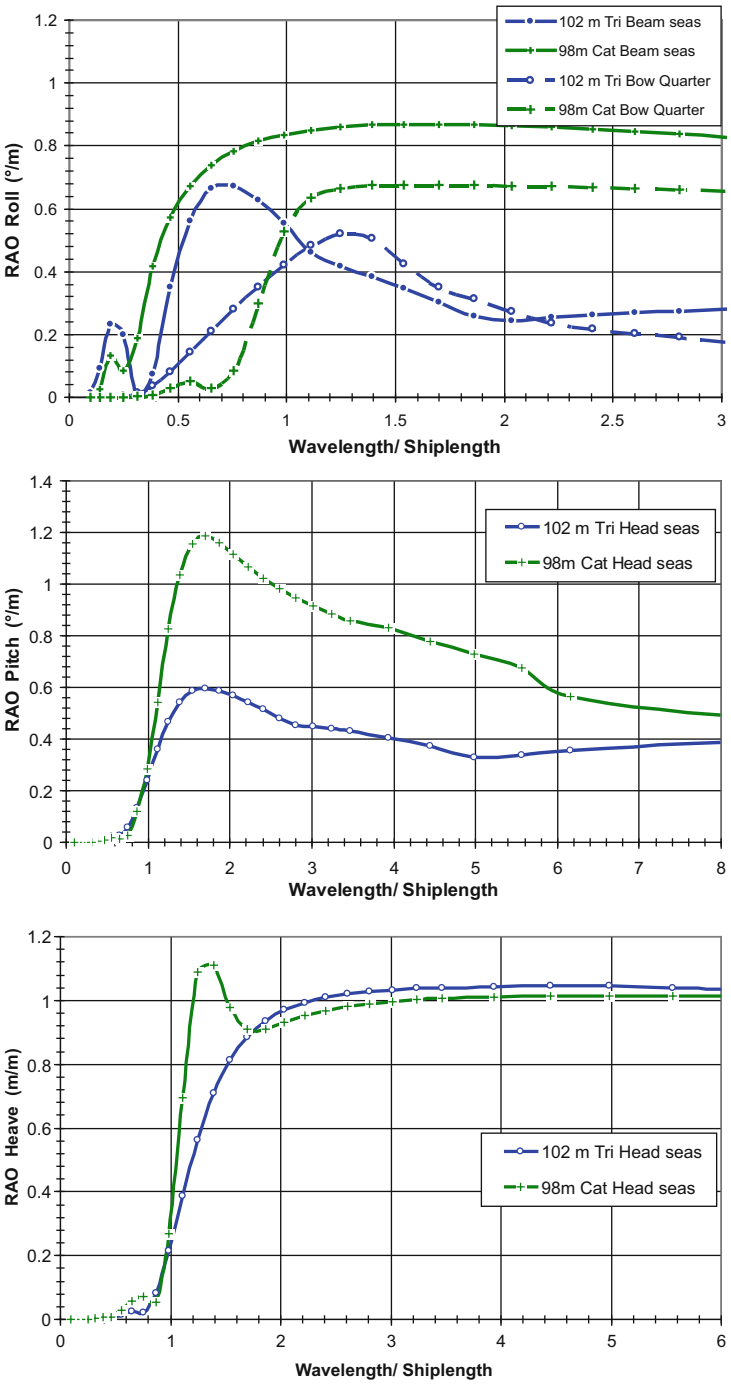

Fig. 10.18 102-m trimaran RAOs: (**a**, **b**) roll and pitch; (**c**, **d**) heave and vertical acceleration

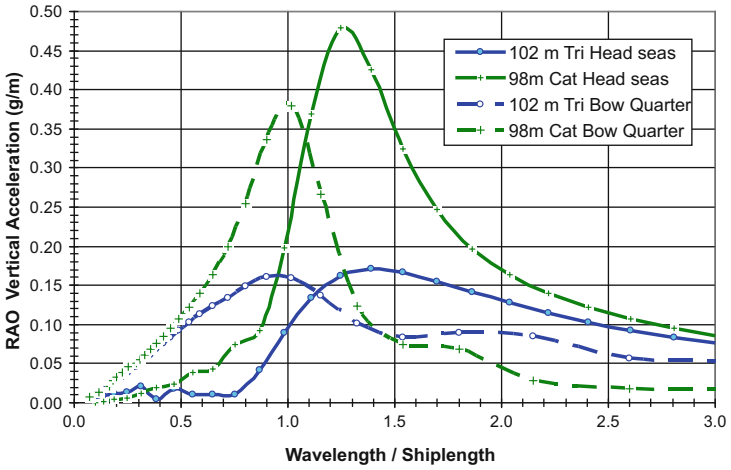

Fig. 10.18 (continued)

Table 10.4 Key data for catamaran and trimaran

		102-m trimaran	98-m catamaran
Lightship	Tons	990	1060
Analyzed deadweight	Tons	340	340
Draft	m	3.2	3.6
Length waterline	m	101.4	90.7
Beam waterline	m	27.23	26.45
Analyzed speed	knots	37	37
LCG	m	35.7	37.64
Vertical centre of gravity	m	7.2	7.08
Roll gyradius	m	6.8	9.25
Pitch gyradius	m	24.45	26.3
Yaw gyradius	m	24.45	22.67

Accelerations and Serviceability: Taiwan Strait

Given the results for a trimaran design potentially suited to an exposed service route, how would the 102-m trimaran fare for Taiwan Strait service? Austal used historical wave occurrence data available from a fixed platform in the center of the strait (Fig. 10.19) using the scatter diagram of Hs and Tz occurrence on the KK platform to produce motion and acceleration statistics for the range of vessel headings. These were then compared with chosen limiting criteria that link to a motion sickness incidence (MSI), where MSI occurrence is less than 10% for the voyage duration. Typical criteria would be vertical and lateral accelerations less than 0.05–0.08 g and roll and pitch less than 4°.

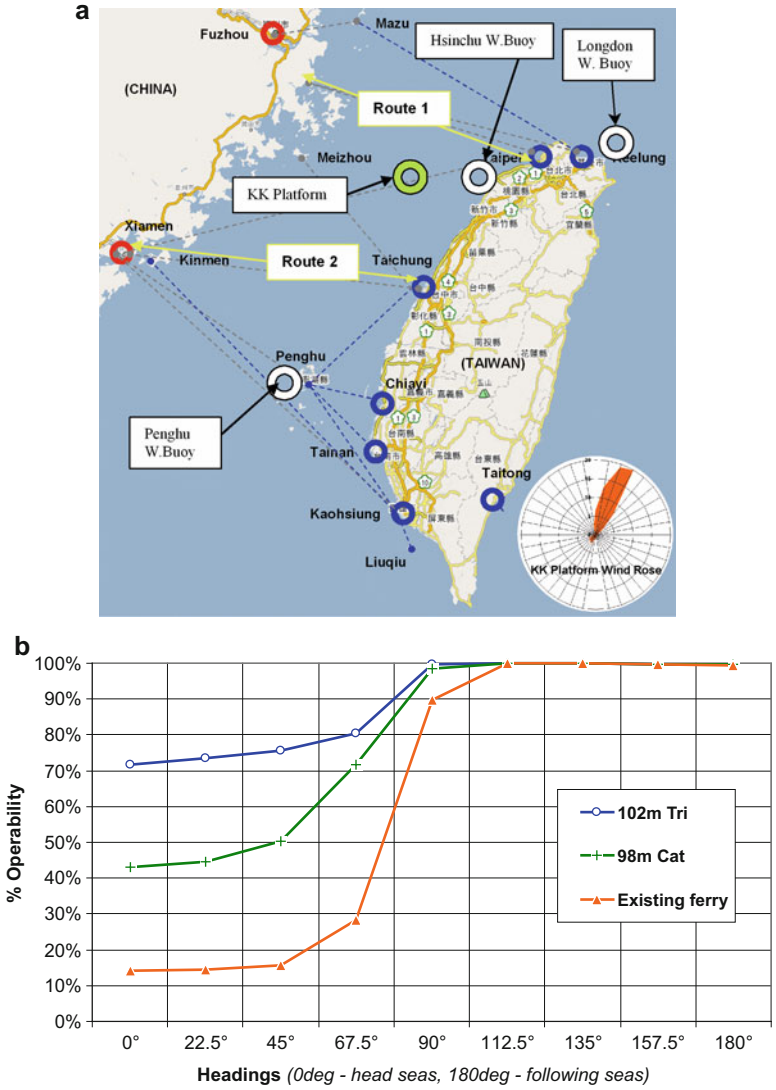

Fig. 10.19 (**a**) Taiwan Strait map; (**b**) trimaran and catamaran operability

It can be seen from the KK platform wind rose in Fig. 10.19a (see bottom right in the figure) that a trimaran navigating the potential route 1 or 2 would face seas on typical headings between 45° and 135°. Figure 10.19b shows that for the 45° heading the trimaran would have 75% uptime, while a catamaran would have 50% and the existing ferry as low as 15%.

The 10% MSI criterion chosen, over the route length which requires a 2-h duration, is a worst-case limit, not accounting for the full geography. If the variation

Fig. 10.20 CMN Ocean Eagle 43 patrol trimaran

in sea conditions across a strait such as this is accounted for, rather than taking the worst case, the operability of all three vessels may be shown to be higher. The relationship between the vessels will nevertheless remain as shown, with the trimaran having a significant advantage over a catamaran or the traditional ferry of a rather smoother ride.

Designer Nigel Irons (see resources) has developed a trimaran design based on a slim central hull and widely spaced sponsons that has been employed on a 35-m vessel for a round-the-world record-setting voyage in 1998 (*Cable & Wireless Adventurer*, subsequently MV *Brigitte Bardot*) and, more recently, together with French shipbuilder CMN, a design for an offshore patrol craft that has been built for the French navy, the *Ocean Eagle 43*. This last vessel is shown in Fig. 10.20. It has a maximum speed of 30 knots ($Fr_L = 0.75$).

It can be seen from the figure that this configuration employs widely spaced sponsons stabilizing a slender central hull that does not extend out to the sponsons in the same way as the Austal and One2three vessels (see *White Rabbit* trimaran, Chap. 13, Fig. 13.15). The vessels clearly have the capability to operate at high speed in extreme wave environments while having a rather lower payload/displacement ratio and useable volume. This is suited for applications in racing, recreation, and offshore patrol. The hull and accommodation structures are in fiber-reinforced plastic.

Craig Loomes of LOMOcean Design, New Zealand, has also designed and worked with shipbuilders on the construction of a number of trimarans, beginning with the 24-m *Earthrace* wave-piercing trimaran (aka *Ady Gil*) and the 22.4-m *Patrol One* based on the same design for operations at up to 32 knots ($Fr_L = 1.08$). The latter vessel has an aft-located superstructure spanning across to the sponsons, which have significant buoyancy below the design waterline and waterplane area to provide significant roll stiffness. Other designs following this concept up to 64 m LOA for offshore patrol have been designed and built (Fig. 10.21).

Fig. 10.21 LOMOcean *Patrol One* trimaran

10.5 Triple Planing Hull

Going back to smaller vessels, instead of the TPC derivative of the catamaran, a configuration might be envisaged with a slim central hull and two outer demihulls of similar length creating a planing trimaran with two tunnels. The TPH craft is such a derivative from a conventional monohull planing craft aimed at improving wave-making drag, wash, and wake, as well as seakeeping quality and planing hull stability. A small prototype of this configuration has been built and tested in China by MARIC [11]. Figure 10.22a shows the frontal view of TPH, and Fig. 10.22b shows the running attitude of TPH after takeoff to planing operation.

Figure 10.23 shows the line and body plans of two variants of the TPH for inland river TPH as shown in the photos (Fig. 10.23a) and for coastal applications (Fig. 10.23b). From the figures one can see that the craft is characterized by the following features:

- Three hulls with sharp form at bow to reduce wave making and improve slamming loads in waves;
- Bow lines that produce low bow wave, wake, and wash and, consequently, impact in river banks or other vessels;
- Tunnels between hulls with contracting cross section from bow to stern so as to capture air with increased static pressure to decrease wetted surface of craft and create turbulence that in addition generates an air lubrication effect combining to decrease drag by up to 11% compared to an equivalent payload planing monohull, according to the prototype test results.

Thus the potential advantages of such craft may be highlighted as follows:

- *Wash and wake elimination*: According to the comparison of test results for such craft model and corresponding planing hull, about 80% of bow waves and 45% of stern waves have been reduced;

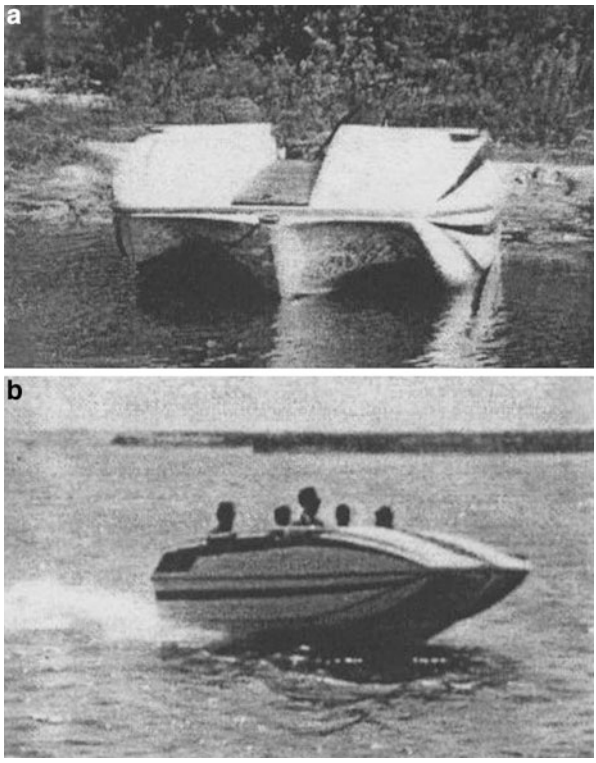

Fig. 10.22 (**a**) Frontal view of MARIC triple planning hull (TPH); (**b**) TPH at speed

- *Fine stability and maneuverability*: Since the craft is supported at three planing surfaces, the craft operates at high speed with fine dynamic stability and course stability. The maneuverability is also fine thanks to the large space between the two propellers, like on a catamaran;
- *Economy*: Fuel consumption can be reduced by about 15% thanks to the air lubrication effect, compared with conventional planing craft;
- *Enhanced riding comfort*: Both crew and passengers enjoy more comfort thanks to reduced slamming, particularly in waves, due to the air cushion effect under the bottom;
- *Payload deck area*: The hull configuration is more rectangular so that passenger accommodation can be simply arranged and create an efficient and economic vessel.

If we consider for a moment the overall configuration of the large vessels for passengers and vehicles, due to the low weight/high volume of such a payload, the wetted hull volume necessary to support the vessel is low compared with the geometric envelope – hence the configurations that have evolved for the large traditional catamarans, the wave piercers, semi-SWATHs, and, latterly, the trimarans. If we consider increasing Fr_L into the planing region, while the TPC

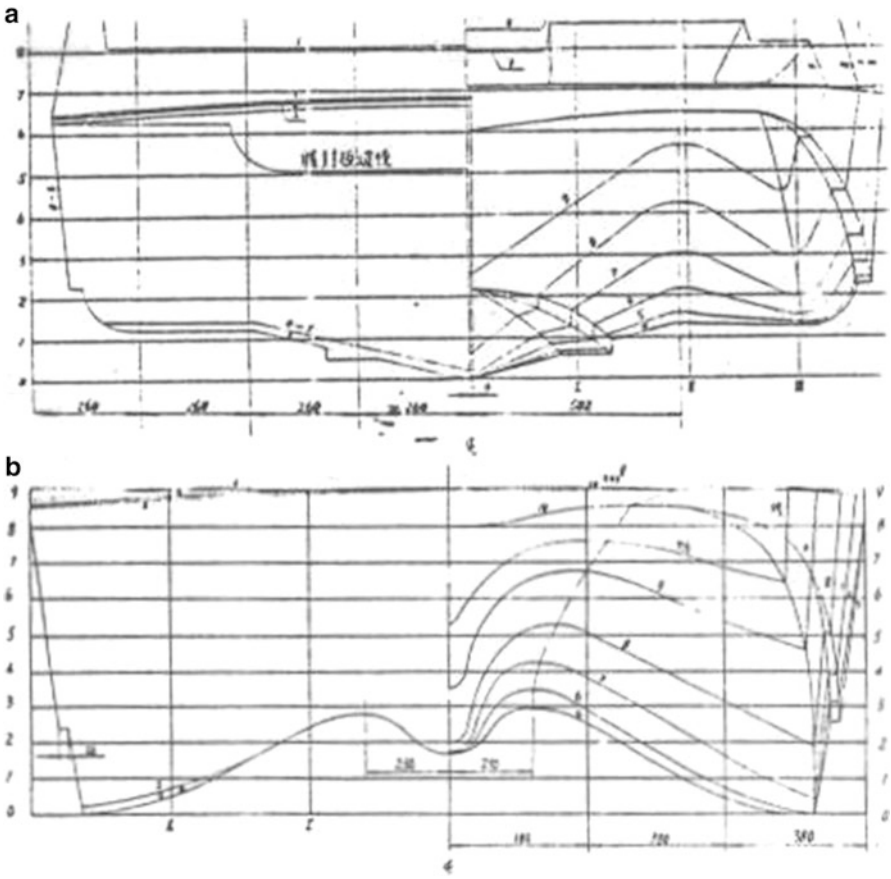

Fig. 10.23 Lines for triple hull craft: (**a**) for inland river craft; (**b**) for coastal TPH

configuration naturally applied to smaller vessels, and if we scale up, the tunnel becomes too large to provide ram air support. If we consider the TPH configuration in the same light, it would suit small high-speed river-taxi-type vessels in the 7- to 15-m size range, perhaps.

The hull forms as shown in Fig. 10.23a, b are convenient to form in GRP but would need to be simplified for construction in aluminum to be economic.

Since the static waterline of both variants has all or most of the lower surface geometry submerged, static stability can be evaluated by treating the vessel as a monohull with a rather complex lower surface profile rather than taking the approach of the catamaran or trimaran considering separate demihulls or hull and sponsons. Preliminary estimates for resistance can follow the same approach, treating the vessel as a planing monohull. The drag reduction of 11% or so would then be useful for acceleration margin through hump speed. The reductions in wave making

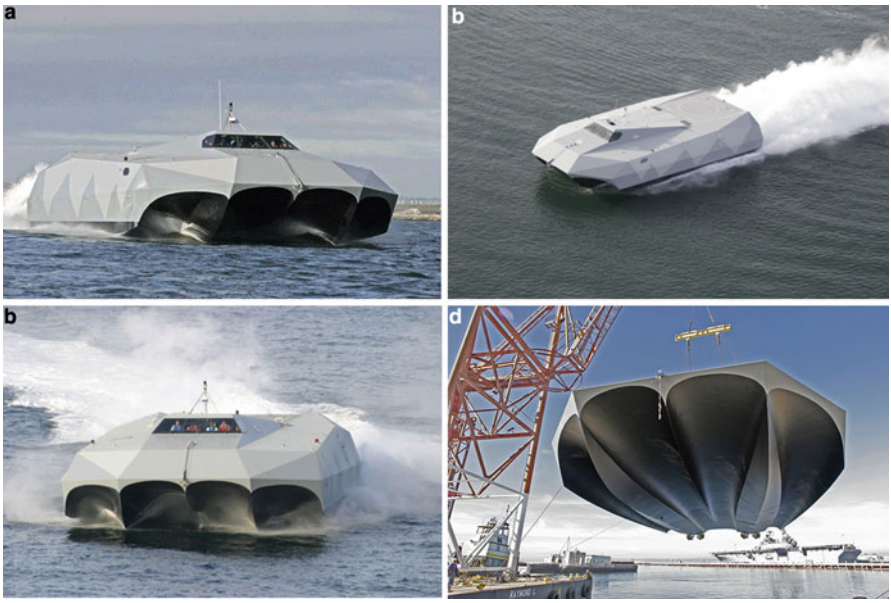

Fig. 10.24 M Craft M80 Stilletto at speed: (**a**) bow form; (**b**) overhead showing wash from surface propulsion and tunnel flow; (**c**) M80 in high speed turn; (**d**) underwater form

suggested previously can then be tested out and determined satisfactory or not through small prototype "real-world" testing.

Many possible tunnel geometries can be applied to such craft. Those shown in Fig. 10.23 might be called gentle geometry variation. A rather more extreme approach to tunnel craft has been developed by M Ship Co. in the USA, which has tested a prototype with two tunnels (single-M craft) and a larger 27-m craft with four tunnels (double-M craft) [12]. The 27-m craft is called the *Stiletto* and is designed for 55 knots in calm water, or $Fr_L = 3.4$ (Fig. 10.24).

Similar to the TPH of MARIC, the M craft has tunnels with decreasing transverse sections but also a roof geometry and cross section change moving back from the bow that encourages entering air to flow in a spiral manner rather than simply afterward. The result is a very turbulent flow regime, air lubrication, and some ram air lift that minimize craft drag at planing speeds. This works well for calm water or small SSs, but in open water the maximum speed drops to 35 knots above SS 3 to 4. The concept may therefore be useful for coastal strike craft or patrol and interdiction.

A smaller version at 12 m length has been built from the single-M design as a fast offshore sport fishing vessel (Fig. 10.25).

This takes us back to the challenge targeted particularly by larger multihull craft – low speed loss and high-quality ride in open-sea conditions. The TPH or M craft configuration may suit sheltered waters to operate at high speed but would not be

Fig. 10.25 M Craft Fisherman 30

suited to the challenge discussed earlier with the large trimaran concept for passenger transport.

What if we accentuate the main hull of a trimaran and adjust the sponson design? The configuration developed by Austal is one such approach. In that case the sponsons are designed as slim stabilizers to essentially a monohull vessel, placed aft for maneuverability, allowing the central hull to have high *L*/*b* for low wave-making resistance while operating in the displacement and semiplaning speed range. A further development for larger vessels might be additional sponsons forward, the pentamaran concept.

10.6 Pentamaran

The pentamaran concept was developed by the company BMT Nigel Gee Ltd., a UK naval architecture consultancy and engineering group. The initial impetus to the concept was a request from a ship operator in 1995 for a large-capacity, high-speed RoRo and freight vessel for routes in the Mediterranean Sea. The company initially looked at a slender monohull stabilized by two short stabilizer sponsons at the stern (Fig. 10.26) after carrying out a parametric study covering monohull, trimaran with three equal hulls, and catamaran form showing that the slender monohull had the lowest drag. Description of the studies in detail is given in reference [13] by Nigel Gee, and we summarize the key points here.

Analysis and model testing of the initial trimaran form showed that the short and broad sponsons did not have positive wave-making interaction with the main hull, while the main hull resistance was primarily friction, since it was so slender. Additionally, the broad sponsons had higher resistance than projected analytically based on the model testing carried out.

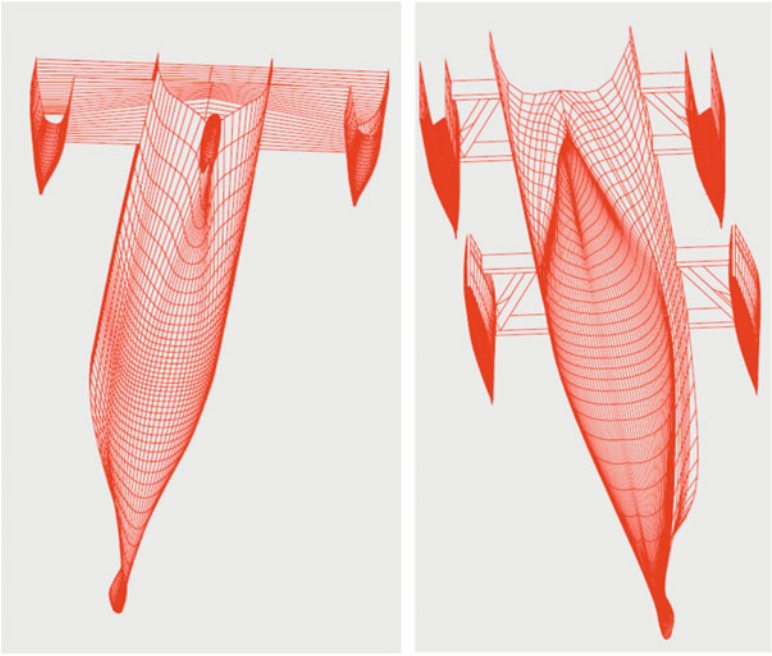

Fig. 10.26 Trimaran and pentamaran development

A design brainstorming session yielded the idea of two further sponsons further forward, not normally immersed at design waterline. The basic idea for stability in roll was that the forward down-moving sponson would enter the water when the emerging rear sponson had just moved above the waterline, so as to smooth the righting moment curve. This arrangement would allow the sponsons to be slimmer and overall drag to be reduced. BMT Nigel Gee has taken out patents for the specific pentamaran configuration. The resulting design was model tested, and results suggested that the installed power requirement servicing the container cargo payload of 13,000 t would meet the ship owner's requirement to be less than 36 MW at a service speed of 30 knots for the 190-m-long vessel.

At that time in the late 1990s there was increasing interest and expected potential market for such a high-speed cargo vessel, but while BMT continued design development, no vessel was taken beyond the design stage. BMT has continued development of the concept focusing on a smaller high-speed car ferry for around 1000 passengers and 250 cars or equivalent cars and trucks (Fig. 10.27 and Table 10.5). This is the same market that Incat and Austal supply with their catamarans, wave-piercing catamarans, and fast trimarans.

In the early 2000s BMT took the pentamaran ferry design much further through a liaison with IZAR, a Spanish shipbuilding company, with the intent to finalize a competitor design for the ferry market [14]. Analysis suggested that a pentamaran of 130 m LOA would have 20% lower power requirements than an equivalent

Fig. 10.27 Pentamaran Superferry design

Table 10.5 Pentamaran design key data from papers

Design	RoRo ferry	Superyacht
Year developed	2002–2005	2008
LOA, LBP, m	175.3, 165	130, 130
BOA m	31.3	30 approx.
Depth, draft, m	10.7, 5.1	8, 5 approx.
Deadweight	800–1000	n/a
Speed, knots	38 max, 36.5 at SS4	40+
Power, kW	4×MAN 16 V 40/50, 4x8000	2×MAN20V8000, 12,000 for cruise and sprint 1×LM2500, 22,000 for sprint
Propulsion	4×KMW 160SII WJ	3×WJ
Max. vertical acceleration	0.2 g at 135 degree wave	n/a

monohull and cost much less than a catamaran for the same duty. BMT also carried out studies of the pentamaran for the US Navy Sealift command, designed a pentamaran frigate, and produced outlines for a pentamaran superyacht, the Super Veloce (Fig. 10.28).

All of these vessels are designed to operate in the Fr_L range of 0.4–0.6 for the main hull, while the sponsons operate in a low planing range (hence the high friction drag and low wave wake and interaction). BMT Nigel Gee proposed several designs

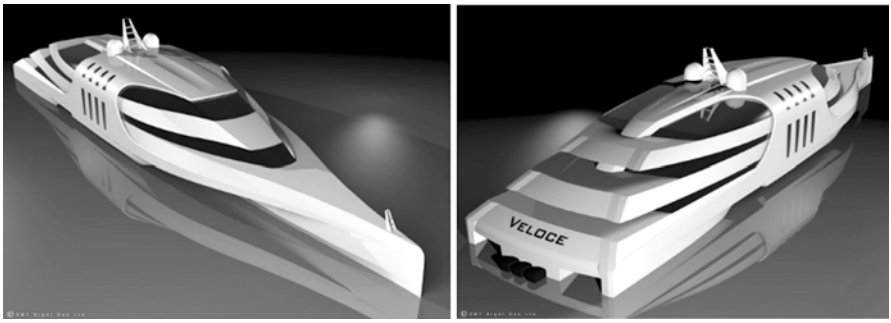

Fig. 10.28 Super Veloce superyacht design

using pentamaran configurations (for which the company holds patents), including the high-speed superyacht design shown in Fig. 10.28.

The Austal configuration has a successful operating track record that would seem to validate the notion that the pentamaran approach may also be successful for SSs where the forward sponsons are not submerged. Where the forward sponsons are submerged through waves, the rear sponsons may also be affected by turbulence caused by the forward sponsons, so that resistance and powering are also affected, and the advantage over the basic trimaran form with elongated slim sponsons may not be significant or even be negative.

The structural arrangement with two separate sponsons on each side is also quite complex, and one wonders whether a simplification could be made to this arrangement and to achieve the same stability function, as follows. Rather than two sponsons, combine the two into a longer single sponson with a canted keel line 40 or 50% above the design waterline, forming a long bow overhang in normal operation. This would have the effect of reducing sponson form drag and water surface "entry loads." Admittedly, the configuration would then be quite similar to that of the Austal trimaran, though with a wedge-shaped sponson in profile. Such a profile could nevertheless also provide a more rapidly increasing roll stability moment in a given SS.

There may be room for multihull configuration development in this space! The main takeaway from the body of work on this configuration is that at the high end of the dimensional scale, there appear real opportunities with careful optimization (see further in the reference material) to design high-speed vessels with realistic powering for longer, more exposed service routes. The fundamental design could remain a slim monohull below planing speed, supported by outboard sponsons that provide roll stability and enable the after half of the vessel upper structure to be enlarged for high-volume payload.

This still leaves us with the question of whether the basic catamaran form can be enhanced for higher speed operation above $Fr_L = 1.0$. In what follows, we consider two alternatives that have been studied and small to medium-size vessels built and tested.

10.7 Hydrofoil-Supported Planing Catamaran

Returning to the catamaran form and looking at much smaller vessels than the container pentamaran, we consider one option to minimize drag for a planing catamaran, as discussed in Sect. 10.2, that of placing hydrofoils across between the keels of the demihulls. This may be termed the hydrofoil planing catamaran (HPC) by MARIC or hydrofoil-supported catamaran (Hysucat) for designs by Professor Hoppe in South Africa.

There are many possible options for using hydrofoils to reduce catamaran drag forces, from simply mounting a foil wing to the keel of a TPC in a suitable position, to mounting foils on retractable legs outboard of the hull of a catamaran at its bow to lift it out of the water, to mounting a foil system on the inside of a catamaran between hulls, to installing a fully submerged foil system to the keels of a fast catamaran so that it operates fully as a hydrofoil at speed. These alternative configurations are shown in Fig. 10.29a–d. Examples of the vessel types are shown in Fig. 10.30.

We have given a summary of the FACAT and Foilcat in [7]. Both are built as high-speed passenger ferries, the FACAT in Russia and the Foilcat in Norway for service in Hong Kong operating alongside a fleet of jetfoil high-speed hydrofoil ferries. Both the FACAT and Foilcat are relatively sophisticated vessels with fully submerged foil systems using controls that actively maintain the foil depth under the water surface. In contrast, our focus here is to look at the relatively simple additions that could be made to a planing catamaran to reduce drag.

Considering first the addition of foils to a TPC, the configuration of a HPC may be as is shown in Fig. 10.29a, which shows the profile, with two hydrofoils located across the keel of the tunnel, so the load on the planing surfaces of the twin hulls at high speed are reduced by the lift of the two hydrofoils located toward the bow and stern, respectively. Figure 10.29b shows the HPC transverse section.

The features of a HPC can be summarized as follows:

- Depending on the geometry of the catamaran, at high speed a ram air cushion layer may be formed within the tunnel, depressing the waterline at the demihull inner sides, thereby decreasing the wetted surface and improving speed performance if the tunnel is in TPC form.
- A partial support is applied to the HPC from the hydrofoils; however, the tunnel width and hydrofoil chord will define the limit to hydrodynamic lift.
- The hydrofoil will benefit from two effects in providing lift: the sidewall end effect and the screen effect owing to the proximity of the water surface that improve its efficiency as a lifting surface. The so-called sidewall effect corresponds to the effective extension of hydrofoil span due to the presence of the sidewalls at the “tips” of the foil, and the so-called solid screen effect is a characteristic of a hydrofoil located close to the air/water surface, which reduces the downwash velocity and induced drag of a three-dimensional hydrofoil, increasing the effective angle of attack and the hydrofoils’ lift.

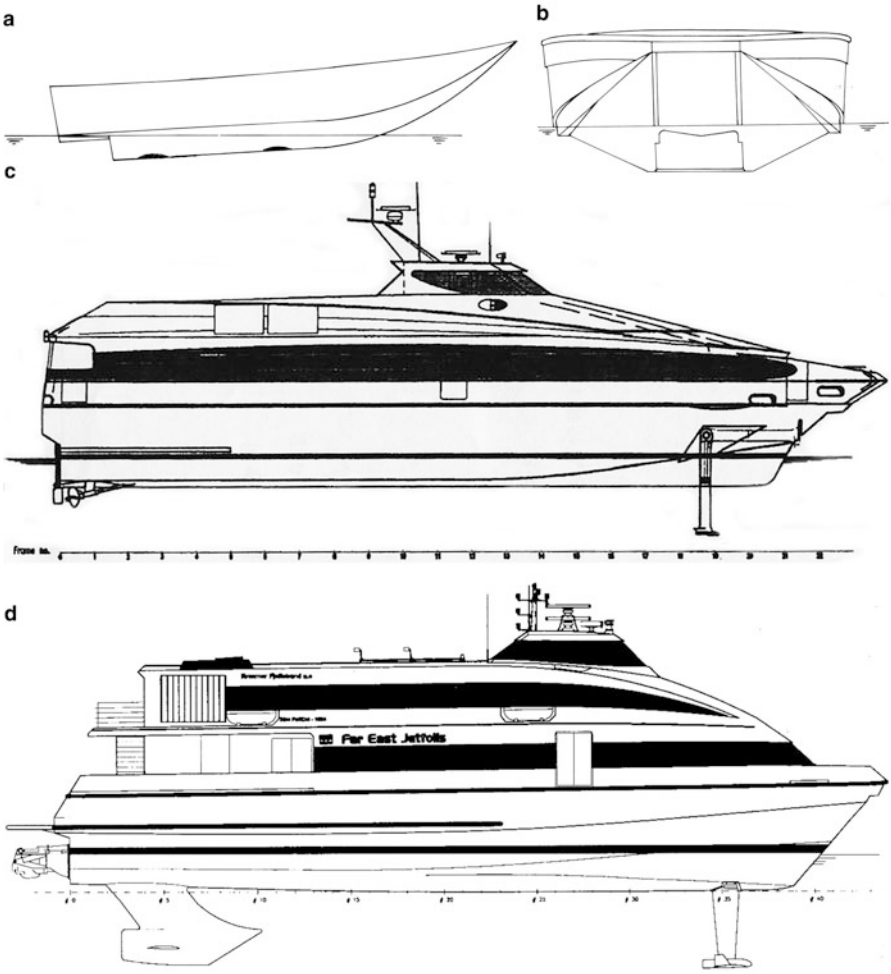

Fig. 10.29 (**a**) Profile of hydrofoil planing catamaran; (**b**) transverse section of HPC; (**c**) FACAT configuration; (**d**) Foilcat configuration

Experimental investigation of a HPC modified from the earlier tested TPC models was also carried out at Harbin Engineering University [15]. The test models were the same as TPC model C. The influence of hydrofoils with the same configuration and installed angle, but with different locations on the model and different model LCG, as well as a different static load coefficient, on drag in calm water were investigated. The test conditions of both TPC and HPC models are listed in Table 10.6.

The test results, presented in Figs. 10.31, 10.32, and 10.33, are as follows:

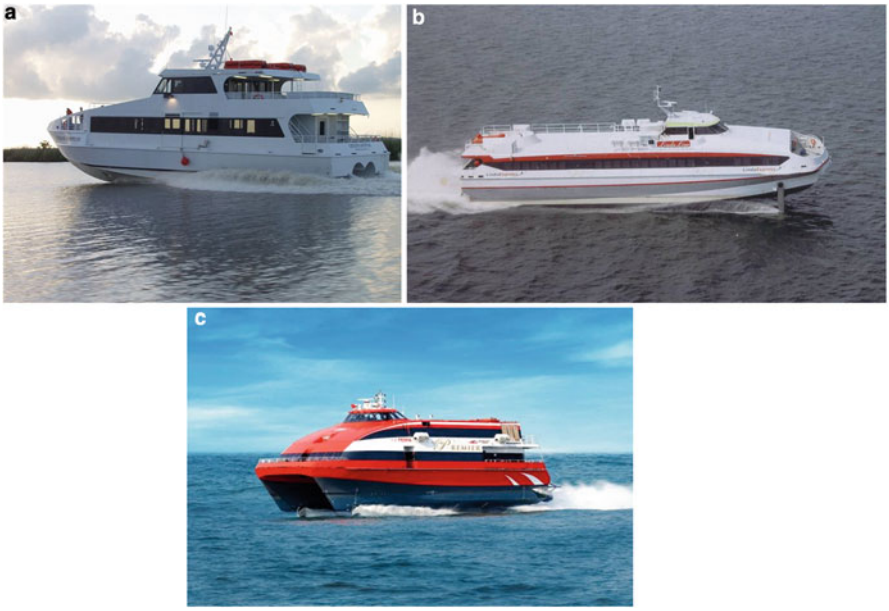

Fig. 10.30 Catamaran Foil assistance configurations: (**a**) Hysucat – Catalina Adventure; (**b**) FACAT; (**c**) Foilcat from HK

Table 10.6 HPC test model scaled characteristics

Craft weight (t)	Location of CG, x_g/L_c	TPC (without hydrofoils)	Hydrofoils at section numbers 4 and 10	Hydrofoils at section numbers 4.5, and 10	Hydrofoils at section numbers 4 and 9.5
4.87	−0.177	3C20	3C19		
5.70	−0.161	3C02	3C04		
5.70	−0.177	3C20			
5.70	−0.191		3C09		
5.70	−0.194	3C01	3C03	3C05	3C06
5.70	−0.205	3C07	3C08		
6.50	−0.177	3C22			
6.50	−0.194	3C21			
7.40	−0.165		3C11		
7.40	−0.170	3C23			
7.40	−0.172		3C10		
7.40	−0.190		3C12		

1. Figure 10.31 shows the comparison of resistance of HPC with TPC models in calm water, and it is found that the HPC resistance is lower than the TPC's at every running condition. Different results are obtained in the case of different

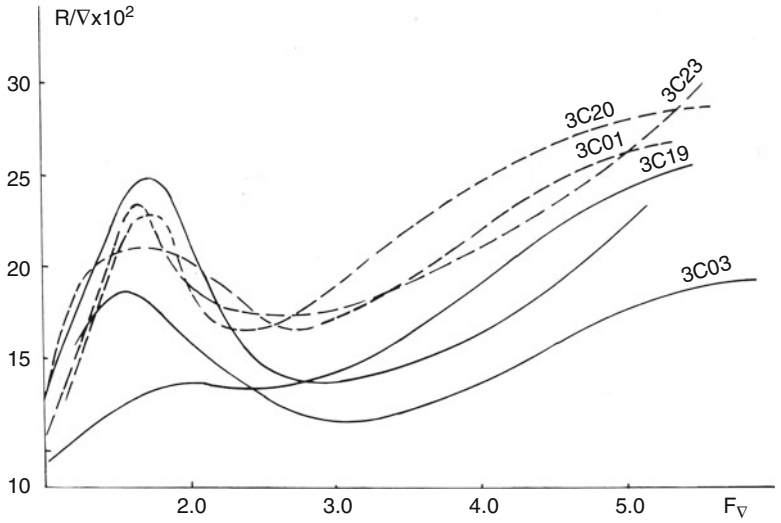

Fig. 10.31 Drag comparison of HPC with TPC models

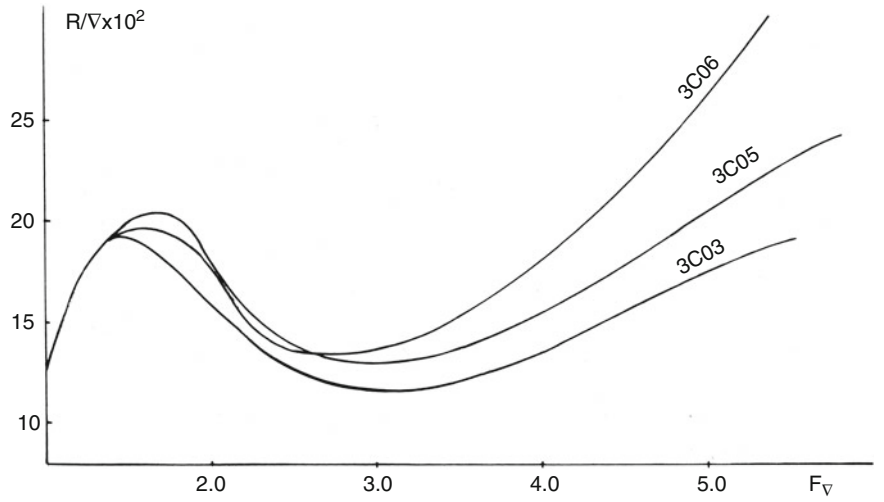

Fig. 10.32 Influence of hydrofoil location on drag

locations for hydrofoils. The maximum decrease of drag is up to approximately 25–35% compared to the TPC after takeoff.

2. Figure 10.32 shows the influence of hydrofoil location on the model drag, and it is found that there is an optimum location for the hydrofoil, which will decrease drag significantly after takeoff (test case 3C03).

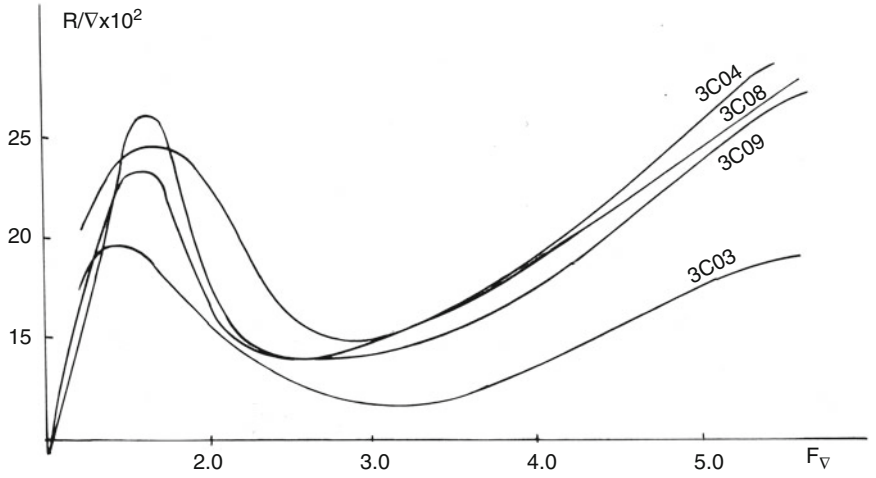

Fig. 10.33 Influence of CG on drag

3. Figure 10.33 shows the influence of LCG on model drag, and it is found that drag is very sensitive to the LCG position, both before and after takeoff. This is similar to other dynamic supported craft. Considering this result from the point of view of foil position relative to LCG, the optimum position of the main lifting foil relative to LCG is an important design parameter.
4. In the case of TPC with well-designed hydrofoils, the drag will be decreased considerably, particularly in craft with a low static load coefficient.
5. HPC designers may be able to optimize performance accounting for varying LCG positions between light weight and fully loaded vessel by adjusting the location and relative dimensioning for fore and rear hydrofoils. It should be noted that a planing craft will also have a changing center of lift as speed increases, and so depending on the proportion of total lift planned to be taken by the foils, the optimum relative position of the foils to the LCG may change.

The study of hydrofoil-supported catamarans has been a focus of Prof. K.G.W. Hoppe and his team at the Marine Engineering Department of the University of Stellenbosch in South Africa since the late 1980s. His work has focused on configurations similar to that of the HPC described earlier, and he has applied the principles to the design and construction of a significant list of projects [16, 17]. Professor Hoppe has investigated various configurations of main lifting foils and support stern foils through analysis and many model tests. Following a systematic initial series of model tests, it was possible to identify configurations of foils that would reduce the drag of a planing catamaran by 30–40% compared with the so-called bare hull catamaran. In addition, the interactions of the foils, primarily the main lifting foil as it passes through waves, were found to stabilize heave motions, giving a smoother ride than the bare hull.

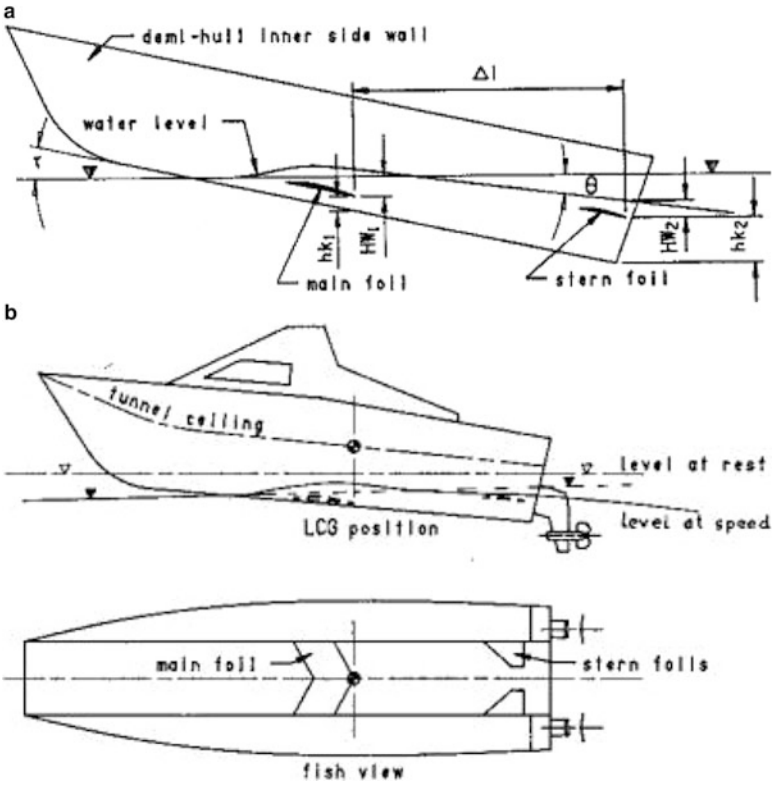

Fig. 10.34 Hysucat diagrams (**a**, **b**)

How does the improvement occur? The reason is that the ratio of drag/lift for a hydrofoil is typically 0.03–0.05, while the same ratio for the planing hulls of a catamaran is 0.25–0.3, a difference of 10 times.

The lifting foil cross section may be a thin "airfoil" section or a c-type section with sharp leading edge. Since the foils operate close under the water surface, the suction pressure over the upper surface will lead to cavitation or air entrainment. The sharp leading edge ensures a stable operation when in the cavitation regime. It may be noted that for effective lift, the immersion of the main foil H_w should be greater than 20–30% of the foil chord depending on the exact foil profile since when immersion is decreased toward the surface, the lift force rapidly declines. This favors a deep V hull section shape as the foil needs to be at or above the keel line for safety.

Professor Hoppe's Hysucat concept is shown in Fig. 10.34a, b. There is a main foil just in front of the LCG and two horizontal or canted fin type foils close to the stern. The forward foil is set above but close to the keel of the demihulls. The trim control foils are set higher and should be consistent with the vessel having a trim similar to the planing trim of the bare hull (except the hull with foils will ride higher

in the water). In larger craft, the rear foils can be actively trimmed to allow for shifting LCG.

The approach taken by Prof. Hoppe to vessel design is outlined in an extensive paper [16] and follow-up [17]. Owing to the complexity of combining the elements of a catamaran and the foils, a combination of analysis and model testing is used. Initially the catamaran base design is prepared, to conform to the payload and other mission requirements and static stability. Following a choice of potential lift support from foils in the range 20–40%, the foil geometry is selected and overlaid on the hull geometry. If the base catamaran design is fixed (perhaps an existing vessel, like many of the projects that have been completed so far by Prof Hoppe's organization), the potential lift proportion will also be limited. If the vessel is a new build, then it is possible to optimize by adjusting the width between the demihulls.

A further explanation of design development and optimization is given in [18] presented to the conference *FAST 95* in Germany. The planing hull hydrodynamics are determined using the semi-empirical methods of Savitsky [19–21] to identify lift, drag, and centers of effort at different trims, hull wetted lengths, and so forth based on the catamaran as a planing hull, but including the friction drag from the submerged vertical walls of the central tunnel.

The hydrofoil lift and drag forces and moments and the effects of interference with the hull are then determined based on data from Hoerner [22, 23] and data for airfoils interpolated from the (US) National Advisory Committee for Aeronautics (NACA) [24]. The effects of inclined flow on the rear foils is taken into account for the forces and moments on these. Once these data are available, a computer routine to determine the balance between forces on the hull from planing and those from the foils is iterated with draft reduced in steps from the hull-only case until equilibrium is reached for vertical forces and then further iteration for the moments accounting for the stern trim foils. The organization has calibrated the analytical procedure with model testing and with actual vessels. For these last, the changes in vessel mass and a number of other parameters as project build is completed had to be considered in a similar manner to the process to be discussed in Chap. 14. For hydrodynamic design purposes, the calibration to model tests is sufficient.

Foil Assisted Ship Technologies, led by Prof. Hoppe, has been involved in a sequence of projects since the 1990s that have built foil-supported catamarans as passenger ferries, utility vessels, and recreational vessels. A sample of four of these are shown in Fig. 10.35. It may be noted that where a vessel is converted, at service speed the vessel will ride higher in the water once planing. This may affect the propulsion system. A stern drive might be adjusted to be slightly lower on the transom to avoid excess ventilation. A waterjet system may have a tendency to intake ventilation in a seaway unless steps are taken to protect from this with longitudinal spray rails or extended keels. Underhull propellers could also see higher cavitation. The bottom line is to check out the propulsion system for the vessel riding at foil-borne draft in the specified seaway. This highlights the challenge in particular with the retrofit of a technology such as this. The concept clearly does have significant potential where it can be incorporated effectively.

Prout Panther 64

Sea Princess

Halter E Cat

Fig. 10.35 Hysucat Project photos: (**a**) Prout *Panther 64*, (**b**) *Sea Princess*, (**c**) *E Cat*, and (**d**) *Nordblitz ferry*

Nordblitz

Fig. 10.35 (continued)

On the US West Coast, designers Teknicraft have employed the technology to minimize the wake from fast catamaran ferries built by the shipbuilder All American Marine Inc. (see resources for links). Following its success in achieving wake reduction when passing an environmentally sensitive area on the route, the ferry operator Kitsap Transit has ordered two more such vessels for the Bremerton–Seattle route.

10.8 Air Cavity Catamaran

The wave-making drag of a catamaran decreases as the length/beam ratio and slenderness of the demihulls increase; however, the friction drag will increase due to increasing demihull wetted area. The optimum catamaran design speed is not too high, say $Fr_L = 0.6$–0.9 for displacement forms.

Using air cushion technology with a catamaran with a full depth cushion between the hulls and flexible seals at bow and stern as SES or air cushion catamaran is one method to reduce the friction drag during high-speed operation above $Fr_L = 1.0$; however, it does introduce machinery for a lift system and skirts with maintenance requirements that have limited its development and acceptance in the conservative marine market.

Many SESs have been built since the 1970s and have provided economical service as passenger ferries. The main operational limitation apart from the machinery issue has been that speed reduction in a seaway was significant. This was where the simple catamaran was able to show an advantage. Later SESs developed for rougher sea conditions had wider demihulls.

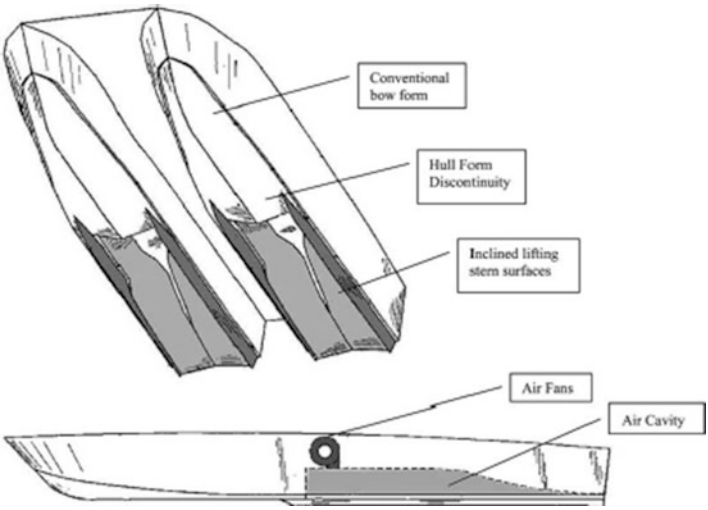

Fig. 10.36 Harley captured air bubble catamaran concept

The question that has arisen since then is whether the main cushion could be discarded and cavities placed at the lower demihull surface to reduce drag. This concept was developed and patented both in the USA and worldwide by Howard Harley in Florida, USA. SES Europe AS was established in 1997 for the purpose of introducing the new patented Harley skirtless SES technology outside the USA [25].

Figure 10.36 shows the configuration of the skirtless catamaran SES by Harley, and it can be seen that the craft comprises a planing twin hull, with planing surface at the bow, a step forward of amidships, and recesses at the rear part of the hulls with twin sidewall extensions on each demihull on the inside of slim inclined planing surfaces so as to form an air cushion in each demihull. The recesses represent 60–70% of the waterline hull length and extend all the way to the transom. The shape of the recess is a constant cross section for some length and tapering to the transom.

The longitudinal fixed keel extensions to the sidewall are also important details, with tests having shown how effectively the sidewalls entrap the air in the air cushion and minimise interaction with the propulsors.

From the figure one can see how the lift fan system is arranged and lift airflow fed into the air cushion during the operation of the craft; however, only 8–15% of the total propulsion power is required for the lift system instead of 20–40% of total propulsion power for a skirted SES owing to lower air leakage. The air will exhaust from the cavity via the transom or transom closure depending on the design, effectively reducing the wetted area of the hulls. Figure 10.37 shows model tests of skirtless monohull SESs in the towing tank of SSPA, Sweden.

Figure 10.38 shows an underwater photo of a catamaran SES model without skirt at 55 knots at full scale, showing the air cushion at the rear part of the model twin

Fig. 10.37 ASV monohull model test showing flattened wake

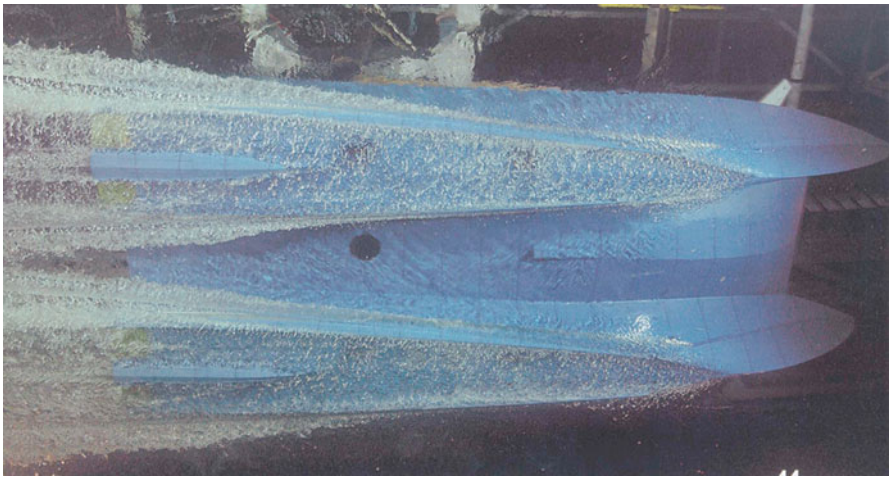

Fig. 10.38 Underwater photo of air cushion catamaran model under test modelling 70 knots

hulls, the air–water spray blown out from the transom, and sidewalls so as to lubricate the wetted surface and reduce the water friction. On this model also two central sponsons can be seen at the stern. This arrangement is convenient for stern-mounted Z-drive propulsion or surface drive. The configuration is not suitable for waterjet drive.

Performance in Calm Water

Based on speed/power measurements on the prototypes and model tests at the Stevens Institute of Technology in the USA and SSPA Sweden AB in Gothenburg, some key full-scale projected data can be given (Table 10.7):

Ride Quality

According to [25], practical observations during testing of the 8 metre and 17 metre prototypes indicate low motions and a soft, comfortable ride. No signs of a so-called

Table 10.7 Leading particulars for the SES without skirts

Length, L, m	7.93	16.77
Weight, W, kg	1600.0	11000.00
Speed, v, knots	45	46
Propulsion power, N_p, kW	84.5	275.7 × 2
Lift power, N_L, kW	13.2	73.5
Total power, N, kW	97.7	624.9
$F_{r\Delta}$	6.83	5.06
Hydrodynamic efficiency		
$K_\eta = \frac{p \cdot v}{N} \left(\frac{\text{kg·km/h}}{\text{kw}}\right)$	3.71	4.08

Fig. 10.39 Wash and wake of SESEU catamaran prototype at 45 knots

cobblestone effect or similar uncomfortable behavior normally seen on conventional SES vessels have ever been observed on either the prototype or the tank testing model. In addition, the impact loads for the craft will be lower than that on a conventional planing hull.

Low Wash And Wake

Figure 10.39 shows the wash and wake of the prototype catamaran in trials. Since most (70–85%) of the hull is lifted out of the water, the surface wave pattern characteristics will be favorable compared with a conventional catamaran. In addition, the demihull beam is smaller than the cushion of conventional SESs, so the surface wave pattern will be generated by the two demihulls rather than the whole vessel beam as with a conventional SES, which has resistance from the catamaran-like side hulls and from the central cushion depression.

For an SES

$$\frac{R_w}{W} = \frac{C_w p_c^2 B_c}{\rho_w g W}, \tag{10.2}$$

where

C_w Wave-making drag coefficient;
p_c Air cushion pressure;
B_c Cushion beam;
R_w Wave drag;
W Weight of craft.

Since the cushion beam will be lower than that of a conventional SES owing to the twin air cushions, the cushion-induced resistance will be much less and the effect of the cushions on the height of the surface wave pattern to the stern of the catamaran should be low.

According to tests, at 40–45, knots this 11-t prototype generated no more than approximately 20 cm wave height at a distance of approximately 30 m from the centerline of the boat (Fig. 10.40). This compares with Fairline or Princess fly-bridge monohulls of the same size, where the wash and wake may exceed 80–100 cm at the top speeds of approx. 28–30 knots.

Note that this concept has also been studied for a long time in Russia [26] for the purpose of improving performance of high-speed vessels in the calmer waters of Russia's extensive rivers and lakes, though mainly applied to monohull vessels rather than catamarans.

The main challenge for this type of craft is the propulsion system operation below the air cushion. The prototypes have demonstrated successfully that drag and powering can be reduced. The concept may well be useful for craft where a complex hull geometry can be formed economically (GRP or CFRP) while large craft in aluminum may become quite a bit more costly. The concept is therefore more suited to smaller vessels requiring a high dash speed.

The use of an air cushion in an underhull cavity to reduce drag can be attractive if the sea conditions for vessel operation are not too challenging. Interisland coastal, lake, or river environments may well be attractive. At more exposed locations, such

Fig. 10.40 SESEU monohull at speed

as where many offshore wind farms are located, the challenge is at a different level. We introduced the SWATH and semi-SWATH configurations that are already in service in Chap. 9. These vessels have service speeds in a range of 20–30 knots maximum. Umoe Mandal has designed and put in service a somewhat faster vessel at the same size of 27 m LOA; it is a full traditional SES with a maximum service speed of 40 knots, as shown in Fig. 10.41 and Table 10.8. While it is clear that the full SES has more complex machinery, including ride control systems and flexible skirts at the bow and stern, for some more remote wind farms the higher speed for personnel delivery may well balance out the overall service provision accessibility and create positive economics. The motion performance during loiter or when docked offshore can also be optimized using variable-geometry lower hull form as for the single-strut SWATH form, so further possibilities for development do exist as operating experience is gained.

10.9 Concept Review and Selection

We have looked at a range of concepts in this chapter, primarily from the viewpoint of hydrodynamic performance. Moving from adjustments of the basic catamaran form, simple lengthening to super slender catamarans has been shown to "fit" with a number of applications such as passenger ferries for rivers and passenger/vehicle ferries. The large trimaran has already found application in exposed environments for both commercial and military uses at high speed.

The hybrid concepts we have looked at show promise, though perhaps in more niche markets. The hydrofoil-supported catamaran can clearly deliver economy for operation in seaways at speeds up to Fr_L 2 or more (Fr_v up to 5). At really high speeds, the "split hull" TPC can be designed for efficient operation up to limits way beyond commercial use with judicious employment of the stepped form and careful aerodynamics for the upper hulls and cross structure.

Racing designers in Florida have taken this art to a high level with low SS speeds up to around 170 knots for Class 1 racing catamarans running with gas turbine power and surface drives.

Some options or combinations seem to add complexity without contributing desired performance improvements. We hope that the insights here will be helpful to readers to avoid projects that have too wide a range of specification options.

The different concepts perhaps represent a toolbox to work with. Let us leave this at that point, before we move on to a discussion of projects and development in Chap. 14, after we have looked at the integration of appendages, propulsion systems, and vessel structural options. Readers may wish to jump forward to that chapter and then return to the detail of the next three chapters to consider them in the context of fitting an overall project together. Once you embark on this more detailed phase, a great deal more work must begin to follow overlapped timescales and become time dependent because of the delivery commitments and the financial constraints that impose themselves on the project. Team work is therefore a key to success!

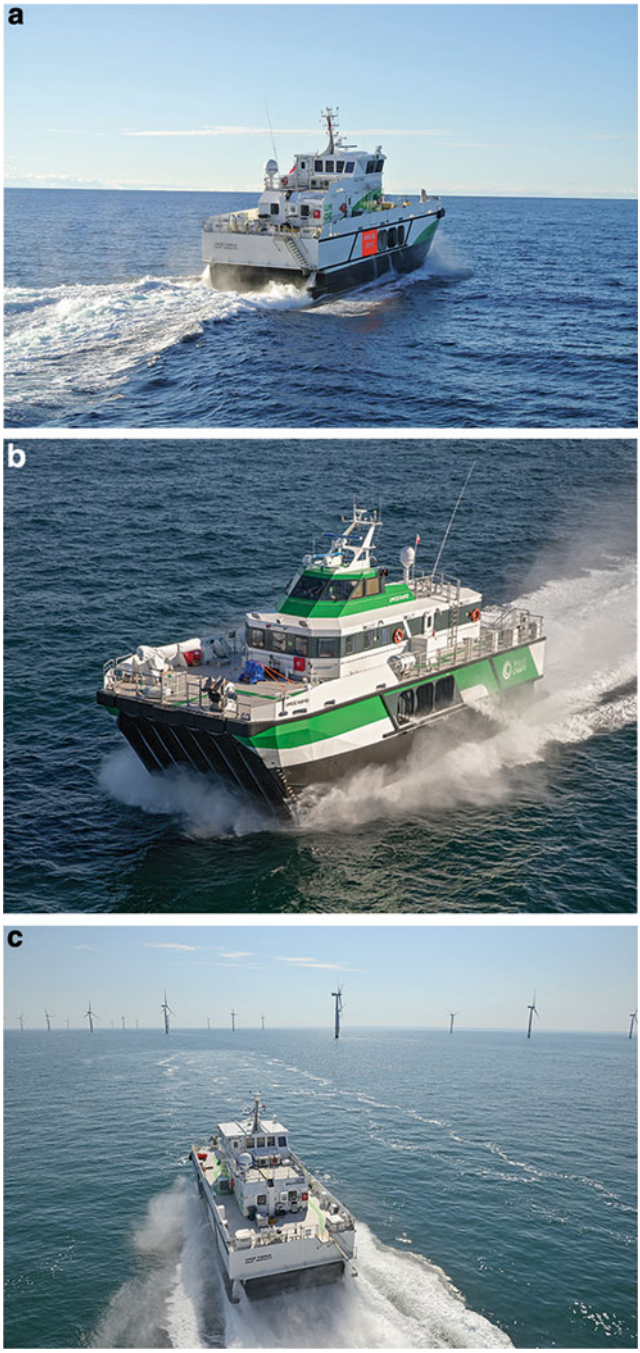

Fig. 10.41 (**a**) Wavecraft Commander SES stern view; (**b**) bow view; (**c**) UMOE SES approaching London array wind farm at speed

Table 10.8 Key data UMOE Wavecraft Commander 27-m offshore wind service SES

Length, LOA, L_{WL}	m	26.6, 23.9
Beam	m	10.4
Draft on cushion	m	0.8
Draft off cushion	m	3.0
Displacement nominal	t	250
Speed, *v*, max, cruise, @1.5 mHs	Knots	42, 38, 30
Fr_L		1.41, 1.28, 1.01
Max. service sea state, Hs	m	3 (2.5 m sig for transfer)
Propulsion power, N_P	kW	2 × 1440
Lift power, N_L	kW	2 × 360
Auxiliary power	kW	2 × 65
Crew		3–4
Passengers, regulated (maximum)		12, 24
Payload total deadweight	te	15
Cargo capacity	te	4
Propulsion		2 × waterjets

References

1. "Cougar 58 f. Catamaran", High speed surface craft, Dec 1982
2. "Cougar Marine plans attempt on Blue Riband", High speed surface craft, Mar/Apr 1985
3. Su YC, Zhao LA (1991) Experimental investigation and analysis on the hydrodynamic performance of the planing catamaran. In: Proceedings of 5th domestic conference on HPMV, Cheng Du (in Chinese)
4. Sato R, Miyata H (1991) Hydrodynamic design of fast ferries by the concept of super slender twin hull. In: Proceedings of FAST 91, Trondheim
5. Nogami H, Miyata H, et al (1992) Fast car ferry by super slender hull. In: Proceedings of 2nd international conference on HPMV, Shen Zhen
6. Itabashi M , Michida R (2000) Performance of IHI SSTH-70 after delivery and future of SSTH, IHI Review
7. Bliault A, Yun L (2010) High performance marine vessels. Springer, New York, USA, ISBN 978-1-4614-0868-0
8. Armstrong NA, Moretti V (2010) The practical design of a 102m trimaran ferry for Taiwan Strait. In: Proceedings, Shanghai HPMV conference, Apr 2010, Shanghai
9. Pattison DR, Zhang JW (1995) Trimaran ships, transactions RINA, The Royal Institution of Naval Architects, London, England, vol 137, pp 143–161 ISSN 0035-8967
10. Armstrong NA, Holden K. A new generation of large fast ferry – from concept to contract reality. In: Proceedings FAST 2003, Athens
11. Lu Q et al (1999) Theory and technical features of planing triple hull. In: Proceedings of 8th domestic conference on HPMV, Apr 1999, Yang-Zhou (in Chinese)
12. Trials programme of M80 starts in California, Fast Ferry International, Mar 2006
13. Gee N, Dudson E, Marchant A, Steiger H. The pentamaran – a new hull concept for fast freight and car ferry applications. BMT Nigel Gee and Associates, Technical paper 09
14. Gee N, Gonzalez JM, Dudson E. The Izar pentamaran – tank testing, speed loss & parametric rolling. BMT Nigel Gee Associates, Technical paper 21

15. Zhao LA, Su YC (1991) Investigation on hydrofoil-planing catamaran. In: Proceedings of 5th domestic conference on HPMV, Nov 1991, Cheng Du (in Chinese)
16. Hoppe KGW. Performance evaluation of high speed surface craft with reference to the Huysucat development, Research Report 1990, published in tow pasrts in Fast Ferry International January 1991 and April 1991. Also available on Hysucraft internet site
17. Hoppe KGW. Recent applications of hydrofoil supported catamarans, published in Fast Ferry International, September 2011. Also available on Hysucraft internet site
18. Hoppe KGW (1995) Optimisation of foil supported catamarans. In: Proceedings FAST 1995, 25–27 Sept 1995
19. The experimental investigation on resistance & seakeeping quality of high speed catamaran, Shiro Matsui, Fast'93, 1993, Yokohama
20. Pham XP, Kantimahanthi K, Sahoo PK. Wave resistance prediction of hard-chine catamarans through regression analysis. In: 2nd international European conference on high performance marine vehicles (HIPER 2001), Hamburg, pp 382–394
21. Sahoo PK, Salas M, Schwetz A (2007) Practical evaluation of resistance of high-speed catamaran hull forms—Part I, Ships and offshore structures. Taylor and Francis, 2:4, pp 307–324. Also available by download from University of Tasmania at www.eprints.utas.edu.au/3601
22. Sahoo PK, Mason S, Tuite A (2008) Practical evaluation of resistance of high-speed catamaran hull forms—Part II, Ships and offshore structures. Taylor and Francis, 3:3 pp 239–245. Also available by download from University of Tasmania at www.eprints.utas.edu.au/7731
23. Hoerner SF, Borst HV (1992) Fluid dynamic lift, 2nd edn. Author, USA, ISBN-13: 978-9998831636
24. Abbot IH, von Doenhof AE (1959) Theory of wing sections. Dover Publications, USA, ISBN-13: 978-0486605869
25. Tudem US (2000) New SES technology-without flexible skirts. In: Proceedings of HPMV'2000 China, 19–23 Apr 2000, Shanghai
26. Sverchkov AV (2010) Krilov shipbuilding research institute, "Application of air cavities on high speed ships in Russia", paper 11. In: International conference on ship drag reduction (smooth ships), Istanbul

Chapter 11
Propulsion and Appendages

11.1 Introduction

We start this chapter by pointing out that a preliminary vessel form has been developed, and a resistance curve in calm and operational conditions has been determined. The aft hull form will take some account of typical dimensions for power units and the intended propulsion device. An initial check is made that there is space in the demihulls to fit the main machinery. Here, we look at the selection and matching process between propulsor and power unit and discuss the design requirements that affect specifications for the suppliers and the design of the engine room area. We will discuss the collation of necessary data on main machinery and the selection and matching of propulsion – propellers and waterjets – with the hull and the machinery. We will also take a look at appendages used for directional control. Fast multihulls operating in open coastal conditions often use stabilizing foils to provide motion damping and tabs or interrupters at the stern to adjust running trim. We touch on these later in the chapter based on recent papers and give supplier references.

First, though, a little background. There are a number of detailed sections in naval architecture textbooks and comprehensive papers on propellers and waterjet propulsion that can form the basis of a study of physical theory and design [1–7]. In addition, several investigations of the integration of waterjets and propellers with hulls to achieve the best possible efficiency have been published in the last two decades. We will give just a brief introduction to the theory of propellers and waterjets and summarize recent research contributions available to us; the references give a more comprehensive treatment. Our objective here is to provide sufficient guidance to select and match machinery that integrates with the vessel design objective and to give references for the reader to follow up on the theoretical side as necessary and work with specialists for detail design.

Analysis and design for propulsion have moved forward from dependence on analytical models supported by cavitation tunnel testing to include the use of

L. Yun et al., *High Speed Catamarans and Multihulls*,
https://doi.org/10.1007/978-1-4939-7891-5_11

computational fluid dynamics (CFD) using solid element finite-element (FE) analysis on computers. Depending on the software used, it is now possible to model vessel hulls with a surrounding water body and an air body above it in a time domain so as to look at fluid flows around a hull and through a propeller or waterjet, either as a propulsion disc representation or a more complete model (see resources, under *propulsion* and *propellers*). The flow through a waterjet can also be modeled with the static machinery for ducting and rotor/stator optimization.

These models are complex and while the FE CFD model can be built using a laptop computer, the time domain solution runs really require higher-level hardware and still (at the time of writing) can take hours to run. Running a series of parametric variations can therefore absorb days of computer time. That is not to imply that CFD is impractical for the individual; there is even some open-source code available suitable for simpler modeling (see resources under *software*). The most likely approach to be taken in such a case is to obtain propulsor characteristic data from the supplier and model the inflow pattern around the propeller or into the waterjet intake so as to investigate the interaction with the stern area of the vessel hull and adjust if necessary. Waterjet and propeller suppliers will then provide support to a client to optimize the propulsor with the hull design. It should be pointed out, though, that the propulsion system vendors are dependent on the vessel designer for the assessment of thrust required for the intended service speed.

The advantage with CFD is that models can be full scale and so do not have the limitation of a free-running hydrodynamic test tank model where Froude scaling can be reliable but the Reynolds number is not scaled. Processes that are primarily related to turbulence in the fluid can therefore be better addressed through CFD.

As mentioned, our starting point is a vessel resistance curve and the hull lines. To translate that into a selection of main machinery, it is necessary to have an initial estimate of the efficiency of the propulsion system at service speed. An open propeller may initially be assumed with an efficiency in the region 0.55–0.65, while waterjet overall efficiency may be slightly higher at 0.65–0.75, including losses due to interaction with the hull. There will be small losses in addition due to the gearbox and transmission, but these may be balanced by system optimization of the hull and propulsor itself, which we discuss in what follows. Once an engine match has been selected for service speed and the propulsor is sized and characteristics defined, it will be possible to look at the operating envelope of thrust and power through the speed range. This will show the margin for acceleration at any speed and verify it is sufficient through the drag hump for vessels intended to operate into the planing region.

Once the engine and propulsor selection has been confirmed, attention can turn to the detailed specifications for the machinery spaces. Requirements are specified by the IMO in the international regulations for high-speed craft (HSC) [8] that have a strong influence on the system design and so we summarize our interpretation of these at the end of the chapter.

11.2 Propellers

Introduction An open-water propeller generates thrust by adding momentum to the water that passes through it. If we consider a diagram of flow streamlines, velocity, and pressure, as in Fig. 11.1, it can be seen that at the propeller disc energy is added giving thrust T. Leading up to the disc velocity is increasing so that dynamic pressure is increasing and static pressure decreasing, in accordance with the Bernoulli equation. Aft of the disc the velocity increases again by an equal amount. The streamlines contract in to the propeller disc and further as they move aft behind the disc until the stream velocity $V = V_a\,(1 + 2a)$ is reached.

The useful work done by the propeller disc is $T \cdot V_a$, while the actual work (or power absorbed) is $T \cdot V_a\,(1 + a)$, and so the efficiency of the disc is the ratio

$$\eta = T \cdot V_a/(T \cdot V_a(1 + a)) = 1/(1 + a).$$

To generate thrust, a propeller has a number of blades with a cross section in a circumferential direction that is similar to a thin airfoil. The foil rotates and has an angle of attack relative to the spiral of its motion in the water as the vessel it is propelling moves forward. The axial vector of its lift force equates to the thrust, while the tangential vector (the drag) represents the torque that has to be applied to drive it.

If we ignore the blades themselves for a moment and just consider the rotational motion they impart, ω, at the disc, there will be another inflow that generates a torque; thus,

$$Q = Ip(\omega_2 - \omega_1) = Ip \cdot \omega(1 - 2a'),$$

where ω_1 and ω_2 are the initial and final rotational velocities of the stream flow. Far upstream $\omega = 0$ and, following a similar logic to the axial induced velocity, the fluid

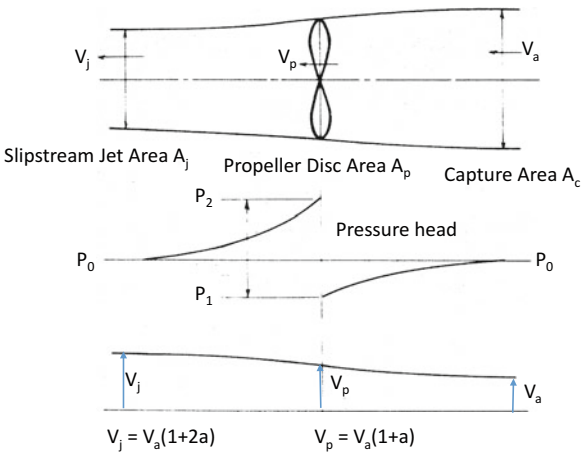

Fig. 11.1 Stream Flow Momentum diagram for propellers

will acquire half its rotational velocity at the disc, so while the disc rotates at ω, the fluid relative rotational velocity will be equal to $\omega \cdot (1 - a')$.

The propeller disc energy balance between torque and thrust is then

$$dT \cdot V_a(1 + a) = dQ \cdot \omega \cdot (1 - a'),$$

so that

$$\eta = dT \cdot V_a/(dQ \cdot \omega) = (1 - a')/(1 + a).$$

Thus an idealized screw propeller will have reduced efficiency in direct proportion to the induced rotational velocity at the disc, in addition to the loss due to the axial velocity inflow at the disc, as shown previously.

If the flow were in an "ideal" fluid, there might be no losses in the system other than those due to the accelerated flow relative to the vessel speed and the rotational losses above. Ideally, if the water screw could operate without any velocity increment, efficiency would be 100%. In this case, at zero speed there would be zero thrust and the vessel could not accelerate. If we look at the theoretical efficiency at different ratios of vessel velocity to jet velocity V_s/V_j, we would obtain efficiency as shown in the plot in Fig. 11.2.

In Fig. 11.2 it can be seen that as the axial velocity increment increases, without including other losses, efficiency reduces almost linearly. If system losses due to real fluid flow around the propeller blades are also included, a further reduction in efficiency is experienced. In addition, the performance with varying jet velocity has a peak that occurs at higher jet relative velocity as other loss factors increase.

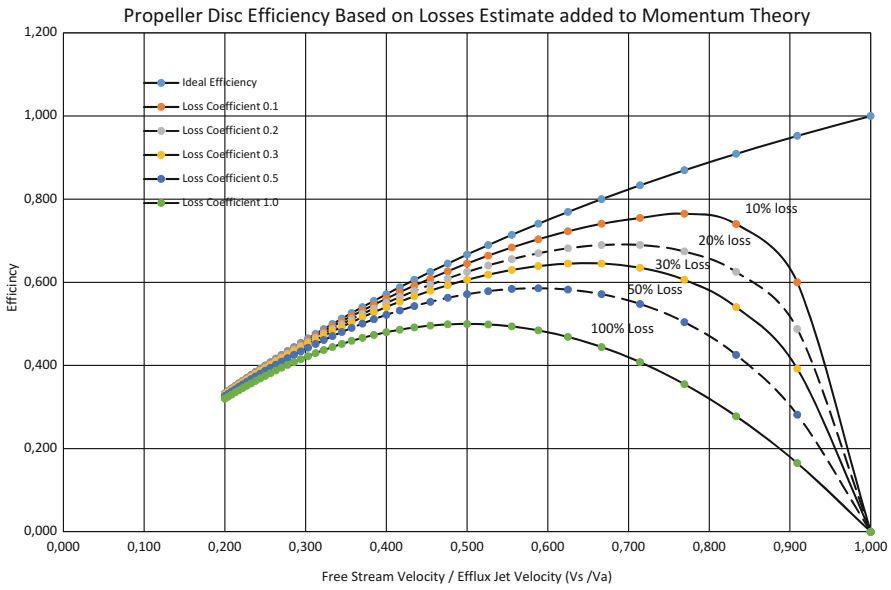

Fig. 11.2 Momentum efficiency diagram

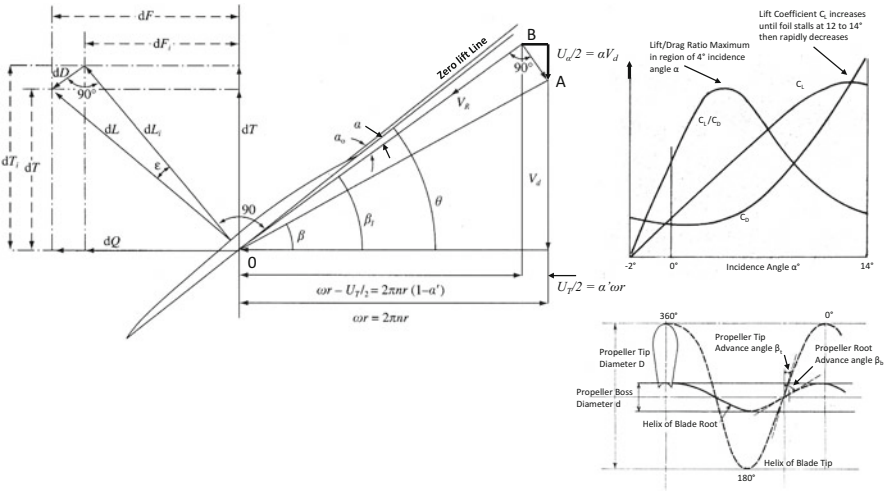

Fig. 11.3 Blade velocity diagram and inset advance spiral, and lift and drag with blade incidence

Typically total losses may be of order 30%, and so the ideal ratio V_s/V_j may be 0.65 and the propeller efficiency around 0.63. Thus, compared to the estimate of vessel total drag, the effective power required from the selected main engine will be an increment of 60%.

So far we are able to get a feel for the efficiency of an ideal open-water propulsor, but how can we move forward to select an appropriate diameter, number of blades, rotational speed, and investigate interaction with the hull of a vessel? For that we need to look at the action of propeller blades in a real fluid. Turning back to how the changes in axial and rotational momentum from actuator disc theory relate to an individual blade, consider the section of a propeller blade and its velocity diagram (Fig. 11.3).

If we consider the propeller blades' spiral rotation, the blade advance should match the spiral. In this case, the vector formed by the axial fluid velocity V_a and the tangential velocity of the blade ($n \cdot \pi \cdot D$) should match. In this case the lift and drag generated by the foil section would be perpendicular and in line with line 0A in the diagram. In order for the foil to generate lift so as to induce the pressure increase across the propeller advancing "disc," it must be oriented with an angle of attack relative to the oncoming flow (angle α). Maximum lift for a thin foil may be at, say, 4° [9, 10]. Since in the axial direction V_a is increased by ($V_a \cdot a$) and the relative rotational velocity is reduced by (($n \cdot \pi \cdot D$) $\cdot\, a'$), the true angle of attack will be reduced from ($\theta - \beta$) to ($\theta - \beta_1$). The lift and drag forces resolve by angle β_1 to the thrust and torque (dT and dQ).

To determine the total thrust and torque from a finite number of blades, the forces on an element are integrated over the radius (Fig. 11.4). Partly owing to the typical spoon-shaped blade geometry, the majority of the thrust is generated on the outer part of the blade with the centroid at approximately $r = 0.7R$.

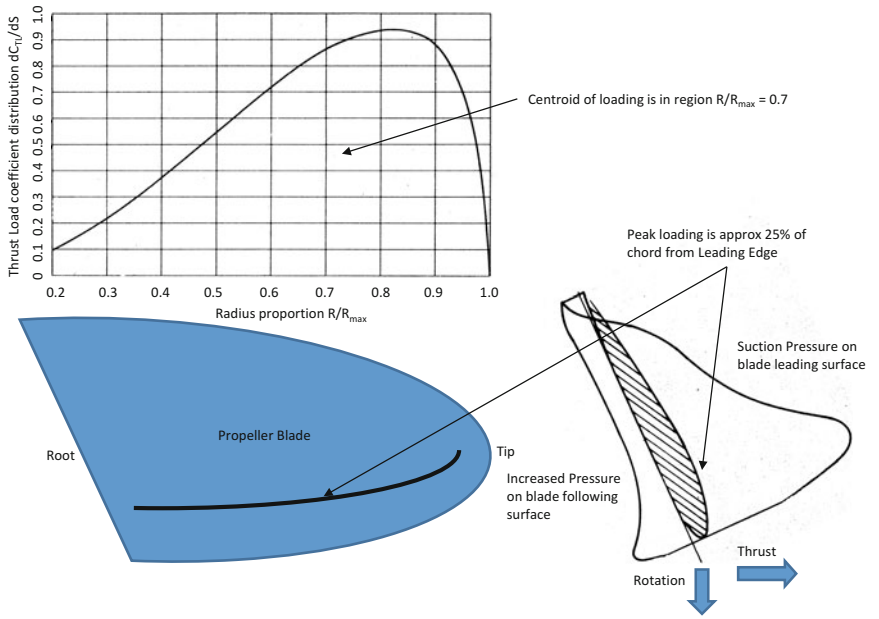

Fig. 11.4 Blade force integration over radius diagram with blade section pressure profile

The blades of a propeller operate as lifting foils, also in a cascade. In a real fluid, a foil will have vortex or circulation flow around the section generating increased pressure on the undersurface and reduced pressure on the upper or forward surface (see section profile in Fig. 11.4, bottom right). In addition, vortices will be generated at the outer edge of the blade. Energy is used in generating the vortices and circulation in addition to the friction force exerted through the blade boundary layers, thereby reducing the efficiency further from the actuator disc estimate.

Determination of performance of a propeller in a real fluid has until recently required scale models to be built and tested in a closed circulating water tunnel (a cavitation tunnel) and the resulting torque and thrust scaled to the prototype. Similar to scaling for ship resistance, nondimensional relationships have been defined to enable a model to be representative, as follows [4]:

$$\text{Advance Ratio}\, J = V/n \cdot D \quad \left(\text{absolute advance ratio}\, \lambda = V/(\pi n D)\right),$$

$$\text{Thrust Coefficient}\, C_\text{t} = T/\left(0.5\rho A_\text{p} {V_\text{a}}^2\right),$$

$$\text{Power Coefficient}\, C_\text{p} = P/\left(0.5\rho A_\text{p} {V_\text{a}}^3\right),$$

$$\text{Thrust Coefficient}\, K_\text{t} = T/\rho \cdot n^2 \cdot D^4 = C_\text{t}\left(\pi J^2/8\right),$$

$$\text{Torque coefficient}\, K_\text{q} = Q/\rho \cdot n^2 \cdot D^5 = C_\text{p}\left(J^3/16\right),$$

$$\text{Propeller Efficiency} = \varepsilon_0 = (J/2\pi)\left(K_\text{t}/K_\text{q}\right) = C_\text{t}/C_\text{p}.$$

By testing a series of geometrically similar propellers with varying blade-area ratios compared to the disc area, blade-section geometry, and outline shape, their characteristics can be plotted. During the twentieth century, such so-called standard series data were developed at a number of marine research institutes in Europe and the USA, allowing designers to rapidly home in on propeller diameter, blade number, and loading that would have minimum risk of cavitation during service speed operation.

The designer will choose a power loading at vessel operational speed and from this identify P/D and J, allowing K_t, K_q, and efficiency to be identified and, thus, the actual power absorbed. Some iteration may then be required to select a combination of diameter and rotational speed that gives a reasonable efficiency while staying within the area to avoid significant face or back cavitation. An example pair of charts is shown in Fig. 11.5a and the selection flowchart in Fig. 11.5b.

For vessel speeds up to about 35 knots, this approach can be successful. Typically a three- or four-blade propeller can be selected. Above 25 knots, a propeller will operate with tip vortices that may also generate cavitation, but with careful selection this can be minimized.

At higher speeds avoidance of cavitation is not possible. Pressure reduction occurs as a rapid decline behind the blade leading edge (Fig. 11.6), and if this reduces to the water vapor pressure at that point, a cavity can form. At full scale it is found that propeller tip vortices begin to show cavitation at vessel speeds of 25 knots, and this can spread inward across the blade as speed increases further. Such cavitation can also be unstable. The result is a loss of thrust and vibration and potential damage to the propeller. As the volume of cavitation increases, interaction with the other blades will also become more significant, with further performance degradation.

Cavitation number at the propeller disc may be approximated by $\sigma = (P_a + \rho gh - P_v) / [0.5\rho\,(V_s(1 + a))^2]$, where P_a is atmospheric pressure, ρgh is water pressure head to propeller submergence, P_v is the local water vapor pressure, and $V_s(1 + a)$ is the axial velocity at the propeller disc. As axial induced velocity increases, that is, propeller loading increases, represented by T_c in Fig. 11.6, so σ decreases.

Above a certain speed depending on the blade loading and speed of advance J (Fig. 11.6), the cavitation will be initiated at the leading edge and will occur across the leading blade surface (suction surface). To minimize this, blades can be designed to overlap so that their surface area is larger than the actuator disc area, reducing pressure loading on the following surface. For medium-speed vessels up to 35 knots it is possible to select a combination of propeller size, blade-area ratio, and revolutions per minute so as to minimize cavitation, but above this a blade section encouraging steady-state full cavitation on the front surface is needed. Several blade geometries are available [6, 7, 11].

Once cavitation is present, care is needed in setting the geometry of the propeller, shaft supports, and both proximity to the hull underside and its shape so as to avoid the development of air entrainment down to the prop (re Suhrbier FAST 95) [12] and [13].

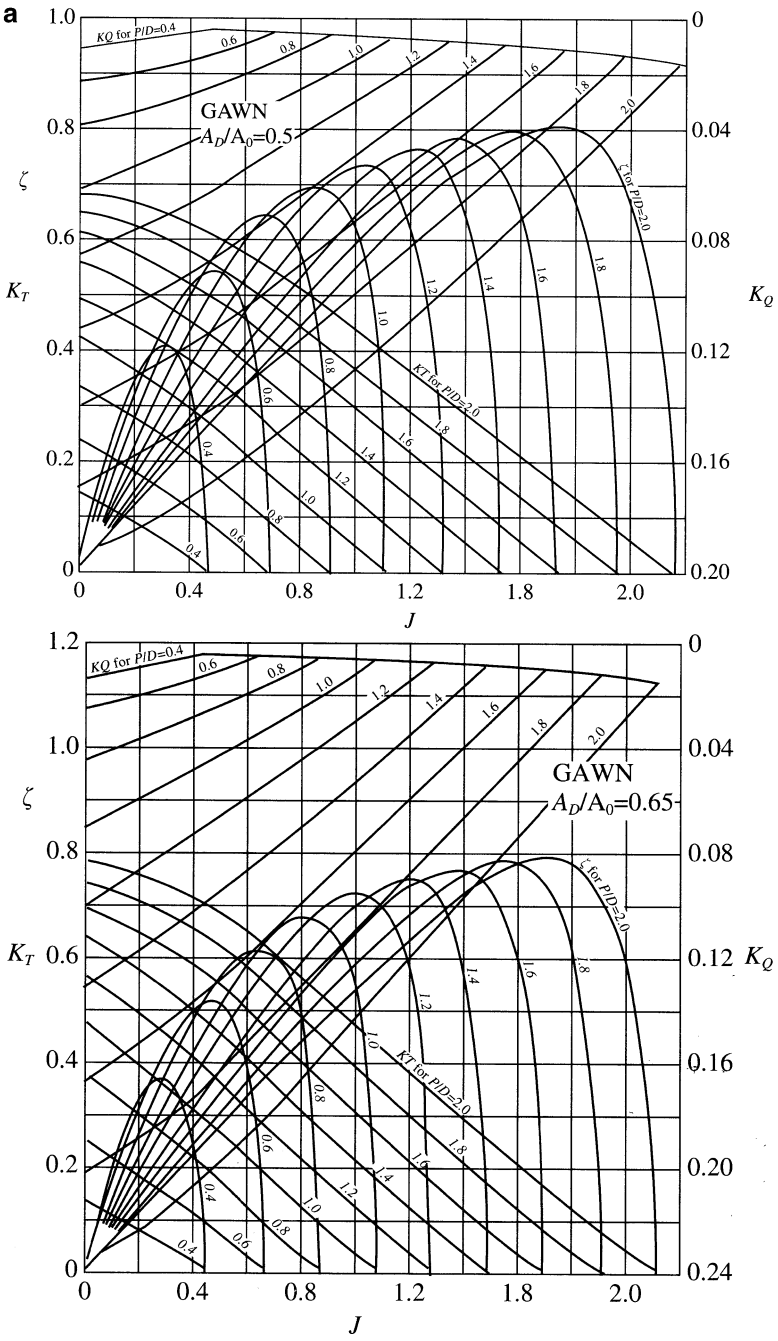

Fig 11.5 (**a**) KTKQ plots for AD/A0 0.5 and 0.65; (**b**) propeller selection procedure

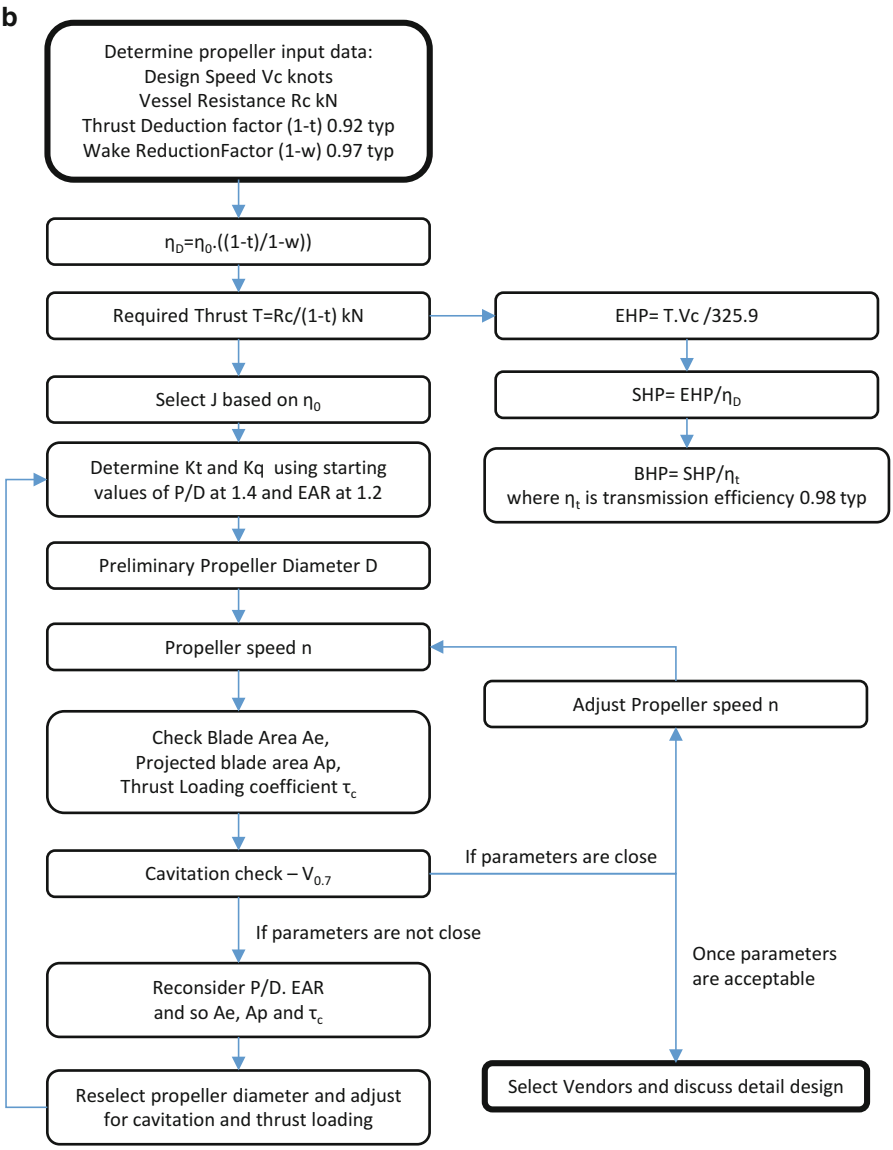

Fig 11.5 (continued)

A fully cavitating propeller operates with suction pressure across the back surface already at vapor pressure, and so higher thrust loadings can only be achieved through higher face pressure. The challenge is that the cavity fills part of the space between the blades, and by definition the pressure from the face of the next blade has to decline to vapor pressure at the cavity-free surface. This favors a smaller number of blades, so the Newton–Rader cavitating propeller series is based on three blade

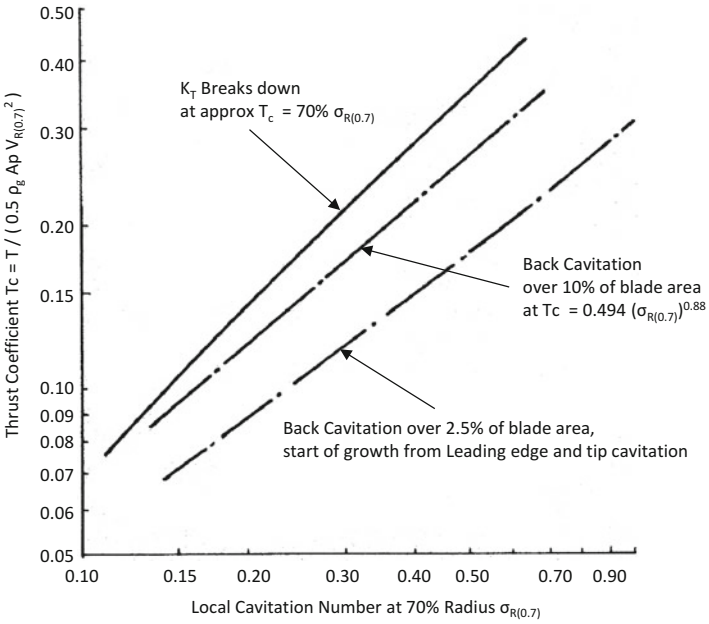

Fig. 11.6 Gawn-Burrill cavitation chart

propellers [11]. Servogear more recently developed a highly skewed blade design for vessels in the 25- to 50-knot speed range and more commonly use a four-blade design.

An approach to propeller selection similar to that described earlier in Fig. 11.5b is followed for fully cavitating propellers, starting with diameter and speed estimates from the desired loading and then iteration using K_t and K_q curves to achieve best possible service speed efficiency. The fully cavitating type of propeller leads to reasonable efficiency at vessel speeds up to about 55 knots, and if the propeller is designed to have controllable pitch (CP), it can also give a reliable thrust margin for transiting vessel hump speed through to planing.

If the vessel service speed exceeds 55 knots (Fig. 11.8), the option is to accept ventilation and instead place the propeller shaft line at the transom base with the propellers aft of the transom and use a blade section and blade-area ratio that works efficiently while the prop is operating fully ventilated – a surface drive [6, 7, 13].

A ventilated propeller operates near or at the water surface and may have a large central boss together with higher blade numbers than cavitating propellers if it is designed as a CP propeller.

Reference [6] describes the development of a propeller of this type absorbing 3300 shp for the US Navy test surface effect ship (SES) 100B craft with maximum speed close to 100 knots, while [13] details measurements on a ventilated propeller designed for another high-speed SES, the SES Corsair tested in Germany some years

later. This propeller was rated at 2090 kW for a vessel speed of approximately 40 knots.

In the commercial and racing world, stern drives with fixed-pitch ventilated propellers have been developed by Rolla/Twindisc, ZF, Francehelices, Flexitab, QSPD, MSA, and Levi (see Fig. 11.7, Table 11.1, and resources to Internet links). Such drives can be designed for vessels in a speed range of 50–100+ knots. The challenge for a designer is the efficiency of such propulsion and, thus, power installation and fuel consumption.

The SES prototype (SES 100B) propulsion described in [6] was found to work well for the power levels related to a 100-t displacement vessel (3300 shp), while scaling up for vessels in the displacement range of 3000 t envisaged for a full-scale SES warship was found to be difficult, and the design competition in the 1970s selected waterjets as the preferred option.

The fully ventilated propellers in the preceding table are designed to operate fully submerged below the waterline at low speeds, rather than having a large boss with its centerline at the static waterline (SWL) like the SES100B propellers. Some of the designs enclose the propeller in a partial cowling (MSA, Levidrives, QSPD, and Flexitab), which protects the propeller and guides flow somewhat. The flow regime through such propellers is nevertheless highly turbulent. Accurate performance evaluation is difficult "on paper" and depends on vendor guidance, particularly for assessment through the speed range.

A view of the application regimes of the different types of propellers discussed is shown in Fig. 11.8.

If a vessel is to operate at Fr_L below 0.4, then a "normal" noncavitating propeller can be selected. In the 0.4–0.8 region, cavitation needs to be taken into account and advice taken from propeller manufacturers (see resources) to select blade loading, speed, and outline shape to give the best possible balance of service speed efficiency with performance through the speed range. Above 0.8 a fully cavitating section needs to be selected. The selected propeller and engine/gearbox combination can then be used to prepare the thrust profile against the drag profile with speed and the thrust margin compared at the vessel hump speed for higher-speed craft and across the speed range for slender vessels. The thrust margin at varying blade angles for a CP propeller can then be reviewed to see whether a fixed-pitch or CP propeller is needed for performance.

Open propellers do not operate in undisturbed water flow since the vessel hull bottom will be directly above. If the top of the actuator disc is too close to the hull, the inflow will be constrained and so performance reduced. Most propellers are driven through shafts that are canted upward to enter the hull through rotating seals to a gearbox and thrust bearing and then to the engine further forward or aft. The shaft angle may be 10–15°, and this introduces variation in the inflow entry to the blades as they rotate, causing pressure pulses that are radiated through the hull. The alternative of a Z drive gearing as used in inboard sterndrives for pleasure vessels is practical for power ratings up to 800 kW for commercial package units but not for larger high-speed vessels.

Twin disc installation in M80

Arnesen propulsion unit

ZF SeaRex units

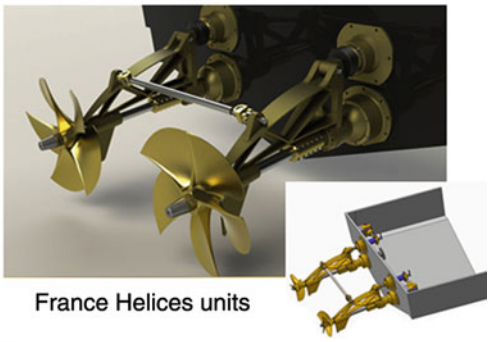

France Helices units

Flexitab XF700 Integrated unit

QSPD integrated unit

MSA STP unit

Levi Drives Unit

Fig. 11.7 Surface drives

Table 11.1 Surface drive range

Surface drive suppliers	Power shp	to .. shp	Steering; elevation
Twindisc (Arneson /Rolla)	500	5000	Hydraulic for both, external to hull, prop shaft universal joint
Francehelices	500	5000	Hydraulic for both, steering mechanism inside hull, prop shaft universal joint
ZF SeaRex	1900	3800	Hydraulic for both, external to hull, prop shaft universal joint
QSPD	300	3000	Rudders/fixed cowl; fixed shaft
Levidrives	200	2500	Rudder/cowl; fixed prop shaft
Flexitab Flexidrive	700	2000	Side rudder/fixed cowl; hydraulic elevation
MSA STP	200	1000+	Hydraulic for both, external to hull, prop shaft universal joint

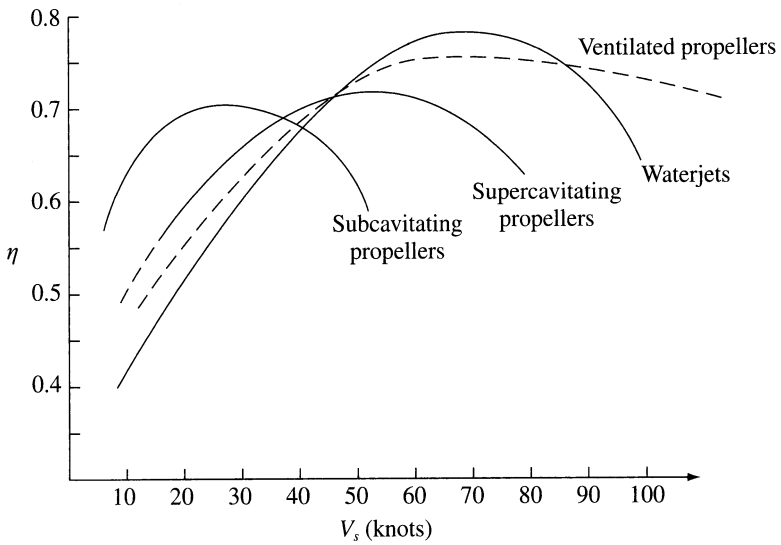

Fig. 11.8 Different propellers' power and speed selection regimes for efficiency

One option that is available is to design the stern part of the hull with a partial tunnel, thereby reducing the shaft angle, and to optimize the propeller blade shape and area for the flow pattern. This is an approach adopted by Servogear (see *Resources*, *propulsion*), who will work together with a designer to arrange the hull to integrate with a variable-pitch propeller system using its specialist approach. This can result in a simple propulsion installation having reduced draft and high propulsive efficiency in a speed range of 20–50 knots. Servogear installations range up to 2000 kW per shaft with propellers up to 1.6 m in diameter. Figure 11.9 illustrates the system. The tunnel is designed based on the inflow geometry at service speed to maximize propulsive efficiency and has to be completed as a joint development with

Fig. 11.9 (**a**) Servogear propeller flow diagram; (**b**) stern view of quadruple installation

the vessel designer. The design has become popular for wind farm service vessels as well as passenger catamaran ferries.

Open propellers operate on free stream flow and have no flow straightening, so aft of the disc flow will be rotating and turbulent, and there will be a substantial body of water with a velocity profile relative to the free stream. The aforementioned design processes aim to maximize the efficiency at service speed by minimizing these effects by keeping blade loading as low as practical and rotational speed also as low as practical. To constrain the size of a propeller and keep transmissions as light as possible so as to integrate with a typical high-speed vessel design, a compromise has to be reached, so propeller selection is normally one of homing in on diameter and blade design that can work with the selected engine and transmission. If this results in too low thrust, a new cycle has to be run with a larger engine size, alternative concepts considered, or the lower service speed accepted as the basis.

At speeds from zero up to service speed a propeller will experience significantly varying flow conditions. Let us consider a propeller running at a constant rotational speed after starting up. At zero vessel speed, entrained water is being accelerated backwards in a spiral to generate thrust in a free stream that is static. If we consider a propeller starting rotation from static, initially the blades will generate the pressure difference between lower and upper surfaces, and so circulation will begin (from high to low pressure), water will be driven through the cascade by the pressure differential and the circulation and will initially form a large-scale rotating circular vortex connecting vortices generated at the blade tips (Fig. 11.10).

As the vessel is accelerated to service speed, the rearward induced water velocity in the free stream decreases relative to global coordinates since relative to the vessel

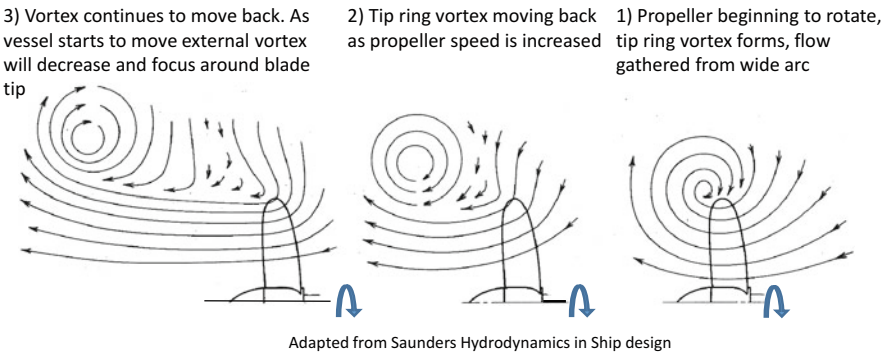

Fig. 11.10 Diagram for propeller operation at zero and increasing speed

the water is traveling rearward at increasing speed. The circular vortices around the propeller blade tips reduce in size, while internal to the vortices pressure diminishes toward vapor pressure. Forward of the propeller disc the entrainment cone decreases, as does that aft of the disc as the axial velocity augmentation "a" reduces down to the design value for the propeller at service speed. Within the disc the angle of attack gradually diminishes, also reducing the thrust developed. At a certain forward speed, thrust will reduce to meet increasing vessel drag. Through this process, including acceleration through "hump speed," the flow under a vessel hull close to the propeller is very turbulent.

If the propeller blades can be varied in pitch, then at low speeds pitch can be reduced and thrust developed with lower power absorbed as the blade geometry is aligned with the lower speed of advance relative to the rotational speed. The blade profile will not be optimized for the low speed condition but will nevertheless operate more efficiently than a fixed-pitch propeller at the same vessel and rotational speed. Since most high-speed vessels have a resistance curve with a "hump" in the region of Fr_L 0.65–0.7, CP propellers can be used to improve acceleration toward service speed. For a multihull where one propeller would be under each demihull, CP propellers also enable easier maneuvering to a quayside at slow speed, when rudders are less effective.

From this description it may be observed that at almost all vessel speeds, quite apart from the thrust developed by a propeller, the region just in front and behind it will have very disturbed flow. Once a designer makes a choice for the service speed condition, it will be important to look at operation across the speed range so as to try to optimize the flow regime and minimize noise and vibration from the propeller and turbulence around the shaft and supports.

A final observation regarding open propellers is that, in general, the arrangement leads to engines being located in the middle section of a hull, which makes control of center of gravity a bit easier. Also, in contrast to a waterjet, there is no internal ducting or entrained water mass in the vessel to account for in mass balance and structural design.

11.3 Waterjets

Introduction Waterjets installed in multihull vessels are located in the compartment next to the transom and comprise a shallow conically shaped inlet duct curved to a pump and stator section that delivers to a nozzle. The ducting geometry is normally fixed, though some very high-speed craft have had a moveable lower lip to the intake to improve performance at low vessel speed. Examples of waterjets are shown subsequently in Fig. 11.11.

The intake is designed to take in water from the vessel underside and deliver it to the pump such that as it enters the pump rotor, cavitation is avoided. The pump then accelerates the water to provide the thrust. Depending on the vessel service speed and size, the pump may be an axial flow, mixed flow, or, where speeds exceed around 50 knots, a two-stage pump, where the first-stage rotor is a helical inducer to raise the "static" pressure head for the main rotor. The propulsion nozzle, protruding from the vessel transom, may be of a parallel geometry or a contracting geometry.

Unlike a free propeller, a waterjet operates inside fixed ducting as a pump. The inlet ducting sucks water in from the flow under the hull and directs it into the pump impellor, where energy is added in a similar manner to a free propeller, except that the blade tips cannot generate free vortices, and so the foil acts more like a wing with infinite span. Downstream of the flow straightener vanes recover the swirl energy imparted by the pump. The pump and vane unit together can deliver close to 100% of the energy into axial momentum so that pump efficiency exceeds 90% before considering turbulence and cavitation of the real fluid. Further downstream of the waterjet nozzle the stream will naturally contract in a vena contractor, unless a contracting nozzle is installed.

At zero vessel speed water will be taken into the intake and accelerated by the pump. As there is no incident velocity, the pump will create a suction pressure ahead of the impellor. If the rotation speed is too high, the pressure reduction could go below vapor pressure and cavitation would begin at the impellor blade's leading edge.

As forward speed is increased, the velocity through the inlet duct will increase. The pump will be able to run at higher speed before cavitation is induced.

If the pump is an axial pump, meaning one designed like a ducted propeller, the inlet duct needs to be designed so that at service speed the flow streamlines are similar to those for a free propeller. While the impellor operates as a pump, the maximum efficiency is at high volume flow and low static head, so at a given thrust rating the tendency will be for larger ducting than a mixed flow pump. At power ratings for small craft this is not an issue, as the benefit is a simpler pump design.

If a mixed flow pump is used, advantage can be taken to use an inlet duct where the velocity is lower than the free stream at high service speed, thereby building some static pressure ahead of the impellor to avoid cavitation and using a higher pressure differential across the system. For a given thrust level the flow path is slightly more compact.

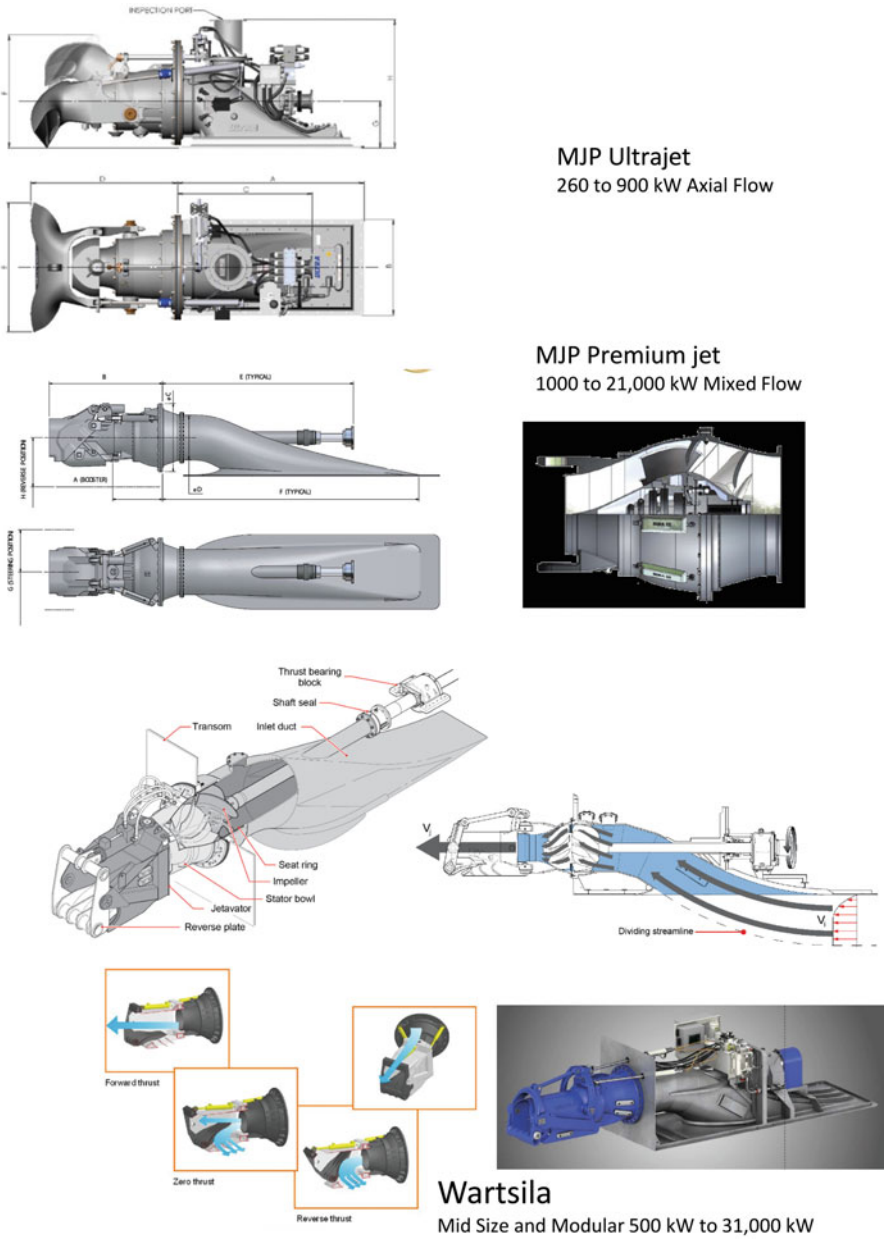

Fig. 11.11 Example waterjets

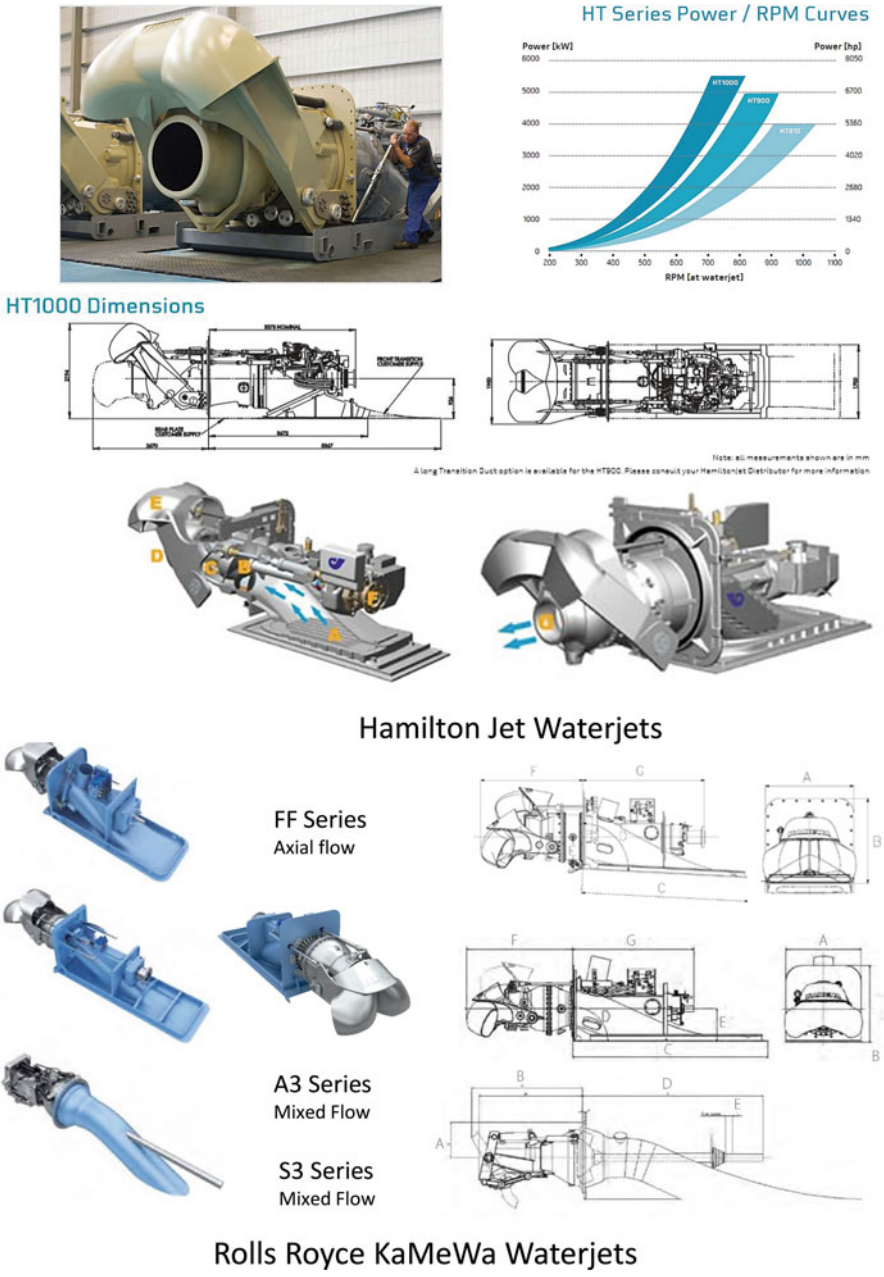

Fig. 11.11 (continued)

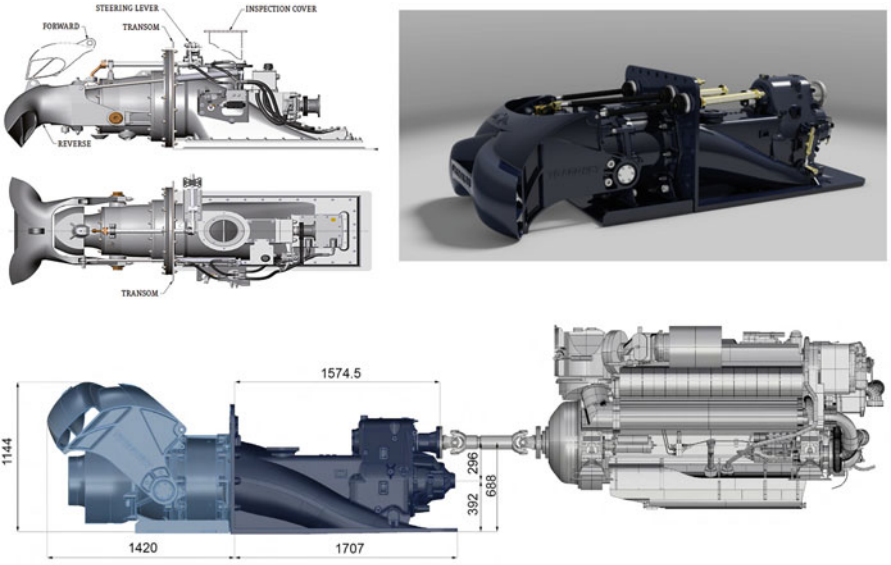

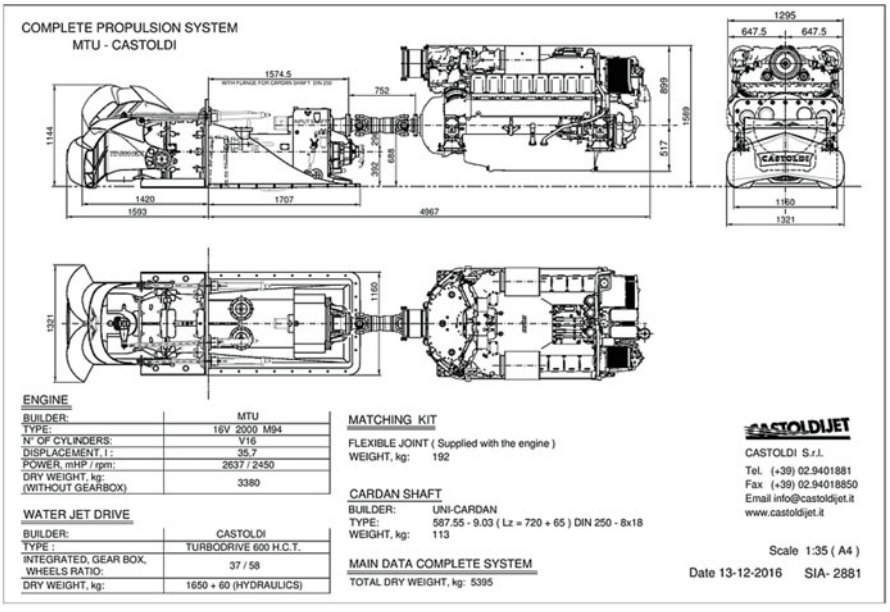

Fig. 11.11 (continued)

This approach has proven successful for large-scale waterjet units, with variations on the theme adopted by Rolls-Royce KaMeWa, Wartsila LIPS, and MJP Ultrajet for units as high as 40 MW power rating and vessel speeds up to 55 knots. A summary of the available jets is shown in Table 11.4 and Fig. 11.19 at the end of this section. Internet links are in the resource section.

Background Theory Similar to propellers discussed previously, the starting point is to consider the propulsor from momentum theory [5, 7] (see Fig. 11.11 above and 11.12 below for comparison). The pump imparts momentum to the fluid, half of that being acceleration as the fluid approaches the rotor disc, and the remainder aft of the rotor. The resulting thrust is the product of the mass flow and jet velocity as noted previously. Since the vessel will be advancing, it is the relative jet velocity that produces the thrust ($V_j - V_s$). The work done to propel the vessel is then

$$\text{Work Done WD} = T \cdot V_s = m' \cdot V_s / \left(V_j - V_s\right).$$

At the same time the work done by the pump is

$$\text{Energy Input} = E = 0.5\, m' \left(V_j{}^2 - V_s{}^2\right).$$

The jet efficiency is then $T \cdot V_s/E$, which reduces to

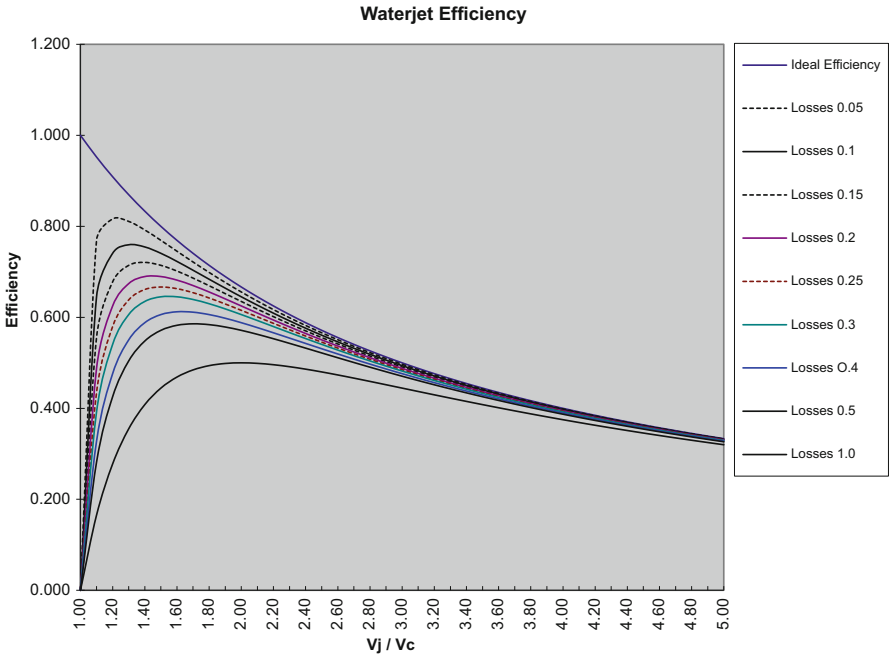

Fig. 11.12 Waterjet theoretical efficiency diagram

$$\eta_j = 2V_s/\left(V_j + V_s\right).$$

$$\text{If we substitute } \mu = V_s/V_j,$$

$$\text{we obtain } \eta_j = 2\mu/(1+\mu).$$

Equating $V_j = V_s\,(1 + b)$ or $V_s\,(1 + 2a)$ as used for the propeller, it can be shown that $\eta_j = 1\,/\,(1 + a)$, similar to a propeller if the impact of inlet ducting, nozzle, and the lifting of water mass into the pump are all ignored and the pump is treated as an actuator disc.

It should be noted that for a propeller we normally refer to the velocity at the actuator disc, whereas for the waterjet we relate to the exhaust jet velocity. This leads to a difference in the subsequent expressions also in comparison with expressions for propellers.

We can define the inlet losses as

$$E1 = 0.5m'V_s{}^2 \cdot (1-\zeta).$$

Nozzle efficiency is a relation of the energy delivered by the jet to that supplied by the pump to the nozzle, so

$$E2 = 0.5m'V_j{}^2 \cdot (1-\eta_n) \text{ is energy loss at the nozzle, so}$$

$$E3 = 0.5m'V_j{}^2 + (1-\eta_n) \times .0.5m'V_j{}^2 \text{is the delivered pump energy}$$

$$= 0.5m'V_j{}^2(1+\xi), \quad \text{where } \xi = (1-\eta_n).$$

Nozzle elevation can be accounted for by a static head, as follows:

$$W_s = m'gH.$$

Then work done:
WD $= m'\,(V_j - (1-w)V_s) \cdot V_s$, where w is the wake fraction for the hull.
While energy supplied by the pump is

$$E4 = m'/2\eta_p\left[V_j{}^2(1+\zeta) - \eta_n(1-w)^2V_s{}^2 + 2gH\right].$$

Efficiency = WD/$E4$.
If both WD and $E4$ are divided by V_j^2, and $\mu = V_s/V_j$ is substituted, we obtain

$$\eta_j = 2\mu\,(1-(1-w)\mu)/\left[1+\xi-(1-\zeta)\,(1-w)^2\mu^2 + 2gH/V_j{}^2\right].$$

If for μ we substitute $(1-w)\cdot\mu$, thereby relating to wake velocity rather than vessel speed, then

$$\eta_j = [1/(1-w)] \cdot 2\mu(1-\mu)/\left[1+\xi-(1-\zeta)\mu^2+2gH/{V_\mathrm{j}}^2\right].$$

So far, we have included the effect of hull wake fraction, inlet losses, nozzle losses, and effect of nozzle height, and we have an expression linking to V_s and V_j. Typically inlet losses may be 15–20%, while nozzle losses can be 1–3%. Wake fraction may be in the region of 3–5%. Using the foregoing relation and plotting efficiency against $V_\mathrm{s}/V_\mathrm{j}$ (μ), plots similar to those in Fig. 11.12 can be obtained. This illustrates that maximum efficiency is obtained when $V_\mathrm{s}/V_\mathrm{j}$ is in a region between 0.65 and 0.75 and the efficiency is also 0.65–0.75.

So far, neither the efficiency of the pump nor the relative rotational efficiency (effect of flow turbulence and vorticity ahead of the pump) has been included. η_p is normally 0.88–0.93, while η_r is close to 0.99. Taking these into account yields

$$\mathrm{OPC} = \eta_j \cdot \eta_p \cdot \eta_r.$$

Using the foregoing example numbers, the resulting Overall Propulsive coefficient (OPC) would be 0.63. The required input power can then be estimated from the required thrust if the transmission efficiency and pump characteristics are known.

Cavitation A pump generates a total head that is a combination of static and dynamic pressure. An axial flow pump operates similarly to a propeller, adding primarily dynamic pressure to the stream. A mixed flow pump adds greater rotational flow so the static head proportion is increased. Since the flow is constrained in a duct, this pressure can be returned to a dynamic pressure increment by a stator blade array and suitable sizing of the duct and boss of the pump leading to the jet nozzle. As the total pressure downstream of the pump is increased, so the suction pressure upstream of the impellor decreases. Similar to a propeller, if the suction pressure reduces to vapor pressure, cavitation will occur at the leading edge of the pump blades. The bubbles may then collapse as the pressure increases across the impellor blades, causing erosion damage.

To avoid cavitation, the relation between the inflow at the impellor and the static head (net positive suction head, or NPSH) has to be maintained with a positive margin above vapor pressure:

$$\mathrm{NPSH} = H_\mathrm{at} + (1-\xi){V_\mathrm{w}}^2/2g - H_\mathrm{i} - H_\mathrm{v},$$

where H_at is atmospheric pressure, H_i is elevation of pump centerline above WL, and H_v is vapor pressure.

There is defined a suction-specific speed for pumps that is essentially a constant, as follows:

$$N_\mathrm{ss} = N Q^{0.5}/(g\,\mathrm{NPSH})^{0.75}.$$

The NPSH increases with vessel forward speed so the pump speed and volume flow may increase. The relation between the changes in N compared with Q will be governed by the pump design.

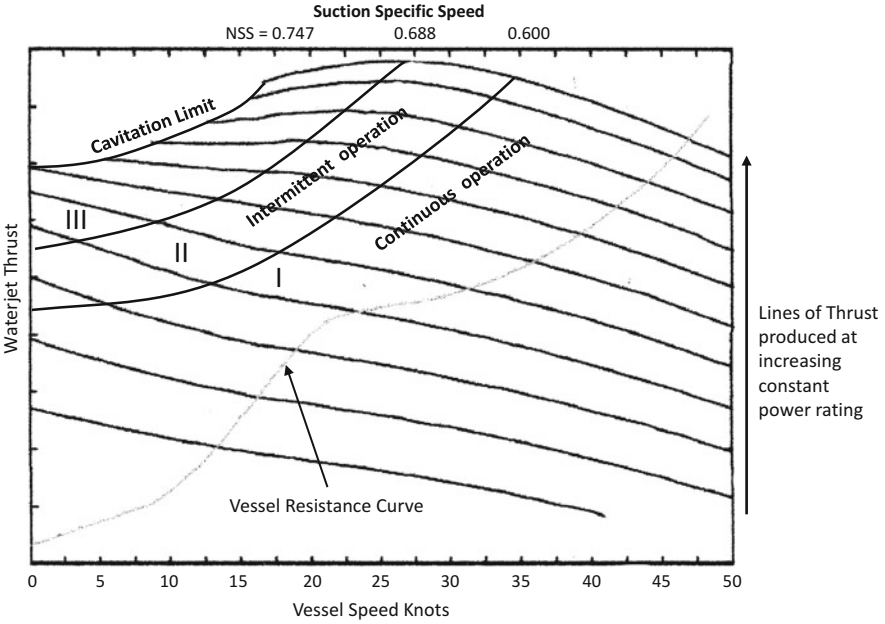

Fig. 11.13 Waterjet power and thrust diagram

The thrust generated by a waterjet pump at constant power input plotted against vessel speed follows a declining curve, as shown in principle in Fig. 11.13. Shown on the same diagram are the regions I, II, and III that bound N_{ss} values of 0.6, 0.688, and 0.747, respectively. Overlaid is an indicative resistance curve for a vessel in calm water. The design matching point is shown at the intersection of the resistance and thrust curves. If vessel speed is reduced at the same power rating, due to increased sea state and vessel resistance, the pump will approach the suction-specific speed. To maintain a margin, the power would need to be reduced. Depending on the shape of the resistance curve, it may be important to match the pump and engine at hump speed or at limiting sea states to ensure a suitable margin against cavitation as well as at service speed. Additionally, if the region of highest efficiency is shown on the power lines, the aim will be to select a pump size where performance falls within the area through as much of the operating range as possible.

Initial Selection To select a waterjet, the following procedure may be helpful. If we know our vessel resistance and speed, the preliminary power estimate can be used to take a first-pass selection; thus:

$$\text{Power kW} = (R \cdot V_s)/(\text{OPC} \cdot \eta_{tr}) \cdot (1 - t). \text{ Initially take } t = 0 \text{ and } \eta_{tr} = 0.97$$

(check for metric units) (Note $1 - t$ is relevant for using the model data . . .)

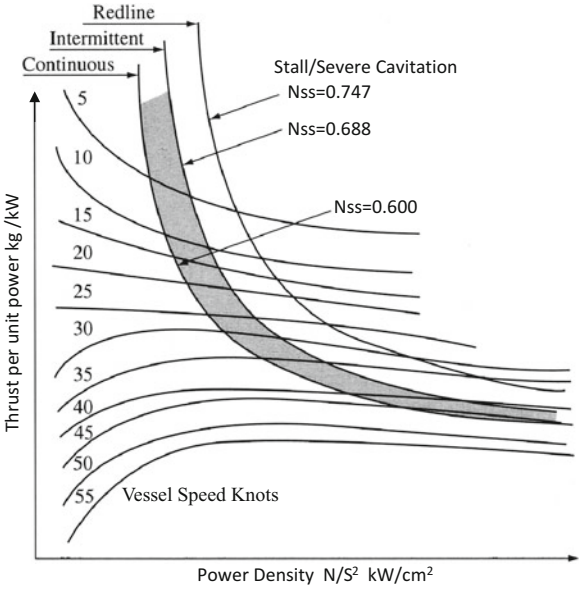

Fig. 11.14 Waterjet thrust with power density and speed

Reference [5] presents a generic diagram to estimate size from thrust and power density derived from commercial waterjet data. Figure 11.14 shows an interpretation of this diagram in metric units. From the previously estimated power the thrust/ kW can be estimated and plotted on the diagram. Reading across to the vessel speed line the pump power density can be read off (kW/S^2 where S is in cm^2). A similar approach can be taken for other vessel speeds based on the resistance curve and using a constant power level to recalculate thrust/kW and obtain revised power loading to plot the thrust curve at constant power. It should be noted that these data are indicative only, and it is best to consult the waterjet manufacturers to obtain actual performance data. Nevertheless, a first estimate can be made.

Knowing the power loading makes it possible to estimate the pump inlet size. Using an assumed relation for nozzle area of 50% of pump inlet size as a first approximation, the jet velocity can be calculated from the inlet velocity, and from that the flow rate.

From this point the jet velocity ratio can be calculated, and, hence, since the other efficiency factors are known, the ideal jet efficiency and η_j accounting for the factors can be checked, and this should equal the initial estimate. If there is a difference, a new estimate can be made. This can also be done to check changes in, for example, nozzle sizing. A flow diagram is shown in Fig. 11.15.

Typical impellor diameters for mixed low pumps are 40% larger than the inlet diameter just upstream. The maximum tip speed recommended for estimation purposes is 46 m/s so as to avoid cavitation and so the pump's revolutions per minute can be estimated. From the power estimate and rotational speed one can look at candidate engines and gearboxes. Before going too far, it is important to check

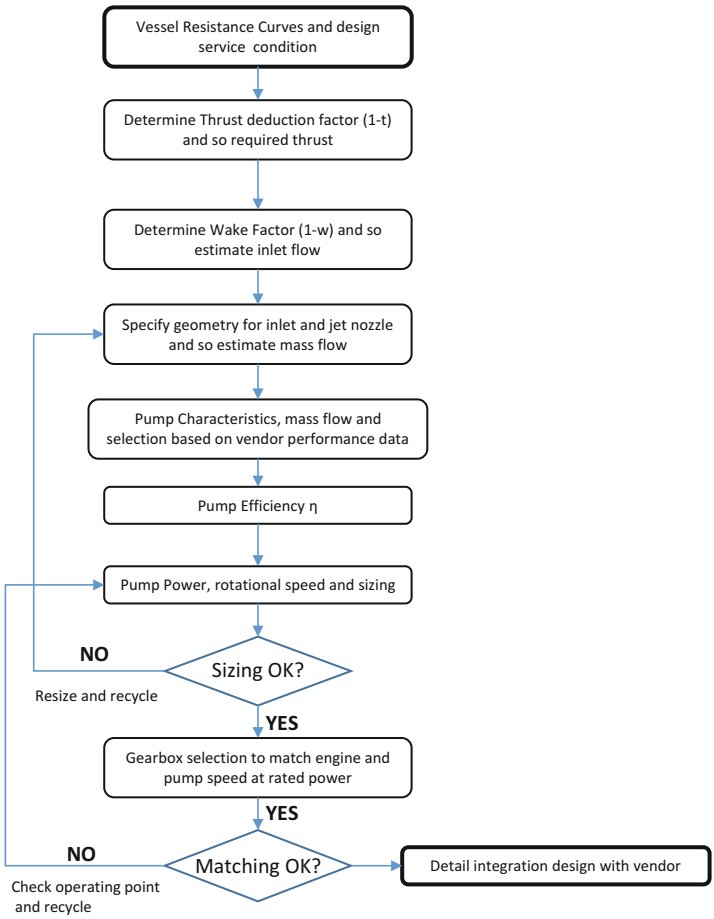

Fig. 11.15 Waterjet selection flowchart

against the waterjet manufacturers' data and confirm a selection before confirming the engine and transmission.

System Efficiency Before looking at commercially available waterjets, we should look a bit more closely at the system efficiencies taken as assumptions earlier and determine whether improvements can be made. If a system can be made more efficient, it can absorb less power for a given thrust and reduce the size of the unit itself as well as the engine to drive it and the fuel needed.

Reference [14] described the optimization of a KaMeWa waterjet system for the record-breaking 67-m-LOA monohull powerboat *Destriero* that crossed the Atlantic at an average speed exceeding 50 knots in 1992. In the paper, the author presents a curve for OPC obtained by KaMeWa for its systems installed in a number of vessels (34). A mean line interpreted from these data is presented in Fig. 11.16. What is

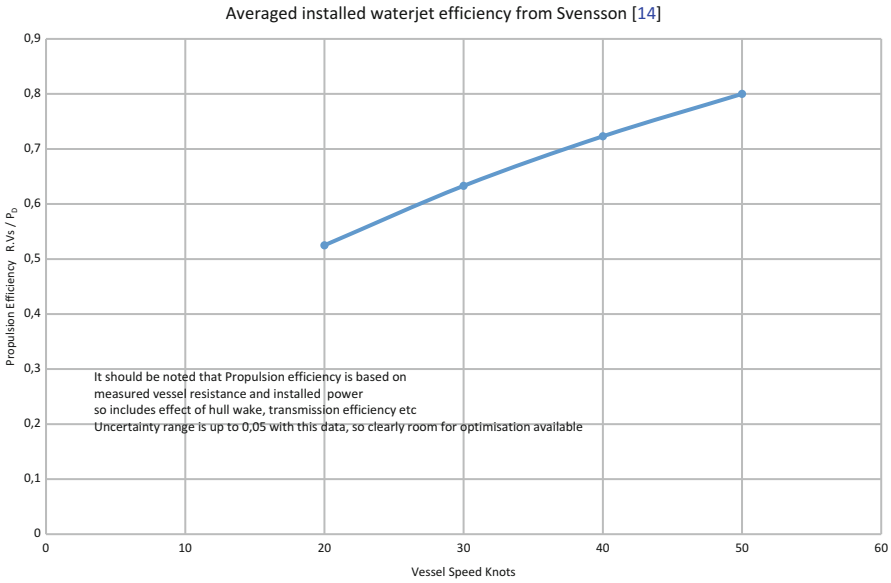

Fig. 11.16 Waterjet practical efficiency, taken from Svensson FAST 91 data

notable is the efficiency trend as vessel speed increases. At a vessel speed of 30 knots, the waterjet system efficiency (eta_D) may be as low as 60%, while at *Destriero*'s 50 knots, a further 15% has been gained. Since pump efficiency is normally in the region of 0.9 or 0.92, clearly the principal gain is due to improvements in inlet efficiency at higher speeds. Research by the major waterjet manufacturers since the 1990s has led to significantly improved waterjet design, with a focus on inflow into the pump through the inlet. The challenge nevertheless remains that for high efficiency a low jet velocity ratio is favored, while to achieve a compact design, the jet velocity ratio should be higher. A mixed flow pump or inducer at high speeds helps the designer in this respect.

Inlet Design Two main issues need to be considered: the ingestion of the hull boundary layer; and the velocity profile through the inlet throat including variation across the cross sections, the pressure profile on the duct surfaces, and the incidence of cavitation both at the lower lip and the forward entry profile.

Boundary Layer The hull boundary layer will have a velocity distribution following a power curve from the free stream at some height from the hull surface down to zero relative to the hull at its surface controlled by water kinematic viscosity. The profile varies with Reynolds number and so is different at model and full scales [15, 16]. At full scale, the following relationship for turbulent flow may be applied for larger craft in the range of 50 m LOA. Reference [17] suggests that for smaller craft 27 m LOA may require a constant of 0.37 instead of 0.27:

$$\delta = 0.27 \cdot x \cdot (V_s/\upsilon)^{-1/6} \text{ and } V_y = V_s(y/\delta)^{-1/7} \text{ for boundary layer.}$$

Here x is the hull length ahead of the waterjet intake and δ is the full height of the boundary layer. Reference [15] indicates that for a catamaran with 50 m ahead of the inlet at 35 knots, δ will be approximately 0.5 m. The velocity quickly rises, and so the layer with significant retardation (>20%) is about 0.15 m from the hull surface.

Hoerner [16] provides a more detailed explanation and experimental data on boundary layer profiles in turbulent flows.

If we are considering an intake for a 55-m vessel, the overall dimensions may be about 2 m length and 1 m breadth at the sole, and so the main effect of the hull boundary layer will be on the upper surface of the intake, facilitating an increase in pressure along the roof. Following our foregoing example, the impellor intake diameter is 0.9 m with an area of 0.636 m^2, so if the duct angle is 25° and the inlet at the hull base is 2.5 m long including the frontal curve, then the throat can be an almost constant area to the aft lip for the streamlines (e.g., Fig. 11.17). At service speed the water ingested into the duct will follow the streamlines shown in Fig. 11.17c, which may extend 0.7 to 0.8 m below the hull going beyond the hull boundary layer. Typical commercial geometries, shown in Fig. 11.20, are similar to this arrangement.

Velocity Profile Figure 11.17 shows streamlines into an intake at low, medium, and high speed. It can be seen that at low speed, water is accelerated from a wide catchment area into the intake. Depending on the power being applied, the flow around the lip may cause cavitation on the inside. The water flow is being accelerated to a high inlet velocity ratio (IVR) (V_p/V_s), and so, as shown in Fig. 11.12, even in the ideal case, the jet efficiency will be low. If the jet is specifically designed for this low speed, it will not be possible to achieve high efficiency unless the relative dimensions and volume are allowed to be increased so as to lower IVR.

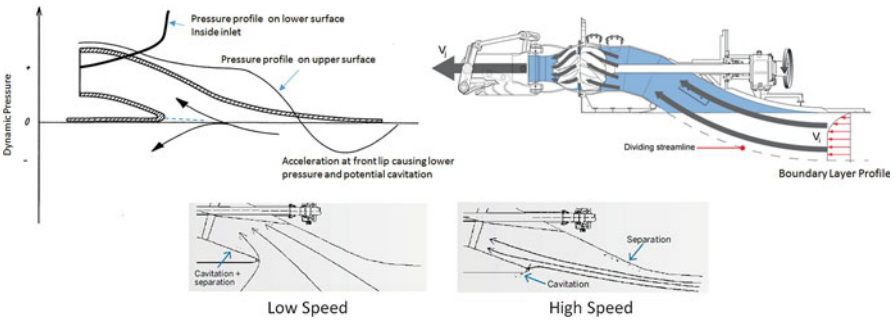

Fig. 11.17 Waterjet inlet profiles and diagrams

The jet at medium speed now has its catchment area forward of the inlet, and it may be that the streamline separation point is just at the nose of the aft lip. To achieve this, the flow into the intake needs to match the external flow at that point; from there the velocity and static pressure can be managed by area variation so as to generate the optimum conditions at the impellor. At high speed, the flow streamlines adjust further, with the streamline separation point moving to the outside of the lip with vortex flow and cavitation on the underside of the lip affecting the pressure on the hull under the waterjet sole.

In addition to ingestion of the hull boundary layer from the hull flowing in over the upper wall of the intake, three other issues affect the flow [18]:

- Pipe flow following curved shape. Compared with the average velocity, the flow speed will be lower on the outside of the bend and faster on the inside of the bend;
- Obstruction resulting from the drive shaft crossing the duct to the impellor. Here the flow has to find its way around a complex geometry causing vortices and internal drag. A rotating shaft can actually improve local flow;
- As speed increases above the optimized design point for a waterjet, the IVR (V_p/V_s) increases, so that flow decelerates through the duct.

A number of research groups have carried out CFD analyses for flow through waterjet systems with the intent of understanding variations in flow regimes. The focus is on the inlet since the performance of the pump and stator and of the jet nozzle is more easily determined through experience with hydraulic pumps and piping systems [18–20]. Examples of CFD studies are given in references [21–23]. The studies have demonstrated that across the inlet area to the impellor there is a high-velocity area at the low part of the duct following from the rear lip and a low-velocity area in the upper part (Fig. 11.18). Reference [21] looked at vessel speeds of 10, 30, and 50 knots, and it is evident that the velocity variation in the inlet is high at low speed and again at high speed, whereas at 30 knots (the design

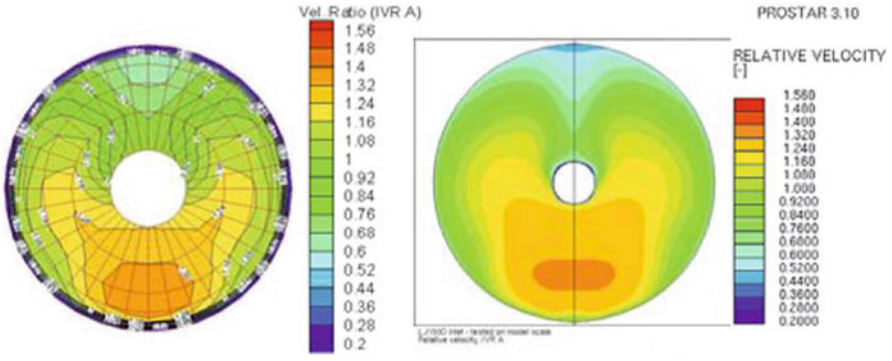

Fig. 11.18 Waterjet inlet profiles at impeller inlet from CFD from Wartsila

optimum point for the example system) the flow distribution was most consistent while still having a velocity gradient from roof to base that gave effective lifting force.

As external dynamic pressure inside the intake increases with speed, the velocity distribution in the intake has the effect of applying positive upward pressure on the intake surfaces, giving a lifting force [14, Fig. 8] that can be as high as the total weight of the waterjet and entrained water.

The Norwegian University of Science and Technology [15] has developed a sizing program to generate the optimum geometry for a flush inlet based on experience from model testing, including self-propulsion tests with waterjet catamarans, to achieve the best possible inlet efficiency.

Leading along from the intake, the water flows past the impellor shaft, which may or may not be inside a cover. The shaft disturbs the flow, though some research [21] suggests that leaving off the shroud so that the rotating shaft interacts with the flow can be beneficial. As the water approaches the impellor at lower vessel speeds [18], the velocity pattern is still evident at the disc, and as speed increased to 50 knots, the velocity profile was almost consistent around the clock.

A comparison of test data against CFD is given in [21]; this work presented results from a detailed CFD analysis of both inlet and pump system. The velocity variation close to the pump inlet was determined from model testing for calibration, and it was shown that the CFD and test results show close agreement.

Based on the results from [20] it may be suggested that an inlet efficiency greater than 0.9 may be achieved with careful design of the vessel's normal service speed. Figure 11.19 shows a plot from the data with efficiency dropping to 0.762 at 10 knots and to 0.78 at 50 knots as the IVR varies from 2.1 to 0.5.

If we assume an inlet efficiency of 0.922 as from [21], this would result in an OPC of 0.634 for a sample vessel calculation at 30 knots. If we compare this with the curve in Fig. 11.16, this suggests 0.625, approximately, which agrees well with our calculations. This suggests that, with care, inlet efficiencies in line with those in Fig. 11.19 can be achieved. Off design point performance will drop away, as

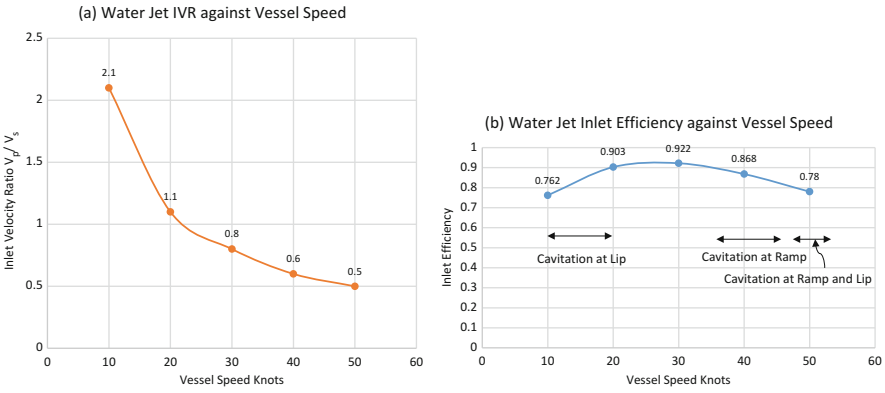

Fig. 11.19 Waterjet inlet efficiencies and IVR

suggested in the figure. For vessel designs in a range above 30 knots, it may be helpful to start with an inlet efficiency of 0.9 for jet selection. While it should be possible to improve on this, particularly for vessels operating in a range of 50 knots, this may best be considered optimization through detailed analysis with CFD rather than initial selection. If the vessel is to be operated below 25 knots, the jet size may grow too large to achieve this high inlet efficiency, so for smaller and slower vessels the original inlet efficiency assumption of 0.8–0.82 may be a realistic start prior to consulting the waterjet manufacturers.

References [23] and [24] detail CFD study followed by manufacture and testing of a waterjet unit in China that verified the accuracy of predictions using the CFD code CFX (see *Resources*, *software*, *ANSYS*).

Reference [22] details a study made in Canada of waterjet performance using a wind tunnel for physical modeling. In this study, the boundary layer for physical testing was carefully measured and compared with the CFD prediction. This work also demonstrated the velocity contours through the inlet duct. The velocity contours aligned with ingestion of the lower-velocity boundary layer along the upper part of the inlet throat and higher-velocity flow at the bottom lip; as the flow passes along the duct, some swirl is induced by the presence of the shaft and the curved centerline such that just ahead of the impellor the flow is more evenly distributed.

It should be noted that most of the CFD studies do not model the actual demihull width. It should be borne in mind by the designer that an inlet will experience other flow perturbations if the sides of the inlet are too close to the hull bottom chines or bilge corner. In the limit, as found with SESs, ventilation can occur and severely affect the inflow. An initial approach may be to allow 75–100% of the inlet width on either side of the inlet to be part of the hull bottom width so as to maintain a high inlet efficiency. Where a second waterjet is in the same hull the spacing between jet inlets may be less, though vendor guidance is important. If this is not practical for the aft hull form selected, CFD analysis will definitely be important, together with manufacturer advice.

Returning to [18], these authors conclude that nonuniform flow within an inlet is unavoidable for waterjet systems. It may be commented, based on the work presented in the other references cited here, that such nonuniformity may be reduced by careful design of the operating conditions, but at lower speeds (and higher speed for sprints perhaps) the nonuniformity will increase, tending to reduce the waterjet efficiency. Further, if a system is to be designed for speeds higher than 55–60 knots, the impellor design will need to move toward an inducer pump, as studied for the US 3KSES in the 1970s [5]. The author suggests that inducer pump design can achieve similar efficiency (around 0.88) to mixed flow pumps and inlet efficiency above 0.8 if attention is taken to changing the inlet shape at the hull base to be rather wider at the first part of the throat so as to ingest more of the boundary layer.

One other issue for waterjet design is that of possible protection from foreign object damage to the impellor. Some waterjets, particularly those for small craft, have an intake grill installed. Waterjet systems for larger vessels do not normally have grillages installed as the risk of foreign body ingestion offshore is low and grillage reduces propulsion efficiency. There may be a logic to installing foreign

object protection for river or lake ferries, as such waterways often contain refuse (e.g., plastic bottles, cans, ropes) that can foul a propeller. This requires discussion with the prospective operator on the risks involved and alternative ways to mitigate the risk.

Nozzle and Exit A waterjet nozzle for larger machines is generally designed as a Pelton type where the flow from the stator already reaches its maximum at the nozzle exit, so the jet is parallel though it has a small velocity variation within the jet. The jet will impinge on the water flow behind the vessel, and having a velocity perhaps twice the vessel speed will create some entrained flow. Being close to or at the water surface the jet will tend to be directed upward by the resistance of the impinged water body, forming the typical "rooster tail" seen as a catamaran accelerates. As mentioned previously, the losses in a nozzle are very small, so an efficiency of 99% is most often assumed.

Waterjet nozzles can be designed with hinges to allow sideways rotation operated by hydraulic rams so as to provide side force for directional control. This is the standard approach to directional control for waterjet vessels. Large craft with two jets in each demihull will often have one jet with a steering nozzle and one jet without, as the forces generated by a single steerable jet are high.

In addition, waterjet suppliers also have designs for reversing systems based on different shapes of bucket that when rotated to cover the nozzle redirect the flow forward. Since this system works while the jet itself is operating for forward thrust, there is no necessity to install reversing gear in the drive train. Again, installation of reversing gear on one jet if there is more than one in a demihull may prove sufficient for slow-speed maneuvering. Examples of the mechanisms can be seen in Fig. 11.11.

Suppliers The main waterjet suppliers and their power/size range are summarized in Table 11.2. Links are provided in the resources section to the company sites and data.

Diagrams illustrating the power ranges for the larger Wartsila and Rolls-Royce KaMeWa waterjets are shown in Fig. 11.20a, b. These nomograms provide a means of initial waterjet selection. Wartsila has a slightly different approach to the selection of its midsize waterjets using a coefficient accounting for hull efficiency on vessels under 50 m in length (see Wartsila Waterjet design guide for midsize waterjets at the company's website). Once a preliminary selection has been made, a designer can refer to the layout drawings and investigate installation in the proposed hull design. Following this, contact with the manufacturer itself is needed to refine the selection and integration with the hull design.

Castoldi has a simplified approach to waterjet selection, as shown in Fig. 11.20c.

Table 11.2 Waterjet suppliers and ranges

Waterjet range	Size designation	Power range kW	Weight range kg Jet (entrained water)
RR KMW S3 series	45–200	800–41,000	725 (577)–44,720 (47633)
RR KMW A3 series	25–63	450–2600	247 (40)–2360 (880)
RR KMW FF series	240–67	260–2000	124 (25)–1545 (703)
Wartsila Modular	910–2180	5500–3100	3700–49,500
Wartsila Midsize	450–810	1250–4300	1400 (450)–3600 (1750)
MJP Premium	350–950	1000–9000	310 (140)–4350 (2800)
MJP Ultrajet	251–452	261–900	153 (33)–643 (120)
Hamilton jet HT	810–1000	4000–5500	Contact supplier
Hamilton jet HM	422–811	750–2800	Contact supplier
Hamilton jet HJ	212–403	250–900	75 (17)–641 (110)
Doen	200/300 series	400–4000	875–3650
Doen	100 series	100–900	85–510
Castoldi Turbodrive	240–600	258–1655	130–1650
Scott Waterjet[a]	612–852	37–705	Contact supplier
American Turbine[a]	T309/SD309/SD312	75–2634	Contact supplier
Berkleyjet[a]	12J	133–371	Contact supplier

[a]These are specialists for sport and utility jet boats

11.4 Main Engines and Drive Trains

Design approach Two types of main engine are available for the fast multihull, the gas turbine, and the diesel or gas engine. There are a number of main machinery suppliers as shown in Table 11.3 below. Some also supply gearbox and transmission components, or work closely with the gearbox and transmission supplier in Table 11.4 so as to provide matching interfaces.

Note that Caterpillar also supplies engines modified to run on liquid natural gas (LNG). MTU is working on optimizing the design of is range for LNG fuel for introduction in 2018/2019. The other suppliers will provide a specific service upon inquiry. Gas turbines can run on LNG, the GE LM2500 is already in service in this form in the Buquebus *Francisco* wave piercer built by Incat. In all cases engines run more cleanly and produce lower emissions.

The first task of the designer, after selecting propulsion machinery, in the case of a catamaran two or four propellers or waterjets, is to determine the main machinery's desired output accounting for initial estimate drive system losses and continuous power rating of the engine, normally set at 85% of maximum for gas engines.

Having made an initial estimate of vessel resistance with speed and propeller or waterjet characteristics so as to deliver the required thrust, the key task for the designer is to select an engine and gearbox combination that can be matched to a selected propulsor so that the thrust curve meets the vessel resistance curve at the desired operation speed (Fig. 11.21). At lower speed, if the resistance curve has a

a

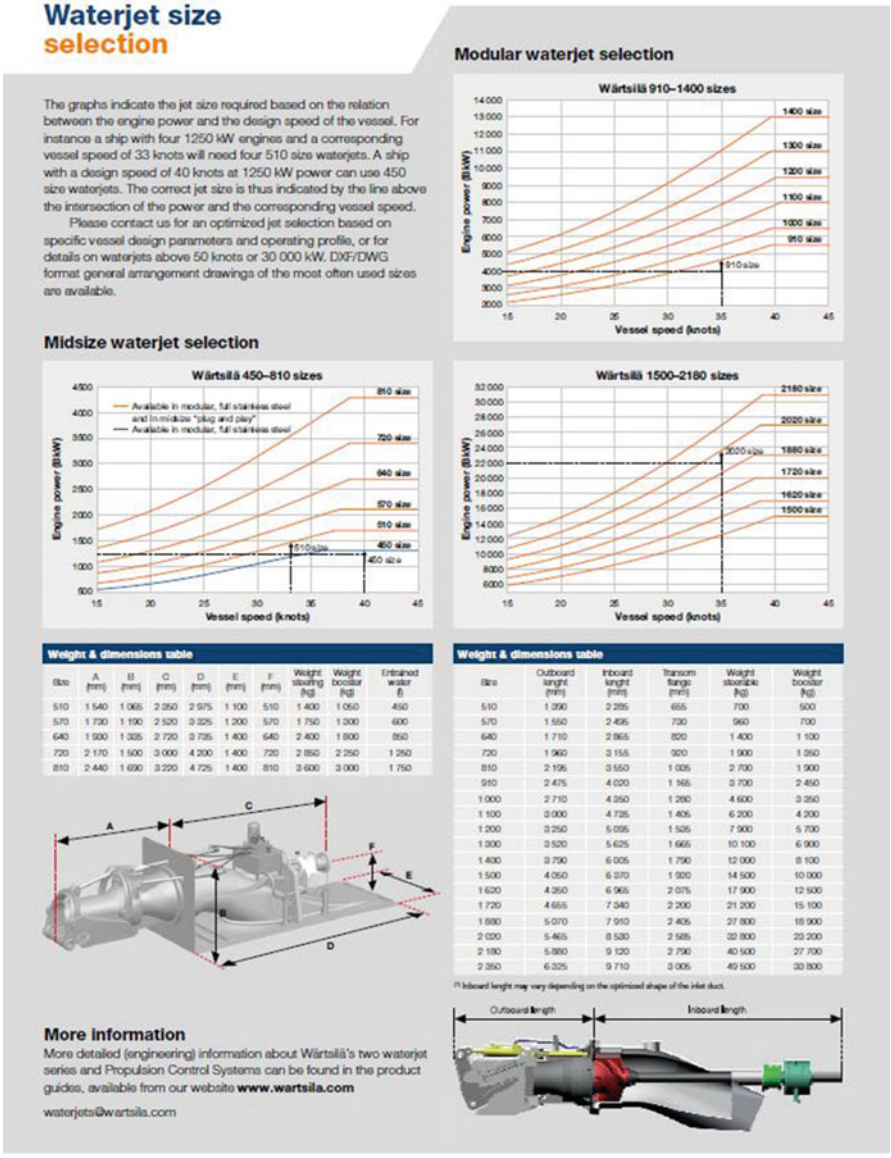

Fig. 11.20 Application diagrams for waterjets, (**a**) Wartsila, (**b**) Roll Royce KaMeWa, (**c**) Castoldi

b

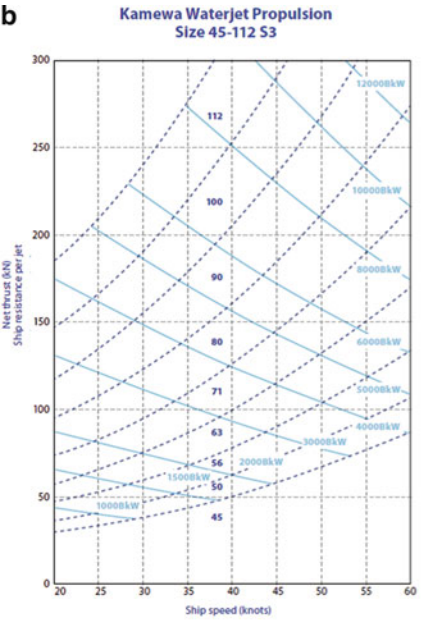

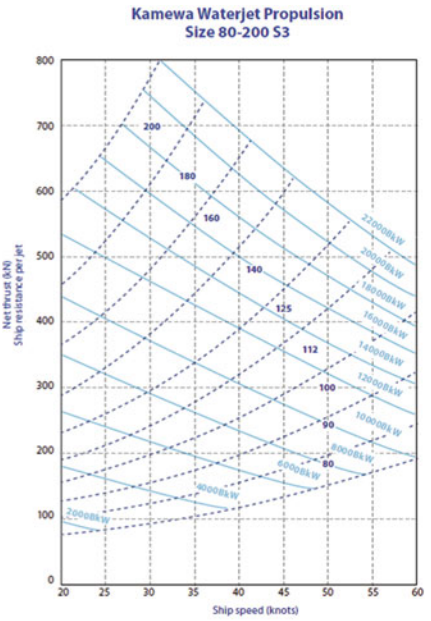

Key features:

- Highest pump performance on the market
- Stainless steel for maximum corrosion and wear resistance
- Impeller, nozzle and inlet duct designs optimised to meet each application's performance demands

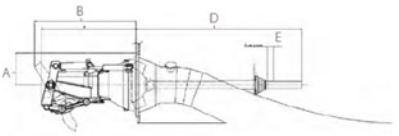

Technical data

Waterjet	Dimensions (mm)				Power range (kW)*	Weight (kg)		
	A	B	D (typical)	E (typical)		Steerable	Booster	EW**
S3-45	410	1318	2450	100	800 - 1790	725	453	577
S3-50	500	1455	2110	100	1000 - 2580	1004	600	750
S3-56	550	1630	2310	100	1200 - 3440	1385	865	1040
S3-63	600	1782	2510	100	1400 - 4300	1882	1172	1490
S3-71	650	2005	2600	100	1500 - 5100	2550	1596	2130
S3-80	700	2269	2800	100	1800 - 6500	3565	2180	3050
S3-90	800	2527	3180	100	2000 - 8500	4820	2940	4340
S3-100	900	2785	3560	100	2500 - 10000	6090	3700	5950
S3-112	1000	3119	3910	100	4000 - 12500	8360	5240	8370
S3-125	1100	3487	4020	100	5000 - 16000	11720	7460	11630
S3-140	1232	3906	4503	100	6000 - 20000	16210	10360	16341
S3-160	1400	4462	5180	100	7000 - 26000	23670	10550	24400
S3-180	1600	5020	5770	100	8000 - 33000	33100	12650	34740
S3-200	1760	5580	6432	100	10000 - 41000	44720	28840	47633

* Depending on speed and operating profile. For performance predictions please contact Rolls-Royce
** Entrained water inside transom

All data subject to change without prior notice

Fig. 11.20 (continued)

c

Model	IMPELLER DIAMETER (INLET) MM	DRY WEIGHT KG	FAST BOATS					SLOW BOATS MAX POWER INPUT, KW
			MAX POWER INPUT KW		MAXIMUM SUGGESTED DISPLACEMENT (TONS)			
			intermittent duty	continuous duty	1 unit	2 units	3 units	
TURBODRIVE 240 H.C.	238	130	309	258	2.5 - 3	6 - 7		96
TURBODRIVE 282	282	182	400	294	3.7	9.2		110
TURBODRIVE 284 H.C.	282	193	441	367	4 - 4.5	10 - 12	17 - 20	136
TURBODRIVE 284 L.V.	282	183	441	367	4 - 4.5	10 - 12	17 - 20	136
TURBODRIVE 340 H.C.	337	307	625	522	6 - 7	15 - 18	26 - 30	193
TURBODRIVE 400 H.C.	400	480	882	736	10 - 12	24 - 28	40 - 50	272
TURBODRIVE 490 H.C.	490	890	1.324	1.103	17 - 20	40 - 50	70 - 83	408
TURBODRIVE 600 H.C.T.	600	1.650	1.986	1.655	38 - 42	94 - 104	160 - 177	800
					THE MAXIMUM SUGGESTED DISPLACEMENT IS PURELY INDICATIVE AS THIS DEPENDS ON HULL SHAPE, LCG, INSTALLED POWER ETC.. PLEASE CONTACT THE COMPANY FOR ADVICE ON ANY APPLICATION.			

Fig. 11.20 (continued)

Table 11.3 Main Machinery suppliers (see Resources for links)

Supplier	Power range kW Low	kW High	Engine type	Typical weight kg/kW ex gearbox
MTU	261	9100	Med.-speed diesel	7.27–3.83
Caterpillar	298	5651	Med.-speed diesel	2.26–5.48
Cummins	224	2893	Med.-speed diesel	2.93–4.59
MAN	537	1397	Med.-speed diesel	2.26–1.69
Scania	184	846	Med.-speed diesel	6.25–1.96
Rolls-Royce		Approx. 30,000	Gas turbine	Skid approx. 0.9
Siemens		Approx. 30,000	Gas turbine	Skid approx. 0.9
GE		Approx. 25,000	Gas turbine	Skid approx. 0.82

Table 11.4 Gearbox and transmission suppliers (see *Resources* for links)

Supplier	Power range approx. kW	Notes	Typical weight t/kW
ZF	500 – 12,000	Various configurations	0.5 to 2.0 w. clutch
Reintjes	500 – 13,500	Various configurations	0.3 to 0.9 ex. clutch
Renk	500 – 10,000	Renk also delivers solutions up to 100,000 kW	0.5 to 2.0 w. clutch
Twindisc	50–2750	Various configurations	0.3 to 0.9 ex clutch

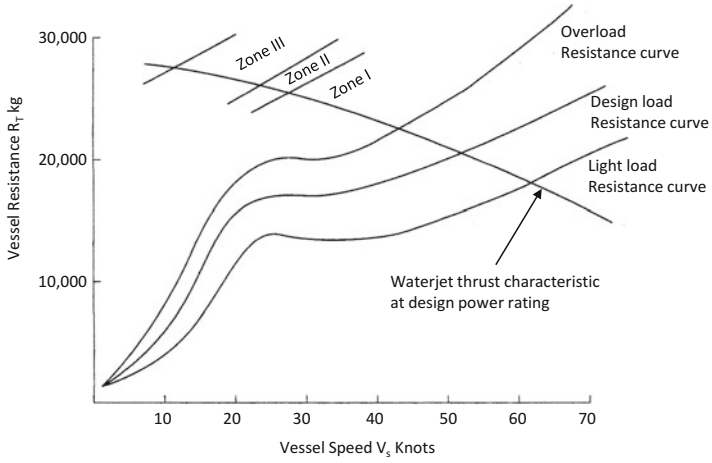

Fig. 11.21 Power and resistance matching curvesa and b

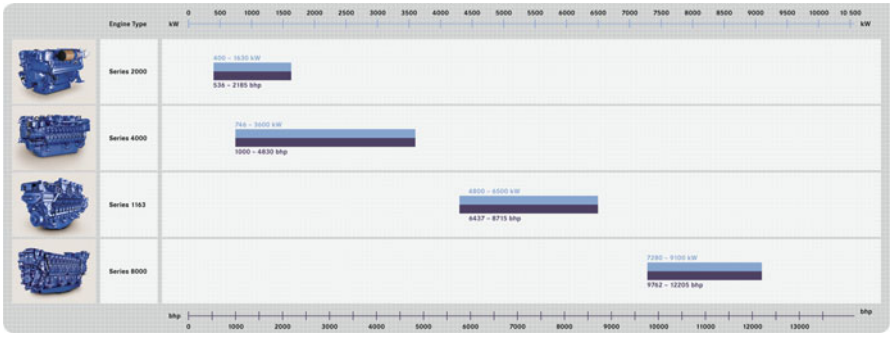

Fig. 11.22 MTU Marine diesel propulsion power plant range

distinct hump, as for a planing vessel, there needs to be appropriate reserve of thrust for acceleration and so a match of engine power to the propulsor requirement at this speed also.

For a waterjet, the selection graphics in Fig. 11.20 give an indication of how the unit size can be selected. From this point vendors provide further graphs of power and impellor speed against vessel design speed. Once this is known and an engine is selected, the transmission gearbox can be selected from the maximum torque of the engine and the speed ratio.

Engines and gearboxes are available as standard existing designs. The task for a designer is to select a waterjet or propeller based on its thrust at service speed and hump speed and match to the closest main engine and gearbox, including a margin.

An example of an engine range from MTU is shown in Fig. 11.22.

Once a candidate engine has been selected, the regulatory requirements impacting its installation in the vessel need to be checked out for the candidate and the ancillaries and controls specified as summarized in Sect. 11.8. This may affect the final selection (Fig. 11.23).

The main engine suppliers listed in Table 11.3 provide application tables for their engine ranges detailing power against rotational speed, while the gearbox suppliers

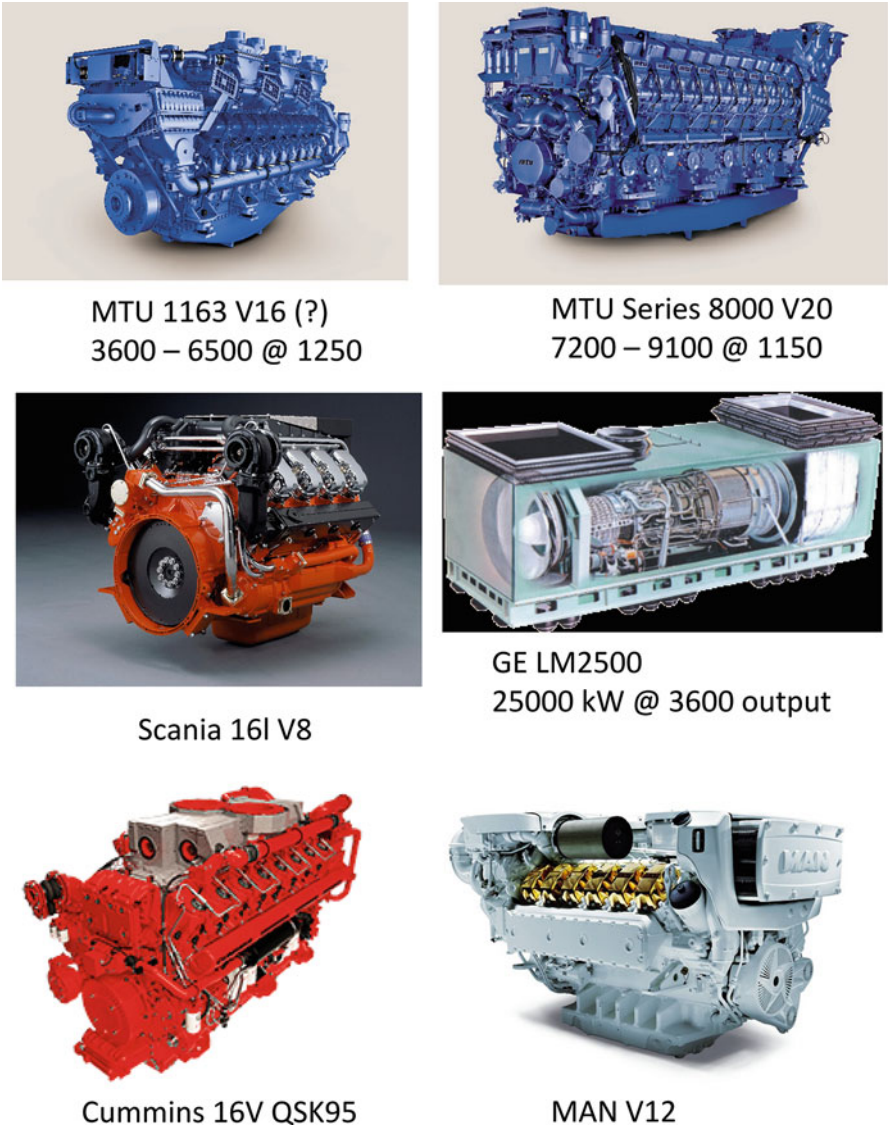

Fig. 11.23 Examples of main machinery

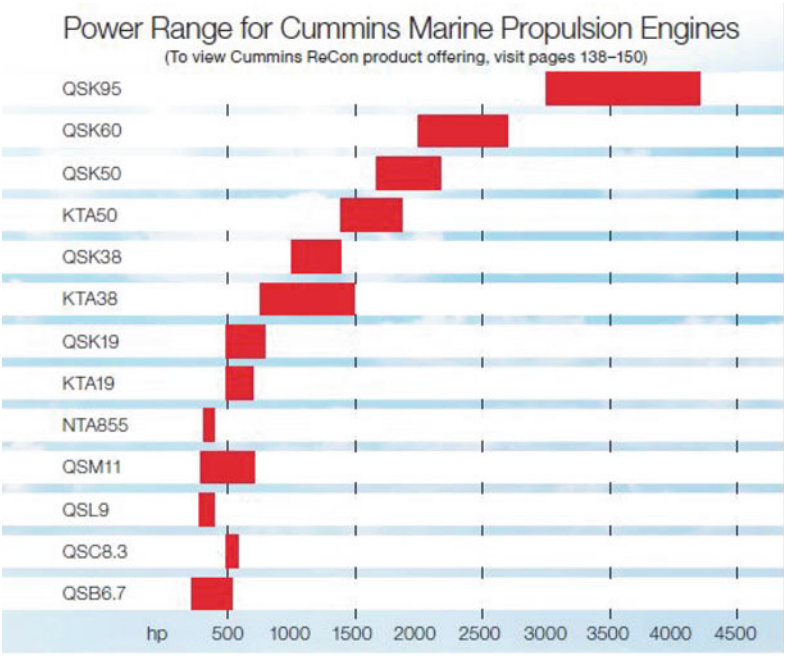

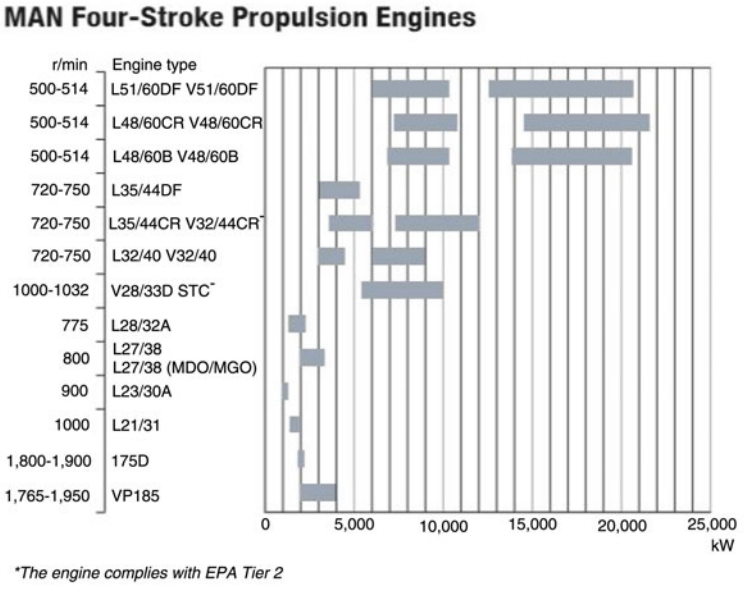

Fig. 11.23 (continued)

in Table 11.4 provide tables of torque and speed for their units as well as more general application charts (Fig. 11.24). Examples of gearboxes are shown in Fig. 11.24b. While the Reintjes VLJ range is tailored to fast ferry application with waterjet propulsion, both that company and the other suppliers have a wide range of configurations of input and output, reduction gearing, integral clutch, power takeoff for ancillaries, and dual input to single output for large ferries, as well as units with a

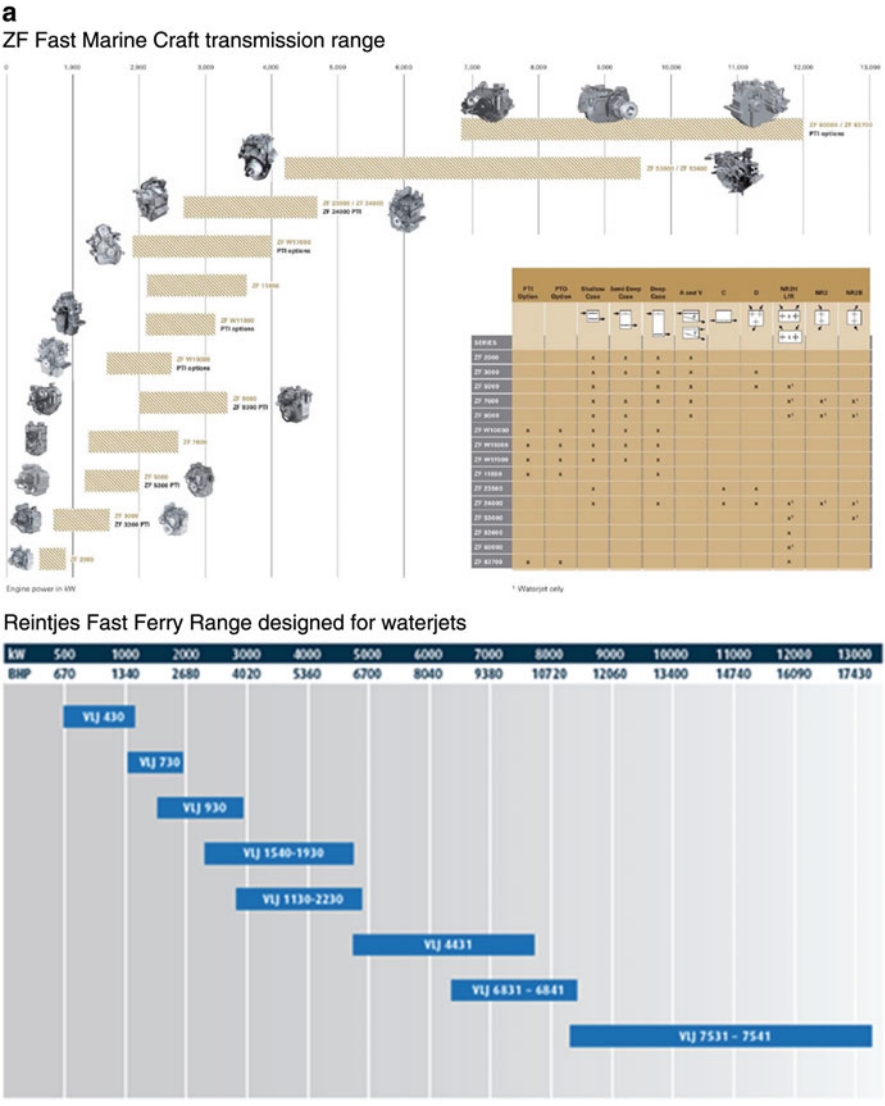

Fig. 11.24 Gearbox range power ranges and examples

b

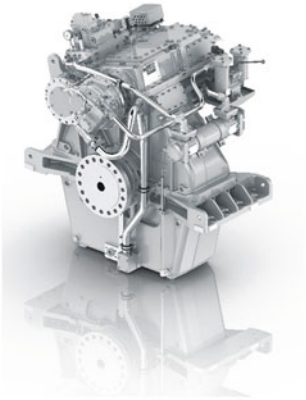

ZF-W10250 Vertical Offset with PTO

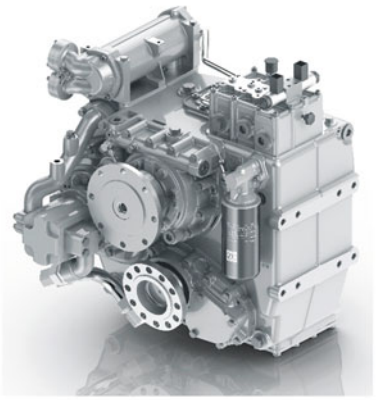

ZF-2000V Vee Drive

Reintjes horizontal offset VLJ

Reintjes Vertical offset VLJ

Renk 275 ASL94 horizontal offset

Renk 273 ASL2 offset double

Fig. 11.24 (continued)

main power input and a secondary input for a smaller engine for slow-speed operations such as may be needed for an offshore patrol vessel.

All the suppliers in Table 11.4 supply gearboxes in fixed configuration and with clutches included. Input and output may be vertically or horizontally offset, and with either power takeoff for ancillaries or with additional input from a second power source. Output shaft may be parallel or angled for V drive (engine behind) or A drive (engine in front). It is necessary to consult the technical data available from each of the suppliers to set up a configuration, but it is clear that just about any internal layout of machinery can be accommodated.

In addition to the engine and gearbox, couplings, drive shafts, and shaft seals need to be considered to assemble a complete drive train. The previously named suppliers together with specialists such as Emerson and Jaure supply these components. Based on the final selection, a general arrangement for the machinery spaces can be developed bearing in mind the auxiliaries that need to be located around the engines. The internal structure to interface with the engine and gearbox mountings can be drawn up to support the local structural analysis that will be completed following global analysis as in Chap. 12.

Once the static and quasi-static extreme cases have been analyzed for the machinery foundations, it will be possible to complete vibration and acoustic analysis. For both diesel engines and for waterjets it is important to identify the frequency hot spots in the vibration energy spectrum. For the engines this provides input to the resilient mountings, while for waterjets the excitation from vorticity between the impellor and stator blades can cause noise, which needs to be attenuated by adjusting the structural stiffness in the integrating structure between waterjet and hull. Guidance is best sought from the manufacturers on the best way to do this for a particular hull geometry and structure.

11.5 Directional Control

Two alternative systems are available for vessel directional control, a traditional rudder behind a propeller or a varying direction of thrust by rotating the propeller or thrust nozzle of a waterjet. Figure 11.25 shows examples of the two systems.

Since all of these devices are located close to the stern, the lever arm to turn the vessel is large and small rotations will provide sufficient force to give the vessel a small turning circle [25]. A traditional rudder will have a separate interface to the hull and structural arrangement. Classification society rules all provide detailed information on sizing and structural design [26–29]; see also *Resources, rules and regulations*.

A propeller-driven vessel will need a controllable pitch (CP) propeller to enable reverse maneuvering, while waterjets, as in Fig. 11.11, can be fitted with reversing buckets that give a strong reverse capability. A multihull can achieve zero speed rotation by differential forward/reverse thrust from the two demihulls, but for the

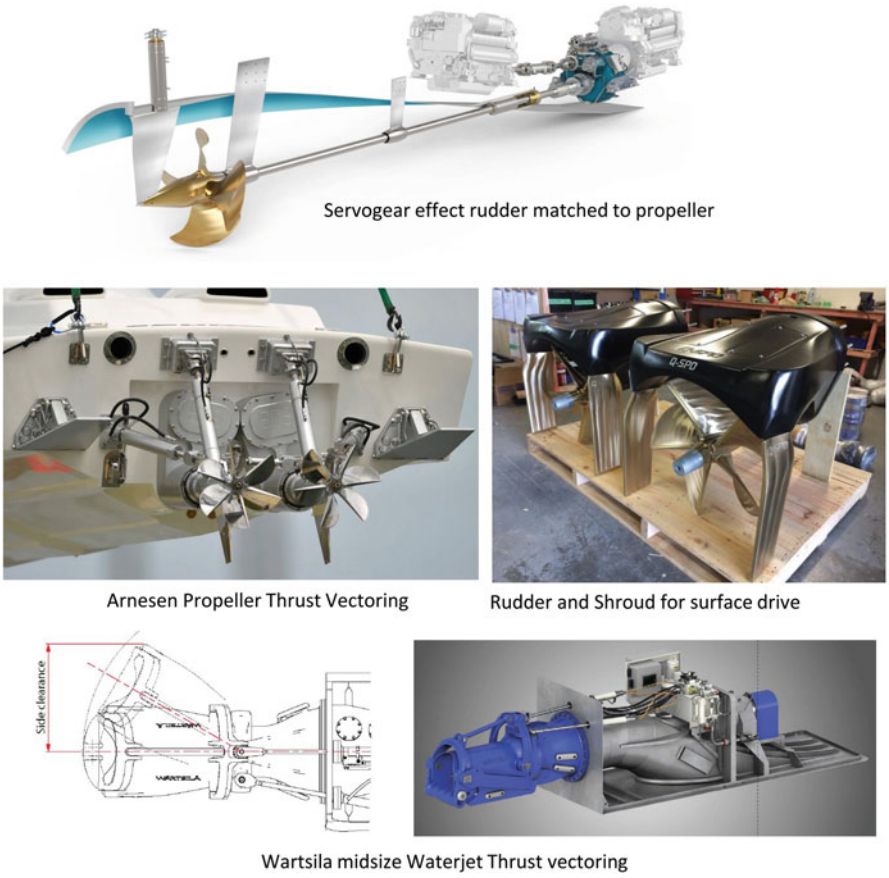

Fig. 11.25 Examples of directional control with rudder and rotating thrust

largest vessel in the range of 100 m LOA and up, it can still be useful to have a small bow thruster to give more precise sideways control for berthing operations.

11.6 Trim Control: Stern Flaps and Interrupters

The generated wave forces on high-speed craft cause increasing bow up trim as Fn_{l} increases through "hump" speed as the generated wave length is twice the vessel L_{WL}. Beyond this as planing is approached natural trim diminishes, but once planing is established above Fr_L 1.0 or so, trim increases again as speed increases further. The bow up trim increases resistance, and so if it can be reduced, this can be optimized. Stern trim tabs and interrupters are the devices that can be employed for this by inducing higher pressure under the hull at the stern. The principle is illustrated in Fig. 11.26a while examples of each are shown in Fig. 11.26b, c.

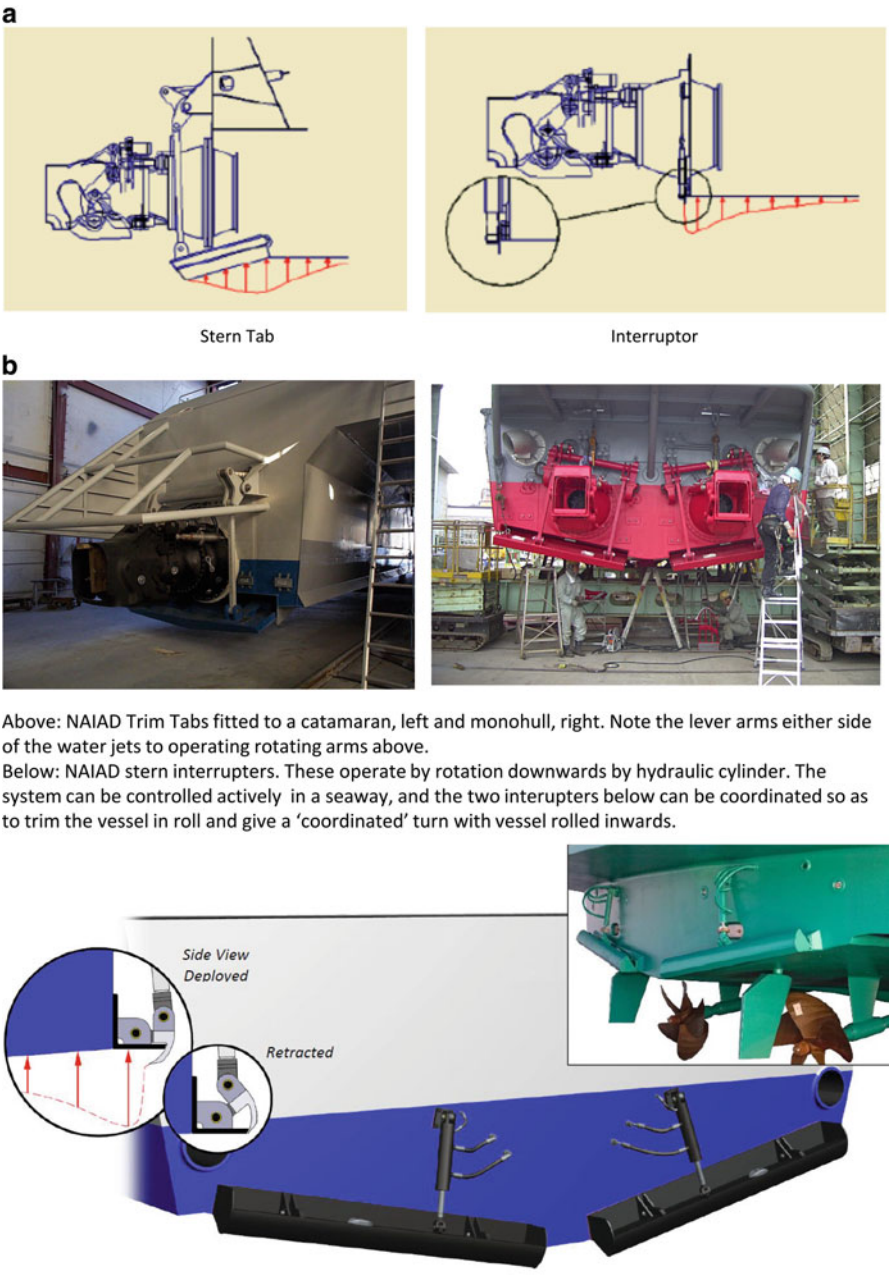

Fig. 11.26 (**a**) Principle of stern tab and interrupter; (**b**) examples of stern trim tab and interrupter devices for trim control

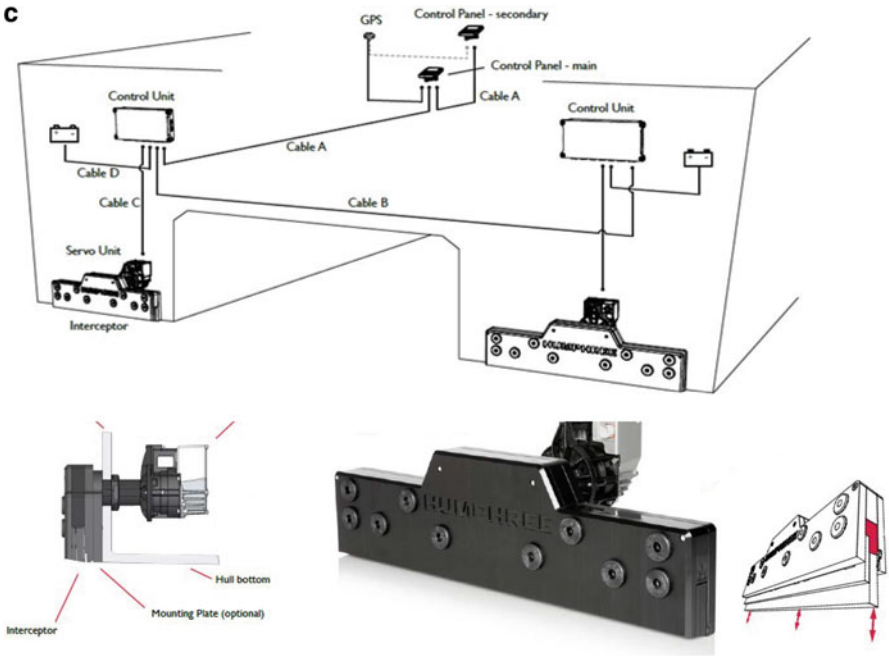

Humphree trim Interrupters for catamaran installation. The system deploys two vertical blades using a geared electrical drive servo in a housing bolted to the vessel transom. Deployment is up to 50mm. Servo can be off centre so as to fit units directly below waterjets

Humphree inteceptors for turning assist. While turning waterjets provides powerful turning moment which is useful at low speed, at high speed it is more efficient to keep the jets in line, and deploy interupters as shown above for course adjustments, so minimising fuel burn. The interrupters are operated coordinated on either side.

Fig. 11.26 (continued)

It is important on fast craft that trim tabs have a sealed hinge at the transom attachment so as not to prompt ventilation, which would reduce the tab's effectiveness. The moment generated is the product of the vertical vector of dynamic pressure on the tab underside and the lever arm to the center of buoyancy plus the increased pressure profile forward of the transom generated by the presence of the tab. For

typical tab dimensions the retardation of flow, and so pressure increase, may lead forward as much as twice the tab chord.

If we consider for a given trim tab force gradually reducing the area of the tab, we would have to increase the angle to achieve the same force; as the tab angle increases above about 15°, it will cause significant vortex flow behind it with recirculation toward the transom. Ahead of the tab it will increase static pressure. If we take this to its limit and simply have a vertical obstacle, it will generate increased pressure under the hull, which will lift it and trim the vessel bow lower. It has been found that this "interrupter" geometry can be a very effective trimming device, while its own intrinsic drag is low, so vessel resistance is reduced.

Adjustment of these two devices can be useful primarily to maintain service speed operating trim with varying longitudinal center of gravity (LCG) in a vessel owing to changes in the payload from one voyage to the next. They are not operated dynamically for damping wave response but nevertheless can be adjusted as vessel speed is increased so as to optimize the dynamic trim as it accelerates through the drag hump and settles at planing speed.

Reference [30] describes the design, installation, and trials of a retrofitted fixed stern flap to a 3720-t displacement FFG7 frigate to assess improvements in resistance and, therefore, power consumption and operating costs. A 10° flap was installed, and it was found to give a 0.5-knot increase in maximum speed at the installed power, so that annual operating costs decreased through lower power usage, correlating to a 10-month payback for the retrofit – clearly a useful performance improvement.

Model testing of interrupter systems is explored in [31] for planing monohull vessels having dead-rise angles of 10°, 20°, and 30°. Effectiveness was found to be higher for the lower dead-rise angles of 10° and 20°. Tests showed that the interrupters had their greatest effect in the region of Fn_{∇} between 1.8 and 2.4. This is exactly the speed region around the drag hump. Commercially, interrupters are available from NAIAD and Humphree (see *Resources*, *Stabilizers and interceptors*), including actuator systems that can give continuous adjustment for dynamic trim correction, as illustrated in Fig 11.26c. Trim tabs are available from several of the transmission and propulsion vendors, for example, Wartsila, Rolls-Royce, Amartech, and Piening.

11.7 Motion Control: Stabilizer and Motion Damping Systems

A strong reason for installing dynamic stabilizer systems on multihulls is to control pitching. In particular for wave piercers, super slender twin-hull (SSTH) and slender trimarans, and semi-small-waterplane-area twin-hull (SWATH) and SWATH forms in longer waves, the use of a bow foil stabilizer can add useful pitching moment damping without significant drag and so reduce bow pitch down effects. There are nevertheless limits to the damping that can be exerted by such devices.

References [32–34] look at the performance of dynamic stabilizer systems and their interactions with large catamaran ferries, and we will discuss their findings to illustrate the recent state of the art.

Reference [32] details an extensive full-scale monitoring program and comparison with analytical motion predictions for an 86-m Incat wave-piercing catamaran ferry that operated across the channel from Weymouth to the UK Channel Islands in 2002. Details of the vessel are given in Appendix 2. This vessel operated at a displacement of 1220 t in sea states up to 3 m significant height. It had hinged tabs at each transom of 8.42 m^2 area and horizontal T foils under each demihull bow at 61.8 m ahead of the transom (14 m behind the bow), each with a wing of 3 m^2. Control movements of the surfaces were $\pm 7^\circ$. Calculated total maximum lifting force at a vessel speed of 37.5 knots was about 65 t, so a maximum added damping force in heave of 5% of displacement. The control system feedback loops of the surfaces were set so that the maximum deflection was used in 3-m seas, which was the operating limit for the vessel. At speeds reduced from the design service speed of 37.5 knots the forces available from the surfaces were lower, so the control loop relationship was set to provide the best possible damping to the vessel response spectrum.

Wave measurement using a forward-looking radar was used, and accelerometers were placed forward, at LCG, aft, and on the beam, with high-speed sampling and fast Fourier analysis instrumentation to derive vessel accelerations and motions during voyages where wave height was above 1 m significant. At this part of the channel there is exposure to Atlantic swells from the west, and the ferry route meant wave directions were predominantly bow quartering. Sufficient data were nevertheless obtained to provide analysis for head seas as well as beam and bow quartering.

The authors made computations to show that setting the control software to operate as a damping mechanism (set so that lift force is set to oppose the vertical velocity of the vessel at that point) gave the best reduction in motion response amplitude operators (RAO), and this was verified. The basis for the BEAMSEA motion program developed at the University of Tasmania is summarized in the paper.

The analytical vessel motion predictions were then compared with the data from voyage measurements, and the computed responses, including the motion controls, were found to correlate well. The maximum effect on pitch and heave response was found to be around the vessel natural periods of response.

Reference [33] presents results from another full-scale motion data gathering exercise and computations were also carried out by personnel from the University of Tasmania and Incat, this time on the 97–m, 1670-t-displacement HSV-2 Swift. This vessel had stern trim tabs and a single retractable T foil mounted to the base of the central bow structure. See Fig. 11.27 for an illustration of a retractable T foil. The system and its controls were supplied via NAIAD Dynamics.

The trials performed on the HSV-2 were part of an extensive program for the US Navy in preparation for its HSV procurement program. The trials analyzed in the reference were carried out by instrumented runs at different headings while operating off the Norwegian coast and in the North Sea east of the UK as part of the program.

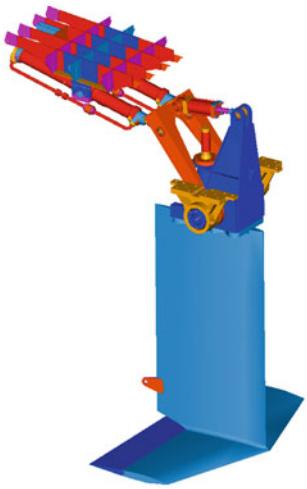

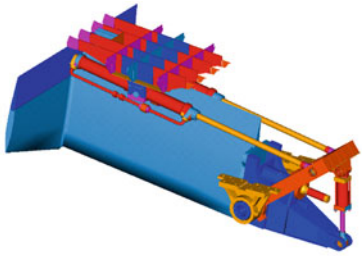

Above: NAIAD Dynamics Motion Damping Deployable T-foil in deployed and stored mode. **Right:** the foil structure showing trailing edge elevator that can be dynamically controlled for optimisation of damping in different seastates using NAIAD cotrol software.

Fig. 11.27 Naiad T foil motion stabilizers

In a similar manner to reference [32], the vessel was fitted with a series of motion sensors, GPS, speed and wave height radar, and data logging. Wave direction was determined from an analysis of the wave slope in relation to the vessel pitch and roll angle, and spectral analysis was carried out to determine the RAOs. Trial runs were made with the T foil deployed and also with it retracted. The BEAMSEA program was again used for analytical prediction of motions, and the T foil was modeled as a damping mechanism in pitch. Good correlation was achieved between the analytical model and the full-scale results for equivalent conditions.

The HSV-2 has a bow with a greater clearance from the SWL than earlier Incat wave piercers with the aim of reducing wave-slamming forces (see Chap. 12 for more on wave slamming).

The results obtained suggested that deployment of the T foil had more effect on damping heave than pitch motions at service speed, though the situation was complex as the vessel had active transom tabs, and these may have had more influence on pitch reduction. Modeling response by taking away the bow shape in

the analytical model also had more of an effect on increasing heave motion rather than pitch.

Clearly there is much to learn still about dynamic motion stabilization of high-speed vessels! In the case of a wave-piercing vessel with a central bow, once it engages with waves, the main task is to restrain downward movement, but the cyclic force response is lower than the vessel SWL, meaning it is in a different phase relationship with the incoming waves compared to the demihulls, so perhaps this influences the vessel response.

Reference [34] presents a theoretical study published in 2004 looking at the effect of T-foil stabilizers and the tradeoff between their drag and motion stabilization. In general, reduced motions may be expected to have a positive impact on vessel power demand, so with judicious design a stabilizer should give an overall positive effect in addition to the motions themselves.

The author presents a linearized slender body analytical model using a boundary element method for resistance and motions of the catamaran vessel investigated operating at speeds of 30, 40, and 50 knots. The catamaran geometry is an idealized vessel, 100 m LOA, with 6-m beam demihulls spaced at 25 m between longitudinal centers, and with a displacement of 1000 t.

The stabilizer T foils were positioned 10 m behind the bows, one on each demihull. The foils themselves had a 1.5-m chord and 6-m span. At 9 m^2 these foils are significantly larger than those installed on the wave piercer in [32].

The author's analytical results indicate that heave response is particularly reduced close to the natural period in heave. In pitch motion the response is dampened significantly in long waves and down to the pitch natural frequency, but above that frequency, that is, smaller sea states, the effect is small.

The effect of foils on vessel drag is small since the presented area and drag coefficient of the foil shape are very low, so drag penalties between 3.55% and 4.7% are projected. The author also considers the effect of unsteady flow conditions on foils as they pass through orbital wave velocities. His calculation suggests that a reduction in effective lift due to oscillatory flow will be 22% at 30 knots for an encounter frequency of 0.8 rad/s or wave period of approximately 2 s. At higher speeds or longer wave periods, the reduction will be smaller, and so overall the consequence of the unsteady lift should be limited.

Considering the results from the three programs referred to earlier, it may be seen that for large multihull vessels active control systems can reduce vessel motions effectively. In addition, analytical tools exist that can be used to assist with the prediction of response. Similar to the modeling of vessel motions and propulsors, it may be expected that CFD tools now available could also assist with this task.

It may be worth noting that active stabilization systems aim to reduce motions and accelerations in sea states up to design limit and at speeds within the certified envelope. If one considers the sea state increasing above the limit for full-speed operation, suggesting that vessel speed is reduced, it is important that vessel motions should allow the vessel to "ride out" a storm. At slower speeds, the effect of a T foil

and stern tab will be reduced; meanwhile, as a storm increases in intensity, the sea state Tz will lengthen, which may increase the effectiveness of the T-foil and heave stabilization.

It may be noted, though, that, depending on the vessel service route, prior to optimizing motions by these active devices, there are opportunities for multihull vessel geometry that can provide first-stage optimization; then it should be considered that the active devices are the refining stage, not that the vessel is dependent on them for operation in high sea states at speed.

IMO HSC Code Chap. 16 distinguishes between systems that must continue operation for safe navigation of the vessel and those that simply improve the ride. A hydrofoil-supported multihull requires the foil system to operate effectively to maintain safe navigation; similarly, a bow-mounted foil system on a wave piercer or trimaran must be effective and reliable. While in both cases the system will improve ride quality, sudden failure would endanger vessel operation.

The key difference is for these systems to look at the potential failure modes and effects and identify how reliability can be achieved so as to reduce the risk to an acceptable level. Most such devices have active controls via trim tabs or elevator surfaces, and so failure of this control should not cause unstable motion of the vessel. To conform to the IMO, alarms should be installed at the vessel bridge so that control failure can be effectively countered by reducing vessel speed or changing direction in a seaway. In the extreme, a failure that occurs while a vessel is at operational speed may represent a case where a crash stop would be initiated, similar to a case where sudden failure of a main engine occurs or a loss of thrust is experienced on one propulsor due to intake blockage or significant propeller blade damage from submerged debris. It may be noted that debris damage is a more likely event for river or estuary operational vessels and may well be a realistic case to consider, depending on the exact location.

The essence here is to carry out a failure modes and effects analysis (FMEA) and then review the impact on design requirements for the stabilizer system and the vessel itself. We provide a summary of the FMEA approach consistent with the requirements of the HSC Code in Text Box 11.1 in what follows.

11.8 *IMO Guidelines*: (IMO HSC Code Chap. 9) Requirements

General The reliability of propulsion machinery is a concern for the IMO since failure could place a vessel in danger during a voyage, so requirements are stated to ensure the normal operation of machinery can be maintained even if essential auxiliaries stop working, for example, the malfunction of:

- Main generators,
- Fuel supply system,

- Lubricating oil system,
- Water cooling system,
- Starting air compressors/receivers,
- Hydraulic, electrical, or pneumatic controls for propulsion machinery.

If one considers the consequences of failures in these systems in an FMEA (Text Box 11.1), the normal result will be to provide backup by duplication unless the system reliability is very high. The backup may not need to maintain 100% operation, for example, if 2 × 75% main generators are installed, the loss of one may still allow for the safe completion of the voyage with internal electrical demand cutback. Fuel and lubrication systems, on the other hand, may require duplicate filter systems.

Main machinery and systems need to be able to operate safely while the vessel is pitched or healed statically by 15° and in addition rolling or pitching by an additional 7.5°, unless the designer can show that its vessel's motions are limited to lower values in extreme conditions by design. For SSTH vessels in pitch, this is likely to be the case, and the same goes for very large multihulls such as the 100 m plus LOA catamarans and trimarans or smaller multihulls that operate in a river or lake environment.

Engines should have two separate means of stopping, actuated from the operator location on the bridge. Any actuators used should be sufficiently reliable to not require duplication.

Engine safety monitoring and control devices should include speed, temperature, and pressures. Monitoring has to be available at the operating station on the bridge and, for Cat B[1] craft, an additional local operator station in the engine room. Protection from overspeed, high temperature, loss of cooling, vibration, and engine overload has to be installed. There must be instrument detection of failure in a liquid cooling system so as to allow machinery to be stopped before catastrophic failure.

The engine design and protective device operation should be such that the engine will not be damaged due to the operation of the emergency device. All safety devices need to have interlock/test functions designed in so as to prevent inadvertent operation causing machinery damage or failure. Boilers and pressure vessels are required to have protection, insulation, and overpressure protection. Fire and explosion safety measures for systems linked to main machinery are discussed in Chap. 13.

Gas Turbines Gas turbine installations need to be designed so that they can operate stably at their design power rating and speed, while also avoiding instability when running up to speed, and when power absorption varies, including protection against surge, stall, or whirling vibration.

[1]Category B craft are those designed to be able to continue when one compartment or one main machinery is damaged, while Category A craft are those that may not be able to continue unaided after such damage and are limited by the IMO to 450 passengers and routing that is within 4 h maximum for rescue by independent resources.

Text Box 11.1 Failure Mode and Effects Analysis Summary
Basic general procedure:

1. Define the system and control elements to be analyzed.
2. Define ground rules and assumptions, including operation probabilities of failure for the control elements and system boundaries.
3. Construct system block diagrams identifying the system elements and control linkages, and model under operation modes, including:

   - Normal operations at service speed,
   - Operation in congested waters,
   - Berthing maneuvers.

   Test response of model to normal operations to ensure it works correctly.

4. Identify failure modes:

   - Loss of function;
   - Rapid change of state (e.g., overspeed, loss of lubrication or fuel);
   - Lack of control, including ability to maintain steady operation;
   - Premature function actions or delayed function actions;
   - Failure to start or cease operation;
   - Others.

   In addition, test the operation of the control model in each of these cases.

5. Analyze failure effects/causes.
6. *Feed results back into the design process to improve response to best possible.*
7. Classify failure effects by severity.
8. Perform criticality calculations.
9. Rank failure mode criticality.
10. Determine critical items in terms of failure consequence.
11. *Feed results back into design process to identify mitigation actions.*
12. Identify means of failure detection, isolation, and compensating provisions.
13. Document the analysis. Summarize uncorrectable design areas, and identify special controls necessary to mitigate risk.
14. Formulate a corrective action plan and acceptance criteria.
15. Follow up on corrective action implementation/effectiveness.

The IMO High-speed Craft Code provides guidance on the following aspects:

- Provision of redundancy,

(continued)

Text Box 11.1 (continued)
- System versus equipment analysis,
- Reporting requirements,
- Probability assessment requirements,
- Definition of corrective actions.

Please refer to resources section also for software, techniques, and training examples.

The gas generator and power turbines in a gas turbine engine should have casings than can contain explosively shed blades.

Gas turbine intakes are designed for high air volume flow. A fast marine vessel has to take account of the need to filter salt from the humid air entering the intakes to minimize the rate of salt buildup on the turbine blades and in addition install arrangements for flushing of the flow paths to clean the blades periodically and maintain engine reliability. Systems are available from vendors such as Sulzer and the main gas turbine suppliers.

To the extent possible, power takeoff shafting needs to be designed to avoid whirling vibration , and connecting joints need to be protected so that a failure cannot result in a shaft causing secondary damage to engine room systems and equipment in the case of failure.

Gas turbines have to be fitted with an emergency overspeed shutdown system, linked to the speed-monitoring instrumentation.

Casings of coolers, intercoolers, and heat exchangers need to be pressure tested on both sides of the circuit.

Diesels Diesel engines will generate higher vibration excitation than a gas turbine, so it is important to investigate the characteristics of the selected engines in terms of the energy spectrum against frequency. This may then be attenuated through resilient mountings. Once the attenuation is applied, the excitation spectrum needs to be applied to the vessel local structure FE model (Chap. 12) to determine whether the structural design needs adjustment so as to ensure the structural natural frequency and harmonics are displaced from the engine energy spectrum (Fig. 11.28). Similar guidance also applies for the transmission system from a diesel engine regarding the shafting and coupling protection against failure modes.

The IMO requires that all high-pressure fuel-delivery lines between fuel pumps and engine fuel nozzles be protected by jacketing tubing against loss of containment by the delivery lines. This is to include failure alarms for the annulus and a means for safe drainage.

Engines with a piston diameter above 200 mm or with crankcase greater than 600 L (0.6 m^3) are required to have explosion relief valves.

Lubricating oil systems, including supply and storage volumes, need to account for the maximum craft roll, pitch, and accelerations so as to avoid spillage and

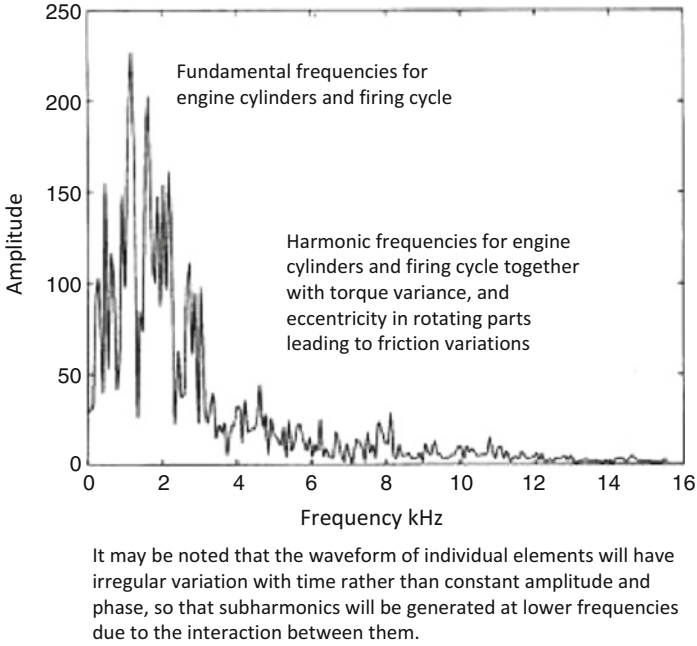

Fig. 11.28 Engine vibration energy spectrum

maintain efficient operation. There should be alarms for low lubricating oil levels and pressure and engine speed limiting in the case of a low-level alarm.

Compressed-air start systems if fitted should be designed to avoid any risk of fire or explosion.

It may also be noted that if a designer adopts LNG as fuel ether to a gas engine (essentially the same as a diesel engine, with much cleaner burn and exhaust) or a gas turbine, the main difference will be that LNG storage must be insulated so as to minimize vaporization under storage, and the fuel system will require a vaporization stage and delivery of the gas to engine cylinder injection. The consequences of damage to tank insulation needs to be considered and mitigation provided to reduce the probability of occurrence to an acceptable level. A significant number of marine craft are now LNG powered, so the design approach is available as a go-by for a designer.

Transmissions Transmission shafts need to be designed bearing in mind, first, the startup torque for the connected propulsor, including engagement impulse from the drive clutch if such a device is installed, then for stiffness so that the natural periods of rotational vibration (whirling) are outside the operating rotational speeds, and finally, that at maximum power rating torsional stresses are acceptable, taking into account a fatigue assessment for the projected typical service life of operational

cycles [35, Chap. 15.6]. Design criteria for operation are required to be set at 105% of the maximum overspeed setting for the engine.

It should be noted that the torque applied to the propulsion device will be resisted by the engine, gearbox, and transmission which will in turn apply loadings to the mountings for each of these to the vessel hull. When analyzing the transmission, the loads at each coupling location or shaft section between steady bearings needs to be determined, and these forces will need to be taken into account when designing the local and global structures. Typically there will be a thrust bearing inboard of the propeller shaft entry or on the drive shaft in the waterjet main housing. Upstream of this the gearbox will apply torque to its mountings, and at the main engine mounts the torque applied to the gearbox will be mirrored by that applied to the engine mounts. Variable-pitch (VP) propellers will apply both push and pull loads, while waterjet systems will have reverse thrust through bucket systems so the reverse thrust is applied to the outer casing of the jet rather than to the impellor drive shaft and through that to the mounting to the transom.

Shafts and couplings should be protected by guards so as to avoid secondary damage to the vessel structure or equipment in case of failure, as noted earlier.

Propulsion and Lift Devices Propulsion devices should be designed to integrate into the vessel main structure. Most important is to analyze the loads that can be applied by the propulsor to the vessel primary structure for its operational envelope, including acceleration, maximum operational speed, and maximum turning moments in the case of steerable waterjets. Once determined, the loads can be used as load cases for application to one of the FE structural models to refine the local design, while the appropriate extreme loads, for example the thrust load at design operational speed plus design margin, will be an important input to the global analysis (Chap. 12).

It is recommended to look carefully at the potential electrolytic action around a propulsion device due to the use of different metals, as well as the potential effects of cavitation erosion and accretion of salt deposits affecting turbulence, vibration, and operational effectiveness. In the case of waterjets, this needs to apply to the casing, including inlet and debris protection grille, and to the submerged jet nozzle, steering equipment, and reversing buckets.

11.9 Concluding Remarks

Currently one of the largest catamaran ferries, the Incat *Francisco*, is powered by gas turbines running on LNG rather than liquid fuel, and as environmental regulations tighten this approach may be of interest also for smaller vessels. The technology advances rapidly at present for LNG-powered trucks, and so this will surely be an option in the near future for river and short distance ferries. The main change for engines operating on LNG is a change to the fuel storage and supply system.

At present electric-powered high speed vessels are limited to hybrid vessels such as a hybrid diesel and battery electric touring catamaran operating out of Bergen [36] and the study for a fully electric 35-knot ferry for San Francisco [37]. It is clear nevertheless that battery electric fast ferries will be joining the fleets in a while. The power train design for these vessels needs a different approach from that for diesel- or gas-turbine-driven multihulls, and this is left to readers to investigate for themselves. For vessels operating short regular transits, it will be possible to have battery topping up at each terminal end stop so as to minimize the battery mass carried by the vessel. This is already being used by ferries in Norway, though not yet fast ferries (as of 2017).

This chapter has been a rather brief walk through propulsion. It will be important for the reader to use the reference material for a full theoretical treatment of the topic and connect with the various suppliers for details of their products and how to select and integrate with the vessel hull design.

Currently tools such as CFD have enabled analytical modeling to give a much more accurate representation of flows around a vessel and through propulsors as well as around stabilizing devices. This does not take away the need for a proper understanding of the underlying fluid dynamics to be able to make the best design choices. What it does do is alter the designers' task toward understanding optimization of FE modeling since, if this is set up right, a model will resolve efficiently, and if not, it might simply fail to reach a stable solution.

Now we will move forward on the basis of having looked at propulsors and made a selection. We have discussed selecting a main engine and transmission and the assembly of the general arrangement, weights, and centers for the machinery compartments, including main tankage.

It might also be worthwhile to take a quick run through the other outfitting elements so as to obtain a view on the weights and distribution of the major equipment (Chap. 13) before going into detail on the structure. If the vessel is an extension of a series, then much information will be available already and have been scaled. If so, this might be retained as preliminary gross estimates, as in Chap. 7, for now, so that we can move on to look at structural design in Chap. 12. We can reconsider refining general outfitting subsequently since, apart from the major structural delineation of spaces, the rest relates to the secondary structural arrangement.

References

1. Hydrodynamics of high-speed marine vehicles, by Odd M Faltinsen, Cambridge University Press, UK, 2005., ISBN 978-0-521-84568-7, 451p
2. Doutreleau Y, Laurens JM, Jodet L (2011) Resistance et Propulsion du navire (Resistance and propulsion of ships – French text). Technosup ENSTA Bretagne, Paris ISBN 978-2-7298-6490-3
3. Capt. H E Saunders (1965/1982) Hydrodynamics in ship design, SNAME, Vol I, Chapters 15, 16 and 17 on propellers and propulsion

4. Principles of naval architecture, SNAME, Chapter V11 sections 11 through 17 on propellers and propulsion devices
5. Allison J (1993) Marine waterjet propulsion. Trans SNAME 101:275–335
6. Allison JL (1978) Propellers for high performance craft. SNAME Mar Technol 15(4):335–380
7. Yun L, Bliault AEJ (2000) Air cushion craft, Chapter 15 Propulsion system design, includes marine propellers, super-cavitating propellers and waterjets for Surface Effect Ships. Hodder Headline/Elsevier/Wiley, UK, ISBN 0 340 67650 7, pp 487–611
8. International Code of Safety for High Speed Craft, IMO, publication IA-185E, ISBN 92789 28014 2402, 2000. Amendments and resolutions after 2000 are available on IMO web site IMO.org
9. Hoerner SF, Borst HV (1992) Fluid dynamic lift, ISBN-13: 978-9998831636, 2nd edn. Publisher by the author, USA
10. Abbot IH, von Doenhof AE (1959) Theory of wing sections. Dover Publications, USA, ISBN-13: 978-0486605869
11. Newton RN, Rader HP (1961) Performance data for propellers for high speed craft. Transactions of Royal Institution of Naval Architects, London, pp 93–118
12. Suhrbier KR. On the influence of fully cavitating propellers on interaction effects and dynamic stability of fast craft, FAST '95 Lubeck-Travemunde, 25–27 Sept, vol 2, pp 795–805
13. Keller M (1995) Full scale measurements on a ventilated propeller, FAST 1995, 25–27 Sept 1995, vol 2, pp 991–102
14. Svensson AR. Description of the water jets selected for 'Destriero', FAST 1991 Trondheim, vol 2, pp 1169–1184, Tapir ISBN 82-519-0962-7
15. Steen S, Minsaas KJ. Experiences from design and testing of waterjet inlets for high speed craft, FAST '95 Lubeck-Travemunde, 25–27 Sept, vol 2, pp 1255–1270
16. Hoerner SF. Fluid dynamic drag. Published by the author, Hoerner fluid dynamics, PO Box 342 Brick Town New Jersey NJ08723, USA, 1965, ISBN-13: 978-9998831636
17. Seil GJ (2000) Computational fluid dynamics optimisation of flush type waterjet inlets. Trans RINA 142:164–181 ISSN 0035-8967
18. Bulten NWH, Verbeek R, van Esch BPM (2006) CFD simulations of the flow through a waterjet installation. Trans RINA 149:141–151 ISSN 0035-8967
19. Alexander KV, van Terwisga T. Controversial issues in waterjet-hull interaction, FAST '95 Lubeck-Travemunde, 25–27 Sept, vol 2, pp 1235–1253
20. Van Terwisga T. The effect of waterjet-hull interaction on Thrust and propulsive efficiency, FAST 1991 Trondheim, vol 2 pp 1149–1167, Tapir ISBN 82-519-0962-7
21. Seil GJ, Fletcher CAG, Doctors LJ. The application of computational fluid dynamics to practical waterjet propulsion system design and analysis, FAST '95 Lubeck-Travemunde, 25–27 Sept, vol 2, pp 1379–1390
22. Murrin DC, Bose N (2006) Waterjet propulsion system tested in a wind tunnel and compared with numerical simulation. Trans RINA 149:1–9 Part B1, ISSN 0035-8967
23. Ding J, Wang Y (2009) Waterjet performance characteristics prediction based on CFD simulation and basic principles of waterjet propulsion. Trans RINA 151:151–174 ISSN 0035-8967
24. Jin S, Wang Y, Wei Y, Fu J (2013) Integration design of waterjet with modern technology. Trans RINA 155:B63–B69 Part B2, ISSN 0035-8967
25. Voulon S, Wesselink AF. Manoeuvrability of waterjet propulsed passenger ferries, FAST '95 Lubeck-Travemunde, 25–27 Sept, vol 2, pp 1131–1156
26. Lloyds Register Rules for Special Service Craft (download from Lloyds Register internet site)
27. Lloyds Register Rules for Trimarans (download from Lloyds Register internet site)
28. DnV Rules for High Speed Light Craft and Naval Surface Craft (download from DnVGL internet site)
29. ABS Rules for Classification of High Speed Craft (download from Eagle (ABS publications) internet site)
30. Cave WL, Cusanelli DS (1993) Effect of stern flaps on powering performance of the FFG-7 class. SNAME Marine Technol 30-1:39–50 ISSN 0025-3316

31. De Luca F, Pensa C (2012) Experimental investigation on conventional and unconventional interceptors. Int J Small Craft Technol Trans RINA 154:65–72 Part B2, ISSN 0035-8967
32. Davis M, R, Watson NL, Holloway DS (2003) Wave response of an 86m high speed catamaran with active T foils and stern tabs. Trans RINA 145:87–106 ISSN 0035-8967
33. Jacobi G, Thomas G, Davis MR, Holloway DS, Davidson G, Roberts T (2012) Full scale motions of a large high speed catamaran: the influence of wave environment, speed and ride control system. Int J Maritime Eng Trans RINA 154:143–155 Part A3, ISSN 0035-8967
34. Doctors L (2004) Theoretical study of the trade-off between stabilizer drag and hull motion. Trans RINA 146:289–298 ISSN 0035-8967
35. A Bliault and L Yun, Theory and design of air cushion craft, 2000, Arnold/Elsevier., ISBN 0 340 67650 7 and 0 470 23621 3 (Wiley), UK, 632 pp
36. A green vision to behold, article in RINA Ship and Boat International Jan/Feb 2017 pp 20-21, 'Vision of the Fjords' hybrid powered touring catamaran by Brødrene Aa (www.braa.no)
37. California green dreamin', article in RINA Ship and Boat International Jan/Feb 2017 pp17-19, 150 pax 35knot all electric catamaran ferry, see study report at the following link for details: http://energy.sandia.gov/transportation-energy/hydrogen/market-transformation/maritime-fuel-cells/sf-breeze/

Chapter 12
Structure Design

12.1 Introduction

So far in this book we have discussed the different configurations of multihull vessels from the point of view of their form, stability, resistance, and motions in waves. Once we have defined the desirable form, the question is how to create the structure that will support the payload and resist the forces that the environment will apply to it. Our purpose with this chapter is to give a summary of the issues connected with the design of a multihull structure, including how this links to the hydrostatic and dynamic analyses and building from the initial estimates of the synthesis in Chap. 7.

To design a structure, we need to identify the static and dynamic loads that will apply to it. The starting point is the static loading, including the hull, superstructure, payload, machinery, and outfit. From that point we need to look at the distribution of buoyancy for the static force balance between the center of gravity (CG) and center of buoyancy (CB) and the moments about these centers to determine static stress distribution in the structure. To obtain the stresses, we need to calculate the cross-section areas and the moments of inertia of the sections to apply the bending moment and shear force.

Dynamically the vessel will be subjected to the forces and moments applied by waves and vessel motion in waves, including slamming forces, and the hydrodynamic pressure variations applied to the hull surface by vessel speed and incident waves' cyclic velocity and pressure gradient. Figure 12.1 below shows this in diagrammatic form.

The structure of a monohull vessel can be likened to a single box beam of varying section. A multihull is a rather more complex structure. Depending on the multihull concept, it has to be treated as a pair or group of beams in the longitudinal direction connected at the top by another box structure, multiple transverse beams, or a combination. In oblique seas, significant out-of-plane forces apply torque to the

L. Yun et al., *High Speed Catamarans and Multihulls*,
https://doi.org/10.1007/978-1-4939-7891-5_12

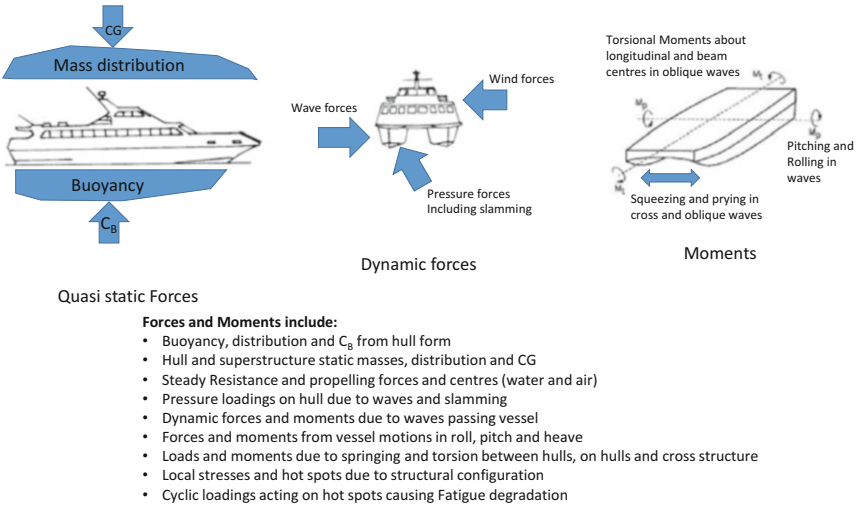

Fig. 12.1 Forces and moments on a multihull

cross structure/superstructure from the hull structures as well as to the hulls themselves.

To develop the structural design of a multihull, a sequence of analyses needs to be followed, supported by results from hydrostatic and dynamic analyses. This design flow is shown as a chart in Fig. 12.2.

If we compare this work with a monohull, the additional tasks are related to the cross structure and the load cases that can be applied to this. If we are designing a trimaran, or even a pentamaran, we still start with the forces on the main hull and then look at the cross structure to the sponsons. If we are designing a hydrofoil supported catamaran, we need to start with the loads that will apply to the base catamaran and then add the point loads that will be developed from the hydrofoils.

Our sequence starts with an estimate for the static loads, which will be done during concept selection before we have an actual structure, so the initial estimate will be based on statistics, as discussed in Chap. 2 and later in more detail in Chap. 7.

Once the concept is selected and we have a geometrical model (for example, in Maxsurf, see Bentley.com in resources), a first estimate of hull shell, frames, bulkheads, and stringers can be prepared. Some decisions have to be made regarding the cross structure to accommodate an open vehicle deck level and more compartmented passenger space above it for larger vessels. Once this is available, the scantlings can be outlined as a bulkhead and longitudinal stringer stiffened box structure.

For smaller passenger vessels the superstructure over the demihulls' main deck and the cross structure will integrate closer with the hulls' structure. The hulls' inner surfaces may simply be continued as curved plating for slender vessels, rather than there being a flat lower "wet deck" to the cross structure. For wave piercers and semi-small-waterplane-area twin hull (SWATH), the forward part of the cross structure

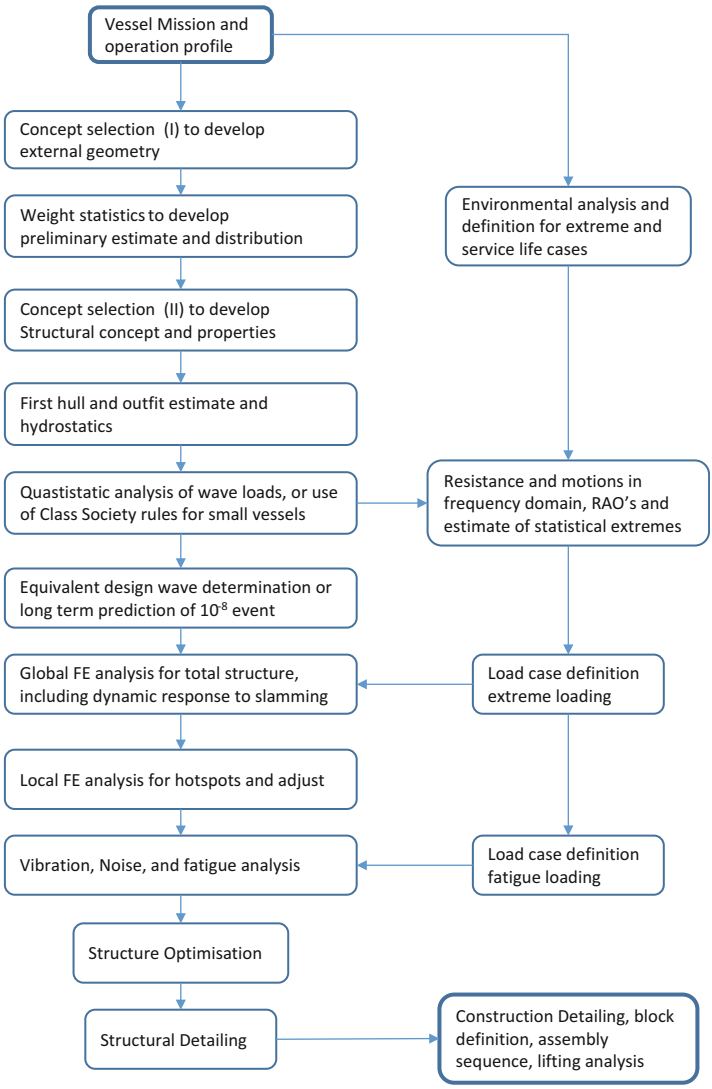

Fig. 12.2 Structural analysis and design activity flowchart (outline list below)

lower surface will need to form a bow shape to deflect solid water from wave crests. We will discuss wave impact later in the chapter.

At this point we need to check with our chosen classification society and regulatory body what criteria they require to be applied to the subsequent structural design load cases and the structural configuration. With that input we can develop our load cases and move the structural analysis forward using a finite-element (FE) structural design package.

The most likely analytical approach of a designer is to follow the procedure recommended by one or another of the classification societies. We will look at the differences in approach starting in Sect. 12.5; meanwhile, let us run through the sequence following the ABS guideline for direct structural analysis [1] and then discuss experience and issues related to the various stages of analysis that have been identified by a number of research projects. First a few thoughts on what needs to be defined to start the analysis.

12.2 Structural Concept Issues for Multihull Craft

The main hull or demihulls of a catamaran form a uniformly supported beam that flexes longitudinally about neutral points approximately 25% in from bow and stern on the waterline.

The demihull beam will have variable stiffness along its length. The initial static deflection in calm water will sag at the longitudinal center of gravity (LCG), with a deflection profile proportional to the beam stiffness at the relevant section along its length. In bow waves of wavelength equal to the length overall (LOA), maximum sagging will occur with the wave peak at bow and stern, and maximum hogging will occur as the wave peak passes amidships. In beam waves with wavelength equal to the centerline separation between demihulls, maximum prying will occur with wave troughs at the centerline and maximum squeezing when the wave peak is at the centerline (Fig. 12.1). For additional explanations of these concepts see [2].

Smaller multihull vessels may have a practical operating limit as specified by DNV GL [3] of a 4-m significant sea state, and so this wave height can be used to test hogging and sagging as quasi-static loading on the structure.

Note that a catamaran, SWATH, and trimaran will all respond differently to quartering seas, producing torsional loads (twisting), as well as squeezing and prying.

The configuration for the cross structure between demihulls on a catamaran can strongly affect the distribution of global loads and stresses. In the limit, a configuration with stiff beams connecting the hulls, with open space between them, would be most structurally efficient. This arrangement will not fully constrain the torsional flexure between hulls in oblique seas or the prying flexure from beam seas unless the beams themselves and the connection to the hulls were rigid in torsion.

Fast sailing catamarans use this arrangement, with very stiff carbon fiber cross beams and tensioned netting for crew to walk on. At the other end of the scale, the cross structure could be a stiffened plate box that constrains the torsional and prying moments. In practice, the structure will be a combination of beam and stiffened plate structures. Heavier structures at bow and stern provide the optimum structural weight.

A catamaran connected by heavy cross beams at bow and stern and lighter intermediate framing will flex, transmitting load from the hulls into the light superstructure through shear forces. If the superstructure is a stiffened box structure,

then it will participate more in the global loads applied via the hulls. Effectively, the center of inertia will be raised, and the hull beam will become stiffer and have a stiffness discontinuity (haunch) at the ends of the superstructure. Careful local detailing is required in these areas, particularly the forward discontinuity to avoid stress concentrations that would lead to reduced fatigue life in that area.

A SWATH will work even more as an "I" beam configuration with unequal flats, with the lower flat of the "I" being the submerged "cylindrical" part of the hull and the upper flat being the main deck box structure.

When planning the structure for a vessel, it is useful to know up front that smaller craft, typically less than 15 m LOA, will need to be designed for stiffness rather than global strength against load criteria. With this in mind the initial structural scantlings may be sized from first principles by considering the quasi-static load cases for head and beam waves of suitable wave length, adding a simple dynamic factor of 50% and measuring this against the allowable stresses published by the appropriate classification society. A review of global and local deflection will indicate whether frame spacing or stringer dimensions or spacing needs adjustment to decrease local deflection. This will then give a head start on the FE analysis, which will be reviewed primarily for deflection against the criteria set by the designer.

Larger vessels will have stresses from the global loading cases that will control their scantlings at the global level, while stiffness may still be a criterion for local areas, for example the vehicle loading deck and main machinery foundations.

Since catamarans utilize the "cross structure" or superstructure to house their payload, the initial form for this will be guided by the requirements for that payload including the "permanent" outfitting. If we consider smaller vessels, particularly slender low wash configurations, the superstructure itself becomes a long box beam extending across the main deck level of the demihulls (see Figs. 12.3 and 12.4 below for illustration of small and large catamaran superstructures).

Fig. 12.3 Small catamaran integrated superstructure

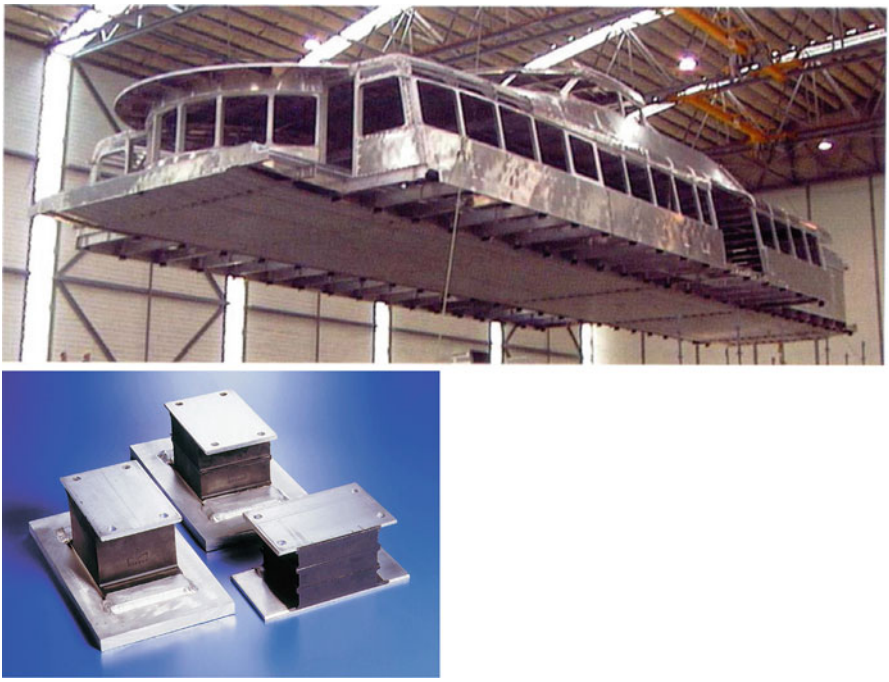

Fig. 12.4 Large catamaran ferry resiliently mounted independent superstructure, and view of resilient mounts used

For passenger ferries, large window areas provide the best passenger experience, but these openings need to be designed so that global loadings are transmitted as stress flows around them. If the main load-bearing structures are at the connection to the demihulls on the inner hull wall, this allows the structure outside of this to be lighter and more consistent with large openings in a stiffened plate. The main issue, then, is the load applied to the frame around the window and suitable resilient mounting for the window in the frame.

Many large catamarans (in the size range above 70 m LOA) are now designed with an upper deckhouse as a rubber isolation structure mounted separately on top of the connecting structure [4, 5]. This configuration also lowers the stresses taken by this part of the structure, assisting a design with substantial window openings.

The hull structure of both catamarans and trimarans in welded aluminum generally comprise a longitudinally stiffened beam with stiffener spacing between 20 and 30 cm depending on the hull dimensions, with web frames at between 50 and 120 cm spacing and main bulkheads between 3 and 5 m. Many shipyards now also have machinery for producing bespoke extruded sections for stiffeners or deck planks, so dimensions can be optimized and welding minimized during construction [4].

Larger catamaran vessels will generally have a longitudinal watertight (WT) bulkhead connecting with the demihulls at the inner longitudinal plating and transversally at bridging structure boundaries.

As discussed in Chaps. 2 and 7, it is useful to take a look at vessels that have already been built, so as to generate ideas for the overall configuration. An overall general arrangement can then be mapped out. At this stage it is necessary also to select main machinery and outfit systems to prepare the vessel specification and allow structural general arrangements to be prepared, weights estimated, and static balance determined, possibly including water ballast to achieve the intended static waterline (SWL).

12.3 Preparation and Analysis

12.3.1 Structural Design and Assessment

There are two objectives to meet: first, to define the scantlings for the vessel structure that can resist the environmental forces while supporting the self-weight and variable payload, and, second, to analyze this structure to verify that it meets criteria for flexure and stress. We discussed a number of issues involved in the configuration of the structure in Sect. 12.2. We now continue to look at the structural analysis. Then we will step back to the guidelines presented by classification societies that allow the initial structural dimensioning to be calculated using rule formulas. The logic with this is to outline first the modeling and detailed analysis that we wish to complete, so that when we prepare the initial structure outline and start building the model, we have these objectives (or any shortcuts we might wish to take if the vessel is a small one, for example) in mind. In particular, the alignment of hydrodynamic and structural modeling can minimize interpolation between models and ensure reliable results.

Three main assessments should be carried out for a large high-speed vessel, the *global and local strength analysis* against design extreme loads, *fatigue analysis* looking at areas of the structure to determine degradation due to stress cycling, and *vibration analysis* to identify structural response to shock loads or excitation from main machinery particularly waterjets that may add to fatigue damage.

In the case of shock loads with pressure rise times less than twice the structural fundamental natural period, the flexibility of the structure may be such that load and response cannot be considered separately. This may affect the oblique case as well as head seas owing to potential squeezing and prying response that will occur if the slamming is from oblique waves. In these cases, the loading applied to the structural model will have to be linked to structural deflection at the nodes where the deflection is obtained from a free vibration analysis of the structure.

If the wave slam has a rise time greater than twice the natural period, then the pressure profile may be added to the other components of the extreme loading case for FE analysis on a quasi-static basis.

An outline of direct structural analysis in line with ABS is shown in Fig. 12.5. We will now discuss each step in turn.

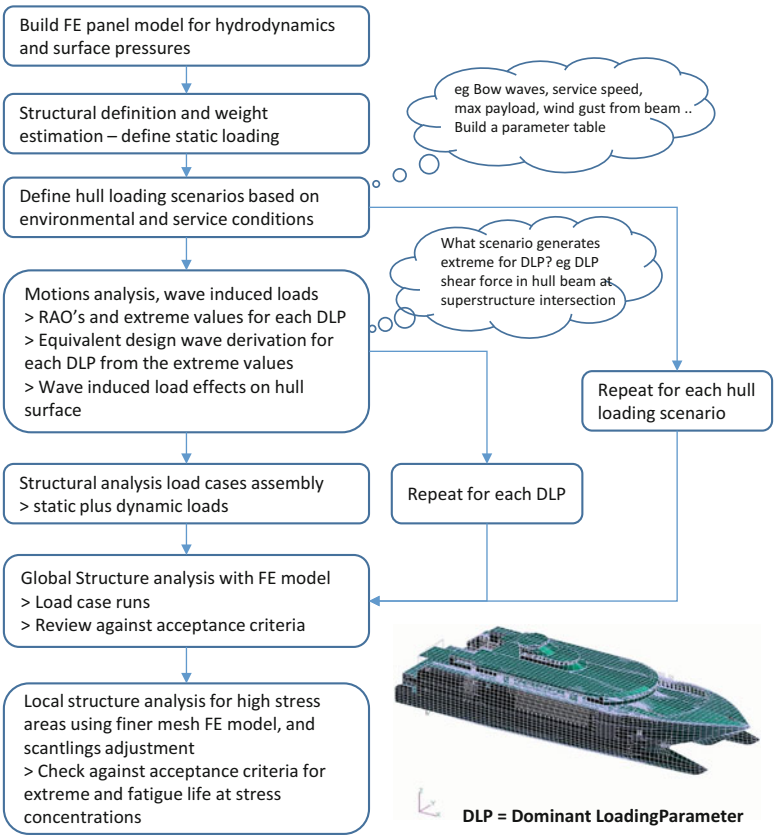

Fig. 12.5 Outline flowchart for direct structural analysis

12.3.2 Environmental and Service Conditions

Early in design development following concept selection, a preliminary analysis will have been carried out for resistance in calm water and for vessel motions in the wave environment. Initial assessment of motions for a concept can be made with a frequency domain analysis and by looking at the unit response amplitude operators (RAOs). To take the selection further, it is necessary to obtain data on the environment expected over the service route or the area for vessel operation.

The motions and loads induced by the seas are generally determined by computer model analysis and physical model testing in regular waves to obtain RAOs through the range of wave frequency, followed by application of the wave energy spectrum applicable for the location, so as to determine the motion response spectrum and the mean (RMS), significant (highest one-third), and maximum predicted motion and loading vectors. A computer model can also give the profile of pressures at the hull surface.

Determination of the vessel response statistics is based on an assumption of linearity with wave amplitude. Where nonlinearity is expected, tests can be carried out [analytically with computational fluid dynamics (CFD) or in a model basin] using an irregular wave spectrum. The challenge, particularly with physical model tests in irregular waves, is that a test run must meet a limited number of waves compared to the full-scale environment, so a number of runs may be necessary to obtain sufficient wave responses to be statistically valid. Equivalently, a computer simulation will need to run sufficiently long to include an appropriate number of waves. The exposure time across the route will give one approach, while an alternative would be to simulate the condition held static for 3 h. Wind wave storms rarely exceed this duration at their extreme. Outside this they are either building or subsiding.

Fortunately, global motions and loadings for multihulls are generally linear with respect to wave amplitude for realistic operational data, including extreme loadings and fatigue loadings, so the use of regular waves and RAOs together with wave statistics is feasible.

High-speed multihull vessels most often operate on fixed routes, so wave statistics should be obtained for that route, from either the potential operator or the environmental agency covering the area.

The route or operational area may include shallows or parts of the route having limited fetch restricting the sea state that can occur or be in open ocean conditions. ABS recommendations for sea spectra to use are JONSWAP, where the service route has limiting factors such as constrained fetch as the peak enhancement (gamma) can be adjusted, while for open ocean either the Pierson–Moskowitz or ISSC/Bretschneider two-parameter spectra will be applicable. Where there is regular underlying swell with significant energy, it is recommended to use the Ochi–Hubble bimodal spectrum, and an alternative here would be Torsethaugen's bimodal spectrum; see [6, 7 and 8 Chap. 8] for more details on wave spectra. Figure 12.6 gives a diagrammatic representation of the determination of motion response from a wave spectrum and RAO profile.

When determining extreme loadings related to the dominant load factors introduced in what follows, the designer will be interested in limiting conditions. Typically statistics are prepared for a given probability of occurrence and storm duration, for example, the 10-year extreme occurrence of a 3-h storm. Based on wind and wave statistics taken over a year or number of years, the Rayleigh distribution can then be used to project the sea state at the selected design interval. The wave energy spectrum for that extreme sea state can then be applied to the vessel RAOs to generate significant and extreme response predictions. See Sect. 12.4 for the approach required by ABS.

Analysis for fatigue will require a scatter diagram for the annual occurrence of sea states and directions, ideally taken from observations at the route or close by. Alternatively, data for a wider area around the operation route can be used. If data for a limited period are used, this is often simply projected forward on a linear basis, ignoring the issue of gradually increasing extreme value expectation. The

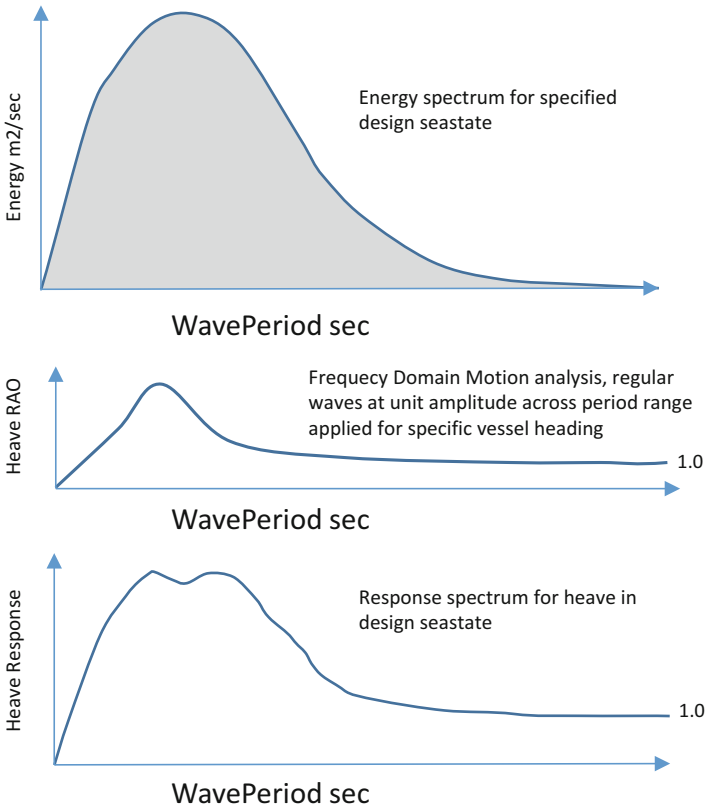

Fig. 12.6 Motions, sea spectra, and extremes

higher frequency waves will create more stress reversals that lead to degradation of structural resistance, so linear projection may be considered a reasonable approach.

The scatter diagram of sea state occurrence can then be translated into a scatter diagram for vessel and structural responses for the calculation of fatigue degradation, usually of points on the structure that are highly loaded and with stress concentrations.

It should be noted that wave statistics are normally gathered by static wave buoys. For a fast vessel the wave encounter frequency will be significantly changed by the service speed, so the data need to be adjusted for this. Further, while some data provide directional sea state information that is important for a permanently moored offshore vessel, a fast multihull will effectively approach the shorter waves in its service environment from straight ahead to around 45° to bow-on, so the omnidirectional scatter diagram is a useful conservative approach, as long as both head seas and an oblique heading are considered for fatigue checks.

12.3.3 Structural Definition and Weight Estimation

Based on vessel general arrangements (Gas), the following definition has to be developed for structural design:

- Hulls' structural GA, including stiffening and bulkheads starting from line plan or model;
- Cross structure, including freight/vehicle payload space;
- Superstructure (and isolation mounting as appropriate);
- Internal outfitting, machinery, and external appendages, including definition of point and distributed loads applied to main structure;
- Material selection, properties, and allowable stresses;
- Static weight estimate, including structure, outfit, water ballast, payload, and consumables under minimum and maximum operating conditions.

12.3.4 Structural Analysis Load Cases

To develop the load cases to be run, the following elements need to be specified:

- Vessel's extreme loading conditions,
- Dominant loading parameters (DLPs) to be considered,
- Environmental conditions to apply.

12.3.4.1 Loading Conditions

The intent is that the design should consider the loading conditions forming a boundary for the vessel's operation, so departure conditions at, for example, full load and full fuel tanks, may define the maximum static loading condition, while a minimum arrival, that is, the lowest defined operational payload together with fuel tanks at a low level and consumables also at the lowest allowable level, will define the minimum static loading condition.

The static loading condition will alter the vessel natural frequency for motion response, so, depending on the shape of the wave energy spectrum, the loading parameters may reach an extreme under different loading conditions. Typically for vessels operating in sea states up to 4 m significant sea state, the period associated with maximum energy will be less than 4 s. The roll, pitch, and heave natural periods for a typical 30-m catamaran may be in ranges of 3, 4, and 6 s, so clearly damping in pitch will be important to that vessel's motions and, hence, structural loading.

These loading conditions will be applied together with the environmental conditions that are expected to generate the extreme stress responses for the particular DLPs.

12.3.4.2 Dominant Loading Parameters

For a multihull vessel, the DLPsinclude the following:

- Midships vertical bending moment (*head seas*)
- Vertical acceleration at bow (*head*)
- Vertical shear force at approx. 0.25 L and 0.75 L from stern perpendicular (*head*)
- Relative vertical velocity along centerline of wet deck for slamming (*head*)
- Longitudinal shear load at centerline of connecting structure (*oblique seas*)
- Vertical and lateral shear at superstructure end discontinuity (*head, oblique*)
- Torsional moment in oblique pitching/rolling motion (*oblique)*
- Splitting moment in yaw during motion oblique to waves (*oblique*)
- Roll motion transverse bending moment (*beam seas*)
- Roll motion vertical and lateral shear forces (*beam seas*)
- Squeezing and prying moment (*beam)*

12.3.4.3 Environmental Conditions to Apply

The preceding DLPs relate primarily to head seas, beam seas, and oblique seas. The approach will be initially to run the structural model in unit waves to obtain the RAOs and to follow this up with application of the spectrum to the design sea condition obtained from location data as discussed earlier so as to integrate the response spectrum and predict the design extreme value. For a specific design the exact oblique angle for wave approach leading to extreme shear and squeeze/pry loadings is difficult to predict, so ABS recommends a series of cases varied by 15° to test the response and then apply the extreme value prediction to the direction with the highest response.

12.3.5 Selection of Load Cases

The load cases selected for analysis should

- Use drafts, loading patterns, and conditions that reflect a vessel's operating conditions;
- Use equivalent design waves or design sea states that generate the vessel extreme responses (see Sect. 12.5, "Loads for Structural Analysis," for explanation)

In addition, DLPs are used to build each load case

The intent is to build a set of load cases around the DLPs, including conditions that would be relevant to each case that is likely to generate extreme response for the dominant parameters. Let us consider key examples and their DLPs:

- *Head waves* – characterized by pitching and vertical acceleration at the bow, with DLPs being amidships vertical bending moment, vertical shear force, vertical shear at longitudinal WT bulkheads, and possibly slamming loads;
- *Beam waves* – causing roll motion generating transverse squeezing and prying forces and moments, vertical and lateral shear; additionally, possible splitting moment in yaw as the vessel is not symmetrical bow to stern, and some torsional moment. This in addition to the static amidships transverse bending moment and shear forces;
- *Oblique head waves* – causing roll and pitch, with DLPs of torsion, vertical bending moment, splitting moment, and vertical and lateral shear.

In each of these examples the vessel maximum static loading and minimum static load may need to be analyzed because the motion and acceleration response will be different.

Faltinsen [8] found that transverse vertical bending moments and shear forces are largest in beam seas (and at zero speed), while the largest pitch-induced bending moment is at 60° to head seas for most wave periods.

12.3.6 Accompanying Load Components

These loadings have to be added to the DLPs for a load case. For the hull plating, resistance to external pressures due to hydrostatic, wave-induced dynamic pressures and vessel velocity has to be determined. Internal to the structure there may be loadings applied locally such as liquid pressures to tank spaces or wheel pressures to vehicle deck.

12.4 Ship Motions, Wave Loads, and Extreme Values

12.4.1 Still-Water Loads

ABS requires the hull girder still-water shear force and bending moment to be determined at a number of stations along the length, taking account of weight distribution and structural discontinuities. A recognized program is to be used (e.g., Maxsurf and Hydromax, LAMP and NLOAD3D, WASIM and HYDROD, GL Shipload) and the bending moment and shear force distribution calculated for both maximum and minimum loaded conditions.

12.4.2 Spectral-Analysis-Based Modeling for Motions and Loads

ABS assumes that a structural FE model will be generated that will be compatible with the hydrodynamic model used for motion analysis such that fluid pressures from the motion model can be applied to the structure's FE model. The seakeeping analysis program must be recognized software (as previously, also see listing of some products in resources at end of book). The assumption is that the motion analysis will be by three-dimensional (3D) potential flow-based diffraction–radiation modeling, generating rigid-body motions in 6° of freedom.

12.4.3 Linear Response: Response Amplitude Operators

For each loading condition selected for analyzing the vessel, ABS expects the RAOs for the six motion components (heave, sway, surge, roll, pitch, yaw), together with those for the DLPs listed earlier in Sect. 12.3, to be determined. This will involve running the motion software for head and beam seas plus a series of oblique directions, for example, 15°, 30°, 45°, 60°, and 75° to bow heading to generate the unit responses or RAOs. The wave frequency range recommended for use is between 0.3 and 1.5 rad/s in increments of 0.05 rad/s, that is, 24 data points to define the RAO curve.

The rigid-body motion and acceleration RAOs will then be determined by the panel-based software and, with the static weight distribution modeled, will be able to generate the bending moment and shear force diagram. From the initial static force analysis the locations of the maxima for the bending moment and shear force can be verified and these locations used to assess the maximum RAOs through the frequency range.

The oblique wave headings are slightly more complicated since, though the same model will enable determination of the torsional load and lateral shear, the heading at which the extreme will occur will depend on the exact geometry of the hull and superstructure.

Thus, from this work with the panel-based model for motion analysis, the core load data can be determined for input to a structural FE model. First, though, the extreme values need to be determined (Fig. 12.7).

12.4.4 Extreme Value Analysis

Once the RAOs for the DLPs are determined based on linear analysis where the water surface is effectively taken as flat at the load case SWL, ABS direct analysis requires the projection of an extreme value based on a most probable extreme at a

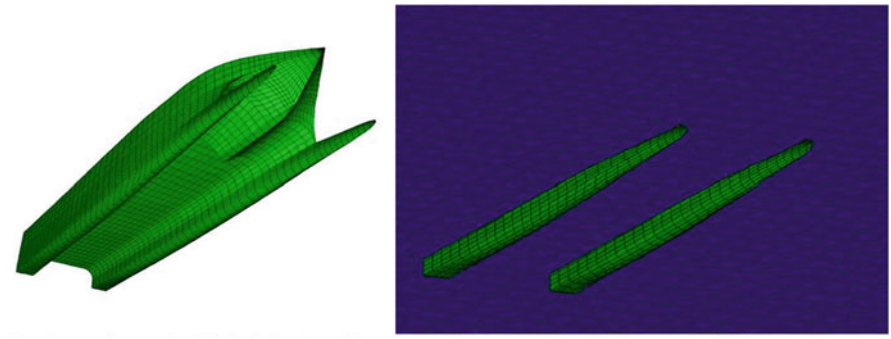

Fig. 12.7 FE panel model for hydrodynamics

probability level of 10^{-8} in terms of wave encounters, where the vessel is assumed to be running at 10 knots. For this a Rayleigh distribution must be used as outlined earlier under environmental conditions.

If we consider a typical multihull ferry operating on a 20-nautical-mile open sea route with average 1–2 m significant seas and running services for 8 h each day and an uptime of 90%, the vessel would meet about 10^8 waves in a 20-year service period.

Interestingly, if the vessel is running at 10 knots average, it would be able to make two round trips a day, and at 35 knots it would be able to make seven round trips. The exposure to waves overall would be similar, while the encounter frequency would be higher for faster vessels. There is an argument therefore to use the vessel normal service speed for commercial vessels, while for military craft it may well be the so-called loiter speed that governs the major part of wave exposure and so would be appropriate for assessing extreme values for such vessels.

For small vessels or those operating in protected environments, giving a limited fetch for wind wave generation, an alternative approach based on a validated short-term extreme value for a route-specific or area-specific environment can be considered. In this latter case the vessel can be classified for operation within a specific limitation. This approach is used by DNV and Lloyd's with a wider listing of specific operations than ABS allows for.

Once the DLP extreme value has been determined, the design equivalent wave amplitude, frequency, and heading need to be determined using the procedure presented subsequently in Sect. 12.5.

12.5 Loads for Structural Analysis

Two approaches to determining the extreme loads on a vessel are proposed: use of equivalent design wave and full nonlinear seakeeping analysis. The formulation for the equivalent design wave approach is given in what follows. This approach is

aimed at setting up a definition of a regular wave that can then be used with a nonlinear seakeeping program such as LAMP [9] to generate motions and wave loads, including wave pressures on the hull above the calm-water line, to input to a FE structural model to determine the structural response.

12.5.1 Equivalent Design Wave Approach

Design equivalent wave is determined from the DLP RAO extreme value at the encounter frequency for each dominant load parameter, as follows. A nonlinear seakeeping analysis in the time domain is carried out using the equivalent design wave as input and running for approximately 20 regular waves to achieve steady-state response and discarding as many as the initial 10 cycles as the starting transient. The output from this model in terms of loads is input to the structural FE model to determine the structure response. Typically, the time domain seakeeping analysis is run under different vessel loading conditions for the different equivalent design waves, producing a series of load cases to apply to the FE structural model.

12.5.2 Formulation of Equivalent Design Waves

The equivalent design wave amplitude is determined by dividing the projected extreme value of the DLP, for example midships vertical bending moment, by its RAO maximum at the appropriate wave heading. The associated wave frequency is that for the RAO maximum at the same heading. See Fig. 12.6 for a diagrammatic representation.

12.5.3 Nonlinear Seakeeping Analysis

The extreme loading is expected to be nonlinear so that it is necessary to model the hull and free surface as panels in three dimensions and determine instantaneous loads in the time domain.

Two mathematical approaches are available, either the Rankine source method for both the hull surface sources and free surface or a mixed source formulation where Rankine sources model the hull surface while the free surface is modeled by a transient Green function (see also Chap. 4).

ABS's own software LAMP can create models using the mixed source approach [9]. Other classification societies also have in-house software available, such as DNV GL WASIM and HYDROD [10], and there is the commercially available AQWA suite [11].

Where access to these resources is not available, an alternative approach to generating the loading inputs to the structural FE model is to follow the guidelines in the Rules for Classification of Lloyd's Register [12, 13], DNV [14], or indeed ABS [15]. We discuss this a little later on in Sect. 12.11.

In the time domain, there will be no hydrostatic restoring force to stabilize the horizontal motions of surge, sway, and yaw, so that drift can occur in FE model results. Nonlinear modeling software generally has the ability to include numerical soft springs that stabilize these motions while having a natural period outside the wave frequency spectrum, similar to the springs employed in wave basin physical testing.

Based on the seakeeping analysis, the ship motion and wave loads occurring at the instant the relevant DLP reaches its maximum can be determined as output. These should be available as pressure and inertial loads over the vessel surface model. Ideally, the hydrodynamic panel model will be aligned to the desired FE model for structural analysis for ease of data transfer without, or at least a minimum of, interpolation.

To make this transfer as effective as possible, it is helpful to plan the structural FE model prior to running a nonlinear seakeeping analysis so as to use the structural FE modeling of the hull surfaces as the starting point for the hydrodynamic model, bearing in mind that for the hydrodynamic model the panels can be larger, so there is a tradeoff between computer model preparation and analysis time for motion analysis against the need to interpolate from a hydrodynamic model to the FE model. Close cooperation between the hydrodynamicist and the structural analyst is called for!

12.6 Global Acceleration and Motion-Induced Loads

12.6.1 Local Acceleration

The local components of acceleration for the solid elements of the vessel lightship weight at their locations need to be determined from the seakeeping analysis for the six motion vectors translated to the *x*-, *y*-, and *z*-axes of the vessel. For roll, pitch, and heave the distance vector from CG must be used, that is,

$$a_{\mathrm{T}}, a_{\mathrm{L}}, a_{\mathrm{V}} = a_{x,y,z} + [\phi, \theta, \gamma] \times R\,(\text{all vectors})$$

where

a	Translational acceleration in vessel coordinates x (T), y (L), z (V);
θ, ϕ, γ	Roll, pitch, or yaw acceleration vector;
R	Distance from CG.

Payload loadings should be evenly distributed over the relevant decks.

12.6.2 Inertial Loads in Structural FE Model

Static: The static load is simply the nodal mass of the structural member or equipment times the acceleration of gravity (g).

Dynamic: We are looking at the extreme case and, hence, instantaneous loading. The vessel, depending on the load case considered, will have a roll or pitch angle. The foregoing accelerations are calculated for the ship fixed coordinate system so the dynamic loadings have to be resolved to the vertical, horizontals, and transverse directions. Thus, excluding wave frequency yaw motion:

$$F_{\mathrm{T}} = m\,(g\,\sin\phi + a_{\mathrm{L}}),$$
$$F_{\mathrm{L}} = m(g\,\sin\theta + a_{\mathrm{T}}),$$
$$F_{\mathrm{V}} = m\,a_{\mathrm{V}},$$

where m is the vessel mass.

12.6.3 Simultaneous Loadings

Having determined the static and dynamic components of load as previously for the light ship weight and payload, we need to transfer these to the nodes of the FE model for analysis. This is done for each load case to be analyzed.

12.7 Internal Tankage

12.7.1 Pressure Components

The fluid pressure from liquids in cargo tankage, fuel tankage, and ballast tankage has to be calculated and applied to the FE model for the extreme loading analysis if the tankage is integral to the vessel primary structure. If it is separate, then the local hull loading below the tankage needs to be considered to identify the local loading on the tank structure itself and translate this to loads at the tank supports interfacing to the global structure.

Note that for the motion analysis the tank contents may have been modeled as static masses. This is reasonable when determining the vessel global motions. Here we are determining the loading at the tank boundaries within the vessel for the stress analysis.

There are two components to consider, the *quasi-static loading component due to the vessel roll and pitch* at the point of extreme motion, which applies hydrostatic pressure on the tank plating, and the *inertial load from the vessel accelerations* in the 6° of freedom.

Both loads have to be combined and distributed to the tank structure boundary nodes in the FE model for the load case being considered. The internal tank pressures at the tank boundaries have to be determined for the vessel motion and acceleration at the instant when the relevant DLP reaches its maximum. For example, in head seas the relevant point is during the design equivalent wave where longitudinal bending moment reaches its peak, including in this case the pitch angle and the vertical and horizontal components of vessel acceleration.

Adjustment between global and vessel coordinates needs to be taken into account for the roll and pitch motion experienced at the moment of the extreme vessel motion from the motion analysis.

The total instantaneous internal tank pressure for each of the tank boundary points may be determined from the following relation as advised by ABS:

$$p = p_o + \rho h_i \left[(g_\mathrm{V} + a_\mathrm{V})^2 + (g_\mathrm{T} + a_\mathrm{T})^2 + (g_\mathrm{L} + a_\mathrm{L})^2 \right]^{1/2},$$

where

p = Total instantaneous internal tank pressure at a tank boundary point;
p_o = Either the vapor pressure or the relief valve pressure setting;
ρ = Fluid density, cargo, or ballast;
ht. = Total pressure head defined by height of projected fluid column in direction of total instantaneous acceleration vector;
a_T, a_L, a_V = Longitudinal, lateral, and vertical wave-induced accelerations relative to craft's axis system at a point on tank's boundary;
g_T, g_L, g_V = Longitudinal, lateral, and vertical components of gravitational accelerations relative to craft's axis system at a tank boundary point:
= $(-\sin \phi, g \sin \theta, g)$;
θ = Roll angle;
ϕ = Pitch angle.

The local acceleration of the tank contents, taken at the CG of the tank, due to ship motions is to be expressed by the following equation:

$$(a_\mathrm{L}, a_\mathrm{T}, a_\mathrm{V}) = a_{\rightarrow} + \Theta \times R_{\rightarrow},$$

where

$(a_\mathrm{T}, a_\mathrm{L}, a_\mathrm{V})$ = longitudinal, transverse, and vertical components of local accelerations at CG of tank contents;
$a_{\rightarrow}$ = Surge, sway, and heave acceleration vector;
Θ = Roll, pitch, and yaw acceleration vector;
$R_{\rightarrow}$ = Distance vector from craft's CG to CG of tank contents.

The accelerations at the tank boundary can be determined in the same way, substituting the distance vector from the vessel CG to the position of the tank boundary.

12.8 Global FE Model Analysis

12.8.1 Three-Dimensional Global Modeling

The starting point for the global FE model is the structural geometry of the vessel. The FE model will then be built from a combination of triangular or rectangular plate elements, beam elements possessing axial, shear, and bending stiffness, and rod elements that have axial stiffness only or axial and bending stiffness. Modeling may use equivalent plate stiffness instead of modeling all stiffeners on a panel bounded by bulkheads or main girders to reduce model size. Care should be taken when developing the model to refine the mesh in areas where rapid changes in stiffness occur, leading to possible stress concentrations. It is helpful to review the extreme loading profiles from the seakeeping model to assist in this process. An example of a FE structural model is shown in Fig. 12.8.

12.8.2 Structural Members

The main structural elements to be analyzed in detail include the following primary structural members that make up the demihulls and cross structure or the main hull, cross structure, and sponsons:

- Bottom and inner bottom plating with associated main girder and stiffener grid;
- Side shell plating, stiffeners, and girders;
- Main deck plating with associated main girder and stiffener grid;

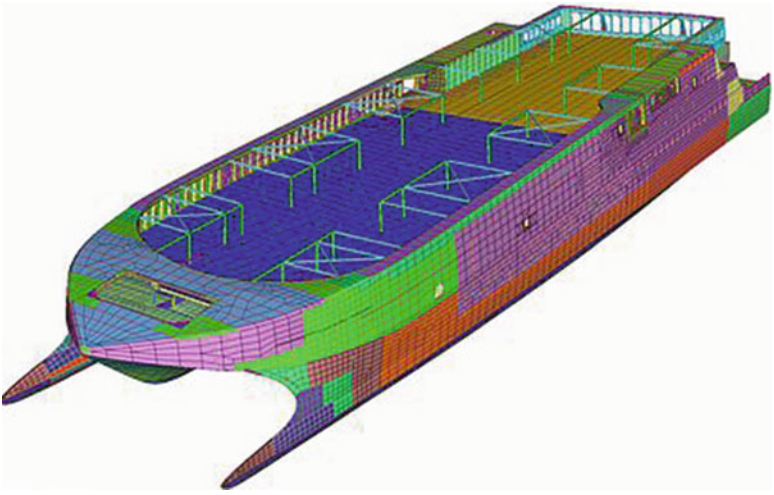

Fig. 12.8 Example FE model for structural analysis

- Longitudinal bulkhead plating and stiffeners;
- Transverse bulkhead plating, stiffeners, and girders;
- Web frames;
- Cross structure deck plating and bulkheads, with girder and stiffener grid;
- Upper superstructure as integral part of cross-structure modeling or linked by nodes at resilient mounts;
- Cross structure central "bow" for wave piercers;
- Sponson shell plating, WT bulkheads, frames, girders, and stiffeners for trimarans or pentamarans.

These should all be built into the global FE model. The intent is that the global stresses should be evaluated to validate the scantlings for the main hull girders and the cross structure, that is, the primary structure, and enable finer mesh models to be built for areas requiring local analysis, for example the reinforcement for main engine mounting, waterjet installation, the "bow" area of a wave piercer under slamming loadings. The global model will include the masses making up the vessel lightweight in addition to the main aforementioned structural members; these, such as the main engines and propulsion machinery, will be represented by the loading applied as point loads to nodes or distributed loads across a series of FE model nodes with the appropriate local acceleration, as in Sect. 12.6, for the motion-induced load.

12.8.3 Equilibrium

The first step with the global FE model is to make an equilibrium check, thus the sum of the static and dynamic loads should balance. If there are any unbalanced forces these need to be investigated and where possible resolved. For high-speed multihull craft the slamming and whipping response and loadings may need to be analyzed and included to obtain balance (see Sect. 12.7 below).

12.8.4 Local Structure Analysis

Similar to the global model, local FE modeling starts with a physical model of the local structure to a suitable boundary identified by nodes in the global model. Considering, for example, the main transverse hull framing, ABS recommends the use of plate elements for transverse web plating, whereas local stiffening is modeled with rod elements with an equivalent cross-sectional area and out-of-plane hull girder plating, also modeled by rod elements with appropriate effective width. The mesh sizing should be as regular as possible and sufficient to represent the stiffness of the local structure operated on by the nodal forces and deflections from the global analysis so as to provide a smooth stress distribution across and along the structure.

Plate elements give the best results if the geometry is square within 2:1, or at least less than 5:1 in low stress areas.

For transverse frames the element grid may be aligned to the stiffener spacing on the main longitudinal plating (bottom, inner bottom, sides, main deck, and upper deck of cross structure).

Local structure stiffeners and panel breakers that are used to prevent buckling and that align with the principal stress direction should be modeled because they will affect the buckling response. Where they are normal to the stress principal direction, they may be ignored for the local FE analysis.

ABS requests that at least the following elements be subjected to local analysis:

- Transverse web frames;
- Main longitudinal girders;
- Bottom, side, and deck longitudinal stringers;
- Horizontal stringers of watertight transverse bulkheads;
- Panels in the slamming areas [especially fiber-reinforced plastic (FRP) panels];
- Haunch at front of cross structure;
- Areas of high stress indicated by global model.

It may also be important to consider the following elements because they are likely to be indicated as areas of high stress in the global model:

- Hydrofoil structural connections to hulls;
- The transition from SWATH or semi-SWATH lower hull-to-strut structure (a significant geometric and stiffness change);
- The internal "corner" area between hull and cross structure (for a trimaran both to central hull and to sponsons).

12.8.5 Additional Analyses

In addition to the global and local analyses for projected extreme loading, the FE model can also be used to carry out the following analyses:

- *Buckling analysis*: In this type of analysis, locally high-stress areas in compression can be tested with increasing load to predict the loading that would result in a buckling failure;
- *Fatigue analysis*: Fatigue degradation has two sources, machinery vibration and wave forces, that is,
  - Vibration from machinery inside the vessel and
  - Dynamic loads from the environment.

  The first task is to identify the natural frequencies of the hull structure in bending and torsion and unit response operators (RAOs), then apply the exciting load spectrum from the waves or machinery to determine the response statistics. A scatter diagram of sea states can then be used to determine the number of cycles

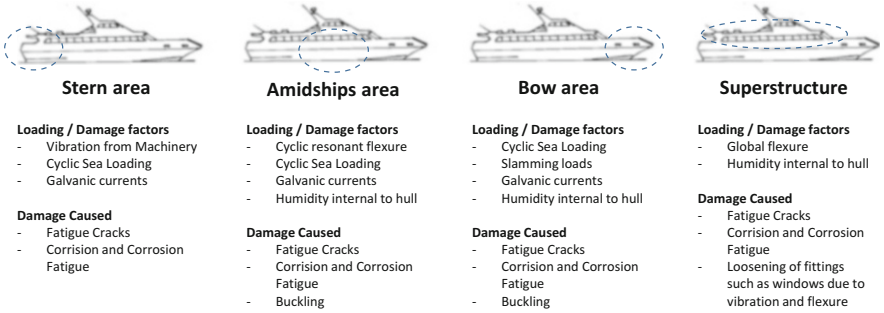

Fig. 12.9 Fatigue in different areas of a multihull

at a given stress level, and from the fatigue damage criterion for the stress ranges the projected damage at operational service life is determined using Miner's rule. It should be noted that, unlike steel, aluminum does not have a fatigue limit, so all parts of the structure will be subject to fatigue degradation as the vessel progresses through its service life. Assessment of highly loaded areas for fatigue degradation is therefore an import issue. Key areas of focus are those subject to wave impact and the forward intersection between hulls and strut or cross structure.

- *Vibration analysis*: The vibration spectrum for the main machinery is applied to the global model via the machinery nodes;
- *Noise analysis*: Similar to vibration analysis;
- *Hydroelasticity*: This is linked to the slamming analysis (Sect. 12.9, looking at responses where deflections are modeled dynamically).

Figure 12.9, interpreted from reference [16], provides an impression of the loadings and cyclic damage created on various parts of the structure of a catamaran. A.Tymifienko carried out a master's project, reported in this reference, looking at the fatigue response of specific catamaran vessels.

12.9 Application of Acceptance Criteria

FE models are expected to be assessed against two failure modes, that of yielding in tension or buckling in compression. Where a fatigue analysis is carried out, the criteria will be against a proportion of the number of cycles to failure.

The vessel may be constructed in steel, aluminum, or FRP, so criteria are given for each material by ABS. The most widely used material is aluminum of "marine quality" suitable for welding. ABS refers to the International Alloy Designation System 5000 series of plates and sheets as these have good corrosion resistance, weldability, and ductility, making them formable (search on internet Wiki: Aluminium_alloy for info).

A rolled or extruded/formed section of aluminum will have a higher strength than the welds used for construction due to the heat-affected zone next to the weld, so the welded joint will determine the criteria for yield strength [cf. ABS rules for materials and welding (part 2) 2–5 A1, Table 2]. This is also a good reason for using extruded beam sections in aluminum as adopted by many shipyards.

12.9.1 Yielding

For plate elements in the vessel structure, ABS applies the von Mises criterion for limiting stress, where

$$\sigma_{\mathrm{HVM}} = \left[s_x{}^2 + s_y{}^2 - s_x s_y + 3\,\tau_{xy}{}^2\right]^{0.5},$$

where

s_x Normal stress in x-direction of element;
s_y Normal stress in y-direction of element;
τ_{xy} In-plane shear stress.

For acceptance, σ_{HVM} should be less than 95% yield for steel and 85% yield for aluminum, and for FRP structures σ_{HVM} is 33% of the lesser of the tensile or compressive strength of the laminate. In addition, the component stresses should all be below the allowable design stresses indicated in what follows for either the global or local condition.

12.9.2 Design Global Hull Girder Stresses

The design stresses are as follows:

12.9.2.1 Global Longitudinal Strength of All Hull Types

σ_a = Design longitudinal bending stress = $[f_p/C.\ Q]$ N/mm^2 (kgf/mm^2, psi);
τ_a = Design shear stress, $[110/Q]$ N/mm^2, $[1.122/Q]$ tf/cm^2, $[7.122/Q]$ Ltf/in.^{2};
f_p = 17.5 kN/cm^2, 1.784 tf/cm^2, 11.33 Ltf/in.^{2},

where

$C = 1.0$ for steel craft,
$= 0.90$ for aluminum craft,
$= 0.80$ for FRP craft;

Q for steel:

$= 1.0$ for ordinary strength steel,
$= 0.78$ for grade H32 steel,
$= 0.72$ for grade H36 steel,
$= 0.68$ for grade H40 steel;

Q for aluminum:

$= 0.9 + q5$ but not less than Q_o;

$q5 = 115/\sigma_y$ N/mm^2,$12/\sigma_y$ kgf/mm^2, $17{,}000/\sigma_y$ psi;
$Q_o = 635/(\sigma_y + \sigma_u)$ N/mm^2, $65/(\sigma_y + \sigma_u)$ kgf/mm^2, $92{,}000/(\sigma_y + \sigma_u)$ psi;
σ_y = Minimum yield strength of unwelded aluminum in N/mm^2 (kgf/mm^2, psi);
σ_u = Minimum ultimate strength of welded aluminum in N/mm^2 (kgf/mm^2, psi);

Q for frp:

$= 400/0.75\sigma_u (41/0.75\sigma_u, 58,000/0.75\sigma_u)$;

Σ_u = Minimum ultimate tensile or compressive strength, whichever is less, verified by approved test results, in N/mm^2 (kgf/mm^2, psi). See Sect. 2-6-5 of the ABS *Rules for Materials and Welding (Part 2) – Aluminum and Fiber Reinforced Plastics (FRP)*. Use the strength properties in the longitudinal direction of the craft.

12.9.2.2 Global Transverse Strength of Multihulls

σ_a Design transverse bending stress, $0.66\sigma_y$ for aluminum and steel craft and $0.33\sigma_u$ for FRP craft, in N/mm^2 (kgf/mm^2, psi);
σ_{ab} Design torsional or combined stress, $0.75\sigma_y$ for aluminum and steel craft and $0.367\sigma_u$ for FRP craft, in N/mm^2 (kgf/mm^2, psi);
τ_a Design transverse shear stress, $0.38\sigma_y$ for aluminum and steel craft and $0.40\tau_u$ for FRP craft, in N/mm^2 (kgf/mm^2, psi),

where
σ_y Minimum yield strength of material, in N/mm^2 (kgf/mm^2, psi); for aluminum the yield strength is to be for the welded condition and to be no greater than $0.7\sigma_{uw}$;
σ_u Minimum tensile or compressive strength, whichever is less, in N/mm^2 (kgf/mm^2, psi);
σ_{uw} Ultimate tensile strength of material in unwelded condition, in N/mm2 (kgf/mm^2, psi);
δ_m Maximum deflection for FRP craft, $\delta_m = (\sigma_a/E)$. LI, in m (in.);

τ_u Minimum ultimate through-thickness shear strength, in N/mm^2 (kgf/mm^2, psi);
L_I Mean span of cross structure, in cm (in.), as indicated in following figure;
E Tensile or compressive modulus of FRP laminate, whichever is less, in N/mm^2 (kgf/mm^2, psi).

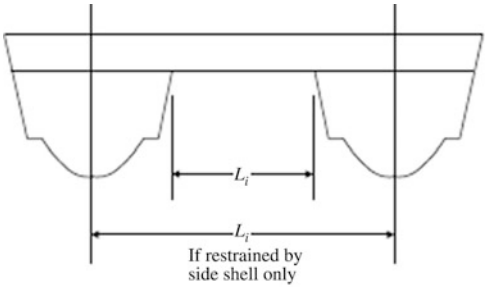

12.9.3 Buckling and Ultimate Strength

ABS requires plate panels, stiffened panels, and primary supporting members to be checked against buckling and ultimate strength using FE model results. The requirements follow the normal procedure for ship strength in that plating that buckles between primary structural members can be allowed as long as the overall structure is not unstable as a consequence, that is, the primary structural members have too little reserve to prevent them also from buckling.

With the exception of areas subject to slamming loads, it is to be expected that the entire vessel structure will stay within the normal elastic stress criteria, particularly including stress concentrations, since if it does not, there may be a problem with fatigue damage to structures in this area. We consider wave slam below.

12.10 Slamming Loads and Structural Response

12.10.1 Slamming Analysis

At the service speed of a high-speed multihull, the relative speed of impact between the bow or front lower surface of the cross structure and incoming waves will cause very high local dynamic pressures. In an extreme case, the vessel local structure of panels and stringers may deflect beyond their elastic limit and in transferring additional load to the surrounding bulkheads and girders cause permanent deflection to these structures as well. In the limit, there may be structural failure leading to flooding, so transverse watertight bulkheads have to be positioned so as to separate areas subject to slamming.

Fig. 12.10 Example(s) of (**a**) high-speed monohull and (**b**) catamaran wave jumping

The designers of fast planing monohull craft have had to deal with this issue when designing the bow shape and structure (Fig. 12.10a). Owing to the sharply angled geometry, the water flow is deflected, reducing the impact pressure compared to a flat surface. In contrast, with a catamaran there is no horizontal cross structure that the upwelling wave can impact (Fig. 12.10b). In addition, the bow shape of a catamaran is somewhat funnel shaped, channeling and accelerating flow.

A slamming analysis to determine the fluid pressures and loading to the structure can be carried out using a nonlinear seakeeping program or a dedicated CFD model. Analytical methods used in the recent past have tended to be based on predictions on a 2D section projected from the motion analysis and have required calibration with

testing or full-scale data. The CFD method can give full 3D results as long as the following advice is followed (cf. ABS guidelines):

- Water-free surface modeling is to be fully nonlinear.
- Air flow is to be modeled including compressibility.
- The structure modeled needs to extend through the superstructure as the loading is upward through this area.
- While for head seas heave and pitch motions only need be considered, for other headings all 6° of freedom need attention.
- The mesh size and time step for the CFD model need to be fine enough to capture the rapid and localized pressure spikes.

Slamming pressures can occur on the bow forefoot of a catamaran or trimaran, the front lower surface of a catamaran cross structure wet deck, particularly close to the internal corners inside of the bows, or over the upper surface of the central bow cross structure arch of a wave piercer.

Once the results from CFD are available, the slamming pressure profile should be mapped to the global FE model. If the slam duration is close to the structural natural period of vibration of the hull girder, then attention has to be paid to the hydroelastic response of the structure (Sect. 12.3) and generally leads to the carrying out of a whipping analysis as follows; otherwise, the instantaneous pressure distribution can be input to the FE model as a quasi-static pressure for the FE analysis. Figure 12.11 shows an example pressure profile for wave slam on the wet deck of a catamaran (courtesy ABS).

12.10.2 Whipping Analysis

Whipping is a transient response of the vessel hull instigated by a shock load such as a slam event. The response is vibration at the structural natural frequency two-node fundamental or harmonics of this. Since the response frequency is much higher than the wave frequency (with typical natural frequency harmonics being between 3 and 1.5 Hz), the whipping analysis can be separate from the global extreme analysis once the exciting pressure pulse load has been defined.

Fig. 12.11 Slamming pressure profile from ABS

The simplest way to determine whipping response is to use a 3D FE model to carry out a free vibration analysis to determine the principal mode shapes for the fundamental and harmonic natural frequencies when the hull structure is excited by the slamming pressure profile. If the damping of the vessel structure is known, then this needs to be applied; if it is not known, ABS recommends using 2–3%. The research discussed in what follows indicates between 3 and 6% for large wave piercers.

12.10.3 Research on Slamming and Whipping Response of Catamarans

The accelerations and loading of high-speed vessels in a seaway have been a concern of naval architects since their advent in the early twentieth century. The initial focus was on planing craft and the dynamic forces that they experienced. While planing monohulls have bow profiles that deflect the flow in higher sea states, they can be lifted substantially or completely from the water surface as they negotiate waves (Fig. 12.10a). The subsequent reentry of the hull into the surface, particularly if it is into a rising wave surface, can cause very high pressures and, hence, local loadings on the hull structure. The impulse nature of the pressure profile can also excite the hull at its structural natural frequency, adding to the pressure and inertial loading from the passing waves.

Captain Saunders gave a detailed exposition on impact forces in reference [17] after treating the hydrodynamics of planing in references [18, 19] from extensive materials he collected in the 1950s. The background mechanics is explained and provides a useful background to the findings from the research into slamming and whipping response discussed in what follows.

Since the 1960s much research has been conducted into the seakeeping of high-speed vessels and suitable guiding criteria. Reference [20] is an example from the early 1980s taking a wide view of the subject that included peak vertical acceleration (slamming acceleration) and bow reimmersion (causing whipping stresses and bow bottom slamming damage) as two key criteria. A comment made at that time was occurrence of frequent slamming was an indicator that operational speed should be reduced.

Reference [21] from 1988, discusses structural analysis of a US Coast Guard (USCG) Island-class patrol boat, a 33-m-LOA semidisplacement vessel with a service speed of 26 knots (Fig. 12.12). The vessel class, developed from a semiplaning offshore patrol vessel design by Vosper Thornycroft in the UK, was intended by the USCG to operate in heavy seas at speed, and so there were concerns about hull integrity over the planned 15-year operating life. A full NASTRAN FE model was created for the steel hull. The peak hydrodynamic pressure distribution was calculated based on methods from Heller and Jasper [22] and applied to it after defining the panel size and minimum plating thickness to avoid yielding. The initial investigations suggested that peak pressures in the bottom panels behind the forefoot

Fig. 12.12 Island-class patrol vessel with annotation for location of slam damage

may exceed yield for the shell plating thickness used depending on the dynamic pressures assumed on the hull panels. It was decided to use 7 lb. (0.16 in., 4.1 mm) steel plating, while the authors' calculations suggested 0.192 in (9 lb or 4.8mm thickness) plating was needed to avoid yield in the 1/10 extreme event. A check against ABS criteria for steel vessels under 61 m suggested 0.26 in. (6.6 mm) would be required.

Model tests at 1/20th scale were carried out to investigate pressures at various locations along the hull as well as motions and acceleration in Pierson–Moskovitz sea states between 6 and 10 ft, or 1.8 m and 3 m significant waveheight. Speeds ranged from 12 to 36 knots. Vertical accelerations in the range 1.1 g were recorded at the model CG during testing. The results appeared to correlate with investigations in other research, while the pressures measured appeared low compared with traditional design methods.

Full-scale trials of the ninth vessel of the class already in service was carried out in high sea states and on one trial experienced a series of heavy slams. A panel between frames 14.5 and 15 at the forward part of the vessel just aft of the forefoot that was strain gauged showed evidence of permanent deformation, and once the vessel was taken out of the water, permanent set was measured, heaviest in the center panel and to a depth up to twice the plate thickness.

The extreme pressures and panel stresses were analyzed and a reliability analysis using Monte Carlo simulation carried out based on the projected operational history of wave encounters using a Poisson distribution to determine the probability of failure (exceedance of yield) with the experimental panel stress data. For the 7 lb. plating a probability of failure of 0.035 was determined, compared to a normal expectation of between 10E-3 and 10E-5. Repeating the analysis with a 9 lb (4.8mm thickness) plate suggested a probability of failure of 3.1E-5, which would be acceptable.

Follow-up analysis of the panel geometry to determine the pressure required to create the permanent set suggested that critical pressure to yield would be 63 psi, while the permanent set would be generated by 114 psi, a factor of almost 2.

It should be noted that in this work, the uncertainty in the correlation of model test data with the full-scale data meant that for reliability analysis, the stress levels were interpreted from the full-scale trails. The end result of this work was that vessels still under construction had their forward bottom plating increased to 9 lb., while for the nine vessels already in commission, additional intercostal stiffening was introduced, reducing the extreme stresses by reducing the aspect ratio of the bow bottom panels from 2:1 to 1:1.

This work gives us a feel for the difficulty in modeling pressures generated once a hull surface out of the water is impacted by a water wave. In the aforementioned case, the ABS rule appears conservative compared with the experience of a paramilitary vessel where operation is expected to continue in rather rougher conditions than a ferry, or at least the ferry would reduce its speed so that the loading itself would be reduced, as is normal practice for commercial vessels.

If we turn to multihull vessels, the bow geometry is rather more complex, and the challenge is how to best form the bow part of the cross structure between the hulls.

In inshore waters, sea states are low enough that the freeboard to underside of the cross structure may be maintained so that waves do not impact. This needs careful review, including the time domain motion analysis mentioned earlier. Multihulls that are to operate on open ocean routes (examples are between the Canary Islands, Taiwan to Mainland China, North to South Island of New Zealand, and across the Bass Strait from mainland Australia to Tasmania) have a more challenging requirement, particularly when you consider that for large craft in the 80- to 120-m-LOA range, service speeds are 40 knots or more, and sea states above 4 m significant can be experienced.

Due to considerable experience of wave slamming to high-speed catamaran and wave-piercer ferries over the last two decades, including structural damage caused to several ferries, a series of studies and results has been published. References [23–27] relate to a sequence of work carried out to model slamming and vibratory response on large wave-piercing catamaran ferries. The work has been substantial and provides valuable insight as the researchers were able to gather full-scale data from ferries in operation as well as from trials and to link this to analysis, 2D scale model drop testing, and 3D model testing in a towing tank with a strain gauged segmented model.

The full-scale data were gathered primarily from two Incat wave piercers, an 86-m (Build No. 42) and a 96-m (Build No. 50) vessel. They are illustrated below in Fig. 12.13a, b.

These catamarans are of the wave piercer type, having a substantial central bow structure that has its keel at some 1 m above the loaded waterline (L_{WL}) extending back some distance, and behind this the wet deck is flat and at a higher level 2.8 m above the waterline. From the profile in Fig. 12.14 it can be seen that if the bow immerses in a wave, it will direct the flow outward, back, and upward toward the curved upper surface connecting with the demihull inner plating.

The purpose of the bow is to provide a buoyancy in larger waves to restrain pitch-down motion since the demihulls' form is so fine. The same action assists against bow pitching down when at speed in following seas, which is an issue for traditional catamarans in heavy following seas.

Fig. 12.13 (**a**) Incat 86-m hull 042; (**b**) 96-m Incat hull 050

A wave piercer is designed to slice through waves rather than react to them, and in short waves this is what happens. As wave length increases beyond vessel LOA, it will begin to profile. At high speed the craft slicing or platforming rather than profiling will cause the bow structure to be impacted directly by an uprising oncoming wave front, and the pressure generated will depend on the relative velocity between the two and the angle of the structure surface and the oncoming wave surface. In the case of the Incat bow design, the bow shape directs the flow up toward

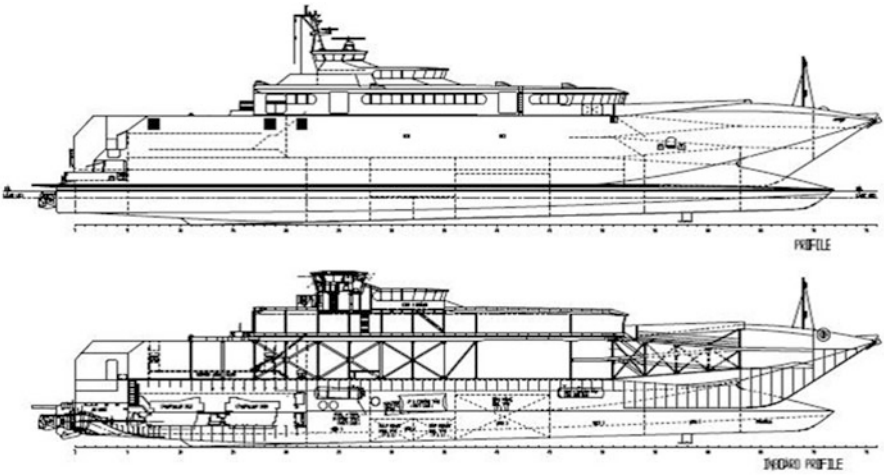

Fig. 12.14 Incat 96-m centerline section and bow profile

the top of the arch. As the wave surface rises and the vessel bow descends, the water fills the arch at the upper internal corner and the deceleration as the water impacts the arch surface causes an impulse pressure. The geometry of the bow is a complex 3D shape, so the flows are as complex. To add to the challenge, when waves engage with a bow structure like this, the upper surface will contain spray (air/water mixture), which is compressible.

It is important to understand that we are talking about severe operating conditions causing this response; nevertheless, ferries operating on exposed routes, such as North to South Island in New Zealand, can experience increasing sea conditions during a voyage that result in slamming.

Whelan [23, 24] collected slam data from full-scale ferries (Incat hulls 42 and 50) that were fitted with strain gauges, accelerometers, and radar wave height measurement, for a total of 10 months of operations, and analyzed data taken from the slam events to relate responses to wave profiles, vessel relative motions, and accelerations.

The work carried out showed that 88% of recorded full-scale slam events were in waves of greater than 2.5 m height. It was also stated that substantial slam events started when wave heights were 2.8 m (relating to wave peaks at reaching 60% of the tunnel height to the wet deck either side of the central bow with the vessel at zero pitch).

The profile of relative motion between the vessel bow and the wave profile through the slam events was analyzed and an average determined so as to be able to use this for model testing. Whelan then scaled the motions, geometry, and masses to carry out drop testing of 2D model bow shapes, including a model of Hull 50, two adjusted profiles, and a series of hard chine bow forms.

The work carried out in [23] and reported in [24] showed by varying the bow cross section geometry for 2D model drop testing that the slam pressures could be

alleviated somewhat by moving the high point of the arch more toward the demihull inner wall. The author also looked at the effect of air entrapment for the drop model and concluded that both at model scale and full scale that the geometry was such that air could escape without being trapped and compressed to create an additional dynamic response, so this was not an issue.

The overall result was that while the characteristic for the slam event could be modeled, the extreme loads recorded at full scale were significantly lower, approximately one-third that of the model. Nevertheless, the full-scale forces measured correlated with the recommended pressures for design by DNV (see Ref. [14] Section 1 C400).

Thomas et al. [25] report on the spectral analysis of full-scale-trial data from Incat vessels 42 and 50 aimed at determining the "whipping" response of these wave-piercing catamarans. Their process was to analyze the strain gauge and pressure sensor measurements from in-service trials to determine the response spectra and further to look at the decay in stress cycles from a slamming event to estimate the structural damping. From the data gathered they found that the primary response was hull longitudinal two-node mode at frequency 2.8 Hz, and a secondary response at 1.3 Hz from lateral torsion for Hull 50, and 2.6/1.5 for Hull 42. To calibrate this, they carried out exciter tests to measure the hull response statically by dropping the vessel's anchor and arresting it on the winch. Responses were close, as shown in Table 12.1. The exciter trials were carried out on Hull 45 – a sister to 42 – as the latter vessel was in operation in the Channel Islands, remote from Tasmania.

FE models of both vessels were built in NASTRAN using plate and bar elements including the superstructure attached to the main hull by its rubber mountings for Hull 50, and a simpler structural raft for Hull 42. The added mass associated with the hull was determined using the method of Salvesen, Tuck, and Faltensen [2]. This mass, similar in magnitude to the vessel displacement, was distributed along the keels of the demihulls at the FE panel nodes.

A comparison was made between the FE mode shapes generated by the natural frequency response analysis and the modes excited at full scale. It was found that the primary two-node longitudinal response dominated and calibrated between the trials and FE modeling.

It was noted that the natural frequency of response decreases as vessel displacement increases, and that, additionally, if mass is changed at locations between nodes, this would change the frequency and, hence, the response. For example, significant local loading at amidships would reduce frequency and response. Equivalently, changing loading at the principal nodes would not affect response other than due

Table 12.1 Incat Catamaran accelerations data from testing

Response frequency, Hz	Hull 42	Hull 45	Hull 50	
	Trials	Exciter	Trials	Exciter
Longitudinal	2.6	3.01	2.8	2.89
Lateral torsion	1.5	n/a	1.3	n/a
Longitudinal from FE ("wet")	2.56	3.0	2.96	2.96
Lateral torsion from FE ("wet")	1.5	1.65	1.5	1.5

to the change in displacement. This gives pause for thought when placing/distributing significant outfitting masses during design.

A further study of the effect of slams and associated whipping response on fatigue life sensitivity was made by assuming the slam events occurred as regular events throughout the operational life. The approach was to generate a set of stress cycles from a slam event based on an assumed decay coefficient (damping) and then aggregate these based on assuming slams at 7.5/h for the 15-year, 5000-h at-sea operational life of the vessel, with a peak impulse at 25% yield stress.

From the analysis of vessels 42 and 50 the damping was estimated at between 0.01 and 0.06, with an overall average of 0.035. Using Miner's law applied to the different stress ranges and number of cycles (as in BS8118, now superseded by BS EN 1999–1-4:2007 + A1:2011 Eurocode 9: Design of aluminum structures, cold-formed structural sheeting) applied to a typical fillet weld within the structure, the authors were able to look at the sensitivity of fatigue life to the damping coefficient. Their findings were that a change from 0.035 down to 0.025 reduced service life by 25% from the whipping stress cycles alone. Additionally, a change between peak stresses at 12.5% yield to 50% yield from the slamming suggested a reduction in fatigue life at the selected weld from 56 down to 0.72 years. This is a significant issue bearing in mind that the slamming impulses investigated are within the linear response domain.

The damping coefficient of 0.035 calibrates with ABS and DNV recommendations. The study showed that whipping response in the elastic region can have a significant impact on fatigue damage and so is important to assess and include in a structural analysis. The question is how to generate a realistic model for impulsive loading without calibrating from the full scale. From Whelan's work it is clear that for the complex geometry of a wave piercer, 2D modeling assists in understanding the mechanism but does not complete the story.

Lavrov et al. [26, 27] have taken the approach of testing a 2.5-m (1:44.8 scale) model in a towing tank in regular waves to investigate hull vibratory response, where the model is constructed in sections with gauged flexible hinges to model the scaled vessel hull hydroelastic response. The model was built to represent a 112-m vessel, Hull 065 (see Appendix 3 for data sheet). The work described in [26] details the development of the strain gauged flexible model and its validation against full-scale vessel characteristics.

This work also started with an investigation of a wave slam that occurred on an earlier 112-m Hull 064 during sea trials. Longitudinal mode response frequency was estimated at 2.44 Hz and damping ratio at 0.065. Prior to its commissioning the response frequency had been estimated at 2.06 Hz, and it was this that was used to calibrate the segmented model to a longitudinal frequency of 13.79 Hz based on scaling by $(L_{FS}/L_{MS})^{0.5}$. The model and structural configuration are shown in Fig. 12.15.

A 3° of freedom mass-spring model was used to predict the required mass and inertia properties of the three model sections. The derivation started from the stiffness of the hull itself and an estimate of the added mass based on semicircular volume related to the waterline breadth at the relevant demihull section. The model

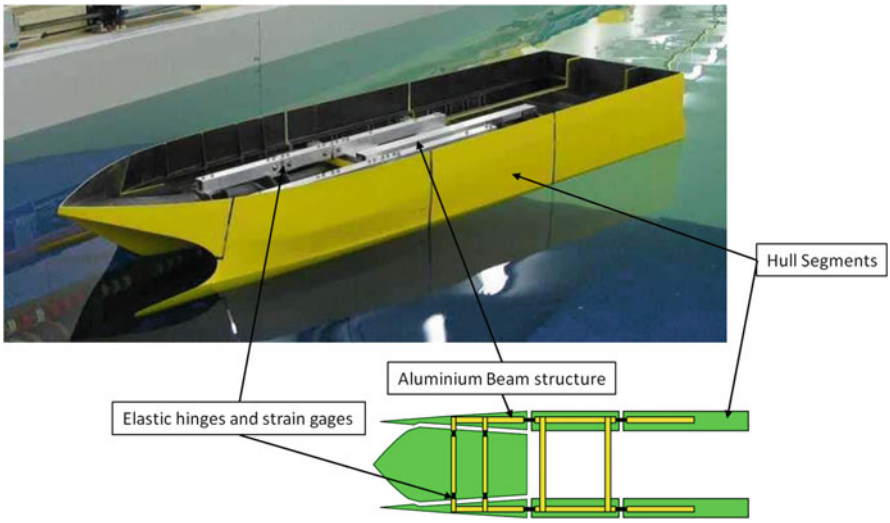

Fig. 12.15 Segmented model (of Incat 065)

was then given an impulse load and mode shape determined for the starboard side hull by measuring the peak strains at the hinges and the instantaneous vertical accelerations. The mode shape was found to correlate with that projected from the theoretical mass spring model used to set up the physical model.

Subsequently, both wet (floating) and dry (hull suspended by long soft elastic straps) vibration tests were carried out by applying impulse loads and measuring the cyclic response and decay. The hinge stiffness's and total model mass were varied separately to investigate the effect on the longitudinal natural period of response, both wet and dry. Runs in calm water at scaled speeds up to Fr_L 0.6 were undergone with the hinge gaps open and then closed by a latex seal.

The effect of the latex seal was to reduce the structural natural frequency by about 1 Hz at all speeds, while the damping showed an upward trend with increasing speed, as shown in Fig. 12.16. This contrasts with the full-scale data suggesting that damping is similar at all speeds, at levels similar to that approached by the model at higher speeds.

Finally, towing tests were carried out in regular waves of heights 60, 90, and 120 mm (2.6, 4.0, and 5.4 m full scale) to investigate responses to slamming impulses. A power spectral analysis was carried out on the strain gauge data for the slam events in these tests to determine the response frequency. Higher wave heights caused greater immersion of the central bow, thereby increasing the added mass and reducing the response frequency.

The conclusion at this stage of the work was that the model setup was able to simulate the full-scale vessel and provide realistic whipping response data to calibrate with wave slamming events.

The same group of authors completed another set of model tests to measure slam loads and trends with wave height and vessel speed [27] using the same model and

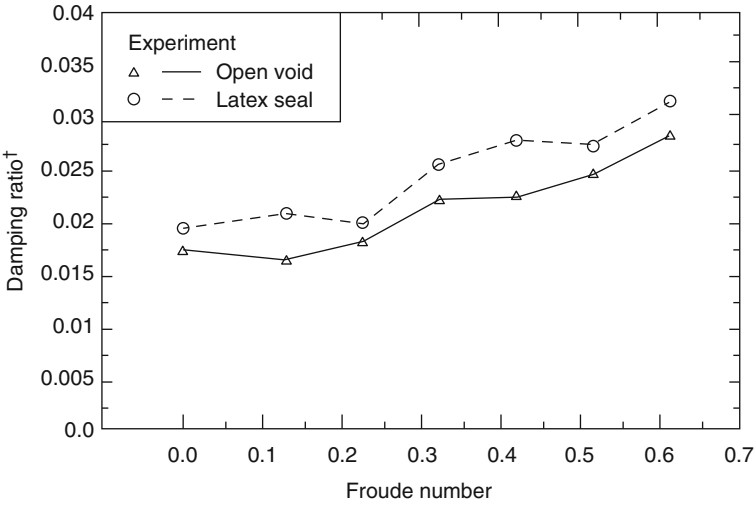

Fig. 12.16 Damping ratio with speed for segmented model with and without gap seals

setup to simulate the 112-m wave piercer. The intent of the work reported here was to look at the slam loadings at different wave heights and speed that would excite the hull vibratory response (rather than looking at the local panel loadings induced). On the basis that severe slams occurred at moderate speed at full scale, it was decided to use a scaled speed of 20 knots, which also to some extent mimics ferry operation in severe weather, with vessel speed being reduced from the maximum service speed of around 40 knots.

The reduced speed is convenient for model towing tank testing in waves, and the use of regular waves removes the question of whether an extreme slam has been measured, which is an issue with the analysis of full-scale testing. The full 3D hydroelastic scale model may provide closer similitude than 2D drop testing in terms of determining overall slam loading.

Model test runs in waves of 30, 45, 60, 90, and 120 mm (1.3, 2.0, 2.6, 4.0, and 5.6 m full scale) were analyzed to determine pitch and heave response with wave frequency and height, and also reduced to RAO values. The pitch response stabilizes at close to 1 below the dimensionless encounter frequency ($\omega_e = \omega\,(L/g)^{0.5}$) of 3 and dies below 0.1 above ω_e of 6. Heave response is a bit more complex but is below 0.2 above ω_e 5 and at 0.8 for ω_e 2.5. The RAOs were found to be similar for all wave heights tested. The heave response showed some variability from linear in the range ω_e 3–4, with higher waves giving higher responses.

At wave heights of 30 and 45 mm slams were not encountered. This correlated with full-scale experience that seas less than 2 m significant wave height (45 mm at model scale) did not cause slamming. The model data exhibited slamming for wave heights of 60 mm and above.

At low encounter frequency the hull loading was dominated by the wave inertial load, while the central bow entered the wave and the water surface passed the bow without the arches filling.

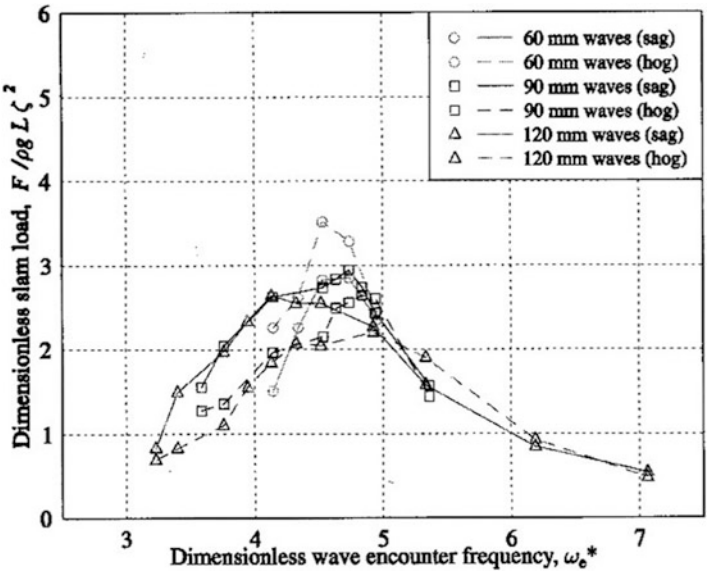

Fig. 12.17 Dimensionless slamming loads versus wave encounter frequency

As wave frequency increased, slamming was experienced and the higher impulsive load was seen to excite the first longitudinal whipping response mode. The slamming load increased with wave height and dimensionless wave encounter frequency up to about 4.5, beyond which slamming forces decreased. An extract of the nondimensional wave slamming force against wave encounter frequency is shown in Fig. 12.17, peaking in the range ω_e 2–3. The peak slamming load monitored was 23.75 kg, which equates to 87% of the model mass, and compares with 93% measured in full-scale vessel trials.

The strain gauge data were analyzed to determine the longitudinal position of the peak loading for both sag (bow up as it enters the wave) and hog (the reflex as the wave passes through the vessel tunnel). It was found that the position was effectively independent of wave encounter frequency and for sag was located just at the rear of the bow arch, while hogging load was centered a little further aft.

The bending moments were also nondimensionalized by relating to wave height ^2 and model length ^2 and found to follow the same profile as the slam loading. When the profile for the loadings with encounter frequency was compared with the heave and pitch RAOs, it was seen that the maximum slam loads and bending response were at higher nondimensional encounter frequencies, ω_e 4.5–5. Rather than simply the motions, it is proposed that the relative motion and acceleration generate the slamming force (as well as the incident geometry of the hull to wave surface). Dimensionless heave and pitch accelerations measured at the model testing were plotted and showed peak response much closer to the slam peak response (in the range 3.5–4.5).

Conclusions from this work are that the model tests were able to simulate the slamming loading and hull structural response and that time domain relative motion and acceleration between the wave profile and the bow are key parameters. This helps to give confidence to FE modeling for overall loading.

Note that following this period of extensive testing and analysis by Incat and Revolution Design Engineers, the arch shape between the central bow and the side hulls was deepened and the curved arch shape adjusted so as to reduce pressure buildup for the larger and faster vessels delivered subsequently.

If we now turn back to ABS guidance, the society recommends nonlinear time domain analysis for wave loads and use of CFD. Tools supported by the society are discussed in references [28, 29] with reference to monohull shipping in extreme conditions. Currently there are limitations to these modeling tools, which are pointed out in the references. They are available directly from ABS internet site.

One further analytical study, this time focusing on a 107-m fast trimaran concept for the US Navy and using the SESAM-based WASIM linear code, is detailed in [30]. The study looked at motions and loadings on the semi-SWATH trimaran (Fig. 12.18). Model tests had earlier been carried out at 1:32 scale looking at motions, and the study using WASIM was to extend the work on a short timescale to see whether the complex form could be optimized. A computer model was built and RAOs from linear analysis generated. Initial results showed that correlation with physical model data obtained from tests in the Webb Institute model basin required input of viscous damping (10% for heave and pitch, 8% for roll). The RAO data were then used in a spectral analysis with PM and JONSWAP spectra for North Atlantic sea state 6, Hs 5 m with Tm 12.4 s and Tz 8.82 s. The analysis was carried out for ship speed zero. RMS values of roll and pitch for the two spectra are given in Table 12.2. Further analysis derived the relative displacement and relative vertical velocity response spectra at a point under the bow so as to be able to apply Ochi's criteria for probability of slamming [31], as below.

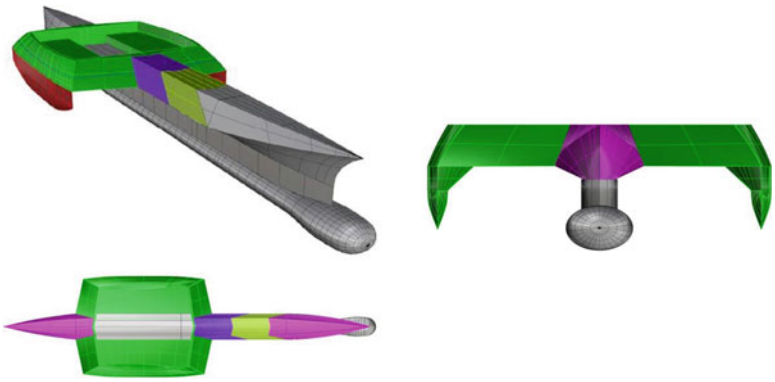

Fig. 12.18 Tri-SWATH

Table 12.2 Tri-SWATH motion data

Sea state 6	RMS roll deg. beam	RMS pitch deg. head	RMS acceleration, g
Pierson–Moskowitz	6.84	2.08	0.11
JONSWAP	7.90	2.10	0.10

The Ochi probability of slamming is calculated as follows:

$$P\{\text{slamming}\} = e^{\alpha},$$

where

$$\alpha = \frac{-d^2}{2m_{0_s}} + \frac{-\dot{s}_{cr}^{\,2}}{2m_{0_{\dot{s}}}}.$$

Here $\dot{S}_{cr} = 0.093\sqrt{\text{gL}}$ is a vertical velocity threshold, Froude scaled from experimental results provided by Ochi. The $m_{0\text{s}}$ and $m_{0_{\dot{s}}}$ are the relative displacement and relative velocity spectral moments at a point located under the keel near the bow, and d is the draft at the design waterline.

From the relative displacement and velocity spectra in head seas the authors projected a probability of slamming of 0.33 for the PM spectrum and 0.35 for the JONSWAP spectrum, which yielded 131 or 134 slams per hour, compared with the Naval Operability (STANAG) criteria they were using for an acceptability of 20 slams per hour based on this method.

The authors commented on the limitations of their approach and the likely overpredictions as a consequence. Their expectation was that at forward speeds additional damping would come into play and reduce motions. The work nevertheless illustrates the challenges in analyzing the response of a complex vessel such as a trimaran and, by inference, that responses such as slamming are nonlinear.

Some additional observations follow. When analyzing the motion response of a trimaran, the pitching response of the main hull and slamming under the forefoot are important to address. For the forefoot area of the main hull the issue is similar to a monohull, with slamming occurring when the bow reenters an upwelling oncoming wave with sufficient relative velocity and the hull surface is at a relatively low angle to the wave surface.

This takes us back to the work in [21]. In addition, a modern fast trimaran of this size will have trim tabs at the transom stern and a stabilization foil under the forefoot, introducing significant damping to longitudinal motions (Chap. 11), thereby reducing the probability of slamming. Finally, for the trimaran there is the possibility of refining the forefoot and bow sections so as to avoid panel orientation beyond 75° from flow direction in locations sensitive to slamming based on Ochi.

From [30] it is clear that the use of nonlinear analysis in the time domain is important for realistic extreme response predictions rather than linear modeling at zero speed, as the researchers themselves comment. It may be realistic also to suggest that for prototype (large) vessels, physical model testing, including wave

loading via pressure sensors or segmented models, is necessary for calibration until CFD techniques have developed further with the help of model testing correlations.

12.10.4 General Observations on Slamming and Whipping Response

If we look back at this very substantial collection of work, some observations may help us to make decisions regarding bow geometry for catamarans. First, it is clear that local slamming pressures can lead to stresses higher than yield unless impulse loading is specifically addressed for multihull vessels of all sizes. This is further backed up by material presented by Faltinsen in [8] Chap. 8. Additionally, from the previously cited work, the bending moments generated by the impulsive loading need to be incorporated into vessel structural design, at least for larger vessels.

The central bow geometry employed on many wave piercers interacts with relatively low waves; the larger the bow, the larger the interaction and, hence, resistance, so the impetus is for a bow as small as practical. How important is the bow to overall motion? How far above SWL should the keel be, and how high should the cross structure underside be? From the aforementioned work, where the bow is substantial and the keel is a meter or so from the SWL, the interaction with oncoming waves is such that they are channeled and the surface "enhanced" to reach significantly above the undisturbed wave profile. An alternative may be highly flared demihull bows above water, but this form would still channel waves flowing between the hulls, enhance the surface elevation, and accelerate the flow.

This takes us to traditional catamarans. For a so-called traditional catamaran, as long as the bow cross structure is above the waves, there is still the wave interaction with the demihull bows, which will direct water flow upward, impacting the cross structure internal corner, causing higher pressure loading, and slamming loads as wave height is increased. While stabilizing foils can reduce motion, in higher-frequency waves, as shown in the studies cited earlier, the relative motion between hull and upwelling wave is the key factor. The bow cross structure is flatter, so the possibility of impulse loading is greater; therefore, strict operating limits are needed to avoid heavy wave interaction. Operating limits can be assessed by time domain simulation and assessment of slam loading against the structural capacity.

There is also potential to consider higher curvature and perhaps chines/spray rails in this demihull bow area so that the wave energy is directed away from the cross structure in a similar manner to planing boat design, even for vessels operating at much lower Froude numbers.

For trimarans, where the cross structure and sponsons are located much further aft, the first concern for slamming is the main hull lower panels aft of the bow forepeak. The sponson bow profile will create channeling to the wave flow as it passes. Since the relative motions and accelerations should be much lower than at the central bow, there is still the potential for slamming forces on the underside of the

cross structure at internal corners to the sponsons in extreme waves, and so careful review of time domain motion analysis is needed to inspect the heave and pitch accelerations and the relative motion between the wave and the sponson/cross structure for extreme waves.

Note that trimarans with forward sponsons may be subject to similar wave enhancement effects and funneling, which would create impact loads on supporting connecting structure, so this favors sponsons being mid or stern located. Stern location can also help to suppress pitch motions, as long as a fine bow form also has damping, normally provided by foils below the keel.

Take care in developing the bow form of catamarans. A central or highly flared bow form may help with plow in down waves, but in normal operating conditions of up to 3-m waves, there may be a balance between wave piercing or fine central bow form and open front so as to not channel waves and create wave enhancement in the funnel form.

This aspect of slamming and hull vibratory response to impulse loading has taken some pages to discuss. The key for a designer is caution in modeling and the interpretation of results. For large vessels the issue cannot be avoided or simplified, as in higher sea states slamming will occur, and, as shown by the work with Incat wave piercers, speed reduction does not remove the problem, and wave height and encounter period (i.e., wave steepness and orbital velocity at the wave surface, including effects of enhancement) are critical parameters.

Smaller vessels will generally be designed for stiffness, so simpler checks of hull shell capacity against conservative slamming pressures may be acceptable. For smaller vessels a simpler approach to structural design is generally taken anyway, and this is where we can move on to look at the classification societies' guidance for design, which includes formulas for slamming pressures.

12.11 Design Using Guidance of Classification Societies and IMO

Our approach in this section assumes that a designer will follow rule guidance for initial scantlings using classification society rules for direct calculation, then, depending on vessel dimensions, decide whether detailed analysis of motions is needed or the design can live with rules and go straight to FE modeling or, for smaller vessels, to use direct simplified structural analysis.

In this section we will give a summary overview from DNV rules and then a commentary for elements of rules from ABS and Lloyd's Register and a sampling of guidance from Turkey and South Korea, these being documents available to the authors at the time of preparation.

We look at sea pressures, accelerations, and their input to determine bending moments and shear forces and then control scantling specifications for the vessel structure. Detailed design of the structure itself is then a specialist subject by itsself that is guided by the extensive rule documents issued by the classification societies, which we leave readers to explore for themselves.

12.11.1 IMO Code of Safety

The IMO Code of Safety for High-Speed Craft [32], Chaps. 3 and 4, provides guidance on buoyancy, stability, and subdivision of hull spaces, general structural requirements, and guidance on the layout of passenger and cargo spaces. Requirements for anchoring, towing, and berthing are also given. These last are cases that need to be checked at least for local loads on a multihull structure.

Chapter 3 gives guidance for global structural design that is generic, along the lines of adequacy for intended use, referring specifically to cyclic loads:

- Not to impair structural integrity for anticipated service life
- Not to hinder functioning of machinery and equipment
- Not to impair ability of crew to carry out its duties

Chapter 4 on accommodation does go into some detail concerning design acceleration levels to be taken into account when considering a collision case based around foundering head-on at speed against a rock extending 2 m above the waterline. Such incidents have happened to catamarans and fast craft. The thinking for the IMO is that the structure experiencing such an event should maintain stable and buoyant condition such that personnel evacuation remains viable. The guidance is summarized in Text Box 12.1.

Text Box 12.1: IMO Guidance on Collision Decelerations

The basis for calculation is vessel at operational speed meeting a vertical rock extending 2 m above vessel SWL.

Horizontal deceleration from the collision, g_{col}, is calculated as follows:

$$g_{col} = 1.2\,(P/g.\Delta),$$

where

Δ = Mean operational displacement (te);
g = 9.806 (m/s^2);
P is the lowest value from either of the the following expressions:

$$P = 460\,(M.C_L)^{0.66}.(E.C_H)^{0.33} \quad \text{or}$$
$$P = 9000.M.C_L(C_H.(T+2))^{0.5},$$

where

Material factor M = 1.0 Al, 0.8 glass-reinforced plastic, 1.3 High Tensile (HT) steel, and 0.95 mild steel;
Length factor $C_L = (165 + L)/245.\ (L/80)^{0.4}$;
Height factor $C_H = (T + 2 + f.\ D/2)/2D$;

(continued)

Text Box 12.1 (continued)

$E = 0.5\ \Delta\ v^2$ (kN.m);
$v =$ Vessel speed (m/s);
$L = L_{WL}$ (m);
$D =$ Vessel girder depth (m);
$T =$ Vessel draft (m);
$f =$ 0 when $T + 2 < D–H_T$,
1 when $D > T + 2 \geq D\text{-}H_T$,
2 when $T + 2 \geq D$;
$H_T =$ Height from underside of tunnel to top of hull girder (m).

The following diagrams give an explanation of factor *f*:

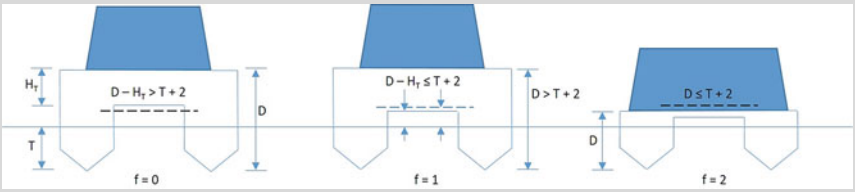

12.11.2 DNV: Initial Structure Dimensioning [14]

Part 3, Chap. 1, of DNV Rules for Classification of High Speed, Light Craft defines the design principles and loads. We provide a summary overview as follows. It should be noted that the full documentation can be downloaded from www.DNVGL.no. It is not our intention below to provide a comprehensive design guide, but rather to indicate the approach to initial scantling estimation for engineers prior to using DNV's documents directly for their work and interact with DNV GL or other classification society through the design process, either as the classification authority or for guidance if another authority will class the vessel.

Subdivision

WT bulkheads shall be provided, with as minimum a collision bulkhead forward and at each end of the machinery space extending upward to a location connecting to a continuous deck and with freeboard. The collision bulkhead shall be positioned between 0.05 *L* and 3 + 0.05 *L* aft of the forward perpendicular, where *L* is vessel L_{WL}.

Scantlings

For craft with $L < 50$ m and $L/D < 12$, the minimum strength standard is normally satisfied for scantlings obtained from local strength requirements. Craft shall be resistant to slamming. Minimum slamming loads are given (Text Box 12.2).

The rules provide a means to estimate design loads that are applicable in strength formulas to be included in calculation methods when the satisfactory strength level is represented by allowable stress or usage factors. The basis is structural response that remains within the elastic region with suitable safety factors.

Wave-induced loads may be determined by calculation, model tests, or full-scale measurement. The determination of dynamic loads is to be based on the long-term distribution of responses over craft operational life.

Note that DNV will not class vessels for operation within a specific geographical area. DNV's approach is slightly different from that of ABS. DNV defines class notation for restricted service from R1 to R6 as follows, while R0 is stated as not applicable for vessels falling into the scope of IMO's Code for High-Speed Craft, meaning ferries and cargo vessels, so designers would have to take additional advice from the society.

Class notation	Condition	Distance to harbor (nautical miles) Winter /summer/tropical			Reduction in Cw, %
R0	Ocean	300	Unrestricted	Unrestricted	0
R1	Ocean	100	300	300	0
R2	Offshore	50	100	250	10
R3	Coastal	20	50	100	20
R4	Inshore	5	10	20	40
R5 and R6	Inland	1	2	5	60
R6	Sheltered	0.2	0.3	0.5	60

where wave coefficient, $C\mathrm{w} = 0.08L \quad \text{for} L < 100\ \text{m},$
$C\mathrm{w} = 6 + 0.02L \quad \text{for} L > 100\ \text{m}.$

Accelerations

DNV provides formulas in Part 3, Chap. 1, Sect. 1.2, "Design Loads," Subsect. B, "Accelerations," to determine minimum design vertical acceleration at CG and horizontal acceleration in surge and in sway due to roll in beam seas. The intent is to determine the combined accelerations for each of the vessel axes due to translation and angular acceleration, treating them as independent processes. The guidance gives formulas allowing for the calculation of the accelerations at vessel CG given the vessel type and basic data regarding the hull characteristics, as summarized in what follows.

Combined accelerations in the vessel vertical, transverse, and longitudinal axes are obtained from the following expression summing the accelerations of the variables 1 to n, where the acceleration variables include the appropriate component of gravitational acceleration:

$$a_{\mathrm{c}} = \sqrt{\sum_{m=1}^{n} a_m^2}.$$

- *Design vertical acceleration*

The design vertical acceleration is intended as the extreme value with a 1% probability of being exceeded in the limiting operating condition. The design vertical acceleration at vessel CG, a_{cg}, may be that obtained from a detailed motion analysis by the designer but will not be less than

$$a_{\mathrm{cg}} = \frac{V}{\sqrt{L}} \frac{3.2}{L^{0.76}} f_{\mathrm{g}} g_0 \quad \left(\mathrm{m/s^2}\right),$$

where a_{cg} and f_{g} are as in the following table. $V/\sqrt{L}$ need not be taken as greater than 3.0.

Factor f_g	Service area restriction notation						
Type	*R*0	*R*1	*R*2	*R*3	*R*4	*R*5	*R*6
Passenger	n/a	1	1	1	1	0.5	0.5
Car Ferry	n/a	1	1	1	1	0.5	0.5
Cargo	4	3	2	1	1	0.5	0.5
Patrol	7	5	3	1	1	0.5	0.5
Yacht	1	1	1	1	1	0.5	0.5
Minimum a_{cg} for all	$1.g_0$	$1.g_0$	$1.g_0$	$1.g_0$	$1.g_0$	$0.5.g_0$	$0.5.g_0$

The accelerations at different locations along the hull length are defined by

$$a_{\mathrm{v}} = k_{\mathrm{v}}.a_{\mathrm{cg}},$$

where k_{v} is a longitudinal distribution factor as follows:

$k_{\mathrm{v}} = 1.0$ from Aft Perpendicular (AP) to amidships;
$k_{\mathrm{v}} =$ Increases linearly from 1.0 amidships to 2.0 at Forward Perpendicular (FP) of vessel.

Given the foregoing design vertical acceleration, DNV provides a relationship to estimate the allowable speed for a vessel in different sea states, as follows:

When $V/\sqrt{L} \geq 3$:

$$a_{\mathrm{cg}} = \frac{k_{\mathrm{h}} g_0}{1650} \left(\frac{H_{\mathrm{S}}}{B_{\mathrm{WL2}}} + 0.084\right) \left(50 - \beta_{\mathrm{cg}}\right) \left(\frac{V}{\sqrt{L}}\right)^2 \frac{L B_{\mathrm{WL2}}}{\Delta} \quad \left(\mathrm{m/s^2}\right),$$

where

H_{s} = Significant wave height (m);
β_{cg} = dead-rise angle at LCG in degrees (minimum 10°, maximum 30°);
B_{WL2} = Waterline breadth at L/2 (m).

For twin- and multihull vessels the total breadth of the hulls (exclusive of the breadth of the tunnels) shall be used for B_{WL2}:

g_0 = Standard acceleration of gravity = 9.81 m/s^2;
k_h = Hull type factor:
monohull, catamaran 1.0; wave piercer 0.9;
surface effect ship (SES) and air cushion vehicle (ACV) 0.8; foil-assisted hull and SWATH 0.7;

When $V/\sqrt{L} < 3$:

$$a_{cg} = 6\frac{H_S}{L}\left(0.85 + 0.35\frac{V}{\sqrt{L}}\right)g_0 \quad (\mathrm{m/s^2}).$$

It is intended by DNV that speed restrictions in sea states as above be applied to vessel operation. In light of the research done on the wave piercers discussed earlier, it may be that reduced speed does not actually lead to reduced accelerations, so a designers must consider carefully the motion response of their chosen vessel configuration in a seaway. It is useful to at least assess the standard limitations that DNV would apply, as a means of comparison with any operability studies that may be carried out initially based on motions and habitability.

- *Design horizontal acceleration*

A vessel should be designed for acceleration in the longitudinal (surge) direction a_l not less than

$$a_l = 2.5\frac{C_W}{L}\left(0.85 + 0.25\frac{V}{\sqrt{L}}\right)^2 g_0,$$

where $V/\sqrt{L}$ need not be taken as being greater than 4.0.

The relationship for acceleration in sea states is proposed as

$$a_l = (1.67)\frac{H_S}{L}\left(0.85 + 0.35\frac{V}{\sqrt{L}}\right)^2 g_0.$$

It should be noted that this acceleration is an estimate of acceleration in a seaway, not deceleration due to impact, as detailed by the IMO HSC code.

It might also be necessary to look at transverse acceleration from forced roll motion in bow heading sea directions, and for this DNV proposes the following formulas:

Period of roll: $T_R = \frac{\sqrt{L}}{1.05+0.175\frac{V}{\sqrt{L}}}$ (s); maximum inclination: $\theta_r = \frac{\pi h_w}{2L}$ (radians);

And the resulting dynamic transverse acceleration: $a_t = \left(2\frac{\pi}{T_R}\right)^2 \theta_r r_r \quad (\mathrm{m/s^2})$,

where h_w is the maximum wave height that 70% of service speed can be maintained, as in the foregoing relations, with a minimum of 0.6 C_W, and r_r is the height above the roll axis, normally taken as the waterline for multihull craft.

Sea Pressures and Forces

External and internal pressures shall be considered those that influence the scantlings of stiffened panels, including static and dynamic sea pressures acting on the hull, internal pressures from tank liquids, and loads from cargo, stores, and equipment.

External dynamic pressures include slamming pressures on lower parts of a vessel. A summary of the approach to slamming for hull forebodies and to cross structures is given in Text Box 12.2.

External sea pressures (separate from slamming) acting on the hull bottom, sides, and weather decks shall not be less than as follows:

- *Load point below waterline*:

$$p = 10h_0 + \left(k_S - 1.5\frac{h_0}{T}\right)C_W \quad \left(\mathrm{kN/m^2}\right);$$

- *Load point above waterline*:

$$p = a\,k_s(C_W - 0.67\,h_0) \quad \left(\mathrm{kN/m^2}\right);$$

h_0 = Vertical distance (m) from waterline at draft T to load point;
k_s = 7.5 aft of amidships,
= 5/CB forward of FP.

Between amidships and FP k_s shall be varied linearly to the 5/CB value at FP:

a = 1.0 for craft's sides and open freeboard deck,

= 0.8 for weather decks above freeboard deck;

C_W = Wave coefficient:
C_w = 0.08 L for $L < 100$ m,
C_w = 6 + 0.02 L for $L > 100$ m.

The minimum sea pressures to be used (kN/m^2) for above-water areas are as follows:

Class notation	Condition	Hull sides	Weather decks	Roofs above 0.1 L from SWL
R0	Ocean	6.5	5	3
R1	Ocean	6.5	5	3
R2	Offshore	6.5	5	3
R3	Coastal	6.5	5	3
R4	Inshore	5	4	3
R5 and R6	Inland	4	3	3
R6	Sheltered	4	3	3

- *Superstructure end bulkheads*

$$p = a k_s (C_W - 0.67 h_0) \quad \left(\text{kN/m}^2\right),$$

$P_{min} = 5 + (5 + 0.05\ L)$ sin α (kN/m^2) for lowest tier of unprotected front;
$P_{min} = 5$ (kN/m^2) for aft end bulkheads;
$P_{min} = 5 + 0.025\ L$ sin α (kN/m^2) elsewhere,

where α is the angle between the bulkhead/side and deck;

h_o, C_W, and k_s as given previously for load point above waterline;

a = 2.0 for lowest tier of unprotected fronts,
= 1.5 for deckhouse fronts,
= 1.0 for deckhouse sides,
= 0.8 elsewhere.

- *Watertight bulkheads with one compartment flooded*

$$p = 10\ h_b \left(\text{kN/m}^2\right),$$

where h_b is vertical distance (m) from load point to top of bulkhead, or to flooded waterline if this is greater.

Additional guidance is given in the rules for pressures due to liquids in tanks, dry cargo, stores, and equipment. The loading on internal structures is calculated by the sum of the static distributed pressure loading and the local acceleration as calculated under accelerations (p. 34).

- *Dry cargo, stores, and equipment*

Standard loading parameters for deck loading may be summarized as follows. The pressure on inner bottom, decks, or hatch covers is defined as

$$p = \rho H (g_0 + 0.5 a_v)\,\text{kN/m}^2,$$

where

a_v = Acceleration at center of area under consideration as in earlier section on accelerations;
H = Stowage height, with standard values for H as in following table:

Deck	Loading (t/m^2)
Weather deck and weather deck hatch covers for cargo	$\rho H = 1.0$
Shelter deck, shelter deck hatch covers, and inner bottom for cargo	$\rho = 0.7$ t/m^3 H = Vertical distance (m) from load point to deck above or top of coaming for hatchways
Platform deck in machinery spaces	$\rho H = 1.6$
Accommodation decks	$\rho H = 0.35$ when not directly calculated, including deck own mass; minimum value if calculated value is 0.25

It should be noted that if weather decks and hatches are designed to take local heavy cargo loads, the design criteria for the deck or hatch shall be the greater of the cargo loading or the sea pressure loading.

For local heavy units the vertical force action on the supporting structures shall be calculated as

$P_v = M\ (g_0 + 0.5\ a_v)$ kN, where M is the mass of the unit in tons.

Text Box 12.2 Slamming Load Calculation from DNV, Part 3, Chap. 1, Sect. 2, Design Loads, Subsection C, Pressures and Forces C200, 300, 400

The *design slamming pressure on the bottom of craft* with speed shall be taken as

$$P_{sl} = 1.3k_l\left(\frac{\Delta}{nA}\right)^{0.3} T_O{}^{0.7}\frac{50-\beta_x}{50-\beta_{cg}}a_{cg}\left(\mathrm{kN/m^2}\right),$$

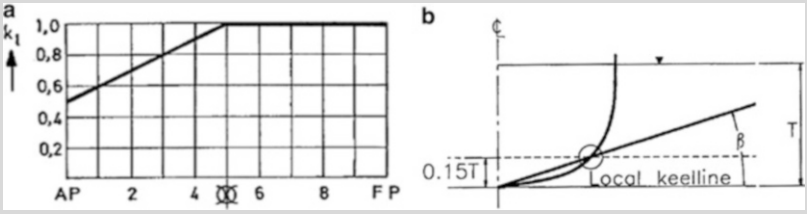

k_l = Longitudinal distribution factor from Fig. A above;
n = Number of hulls, 1 for monohulls, 2 for catamarans; trimarans and other multihulls will be specially considered;
A = Design load area for element considered in m^2, where A shall not be taken greater than 2.5 s^2 m^2 for plating; for stiffeners and girders, A is taken as the product of (spacing x span); for any structure A need not be taken to be less than 0.002 Δ/T;
T_O = Draft at $L/2$ in meters at normal operation condition at service speed;
Δ = Fully loaded displacement in tons in salt water on draft T;
βx = Dead-rise angle in degrees at transverse section considered (minimum 10°, maximum 30°);
β_{cg} = Dead-rise angle in degrees at LCG (minimum 10°, maximum 30°);
a_{cg} = Design vertical acceleration at LCG (av calculated at LCG).

Note that for round bilge sectioned vessels with no pronounced dead-rise angle, βx and βcg can be estimated as in the preceding Fig. B, taking a line from keel to the intersection of a line at 15% of vessel draft T.

All craft shall be designed for a *pitching slamming pressure on bottom* as follows:

(continued)

Text Box 12.2 (continued)

$$P_{sl} = \frac{21}{\tan(\beta_x)} k_a k_b C_W \left(1 - \frac{20T_L}{L}\right) \left(\text{kN/m}^2\right);$$

βx is as previously;

k_a = 1 for plating,
= 1.1–20 lA/L; maximum 1.0, minimum 0.35 for stiffeners and girders, where
lA = longitudinal extent (m) of load area;

k_b = 1 for plating and longitudinal stiffeners and girders,
= L/40 l + 0.5 (maximum 1.0) for transverse stiffeners and girders, where
l = span (m) of stiffener or girder;

T_L = lowest service speed draft (m) at FP measured vertically from waterline to keel line or extended keel line.

Above pressure shall extend within a length from FP by $(0.1 + 0.15(V/L^{0.5}))$. L, where

$V/L^{0.5}$ need not to be taken to be greater than 3.

ps$l$ and may be gradually reduced to zero at 0.175 L aft of the aforementioned length.

Pitching slamming pressure shall be exposed on elements within the area extending from the keel line to the chine, the upper turn of bilge (above line in Fig. B), or pronounced spray rail.

Text Box 12.2 Continued: Slamming Loads Fore and Side Body

Forebody sideand bow impact pressure shall be taken to be as follows (kN/m^2):

$$P_{sl} = \frac{0.7LC_L C_H}{A^{0.3}} \left(0.6 + 0.4\frac{V}{\sqrt{L}} \sin\gamma \cos\left(90^\circ - \alpha\right) + \frac{2.1a_0}{C_B}\sqrt{0.4\frac{V}{\sqrt{L}} + 0.6\sin\left(90^\circ - \alpha\right)\left(\frac{X}{L} - 0.4\right)}\right)^2,$$

where $V/\sqrt{L}$ need not be greater than 3;

A = Design load area for element considered (m^2);
For plating A shall not be taken to be greater than = 2.5 s^2 (m^2),
For stiffeners and girders A need not be taken to be smaller than e^2 (m^2),
In general, A need not be taken to be smaller than L B_{WL}/1000 (m^2);

(continued)

Text Box 12.2 (continued)

e = Vertical extent of load area, measured along shell perpendicular to waterline;
x = Distance (m) from AP to position considered;
C_L = Correction factor for length of craft,
= $(250\ L - L^2)/\ 15{,}000$. L is not to be taken to be longer than 100 m;
C_H = correction factor for height above waterline to load point,
= $(1–0.5\ h_0\ /\ C_W)$, where Cw may be reduced as in the guidance for calculation of slamming loads on the hull bottom at beginning of this text box;
h_0 = Vertical distance (m) from waterline at draft T to load point;
α = Flare angle taken as the angle between side plating and a horizontal line, measured at point considered (Fig. C);
γ = Angle between waterline and longitudinal line measured at point considered (Fig. D);
a_0 = Acceleration parameter:

$$a_0 = 3.\ C_W/L + C_V.\ V/L^{0.5}, \text{ where } C_V = L^{0.5}/50 \text{ with maximum } 0.2.$$

Forebody side and bow pressure shall not be taken to be less than the calculation of the external sea pressure. The impact pressure is to be calculated for longitudinal positions between 0.4 L and the bow.

In the vertical direction, the impact pressure shall extend from the bottom chine or upper turn of the bilge to the main deck or vertical part of the craft's side. The upper turn of the bilge shall be taken at a position where the dead-rise angle reaches 70°, but not higher than the waterline.

If no pronounced bottom chine or upper turn of the bilge is given (V shape), the impact pressure shall extend from the keel to the main deck or vertical part of the craft's side.

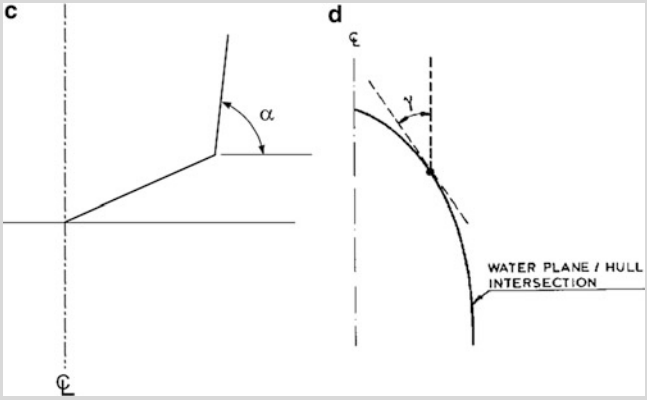

Text Box 12.2 Continued: Slamming Loads on Flat Cross Structures
The design slamming pressure on flat cross structures (catamaran tunnel top, etc.), shall be taken as

$$P_{sl} = 2.6k_t\left(\frac{\Delta}{A}\right)^{0.3} a_{cg}\left(1 - \frac{H_C}{H_L}\right)(\mathrm{kN/m^2}),$$

where

A = Design load area for element considered as in the guidance for calculation of slamming loads on the hull bottom at beginning of this text box;
H_C = Minimum vertical distance (m) from WL to load point in operating condition;
k_t = Longitudinal pressure distribution factor according to Fig. E below;
H_L = Necessary vertical clearance (m) from WL to load point to avoid slamming,
= 0.22 L (k_c – 0.8 L/1000);
k_c = Hull type clearance factor, which is
0.3 for catamaran, wave piercer, foil-catamaran, SES, ACV, hydrofoil;
0.5 for SWATH.

Slamming pressure shall not be less than the sea pressure according to the calculation for vessel side above the WL; see sea pressure calculation preceding this text box.

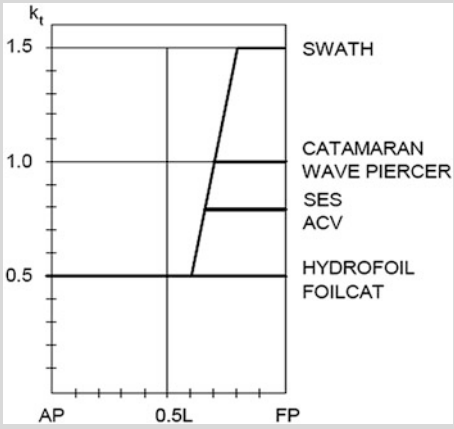

Hull Main Girder Design Loads
DNV advises that for vessels with a hull form having $L/D < 12$ and a length less than 50 m, the minimum strength standard for scantlings is normally satisfied by the local

strength requirements. For other vessels longer than 50 m and having $L/D > 12$ for the demihull main beam structures, the following approach is needed to determine the main hull girder dimensions.

It may be noted that we are considering high-speed, semiplaning craft that have significant dynamic lifting force or planing craft that are completely supported by dynamic forces. The approach is therefore to initially assess potential "slamming forces" based on a vessel reentering waves of the same length as the vessel with the wave peak either at the bow and stern or at amidships. The landing area is first assessed, and then the bending moment can be calculated. The landing area is defined as follows:

$$A_R = k\Delta\left(\left(1 + 0.2\, a_{cg}/g_0\right)/T\right) \quad \left(m^2\right),$$

where

k = 0.7 for crest landing and 0.6 for trough landing;
Δ = Displacement (t);
a_{cg} = Vertical design acceleration at LCG.

For a crest landing with the midship area loaded the bending moment is

$$M_B = \frac{\Delta}{2}\left(g_0 + a_{cg}\right)\left(e_w - \frac{l_s}{4}\right)(\text{kNm}),$$

where

e_w = 0.5 of distance between LCG of fore half-body and LCG of aft half-body of vessel (m),
= 0.25 L if not known (0.2 L for hollow landing);
l_s = Longitudinal extension of slamming reference area,
$= A_R/b_s$;
b_s = Breadth of slamming area,
$= 2 \times b$ where b is demihull beam for catamarans.
It should be noted that $(e_W - l_s/4)$ should not be taken to be less than 0.04 L.

For hollow (trough) landing with bow and stern area loaded

$$M_B = \frac{\Delta}{2}\left(g_0 + a_{cg}\right)(e_r - e_w),$$

where A_R is in this case divided into two parts at each end of the hull(s):

e_r = Mean distance from center of $A_R/2$ end areas to vessel LCG (m),

and $(e_r - e_w)$ is not to be taken to be less than 0.04 L.

Hogging and Sagging Bending Moments
For all vessel configurations, analysis of design bending moment on the hulls is intended to be based on the wave inertia forces, including effects from the vessel pitch angle. For the initial design for twin-hull craft (in kNm):

Mtot hog $= M$sw + 0.19 $C_W L^2$ (B_{WL2} + $k_2 B$tn) CB;
Mtot sag $= M$sw + 0.14 $C_W L^2$ (B_{WL2} + $k_3 B$tn) (CB + 0.7);
Msw = Still-water moment in most unfavorable loading condition in kNm [(Note 1)],
= 0.5 Δ L (kNm) in hogging if not known,
= 0 in sagging if not known [(Note 2)];
additional correction of 20% to be added to the wave sagging moment for craft with large flares in the bows of the vessel;

B_{WL2} = Greatest molded breadth at fully loaded waterline measured at L/2;
B_{tn} = Breadth (m) of cross structures (tunnel breadth);
k_2 and k_3 = Empirical factors for effect of cross-structure immersion in hogging and sagging waves; if no other value is available, then the designer shall use

$$k_2 = 1 - \frac{z - 0.5T}{0.5T + 2C_W}, \text{minimum } 0,$$

$$k_3 = 1 - \frac{z - 0.5T}{0.5T + 2.5C_W}, \text{minimum } 0;$$

$k_4 = 0.25$ in general, when V is maximum speed of craft,
= 0.35 when V is taken as the slowed-down speed;

z = Height (m) from baseline to wet deck (top of tunnel).

Notes

1. Documentation of the most unfavorable still-water conditions shall normally be submitted for information.
2. If the still water moment is a hogging moment, 50% of This moment Can be deducted Where the design sagging moment Mtotsag is calculated

Shear Forces from Longitudinal Bending

The vertical hull girder shear force may be related to the hull girder bending moments as follows:

$$Q_b = \frac{M_B}{0.25\text{L}}(\text{kN}),$$

where M_B is the bending moment in kNm.

Axial Loads

Axial loads from surge acceleration (= Δ. a_l), thrust, and sea end pressures may have to be estimated and added together in most exposed areas, for example, the forebody for buckling control. The value of surge acceleration (a_l) advised is to be not less than $0.4g_0$ for $V/\sqrt{L} > 5$and not less than $0.2g_0$ for $V/\sqrt{L} < 3$ with linear interpolation between these speed ratios.

Combination of Hull Girder Loads
The hull girder load vertical bending, vertical shear, and torsion shall be considered according to the following combinations:

- 80% longitudinal bending and shear + 60% torsion,
- 60%% longitudinal bending and shear + 80% torsion.

The hull girder load transverse vertical bending moment and pitch connecting moment shall be considered according to the following combinations:

- 70% transverse bending + 100% pitch connecting,
- 100% transverse bending + 70% pitch connecting.

The following formulas for twin-hull loadings can be applied to generate the preceding loading combinations.

Twin-Hull Loads
The transverse strength of twin-hull connecting structure may be analyzed for moments and forces specified in what follows.

- *Transverse vertical bending moment*

For craft with $V/\sqrt{L} > 3$ and $L < 50$ m, the twin-hull transverse bending moment may be assumed to be

$$M_S = \frac{\Delta\, a_{\mathrm{cg}} b}{s}\ (\mathrm{kNm}),$$

where

$b =$ Transverse distance between centerlines of the two demihulls;
$s =$ Factor given in following table.

Service restriction	s	q
*R*4 to *R*6	8.0	6.0
*R*3	7.5	5.5
*R*2	6.5	5.0
*R*1	5.5	4.0
*R*0	4.0	3.0

For vessels with $L \geq 50$ m, the twin-hull transverse bending moment shall be assumed to be the greater of

$$\text{or } M_{\mathrm{S}} = M_{\mathrm{S0}}\left(1 + \frac{a_{\mathrm{cg}}}{\mathrm{g}_0}\right)(\mathrm{kNm})$$

$$M_{\mathrm{S}} = M_{\mathrm{S0}} + F_{\mathrm{y}}(z - 0.5\mathrm{T})(\mathrm{kNm})$$

where

M_{S0} = Still-water transverse bending moment (kNm);
z = Height from baseline to neutral axis of cross structure (m).

For vessels larger than $L \geq 50$ m, the twin-hull still-water transverse bending moment can be assumed to be as follows:

$$M_{S0} = 4.91\Delta\left(y_b - 0.4^{0.88}\right)\text{(kNm)},$$

where

Δ = Displacement (t);
y_b = Transverse distance (m) from vessel centerline to local centerline of one demihull;
B = Beam overall (m);
Fy = Horizontal split force on immersed hull

$$= 3.25\left(1 + 0.0172\frac{V}{\sqrt{L}}\right)L^{1.05}T^{1.30}(0.5\,B_{WL})^{0.146} \cdot \left[1 - \frac{L_{BMAX}}{L} + \frac{L_{BMAX}}{L}\left(\frac{B_{MAX}}{B_{WL}}\right)^{2.10}\right]H_1\,\text{(kN)};$$

H_1 = Minimum of 0.143 B or Hs max;
B_{WL} = Maximum width (m) in waterline (sum of both hulls);
B_{MAX} = Maximum width (m) of submerged part (sum of both hulls);
L_{BMAX} = Length (m) of part of hull where $B_{MAX}/B_{WL} > 1$;
$HS,_{MAX}$ = Maximum significant wave height in which vessel is allowed to operate (m).

$V/\sqrt{L}$ need not be greater than 3 for the calculation.

An explanation of the different breadths depending on hull configuration is shown in Fig. 12.19, applying particularly for semi-SWATH craft.

- *Vertical shear force between demihulls*

The vertical shear force in the centerline between twin hulls may be assumed to be

$$S = \frac{\Delta\, a_{cg}}{q}\,\text{(kN)},$$

where q is as in the preceding service restriction table.

- *Pitch connecting moment*

The twin-hull pitch connection moment (see M_p in figure below) may be assumed to be

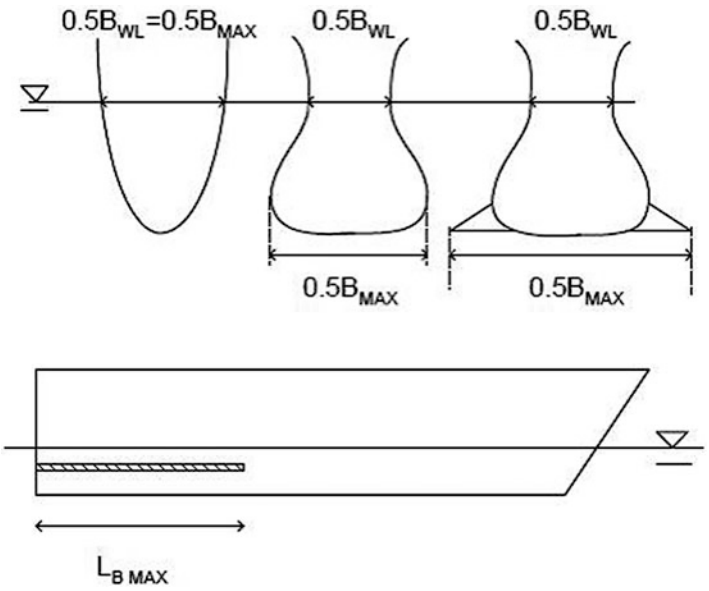

Fig. 12.19 Dimensions for semi-SWATH forms

$$M_{\mathrm{P}} = \frac{\Delta a_{\mathrm{cg}} L}{8}\,(\mathrm{kNm}).$$

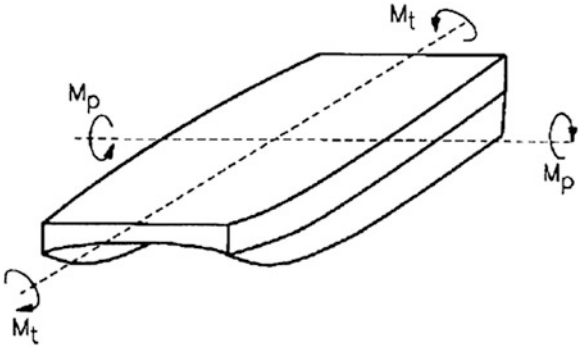

- *Torsion connecting moment*

  The twin hull torsion connecting moment M_{t} in the figure may be assumed to be

$$M_t = \frac{\Delta a_{cg} b}{4} \text{ (kNm)},$$

where b is the distance between the two demihull centerlines.

Structural Design

DNV guidelines for structural design are contained in Chap. 3 of its rules, for aluminum structures (steel is covered in Chap. 2 and FRP in Chap. 4, each covering similar ground). Guidance is given on allowable design stresses related to the selected materials, including the effects of welding in the case of steel and aluminum and joint design in the case of FRP.

The starting point is the midship section modulus for hull girder strength, with the requirement stated as

$$Z = M/\sigma x \text{ 10E3 cm}^3,$$

where

M = Longitudinal midship bending moment (kNm), which is the greatest of the following combinations:

- = sagging or hogging bending moment,
- = hollow landing or crest landing bending moment,
- = maximum still-water + wave bending moment for high-speed displacement craft and semiplaning craft in displacement mode,
- = maximum total moment for multihull with hydrofoil on foils;

σ = 175 × f_1 N/mm^2 in general for aluminum, where

f_1 = material safety factor, specified in Table B1 of Sect. 2 in Part 3, Chap. 3.[1]

The effective section modulus excludes superstructures that do not form a strength deck for the vessel longitudinal section.

When considering shear strength, the allowable stress is defined as

τ = allowable bending stress/1.732051.

Guidance is given for the calculation of plating and stiffener characteristics, pillars, bulkheads, girders, weld connections, and direct strength calculations for all the main members. For applicable grades of aluminum plate, strip and profiles at different temper factors of safety are specified, which are then included in the calculation of allowable stress for the structural members. NV-5383 sheet and plate has an SF (f_1) of 0.89 and 0.64 in the welded condition, for example.

[1]Table B1 provides design safety factors for various grades of aluminum in wrought, extruded, and welded conditions. Equivalent data are also provided for steel and for FRP materials in other chapters. The factors for aluminum vary between 0.27 and 0.9, so consultation of the rules is recommended!

For multihull vessels, following dimensioning scantlings based on longitudinal loading cases, attention has to turn to design for transverse strength considering bending and shear strength in beam seas and, finally, torsional load cases. It is simplest to take this last condition in the FE analysis once the model has been built for large vessels.

12.11.3 ABS: Initial Structure Dimensioning [15]

We used the ABS guideline on direct analysis methods in earlier sections of this chapter to assist in walking through the fundamental structural design process. ABS provides guidance similar to that of DNV, summarized earlier, on structural configuration and dimensioning using a rule-based approach, and to that of Lloyd's Register. ABS covers the use of steel, aluminum, and FRP together in the one part of their rules (Part 3, "Hull Construction and Equipment").

ABS begins by giving guidance on the application of the direct analysis method to structural design, including advice on building FE models for FE analysis before continuing in Chap. 2 with rule-based guidelines for overall modulus and global stress requirements.

ABS has an approach to minimum modulus for vessels of different lengths and displacements to fulfill requirements, as summarized in what follows.

Where vessels are greater than 61 m LOA, ABS also specifies wave bending moment, still-water bending moment, and slamming bending moment formulas and a midship section modulus for the central 40% of the vessel based on equations similar to those of DNV, where the bending moment used is the maximum of wave and still-water moment in hogging or sagging or the slamming moment on its own, if that is greater.

ABS provides guidance envelopes of bending moment and shear force distribution along the craft length for vessels over 61 m. A detailed section for determining the primary strength for twin-hulled craft, including an analysis of cross structures, is provided. The allowable stresses are reduced to account for the simplification in analysis in this case, while the procedure may be useful to set up early scantlings for later optimization. Rule-based equations are provided for external pressures below the waterline and above, including slamming pressures on cross structures. The approach is similar to that of DNV, while the makeup of elements in the equations is slightly different. The ABS guidance is summarized in what follows.

It is possible, therefore, to check whether operational limitations set by the classification society are appropriate or appear conservative at this stage and then to make preliminary structural dimensioning of a multihull structure based on these rules, including the main hull girder structures and cross structure. For larger vessels more detailed analysis to develop the final design based on the direct method discussed earlier in this chapter is necessary.

We do wish to emphasize that the material shown here is a summary of very detailed guidance given by DNV GL, ABS, and Lloyd's Register, and it is that

material that should be consulted first by a designer before proceeding with a design. Owing to the different approaches taken by the societies, it is helpful to take a look across all the guidances as they give useful insights for designers.

Continuing with the ABS approach to initial calculation, therefore, we begin with section modulus calculation.

Section Modulus Calculation

- *Vessels up to 61 m long:*

Required section modulus (SM) at amidships of the primary hull girders is as follows:

$$\mathrm{SM} = C_1 C_2 L^2 B (C_\mathrm{b} + 0.7) K_3 C\, Q \qquad \mathrm{cm}^2 - \mathrm{m},$$

where

$C_1 = 0.044\,L + 3.75 \qquad L < 90$ m,
$\quad = 10.75 - ((300 - L)/100)^{1.5} \quad L \geq 90$ m;

$C_2 = 0.01$steel, 0.01 aluminum, 1.44×10^{-4} fiber-reinforced hulls;
L = Length of craft (m);
B = Breadth (m) (sum of demihull breadth for catamarans);
V = Maximum speed (knots) in calm water for loading conditions under consideration;
C_b = Block coefficient at design draft, based on length, L, measured on design load waterline; C_b is not to be taken to be less than 0.45 for $L < 35$ m or 0.6 for $L \geq 61$ m; C_b for lengths between 35 m and 61 m is to be determined by interpolation;
K_3 = (0.7 + 0.3 $[(V/\sqrt{L})/2.36]$);
C = 1.0 for steel, 0.9 for aluminum, and 0.8 for fiber-reinforced hull craft.

Q is defined as follows:

Steel = 1 mild steel, 0.78 H32, 0.72 H36 grades, for other grades $\mathrm{Q_{other}}$ will be as follows:
Q_other = $490/(\sigma_y + 0.66\sigma_u)$ $[50/(\sigma_y + 0.66\sigma_u)$, $70{,}900/(\sigma_y + 0.66\sigma_u)]$, where yield strength σ_y is not to be greater than 70% ultimate strength σ_u.

Aluminum

Q = $0.9 + q_5$ but not less than Q_o;
q_5 = $115/\sigma_y$, $(12/\sigma_y$, $17{,}000/\sigma_y)$;
Q_o = $635/(\sigma_y + \sigma_u)$, $(65/(\sigma_y + \sigma_u)$, $92{,}000/(\sigma_y + \sigma_u))$ N/mm^2 (kgf/mm^2, psi);
σ_y = Minimum yield strength of welded aluminum (not to be greater than $0.7\sigma_u$);
σ_u = Minimum ultimate strength of welded aluminum in N/mm^2 (kgf/mm^2, psi).

Fiber-Reinforced Plastic

Q = 400/0.75σ_u, (41/0.75σ_u, 58,000/0.75σ_u);
σ_u = Minimum ultimate tensile or compressive strength, whichever is less, verified by approved test results (N/mm^2) (kgf/mm^2, psi); strength properties in longitudinal direction of craft are to be used.

- *Vessels exceeding 61 m in length:*

Required SM for 0.4 L around amidships of the primary hull girders is as follows:

$$\mathrm{SM} = [M_t C\, Q\,]/f_p \quad \mathrm{cm}^2 - \mathrm{m},$$

where[2]

Material qualities C and Q are as defined previously:

f_p = 17.5 kN/cm2, (1.784 tf/cm^2, 11.33 Ltf/in^2);
M_t = Maximum total bending moment, to be taken as the greatest of the following:

$= M_{\mathrm{swh}} + M_{\mathrm{wh}}$,
$= -M_{\mathrm{sws}} - M_{\mathrm{ws}}$,
$= M_{sl}$;

M_{sws} = Maximum still-water bending moment in sagging condition;
M_{swh} = Maximum still-water bending moment in hogging condition.

Where detailed calculations are not available the following may apply:

$M_{\mathrm{sws}} = 0$;
$M_{\mathrm{swh}} = 0.375\, f_p C_1 C_2 L^2 B\, (C_b + 0.7)$;

M_{wh} = Maximum wave-induced bending moment in hogging condition;
M_{ws} = Maximum wave-induced bending moment in sagging condition.

Where detailed calculations are not available the following may apply:

$M_{\mathrm{ws}} = -k_1 C_1 L^2 B\, (C_b + 0.7) \times 10^{-3}$;
$M_{\mathrm{wh}} = + k_2 C_1 L^2 B\, C_b \times 10^{-3}$;

Where $k_1 = 110\ (11.22, 1.026)$ and $k_2 = 190\ (19.37, 1.772)$
M_{sl} = Maximum slamming-induced bending moment;
$M_{\mathrm{sl}} = C_3\, \Delta \left(1 + n_{\mathrm{cg}}\right) (L - l_s)$ kN-m (tf-m, Ltf-ft),

where

C_3 = 1.25 (0.125, 0.125);
Δ = Full load displacement, in metric tons (long tons)
l_s = Length of slam load (m) (ft),
$= A_R/B_{\mathrm{WL}}$;

[2]Note: moments are in kN-m (and tf-m, Ltf-ft where applicable).

A_R $= 0.697\Delta/d$ m^2 ($25\Delta/d$ ft^2);
B_{WL} = Waterline breadth at LCG (m) (ft) (sum of demihull breadths for catamarans);
d = Hull depth;
n_{cg} = Maximum vertical acceleration (g), but $(1 + n_{cg})$ is not to be taken to be less than as follows: for vessels Δ 180 te, 3 g, 400 te 2 g, and above 1200 te 1 g. The values should be linearly interpolated for displacements between these values.

Catamaran Shear Strength
The nominal total shear stresses due to still-water and wave-induced loads are to be based on the maximum algebraic sum of the shear force in still water, F_{sw}, the wave-induced shear force, F_w, and the slam-induced shear force, F_{sl}, at the location being considered. The thickness of the side shell is to be such that the nominal total shear stress is not greater than $11.0/Q$ kN/cm^2 ($1.122/Q$ tf/cm^2, $7.122/Q$ Ltf/in.^{2}), where Q is as defined in Section Modulus calculation above. Consideration is also to be given to the shear buckling strength of the side shell plating.

Wave Shear Forces
Wave-induced positive and negative shear force is defined as follows:

$F_{wp} = + k F_1 C_1 L B (C_b + 0.7) \times 10^{-2}$ for positive shear force,
$F_{wn} = -k F_2 C_1 L B (C_b + 0.7) \times 10^{-2}$ for negative shear force,

where

F_{wp}, F_{wn} = Maximum shearing force induced by wave, in kN (tf, Ltf);
k = 30 (3.059, 0.2797);
$F_1 F_2$ = Distribution factor as shown in following figures;
B = Sum of catamaran demihull beams.

Slam-Induced Shear Force
Slam-induced positive and negative shear force is defined as follows:

$F_{sl} = C_4 F_1 \Delta (n_{cg} + 1)$ kN (tf, Ltf) for positive shear force,
$F_{sl} = C_4 F_2 \Delta (n_{cg} + 1)$ kN (tf, Ltf) for negative shear force,

where

C_4 = 4.9 (0.5);
Δ = Full load displacement in metric tons (long tons);
n_{cg} = Maximum vertical acceleration as defined in Section Modulus calculation above.

Shear Strength
Shear stress in the side plating of demihulls can be obtained from the greater of

$$f_s = (F_{sw} + F_w)m/2t_s I \quad \text{or} \quad f_s = F_{sl}\, m/2t_s I,$$

where

f_s = Nominal total shear stress, in kN/cm^2 (tf/cm^2, Ltf/in.^{2});
I = Moment of inertia of hull girder section, in cm^4 (in.^{4}), at the section under consideration;
m = First moment about neutral axis of area of effective longitudinal material between horizontal level at which shear stress is being determined and vertical extremity of effective longitudinal material, taken at section under consideration, in cm^3 (in.^{3});
t_s = Thickness of side shell plating at position under consideration, in cm (in.);
F_{sw} = Hull-girder shearing force in still water, in kN (tf, Ltf);
F_w = F_{wp} or F_{wn} = F_1 or F_2 as specified by figure 12.20, depending on loading;
F_{sl} = Slam-induced shear force, in kN (Ltf), as indicated earlier; the slam-induced shear force is to be applied in both the hogging and sagging conditions.

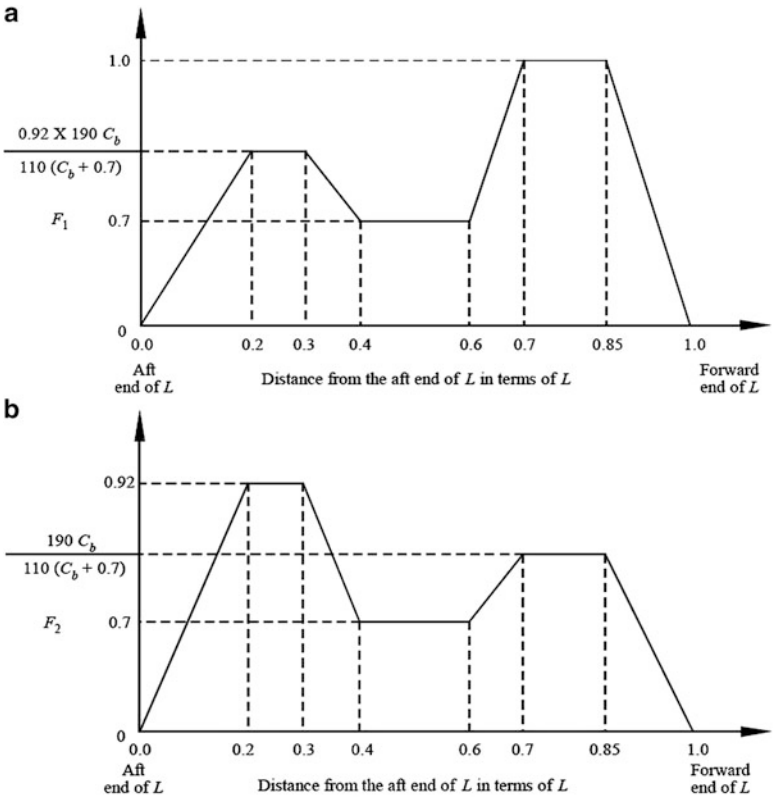

Fig. 12.20 (**a**) Shear force distribution – positive; (**b**) shear force distribution – negative

Catamaran Transverse Loadings

The transverse primary hull loadings in bending torsion and shear are determined by the following equations:

$$M_{\text{tb}} = K_1 \Delta B_{\text{cl}}\left(1 + n_{\text{cg}}\right) \quad \text{kN-m} \quad (\text{kgf-m, ft-lb}),$$
$$M_{\text{tt}} = K_2 \Delta L\left(1 + n_{\text{cg}}\right) \quad \text{N-m} \quad (\text{kgf-m, ft-lb}),$$
$$Q_t = K_1 \Delta \left(1 + n_{\text{cg}}\right) \quad \text{kN} \quad (\text{kgf, lb}),$$

where

M_{tb} = Design transverse bending moment acting upon cross structure connecting hulls;
M_{tt} = Design torsional moment acting upon transverse structure connecting hulls;
Q_t = Design vertical shear force acting upon transverse structure connecting hulls;
K_1 = 2.5 (0.255, 0.255);
K_2 = 1.25 (0.1275, 0.1275);
Δ = Craft displacement (t) (kg, lb);
B_{cl} = Distance between the hull centerlines, in meters (feet);
L = Length of craft, in meters (feet);
n_{cg} = Vertical acceleration at craft's CG, as in earlier definition.

The designer is then expected to show that the structure meeting the SM requirements given earlier will meet the following design stress requirements:

n_{cg} = Vertical acceleration at craft's CG as in previously given definition;
σ_a = Design transverse bending stress, 0.66 σ_y for aluminum and steel craft and 0.33 σ_u for FRP craft, in N/mm^2 (kgf/mm^2, psi);
σ_{ab} = Design torsional or combined stress, 0.75 σ_y for aluminum and steel craft and 0.367 σ_u for FRP craft, in N/mm^2 (kgf/mm^2, psi);
τ_a = Design transverse shear stress, 0.38 σ_y for aluminum and steel craft and 0.40 τ_u for FRP craft, in N/mm^2 (kgf/mm^2, psi).

The transverse bending and shear stress that shall be lower than the preceding values for the cross structure are as follows:

$\sigma_t = 10\ M_{\text{tb}}/\text{SM}_{\text{t}}$ N/mm^2;
$\tau_a = 10\ Q_t/A_t$ N/mm^2, where A_t is the shear area of the cross structure.

The elements to be included in the calculation of the transverse section modulus (SM_{t}) and moment of inertia (I_t) are the main deck and bottom plating, wet deck transverse stiffeners, transverse bulkheads or web frames that traverse the connecting structure and are effectively part of the demihull structure, transverse box beams that continue into the demihulls and continuous transom plating, and horizontal stiffening.

It should be noted that the maximum bending stress should be less than the allowable torsional stress on the structure.

Author's Note The torsional stresses in the cross structure will be determined by applying the torsional moment operating about the torsion centre. Longitudinally this is located on the longitudinal centerline, at the longitudinal neutral point determined by the integration of $\partial(k_i x_i)\ /\partial(k_i)$, where $k_i = EI_e/l_e^3$ is the element stiffness and x_i is the distance of the element from FP. Vertically the neutral point is located at the neutral point of the cross structure in bending.

12.11.4 Lloyd's Register: Initial Structure Dimensioning [12, 13]

Lloyd's Register (LR) publishes two rules documents: Classification of Special Service Craft and Classification of Trimarans. Guidance on hull structural dimensioning is given in separate parts for steel, aluminum, and composite materials.

LR also classifies vessels according to service groups 1 through 6, having similar restrictions to the DNV classifications.

In Chap. 2, Sect. 2.5, on general design, LR specifies the minimum height for the vessel bow form based on height from summer load waterline to the top of the exposed deck on the side at the FP to be at least as follows:

$$H_b = \left(6075\left(\frac{L_L}{100}\right) - 1875\left(\frac{L_L}{100}\right)^2 + 200\left(\frac{L_L}{100}\right)^3\right) x\left(2,08 + 0,609C_b - 1,603C_{wf} - 0,0129\left(\frac{L_L}{d_1}\right)\right),$$

where

H_b = Minimum bow height;
L_L = Load line length (m);
d_1 = Draft at 85% of hull depth D (m);
A_{wf} = Waterplane area forward of $L_L/2$ at draft d_1 (m);
B = Molded breadth (m);
C_b = Block coefficient as defined in load lines convention
C_{wf} = waterplane area coefficient forward of $L_L/2$, where
$C_{wf} = A_{wf}/((L_L/2).\ B)$.

LR specifies a minimum significant wave height for determining load and design criteria as follows:

Service group	Description	Distance to refuge	Min. sea state Hsig
G1	Sheltered	5 nautical miles	0.6
G2	Coastal	20	1.0
G2a	Coastal	60	1.5
G3	Specified operation area	150	2.0
G4	Specified operation area	250	4.0
G5	Specified operation area	350	4.0
G6	Yachts and patrol craft	Unrestricted	4.0

LR provides formulas for rule calculation of acceleration, pressure and pressure combination, impact loads from slamming on hull bottom, foils and forebody structures, and cross-deck structures.

For many of the calculations LR specifies a service area restriction factor, G_f, which varies from 0.6 for G1 to 1.25 for G6, as well as a service factor, S_f, for different missions: more exposed missions like patrol craft, pilot boats, and workboats are subject to S_f of 1.2, 1.25, and 1.25, respectively. A similar approach is adopted for adjusting wave bending moments and shear forces for hull girder strength determination. Local design criteria are then covered in Chap. 4, which is dedicated to multihull craft covering catamaran, multihull, and SWATH forms.

Detailed scantling determination is covered in Part 7, Chap. 4, for multihull vessels in aluminum, and this specifies minimum thickness requirements for plating and stiffeners and provides detailing guidance.

The LR rules for trimarans [13] follow a similar coverage for environmental loads and scantling determination (Parts 5 and 6). Rule formulas are provided for sea pressure, motion and acceleration, longitudinal bending moment, and shear force calculation, as well as horizontal bending moment, torsional moment, cross-deck splitting moment, and shear force.

The global strength requirements for trimarans follow the same approach as for special service craft, including guidance on cross-deck strength.

Impact pressures by rule calculation are covered for bottom impact that follows the approach of Ochi [31] and for impact to bow and cross-deck structures above the waterline. The slamming pressures are all based on relative velocity, with a starting estimate if the extreme estimate of relative velocity is not available to the designer. For information, in what follows we summarize this calculation for bow flare and wet deck slamming.

Trimaran slamming from LR rules for trimarans V1 Part 5, Chap. 5, pp. 41 and 42.

Bottom impact pressure due to slamming, IP_{bi}, is to be derived using the method given in what follows. This method will produce impact pressures over the whole of the underwater plating region:

$$IP_{bi} = f_{bi}\left(19 - 2720\,(T_x/L_{WL})^2\right)\sqrt{(L_{wl}V_{sp})}\ \ \mathrm{kN/m^2},$$

where

f_{bi} = 0.09 at forward end of L_R, and 0.18 from 0.9 to 0.8 of L_R;
L_R = Lloyd's rule length of main hull, 97% of L_{WL} at design draft starting at stem;
T_x = Local draft from keel to design waterline at longitudinal position under consideration;
V_{sp} = The greater of the cruising speed or two-thirds the sprint speed, in knots. For ships where it is not required to maintain high speeds in severe weather, the value of V_{sp} may be specially considered.

Bow flare slamming, at waterline, declining to 40% at weather deck level:

$$IP_{\mathrm{bi}} = 0.18\left(19 - 2720\,(T_{\mathrm{x}}/L_{\mathrm{WL}})^2\right)\sqrt{(\,L_{\mathrm{WL}}V_{\mathrm{sp}})}\ \ \mathrm{kN/m^2}\ \ \text{at } 0.9\,L_{\mathrm{R}}.$$

Wet deck slamming

$$IP_{\mathrm{bi}} = f_{\mathrm{imp}}k_{\mathrm{f}}V_{\mathrm{R}}V_{\mathrm{sp}}(1 - (\,G_{\mathrm{A}}/1.29\,H)),$$

where

f_{imp} = One-third for leading edge of wet deck, one-sixth for underside of wet deck;
k_{f} = Longitudinal distribution factor 2.0 for forward one-quarter and 1.0 elsewhere;
V_{R} = Relative vertical speed in knots = $(8H/\sqrt{\mathrm{L}_{\mathrm{WL}}})$ + 2 knots;
G_{A} = Air gap from wet deck underside to design waterline;
H = Minimum significant wave height (m)

where H = 0.6 (G1 service), 1.0 (G2), 2.0 (G3), and 4.0 for G 4,5 and 6;

V = Maximum service speed in knots;
P_{des} = Combined pressure Vol. 1, Part 5, Chap. 5-3-2.

Minimum Weather Deck Pressure

$$P_{\mathrm{D}} = 6 + 6\,f_{\mathrm{L}}f_{\mathrm{WV}}\ \ \mathrm{kN/m^2},$$

where

f_{L} = Location factor = 1+ 4 $(x_{\mathrm{WL}}/L_{\mathrm{WL}})$ – 0.75) but not less than 1.0;
f_{wv} = Wave height factor for service area or group;
x_{wl} = Longitudinal distance (m), measured forward from aft end of $\mathrm{L_{WL}}$ to position of CG of item being considered.

The restriction with using the LR trimaran guideline at time of publication (2018) is that it is written for steel vessels, so interpretation regarding the allowable stresses would be required for aluminum or FRP. This might be achieved by cross reference to the sections on special service craft rules for multihull craft and comparison with the guidance from DNV GL and ABS.

12.11.5 Turk Loydu (TL) [33]

This Turkish classification society provides guidelines for high-speed craft in Chap. 7 of its rules. The guidance covers high-speed craft as defined in the IMO HSC Code. They spend some time discussing physical damage in Sect. 7.2 on buoyancy, stability, and subdivision, which is useful to consider compared with the basic grounding case considered in the IMO as this discussion is more extensive.

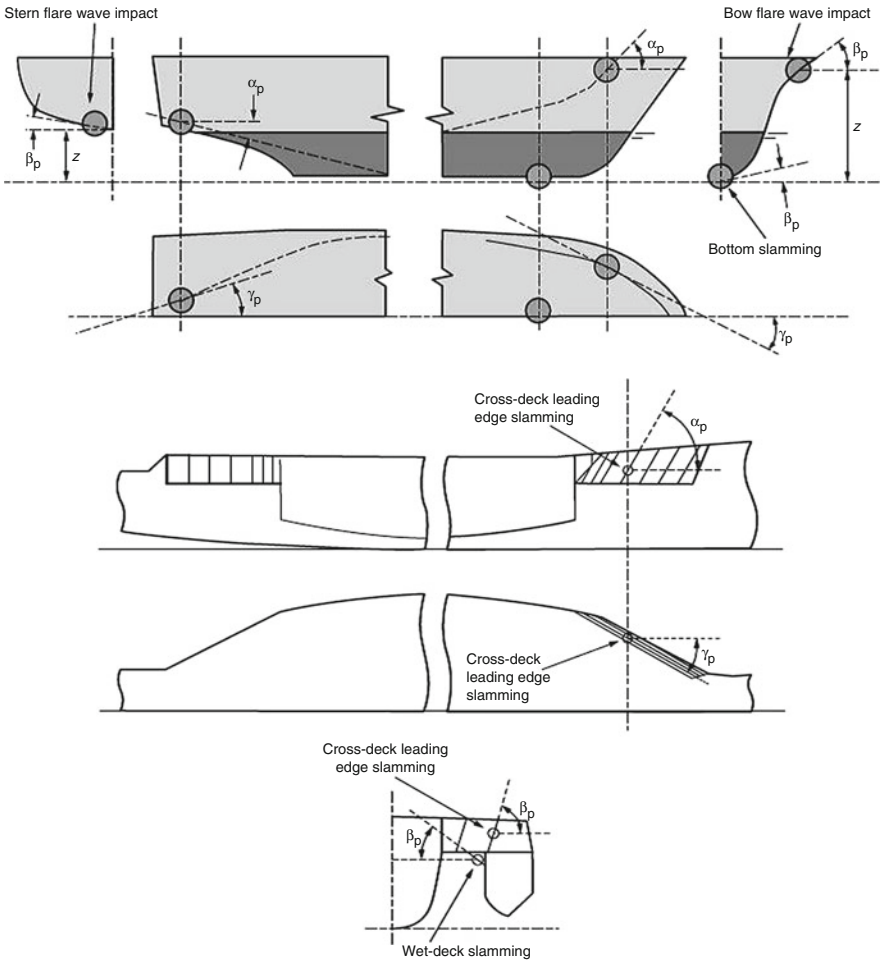

Fig. 12.21 Lloyds Register definition diagram for wave slam locations

Guidelines for the assessment of design vertical and horizontal accelerations are given, simply related to the vessel service, L_{WL}, and service speed. Having determined this, which is assumed to equate to the highest 1% acceleration in the most severe sea state expected, TL gives formulas using the CG acceleration to specify the limiting Hs imposed by the acceleration value. This same acceleration value is used to determine bending moment and shear force on hulls from accelerations. These are then added to the still-water moment and moments applied by static masses that make up the vessel structure and equipment.

Impact loading from slamming is treated as local loading, that is, separately from the global loading above. This is similar to the approach of LR, ABS, and DNV for determining loading. Guidance is provided for bottom slamming and wet deck slamming for catamarans.

The structural response to slamming is a matter of whether the loading can be added to the FE model quasi-statically (most likely for small vessels) or whether a whipping response is excited so that vibration analysis is required to determine extreme structural response (most likely for large vessels).

Further guidance is also given on the design of structural details, welds and joints for FRP structure, and the dimensioning of plating, girders, stiffeners, bulkheads, decks, and deck supporting members.

12.11.6 Other Reference Materials

Documentation that may be useful for design, including structural design of smaller craft, is available from the Korean Register (Guidance for Recreational Crafts) [34] and guidelines from the UK Marine and Coast Guard Agency [35]. The Korean Register document covers craft with lengths of 2.5 to 24 m in steel, aluminum, wood, and FRP. Similar rules are available for vessels in this size range also from ABS, LR, and DNV.

12.12 Concluding Thoughts on Primary Structure

The USCG commissioned a comparative study [36] of the rules for high-speed craft by American Bureau of Shipping, Det Norsk Veritas, Germanischer Lloyd, Nippon Kokkan kk, RINA Spa, and Lloyds Register that was reported in 2005. A detailed review was carried out using an example monohull for ferry or patrol missions, and the scantlings determined by the rule set were compared. The SNAME paper summarizing the results concluded that the rules were generally aligned, while for commercial vessels designed according to DNV the vertical accelerations were lower, leading to global girder strength rather than local scantlings being the controlling factor. For patrol craft, accelerations were comparable, while the DNV longitudinal bending moment was the highest. Bottom dead rise affected the design more for DNV than ABS. ABS required heavier scantlings forward of amidships.

The comparison was for one design, and in both cases, since it is the initial rule-based calculations that were used, it illustrates that detailed FE analysis and a challenge to both the input data and the structural modeling are necessary to produce a robust and at the same time optimized design for a large high-speed multihull.

From the authors' review of the material, it appears that there are useful elements that can be taken from the different rules for the initial structural design. A spreadsheet format, together with drawings, will be useful to work around adjusting the initial concept toward a design that can be incorporated into FE analysis. It is best that individual designers build the calculation sheet to suit their needs as many possible choices exist for the different design elements. LR has a software tool that can be downloaded and performs this work directly based on its approach.

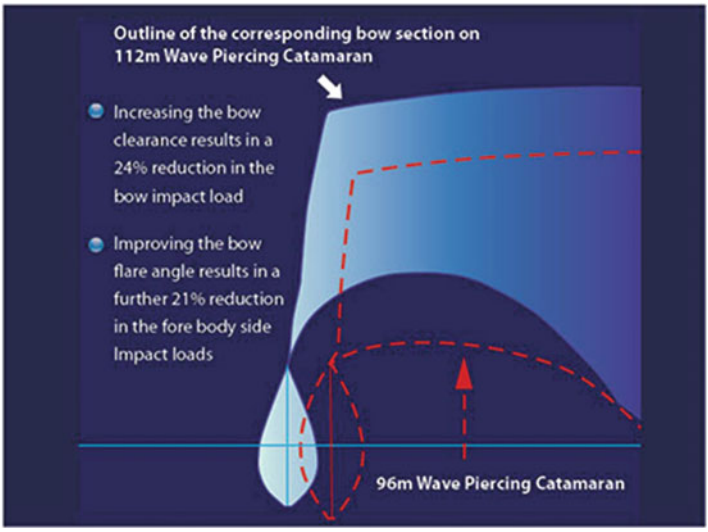

Fig. 12.22 Incat super bow

Once the structure has been outlined, in parallel with the FE work, which is by its nature painstaking and time consuming, the internal outfitting may be considered, as we discuss in the next chapter.

Returning to hydrodynamic forces and wave-piercing vessels, following the extensive research discussed earlier, Incat has taken this work and incorporated a revised bow geometry in its 112-m vessels, as shown in Fig. 12.22. By making the bow arch higher and the bow flare sharper, the company has been able to reduce impact loads by a significant amount, which can feed back into the structural design as well as bring greater comfort to passengers.

References

1. ABS Guidance Notes – Direct Structural analysis for High Speed Craft, download from ABS internet site (Eagle.org), see resources
2. Cook SM, Crauser P, Klaka K (1999) Investigation into wave loads and catamarans, Curtin University, Australia, Hydrodynamics of High Speed Craft Conference, RINA 24-25 Nov 1999, London UK
3. DNV Rules for Classification of High Speed, Light Craft and Naval Service Craft, Part 3, Chapter 1, Jan 2011
4. Armstrong NA, Catamarans, Chapter 46 of US Society of Naval Architects and Marine Engineers (SNAME) Ship Design and Construction, edited by Thomas Lamb (2003) ISBN 0-939773-40-6 (Vol I), ISBN 0-939773-41-4 (Vol II)
5. Mackay Rubber Mountings at www.mackayrubber.com.au
6. Newman JN (1977., ISBN 0-262-14026-8) Marine Hydrodynamics. MIT Press, pp 311–325

7. Jenkins GM, Watts DG (1968) Spectral analysis and its applications. Holden Day Inc,, Library of Congress No 67.13840
8. Hydrodynamics of High-Speed Marine Vehicles, by Odd M Faltinsen, Cambridge University Press 2005, ISBN 978-0-521-84568-7, 451 pages
9. Shin YS, Belenky VL, Lin WM, Weems KM, Engle AH, Non-linear Time Domain Simulation Technology for Seakeeping and Wave-load Analysis for Modern Ship Design, ABS Technical Papers 2003, available by download from ABS internet site Eagle.org
10. DnV GL Wasim and Hydrod, refer to link under DnVGL in resources
11. AQWA refer to internet link for ANSYS AQWA in resources. As at link www.ansys.com/Products/Structures/ANSYS-Aqwa
12. Lloyds Register Rules for Special Service Craft (download from Lloyds Register internet site)
13. Lloyds Register Rules for Trimarans (download from Lloyds Register internet site)
14. DnV Rules for High Speed Light Craft and Naval Surface Craft (download from DnVGL internet site)
15. ABS Rules for Classification of High Speed Craft (download from Eagle (ABS publications) internet site)
16. Tymofienko K, Fatigue tool sensitivity analysis and design curves, IP501909 Master's Thesis NTNU, Aalesund 02.06.2016 (Spectral fatigue analysis following DnV requirements on Damen catamaran ferry)
17. Capt. H E Saunders, Hydrodynamics in ship design, Vol III, SNAME, 1965/1982, Chapter 16 Impact and other reactions between waves and a ship
18. Capt. H E Saunders, Hydrodynamics in ship design, Vol I, SNAME, 1965/1982, Chapter 30 The behavior of planing craft
19. Capt. H E Saunders, Hydrodynamics in ship design, Vol II, SNAME, 1965/1982, Chapter 53 Quantitative data on dynamic lift and planing
20. Mandel P, Seaway Performance Assessment for Marine Vehicles, DTNSRDC, Bethesda, MD, AIAA 6th Marine Systems Conference September 14-16 1981, Seattle, pp 11.
21. Purcell ES, Allen SJ, Walker RT, Structural Analysis of the U.S. Coastguard Island Class Patrol Boat, SNAME Annual Meeting November 9-12 1988 Paper No 7, pp 23
22. Heller SR, Jasper NH, On the structural Design of Planing Craft, Transactions RINA, July 1960
23. Whelan JR, Wet deck slamming of high speed catamarans with a centre bow, Doctoral Thesis at University of Tasmania, July 2004 – Thesis backing up ref 12-15 done under Prof Davis and Dr Holloway, supported by Incat and Australian Research Council.
24. Davis MR, Whelan JR (2006) Modelling wet deck slamming of wave piercing catamarans. Transactions RINA:119–140 ISSN 0035-8967
25. Thomas G, Davis M, Holloway D, Roberts T (2003) The whipping vibration of large high speed catamarans. Transactions RINA:289–304 ISSN 0035-8967
26. Lavroff J, Davis MR, Holloway DS, Thomas G (2009) The vibratory response of high speed catamarans to slamming investigated by hydro-elastic segmented model experiments, Report DOI 10.3940, Transactions RINA. pp 183–193, ISSN 0035-8967
27. Lavroff J, Davis MR, Holloway DS, Thomas G (2011) Determination of wave slamming loads on high speed catamarans by hydro-elastic segmented model experiments, (DOI No 10.3940) Transactions RINA, vol 153. pp A185–197, ISSN 0035-8967
28. Shin YS, Belenky VL, Lin WM, Weems KM, Engle AH (2003) Non Linear Time Domain Simulation Technology for Seakeeping and wave load analysis for modern ship design. ABS Technical Papers, pp 257–281
29. Sungeun PK (2011) CFD as a seakeeping tool for ship design. ABS, International JNAOE 3:65–71
30. Onas AS, J Falls I Stojanovic, Seakeeping analysis of a SWATH type trimaran using potential flow, (DNV WASIM from SESAM) US Naval Research N00014-10-1-0652
31. Ochi MK Prediction of occurrence and severity of ship slamming at sea, Fifth Symposium of Naval Hydrodynamics, Bergen, Norway, pp 549–559

32. International Code of Safety for High Speed Craft, IMO, publication IA-185E, ISBN 92789 28014 2402, 2000. Amendments and resolutions after 2000 are available on IMO web site IMO. org.
33. Turk Loydu – Rules for High Speed Craft, Chapter 7, (download from Turk Loydu internet site)
34. Korea Register of Shipping Rules for High Speed and Light Crafts and also Rules for Recreational Craft at www.krsusa.cloudapp.net/Files/KRRules/KRRules2016/KRRulesE.html
35. The Merchant Shipping (High Speed Craft) Regulations 2004, UK Statutory Instruments 2004 No 302, ISBN 0-11-048699-4. (Application of IMO HSC Code in UK)
36. Stone KF, Novak DS, Comparative structural requirements for High Speed craft, USCG Ship Structure Committee Report SSC-439, 2005, and SNAME Transactions 2006 pp 310 – 326.

Chapter 13
Systems, Safety, and Layout

13.1 Introduction

In this chapter we will focus on the outfitting required for the safety and comfort of passengers, crew, and cargo payload and safe operation of the vessel itself. This design input shapes the superstructure internally from the payload and externally from functional aspects. This is then further influenced by aerodynamic forces for external shape, and for ferries and superyachts also by "style." The starting point are the IMO requirements, followed by the rules applied by classification societies, see references [1–10].

We will discuss the systems that need to be supported, for example, the environment in the passenger cabins, and present a brief discussion on internal architectural design. This last item will link closely with the requirements of the operator, so it will be necessary to consult with them before going too far in designing the interior. If the vessel is for an individual client, for example if it is to be operated as a superyacht, then an approach to the internal outfitting that is different from the approach to outfitting a ferry will be necessary. Some of the layout considerations are affected by design in terms of collision, and this relates back to structural design and Chap. 12.

Our aim is to illustrate the key guidelines that form the design framework, with some illustrations from existing vessels. Within the overall framework, a designer often has a range of options. One example is the choice of how vehicles enter and leave a vessel or how passengers enter and leave. This will be influenced by the route and port facilities.

Our approach in this chapter is that of project leader rather than specialist, so suffice it to identify requirements and guidance to allow specialist engineers to integrate with the vessel overall design. In addition to the references, you will find key resources and links listed with the reference details at the end of this book.

L. Yun et al., *High Speed Catamarans and Multihulls*,
https://doi.org/10.1007/978-1-4939-7891-5_13

13.2 Layout, Safety, and Emergency Systems

13.2.1 Layout and Seating

The vessel configuration and deck layout are primarily set by the mission. For example, larger craft have the following basic missions:

Ferry	Passenger or passenger and vehicle
Utility vessel	Wind farm maintenance, offshore crew or supply, or offshore patrol/interdiction
Superyacht	Leased out or individual owner
Naval	Patrol military outfit, fast strike military outfit, or power projection

Internally the starting point is the payload, that is, vehicles, freight, and function modules generally at the main deck level, and on the next level(s) the passenger and crew spaces. During our initial selection phase we will have defined this requirement and summarized it in a data sheet (Chaps. 2 and 7 and Appendix 4). The global assessment of the deck space will have been made by reference to existing vessels. An example for a passenger ferry is given in Fig. 13.1, a large passenger and car ferry (Fig. 13.2), and a wind farm service vessel (Fig. 13.3).

Part of the layout and associated outfit will be influenced by the mission duration as well as the function listed earlier. Thus, a larger ferry may need to make longer voyages and not just serve as a kiosk for food and drinks with the associated pantry or stock room; it may be necessary to have fast food locations and sitting areas or even a full restaurant, areas for games and amusement, kids' play areas, a move theater, or video game rooms. The crew may stay on board for multiple voyages or,

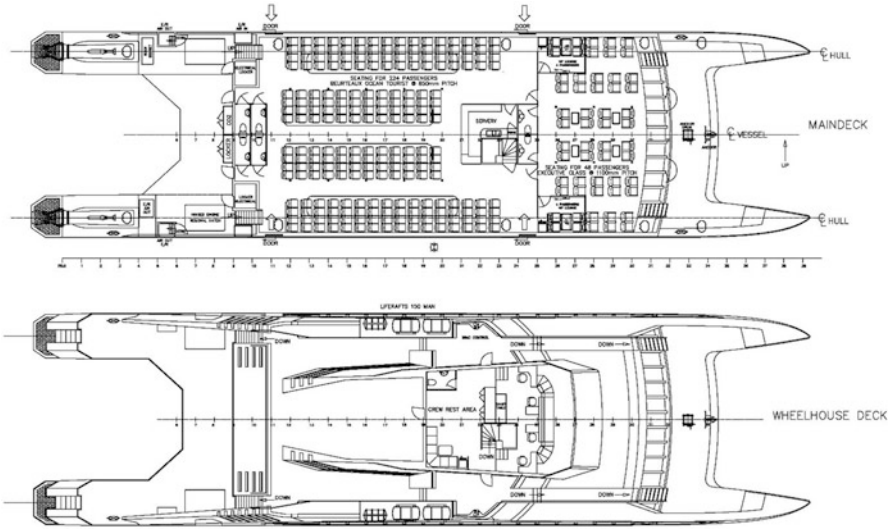

Fig. 13.1 Passenger ferry layout AdHoc designs 47-m super slim

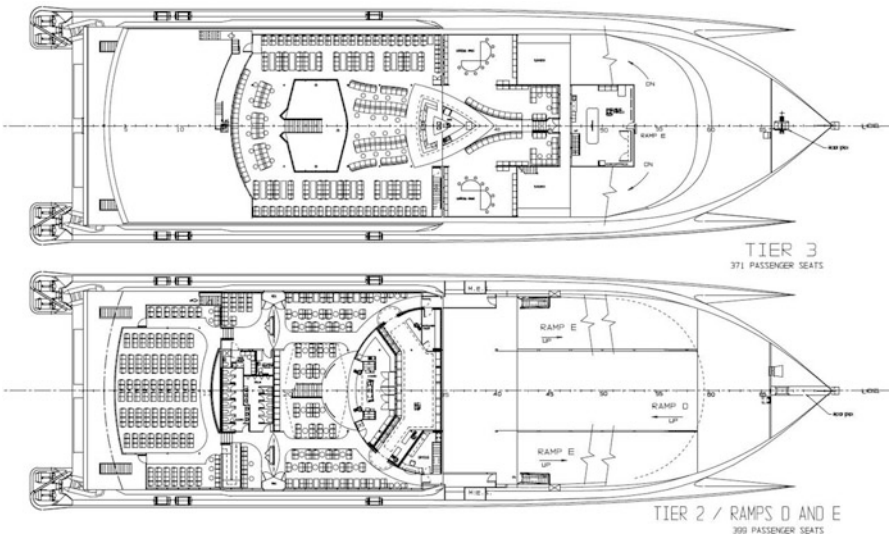

Fig. 13.2 RoPax ferry layout passenger decks Incat 046 91 m

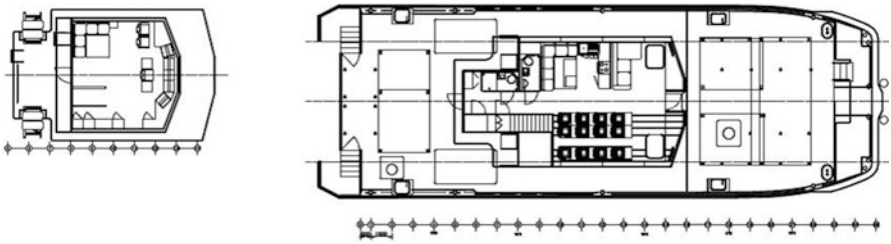

Fig. 13.3 South Boats 26-m wind farm support catamaran deck layouts

in the case of utility, naval, or superyacht missions, for periods of duty, necessitating crew living accommodations and the installation of a navigation bridge.

It should be noted that the passenger deck layouts above are extracts. Full data sheets for these vessels can be found on the websites for Incat, Adhoc Designs, and South Boats.

For passenger vessels the IMO requires that for vessels above 450 passengers there must be at least two separate zones, with each zone being no longer than 40 m and with separate safe areas in case of fire. The separate safe zone can be the alternate passenger area providing the space can accommodate the total number of passengers for emergency purposes. Escape facilities from each zone should then be capable to service the full requirements of the passenger capacity.

Ideally, before finalizing the overall configuration and structure design, we need to review the space requirements in detail. First, a few thoughts are in order

Fig. 13.4 Passenger ferry internal views **a**, **b**, and **c**

regarding passenger spaces. For short voyages the typical seating plan will be three or four abreast in line sitting next to windows, a corridor inside, and then an internal block of seats. Depending on the size of vessel, there may be another access corridor centrally.

Figure 13.4a shows a shot from a catamaran operating out of Stavanger as a bus traveling up to Bergen (Flaggruten). You can see that the seat pitch is quite close, not down to aircraft levels, but close nevertheless. On the smaller vessels such as this the baggage is stored in a space close to the exits on either side toward the stern. Figure 13.4b, shows a view of another catamaran serving the Kristiansund–Trondheim route, and Fig. 13.4c shows a view from inside a sightseeing catamaran in the Stavanger area on the way to Lysefjord (looking toward the stern).

On the larger RoPax vessels most people's baggage will stay in their vehicles. It is important, though, for a designer to consider a passenger's needs while on the trip. You can see in Fig. 13.4 that there are plenty of power sockets for laptop or phone charging (the trip to Bergen is over 4 h). Many of the groups of six face each other with a table between them. On other vessels aircraft-style seatback tables are installed. It is also now normal to have screens located so that all passengers can see them to play the safety video, provide trip information, and show advertising and news on board. We will touch on this topic later in the section on electronics.

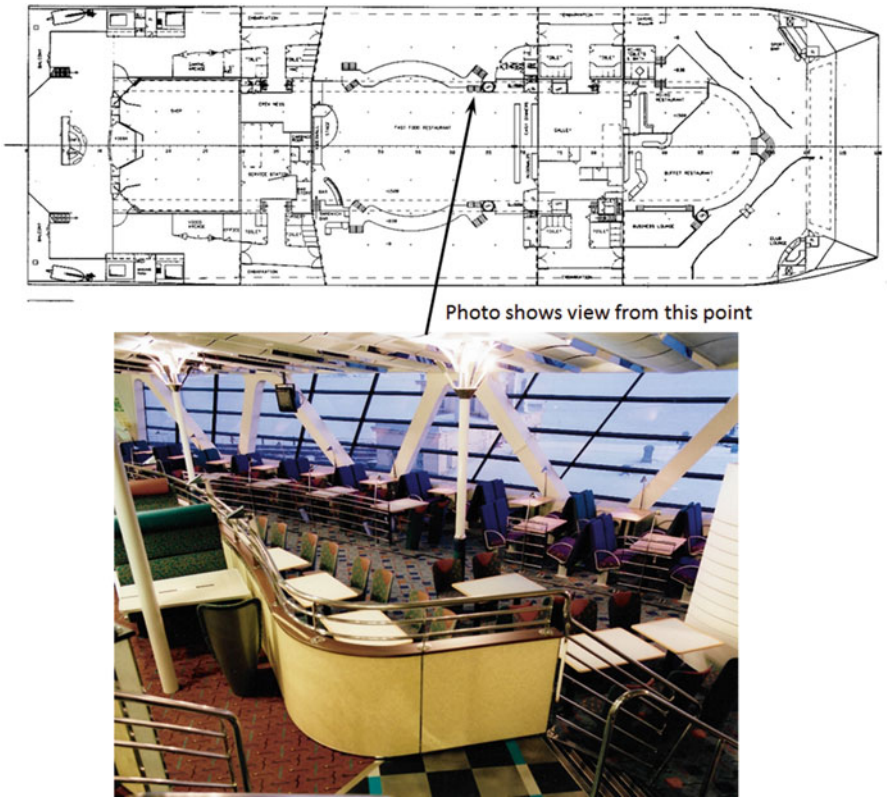

Fig. 13.5 Stena Craft HSS 1500: (**a**) internal view (**b**) deck layouts

At many locations now it is also expected to have Wi-Fi available for those on board, as well as a locked system for vessel operations. Depending on the operator, lifejackets may be of the foam type stored close to exits or the self-inflating kind stored under seats. Seat manufacturers supply both options. A short list of seat manufacturers and their links appears in the resource section.

In larger vessels, depending on the voyage length, the passenger seating may have wider spacing and be laid out more informally (Fig. 13.2). In the HSS semi-SWATH vessels that used to connect Ireland to Scotland and Wales, the craft have sufficient space above the vehicle deck to accommodate a full suite of entertainment spaces, including movies, duty-free shops, fast food snack bars, and video games, as well as a bar and casino (see Fig. 13.5 below for the layout).

The IMO HSC [10, Chap. 4] specifies limitations on the location of passenger spaces and crew accommodations. The passenger spaces must be behind the area of the hull that may be damaged by collision, as discussed in Sect. 12.11.1 in Chap. 12. Thus the main cabin must be behind the main watertight bulkheads at bow and stern

Table 13.1 Guidelines for passenger areas

Description	$G_{col} < 3$	G_{col} 3 to 12	$G_{col} > 12$
Seat back Forward or Back facing allowed in all cases	Low or high	High + Protective padding and deformation	High + Protective padding and deformation
Seat Belts	None required	Lap Belts for forward facing seats where no protective structure forward	3 point belt or shoulder harness belts for forward facing seats. No belts in backward facing seats
Sofas	allowed	Not allowed	Not allowed
Tables	Allowed	Tables with protective features, dynamic tested	Not allowed
Projecting Objects	Padding required	Padding required	Padding required -Specially approved
Kiosks, Bars etc requirements	No special requirements	On aft side of bulkheads or specially approved arrangements	To be specially approved arrangements
Baggage	No special requirements	To be placed with protection forward	To be placed with specially approved protection forward
Large masses	Restraint and positioning to be considered for collision case	Restrainment and positioning to be considered for collision case	Restrainment and positioning to be specially approved

to allow for potential structural damage from a collision at speed. The main issue is the effect of deceleration forces on passengers or cargo.

This is also a key consideration for furniture installations in accommodations. The IMO provides constraints as in Table 13.1 below.

Seating and seating design

Fast ferries need to have a seat available for each passenger and crew member for which it is certified. If the vessel is to operate in heavy weather with a reduced number of passengers or cargo, then this can be taken into account, for example, in terms of the necessity for seat belts. The layout around seats shall not obstruct access in any situation, so designers need to take account of emergency evacuations and facilities allowing access to disabled people such as ramps into saloons and lifts from the vehicle deck to passenger saloons for larger vessels.

It is stressed that seats, and furniture in general for that matter, are designed to minimize the possibility of injury to people, including trapping. The design of upholstery can help this, as can curved corners. With the exception of handrails in gangways, protruding handles and ledges should be avoided as much as possible.

In general it may be expected that passenger vessels for estuary or river use will have a simple seating layout and for larger such craft a little more space centrally and aft for a kiosk and utilities. Gangways will need to be wide enough for people to pass each other as well as allowing wheelchair navigation to parking places. Short-trip vessels in Norway tend to have an open deck toward the stern, allowing passengers to get some fresh air, while short-trip and excursion vessels in Australia also often have an upper open deck that passengers can visit. Many vessels also have a smaller

Table 13.2 Static forces for seat design

Force direction	Force kN	Height above seat	Notes
Forward	2.25	350 mm	Horizontal to seat back
Aft	1.5	350 mm	
Transverse	1.5	At level of seat	Horizontal to seat bottom
Down	2.25	350 mm	Uniform over seat bottom
Up	1.5	350 mm	Uniform over seat frame

Note 1: If there is more than one seat to a frame, forces are to be aggregated
Note 2: Forces to be applied by round cylinder diameter of 164 mm and length equal to seat width with transducer to monitor force

"upper class" lounge for those wanting extra comfort. It may be noted that the seat suppliers in our resource list offer seats with differing levels of comfort to meet this demand.

When designing a vessel, the designer will need to look at the local loading imposed by seating and other factors to the passenger cabin deck to check panel loadings and aggregate the loads to feed in to the global and local Finite Element (FE) structural models.

All seats must be able to withstand static forces, as in Table 13.2, for craft with a design collision load of less than 3 g. The seating must be tested by the manufacturer to receive certification.

A seat will be acceptable if results from the tests show:

1. Permanent displacement is <400 mm.
2. No part of the seat or frame becomes detached.
3. Seat and frame remain firmly retained and locking systems remain locked.
4. Rigid parts of the seat that an occupant may contact should have as a minimum a curved surface with a radius of at least 5 mm.

Where the vessel has a design collision load of 3 g or greater, seats shall conform to the following:

- The seat-supporting structure and attachment, seat belts, or harness shall be designed for the maximum g force in the appropriate direction, bearing in mind whether the seats are forward, aft, or transverse facing.
- Acceleration pulse for design should be representative of collision history (i.e., should mirror the time domain history from analysis as in Chap. 12). If this is not known a time history as shown below can be used (Fig. 13.6).
- Tests should be carried out with seating attached to a base frame simulating the vessel deck structure strength and stiffness as mcuh as possible.
- Tests should be conducted with instrumented test dummies (type 'II', type 'Hybrid II' or better), and all seats in group seating shall be filled. If they are in a group, the dummy with the highest injury potential is to be instrumented. Tests are to be in accordance with national standards appropriate to the vessel's operation.

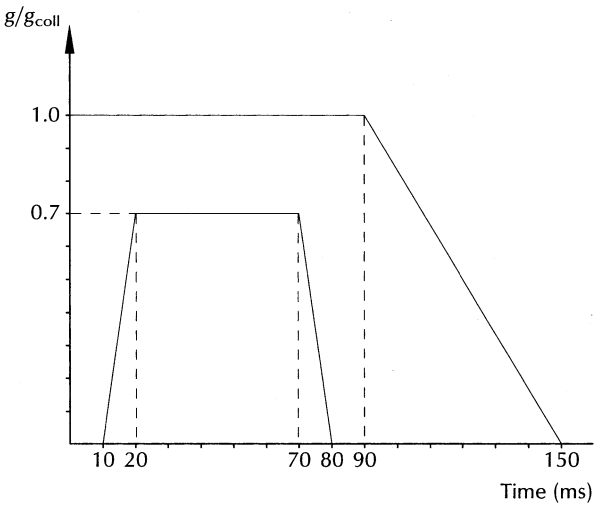

Fig. 13.6 Time history for seat deceleration in collision

The IMO provides detailed injury criteria for accelerations and forces applied to a passenger that should not be exceeded in a collision event. This includes criteria for accelerations and loads to the head, neck, pelvis, femur, and thorax. To determine the forces, it is necessary to determine decelerations that would be applied to the seating and apply these data to a physical test dummy and the seating as noted earlier. Such tests are controlled by national and international standards such as ECE 80, ADR 66/00 in Australia, and NCHRP Report 350 in the USA. Both the guidance and the test procedures are specialized, and so readers are referred to Annex 9 of the HSC code in the first instance. Seat manufacturers will be familiar with the procedures and will be able to give guidance and provide or arrange for suitable test facilities and data recording. Key issues for the designer to ensure the seating will be acceptable are as follows:

1. Seat unit, tables, and so forth must stay intact and attached to mountings without deformation that causes the occupant to be injured or trapped.
2. Lap belt must stay reliably on pelvis, harness must stay reliably on shoulder area restraining the occupant, and release mechanisms must be operative after test.
3. Criteria defined in HSC Code Annex 9 are fulfilled through full-scale testing with instrumented dummies.

Equipment and Baggage

Equipment and baggage in public and operational spaces where personnel are present should be positioned and secured so as to safely remain in position during design collision event (Chap. 12). It is important to note that if a baggage space is used to stack bags and suitcases, the unit load could be significant, so it is best to check the local framing around the storage space for the anticipated loading.

Safety equipment should be stored and restrained such that following design collision it is accessible and useable for rapid evacuation of passengers and crew as

appropriate. Attachments and restraints including wall structures need to safely withstand the forces from equipment weight and the collision deceleration for the given craft.

13.2.2 Exit and Evacuation

It is normal to arrange crew accommodations and facilities centrally under the wheelhouse or directly behind it and centrally toward the stern on the main passenger deck level. This allows crew quick access to the muster points adjacent to the vessel main exits, which will also be used for evacuation. The life rafts and access chutes will be launched automatically by crew from inside these positions. Very large multihull vessels may need more than one emergency exit on each side of the vessel if passengers are to be evacuated safely within a reasonable time frame.

The IMO requests ("should have") at least two exits at each end of the public space. Taking account of the typical vessel layout, this may lead to an exit for emergencies at amidships as well as one toward the stern as used for day-to-day entry and departure on each side of the vessel, though this is not a normal arrangement, as reflected in vessel data sheets in Appendix 3. There shall be handholds along both sides of passageways so that passengers can steady themselves while moving.

Door/hatch/hydraulic ramp latching arrangements at exits need to be clearly labelled so as to avoid confusion in an emergency regarding how to release and activate. Facilities should be available for release, opening, and activation from both inside and outside.

Space should be available by the exit for crew to operate the emergency system for evacuation chutes or slides and life rafts and provide passenger assistance to evacuate wearing life vests. Handholds, antiskid floor coverings, seamless chute/slide connections, and appropriate steps should be in place or be deployed with evacuation slides or chutes so that passengers can safely disembark without catching clothing. Signage and lighting for evacuation should be clear and visible during the day and at night and linked to emergency power systems in case of a main power failure. Figure 13.7 shows examples from a 33-m passenger river ferry, a 74-m Incat waver piercer RoPax ferry, and the 99-m Francisco.

Evacuation timing The IMO devotes some effort on this in the HSC code, focused around time to evacuate in case of a fire on board. The intent is to allow passengers to evacuate in one-third of the time that the structural fire protection is rated for minus 7 min, that is,

$$\text{Evacuation time} = (\text{SPF-7})/3 \text{ min, where SPF is structural protection time}$$

If we assume that the fire protection is from the machinery spaces and is designed for 37 min, our evacuation time will be 10 min. If we have 100 people on board, this

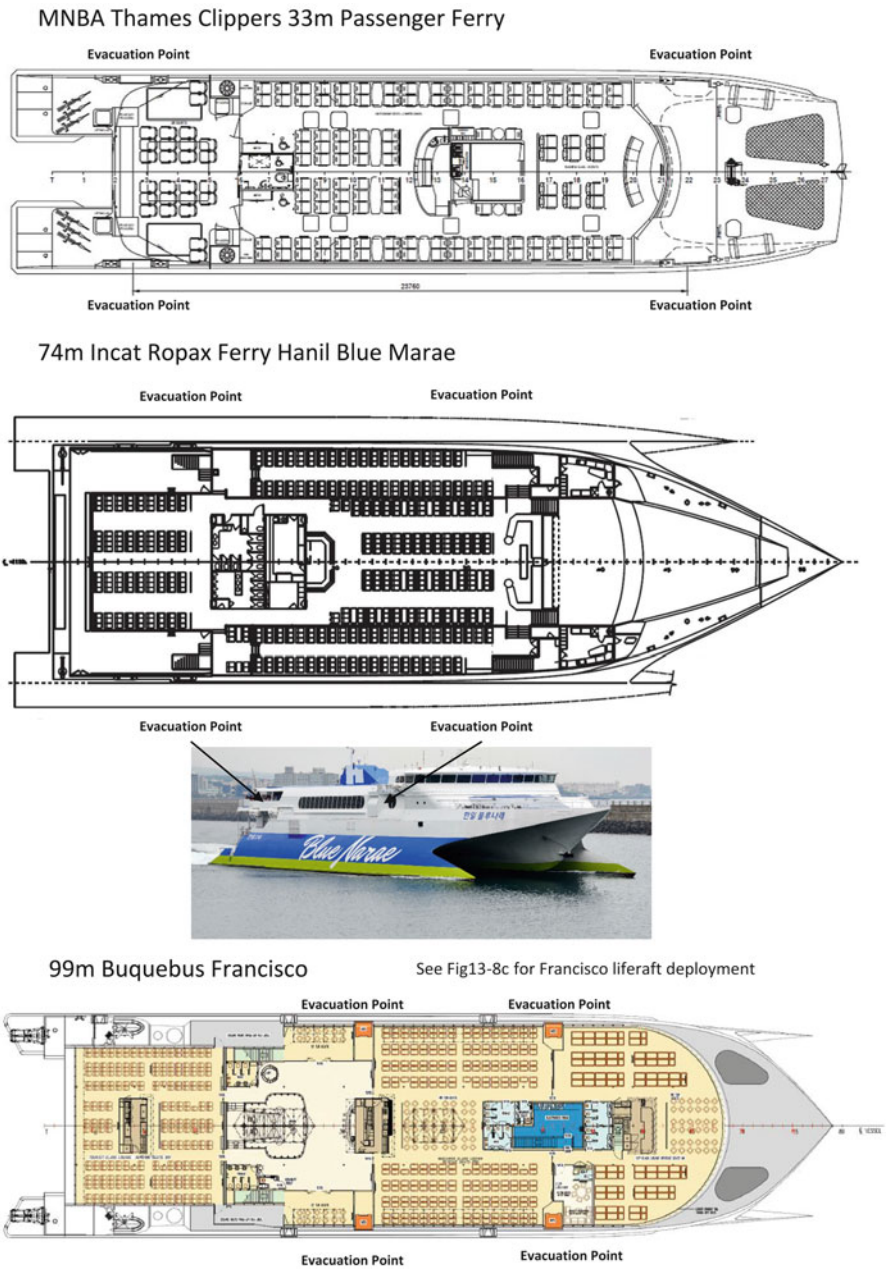

Fig. 13.7 Example escape routing diagrams: (**a**) Thames Clippers 33-m ferry; (**b**) Incat 74-m RoPax wave-piercer Hanil Blue Marae, S Korea, deck layout and photo; (**c**) Incat 99-m RoPax ferry Francisco passenger main deck layout and exits

means the arrangements need to allow the evacuation system deployment, perhaps in 2–3 min to be inflated and ready, and then send 15 people down the chutes or slides each minute.

DNV GL has a CAD-based system, called AENEAS, for analyzing passenger evacuation based on the vessel cabin layout [11].

It should be noted that escape from a river passenger ferry, where the freeboard may be 1 or 2 m and so transfer to a life raft may be almost direct, will be a very different challenge from the evacuation of a large passenger and vehicle ferry. In the latter case the whole escape system needs to be integrated, with inflatable chutes allowing passengers access down to the life raft, which itself will hold a large number of people. The designer therefore needs to take care to design internal access corridors, areas around the emergency exit, and the escape system itself.

Controlling the passenger flows and operation of the equipment at emergency evacuation points also needs care, with design for allocation of responsibilities to crew members that can be logical and therefore clear to passengers without special instruction, so as to avoid confusion and consequent delays in evacuation. While evacuation trials may indicate a safe process, in a real-life situation there will always be some confusion, personal fears, and errors of movement made by passengers. Some passengers may also receive injuries in case of a collision or sudden stop of the vessel. Some consideration of extraction of injured persons may therefore also be useful. Usually the result of working through such an exercise is that the vessel layout will appear comfortable to passengers in terms of access to seating and the cabin layout as such.

13.2.3 Accommodation Noise Levels

Noise level in accommodations should not exceed 75 dBA based on HSC guidance. This is actually loud, and modern large craft have levels down in the 60 dBa range. Vibration can be an issue, which is why Incat uses rubber mountings in passenger accommodation upper superstructure (see more on this in Chap. 12, Fig. 12.4, and see resources for supplier and specifications). The wheelhouse recommendation is 65 dBA, and here again it will better be in low the 60 or even upper 50 dBa range if possible for comfort, particularly on longer voyages. Once passengers are on board, on the one hand they act as a sound absorber, while on the other hand conversation can raise noise levels. The contradiction is that if a cabin is quiet, then conversation stays quiet, while if it is noisier, people will tend to speak louder so as to be heard, thereby further raising overall noise level. If the vessel is large and has several lounges, it is possible to arrange one to be a quiet(er) room, most likely the executive lounge.

One other observation is that the main structural material has an impact on noise attenuation generally. A fiber-reinforced-plastic vessel will be naturally quieter, as both the reinforced plastic and the structure design based on foam sandwich for frames, floors, and bulkheads provide considerable noise attenuation. An aluminum

or steel structure efficiently transfers vibration and noise in comparison and so must be insulated.

In resources, under marine interiors, you will find several designers and suppliers of panels and insulation for fire protection and sound insulation.

13.2.4 Fire Safety

The basic principles for design against the risk of onboard fire (IMO HSC Chap. 7) are as follows:

- If a fire occurs in one space, the effectiveness of detection and extinguishing capabilities and safety systems is maintained in unaffected spaces.
- Passenger accommodation is segregated so that if there is an event in one area, passengers will have alternative escape routes to a safe area.
- The vessel is subdivided by fire-resistant boundaries.
- Use of combustible materials and materials generating smoke and toxic gases in a fire is avoided so far as possible and restricted concerning passenger furnishings.
- A fire can be detected and extinguished within a bounded compartment.
- Escape routes and access to firefighting equipment is protected.
- Firefighting equipment is readily available.
- During a voyage, vehicle and cargo spaces can only be entered by authorized crew members, who may by request accompany a passenger for access.

IMO guidance is that liquid fuel with a flash point below 43 °C is not recommended and not below 35 °C for gas turbines [IMO HSC 7.5.1 to 6].

Designers are requested to consider the source and potential spread of fire and provide segregation so that there will be a safe haven. Enclosed spaces such as movie theaters are indicated as not being permitted, so a special exemption would be required. Any installed galleys would have to meet the requirements of chapter II-2 of the IMO convention on the Safety of Life at Sea. The transport of dangerous goods is subject to compliance with II-2/53 and 54 of the IMO convention.

Space Classification

The different spaces aboard a vessel are categorized as follows, with the requirements for fire protection duration as in the two subsequent tables:

1. Major hazard – machinery, vehicle, dangerous goods, storerooms containing flammable liquids, special-category spaces
2. Moderate hazard – auxiliary machinery, bonded stores, crew and service spaces
3. Minor hazard – low-risk auxiliary machinery, cargo, fuel tank spaces, tanks, and voids
4. Control stations
5. Evacuation stations – external stairs and open decks used as escape routes, muster stations, open deck spaces and enclosed promenades by lifeboat and life raft

embarkation and lowering stations, vessel side down to waterline at lightweight displacement adjacent to life raft and evacuation slide or chute
6. Open spaces at areas other than in item 5

Note that the following table shows requirements between spaces of a given category. For example, 1/1 is between two major risk category spaces, where 60 min fire protection is required on both sides of the dividing bulkhead or deck. Where a boundary does not need fire insulation but shall be smoke tight is indicated by gray shading.

Passenger Craft

Space	1	2	3	4	5	6
1 Major	60/60	60/30	60/na	60/na	60/na	60/na
2 Moderate		30/30	30/na	60/na	30/na	Inside
3 Minor				30/na		Inside
4 Control stations		30/30				inside
5 Evacuation						inside
6 Open						

Cargo Craft

Space	1	2	3	4	5	6
1 Major	60/60	60/30	60/na	60/na	60/na	60/na
2 Moderate		30/30 smoke	30/na	60/na	30/na	inside
3 Minor				30/na		inside
4 Control stations		30/30				inside
5 Evacuation						inside
6 Open						na

Fire Divisions

Designers should consider the location of fire divisions and the presence of water on the other side of the division, potentially providing a cooling effect by heat transfer. In such a case, insulation may not be appropriate.

Firefighting divisions must comply with the following requirements:

- Constructed of noncombustible or fire-resistant materials, fire insulated, and suitably stiffened to maintain load-carrying capabilities within rated time period
- Prevent passage of flames and smoke within rated time period
- The fire division has to have sufficient insulation that on opposite side to teh fire teh bulkhead must not have an average temperature greater than 139 °C, and an extreme temp anywhere on it of higher than 180 °C
- Be certified by testing

The main load-carrying structures that are also fire divisions should be able to resist fire for 60 min without losing their structural integrity. Designers should

consider load distribution along such members so as to avoid stress concentration that may be a cause for collapse in case of fire.

When constructed of aluminum, they should be insulated to avoid having the core temperature rise above 200 °C within the 30 or 60 min period. Where construction is of a composite material, the insulation shall be such that the temperature in the core material stays below that where deterioration of the structure's load-carrying capacity may occur.

It should be noted that doors and penetrations should provide fire protection equivalent to the fire-resistant boundary walls. Machinery spaces must have a complete enclosing boundary that is fire resistant.

Structural Fire Protection

The main structure shall be protected for 60 min. Lesser structures may be protected for no less than 30 min. Where there is uncertainty about the classification of a space and boundary, the most stringent requirements should be applied. The upper side of special-category space decks does not need insulation.

The main structure shall be made of noncombustible materials or approved fire-restricting materials provided they have been tested and preapproved. It may be noted that while steel can resist the temperature of a hydrocarbon fire for a short period, unprotected insulation is necessary to give 30–60 min protection to avoid structural degradation or collapse. Aluminum has a much lower resistance to such fires, and so fire insulation is critical to maintaining structural integrity for the required period. In the case of composite construction, selection of appropriate resin composition is important so as to provide fire-retardant properties for the structure itself, while the insulation needs to be in place to ensure the safe duration of 30 or 60 min to allow personnel evacuation.

Outfitting materials

Where insulation could come into contact with flammable liquids or vapors, the material should be fire resistant, impermeable to vapors or liquids, and have low flame-spread characteristics.

Fire-resistant materials are defined as those with

- Low flame-spread characteristics
- Limited heat flux
- Limited heat release
- Gas and smoke release low enough to avoid danger to passengers and crew

Furniture should also be constructed from noncombustible or fire-resisting materials while curtains or drapes should conform to IMO Resolutions A471 and 563 concerning resistance to the propagation of flames. Upholstery must be flame resistant in accordance with A652, and bedding must be in accordance with A688.

Primary deck coverings must comply with A653 and A687 for flame resistance and propagation resistance.

Exhaust gas pipes/ducts should be insulated, and all compartmentation that the ducts pass through should be insulated by noncombustible material. The insulation

design shall account for operating and design emergency temperatures within ducts. The design of exhaust manifolds or pipes should be such as to safely discharge and disperse hot exhaust gases.

Stairs and elevators

Internal stairways connecting between deck levels should have smoke- and fire-insulated divisions/doors between the levels at a minimum at the top or bottom. Where connecting multiple decks the entrance to each level should be protected by a fire division, while the stairway itself will be an enclosed fire- and smoke-protected space.

Tunking for the elevators should also be fire- and smoke-protected spaces and include the entrances to each deck level.

Air spaces between suspended ceilings, paneling, or linings should be fitted with close-fitting draft stops less than 14 m apart so as to avoid having a fire draw oxygen from a remote location, reducing the effect of fire-extinguishing measures locally.

Ventilation

Ventilation systems installed in high-speed craft should have main inlets and outlets that can be closed from outside the space being ventilated. Those systems ventilating hazardous areas should be able to be operated remotely from a continuously manned control station.

The ventilation system operation should be set up with controls outside each space that is separately ventilated and those in hazardous areas operated remotely from a continuously manned control station. Controls for hazardous areas should be separate from those for general areas.

Hazardous-area and muster-area ventilation should be separate from systems for other areas, and the vent ducting should not pass through these other areas, just as ducting for general areas should not pass through hazardous areas. Basically, the systems need to be carefully segregated in the vessel. Think of the engine room and machinery rooms as areas to be "self-contained" and protected as far as is practical. If a duct must pass through a fire wall and hazardous area, then failsafe automated fire dampers will have to be fitted at the penetration spot. Such dampers will also need to have a manual closure available on the "safe" side of the penetration. Where ducts penetrate a deck, the protection should be such that deck integrity is not affected and smoke/vapor will not pass through.

Fuel and Flammable liquids

Tanks should be separated from passenger, crew, and baggage compartments by vapor-proof enclosures, ventilated from the outside, and suitably drained.

Fuel tanks should be in separate areas away from major fire hazards. Fuel pipes should be protected by stop valves directly by tankage operable outside the space where a fire may occur (the tankage space or the engine room). Fuel piping should be of steel or alternative certified material. Use of flexible piping should be avoided.

Pipes, valves, and couplings conveying fuel of flammable liquids should be installed away from hot surfaces, engine air intakes, electrical equipment, and

potential ignition sources and be shielded to prevent leakage from contacting such ignition sources. It is necessary to consider the vessel at speed in a seaway in this context, rather than the vessel static.

Where fuel with a flashpoint below 43 °C is used, the following precautions shall be taken:

- Tankage shall be a minimum of 760 mm inside the hull side and bottom plating, decks, and bulkheads.
- There shall be overpressure protection with relief valves and overflow protection that discharges to a safe location.
- Spaces containing tanks shall be ventilated with a minimum of six air changes per hour, and equipment and electrical system for this shall be certified intrinsically safe.
- Vapor detection shall be installed in all spaces containing fuel lines, with alarms at continuously manned control stations (most likely the wheelhouse).
- Internal fuel tanks should have save-all gutters for spillage.
- Tank content status shall be available by safe and efficient means, including monitoring for tank filling. Gauge glasses are prohibited.
- Bunkering shall take place when no passengers are present at approved refueling facilities with firefighting facilities available.

Fire Detection and Extinguishing

Firefighting on a vessel needs to consider the cause first, then the space to be protected and the potential occupants, and the potential progress of the fire and how to reduce available energy so as to extinguish it. A risk and consequence analysis will assist in pinpointing these issues to allow a specialist engineer to subsequently design the detection and firefighting system for the vessel.

In an enclosed space such as an engine room, the key aim is first to shut off any source such as fuel leakage and electrical energy and then exclude oxygen by CO_2 blanketing or something similar. Local electrical fires should not be fought with water, so dry powder or foam system extinguishers are important for these spaces. In large "open" areas such as passenger saloons, the expectation is a combination of local "hand" extinguishers and hose-based firewater supplied via a dedicated pair of firewater pumps powered by main and uninterruptible power supply (UPS) systems for security. The firewater system is really the system of last resort.

Passenger vessels require a fixed water sprinkler system in public spaces, service areas, storage rooms, and closed spaces other than those containing flammable liquids. Other large vessels with crew cabins and living facilities (e.g., military vessels) may also require an automated sprinkler system in these spaces similar in function to systems installed on large cruise liners. The main controls are generally operated from the bridge, with locally operable controls from adjacent fire areas for each space protected, while the system should be segregated for the different passenger zones.

Care should be taken, though, for protection systems in galley spaces due to the presence of flammable fats, and so in these spaces reversion to foam extinguishing designed specifically for this type of fire needs to be applied.

All enclosed spaces with major or moderate fire hazards must be protected with a smoke detection system and manual call points to inform the main control position on the bridge of the vessel. Main machinery rooms should also have instrumented leak and vapor detection for flammable fluids, as noted previously, and be supervised by TV cameras monitored from the bridge. There should also be a manual call point to bridge at the exits from these spaces.

Manual call points should be installed in all separate spaces on the vessel, normally at the entrance/exit to the spaces, and be no more than 20 m apart in corridors.

Smoke and fire detection should be installed in all corridors, stairways, and escape routes. Consideration should be given to detection also for ventilation ducts. The placement of detectors shall conform to the following table unless testing shows they can be varied:

Type of detector	Max. floor area per detector (m^2)	Max. distance between centers (m^2)	Max. distance from bulkheads (m)
Heat detector	37	9	4.5
Smoke detector	74	11	5.5

Smoke detectors should operate at between 2% and 12.5% obscuration/m
Specification stipulate that heat detectors should operate at 54–78 °C

Fixed fire detection and protection should be supported from power linked from two sources, the main power and a separate dedicated supply from the emergency power system (often referred to as the UPS), so that in case of a main power failure the systems will be fully functional. Fault detection and indication at the bridge shall be part of these systems. Cabling shall avoid machinery spaces as much as possible, with the exception of coupling to the power supply. The UPS is normally located in a dedicated "safe" area (see subsequent discussion).

Instrumentation for detectors and manual call point status and warning should start with a visual signal and have an audible warning after at most 2 min if not acted upon. There should be an alarm sounding system from the bridge to all craft spaces that could contain personnel.

Indication and operational controls on the bridge and any other local operation stations shall be arranged in logical groups for the vessel layout and located so as to facilitate efficient and accurate response to an emergency. The grouping of indication and controls for hazardous areas shall be separate from those for other spaces. Extinguishing should be operable from the control position on the bridge.

The designer should carefully consider the grouping of spaces for fire detectors and indication. The interest will generally be to minimize the number of instruments while allowing an accurate determination of location. Care is needed for large open spaces, and so it is recommended to take advice from a specialist who may be able to advise on optimized detector locations once a risk assessment has been conducted

and hazard scenarios determined. This part of design takes some specialization to get it right so as to be efficient as well as reliable and as simple as possible! Overinstrumentation may not lead to improved detection, and subsequent complexity may even cause confusion in an actual emergency.

Where a gas (CO_2) system controlled from the bridge is installed, it needs to have the capacity for second discharge from a local manual operation site outside the space. If two independent systems are installed, one shot is sufficient for each. Lines from extinguishing medium-containing cylinders to the protected space shall have marked control valves outside the space (this assists function testing) and nonreturn valves in the discharge lines between cylinders and manifolds. Piping and nozzle placement shall be such as to give uniform distribution of the medium in the space being protected. Machinery rooms need careful review of placement so as to be operational as quickly as possible. Remember that CO_2 gas is heavier than air and so will fill from the lowest points. Consider the complex internal structure and equipment so as to avoid leaving air pockets.

Installation of an audible warning of extinguishing medium release into a potentially manned space prior to release to allow evacuation is essential. Automatic release of extinguishing medium should not be possible (manual initiated system from bridge or manual operating point). Clear instructions should be located at all operation points.

Extinguishing material containers (e.g., bottles) must be located outside protected spaces and be certified for use by the appropriate authority. Fixed container spaces should be located adjacent to the superstructure exterior with access from outside for inspection, replacement, or recharging.

CO_2 systems

The minimum volumes of extinguishing material as required by the IMO are based on a coverage of 0.56 m^3/kg of stored compressed gas. The gas should be able to fill 30% of the largest cargo space and 35% of the gross volume of machinery spaces at a delivery rate such that 85% of the discharge is completed within 2 min for a specific event. Delivery by the system upon activation should be a two-stage discharge, first activation of the system from the container to fill the manifold and second delivery into the space to be protected. Controls should be located in a protected release box outside the space as well as on the bridge.

Firewater systems

Two independent pumps with a minimum of 25 m^3/h or two-thirds capacity of bilge pumps should be installed, with each pump able to operate two hydrants simultaneously. Pumps should be installed in separate locations so both cannot be knocked out together, meaning they should be placed in opposite hulls. The vessel should have a fire main feeding hydrants and isolation valves to separate the section within the machinery spaces containing the fire pumps. This is so that one pump can be isolated and the other can feed the fire main. Fire hoses shall be available and stored nearby to be connected to hydrants.

Note that if a firewater system is activated, significant volumes of water will be spread over deck areas in a short time period. To avoid danger to vessel stability, the designer needs to consider where the firewater will migrate and ensure that it can discharge overboard or drain to a location where it can be pumped overboard; pumping should be available for this, together with or in addition to general bilge pumping facilities. This applies also for special-category spaces.

Portable and local equipment
At least five portable fire extinguishers, including one outside each machinery space, are required.

Special-category spaces (Vehicle Area in particular)
The intent behind these spaces is for a fixed firefighting system to be installed, and the status of doors and closures that are automatic is indicated at the bridge. Water fog and foam systems are mentioned by the IMO. The requirement is for effectiveness against a flowing petrol fire demonstrated to the vessel's registration authority. A requirement for at least three water fog applicators is mentioned. In addition, a requirement is given for a portable foam applicator system with a 20 L tank that can be connected to the local fire main system or be used with portable foam applicators for roaming use in the special-category space. There should also be local portable fire extinguishers (one every 15 m) in the space.

Ventilation of these spaces should be sufficient for 10 air changes per hour while under way and 20 changes per hour while at port during loading and unloading operations. The ventilation system for these spaces must be separate from other systems, and its status must be able to be monitored and controlled and closed off in emergencies from the bridge and a control station must be located outside the space. Duct and damper materials must be steel.

Electrical equipment in such spaces should normally be of EX standard (safe for use in hazardous areas) to minimize ignition source risks.

13.2.5 Lifesaving Appliances and Arrangements

The IMO (HSC Chap. 8) requires that all lifesaving equipment conform to Part C, Chap. III of the SOLAS Convention and that it be tested and approved by the governing authority for vessel operation:

- Two very high frequency (VHF) radios on every passenger craft
- One radar transponder on each side of craft or one in each survival craft
- Communications to control, muster, and embarkation stations
- One life buoy on each side with 30-m line
- Life jackets for all passengers and crew, minimum 10% for children
- Immersion suits for crew acting for escape

The vessel should have survival craft located outside close to embarkation stations, with equal capacity on each side, the location being a safe and accessible position even when the craft is damaged. Designers need to take care for launching of survival craft in terms of proximity to propellers and water jets at the stern, craft overhangs that may impede the use of chutes or slides, exhausts, and water outlets below the craft waterline.

Access to survival craft shall be via chute or slide unless (for small craft) deck is less than 1.5 m freeboard above the water surface. There needs to be at least two survival craft of 100% capacity, with additional craft for not less than 10%. Often there will be more than two survival craft launched together and linked. Examples of deployed rafts and chutes are shown in Fig. 13.8. There are a number of specialist suppliers of survival equipment that is tested and certified according to both IMO and major maritime country regulations suitable for use in high-speed multihull ferries. Internet links are given in the resources at the back of this book.

One rescue boat is needed for vessels operating under IMO rules (i.e., in exposed waters rather than rivers) and two boats for ferries with capacity over 450 persons with one stored for deployment on each side, with the exception of craft less than 20 m in length (or river vessel). The rescue boat must have the capability to get a helpless person on board. The bridge needs to be constructed such that one can observe a rescue operation from it, and recovery should be possible in the worst operating conditions.

The rescue boat should be able to be boarded from its stored position and recovered from the sea when fully loaded. It should be located and stored so startup is possible within 5 min even in case of collision. It is assumed that rescue boats will eventually marshal the survival craft. If a craft has many small survival life rafts, then each rescue boat may not be designed to handle more than 10 rafts, though if a boat can actually tow 2 or more, then the IMO allows that it could marshal up to 12. This aspect needs some serious thought where a ferry for several hundred passengers is being designed, so as to balance the practicality of life raft size, ease of access and therefore pace at which passengers can be off-boarded, and the eventual shepherding of these same life rafts once passengers and crew have completed the deployment and transfer process.

Note that vessels working in estuaries or rivers will generally be smaller craft and so many of the requirements discussed previously as required by the IMO are for vessels that will operate in international waters and generally an exposed environment distant from port or early rescue by other parties (independence of action). For such smaller craft a designer should consider the possible means of recovery from an incident, whether collision or fire, and propose measures to provide personnel rescue and fire extinguishing. Some rivers have high flow rates also, both downstream in upper reaches (e.g., Yangtze and tributaries) and in inner estuaries during flood tide, and so rescue system design needs to consider currents rather than extreme waves as for an offshore vessel.

Note also that the IMO allows sheltered voyage craft in warm climates to have open life rafts (Annex 10 of the SOLAS convention) for vessels with less than 450 passengers.

Fig. 13.8 (**a**) Closed Life rafts; (**b**) open life rafts; (**c**) multiple exits

13.3 Functional Systems

13.3.1 Anchoring, Towing, and Berthing (IMO Chap. 6)

The basis for high-speed craft is that anchoring is for emergency use only. Main facilities are for berthing a vessel at a quay for loading and unloading. The designer nevertheless needs to establish locations for anchoring and mooring fairleads, cleats, and bollards suitable for the port facilities to be designed for it or be available. This equipment needs to attach to a vessel's primary structure via foundations that are designed for the realistic forces due to current, wind, and waves at the terminal or temporary mooring. Space, storage, and handling arrangements for ropes will need to be provided.

Vessels should have at least one anchor, cable, and warp, with a winch facility for launching and recovery, storage space for equipment, and a safe working area for personnel to perform anchoring or recovery. This may be a relatively simple affair with a hand winch for small river craft or a rather more substantial installation for a 100 m RoPax catamaran. The working area should be illuminated and protection from cable and machinery provided for personnel safety. Communication shall be available with the bridge by hand radio or fixed intercom. When retrieved, the anchor should be retained in place securely against operational conditions.

Towing arrangements should be available to respond to the worst operational conditions. If from more than one point, the vessel should have its own bridle. The maximum towing speed needs to be determined and structures and equipment designed to be safe when these loads are being towed by a tow vessel in a seaway. Towing lines to a recovery tug are set quite long so as to give flexibility, avoiding snatch loads in the system.

Special attention is needed to ensure that fairleads and structure in terms of berthing lines, anchor cables and warps, and towline arrangements provide smooth guidance and avoid the possibility of snagging or chafing.

Note that many ferries have protected berthing arrangements designed for them and maintain thrust to stay in place rather than deploying an arrangement of berthing lines. The requirements of the operator need to be discussed in this connection. Water-jet installations can normally provide reverse thrust to back up against a berth, though in certain situations where side winds or currents are a challenge, bow thrusters may assist in maintaining position as an alternative to a bow warp.

13.3.2 Auxiliary Systems (IMO Chap. 10)

Piping, valves, and fittings need to be designed so that system capability (working pressure) is no greater than the design capability of the weakest item. Piping and tankage should be designed with a suitable margin against maximum working pressure. Normally systems should be tested to at least working pressure or 110%.

Where there is the possibility for excess pressure, for example, vapor in a tank header or liquid expansion due to temperature in a system, relief systems should be designed and, in case of tankage overflow, protection provided. Materials used should be compatible with the internal fluid. Nonmetallic pipe may be considered for certain systems, low-pressure water and bilge for example, particularly if the vessel structure itself is nonmetallic. Integrity of the watertight compartmentation of the vessel must be maintained.

Fuel, Lubricating oil, hydraulic oil and inflammable liquids
These systems should preferably be steel or corrosion-resistant metallic tubing appropriate to the system pressure, with a minimum possible joints or connections between supply and user equipment. The routing should be such that inspection is readily available at all times. Where a flexible hose must be used for a connection to a piece of equipment, this must be approved by the authority that the vessel will operate under.

Where machinery compartments have daily service tankage (for example, for auxiliary services), this should be provided with means to prevent overflow. Where fuel oil purifiers are installed, these should be in a separate area for the purifiers and heaters, with facilities to prevent as well as contain spillage. If any fuel oil tanks have heating arrangements, these will need to have thermostatic controls and alarms in case of control failure.

Bilge and Drainage
All watertight compartments in the vessel hull will need to have drainage and pumping facilities connected. This will normally entail piping, valves, and ring main or possibly a manifold system connected to a self-priming bilge pump for each hull of a catamaran. The system needs to be independent of any other water system and such that bilge water is pumped from a compartment and direct overboard without the possibility of filling another compartment.

The IMO requires the bilge main to have a diameter of at least

$$d = 25 + 1.68(L \cdot (B + D))^{0.5},$$

where

d is the internal diameter of the bilge main;
L, B, and D are vessel (demi) hull LOA, BOA, and molded depth.

A minimum of two bilge pumps should be installed in each hull, each sufficient to pump water through the system at a rate of at least 2 m/s with a 20% design margin. One of the pumps should be connected to the emergency power supply. Pumps should be located in such a manner that one pump is always available for any compartment in an emergency. Suction branch piping should be greater than 25 mm in diameter and fitted with inlet strainers. Nonreturn valves should be fitted at the manifold and bilge pump suction pipe or hose.

For smaller vessels without a bilge main, individual submersible pumps may be installed in hull compartments other than the closed compartments forward of the passenger facilities. In addition, one portable pump should be available, powered from the emergency power supply if available, to access spaces. The capacity for each of the fixed pumps is defined by

$$Q_n = Q/(N-1)\ \text{t/h and should be greater than 8 t/h,}$$

where the total volume requirement Q is the 2.4 times the volume determined by 2 m/s flow through a bilge main diameter d above for the actual vessel. For a catamaran this will be calculated for each demihull separately.

Ballast system
If the vessel is fitted with ballast tanks and pumping in order to maintain trim this system should be independent of other water systems if ballast is water and should use dedicated compartments that do not have possibility for entry of hydrocarbon oils so as to avoid so as to avoid discharge of oil pollution to sea.

Intakes and Exhaust
The main issue here is to control the airflow by positioning of intakes and with filtration so as to avoid ingestion of salt from vapor in the air at sea. Gas turbines require a considerable airflow and so marine vessels must have significant sized 'knit mesh' type filters (see resources) that are able to be cleaned by freshwater back flushing on a regular basis.

Exhaust discharges should be separated from intakes such as for ventilation and arranged so that gasses are directed away from vessel personnel accesses. If the vessel is a superyacht or military vessel there may also be an issue of hot exhaust plume emission in proximity of helicopter landing trajectory. Specific studies may be carried out to clarify acceptability, see Chap. 7.

13.3.3 Control, Alarm, and Safety Systems (IMO Chap. 11)

A high-speed multihull will have the ability to remotely control and monitor from the bridge the main propulsion engines, water-jet hydraulic systems for direction, forward and reverse, trim tabs or interrupters, forward stabilizing hydrofoils, and the internal service systems, including the safety systems discussed earlier. To achieve this, there will be control loops, and necessary backup duplication, with instrumentation and actuation at the hardware location and integrated control systems within the bridge compartment. All the aforementioned equipment will be controlled by digital microprocessors and may, if required, be linked to a data monitoring system to allow health and performance monitoring.

During berthing and loading, a vessel will have personnel performing operations externally or at the passenger or vehicle entrance ramps using local operating

Fig. 13.9 Hydraulic ramp illustrations – showing bow ramp down and up, and rear ramp down and up

stations. The status of any equipment such as hydraulic operated ramps (Fig. 13.9) should be able to be monitored by command on the bridge by instrumentation or on smaller vessels by radio communication. It is normal for this equipment to be arranged for local operation only so that a human guard is available, with status monitoring on the bridge for larger vessels.

Where a function can be operated from the bridge or a local station, there should be an indication on the bridge of control being selected locally so that command are aware of the status and action will not be attempted from both locations.

It is expected by the IMO that the bridge will have controls for the following emergency systems:

- Activating fire-extinguishing systems including closure of ventilation openings and stopping of ventilation machinery
- Stopping main and auxiliary engines and machinery
- Fuel-supply shutoff to main and auxiliary machinery
- Disconnection of power sources for the normal power system using latched switches

Also on the bridge there should be alarms connected to the controls so that malfunction or out-of-envelope unsafe conditions are warned about to the command by both visual and audible means. A condition can be accepted to remove the audible

alarm while the visual should remain until the fault is corrected. Key alarms that should be in full view throughout vessel operation to bridge crew are those for fire detection, loss of electrical power, engine overspeed, and overheating of any permanently installed NiCad of NiMH batteries.

Additional alarms that should be available to operating crew on the bridge are:

- Monitors for exceedance of limit values for vessel, machinery, or systems operating parameters (for example, monitoring of vessel motion or accelerations if available)
- Failure of power source
- Power failure to directional, trim, or stability devices
- Automatic bilge pump startup
- Failure of compass system (or GPS)
- Fuel tank low level or overflow
- Failure of navigation lights
- Fluid low levels for any critical systems (e.g., hydraulic fluid reservoirs)
- Failure of ventilation fans to hazardous spaces including vehicle decks
- Fuel line failure

Where shutdown of systems is controlled by automated processes, the commencement of automated shutdown should be indicated by audible/visual alarm and a manual override should be available for all cases apart from those where intervention would cause failure or explosion.

13.3.4 Electrical Installations (IMO Chap. 12)

Electrical and instrument systems on a fast multihull should provide services to maintain normal operation and environmental control of the vessel based on the premise that main auxiliary generators will provide normal service while services essential in an emergency are provided through the same circuits by essential service generators or battery supply or dedicated emergency circuits. A failure modes and effects analysis (FMEA) should be carried out to assess the scenarios for the vessel, evaluate the consequences for the electrical circuitry, and define requirements for the main and emergency circuits to minimize the risk of failure.

Essential services where failure may cause serious damage to the craft (for example, bilge pump systems) should be fed by two independent circuits designed to avoid double jeopardy.

Interruption of essential or emergency system circuits should occur only via latched breakers so as to avoid unintended operation.

Electrical machines should be protected by double insulation or suitable grounding to prevent exposed metal surfaces from becoming live in fault conditions.

Cable sheathing, joints, and terminations shall be flame retardant and, when in hazardous areas, flame resistant. Circuits shall be protected against short-circuit overload by suitable protective devices such as circuit breakers or fuses.

Nonmetallic vessels
These vessels shall have electrical systems where voltage does not exceed 500 V for main service power and 250 V for lighting, communications, and power sockets. Careful attention is drawn to providing circuit segregation so that power to each circuit and subcircuit and from all electrical plants can be cut off to prevent danger. The circuits should be double insulated rather than grounded. Designers should consider the possible effect of lightning strike on the vessel and static electricity generation due to fluid flow in metallic pipes when designing electrical continuity and grounding to sea. Primary lightning conductors should have a cross section of 50 mm^2 copper or equivalent in aluminum while secondary conductors should have a minimum cross section of 5 mm^2 copper or equivalent. Continuity should be such that resistance does not exceed 0.05 ohms as a basis for design.

Main Power Source
At least two generating sets need to be installed. The sets may be either (preferably) $2 \times 100\%$ for vessel normal conditions or $2 \times X\%$ where X is a power level sufficient to supply normal operation and safety of the vessel itself and minimum services for habitability (sanitary, fresh water, ventilation and heating, refrigeration, and cooking).

Design of the electrical system and generators should take account of the necessity to restart the main engine from dead craft condition, and the selected configuration should be able to be shown as reliable for all failure scenarios of the main engines.

Switchboards need to be in separate spaces from the generator and transformer spaces, not in an enclosure in the same space.

Main bus bars should normally be divided in two sections, each with a circuit breaker and power supplies equally divided as much as possible.

Emergency Power source
The emergency power source should be a self-contained system and the generator, transformer, transitional power source (battery system starting if main generator fails), emergency power, and lighting switchboards should all be above the waterline level in vessel damaged state so as to operate successfully in an emergency. The location of the equipment should be separated from the main machinery and electrical distribution spaces, and additionally the power distribution system should also be separated from the main power distribution network so far as practical, to avoid double jeopardy failure scenarios.

Emergency power may be from a battery or a generator. When from a generator, it shall start automatically upon failure of the main power supply and be on load within 45 s. Additionally, in this case there needs to be a transitional power source bridging between failure of the main supply and startup of emergency generation.

If the emergency supply is battery powered, it must be capable of automatically connecting to the emergency system in case of failure of the main power source and to supply the emergency load for the design period (transition or emergency period) and maintain voltage within 12% of nominal levels. Emergency switchboards are

best in separate compartments, whether battery or engine, and the IMO will allow emergency switchboard to be colocated with a generator. Where batteries are used for emergency supply, they should be kept charged at all times by supply from the main power system, with overcharge and overheat monitoring.

Emergency generating sets should be able to start reliably at zero degrees or the minimum temperature for the operating location if this is less. Preheating may need to be installed. Starting equipment must be able to supply for three consecutive starts, with an effective manual start or a secondary start system for another three starts within 30 min installed. Electric and hydraulic systems should be controlled from the emergency switchboard, while the starting energy source should be in the same compartment as the generator. A compressed air system would be from either main or auxiliary air receivers through nonreturn valves at the emergency generator space or by a local emergency air compressor.

Emergency Power Supply Requirements
In general, there needs to be duplicated circuits for the emergency system supply to essential services arranged such that via bus bar selection the equipment can be fed from the main power circuit or, if all or part of that circuit is knocked out, switched to the emergency circuit. There needs to be automatic shutdown of nonessential services in case of emergency or, for smaller and less complex vessels, a clear list close to circuit breakers to allow this to be achieved manually.

For smaller IMO Category A (B) vessels the power supply shall operate safely supplying the following:

- For at least 10 (10) min
  - power drives for directional controls
- For at least 30 min (B only)
  - powered watertight doors and indicators
- For 4 (4) h intermittent service
  - signaling lamps and craft whistle if not independently powered
- For at least 5 (12) h
  - Emergency lighting at stowage of lifesaving equipment and crew firemen equipment, escape routes and disembarkation, passenger spaces, main and emergency machinery spaces, steering gear, control stations, navigation lights, internal communication systems, fire detection, alarms and extinguishing, radio systems, essential powered instruments, and propulsion controls
- For at least 12 (12) h
  - “not under command” lights

The IMO notes that on passenger vessels there should be supplementary emergency lighting that can last at least 3 h after all other supply fails, sufficient for

passenger escape. Additionally, segregation of distribution systems should be such that in an emergency event affecting a complete "vertical zone" this should not interfere with the emergency services in other zones. This affects routing and protection of cables through vessel segregated zones.

Cargo vessels must meet the same requirements as Category B vessels mentioned earlier.

Steering and stabilizers – loss of control power
Where steering or stabilization is dependent for safe performance on the functioning of a single device, the power to this device should be served by two independent circuits to provide a failsafe system. For a multihull vessel, steering by water-jet systems or multiple rudders may obviate this situation; nevertheless, it does point to another scenario for FMEA, where the designer should look at the consequences of power failure to the control and stabilization devices. It may be possible for an individual device to fail to a "safe" state where vessel control deviation is minimized. When the failure is to a bow foil damping system, it may simply be sufficient for the failure to be annunciated at a monitor on the bridge so that the commander can take action to adjust vessel speed or handling to compensate for the loss of the ability to actively control the stabilizer via an automated feedback system.

13.3.5 Navigational Equipment (IMO Chap. 13)

The minimum requirements specified for safe navigation are as follows. Note that the requirements of the local administration may allow safety to be met by other means.

- *Compasses*
  Magnetic compass in a binnacle with correction capability and protected from magnetic interference, readable from steering position. In addition, smaller vessels for less than 100 passengers should have an instrument suitable for the vessel speed, motion characteristics, and area of operation to provide a heading reference superior to that of the magnetic compass. Large vessels should have a gyrocompass suitable for the craft characteristics.
- *Speed and distance measurement*
  Vessels should have speed and distance measurement for reliable measurement at the design speed and environment. Often radar devices are installed for speed and GPS for positioning.
- *Echo sounding*
  Vessels should have an echo sounder for use at slow speeds and assistance for navigation in confined waters.
- *Radar*
  Vessels should have at least one X band azimuth–stabilized radar, while vessels for more than 450 passengers or greater than 500 t gross tonnage require

a second radar installation. One radar should include facilities for course plotting. Note that radar may also be used in a SAR operation if the vessel is involved.

- Electronic positioning

  Where operation is in a location where electronic positioning is available, a system should be installed. Currently there are electronic chart and location systems available using GPS satellites for most global coastal areas, so these systems have become the primary means of positioning with radar giving information on local traffic in the same area.

- *Rate of turn and rudder position indication*

  A rate of turn indicator should be installed to warn the commander if the vessel design limit is being reached. Rudder position should also be annunciated or, alternatively, the position of the steering thrust from water jets or steerable propulsor (z-drive or podded propulsor)

- *Steering and propulsion*

  Steering wheel, tiller, or joystick movement should be in the same direction as vessel direction change. The propulsion system indication should have physical or electronic indication of status/mode.

- *Searchlight*

  At least one steerable searchlight operable from the command station and one battery-powered portable searchlight stored on the bridge

- *Automatic pilot*

  For vessels that operate on longer voyages at locations where traffic is low density, an automatic pilot can be a help to command. The IMO recommends its installation. Designers should carefully consider the vessel mission and, when the use of autopilot will be appropriate, consulting with operator and local regulatory bodies. For a high-speed vessel, in addition to the local traffic, changes in sea and wind conditions can importantly affect the requirements for safe navigation, perhaps reducing speed, adjusting track, and so on, and so autopilot may be a rarely used tool.

- *Night Vision*

  For vessels that will operate at night, the designer will need to consider night lighting for the bridge, and for operation in locally trafficked waters (coastal, estuarine, river) consideration given to night vision equipment so that the commander can work together with the radar operator for collision avoidance.

  The designer may wish to consult with the operator on his procedures for nighttime and fog conditions so as to design the equipment and its operation for navigation and collision avoidance for optimum effectiveness when used in concert.

The designer should consider the need for communications and instrumentation required for command in cases where wing positions are available to the commander. Alternatively, video camera locations and operation as well as screens in the bridge need to be reviewed. At the time of writing, one may expect a video system allowing the commander and crew to view all major entrances, saloons, car or cargo deck, sides, and stern of the vessel for close maneuvering and berthing; this

may now extend to proximity sensors for docking and, perhaps, in the short term linkage between these and the propulsion system so as to automate the final docking sequence once the quay parameters have been recorded and "learned" by the system.

13.3.6 Radio Communications (IMO Chap. 14)

Remember here that the IMO is relating to international waters, so generally exposed environments relatively remote from safe havens or rescue facilities. Equipment needed for river or close estuarine operation can be simplified, but we will summarize the full installation first.

The key purpose of the radio installations is as follows:

- Two separate means of transmitting ship-to-shore distress alerts, receiving alerts from shore about other vessels, and the ability to make ship-to-ship distress alerts
- Transmission and receipt of communications for search and rescue coordination both off and on scene, both from shore and bridge to bridge
- Transmission and receipt of maritime safety information and general communications to shore and to other vessels

Typical installations will include the following:

- Radiotelephone distress frequency watch receiver operating at 2182 kHz
- VHF radio with digital selective calling (DSC) on international Channel 70 with continuous watch on this channel together or separately, and telephony on Channels 6, 13, and 16
- Radar transponder operating at 9 GHz available for emergency deployment in survival craft if necessary
- NAVTEX receiver for maritime safety information or equivalent Inmarsat system depending on location of operation
- Satellite emergency position indicating radio beacon (Satellite EPIRB) working at 406 MHz to polar satellite service or Inmarsat in the 1.6 GHz band able to be taken on survival craft operated manually or floating free and automatically operated in water contact

It should be noted that the IMO provides variations to the foregoing list depending on where the vessel operates, basically if the area is within range of different coastal watch stations, so as to enable efficient communication. Outside this vessels become dependent on Inmarsat and standards allowing ship-to-ship communication. Once again, vessels operating in rivers or estuaries exclusively will have somewhat different requirements, set by local authorities, and so these should be consulted before completing the specification.

A small project-oriented note here: radio communications generally require licenses, and these take a little time to be approved. Coordination is required between the vessel designer/builder and the operator to ensure the necessary licenses are in

place before the vessel is delivered! Approval may also require equipment operational testing with an authority. Please don't forget to plan for this.

Power for the radio systems must be an uninterruptable supply with transition from main supply to the backup as required.

Bearing in mind the dependence of the vessel on these systems to maintain safety, the designer should consider equipment reliability and failure scenarios so as to devise a balance of maintenance routines and equipment duplication so that the basic aforementioned requirements can be met for all voyages undertaken. The duplication may be via spares, duplicate equipment maintained on shore, duplicate equipment on board, or onboard maintenance of a single piece of equipment. The selected option needs to be validated with local authorities.

13.3.7 Bridge Layout

The bridge should be located so that direct visual access is available, if possible around the entire vessel. The IMO specifies blind sectors from ahead to 22.5° aft of the beam and less than 20° on either side with individual blind sectors less than 5° and individual windows greater than 10° wide. The navigator should when seated be able to see the sea surface forward of one craft length from the bow. Aft of this there may well be a passenger saloon or crew spaces, so view of the stern will depend on video.

If there is a separate docking workstation associated with the bridge, the navigator should be able to see enough of the vessel side/stern to safely dock the craft. Some of this may well be difficult to "see" directly from a bridge, but the combination of a docking personnel with radio at the stern and video surveillance should ensure safe operation. Once again, sensing technology and IT advanced quickly in the period 2010–2017, so this technology should help to simplify systems and manning responsibilities going forward.

The bridge should have a layout with workstations as follows:

- Commander with main propulsion, direction, trimming, and dynamic stabilizing controls together with compartment video, internal communications, and external radio communications
- Navigator with radar, position and charting, and electronic or chart table close by
- Separate station for main and auxiliary power performance monitoring
- Separate panels for safety systems, electrical systems, and internal environmental controls that require active oversight

Instrument and electrical system cabinets will normally be located in a utility room below or behind the bridge, with the annunciation of status sent as digital signals to suitable logic diagrams on selectable screens at bridge level.

The bridge should also normally have storage for operating crew life jackets or full suits, mobile emergency equipment, vessel documentation, and reference manuals.

Once again this applies to large vessels that operate under the IMO. For river or estuarine operation, smaller vessels may operate more like a bus or coach, so the focus would be on the needs of the commander and requirements of the local authority.

13.3.8 Service Spaces

On larger vessels there will be a significant service crew supporting the maintenance of refreshment, cleaning, and environment systems, entertainment system operations, and commercial controls and associated service/storage spaces. There may also be a need for spaces such as a restroom for onboard cleaning staff.

A purser's office may be required, located close to local equipment rooms for electrical distribution, instrument cabinets, HVAC, and fire safety. These will generally be located on the same decks as the main passenger level. Sizing and location will depend on the size of the vessel and consequent service power and system requirements, so it is recommended that designers first identify the electrical load requirements from the sum of the main users and essential users and on that basis determine the necessary control cabinet sizing. A nominal cable routing as well as HVAC ducting layout will help to identify the location that would entail the least amount of cabling and ducting, and from this the overall layout can start to be refined.

13.3.9 Cargo Handling Including Vehicle Ramps etc.

With the exception of the smaller river passenger vessels, probably the key starting point is that you will need to provide some kind of ramp access to the vessel. Both for speed of deployment and security a system deployed from the vessel is preferred, usually hydraulically driven, for example, like those in Fig. 13.9. The structure is likely to be "bespoke" in terms of both vessel access and the quaysides to be visited, but it will essentially comprise a ramp structure of aluminum beams and section, grated floor, a tubular hinge, and stanchions/handrails on each side. Deployment and retrieval will be performed with long-stroke hydraulic actuators that function much like hydraulically operated watertight door mechanisms but in the vertical plane.

For smaller river craft the same lift and lower or slide in and out to the vessel deck for a very light ramp might also be a simple rope or chain and pulley. That is perhaps the simplest level.

At the other end of the scale we have vehicle ramps at the stern of very large catamarans. In essence, though, they have the same mechanism of hydraulic actuator deployment and retrieval up to closing and a locking mechanism for safety during voyages. The difference is the structure scale and the loads they must carry, since they will have to be able to support perhaps 50% of the weight of a 40-t truck as the

tractor rear wheels or trailer rear wheels cross it, applying point loads at the wheel pattern. Perhaps the most complicated ramp installed to date has been that for the HSV2, an Incat wave piercer that was leased by the US Navy for evaluation for a number of years prior to final selection of the design of the HSV vessel program in 2008 (check) (Fig. 13.10). The reason it was so complex was that it had to allow vehicle delivery while the vessel was moored alongside a quay, where the quayside was unprepared for the vessel itself, essentially at any location worldwide where the vessel could approach a quayside. The vessel and the ramp were to provide valuable service across many countries during its US naval deployment. For comparison Fig. 13.10 also shows two typical examples of large stern ramps/doors on Incat and Austal ferries.

Thus, ramp design may be a significant structural design exercise but is simply a factor of the geometry, and once the structure has been dimensioned, the key points for a multihull designer are simply the weight, effect on vessel weights and centers, and the cost factor for the owner.

Once vehicles or cargo are on board and arranged in the vehicle deck, the final issue to consider is securing the cargo in place. At sea a multihull will pitch perhaps 5–10° maximum in normal service, and maybe up to 5° in roll. The accelerations should stay below 0.3 g.

When you apply the brakes on a car, you will stay below 0.1 g, apart from emergency. The brakes on a vehicle can normally apply restraint up to 1 g deceleration, but restraining a static vehicle depends on the friction force available from the statically braked wheels. Trucks have air (release) parking brakes on both the tractor and trailer wheels, which makes for a relatively safe system. Most cars, including MPVs and pickups, have a parking brake on just the two rear wheels, so for safety it is important that such a vehicle also be left in gear so that all four wheels are effectively locked.

The designer's challenge is then to work out the factor of safety against vehicle movement for the tires to the deck based on the friction factor between the deck surface and the tire taking an average wear factor for tires, braked footprint, and load and a safety factor. This last may need to be at least 50%. It is best to be conservative here rather than have vehicles move and cause damage. Needless to say, a deck with a rough surface, whether a grit containing coating or a patterned plate and nonslip coating, will provide much better grip. Once the motion limits of the craft are determined from hydrodynamic analysis, a choice can be made about whether additional security such as chocks or restraints need to be made available for vehicles on a high-speed multihull. It may well be that these are used only when a voyage is undertaken with sea state above certain conditions, meaning infrequently used. The main thing is to have the facility, to avoid unnecessary voyage cancellations. The IMO HSC code just states that adequate restraint is to be provided for cargo (see IMO HSC Chap. 4.9.1).

Before assessing the loading from the assembled vehicles, the designer needs to look at the maneuvering of vehicles onto, inside, and coming back off the vessel via loading ramps. If the approach is to drive on and reverse off, this may suit small cars but not trailers or trucks and buses. Larger vessels have enough room for vehicles to

Fig. 13.10 (**a**) Austal ferry *Maria Dolores* stern ramp; (**b**) USN HSV2 rear ramp and crane; (**c**) trimaran Fred Olsen Benchijigua leaving Los Cristianos with stern simple closure and folding barrier

circle around inside the vehicle bay, though trucks may still be difficult to design for as their turning circle is significant. If maneuvering is difficult, the terminal loading time will be affected, so careful discussion with the operator is required to make sure the vessel-to-port interface is made as efficient as possible, not just by the ramps, but also by the onboard traffic flow, including sequencing the procedure for loading and positioning of different size vehicles.

13.3.10 Personnel Access Systems for Offshore Transfer

Personnel access to offshore wind farm structures can be rather more challenging than quayside access. The personnel access will be a small platform somewhat higher than a vessel forecastle due to the exposed wave environment. A wind farm vessel will nose bow on to a fender system and use power to maintain contact below this. In calm weather, personnel can cross directly to ascend a fixed stairway or ladders, but in swell and heavier weather vessel motions make this a dangerous exercise. The ability to transfer personnel can therefore constrain operator maintenance and so turbine reliable uptime and a safer alternative are seen as means to improve wind farm operations and minimize overall costs. The motion-stabilized stairway is necessary for safe personnel transfer in these heavier conditions.

An example of a system of this type is that developed for the operator Wind Transfers Ltd. by BMT, Houlder, and ICS. The hardware is an articulated stairway mounted on the bow deck of the catamaran, while software developed by ICS monitors the vessel heave, roll, and pitch to activate hydraulic cylinders maintaining the position of the stairway's outer end connecting with the wind turbine structure. Figure 13.11 shows a diagram of the access and a photo of the installation prototype, while Fig. 13.12 shows trials in 2014 with an enhanced bow roller system mounted on the vessel bow.

The prototype was tested in 2012, and the system has been under trial since 2014. One challenge is the mass of the system and its effect on the relatively small and light catamarans currently used for such service – in the range 18–28 m LOA. The current development has shown the practicality of such a system, so optimization of the structural design for low mass and compact storage on the fore deck to minimize impact on the commander's forward vision, as well as higher reach, are clear targets for system development. A second issue is the space occupied by the access is also valuable real estate for maintenance and spare equipment to be lifted to the turbine by winch or crane once maintenance personnel are transferred.

One can envisage development of these vessels with more aft deck space and dynamic positioning capability to deliver this functionality as the industry matures over the coming decades. Recently also offshore wind farms have incorporated central utility platforms for transmission to shore, minimizing seabed power cabling. Personnel transport and transfer to these platforms will provide additional opportunities and challenges to the catamaran industry.

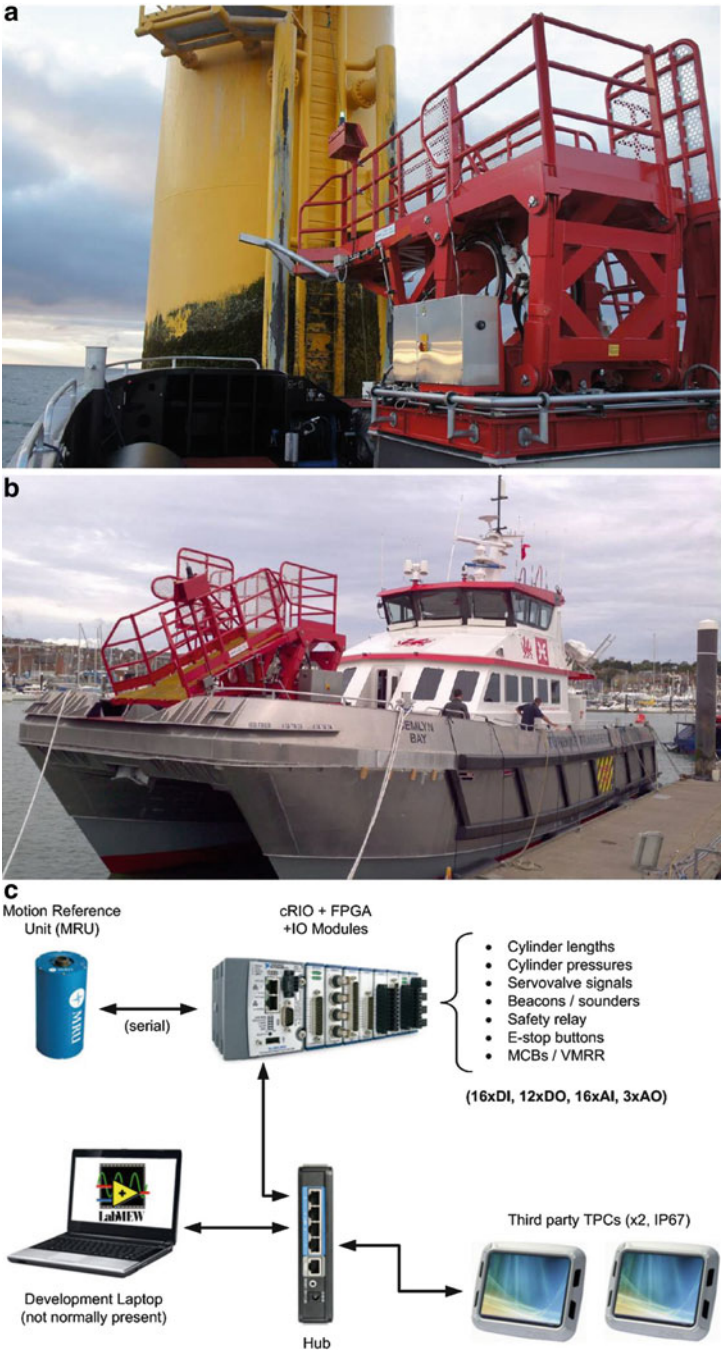

Fig. 13.11 (**a**–**c**) TAS diagram and photos of prototype

Fig. 13.12 Houlder TAS on wind farm vessel at turbine trials 2014

13.4 Architectural Design and Style

Turning to the overall shape and styling of a multihull superstructure, there is much to consider. We discussed aerodynamic influences in Chap. 7 and so will focus on the user perspective here. Let us look at the external issues first and then internal design.

External style

You will see from the images of recent vessels in this book and on the websites of builders that ferries are designed with bow and forward superstructure shaping that gives a low aerodynamic drag; in addition, the bow area is enclosed without open decks on larger vessels and with passenger accommodation at a higher level above the vehicle deck, allowing forward-raked windows as well as large windows along the side and at the rear. Smaller ferries may have an access ramp at the bow (Fig. 13.9) and the designs are rather more varied depending on the access requirements for boarding passengers.

The stern area is influenced by the specification for access by vehicles, freight, and passengers, open deck areas for crew access to guide docking maneuvers, and connection of hoses for fuel bunkering (Fig. 13.10). Smaller passenger vessels often have an open stern deck area with passenger access, while river and sightseeing vessels have open upper decks (Fig. 13.13).

The combination of structural configuration and paint scheme on modern vessels provides a rakish appearance, which is inviting for passengers. This is an important part of the overall experience for the customer of a ferry or excursion vessel operator.

Fig. 13.13 (**a**) River bus with open upper deck (Sydney); (**b**) Thames River bus with closed passenger cabin on single-level deck

From a naval architect's point of view, this is a first important step. The next is the experience internally. Once passengers have entered the cabin, it is important that they have sufficient room in passageways to negotiate, taking into consideration not just baggage but also children, and that wheelchair-bound passengers can find a place. This means passageways 75–90 cm wide. To avoid traffic jams, additional open spaces next to exits, by kiosks, and toward the bow will be necessary. Consider the vessel details in Appendix 3 for some indications.

Internal furnishings and decoration need attention with respect to both appearance and ease of cleaning. There are a wide variety of cultural norms worldwide for internal space decoration, so I would not wish to suggest one particular style. It is nevertheless generally accepted that colors toward the red end of the spectrum are "hot" in the sense of setting people's mood, neutral colors give an equivalent response while being also calming, and blue colors and lighting are "cooling" or clinical. Dark colors, toward brown and black, are not helpful in emergency situations as they absorb rather than reflect light, so it is better to have a light neutral color and matt surface for most of the furnishings, as green emergency exit guides will be clearly visible, for example. Advertisement material and other notices will also then stand out clearly and draw passengers' attention.

The next issue to approach is layout of facilities on board. All but the smallest vessels will need to have some kind of wash room on board for passengers. The size and facilities will depend on the number of passengers on board. A rule of thumb may be one toilet per 50 passengers with a wash bowl and drying towels or drying machine, though this will also depend on voyage length. Operators can normally advise on requirements in this regard. Apart from an area for baggage, in the main passenger areas there is the question of seat and table groupings rather than simple seat rows where a vessel has the available deck space due to the provision of vehicle space in the deck below. A wide variety of seating, tables, and furnishings are available from specialist companies. A sample of links is given in the resources at the back of the book as a starting point.

It may be useful for the designer to make a checklist of passenger expectations for a typical journey in terms of time spent on various activities so as to tailor the outfit to provide a positive experience. Examples may be simply sitting and viewing outside for the duration of 30-min or so trip, with commentary from a crew member or announcements at "bus stops" for a river or harbor craft (in which case audio equipment will be needed so passengers can hear but that will not be too loud). On larger vessels passengers may sit for a period, read, watch video on a laptop, sleep, walk around the vessel, visit kiosks (how fast should service be set up for?), eat (at a table or in their seat? What facility is there for trash?), sit at group seating with friends or family for conversation, or chase children who need to release energy.

The designer will need to review the normal placement of crew and the sequence of passenger movements in case evacuation becomes necessary. This includes the ability to deliver life jackets to all passengers and instruct/assist parents to put jackets on children, while other crew members deploy life rafts and access slides or chutes. This may well give good guidance for life jacket storage locations and areas around them, as if they are too close to exits, there will definitely be a jam as people try to

put them on and others lean forward in an attempt to grab one for themselves. Think of these as ergonomics studies. The aim is for a design where nobody (other than the designer, that is) questions it, because it just works. For general passenger behavior and experience, there will be positive feedback after a while ("that boat was comfortable, quiet, etc."), while emergencies are something only the operator and designer will give much thought o, other than passengers listening to the safety announcements every time a vessel is boarded (and hopefully taking in the information; this can make all the difference in an emergency. Think about it, when did you last really take notes on a trip? Yes, some announcements are boring and are ignored, so design announcements that will get people's attention because some really do matter). Think back to announcements that you still remember, like that tune you can't get out of your head. Yes, this is an issue for a multihull designer, as safety is number one! Announcements can now also be made on video screens, and these should be simple enough to understand when standing at the opposite end of the compartment; otherwise, they will not be followed or absorbed.

Finally, both for external and internal design we have the "superyacht" challenge. Some catamarans and trimarans have already been built as superyachts (Figs. 13.14 and 13.15). For a designer, a commission for a vessel of this type opens up the possibility of a more extreme specification, whether in relation to vessel speed, external styling, or internal outfit. That said, since most such yachts are used for "cruising" and entertaining while at anchor, really high speeds will more likely be needed for smaller luxury vessels – an extension of the fast cabin cruiser concept where the owner enjoys helming such a vessel. Larger vessels are designed for operation by a permanent crew, whether for a single owner or a chartering company.

This brings us to the design of the internals of such vessels in comparison to a fast ferry. Smaller craft may be operated by the owner and friends or a short-term crew. So for a catamaran, this means personnel cabins forward on the main deck, galley and dining, plus an open area deck aft, navigation bridge, and open deck aft on the deck above. All these facilities would follow marine recreation boating practices and be of lightweight construction.

Larger superyachts have a wholly different approach to internal outfitting since a key attribute is the ability to impress visitors, whether the vessel is being chartered for a short while or belongs to a wealthy individual. Perhaps the best guideline here is that if a commission is received for a superyacht multihull, it will be best to approach internal designers who have a track record of outfitting such vessels and select one who is favorably disposed toward the multihull concept that you are proposing as well as some knowledge about the owner or chartering company. The challenge from that point will be striking a balance between the mission statement and expectations of the prospective owner, the vision of the interior designer, and the cost/performance envelope that you are able to deliver. Initial ideas and links to specialists may be found in publications such as [12].

Some thoughts on the design of multihull superyachts' hull form provided by a specialist SABDES are as follows:

"Superyacht styling when applied to a multihull platform is an interesting challenge. It involves all the same processes of creativity as applied to designing on a

Fig. 13.14 Catamaran super yachts: (**a**) Curvelle Quaranta; (**b**) Sabdes concept

monohull platform, and can open up the ability to offer unique features more difficult to create in a monohull; one obvious example would be having the ability to raise and lower the guest tender directly under the main guest deck between the port and starboard hulls, in the case of a catamaran.

Putting the pros and cons of various features aside for the purpose of focusing on an exterior styling solution is a subject that SABDES Design finds very important to get right with a client. SABDES have good experience with catamaran and wave-

Fig. 13.15 Trimaran superyacht *White Rabbit*

piercer vessel design, having worked with Incat and Revolution Design on various commercial vessels, yet when we apply our thinking to multihull superyacht styling, we take a more holistic approach.

For example, on catamaran design, one important aesthetic we have explored is to offer a tapered forward hull form. We previously developed for a client a 50 m design using asymmetrical cross section hulls. This gave the vessel a much less 'blocky' look than traditional symmetrical hull cats because it allowed us to curve the hulls right to the inboard side of the hulls, more like a fast ocean racing power catamaran, and not just to the hull centres. This offers a subtle yet important aesthetic improvement, especially when viewed from forward three quarter views.

SABDES don't steer away from basing superyacht multihulls on a commercial style hull form, especially if it's a well-proven one; it's just that we feel there are reasons that amongst the world's superyacht fleet, only a small percentage are multihulls, and we are genuinely excited by multihulls, and especially cats, and aim to offer positive and innovative design inputs as we would like to see many more!

One avenue of research and innovation we are exploring is developing full tapered bow catamarans, ones that have a monohull bow morphing into port and starboard catamaran pods by a gradually reducing chine seen in profile and an exaggerated raked stem.

Our feeling is that generally yacht owners either love multihull superyachts or they don't. Even though multihull superyacht aesthetics above the sheer line have in

the past been aligned closely with monohull superyachts, though they are wider, there is some stigma that keeps many potential yacht owners from considering multihull superyachts, including wave piercer and trimaran superyachts, SWATH, etc., despite the fact that, arguably, multihulls have many advantages.

So to completely remove any stigma multihull designs may have, we at SABDES attempt a fresh approach to conceptualizing the look of multihulls. Customers have told us 'it needs to look more like a monohull', and we take that comment seriously, but we also try to determine the unique superyacht identity that multihulls can offer rather than meld simply into a monohull formula."

The messages imparted here are that client expectations and desires need to be met, while channeling those expectations to deploy the attributes of the multihull to best effect. Unless the style is impactful, it is not going to be accepted by someone who by definition probably has an outsize ego or a charter company aiming to appeal to those same individuals. The vessel will have to offer utility and performance that are superior to those of the alternatives, whether other multihull designs or monohull vessels. The definition of that superiority depends on the mission, so we return to the importance of defining, as much as possible, the operating mission of the vessel.

We have not discussed specifically the complex subject of military outfitting here. At one level the same rules apply, since personnel safety remains the number one priority, and making arrangements for containerized functional outfit modules can be considered an extension of the approach to locking down trucks.

Electronic outfitting is much more complex for military communications and data acquisition but still follows the principles of duplication and separation of circuitry, fire protection, and, in this case, a new issue to consider, blast protection. This, last together with weapons outfitting, is something that military organizations around the world keep confidential.

Some vessels, notably the US Navy's LCS trimarans, have helicopter landing facilities on the upper deck aft. The design of aircraft interface and support is another specialized subject where for military operations the organization itself will have its own guidelines, but the basic requirements can be gleaned from civil aviation authorities and maritime regulation authorities.

The key issues for a helideck on a marine vessel will be the size, shape, markings and structural integrity in case of a helicopter crash, and wind environment at the helideck for a vessel in operation (particularly turbulence behind the vessel superstructure, which may destabilize a helicopter as it transits sideways to the deck from its initial position to one side prior to final landing). When designing the landing area and associated hanger or service facilities, the requirements must be met for onboard maneuvering, storage and maintenance areas for the aircraft, its equipment, payload items, and safe fueling.

Naval vessels are changing to incorporate the ability to deploy a range of unmanned vehicles, both aviation and surface and submarine units. The considerations in incorporating these were summarized in a paper to the RINA Warship 2006 conference [13-3]. The paper gives useful insights into the various unmanned vehicles considered at the time of publication for the UK Royal Navy. The marine vehicles (AMVs or AUVs) require deployment and recovery from the sea surface

while the aircraft (UAVs) would require facilities similar to those for smaller piloted aircraft.

The storage and mechanical handling of marine craft on board is a more complex task than a helideck and hangar for a helicopter, as there are options for using a stern dock or arrangement between catamaran hulls, employing a deck hatch toward the stern to operate as a "moon pool" for deployment with a crane or winch and guide frame. Alternatively, a crane, A-frame, or davits could be used for deployment over the side of the vessel. Also, an AMV or AUV could be deployed from the external main deck or a hatch arranged closer to the SWL on the hull side so that the unit could be slid out on a frame, attached to the davit or crane, and lowered directly. The use of cranes, an A-frame, or davits may also simplify transfer ashore where facilities are minimal. See Appendix 2 for this author's initial item list to consider in the data sheets.

Another issue for such equipment is its control. Much like the outfit for a subsea ROV vessel for the offshore industry, it will be necessary to have a fully fitted operation room with the pilot control stations and visualization both through vehicle-mounted cameras and also location mapping, velocity, condition monitoring, and sensor data recording for the designed missions.

Going back to the superyacht configuration, the designer of these vessels faces a challenge similar to that of incorporating helicopter facilities for larger vessels, the storage, maintenance, and mechanical handling on board, and the deployment/recovery of various "toys" that have become a common feature, from jet skis, to small viewing submarines, to small sailboats, for example.

The superyacht crew may not have the same control and data handling requirements for "toys," but it may well have a need for deployment monitoring from the bridge and tracking once outside the vessel so as to maintain safety for both the operator of the toy and the mother vessel.

13.5 Summary

This chapter has focused on the internals of a multihull's superstructure. These systems probably use up as much as 30% of the project budget, likely costing as much as the hull or the engines and propulsion; thus, the design needs to be right so as to have an economical vessel.

Second, if the designer doesn't get it right, the vessel will not receive a permit to operate, and correcting issues at a later stage can become very costly and caused unplanned expenditures.

Then there is the customer – the passenger; if the internal environment is not comfortable even before the voyage starts, the operator will not have repeat customers. Finally, the operating environment on the bridge must be right, since if it is not set up right, vessel control may not be reliably safe.

Procurement of most of the equipment and bulk related to these systems needs to be conducted in parallel with construction of the hull and superstructure, and the

system design cannot happen too long after the primary structure is designed, as there will be a long list of attachments and secondary structure needed to allow installation to proceed – a careful interface design is just as crucial.

Then we have the fact that piping and cable installation tends to be time consuming, and instrument system loop testing before startup is always on the critical path and, once again, time consuming. To test instrumentation and controls, you need power and all the functional equipment mechanically complete, so by definition it is always last. Rush this stage, and you risk having faults during trials and workup. On the other hand, since it is the last bit of the critical path, there will always be time pressure.

If this sounds negative, let us just turn the preceding thoughts upside down, and you have every excuse to spend some time working on the vessel "systems" and ensuring a smooth project delivery! The greatest reward of all is a happy customer.

Now we will turn to project execution itself, assembling the technical jigsaw puzzle and managing all the stages from design through contract tendering and award, construction, and project delivery.

References

1. DNV rules for classification of high speed, light craft and naval service craft, Part 3, Chapter 1 (2011)
2. DNV GL Wasim and hydrod, refer to link under DNV GL in resources
3. Lloyd's register rules for special service craft (download from Lloyd's register internet site)
4. Lloyd's register rules for trimarans (download from Lloyd's register internet site)
5. DnV rules for high speed light craft and naval surface craft (download from DnVGL internet site)
6. ABS rules for classification of high speed craft (download from Eagle (ABS publications) internet site)
7. Turk Loydu – rules for high speed craft, Chapter 7, (download from Turk Loydu internet site)
8. Korea register of shipping rules for high speed and light crafts and also rules for recreational craft at www.krsusa.cloudapp.net/Files/KRRules/KRRules2016/KRRulesE.html
9. The merchant shipping (high speed craft) regulations 2004, UK Statutory Instruments 2004 No 302, ISBN 0-11-048699-4. (Application of IMO HSC Code in UK)
10. International code of safety for high speed craft, IMO, publication IA-185E, ISBN 92789 28014 2402, 2000. Amendments and resolutions after 2000 are available on IMO web site IMO.org
11. DnVGL evacuation software AENEAS, refer to link https://www.dnvgl.com/services/aeneas-the-standard-in-passenger-evacuation-analysis-48508 for details
12. Megayachts – concept, design, construction volume 17 2016, Annual published by Boat International Media Limited, London, ISBN 1-898534.67-X

Chapter 14
Project Delivery

14.1 Introduction

We have taken you, the reader, on a journey through the main technical characteristics of a range of multihull vessels, focusing on the catamaran and determination of performance for high-speed applications. The last three chapters looked at the outfitting and structural aspects necessary to bring a design together for construction.

In this chapter, our aim is to link these elements into a project delivery process. The purpose of this is to discuss the need to strike a balance between the different elements that go into delivering a successful outcome for the designer and shipyard – a vessel that meets the operator's requirements. This may start with a simple purpose but can easily develop into a complex set of requirements that may overlap or compete, particularly if a roadmap is not set up in advance to keep you on track. Not everything can be decided and fixed at the start, so clarifying the key decision-making steps and timeline are important for managing expectations and planning the work.

To some extent, we will be referring back to technical subjects detailed out in earlier chapters, so think of this as a recap, plus a high-level how-to set of thoughts on project management.

It is important to state here that the following discussion does not represent the specific process used by the companies listed among the resources at the back of this book; rather, it is an approach that grew out of the author's background experience in project management. It is believed to represent good practice applicable particularly to larger-vessel projects and, in simplified form, to smaller vessels.

To deliver a successful project, one must be sensitive to the points where optimization must be stopped and where a design (element) must be frozen, and in particular one must recognize that vendors do need to be actively communicated with and assertively followed up for progress.

Additionally, quality needs to be cross-checked, probably more than once in each phase! "Show me don't tell me" is particularly powerful as a concept in this regard.

L. Yun et al., *High Speed Catamarans and Multihulls*,
https://doi.org/10.1007/978-1-4939-7891-5_14

Remember that this means a procurement contract will require that the designer/builder have inspection rights with vendors and possibly hold points for equipment test, as these rights cannot be "assumed"; once equipment or material is in logistics or receipt inspection, it is too late.

Let us take as our starting point that we have a potential business client who needs a vessel to perform a marine service involving passengers and freight or equipment delivered at a service speed exceeding 25 knots in service condition to a terminal or offshore work site. The service may also include berthing or station keeping in an exposed environment. Take a look at the project road map in Fig. 14.1, and compare it with Fig. 2.14 covering the concept select phase and Fig. 7.1 showing the main design flow. We will discuss the stages along this roadmap in the following sections.

14.2 Setting Targets

Given our starting point, we need a little more information from the client to help us with candidate concept options. We need to know enough to validate that a multihull concept of some kind is appropriate.

In Chap. 7 we discussed developing the functional specification data sheets presented in Appendix 2 as Tables 2.1 and 2.2. Before moving forward we need to establish these basic metrics. We can then use the information from Chap. 2, or equivalent data, to make a first-pass selection of candidates. Chapter 2 summarized many of the key characteristics for multihull vessel concepts to assist in selecting the most appropriate configuration.

Our next task is to put limits around the main delivery parameters for our project. How much time do we have to deliver the prospective client's vessel? Within that period can we fit the sequence of tasks for screening (Fig. 2.14), initial design in the select phase (Fig. 7.1), and procurement, detailed design, and shipyard construction (Fig. 14.1)?

Each of these phases requires some investigation to define the deliverables and verify the timescale for each main activity together with linkages between activities. Some may be in parallel or overlap, with one task controlling the start and one controlling the finish and ability to move forward, while others may simply link sequentially. Working through the logic should lead to a single sequence of activities that is the "critical path" defining the minimum possible project duration. Since there are always holdups or changes here and there, additional "float" needs to be added between tasks that have high schedule risk. Other tasks that are off the critical path will by definition have "float" as their duration will be less than that required to link to their successor activity. The main deliverable dates along our critical path should also define our main milestones. This process is applicable in principle to any large engineering project, so what are the special issues for a multihull project?

The first issue is to ensure the candidate selection is robust. Initially this is about taking the time to consider the different multihull configurations in relation to the mission definition, then, where a configuration is selected, to investigate hull spacing

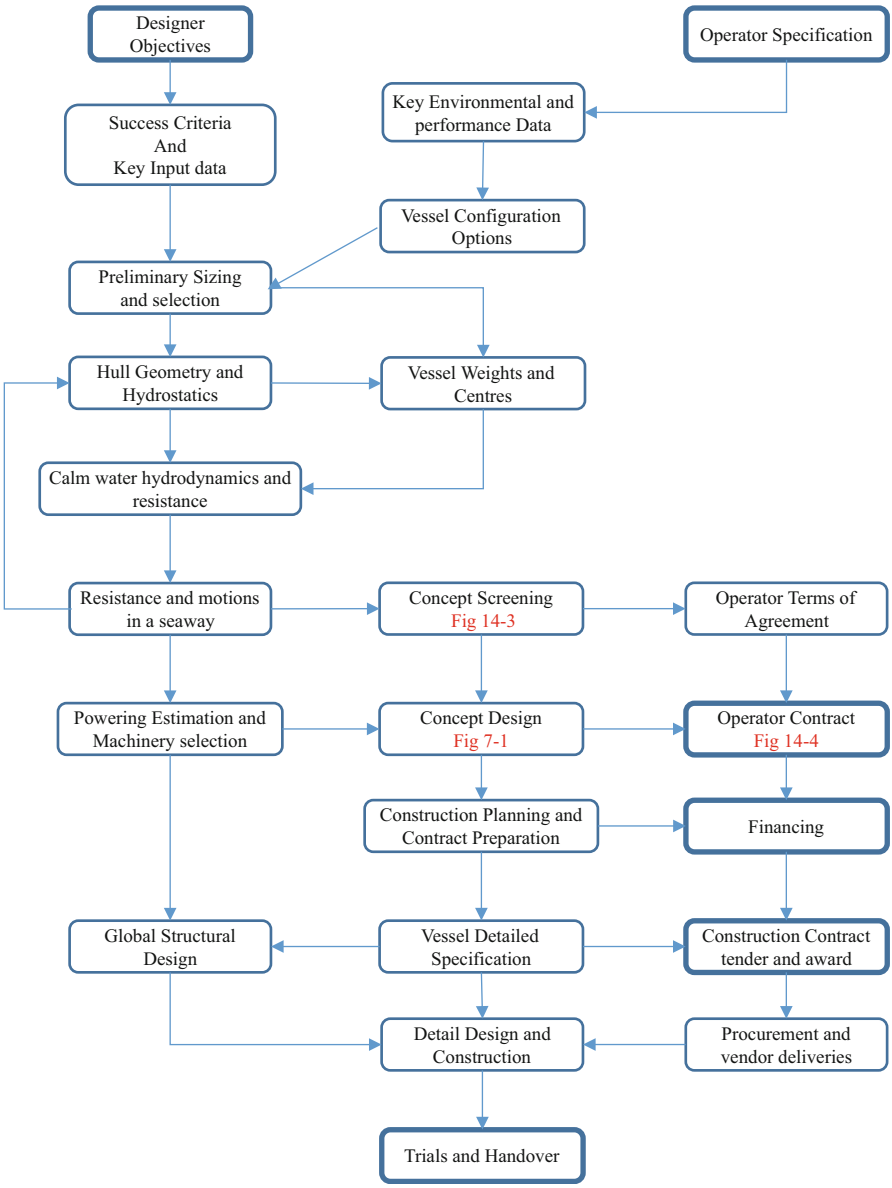

Fig. 14.1 Fast multihull project roadmap

and slenderness options. If this phase is completed diligently, the initial design and detailed design phases should then be a process of steady refinement. If there are surprises along the way, it will be useful to check back to the functional specification data sheets to make sure the data are robust or, alternatively, whether they should be adjusted.

The second issue is whether the selection candidates can be initially dimensioned by reference to existing vessels. It is worthwhile making a search for similar sized vessels. While there may not be examples to the exact mission, use the nearest available, and these can help with making first estimates of design parameters, as discussed in Chap. 7.

The third issue is how far the designer needs to take hydrodynamic analysis and optimization before fixing the general arrangement and moving forward to detailed design. Computer software such as Maxsurf can provide motion estimates, as well as hydrostatics, and structural design data. If demihull geometry and spacing need verification, a series of "runs" can be carried out quickly using computer analysis. Is this sufficient, or will a model test series be required? A model test program can take several months to complete and so needs careful planning relative to the design phase.

Most of the major multihull designs referred to in this book have been developed as members of a series of similar designs, with the prototype undergoing both analysis and model testing, and where possible correlation with data taken from instrumented field trials or operations. Scaling a design up to increase passenger or freight capacity can be done with a simplified process.

So at this point we should have the Project Definition including a descriptive Mission, the functional specification data sheets in prototype form, an overall Project Roadmap identifying the key milestones or decision points, and project plan Gantt charts showing linked activity delivery against a calendar. An example for concept screening phase is shown in Fig. 14.2.

Before moving on from this, it is useful to look at the main milestones and decide on the action if a milestone is delayed including what schedule float should be planned. If this is agreed on up front, it will avoid delays creating emergencies on a project. One example would be for delivery dates of main equipment for installation from a vendor. One strategy may be to build in more float for that vendor's delivery or, if this is not possible, identify the additional payment that would be possible to speed up the delivery. Both of these decisions need information on the vendor's previous performance, order book, and manufacturing flexibility. At this initial stage vendors are not selected, so some simple assumptions need documenting and timing for refresh and adjustment as the project moves forward to be agreed upon.

Another important item is to identify the key requirements of regulatory bodies and classification societies, the points in the project where information is required for review and approval, and the time that the body will take to respond. This could affect the detailed design phase planning. In addition, certain physical tests are often required before a vessel can be allowed to enter service, for instance, stability and emergency evacuation. This last needs to be built into the planning for trials and operator acceptance, including some time for adjustments or retest so as to have a "safe" schedule.

A final element that needs attention at this point is the potential expenditure profile. In the simplest case, where a designer or shipyard is to build a prototype or vessel for "stock," this will be necessary to develop the project financing proposal to present to the bank or investors. This may also be done in steps if a designer or

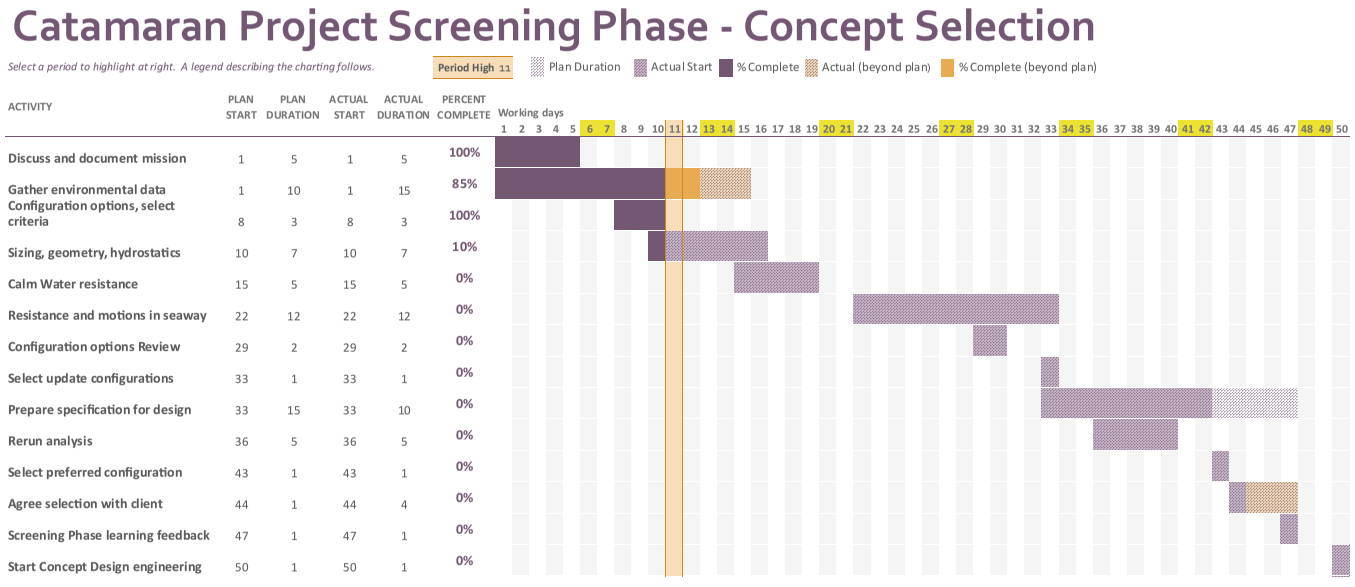

Fig. 14.2 Gant diagram chart for screening

shipyard wishes to prepare a vessel design that will be marketed to potential users before committing to a detailed design.

Major commitments are made once main mechanical equipment and construction materials are procured, with staged payments through to delivery. A number of these payments may be required before a construction contract can be formalized with an operator in order to have the main equipment available for the shipyard construction schedule.

In this case, there are three options. The simplest is for the project manager (either the engineering practice or the shipyard) to arrange purchase orders with cancellation clauses linked to the main construction award and to allow for project financing through a commercial lender. The alternative is for the operator to take responsibility for the free issue of this equipment to the shipyard for installation. This latter may be useful for an operator if the vessel is one of a series, and having a direct relationship with the main propulsion vendor may be useful for after-sales service and maintenance.

It should be noted that once the main engine selection has been made and committed to procurement, the engine ratings set a limit on vessel performance, so this is a key milestone!

An operator will generally want to back load his payments to link to vessel construction progress, with the retention of final payments until trials have been passed and regulatory approvals given. A shipyard would normally like payments front loaded so as to avoid separate project financing. If the project is run by an engineering practice, then project financing will be necessary to close the gap between the delivery side (engineering, procurement, and shipyard construction) and the operator client. Project finance takes a little time to arrange, and so this is another task that needs to be in the project roadmap and plans.

The roadmap in the foregoing Fig. 14.1 incorporates these into the project delivery process. To work through all the key decision points, it is also helpful to check, probably in two parts, first what the client wants and second what you need to deliver for the client's requirement to be met referring to the mission description and the functional specification.

Thus, for our project we now have our mission, initial specifications, roadmap, first-pass project plans as Gantt charts, and an investment profile. Let us move forward to look at the configuration alternatives.

14.3 Looking at the Alternatives: Concept Screening

Once the main framework for the project has been set up as suggested in Sect. 14.2, it is possible to look at the first task – selecting candidates from the range of concepts to be considered – concept screening. Much of the detail to be considered is covered in Chap. 2, suffice it here to say that it is important to follow a flowchart such as that in Fig. 14.3 to set up realistic options and document the reasoning for selecting

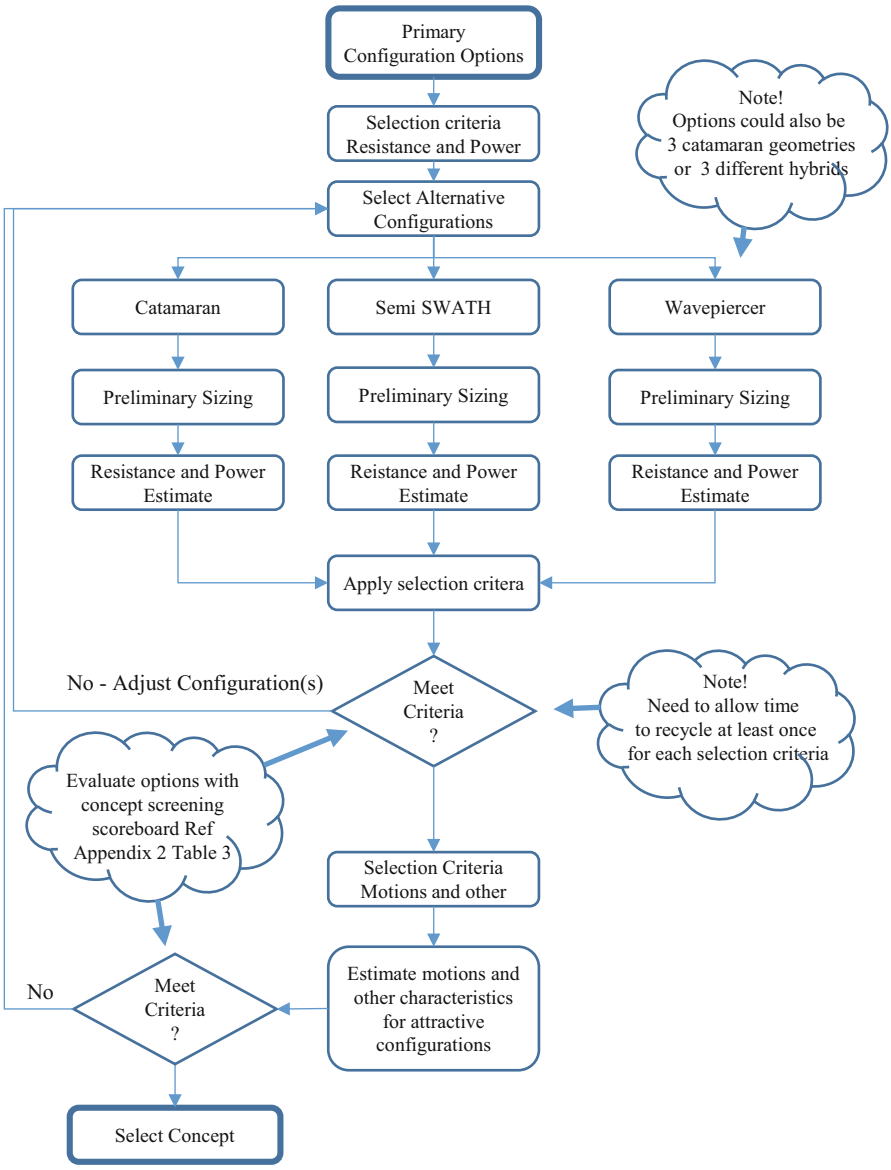

Fig. 14.3 Concept screening flowchart

between suboptions such as water jet versus open propeller propulsion and the use of stabilizing surfaces.

The first step to this is to set up a scoreboard for vessel attributes based on the mission and specification data and screening out the designs that simply will not deliver; see in Appendix 2 the data sheet examples and the template scoreboard.

An example could be a high-speed river ferry, which needs shallow draft, easy berthing, and low wash. Here a super slender asymmetric demihull catamaran propelled by water jets may be the first option, with variants being different demihull spacing. While a speed of 25–30 knots may be important, planing speed or the use of hydrofoils to reduce powering may not be desired due to higher wash generation, so the alternatives can be limited to demihull spacing and slenderness.

An alternative sample may be a ferry service across open water between cities, where a catamaran, waver piercer, or trimaran might all be potential candidates, depending on the distance and, hence, the voyage duration and the environment along the route.

Concerning the environment along a route, this may have significant variation. Note that the coast of Norway is less challenging than it might at first seem because most of the routes are protected by a whole series of islands that keep the seas short, with short crossings of areas open to the ocean. This contrasts with ferry exposure to open ocean conditions to cross the Channel between the UK and France or across the Taiwan Strait. A review of motions for such services based on sea state and acceptability based on the different sections of route length will help to set criteria for concept selection for such services.

In terms of potential cost, if the most favored technical concept appears likely to be expensive, it may be possible to improve motion response of less expensive options through the use of stabilizers. Alternatively, cost-reducing alternatives for the construction of the top-scoring technical alternative may be available through shipyard competitive tenders, alternative materials or material supplies, or hull construction at a low-cost shipyard, and separate outfitting .

Having reviewed the alternatives with the scoreboard and made a selection, whether for a single type of multihull and geometry variations or for a competition between multihull types or hybrids, the next step is to derive potential dimensions and characteristics from vessels already built as a starting point.

This initial screening stage can be done quickly, as there is no in-house design work to carry out. Once the basis for the initial analysis has been set up, it will be important to check out the resources that are available for carrying out parallel concept developments for final selection at the end of the phase – concept selection. Recall here a basic requirement for successful projects – “plan the work, and then work the plan.” If resources are not available to cover parallel tasks, either the project schedule needs adjusting to cope with these in sequence or the concept-selection phase should involve analyzing the highest-rated concept first and working on the next alternative only if the first one fails against project objectives.

14.4 Concept Design Phase

The starting point for this phase are the function specification data sheets prepared in the last section. If more than one multihull concept is being considered beyond screening, a preliminary design schedule needs to be prepared for each, with steps along the way to check that the concept remains inside the target envelope.

Based on the data sheets it is necessary first to prepare a line plan and from that generate the hydrostatic data to verify acceptable static stability, as discussed in Chap. 3.

At this stage it is necessary to check that LCG and LCB are in an appropriate location for the concept. We have seen that for planing vessels and for vessels using hydrofoils, performance is sensitive to these locations (see Chap. 4 for planing vessels and Chap. 10 for hydrofoil support). If the statics suggest the metacenter is too high in roll, there are options to look at demihull spacing or to adjust the demihull waterplane area both above and below the design draft.

LCG is an estimate at this stage, but it does need to be backed up by a simple analysis addressing the key items of mass, such as the hull, main engines and propulsion, fuel and water tankage, superstructure, and the main cargo of vehicles or freight. We presented a sheet for this estimation in Chap. 12. This sheet will need to be updated and detailed out as vessel design progresses.

Once the hydrostatics have been prepared, it is possible to move on to resistance estimation. Depending on the vessel geometry, it may be useful to conduct an analytical estimate, as reviewed in Chap. 4, before modeling the vessel in software such as Maxsurf so as to be able to critique the vessel-induced wave making and enable optimization choices. This is particularly important for vessels operating in a river or estuarine environment where wash is a key consideration.

Typically with a slender catamaran the demihull spacing will strongly influence the wave making and the resistance at service speed, and so some variation is worthwhile investigating, including asymmetrical demihull forms.

A wave piercer is normally designed with wide spacing and will have a complex geometry for the demihulls and the bridging or above the water central hull, so it is easier to set up a model in one of the major software packages (see resources at end of this book) and run resistance analyses for the potential geometry adjustments. Once the geometry has been selected based on resistance, a cross check with the hydrostatics must be made.

A trimaran is a rather more complex configuration to develop, and presently there are few designs to refer to. An introduction was given in Chap. 10. Once the dimensions and form of the main hull have been selected, the dimensions and form of the sponsons can be adjusted significantly to alter the cargo deck arrangement, provide the desired static righting curve, and orient wave making from sponsons toward the main hull to minimize wash.

If hydrofoils are to be used for support on a planing catamaran, following the setting out of the hull lines, the main support foils and stern control foils must be estimated. While vessels designed from the ground up have been very successful, the conversion of an existing high-speed catamaran ferry in China showed that while speed and power improvements were gained, the lower immersion of the water-jet intakes produced problems of vapor ingestion and pump cavitation in a seaway so that the catamaran had to be returned to its original state without a foil configuration. Consideration of the propulsor as an integral part of the configuration design is a more sensitive issue for this concept.

This takes us to the selection of the main propulsion for the vessel based on resistance calculations. A review of potential vendors is needed first (Chap. 11). A choice of engine and propulsor must be made to match as close as possible the vessel resistance estimate at service speed adjusted by the power to thrust efficiency of the selected system, using data from the vendors. When this is confirmed, the weights and centers can be checked, and a vendor market estimate for procurement costs should be possible.

A designer will go through these options so as to prepare updated lines and initial structural layout at this stage and, hence, make an update of the weight and center analysis, as discussed in Chap. 7 and in more detail in Chap. 12. Once this material is available, it should be possible to work through the scoreboard again and determine the most efficient configuration from that point forward.

Unless the vessel is part of an existing vessel design series, it is advisable to carry out a model test program at some point to provide correlation with the computer predictions for resistance, including the effects of wave interaction between demihulls or hull and sponsons, and the motions in waves. This will also allow for validation of the configuration selection.

If the selection of a single base configuration at this point is uncertain using the analytical performance data, it may be necessary to carry out model tests as part of this phase so as to make a clear decision prior to discussions with shipyards or the construction department.

If the concept selection was clearer, then the model tests can be planned out in the later part of this selection phase and tendered to model test basins while the shipyard and construction review is going on, so as to carry the tests out early during detailed design after incorporating any necessary updates based on the construction review.

Once a selection regarding the configuration has been made, it is time to talk with the shipyard's construction department, if the designer is on a shipyard design team. A review of the vessel structural proposal can be carried out and an initial estimate of construction schedule prepared for discussion with the client. If the designer is independent of a shipyard, first a review of potential construction yards is required, along with an initial enquiry to obtain expressions of interest, and then project details must be sent out for the interested yards to respond with their delivery proposals.

The discussions with the construction department or shipyard can then focus on what is necessary to optimize the selected vessel design from the construction point of view and its potential impact on form and performance. The construction philosophy must be agreed on before the detailed structural design is carried out.

The outcome for this concept selection phase is an outline of the vessel to be designed and constructed to meet client requirements. The responses from construction department or candidate construction shipyards should be enough for a detailed project plan and estimate to be made. Now we know what we want to build. How do we get there? Let us take a look at the assembly of a project plan before going into detailed design, as this work is needed in parallel to the concept selection work.

14.5 Project Plan, Construction, Lifecycle Costs/Economics

First a word on the project plan. From the point of view of the designer, we are already in a plan – the roadmap for the whole process (Fig. 14.1). Armed with our concept selection and feedback from both shipyard construction and the prospective client on the preliminary design, we are homing in on what we aim to build.

Before we move into the design of our selected vessel, we now need a more detailed plan and schedule that can become part of the formal contract with the client and an internal service agreement with construction or a formal contract with a shipyard. It will be necessary to discuss and agree on this plan prior to starting the detailed design and for it to be signed off on and incorporated into the contracts, with an updated revision at a milestone during detailed design (see the roadmap in Fig. 14.1) as the most likely kick-off for the main structure fabrication once the detailed construction plan is available from the shipyard or construction department.

In addition, it will be necessary to determine the project financing required in order to fill the gap between commitments to procurements and payments for construction milestones, and staged payments by the client.

In the limit - rather than paying in stage payments the ultimate limit is a single payment at delivery, the whole project will have to be financed. In this case, the client's price will be higher for the cost of capital employed and coverage of the risk of nonacceptance that must be covered through insurance. The cost of that insurance will be closely linked to articles in the delivery contract.

Development of the project plan and schedule is a natural part of the concept selection phase and may influence the final selection. As can be seen from Fig. 14.4 below, a number of other technical and commercial inputs to the contracts need to be addressed at the same time as the preliminary design work is being completed so that deliverables are fully defined and costs and economics can be assessed. These may include the following items:

Base Vessel Cost Estimate

- Design and procurement, including
  - Procurement of permanent outfit
  - Procurement or receipt and installation of payload-related outfit
- Construction and delivery, including
  - Mechanical completion and commissioning
- Project management including
  - Procurement quality control and expediting
- Indirect cost elements
  - Project-specific services, offices, software, and so forth

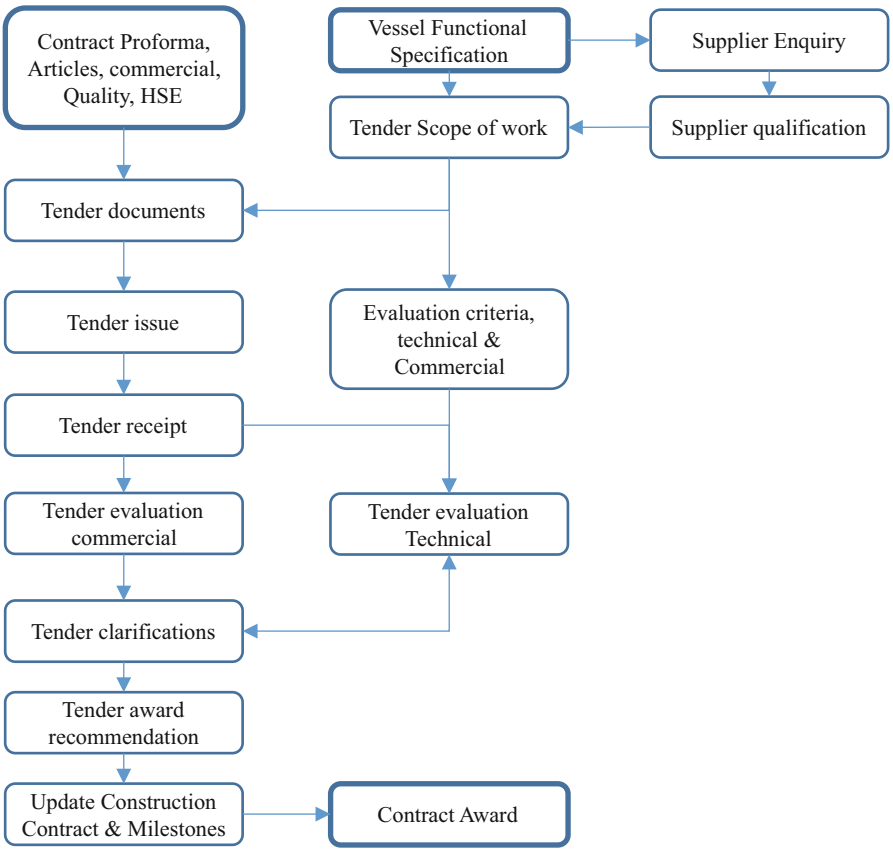

Fig. 14.4 Construction contract preparation flowchart

Client Handover Requirements

- Deliveries including maintenance and spare parts planning proposal, personnel training, and so forth prior to vessel delivery
- Vessel trials, acceptance, and delivery process, including terminal compatibility and turnaround times between services
- Warranty period

Operation Lifecycle Costs

- Terminal usage including personnel and vehicle access, parking, and boarding control
- Services and consumables, including
  - Most craft – daily internal cleaning, replenishment of consumables
  - Fuel and water supply routines
  - Onboard sales supplies
  - Harbor/terminal interface and costs (more complex for larger craft)

- Maintenance and spare parts inventory management, setup, and operation
  - Annual or regular slipping and docking for hull cleaning
  - Engine, gearbox, and water jet/propeller/thruster routines (manufacturer)

Obsolescence Planning and Sell-On

- Expected life to replacement or redeployment and estimate of residual value at that point

While some owners may wish to develop operations and cost of ownership economics themselves, the aforementioned subjects as such will need to be discussed with the designer. It would be helpful if the designer could develop a knowledge of the costs and the financial factors that influence an operator's economic model, even if this is done as a reverse engineering exercise, as this can give insights into operator preferences.

The view of an operator will be different if he has a long-term contract for a ferry service with a local authority compared with starting up a new route as a purely commercial venture, where they may have to find a different route for the vessel(s) if the commercial model proves less economic than necessary to finance the operation. In the first case, financing for the operation is low risk, while for the latter case external financing may entail higher costs to the operator.

Operational service failures are important to get feedback from by the vessel designer and builder (and keep a dossier), as they will need to give an explanation on the reasons for such failures to subsequent prospective clients.

Figure 14.4 indicates the activities toward the end of concept design where the detailed plan together with the cost estimates and economics are prepared, leading to contract preparation and discussions.

Figure 14.5 shows a concept design phase plan. As detailed design proceeds, the uncertainties in performance, construction, and outfitting will decrease, so that the delivery cost and vessel economics can be estimated more precisely. During detailed design the schedule may therefore be updated. One potential milestone for updating the schedule would be the point at which model tests are completed and the results incorporated into the design. There would be a second update at or close to the end of detailed design when the shipyard contract or service agreement with the construction department of the shipyard is formalized based on so-called approved for construction (AFC) drawings and documents.

The decision regarding the timing of the main contracts is related to the level of uncertainty with respect to design growth and overall project risk margins borne by the designer and constructor versus the ability to finance the project to that point.

The contract with the client will be signed prior to the start of detailed design and will incorporate the designer/shipbuilder's "sunk costs" up to the point of signing the main contract and either including these in an up-front payment or as part of the stage payments. If the designer is an independent organization, this development phase may have been financed separately as a fully or partly funded engineering study by the client.

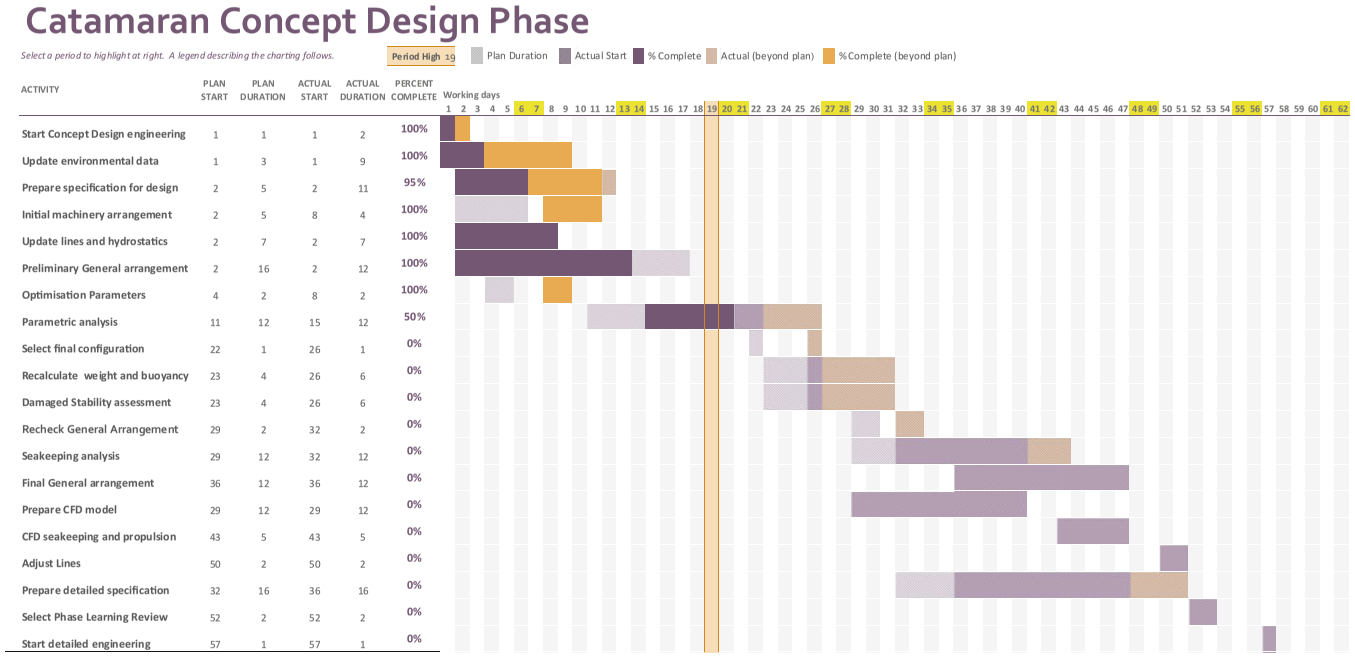

Fig. 14.5 Gantt chart for concept design phase

In either case, if the organization (shipyard or independent) intends to develop a vessel class with the design, the development costs up to this point may be spread across the expected vessel market, with the refunding from vessel projects being aggregated at net present value to avoid hidden economic loss.

Returning to the preparation of the plan and its agreement, the best time to start is while the weights and centers are being updated for the preliminary designs. Many tasks are generic with resource and duration related to the vessel size. The plan should include the main elements shown in Fig. 14.5 and then be updated with a more detailed plan for the construction phase during discussions with the construction department or shipyard so as to reflect the construction philosophy and schedule risks.

It is worthwhile discussing how to define the content of these main activities, the resources and interlinks. A naval architect is not normally an expert planner, while planners need significant information to develop a reliable plan and schedule (do not allow planners to make assumptions on their own – a good planner will always cross-check all data with the activity owner, hopefully using open questions to ensure the context is also correct!). The key here is for the engineer to be clear about the task deliverable definition, resources, schedule risk, and the schedule float necessary to deliver with at least 75% confidence (a 50/50 level of confidence is too risky).

Once the overall plan has been defined using planning software such as Microsoft Project [1] or Primavera PS6 [2] (or spreadsheet template tools for simpler projects), the critical path(s) can be identified and reviewed. Some links are in the resource section, while [3] is an example of a detailed textbook on project planning for engineering and construction projects following UK and European standards.

Simpler tools can be used to analyze the activity linkages in a forward pass, while "heavier duty" tools such as Primavera make a backward pass also to cross-check. If you (or a project planner working for you) use a simpler tool, it is worthwhile reviewing manually your planning model backward from the delivery, working from the critical path, checking that tasks are linked to it to ensure float is greater than zero, and stepping out to these secondary tasks to make sure that the sequence leading to them also has positive float.

Float on the critical path itself can be inserted and managed in several ways. Appropriate float can be attached to each critical path task or a "hammock" float added in to each major project milestone, or the float can simply be added as a single item prior to delivery. There are pros and cons with each of these approaches. The last approach will lead to a project that will progressively look more delayed compared with the original plan (which will not give a client confidence). The first approach aligns with the work for developing the plan in the first place, but normally the confidence level is simply built into the activity duration as a margin by the engineer or planner, so it makes sense to place "float" tasks just prior to significant milestones where a string of activities results in a building block or vendor delivery. The float can be assessed by discussion of the task string using a logical approach or by probabilistic schedule modeling using a specialized planning tool (Primavera PS has a routine built into the system for this).

A sample project schedule for a concept design phase including inputs from concept screening phase is shown in Fig. 14.6 below identifying float activities at milestones.

So what are we trying to achieve with our project plan? The delivery schedule is a core element, but this can only come together once the construction philosophy has been defined, as well as the concept being selected. By this time, at the end of concept selection, the designer, construction department or candidate shipyards, and client will all have an idea of what the vessel should look like and how to build it.

As mentioned earlier, the expectations of all parties will be to be able to identify their roles and deliverables so as to enable contractual agreement between the parties. The contracts will be able to be signed and work started once financing has been confirmed, contingent on the contracts.

If the designers are part of a shipyard, the construction philosophy will already be known, and this will be incorporated into the planning and contract proposal from the design department to the client.

If the client contract involves a designer, it would need to be "back to back" with a shipyard contract or memorandum of understanding (MOU). To commit to a construction contract, the shipyard will need the structural arrangement agreed to and the design flexibility available for construction detailing and optimization. Particularly if the construction is to be tendered to multiple shipbuilders, there needs to be time for proposals to be prepared and evaluated. An example activity string is shown in Fig. 14.4. It is important that sufficient time is allowed for this work, as the initiation of detailed design indicates a commitment to the project, and any delays that arise compared with the agreed project plan will incur costs and possibly penalty payments.

14.6 Detailed Design

Having made the vessel concept selection and completed preliminary design, followed by vessel specification updates, and development of the input to a project plan, schedule, and delivery contracts, we are now ready to follow through, in two phases, first completing the detailed design and procurement for the vessel, and then completing construction.

A detailed design schedule is outlined in Fig. 14.6 below. Detailed design is constrained by two major inputs – specification data for equipment and systems and materials data including the hull and superstructure primary structure material and the jointing specification whether that be weld specifications or nonmetallic joint design standards. Once these are known, the design schedule will depend on people, resources, and expertise. In both cases it is important to consider the risks for delays due either to a lack of information from vendors or resource constraints during the main design period.

It is convenient for both designer and shipyard construction to have a schedule of milestones and reviews that cover, for example, the following types:

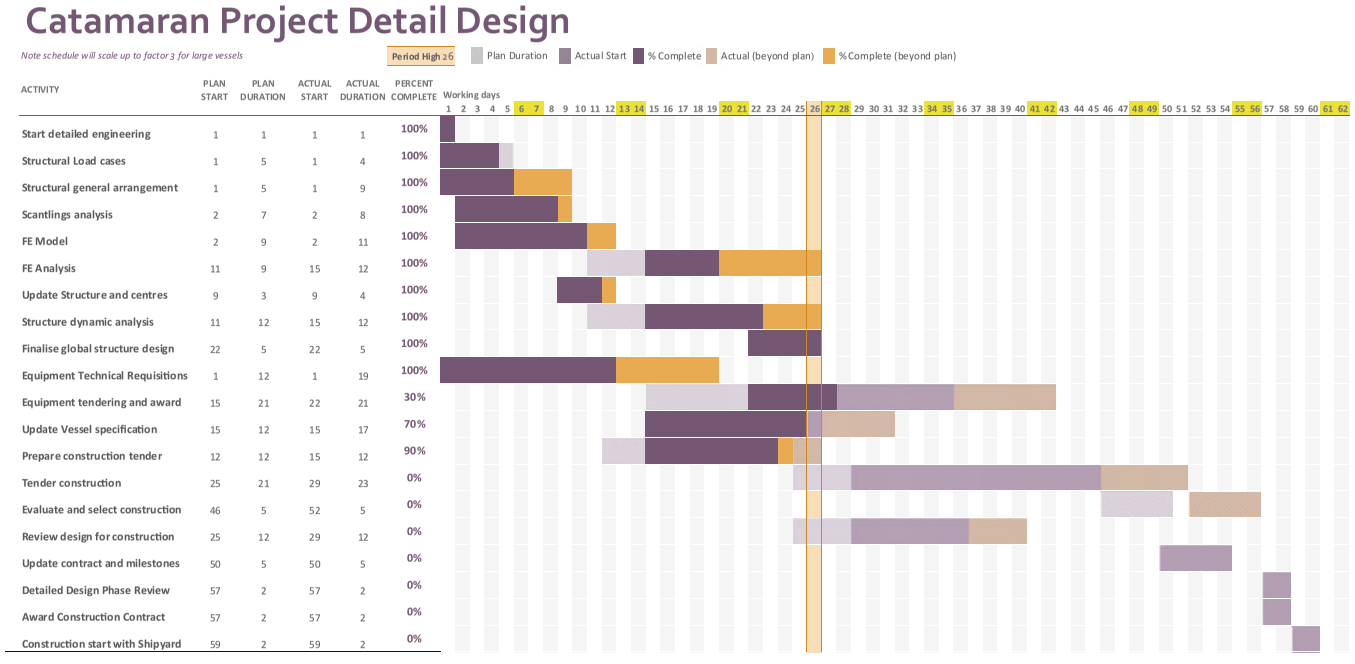

Fig. 14.6 Gantt chart for detail design

- Structural model hot spot review after stress analysis, hull, superstructure, and interconnection
- System reviews for fluid piping, hydraulics, electrical system, instrumentation, and HVAC
- System review for main machinery after general arrangements for assessment of maintenance access
- Layout and architectural outfit review for passenger spaces, freight and vehicle spaces, and crew and utility spaces
- Safety review following system design to validate against regulations
- Performance review to check that this remains on target and adjust design of stabilizer systems if appropriate

Completion of these reviews will enable the designer or design department to give the go-ahead to the construction design department or the shipyard design department to continue and complete the design for construction by freezing the specifications. The detailed design schedule will then have in its later period a sequence of AFC dates. These define the starting point for the shipyard to begin fabrication and construction, assuming the materials needed are available on site.

While "stock" materials may be immediately available, it is likely that many vessel-specific items will need to be procured. The lead time for their delivery will then affect the construction schedule and, perhaps, some sequencing.

Bulk items (e.g., piping, structural materials) are normally available quickly, while instrumentation has a much longer lead time, and the main mechanical equipment (main engines, propulsion, generators) may have to be committed in the concept design phase, or at least the main contracts must be signed immediately in order to meet client delivery requirements.

As was mentioned in the previous section, model testing for the selected concept might be carried out early in the detailed design phase. If the delivery schedule is not tight then it is convenient to carry out testing at this time and ensure the hydrodynamic design is the best possible. This may also be guided by financial constraints if the concept phase is carried out as a study funded by the prospective client.

Once this work is completed, the vessel's overall configuration must be considered frozen. The issues affecting vessel performance from the detailed design phase will then be the weight growth of the hull structure and architectural outfitting and eventually the performance in operation of the propulsion system – motor(s) and propulsor(s) combined.

Ideally, a project will have a growth allowance for weight increase (at the detailed design phase, perhaps 5%), and the main propulsion will have a track record of previous installations so that the thrust efficiency and margin for accelerating to service speed will be sufficient to maintain contract service performance.

Once the vessel itself has completely reached approved for construction (AFC) status, attention in the design department turns to monitoring the ongoing construction activities and to receiving all the data from vendors, including recommended spares to prepare the operating and maintenance manuals for the vessel, procuring the spares necessary for commissioning the vessel, and initial holding of spares by the operator.

14.7 Construction

This book looks at the fast multihull design from the naval architecture point of view – a project management perspective – rather than the details of construction, so we stay at the overview level. It is important nevertheless to look at the construction process and see how it interacts with design, so that the designer can learn from feedback and, where necessary, guide construction to ensure that quality is maintained relative to technical specifications. The construction schedule developed by the shipyard's construction design department will look at things at a much greater level of detail and with shorter timespan activities so as to effectively coordinate fabrication and construction on a day-to-day basis.

It can be seen from Figs. 14.6 and 14.7 that detailed design and construction are not sequential but have considerable overlap. Design of much of the outfitting systems will be phased later than the main hull structure. The installation sequence will generally follow construction of the main hull or demihull structures and the bridging structure. Larger vessels are assembled from hull blocks constructed in parallel in a fabrication hall. The main superstructure will also be fabricated in a hall as a single unit or in sections. The hull sections will be assembled and main engines and propulsion installed while access is simplest. If the upper-level superstructure is to be resiliently mounted to the main hull structure, this last must be structurally complete before the two units are mated. Preinstallation of piping and ducting sections to the hull or superstructure blocks can be convenient to minimize overall vessel construction schedule as long as the spool hookup is carefully planned for access.

Weight monitoring should be carried out regularly throughout construction. This is important for the build and also produces valuable data for future designs. If a vessel is being built by the shipyard at which it is also designed, then such data should be available from the outset of concept design so that allowances and margins can be refined to minimize construction costs as well as ensure the vessel meets its performance specifications.

Once the vessel is in construction, the main follow-up issue for the designer is to quality-assure construction against technical specification. This progresses from bulk-material quality for structural fabrication, through welding, jointing, and non-metallic material layup, to quality of vendor deliveries, equipment and system installation and function testing, architectural installation, and area completions. An efficient system for the documentation and acceptance of completion from construction to mechanical completion, function testing, and eventual system startup is an important tool for all parties, including classification societies and regulatory bodies that must approve the vessel.

The activities related to these tasks also require careful planning and interaction between design and construction. Electrical circuit and instrument loop testing can be time consuming, particularly where faults are found. Correcting faults is not usually a problem; the issue is tracing the cause, which is where the designer can help. Vibration and transmitted noise from machinery can be another time-

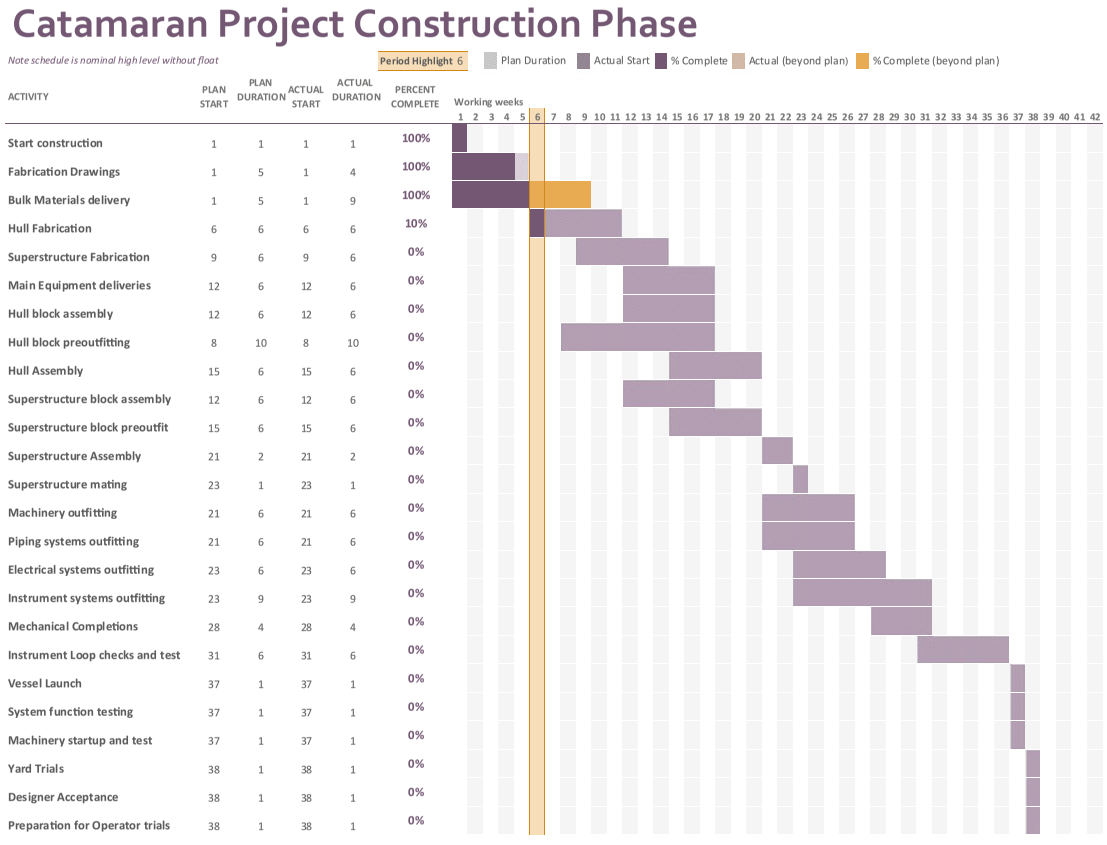

Fig. 14.7 Gantt chart for construction phase

consuming problem, whose solution in this case entails finding a simple solution to dampen out the noise. HVAC ducting can be an annoying source here, as it can serve as a medium for transmitting noise to passenger or personnel areas (in the "old days" ships used to have a speaking tube for communication from engine room to bridge).

Construction needs to have some float at least to "problem solve" in the later part of construction, and designer input to help solve such issues also needs planning – so the project should not let the designers go too early!

The designer or engineering department will normally take on the responsibility of preparing operating and maintenance manuals. Completion of these will depend on the receipt of vendor documentation for operation, maintenance, and spares. It is normal for these data to be assertively followed-up. As the key focus of a vendor is delivery of the hardware for their payment. Retention of the documentation is useful but is not a guarantee of efficient delivery, so it will still be necessary to chase.

14.8 Trials, Handover, Operation, and Feedback

Once the construction, mechanical outfitting, and functional testing have been completed while the vessel is at quayside, sea trials can be carried out, initially by the shipyard and subsequently with the owner. A sequence of runs at different payloads and in different sea states will need to be run to verify performance against specifications.

During this testing, adjustments may need to be made to the main machinery, so vendor representation may be necessary for a specified period. Vendor attendance can also be used to verify that installation is to specifications, that the transmission is aligned, and on initial runs that machinery vibration and noise is within specifications. A summary schedule for commercial vessel trials and handover is shown in Fig. 14.8.

Vessel trials in different sea states will allow adjustment to stabilizers and trimming mechanisms and measurement of motions and accelerations.

Once the program agreed to with the owner is complete, the vessel will be delivered to its operating base, either by self-propelled voyage or as freight aboard a suitable break bulk cargo ship.

If it is a military vessel, there will be an intermediate stage where the vessel will have its mission outfit installed, followed by trials for operating this equipment. This phase may be almost as lengthy as the initial vessel build.

Once delivered to the operating location, the vessel will have to complete trials for interface to the quay facilities, passenger and vehicle loading (perhaps using operator company personnel), and trials for deployment of evacuation life rafts and successful passenger transfer in order to win approval by local marine regulatory authorities. Once these trials are all passed, operations can start.

The designer and builder will retain an interest in the vessel for at least the first year or two while warranty is still in place, with back-to-back warranties for items such as the main engines, propulsion and electronic equipment.

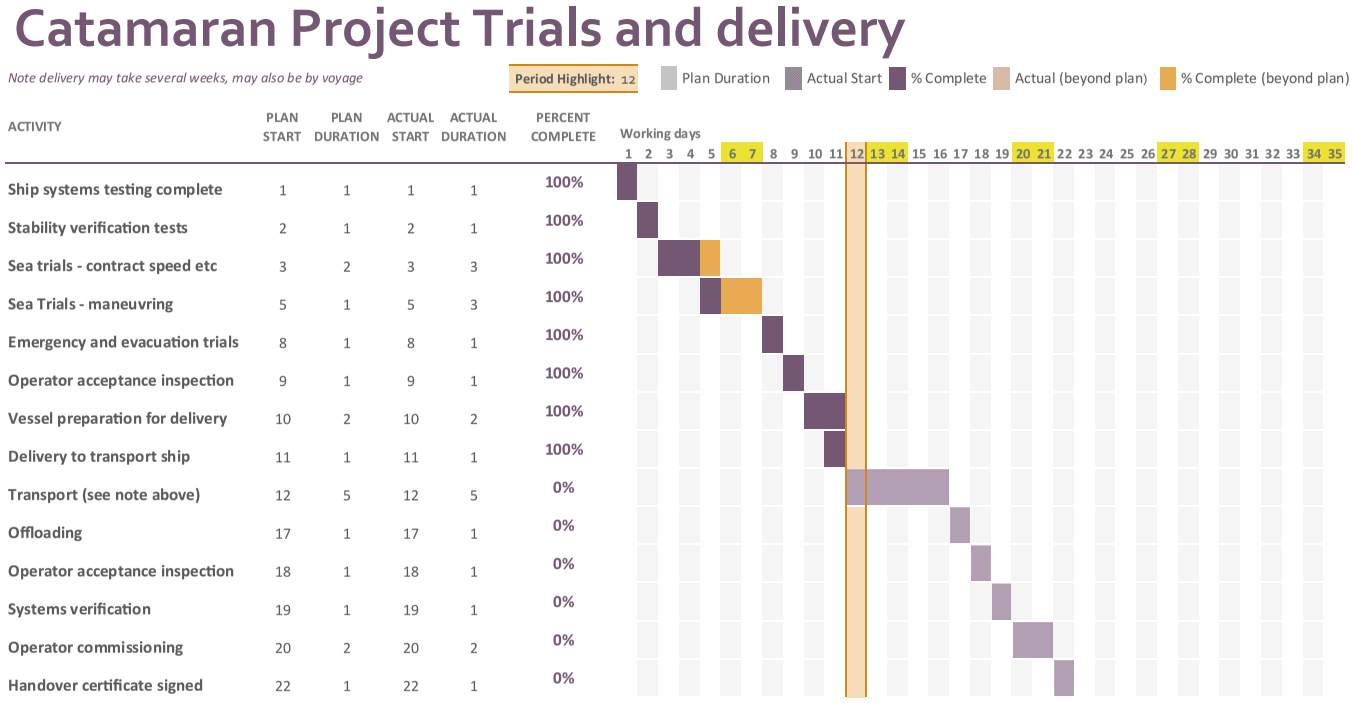

ACTIVITY	PLAN START	PLAN DURATION	ACTUAL START	ACTUAL DURATION	PERCENT COMPLETE
Ship systems testing complete	1	1	1	1	100%
Stability verification tests	2	1	2	1	100%
Sea trials - contract speed etc	3	2	3	3	100%
Sea Trials - maneuvring	5	1	5	3	100%
Emergency and evacuation trials	8	1	8	1	100%
Operator acceptance inspection	9	1	9	1	100%
Vessel preparation for delivery	10	2	10	2	100%
Delivery to transport ship	11	1	11	1	100%
Transport (see note above)	12	5	12	5	0%
Offloading	17	1	17	1	0%
Operator acceptance inspection	18	1	18	1	0%
Systems verification	19	1	19	1	0%
Operator commissioning	20	2	20	2	0%
Handover certificate signed	22	1	22	1	0%

Fig. 14.8 Gantt chart for trials and delivery

14.9 A Successful Multihull Project

A successful project usually results from having a team whose members work well together. In such cases, the team must include the operator client, the naval architects (designers and project management), and the shipyard or shipyard detailed design and construction departments. While contractual arrangements or service agreements between them will be in place, a loss to one is a loss to all. Since errors do occur across the whole range of tasks, the risks from these need to be understood and mitigation put in place. With defined mitigation as backup, a project can progress successfully.

Planning and executing such a project is not a static exercise, and that is one reason we have walked through the different phases looking at plans for each of them. The main thing is to recognize that knowledge is developed and refined in a stepwise manner, so unless a vessel like the one in the present project has already been built by the same shipyard, uncertainty needs to be considered a bit like a funnel.

Planning is about establishing a reliable linkage between technical definition, resources, and schedule. Where activities can be run as separate processes from the resource point of view, as long as a technical definition is available, the work can proceed in parallel. Until a task is completed (including necessary quality control), there will remain some uncertainty. Once it is complete, though, there is no further need for float or contingency against that task. Because of this, the schedule float can steadily be managed to zero at delivery, and the cost contingency can follow the same process. It is usual in projects for the contingency and float management to be reviewed at major milestones, for example at the start of fabrication and upon completion of the hull/superstructure assembly.

A prototype or first of class will require the maintenance of greater contingency and float until later in the project (do not relinquish it too early, only to regret it later). The better the risk profile is understood, the easier it is to refine the management process.

Where float or contingency is not explicitly specified, it is useful for a design department or designer to carefully monitor the outcome of a procurement or task to compare with the original baseline plan and estimate. In this way guidance can be built up for float and contingency management in subsequent projects. That is not to say that one should simply replicate. It serves as a basis for review and the implementation of an improvement process. To improve, one needs to know what can be changed and what is the potential for making changes. One area is actually avoiding change once design is frozen. It is important to compare against the original baseline plan, not staged updates. Particularly for a prototype there will be considerable change, and it is important that these lessons be accepted, not hidden or explained away. This can be applied to an integrated shipyard, a designer, or a shipyard using a designer's plans and support.

Where changes are shown to be needed, change management is important to implement as a formal process once design elements are frozen. For this to be

successful, it is necessary to have a definition of a change written into the contract. If the vessel is built at a shipyard by contract with a designer, the shipyard will be keen to have this well defined. If the project is within a shipyard, this will need to be written into the service agreement between the construction department and design and the status regularly monitored by both teams.

14.10 Closing Out

This chapter has been all about the process and the controls needed to manage a project involving a multihull vessel. We have reviewed the process in a generalized way. For smaller vessels many of the phases can be simplified. The principles apply nevertheless. It is recommended to look at the issues referred to here and address them all up front, simplifying where it is applicable. The main thing is to recognize that the whole process is one of positively managing steadily reducing uncertainty and risk. If a measurable reduction in risks for the project as it progresses is not achieved, then the project is not under control and needs reassessment rather than soldiering on in hope. Milestone reviews are a useful way to ensure control is maintained in a stepwise fashion.

The first key risk that the designer must manage is selecting the "right" concept to take into preliminary design. With a multihull vessel there is the possibility of "optimizing" vessel motions in a seaway at normal operating speed and in normal sea conditions, so operator expectations must be managed carefully as to how much can be achieved. The concept selection needs to be robust – do not aim too high too early – give yourself some room for maneuvering. Nevertheless, do set some targets. Think also in terms of a vessel design series; the second and following vessels in a series or class can build in many lessons from the first model or prototype, – so long as the lessons are captured for future use!

There are lots of options to consider, and while they do have to be addressed, it is important to close them down as efficiently as possible once the choices have been agreed upon from screening.

The second key risk is delivery schedule and cost. The operator will have commitments for vessel service operation that mean project delays will be costly to them. Both schedule delays and design changes will result in costs that cannot be reclaimed by the designer and will eat into project return. The contracts set up at the end of concept selection and preliminary design are what controls these last elements, so this phase leading up to contract commitment is crucial to success on all sides.

Another issue here is that if a design is developed by a naval architectural house and is to be built as a standard design, it will be important that agreements with shipyards and suppliers take this opportunity into account, as otherwise the benefits of repetition will not be realized, at least by the naval architect and client. A shipyard and suppliers may have considered each vessel as a one-off contract, with its startup and closeout costs.

Shipyard experience with high-speed vessels and multihulls in particular is a key to success. This is now widespread across the globe. Yards do have a tendency to specialize, so there are a number that specialize in very large vessels, another group building smaller passenger ferries for example, and another one building vessels for the offshore wind farm maintenance market. We have compiled a list (please consider this an incomplete sample!) of designers and shipyards for initial reference, valid at the time of publication. These appear in the resource listing at the end of this book, together with their website addresses.

A design will not come together efficiently unless a design group and project team have a plan to follow and criteria to make timely decisions, as discussed here. I have placed the chapter on project management at the end of the book, though in actual fact it is the first issue that needs to be addressed by a naval architect. "Plan the work and then work the plan" is one good way to look at it, while pulling a plan together and delivering it requires teamwork and commitment, not just a planning specialist.

You will also probably be scanning this as you are about to put the book down, having also run through the final chapter at a good clip. I would invite you to take a look again after letting things sink in somewhat and after you've given your idea for an amazing new design to mature. Follow the roadmap, and it will take you back logically to the sequence followed by Chaps. 2, 3, 4, 5, 6, 7, 11, 12, and 13. Between Chaps. 8, 9, and 10 it may be useful as a means of considering alternative configuration options.

This, I suppose, is what makes this a textbook – it is a tool rather than simply a descriptive text. I hope that it will really be useful in that respect.

These days, a textbook can make a statement at a particular point in time. In contrast, we now have a constantly developing resource on the Internet. I have gathered a collection of reference locations in the resource section. They cover the main actors in the business, which should minimize the time it takes you to home in on most topics. What it does not do is lead you through the often not so logical structure of the sites. There is such a variety that the best advice is to take your time and dig around, using different search criteria as you might when using a browser as such. There is a wealth of material there. The classification societies all have their material available directly for download, while the IMO does require that you order and pay for its documents.

One other area where a membership or access through a university library is needed is materials published by the UK Royal Institution of Naval Architects (RINA) and the US Society of Naval Architects and Marine Engineers (SNAME); I have used both of these resources throughout the book. Much of the material by these societies is now available online on their websites, so enquiry on the societies' websites can be one approach. Universities are now putting much of their research into online repositories, some open and some closed, which is where reports by Southampton University are available, for example. Today's university students are no doubt completely up to speed on these sources!

An area more difficult to access easily is computer modeling. A whole range of tools are now available, and the main ones are all proprietary and at budget levels only supported by a commercial organization or a university. Learning to work with

the software, whether for hydrostatics, dynamics, or structures, is a competence requiring patience and commitment. University courses now include exercises in using the more popular tools to prepare models and run statics and dynamics. These can enable a student to experiment with demihull forms and vessel configurations, all the while getting used to the techniques of choosing appropriate element types and sizing and to optimizing the time taken to reach steady state or equilibrium.

The market is changing as this book goes to press, the vessel type is now embedded globally in the passenger and RoPax ferry market, and while this continues to develop, it is areas such as offshore crew and material transfer that are still developing and exploring the full range of configurations from SWATH to catamarans to trimarans and SESs.

LNG as a fuel has taken a step forward for the largest vessels, while hybrid and electrical powering is now practical for smaller passenger multihulls, at least at the lower end of the speed range. The development of power trains and battery storage systems is a work in progress in the car and truck markets at present, but should be economically attractive for local fast passenger ferries before too long. Society's rapidly increasing demand for a transition to renewable resources and zero-emissions powering will probably lead to requirements that ferries in the next cycle of vessel replacement produce zero emissions. The current round of development will then follow the traditional route to operation in the developing world.

I hope that readers will accept this book as a useful naval architecture tool and find it thought provoking. If they do, it might just be the spark for some new ideas, which would be a very rewarding result, indeed!

Alan Bliault
Sola
February 2018

References

1. Chatfield C, Johnson T (2013) Microsoft project 2013 step by step. Microsoft Press, USA ISBN: 978-0-7356-6911-6
2. Harris PE (2015) Planning & control using primavera P6 oracle primavera P6 versions 8.1 to 8.4. Eastwood Harris Pty Ltd, Victoria ISBN: 978-1-925185-02-7
3. Lester A (2007) Project management, planning and control, 5th edn. Elsevier, Holland ISBN: 978-0-7506-6956-6

Resources

In what follows, we list a selection of publications that give regular information on multihull vessels and a selection of Internet sites that can form a starting point for technical search. First the publications.

Publications

Fast Ferry Information
Fast Ferry HPMV database details of vessels, designers, shipyards, operators, and general information updated regularly and with a quarterly newsletter for fast ferries. Visit www.fastferryinfo.com for details. Published by Fast Ferry International, ISSN 0954 3988, 10 times annually up until end of 2011.

Ship and Boat International
The Royal Institution of Naval Architects (RINA), London, ISSN 0037 3834. Also Warship Technology published by the RINA, ISSN 0957 5537. Both journals have articles on high-speed craft. Find the RINA at www.rina-org.uk.

FAST Series of Marine Conferences on Fast Sea Transportation
These biennial conferences cover design and technology research for all types of HPMV. The papers have become steadily more analytical since the first conference in Trondheim in 1991. Visit www.fast2017.com for more details or do a search on "Fast Sea Transportation Conference."

Shippax Journal and Database
General ferry website and journal, ferry database at www.shippax.com. Includes regular fast ferry news data.

L. Yun et al., *High Speed Catamarans and Multihulls*,
https://doi.org/10.1007/978-1-4939-7891-5

Norwegian Shipping List
Illustrert Norsk Skipsliste, annual publication of three volumes in January each year, Publisher Shipping Publications AS, ISBN-10/ 978-82-90528-28-0. Volume 2 lists current ferries/fast ferries, navy, and pilot vessels in service in Norway, including fast catamarans. Refer also to database at www.skipslistene.no.

Boat International
Boat International Media Ltd., London, UK, ISSN 0264 9138. Monthly magazine focusing on superyachts and chartering. Go to www.BoatInternationalMedia.com for details.

Yachts France, Lux Media Group, Cannes, France

Monthly magazine focusing on fast motor yachts and superyachts. Go to www.luxmediagroup.com for details.

An annotated selection of websites that are useful for following up is given below. The sites are grouped by subject area. Please note that the listing is not exhaustive. The idea is to give you a place to start. We have also given additional direction to pages that are directly useful as many of the sites for large companies or groups have different ways of presenting their information, and finding the area for information relevant to our subject of fast multihull vessels is not always intuitive.

It is also important to note that companies do change, getting absorbed into larger organizations, and some more specialist organizations seem to have passed further on to different larger organizations. Our advice is that if the link doesn't work for you, try searching on the main name and see if parts of the address have been changed, perhaps .co.uk to .com, for example. Please do be careful to check that a site is genuine if searching on keywords, as there are many fakes out there. It is important to have virus protection installed on your computer. Happy hunting!

Societies
The best societies to start with are RINA and SNAME, as they publish research papers and technical journals. A keyword search will turn up useful information put out by many other societies and special interest clubs.

www.RINA.org.uk	Royal Institution of Naval Architects (London, UK)
www.SNAME.org	Society of Naval Architects and Marine Engineers (NY, USA)
www.foils.org	International Hydrofoil Society
www.MARIN.nl	Netherlands Test Basin and Hydrodynamic Research

General

www.usn.mil	US Navy
www.uscg.mil	US Coast Guard
www.ONR.Navy.mil	Office of Naval Research, USA
www.royalnavy.mod.uk	British Royal Navy
www.theblueriband.com	History and ship information of Blue Riband Trophy
www.janes.com	Search on High-Speed Marine Transportation for further details
www.pvs.kcc.edu	Hawaiian voyaging traditions . . .

Universities

www.NTNU.no	Trondheim University and Test Basin
www.engineering.unsw.edu.au	University of New South Wales at /mechanical-engineering/Naval Architecture. Professor Laurie Doctors and his book on the hydrodynamics of high-performance marine vessels (see books below). Degree now suspended.
www.utas.edu.au/	University of Tasmania, Marine Technology and Naval Architecture, with extensive list of research papers available on request at www.eprints.utas.edu.au.
www.ucl.ac.uk	Search under /mecheng, /our-courses, /postgraduate/naval-architecture for courses, research, and contacts
www.southampton.ac.uk/	Search under engineering maritime engineering, ship science, naval architecture for naval architecture courses and contacts
www.wumtia.soton.ac.uk	/about-us/published-papers/high-speed-craft-code-review for high-speed craft reviews by Southampton University, including wind heeling moment research
www.theses.gla.ac.uk	University of Glasgow library and repository for theses; look under Sect. v for naval and naval architecture
www.wegemt.com	European universities' summer school papers, includes HPMV
www.boatdesign.net/	At web/schools.htm giving useful list of schools for naval architecture

Catamarans and Trimarans

www.austal.com	Austal Catamarans
www.amd.com.au	Advanced Marine Designs – wave piercer specialists
www.incat.com.au	International Catamarans – wave-piercing catamarans
www.revolutiondesign.com.au	Incat's design group
www.incatcrowther.com	Catamaran designer and builders linked to Incat, UK, USA, Australia
www.kvichak.com/	Builder on US West Coast, works with Incat Crowther
www.gladding-hearn.com	/product/catamaran-ferries/ catamaran ferries and wind farm vessels

(continued)

www.damen.com	Damen Shipyard – catamarans
www.cocoyachts.com/	Design house based in Gorinchem, Netherlands, that works with Afai and others for ferries in China
www.fjellstrand.no/	Fjellstrand
www.batservicemandal.no	Go to /vessels for full listing and details including wind farm, Danube, Norway coastal, and so forth
www.um.no	Umoe Mandal, designers and builders of catamaran ferries and surface effect ships (SESs) for wind farm service (see also www.wavecraft.no)
www.braa.no/	Brødrene Aa, builders of composite hull fast catamaran ferries and others
www.oma.no/	Oma båtbyggerie, builds aluminum fast ferry and utility catamarans
www.rodriquezconsulting.com	Consulting arm of Rodriquez, hydrofoil pioneer and catamaran designer in 1980s and 1990s; based in London and focusing now more on superyacht and internal outfitting
www.intermarine.it/en/homepage	Construction group of Rodriquez for hydrofoils, catamarans, trimarans, and so forth; has also developed stabilization foil systems for multihull fast ferries, initially in-house. Now produces fins, intruders, and T foils
www.wangtak.com.hk	Go to /html_en/shipbuilding.html for fast ferries; builds in Guangzhou
www.afaisouth.com/en	Afai Southern Shipyard, part of CSIC, works with Damen and CoCo Yachts, as well as AMD for fast catamarans; builds ferries and patrol vessels
www.aresaboats.com	/boats/passenger-vessels/aresa—fcat range from Spain shipyard
www.cheoylee.cn	Catamaran passenger ferry models 18 to 32 m at following location
	/?_page=models&_func=commercial_list&_lang=en&_para[]=9
	Works with Incat Crowther and Cummins engines, based in Hong Kong
www.harleyshipbuilding.net	Designer and builder of air cavity catamarans
www.mobimar.com/	Boat builder in Turku, Finland; designs and builds catamaran and trimaran vessels in range of 12–35 m for utility, wind farm access, and ferry vessels

Designers

www.amd.com.au	Advanced Multihull Design consultancy
www.one2three.com.au	Cat and trimaran designers
www.marinteknik.se/	Designers of catamaran ferries now under www.Bokseng-ipl.com as Marinteknik International Pte. Ltd., Singapore
www.bmtng.com	Site for BMTNigelGee catamarans, SWATHs, and a wide selection of fast ferries and utility vessels
www.gdlcs.com	General Dynamics site for LCS program
www.adhocmarinedesigns.co.uk	Personnel from former FBM catamaran builder in Cowes, now supporting wind farm vessels and ferries; uses QinetiQ design software

(continued)

www.QinetiQ.com	Site test basin and design analysis, navy built on PLM from Siemens
www.multi-maritime.no	Norwegian Designer of fast craft and catamarans at /mmdesign/high-speed-vessels/
www.amdesign.co.th	Albatross Marine Design site for designers of catamarans and fast vessels
www.mpyd.net	Michael Peters Yacht Design, racing heritage, race boats – fast cats
www.invincibleboats.com	Ventilated stepped V hulls as from mpyd
www.aeromarineresearch.com	Tunnel boats – HS cats, design books, and software
www.revenger.co.uk	Stepped hull Rigid Inflatable Boat (RIB)s
www.lornecampbelldesign.com	Planing and racing craft – cf. presentation on steps
www.alionscience.com	Owner of Proteus but site doesn't link
www.proteusengineering.com	Naval architects – motion analysis and other ship design tools, as previously, for download
www.cdicorp.com	/engineering/government-services/naval-architecture-advanced-ship-design/ including Band Lavis Group working on ACV and catamarans and others
www.nigelirens.com	Nigel Irens consultancy, extreme trimaran designs
www.cmn.group.com	CMN in France – Nigel Irens extreme trimarans
www.multihulldesigns.com	Kurt Hughes Sailing Designs for multihulls and others; designer supplies plans and so forth, including for yards to build ferries e.g., a 61-ft ferry at 28 knots; in Seattle, WA, USA
www.sabdes.com	Designer of concept and superyachts and interior/exterior styling for including Incat, Hysucat; based in Hobart and Melbourne
www.keelmarine.com	Naval architects, designs wind farm catamarans

For Catamaran Operations (A Small Sample)

www.turbojet.com.hk	Hong Kong operator of cats and foilcat
www.kumamotoferry.co.jp	All about ocean arrow SSTH/70 (option LFS of screen)
www.alilauro.it/flotta	Italian fast ferry operator
www.Pentlandferries.com	Ferry operator of semi-SWATH
www.corsicaferries.com	Corsica Ferries, fast Ropax ferry operator
www.torghatten-nord.no	Fast catamaran ferry operators in Norway, Nordland and Troms area
www.caspmarine.com/	Offshore fast transfer, including catamarans
www.wm-offshore.com/fleet/	Offshore fast transfer, including catamarans

(continued)

www.seacormarine.com/	Offshore fast transfer, including catamarans
www.swire.com.sg	Offshore fast transfer, including catamarans, at /Fleet.aspx#sub8

For Catamaran Construction (A Sample)

www.strategicmarine.com	Catamaran builders in Australia, Singapore, Vietnam for ferry, wind farm, and utility service
www.wightshipyard.com/	Isle of Wight shipyard specializing in fast ferries, built Redjet 6 in 2016, and 2 40m vessels for Thames Clippers in 2017; design is by One2three Naval Architects; works out of ex BHC facility in West Cowes.
www.aba-global.com	Aluminium Boats Australia, builders of catamaran ferries and fast craft, works with designers One2three
www.gladding-hearn.com/	Catamaran ferry builders, works with Incat Crowther
www.gulfcraft.com	Shipyard with catamarans at /catamarans
www.ozatashipyard.com	Shipyard with catamaran project at /w9675-nb-35-carbon-catamaran.html
http://samalu.com/	Sam Aluminium Engineering, Singapore, with 20 m cat project in 2017
www.wightshipyard.com	Builders of catamaran passenger ferries
www.bokseng-ipl.com	Builders of Marinteknik catamarans, at /marinteknik.html
www.allamericanmarine.com	Builders of passenger catamaran ferries, foil assist, and others
www.metalsharkboats.com	Builders of fast catamaran ferries and utility craft to Damen and Incat Crowther designs

SWATH

www.swath.com	SWATH International Ltd. of Bethesda, MD
www.navships.com	Navatek, designers of SWATH and submerged buoyancy craft
www.navatekltd.com/	Alternative site for Navatek
www.abeking.com	Abeking and Rasmussen, SWATH design and build
www.DanishYachts.com	Danish Yachts, design and build of CFRP SWATH (try Facebook also)

Cats with Foils

www.hysucraft.com	Hysucraft foil-supported catamaran development
www.fastcc.hysucraft.com	New site (old still operates)
www.hysucat.com	US foil-assisted RIB cats and fisher craft
www.teknicraft.com	NZ foil-assisted cats
www.missionkraft.com	UK designers of cats and foil-supported cats

Wind Farm

www.southboatsiow.com	Aluminum wind farm catamaran and workboat shipbuilder
www.alicatworkboats.com	Works in partnership with South Boats. Try /alicat-vessel-datasheets
www.safehavenmarine.com	Wind farm and utility cats in range 12 to 18 m and 24 to 30 knots
	Note Austal, Damen, Danish Yachts, Abeking & Rasmusen, and Umoe Mandal all design and build wind farm boats; a sample of operators follows
www.seacatservices.co.uk/	Uses boats from South Boats IOW with Servogear propulsion. Spec sheets for all their craft available on site. Forward open deck helps to load and unload container or gear as it noses to structure
www.turbinetransfers.co.uk/	Wind farm catamaran operators from Anglesey. Useful videos showing vessels at speed, operation of TAS system, personnel transfer, equipment lift, heavy seas, with semi-SWATH hull form from BMT, diving, and so forth. Includes film of what can go wrong (boat landing gone wrong) and boat recovery
www.Odfjellwind.com	Odfjell Wind Service, operates a fleet of fast SWATH wind farm service vessels
www.marintimecraft.co.uk	Maritime Craft Services, operates fleet of catamaran wind farm service vessels
www.n-o-s.eu	Northern Offshore Services, operators of a fleet of catamaran utility and wind farm vessels including SWATHs
www.Offshoreservice.de	EMS Maritime Offshore Service based in Emshaven; operates wind farm service catamarans and SWATHs

Personnel Transfer Systems

www.ampelmann.nl/	Hydraulic walk-to-work systems for personnel transfer offshore
www.houlderltd.com	Turbine access system developed with BMT and Turbine Transfers vessel operators, at /tas-turbine-access-system-steps-access-challenge/

Specials

www.americascup.org	America's Cup catamarans including videos
www.aeroyacht.com	Foiling cat yachts
http://www.class-1.com/	Class 1 offshore powerboat site, including high-speed catamarans

(continued)

http://xcatracing.com/	Xcat World offshore racing series site – exciting videos
http://cowestorquaycowes.co.uk/	Cowes Torquay classic offshore race site, now monohulls only
www.solarnavigator.com	Trimaran from N Irens
www.curvelle.com/	Catamaran superyacht designers – Quaranta
www.energy.sandia.gov	Hydrogen fuel cell catamaran study 35-knot, 150-pax ferry for San Francisco Bay area. Report available at
	/transportation-energy/hydrogen/market-transformation/maritime-fuel-cells/sf-breeze/
www.pvs.kcc.edu	Hawaiian voyaging traditions . . .

Rules and Regulations

www.lr.org	Lloyd's Register classification society
www.dnvgl.com	DNV classification society – high-speed service craft rules
www.eagle.org	ABS rules at /rules-and-resources/rules-and-guides.html
www.turkloydu.org/en-us	Lloyd's Turku classification society home page, go to /publications/turkloydu-rules.aspx# for regulations, part C High Speed Craft
www.krs.co.kr	Korean Register of Shipping classification society, technical rules listing – GB11 for HSC, GC06, and 07 for recreation and WIG
Rules at http://krsusa.cloudapp.net/Files/KRRules/KRRules2016/KRRulesE.html	
www.ccs.org.cn	China classification society, go to /ccswzen/font/fontAction!moudleIndex.do for high speed craft rules
www.gov.uk/	UK Maritime and Coast Guard Agency, go to guidance/high-speed-craft-construction-and-maintenance-standards#construction-standards-for-high-speed-craft
www.amsa.gov.au	Australian Marine Standards Association
www.sjofartsdir.no/en	Norwegian Maritime Authority, go to /shipping/legislation/#regulations
www.bureauveritas.com	Home page at /home/our-services/classification/
www.veristar.com/portal	/veristarinfo/detail/generalinfo/giRulesRegulations/bvRules/rulenotes for full rules listing, including HSC and others, items in red can be downloaded. Also link to erules. Erules loads a popup application also – takes too long for me. Note 396 is joint between BV, GL, and RIN from 2002 and so links also to DNV rules

International Organizations

www.ittc.info/	International Towing Tank Conference home page – source for guidance on model testing and hydrodynamic analysis including CFD for vessel and propulsors. Go to the publications list for PDFs of key procedures and guidelines. Full reports of each ITTC are available in the downloads section
www.imo.org/en	Home page for International Maritime Organisation – HSC Code and updates – HSC Code, can buy paper or electronic

Software

www.bentley.com	Maxsurf is at extension /en/products/brands/maxsurf. Hydromax is also documented on the site. Maxsurf is for hull modeling and statics, and Hydromax is for wave generation and drag
www.dnvgl.com/services	Go to /services/global-fe-analysis-software-shipload-18522 for DNVGL shipload, or /linear-and-non-linear-hydrodynamic-analysis-of-vessels-including-forward-speed-wasim-2413 for linear and nonlinear hydrodynamic analysis or /hydrodynamic-analysis-and-stability-analysis-sesam-hydrod-2410 for stability and linear hydrodynamic analysis or /marine-project-management-efficient-collaboration-in-ship-design-shipbuilding-and-aftermarket-synergi-project-18373 for Synergi Project Management
www.proteusengineering.com/	Fastship/for hull dev/Visual SMP ship motions prog from USN using strip theory. US-based with Alion
www.alionscience.com	Owners of Proteus – use Navcad resistance and powering (from Hydrocomp) GHS for stability and hydrostatics (from Creative Systems) and Visual SMP for seakeeping
www.hydrocompinc.com	Navcad speed and power, using 2D theory based on volume rather than surface ordinates
www.ghsport.com	Creative Systems Inc, General HydroStatics programs, used by Navatek and Damen
www.autoship.com	Detail design software
www.aerohydro.com	Multisurf 3D design and interface to WAMIT – note modeling, not structural, and depends on WAMIT for motions
www.boatdesign.net	Information network for boat design; useful site and software links
www.aeromarineresearch.com	Information site for power boat design including tunnel hull catamaran planing craft
www.hawaii-marine.com/templates/	Various spreadsheets for hydrostatics and planing hull resistance calcs including Savitsky (outside EU only to individuals)
www.aveva.com	Aveva Marine comprehensive naval architecture for ship projects, hull and outfitting design, including project workflow – initial – design for hull form, structure, and hydrostatic and dynamics, followed by materials, drafting, PDMS, systems, and fabrication setup as used by Hyundai and others
www.delftship.net	Hull modeler and hydrostatics, free and professional at eur150, plus extensions ref Danish Yachts
www.wumtia.soton.ac.uk/software	Southampton University Wolfson Unit Marine Design Software – free and to purchase. The free shipshape program can output to DXF as well as their own format for further processing

(continued)

www.rhino3d.com/	Rhino 3D modeler and rendering software available for PC and MAC. Eur 995 for full software or Eur 1700 for whole package. Works with NURBS surfaces, for example
www.orca3d.com	Builds on rhino modeling and provides hull design and fairing, hydro and stability, speed and power, and weight/cost tracking for around USD 3000
www.autodesk.com/products	Autodesk site for CAD products and integration with Solidworks and Nastran FEM
www.autodesk.com/navisworks	Autodesk CAD and Navisworks viewer and project management
www.solidworks.com/	CAD modeling suite
www.SSI-corporate.com	ShipConstructor 2017 based on AutoCAD and Navisworks, linking to modules mechanical, P&ID, Plant 3D, use for detailed systems design
www.napa.fi	Finnish company supporting major shipyards, also Far East links with AutoCAD
www.ptc.com	Software design site
www.adina.com/	FEM suite, German origin, with nonlinear analysis
www.plm.automation.siemens.com/en_us/	Siemens PLM home page with access to all products
www.mdx.plm.automation.siemens.com/star-ccm-plus	Siemens Star CD and CCM+ etc fluid simulation software for internal and general turbulent flows, earlier CDadapco Star CD and CCM+, now integrated into Siemens design automation solutions
www.paramarine.qinetiq.com/products/paramarine/Pages/default.aspx	Qinetiq Paramarine software builds on Siemens PLM parasolid modeling. Seakeeping via 2D Rankine source approach for frequency domain response, also has structural model aimed at naval projects; also used by Adhoc Marine and Keel Marine for wind farm catamaran design
www.mscsoftware.com	Home for finite element–based software including Nastran Structural design FEM software linear, fatigue and nonlinear, and multiple linked structures
www.ansys.com	At /Products/Structures/ANSYS-Aqwa
	Diffraction-based software for wave loads and links to ANSYS ASAS suite for structural analysis
www.ansys.com	At /Products/Fluids/ANSYS-Fluent
	CFD software tools including Fluent and CFX. Fluent is general modeling while CFX covers turbomachinery. Used by Navatek see brochure
www.openfoam.com/	Open-source CFD software – also has visual CFD
https://www.cfd-online.com	Go to /Wiki/Main_Page for lots of info, sources both open and commercial including mesh generation , visualization, etc.
www.sunrise-sys.com	Suppliers of pipenet piping system modeling for flow analysis including firewater sprinklers; go to /index.asp

(continued)

www.swan.tudelft.nl/	SWAN software from TUI Delft freely available for wave generation modeling in coastal areas and inland waters, so useful for wave wash
www.ptc.com	Mathcad software, also links to Solidworks
www.mathworks.com	MATLAB for solving matrix-based problems
www.strand7.com/	FE software with useful images in gallery showing twisted cat. Aimed at smaller companies
www.reliasoft.com/products.htm	Reliability and FMEA software tools
www.fmea-fmeca.com	Information site on FMEA/FMECA and industry standards for FMEA

Planning Software

www.products.office.com	At /en-us/project/project-and-portfolio-management-software for Microsoft Project
www.oracle.com/applications/	At primavera/products/project-management for details of Primavera P6
www.smartsheet.com/	At top-project-management-excel-templates for Excel-based system for smaller projects and for collaboration

Propulsion Waterjets

www.wartsila.com	Wartsila water jets in range 4500 to 26,000 kW incorporates LIPS from earlier, look under propulsion products for water jets; in Holland
www.marinejetpower.com	Successor to MJP at /index2.php including Ultrajet range, see history
www.rolls-royce.com/marine/	Rolls-Royce subsidiary KaMeWa waterjets in power range from 100 kW to 40 mW (under /propulsors/waterjets)
www.hamiltonjet.com	Hamiltonjet waterjets up to approx. 4000 kW
www.castoldijet.it/en	Castoldijet waterjets up to 1987 kW at /waterjet_en/applications_en.html
www.namjet.com/	Site for North American Marine Jet, suppliers of jets 387 to 1016 m in diameter for utility and small ferries. Axial pump design, and electrical controls not hydraulic for improved reliability
www.scottwaterjet.com	At /products/index.html, New Zealand supplier for smaller jet units in range 50 to 2000 shp
www.rbbi.com	At /links/drives/waterjet.htm list of waterjet manufacturers world-wide with links
www.berkeleyjet.com/	US manufacturer for planing craft in power range 205 to 430 shp
www.americanturbine.com/	Another supplier similar to Berkleyjet for jet boats, mixed flow jets including inducers and aluminum intakes can be welded in to aluminum hulls
www.doen.com/	Dutch manufacturer of waterjets in range 100 to 4000 kW

Propellers

www.servogear.no/	Classic propellers for fast ferries, in hull partial tunnel (Norway)
www.wartsila.com	At /products/marine-oil-gas/propulsors-gears, though oriented to large ferries and ships (Finland)
www.rolls-royce.com/marine	KaMeWa is now part of Rolls-Royce Marine under propulsion; continues to supply propellers for fast vessels including CP and supercavitating
www.elicheradice.com	At /page.php?pageid=PHOME001 home page for propeller, Shaft and skeg supplier in Italy including surface drives (they say)
www.piening-propeller.de/en/	Propellers and propulsion packages (e.g., gearbox, shaft), also high speed
www.qmarine.co.nz	At /products/propulsion-systems inc surface drives and market MJP waterjets
www.tuprop.com/	Tunnel propeller system, mounted on transom to 1000 shp for utility and fast boats, site for MSA Marine systems GmbH
http://www.andritz.com	At /products-and-services/pf-detail?productid = 9659, for EscherWyss CP high-speed propeller systems
www.amartech.nl/products	Propeller and transmission designer and manufacturer
www.bruntons-propellers.com/	Smaller propeller manufacturer, has built props for many high-speed craft, builds up to 3000 KW, while sister company Stone Marine builds larger propellers
www.teignbridge.co.uk/	Propeller manufacturer including high-speed propellers and surface drive propellers
www.miwheel.com/	Michigan Wheel – various propeller series for outboards, inboards, and speeds in range up to Fn about 0.7, I think; they are big
www.volvopenta.com	Search on IPS system for their integrated engine and rotatable contrarotating puller propeller drives in range to 740 kW, with control system

Surface Drives

www.Rolla-propellers.ch	Rolla propellers (also analytical consultants) for surface drive and fully submerged high-speed propellers (Italy)
www.Arneson-industries.com	Arneson surface drives – the complete drive system (USA)
www.zf.com	ZF Searex surface drive
www.francehelices.fr	Surface drive system and propeller manufacturer
www.q-spd.com/	Surface drive manufacturer supplied by Qmarine above
www.levidrives.com	Levi surface drives and propellers. Drive unit has fixed prop and cover that doubles as rudder mechanism
http://msa-marine-systems.com/	Tunnel surface drives in range to around 2000 kW. Drive unit hinged for both trim and turning

Engines

www.deutz.com	Engines up to around 600 shp air and water cooled, still independent
www.mtu-online.com	Go to products, engine-program diesel engines for marine main propulsion, passenger ships and ferries for engines for marine and fast ferries in range up to 9000 kW, now part of RR, yes, but independent in group; includes Detroit Diesel now also
www.cat.com	Go to /en_US/by-industry/marine.html. Main base is Germany, which is descendant of MWM (now Caterpillar Energy Solutions GmbH), used by LCS project etc.
www.marine.man.eu	MAN engines, go to /applications/ferries
www.cumminsengines.com	Main site for marine, go to resources to download data sheets and other documents
www.rolls-royce.com	Go to /products-and-services/marine/product-finder/diesel-and-gas-engines.aspx#section-featured-product to locate med speed (Bergen) diesels, propulsion pods, and so forth, as well as KaMeWa waterjets and CP Propellers
www.energy.siemens.com/hq/en	Go to /fossil-power-generation/gas-turbines. Siemens use RR as core drivers 4–50 mW
www.scania.com/global/en	At /global/products-and-services/engines/our-range/marine-engines.html for marine engines up to 1150 bhp. Eight Di13 engines being used in ferries on Potomac, for example, by Metal Shark
www.geaviation.com/marine/	GE marine site for gas turbines and diesels. Gas turbines 4.5 to 42 MW, diesels are medium speed and heavy
www.dieselturbo.man.eu/	MAN B&W diesel site, mainly large, slow diesels for ships
www.volvopenta.com	Engines and integrated propulsion stern drives
www.yanmarmarine.com	Powerboat and commercial marine diesels up to 4480 kW
www.mercurymarine.com	Outboards and sterndrives to 550 bhp
www.suzukimarine.com	Outboards up to 350 bhp
www.evinrude.com	Outboards up to 300 bhp

Intake Filtration

www.sulzer.com/en	Go to /Products-and-Services/Separation-Technology/Separators for knitmesh filters
www.knitted-mesh.com	Chinese supplier of knitted mesh products including demister materials

Service Suppliers and Marine Equipment Suppliers

www.frydenbo-industri.no	Go to /eng/engines/deutz/deutz-marine-engines and others in Norway
www.european-diesels.co.uk	Go to /engines/ for service and spare range including Ruston, Bergen diesel, Dorman, Perkins, and English Electric
	Ruston sold to Siemens, but diesels seem to have stopped, so only spares now

(continued)

www.vetus.com/	Suppliers of equipment and outfitting for boats and smaller vessels ranging from engines and ancillaries to windows to fire retardant insulation materials (under engines and around)

Gearboxes and Transmission

www.reintjes-gears.de	Reintjes, also propulsor plus PDFs of vessels
www.zf.com	Go to /corporate/en_de/products/further_product_ranges/marine/index.html for marine gearboxes and fast ferries, and others; also do fixed pitch propellers and tunnel thrusters
www.twindisc.com	At /marine-products/ for gearboxes and transmission, trim tabs, propellers, and other products. Parent to Rolla and Arneson
www.prm-newage.com	At /c1-marine-gearbox for marine gearboxes at smaller power end of market
www.renksystems.com	Marine at /renk-marine-gears.php; has supplied also US Navy LCS
www.renk.biz/home-en.html	Renk main site, go to vehicle transmissions and products to find marine transmissions and download brochure
www.renk-maag.ch/en/company/	Renk Swiss subsidiary providing high-performance gearboxes
www.regalpts.com	Jaure s.a. specialist in marine transmission shafts and couplings at /industries/marine/Pages/marine.aspx
	Note that Rolls-Royce, Wartsila, and MAN also provide transmission components or integrated systems

Stabilizers and Interceptors

www.humphree.com/	Interceptors and stabilizers, electric
www.naiaddynamics.com/	Successor to Maritime Dynamics, designers of stabilization systems for fast marine vessels including forward T foils and stern tabs, with active control systems
Rolls-Royce, and Servo gear also deliver stabilizers, and check this site for other potential suppliers: www.nauticexpo.com/boat-manufacturer/stabilizer-19818.html	

Seat Manufacturers

www.eknes.no	Eknes classic seating for fast ferries
www.beurteaux.com/	Supplier of fast ferry seating for more than 900 vessels
www.westmekan.com/no	Suppliers of ferry seats and propulsion gear out of Nordfjordeid
www.pacificmarine.net	/marine-deck/marine-seats/ferry-passenger-seats.htm. US company for seats and other internals for ferries
www.deltafurniture.com	at /passenger transportation/ferry seating Ferry seating and passenger transport specialist – Canada location
www.ferryseating.com/	China supplier

(continued)

www.ferryseat.com/	Sanhui, another Chinese factory with IMO HSC-certified seats
www.springfieldmarine.co.uk	UK supplier of ferry seats, crew transfer and suspension seats for crew, and so forth
www.grammer.co.uk/home.php	Grammer seats for suspended marine and all sorts of transport (not pax seats)

Marine Interiors

Safety Outfitting and Other Items

www.surviteczodiac.com	Survivetec group, main company in France
www.rfd.co.nz	Survivetec – NZ – evacuation and survival gear
www.Viking-life.com	Evacuation and life rafts
www.lsames.com	Evacuation and life rafts
www.actionair.co.uk	HVAC duct marine fire dampers for rectangular or round ducting

Rubber Mountings

www.mackayrubber.com.au	Rubber mounts for top superstructures for Incat, Austal, and others, as well as complete industrial range of vibration isolation
http://isoflextech.com	Suppliers of isolation rubber mounts for machinery, superstructures, and wheelhouses for commercial vessels
www.nauticexpo.com	Site for ships and yacht windows and various other marine outfitting equipment

Marine Fire and Sound Insulation

www.glava.no	Go to /marine-offshore/solutions for insulation, fire protection, and other items
www.promat-marine.com/en	Marine fire and noise insulation

Marine Architectural Panels Including Suspended Ceilings

www.duflex.com.au	/duflex2/products/featherlight for FRP panels
http://www.lautex.com	marine ceilings with sound absorption
http://dampa.com	/marine/products/ marine ceiling panels and design; supplies Austal, on 126 m trimaran
www.ceilingworks.com.au	Ferry internal suspended ceilings, etc.
www.altrofloors.com	Maritime safety flooring at /floors/transport-floors/Maritime

Marine Interior design

www.speargreen.com.au/	Interior design specialist for fast ferries, out of Sydney since 1993. Also does naval architecture. Worked with AMD and Austal for Oman, for example
www.arosmarine.com/en	Marine outfitting contractor, does installation – interesting is "proven brands" banner bottom left on page
www.kaefer.com	/Accommodation.html, another contractor for installation, especially for cruise ships and others with range of own brand equipment as well
www.alusys.com.sg/	Singapore-based internal outfitting contractor including for ferries

General Reference Materials

University of Southampton Reports from www.eprints.soton.uk.

Use refined search and author name, sort on year to get easiest usable results. The reports below are a sample, as the R&D was quite extensive over the 1990s and 2000s

Ship Science Report No. 71, March 1994, A. F. Molland, J. F. Wellicome and P. R. Couser

Resistance experiments on a systematic series of high-speed displacement catamaran forms: variation of length-Displacement ration and Breadth-Draught ratio.

Ship Science Report No. 72, March 1994, A. F. Molland, J. F. Wellicome and P. R. Couser

Theoretical prediction of the wave resistance of slender hull forms in catamaran configurations.

Ship Science Report No. 89, December 1995, J. F. Wellicome, P. Temarel, A. F. Molland, and P. R. Couser, Experimental Measurements of the seakeeping characteristics of fast displacement catamarans in long crested head seas.

Ship Science Report No. 106, January 1999, J. F. Wellicome, A. F. Molland, J Clic and D. J. Taunton

Resistance Experiments on a high-speed displacement catamaran of Series 64 form

Ship Science Report No. 118, October 1999, J. F. Wellicome, A. F. Molland, J Clic and D. J. Taunton

Experimental measurements of the seakeeping characteristics of fast 4.5 m displacement catamarans in open irregular seas

Ship Science Report No. 122, December 2001, A. F. Molland, P. A. Wilson and D. J. Taunton

A systematic series of experimental wash wave measurements for high-speed displacement monohull and catamaran forms in shallow water.

Ship Science Report No. 123, December 2002, A. F. Molland, P. A. Wilson and D. J. Taunton

Further experimental wash wave measurements for high-speed displacement catamaran forms in shallow water.

Ship Science Report No. 124, December 2002, A. F. Molland, P. A. Wilson and D. J. Taunton

Experimental measurement of the wash characteristics of a fast displacement catamaran in deep water.

Ship Science Report No. 125, November 2002, A. F. Molland, P. A. Wilson and D. J. Taunton

Theoretical prediction of the characteristics of ship generated near field wash waves.

Ship Science Report No. 127, 2003, A. F. Molland, P. A. Wilson and D. J. Taunton

Resistance experiments on a series of high-speed displacement monohull and catamaran forms in shallow water.

A Sample of Useful Additional Reference Papers

1. Band Lavis Final Report, Programme Element No 2.18 – Development of a route or mission dependent approach for the calculation of rational structural dynamic loads for high speed multihulls. Band Lavis and Associates, Report No 727-1 Oct 2002, CCDoTT Fiscla 2001 Subcontract DTMA91-97-H00007 – STRUCTURE Ibook
2. J T Tuitman, F X Sireta, S Malenica and T N Bosman, Transfer of non-linear seakeeping loads to FEM Model using quasi-static approach ISOPE, IOPEC 2009, Osaka, Japan June 21-26, ISBN 978-1-880653-53-1 ISSN 1098-618
3. Catamarans – Technological limits to size and appraisal of structural design information and procedures, Ship Structure Committee Report SSC-222 1971 available at www.shipstructure.org
4. Structural Loading prediction for high speed planing craft, Ship Structure Committee Report SSC-471, 2015 available at www.shipstructure.org.
5. The specialist Committee on Waterjets, Final Report and Recommendations to the 22nd International Towing Tank Conference, 1999 available at www.ITTC.info/
6. F Cheng, C Mayoss, T Blanchard, The Development of Trimaran Rules, Lloyd's Register Technical Papers, 2006, available on request from Lloyd's Register Publications Department.
7. H Peng, Numerical Computation of Multi-hull ship resistance and motion, part of PhD thesis at Dalhousie University, Canada, 2001, available at the National Library of Canada, http://www.collectionscanada.gc.ca/obj/s4/f2/dsk3/ftp05/NQ63482.pdfs
8. S M Cook, P Couser, K Klaka, Investigation into wave loads and catamarans, hydrodynamics of high-speed craft conference, RINA 24-25 November 1999, London, UK
9. P R Couser, A F Molland, N A Armstrong, I K A P Utama, Calm water powering predictions for high speed catamarans, FAST 1997, 12 to 23 July 1997, Sydney, Australia

10. T Hansvik, Use of interceptors and stepped hull to improve performance of high speed planing, High Speed Craft – ACVs, WIGs, and Hydrofoils Conference at RINA 31 October–1 November 2006

Recent Textbooks in the Same Subject Area

1. Hydrodynamics of High Performance Marine Vessels, Professor Laurence J Doctors, two volumes, available at Amazon.com, 888 pp, 2016, ISBN-13 978-15112244717
2. Performance by Design – Hydrodynamics for High-Speed Vessels, D J Blount, published by Donald J Blount and Associates, 342 pp, 2014, ISBN-10-0989083713
3. Practical Design of Advanced Marine Vehicles, Chris B McKesson, 392 pp, 2014, ISBN 13 978-1497396890

Appendix 1

Sample Early Vessel Data

The table below gives an impression of the historical timeline to the design of early multihull and some early steam-powered craft before the design of high-speed catamaran ferries took off in the 1980s. The vessels from the 1960s shown here are large utility vessels with mission aimed at improved motion in seaways rather than speed.

L. Yun et al., *High Speed Catamarans and Multihulls*,
https://doi.org/10.1007/978-1-4939-7891-5

Table A1.1 Historical summary

Name	Year built	Country	Designer/Builder	Owner/ Operator	LOA (ft)	BOA (ft)	Displt. tons	Propulsion	HP	Speed (knots)
Simon & Jude	1662	England	Sir William Petty	Sir William Petty	20	9	n/a	Sail	n/a	n/a
Experiment Catamaran	1664	England	Sir William Petty	Sir William Petty	n/a	n/a	Appro×150	Sail	n/a	n/a
St. Michael the Archangel	1684	England	Sir William Petty	Sir William Petty	50	12	n/a	Sail	n/a	n/a
Edinburgh	1787	Scotland	Patrick Miller	Patrick Miller	60	14.5	n/a	Sail and hand-turned paddle wheels	Sails and men	n/a
Experiment of Leith, Sail and manpowered catamaran	1788	Scotland	Patrick Miller	Patrick Miller	100	40	n/a	4 central pad-dles by winch	Sails and men	4.3
Clermont steam ferry	1807	USA	Robert Fulton	Robert Fulton North River Ferries	80	30	118	Steam (paddle wheels)	20	4
Jersey steam ferry	1812	USA	Robert Fulton	Robert Fulton	80	30	118	Steam (paddle wheels)	20	4
York steam ferry	1813	USA	Robert Fulton	Robert Fulton	80	30	118	Steam (paddle wheels)	20	4
Nassau steam ferry	1814	USA	Robert Fulton	NY & Brook-lyn Steamboat Ferry	80	30	120	Steam (paddle wheels)	120	12
Demologos (Fulton the First)	1814	USA	Robert Fulton	US Navy	153	58	1450	Steam (paddle wheels)	120	8
Aetna steam ferry	1817	England	Dawson & Co	Batman	63	28	68	Steam (paddle wheels)	22	5.5
Gemini	1850	England	Peter Barie/ Robin-son & Russell	n/a	157	27	n/a	Steam (paddle wheels)	50	n/a

USS Benton Ironclad River Gunboat	1864	USA	St Louis Shipyard, Missouri	US army western gunboat flotilla	202	72	2600	2 × steam to stern Paddle wheel	n/a	5.5
Castalia Steam ferry	1874	England	Capt..WT. Dicey/ Thames Iron Works	English Channel	290	60	n/a	Steam (2 paddle wheels)	250	10.5
Calais-Douvres Steam ferry	1877	England	Capt. W.T. Dicey/ Hawthorne	English Channel S.S. Company	302	62	192	Steam (paddle wheels)	2400	11
Thomas Pickles New Orleans Ferry	1892	USA	Thomas Dunbar/ Howard Shipyard Jeffersonville	Algiers Public Service Co	125	77	237	Steam (aft paddle wheels)	474	n/a
SMS Vulkan	1910	Germany	Howaldswerft	German Navy	280	54	n/a	Steam	1200	12.3
Kommuna *(ex Volkhov)*	1913	Russia	Putilov Shipyard St Petersburg	Russian Black Sea Fleet	315	60	3100	Diesel (2)	1200	10
"Algeria" and "New Orleans" Ferries	1925	USA	n/a	New Orleans Ferries	150	67	500	Steam	n/a	12
Venturi	1949	USA	Gar Wood Enterprises	Gar Wood	186	40	n/a	Diesel	4800	20
"1960" Class	1960	USSR	Gorki Shipyard	Russian Navy	236	49	1000	Diesel (2)	1080	14.5
"Rest Class"	1962	USSR	Gorki Shipyard	Russian Navy	146	46	282	Diesel (2)	500	11
E.W. Thornton Offshore Drill Rig	1962	USA	Friede. Goldman/ Levingston Shipbuilding Co	Reading & Bates Offshore Drilling Co.	278	105	6100	Diesel (2)	3000	12
Caribbean Twin	1962	USA	Twin Hull Boat Co.	n/a	70	28	180	Diesel (2)	700	12
Sea Palace	1964	Japan	Nippon Kokan	n/a	137	42	410	Diesel (2)	1300	15
Ker-Ogly	1966	USSR	Krasno Sormova Shipyard	n/a	425	164	11370	Diesel (6)	6000	10

(continued)

Table A1.1 (continued)

Name	Year built	Country	Designer/Builder	Owner/ Operator	LOA (ft)	BOA (ft)	Displt. tons	Propulsion	HP	Speed (knots)
Ridgely Warfield	1967	USA	Bethlehem Steel Co	Chesapeake Bay Inst.	106	34	162	Diesel (2)	2300	18
Eksperiment	1968	USSR	Svyetlovsky Ship Repair Yard	n/a	130	60	945	Diesel (2)	600	9
Duplus Diving support vessel	1968	Holland	Trident Offshore/ Boele's Scheepswerken	Netherlands Offshore Co.	131	56	1450	Diesel-Electric (2)	1698	8
Pigeon (ASR-21) Subsea Surveillance	1969	USA	Alabama Drydock and Shipbuilding Co.	US Navy	251	86	4200	Diesel (4)	6000	15
Hiryu Patrol Vessel	1969	Japan	Nippon Kokan	Maritime Safety Agency	90	34	235	Diesel (2)	2200	13
Hayes (T-Agor-16) Subsea surveillance	1971	USA	Todd Shipyard Seattle	US Navy	247	75	3100	Diesel (2)	4800	15

Appendix 2

L. Yun et al., *High Speed Catamarans and Multihulls*,
https://doi.org/10.1007/978-1-4939-7891-5

Table A2.1 Data Sheet 2-1 Initial Data

Mission		**Option 1**	**Option 2**	**Option 3**	**Option 4**	**Notes**
Insert description						Key characteristics required, perhaps attach document
Max voyage distance	Nm					Alternatively define endurance required
Max sea state expected	Sig.m					Document all environmental data available for area
Voyage average duration	Hr/min					To estimate service speed
Initial service speed estimate	Kph					Use a factor 1.1 to allow for unknowns related to the route
Dash speed requirement and duration	Kph					For utility or military vessels
Payload data	**No**	**Unit mass**	**Total mass**			
Passengers plus Crew	nn					Use to estimate deck area required
Trucks	nn					Use to estimate deck area required
Cars	nn					Use to estimate deck area required
Freight	tonnes					Use to estimate deck area required
Consumables (commercial)	tonnes					Stock for onboard kitchen, shops, kiosk
Fuel	tonnes					Volume based on power and duration from statistics
Ballast water and other liquids	tonnes					Estimate from existing vessel data statistics
Vessel type options	Options for each characteristic					
Speed Regime (Fr_l)	<0.4	0.4–0.75	0.75–1.0	>1.0		Displacement, dynamic, semi-planing and planing
Catamaran	Normal	SSTH	S-SWATH	SWATH	Wpiercer	Configuration main concept
Trimaran	Normal	Stabilised monohull				Stability = stabilised monohull trimaran
Hydrofoil support	Keel	Sub-keel				Can also be to trimaran
Other configurations	Hybrid, air cushion, etc.					Provide description of concept, e.g. air cushion support

Initial estimate of key data		Give data and basis				Notes
LWL	m					Trimarans give main hull, and sponsons
BWL	m					Overall beam across demihulls, or trimaran sponsons
Trimaran main hull Bwl	m					Breadth of main hull
Demihull or sponson Bwld	m					Depth of demihull or trimaran sponson
Demihull or sponson spacing	m					Give distance between centres and to centreline
Draft at DWL	m					Main hull for trimarans
Freeboard at DWL	m					Main hull for trimarans
Sponson draft at DWL	m					For trimarans
Sponson freeboard at DWL	m					For trimarans
Initial estimate displacement	tonnes					Estimate from existing vessel data statistics
Initial estimate installed power	kW					Estimate from existing vessel data statistics

Table A2.2 Data Sheet 2 - Detailed Design Selection

Main particulars - Page 1 of 3	**Dims/ specification**	**Description (to be completed by designer!)**	**Notes**
Estimated payload	*tonnes*	Estimate from selection process	Italicised elements will require analysis
Light ship displacement	*tonnes*	Estimate from selection process	Other items specify and adjust with analysis
Design displacement	*tonnes*	Estimate from selection process	
LOA	m	Based on selected configuration	
LWL	m	Based on selected configuration	
BOA, B	m	Based on selected configuration	
Demihull beam, b	m	Based on selected configuration	
Spacing to demihull centreline, c	m	Based on selected configuration	
Depth to main watertight deck, T	m	Based on selected configuration	
Draft at full payload, SWL, d	m	Based on selected configuration	
Freeboard to main watertight deck, h	m	Refer Chapter 3 and IMO requirements	
Amidships tunnel height above keel, H_t	m	At least service (Hsig/1.8) above SWL (?)	
Key coefficients			
CB		Based on selected configuration	This may be adjusted in following design phase
CP		Based on selected configuration	This may be adjusted in following design phase
L/b, demihull fineness		Based on selected configuration	This may be adjusted in following design phase
Additional coefficients		Other coefficients important to the particular design	
Structural specification			
Hull material	Material	Steel/Al/CFRP/combination	Final selection also involves client
Deckhouse/superstructure	Integrated/ isolated	Isolation requires interface design for structures	Will require characteristics from specialist vendors
Cathodic protection	Underwater outfit	Dissimilar metal alloys propulsion and appendages	Will require corrosion analysis and cathodic protection

Non-structural panels and noise insulation	m^2 and tonnes	Based on accommodation spaces layout	At this stage is overall mass and CG based on specification
Machinery space insulation and fire protection	m^2 and tonnes	Based on machinery spaces layout	At this stage is overall mass and CG based on specification
Estimated structural mass primary structure	*tonnes*		
Estimated structural mass secondary structure	*tonnes*		
Tankage capacities			
Fuel oil (and/or LNG)	M^3, no tanks	May require pumping or monitoring for transfers	LNG tankage also requires boiloff control
Potable water	M^3, no tanks	Fill/drain/clean requirements?	Disposal?
Main engine lube oil	M^3, no tanks	Fill/drain/clean requirements?	Removal and disposal of spent liquid?
Gear oil	M^3, no tanks	Fill/drain/clean requirements?	Removal and disposal of spent liquid?
Hydraulic oil	M^3, no tanks	Fill/drain/clean requirements?	Removal and disposal of spent liquid?
Coolant	M^3, no tanks	Fill/drain/clean requirements?	Removal and disposal of spent liquid?
Waste oil	M^3, no tanks	Fill/drain/clean requirements?	Removal and disposal of spent liquid?
Grey water	M^3, no tanks	Fill/drain/clean requirements?	Removal and disposal of spent liquid?
Sewage	M^3, no tanks	Fill/drain/clean requirements?	Removal and disposal of spent liquid?
Bilge slop tank	M^3, no tanks	May require pumping or monitoring for transfers	Disposal?
Total liquid deadweight	*tonnes*		
Main particulars Page 2 of 3	**Dims/ specification**	**Description**	**Notes**
Main power and propulsion			
Main engines, diesel, LNG/gas, electric	n x power rating, kW	Turbine/reciprocating/electric, no off, power, vendor	Will require speed/torque/power curves
Propulsion auxiliary systems	Type	Diesel, LNG/gas, electric	Electric will require battery dimensions/weight estimate
Gearboxes	Type	V, Z, A, combining, secondary t/o	Will require power and speed/torque curves

(continued)

Table A2.2 (continued)

Transmission shafting and supports	Material	Length, bearings, restraint, mass, dynamics	
Propulsion	Propeller spec	Sub cav, super cav, surface ventilated	Will require speed matching via gearbox
or	Waterjet spec	Axial, mixed flow, direction and reverse	Will require speed matching via gearbox
Bow thrusters	Thruster spec	Tunnel, rotating, powering, control	May be electric, hydraulic or direct drive
Estimated total mass	*tonnes*		
Power generation and distribution			
Auxiliary power generation	Functional spec	Generator set 2 x Onan MDKBR 19.5 kW	
Emergency power system	Functional spec	Emergency generators or battery backup	
Distribution system	Functional spec	Network 24V DC, 230V 50 Hz AC	
Electrical propulsion, battery/ transformation	Functional spec	MWh capacity, dimensions, mass, cooling	Will require specialist design support
Shore side power delivery	Functional spec	MWh capacity, dimensions, mass, cooling	Power for battery charging including interface
Estimated total mass	*tonnes*		
Instrumentation and control			
Main engine control and monitoring	Functional spec	Bridge and local operating stations	
Auxiliary and emergency power monitor	Functional spec	Bridge and local operating stations	
Bridge navigation outfit	Functional spec	GPS location, compass, autopilot etc	
Satellite and telecommunications	Functional spec	Satellite and radio telecoms, Internet for secure vessel operations	

Fire detection system	Functional spec	Smoke and heat detection, by compartment	
Accommodation systems monitoring	Functional spec	Electrical/instrument status, gangway and compartment closure status	
Public address	Functional spec	Locations and override to entertainment systems	
CCTV	Functional spec	Camera locations and supervisory system	
Navigation lighting	Functional spec	As per IMO	
Searchlights	Functional spec	Per client specification	
Estimated total mass	*tonnes*		
Trim and direction control, motion damping			
Stern mounted tabs or intruders	Functional spec	Sizing, power, control system	Will be based on model testing and analysis
Bow T foils, central or under bow	Functional spec	Fixed/retract, sizing, power, control	Will be based on model testing and analysis
Trim and damping control system	Functional spec	Fixed/retract, sizing, power, control	Will be based on model testing and analysis
Rudders, steering intruders	Functional spec	Sizing, power, control system	Possible integration of rudder with propeller
Estimated total mass	*tonnes*		
Deck layout and equipment			
Anchor equipment	Functional spec	Anchors, chains, chain winches and guides	Anchor, chain and winch via IMO and class requirements
Bow fendering	Functional spec	Rollers, fixed rubber, shaping	Define interface to quays or offshore structure

(continued)

Table A2.2 (continued)

Side and stern fendering	Functional spec	Fixed rubber, inflated deployable	Define quayside interface
Personnel access – bow	Functional spec	Powered ramp, offshore transfer system	Passengers to quayside, or access to offshore structure?
Personnel access – side decks aft/ forward	Functional spec	Powered gangway, power, control	To dedicated quayside facility, or other interface?
Personnel access – stern	Functional spec	Powered gangway, power, control	To dedicated quayside facility, or other interface?
Vehicle access – stern and/or bow	Functional spec	Powered ramps, power, control	To dedicated quayside facility, or other interface?
Vehicle decks, area, clearance heights, lanes	Functional spec	Deck loading, tie-downs, ramps, lane spacing	Vehicle drive on, round and off needs drawing up
Main particulars page 3 of 3	**Dims/ specification**	**Description**	**Notes**
Deck capacities	**Area m^2, load t**	**Other arrangements**	
Open fore deck	nn, mm	Tie-down for containers and cargo	10ft or 20ft containers? ISO mounts
Open aft deck	nn, mm	Tie-down, Craneage, deck protection	10ft or 20ft containers? ISO mounts
Mob recovery system	Functional spec	Mob boat cradle and launch davits	Boat location and winch powering/control
Aviation interface, deck location	nn, mm	Helicopter landing area, tie-downs, and interface	Helicopter specifications?
Estimated maximum payload	*tonnes*		
Life saving equipment	**Number**		
Life buoys, lifejackets	nn, nn		
Immersion suits (crew, and utility vessels)	nn		
Life rafts	4 × nn persons		

Fire fighting			
Fixed system machinery areas	Functional spec	CO_2 fixed Fi-Fi system in engine rooms	Refer IMO
Fixed system passenger/vehicle areas	Functional spec	Distributed sprinkler systems	
Fire hose system	Functional spec	Hose reels internal and/or external	
Portable equipment	Functional spec	Fire extinguishers, no and placement	
External monitors	Functional spec	Volume flow rate, pressure	External fire monitors may be required for off-shore vessels
Estimated total mass	*tonnes*		
Personnel accommodation and outfitting	**Capacity, persons**	**Area m^2**	**Specification**
Bridge, crew	nn	nn	Crash tested suspension seats
Main saloon, passengers	nn	nn	Seats and tables, standard
Aft saloon, passengers	nn	nn	Seats and tables, standard
Upper saloon, passengers	nn	nn	Seats and tables, executive
Kiosk, staff	nn	nn	Summary specification of outfit?
Cafe and dining room, including galley	nn	nn	Summary specification of outfit?
(Duty free) shop	nn	nn	Summary specification of outfit?
Wash rooms (main saloons, and for crew)	nn	nn	Clarify location(s), outfit, and access inc barriers for access privacy
Emergency evacuation spaces	nn	nn	Access to exits, assembly areas, life jacket and suit storage
Crew spaces	nn	nn	Specify cabins, spaces, etc.
Galley and crew mess area	nn	nn	Galley and crew mess area and outfit specification

(continued)

Table A2.2 (continued)

Utility spaces, commercial	Capacity m^3	Shelving m^2	Storage compartments for sales items
Utility spaces cleaning	Capacity m^3	Shelving m^2	Storage compartments for cleaning, trash, etc.
Luggage area capacity m3 and shelving m2	Capacity m^3	Shelving m^2	Summary specification for shelving, restraints, etc.
Stairs and lifts between decks	Capacity, persons	Stairway dimensions and handrailing	
Electronic outfit for passenger use	Functional spec	Entertainment and communications	GPS, telecoms, Internet, Wi-Fi, satellite TV
Air conditioning and heating	Functional spec	Specification by compartment	Compartment volume, temperature range and heating/cooling kW
Internal lighting	Functional spec	Specification by compartment	Estimate of lumens required and number of points
External lighting for vehicle/personnel access	Functional spec	Specification by deck location and area	Estimate of lumens required and number of points
Estimated total mass	*tonnes*		

Note 1: Military or paramilitary vessels will require additional specifications for weapons, data systems, battle hardening, subsea and aviation equipment and interfaces

Note 2: Objective of this datasheet/book is to document specifications, estimates of mass, locations and centres of mass items. Both targets and actual are useful to document

Table A2.3 Concept screening scoreboard Concept identification: concept 1

	Scoring	**Weight**	Better	Meets	Less than	**Total**
Item	Description		15–10	10	10–5	
1	Payload delivery (deck areas, passengers, vehicles other issues)	3			9	27
2	Speed/service sea state	3	12			36
3	Motions/comfort/speed degradation	2	12			24
4	Powering/fuel consumption	2			9	18
5	Acquisition cost based on specification	6			7	42
6	Terminal/onshore interface	2	12			24
7	Operating cost	2			9	18
	Total	20				189

Evaluation of acceptability

Score 200 or better is acceptable to continue, if score lower needs concept revision, if score less than 180 concept to be rejected

Concept screening actions:

In this example case acquisition cost is critical and so must be addressed to be accepted to move forward in this example

Reduced capital cost may also lower operating cost, to be tested

Powering and payload delivery may be optimised later as close to a 'meeting' score

Notes

a. It may be noted that scoring categories may be adjusted, weights adjusted, and rejection score adjusted

The basis for the scoring in each category needs to be defined and accepted by management, based on data realism prior to evaluation

b. The key principle is that all concepts being screened should be subject to same scoring and weights, etc.

c. There must be an agreed lower bound, determined by evaluation of consequences to not 'meeting' each category requirement

d. The scoring is a management tool to give direction to the selection process, not an analytical process!

e. It is not precise but better than personal views as the scoring can be debated relative to the concept

f. Scoring can be done by team members individually and the range of results used for debate on ways forward

g. Costs at this stage may be evaluated on basis of cost/ton from shipyards, and cost/ton.knot from operators

h. Once scores and actions are available for each concept that is not rejected, they can be prioritised and rejection criteria adjusted for second round review

Appendix 3

Sample Vessel General Arrangements and Specifications

Included on following pages are general arrangements and data sheets for vessels listed below. They are a sample for recent high-speed catamarans and trimarans at varying sizes and for varying missions. Some key data are also listed.

	Vessel	Designer/Builder	Type/Mission
1	Fred Olsen Benchijigua	Austal	127 m Trimaran RoPax ferry
2	Oman National Ferries Company *Shinas* and *Hormuz*	Austal	65 m ferry and utility catamaran
3	Buquebus *Francisco*	Incat	99 m wave piercer RoPax ferry
4	MNBA Thames Clipper Neptune & Galaxy	One3three/Incat	35 m Hunt class super slender catamaran passenger ferry
5	Seacor *Panther*	Incat Crowther/Gulf Marine	57 m offshore supply catamaran
6	Seacat *Enterprise*	South Boats	27 m catamaran HSUV
7	MCS SWATH1 and SWATH 2	Adhoc Marine Designs/ associate shipyard	Typhoon 26 m SWATH HSUV

Many thanks are due to the following organizations for permission to reproduce this technical material:

- Austal, Henderson, Western Australia for permission to use the data sheets for *Benchijigua* trimaran and *Shinas* catamaran
- Incat Australia, Hobart, Tasmania, for permission to use the data sheets for *Francisco* and the minispec for the 33 m *Thames Clipper* ferry
- One2three Naval Architects, Sydney, Australia, for permission to use the GA for the 33 m *Thames Clipper* ferry
- Seacor Marine, Houma, LA, USA, for permission to use the data sheet for Seacor *Panther*

L. Yun et al., *High Speed Catamarans and Multihulls*,
https://doi.org/10.1007/978-1-4939-7891-5

- South Boats, Cowes Isle of Wight, UK, for permission to use the data sheet for Seacat *Enterprise*
- Adhoc Marine Designs, Newport, Isle of Wight, for permission to use the data sheet for the MCS SWATH1 and 2

With permission of Seacor we include the detailed specification sheet for one of their offshore service vessels, the Leopard. This specification gives a useful idea of the information designers need to consider when developing their own specification sheets for a utility vessel. A similar level of detail is available from the data sheets for the two HSUVs. Slightly simpler information is presented for the ferries, sufficient we hope for a designer to start a thought process for specification and to consider how to determine the details of LNG fuel systems, control systems for stabilizers, or interfaces to helicopter landing control and other emergency facilities as installed on Shinas and Hormuz.

The resources section should allow location of potential supplies and specifications for much of the outfit equipment over the Internet.

Fred Olsen 127-m Trimaran Ferry Benchijigua

PRINCIPAL DIMENSIONS

Length overall	126.7 metres
Length (waterline)	116.9 metres
Beam (moulded)	30.4 metres
Depth (moulded)	8.2 metres
Hull draft (approx.)	4.2 metres

PAYLOAD AND CAPACITIES

Passengers	1,291
	Outdoor seating for 128
Crew	35
Vehicles	341 cars
Heavy vehicles	450 truck lane metres and 123 cars
Centre lanes between pillars	4.6 metres
Trucks under raised mezzanine deck	4.2 metres
Trucks aft of raised mezzanine deck	4.6 metres
Cars under mezzanine deck	2.0 metres
Cars over mezzanine deck	2.0 metres
Maximum deadweight	1,141 tonnes
Maximum axle loads (centre lanes)	15 tonne/dual axle
(outer lanes)	12 tonne/dual axle
(mezzanine lane)	0.8 tonne/dual axle

PROPULSION

Main engines	4 x MTU 20V 8000 M70
	4 x 8,200 kW @ 1,095 rpm
Gearboxes	2 x Renk ASL65
	1 x Renk ASL2x80
Waterjets	2 x KaMeWa 125 S11
	1 x KaMeWa 180 B11

PERFORMANCE (with Ride Control fitted)

Speed (100% MCR)	40.5 knots
Fuel	145,000 litres

CLASSIFICATION

Germanischer Lloyd
✠ 100 A5, HSC-B OC3 Highspeed Passenger/Ro.Ro Type, MC, AUT
Spanish Flag Authority

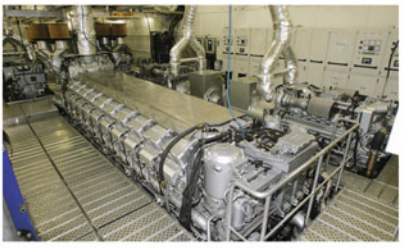

PROFILE

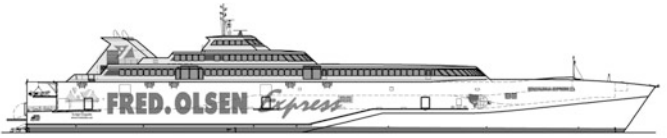

BRIDGE DECK

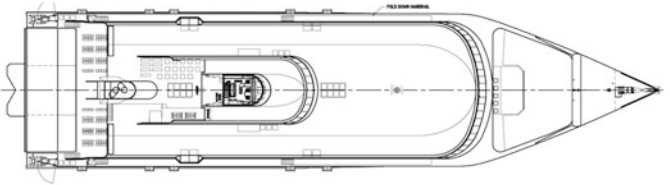

OBSERVATION DECK

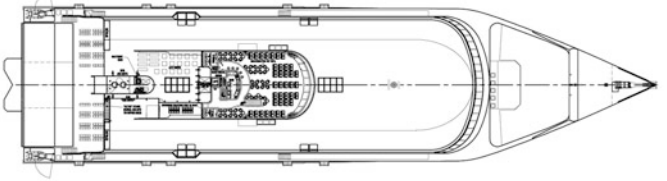

UPPER DECK

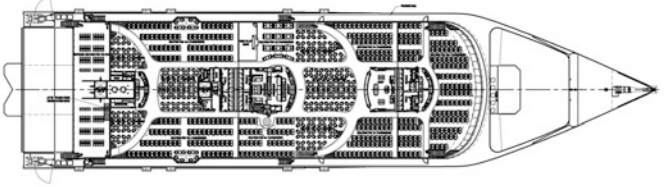

MEZZANINE DECK

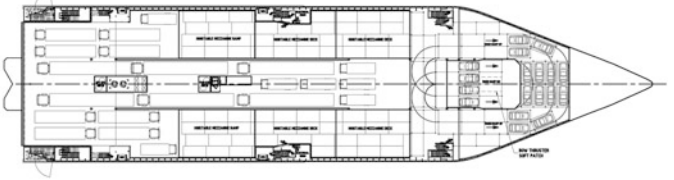

MAIN DECK

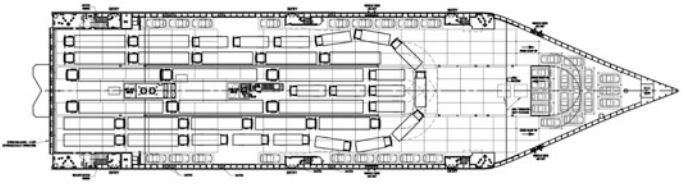

HULL

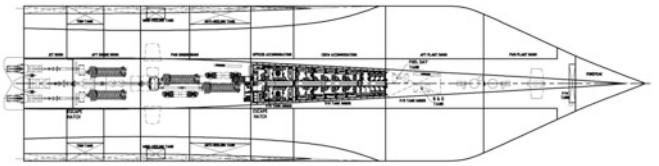

Oman National Ferries Company Shinas *and* Hormuz

PRINCIPAL DIMENSIONS

Length overall	64.8 metres
Length (waterline)	61.1 metres
Beam (moulded)	16.5 metres
Hull depth (moulded)	6.2 metres
Hull draft (maximum)	2.1 metres

PAYLOAD AND CAPACITIES

Passengers	208
Crew	12
Vehicles	56 or 54 truck lane metres plus 34 cars
Maximum axle loads	
Aft main deck	9 tonnes (single wheel) 12 tonnes (dual wheel)
Remainder of main deck	3 tonnes (single wheel)
Vehicle deck clear height	3.1 metres
Helicopter	Agusta Westland AB139 or equivalent
Fuel	44,000 litres

PROPULSION

Main engines	4 x MTU 20V 1163 TB73L 4 x 6,500 kW
Gearboxes	4 x Reintjes
Waterjets	4 x Kamewa 90 SII

PERFORMANCE

Service speed (95% MCR)	51.5 knots

CLASSIFICATION

Det Norske Veritas / IMO HSC 2000

PROFILE

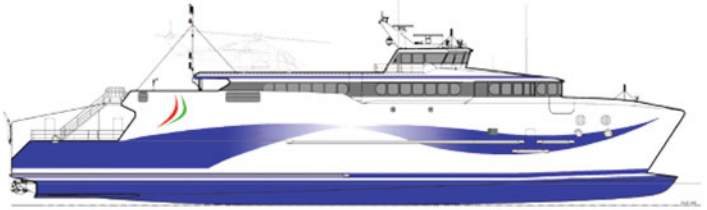

BRIDGE DECK

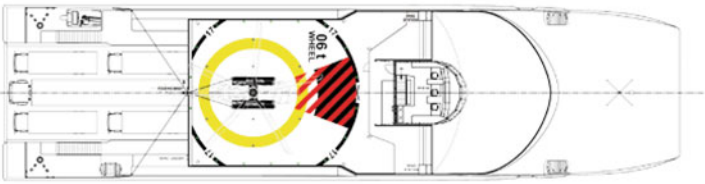

UPPER DECK

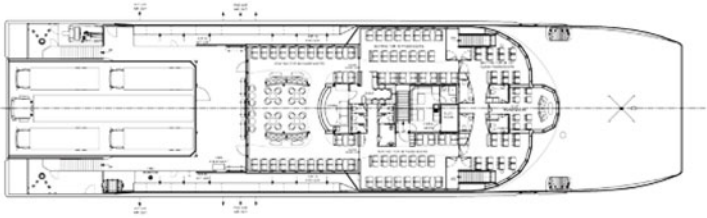

MAIN DECK

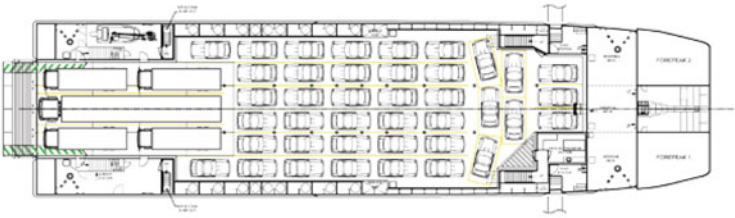

HULLS

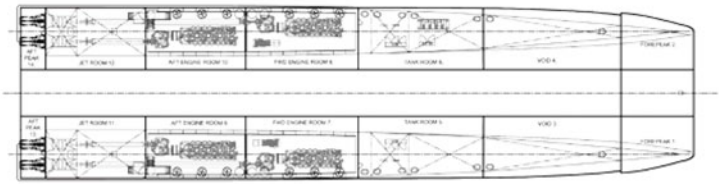

Buquebus 99-m Wave-Piercer Ropax Ferry Francisco *Fueled by LNG*

99m HULL 069

incat
www.incat.com.au

Hull 069

99m Wave Piercing Catamaran

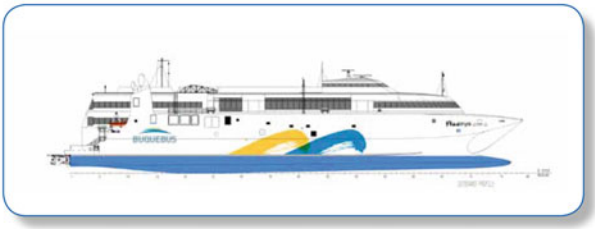

General Particulars

Yard No:	069
Designer:	Revolution Design Pty Ltd.
Builder:	Incat Tasmania Pty Ltd.
Class Society:	Det Norske Veritas
Certification:	DNV + IAI HSLC R4 CAR FERRY B GAS FUELLED EO
Length overall:	99.00m
Length waterline:	90.54m
Beam (overall)	26.94m
Draft (design)	2.98m
Deadweight:	450 tonnes
Speed:	51.8 knots @ 450 tonnes deadweight, 100% MCR Lightship trial speed: 58 knots @ 100% MCR

Capacities

Passenger Capacity: maximum1024 persons (passengers and crew)
Tier 2 Passenger Deck is divided into three areas as follows:
- T2 Aft Lounge (Economy Class) with seating areas and Bar/Kiosk.
- T2 Duty Free Shop Lobby with Male/Female Toilets
- T2 Duty Free Shop.

Tier 3 Passenger Deck is divided into four areas as follows:
- T3 Aft Lounge (Tourist Class) with seating areas and Bar/Kiosk.
- T3 Main Foyer with Reception Area, Business Lounges (P&S), Male/Female Toilets and Disabled Toilet/Mothers Room.
- T3 Mid Lounge (Business Class) with seating areas Bar/Kiosk, Male/Female Toilets.
- T3 Forward Lounge (First Class) with seating areas, Bar, VIP Lounge and Male/Female Toilets.

The Tier 4 wheelhouse and Tier 3 lower wheelhouse are accessed from the T3 Forward Zone.

Vehicle Capacity: 150 car spaces at 4.5m long x 2.3m wide.
Tier 1 Vehicle Deck clear height: 2.3m
Tier 1 Vehicle Deck: Axle load: 2.0 tonne per axle

Vehicle Access: Via shore based stern ramps across transom.

Tankage

Fuel Oil (main storage) 2 x 70,000 (approx) litres
Fuel Oil (generator header tanks) 2 x 1,240 litres
LNG (main storage) 2 x 40m3
Fresh Water: 1 x 5,000 litres
Black & Grey Water: 1 x 5,000 litres
E/R Oily Water: 2 x 160 litres
Bilge Holding: 1 x 1,000 litres
Aft Hydraulic Oil: 2 x 400 litres
Fwd Midships Hydraulic Oil: 1 x 200 litres

Construction

Design - Two slender, aluminum hulls connected by a bridging section with centre bow structure at the forward end. Each hull is divided into nine vented, watertight compartments divided by transverse bulkheads. Two compartments in each hull are prepared as fuel tanks with an additional compartment prepared as a long range tank.

Air Conditioning

Reverse cycle heat pump units throughout are capable of maintaining between 20-22 deg C and 50% RH with a full passenger load and ambient temperature of between 0 deg C and 35 deg C and 60 % RH.

Safety & Evacuation

Four Marine Evacuation Stations (MES), two port and two starboard, each MES is capable of serving a total of up to 256 persons. A total of nine, 128-person open reversible life-rafts are fitted.

Machinery

Gas Turbines: Two (2) GE Energy LM2500 marine gas turbines rated at 22MW each.

Water Jets: Two (2) Wartsila LJX 1720 SR waterjets are configured for steering and reverse.

Gensets: 4 x Caterpillar C18 340 ekW generators fitted with marine brushless self-excited alternators, arranged for automatic start-up and paralleling, provide power for all passenger and ship services. The electrical control system considers one genset is maintained as a standby set.

GT Gensets: 2 x Caterpillar C9 200 ekW generators fitted with marine brushless self-excited alternators provide electrical power for gas turbine services. Each GT genset is considered independent.

Trim Control: A hydraulically operated trim tab is fitted at the aft end of each hull to allow adjustment of the running trim of the vessel.

Hydraulics - Three hydraulic power packs, one forward and two aft, all alarmed for low level, high temperature, filter clog and low pressure, supply hydraulics for capstans, trim tabs, steering and stern ramp.

Electrical

Distribution - 415V, 50 Hz. 3 phase. 4 wire distribution with neutral earth allowing 240 volt supply using one phase and one neutral. Distribution via distribution boards adjacent to or within the space they serve. 200-amp 415V 3-phase shore power connection point fitted in starboard anteroom.

Details provided are based on original design and certification.
For information on Incat representatives in your region contact head office

18 BENDER DRIVE DERWENT PARK HOBART TASMANIA 7009 AUSTRALIA P: +61 (0) 3 6271 1333 F: +61 (0) 3 6273 0932 E: INCAT@INCAT.COM.AU

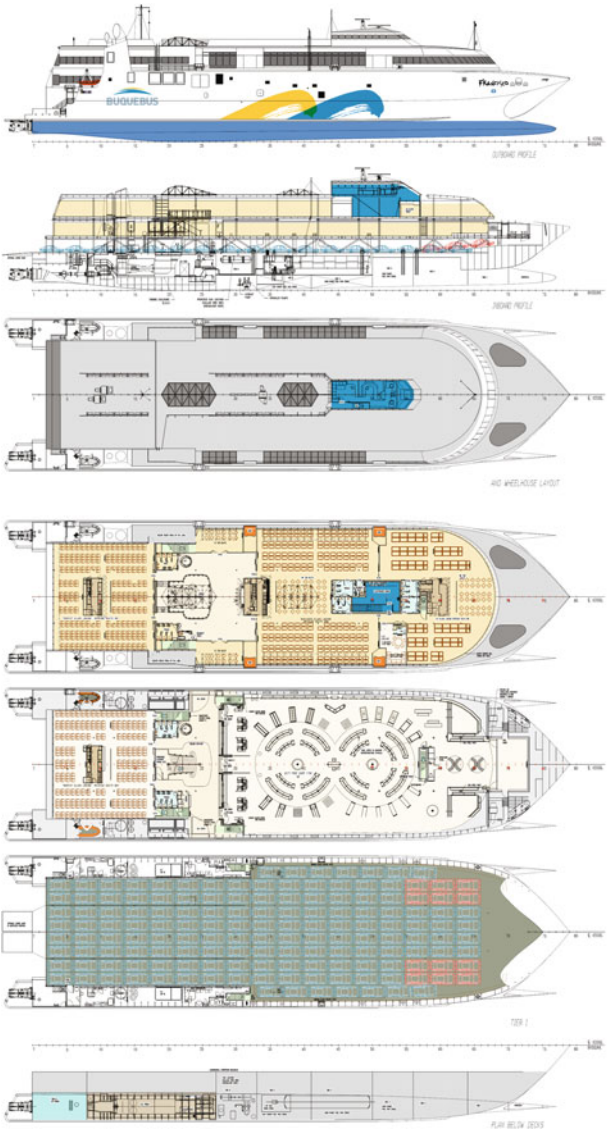

BUQUEBUS

99m

LOA:	99.00 m
LWL:	90.54 m
Beam:	26.94 m
Draft:	2.98 m
Deadweight:	450 tonnes

Capacity:
Over 1000 passengers
and 150 cars.
Duty free shop over
1100 square metres

Engines:
GE Gas Turbine LM2500
2 x 22 MW Total power
44 MW

Waterjets:
Wartsila LJX 1720SR

Gearbox:
Renk: Bus 175

MNBA 33-m Super Slender Catamaran Ferry Thames Clipper

35m HULL 076

www.incat.com.au

Hull 076

35m Passenger Catamaran

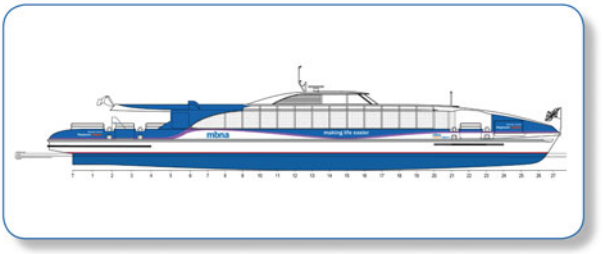

General Particulars

Yard No	076
Designer	One2Three
Builder	Incat Tasmania Pty Ltd.
Society	DNV·GL
Class Notation	DNV +1A1 HSLC Passenger R4 EO
Flag	United Kingdom
Speed	Over 25 knots at full displacement 30 knots at light displacement
Regulations	HSC Category A with MCA Equivalences appropriate to operation in UK Category C waters

Principal Dimension

Length Overall	35.37m
Length Waterline	32.45m
Beam Moulded	8.30m
Hull Depth Moulded	2.15m
Load Draft	1.00m

Capacities

Passengers	150
Crew	3

Tankage

Diesel Fuel	2 x 1500 Litres
Fresh Water	500 Litres
Black water	500 Litres

Deadweight

Full Load Deadweight:	
Passengers (150 @ 80kg each)	12.00 Tonnes
Crew (3 @ 80kg each)	0.24 Tonnes
Fuel 100% (usable volume)	2.04 Tonnes
Fresh Water 100%	0.50 Tonnes
Sullage 10%	0.05 Tonnes
Bar Provisions	0.20 Tonnes
Stores	0.10 Tonnes
Total (100% Deadweight)	15.13 Tonnes

Construction

The hull construction is of marine grade aluminium.
The hull form is semi-round bilge with symmetric hulls.

Machinery

Main Engines	2 x Scania DI16 072M marine diesel engines, rated at 625kW (850hp) @ 2300rpm
Gearboxes	2 X ZF2000, reversing with PTO
Waterjets	2 x Rolls Royce/Kamewa 40A3
Generators	2 x Kohler 33EF0ZDJ

Electrical

Electrical System	415/240V 50Hz AC supplied by two diesel alternators, located in the engine rooms 24V DC for emergency back-up and controls of machinery

Air Conditioning

Passenger Space	3 x Independent air cooled packaged units and ceiling cassettes
Wheelhouse	1 x Independent compact type air cooled cassette
Ambient Temperatures	+35°C to -10°C

Safety and Evacuation

Liferafts	2 x LSA 128 person open-reversible 1 x RFD Ferryman 30 person
Life Jackets	165 adult and 16 child Premier 2010
Medical supplies	2 x Category C First Aid packs
MISC equipment	2 x Jason cradle

Navigation and Communication

Radar	Furuno NavNet DRS4A, 48nm
Compass	Platismo Offshore Class B
Speedlog	Walker 7070MK2F
GPS	Furuno GP-170, 6"LCD
Radios	2 x Sailor 6222 VHF/DSC 4 X ICOM IC-M35 VHF handheld
AIS	Thames AIS
Public Address	Gitiesse Imcos PA/GA
Control/Monitoring	Maps/Böning AMS

Details provided are based on original design and certification.
For information on Incat representatives in your region contact head office

18 BENDER DRIVE DERWENT PARK HOBART TASMANIA 7009 AUSTRALIA P: +61 (0) 3 6271 1333 F: +61 (0) 3 6273 0932 E: INCAT@INCAT.COM.AU

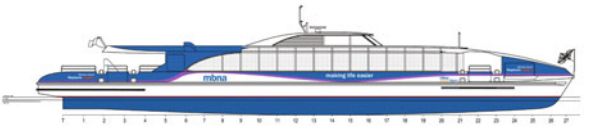

Profile View

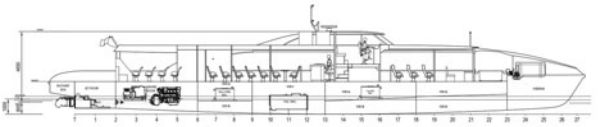

Centreline Profile

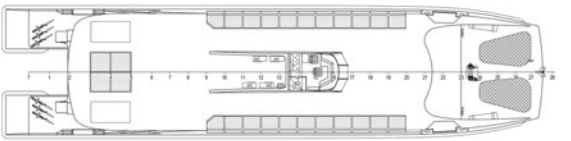

Upper Deck

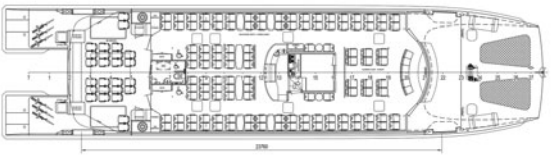

Main Deck

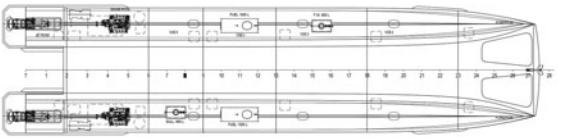

Below Decks

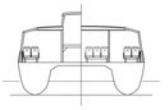

Typical Section

One 2 three
NAVAL ARCHITECTS

PRINCIPAL PARTICULARS

Length Extreme	35.37 m	Draft	1.69 m
Length WL	32.69 m	Fuel	2x1500 L
Beam (Overall)	8.80 m	Fresh Water	600 L
Beam (Moulded)	8.30 m	Sullage	600 L
Depth (Moulded)	2.15 m	Seats	330
		Internal - Tourist	300
		Internal - Business	18
		External	10
		Internal Seats - Boatmans "Tourist"	2
		- Boatmans "Club"	2
		External Seats - Boatmans "Outdoor"	2

33m PASSENGER CATAMARAN
GENERAL ARRANGEMENT

02 JUNE 2015

One 2 Three Pty Ltd | 11 Phillips Rd | Kogarah | NSW | 2217 | Australia | Tel: +61-2-9553-0366 | Fax: +61-2-9553-0344 |design@one2three.com.au

DRAWING # 13049-0002 REVISION AF A1 SHEET SCALE 1:100

General Arrangement of Seacor Panther

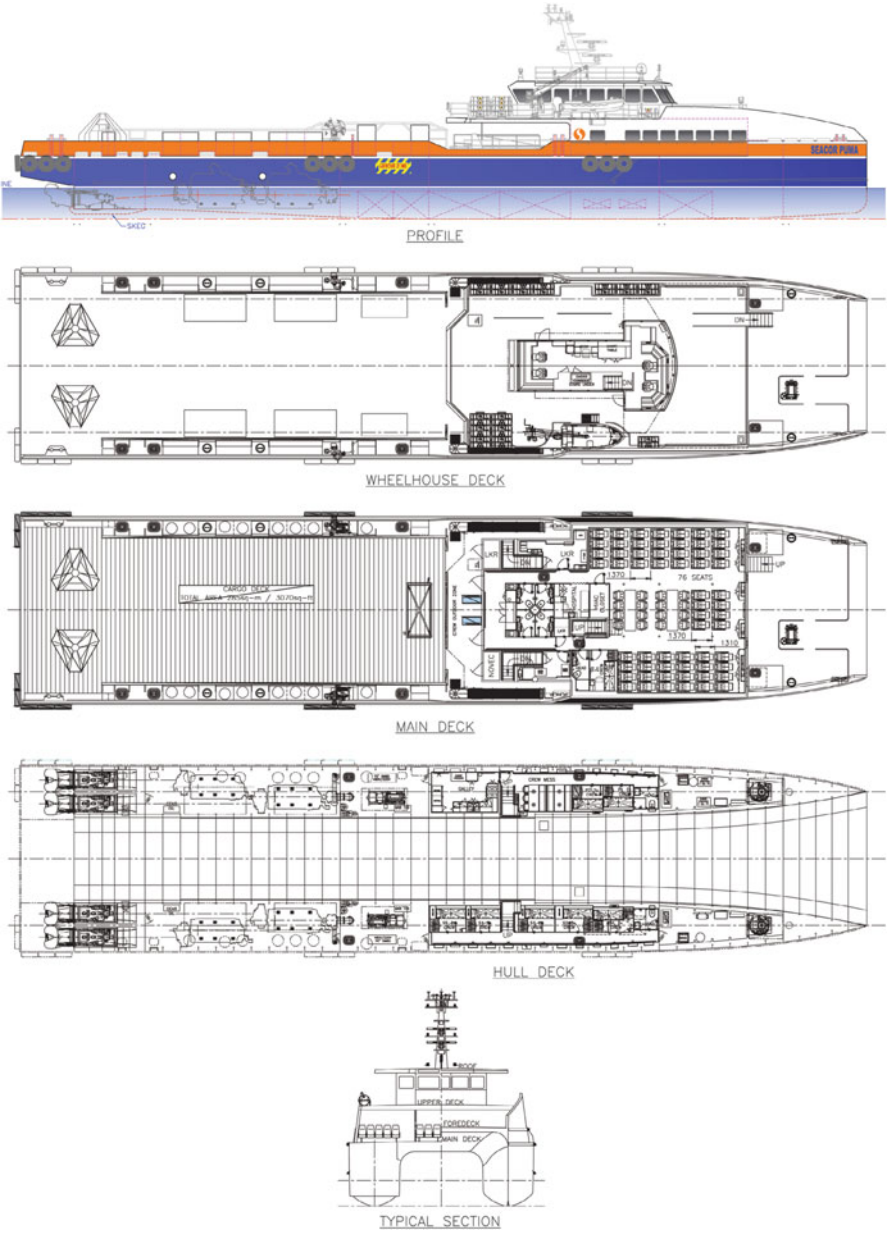

Seacor Panther *Specification Sheets*

MAIN PARTICULARS

LENGTH OVERALL	187.82 ft	57.25 m	LIGHT DRAFT	5.74 ft	1.75 m
LENGTH BP	176.00 ft	53.64 m	LOADED DRAFT	8.79 ft	2.68 m
BEAM	41.00 ft	12.50 m	SUMMER FREEBOARD	6.51 ft	1.98 m
DEPTH	14.33 ft	4.37 m	LIGHTSHIP	322.00 Lt	327.17 Mt

CAPACITIES

FUEL OIL	25,437 USG	96.3 m^3
POTABLE WATER	6,870 USG	26.0 m^3
MAIN ENGINE LUBE-OIL	1,600 USG	6.1 m^3
SEWAGE	680 USG	2.6 m^3
GEAR OIL	192 USG	0.7 m^3
WASTE OIL	800 USG	3.0 m^3
COOLANT	90 USG	0.3 m^3
HYDRAULIC OIL	100 USG	0.4 m^3
JET OIL TANK	113 USG	0.4 m^3
GREY WATER	680 USG	2.6 m^3
BILGE SLOP TANK	800 USG	3.0 m^3
DEADWEIGHT	255.03 Lt	259.12 Mt

CARGO DECK

TONNAGE	200 Lt	203.2 Mt
STRENGTH	540.0 lb/ft^2	2.6 Mt/m^2
LENGTH	94.25 ft	28.7 m
WIDTH	9.75 ft	3.0 m
CLEAR AREA	3,084 ft^2	286.5 m^2
CLEAR AREA W/ GENERATOR	3,000 ft^2	278.7 m^2

TONNAGE

	INT
GRT	491 ITC
NRT	147 ITC

MACHINERY

MAIN ENGINES	Cummins QSK95 rated 4000 hp IMO Tier II Engines
BRAKE HORSEPOWER	16,000 hp
REDUCTION GEARS	4 - Twin Disc MGX62500 SC
RATIO	2.111:1
PROPULSION	4 - Hamilton Jet HM810
GENERATORS	2 - 290 KW paralleling IMO Tier II Engines
GENERATOR DRIVES	2 - Cummins QSM11 DM SWAC
DECK GENERATOR	1 - Cummins QSM11 - 270KW
BOW THRUSTER	2 - Veth VL-180
OIL WATER SEPERATOR	1 - US-500-C Bilge Water Separators
FUEL CENTRIFUGE	2 - MAB 103
WATER MAKER	Aquamatic 1800 USG per day

PERFORMANCE

MAXIMUM SPEED	40 Kts
CRUISING SPEED	35 Kts

DISCHARGE RATES

	GPM @ FT	M^3/HR @ M
FUEL OIL	180 60	

This specification is based on construction plans and calculations at building and is believed to accurately reflect the vessel. However, such accuracy cannot be guaranteed.

ACCOMMODATIONS — CABINS: 8 — BERTHS: 16

GALLEY	Seating for 15
TELEVISION	3 - with VCR/DVD combo in passenger area 2 - with VCR/DVD combo in Galley / Mess
REFRIGERATOR/FREEZER	2 - refrigerators & 3 - freezers - 21 cu ft
A/C & HEATING	4 Technicold units - 90,000 BTU eachl
PASSENGER AREA	76 First Class Seats total Noise Supression Insulation Fitted for Passenger Comfort
HOSPITAL	1 bed
PASSENGER HEAD	4
WASHER / DRYER	2 sets
BEVERAGE/SNACK BAR AREA	Located in Passenger Area/Main Deck Microwave, Coffee Pot, Beverage Cooler

ELECTRONICS & CONTROLS

COMPASS	1 - Magnetic & 3 - Gyro
DEPTH RECORDER	1 - Furuno FE800
ENGINE / GEAR CONTROLS	Hamilton Jet
EPIRB 406 MHZ	Sailor SGE-406II
GPS	Furuno GP170
RADAR - ARPA	2 - Furuno FAR2127 (Arpa Enabled)
GMDSS	Furuno A3 Console
STEERING	Hamilton Jet
AUTOPILOT	Simrad Type AP-70
VHF	4 - ICOM M506
INTERNAL TELEPHONE	PHONTECH BTS4000
PA SYSTEM	PHONTECH SPA1500
HAILER	Furuno LH3000
DYNAMIC POSITIONING	Kongsberg SDP21 / KPOS / ABS Class 2
NAVTEX	Furuno NX 700B
INTERNET E-MAIL	VSAT
VESSEL MONITORING SYSTEM	CSP
AIS	Furuno FA150
DP REFERENCES	2-CNav 3050, 1-Radius, 1-CyScan
BNWAS	Furuno BR500

SPECIAL EQUIPMENT

FIRE FIGHTING	Novek 1230
EXTERNAL FIRE FIGHTING	10,600 GPM total 2 - Jason Monitors @ 5300 GPM each & 2 - Jason Pumps 1 fitted with foam
FIRE DETECTION	Smoke and Heat Detection per ABS
LIFE RAFTS	14 x 25 man inflatable rafts
RESCUE EQUIPMENT	FRC with Jacobs Ladder
FUEL METER	2 - fuel meter with ticket printer
SEARCHLIGHTS	3 - remote control
CCTV MONITOR	Fitted
DECK LIGHTING	10 - LED Fixtures

r20170518

SPECIAL EQUIPMENT (CONTINUED)

SEWAGE TREATMENT	2 - Headhunter IMO MEPC 159(55)
RIDE CONTROL	Maritime Dynamics
MSI DISPLAY	Maritime Dynamics
WIRELESS INTERNET ACCESS	Fitted
FIXED BOARDING RAMPS	1 - Starboard
SATELLITE TV	Fitted
DECK POWER RECEPTACLES	3 - 480 volt - 3 phase
ANCHOR WINCH	HIDROMARIN MPC-1600
CLEARSPRAY DISPERSANT SYSTEM	21.4 m of boom
FRC/DAVIT	Ned Deck Sch 12-3.5R RSQ450A Rescue Boat w/ Yanmar D27 diesel outboard
ANCHOR	SHHP Pool 202KG
SURFER LANDING	
FROG 10	2

DOCUMENTATION

CLASS	A1 HSC Crewboat Restricted Service+ + AMS + DPS2+ Fire Fighting Capability
OFFICIAL NUMBER	6957
RADIO CALL SIGN	V7FN8
DP CLASS	ABS - DP2
ERN	85, 82, 5, 5
VESSEL DELIVERY DATE	Jun-17
IMO#	9805879
ABS ID	YY268268
MMSI #	538006957
FLAG	Marshall Islands
IOPP/SMPEP	YES
HOME PORT	Majuro, MI
KEEL LAID	Apr-16

r20170518

Seacat Services, Seacat Enterprise*, South Boats 27-m High-Speed Utility Vessel*

General Arrangement

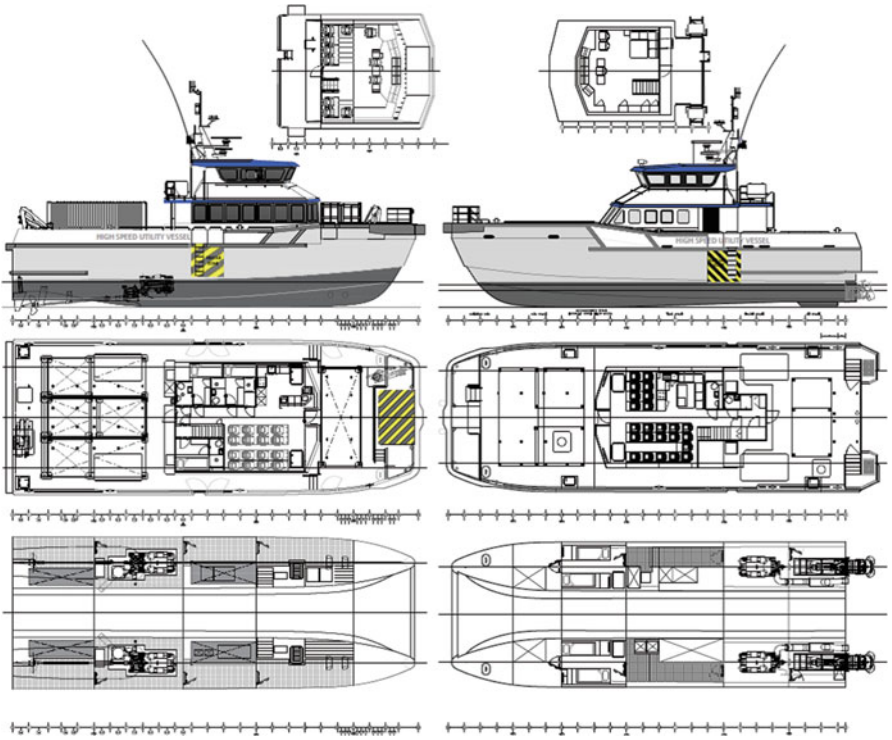

Specifications

Length overall: 26.93 m, Max Beam: 9.40 m, Draft: 2.04 m, GRT: 123.6 t

Capacities	
Fuel oil	37,000 L
Fresh water	1,500 L
Gray/black water	1,500 L
Free work deck area	124 m^2
Max. deck load	2.0 t/m^2
Deck cargo (balanced with fuel load)	40 t
Crew	<4 persons
Industrial personnel	<24 persons

Performance
Speed (max) 25.0 knots (550 L/h)
Speed (high) 22.0 knots (500 L/h)
Speed (low) 19.0 knots (430 L/h)

Propulsion system	
Main engines	2 × MTU 12V-2000-M72
Total power	2 × 1080 kw (2 x 1450 hp)
Gearboxes	2 × Servogear HD295 3.3:1
Propulsion	2 × Servogear 1175mm CPP Ecoflow Propulsion or 2 × Waterjets/ FPP/IPS
Bow Thrusters Hercules	4 × HHBT45, each 45 hp
Electrical equipment	
Network 24V DC, 230V 50 Hz AC	
Generator set 2 × Onan MDKBR 19.5 kW	
Deck Layout and Equipment	
Anchor equipment	1 × 225 kg SHHP with chain and line, AAW-150 winch
Bow fendering	RG Seasight composite rubber
Secondary access (option)	Osbit Maxccess/offshore transfer devices, tube docking device
Fore deck 34 m^2 (max. 10 te)	TMP 500 L
	1 × 20ft ISO Container mounts
Aft deck 80 m^2 (max. 30 te)	Effer 275 M crane
	3 × 20 f. or 4 × 10 f. ISO container mounts
Mob recovery system	Fibrelight cradle c/w ship-mounted davit

Lifesaving equipment
Life buoys 6
Life jackets 30
Immersion suits 30
Life rafts 4 × 16 persons
Fire fighting
CO_2 fixed Fi-Fi system in engine rooms
Portable hand-operated Fi-Fi in other areas
Consillium fire detection throughout
2 × DESMI hydraulic saltwater Fi-Fi c/w hose and nozzle
Optional Fi-Fi monitors
Accomodation
24 × Seat saloon, 3 × Seat bridge
Crash-tested suspension seats (as photo on right)

Welfare
Soft mounted deckhouse to minimize exposure to noise vibration
Noise levels < 60 dBA
Air conditioning and heating
Washing machine and tumble dryer
Luggage area
3 × twin crew cabins ensuite
Drying room, technician's head, with toilet, urinal, sink, and hand dryer.
Galley and crew mess area with water boiler, coffee machine, microwave oven, hob, fridge, and freezer
3 × TVs, playstation4, DVD player, radio, MP3, satellite TV, 4G Internet, VSAT

Maritime Craft Services SWATH 1

Adhoc Marine Designs Typhoon-Class High-Speed Utility Vessel

General Arrangement

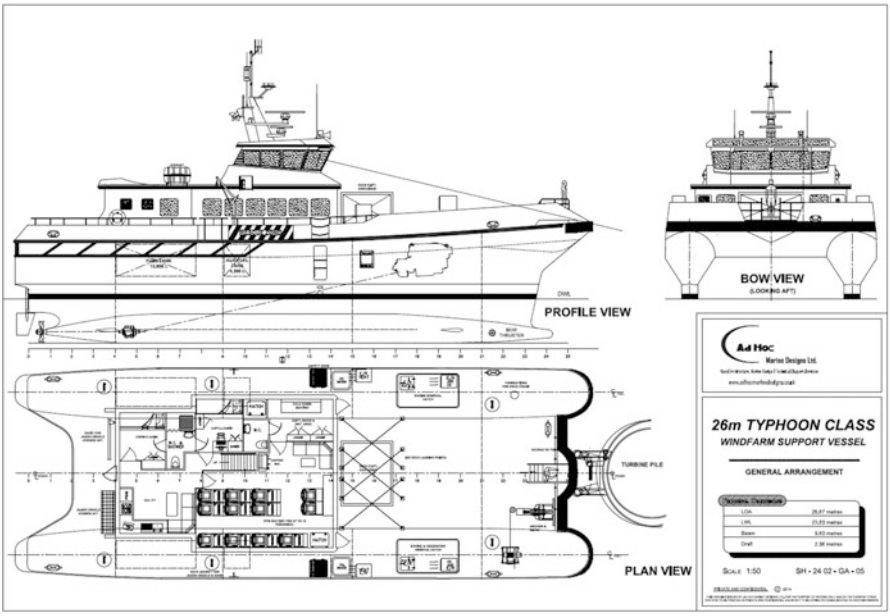

Specifications

General	
Type	Typhoon Class SWATH
Built	2016
Class	Bureau Veritas 1@Hull MCA
	Category 1
Flag	UK
Dimensions	LOA:26 m; BOA:9.8 m; Draft:2.1 m
Displacement	5 t
GRT	TBC
Post of Registry Glasgow	

Tank capacities	
Fuel oil	19.5 m^3
Fresh water	1.96 m^3
Dirty oil	0.196 m^3
Sewage	0.5 m^3
Ballast	21 m^3
Bilge/black water	0.196 m^3
Hydraulic oil	0.7 m^3
Performance	
Sprint speed	24 knots
Cruise speed	22 knots
Propulsion	
Main engines	2 × MAN D2862 LE 466
Total power	2 × 1029 kW
Gearbox	ZF 3050A
Propellers	Hundested CPP
Bow thrusters	2 × 50 kW
Auxiliary equipment	
Main generators	2 × Kohler 28EFOZD
Capacity	2 × 28 kW 230/400V@50Hz
Stabilizers	4 × fins by Island Engineering
Ballast system	Servowatch
Deck	
Deck crane	Palfinger PK4501 (space available)
Deck capacity	5 te
Deck clear area	95 m^2
Fixing points for 3 m length ISO container	
Accommodation	
Heated and air-conditioned passenger saloon with suspension seats for 12 passengers completed with work tables and Euro 230 V sockets	
Pantry area with amenities, shower, and toilets	
Crew maximum 6 persons	
Navigation equipment	
Searchlight	2 × colorlight LED
Magnetic compass	Sestrel major binnacle
Satellite compass	Furuno SC50
Gyro compass	Furuno GC80
GPS	Furuno GP150
Radar	2 × Furuno 2117BB
ECDIS	Furuno FMD3100
Autopilot	Navitorn NT888G
AIS	Furuno FA150
Echosounder	Furuno FE700
VHF/DSC	2 × Sailor 6222

(continued)

Navigation equipment	
VHF Handheld	Jotron TR20
SSB	Sailor 6310
Navtex	Furuno NX7008

Index

L. Yun et al., *High Speed Catamarans and Multihulls*,
https://doi.org/10.1007/978-1-4939-7891-5